Peptides

Copenhagen 2010: Tales of Peptides

The Proceedings of the Thirty-First European Peptide Symposium

Michal Lebl
Morten Meldal
Knud J. Jensen
Thomas Hoeg-Jensen

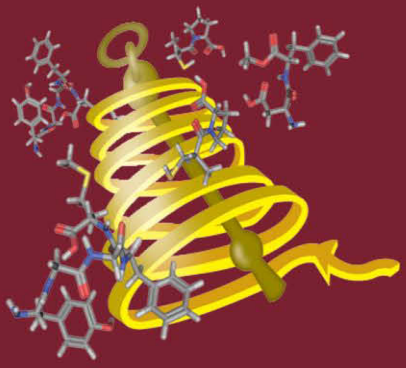

Peptides 2010

Tales of Peptides

Proceedings of the Thirty-First European Peptide Symposium

Peptides 2010

Tales of Peptides

Proceedings of the Thirty-First
European Peptide Symposium

Peptides 2010

Tales of Peptides
Proceedings of the Thirty-First
European Peptide Symposium
September 5-9, 2010, Copenhagen, Denmark

Edited by
Michal Lebl
Prompt Scientific Publishing, San Diego, CA, USA
michallebl@gmail.com
Morten Meldal
Carlsberg Laboratory, Copenhagen, Denmark
mpm@crc.dk
Knud J. Jensen
University of Copenhagen, Faculty of Life Sciences, Denmark
kjj@life.ku.dk
Thomas Høeg-Jensen
Novo Nordisk A/S, Maaloev, Denmark
tshj@novonordisk.com

European Peptide Society

ISBN 0-9715560-5-9

Published by the European Peptide Society

Sold and distributed by www.lulu.com

Produced by Prompt Scientific Publishing,
www.promptpublishing.com, San Diego, U.S.A.

Introduction

We had the distinct honor to jointly host the 31st Symposium of the European Peptide Society and we hope that you had an exciting experience at the Symposium. The 31EPS took place at the Bella Center located just outside Copenhagen City near the Airport. It is the largest conference facility in the region and provides all the necessary facilities for a successful conference. In close collaboration with the Scientific Committee we composed an exciting four day event for you and we believe we identified some of the most important new results in peptide science for oral presentation during the meeting. There was provided for an excellent exhibition event at the 31EPS and the general feeling was that exhibitors were thrilled to have such good contact to participants. EPS and the organizers would like to sincerely thank the sponsors of this event for their significant contributions and support of the field of Peptide Science.

The four-day format was new at 31EPS. The symposium had 882 participants, 600 abstract submissions and 78 lectures. We therefore had an intense program Monday to Thursday, enabling participants to return Thursday night or Friday morning as their flight connections allowed. The traditional social events on Wednesday was not arranged, instead we expected that participants with an interest in Copenhagen culture would arrange tours on their own before or after the meeting. The 31EPS was followed by the 31EPS-Satellite Symposium on Cell Penetrating Peptides, a two-day mini-symposium at the Panum Institute, University of Copenhagen.

On the social side There was a welcome reception at the Bella Center Sunday night and the gala farewell dinner at Langelinie Pavillionen Wednesday evening which included entertainment with the famous Captain Hoffers Show Band. The City of Copenhagen offered a visit with servings to the City Hall at the center of Copenhagen on Tuesday evening. This was arranged at the same time as the Speakers Dinner took place at the historic Carlsberg Museum.

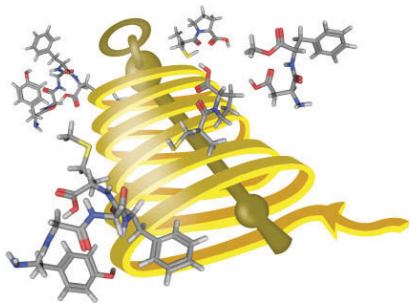

The 31EPS Logo The Logo is based on a novel of the famous Danish author, H. C. Andersen. in this less known but beautiful story titled “The Bell” H. C. Andersen in the most fascinating manner shows us how those and only those who search the truth with perseverance and passion shall find it and have a life experience, in which they unite

with our universe. We thought this story has a lot in common with the slow process of unraveling the true nature of peptide biology and thus the Logo.

The picture of the three relaxed 31EPS Co Chairs, Morten Meldal (second to the right) Knud J Jensen (to the left) and Thomas Hoeg-Jensen (to the right) in the merry company of Tom Muir and Anette Beck-Sickinger after one of the sessions.

Morten Meldal **Knud J. Jensen** **Thomas Hoeg-Jensen**

Co Chairs of 31EPS

Scientific program

In planning the 31st EPS, the organizers aimed at creating the strongest possible scientific program broadly within peptide science. There was more emphasis on new, enabling developments in peptide chemistry than in some previous peptide symposia. in addition the organizers wanted to highlight peptides as drugs and had a dedicated session towards this topic, chaired by Thomas Hoeg-Jensen and Waleed Danho.

The plenary and invited speakers were Herbert Waldmann, Tom W. Muir, Ernest Giralt, William F. DeGrado, Ivan Huc , Fernando Albericio, Horst Kessler, Paul Alewood, Annette Beck-Sickinger, William Lubell, Ronald Raines, and Richard DiMarchi, who were invited to present the latest developments in peptide science from around the world. in addition the two awardees, Helma Wennemers and Stephen B. H. Kent contributed to the strong program. The speakers were invited to present new developments in peptide synthesis, both in SPPS and in ligation methods, peptide chemical biology including the role of farnesylation and palmitoylation, peptide medicinal chemistry, foldamers related to peptides, structural aspects of peptides and proteins and more.

The scientific committee ranked all abstracts. Based on their ranking, the speakers for the oral and young investigator presentations were selected.

The young investigator sessions as well as the Zervas and Rudinger award sessions were all integrated into the main program to encourage attendance. The sessions covered were: Peptide biochemistry and biology; synthetic chemistry of amino acids and peptides; young investigator session; general peptide science; ligation; peptides as drugs; peptidomimetics; protein design and protein modification; peptide materials and peptide properties; antibacterial and cell penetrating peptides; lipopeptides; signaling, hormones and neuro-peptides; peptide biology; chemical biology and proteomics. Needless to say, the actual lecture topics covered a wider range than this. The parallel sessions Monday and Wednesday were a success, in spite of some initial technical problems on Monday afternoon.

In summary, there were 5 plenary lectures, 7 invited lectures, 2 award lectures, 12 young investigator lectures and 52 oral presentations. Finally, as mentioned above there were close to 600 poster presentations, and two afternoons in the program were dedicated to poster sessions. There were generally lively discussions after lectures, which contributed to a scientifically very strong program.

Production Team Remarks

This year's proceedings production was a test about readiness of European Peptide Society members to accept the new technologies allowing the book to be published three months after the symposium, or earlier. Besides the speed of production, reduction of the book cost was an additional goal. Manuscripts were accepted through the internet page and entered into the database. This process allowed creating indexes on the fly and simplified communication with authors. Manuscripts were available for proofreading six weeks after submission and the finalized book was available on the website for downloading 10 weeks after the symposium. The "real book" is available from "just in time" printing process at www.lulu.com. Due to the fact that the European Peptide Society is a nonprofit organization, there is no margin charged for the book, and all members can order it for production cost (we recommend comparing the price with the price of previous symposium volumes).

Our thanks go to all authors who delivered manuscripts of a high technical quality before the deadline. If everybody would adhere to the guidelines for manuscript preparation, we could have it ready much earlier. Figures in which the size of the fonts is at the level of the size of polystyrene solid phase support, are the most prevalent problem in submitted manuscripts. Authors should understand that some of the graphs looking good at the poster size are far from ideal for book page size. Some of the figures were replaced by authors during the proofreading, but there are still a lot of figures requiring a microscope for deciphering the text in printed version. Fortunately, most of the readers of the symposium proceedings actually download the pdf file and therefore can enlarge the page to readable size. We urged authors not to submit color version of the figures, however, it was probably an unreasonable request. Even though in print these figures will be represented in shades of gray (sometimes very light gray representing yellow color), the downloaded pdf file keeps the information content intact.

Our company, Prompt Scientific Publishing, produced the proceedings of the 17th, 18th, and 21st American Peptide Symposia testing different production technologies. We believe that providing the information in both printed and electronic form is an ideal process. The speed is the most important factor – the value of the book of proceedings two years after the symposium is close to zero. We still believe that with the combination of the new technologies and author's cooperation we can deliver the proceedings book at the time of the symposium. Hopefully, once authors realize that their manuscript can be published very quickly, the next volume of proceedings will cover an even higher percentage of the presented work than this one.

We want also to thank the co-editors for delivering their part of the work promptly – it just proved the fact that being in three countries (Denmark, Czech Republic, and USA) on two continents does not have to slow the communication at all.

Roseann Story-Lebl
Michal Lebl

Message from the Chairman of the European Peptide Society

The 31st European Peptide Symposium, the most recent biennial symposium organized under the auspices of the European Peptide Society was again a great success. A highly international group of 882 scientists from all over the world met in Copenhagen, Denmark in September.

For several reasons, this 31st European Symposium has been a special one. The scientific program offered to the participants was of very high quality. Although structural aspects and biology of peptide and protein science were well represented, the program left a large place to all branches of chemistry.

During the Council meeting of the European Peptide Society (EPS) on Monday a large number of newly elected Representatives of peptide communities from different countries had a chance to meet for the first time in Copenhagen. According to the statutes of the Society it was also the time to elect new members of the Executive Committee. The Council expressed its appreciation to retiring members. Professor Ettore BENEDETTI from Italy has been the treasurer of the EPS for 4 years, after being a member of the Executive Committee for 4 years. Professor Anna-Maria PAPINI from Italy has been elected as Treasurer of the EPS. Professor David ANDREU from Spain, who acted as the Scientific Affairs Officer of the EPS for 2 x 4 years, has been replaced by Professor Solange LAVIELLE from France. Both of them, beyond their involvement in their respective duties, have significantly and tremendously been committed for the European Peptide Society. Professor Jean MARTINEZ, being a member of the Executive Committee since 1990, having acted first as Scientific Affairs Officer for 4 years (1998-2001) then for 8 years (2002-2010) as President of the EPS, leaves the presidency to the new elected President, Professor Ferenc HUDECZ from Hungary. Professor Hudecz served the Society as Secretary for 2 x 4 years (2000-2008).

I would like to warmly thank all members of the Council I had the chance to work with; they all were of great help in running the Society duties. A special mention is to the colleagues of the Executive Committee who really efficiently assisted me in the Society, always in a very friendly atmosphere. I would also like to address my thanks to all colleagues of the American, Chinese, Japanese, Korean, Australian and Indian Peptide Societies for their contribution to the International Peptide Society. Last but not least, my warm thanks to all members of the European Peptide Society who have made my period of Presidency so pleasant.

One of my last duty as the President of EPS will be to congratulate and thank our colleagues Thomas HOEG-JENSEN, Knud JENSEN, Morten MELDAL, organizers of the 31st European Peptide Symposium in Copenhagen and their teams, for offering to the peptide community a so attractive scientific week around peptide and protein science.

I and the newly elected President wish the new EPS council, the new Executive Committee, all of you, the European Peptide Society and Peptide Sciences, a great success for the future.

Preceeding chairman of EPS, Professor
Jean Martinez
Laboratoire des Aminoacides, Peptides et Protéines , Faculté de Pharmacie
CNRS-UMR, BP 14491,
Av. Charles Flahault
F-34093 Montpellier Cedex 5
FRANCE

Present chairman of EPS, Professor
Ferenc Hudecz
Research Group of Peptide Chemistry
Department of Organic Chemistry
Eötvös Loránd University
Pázmány Péter sétány 1A
H-1117 Budapest, Hungary

31st EUROPEAN PEPTIDE SYMPOSIUM

September 5-9, 2010
Copenhagen, Denmark

Co-Chairs

Morten Meldal
Carlsberg Laboratory, Copenhagen
mpm@crc.dk
Knud J. Jensen
University of Copenhagen, Faculty of Life Sciences, Copenhagen
kjj@life.ku.dk
Thomas Høeg-Jensen
Novo Nordisk A/S, Maaloev
tshj@novonordisk.com

Local organizing Committee

Jens Buchardt
Paul R. Hansen
Peter Heegaard
Phaedria St. Hilaire
Birthe Kragelund
Thomas E. Nielsen
Kristian Strømgaard

International Scientific committee

Fernando Albericio
David Andreu
Annette G. Beck-Sickinger
Paul Cordopatis
Ronald Frank
Yoshiaki Kiso
Hilkka Lankinen
Tom Muir
Anna-Maria Papini
Antonello Pessi
Claudio Toniolo
John Wade

EPS Travel Grants

25 young investigators were selected as recipients of travel awards, funded by the European Peptide Society. Investigators with oral or poster presentations and long travels were prioritized in the selection process as performed by the 31EPS chairmen.

List of 31st European Peptide Symposium Sponsors

The 31st European Peptide Symposium was made possible through the generous support of the following organizations:

Novo Nordisk	Platinum Sponsorship
Biotage	Gold Sponsorship
CEM	Gold Sponsorship
Jupiter Bioscience	Gold Sponsorship
Polypeptide Laboratories	Silver Sponsorship, Rudinger Award
Bachem AG	Zervas Award
Escom Science Foundation	E. & B. L. Schram Awards
Merck Bioscience	
Aapptec	
John Wiley & Sons	
Waters	
Cambridge Isotope Labs	

List of 31st European Peptide Symposium Exhibitors

Aapptec
Activotec
Agilent Technologies
AkzoNobel/Kromasil
Almac Sciences
AmbioPharm Inc
Americam Peptide Company Inc.
Bachem AG
BCN Peptides S.A.
Biotage
C S Bio Co.
C.A.T. Gmbh & Co KG
CEM CORPORATION
CLB Biopharma LLC
CPC Scientific
Creosalus
Dionex
European Peptide Society
Genzyme Pharmaceuticals LLC
Gl Biochem
Grace Davison Discovery Sciences
Hybio Pharmaceutical Co. Ltd
INTAVIS AG
Iris Biotech GmbH
Jupiter Bioscience Limited
LONZA
Merck Chemicals LTD
Mettler-Toledo A/S
Nagase GmbH
Neuland Laboratories Ltd
ORPEGEN Peptide Chemicals
PCAS BioMatrix Inc.
Peptides International
PEPTISYNTHA
Phenomenex
PolyPeptide Laboratories A/S
Polypure AS
Protein Technologies Inc.
RAPP Polymere GmbH
Reanal Finechemical
Senn Chemicals AG
Sussex Research
Synthetech Inc
Tianjin Nankai Hecheng S&T
Varian Inc.
Waters
YMC Europe

The European Peptide Society

The European Peptide Society was founded in 1989, primarily in order to ensure that the valuable but informal European Peptide Symposia should be continued on a sound basis. The Statutes state that it is a non-profit association established for the public benefit to promote in Europe and in certain neighboring countries the advancement of education and in particular the scientific study of the chemistry, biochemistry, and biology of peptides.

Its most important activity is the organization in Europe of the biennial international symposium which regularly attracts about 1000 participants from all over the world. The Proceedings are published biennially. Although the early symposia (from 1958 onwards) were necessarily devoted largely to the development of chemical methods for the synthesis of peptides, the programs now extend to the biology of peptides, and include, for example, structure-activity relationships, conformational studies, peptide vaccines, and the immunology of peptides.

The Society also supports financially smaller local meetings and workshops. The governing body of the Society is the Council. Each constituent country which has the required minimum number of members the Register of the Society has one representative on the Council. Council elects from ordinary members of the Council or from co-opted members of the Council a Chairman, a Secretary and a Treasurer each for a period of four years. Council also appoints an Executive Committee consisting of the Chairman of the Council, the Secretary, the Treasurer, the Scientific Affairs Officer and one ordinary member. The Society has a membership of about 1200 (from some 30 countries) who pay no subscription at present. The principle was established at the outset that there would be no subscription in order to ensure that all peptide scientists in Europe would be able to enroll.

The Council introduced the following rules in 2002. For the acceptance of application for membership one full paper published in peer-reviewed journal or two publications in Proceedings of International meetings related to peptide science or one accepted patent are required. Members are receiving the Newsletter and have the right to nominate/elect National Representative of the country. For the acceptance of application for temporary membership no written record in the field is needed, but the applicant must be supported in writing by a member of the Society. Temporary members are receiving the Newsletter. Temporary membership will be automatically cancelled after 3 years or renewed upon written request. For consideration of travel grant application at EPS meetings or at EPS supported meetings there is no EPS membership required.

The only current income to the Society is from sponsorship contributions, a small per capita contribution from the registration fee of the biennial symposia, and advertising in, and with, the Society's Newsletter. of these sources, sponsorship is the most important, and indeed the continued viability of the Society as currently organized is completely dependent on the support of Sponsors. The Society's outgoings at present comprise production and circulation expenses connected with its six-monthly Newsletter, expenses of its annual Executive Committee Meeting (which are very modest), other administrative expenses (which are minimal), and the subsidy of small scientific meetings in the field. It does not contribute to the costs of the *Journal of Peptide Science*: although this is the Society's official journal, it is

published by John Wiley & Sons as a financially independent operation. None of the Society's Officers receive any benefit from their offices; the Society has no employees or administrative overheads apart from postage etc; its accounts are professionally audited and are available to any interested Sponsor or potential Sponsor.

Society members may subscribe to the Journal of Peptide Science at a greatly reduced rate. In addition, the Society circulates a Newsletter which contains brief reports of meetings and other news, book reviews, and lists, and a calendar of relevant symposia. The Society administers the Josef Rudinger Memorial Lecture Award and the Leonidas Zervas Award, and a fund to assist younger members to attend symposia. It has close and cordial relations with the other Peptide Societies. At present membership is free to academic and individual industrial applicants giving evidence (by listing published papers or patents) of their commitment to scientific research in this field.

European Peptide Symposia

Symposium	*Year*	*Location*
1st	1958	Prague, Czechoslovakia
2nd	1959	Munich, GFR
3rd	1960	Basel, Switzerland
4th	1961	Moscow, Russia
5th	1962	Oxford, UK
6th	1963	Athens, Greece
7th	1964	Budapest, Hungary
8th	1966	Noordwijk, The Netherlands
9th	1968	Orsay, France
10th	1969	Abano Terme, Italy
11th	1971	Vienna, Austria
12th	1972	Reinhardsbrunn, GDR
13th	1974	Kiriyat Anavim, Isreal
14th	1976	Wepion, Belgium
15th	1978	Gdansk, Poland
16th	1980	Helsingor, Denmark
17th	1982	Prague, Czechoslovakia
18th	1984	Djuronaset, Sweden
19th	1986	Porto Carras, Greece
20th	1988	Tubingen, GFR
21st	1990	Barcelona, Spain
22nd	1992	Interlaken, Switzerland
23rd	1994	Braga, Portugal
24th	1996	Edinburgh, UK
25th	1998	Budapest, Hungary
26th	2000	Montpellier, France
27th	2002	Sorrento, Italy
28th	2004	Prague, Czech Republic
29th	2006	Gdansk, Poland
30th	2008	Helsinki, Finnland
31st	2010	Copenhagen, Denmark

The Josef Rudinger Award

This award is presented "in commemoration of Josef Rudinger's role in the foundation of the European Peptide Symposia and of diverse contributions he made to peptide chemistry". There is no restriction as to nationality, age or position of those nominated, but they must be distinguished.

2010 Stephen B. H. Kent
University of Chicago, USA

2008 Horst Kessler and **Manfred Mutter**
Technical University of Munich, Germany
University of Lausanne, Switzerland

2006 Ettore Benedetti and **Claudio Toniolo**
University of Napoli "Frederico II", Italy
University of Padova, Italy

2004 Luis Moroder
Max-Planck-Institute für Biochemie, Martinsried, Germany

2002 Sándor Bajusz and **Kálmán Medzihradszky**
IVAX-Institute of Drug Research, Budapest, Hungary
Department of Organic Chemistry, Eötvös L. University, Budapest, Hungary

2000 Bernard P. Roques
INSERM, CNRS, Paris, France

1998 Shumpei Sakakibara
Peptide Institute, Osaka, Japan

1996 Ralph Hirschmann
University of Pennsylvania, Philadelphia, USA

1994 Robert C. Sheppard
MRC, Cambridge, United Kingdom

1992 Viktor Mutt
Karolinska Institute, Stockholm, Sweden

1990 R. Bruce Merrifield
The Rockefeller University, New York, USA

1988 Erich Wünsch
Max-Planck-Institüt für Biochemie, Münich, Germany

1986 Robert Schwyzer
ETH Zürich, Switzerland

The 2010 Leonidas Zervas Award

The *Leonidas Zervas* Award is presented "to the scientist who has in the opinion of the Council of the Society made the most outstanding contribution to the chemistry, biochemistry, or biology of peptides in the five years preceding the date of selection". There is no restriction as to nationality or position of the candidate, but regulations give preference to younger candidates.

2010 Helma Wennemers
University of Basel, Switzerland

2008 Anna Maria Papini
University of Florence, Italy

2006 Carlos García-Echeverría
Novartis Institutes for BioMedical Research, Basel, Switzerland

2004 Helene Gras-Masse
Institut Pasteur de Lille, France

2002 Thomas W. Muir
Rockefeller University, New York, USA

2000 Antonello Pessi
Instituto di Ricerche di Biologica Moleculare P. Angeletti, Rome, Italy

1998 Annette G. Beck-Sickinger
ETH Zürich, Switzerland

1996 Morten Meldal
Carlsberg Laboratory, Valby, Denmark

1994 Ernest Giralt and **Fernando Albericio**
University of Barcelona, Barcelona, Spain

1992 Günther Jung
University of Tübingen, Tübingen, Germany

1990 Michal Lebl and **Jean Martinez**
Czechoslovak Academy of Sciences, Prague
CNRS, Montpellier, France

1988 Alex Eberle
University of Basel, Basel, Switzerland

Young Investigators' Symposium

The young investigator symposium featured 12 participants, who were preselected from over one hundred requests for oral presentations. The quality of the oral presentations was first rate and ranged on a variety of subjects featuring the chemical, biological and medicinal aspects of peptide science. The young investigators presented their research effectively and responded to questions in a clear and informative manner, which inspired further discussion. Judging the presentations was a difficult task in light of the excellent performance from all of the participants. The judges were relieved to be able to compliment the Dr. Bert L. Schram Young Investigator Awards, which were generously given by ESCOM, with four honorable mention distinctions with complementary books generously donated by Wiley Publishers. Special thanks goes to Professors Carlo Unverzagt, University of Bayreuth, Paul Cordopatis, University of Patras and William D. Lubell, Université de Montréal, who helped to preside over the session and assist in the judging.

Dr. Bert L. Schram Young Investigator Award Winners:

J. Clark, The University of Queensland: "The Engineering of an Orally Active Conotoxin for the Treatment of Neuropathic Pain"

K. Holland-Nell, Carlsberg Laboratory: "Clicking Peptides: Disulfide Bond Mimetics by the CuAAC Reaction"

Honorable Mentions:

C. M. M. Mas Moruno, Technische Universität München: "Enhancement of Receptor Selectivity of Cilegitide by Multiple N-Methylation"

V. A. Ahrens, Leipzig University: "Promising Tools for Breast Cancer Therapy: Carborane-Containing NPY Analogs"

C. Heinis, EPFL, Lausanne: "Bicyclic Peptides with Tailored Binding Specificity"

J. M. Arsenault, Université de Sherbrooke: "Cellular Expression of the Angiotensin II Type 1 Receptor Containing the Non-canonical Photolabelling Amino Acid Bpa"

Dr. Bert L. Schram Poster Awards:

The poster award winners were selected by the 31EPS local organizing committee, which acted as poster referees as chaired by Kristian Strømgaard.
The following two posters were selected as winners of the Dr. Bert L. Schram Poster Awards:

Dr. Bert L. Schram Poster Award Winners:

Jordan Fletcher, University of Bristol (Woolfson lab), poster 487: Building blocks for synthetic biology: A basic set of coiled coils of defined oligomeric state. This poster transparently presented a basic set of coiled coils with a tunable oligomericity that has applications in many areas of peptide science. The scientific content was of high quality, the layout of the poster easily guided the reader and the clarity of the illustrations communicated the goal and the conclusions of the work elegantly.

Richard Raz, FMP Berlin (Rademann lab), poster 134: Fmoc solid phase synthesis of peptide thioesters and thio acids for native chemical ligation employing a tert-butyl thiol linker. Synthesis of peptide thioesters for native chemical ligation is a challenging problem in Fmoc solid-phase peptide synthesis. This poster presented an elegant Fmoc compatible strategy for the synthesis of peptide thioesters and thioacids. The science was clearly described, the results were visually well organized and the organization of the poster communicated the importance of the work clearly.

Honorable Mentions:

L. Stella University of Rome, Italy: Effect of helix kink on the activity and selectivity of an antimicrobial peptide

U. Hjørringgaard, Århus University, Denmark: Cyclodextrin Scaffolded Alamethicin with highly efficient Channel-forming Properties

R. H. Hasset, University of Leipzig, Germany: Rational Insights in peptide affinity towards inorganic surfaces.

T.M.H. Hackeng, Maastricht University, Holland: Increasing immunogenicity of murine vitamin K dependent protein S through multivalent association of native-folded protein domains

Table of Contents

Proceedings of the 31st European Peptide Symposium
Michal Lebl, Morten Meldal, Knud J. Jensen, Thomas Hoeg-Jensen (Editors)
European Peptide Society, 2010

$n\rightarrow\pi^*$ Interactions in the Molecules of Life

Amit Choudhary[1] and Ronald T. Raines[2]
[1]Graduate Program in Biophysics; [2]Departments of Biochemistry and Chemistry, University of Wisconsin–Madison, Madison, WI, 53706, U.S.A.

Introduction

Noncovalent interactions modulate the structure, function, and dynamics of the molecules of life [1]. We have discovered a noncovalent interaction in proteins and nucleic acids, termed the $n\rightarrow\pi^*$ interaction, in which the lone pair (n) of a donor group (typically a carbonyl oxygen) overlaps with the antibonding orbital (π^*) of an acceptor group (typically a carbonyl group) (Figures 1A and 1B) [2]. The $n\rightarrow\pi^*$ interaction is reminiscent of the approach of a nucleophile to an electrophilic carbon along the Bürgi–Dunitz trajectory [2a] and analogous to a hydrogen bond, which likewise involves the delocalization of a lone pair of an acceptor over an antibonding orbital (σ^*) of a donor [3]. The stereoelectronic constraints necessary for an energetically meaningful $n\rightarrow\pi^*$ interaction are met in several fundamental protein secondary structures, such as α-, 3_{10}-, and polyproline II helices, and twisted β-sheets. A signature of the $n\rightarrow\pi^*$ interaction in proteins is a short $O_{i-1}\cdots C'_i$ contact [2b, 2d]. It has been argued that the attractive C=O···C=O interaction is primarily a dipole–dipole (Figure 1C) [4] or a charge–charge interaction (Figure 1D) [5]. We used a peptidic model system (Figure 2) to explore the nature of this interaction. Regardless of the origin of the interaction between the adjacent carbonyl groups, the interaction stabilizes the *trans* conformation preferentially over the *cis* conformation. Thus, the value of $K_{trans/cis}$ reports on the strength of the C=O···C=O interaction.

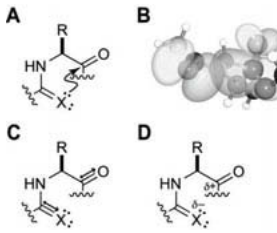

Fig. 1. Plausible C=X···C=O interactions [2d].

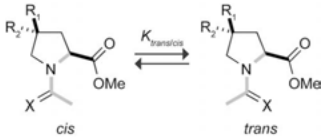

1: X=O, R_1=H, R_2=H **4**: X=S, R_1=H, R_2=H
2: X=O, R_1=F, R_2=H **5**: X=S, R_1=F, R_2=H
3: X=O, R_1=H, R_2=F **6**: X=S, R_1=H, R_2=F

Fig. 2. Compounds used to examine the C=X···C=O interaction [2d].

Results and Discussion

To distinguish between a charge–charge interaction and an $n\rightarrow\pi^*$ interaction, we envisaged the replacement of O_{i-1} with sulfur, S_{i-1}, in this model system [2d]. A charge–charge interaction would be attenuated because sulfur is less negatively polarized than oxygen, whereas the $n\rightarrow\pi^*$ interaction would be strengthened because sulfur is a softer base than oxygen. An increase in $K_{trans/cis}$ is observed from this isosteric substitution. Hence, the stabilization of the *trans* conformation cannot be due to a charge–charge interaction. Another signature of the $n\rightarrow\pi^*$ interaction is the pyramidalization of the acceptor carbonyl group. The degree of pyramidalization, like $K_{trans/cis}$, should increase with the strength of the $n\rightarrow\pi^*$ interaction. We employed a subtle means to alter the strength of the $n\rightarrow\pi^*$ interaction [6]. In accord with a potent $n\rightarrow\pi^*$ interaction, a positive correlation is observed between the degree of acceptor carbonyl pyramidalization and the value of $K_{trans/cis}$.

Next, we reasoned that the replacement of the C=O acceptor with a C–F bond would retain the dipole–dipole interaction but attenuate the $n\rightarrow\pi^*$ interaction [7]. This substitution with an amide bond isostere, the fluoroalkene isostere, leads to reversal of the conformational preference from *trans* to *cis*. Such reversal of the conformational preference cannot be explained by classical electrostatic models. It is plausible that this conformational reversal stems from closed shell repulsion between the lone pair of the donor (O_{i-1}) and the π-orbital of the fluoroalkene isostere. Such closed shell repulsions are countered by an $n\rightarrow\pi^*$ interaction in amides, which are absent in their fluoroalkene isostere.

Our computational studies indicated significant $n\rightarrow\pi^*$ interaction in certain regions of the Ramachandran plot [8]. This expectation was validated by a statistical analysis of a

large, non-redundant subset of protein structures determined to high resolution (Figure 3). Moreover, these studies indicated that $n\rightarrow\pi^*$ interactions are abundant and especially prevalent in common secondary structures such as α-, 3_{10}-, and polyproline II helices, and twisted β-sheets. As the adjacent carbonyl dipoles repel each other in an α-helix, the $n\rightarrow\pi^*$ interaction likely plays an important role in helix nucleation. Other signatures of the $n\rightarrow\pi^*$ interaction such as pyramidalization of the acceptor carbonyl carbon [9], considerable carbonyl bond lengthening [10], and polarization of its π-electron cloud [10] have been observed in the α-helices of high-resolution protein structures. Occasionally, β-strands have a bulge - an amplified right-handed twist - resulting in local disruption of the β-sheet structure. Such β-bulges are involved in the dimerization of immunoglobulin domains and can assist in enclosing the active sites of proteins. Two common types of β-bulges, the G1 and wide types, adopt φ and ψ dihedral angles indicative of considerable $n\rightarrow\pi^*$ interactions. The conformational stability of the collagen triple helix has already been attributed in part to the $n\rightarrow\pi^*$ interaction [11]. Interestingly, the absence of 4*S* diastereomer of hydroxyproline from collagen has been attributed in part to a strong $n\rightarrow\pi^*$ interaction that provides it with unusual conformational features [12].

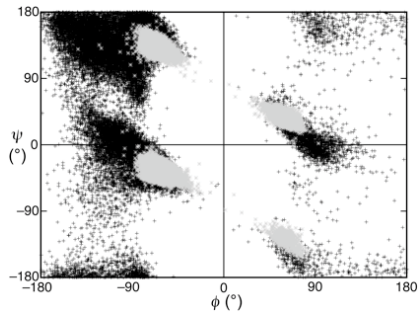

Fig. 3. Ramachandran map of $n\rightarrow\pi^*$ interactions (gray) in proteins [8].

In addition to its widespread occurrence in proteins, the $n\rightarrow\pi^*$ interaction has been postulated to play an important role in the origin of life [13] as well as modulating the conformational and physical properties of aspirin [9]. Finally, we note that $n\rightarrow\pi^*$ electronic delocalization likely plays a role in many protein–ligand interactions and catalytic processes.

Acknowledgments

This work was supported by grant R01 AR044276 (NIH). We thank Profs. G.R. Krow, S.J. Miller, J.D. Sutherland, and D.N. Woolfson for collaborative interactions, and F.W. Kotch, I.A. Guzei, L.C. Spencer, B.R. Caes, C.N. Bradford, and M.D. Shoulders for contributive discussions.

References

1. Anfinsen, C.B. *Science* **181**, 223-230 (1973).
2. (a) DeRider, M.L., et al. *J. Am. Chem. Soc.* **124**, 2497-2505 (2002); (b) Hinderaker, M.P., Raines, R.T. *Protein Sci.* **12**, 1188-1194 (2003); (c) Hodges, J.A., Raines, R.T. *Org. Lett.* **8**, 4695-4697 (2006); (d) Choudhary, A. et al. *J. Am. Chem. Soc.* **131**, 7244-7246 (2009).
3. Weinhold, F. *Adv. Protein Chem.* **72**, 121-155 (2005).
4. (a) Diederich, F. et al. *Angew. Chem. Int. Ed.* **44,** 1788-1805 (2005); (b) Diederich, F., et al. *Proc. Natl. Acad. Sci. U.S.A.* **105**, 17290-17294 (2008).
5. (a) Milner-White, E.J., et al. *J. Mol. Biol.* **248**, 361-373 (1995); (b) Milner-White, E.J., et al. *J. Mol. Biol.* **248**, 374-384 (1995).
6. A 4R electron-withdrawing group (EWG) brings the O_{i-1} or S_{i-1} donor and $C_i{=}O_i$ acceptor closer; a 4*S* EWG increases the distance between the donor and acceptor.
7. Jackobsche, C.E., et al. *J. Am. Chem. Soc.* **132**, 6651-6653 (2010).
8. Bartlett, G.J., et al. *Nat. Chem. Biol.* **6**, 615-620 (2010).
9. Choudhary, A., et al. unpublished results.
10. Lario, P.I., Vrielink, A. *J. Am. Chem. Soc.* **125**, 12787-12794 (2003).
11. Shoulders, M.D., Raines, R.T. *Annu. Rev. Biochem*. **78**, 929-958 (2009), and references therein.
12. Shoulders, M.D., et al. *J. Am. Chem. Soc.* **132**, 10857-10865 (2010).
13. Choudhary, A., et al. *ACS Chem. Biol.* **5**, 655-657 (2010).

Proceedings of the 31st European Peptide Symposium
Michal Lebl, Morten Meldal, Knud J. Jensen, Thomas Hoeg-Jensen (Editors)
European Peptide Society, 2010

Mimicry Effect of the Neo-Epitope [Asn^{641}(Glc)]FAN(635-655) with CSF114(Glc) Detecting Autoantibodies in Multiple Sclerosis

Shashank Pandey[1,2], Elisa Peroni[1,3], Maria Claudia Alcaro[4], Fabio Rizzolo[1,2], Mario Chelli[1,2], Paolo Rovero[1,2,4], Francesco Lolli[1,5], and Anna Maria Papini[1,2,3]

[1]Laboratory of Peptide & Protein Chemistry & Biology, Polo Scientifico e Tecnologico, University of Florence, 50019, Sesto Fiorentino (FI), Italy; [2]Department of Chemistry and CNR ICCOM, Via della Lastruccia 3/13, University of Florence, I-50019, Sesto Fiorentino (FI), Italy; [3]Laboratoire SOSCO-EA4505, Universitè de Cergy-Pontoise, Neuville-sur-Oise F-95031, Cergy-Pontoise, France; [4]Toscana Biomarkers Srl, via Fiorentina 1, I-53100, Siena, Italy; [5]Department of Neurological Sciences & Azienda Ospedaliera Careggi, Viale Morgagni 34, University of Florence, I-50134, Firenze, Italy; [6]Department of Pharmaceutical Sciences Via Ugo Schiff University of Florence, I-50019, Sesto Fiorentino (FI), Italy

Introduction

Multiple sclerosis (MS) is an inflammatory demyelinating disease of the central nervous system (CNS) whose pathogenesis has not been yet elucidated, even if an autoimmune mechanism against myelin antigens is thought to contribute to its immunopathological mechanism. Anyway, the target antigens responsible for inflammation and demyelination remain elusive. Different self-proteins have been investigated as potential targets for T or B cells in MS [1-4]. We demonstrated for the first time, the possibility of using the glycosylated peptide CSF114(Glc) to identify specific autoantibodies in Multiple Sclerosis patients' sera [5,6].

We report herein, the mimicry effect of CSF114(Glc) with neo-epitope peptides and the potential of this artificially N-glucosylated peptide sequence in identifying native peptides detecting autoantibodies.

Results and Discussion

Some fragments of the nervous system proteins containing *N*-glycosylation consensus site (Asn-Xaa-Ser/Thr) were selected by primary as well as tertiary structure alignment of CSF114(Glc) using SwissProt database.

Selected fragments were peptides of Factor Associated with Neutral sphingomyelinase activation Asn^{641}FAN(635-655); Oligodendrocyte Myelin glycoprotein Asn^{192}OMgp(186-204) and Nogo receptor [Asn^{179}]NogoR(173-191), which displayed 8/21, 3/21, and 5/21 residues homology with CSF114(Glc), respectively (Table 1).

It was possible to synthesize peptide fragments only by microwave-assisted peptide and glycopeptide synthesis introducing Asn(Glc) at the requested position by the building block approach using Fmoc-Asn(GlcOAc$_4$)-OH. The neo-glycopeptides were analyzed in SP-ELISA on sera of clinically definite MS patients (Figure 1a) compared to Normal Blood Donors (data not shown).

Table 1. Neo-peptide epitopes

Glycosylated peptides	*Sequences*
[Asn^{641}(Glc)]FAN(635-655)	G I T V S R **N G S** S V F T T S Q D S T L K
[Asn^{192}(Glc)]OMgp(186-204)	T L I N L T **N L T** H L Y L H N N K F T F I
[Asn^{179}(Glc)]NogoR(173-191)	T F R D L G **N L T** H L F L H G N R I S S V
CSF114(Glc)	T P R V E R N G H S V F L A P Y G W M V K

(N X T/S)=N-glycosylation consensus sequence

The aberrantly glucosylated peptide [Asn^{641}(Glc)]FAN(635-655) showed similar reactivity to CSF114(Glc) and appeared to be the preferred ligand in comparison to [Asn^{179}(Glc)]NogoR(173-191) and [Asn^{192}(Glc)]OMgp(186-204) in the solid-phase conditions of ELISA for MS autoantibody recognition (Figure 1a).

Moreover, affinity purified anti-[Asn^{641}(Glc)]FAN(635-655) IgGs showed cross reactivity with CSF114(Glc) in SP-ELISA (Figure 1b) and the complex of affinity purified anti-CSF114(Glc) antibodies and CSF114(Glc) could be inhibited by [Asn^{641}(Glc)]FAN(635-655) in competitive ELISA The same result was obtained with the complex of anti-[Asn^{641}(Glc)]FAN(635-655) Abs and the corresponding glycopeptide fragment using CSF114(Glc) as inhibitor (Figure 1 c-d).

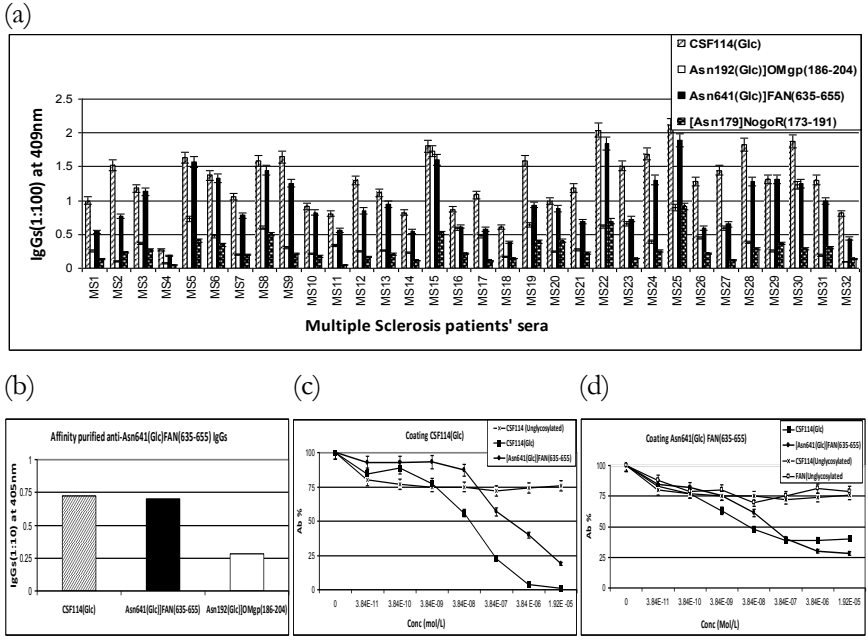

Fig. 1. (a) SP-ELISA for autoantibody detection (IgGs) on MS patients' sera to the selected neo-peptide epitope fragments. (b) SP-ELISA on affinity purified anti-[Asn^{641}(Glc)] FAN(635-655) IgGs showing a mimicry effect with CSF114(Glc). (c) Inhibition ELISA of anti-CSF114(Glc) IgGs. (d) Inhibition ELISA of anti-[Asn^{641}(Glc)]FAN(635-655) IgGs.

These results let us to hypothesize a mimicry effect of [Asn^{641}(Glc)]FAN(635-655) with CSF114(Glc).

Acknowledgments

Italian government scholarship for biotechnology 2008 (India) and MIUR scholarship 2009 (Italy) to S.P., Ente Cassa Risparmio di Firenze (Italy) as well as Chaire d'Excellence 2009-2013 (France) to A.M.P. are gratefully acknowledged for financial support.

References

1. Hohlfeld, R. *Brain* **120**, 865-916 (1997).
2. Bauer, J., Rauschka, H., Lassmann, H. *Glia* **36**, 235-243 (2001).
3. Brosnan, C.F., Raine, C.S. *Brain Pathol.* **6**, 243-257 (1996).
4. Cross, A.H., Trotter, J.L., Lyons, J. *J. Neuroimmunol.* **112**, 1-14 (2001).
5. Mazzucco, S., Mata, S., Vergelli, M., Fioresi, R., Nardi, E., Mazzanti, B., Chelli, M., Lolli, F., Ginanneschi, M., Pinto, F., Massacesi, L., Papini, A.M. *Bioorg. Med. Chem. Lett.* **9**, 167-172 (1999).
6. Carotenuto, A., D'Ursi, A.M., Nardi, E., Papini, A.M., Rovero, P. *J. Med. Chem.* **44**, 2378-2381 (2001).

Proceedings of the 31st European Peptide Symposium
Michal Lebl, Morten Meldal, Knud J. Jensen, Thomas Hoeg-Jensen (Editors)
European Peptide Society, 2010

Cyclic Peptides with a Diversely Substituted Guanidine Bridge: Synthesis, Structural and Biological Evaluations of Model Peptides

Youness Touati Jallabe[1], Engin Bojnik[2], Laurent Chiche[3], Abdallah Hamzé[1], André Aumelas[3], Nga N. Chung[4], Peter W. Schiller[4], Dorothée Berthomieu[5], Sandor Benyhe[2], Vincent Lisowski[1], Jean Martinez[1], and Jean-François Hernandez[1]

[1]Institut des Biomolécules Max Mousseron, CNRS UM5247, Universités Montpellier 1 and 2, Montpellier, 34093, France; [2]Institute of Biochemistry, Biological Research Center, Szeged, 6726, Hungary; [3]Centre de Biochimie Structurale, Montpellier, 34090, France; [4]Laboratory of Chemical Biology and Peptide Research, Montreal, H2W 1R7, Canada; [5]Institut Charles Gherardt, MACS, Montpellier, 34296, France

Introduction

In addition to occurring in numerous natural compounds, cyclization is often used in peptide chemistry to generate peptides with higher stability, potency and selectivity, by constraining the peptide backbone. Cyclization can be achieved through various bridging bonds, between peptide ends and/or side-chains. In the later case, it mostly involves a disulfide bond, but there can be many other possibilities. But, once cyclized, these bridges do not allow further structural variation. We developed cyclized peptides with a diversely substituted guanidine bridge and showed using model peptides that this variability might modulate their conformation and biological activity.

Results and Discussion

The guanidine bridge is formed between the side-chains of two diaminoacyl residues and the extra-cyclic nitrogen can be non- (R^1, R^2 = H), mono- (R^1 = H, R^2 = Alk) or di-substituted (R^1, R^2 = Alk). Their synthesis followed a convergent solid phase strategy (Scheme 1). First, a peptide containing two orthogonally protected diaminoacyl residues was assembled on a low loaded support. The alloc group was then selectively removed and the free amino group was converted into isothiocyanate using di-(2-pyridyl)-thionocarbonate. After Mtt removal, intramolecular reaction afforded the cyclic peptide with a thiourea bridge. The guanidine bridge was obtained just before cleavage by treating the S-methyl intermediate with various amines. LC-MS analyses showed that the major peak contained the expected compound and that the main purity corresponded to a dimerisation product. The dimer proportion was found to decrease when decreasing the cycle size. Then, we were able in some case to largely diminish this secondary species by adding LiCl in the cyclization mixture.

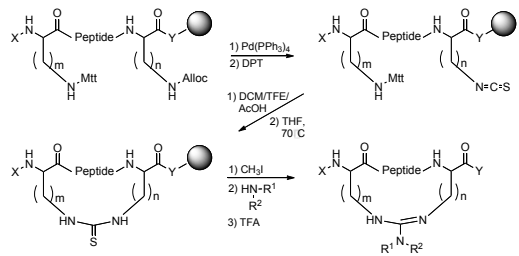

Scheme 1. Solid phase strategy.

With respect to its planarity, we anticipated that the guanidine bridge could adopt four different orientations inside the peptide cycle (Figure 1) and we hypothesized that the degree of guanidine substitution might influence this orientation and therefore peptide conformation. A series of proline-containing and RGD-related cyclic analogues of various sizes and with a diversely substituted guanidine bridge was prepared and studied by 2D-NMR

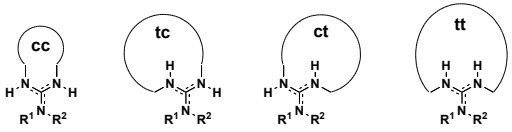

Fig. 1. c = cis, t = trans.

Table 1. Proline cis/trans ratios of RGD-related analogues (m,n=1) calculated from NMR spectra[a] and preferred guanidine orientations according to a molecular modeling study

X	*NH_2*	*NH-Me*	*Pyrrolidine*
Pro cis/trans	65:35	90:10	20:80
Preferred guanidine orientation(s)b,c	tc (Cis) ct (Trans) tt (Trans)	tc (Cis) ct (Trans)	cc (Trans) ct (Trans) tc (Cis)

[a] Water, 700 MHz, 320 K; [b] From the most to the least preferred; [c]The proline conformation preferred for each guanidine orientation is given in brackets

(Figure 2). The Asp-Pro peptide bond showed both cis and trans conformations. The proline cis/trans ratio was measured and found to vary significantly as a function of the degree of bridge substitution, at least for the shortest analogues (m = n = 1) (Table 1). In particular, an inversion of this ratio was observed between the mono- and the di-substituted analogues. To explain these results, a molecular modeling study (Vconf, Verachem LLC) helped by quantum chemical computations was performed. As it could be expected, this study indicated that the guanidine orientation could be driven by potential steric clashes between substituents. As a result, the cc orientation is disfavored for non- and mono-substituted analogues while the tc and ct isomeries are the only ones favored for the mono-substituted analogue (Table 1). The di-substituted analogue is a special case as steric clashes should occur for all orientations but the cc orientation appeared as the most favored. The study also indicated that, for unknown reasons, each guanidine orientation would favor either cis or trans proline. For instance, the tt and cc orientations were preferentially associated with a trans proline, while a cis proline was preferred for the tc isomer. Taken together, the modeling results were in accordance with NMR data.

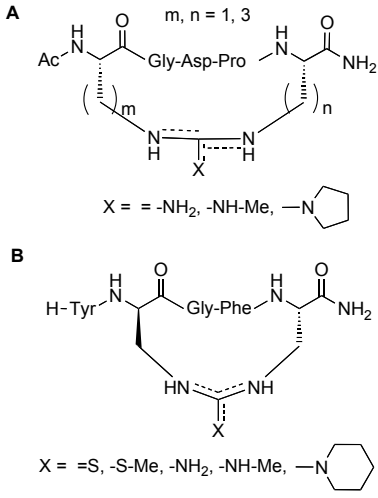

Fig. 2. A, RGD-related cyclic analogues. B, Enkephalin cyclic analogues.

As we showed that the degree of guanidine bridge substitution could modulate the conformation of a given peptide, we explored its potential influence on the biological activity of another model peptide. A series of enkephalin cyclic analogues was prepared (Figure 2). They were submitted to various biological assays, including binding to mu and delta opioid receptors and functional assays (G-protein activation, GPI and MVD bioassays). All compounds were found more or less selective for the mu receptor and full agonists. A significant variation in mu affinity and selectivity for this receptor was evidenced between non- (Ki = 19 nM; delta/mu = 39), mono- (Ki = 1.5 nM; 41) and di-substituted (Ki = 107 nM; 10) analogues. NMR study is currently performed to try to explain these variations. Then, it is interesting to note that the analogue with a thiourea bridge possessed a very good affinity for the mu receptor with a Ki of 0.4 nM but with a mu selectivity of only 13 fold.

In conclusion, guanidine bridges appeared as interesting tools to build cyclic peptides with substitution-dependent cycle conformations. At least for short cyclic peptides, we showed that, for a same sequence, a diversely substituted bridge could modulate the conformation and the biological activity of a peptide. Then, the ability to prepare such analogues together with the thiourea and S-methyl-isothiourea intermediates from a unique precursor makes our solid phase method a powerful tool to rapidly attain large diversity.

Acknowledgments
We thank Pierre Sanchez for mass spectrometry analyses.

Proceedings of the 31st European Peptide Symposium
Michal Lebl, Morten Meldal, Knud J. Jensen, Thomas Hoeg-Jensen (Editors)
European Peptide Society, 2010

Photolabile Protecting Groups Based on Novel Thiocoumarins and Thioquinolones: Synthesis and Photorelease of a Model Amino Acid Conjugate

Andrea S.C. Fonseca, M. Sameiro T. Gonçalves, and Susana P.G. Costa

Centre of Chemistry, University of Minho, Campus of Gualtar, 4710-057, Braga, Portugal

Introduction

Photocleavable protecting groups are an interesting alternative to classical acid- and base-labile groups and have been given particular attention in research areas related to synthetic and combinatorial chemistry. Since the use of light can provide spatial and temporal resolution in the photorelease process, these groups have also been used for elucidating signaling mechanisms in biological and metabolic processes within cellular systems, and for drug delivery with photoresponsive prodrugs. In recent years, a need for new light-sensitive protecting groups has evolved considering their importance, for example in molecular caging, towards the design of more efficient protecting groups that allow orthogonal deprotection/cleavage for application in biomolecules. To be useful in biological experiments, a photolabile (caging) group must undergo photolysis rapidly, in high yield, and at wavelengths not detrimental to the biological system [1]. Coumarin derivatives are well established photolabile protecting groups that have been used in the protection of various functional groups [2] whereas quinolone derivatives were recently reported by us as carboxyl protecting groups cleavable by light [3].

Considering our promising findings on the comparison of a series of substituted coumarins and quinolones [3], and the fact that the replacement of the carbonyl group by a thiocarbonyl group at the heterocycle should induce a shift towards longer wavelengths in the molecule's photoresponsive properties (desirable for bioapplications), we now extend this research to the synthesis of fluorescent conjugates based on novel thiocoumarins and thioquinolones, using phenylalanine as a model amino acid.

Results and Discussion

The synthesis of the thionated coumarin and quinolone derivatives **2** was accomplished by reaction of the corresponding model phenylalanine conjugates **1** previously obtained [3] with Lawesson's reagent, by refluxing in dry toluene. Following purification by silica gel column chromatography, conjugates **2a-d** were obtained in fair to good yields (Figure 1, Table 1). The present compounds were chosen in order to evaluate the influence of the nature of the heterocycle and the position of the methoxy substituent at the heterocyclic moiety on the photocleavage properties of the conjugates. Full characterisation by the usual spectroscopic techniques was performed. The replacement of the carbonyl at the heterocycle by a thiocarbonyl (leaving the remaining carbonyl groups in the conjugate unchanged) was supported by IR spectroscopy (absorption bands between 1255-1290 cm^{-1}) and confirmed by ^{13}C NMR spectra with the signals of the thiocarbonyl carbon between δ 181.88 and 197.11 ppm. UV-vis spectroscopy characterization was carried out in absolute ethanol and by comparison with the data reported for precursor conjugates **1**, the thiocarbonyl conjugates **2** displayed an UV-vis absorption band with a bathochromic shift as expected (73 nm for thiocoumarin **2a** and *ca*. 50 nm for thioquinolones **2b-d**).

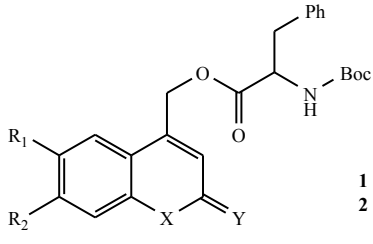

a X = O R_1 = H R_2 = OCH_3
b X = NCH_3 R_1 = H R_2 = H
c X = NCH_3 R_1 = OCH_3 R_2 = H
d X = NCH_3 R_1 = H R_2 = OCH_3

*Fig. 1. Synthesis of conjugates **2**. Reagents: a) Lawesson's reagent, toluene, reflux.*

*Table 1. Yields, UV-vis absorption data, irradiation times (t_{irr}, in min) and rate constants (k, in min^{-1}) for the photolysis of conjugates **2a-d** at different wavelengths in MeOH/aq. HEPES buffer (80:20)*

Cpd.	Yield (%)	UV-vis λ_{max} (nm)	254 nm		300 nm		350 nm		419 nm	
			t_{irr}	k	t_{irr}	k	t_{irr}	k	t_{irr}	k
2a	73	395	30.0	0.10	100.7	0.03	45.7	0.07	36.6	0.08
2b	80	384	8.3	0.35	10.3	0.30	10.4	0.28	9.8	0.32
2c	74	401	0.5	4.74	0.7	4.49	0.5	6.61	0.4	7.19
2d	50	385	0.5	6.22	0.7	4.06	0.6	4.94	0.6	5.10

The photocleavage of thiocoumarin **2a** and thioquinolone **2b-d** phenylalanine conjugates was studied in MeOH/aq. HEPES buffer (80:20) at different wavelengths of irradiation, in a Rayonet RPR-100 reactor with lamps of 254, 300, 350 and 419 nm, resulting in the quantitative release of Z-Phe-OH and photo by-products related to the heterocycle. Cleavage kinetics parameters were obtained from plots of peak area, determined by HPLC/UV monitoring, of the starting material *versus* irradiation time, with a linear correlation suggesting a first order reaction. Rate constants were obtained by the linear least squares methodology for a straight line. The irradiation time was the time necessary for the consumption of the starting material until less than 10% of the initial area was detected (Table 1).

It was found that the thiocarbonyl analogues **2** cleaved significantly faster and at longer wavelengths than the precursor carbonyl compounds **1** [3] and within the thionated series, the quinolone conjugates released the amino acid more efficiently when compared to the coumarin conjugate (between 60-140 times faster depending on the wavelength, compare **2a** with **2d**). Considering the influence of the methoxy substituent at the quinolone moiety, the results indicated that it had a positive effect on the photocleavage properties of the corresponding conjugates (between 14-20 times faster, compare **2b** with **2c** and **2d**). The position of the methoxy group was irrelevant for the rate constant at all wavelengths of irradiation (compare **2c** and **2d**).

In summary, thionated coumarin and quinolone phenylalanine conjugates **2** were readily obtained in fair to good yields through a one-step reaction and upon photolysis it was found that the thionated conjugates **2** cleaved significantly faster than the parent conjugates **1** at 419 nm [3] and cleavage kinetics parameters were obtained. The cleavage of the ester bond and the quantitative release of the amino acid in short irradiation times at all considered wavelengths of irradiation suggests that thionated quinolone derivatives **2b-d** may be considered as promising alternatives as photocleavable protecting groups for carboxylic acids. Fast photolysis at 419 nm for quinolone conjugates **2b-d** is particularly interesting, since this wavelength is the most suitable for practical caging strategies as it avoids cell damage due to short wavelengths.

Acknowledgments

Thanks are due to *Foundation for Science and Technology* (FCT-Portugal) for financial support through project PTDC/QUI/69607/2006 (FCOMP-01-0124-FEDER-007449) and a PhD grant to A.S.C. Fonseca (SFRH/BD/32664/2006). The NMR spectrometer Bruker Avance III 400 is part of the National NMR Network and was purchased in the framework of the National Program for Scientific Re-equipment, contract REDE/1517/RMN/2005 with funds from POCI 2010 (FEDER) and FCT.

References

1. Mayer, G., et al. *Angew. Chem. Int. Ed*. **45**, 4900-4921 (2006).
2. (a) Hagen, V., et al. *Angew. Chem. Int. Ed*. **44**, 7887-7891 (2005); (b) Geissler, D., et al. *Angew. Chem. Int. Ed*. **44**, 1195-1198 (2005); (c) Furuta, T., et al. *ChemBioChem* **5**, 1119-1128 (2004); (d) Shembekar, V.R., et al. *Biochemistry* **46**, 5479-5484 (2007); (e) Gilbert, D., et al. *ChemBioChem* **8**, 89-97 (2007); (f) Fonseca, A.S.C., et al. *Tetrahedron* **63**, 1353-1359 (2007); (g) Fernandes, M.J.G., et al. *Tetrahedron* **64**, 3032-3038 (2008); (h) Soares, A.M.S., et al. *Amino Acids* **39**, 121-133 (2010).
3. Fonseca, A.S.C., et al. *Amino Acids* **39**, 699-712 (2010).

Proceedings of the 31st European Peptide Symposium
Michal Lebl, Morten Meldal, Knud J. Jensen, Thomas Hoeg-Jensen (Editors)
European Peptide Society, 2010

Amino Acid Coupling Reactions in Aqueous Environment Using Microwave Assistance Heating

Athanassios S. Galanis[1], Morten Grøtli[2], and Fernando Albericio[3]
[1]Department of Pharmacy, University of Patras, Patra, 26504, Greece; [2]Department of Chemistry, University of Gothenburg, Gothenburg, 41296, Sweden; [3]Institute for Research in Biomedicine, Barcelona Science Park, Barcelona, 08028, Spain

Introduction

The solid-phase method is the principal method for peptide synthesis, but it requires a large amount of organic solvent. As the safe disposal of organic solvent waste is an important environmental issue, as well as the increase of the synthesis cost, a method for peptide synthesis in water would be desirable. Thus, the aim of this project is to replace costly organic solvents for peptide synthesis with inexpensive, environmentally-benign solvents, such as water. We previously reported the solid phase peptide synthesis in aqueous environment using microwave heating, Boc-derivatives and the mixture of HONB/EDC as coupling reagents [1,2]. In the following, we present the studies of the twenty native amino acids coupling reaction using commercial available Boc-derivatives. Moreover, comparison among the microwave heating efficiency and the conventional thermal heating method is also reported.

Results and Discussion

The concept of this work was the use of microwave influence for SPPS in water. Obviously, the major issue was the amino acids coupling reaction efficiency in water. In order to develop a strategy that could be easily applied in every laboratory or in industry, the evaluation of commercial available amino acid derivatives and reagents or derivatives that could be easily synthesized, was performed. Thus, the Fmoc and Boc amino acids were evaluated, even though those groups are hydrophobic. Furthermore synthesis and evaluation of several azido acids was carried out, as azido group is an hydrophilic group, can be used as alternative N^{α}-protecting group, and azido acids derivatives can be easily synthesized. Regarding the solid support, the poly (ethylenglycol) type resins were used, as they are more hydrophilic compared to polystyrene resins. Several coupling reagents were evaluated, starting with the N-(3-dimethylaminopropyl)-N'-ethylcarbodiimide (EDC) that is an excellent water soluble carbodiimide, following by studies of several additive reagents efficiency. In coupling reaction experiments, Tentagel and ChemMatrix resins were used as solid support with a pre-attached Rink amide linker, EDC carbodiimide with or without the presence of additive reagents, applying microwave irradiation to elevate the temperature up to 80 degrees for 10 to 30 min. The coupling reactions of all experiments were performed on solid phase and each amino acid derivative was reacted to a pre-synthesized dipeptide of Gly-Phe bound onto the RAM-TentaGel/ChemMatrix resin (Figure 1).

Among the amino acid derivatives that were studied, Boc-amino acids provided by far better results compared to Fmoc- and azido acid derivatives. However, active esters stability studies, showed that the esters are not stable in water at elevated temperature. Thus, short reaction time (up to 10 min) were essential, in order to avoid byproducts detected when extended time was applied. Among the coupling reagents that were studied, the mixture of EDC / HONB (N-hydroxy-5-norbornene-2,3-dicarboxylic acid imide) provided the better results as the reactions were completed and traces of byproducts were only detected in some cases. After optimization of coupling conditions, the reactions of each Boc-amino acid derivative was performed using microwave assisted heating at 70 ^{o}C for 7min (two couplings; Table 1). Except for the derivatives in which the Bzl group is

Fig. 1. Coupling reaction experiments. Each derivative was coupled onto a Gly-Phe bound on resin dipeptides and the targeted tripeptide product was analyzed by HPLC after the cleavage from the resin.

Table 1. Purity of the targeted tripeptides after coupling reactions of Boc-derivatives onto a Gly-Phe bound on resin dipeptide. Two (2) reactions were performed in water using microwave technology (TentaGel or ChemMatrix resin, EDC/HONB (5eq), 70 °C; 7min)

Derivative	*Starting material* H_2N- GF	*Targeted tripeptide* Boc-aa -GF
Boc-Ala-OH	-	99.4%
Boc-Arg(Tosyl)-OH	-	100%
Boc-Cys(Acm)-OH	-	96%
Boc-Gly-OH	-	100%
Boc-Leu-OH	-	98%
Boc-Lys(2ClZ)-OH	-	96%
Boc-Lys(Alloc)-OH	-	93%
Boc-Phe-OH	-	97%
Boc-Pro-OH	-	100%
Boc-Ser-OH	-	94%
Boc-Trp-OH	-	97%
Boc-Tyr-OH	-	97%
Boc-Val-OH	-	92%
Boc-Asn(Bzl)-OH	35%	54%
Boc-Asp(OBzl)-OH	11%	84%
Boc-Gln(Bzl)-OH	23%	61%
Boc-Glu(OBzl)-OH	14%	78%
Boc-His(Tosyl)-OH		n.d.
Boc-Ile-OH	-	83%
Boc-Met-OH	3%	87%
Boc-Thr(Bzl)-OH	-	88%

used for side chain protection, almost all provided complete reactions and high yield and purity targeted tripeptides. Thus, alternative side chain protected derivatives are under investigation for their efficiency for coupling reactions in water at elevated temperature. Another critical issue was the use of the zwiterronic detergent TritonX100 that enhances the swelling properties of the poly (ethylenglycol) type resin and increases the solubility of the peptides.

In order to study if this novel strategy can be applied using conventional thermal heating, coupling reaction of Boc-derivatives were performed using a hot plate, applying the same temperature as in the microwave promoted coupling. Similar results were obtained. In conclusion, SPPS can be applied using water as solvent at elevated temperature (by thermal or microwave heating) and further studies are essential in order to optimize the coupling reaction efficiency in water. The synthesis of the Leu-Enk pentapeptide has been successfully performed using this new developed environmental friendly strategy [2].

Acknowledgments

A.S.G. acknowledges a MARIE-CURIE Intra-European-Fellowship- Project No 040451.

References

1. Galanis, A.S., Albericio, F., Grøtli, M. (Hilkka Lankinen Eds.) *Peptides 2008 (Proceedings of the 30th European Peptide Symposium)*, Finland, 2008, pp. 164-165.
2. Galanis, A.S., Albericio, F., Grøtli, M. *Org. Lett.* **11**, 4488-4491 (2009).

Proceedings of the 31st European Peptide Symposium
Michal Lebl, Morten Meldal, Knud J. Jensen, Thomas Hoeg-Jensen (Editors)
European Peptide Society, 2010

Bis-Azobenzene Photoswitchable α-Amino Acids for Nanomaterials Applications

Alessandro Moretto[1], Marco Crisma[1], Paola Fatás[2], Gema Ballano[2], Ana I. Jimenéz[2], Carlos Cativiela[2], and Claudio Toniolo [1]

[1]ICB, Padova Unit, CNR, Department of Chemistry, University of Padova, Padova, 35131, Italy; [2]Department of Organic Chemestry, ICMA, University of Zaragoza-CSIC, Zaragoza, 50009, Spain

Introduction

The photoisomerization of an azobenzene moiety between the extended (*trans*) and compact (*cis*) conformations (Figure 1) is reversibly triggered by light at two different wavelengths [1-3]. The resulting modifications in the molecular 3D-structures have been extensively exploited to photoswitch transformation in chemical species reversibly for various types of applications, *e.g.* in the construction of optoelectronic devices [4].

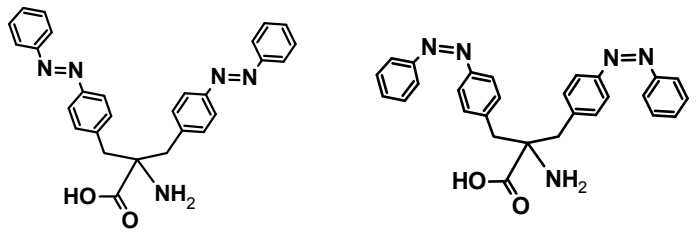

trans *cis*

Fig. 1. The trans and cis forms of the C^{α}-tetrasubstituted α-amino acid pAzoDbg synthesized and studied in this work.

Results and Discussion

Here, we describe synthesis and chemical characterization of the two achiral, C^{α}-tetrasubstituted, α-amino acids, each characterized by two azobenzene moieties covalently linked to their α-carbon atom, *bis*[4-(phenylazo)benzyl]Gly (*p*AzoDbg) and its 3-(phenylazo)benzyl (*m*AzoDbg) analogue. These "albatros-like" compounds were characterized by UV-Vis spectroscopy and, one of them, by X-ray diffraction as well.

We found that both compounds undergo multiple, reversible isomerizations in a variety of solvents by irradiation with Vis light (to *trans*) or UV light (to *cis*) (Figure 2). However, when the α-amino acids are dispersed in a paraffin medium, their photoswitch

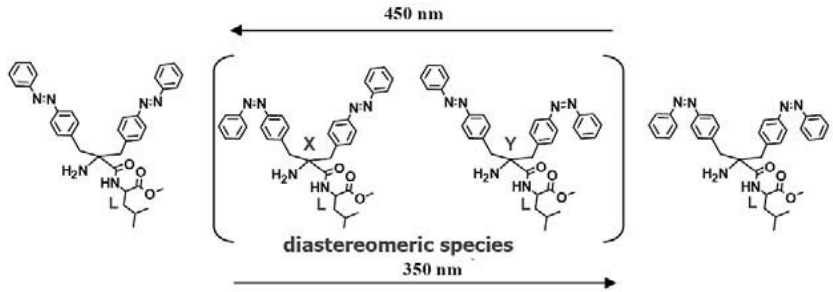

Fig. 2. Mechanism of light-driven, trans/cis isomerization via the intermediate (X)-H-pAzoDbg-L-Leu-OMe (cis-trans)/(Y)-H-pAzoDbg-L-Leu-OMe (trans-cis) diastereomers.

processes are blocked. Interestingly, using HPLC and NMR, we were also able to unravel an intermediate state in the interconversion process, namely the racemate of the *trans*/*cis* and *cis*/*trans* configurational isomers. This phenomenon was further, albeit indirectly, demonstrated by photoisomerization of the chiral dipeptide based on one azobenzene-residue with H-L-Leu-OMe, which afforded two diastereomeric intermediates, as detected by HPLC and verified by NMR. We are currently extending this study to more complex molecular systems, where the two amino acids, appropriately N^{α}-functionalized, are bound to various type of nanoparticles.

References

1. Pieroni, D., Fissi, A., Angelini, N., Lenci, F. *Acc. Chem. Res.* **34**, 9-17 (2001).
2. Denschlag, R., Schreier, W.J., Rieff, B., Schrader, T.E., Koller, F.O., Moroder, L., Zinth, W., Tavan, P. *Phys. Chem. Chem. Phys.* **12**, 6204-6218 (2010).
3. Backus, E.H.G., Bloem, R., Donaldson, P.M., Ihalainen, J.A., Pfister, R., Paoli, B., Caflisch, A., Hamm, P. *J. Phys. Chem.* **B 2010**, 114, 3735-3740 (2010).
4. Irie, M. *Bull. Chem. Soc. Jpn.* **81**, 917-926 (2008).

Proceedings of the 31st European Peptide Symposium
Michal Lebl, Morten Meldal, Knud J. Jensen, Thomas Hoeg-Jensen (Editors)
European Peptide Society, 2010

Stabilization of β Turn Conformation in Melanocortin-Like Peptide by Click Side Chain-To-Side Chain Cyclization

Chiara Testa[1,2,3], Stefano Carganico[1,2,3], Francesca Nuti[2,3], Mario Scrima[4], Anna Maria D'Ursi[4], Marvin L. Dirain[5], Nadeje Lubin Germain[1], Carrie Haskell-Luevano[5], Michael Chorev[6,7], Paolo Rovero[2,8], and Anna Maria Papini[1,2,3]

[1]Laboratoire SOSCO – EA4505 Université de Cergy-Pontoise Neuville-sur-Oise, 95031, Cergy-Pontoise, France; [2]Laboratory of Peptide & Protein Chemistry & Biology, Polo Scientifico e Tecnologico, University of Florence, I-50019, Sesto Fiorentino (FI), Italy; [3]Department of Chemistry "Ugo Schiff", University of Florence, I-50019, Sesto Fiorentino (Fi), Italy; [4]Department of Pharmaceutical Science, Via Ponte Don Melillo 11C, Salerno, I-84084, Italy; [5]Department of Pharmacodynamics, University of Florida, Gainesville, FL, 32610, U.S.A.; [6]Laboratory for Translational Research, Harvard Medical School, One Kendal Square, Building 600, Cambridge, MA, 02139, U.S.A.; [7]Department of Medicine, Brigham and Women's Hospital, 75 Francis Street, Boston, MA, 02115, U.S.A.; [8]Department of Pharmaceutical Science, Polo Scientifico e Tecnologico, University of Florence, Via Ugo Schiff 3, I-50019, Sesto Fiorentino (Fi), Italy

Introduction

Interaction of linear and flexible peptides with their macromolecular target, such as GPCRs, involves a limited number of closely related conformations that are recognized by, bind to and either activate or block the biological activity of these targets. Hence, the so called bioactive conformation represents only a small subset of the larger ensemble of accessible conformations which are in a dynamic equilibrium. A growing arsenal of structural rigidifications offers means to capture and stabilize the biological conformation of linear peptides in an effort to enhance target specificity, biological potency, binding affinity and metabolic stability [1,2]. Herein we report on the extension of an innovative strategy for stabilization peptide β-turn conformation by side chain-to-side chain cyclization employing a bridge containing a [1,2,3]triazole [5-8].

Results and Discussion

Melanocortin GPCR receptors (MCRs) are involved in many biological pathways, including sexual function, feeding behaviour, energy homeostasis and pigmentation, making them potential targets for drugs to treat diseases such as obesity and sexual dysfunction. Therefore, understanding the bioactive conformation of the ligand and the structure of the receptor–ligand complex is crucial to design more potent and MCR-subtype selective ligands. MT-II is a potent long acting non-selective super-agonist of MCRs, characterized by lactam bridge between residues Asp^5 and Lys^{10} stabilizing a type-II β turn structure that is critical for its bioactivity [3]. The minimal active sequence is identified by the tetrapeptide His^6-D-Phe^7-Arg^8-Trp^9 [4], which is included in the cyclic portion formed by lactam ring. In previous work [5] we designed and studied a new intramolecular side chain-to-side chain [1,2,3]triazolyl-bridged modification. This 1,4-disubstituted [1,2,3]triazolyl moiety is bioisosteric to the peptide bond and was recently introduced by us as an α-helix stabilizing rigidification replacing the *i*-to-*i+4* side chain-to-side chain bridging lactam in peptides derived from parathyroid hormone-related protein (PTHrP). In the current study, we applied the [1,2,3]triazolyl-bridging strategy to stabilize a β-turn conformation in MT-II by replacing the lactam bridge with a *i*-to-*i+5* side chain-to-side chain cyclization via Cu^I-catalyzed azido-to-alkyne 1,3-dipolar cycloaddition (CuAAC) generating 1,4-disubstituted [1,2,3]triazolyl-containing ring structures. In this context, we have developed synthesis of N^{α}-Fmoc-ω-azido-α-amino- and N^{α}-Fmoc-ω-ynoic-α-amino acids (Figure 1) by diazo-transfer of the N^{α}-protected ω-amino-α-amino acids [6,7] and by alkylation of a Ni(II) complex of the Schiff base derived from glycine

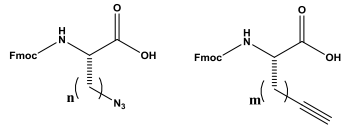

Fig. 1. Azido and Alkynyl Amino acid building blocks for Fmoc-tBu SPPS.

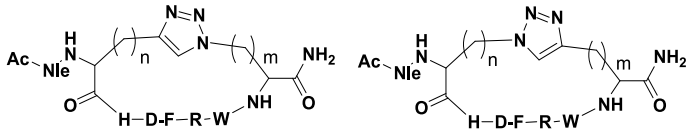

Fig. 2. Schematic representation of all the possible MTII peptide analogs cyclized by [1,2,3]triazolyl-containing bridges that vary in the size of the bridge and the position and direction of the triazolyl moiety within the ring. In the notation tb stands for [1,2,3]triazolyl-bridged, the superscripts m and n define the number of methylenes connecting the triazole moiety to the N- and C-proximal bridge heads and the numbers in the bracket identify the orientation of the triazolyl within the bridge.

and a chiral inducer with alk-ω-ynyl bromides respectively [8]. Clicked MT-II analogs I-IV presenting different permutations of bridges containing 5 methylenes and a triazolyl moiety were synthesized by a combination of solid phase assembly of the linear peptide precursor I'-IV' and were followed by solution phase CuAAC. The adenylate cyclase activity (EC_{50}) of the linear precursor I'-IV' and cyclic MTII peptide analogs I-IV was evaluated in the murine melanocortin receptors mMC1R, mMC3R, mMC4R and mMC5R (Table 1). Indeed the cyclic peptides are more potent than their linear precursors confirming that conformational stabilization in the form of side chain-to-side chain cyclization enhances *in vitro* potency. Moreover, the clicked cyclic peptides have similar potency compared to the parent lactam-containing MTII analog. There are indications of emerging selectivity toward receptor subtypes but these need to be further optimized.

*Table 1. Biological activity (EC_{50}) of the MTII peptide analogs towards the principal murine melanocortin receptors. *Lin stands for linear precursor.*

	Peptide	*mMC1R*	*mMC3R*	*mMC4R*	*mMC5R*
		EC_{50} (nM)	*EC_{50} (nM)*	*EC_{50} (nM)*	*EC_{50} (nM)*
	MTII	-	0.33	0.04	0.27
I	$(tb4^{1},1^{4})$MTII	-	3.14	1.62	1.93
II	$(tb1^{4},4^{1})$MTII	-	3.70	0.58	1.76
III	$(tb4^{2},1^{3})$MTII	0.11	0.59	0.15	0.47
IV	$(tb1^{3},4^{2})$MTII	0.51	2.95	0.36	2.30
I'	Lin[Nle^{5}(δ-N_3),Pra^{10}]MTII*	1.04	3.67	0.71	6.62
II'	Lin[Pra^{5},Nle^{10}(δ-N_3)]MTII	0.58	4.13	0.43	3.91
III'	Lin[$hAla^{5}$(γ-N_3),Nva^{10}(δ-yl)]MTII	1.25	8.57	1.48	12.4
IV'	Lin[Nva^{5}(δ-yl),$hAla^{10}$(γ-N_3)]MTII	2.11	9.90	1.35	11.8

In summary, our studies support our contention that the [1,2,3]triazolyl-bridged peptides achieve conformational stabilization that enhances their *in vitro* potency. In the future we will continue to fine-tune this modification to improve receptor-subtype selectivity.

Acknowledgments
The present work has been supported by the Agence Nationale de la Recherche chaire d'Excellence 2009-2013 (France).

References

1 Henchey, L.K., Jochim, A.L., Arora, P.S. *Current Opinion in Chemical Biology* **12**, 692 (2008).
2 Kim, Y.W., Verdine, G.L. *Bioorganic and Medicinal Chemistry Letters* **19**, 2533 (2009).
3 Al-Obeidi, F., de Lauro Castrucci, A.M., Hadley, V.J. *J. Med. Chem*. **32**, 2555-2561 (1989).
4 Ying, J., et al. *Biopolymers* **71**, 696-716 (2003).
5. Cantel, S., et al. *J. Org. Chem.***73**, 5663-5674 (2008).
6. Le Chevalier Isaad, A., Papini, A.M., Chorev, M., Rovero, P. *J. Pept. Sci.* **15**, 451-454 (2009).
7. Le Chevalier Isaad, et al. *Eur. J. Org. Chem.* **31**, 5308-5314 (2008).
8. Scrima, M., et al. *Eur. J. Org. Chem.* 446-457 (2010).

Proceedings of the 31st European Peptide Symposium
Michal Lebl, Morten Meldal, Knud J. Jensen, Thomas Hoeg-Jensen (Editors)
European Peptide Society, 2010

Impact of Ionic Liquids on the Conformation of Peptides Studied by HR-MAS NMR Spectroscopy

Annekathrin Richardt, Carmen Mrestani-Klaus, and Frank Bordusa
Institute of Biochemistry and Biotechnology, Martin-Luther-University Halle-Wittenberg, Halle, 06120, Germany

Introduction

Ionic liquids (ILs) have attracted a rapid use as popular solvents in chemistry and biocatalysis as well. They exhibit melting points lower than 100°C, low vapor pressure and are mostly more viscous than classic solvents. In our research, we used ILs as reaction medium additives in the protease-mediated synthesis of proteins [1]. In the attempts to explain the altered enzyme activities on the basis of a hypothetical effect of ionic liquids on the spatial structure of the biocatalyst or peptide and protein targets, the impact of ILs on the *cis/trans* ratio of Xaa-Pro peptide bonds was studied by solvent jump experiments [2]. Consequently, direct interactions between dissolved peptides and ILs have to be investigated in order to understand how ionic liquids influence the structure of peptides.

For this purpose, conventional high-resolution ^{1}H NMR measurements of IL/peptide systems were initially performed. However, these experiments did not lead to useful results due to extremely low peptide signal resolution and line-broadening effects caused by the high IL viscosity. Therefore, HR-MAS (high-resolution magic angle spinning) NMR spectroscopy has been successfully applied here as efficient, powerful and IL-compatible analytical method to facilitate structural analysis of IL/peptide systems on a molecular level.

Results and Discussion

The present study was focused upon investigations of peptide/IL systems using the model tetrapeptides Ala-Xaa-Pro-Phe (Xaa = Ala, Glu, Gly, Lys, Phe) that exhibit high water as well as IL solubilities. As ionic liquids, 1-ethyl-3-methylimidazolium diethylphosphate [EMIM][Et_2PO_4], 1,3-dimethylimidazolium dimethylphosphate [MMIM][Me_2PO_4] and 1-ethyl-3-methylimidazolium trifluoroacetate [EMIM][CF_3CO_2] were chosen (Figure 1).

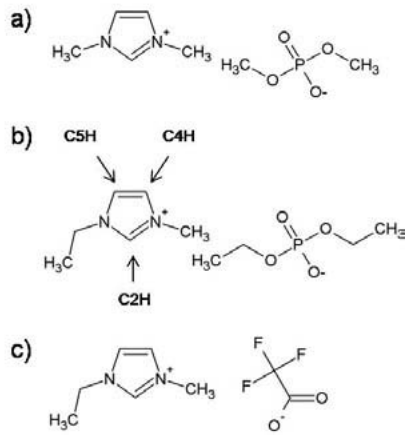

Fig. 1. Structures of the ionic liquids: a)[MMIM][Me_2PO_4] b)[EMIM][Et_2PO_4] c)[EMIM][CF_3CO_2].

In general, imidazolium-type ILs are frequently used, most investigated, commercially available and well water miscible. They represent ideal model systems for structural investigations using NMR spectroscopy since imidazolium ring protons are highly sensitive to the chemical environment.

In order to get evidence of direct interactions between the ILs and peptides as well as of IL-induced conformational changes of the dissolved peptides, we utilized proton chemical shift difference values ($\Delta\delta$). Accordingly, high-resolution NMR spectra of the peptides and of the ILs were recorded separately in aqueous solution as a point of reference. Afterwards, NMR spectra of different IL/peptide mixtures were acquired. Complete resonance assignment of both the ILs and the peptides as well as of the IL/peptide systems was done by applying conventional two-dimensional NMR techniques (Figure 2a). The proton chemical shifts were extracted from the spectra as basis for the determination of chemical shift differences between the reference systems in aqueous solution and the IL/peptide systems. *cis/trans* peptide isomer ratios were determined via integration of well-resolved signals in the ^{1}H NMR spectra.

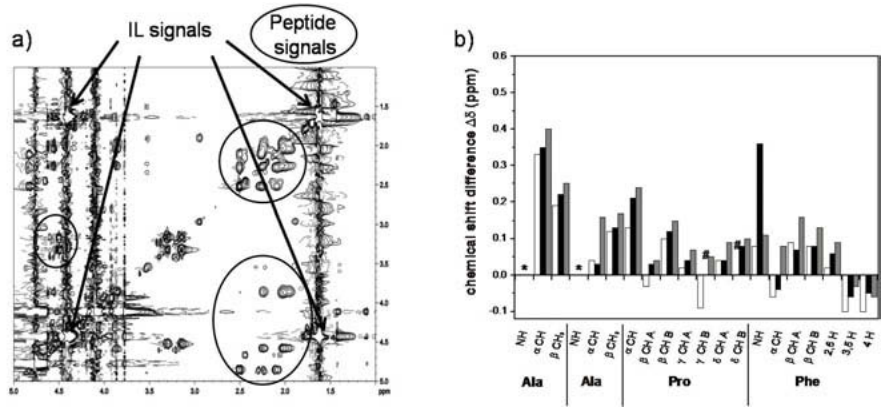

Fig. 2. a) Part of the 400 MHz HR-MAS TOCSY spectrum of AEPF dissolved in 70% [EMIM][Et_2PO_4]/30% D_2O(v/v), 303 K, spinning rate 6 kHz. b) ^{1}H NMR chemical shift differences of the peptide AAPF dissolved in [EMIM][Et_2PO_4] (white), [MMIM][Me_2PO_4] (black) and [EMIM][CF_3CO_2](grey). could not be assigned. # no Δδ.*

As a result, a large quantity of proton chemical shift differences has been obtained indicating that the peptides strongly interact with ILs. For the ionic liquids, we found small Δδ what might be connected to the large excess of the ILs in the mixtures with ratios of up to 40:1. However, the data agree with the reported fact that chemical shifts of imidazolium ring protons depend on the IL concentration as well as anion structure [3]. In Figure 2b, Δδ values are presented graphically for one example peptide, AAPF. In the bar graphs, Δδ is shown for each proton of each amino acid in the peptide sequence. Since Δδ values are indicators of the interaction between ILs and peptides, the strength of the interactions correlates with the bar height. We can conclude that the strength of the interaction depends on the IL chosen as well as on the position of the proton in the peptide sequence. The strongest effects for all peptides occur with [EMIM][CF_3CO_2] pointing to a specific role of the ionic liquid anions for IL/peptide interactions. Furthermore, most amide protons of each single amino acid shifted considerably downfield displaying that the interactions with the ILs are fairly strong along the peptide backbone and may be caused by hydrogen bonding with the solvent anions [4]. Upfield shifts for Pro and Phe aromatic side chain protons were obtained (see Figure 2b) likely arising from ring stacking with imidazolium ring protons.

We also found an influence of ILs on the *cis/trans* equilibrium of Xaa-Pro peptide bonds what is in agreement with solvent jump experiment data mentioned above. The *cis/trans* equilibrium seems to depend on the nature of the amino acid in position Xaa. Compared to water, ionic liquids favour the *trans* isomer. It is of special interest that different Δδ values between the two conformers *cis* and *trans* were obtained, particularly at position Xaa. Summarizing, these results clearly show that the remarkable impact of ILs on the *cis/trans* equilibrium relies on direct conformer-specific IL/peptide interactions.

From our future work we can expect detailed insights into the molecular reasons for interactions of ionic liquids with peptidic structures that may help to explain effects already found in protein folding or enzyme catalysis.

Acknowledgments
We acknowledge financial support by the Deutsche Forschungsgemeinschaft (DFG) within the priority program SPP 1191, grant BO 1770/4-1.

References

1. Wehofsky, N., Wespe, C., et al. *ChemBioChem* **9**, 1493-1499 (2008).
2. Wespe, C., *Ph.D. thesis*, Martin-Luther-University Halle-Wittenberg, Halle, 2009.
3. Bonhôte, P., Dias, A.-P., et al. *Inorg. Chem.* **35**, 1168-1178 (1996).
4. Hesse, M., *Spektroskopische Methoden in der organischen Chemie*. 2nd ed., Thieme Verlag, Stuttgart, 1984.

Proceedings of the 31st European Peptide Symposium
Michal Lebl, Morten Meldal, Knud J. Jensen, Thomas Hoeg-Jensen (Editors)
European Peptide Society, 2010

Next Generation Peptide Microarrays

F. Ralf Bischoff[1], Frank Breitling[2], and Volker Stadler[1]
[1]PEPperPRINT GmbH, Heidelberg, 69123, Germany; [2]Karlsruhe Institute of Technology, Institute for Microstructure Technology, Eggenstein-Leopoldshafen, 76344, Germany

Introduction

In recent years, DNA chips have revolutionized genome research. A similar trend is predicted for peptide chips in proteome research. Their use ranges from the characterization of sera, enzymes and antibodies through the screening of new protein biomarkers up to the development of peptide-based drugs and vaccines. Due to complex manufacturing processes, however, available peptide chips fall short of the spot density and thus information content of corresponding DNA chips by far. To eliminate these obstacles, we developed a new combinatorial technique with amino acids embedded in solid "amino acid toner" particles [1]. These toners are printed onto glass slides with micron resolution, using a custom-made 20-colour laser printer [2]. With all the different amino acid particles finally printed, they are melted at once to initiate coupling. Repeated printing and melting eventually result in custom peptide microarrays with presently 5,440 spots on microscope slides, and up to 156,000 spots on larger slides.

Results and Discussion

Since more than 15 years, peptide arrays were predominantly synthesized by means of the spotting technique developed by Ronald Frank [3]. Thereby activated amino acids are dissolved in a solvent like DMF, and spotted onto cellulose substrates for combinatorial synthesis of up to 25 peptides per cm^2. Working with liquid droplets, however, limits the array resolution due to evaporation effects and spreading on the support. To generate custom peptide microarrays with higher spot densities and thorough flexibility at a significantly reduced material need, we developed a new combinatorial technique which is based on the laser printing of "amino acid toner particles". Our approach is sketched in Figure 1 (left): First, amino acid toners are printed with high resolution onto a solid support (a), followed by melting of the toner particles to release the embedded amino acids what initiates coupling (b). Residual material is then removed by washing (c), before N-terminal Fmoc-protecting groups are cleaved from the growing peptide chains (d). Repeating this cycle of synthesis (a-d) finally results in combinatorially synthesized peptide microarrays.

The amino acid toners are manufactured by sophisticated milling and sieving processes [1]. They are composed of Fmoc amino acid pentafluorophenyl esters as monomers, a toner resin, a higher homologue of standard solvents for peptide synthesis (ditolyl sulfoxide and diphenyl formamide instead of DMSO and DMF), and of charge control additives which enable the generation of defined surface charges required for the laser printing process. Their physical properties have been carefully adjusted to color toners from the OKI C7400 series (Figure 1, middle). The first generation peptide laser printer has been developed in collaboration with Fraunhofer IPA and contains commercially available printing units of the same OKI series (Figure 1, right). Instead of the 4 printing units of a conventional color laser printer, the peptide laser printer consists of 20 printing units for the 20 most important L-amino acids combined with a linear stage to enable repetitive printing with micron resolution [2]. Furthermore, the amino acid toners can be printed not only on cellulose sheets and polymer foils, but also on glass slides as peptide chip substrates.

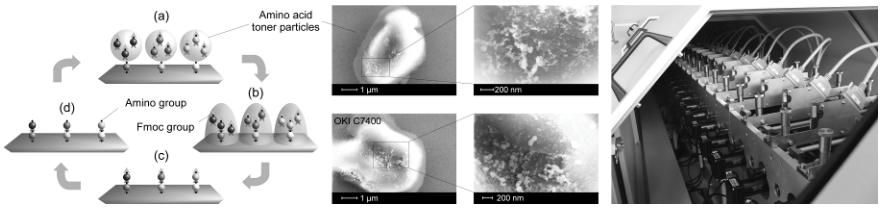

Fig. 1. Combinatorial synthesis of peptide microarrays by amino acid toner particles (left); SEM images amino acid toners in comparison with high-end toners of the OKI C7400 series (middle); peptide laser printer with OKI printing drums arranged in a row.

Once printed, the amino acid particles are melted at 90°C to liquefy the solid toner matrix and to induce combinatorial peptide synthesis. Due to these unusual reaction conditions in terms of solvent and temperature, we also investigated couplings yields and unwanted side-reactions like racemization and aspartimide formation that might have been induced by elevated temperatures [2]. Stepwise coupling yields were determined by Fmoc deprotection and UV/Vis spectrometry, and compared to peptide synthesis in DMF. On two-dimensional glass slides coated with a thin polymer film [4], and without pre-swelling, repetitive coupling yields were 90% on average for our toner-based approach which was equivalent to coupling in DMF on the same slides. To get close to maximum yields even with 15-20mer peptides, we thus typically carry out double couplings and acetylate residual amino groups after each coupling step to truncate unreacted sequences. Furthermore, the peptide integrity could be verified by mass spectrometry and HPLC. These methods did not reveal any major signals besides the full-length peptides, which indicates that heat-induced side reaction did not occur to a measurable extent.

The peptide laser printer enables the combinatorial synthesis of peptide microarrays with 5,440 peptides per microscope slide and up to 156,000 peptides on larger slide formats. We meanwhile applied these peptide microarrays for epitope mapping of antibodies with amino acid resolution (Figure 2a), the screening of peptide target binders, the characterization of kinases and proteases, the analysis of serum responses upon immunization (Figure 2b), and the screening of serum biomarkers. The mapping of antibody epitopes and serum analysis after immunization is done by translation of the target protein into an array of overlapping peptides. This chip is incubated with the antibody or serum sample, followed by staining with secondary and control antibodies (Figure 2, spot frames). Due to the high spot densities, we can reduce sample consumption to 5-10 µL per antibody or serum. In other approaches, we used libraries of stochastic peptides, i.e. non-natural sequences which are generated by a computer algorithm. Incubated with a monoclonal Flag antibody, we were e.g. able to identify peptide binders with a certain similarity to the wild-type epitope (DYKDDDDK) from a library of 9,000 different 15mer peptides. These binders were then permuted in a consecutively synthesized chip and again stained with the Flag antibody to finally reveal the consensus motif DYK from an initially random library.

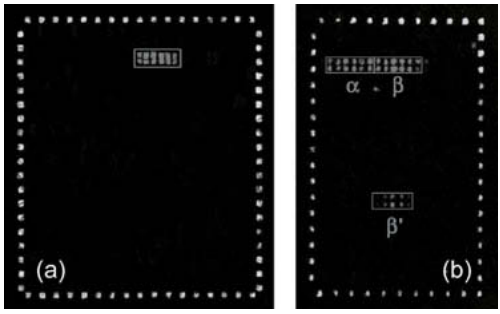

Fig.2. Epitope mapping of a monoclonal antibody with amino acid resolution (a); analysis of serum responses after immunization against two homologue protein antigens (b).

A second generation of the peptide laser printer is presently put into operation and will be able to increase chip content to ~ 20,000 peptides per microscope slide and ~500,000 peptides on larger slides. Custom peptide microarrays are made available by PEPperPRINT, a spin-off of the German Cancer Research Center in Heidelberg. PEPperPRINT also provides comprehensive epitope mapping and R&D services for peptide discovery and development.

Acknowledgments

We thank our co-workers at the research group "Chip-Based Peptide Libraries at the German Cancer Research Center and at PEPperPRINT and the Fraunhofer IPA for their contribution. This work was supported by grants from the Federal Ministry of Education and Research (0315642A) and the European Union (Grant Agreement Number 223243)

References

1. Beyer, M., et al. *Science* **318**, 1888 (2007).
2. Stadler, V., et al. *Angew. Chem. Inter. Ed*. **47**, 7132 (2008).
3. Frank, R., *Tetrahedron* **48**, 9217 (1992).
4. Beyer, M., et al. *Biomaterials* **27**, 3505 (2006).

Proceedings of the 31st European Peptide Symposium
Michal Lebl, Morten Meldal, Knud J. Jensen, Thomas Hoeg-Jensen (Editors)
European Peptide Society, 2010

Imide-Click Ligation and Click-Unclick Peptide-Based Prodrug Strategy

Reda Mhidia[1], Nicolas Bézière[1], Nicole Pommery[2], Annick Blanpain[1], and Oleg Melnyk[1]

[1]CNRS UMR 8161 Institut Pasteur de Lille, Univ. Lille Nord de France, IFR 142, Lille, 59021, France; [2]Univ. Lille Nord de France, Lille, 59006, France

Introduction

Polypeptide-drug conjugates are frequently used for targeting drugs to specific biomarkers. Release of the active substance at the delivery site can be triggered by a specific biochemical event. In particular, the design of self-immolative linkers, whose fragmentation is triggered by a specific enzyme, is of utmost interest. However, preparation of such carrier-linked prodrugs requires multi-step procedures and complex protection schemes. We disclose here a novel strategy named click-unclick allowing the easy assembly and the controlled disassembly of peptide-based prodrugs (Figure 1) [1]. First, a click-type reaction, i.e. imide ligation between a peptide thioacid and an azidoformate derivative of the drug, allows the formation of an imide linker between a drug and a peptide carrier. The second unclick step is defined as a process leading to the elimination of the linker by intramolecular cyclization and to the release of the drug. Essential to the unclick concept is the participation of the bond formed by click chemistry in the disassembly mechanism.

Results and Discussion

The reaction of thioacids with electron-deficient azides such as sulfonyl azides gives access to the corresponding amides in good yield [2,3]. Azidoformates have been scarcely studied in this field. The strategy described in Figure 1 involves as a first step an imide ligation between peptide thioacid carrier **1** and a drug activated by an azidocarbonyl group **2**. Ligation proceeds very cleanly at pH 2.5. At this pH, ε or α-amino groups are protected by protonation. At higher pH, azidoformate **2** was able to react partially with amino groups. No side reactions with amino acids such as His, Tyr, Ser, Asn or Glu have been observed. The compatibility of imide ligation with Cys remains to be established since this amino acid has been shown to be incompatible with sulfo-click ligation between thioacids and sulfonyl azides [3]. Imides such as **3** can be purified by RP-HPLC using water/acetonitrile linear gradients containing TFA and lyophilized without detectable degradation. Imide ligation features most of the characteristics displayed by click reactions: the reaction is chemoselective, racemization free, gives good yields using simple reaction conditions in water, requires only readily available starting materials. It is illustrated in Figure 1 with the synthesis of imide 3. The modest yield of 28% is due to the small scale of synthesis (few mgs). Isolated yields are usually in the range 50-60%. Conjugate **3** features a masked

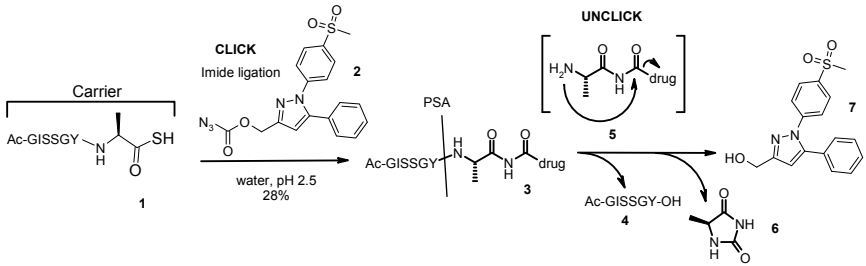

Fig. 1. Illustration of the click-unclick strategy. An imide-click reaction allows the chemoselective and racemization free assembly of peptide-drug conjugate. The drug is unclicked by the action of an enzyme.

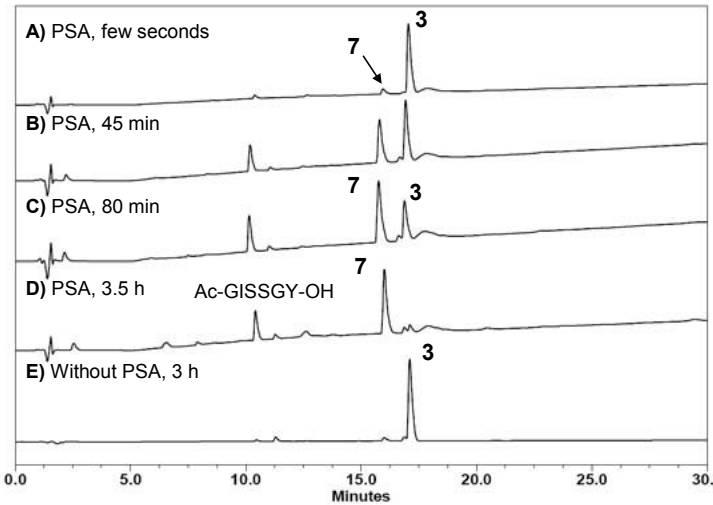

Fig. 2. Unmasking of the drug using an endopeptidase (PBS pH 7.4, 37°C). Conjugate 3 (40 µM) was incubated with (A-D, 10 µg/mL) or without (E) PSA. RP-HPLC analysis of the reaction mixtures on a C18 Nucleosil column (215 nm).

COX-2 inhibitor and a peptide substrate for prostate specific antigen (PSA). COXs are involved in a number of diseases. In particular, COX-2 is over-expressed in prostate cancer, and is considered as a molecular target in this disease. PSA is an chymotrypsin-like endopeptidase which is relatively specific to prostate tissue and overexpressed in prostate cancer cells. This enzyme has been used by several groups for vectorization of anticancer drugs because PSA is active only in the prostate cells microenvironment.

Next, conjugate **3** was incubated with PSA, which cleaves after Tyr residue present in the penultimate position (Figure 2A, D). Figure 2A-D shows that unmasking of **7** was almost complete after 3h of PSA digestion ($t_{1/2}$ ~ 40 min). Unmasking of **7** occurred in the mixture because rearrangement of intermediate **5** (Figure 1) did not occur in the eluent used for RP-HPLC analysis (pH 2) due to protonation of the amino group. Stability of **5** in acidic media was confirmed with a reference compound obtained by reacting Boc-Ala-SH with azidoformate **2**, followed by Boc removal in TFA. We have also demonstrated the formation of hydantoin **6** in stoichiometric amounts. The early eluting peak in Figure 2A,D corresponded, by LC-MS, to peptide Ac-GISSGY-OH, showing the Tyr-Ala peptide bond cleavage by PSA. The buffer alone led to the release of a small proportion of **7** due to slow hydrolysis or degradation of the imide bond in water (Figure 2E, $t_{1/2}$ ~ 15 h).

In conclusion, imide ligation is a useful ligation method in peptide chemistry which allowed the facilitated assembly of peptide-drug conjugates and the design of a novel self-immolative linker.

Acknowledgments

We thank financial support from Région Nord Pas-de-Calais and from Cancéropôle Nord-Ouest. We thank Emmanuelle Boll (CNRS) for NMR experiments.

References

1. Mhidia, R., Beziere, N., Blanpain, A., Pommery, N., Melnyk, O. *Org. Lett.* **12**, 3982-3985 (2010).
2. Shangguan, N., Katukojvala, S., Greenberg, R., Williams, L.J. *J. Am. Chem. Soc.* **125**, 7754-7755 (2003).
3. Rijkers, D.T., Merkx, R., Yim, C.B., Brouwer, A.J., Liskamp, R.M. *J. Pept. Sci.* **16**, 1-5 (2010).

Proceedings of the 31st European Peptide Symposium
Michal Lebl, Morten Meldal, Knud J. Jensen, Thomas Hoeg-Jensen (Editors)
European Peptide Society, 2010

Designed Hairpins Modulate the Amyloidogenesis of Alpha Synuclein: Inhibition and Diversion to Non-Amyloid Aggregates

Niels H. Andersen[1], Kelly N.L. Huggins[1], Marco Bisaglio[2], and Luigi Bubacco[2]

[1]*Department of Chemistry, University of Washington, Seattle, WA, 98195, U.S.A.;*
[2]*Department of Biology, University of Padova, Padova, 35121, Italy*

Introduction

At the previous EPS symposium we reported that designed β hairpins bearing cross-strand pairs of Trp and Tyr residues inhibit the aggregation of human pancreatic amylin (hAM); the inhibition was evidenced by 2 to 8-fold increases in the lag time to amyloid fibril formation as measured by thioflavin-T (ThT) fluorescence and the timescale for the evolution of a β-structure CD spectrum [1]. Those conclusions have since been confirmed by additional studies including TEM imaging of the fibrils. The effects of the hairpins used in that study, and additional peptides, upon the aggregation of α synuclein (α-syn, the amyloid-producing species associated with Parkinson's disease) has now been examined. Hairpins also modulate the aggregation α-syn, but by a different mechanism and with different structure activity relationships.

Results and Discussion

To date, the effects of 18 7-18 residue peptides on amyloid fibril formation by α-syn have been examined. In this preliminary account, we will present the data for two hairpins (WW2 and YY2) as well as a species with a Trp-flanked turn (μPro1, with the same WI**p**GKW core sequence as WW2), comparing this to the aggregation assay results for α-syn in the absence of added peptides as well as in the presence of selected peptide controls. The peptide sequences are collected in Scheme 1. In the case of hAM, WW2 was the most potent inhibitor of hAM aggregation, showing effects at equimolar concentrations while rat amylin [2] required a 6-fold concentration to effect any retardation of aggregation onset. Hairpin WW2 effected at 70% reduction in hAM fibril yield and increased the lag time by a factor of 6 when present in a 2-fold excess. In contrast, μPro1 addition increased the fibril yield (120% of control by the ThT assay) and caused a decrease in the lag time.

YY2	KKLTVY-I**p**GK-YTVSA
WW2	KKLTVW-I**p**GK-WTVSA
control	KKLTVW-I
μPro1	C_2H_5CO-W-I**p**GK-WTG

*Scheme 1. Peptide names and sequences- lower case **p** = D-Pro.*

Our α-syn aggregation assay conditions (100 μM α-syn in 1.5 vol-% HFIP) yield reproducible amyloid formation with the onset of β structuring (by CD and ThT fluorescence) occurring in 6 h and complete after 16 h (Figure 1). While many hairpins drastically altered the course and results in this assay, μPro1 (which enhanced fibril formation for hAM) was entirely without effects on α-syn aggregation. This (or a small increase in the lag time coupled with modest levels of inhibition as measured in the ThT fluorescence assay) was also observed for other hairpins bearing a W-loop-W unit but with

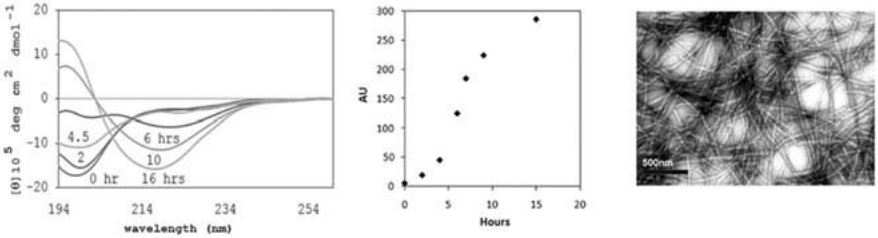

Fig. 1. The course of amyloid formation and the fibril TEM for α-synuclein controls.

short β strands. In contrast, numerous analogs of KKLTVS-IXGK-KITVSA and other hairpin scaffolds with 5-7 residue long β strands, led to accelerated production of insoluble aggregates. This was always accompanied by a decrease in the ThT fluorescence signal and intensity of the β CD signature (versus the uninhibited control) at the 16 h point in the assay. Peptides WW2 and YY2 were the most effective "inhibitors". We attributed these observations to the formation of insoluble non-amyloid species. To verify this, we relied on TEM imaging and Congo red (CR) staining of the final assay mixtures with complete dispersion of the precipitates so that all species present would be observed in the images. The right panel of Figure 1 shows the amyloid fibrils observed in an uninhibited control. In such controls (and in the presence of μPro1 and other peptides that did not reduce the ThT fluorescence response), CR staining is observed with the bright green birefringence that is diagnostic of amyloid species. Aggregation experiments with WW2 and YY2 inihibition failed to display fibrils of normal morphology by TEM and displayed little CR staining and no green birefringence. TEM images appear below (Figure 2 - compare with Figure 1).

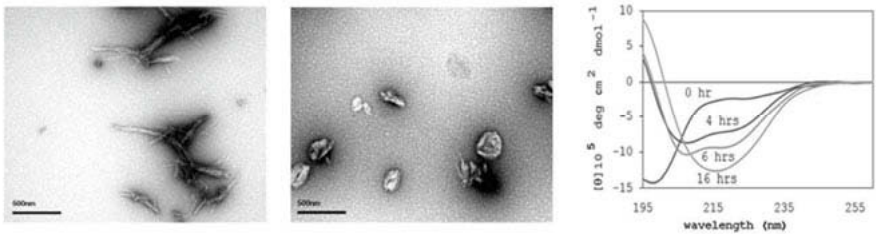

Fig. 2. TEM image for: WW2 inhibition (left); YY2 inhibition (middle); CD spectra with KKLTVWI (right).

The limited formation of short thick fibrils was observed for most hairpins that decreased the time to cloudiness in the assay: illustrated for peptide WW2 which produced immediate cloudiness in assays initiation by the addition of HFIP (to a 1.5% final concentration). Peptide YY2, in contrast, afforded circular (spherical?) structures in the TEM images.

Of interest, KKLTVWI, the single strand control for hairpin WW2, which increases the lag time to fibril formation but eventually yields fibrils of normal morphology and CR staining characteristics, displayed a different time course of CD spectral changes (Figure 2). At intermediate times in the assay, the CD spectrum indicates the formation of a highly helical state. We anticipate that both solution-state NMR and 2D IR [3] studies of amyloidogenesis in the presence of hairpins and other peptides will provide details regarding the initial binding sites for the inhibitors and the alterations in the amyloidogenesis pathway that result.

Conclusions

For the amyloidogenesis inhibition with either hAM or α-syn, hairpins with strand lengths of a least 5 residues are required. In the case of hAM, the presence of cross-strand W/W (or less effectively Y/Y) pairs at non-H-bonded sites is required for inhibition as detected by either lag time prolongation or reduced fibril yield (TEM and ThT assays). In the case of α-syn, long hairpins result in the formation of non-amyloid aggregates. This diversion of the preamyloid state is enhanced by Trp and Tyr residues in the hairpin strands, but can also be observed with hairpins lacking the aromatic sidechains.

Acknowledgments

Work at U.W. was supported by grant 3R01GM59658-8S1 (NIH); some of the hairpins were designed in and were available from prior NSF supported (CHE-0650318) studies.

References

1. Huggins, K.N.L., Andersen, N.H. In Lankinen H., (Ed.) *Peptides 2008 (Proceedings of the 30th European Peptide Symposium)* 2010, p. 590.
2. Cao, P., Meng, F., Abedini, A., Raleigh, D.P. *Biochemistry* **49**, 872-881 (2009).
3. Shim, S.-H., Gupta, R., Ling, Y.L., Strasfeld, D.B., Raleigh, D.P., Zanni, M.T. *PNAS U.S.A.* **106**, 6614-6619 (2009).

Proceedings of the 31st European Peptide Symposium
Michal Lebl, Morten Meldal, Knud J. Jensen, Thomas Hoeg-Jensen (Editors)
European Peptide Society, 2010

Selective Targeting of Extracellular Cyclophilins by Novel Cyclosporin A Derivatives

Miroslav Malešević[1], Jan Kühling[1], Viktoria Kahlert[1], Frank Erdmann[1], Molly A. Balsley[2], Michael I. Bukrinsky[2], Stephanie L. Constant[2], and Gunter Fischer[1]

[1]Max Planck Research Unit for Enzymology of Protein Folding, Halle (Saale), 06120, Germany; [2]Department of Microbiology, Immunology, and Tropical Medicine, The George Washington University, Washington, DC, 20037, U.S.A.

Introduction

Cyclosporin A (CsA), a cyclic undecapeptide extracted from the fungus *Tolypocladium inflatum*, is an indiscriminately tight binding inhibitor of Cyclophilins (Cyps). Cyclophilins together with parvulins and FK-506 binding protein belongs to the family of peptidyl-prolyl *cis/trans* isomerases (PPIases EC 5.2.1.8). These ubiquitous chaperone enzymes, that influence de novo protein folding, and refolding of denatured proteins, are found in virtually all organisms. There are 20 different human Cyp isoforms; the most abundant member of them is cyclophilin A (CypA, Cyp18). Cyp A and Cyp B are also extracellular enzymes that cause chemotactic responses of eosinophils, neutrophils, and T-cells (mediated by the PPIase active site of cyclophilins) probably through the CD-147 receptor. The mechanism and stimuli needed for Cyp release from cell is unknown. However, elevated levels of Cyp have been detected in different inflammatory diseases, like asthma, severe sepsis, rheumatoid arthritis, or psoriasis.

Although human Cyps are involved in a multitude of cellular functions like cell growth, proliferation, and motility, Cyp-inhibitors, like e.g. CsA, are considered as possible antiviral or antiparasitic therapeutics. Also, Cyp inhibition is a promising strategy for treating several pathological processes like cancer or inflammatory diseases. However, major obstacles for a broader use of Cyp inhibitors are lack of selectivity and immunosuppression.

Results and Discussion

A novel CsA derivative (Figure 1) for selective targeting of extracellular Cyps was designed and synthesized [1]. A trifunctional template, obtained from trimesic acid [2], was functionalized with the fluorescent marker 5(6)-carboxytetramethylrhodamine and a side chain-extended [D-Ser8]-CsA analog. The remaining third position was occupied with a highly negatively charged $(D\text{-}Glu)_6$-Gly-OH moiety, which was used to improve the derivative solubilities at physiological conditions and to diminish its cell permeabilities. As a cell-permeable reference, (Cs9-Rhd), the same [D-Ser8]-CsA analog and 5(6)-carboxytetramethylrhodamine connected with the cadaverin linker [3], was synthesized.

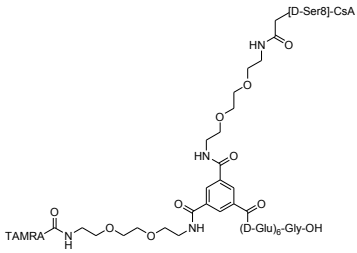

Fig. 1. The novel CsA derivative MM-218.

Both confocal laser scanning microscopy (Figure 2) and fluorescence-activated cell sorting experiments confirmed the cell impermeability of the MM-218 compound. Contrary, the Cs9-Rhd was accumulated mostly in the cell cytoplasm. However, fluorescent clusters were observed on the cell membrane upon incubation with both compounds. In a protease-coupled PPIase assay [4] MM-218 (Ki=1.8± 0.6 nM CypA, 1.3 ± 0.5 nM CypB) and Cs9-Rhd (Ki=4.3±0.5 nM CypA, 12.0± 2.8 nM CypB) were even better reversible Cyp inhibitors than CsA itself (Ki=8.4±2.5 nM CypA, 6.9±2.1 nM CypB). However, in a RII phosphopeptide dephosphorylation assay [3], the Calcineurin (CaN) was best inhibited by a CsA/CypA binary complex (MM-218/CypA Ki=26.2 ±1.2 μM, Cs9-Rhd/CypA Ki=0.8±0.1, CsA/CypA Ki=0.09±0.005 μM). Probably because of its cell impermeability the MM-218 compound could not inhibit the proliferation of the concanavalin A stimulated splenic lymphocytes and appeared to be non-immunosuppresive

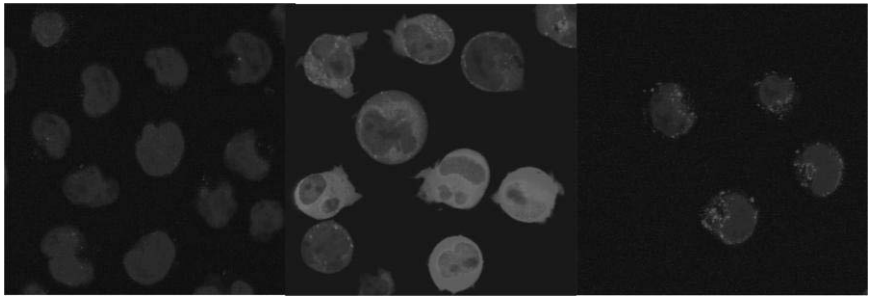

Fig. 2. Confocal microscopy of Jurkat cells incubated with Cs9-Rhd or MM-218.

in the mixed-lymphocyte assay with human peripheral blood mononuclear cells. Cs9-Rhd and CsA itself were, as expected, immunosuppresive in both assays. Additionally, MM-218 has been non-cytotoxic in tested concentrations. The cell-impermeable compound MM-218 was also stable to proteolytic degradation as confirmed by an unchanged HPLC-MS profile of this substance during 96 h incubation time at 37°C in the mouse serum. In a chemotactic assay MM-218 completely inhibited activated mouse CD4+ T-cell migration in response to CypA and CypB, but not in response to chemotactic cytokine RANTES. The full advantage of this stable, non-immunosuppresive but potent extracellular Cyp inhibitor was shown in mouse model of asthma, where a drastic reduction of leukocyte numbers only in the lung tissue and airways of asthmatic mice upon intervention with MM-218 was observed [5]. Moreover, it was shown that MM-218 intervention significantly reduces hyperreactivity, in a mouse model of acute allergic asthma, as confirmed by measuring the lung airway resistance and compliance of mice primed with ovalbumin and challenged with increasing doses of methacholine [5]. The asthmatic mice group treated i.p. with MM-218 showed similar airway resistance and lung compliance to those of naïve mice.

The important advantage of this novel CsA derivative, MM-218, over CsA itself for the study of inflammatory diseases is that all effects resulted from inhibiton of different nuclear transcription factors, calcineurin, intracellular Cyps or other diverse intracellular CsA interaction partners could be completely excluded. The effects observed upon MM-218 intervention in asthmatic mice model could be assigned to inhibition of extracellular Cyps.

In modern drug design, selectivity gains ever-growing scientific attention. As a consequence of their selectivity, therapeutic agents could act at low concentrations with minimal or no side effects. In particular, selectivity could be achieved even for non-selective enzyme inhibitors by their targeting to a specific cell population or cell compartment. In this work, selectivity for extracellular Cyps was achieved by derivatization of the non-selective CsA molecule with oligo D-Glu peptide. It was clearly shown that this modification of CsA led to drug improvements in terms of: better solubility, no side effect, lower drug doses, no immunosuppression.

It could be concluded that selective targeting of extracellular Cyps is a powerful approach to i) study Cyp functions in physiological and pathological processes and ii) develop novel improved anti-inflammatory drugs.

Acknowledgments
Supported by SFB 610 (Deutsche Forschungsgemeinschaft) and AI067254 (National Institutes of Health).

References

1. Malešević, M., et al. *Angew. Chem. Int. Ed.* **49**, 213-215 (2010).
2. Malešević, M., Lücke, C., Jahreis, G. In *Peptides 2004, Proceedings of the Third International and Twenty-Eighth European Peptide Symposium*, Kenes International, Israel, 2005, p. 391.
3. Zhang, Y., et al. *J. Biol. Chem.* **280**, 4842-4850 (2005).
4. Fischer, G., et al. *Biomed. Biochim. Acta* **43**, 1101-1111 (1984).
5. Balsley, M.A., et al. *J. Immunol.* Submitted.

Proceedings of the 31st European Peptide Symposium
Michal Lebl, Morten Meldal, Knud J. Jensen, Thomas Hoeg-Jensen (Editors)
European Peptide Society, 2010

Design of Peptidyl-Inhibitors for Glutathione Transferase (GST) Useful in Targeted Cancer Chemotherapy

Irine Axarli[1], Georgia A. Kotzia[1], Christos Petrou[2], Paul Cordopatis[2], Nikolaos E. Labrou[1], and Yannis D. Clonis[1]

[1]Laboratory of Enzyme Technology, Department of Agricultural Biotechnology, Agricultural University of Athens, 75 Iera Odos Street, GR-11855, Athens, Greece; [2]Laboratory of Pharmacognosy and Chemistry of Natural Products, Department of Pharmacy, University of Patras, GR- 26500, Patra, Greece

Introduction

GSTs [1-4] have emerged as a promising therapeutic target because specific isozymes are overexpressed in a wide variety of tumours and may play a role in the aetiology of other diseases, including neurodegenerative diseases, multiple sclerosis and asthma. A common problem encountered in cancer chemotherapy is the appearance of chemotherapeutic resistant tumour cells. A possible origin for the problem appears to be an increase in the expression of total GST activity. It is plausible that GSTs serve two distinct roles in the development of drug resistance via direct detoxification as well as acting as an inhibitor of the mitogen-activated protein (MAP) kinase pathway. In addition to glutathione conjugating activity, GSTs exhibit sulfonamidase activity and catalyze the GSH-mediated hydrolysis of sulphonamide bonds. Such reactions are of interest as potential tumour-directed pro-drug activation strategies [3].

Results and Discussion

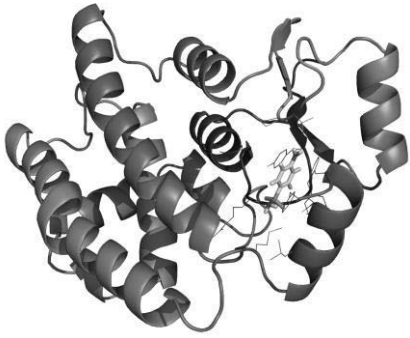

Fig. 1. Interaction of sulphanilamide lead-ligand with hGSTA1-1 from docking calculations. Side-chains of specific residues contributing to sulphanilamide binding are presented as thin stick. The ligand is shown as thick stick.

Human GSTA1-1 (hGSTA1-1) was cloned and expressed in *E. coli* (10-20% of soluble *E. coli* protein). The enzyme is a homodimeric protein. Each monomer has two domains, an α/β-domain that includes $\alpha1$-$\alpha3$ helices and a large α-helical domain comprising helices $\alpha4$-$\alpha9$. The former contains the GSH-binding site (G-site) on top of the α-domain. A hydrophobic pocket (H-site) lies between the domains in which a hydrophobic substrate binds and reacts with GSH (Figure 1). The recombinant enzyme was purified to homogeneity in a single-step by affinity chromatography on immobilized glutathione. GSTs exhibit sulphonamidase activity and catalyze the GSH-mediated hydrolysis of sulphonamide bonds to form the corresponding amine (Figure 2). In the present work we report the design and synthesis of chimaeric sulphonamide-derivatives which can be activated by the model human isoenzyme GSTA1-1 (hGSTA1-1). These chimaeric molecules consist of (i) a bombesin-moiety (Table 1) (analogues [Leu^{13}]-bombesin, [Phe^{13}]-bombesin and [Ser^{3},Arg^{10},Phe^{13}]-bombesin) as a structural element determining the drug selectively to tumour cells, able to recognize bombesin receptors present on the tumour cell surface, and (ii) an aromatic sulfonamide moiety. Sulfonamide bombesin analogues were synthesized by Fmoc solid phase methodology [5] utilizing Rink Amide MBHA resin [6] as the solid support.

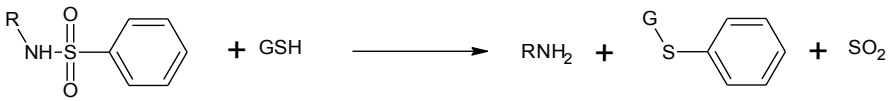

Fig. 2. Sulfonamide cleavage by hGSTA1-1.

Table 1. The general structure of the sulfonamide bombesin analogues and the primary structure of bombesin and its analogues, R = C_6H_5-SO_2-

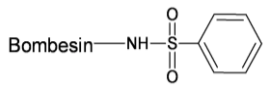

Bombesin	pGlu-Gln-Arg-Leu-Gly-Asn-Gln-Trp-Ala-Val-Gly-His-Leu-Met-NH_2
R-[Leu^{13}]-bombesin	C_6H_5-SO_2-Glu-Gln-Arg-Leu-Gly-Asn-Gln-Trp-Ala-Val-Gly-His-Leu-Met-NH_2
R-[Phe^{13}]-bombesin	C_6H_5-SO_2-Glu-Gln-Arg-Leu-Gly-Asn-Gln-Trp-Ala-Val-Gly-His-Phe-Met-NH_2
R-[Ser^3,Arg^{10},Phe^{13}] -bombesin	C_6H_5-SO_2-Glu-Gln-Ser-Leu-Gly-Asn-Gln-Trp-Ala-Arg-Gly-His-Phe-Met-NH_2

Stepwise synthesis of the peptide analogues was achieved with diisopropylcarbodiimide/1-hydroxybenzotriazole (DIC/HOBt) in dimethylformamide (DMF) as coupling agents [7]. In order to achieve the prodrug formation, pGlu residue from the N-terminal of the native bombesin sequence was replaced by Glu which has a free amino group available to coupling with another group. Coupling of benzenesulfonyl group with the free amino-terminal and formation of the sulfonamide bond was achieved using N-methylmorpholine. After the completion of the synthesis, the resin was treated with a TFA (trifluoroacetic acid) solution to liberate the fully deprotected crude peptide conjugates. All the products were purified by gel filtration chromatography on Sephadex G-15. Final purification was achieved by preparative high performance liquid chromatography (Lichrosorb RP18 column). ESI-MS analysis confirmed the expected peptide formulae.

To analyze the sulfonamidase activity, a collection of different classes of GST isoenzymes were investigated using sulfanilamide (4-aminobenzenesulfonamide) as a model substrate. In particular, GSTs belonging to class alpha [human GSTA1-1, (hGSTA1-1); mouse GSTA4-4, (mGSTA1-1)], pi [human GSTP1-1, (hGSTP1-1)], sigma [*Schistosoma japonicum* GST, (SjGST); human spleen haematopoietic prostaglandin D synthase, (PDS-GST)], tau [*Glycine max* GST, (GmGSTU4-4)] and phi (*Zea mays* GST I) were examined. The higher sulfonamidase activity was observed for hGSTA1-1. This observation is of particular importance since this isoenzyme is expressed in several tumours and therefore may represent a therapeutic molecular target in cases where tumour-protective effects depends upon hGSTA1-1 activity. After hGSTA1-1-mediated cleavage of the sulfonamide bond of the chimaeric molecule (pro-drug), the released aromatic sulfonamide moiety is conjugated with GSH, thus leading to a S-aromatic-glutathionyl conjugate which is a strong inhibitor for GST. This inhibition was found to be of a competitive-type with respect to GSH (K_i = 5.1±0.8 μM) and of a non-competitive type with respect to the aromatic substrate CDNB (K_i = 8.6±0.7 μM). This effect may reduce the drug resistance of cancer cells.

Acknowledgments
This work was partially supported by the Hellenic General Secretariat for Research and Technology.

References

1. Labrou, N.E., Mello, L.V., Clonis, Y.D. *Biochem. J.* **358**, 101-110 (2001).
2. Labrou, N.E., Karavangeli, M., Tsaftaris, A., Clonis, Y.D. *Planta* **222**, 91-97 (2005).
3. Axarli, I., Labrou, N.E., Petrou, C., Rassias, N., Cordopatis, P. Clonis, Y.D. *Eur. J. Med. Chem.* **44**, 2009-2016 (2009).
4. Labrou, N.E., Kotzia, G.A., Clonis, Y.D. *Protein Eng. Des. Sel*. **10**, 741-748 (2004).
5. Fields, B.G., Noble, L.R. *Int. J. Pept. Prot. Res*. **35** 161-214 (1990).
6. S. Aventis, European Patent 322348 and US Patent 5124478.
7. Köning, W., Geiger, R. *Chem. Ber.* **103,** 788-798 (1970).

Proceedings of the 31st European Peptide Symposium
Michal Lebl, Morten Meldal, Knud J. Jensen, Thomas Hoeg-Jensen (Editors)
European Peptide Society, 2010

Exploring the HBV Envelope Protein for Liver-Specific Drug Targeting

Thomas Müller[1], Alexa Schieck[1], Barbro Beijer[1], Anja Meier[2], Uwe Haberkorn[1], Stephan Urban[2], and Walter Mier[1]

[1]Department of Nuclear Medicine, University Hospital Heidelberg, Im Neuenheimer Feld 400, 69120, Heidelberg, Germany; [2]Department of Molecular Virology, University Hospital Heidelberg, Im Neuenheimer Feld 350, 69120, Heidelberg, Germany

Introduction

Many pharmaceuticals used today do not exhibit a specific targeting to their site of action. We are currently developing a novel drug, named Myrcludex B, against hepatitis B virus infections [1]. It is derived from the 47 N-terminal amino acids of the large hepatitis B envelope protein and is myristoylated at the N-terminal (Myristoyl-HBVpreS/2-48). The peptide accumulates exclusively inside the liver; already 10 minutes after intravenous injection, 88% of the injected peptide was found inside the liver (Figure 1). In *in vitro* FACS experiments it was shown that the peptide binds specifically to various liver cell lines including primary human hepatocytes. Encouraged by these findings, the peptide is now further investigated as a possible drug carrier for targeting different drugs to the liver. In order to demonstrate the versatility of this carrier concept, different compounds were selected. Penicillin was chosen as a representative of antibiotics. The antimalarial primaquine was selected, because it is known to eradicate persisting forms of the parasite inside the liver. Doxorubicin is a standard chemotherapeutic against hepatocellular carcinoma but leads to severe side effects. The advantage of drug targeting is the lower amount of drug required for therapy accompanied by a reduction of side effects.

Results and Discussion

Biodistribution studies revealed that all the synthesized drug conjugates predominantly target the liver. However, the pharmacokinetic behavior is altered depending on the conjugated drug. Especially in the case of the doxorubicin derivative, the excretion was much faster compared to the peptide itself. Although the initial liver uptake 10 minutes post injection was comparable (93% versus 88% for Myristoyl-HBVpreS/2-48), 1 hour post injection the amount inside the liver had already decreased significantly to 51% versus 81% (Figure 2). However, in the case of the penicillin derivative, the excretion kinetics are comparable to Myristoyl-HBVpreS/2-48 but the absolute values are significantly lower.

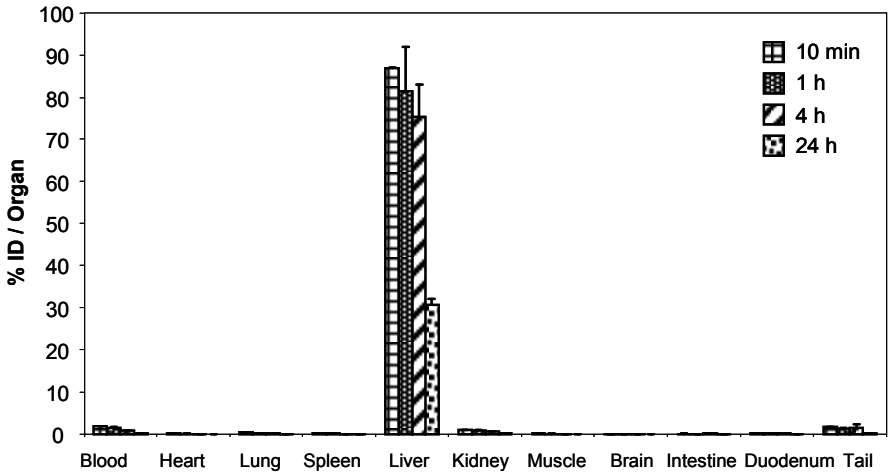

Fig. 1. Biodistribution of radioactively labeled Myristoyl-HBVpreS/2-48 in female NMRI mice.

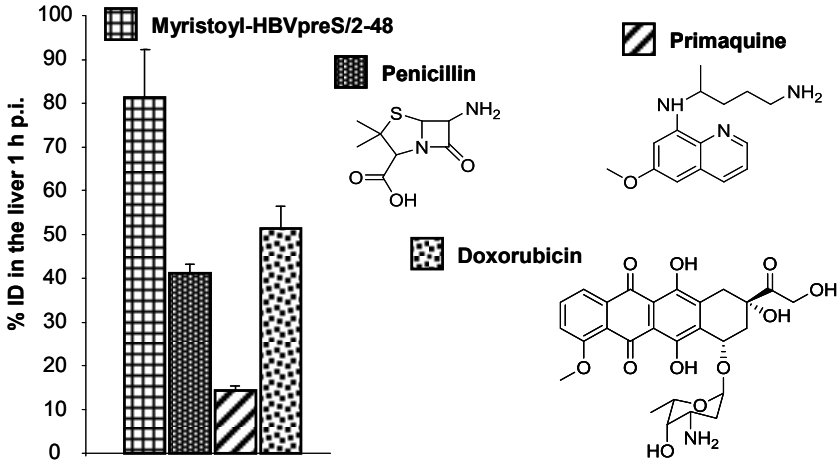

Fig. 2. Biodistribution data of the different derivatives 1 h after intravenous application in female NMRI mice.

Furthermore, it was shown that the liver specificity arises from the particular sequence of the peptide. For example, in the case of the primaquine derivative, a mutant with only two exchanges at positions 11 and 13 for the respective D-amino acid did not show the liver-specific uptake.

All peptides were synthesized by employing automated Fmoc/tBu peptide synthesis with HBTU/DIPEA activation. After the peptide synthesis and the coupling reactions, purification was carried out by RP-HPLC. All peptides and conjugates were obtained in high purity and the yield of the conjugation reaction was determined. For penicillin and the primaquine derivatives, a peptide with an additional C-terminal cysteine was synthesized. Penicillin was coupled as a bromoaceto derivative [2] to the cysteine residue forming a thioether bond with a yield of 45%. Primaquine was first reacted with Boc-Cys(NPyS)-OH, and secondly, the amine was deprotected with TFA. The NPyS protecting group can react selectively with thiols forming a disulfide bond [3], in this case to the cysteine side chain with a yield of 56%. In the case of doxorubicin, it was important to leave the amine at the saccharide part intact [4]. The amine was Fmoc protected and then the Fmoc-protected doxorubicin was reacted with glutaric acid anhydride in order to yield a free carboxylic acid for coupling. This derivative was then coupled to a shortened peptide only containing one lysine residue by standard HBTU/DIPEA activation. After Fmoc deprotection, the final conjugate was obtained with a yield of 45%. In conclusion, the peptide Myristoyl-HBVpreS/2-48 has been shown to be a versatile drug carrier and all conjugates were synthesized in high purity and good yields.

Acknowledgments
The authors gratefully acknowledge the Bundesministerium für Bildung und Forschung (BMFB) for finacial support (grant 01GU0702).

References

1. Petersen, J., et al. *Nature Biotechnology* **26**, 335-341 (2008).
2. Li, S., Roberts, R. *Chemistry and Biology* **10**, 233-239 (2003).
3. Matsueda, R., et al. *Chemistry Letters* **10**, 737-740 (1981).
4. Nagy, A., et al. *PNAS* **93**, 7269-7273 (1996).

Proceedings of the 31st European Peptide Symposium
Michal Lebl, Morten Meldal, Knud J. Jensen, Thomas Hoeg-Jensen (Editors)
European Peptide Society, 2010

Biocompatible Triazole Ligations via 1,3-Dipolar Cycloadditions of Peptidyl Phosphoranes and Azido Peptides

Jörg Rademann[1,2*] and Ahsanullah[2,3]

[1]Medicinal Chemistry, Leipzig University, 04103, Leipzig, Germany; [2]Leibniz-Institut of Molecular Pharmacology, Robert-Rössle-Str. 10, 13125, Berlin, Germany; [3]Institute of Chemistry and Biochemistry, Free University Berlin, Takustr. 3, 14195, Berlin, Germany

Introduction

Recently, we have found a versatile and practical approach for the integration of C-acylation steps within classical, Fmoc-based N-acylation, i.e. peptide chemistry [1]. The resulting C-terminal peptide electrophiles have served as valuable synthetic intermediates in C-terminal variation and heterocyclic-derivatization of peptides [2].

Peptidyl phosphorane, a C-terminal peptide electrophile, can also act as a dipolarophile and participate in 1,3-dipolar cycloaddition reactions. Among dipole partners, azido group would be an obvious choice because triazole will be the resultant product in that case and triazole ligations have found wide range use in all the disciplines of chemistry. Catalytic versions of Huisgen's 1,3-dipolar cycloadditon (azide-alkyne cycloaddition) result in regioselective triazole formation especially, Cu-catalyzed triazole ligation has become very popular over the recent years. Metal catalysis, however, limits their use as biocompatible ligation although strain-promoted triazole ligation has been discovered as an alternate to avoid metal catalysis but regioselectivity is lost in that case. Thus, azide-phosphorane triazole ligation, avoiding metal catalysis but retaining regioselectivity, is an exciting extension in peptide ligation methods.

Results and Discussion

Polymer-supported triphenylphosphine was alkylated with *tert*-butyl bromo acetate and resulting phosphoranylidene acetate was acylated with activated amino acid through racemization-free C acylation and the peptide chain was elongated through Fmoc-based solid phase peptide synthesis (SPPS), as shown in Figure 1. After N-acetylation of the amino terminus of the peptide chain or coupling azido acid at the N-terminus, the *tert*-butyl ester was saponified with TFA. Ester cleavage proceeds with instantaneous decarboxylation resulting in peptidyl phosphorane or azido-peptidyl phosphorane depending on N-terminus of peptide chain, as shown in Figure 2.

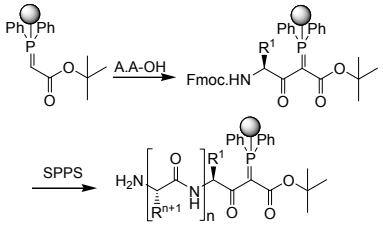

Fig. 1. Synthesis of polymer-supported peptidyl phosphoranes.

In addition to their use in synthesis of various peptide electrophiles and peptide-heterocycle chimera, peptidyl phosphoranes can act as dipolarophile and react with azide dipole in triazole ligation.

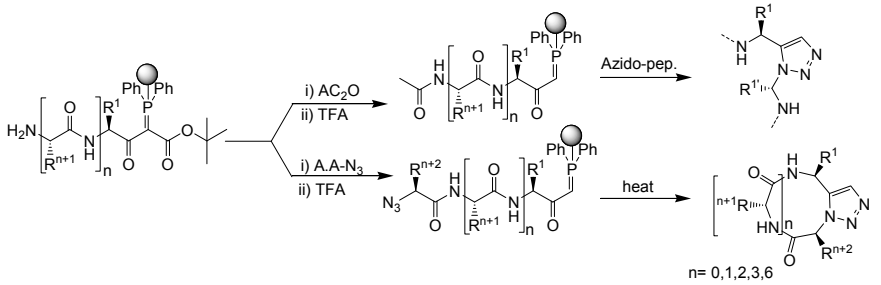

Fig. 2. Triazole ligation for peptide turns and cyclopeptides with cis-locked triazole ring incorporated.

Peptidyl phosphoranes were first reacted with electron deficient azides such as triflic azide, tosyl azide, 4-nitro benzoyl azide and 4-carboxyl phenyl azide. The cycloaddition reaction proceeded smoothly in unpolar solvents at room temperature with complete regioselectivity in favor of 1,5-disubstituted triazole. The reaction, however, needed polar solvents and gentle heating in case of relatively electron rich azides such as benzyl azide, methyl 2-azido acetate and 2-azido-acetamide but still with good yield and complete regioselectivity. This reactivity trend and effect of solvent polarity reflects polar transition state involved and LUMO controlled 1,3-dipolar cycloaddition. Finally, this reaction was used for short peptides ligation by heating peptidyl phosphoranes with azido peptides in polar solvents like THF and DMF. The potential of ligation products, with 1,5-triazole incorporated, to form stable conformations in solution was investigated using 2D-ROESY spectroscopy and molecular dynamic simulations. All the structures consistently indicated a turn-like bend in short peptides [3]. Thus, the triazole ligation method established has potential to introduce β-turn in short peptide chains. Moreover, the reaction is devoid of any metal catalysis and has potential to be developed as biocompatible ligation. In this context soluble peptidyl phosphoranes were synthesized and used in azido-phosphorane triazole ligation in aqueous medium at room temperature.

Azido-peptidyl phosphoranes in principle can undergo either intra-molecular or intermolecular reactions, the first resulting in triazolyl-cyclopeptide through cyclative cleavage as shown in Figure 2. When, however, azido-dipeptidyl phosphoranes were heated in DMF, they delivered exclusively dimeric products. In contrast to this, the azido-tripeptidyl phosphoranes yielded a mixture of monomeric and dimeric triazolyl-cyclopeptides through competition between intra-versus inter-site reactions. It might be possible to minimize inter-site reactions by using a more rigid resin with higher percentage of cross linker. To test the assumption, macroporous polystyrene resin (20% divinyl benzene) was used instead of microporous polystyrene (2% polystyrene) and a major shift towards monomeric product (intra-site reaction) in case of azido-tripeptidyl phosphorane was observed. Azido-dipeptidyl phopsphoranes, however, still resulted in the formation of dimeric products (inter-site reaction) despite of using the macroporous resin. This observation indicates that azido dipeptides are too short to be cyclized through cyclative cleavage and inter-site cyclization is strongly favoured in this case. As expected, azido-tetrapeptidyl phosphoranes resulted in monomeric triazolyl-cyclopeptide either exclusively or with minor dimeric product formation. To test the potential of cyclative cleavage for relatively longer peptide chains, azido-penta- and octa-peptidyl phosphoranes were cyclized in relatively good yield [4]. The cyclization method completely avoids formation of soluble, non cyclized and oligomeric by-products and is superior to solution phase cyclizations. The method provides an easy access to cyclopeptides with locked *cis*-peptide mimetic.

Acknowledgments

This work was supported by the Deutsche Forschungsgemeinschaft (Ra895/2, FOR 806, SFB 765), Boehringer Ingelheim Pharma, the Fonds der Chemischen Industrie, the Deutscher Akademischer Austauschdienst and the Higher Education Commission of Pakistan (by a stipend to A.).

References

1. a) Weik, S., Rademann, J. *Angew. Chem.* **115**, 2595-2598 (2003); *Angew. Chem. Int. Ed.* **42**, 2491-2494 (2003); b) El-Dahshan, A., Weik, S., Rademann, J. *Org. Lett.* **129**, 12670-12671 (2007).
2. a) El-Dahshan, A., Ahsanullah, Rademann, J. *Biopolymers:Peptide Science* **94**, 220-228 (2010); b) El-Dahshan, A., Nazir, S., Ahsanullah, Ansari, F.L., Rademann, J. *Eur. J. Org. Chem.* In press (2010).
3. Ahsanullah, Schmieder, P., Kühne, R., Rademann, J. *Angew. Chem. Int. Ed. Engl.* **48**, 5042-5045, (2009).
4. Ahsanullah, Rademann, J. *Angew. Chem. Int. Ed. Engl.* **49**, 5378-5382, (2010).

Proceedings of the 31st European Peptide Symposium
Michal Lebl, Morten Meldal, Knud J. Jensen, Thomas Hoeg-Jensen (Editors)
European Peptide Society, 2010

Peptide Fragmentomics

Alexander A. Zamyatnin[1,2]

[1]A.N.Bach Institute of Biochemistry, Russian Academy of Sciences, Moscow, 119071, Russian Federation; [2]Universidad Técnica Federico Santa Maria, Departamento de Informática, El Centro Cientifico Tecnologico de Valparaiso, Valparaiso, 1680, Chile

Introduction

Natural fragmentation of biological molecules including peptides is well known. Fragmentary structural organization is characteristic of both the simplest and most complex biological molecules. There are numerous examples showing that relatively small natural physiologically active substances are fragments of larger ones. A steady increase in the number of publications dealing with protein fragment structure and function has been seen in recent years. For some proteins there are already hundreds of fragments that have been studied in detail. Thereupon the term "fragmentomics" is grounded and defined, the bases and determination are given for the notion of the "fragmentome" as a set of all fragments of a single substance, as well as for global fragmentome of all chemical components of living organisms [1,2]. The computer analysis of structure and functions of food protein fragments was performed in this work

Results and discussion

The data of SwissProt database [3] containing primary structures of proteins were used as an object of investigation. Their sequences were compared with EROP-Moscow information on structure and functions of regulatory oligopeptides [4] using specially created computer programs [1,2].

The input data were the complete amino acid sequences of the proteins used as a source of fragments. The initial sequence was fragmented in a stepwise manner. e.g, in the case of dipeptide fragments, this procedure produced fragments with the following numbers of amino acids from the N-terminus – 1–2, 2–3, and so on until the fragment that started at the second residue from the C-terminus. The cases when the amino acid sequence of a fragment coincided with the primary structure of a natural oligopeptide were recorded. This method was used to reveal protein regions identical to a regulatory oligopeptide with known functions. For this theoretical analysis we selected subunits of bovine casein as the most representative in experimental studies.

This protein consists of four subunits (α-1s, α-2s, β, and κ) containing from 169 to 209 amido acid residues. Amino acid residue composition of α-2s and κ subunits includes all 20 standard amino acid residues, while no cysteine residue is present in subunits α-s1 and β. Computer fragmentation has shown that many small fragments are repeated both in a separate and in different casein subunits. Most frequent were the dipeptide EE fragments in subunits α-s1, α-s2, and β. The largest repetitive structures were heptapeptide fragments SSSEESI that are present twice in β subunit.

It can be supposed that the variety of fragmentome structures is the basis for variety of the fragment functions. In the case of casein, 60 fragments were obtained experimentally by different researchers and included in the EROP-Moscow database together with functional characteristics. Most of these fragments are enzyme inhibitors (angiotensin-converting enzyme and cathepsin). The most representative are fragments of β-subunit. A special group of four fragments formed of this subunit region (60-70) was named casomorphins earlier according to their opioid activity. In the same subunit, the function of enzyme inhibitors was detected in four fragments of the region 43-66.

Computer analysis allowed detection of functional properties in different fragments. It appeared that 22 different dipeptide and 12 tripeptide casein fragments were fully identical to natural non-casein oligopeptides obtained from different kingdoms of living organisms. In total, they present 77 regions in all casein subunits and many of them are beyond the limits of amino acid sequences of experimentally obtained structures. Spectrum of their functions is also diverse. Comparison of data in some cases confirms retention of functional properties after fragment shortening. Thus, fragment 31-32 (VF) of α-s1 subunit obtained from muscle of *S. melanostictus*, is a part of fragment 23-34 of the same casein subunit and both exhibit function of enzyme inhibitor. However, fragment subdivision is accompanied by alteration of functional properties both in the case of fragment 34-35 (RY) of κ-subunit

obtained from the same sardines and of fragment 33-38 of the same casein subunit, for which functions of enzyme inhibitor and neuropeptide were found, respectively.

Due to the presence of proteolytic enzymes within cells and in extracellular medium of a living organism, continuous degradation of peptide structures takes place. Four hundred different types of peptide bonds are cleaved with different probability, and this can result in a continuously changing mosaic of numerous fragments of endogenous proteins. In a limiting case, formation of a complete fragmentome of each of them is possible.

Formation of a complete fragmentome is quite probable during digestion when exogenous proteins are supplied with food. Thus, exogenous fragments are added to the pool of endogenous fragments. Due to partial repetition of amino acid sequences these regulators can be formed in significant amounts and noticeably influence different processes of metabolism. In particular, detection of enzyme inhibitors among them shows that the process of food protein cleavage can be inhibited by proteolysis products. Besides, fragments only just formed in the gastrointestinal tract and exhibiting antimicrobial properties are able to take part in regulation of the microflora balance. Thus, usual consideration of food proteins as an energy source can be appended by regulatory properties of their fragments because fragmentation within an organism can result in generation of a dynamically developing pool of exogenous regulatory oligopeptides, functions of which can change during formation of smaller fragments. The existence of the endogenous–exogenous pool of regulatory molecules makes wider the sense and content of the hypothesis concerning a functionally continuous totality (continuum) of natural oligopeptides [5].

Accumulation of data on structure and functions will make it possible to characterize more completely the functional abilities of numerous protein fragments, to approach understanding their role in evolution and to use them in practice. Possible practical importance of the use of natural fragments is in dietology, therapy, as well as in sanitary hygiene and cosmetics. Recording functional properties of nutritive protein fragments can suggest to dieticians what food is preferable for patients, and to pharmacologists what peptide fragments are reasonable to use as drugs or food additives.

Due to improvement of research methods, including computer analysis, our knowledge of structural and functional properties of the global fragmentome is intensively growing. This knowledge is still not enough for complete understanding of the regulatory role of fragments in living organisms. Nevertheless, already now it is possible to formulate ideas concerning structure–functional fragmentomics of natural peptides and other substances.

Acknowledgments

This work was supported by the Russian Academy of Sciences Presidium program "Molecular and Cell Biology" and by the Chilean National Research Foundation FONDECYT (Grant No. 1080504).

References

1. Zamyatnin, A.A. *Biophysics* **53**, 329-335, (2008).
2. Zamyatnin, A.A. *Biochemistry (Moscow)* **74**, 1575-1585 (2009).
3. Boeckmann, B., Bairoch, A., et al. *Nucleic Acid Res*. **31**, 365-370 (2003).
4. Zamyatnin, A.A., Borchikov, A.S., et al. *Nucl. Acids Res*. **34**, 261-266 (2006).
5. Ashmarin, I.P., Obukhova, M.F. *Biochemistry (Moscow)* **51**, 531-545 (1986).

Proceedings of the 31st European Peptide Symposium
Michal Lebl, Morten Meldal, Knud J. Jensen, Thomas Hoeg-Jensen (Editors)
European Peptide Society, 2010

Molecular Knots as Templates for Protein Engineering: The Story of Lasso Peptides

Kok-Phen Yan, Séverine Zirah, Yanyan Li, Christophe Goulard, Rémi Ducasse, Alain Blond, Jean Peduzzi, and Sylvie Rebuffat

Muséum National d'Histoire Naturelle, Centre National de la Recherche Scientifique, Molécules de Communication et Adaptation des Microorganismes, FRE 3206 CNRS-MNHN, Paris, France

Introduction

Lasso peptides are unusual ribosomally synthesized peptides from bacteria with an original structure forming a molecular knot. The N-terminus is covalently linked to the carboxyl side chain of an Asp or Glu residue at position 8 or 9, forming a macrolactam ring, which is threaded by the C-terminal tail, thus forming a lasso. The lasso structure is stabilized by sterical constraints that maintain the C-terminal tail within the ring and/or one or two disulfide bridges (Figure 1) [1-5].

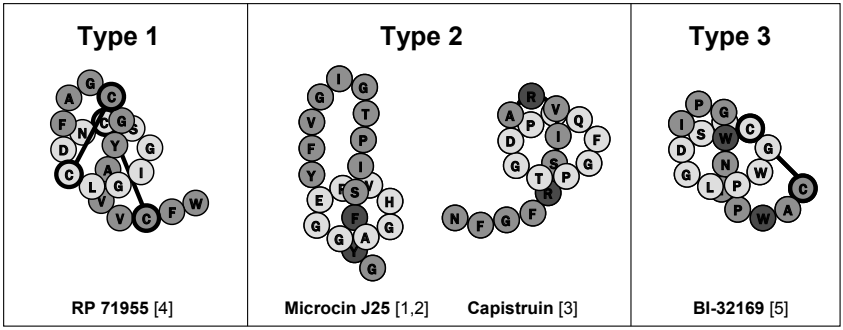

Fig. 1. Sequences and topology of type 1 (2 disulfide bridges), 2 (no disulfide bridge) and 3 (1 disulfide bridge) lasso peptides. The macrolactam ring, C-terminal tail and bulky residues located above and below the ring are indicated in soft grey, grey and dark grey, respectively. The disulfide bridges are shown in black.

Microcin J25 (MccJ25, Figure 1) is a lasso peptide produced by *E. coli* AY25 that exerts potent antimicrobial activity against *Salmonella* and *Escherichia* species [6]. The lasso structure of MccJ25 is stabilized by two aromatic residues (F_{19} and Y_{20}) located on each side of the ring. MccJ25 is apportioned into a loop (V_{11}-P_{16}) and a ring (Figure 1), which are involved in the import into target cells via interaction with the siderophore receptor FhuA [7], and in the inhibition of the RNA polymerase, which is its intracellular target [8], respectively. The gene cluster encoding MccJ25 is composed of four genes *mcjA, mcjB*, *mcjC* and *mcjD*. The reconstitution of MccJ25 *in vitro* from its precursor McjA incubated with the maturation enzymes McjB and McjC in the presence of ATP and Mg^{2+} [9] paved the way for the characterization of the biosynthesis of lasso peptides. We present here our recent results on the biosynthesis process of MccJ25 and on structure/activity relationships based on rationally-designed variants of MccJ25.

Results and Discussion

Site-directed mutagenesis on the genes encoding the maturation enzymes identified the catalytic sites involved in the maturation process and the respective roles of McjB and McjC. McjB is a cysteine protease involved in the cleavage of the leader sequence of McjA, while McjC is responsible for both the activation of Glu8 and the subsequent cyclization step. Deletions in the leader region of McjA showed that the 6 last residues before the cleavage site are important for the maturation, in agreement with the results from Link and coll. [10].

MccJ25 variants were produced by site-directed mutagenesis on the gene *mcjA* encoding the precursor. We designed a panel of analogous peptides with modifications on the ring, the loop, or the C-terminal tail region separately, in order to examine the effects of such modifications on the lasso structure and the antibacterial activity. A combination of methods was developed to unambiguously characterize the lasso topoisomers and differentiate them from the cyclic branched structure that could be adopted by some of the generated variants. As a reference for a non-lasso peptide, we used the synthetic cyclic branched topoisomer of MccJ25 (MccJ25-lactam) that contains the macrolactam ring, but a free C-terminal tail. The results were rationalized in terms of structure/activity relationships. Due to its lasso structure, MccJ25 presents an original comportment when submitted to tandem mass spectrometry (MS/MS) experiments. In particular, MS/MS of MccJ25 generates lasso-specific two-peptide product ions (Figure 2 A-B). Carboxypeptidase Y digestion of MccJ25 and its variants monitored by LC-MS, showed a wide fragmentation extent for the cyclic-branched peptides, while lasso peptides revealed resistant to proteolysis (Figure 2C).

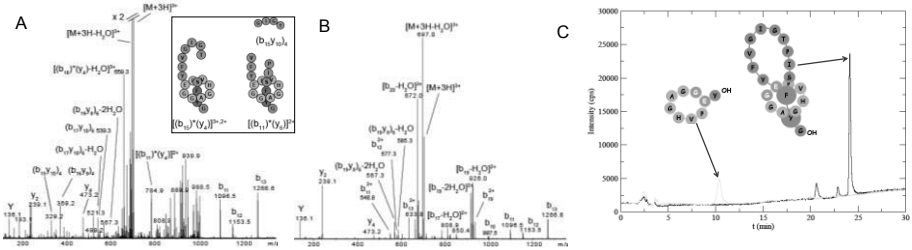

Fig. 2. Differentiation of lasso and non-lasso topoisomers. A: MS/MS spectrum of MccJ25, showing typical two-peptide product ions. B: MS/MS spectrum of MccJ25-lactam. C. LC-MS profiles of MccJ25 (black) and MccJ25-lactam (grey) carboxypeptidase Y digestion mixtures fragments after 3 hours.

Our results indicate that the size of the ring and the presence of the bulky residue Y_{20} below the ring and of the C-terminal residue G_{21} are particularly critical for maintaining the lasso structure. Taken together, our results identified key elements involved in the maturation of lasso peptides on one hand, and positions that display tolerance for the rational design of lasso peptide modifications on the other hand, showing that lasso peptides constitute attractive tools for the future development of bioactive peptides.

Acknowledgments
This work is supported by ANR BLAN-NT09-692063.We thank the mass spectrometry platform of the MNHN for access to the ESI-Qq-TOF spectrometer.

References

1. Rosengren, K.J., Clark, R.J., Daly, N.L., Göransson, U., Jones, A., Craik, D.J. *J. Am. Chem. Soc.* **125**, 12464-12474 (2003).
2. Wilson, K.A., Kalkum, M., Ottesen, J., Yuzenkova, J., Chait, B.T., Landick, R., Muir, T., Severinov, K., Darst, S.A. *J. Am. Chem. Soc*. **125**, 12475-12483 (2003).
3. Knappe, T.A., Linne, U., Zirah, S., Rebuffat, S., Xie, X., Marahiel, M.A. *J. Am. Chem. Soc.* **130**, 11446-11454 (2008).
4. Frechet, D., Guitton, J.D., Herman, F., Faucher, D., Helynck, G., Monegier du Sorbier, B., Ridoux, J.P., James-Surcouf, E., Vuilhorgne, M. *Biochemistry* **33**, 42-50 (1994).
5. Knappe, T.A., Linne, U., Xie, X., Marahiel, M.A. *FEBS Lett.* **584**, 785-789 (2010).
6. Rebuffat, S., Blond, A., Destoumieux-Garzón, D., Goulard, C. and Peduzzi, *J. Curr. Protein Pept. Sci.* **5**, 383-391 (2004).
7. Destoumieux-Garzón, D., Duquesne, S., Peduzzi, J., Goulard, C., Desmadril, M., Letellier, L., Rebuffat, S., Boulanger, P. *Biochem. J.* **389**, 869-876 (2005).
8. Mukhopadhyay, J., et al. *Mol. Cell* **14**, 739-751 (2004).
9. Duquesne, S., et al. *Chem. Biol*. **14**, 793-803 (2007).
10. Cheung, W.L., Pan, S.J., Link, A.J. *J. Am. Chem. Soc*. **132**, 2514-2515 (2010).

Proceedings of the 31st European Peptide Symposium
Michal Lebl, Morten Meldal, Knud J. Jensen, Thomas Hoeg-Jensen (Editors)
European Peptide Society, 2010

Cryptides: Receptors and Signaling Mechanisms for Novel Neutrophil-Activating Peptides Hidden in Mitochondrial Proteins

Hidehito Mukai[1], Tetsuo Seki[2], Yoshinori Hokari[2], Akiyoshi Fukamizu[2], and Yoshiaki Kiso[1]

[1]Department of Medicinal Chemistry, Center for Frontier Research in Medicinal Science, Kyoto Pharmaceutical University, Kyoto, 607-8412, Japan; [2]Graduate School of Life and Environmental Sciences, University of Tsukuba, Tsukuba, Ibaraki, 305-8577, Japan

Introduction

The physiological roles of fragmented peptides that are simultaneously produced during maturation and degradation of peptidergic hormones, neurotransmitters, and modulators have recently been of particular interest. Namely, biologically active peptides are matured by specific proteolytic cleavages of their precursor proteins which have no biological functions, and then degraded by various proteases. During these processes, many fragmented peptides are also produced from the same precursor proteins. Although the physiological importance of these fragmented peptides has not been well elucidated yet, they may have various unexpected biological functions.

Recently, we purified and identified novel neutrophil-activating peptides mitocryptide-1 (MCT-1) and mitocryptide-2 (MCT-2) (Figure 1) that were cleaved from mitochondrial cytochrome *c* oxidase subunit VIII and cytochrome *b*, respectively [1-4]. We also found many neutrophil-activating peptides derived from various mitochondrial proteins [3-5]. Moreover, peptides produced from not only mitochondrial but also other proteins such as hemoglobin were shown to regulate a variety of biological functions including cell proliferation [2,5-7]. These lines of evidence proposed that such fragmented peptides play critical roles including triggering inflammatory responses and healing damaged tissues. We therefore named these functional "cryptic" peptides that are hidden in protein structures as "**cryptides**" [3-5]. Here, we present the discovery of various cryptides that activate neutrophils. We also report our investigation on receptors and intracellular signaling mechanisms for these identified cryptides.

Results and Discussion

Neutrophil is one of the leukocytes involved in innate immunity by destructing and removing infectious organisms and toxic cell debris. Once tissue injury occurs due to infection or internal cell damage, neutrophils immediately migrate to the sites to scavenge toxic substances, i.e., they produce superoxide and digestive enzymes, and phagocytose toxic cell debris and infectious microorganisms. Although some chemokines such as interleukin 8 produced by surrounding tissues are known to induce migration and activation of neutrophils, these are synthesized, however, *after* the inflammatory stimulation. Moreover it has not been known for a long time what factors promote immediate neutrophil migration to the early stage inflammatory sites caused by tissue damage. Therefore, since 1993, we have attempted to purify neutrophil-activating factors from healthy organs. After intensive studies for more than 6 years, we finally purified and identified two novel mitochondrial protein-derived bioactive peptides MCT-1 and MCT-2 (Figure 1) that efficiently induce neutrophilic migration and activation at nanomolar concentrations [1-4].

Mitocryptide-1 (derived from C-terminal of cytochrome *c* oxidase subunit VIII):

Leu – Ser – Phe – Leu – Ile – Pro – Ala – Gly – Trp – Val – Leu – Ser –
His – Leu – Asp – His – Tyr – Lys – Arg – Ser – Ser – Ala – Ala

Mitocryptide-2 (derived from N-terminal of cytochrome *b*):

Porcine: formyl – Met – Thr – Asn – Ile – Arg – Lys – Ser – His – Pro –
Leu – Met – Lys – Ile – Ile – Asn

Fig. 1. Amino acid sequences of mitocryptides purified from porcine hearts.

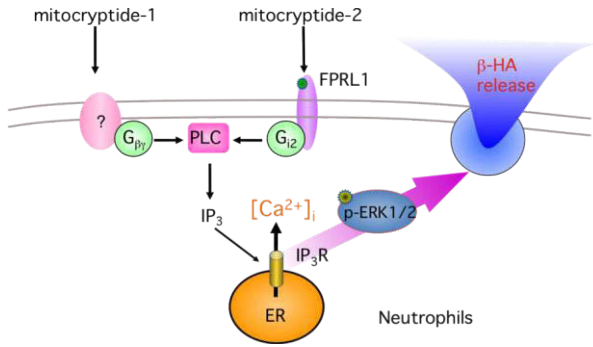

Fig. 2. Proposed signaling mechanisms of neutrophilic functions induced by mitocryptides.

To identify receptor molecules for the mitocryptides, we crosslinked these peptides with intact neutrophilic-differentiated HL-60 cells, and found that MCT-1 was bound to molecular complexes which consisted of at least five different proteins. Moreover, the receptor molecule for MCT-2 in neutrophilic-differentiated HL-60 cells was shown to be formyl-peptide receptor like-1 (FPRL1) because the attenuation of FPRL1 expression by its siRNA largely attenuated MCT-2-induced β-hexosaminidase (β-HA) release from the cells. We also investigated their intracellular signaling mechanisms, and demonstrated that the neutrophilic function of β-HA release was induced by G_i- or G_o-protein-dependent intracellular signaling events including $[Ca^{2+}]_i$ increase and ERK1/2 phosphorylation (Figure 2). We are now investigating each protein that forms receptor-protein complexes for MCT-1. We are also comprehensively identifying many cryptides by bioinformatic approach.

Acknowledgments
The present study was supported by research grants from the Ministry of Education, Culture, Sports, Science and Technology, Japan (No. 21603014; 40089107) and a supplementary research aid from Nippon Boehringer Ingelheim Co., Ltd.

References

1. Mukai, H., Hokari, Y., Seki, T., Nakano, H., Takao, T., Shimonishi, Y., Nishi, Y., Munekata, E. In Lebl, M., Houghten, R.A. (Eds.) *Peptides: The Wave of the Future (Proceedings of the Second International and the Seventeenth American Peptide Symposium)*, American Peptide Society, San Diego, 2001, pp 1014-1015.
2. Mukai, H., Matsuo, Y., Kamijo, R., Wakamatsu, K. In Chorev, M., Sawyer, T.K. (Eds.) *Peptide Revolution: Genomics, Proteomics & Therapeutics (Proceedings of the Eighteenth American Peptide Symposium)*, American Peptide Society, San Diego, 2004, pp 553-p555.
3. Mukai, H., Hokari, Y., Seki, T., Takao, T., Kubota, M., Matsuo, Y., Tsukagoshi, H., Kato, M., Kimura, H., Shimonishi, Y., Kiso, Y., Nishi, Y., Wakamatsu, K., Munekata, E. *J. Biol. Chem.* **283**, 30596-30605 (2008).
4. Mukai, H., Seki, T., Nakano, H., Hokari, Y., Takao, T., Kawanami, M., Kiso, Y., Shimonishi, Y., Nishi, Y., Munekata, E. *J. Immunol.* **182**, 5072-5080 (2009).
5. Ueki, N., Someya, K., Matsuo, Y., Wakamatsu, K., Mukai, H. *Biopolymers (Pept. Sci.)* **88**, 190-198 (2007).
6. Ivanov, V.T., Karelin, A.A., Philippova, M.M., Nazimov I.V., Pletnev, V.Z. *Biopolymers (Pept. Sci.)* **43**, 171-188 (1997).
7. Gomes, I., Grushko, J.S., Golebiewska, U., Hoogendoorn, S., Gupta, A., Heimann, A.S., Ferro, E.S., Scarlata, S., Fricker, L.D., Devi, L.A. *FASEB J.* **23**, 3020-3029 (2009).

Proceedings of the 31st European Peptide Symposium
Michal Lebl, Morten Meldal, Knud J. Jensen, Thomas Hoeg-Jensen (Editors)
European Peptide Society, 2010

mCD4-HS12: Closing and Locking Doors for HIV-1 Entry

F. Baleux[1*], P. Clayette[2], F. Arenzana-Seisdedos[3], D. Bonnaffe[4], and H. Lortat-Jacob[5]

[1]Institut Pasteur, URA CNRS 2128, Unité de Chimie des Biomolécules, Paris, 75015; [2]SPI-Bio, Fontenay aux Roses, 92260; [3]Institut Pasteur, INSERM U819, Unité de Pathogénie Virale, Paris, 75015; [4]UPS, UMR 8182, ICMO, Orsay, 9400; [5]IBS, UMR 5075, Grenoble, 38027, France

Introduction

HIV entry is mediated by sequential attachment of gp120 viral glycoprotein to CD4 cell receptor then GPCR cell coreceptor, mainly CCR5 or CXCR4. Following CD4 attachment, gp120 undergoes conformational changes that expose the CD4 induced epitope (CD4i), which in turn, binds to coreceptor. Besides binding to CD4 and GPCR, HIV also binds to glycosaminoglycans at the cell surface, mainly heparan sulfates (HS). Moreover, the CD4i epitope contains heparin binding sites (HBS) that can be targeted by short HS fragments [1,2].

Results and Discussion

An original and new concept has been developed to inhibit attachment and entry of HIV-1: mCD4-HS12 [3]. Composed of a miniCD4 peptide covalently linked to a synthetic sulfated dodecasaccharide, this bis-acting molecule binds to gp120, expose the CD4i epitope which in turn, is locked by the polyanionic part HS12 (Figure 1). Based on mCD4/gp120 structure [4], a new miniCD4 peptide was designed, bearing a single lysine residue suitably located to reach the CD4i heparin binding site (R419, K421, K432). After mCD4 Fmoc solid phase peptide synthesis, a maleimide moiety was introduced on the Lys5 side chain. The synthetic sulfated dodecasaccharide was derivatized by a thioacetyl group. Hydroxylamine treatment generates the free thiolated HS12 that reacts with maleimide activated mCD4, affording the mCD4-HS12 conjugate. This molecule fully inhibits the binding of sCD4-gp120 complex to 17b mAb (often used as coreceptor surrogate) when evaluated by Biacore experiments. More interestingly, mCD4-HS12 turned out to be a potent antiviral molecule when evaluated *in cellulo* (Table 1).

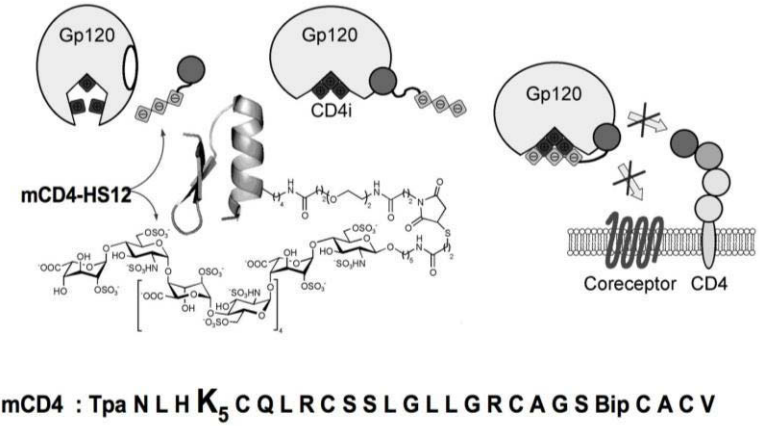

Fig. 1. mCD4-HS12 mode of action.

Table 1. mCD4-HS12 antiviral activity in PBMC

	Ba-L (R5)			89.6 (R5/X4)			LAI (X4)		
	ED_{50} (nM)	ED_{70} (nM)	ED_{90} (nM)	ED_{50} (nM)	ED_{70} (nM)	ED_{90} (nM)	ED_{50} (nM)	ED_{70} (nM)	ED_{90} (nM)
mCD4g	> 500	> 500	> 500	nd	nd	nd	244±18	377±169	560±222
HS_{12}	> 500	> 500	> 500	nd	nd	nd	> 500	> 500	> 500
mCD4-HS_{12}	2.4±1.9	4.9±0.3	**11.1**±7.6	4.5±0.7	5.2±0.6	**6.5**±0.8	1.4±0.9	2.05±0.55	**3.0**±0.65
AZT	6.6±0.8	14±8.1	45±44	2.1±0.15	4.0±1.0	12.3±8.2	1.8±0.85	2.75±1.3	5.6±2.5

This molecule is conceptually distinct from any other existing ones, displays low nM affinity for gp120, and inhibits the binding of HIV-1 to cell surface CD4, CCR5, CXCR4 and HS, the major ligands involved in virus attachment and entry. This innovative compound, which displays strong anti viral activity (IC_{50} 2 to 5 nM) is the first molecule targeting the coreceptor binding site of gp120. A remarkable characteristic of mCD4-HS_{12} is its ability to neutralize HIV-1 in a coreceptor independent manner (inhibition of CCR5-, CXCR4- and dual- tropic HIV-1 stains). This is a significant advantage since the efficacy of CCR5-specific antagonists could be jeopardized by the emergence of more aggressive viral strains that utilize CXCR4 and for which no inhibitors are yet available. This molecule, acting very early in the viral life cycle, has potential for both prevention and therapy following topical and/or parenteral application.

Ongoing work is on simplifying the HS part of the molecule. Indeed, a conjugate containing an acidic peptide, mCD4-GPR1, still displays nanomolar antiviral activity (200nM). HS12 replacement by heparin mimic peptides is under investigation, as well as more general replacement by polyanionic compounds.

Acknowledgments
This work was supported by ANRS agency.

References

1. Vives, R.R., Imberty, A., Sattentau, Q.J., Lortat-Jacob, H. *J. Biol. Chem.* **280**, 21353-21357 (2005).
2. Crublet, E., Andrieu, J.P., Vives, R.R., Lortat-Jacob, H. *J. Biol. Chem.* **283**, 15193-15200 (2008).
3. Baleux, F., Loureiro-Morais, L., Hersant, Y., Clayette, P., Arenzana-Seisdedos, F., Bonnaffe, D., Lortat-Jacob, H. *Nat. Chem. Biol.* **5**, 743-748 (2009).
4. Huang, C.C., Stricher, F., Martin, L., Decker, J.M., Majeed, S., Barthe, P., Hendrickson, W.A., Robinson, J., Roumestand, C., Sodroski, J., Wyatt, R., Shaw, G.M., Vita, C., Kwong, P.D. *Structure* **13**, 755-768 (2005).

Proceedings of the 31st European Peptide Symposium
Michal Lebl, Morten Meldal, Knud J. Jensen, Thomas Hoeg-Jensen (Editors)
European Peptide Society, 2010

Use of Ester-Containing Peptides Toward Understanding the Functions of Amyloid Beta Peptide and Human Insulin

Youhei Sohma[1,2], Stephen B. H. Kent[2], and Yoshiaki Kiso[1]
[1]Department of Medicinal Chemistry, Center for Frontier Research in Medicinal Science, Kyoto Pharmaceutical University, Kyoto, 607-8412, Japan; [2]Department of Biochemistry and Molecular Biology, Institute for Biophysical Dynamics, The University of Chicago, IL, 60637, U.S.A.

Introduction

Chemical synthesis of peptides/proteins provides an efficient and versatile tool for elucidating in unique ways the molecular basis of function. This paper represents new insights into the utility of ester-containing peptides toward understanding the functions of bioactive peptides/proteins.

Results and Discussion

Ester Insulin

As a minimal surrogate for proinsulin we designed and synthesized an 'ester insulin' precursor in which the A- and B-chains of insulin are covalently connected via an ester bond between the beta-hydroxyl group of ThrB30 and the gamma-carboxyl group of GluA4 [1]. The ester linkage made the precursor molecule as favorable for folding/disulfide formation as does the 35 amino acid residue C-peptide in proinsulin. Folded ester insulin was readily saponified to give insulin with full biological activity.

With suitable optimization of its preparation, ester insulin may prove to be the key to a simple and effective route to the total chemical synthesis of insulin. The ester insulin precursor polypeptide could be made by any of several synthetic routes, including the hybrid solution-solid phase methodology used for the cost effective large-scale manufacture of long peptides. We believe that ester insulin will be a useful intermediate for the efficient generation of insulin analogues in the research laboratory and for cost-effective chemical manufacture of human insulins.

O-Acyl Isopeptide of Amyloid Beta Peptides

Replacing the native amide (*N*-acyl moiety) by an ester (*O*-acyl moiety) at beta-hydroxyl group of Ser or Thr residue (designated "*O*-acyl isopeptide") changes the physical property of the native peptide [2]. Additionally, due to the presence of an additional amino group, the *O*-acyl isopeptide is generally hydrophilic. The target peptide is then generated from the corresponding *O*-acyl isopeptide via an *O*-to-*N* intramolecular acyl migration.

Based on the *O*-acyl isopeptide method, we are establishing an *in situ* system in which monomer amyloid beta peptide (Abeta) 1-42 is quickly produced from the water-soluble *O*-acyl isopeptide possessing an ester bond at the Gly^{25}-Ser^{26} sequence [3]. The generated monomer Abeta1-42 showed random coil-to-β-sheet conformational change, oligomerization, amyloid fibril formation and cytotoxicity. The intense and uncontrollable self-assembling nature of Abeta causes difficulties in preparing monomer Abeta, resulting in irreproducible or discrepant study outcomes. Thus, the *O*-acyl isopeptide system has been used in Abeta-related Alzheimer's disease research to more clearly explain the functions of Abeta. Further studies with Abeta mutants enabled us to identify new functions of amyloid beta peptides.

Acknowledgments

We are grateful for Drs. Atsuhiko Taniguchi and Hidehito Mukai (Kyoto Pharmaceutical University) for their collaborations throughout the study of *O*-acyl isopeptide.

References

1. Sohma, Y., Hua, Q-X., Whittaker, J., Weiss, M.A., Kent, S.B.H. *Angew. Chem. Int. Ed.* **49**, 5489-5493 (2010).
2. Sohma, Y., Sasaki, M., Hayashi, Y., Kimura, T., Kiso, Y. *Chem. Commun.* 124-125 (2004).
3. Taniguchi, A., Sohma, Y., Hirayama, Y., Mukai, H., Kimura, T., Hayashi, Y., Matsuzaki, K., Kiso Y. *ChemBioChem* **10**, 710-715 (2009).

Proceedings of the 31st European Peptide Symposium
Michal Lebl, Morten Meldal, Knud J. Jensen, Thomas Hoeg-Jensen (Editors)
European Peptide Society, 2010

The Dynamic Ras Cycle

Christian Hedberg[1], Herbert Waldmann[1], and Frank Dekker[1,2]
[1]Max-Planck Institute of Molecular Physiology, Department of Chemical Biology, Otto-Hahn-Strasse 11, D-44227, Dortmund, Germany; [2]Current address: University of Groningen, Institute of Pharmacy, Department of Therapeutic Gene Modulation, Antonius Deusinglaan 1, NL-9713 AV, Groningen, Netherlands

Introduction

The Ras proteins are small membrane-associated signal transducing GTPases that play an important role in controlling numerous cellular processes, such as growth, division and differentiation. Mutations in Ras-proteins are present in approximately 30% of all human cancers. Single-residue mutations in the GTPase switch region of H- and N-Ras result in constant oncogenic activation of the MAP-kinase signaling pathway, which frequently occurs in melanoma, leukemia and small intestine cancers, thus resulting in a negative survival prognosis for affected patients [1].

Results and Discussion

To display proper biological function, N-and H-Ras proteins need to be S-farnesylated and S-palmitoylated at the C-terminus to attach at the plasma membrane. A single lipid modification leads to membrane affinity; addition of a second lipid results in membrane anchoring. S-farnesylation is a static modification that provides the initial affinity, whereas S-palmitoylation is reversible and results in stable anchoring. The state of modification controls the spatiotemporal localization of the Ras-protein through cycles of palmitoylation-depalmitoylation, thus regulating the signal transduction event by cycling the Ras-protein between the Golgi and the plasma membrane. The dynamic nature of the cycle through S-palmitoylation is driven by palmitoyl transferases (PAT-activity) at the Golgi and thioesterase enzymes which are distributed in the cell (APT-activity). The H-and N-Ras cycle proceeds in four distinct steps (Figure 1). Initially, farnesylated Ras partitions to membranes (a). Subsequent kinetic trapping at the Golgi by S-palmitoylation leads to stable anchoring (b). In a third step, the Ras-protein is transported to the plasma membrane by the secretory pathway (c), where it exhibits its signaling activity. The Ras-protein is subsequently released from the PM by depalmitoylation (d), allowing again for partioning into the endo-membranes, which closes the cycle [2]. Considering the dynamics of the cycle, it indicates that inhibitors of palmitoylation, as well as depalmitoylation, would alter the steady state localization of Ras and thus affect Ras signalling.

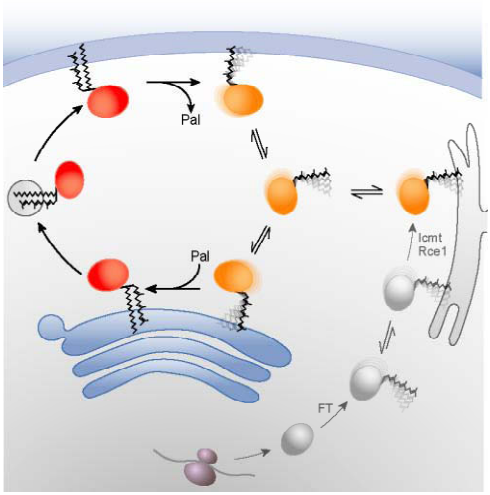

Fig. 1. Schematic illustration of the Ras cycle dynamics. Pal = Palmitoyl. We conclude that the de-/repalmitoylation cycle allows continuous trafficking between the PM and Golgi, which determines the spatio-temporal signalling profile of H- and N-Ras (amplitude, duration, coupling to different signalling pathways/effectors).

We recently showed that acyl protein thioesterase 1 (APT1, aka Lypla1) [3] is a major contributor to intracellular thioesterase activity essential for depalmitoylation of H- and N-Ras proteins *in vivo* [4]. We employed fluorescently-labeled fully lipidated semi-synthetic Ras-proteins (Figure 2a) as tools to probe the dynamics of the acylation cycle. In

parallel, we developed the cell-permeable small molecule APT1-inhibitor denoted Palmostatin B (Figure 2b) through the knowledge-driven PSSC approach [5]. By combining the semi-synthetic protein tools with the conditional chemical knockdown of APT1, we could observe the inhibition of H- and N-Ras depalmitoylation events by live confocal microscopy. Short-term Palmostatin B knockdown of APT1 prevents Ras activation on the Golgi, which enables studies on compartment specific signalling. Alternatively, long term Palmostatin B treatment disturbs H- and N-Ras precise steady state localization, causing unspecific entropy driven redistribution to endomembranes, thus down regulating global Ras signalling. This is reflected by the phenotypic back transformation of oncogenic Ras transformed MDCKf3 cells, as well as reduction in Erk phosphorylation. We verified the long-term effect by siRNA mediated inhibition of APT1 expression in MDCKf3 cells and observed similar Ras-delocalization and phenotypic reversal. In summary, we have demonstrated that Palmostatin B is an excellent tool to dissect Ras-protein dynamics in a time-dependent manner *in vivo*.

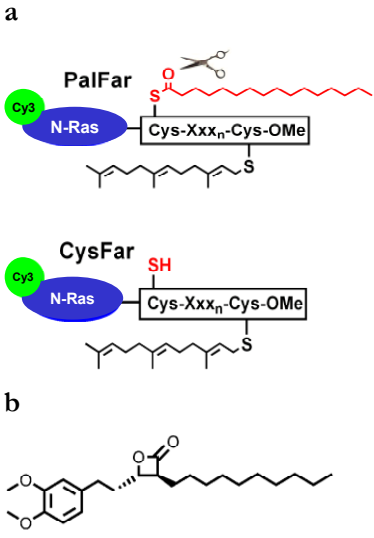

Fig. 2. (a) Semi-synthetic lipidated N-Ras protein probes. The scissors indicate site of APT1 depalmitoylation. (b) Palmostatin B, a potent small molecule inhibitor of APT1.

The development of APT1 inhibitors has gained little attention in pharmaceutical industry, as it has intuitively been expected that inhibition of depalmitoylation would increase the portion of Ras in active palmitoylated form, which would facilitate oncogenic signalling. However, the discovery that dynamic palmitoylation / depalmitoylation events are required to maintain proper Ras localization indicates that inhibition of Ras depalmitoylation will attenuate Ras-mediated signalling, thus making the depalmitoylation event more attractive to target, compared to the palmitoylation step. In a recent study, we have found the palmitoylation-reaction of proteins at the Golgi to be a rather unspecific generic sorting machinery for palmitoylated proteins, thus being unwanted to target by small-molecule inhibitors [6]. Furthermore, it opens a new and unexpected entry towards further development of conceptually new approaches in oncology that target depalmitoylation specifically. However, the selectivity of both Palmostatin B and the enzyme APT1 remain to be investigated further. It can be expected that many biological functions are regulated by reversible palmitoylation events controlling protein localization and that additional thioesterases will be identified in the near future. Such a development will further increase the importance of thioesterase inhibitors such as palmostatin B, as well as of semi-synthetic lipidated proteins to probe biological function *in vivo*.

Acknowledgments

We thank all our collaboration partners, listed as co-authors in references 1-2 and 4-6, as well as the funding agencies supporting the Ras-project over the years, in particular DFG through SFB 642, Alexander von Humboldt Foundation and the Max-Planck Gesellschaft.

References

1. Waldmann, H., Wittinghofer, A. *Angew. Chem. Int. Ed.* **39,** 4192-4214 (2000).
2. Rocks, O., et al. *Science* **307**, 1746 (2005).
3. a). Sugimoto, H., Hayashi, H., Yamashita, S. *J. Biol. Chem.* **271**, 7705 (1996); b). Duncan, J.A., Gilman, A.G. *J. Biol. Chem.* **273**, 15830 (1998).
4. Dekker, F.J., et al. *Nat. Chem. Biol.* **6**, 449 (2010).
5. Dekker, F.J., Koch, M.A., Waldmann, H. *Curr. Op. Chem. Biol.* **9**, 232 (2005).
6. Rocks, O., et al. *Cell* **141**, 458. (2010).

Proceedings of the 31st European Peptide Symposium
Michal Lebl, Morten Meldal, Knud J. Jensen, Thomas Hoeg-Jensen (Editors)
European Peptide Society, 2010

Synthesis of Biaryl Cyclic Peptides Through Solid-Phase Borylation and Cyclization by a Suzuki-Miyaura Cross-Coupling

Ana Afonso, Marta Planas, and Lidia Feliu
LIPPSO, Department of Chemistry, University of Girona, Girona, 17071, Spain

Introduction

Cyclic peptides containing a biaryl bridge are widespread in nature. They possess diverse structural features and range from monocyclic to bicyclic to the structurally complex polycyclic glycopeptide antibiotics. These macrocycles have attracted considerable interest due to the significant biological activities that most of them exhibit, including proteasome inhibition, and antimicrobial or cytotoxic activities [1].

Within our current research on the synthesis of biaryl peptides, we focused our attention on the solid-phase preparation of peptides containing a biaryl bond between the side chains of two aromatic amino acids. Recently, we have reported the synthesis of biaryl peptides involving the borylation on solid support of a phenylalanine followed by the Suzuki-Miyaura cross-coupling with a variety of aryl halides [2,3]. Here we report the application of this methodology to the synthesis of biaryl cyclic peptides.

Results and Discussion

Borylation of Boc-Phe(4-I)-Leu-Leu-Rink-MBHA (**1**) [2], Boc-Tyr(3-I,OMe)-Leu-Leu-Rink-MBHA (**2a**) and Boc-Tyr(3-I,OSEM)-Leu-Leu-Rink-MBHA (**2b**) was performed using Miyaura conditions (Schemes 1 and 2). After each experiment, the resin was cleaved with TFA/H_2O/TIS and the crude reaction mixture was analyzed by HPLC and mass spectrometry. The corresponding boronates were obtained in high purities (70-99%).

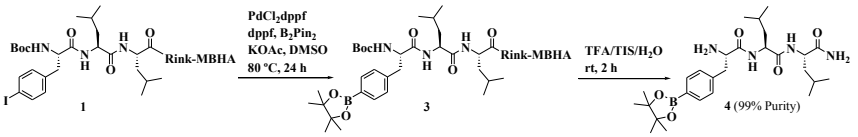

*Scheme 1. Miyaura borylation of Boc-Phe(4-I)-Leu-Leu-Rink-MBHA (**1**).*

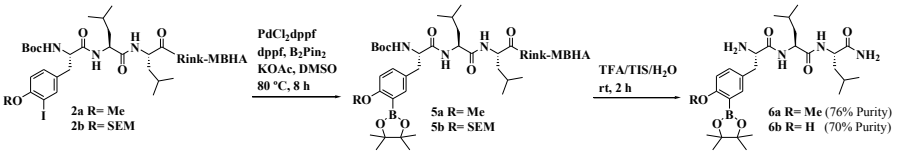

*Scheme 2. Miyaura borylation of Boc-Tyr(3-I,OMe)-Leu-Leu-Rink-MBHA (**2a**) and Boc-Tyr(3-I,OSEM)-Leu-Leu-Rink-MBHA (**2b**).*

Boronopeptidyl resins **3** and **5b** were arylated with a conveniently protected 4-iodophenylalanine, 3-iodotyrosine or 4-bromohistidine via a Suzuki-Miyaura cross-coupling (Schemes 3 and 4**).** Reactions were carried out under microwave irradiation. Except for **9c**, the expected biaryl tetrapeptides were obtained in moderate to good purities after cleavage (Table 1). Compound **8,** which is a common side-product of cross-coupling reactions, was also detected.

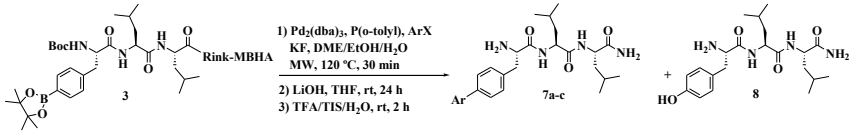

*Scheme 3. Suzuki-Miyaura arylation of Boc-Phe(4-BPin)-Leu-Leu-Rink-MBHA (**3**).*

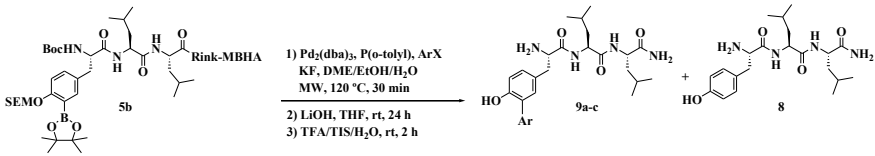

*Scheme 4. Suzuki-Miyaura arylation of Boc-Tyr(3-BPin,OSEM)-Leu-Leu-Rink-MBHA (**5b**).*

*Table 1. Arylation of resins **3** and **5b** under microwave irradiation*

ArX	*Peptide*	*Peptide purity (%)*[a]	***8** (%)*[a]
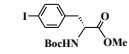	7a	91	8
	9a	55	16
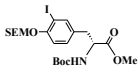	7b	57	12
	9b	45	18
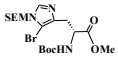	7c	40	8
	9c	18	60

[a]*Percentage determined by HPLC at 220 nm from the crude reaction mixture*

Linear precursors containing the corresponding amino acid boronate and the haloaryl residue were prepared using the Miyaura conditions previously optimized. Then, cyclization via a Suzuki-Miyaura cross-coupling was performed under microwave irradiation. After cleavage, biaryl peptides **10-15** were obtained in moderate to good purities.

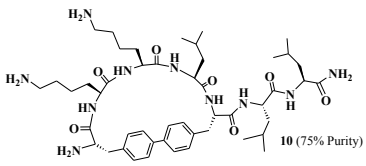

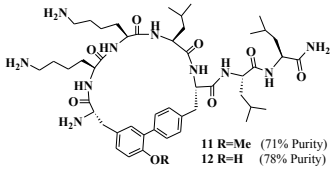

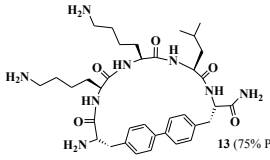

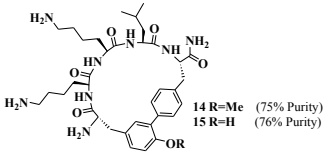

The above methodology was extended to the synthesis of biaryl cyclic peptides of different sizes. Biaryl peptides were obtained in purities ranging from 35 to 67%.

Acknowledgments
Ana Afonso is recipient of a predoctoral fellowship from the MICINN of Spain. This work was supported by grants AGL2006-13564-C02-02/AGR and AGL2009-13255-C02-02/AGR (MICINN of Spain).

References

1. Feliu, L., Planas, M. *Int. J. Pept. Res. Ther.* **11**, 53-97 (2005).
2. Afonso, A., Rosés, C., Planas, M., Feliu, L. *Eur. J. Org. Chem.* 1461-1468 (2010).
3. Miyaura, N., Suzuki, A. *Chem. Rev.* **95**, 2457-2483 (1995).

Proceedings of the 31st European Peptide Symposium
Michal Lebl, Morten Meldal, Knud J. Jensen, Thomas Hoeg-Jensen (Editors)
European Peptide Society, 2010

Synthesis and Characterization of FlAib, a Completely Rigidified Benzophenone Containing α-Amino Acid

Karen Wright[1], Antonio Blanco Alvarez[1], Marco Crisma[2], Alessandro Moretto[2], Fernando Formaggio[2], and Claudio Toniolo[2]
[1]ILV, UMR CNRS 8180, University of Versailles, Versailles, 78035, France; [2]ICB, Padova Unit, CNR, Department of Chemistry, University of Padova, Padova, 35131, Italy

Introduction

Photoreactive amino acids with benzophenone side chains, such as the widely used Bpa [3-(4-benzoylphenyl)alanine] (Figure 1) [1], have been used as photoprobes for the covalent modification of enzymes and receptors in protein-mapping studies. However, results of photocross-linking experiments need to take into account the high flexibility of the Bpa side chain [2]. Since incorporation of a cyclic structure into the amino acid side chain reduces flexibility, we have designed and synthesized an extremely highly constrained fluorenone-containing amino acid, FlAib (2-amino-1,2,3,6-tetrahydro-6-oxocyclopenta[*c*]fluorene-2-carboxylic acid) (Figure 1), belonging to the sub-class of the $C_i^{\alpha} \leftrightarrow C_i^{\alpha}$ cyclized, C^{α}-tetrasubstituted α-amino acids, which are known to induce β-turn and helix formation in peptides [3]. A more flexible residue of this family, BpAib (2-amino-5-benzoyl-2,3-dihydro-1*H*-indene-2-carboxylic acid) (Figure 1), was already prepared and studied by our groups [4].

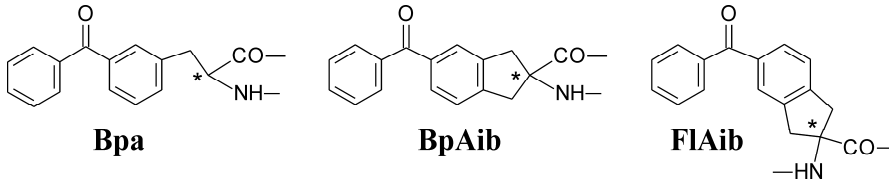

Fig. 1. Chemical structures of Bpa, BpAib, and FlAib.

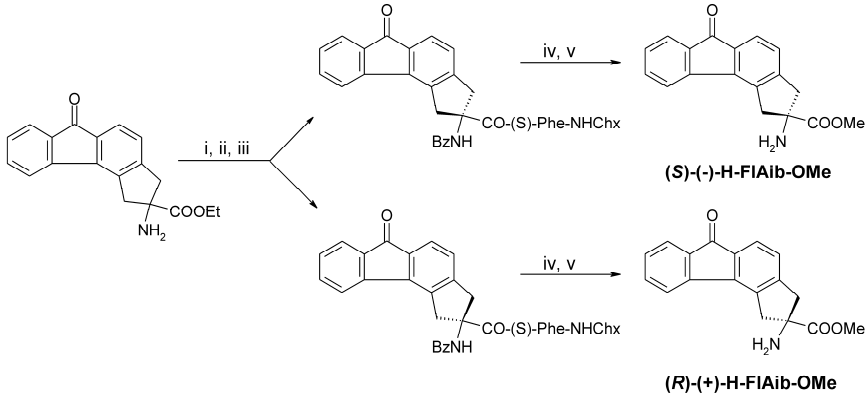

Fig. 2. Scheme followed for the resolution of the diastereomeric mixture of FlAib. (i) Bz_2O, MeCN; rt. (ii) NaOH, THF/MeOH/H_2O; 60°C. (iii) H-(S)-Phe-NHChex, HATU, DIEA; THF; rt. (iv) 10 M HCl, dioxane; 100°C. (v) $SOCl_2$; MeOH; rt.

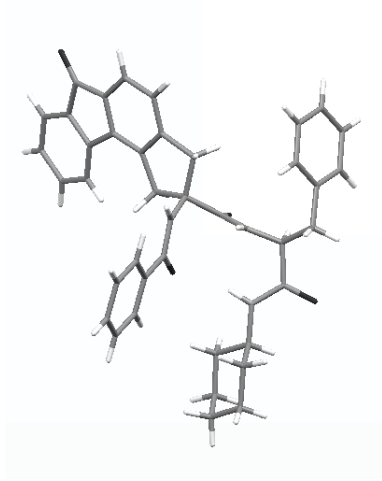

Fig. 3. X-Ray diffraction structure of Bz-(R)-FlAib-(S)-Phe-NHChx.

Results and Discussion

The 3,4-dimethyl-fluorenone structure required for the synthesis of FlAib was obtained by diazotization of the corresponding dimethyl-aminobenzophenone (prepared from the known 2-amino-3,4-dimethylbenzoic acid). Bromination of the side chains of this dimethyl-fluorenone gave 3,4-(*bis*)bromomethyl-fluorenone, which was used in the *bis*(alkylation) of ethyl-isocyanoacetate under phase-transfer conditions to give the cyclic, racemic amino acid H-FlAib-OEt (OEt, ethoxy) after acid hydrolysis. N^{α}-Benzoyl (Bz) protection, saponification of the ester function, and coupling with H-(*S*)-Phe-NHChx (Chx, cyclohexyl) gave two dipeptide diastereomers (Figure 2) which could be resolved by crystallization and chromatography.

A crystal of one of these diastereomers, Bz-(*R*)-FlAib-(*S*)-Phe-NHChx, subjected to X-ray diffraction analysis, allowed the assignment of the absolute configuration of the FlAib residue (Figure 3). The (*R*)-FlAib residue is able to induce a (type-I) β-turn in the molecule, thus behaving as an (*S*)-protein amino acid.

References

1. Kauer, J.C., Erickson-Viitanen, S., Wolfe, H.R., Jr., DeGrado, W.F. *J. Biol. Chem.* **261**, 10695-10700 (1986).
2. Saviano, M., Improta, R., Benedetti, E., Carrozzini, B., Cascarano, G.L., Didierjean, C., Toniolo, C., Crisma, M. *ChemBioChem* **5**, 541-544 (2004).
3. Toniolo, C., Crisma, M., Formaggio, F., Peggion, C. *Biopolymers (Pept. Sci.)* **60**, 396-419 (2001).
4. Wright, K., Moretto, A., Crisma, M., Wakselman, M., Mazaleyrat, J.-P., Formaggio, F., Toniolo, C. *Org. Biomol. Chem.* **8**, 3281-3286 (2010).

Proceedings of the 31st European Peptide Symposium
Michal Lebl, Morten Meldal, Knud J. Jensen, Thomas Hoeg-Jensen (Editors)
European Peptide Society, 2010

Straightforward Syntheses of Deuterated Precursors to be Used as Powerful Tracers under Fermentative Conditions

Florine Cavelier[1], Aurélie Roland[2], Alain Razungles[2], and Rémi Schneider[3]

[1]IBMM UMR CNRS 4247, Montpellier, 34095, France; [2]UMR 1083 Sciences Pour l'œnologie INRA-SupAgro-Université Montpellier I, Montpellier, 34060, France; [3]Institut Français de la Vigne et du Vin, Montpellier, 34060, France

Introduction

The *S*-3-(hexan-1-ol)-glutathione (G3MH, **1**) and *S*-3-(4-methylpentan-2-one)-glutathione (G4MMP, **2**), initially identified in Sauvignon Blanc grapes [1,2], were presumed to be precursors of powerful odorant thiols found in wines: the 3-mercaptohexan-1-ol (3MH) [3] and the 4-mercapto-4-methylpentan-2-one (4MMP) [4] respectively. These thiols, also called varietal thiols, were reminiscent of grape fruit and blackcurrant bud and contribute positively to the fruity notes of young wines. The biogenesis of such thiols in wine is very complicated and not entirely understood. To bring new insights in the 3MH and 4MMP biogenesis, labeled analogues of G3MH and G4MMP were synthesized and used as tracers in fermentation experiments to investigate potential relationship with these thiols under enological conditions.

Results and Discussion

This study intended to provide few amounts of deuterated analogues of glutathione conjugates occurring in grapes. First synthesis of **1** in deuterated form required lengthy (7 steps) and tedious efforts in order to obtain the desired product with a very moderate yield [5]. Other work reported the direct synthesis of **1** and **2** using a conjugate addition of glutathione on *(E)*-2-hexenal with pyridine giving pure products in satisfactory yields [6]. Unfortunately, we did not succeed in reproducing this reported synthesis. Therefore, we developed a new strategy for the **1**-d_2 synthesis in racemic form as well as for the **2**-d_{10}.

Conjugate addition of glutathione on the *(E)*-2-hexenal led to **1** after a reduction step with sodium borohydride (Figure 1). The conjugate addition was the only limiting step (incomplete, generation of by-products), whereas the reduction facilitated the production of the expected compound in good yield and purity as already reported [5,6]. To improve the global reaction yield and the purity of the desired product, investigations were necessary in order to optimize the conjugate addition [7]. The optimal conditions were thus defined: room temperature, slow addition of *(E)*-2-hexenal in 3 portions, pH=8 (phosphate buffer), stirring for 10 h. Then, the same conditions, including an additional reduction step with sodium borohydride, were applied to the formation of **1**-d_2 with the *(E)*-2,3-[$^2H_2$]-2-hexenal as starting material [6].

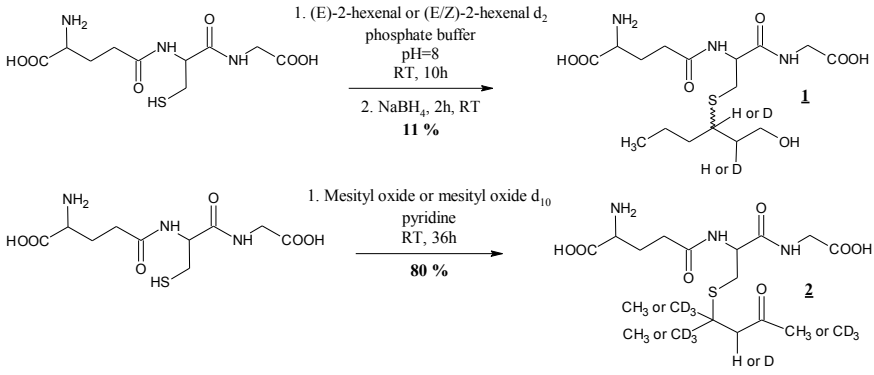

*Fig. 1. Synthesis of natural and labeled G3MH (**1**) and G4MMP(**2**).*

Table 1. Molar conversion yields of glutathionylated precursors into corresponding thiols under enological conditions

Precursor	*Spiking (µg/L)*	*Molar conversion yields (%)*	
		Synthetic medium	*Sauvignon Blanc*
G3MH	12		4.4
	15	0.6	
	75	0.6	
	150	0.6	
G4MMP	1.8	nc*	0.3

**not calculated*

The direct synthesis of **2**-d_{10}, adapted from a published protocol [6], was inexpensive and effective (yield close to 80%). This established protocol was optimized and it can be easily carried out by non-specialists.

To investigate potential relationship between glutathione conjugates and varietal thiols, a synthetic and a Sauvignon Blanc must were spiked with **1**-d_2 at several concentrations and with **2**-d_{10} at 1.8 µg/L (Table 1). Fermentation processes were conducted at laboratory scale with VIN13 (10g/hL) as yeast strain at 20°C. At the end of fermentation, synthetic and Sauvignon Blanc wines were extracted and analyzed according to well optimized and published methods [8-9] by GC-MS and GC-MS/MS.

In the first experiment, the formal identification of 3MH-d_2 in both synthetic and Sauvignon Blanc wines (same retention time and similar spectral data such as the reference compound) proved the direct relationship between **1** and 3MH under enological conditions. The molar conversion yield of **1**-d_2 into 3MH-d_2 was lower under synthetic than natural conditions as already reported for the cysteinylated precursor of 3MH [10] (Table 1). The conversion of **1**-d_2 into 3MH d_2 did not depend on the initial concentration of precursor in must.

In the second experiment, the identification of 4MMP-d_{10} in synthetic and natural wines demonstrated the relationship between **2** and 4MMP under enological conditions. Standard additions of 4MMP d_{10} were performed in Sauvignon Blanc wine in order to estimate the molar conversion yield: 0.3% (Table 1). Both *S*-glutathione conjugates **1** and **2** represent the second major precursors of 3MH and 4MMP respectively and opened avenue for additional studies on varietal thiols biogenesis in wine.

Acknowledgments

We thank Interloire, Institut Français de la Vigne et du Vin and Sicavac for technical and financial support. Supported by CIFRE fellowship (Interloire, Interprofession des vins du Val de Loire).

References

1. Fedrizzi, B., et al. *J. Agric. Food Chem.* **57**, 991-995 (2009).
2. Peyrot des Gachons, C., Tominaga, T., Dubourdieu, D. *J. Agric. Food Chem.* **50**, 4076-4079 (2002).
3. Tominaga, T., Furrer, A., Henry, R., Dubourdieu, D. *Flavor Fragrance J.* **13**, 159-162 (1998).
4. Darriet, et al. *Flavor Fragrance J.* **10**, 385-392 (1995).
5. Roland, et al. *Food Chem.* **121**, 847-855 (2010).
6. Grant-Preece, et al. *J. Agric. Food Chem.* **58**, 1383-1389 (2010).
7. Roland, et al. *J. Agric. Food Chem.* accepted for publication (2010).
8. Schneider, et al. *J. Agric. Food Chem.* **51**, 3243-3248 (2003).
9. Rodriguez-Bencomo, J.J., Schneider, R., Lepoutre, J.P., Rigou, P. *J. Chromatogr. A.* **1216**, 5640-5646 (2009).
10. Subileau, M., Schneider, R., Salmon, J.M., Degryse, E. *J. Agric. Food Chem.* **56**, 9230-9235 (2008).

Proceedings of the 31st European Peptide Symposium
Michal Lebl, Morten Meldal, Knud J. Jensen, Thomas Hoeg-Jensen (Editors)
European Peptide Society, 2010

Tert-$BuNH_2$ as an Efficient Reagent for the Deprotection of Fmoc Protected Amino Acids

Armin Arabanian[1,2] and Saeed Balalaie[1]

[1]Peptide Chemistry Research Center, K.N. Toosi University of Technology, Tehran, 15875-4416, Iran; [2]Tofigh Daru Res. & Eng. Co., 61st St. km 18 Karaj Highway, Tehran, 37515-375, Iran

Introduction

The protection and deprotection of the amine group is essential for the condensation of α-amino acids via amide bond in a defined sequential order. All amino protecting groups are fundamentally suitable for masking the α-amino group of amino acids, but it is very important that the repetitive steps proceed rapidly in high yields and with minimal side reactions to prevent formation of by-products. N^{α} Deprotection is one of the major steps in SPPS with consideration of orthogonality. The Fmoc/*t*Bu method was introduced by Atherton and Meienhofer and is based on an orthogonal protecting group strategy, using the base labile Fmoc group for protection of the α-amino group and acid labile side-chain protecting groups and resin-linkage agents [1]. In Fmoc/*t*Bu SPPS, a 20% V/V solution of piperidine in DMF is used as an efficient condition for Fmoc-deprotection. The details about the mechanism were clarified. It was shown that, in some cases the standard treatment with 20% piperidine in DMF may not always be effective and need a stronger base such as DBU. Piperidine is not only an expensive reagent, but also a controlled substance according to the *92/109/EC* recommendation, and also there are some reports about the effect of piperidine on mutation and DNA destruction. According to these drawbacks, Leondiadis reported using of 5% piperidine for Fmoc-deprotection [2].

Results and Discussion

Finding a suitable reagent for Fmoc-deprotection is an interesting subject in peptide synthesis chemistry. In this work, we report experimentally a simple procedure for the N^{α} deprotection using *t*-$BuNH_2$ to remove Fmoc in SPPS. Recently, *t*-$BuNH_2$ was used for the selective cleavage of carbamates [3]. To examine the possibility of using *t*-$BuNH_2$ solution, different percentages of it were used. We applied 25, 10 and 5% *t*-$BuNH_2$ solution for the Fmoc-deprotection from different Fmoc-protected amino acids. Meanwhile, we checked the rate of Fmoc-deprotection and the sample was collected after 2, 5, 10 and 20 min. The protected amino acids on 2-chlorotrityl chloride resin were selected as starting materials and removal of Fmoc group was controlled by using UV absorption at 301 nm. The details about Fmoc-deprotection from two amino acids (Leu and Met) which were supported on resin were summarized in Tables 1 and 2.

According to these data, *t*-$BuNH_2$ in DMF provided the same result like piperidine for the Fmoc-deprotection. For example, we tested the use of 5% *t*-$BuNH_2$ solution and after 20 min, more than 90% of the Fmoc group was removed. The Fmoc-deprotection using *t*-$BuNH_2$ is slower than piperidine, but when 25% *t*-$BuNH_2$ was used, the same results as

Table 1. Fmoc-deprotection using t-$BuNH_2$ for Fmoc-Leu-Resin

Base		*Fmoc-deprotection (%)*			
		T=2 min	*T=5 min*	*T=10 min*	*T=20 min*
Piperidine/DMF	5%	53.8	83.6	92.8	97.5
	10%	77.6	86.2	89.7	98.2
	25%	81.6	95.1	98.6	100.0
t-Butylamine/DMF	5%	30.0	51.4	65.2	92.8
	10%	31.3	64.4	76.0	95.2
	25%	60.8	85.1	90.4	100.0

with piperidine were obtained. For checking the *t*-$BuNH_2$ scope, limitation and diversity, we checked it for the synthesis of Leu- and Met-enkephalin (Figure 1). The results were comparable to piperidine.

In conclusion, *t*-$BuNH_2$ solution in DMF could be used instead of piperidine in DMF in SPPS for Fmoc group removal from the resin-bound peptides. This can provide convenience and lower cost peptide synthesis because piperidine is not only an expensive reagent but also is a controlled substance. Meanwhile the diversity of this methodology was checked using different protected amino acids.

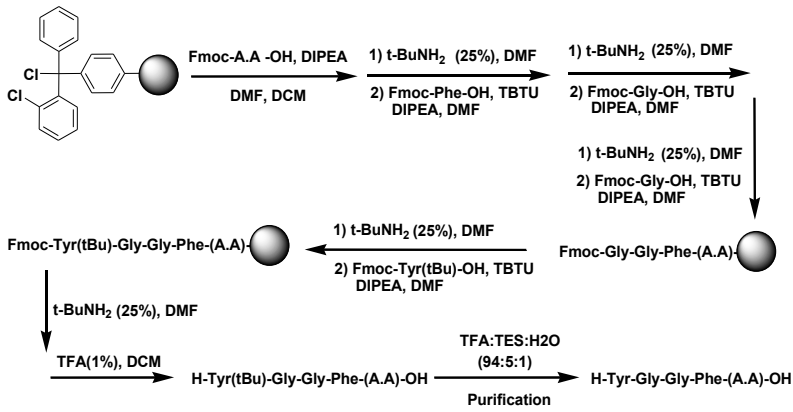

Fig. 1. Solid phase synthesis of enkephalins by using of t-$BuNH_2$ for Fmoc-deprotection.

Table 2. Fmoc-deprotection using t-$BuNH_2$ for Fmoc-Met-Resin

Base		*Fmoc-deprotection (%)*			
		T=2 min	*T=5 min*	*T=10 min*	*T=20 min*
Piperidine/DMF	5%	51.2	79.5	89.8	96.1
	10%	76.2	82.4	91.1	97.6
	25%	81.4	94.2	97.6	100.0
t-Butylamine/DMF	5%	29.1	48.5	66.2	90.0
	10%	32.3	62.5	78.3	96.1
	25%	60.7	81.6	88.4	100.0

Acknowledgments
We would like to thank Tofigh Daru Research & Eng. Co. for kind cooperation. A part of this research work was supported by research council of K. N. Toosi University of Technology is gratefully acknowledged

References

1. Moroder, L., Felix, A., Toniolo, C. (Eds.) *Synthesis of Peptides and Peptidomimetics,* Vol E 22a, Thieme, Stuttgart, 2004.
2. Leondiadis, L., Zinieris, N., Ferderigos, N. *J. Comb. Chem.* **7**, 4-6 (2005).
3. Suarez-Castillo, O.R., Montiel-Ortega, L.A., Melendez-Rodriguez, M., Sanchez-Zavala, M. *Tet. Lett.* **48**, 17-20 (2007).

Proceedings of the 31st European Peptide Symposium
Michal Lebl, Morten Meldal, Knud J. Jensen, Thomas Hoeg-Jensen (Editors)
European Peptide Society, 2010

Peptide Diketopiperazine Thioester Formation at the Cys-Pro-Cys Position

Toru Kawakami, Sakiko Shimizu, and Saburo Aimoto
Institute for Protein Research, Osaka University, Suita, 565-0871, Japan

Introduction

The peptide thioester is one of the key intermediates in protein synthesis by the ligation strategies, such as the thioester method [1,2] and native chemical ligation [3,4]. The focus of our research has been on the use of the *N* to *S* acyl shift reaction for preparing peptide thioesters. In previous studies, we reported on the thiol-auxiliary mediated thioester formation [5,6] and on the diketopiperazine (DKP)-thioester formation by the use of a Cys-Pro ester (CPE) unit [7,8]. The peptide containing the CPE unit can be directly utilized in a ligation reaction with a peptide containing a cysteine residue at the N-terminus (Cys-peptide) in a one pot reaction. In this reaction, the ester group played a crucial role as a leaving group at the DKP-forming step. The next step is to design a general sequence that leads to thioester production without an ester moiety, which would make it possible to use genetically engineered proteins as peptide thioester precursors. We report herein on the formation of a peptide DKP thioester using a peptide containing a Cys-Pro-Cys sequence (CPC peptide) [9].

Results and Discussion

We initially prepared a peptide library, H-Ala-Lys-Leu-Arg-Phe-Gly-Cys-Pro-*Xaa*-*Xbb*-*Xcc*-Arg-NH_2 (**1**), in which the Cys-Pro sequence was fixed and the *Xaa*-*Xbb*-*Xcc* region contained random sequences of 3 amino acid residues consisting of Asn, Asp, Cys, Gln, Gly, His, Leu, or Ser. The library was treated with an excess amount of H-Cys-Tyr-NH_2 (**2**) in a carbonate buffer at pH 8.2. A ligated product, H-Ala-Lys-Leu-Arg-Phe-Gly-Cys-Tyr-NH_2 (**3**), would be expected to be produced, if the active sequence is contained in the library. A library **1a**, in which the *Xaa* residue was fixed with 8 different amino acid residues respectively, and *Xbb* and *Xcc* contained random residues, was treated with peptide **2**. When a Ser or Cys residue was located at the *Xaa* position, the ligated product **3** was observed as a small but distinct peak by RP-HPLC and by mass spectroscopy. When a Ser residue was located at the *Xaa* position and the *Xbb* or *Xcc* position was fixed with the 8 different amino acid residues respectively, the results were similar; a signal corresponding to peptide **3** was observed in the majority of cases. These findings suggest that only Ser or Cys residues at the *Xaa* position are essential and that the ligation reaction proceeds *via* the following steps (Figure 1): An *N-S/O* acyl shift reaction at the second Ser or Cys residue of a peptide **4** containing Cys-Pro-Ser/Cys sequence (path ***b***) would produce a (thio)ester structure at the C-terminus, as shown in structure **5b** which contains a similar structure to the CPE unit. Once the CPE structure is constructed, the DKP thioester formation (structure **7**) might occur *via* an *N-S* acyl shift reaction at the first Cys residue (path ***a***), followed by DKP formation (path ***c***). The order of the acyl shift reactions ***a*** and ***b*** would not be critically important. Finally, the native chemical ligation reaction of thioester **7** proceeds with a Cys-peptide **9** to give the ligation product **10**.

A Ser or Cys residue at the *Xaa* position in the library was required for the ligation, whereas the reaction proceeded in low yield under neutral conditions. Next, some of the selected peptides were treated in an acid solution since the equilibrium between a thioester and an amide forms at a Cys site shifts in favor of the thioester under the acidic conditions [10]. As a result, when a peptide, H-Ala-Lys-Leu-Arg-Phe-Gly-Cys-Pro-Cys-NH_2 (**4a**) was incubated in a 0.1 M HCl solution at 110 ºC in an evacuated sealed tube for 2 h, the mass number corresponding to peptide DKP thioester **7a** was observed and the isolated yield was 12%. In this condition a hydrolysis product, H-Ala-Lys-Leu-Arg-Phe-Gly-OH (**11**) was observed, while the CPC peptide **4a** was remained. When peptide **4a** was treated with heptafluorobutyric acid vapors at 110 ºC in an evacuated sealed tube for 4 h [11], the DKP thioester product **7a** was isolated (9 %) with its epimer in the DKP moiety (12%), in which CPC peptide **4a** disappeared and the production of hydrolysis peptide **11** was reduced. When this crude mixture was reacted with an excess amount of Cys-peptide **2** to give a single ligated isomer **3** in a yield of 17% based on CPC peptide **4a**.

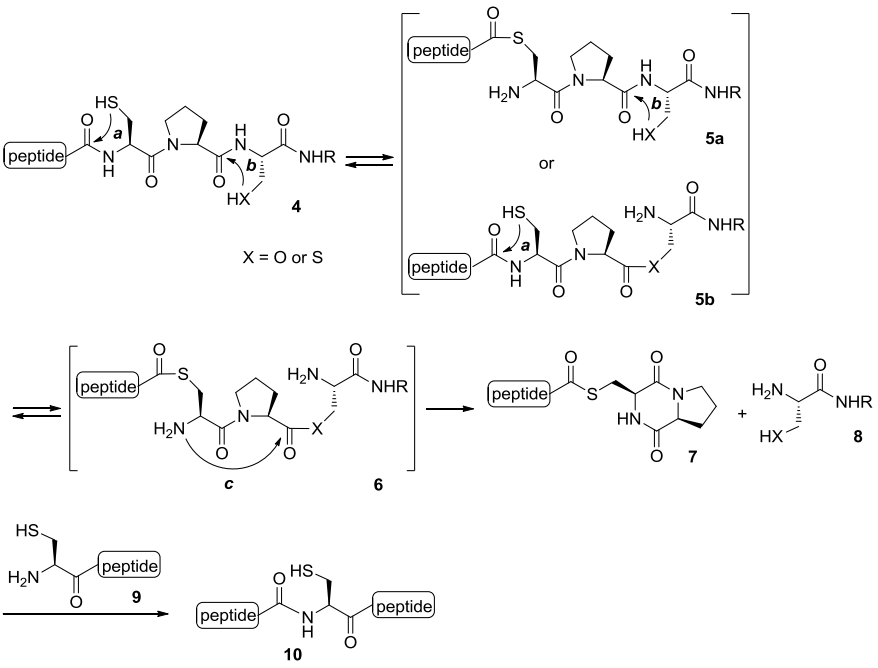

Fig. 1. Formation of a DKP thioester via an intramolecular N to S/O acyl shift reaction.

In conclusion, a peptide containing a Cys-Pro-Cys (CPC) sequence can be transformed into a peptide DKP thioester *via* the *N-S* acyl shift reaction. The DKP thioester-forming reaction requires acidic conditions and high temperature at this stage. Current efforts are directed toward searching the mild reaction conditions. Recombinant proteins containing the CPC sequence would be used for the production of the peptide thioesters.

Acknowledgments
This research was supported, in part, by The Naito Foundation and Grants-in-Aid for Scientific Research from the Ministry of Education, Culture, Sports, Science and Technology, Japan.

References

1. Hojo, H., Aimoto, S. *Bull. Chem. Soc. Jpn.* **64**, 111-117 (1991).
2. Kawakami, T., Kogure, S., Aimoto, S. *Bull. Chem. Soc. Jpn.* **69**, 3331-3338 (1996).
3. Dawson, P.E., Muir, T.W., Clark-Lewis, I., Kent, S,B,H. *Science* **266**, 776-779 (1994).
4. Tam, J.P., Lu, C.-F., Shao, J. *J. Proc. Natl. Acad. Sci. U.S.A.* **92**, 12485-12489 (1995).
5. Kawakami, T., Sumida, M., Nakamura, K., Vorherr, T., Aimoto, S. *Tetrahedron Lett.* **46**, 8805-8807 (2005).
6. Nakamura, K., Kanao, T., Uesugi, T., Hara, T., Sato, T., Kawakami, T., Aimoto, S. *J. Pept. Sci.* **15**, 731-737 (2009).
7. Kawakami, T., Aimoto, S. C*hem. Lett*. **36**, 76-77 (2007).
8. Kawakami, T. Aimoto, S. *Tetrahedron* **65**, 3871-3877 (2009).
9. Kawakami, T., Shimizu, S., Aimoto, S. *Bull. Chem. Soc. Jpn.* **83**, 570-574 (2010).
10. Nakamura, K., Sumida, M., Kawakami, T., Vorherr, T., Aimoto, S. *Bull. Chem. Soc. Jpn.* **79**, 1773-1780 (2006).
11. Tsugita, A., Takamoto, K., Kamo, M., Iwadate. H. *Eur. J. Biochem.* **206**, 691-696 (1992).

Proceedings of the 31st European Peptide Symposium
Michal Lebl, Morten Meldal, Knud J. Jensen, Thomas Hoeg-Jensen (Editors)
European Peptide Society, 2010

Fmoc Deprotection by *tert*-Butylamine in Solution and in the Synthesis of Cyclic Part of Oxytocin-Like Peptides

Martin Flegel[1,3], Zuzana Flegelová[2], Petr Maloň[3], Sixtus Hynie[1], and Věra Klenerová[1]

[1]1st. Faculty of Medicine, Charles University in Prague, Prague 2, Albertov 4, 12800, Czech Republic; [2]Vidia spol.s.r.o, Nad Safinou II. 365. Jesenice u Prahy-Vestec, 25242, Czech Republic; [3]IOCB, Flemingovo n. 2 Prague 6, 16610, Czech Republic

Introduction

The Fmoc protecting group is usually cleaved at basic conditions by 20% piperidine in DMF [1]. For deprotection of difficult sequences diazabicycloundecene (2 % DBU in DMF) is often used. Both commonly used agents are unfortunately not very suitable in the alternative liquid phase synthesis. Therefore there is a permanent effort and search for the agents easily removable during inevitable intermediates isolation [2]. The cyclic part of oxytocin H-c(Cys-Tyr(I_2)-Ile-Gln-Asn-Cys)-NH_2 was manually synthesized on the solid phase. For the Fmoc group removal both 20% piperidine in DMF and 30% of *tert*-butylamine (TBA) in DMF were compared. TBA in the mixture with 1-octadecanethiol (C18-SH) was then used for deprotection of some Fmoc-AA derivatives to study the cleavage condition affordable for liquid phase. The choice of the model peptide was motivated by its possible exploitation either for CD spectral measurement and/or for biological effects in CNS during the study of stress. It was also desirable to develop a simple method for the iodination of Tyr residue.

Results and Discussion

Fmoc-Cys(Trt)-Tyr(tBu)-Ile-Gln(Trt)-Asn(Trt)-Cys(Trt)-Rink-resin was synthesized in two batches employing the usual scheme. Fmoc derivatives were used in 3 eq. excess, DIC/HOBt was used for coupling and deprotection was carried out for 5 and 20 min in 20% piperidine /DMF solution. The analogous scheme was applied in the second batch, where 30% TBA in DMF with 0.1% dithiothreitol (DTT) for 5 and 40 min was used for the Fmoc removal (Table 1).

The peptides were then detached from the resin in the cocktail of 95%TFA, 3% anisole and 2% water in 3 hours, precipitated by diethylether, dissolved in methanol, acidified by AcOH (pH 4.5, 1 mg/ml), and oxidized by 1% iodine in MeOH to create a disulfide bridge. After 30 min the yellowish solution was decolorized by ascorbic acid, and the solution gently evaporated at 40° C in vacuum. The residue was dissolved in water, desalted and purified on HPLC column. The peptides were then freeze dried. In both batches the peptide iodinated in the Tyr aromatic ring was surprisingly found as the main product.

Some Fmoc derivatives of Tyr(tBu), Trp, Gln(Trt), Nal, and Cys(Trt) were chosen for the study of the cleavage reaction in solution. For all of them the Fmoc group was fully removed with TBA in 30-60 min. To scavenge dibenzofulvene (DBF), DTT [6] or C18-SH was added in 5-10 molar excess to 30% solution of TBA in ACN or in 100%TBA.

The isolation process in solution approach using TBA was found to be easier. DBF, as the primary product of the Fmoc elimination is a very reactive intermediate, which in the reversible Michael addition reacts with nucleophiles to form adducts with piperidine, primary or secondary amines, or preferably with the soft nucleophiles such as thiols. In the solid phase, large excess of the base guarantee full conversion of DBF to piperidine adduct. In the liquid phase other methods can serve this purpose. Easy and friendly reaction conditions and isolation of the pure intermediate are of importance.

Table 1. Monitoring of peptide synthesis

mmol/g (Fmoc Release)	Piperidine	0.60	0.61	0.61	0.61	0.64	0.68
	Sequence	C	Y	I	Q	N	C
	tert-Butylamine	0.61	0.63	0.64	0.69	0.73	0.73

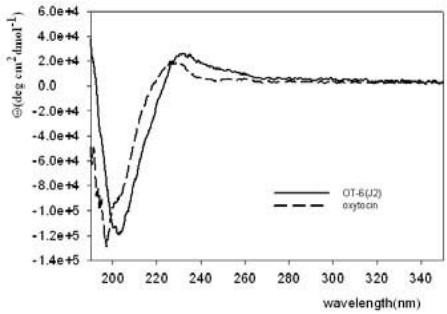

Fig. 1. CD spectrum of oxytocin (OT).

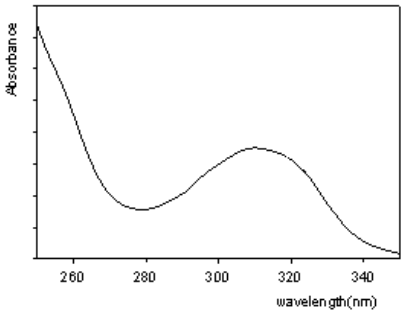

Fig. 2. UV spectrum of tocinamide I2 (OT6I2) and tocinamide I2(OT6I2).

Hydrogenolysis (Pd/C) [3,4], various bases [1,2], $AlCl_3$/Toluene [5], catalytic amount of DBU/C8SH [6], MeONa/mercaptoacetic acid [7], elevated temperature (130 ^oC) [8] and resin bound piperazine and other resin supported scavenging agents were tested. DBF at higher concentration polymerizes and if not fully scavenged, reacts reversibly with the amino groups on the peptide chain producing secondary peptide-amines. *Tert*-butylamine has the properties convenient for Fmoc deprotection. It is a strong base (pK_a 10.7), and its reactivity towards amide formation is limited due to its bulky chain. Boiling point of TBA is 46^oC and therefore it can be evaporated very easily.

TBA solutions (30% in DCM, THF, dioxan, DMF, ACN), or neat TBA were used for Fmoc deprotection in solution synthesis. Peptides having free amino group can be usually precipitated by ether, heptane, or petroleum ether from the reaction mixture. For the improvement of solubility in these solvents, DBF should be scavenged by C18-SH to form an adduct which can be then easily extracted. Unpleasant odor of C18-SH is well acceptable in comparison to other commonly used thiols.

Circular dichroism of the diiodinated compound OT6I2 (measured on Jasco J-815 spectrometer in neutral buffer (PBS 10mM pH = 7, quartz cell 0.1cm) shows the intense negative band at 190-210 nm and the smaller positive band at 220-250 nm, both nearly identical to CD spectra of oxytocin (see Figure 1). Finding these bands red shifted by about 10 nm for OT6I2 as compared to OT conforms to the effect of iodinated tyrosine aromatic ring. The band due to iodinated tyrosine nucleus is also discernible in absorption spectrum at ~310 nm (range 280-350 nm, measured on Jasco J-815 spectrometer in neutral buffer (PBS 10mM pH = 7, quartz cell 1cm). A similarity between CD spectra of the complete OT nonapeptide and just the ring part with the modified tyrosine indicates that a conformation of both cyclic parts remains similar and the C-terminal tripeptide of oxytocin has only a minor effect on its spectral properties.

Acknowledgments

The investigation was supported by MSM 0021620806 G.A. Czech. Acad. Sci. KAN 200520703 and 200100801 and by Grant Z4 055 0506.

References

1. Fields, G.B. *Methods in Molecular Biology 35, Peptide Synthesis Protocols*, (Pennington M.W., Dunn, B.M., Eds.), Humana Press (1994).
2. Takahashi, D., patent application number 20100184952 USPC Class 530333.
3. Carpino, L.A., Han, G.Y. *J. Org. Chem*. **37**, 3404-3409 (1972).
4. Maegawa, T., Fujiwara, Y., Ikawa, T., Hisashi, H., Mongushi, Y., Sajiki, H. *Amino Acids* **36**, 493-499 (2009).
5. Leggio, A., Liguori, A., Napoli, A., Siciliano, C., Sindona, G. *Eur. J. Org. Chem*. 573-575 (2000).
6. Sheppeck, J.E., Kar, H., Hong, H. *Tetrahedron Letters* **41**, 5329-5333 (2000).
7. De Marco, R., et al. *Amino Acids* DOI 10.1007/s00726-009-0267-2.
8. Hoeck, S., Marti, R., Riedl, R., Simeunovic, M. *Chimia* **64**, 200-202 (2010).

Proceedings of the 31st European Peptide Symposium
Michal Lebl, Morten Meldal, Knud J. Jensen, Thomas Hoeg-Jensen (Editors)
European Peptide Society, 2010

Radical Scavenging Activity of Hydroxycinnamoylamides of Amino Acids - Precursors of Biogenic Amines

Maya G. Chochkova[1], Hristina G. Nikova[1], Galya I. Ivanova[2], Lyubomir N. Georgiev[1], and Tsenka S. Milkova[1]

[1]South-West University "Neofit Rilski", Blagoevgrad, 2700, Bulgaria; [2]Requimte, Polo da Universidade do Porto, Departamento de Química, Rua do Campo Alegre, Porto, 4169-007, Portugal

Introduction

Oxygen is a molecule that humans and the other aerobics require to maintain their lives. However, it creates a paradox, because this molecule is essential for the survival, being at the same time potentially harmful. During normal metabolism, unconsumed oxygen molecules could be changed to free radicals such as superoxide ($O2^-$, OOH•), hydroxyl (OH•) and peroxyl (ROO•) radicals. Excessive production of these species beyond the antioxidant defense system of the body can cause oxidative stress [1,2]. This phenomena is a key factor to the pathogenesis of various disorders in human body, including cancer, atherosclerosis, malaria, and rheumatoid arthritis and neurodegenerative diseases [3,4]. Thus, the development of different type antioxidants, which can block the production or scavenge the obtained free radicals, has attracted the attention in the recent years. Amongst the various groups of antioxidants, our attention was focused on hydroxycinnamic acid amides, because more of these compounds are naturally occuring and have a stable structure after the free radicals are quenched.

Results and Discussion

In order to estimate the influence of different incorporatated amino components in hydroxycinnamoylamides towards DPPH radical, two type of amides were obtained (Table 1).

Table 1. Synthesized hydroxycinnamic acid amides

Compound		Substituent R`	Substituent R``	Substituent Y
1	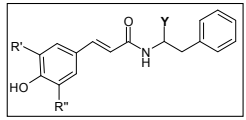	OH	H	H
2		OCH_3	OCH_3	H
3		OCH_3	H	H
4		OCH_3	OCH_3	$COOBu^t$
5		OCH_3	H	$COOBu^t$
6	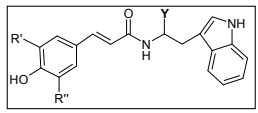	OH	H	H
7		OCH_3	OCH_3	H
8		OCH_3	H	H
9		OH	H	COOMe
10		OCH_3	OCH_3	COOMe
11		OCH_3	H	COOMe

The free radical scavenging activities (RSA) of amides (**1–11**) and standards such as ferulic, sinapic, caffeic acids were determined using a DPPH method [5] (Table 2). The method is based on the reduction of alcoholic DPPH* solution in the presence of a hydrogen-donating antioxidant due to the formation of the non-radical form DPPH-H.

Table 2. Results of evaluation of radical scavenging activity of hydroxycinnamoylamides

	(%) RSA					
	0.9 mM		1.8 mM		3.6 mM	
	Reaction time (min)					
AH	10'	20'	10'	20'	10'	20'
Caffeic acid (Caf A)	**23.8 ± 0.4**	**24.01 ± 0.04**	**35.9 ± 0.9**	**38.9 ± 4.5**	**79.3 ± 2.3**	**83.9 ± 3.9**
(1) Caf A-phenylethylamine	41.85±1.55	44.29±1.55	77.33±2.33	80.37±2.31	93.43±0.09	94.21±0.96
(6) CafA - tryptamine	30.72±2.15	33.25±2.50	59.12±2.05	63.13±2.09	90.41±0.37	90.82±0.36
(9) CafA -Trp-OCH_3	27.1 ± 2.1	28.7 ± 2.2	44.6 ± 1.7	50.4 ± 1.7	80.1 ± 8	87.9 ± 0.3
Sinapic acid (SA)	**16.1 ± 0.5**	**17.2 ± 0.3**	**26.5 ± 0.1**	**31.9 ± 0.1**	**69.0 ± 1.8**	**69.6 ± 1.0**
(7) SA- tryptamine	8.76±0.30	9.90±0.30	16.58±1.22	18.33±1.17	33.67±1.11	39.25±1.03
(2) SA- phenylethylamine	11.83±0.89	13.40±0.72	22.00±0.35	24.07±0.10	37.99±3.20	41.06±3.55
(10) SA–Trp– OCH_3	8.6 ± 0.7	12.9 ± 0.8	14.0 ± 0.05	15.2 ± 0.8	32.5 ± 0.01	39.5 ± 1.1
(4) SA-Phe-OBu^t	12.0 ± 0.1	13.2 ± 0.1	20.0 ± 1.6	24.9 ± 0.6	36.8 ± 3.4	40.2 ± 4.9
Ferulic acid (FA)	**12.0 ± 0.1**	**13.8 ± 0.3**	**21.0 ± 0.2**	**25.1 ± 0.4**	**36.7 ± 0.1**	**44.3 ± 0.1**
(11) FA –Trp– OCH_3	2.5 ± 1.0	4.52 ± 0.05	5.2 ± 0.1	9.9 ± 0.1	6.8 ± 0.7	13.4 ± 0.5
(5) FA-Phe-OBu^t	7.5 ± 0.2	10.4 ± 0.2	11.4 ± 1.8	17.8 ± 1.3	16.4 ± 1.6	29.3 ± 0.2
(8) FA-tryptamine	11.09±1.47	13.68±1.67	20.86±0.30	23.04±0.38	33.12±1.43	37.46±1.61
(3) FA-phenylethylamine	11.31±0.33	13.36±0.42	20.34±1.37	23.42±1.46	33.89±1.26	38.85±1.41

% RSA—percent radical scavenging activity;
% RSA =[($Abs_{516nm\ (t=0)}$ - $Abs_{516nm(t=\ t')}$) x 100/$Abs_{516nm(t=0)}$], as proposed by Nenadis et al. [5].

The DPPH assay results showed that the type of amino component (aromatic amines or their corresponding amino acid precursors) in the 3-phenylpropenoylamides affected insignificantly the antioxidative activity. All hydroxycinnamic acid amides of phenylethylamine were the most potent compounds, especially N-caffeoyl-phenylethylamine. With the exception of caffeoylamides, all tested hydroxy-cinnamoylamides have shown lower RSA than the corresponding free phenolic acid.

Acknowledgments
For the support of this work we are grateful to the contracts: VUL-304/07 and SRP-C2.

References

1. Halliwell, B. *Biochemical Society Transactions* **35**, 1147-1150 (2007).
2. Sortino, C., Politi, M., Morelli, I., Mendez, J. *J. Ethnopharmacol*. **79**, 379-381 *(*2002).
3. Maxwell, S.R. *Drugs* **49**, 345-361 (1995).
4. Aruoma, O.I. *JAOCS* **75**, 199-212 (1998).
5. Nenadis, N., Boyle, S., Bakalbassis, E.G., Tsimidou, M. *JAOCS* **80,** 451-458 (2003).

Proceedings of the 31st European Peptide Symposium
Michal Lebl, Morten Meldal, Knud J. Jensen, Thomas Hoeg-Jensen (Editors)
European Peptide Society, 2010

Repetitive Cleavage of Aib-Peptides by Trifluoroacetic Acid

Hans Brückner[1], Christoph Theis[1], Thomas Degenkolb[1,2], Renate Gessmann[3], and Michael Kokkinidis[3]

[1]Research Center for BioSystems, Land Use and Nutrition (IFZ), Department of Food Sciences, University of Giessen, Giessen, 35392, Germany; [2]Department of Entomology (IFZ); [3]Institute of Molecular Biology and Biotechnology (IMBB), FORTH, Heraklion, 71110, Crete, Greece

Introduction

Crystalline, synthetic *homo*-Aib-peptides of the general structure Z-$(Aib)_n$-O*t*Bu (n = 3–11) form consecutive β-turns of type III resulting in full turns of (3_{10})-helices for n = 5, 8, and 11 (Aib, α-aminoisobutyric acid, 2-methylalanine) [1]. Native **peptaibols** are helical, fungal peptides containing Aib as well as proteinogenic amino acids and a *C*-terminal 2-amino alcohol. Natural peptides lacking the amino alcohol are named **peptaibiotics** [2,3]. Peptide bonds formed by proteinogenic amino acids are commonly stable against TFA at moderate temperature, whereas those formed by Aib are less resistant. We present a study and propose a mechanism concerning the cleavage of synthetic Aib-peptides by anhydrous TFA.

Results and Discussion

Anhydrous TFA (100 µl) was added to 0.1 mg of each peptide (Figure 1). Solutions were kept at 37 °C for 0.5 – 26 h. Dried residues were dissolved in MeOH, and the resulting cleavage products were analyzed by RP-HPLC and online ESI-CID-MS. Details of the crystal structures and synthesis of peptides are described in references [1c] and [4], respectively. For the crystal structures of Z-$(Aib)_{10}$-O*t*Bu and Z-$(Aib)_7$-O*t*Bu see Figure 2.

Release of regular series of Z-$(Aib)_{10\text{-}5}$-OH from synthetic Z-$(Aib)_{10}$-O*t*Bu within 0.5 h was recognized (Figure 1). Concomitant formation of H-$(Aib)_{10\text{-}3}$-OH was also observed. After 3 h, a regular series Z-$(Aib)_{7\text{-}3}$-OH from Z-$(Aib)_7$-O*t*Bu was formed. However, cleavage of the Z-groups also occurred. From Ac-$(Aib)_{10}$-O*t*Bu *C*-terminal Aib-residues were cleaved but *N*-terminal Ac-$(Aib)_5$-OH was still observed after 8 h. Based on these data, a repetitive cleavage mechanism of *homo*-Aib-peptides *via* formation of *C*-terminal oxazolones has been proposed (Figure 2). Related mechanisms have been discussed in the literature [6]. In native peptaibols very fast cleavage of the Aib-Pro bonds was observed as well as scission of certain Aib-Aaa (Aaa = Gly, Ala, Gln) and Aib-Aib bonds. Considerable agreement was noticed with the formation of regular *b*-series of positive acylium or oxazolonium ions resulting from ESI-MS (Figure 2).

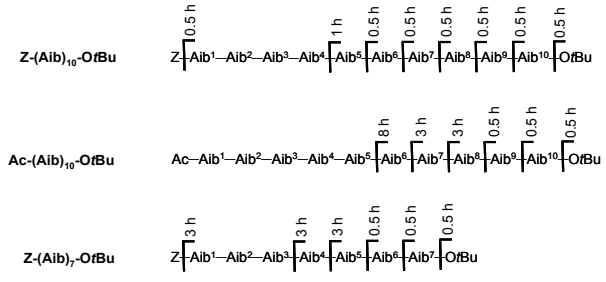

Fig. 1. Structures of homo-Aib-peptides analyzed. Preferred cleavages of peptide bonds at certain time intervals are indicated.

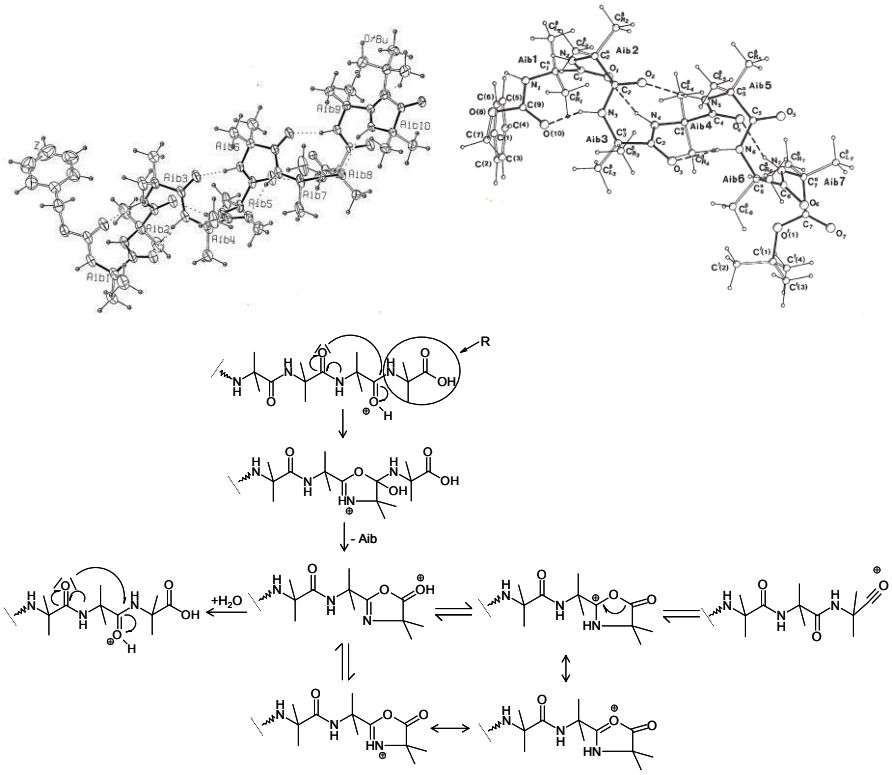

Fig. 2. Above: (3_{10})-helical crystal structure of Z-$(Aib)_{10}$-OtBu (left) [4] and Z-$(Aib)_7$-OtBu (right) [1c]; Below: proposed C-terminal cleavage mechanism of homo-$(Aib)_n$-peptides via repetitive intermediate formation of oxazolinolium/oxazolinium (oxazolonium) ions after treatment with TFA. The resulting homo-$(Aib)_{n-1}$ –peptides (left side) and related formation of the b-series of positive fragment ions under gas phase conditions of ESI-MS (right side) are displayed. Encircled R represents an α-aminoisobutyryl residue [5].

References

1. (a) Benedetti, E., et al. *J. Am. Chem. Soc.* **104**, 2437-2444 (1982); (b) Toniolo, C., Benedetti, E. *Trends Biochem. Sci. (TIBS)* **16**, 350-353 (1991); (c) Vlassi, M., Brueckner, H., Kokkinidis, M. *Acta Cryst.* **B49**, 560-564 (1993); (d) Geßmann, R., Brückner, H., Kokkinidis, M. *Acta. Cryst.* **B54**, 300-307 (1998); (e) Gessmann, R., Brückner, H., Petratos, K. *J. Pept. Sci.* **9**, 753-762 (2003).
2. Toniolo, C., Brückner, H. (Eds.) *Peptaibiotics - Fungal Peptides Containing α-Dialkyl α-Amino Acids.* Verlag Helvetica Chimica Acta, Zürich and Wiley-VCH, Weinheim, 2009.
3. Degenkolb, T., Brückner, H. *Chem. Biodivers.* **5**, 1817-1843 (2008).
4. Geßmann, R. *Dissertation*. Universität Hohenheim, Stuttgart, Germany, 1999.
5. Theis, C., Degenkolb, T., Brückner, H. *Chem. Biodivers.* **5**, 2337-2355 (2008).
6. (a) Obrecht, D., Heimgartner, H. *Helv. Chim. Acta* **70**, 329-338 (1987); (b) Creighton, C.J., Romoff, T.T., Bu, J., Goodman, M. *J. Am. Chem. Soc.* **121**, 6786-6791 (1999).

Proceedings of the 31st European Peptide Symposium
Michal Lebl, Morten Meldal, Knud J. Jensen, Thomas Hoeg-Jensen (Editors)
European Peptide Society, 2010

Antioxidant Potential of Phenolic Acid Amides of Aromatic Amines

Lyubomir Georgiev[1], Iskra Totseva[2], Katya Seizova[2], Emma Marinova[2], Maya Chochkova[1], and Tsenka Milkova[1]

[1]South-West University "Neofit Rilski" Blagoevgrad 2700, Bulgaria; [2]Institute of Organic Chemistry with Centre of Phytochemistry, Bulgarian Academy of Sciences, Sofia 1113, Bulgaria; [3]Institute of Molecular Biology "Roumen Tsanev", Bulgarian Academy of Sciences, Sofia 1113, Bulgaria

Introduction

The lipid peroxidation is one of the important primary events in the free radical-mediated oxidative damage of biological membranes and tissues. Antioxidants are organic molecules which can avoid or delay the progress of lipid oxidation. Hydroxycinnamic acid compounds are widely distributed in the plant kingdom. They have been described as chain-breaking antioxidants, probably acting through radical-scavenging, which is related to their hydrogen-donating capacity, and their ability to stabilise the resulting phenoxyl radical [1]. On the other hand, some studies indicated that catecholamines and related compounds may possess antioxidant activity that seems to be correlated with the numbers of hydroxyl groups and their position on the benzoic ring [2,3].

The aim of the present investigation was to elucidate the antioxidative activity of eight synthesized cinnamoyl- and hydroxycinnamoyl amides of biogenic amines during oxidation of pure (depleted from pro- and antioxidative micro components) triacylglycerols of sunflower oil at 100ºC whose oxidation mechanism is well known. The results obtained were compared with the inhibiting effects of the main hydroxycinnamic acids.

Results and Discussion

Pure triacylglycerols of sunflower oil (TGSO) were obtained by cleaning the sunflower oil sample from pro- and antioxidants and trace metals by adsorption chromatography [4].

Oxidation was carried out at 100°C (±0.2°C) in the dark by blowing air through the samples (2 g) at a rate of 50 ml/min. Under these conditions the process took place in a kinetic regime, i.e. at a sufficiently high oxygen concentration at which the diffusion rate did not influence the oxidation rate. The process was followed by withdrawing samples (ca 0.1 g) at various time intervals and subjecting them to iodometric determination of the primary oxidation products (peroxides) concentration, i.e. the peroxide value (PV) [5]. The coefficient of variation for PV determination was 7-8% irrespective of the measured value. Kinetic curves of peroxide accumulation were plotted.

The effectiveness of the additives in the lipid systems was estimated on the basis of the induction period (IP) which was determined by the method of the tangents. That means the tangents are applied to the two parts of the kinetic curves. The coefficient of variation ranged from 6 - 13% and was inversely related to the induction period. The reported IP values result from three independent experiments. The effectiveness was expressed as stabilization factor F:

$$F = IP_{add} / IP_o$$

where IP_{add} is the induction period in the presence of the tested additive, and IP_o is the induction period of the control sample.

The cinnamoyldopamine, p-coumaroyldopamine feruloyldopamine, sinapoyl-dopamine, caffeoyldopamine, caffeoyltyramine, caffeoylphenylethylamine, and caffeoyl-tryptamine were evaluated for their antioxidant effectiveness at the concentration $1x10^{-3}$ M during autoxidation of pure triacylglycerols of sunflower oil (TGSO) at 100°C. After processing all the kinetic curves of peroxide accumulation obtained the values for the stabilization factor (F) were determined. A value of F = 1 corresponds to no antioxidant activity. The results obtained are presented in Figure 1. A comparison with the effectiveness of caffeic (CA), sinapic (SA) and ferulic (FA) acids at the same

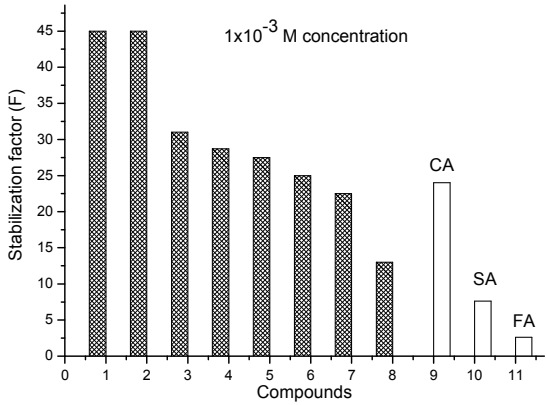

Fig. 1. Stabilization factor of caffeoyldopamine (1); cinnamoyldopamine (2); caffeoylphenylethylamine (3); p-coumaroyldopamine (4); caffeoyltyramine (5); caffeoyltryptamine (6); feruloyldopamine (7) and sinapoyldopamine (8) during oxidation of TGSO. For comparison F for caffeic acid (CA); sinapic acid (SA) and ferulic acid (FA) at the same concentration are given.

concentrations is given. Cinnamic and p-coumaric acids were inactive during these oxidation conditions.

From the Figure 1 is seen that all compounds possessed excellent antioxidant effectiveness, higher or comparable with this of the caffeic acid. The antioxidant activity decreases in the following order: caffeoyldopamine ≅ cinnamoyldopamine > caffeoylphenylethylamine > p-coumaroyldopamine > caffeoyltyramine > caffeoyltryptamine ≈ caffeic acid > feruloyldopamine > sinapoyldopamine. The results showed that in contrast to the hydroxycinnamic acids, the presence of methoxy groups in the molecules of feruloyldopamine and sinapoyldopamine decrease antioxidant effectiveness.

Acknowledgments
For the support of this work we are grateful to contracts VUL-304/07 and SRP-C2.

References

1. Siquet, C., Pavia-Martins, F., Lima, J.L.F.C., Reis, S., Borges, F. *Free Radical Res.* **40**, 433-442 (2006).
2. Yen, G.C., Hsieh, C.L. *Biosci. Biotechnol. Biochem.* **61**, 1646-1649 (1997).
3. Sofic, E., Denisova, N., Yodium, K., Vatrenjak-Velagic, De Filippo, C., Mehmedagic, A., Causevic, A., Cao, A., Joseph, J.A., Prior, R.L. *J. Neutral Transm.* **108**, 541-557 (2001).
4. Yanishlieva, N.V., Marinova, E.M. *Food Chem*. **54**, 377-382 (1995).
5. Yanishlieva, N.V., Popov, A., Marinova, E.M. *Compt. rend. Acad. bulg. Sci.* **31**, 869-8712 (1978).

Proceedings of the 31st European Peptide Symposium
Michal Lebl, Morten Meldal, Knud J. Jensen, Thomas Hoeg-Jensen (Editors)
European Peptide Society, 2010

Solid Phase Synthesis and Characterisation of a Platelet-Derived Growth Factor Receptor (PDGFR) Specific Affibody Molecule

Bård Indrevoll, Roger Bjerke, Dimitrios Mantzilas, Erlend Hvattum, and Astri Rogstad
GE Healthcare AS, 0401, Oslo, Norway

Introduction

A 66 amino acid PDGFR specific Affibody [1] peptide was prepared by microwave-assisted automated solid-phase synthesis. The peptide was assembled on a 100% PEG resin affording good purity and acceptable yield of crude Affibody. Fmoc-deprotection steps were carried out using piperazine in order to suppress aspartimide formation [2]. Pseudo-proline was incorporated in the peptide backbone. The identity of the synthetic Affibody was confirmed by TOF-MS. The secondary structure content was compared with its recombinant counterpart [3] using circular dichroism (CD) and the biological activity assessed by fluorescence polarisation (FP) and surface plasmon resonance (SPR) techniques.

Results and Discussion

Affibody molecules, members of the family of antibody mimetics, are small high affinity proteins engineered to bind specifically to a large number of target proteins [4]. Affibody molecules are composed of three alpha helices and lack disulfide bridges. The three-helix bundle structure is one of the fastest folding protein structure known [5]. The purpose of this study was to evaluate the feasibility of preparing a 66 amino acid Affibody peptide (GSSLQVDNKF NKELIEAAAE IDALPNLNRR QWNAFIKSLV DDPSQSANLL) by solid-phase synthesis and to compare the synthetic peptide with its recombinant counterpart with respect to secondary structure and biological activity.

Solid-phase synthesis was carried out on a CEM Liberty microwave peptide synthesiser using Fmoc/tBu strategy starting with 0.05 mmol NovaPEG Rink amide resin (0.67 mmol/g). Single couplings of amino acid (0.5 mmol) using HBTU (0.45 mmol)/HOAt (0.45 mmol)/DIPEA (1 mmol) in NMP were employed except in the case of Arg(Pbf) residues where double couplings were used. A pseudo-proline dipeptide was incorporated for Lys^{37}-Ser^{38}. Fmoc-deprotection was carried out using 5% piperazine/0.1 M HOAt in NMP. The peptide was cleaved from the resin by 2.5% water, 2.5% EDT, 2.5% TIS, 92.5% TFA (10 mL) affording 148 mg (41%) crude Affibody. No aspartimide formation was observed.

Purification by HPLC on a Phenomenex Luna 5µ C18 (2) column applying gradient elution (20-50% B over 40 min where A = H_2O/0.1% TFA and B = ACN/0.1% TFA) afforded 49 mg (14%) pure lyophilised Affibody. MS analysis of the product was performed on a QTof-micro mass spectrometer operating with ESI^+ (expected for $C_{315}H_{511}N_{91}O_{102}S$: 1034.8 ($MH_7^{7}$+), 1207.1 ($MH_6^{6}$+), 1448.4 ($MH_5^{5}$+), 1810.2 ($MH_4^{4}$+); *m/z* found: 1034.8, 1207.2, 1448.4, 1810.0). Analytical HPLC (Figure 1) was run on a Phenomenex Luna 3µ C18 (2) 20 x 2 mm column (20-50% B over 5 min; A = H_2O/0.1% TFA and B = ACN/0.1% TFA; 0.6 mL/min; UV 214 nm).

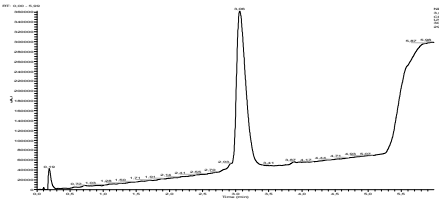

Fig. 1. Analytical HPLC chromatogram of purified synthetic Affibody.

Fluorescence polarisation (FP) analyses were performed on a Tecan Safire FP plate reader at ex635/em678 nm using PBS (pH 7.5) with 0.01% Tween-20 as binding buffer. The concentration of CyDye-labelled synthetic Affibody was 5 nM and the concentration of rhPDGFR β (R&D Systems) was varied from 0 to 250 nM. Binding of labelled Affibody to the PDGF receptor was observed (Figure 2). The labelled Affibody has a MW that is at the limit of what can be detected in the FP assay (>8 kDa). Hence, no reliable Kd value was calculated.

Table 1. SPR kinetic variables calculated using 1:1 Langmuir binding model

Variable	*Value*	*Unit*
k_a	1.1×10^{6}	1/Ms
k_d	2.1×10^{-3}	1/s
K_D, synthetic	1.9×10^{-9}	M
K_D, recombinant	0.5×10^{-9}	M

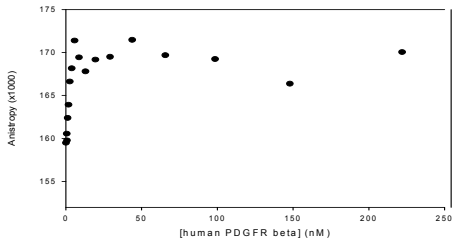

Fig. 2. FP plot of labelled synthetic Affibody.

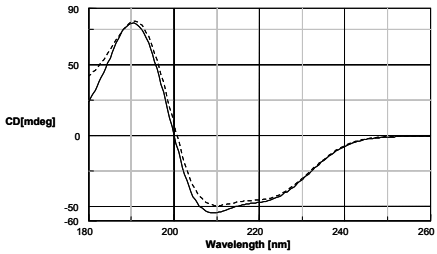

Fig. 3. CD spectra of synthetic (solid line) and recombinant (broken line) Affibody.

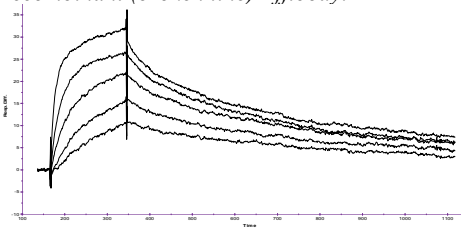

Fig. 4. SPR sensorgrams for synthetic Affibody.

Circular dichroism (CD) spectra were recorded at ambient temperature on a Jasco J-715 spectropolarimeter equipped with a 0.1 cm 100-QS Supracil cuvette. The concentration of Affibody was 0.2 mg/mL phosphate buffer (pH 7.4). Synthetic and recombinant Affibody gave similar spectra, both showing characteristic alpha-helix features (Figure 3).

Surface plasmon resonance (SPR) analyses was performed on a BiaCore 3000 equipped with a CM5 chip activated using EDC and NHS. The rhPDGFR β protein (10 µg/mL acetate buffer, pH 4.0) was passed over the surface for 7 min at flow rate 10 µL/min using 10 mM HEPES buffer containing NaCl, EDTA and surfactant P20 (pH 7.4). Affinity and kinetic study were performed at immobilisation of 1.6 µg/mL rhPDGFR β at the response level 3100 RU. The concentration range of Affibody was 0.01–1 µg/mL. Each concentration was injected in triplicate. Injection time was 3 min at a flow rate of 30 µL/min, dissociation time was 15 min (Figure 4). The K_D value for the synthetic Affibody obtained from the SPR kinetics was similar to the K_D value reported for the recombinant counterpart (Table 1).

Conclusion

The PDGFR specific Affibody was synthesised in good purity and acceptable yield. The synthetic Affibody was comparable with its recombinant counterpart with respect to secondary structure content and biological activity.

References

1. Marino, M.E., et al. *U.S. Patent Appl.* 20090191124 (2009).
2. Palasek, S.A., et al. *J. Pept. Sci*. **13**, 143-148 (2007).
3. Samples of recombinant PDGFR specific Affibody and K_D data for recombinant PDGFR specific Affibody were provided by Affibody AB, Sweden.
4. Nord, K., et al. *Nature Biotechnol*. **15**, 772-777 (1997).
5. Arora, P., et al. *Protein Sci*. **13**, 847-853 (2004).

Proceedings of the 31st European Peptide Symposium
Michal Lebl, Morten Meldal, Knud J. Jensen, Thomas Hoeg-Jensen (Editors)
European Peptide Society, 2010

Racemization of Amino Acids on Heating with Sugars or (Hydroxyalkyl)aldehydes or -ketones

Hans Brückner
Research Center for BioSystems, Land Use and Nutrition (IFZ), Department of Food Sciences, University of Giessen, Giessen, 35392, Germany

Introduction

Previously, we have reported on the racemization (epimerization) of α-amino acids (AAs) on heating with saccharides in aq. AcOH [1,2]. It was postulated that it occurs at early stages of the Maillard (**MR**) reaction. It starts with the reversible formation of Schiff bases (**SB**s) and proceeds via formation of 1-amino-1-deoxy-2-ketoses from aldoses (**A**madori **r**earrangement **p**roducts, **ARP**s) or 2-amino-2-deoxyaldoses from ketoses (**H**eyns **r**earrangement **p**roducts (**HRP**s) [3]. Here, it is shown that (α-hydroxalkyl) aldehydes or (α-hydroxyalkyl)ketones in general induce racemization. Based on these data, a feasible racemization mechanism for AAs via formation of cyclic lactones is presented.

Results and Discussion

Mixtures of L-Ala, D-sugars, and aldehydes/ketones were heated at 130 °C in 1 M AcOH. (Table 1). Racemized Ala was isolated via cation exchanger, and enantiomers were quantified on Chirasil-L-Val [1,2]. From data the following conclusions are drawn: both aldoses and ketoses cause racemization of L-Ala. Fastest racemization was induced by glyceraldehyde, methylglyoxal monohydrate, and pyridoxal. In comparison to ribose, 2-desoxyribose induces less racemization indicating the relevance of the α-position of the hydroxyl groups in aldehydes and ketones. The polyalcohol sorbitol does not promote racemization. From the data, the reversible formation of SBs and lactones thereof that show prototropy (tautomerism) is deduced (Figure 1). In equilibrium release of racemized L-Ala (or other chiral α-AA) as the result of keto-enol tautomerism occurs. The mechanism is also applicable to ARPs and HRPs generated in the course of the MR. From ARPs 7-ring ε-lactones can be formed (or 6-ring δ-lactones via previous 1,2-enaminolisation) whereas from HRPs formation of 6-ring δ-lactones is possible (see Figure 1). The aldimine of L-Ala and pyridoxal might form an ε-lactone with the phenolic group. Release of racemized AAs on heating of dry, chemically synthesized and opically pure ARPs is attributed to dehydration according to the lactone mechanism or/and direct proton abstraction from the C^{α}-atom of the AA conjugate [4,5]. For racemization of AAs in the MR see also [6].

Table 1. Relative quantities of D-Ala [%D = 100D/(D+L)] resulting from the reaction of L-Ala (5 mM) and sugars/aldehydes (500 mM) in 1 M aq. AcOH at 130 °C; n.d, not determined; n.m., not measurable owing to destruction of Ala; content of Ala is decreasing by orders of magnitude during the course of the experiments and browning is increasing.

Reactand	*Time (hours)*								
	1	*3*	*8*	*15*	*24*	*48*	*72*	*96*	*120*
Sorbitol	0.15	0.23	0.84	1.50	2.72	4.26	6.53	7.43	n.d.
Fructose	0.24	1.54	5.56	17.9	24.6	39.5	36.2	35.0	n.d.
Glucose	0.14	0.44	0.96	2.23	3.39	10.4	24.1	36.3	40.8
Galactose	0.29	1.02	2.52	3.76	11.0	18.9	33.0	40.5	40.4
Xylose	0.31	1.04	3.23	8.18	13.9	34.3	42.8	44.1	41.5
Ribose	0.82	2.41	6.61	17.3	27.6	40.8	40.7	35.7	n.d.
2-Deoxribose	n.d.	1.25	3.01	2.85	4.62	11.3	13.5	12.8	13.0
Glyceraldehyde	n.d.	n.d.	27.7	34.7	32.6	30.0	n.d.	n.d.	n.d.
Methylglyoxal	38.6	36.0	42.1	36.6	38.0	28.9	30.9	31.6	37.9
Pyridoxal	36.4	41.8	21.3	n.d.	11.5	n.m.	n.m.	n.m.	n.m.

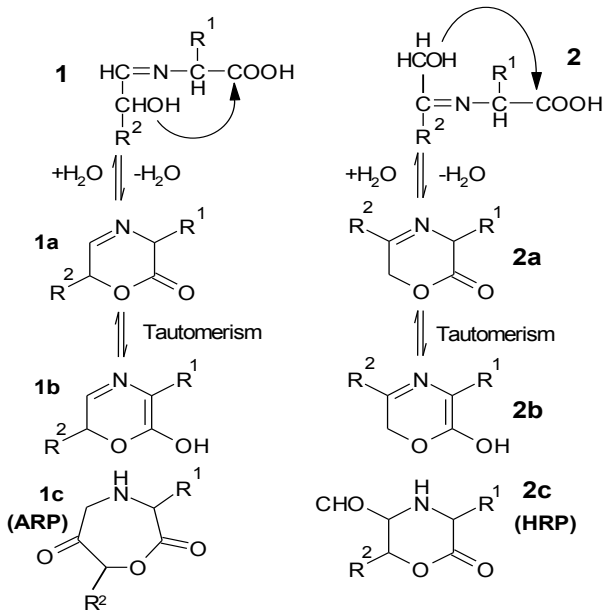

*Fig. 1. Proposed racemization of amino acid (AA) enantiomers. Shown are general open-chain structures of Schiff bases resulting from the reaction of AAs with aldoses **1**(series triose to hexanoses) or (hydroxyalkyl)aldehydes, or ketoses **2** (series tetrulose to hexuloses) or (hydroxyalkyl)ketones. Tautomerism of δ-lactones **1a, 1b** and **2a, 2b** formed from **1** and **2**, respectively, are displayed. Structures of the rearrangement products generated from **1** and **2** are shown in **1c** (ARP) and **2c** (HRP). R^1 = AA side chain; R^2 = sugar residues; for methylglyoxal monohydrate (1,2-dihydroxyacetone) R^2 = methyl in **2**, **2a** and **2b** and two hydroxyl groups are bound to C^1 of **2**.*

Acknowledgment
Special thanks to Prof. Carlo Unverzagt, University of Bayreuth, for valuable discussion of mechanistic aspects at the occasion of the 31 EPS.

References

1. Brückner, H., Justus, J., Kirschbaum, J. *Amino Acids* **21**, 429-433 (2001).
2. Brückner, H., Kirschbaum, J., Pätzold, R. In Benedetti, E., Pedone, C. (Eds.) *Peptides 2002 (Proceedings of the 27th European Peptide Symposium)*, Edizioni Ziino, Napoli, 2002, p. 54-55.
3. Hofmann, T. *Eur. Food Res. Technol.* **209**, 113-121 (1999).
4. Pätzold, R., Brückner, H. *Eur. Food Res. Technol.* **223**, 347-354 (2006).
5. Pätzold, R., Brückner, H. *Amino Acids* **31**, 63-72 (2006).
6. Kim, J.-S., Lee, Y.-S. *Food Chemistry* **108**, 582-592 (2008).

Proceedings of the 31st European Peptide Symposium
Michal Lebl, Morten Meldal, Knud J. Jensen, Thomas Hoeg-Jensen (Editors)
European Peptide Society, 2010

Nicotianamine and Thermonicotianamine: Supported Synthesis and Chelation Ability

Manuel Larrouy, Jean Martinez, and Florine Cavelier
Institut des Biomolécules Max Mousseron, UMR 5247 CNRS-UM1-UM2, Place E. Bataillon, Case Courrier 1703, 34095, Montpellier, France

Introduction

The nicotianamine (NA), which was first isolated from the leaves of *Nicotiana Tabacum* L [1] is known as a key biosynthetic precursor of phytosiderophores. Various studies have proved that NA plays a significant role in the plants physiology as iron, nickel or zinc transporter [2].

Due to the importance of NA, we developed a new method to provide easily and quickly synthetic NA [3-9] and analogues for structure-activity relationship studies on the complementation of Nicotianamine Synthase (NAS) deficient tomato mutant "*Chloronerva*". Using this method, we also synthesized a new natural analogue of NA, the thermonicotianamine (tNA) [10], that was found in the active site of an archeal NAS like enzyme [11-12]. Chelating ability of this compound was compared to that of NA by MS analysis of metal-ligand complexes [13].

Results and Discussion

This novel approach involved a first moiety anchored on Wang resin and bearing a free amine and on the other part, an aldehyde with suitable protecting groups on all other functions (Scheme 1). This later building block will be used twice to construct NA from the left to the right part of the molecule (Scheme 2). This new method provided NA, the new natural analogue tNA and non-natural analogues in high yields and purity.

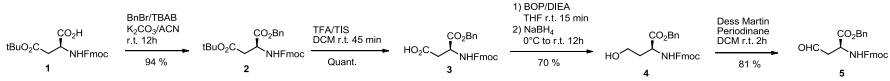

Scheme 1. Synthesis of the aldehyde moiety.

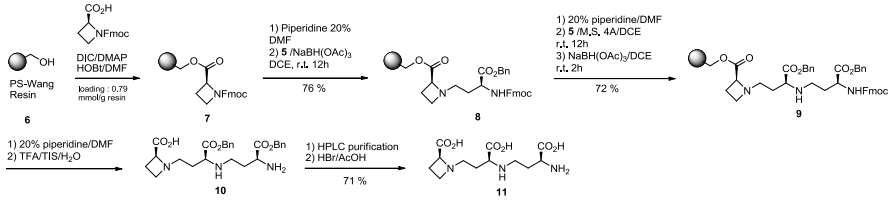

Scheme 2. Supported synthesis of Nicotianamine.

Chelating ability of tNA was investigated and compared to that of NA by MS analysis. It appeared that NA and tNA are able to chelate quantitatively Cu(II), Ni(II) (Figures 1 and 2) and Co(II) at pH = 7.5. Competition studies of metal chelation with NA and tNA showed that Cu(II) complexes are formed first, whereas Ni(II) complexes are thermodynamically more stable. Moreover tNA seemed to chelate Cu(II) preferentially.

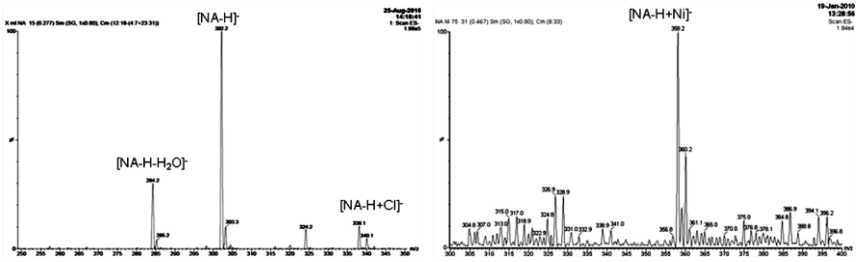

Fig. 1. NA free of metal (left) and NA-Ni(II) chelate (right). MS ESI.

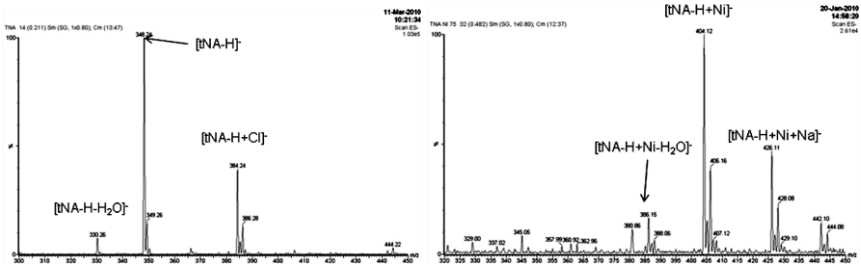

Fig. 2. tNA free of metal (left) and tNA-Ni(II) chelate (right). MS ESI.

Conclusion

We successfully achieved the synthesis of NA, tNA and analogues using an original solid supported methodology and showed the chelating abilities of tNA *in vitro*.

Further studies on metal transport in plant with NA, tNA and non-natural analogues are in progress. The physiological role of the tNA in its host will be also investigated in order to verify the existence of a phylogenetic evolution in metal chelation.

Acknowledgments

This work was supported by the Agence Nationale de la Recherche.

References

1. Noma, M., et al. *Tetrahedron Lett.* **22**, 2017-2020 (1973).
2. Stephan, U.W., et al. *Physiol. Plant* **88**, 522-529 (1993).
3. Fushiya, S., et al. *Heterocycles* **15***,* 819-822 (1981).
4. Ripperger, H., et al. *J. Prakt. Chem.* **329**, 231-234 (1987).
5. Matsuura, F., et al. *Tetrahedron* **50**, 9457-9470 (1994).
6. Shiori, T., et al. *Heterocycles* **44**, 519-530 (1997).
7. Klair, S.S., et al. *Tetrahedron Lett*. **39**, 89-92 (1998).
8. Miyakoshi, K., et al. *Tetrahedron* **57**, 3355-3360 (2001).
9. Bouazaoui, M., et al*. Eur. J. Org. Chem*. (2010) in press.
10. Dreyfus, C., et al. *patent* FR0901574, (2009).
11. Dreyfus, C., et al. *Acta Cryst.* **F64**, 933-935 (2008).
12. Dreyfus, C., et al. *Proc. Nat. Acad. Sci.* **106**, 16180-16184 (2009).
13. Rellán-Alvarez, R., et al. *Rapid Commun. Mass Spectrom*. **22**, 1553-1562 (2008).

Proceedings of the 31st European Peptide Symposium
Michal Lebl, Morten Meldal, Knud J. Jensen, Thomas Hoeg-Jensen (Editors)
European Peptide Society, 2010

Tert-Butylation of Hydroxyl Group Using MTBE

Sorour Ramezanpour and Saeed Balalaie*
Peptide Chemistry Research Center, K. N. Toosi University of Technology, Tehran, P.O.Box 15875-4416, Iran; balalaie@kntu.ac.ir

Introduction

Amino acids with hydroxyl group in side chain exert special functions in biologically active peptides and proteins. Serine, threonine and tyrosine are amino acids which contain hydroxyl group in side chain. In serine and threonine proteases, these two amino acids are involved in the catalytic mechanism. Meanwhile, there are different unusual amino acids such as hydroxy proline with hydroxyl group. Protection of hydroxyl group in the side chain is an essential role for selection of synthesis strategy.

The protecting groups of hydroxyl moieties can be classified into three different types, namely alkyl ethers, carbonic acid esters, and silyl ethers[1].

The protection of hydroxyl group as benzyl ether or *tert*-butyl ether are the most frequently applied protection methods. *Tert*-Butyl ethers could be formed using isobutylene with *p*-toluenesulfonic acid or a concentrated inorganic acid and with different starting materials [1]. This gaseous reagent is volatile and its use can generate high pressures, therefore using isobutylene as a reagent in the laboratory has some disadvantages.

Results and Discussion

The synthesis of *t*-butyl ether usually require isobutylene cylinder and suffer from drawbacks such as laborious synthesis procedure. Thus, the development of a method for synthesis of *t*-butyl ethers using cheap reagents would be desirable. Following our research work about the novel methodologies in synthesis of amino acid derivatives, we concentrated on the new approach for the synthesis of O-*tert* butylated serine derivatives. Herein, we wish to report methyl *tert*-butyl ether (MTBE) as a starting material for the *in situ* generation of isobutylene in the presence of acid. First of all, the starting material [2] was prepared according to the following reaction; a) formation of Z-Ser-OH using Z-ONSu b) protection of C-terminal using *p*-nitro benzyl bromide (Scheme 1).

The role of methyl *t*-butyl ether as a *tert*-butylating agent using different acids and also using different starting materials was investigated. In this approach, reaction of methyl *t*-butyl ether with Z-Ser-ONbz and also $Cl^- H_3N^+$-Ser-OMe was carried out under different reaction conditions.

Firstly, reaction of Z-Ser-ONbz with MTBE or isobutylene in the presence of 60% $HClO_4$ were carried out and the desired *O*-tert butyl ether was formed in 20% and 80% yields, respectively (Scheme 2).

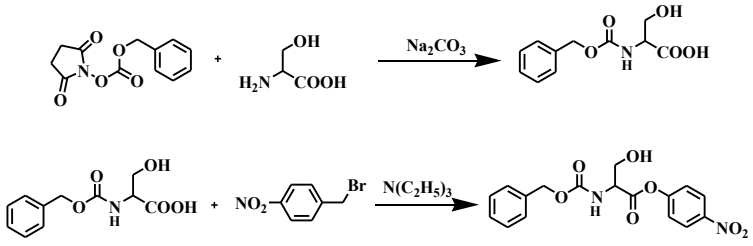

Scheme 1. Synthesis of Z-Ser-ONbz.

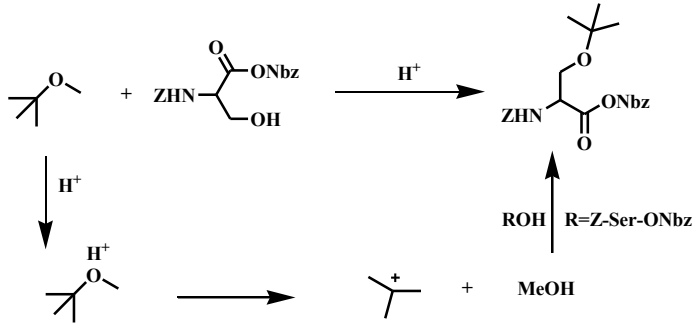

Scheme 2. Mechanism of cleavage MTBE and synthesis of t-butyl ether.

In another experiment, reaction of $Cl^-H_3N^+$-Ser-OMe [3] was carried out using *p*-toluenesulfonic acid with MTBE or isobutylene, but the yield of the desired ether were 10% and 40% respectively. Changing the acid from concentrated inorganic acid to mild silica sulfuric acid leads to low yield of the product.

We described that MTBE could be used as a reagent for *tert*-butylation of free hydroxy group in serine. The yield using this reagent was lower compared to isobutylene, but it is cheaper and the reaction conditions are mild. The proposed mechanism involves the formation of *tert*-butyl cation and finally formation of *O-tert*-butylated product. In spite of the low yield of *O-tert*-butyl ether with MTBE it has some advantages compared to isobutylene. The simplicity of MTBE as a reagent, low cost of the reagent and mild nature of MTBE compared to isobutylene is an attractive point of the protocol described here. All of reactions with MTBE were done at room temprature and atmospheric pressure.

Acknowledgments

This reaction project was supported by Tofigh Daru research company (TODA Co) and we would like to thank Dr. S. Omidvar and Dr. A. Arabanian for financial support**.**

References

1. Reissmann, S., Steinmetzer, T., Greiner, G., Seyfarth, L., Besser, D., Schumann, C. *In Synthesis of Peptides and Peptidomimetics;* Eds. Felix, A., Moroder, M., Toniolo, C. Thieme, Stuttgart, 2004, E22A, 347-387.
2. Wunch, E., Jentsch, J. *Chem. Ber*. **97**, 2490 (1964).
3. Adamson, J., Blaskovich, M.A., Groenevelt, H., Lajoie, G.A. *J. Org. Chem*. **56**, 3447 (1991).

Proceedings of the 31st European Peptide Symposium
Michal Lebl, Morten Meldal, Knud J. Jensen, Thomas Hoeg-Jensen (Editors)
European Peptide Society, 2010

Synthesis of New Polymer Matrices Including Amino Acids

Dantcho L. Danalev[1,2], Jean-Marie Ringeard[1], Stéphane Serfaty[1], Jean-Yves Le Huérou[1], Emmanuel Caplain[1], Lyubov K.Yotova[2], and Pascal Griesmar[1]

[1]Université de Cergy-Pontoise, Cergy-Pontoise, France; [2]University of Chemical Technology and Metallurgy, Sofia, Bulgaria, dancho_danalev@yahoo.com

Introduction

Water is the main constituent of all living things. Many of them can even live only in the water. They change the environment by their abstraction and their releases. Finally, life grows only at low temperature (below 100 °C). However, in this temperature range, water and aqueous media are the optimal condition for corrosion of metals. It is therefore natural that there is interaction between life and corrosion.

Microbiologically induced corrosion (MIC) is a term that is used for a phenomenon where corrosion is caused and develops under the influence of microorganisms [1]. The microorganisms taking part in this process are mainly bacteria [2,3]. Other organisms which could induce MIC are fungi that give off acids or algae that form electrochemical cells [4]. All of this results in MIC. It is considered that 20% of the damages caused by corrosion are due to MIC [5]. Such damages often occur in the aviation industry and are a serious problem today. The water standing at the bottom of the fuel tank creates a favorable environment for the development of microorganisms. They can be aerobic and anaerobic. The aerobic ones tend to produce acid metabolite products which cause corrosion. The anaerobic microorganisms also cause corrosion as they trigger oxidation-reduction reaction. The most often occurring microorganisms contaminating the fuels are the philamentous fungi *Hormoconis resinae*, of the genus *Cladosporium*, *Aspergillus, Fusarium*, yeast of the genus *Candida, Rhodotrula* and bacteria of the genus *Pseudomonas, Acinetobacter, Flavobacterium*. The listed microorganisms are found in different consortia depending on the geographic location, composition of the fuels and the temperature. They form biofilms on the surface of the tanks. The revealing of the composition of the formed biofilms and their role in the corrosion process could turn out to be an important and promising factor in the monitoring of this adverse process. By definition, the biofilms (BF) are structurally and functionally defined communities of microorganisms on various natural and artificial surfaces (Figure 1). BF have a complex structure including cells and substances secreted from them – mainly exopolymer substances (EPS), and a network of microchannels through which water, nourishing and waste substances circulate.

One of the most important factors influencing the formation of BF is the matrix to which the microorganisms attach. Its influence is affected by the structure of its surface, physicochemical properties, the thickness and the hydrodynamic effects which are dependent on the type of the flow, laminar or turbulent. Another important factor is the liquid environment – composition, ion strength, temperature, pH. Not least important is the influence of the properties of the cells and between cells – hydrophobicity of their surface, intrinsic electrical and mechanical interactions, exopolymer substances, etc.

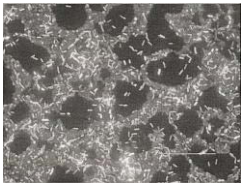

Fig. 1. Polymicrobial biofilms grown on stainless steel surfaces.

Studies on the biodegradation of morpholine and its derivatives Poupin et al. found that one of its analogues thiomorpholine has strong bactericidal properties [6]. This could be used successfully to fight against microbial induced processes by establishing appropriate modified amino acids and their use as protective layer in the tanks and other metal deposits. As part of a diet, proteases which normally function in the bacterial cell would lead to a release of the thiomorpholine, highly toxic to bacteria and their immediate death (bactericide properties).

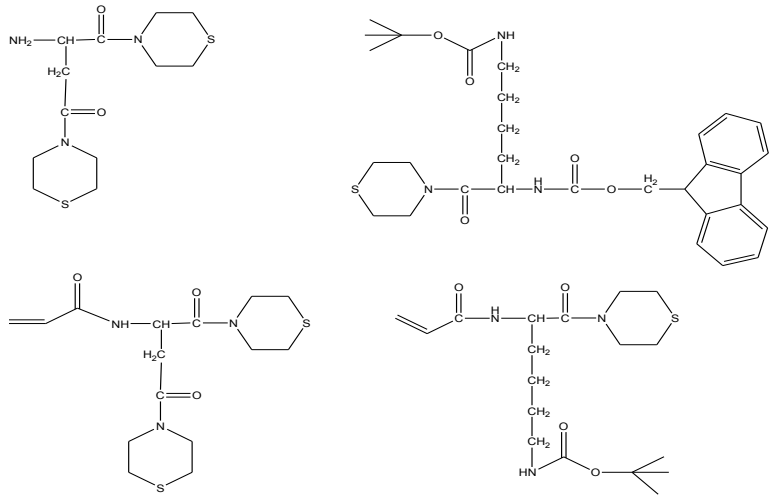

Fig. 2. Structure of morpholinoaspartic acid and morpholinolysine (A) and acrylic acid modified monomers (B).

Results and Discussion

Herein, we report the creation of new hybrid materials with bactericide and bacteriostatic properties based on modified amino acid, incorporated in polymer matrices. Two amino acids (Asp and Lys) were chosen to be modified by thiomorpholine incorporation. This choice was done because of both their different properties (the first one is acid and the second one is basic) and literature data that they could be used as a media for bacteria proliferation. Compounds presented in Figure 2A and 2B were synthesized. These compounds were synthesized using standard coupling procedures in solution by means of TBTU as a coupling reagent. In order to obtain acrylamide derivatives of modified amino acids which can be further polymerized and a new hybrid material to be created, the chloride of acrylic acid was incorporated to N^{α}-amino group of Asp and Lys modified with thiomorpholine. A Schotten-Baumann reaction was used in presence of Et_3N as a base. The polymerizations were induced by AIBN (azobisisobutyronitrile) in DMF at 60^{o}C.

The studies of visco-elastic properties of newly synthesized matrices are in progress. A new technique employing shear waves in the ultrasound range (the so-called "Thickness Shear Mode" technique) is used [7]. This technique is a sensitive method to detect the modification of the structure of the polymer during its formation. It allows to track the rheological parameters of a polymer matrices during the process of formation under the liquid to gel phase by investigation of the following parameters:

- the complex shear modulus (G'(ω), G"(ω) at high frequency giving information about the viscoelasticity of the polymer.
- the complex permittivity (ε'(ω),ε"(ω)) in the radiofrequency region.

References

1. Setareh, M., Javaherdashti, R. *Mater. Corrosion* **54**, 259-263 (2003).
2. Little, B.J., Wagner, P. *Mater. Perf.* **36**, 40-44 (1997).
3. *Cooling Water Treatment Manual, 3rd ed.*, TPC1 Publication, NACE International Publications, Houston, TX.
4. The Institute of Materials, U.K. *A Working Party Report on Microbiological Degradation of Materials and Methods of Protection*, European Federation of Corrosion Publication No. 9, 1992.
5. Flemming, H.-C. *Economical and Technical Overview, Microbially Influenced Corrosion of Materials*, E. Heitz, H.-C. Flemming, W. Sand, Ed., Springer-Verlag, Berlin, 1996.
6. Poupin, P., et al. *Applied and Environmental Microbiology* **64**, 159-165 (1998).
7. Ould-Ehssein, C., et al. *Ultrasonics* **44**, 875-879 (2006).

Proceedings of the 31st European Peptide Symposium
Michal Lebl, Morten Meldal, Knud J. Jensen, Thomas Hoeg-Jensen (Editors)
European Peptide Society, 2010

Convenient Synthesis of Tfm-Dipeptides from Unprotected Enantiopure α-Tfm-Proline and α-Tfm-Alanine

Grégory Chaume, Nathalie Lensen, Caroline Caupène, and Thierry Brigaud

Laboratoire SOSCO, Université de Cergy-Pontoise, 5, mail Gay Lussac, Cergy-Pontoise, F-95000, France

Introduction

The major disadvantages of peptides as therapeutic agents are their rapid degradation by peptidase and their low lipophilicity. In this context, α-trifluoromethyl-α-amino acids (α-Tfm-AAs) are very attractive compounds for the design of biologically active molecules [1]. Their incorporation into peptides increases chemical and thermal stability, resistance to protease degradation and enhances hydrophobicity giving a better affinity for lipid membranes [2]. Moreover, their incorporation into peptides induces particular conformational stabilisations and better auto-assembly [3]. In addition, labeled ^{19}F peptides are of a big interest for structure elucidation and biochemical process investigations [4]. In the course of our studies, we have recently reported efficient and scalable methodologies for the synthesis of enantiopure α-Tfm-AAs [5-9]. Here, we report the synthesis of highly lipophilic dipeptide building blocks from enantiopure α-Tfm-AAs [10].

Results and Discussion

Thanks to a convenient gram-scale strategy for the synthesis of (*S*)- and (*R*)-α-Tfm-prolines [12], we were able to undertake a methodological study in order to incorporate this promising unnatural amino acid in a peptide chain. We anticipated that α-Tfm-AAs should be deployable in peptide coupling reactions without protection of their nitrogen atoms due to the strong deactivation of the amino group by the CF_3 group. The peptide coupling methodological study allowed us to establish the best coupling conditions to avoid the formation of the diketopiperazine side product and to optimize the coupling yield. Thus, one equivalent of α-Tfm-proline is added to two equivalent amount of the non-fluorinated amino acid in the presence of the coupling reagents HOBt/EDCI. These optimized conditions were then successfully applied to the coupling of various amino acids with unprotected α-Tfm-proline (Figure 1). The enantiopure dipeptides derived from unprotected (*S*)-α-Tfm-proline and alanine, valine, phenylalanine and leucine were conveniently obtained in good yields (76-95%) without any traces of diketopiperazine. The coupling reaction starting from unprotected (*R*)-α-Tfm-proline was also very efficient.

In order to extend the methodology to acyclic α-Tfm-AAs, the coupling of α-Tfm-alanine [8] was investigated. Coupling reactions between unprotected (*R*)-α-Tfm-alanine and non-fluorinated α-amino acids were achieved following the same procedure designed for α-Tfm-proline. The corresponding dipeptides were conveniently obtained in 77-82% isolated yields without formation of diketopiperazine (Figure 2).

As a proof-of-concept of the incorporation of enantiopure α-Tfm-AAs into peptide chains, coupling reaction of the (*R*)-α-Tfm-Ala-L-Leu-OBn dipeptide at its *N*-terminus was

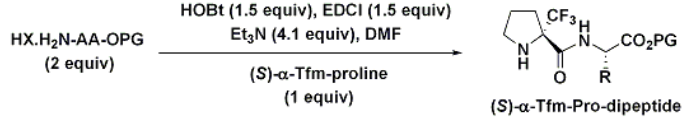

X	R	PG	α-Tfm-Pro	Yield (%)
OTs	Me	Bn	(*S*)	95
OTs	Me	Bn	(*R*)	87
Cl	*i*-Pr	*t*-Bu	(*S*)	87
Cl	Bn	*t*-Bu	(*S*)	76
OTs	*i*-Bu	Bn	(*S*)	80

Fig. 1. α-Tfm-Proline containing dipeptides.

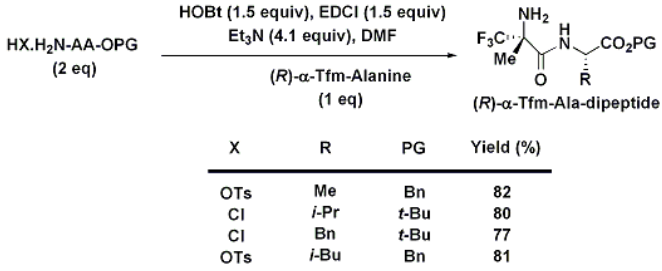

X	R	PG	Yield (%)
OTs	Me	Bn	82
Cl	*i*-Pr	*t*-Bu	80
Cl	Bn	*t*-Bu	77
OTs	*i*-Bu	Bn	81

Fig. 2. α-Tfm-Alanine containing dipeptides.

investigated. Because of the strong deactivation of the amino group and the steric bulkiness of the CF_3 group, specific activation methods (mixed anhydrides [11] or amino acid bromides [12-14]) were already reported in the literature for *N*-terminal couplings of α-Tfm-AAs. In order to elaborate a tripeptide building block suitably protected for peptide synthesis, we decided to perform the coupling reaction with an Fmoc-protected amino acid chloride. The corresponding tripeptide was obtained in 74% yield without any epimerization (Figure 3).

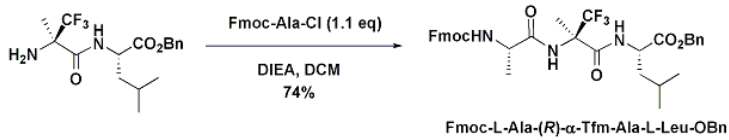

Fig. 3. α-Tfm-Alanine containing tripeptide.

Acknowledgments
We thank Central Glass Company for financial support. We also thank the French Fluorine Network.

References

1. Ojima, I. *Fluorine in Medicinal Chemistry and Chemical Biology* Wiley, 2009.
2. Koksch, B., Sewald, N., Hofmann, H.-J., Burger, K., Jakubke, H.-D. *J. Pept. Sci.* **3**, 157-167 (1997).
3. Jäckel, C., Koksch, B. *Eur. J. Org. Chem.* 4483-4503 (2005).
4. Maisch, D., Wadhwani, P., Afonin, S., Bottcher, C., Koksch, B., Ulrich, A.S. *J. Am. Chem. Soc.* **131**, 15596-15597 (2009).
5. Huguenot, F., Brigaud, T. *J. Org. Chem.* **71**, 7075-7078 (2006).
6. Huguenot, F., Brigaud, T. *J. Org. Chem.* **71**, 2159-2162 (2006).
7. Chaume, G., Van Severen, M.C., Marinkovic, S., Brigaud, T. *Org. Lett.* **8**, 6123-6126 (2006).
8. Chaume, G., Van Severen, M.C., Ricard, L., Brigaud, T. *J. Fluorine Chem.* **129**, 1104-1109 (2008).
9. Caupène, C., Chaume, G., Ricard, L., Brigaud, T. *Org. Lett.* **11**, 209-212 (2009).
10. Chaume, G., Lensen, N., Caupène, C., Brigaud, T. *Eur. J. Org. Chem.* 5717-5724 (2009).
11. Koksch, B., Quaedflieg, P.J.L.M., Michel, T., Burger, K., Broxterman, Q.B., Schoemaker, H.E. *Tetrahedron: Asymmetry* **15**, 1401-1407 (2004).
12. Dal Pozzo, A., Bergonzi, R., Ni, M. *Tetrahedron Lett.* **42**, 3925-3927 (2001).
13. Dal Pozzo, A., Ni, M., Muzi, L., de Castiglione, R., Mondelli, R., Mazzini, S., Penco, S., Pisano, C., Castorina, M., Giannini, G. *J. Med. Chem.* **49**, 1808-1817 (2006).
14. Dal Pozzo, A., Ni, M., Muzi, L., Caporale, A., de Casteglione, R., Kaptein, B., Broxterman, Q.B., Fromaggio, F. *J. Org. Chem.* **67**, 6372-6375 (2002).

Proceedings of the 31st European Peptide Symposium
Michal Lebl, Morten Meldal, Knud J. Jensen, Thomas Hoeg-Jensen (Editors)
European Peptide Society, 2010

Concise Access to (*S*)- and (*R*)-α-Tfm Serine and α-Tfm Aspartic Acid From Chiral Trifluoromethyloxazolidines (Fox)

Julien Simon, Thuan Nguyen, Grégory Chaume, Evelyne Chelain, Nathalie Lensen, Julien Pytkowicz, and Thierry Brigaud
Laboratoire SOSCO, Université de Cergy-Pontoise, 5, mail Gay Lussac, Cergy-Pontoise, F-95000, France

Introduction

α-Trifluoromethylated amino acids (α-Tfm AAs) are current synthetic targets due to the unique physical and biological properties imparted by the fluorinated group. However, their preparation in enantiopure form remains a challenge [1-3]. Our group is involved in the development of efficient synthetic routes for the preparation of enantiopure α-Tfm AAs starting from chiral CF_3-oxazolidines (Fox) or imines [4-9] and their incorporation into a peptide chain [10]. We will report here the straightforward preparation of both enantiomers of α-Tfm-serine and α-Tfm-aspartic acid in enantiopure form starting from oxazolidines derived respectively from ethyl trifluoropyruvate and ethyl 4,4,4-trifluoroacetoacetate (ETFAA). The key step of both synthesis involves a Strecker-type reaction.

Results and Discussion

The synthesis of both enantiomers of α-Tfm-serine started with the preparation of the chiral CF_3-oxazolidine derived from ethyl trifluoropyruvate and (*R*)-phenylglycinol (Figure 1). We already reported that when using $LiAlH_4$ as reducing reagent, the ester reduction of the oxazolidine was accompanied with its ring opening [11]. Nevertheless, we hypothesized that the use of a less reactive reducing reagent should allow the chemoselective reduction of the ester group thank to the high degree of activation of the ester moiety by the CF_3 group. Thus, using $NaBH_4$, the ester group of the oxazolidine was selectively reduced. A

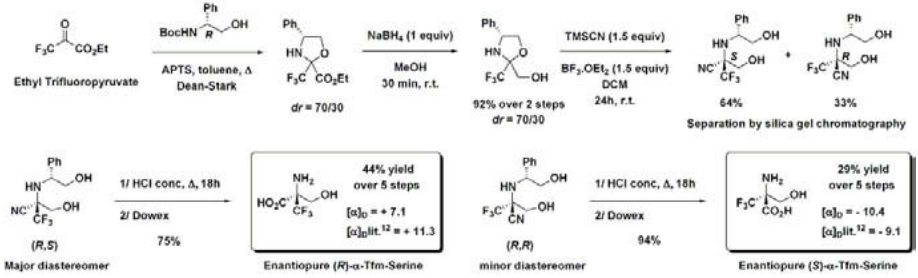

Fig. 1. Synthesis of (S)- and (R)-α-Tfm-Serine in enantiopure form.

Strecker-type reaction was then successfully performed to afford the corresponding amino nitriles. After separation of the respective major (*S*,*R*) and minor (*R*,*R*) diastereomer by silica gel chromatography, the clean removal of the chiral auxiliary and hydrolysis of the nitrile group occurred in a one step procedure using concentrated HCl to afford respectively the (*R*)- and the (*S*)-α-Tfm-serine in enantiopure form and in good overall yield. Absolute configuration was attributed thanks to correlation with the optical rotation reported in the literature [12].

The straightforward access of both enantiomers of α-Tfm-aspartic acid involved the preparation of the ethyl 4,4,4-trifluoroacetoacetate-based CF_3-oxazolidine. Following a

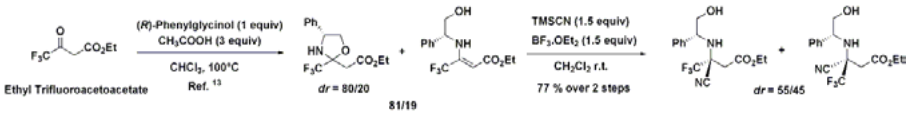

Fig. 2. Strecker-type reaction from ethyl 4,4,4-trifluoroacetoacetate-based CF_3-oxazolidine.

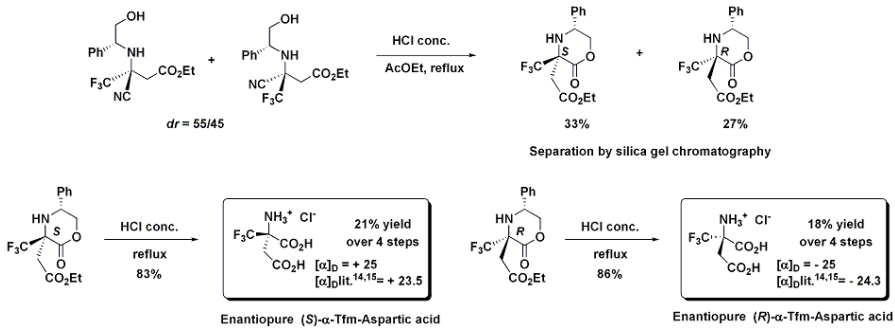

Fig. 3. Synthesis of (S)- and (R)-α-Tfm–Aspartic Acid in enantiopure form.

described procedure [13], the expected CF_3-oxazolidines were obtained in a 80/20 diastereomeric ratio in mixture with the enamine derivative (Figure 2). The crude mixture was then engaged in the Strecker-type reaction to afford the corresponding amino nitriles.

At this stage, an acidic treatment of the amino nitriles in ethyl acetate allowed the hydrolysis of the cyano group and the formation of the corresponding morpholinones (Figure 3). A concentrated HCl treatment of the separated (*S*,*R*) and (*R*,*R*) diastereomers provided the clean removal of the chiral auxiliary and the hydrolysis of the ester group to give respectively the (*S*)- and the (*R*)-α-Tfm aspartic acid in enantiopure form and in good overall yield. The absolute configuration was again determined by correlation with the optical rotation reported in the literature [14,15].

Acknowledgments

We thank Central Glass Company for financial support. We also thank the French Fluorine Network.

References

1. Smiths, R., Cadimaco, C.D., Burger, K., Koksch, B. *Chem. Soc. Rev.* **37**, 1727-1739 (2008).
2. Kukhar, V.P., Soloshonok, V.A. *Fluorine Containing Amino Acids: Synthesis and Properties.* Wiley, New York, 1995.
3. Brigaud, T., Chaume, G., Pytkowicz, J., Huguenot, F. *Chim. Oggi.* **25**, 8-10 (2007).
4. Lebouvier, N., Laroche, C., Huguenot, F., Brigaud, T. *Tetrahedron Lett.* **43**, 2827-2830 (2002).
5. Huguenot, F., Brigaud, T. *J. Org. Chem.* **71**, 2159-2162 (2006).
6. Huguenot, F., Brigaud, T. *J. Org. Chem.* **71**, 7075-7078 (2006).
7. Caupène, C., Chaume, G., Ricard, L., Brigaud, T. *Org. Lett.* **11**, 209-212 (2009).
8. Chaume, G., Van Severen, M.C., Ricard, L., Brigaud, T. *J. Fluorine Chem.* **129**, 1104-1109 (2008).
9. Chaume, G., Van Severen, M.C., Marinkovic, S., Brigaud, T. *Org. Lett.* **8**, 6123-6126 (2006).
10. Chaume, G., Lensen, N., Caupène, C., Brigaud, T. *Eur. J. Org. Chem.* 5717-5724 (2009).
11. Pytkowicz, J., Stéphany, O., Marinkovic, S., Inagaki, S., Brigaud, T. *Org. Biomol. Chem.* ASAP DOI: 10.1039/C0OB00424C (2010).
12. Bravo, P. Viani, F., Zanda, M., Soloshonok, V.A. *Gazz. Chim. Ital.* **125**, 149-150 (1995).
13. Ishida, Y., Iwahashi, N., Nishizono, N., Saigo, K. *Tetrahedron Lett.* **50**, 1889-1892 (2009).
14. Lazzaro, F., Gissot, A., Crucianelli, M., De Angelis, F., Bruché, L., Zanda, M. *Lett. Org. Chem.* **2**, 235-237 (2005).
15. Lazzaro, F., Crucianelli, M., De Angelis, F., Frigerio, M., Malpezzi, L., Volonterio, A., Zanda, M. *Tetrahedron: Asymmetry* **15**, 889-893 (2004).

Proceedings of the 31st European Peptide Symposium
Michal Lebl, Morten Meldal, Knud J. Jensen, Thomas Hoeg-Jensen (Editors)
European Peptide Society, 2010

CF_3-Pseudoprolines: Synthesis and Conformational Study of Hydrolytically Stable Proline Surrogate Containing Dipeptides

Olivier Barbeau[1], Caroline Caupène[1], Debby Feytens[2], Grégory Chaume,[1] Philippe Lesot[3], Emeric Miclet[2], and Thierry Brigaud[1]

[1]Laboratoire SOSCO, Université de Cergy-Pontoise, 5, mail Gay Lussac, Cergy-Pontoise, F-95000, France; [2]Laboratoire des biomolécules, Université Pierre et Marie Curie, UMR 7203, 75005, Paris, France; [3]RMN en Milieu Orienté, ICMMO, UMR CNRS 8182, Bat. 410, Université Paris Sud 11, Orsay, 91405, France

Introduction

The incorporation of proline derivatives is known to restrict the peptide bond *cis*/*trans* isomerization, to control the protein folding and consequently to modulate the biological activity of peptides. Pseudoproline residues (ΨPro) proved to be versatile tools for overcoming the aggregation encountered during solid phase peptide synthesis.[1,2] They also turned out to be inducers of β-turns containing predominantly *cis*-amide bond and useful tools in peptide cyclization. Our group is interested in the development of efficient routes for the preparation of enantiopure α-trifluoromethylated amino acids (α-Tfm AAs), [3,4] particularly pyrrolidine-type α-Tfm AAs [4-6] and their incorporation into a peptide chain [7]. Here, we will report the preparation of various CF_3-ΨPro as well as the methodological study developed to optimize the synthesis of various *C*-terminal and *N*-terminal CF_3-ΨPro containing dipeptides. Their conformation and their stability toward hydrolysis have been also studied and will be detailed.

Results and Discussion

Three CF_3-ΨPro esters were conveniently prepared through the condensation reaction of trifluoroacetaldehyde ethyl hemiacetal or trifluoroacetone with serine or cysteine ester derivatives (Figure 1) [8]. The isolated diastereomerically pure CF_3-ΨPro esters are extremely stable thanks to the strong electron-withdrawing effect of CF_3 group. Therefore, there is no epimerization at the C-2 center of the oxazolidine ring through ring-opening and ring-closing equilibrium.

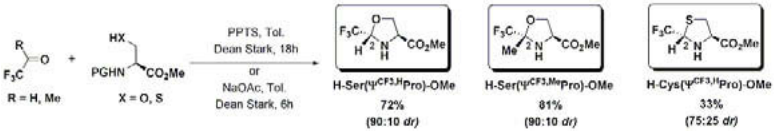

Fig. 1. Preparation of the CF_3-pseudoprolines.

Then, we turned our attention to the incorporation of CF_3-ΨPro units into a peptide chain. First, we studied the coupling reaction at their *C*-terminus position. After saponification, the reaction of both diastereomers of H-Ser($\Psi^{CF3,H}$pro)-OMe with L-alanine using standard peptide coupling reagents gave the corresponding dipeptides in moderate to good yield, depending to the absolute CF_3 configuration (Figure 2). It should be noticed that the protection of the CF_3-ΨPro amino group is not required due to the deactivation imparted by the CF_3 group.

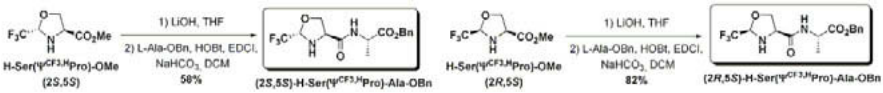

Fig. 2. Preparation of N-terminal CF_3- ΨPro containing dipeptides.

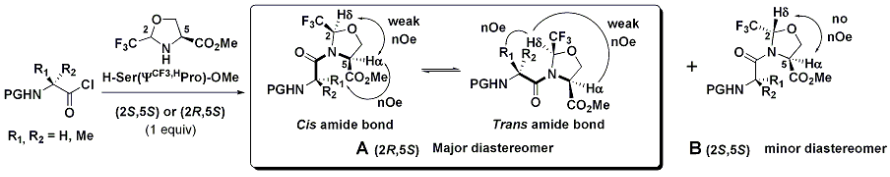

Amino acid (equiv)	Ψpro	Yield	A/B	*cis/trans* amide bond ratio of A[b]	Pdt
Nbs-Ala-Cl (7)	(2*S*,5*S*)	89%[a]	(85/15)	47/53	Nbs-Ala-Ser($\Psi^{CF3,H}$Pro)-OMe
Nbs-Ala-Cl (7)	(2*R*,5*S*)	91%[a]	(73/27)		
Nbs-Aib-Cl (7)	(2*S*,5*S*)	66%[a]	(100/0)	100/0	Nbs-Aib-Ser($\Psi^{CF3,H}$Pro)-OMe
Fmoc-Gly-Cl (1.1)	(2*S*,5*S*)	98%	(100/0)	39/61	Fmoc-Gly-Ser($\Psi^{CF3,H}$Pro)-OMe
Fmoc-Gly-Cl (1.1)	(2*R*,5*S*)	97%	(100/0)		
Fmoc-Ala-Cl (1.1)	(2*S*,5*S*)	89%	(82/18)	86/14	Fmoc-Ala-Ser($\Psi^{CF3,H}$Pro)-OMe
Fmoc-Ala-Cl (1.1)	(2*R*,5*S*)	84%	(91/9)		
Fmoc-Aib-Cl (2)	(2*S*,5*S*)	28%	(100/0)	100/0	Fmoc-Aib-Ser($\Psi^{CF3,H}$Pro)-OMe
Fmoc-Aib-Cl (3)	(2*R*,5*S*)	45%	(100/0)		

[a] 1 equiv of collidine was used for the coupling reaction
[b] ratio determined by ^{19}F & ^{1}H NMR in $CDCl_3$ at 273K

Fig. 3. Preparation of C-terminal CF_3-ΨPro containing dipeptides and cis/trans isomerization.

Coupling reactions at the deactivated *N*-terminal position were first performed following a reported procedure [9] and required the use of amino acid halides. Optimization of the reaction allowed the Fmoc-peptide synthesis in base free condition in excellent yield with glycine and alanine (Figure 3). A moderate yield was obtained for the bulky Aib amino acid. In all cases, starting from (2*R*,5*R*)- or (2*R*,5*S*)-oxazolidine, an epimerization occurred at C_2 center to give the major (2*R*,5*S*)-oxazolidine containing dipeptide diastereomer **A**. This result was confirmed by nOe experiments showing the presence of nOe signal between Hα and Hδ. Conformational study of the *cis*/*trans* isomerization ratio of the amide bond for **A** by nOe indicates that the *cis* conformation is largely favored from the moment that R_1 group is not H.

Acknowledgments
We thank the CNRS for the grant to O.B. and Central Glass Co. for financial support and the gift of trifluoroacetaldehyde hemiacetal. We also thank the French Fluorine Network.

References

1. Dumy, P., Keller, M., Ryan, D.E., Rohwedder, B., Wohr, T., Mutter, M. *J. Am. Chem. Soc.* **119**, 918-925 (1997).
2. Keller, M., Sager, C., Dumy, P., Schutkowski, M.; Fisher, G.S., Mutter, M. *J. Am. Chem. Soc.* **120**, 2714-2720 (1998).
3. Huguenot, F., Brigaud, T. *J. Org. Chem.* **71**, 7075-7078 (2006).
4. Chaume, G., Van Severen, M.C., Marinkovic, S., Brigaud, T. *Org. Lett.* **8**, 6123-6126 (2006).
5. Chaume, G., Van Severen, M.C., Ricard, L., Brigaud, T. *J. Fluorine Chem.* **129**, 1104-1109 (2008).
6. Caupène, C., Chaume, G., Ricard, L., Brigaud, T. *Org. Lett.* **11**, 209-212 (2009).
7. Chaume, G., Lensen, N., Caupène, C., Brigaud, T. *Eur. J. Org. Chem.* 5717-5724 (2009).
8. Chaume, G., Barbeau, O., Lesot, P., Brigaud, T. *J. Org. Chem.* **75**, 4135-4145 (2010).
9. DalPozzo, A., Bergonzi, R., Ni, M. *Tetrahedron Lett.* **42**, 3925-3927 (2001).

Proceedings of the 31st European Peptide Symposium
Michal Lebl, Morten Meldal, Knud J. Jensen, Thomas Hoeg-Jensen (Editors)
European Peptide Society, 2010

Solid Phase Synthesis Substituted Peptide Amides on Aryl Hydrazine Resin

Witold A. Neugebauer[1], Anna Kwiatkowska[2], Xue Wen Yuan[1], and Robert Day[1]

[1]Institut de pharmacologie de Sherbrooke, Université de Sherbrooke, Sherbrooke, J1H 5N4, Québec, Canada; [2]Faculty of Chemistry, University of Gdańsk, Sobieskiego 18, 80-952, Gdańsk, Poland

Introduction

Solid phase syntheses in classical approach starts with attachments of the first amino acid to resin for free acid to form an ester link or an amide bond to form a peptide amide. Such an approach could be applied when *C*-terminal residue desired peptide does possess at *C*-terminus a functional group (carboxyl group). Y. Kwan, et al. [1] presented an approach to synthesize p-nitroanilides and other anilides analogues using aryl hydrazine resin. We used [2] a very similar approach to synthesize Pyr-Arg-Thr-Lys-Arg-AMC with a slightly modified procedure. Presently, we show application of this procedure for synthesis *C*-terminal aliphatic amides on solid phase manner. Peptide less *C*-terminal residue (amine) is synthesized on 4-Fmoc-hydrazinobenzoyl AM NovaGel resin (Novabiochem). *N*-terminal residue of the sequence should not be exposed with free amino group for the cleavage/amidation step.

Methods

Peptide synthesis: The peptide synthesis procedure (Figure 1) is based on solid-phase continuous flow (Fmoc) strategy on aryl hydrazine resin. A whole sequence less *C*-terminus amine residue was assembled. When this synthesis is completed, the fully protected peptide aryl hydrazine resin is oxidized with NBS in presence of pyridine. The resulting acyl diazene resin is then cleaved by peptide displacement at *C*-terminus with amine. The protected peptide amide is then deprotected with TFA and purified (C18 chromatography column acetonitrile gradient in water with 0.1% TFA). Finally peptide amides were identified by MALDI mass spectrometry and their purity determined by analytical HPLC.

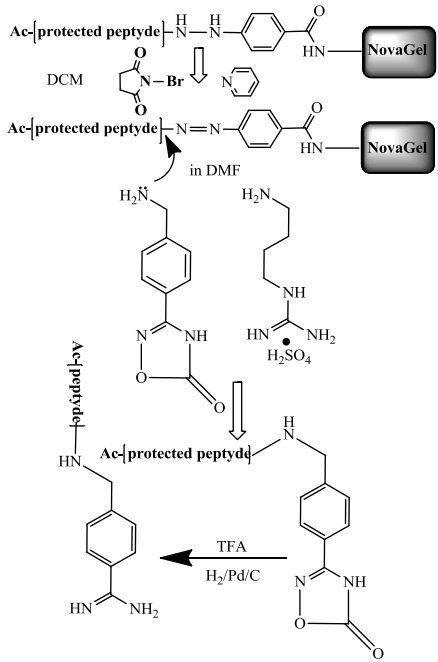

Fig. 1. Scheme of general synthesis of peptide-substituted amide.

Results and Discussion

Cleavage/displacement reaction efficiency depends on amine nucleophilicity which in case of aromatic amines is not significant. Aliphatic amines should have much more nucleophilicity than aromatic amines (aniline, AMC) and therefore should react faster and more efficient in the described procedure. In our approach we used

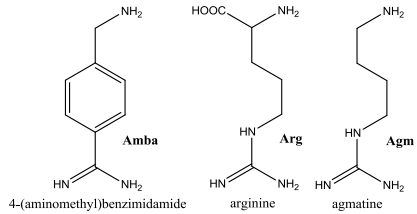

Fig. 2. Structure of arginine mimetics.

aliphatic amines (Figure 1) as decarboxyl amino acid derivatives, which could mimic (Figure 2) peptide *C*-terminus residue. Several peptide substituted amides were efficiently synthesized on solid-phase. As an example of usefulness this method, we present two new analogues of our previously developed PACE4 inhibitor: *Ac*-LLLLRVKR-NH_2 [3]. *C*-terminus arginine amide we replaced with substituted amines [arginine mimetics (Figure 2)]: agmatine (Agm) and 4-(aminomethyl)benzimidamide (Amba) [4] and our new inhibitors, *Ac*-LLLLRVK-*Agm*; *Ac*-LLLLRVK-*Amba,* were tested as convertase inhibitors with improved K_i in particular for PACE4 (Table 1).

Table 1. Inhibitory constant [K_i] of synthesized analogues

Peptide	*K_i [nM] against PACE4*
Ac-LLLLRVKR-NH_2	18.72
Ac-LLLLRVK-*Agm*	11.77
Ac-LLLLRVK-*Amba*	0.24

The yield of the crude product from this reaction was reasonably good, however a significant amount of brominated side products were detected. Such bromination might be caused by active bromine of NBS and maybe alternative hydrazide oxidation to diazene with Cu (II) acetate could be used. The *C*-terminal modified peptides were obtained and epimerization was not noticed. Biological activity of synthesized inhibitors confirmed their stereo chemical purity. The aryl hydrazide resin-linker is one of the most useful resins for the synthesis of chemically *C*-terminally modified peptides [5] to amides, substituted amides, nitroanilides, thioesters, acids and esters [6]. The aryl hydrazide resins were also used for the solid-phase head-to-tail peptide cyclization [7].

Acknowledgments
This work is supported by research grants to RD from the Canadian Institutes of Health Research (CIHR) and the Ministère du Développement Économique, de l'Innovation et de l'Exportation (MDEIE) du Québec.

References

1. Kwon, Y., Welsh, K., Mitchell, A.R., Camarero, J.A. *Organic Letters* **6**(21), 3801-3804 (2004).
2. Neugebauer, W.A., Parent, A., Yuan, Xue Wen, Day, R. *Adv. Exp. Med. Biol*. **611**, 371-372 (2009).
3. Day, R., Fugère, M., Neugebauer, W.A. International patent application no. PCT/CA2009/000935; Jan 14, 2010.
4. Becker, G.L., Sielaf, F., Than, M.E., Lindberg, I., Routhier, S., Day, R., Lu, Y., Garten, W., Steinmetzer, T. *J. Med. Chem.* **11,** 1067-1075 (2010).
5. Woo, Y-H., Michell, A.R., Camarero, J.A. *Int. J. of Peptide Res. and Therapeutics* **13**, (1-2) 181-190 (2006).
6. Peters, C., Waldman, H. *J. Org. Chem*. **68**, 6053-6055 (2003).
7. Rosenbaum, C., Waldman, H. *Tetrahedron Letters* **42**, 5677-5680 (2001).

Proceedings of the 31st European Peptide Symposium
Michal Lebl, Morten Meldal, Knud J. Jensen, Thomas Hoeg-Jensen (Editors)
European Peptide Society, 2010

Solid-Phase Synthesis of *C*-Terminus Chloromethyl Ketone Peptides

Witold A. Neugebauer[1], Nabil G. Seidah[2], Delia Susan-Resiga[2], Xue Wen Yuan[1], and Robert Day[1]

[1]Institut de pharmacologie de Sherbrooke, Université de Sherbrooke, 3001, 12e Avenue Nord, Sherbrooke, J1H 5N4, Québec, Canada; [2]Institut de recherches cliniques de Montréal 110 West Pine Ave, Montreal, H2W 1R7, Québec, Canada

Introduction

Halomethyl ketones and in particular chloromethyl ketones are important tools in enzyme inhibitory studies. Chloromethyl ketones of amino acids, their analogues and peptides are the most commonly used. There are numerous ways to make halomethyl ketones of amino acids or peptides in solution. A transformation of molecules such as amino acids to their chloromethyl ketones in classical organic synthesis is relatively easy. Peptide chloromethyl ketone preparations give more problems due to peptide solubility, stereochemistry when couples from C-side of the peptide or peptide direct transformation to chloromethyl ketone. Solid-phase synthesis of peptide chloromethyl ketone would eliminate most of those problems. Classical solid phase synthesis of such chloromethyl ketone peptide could not be applied due to missing C-terminal carboxyl group. A new strategy, used by Kwon, et al. [1] to build a peptide on special aryl hydrazine resin (Figure 1) and cleave assembled peptide sequence (without the last C-terminal chloromethyl ketone) with hydrochloride of chloromethyl ketone residue was used. Synthesized peptides: subtilisin/kexin-like isozyme-1 SKI-1 [called also Site-1 protease] inhibitors (Figure 2) were tested on their inhibitory potency (Figure 3).

Methods

Peptide synthesis: Peptides were synthesized (Figure 1) using continuous flow synthesizer with Fmoc strategy. The protected peptide-resin less C-terminal chloromethyl ketone residue was then mildly oxidized to diazene and displaced from the resin with amino acid chloromethyl ketone derivative. Solvent was evaporated and peptides were then deprotected (TFA/TIPS/water). Peptide salts were precipitated in anhydrous ethyl ether, filtered, dissolved in 25% acetic acid and lyophilized. The crude peptides were finally purified by C18 column chromatography in acetonitrile gradient in water with 0.1% TFA. Peptide identities were confirmed by MALDI mass spectrometry and their chromatographic purity verified by analytical HPLC.

Source of recombinant hSKI-1: Soluble human SKI-1, lacking the transmembrane domain and cytosolic tail, hSKI-1-BTMD, was isolated from overnight media of HEK 293 cells infected with a recombinant vaccinia virus (VV) vector, VV:hSKI-1-BTMD. Upon collection and cell debris removal by centrifugation, the media was concentrated 5-fold on an Amicon Ultracel 30K (Milipore) and stored at -20°C as a 20% glycerol solution. Overnight media from HEK293 cells infected with vv:wild type (WT) that was prepared as above was used as a background activity control.

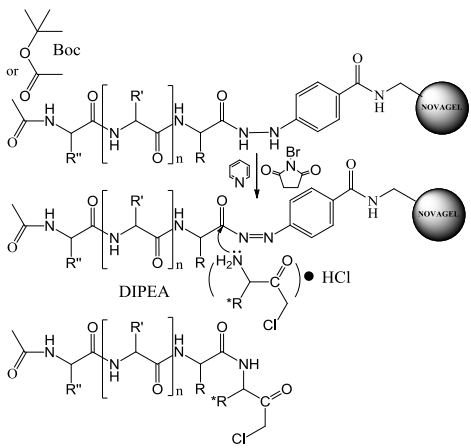

Fig. 1. Scheme of general peptide-chloromethyl ketone synthesis.

In vitro enzymatic assay: Reactions were performed at 37°C in 100 ml. Each reaction mixture consisted of: buffer (25 mM TRIS-HCl, 25 mM MES, 1 mM $CaCl_2$, adjusted to pH 7.5), 40 ml vv:hSKI-1-BTMD or vv:WT, 20 mM inhibitor peptides or DMSO in equi-valent volume, and 200 mM fluorogenic

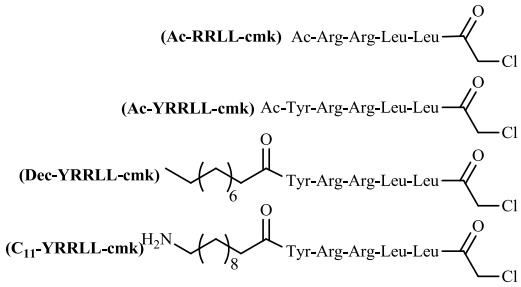

Fig. 2. Synthesized -chloromethyl ketone peptides.

substrate Ac-RRLL-MCA. The inhibitor peptides (RRLL-cmk derived peptides I-IV and Dec-RRLL-cmk) stock solutions were prepared in DMSO at 10 mM peptide concentration. The solutions containing vv:hSKI-1-BTMD or vv:WT and inhibitor peptides or DMSO were pre-incubated for 20 min at 37°C prior to initiation of the reaction by addition of the fluorogenic substrate Ac-RRLL-MCA. Enzymatic activity measurements were performed by monitoring the liberated AMC group with a SpectraMax Gemini EM microplate spectrofluorometer (Molecular Devices) (λ_{ex}=360 nm; λ_{em}=470 nm with a cutoff filter set at 435 nm). For each inhibitor, the background activity measured in the presence of vv:WT was subtracted from the enzymatic activity measured in the presence of vv:hSKI-1-BTMD.

Results and Discussion

Any given peptide sequence can be synthesized as chloromethyl ketone (with available amino acid chloromethyl ketone derivative) in the described way. As an example, we synthesized several SKI-1 inhibitors and demonstrated their inhibitory potency and validation of used procedure (Figure 3).

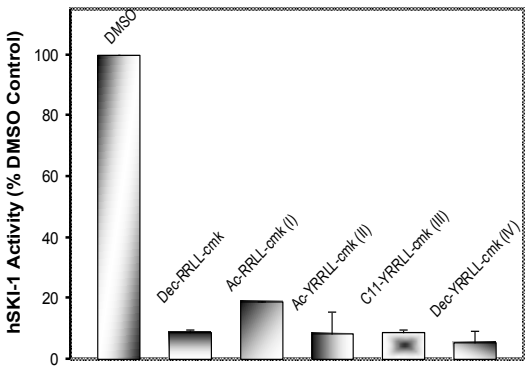

Fig. 3. The RRLL-cmk derived peptides I-IV and Dec-RRLL-cmk show similar inhibitory activity of the in vitro processing of Ac-RRLL-MCA by SKI-1. Inhibitor peptides (20 mM) or DMSO (control) and hSKI-1 were preincubated for 20 min at 37°C before initiation of the reaction by addition of 200 mM fluorogenic substrate, Ac-RRLL-MCA. hSKI-1 activity is expressed as % of the activity measured in the presence of DMSO control (averages, n=2, ± S.D.).

Acknowledgments

This work is supported by research grants to RD and NGS from the Canadian Institutes of Health Research (CIHR) and the Ministère du Développement Économique, de l'Innovation et de l'Exportation (MDEIE) du Québec.

References

1. Kwon, Y., Welsh, K., Mitchell, A.R., Camarero, J.A. *Organic Letters* **6**(21), 3801-3804 (2004).

Proceedings of the 31st European Peptide Symposium
Michal Lebl, Morten Meldal, Knud J. Jensen, Thomas Hoeg-Jensen (Editors)
European Peptide Society, 2010

Photo-Uncaging of Neurotransmitter Amino Acids From Fluorescent 5,6-Benzocoumarinyl Precursors

Maria José G. Fernandes, M. Sameiro T. Gonçalves, and Susana P.G. Costa

Centre of Chemistry, University of Minho, Campus of Gualtar, 4710-057 Braga, Portugal

Introduction

Photoactivable precursors of bioactive molecules (caged compounds) are important research tools for tracking molecular dynamics with high spatiotemporal resolution in biological systems [1]. A diversity of structures, such as 2-nitrobenzyl [2], 1-(4,5-dimethoxy-2-nitrophenyl)-ethyl [3], 4,5-dimethoxy-2-nitrobenzyl [4], 6-bromo-7-hydroxy-coumarin-4-yl-methyl [5], 7-[(diethyl-amino)-coumarin-4-yl]-methyl [6] and 7-dinitro-indolinyl [7] have been evaluated as caging groups for the photo-regulation of calcium ions, neurotransmitters, carboxylic acids, proteins, nucleotides, peptides, RNAs and DNAs [8].

Having in mind these facts and as a continuation of our work related with the investigation of alternative photolabile protecting groups [9], we now report the evaluation of the release under irradiation of β-alanine, tyrosine, 3,4-dihydroxyphenylalanine (DOPA) and glutamic acid neurotransmitters from the corresponding 5,6-benzocoumarinyl fluorescent conjugates. Photo-uncaging studies were carried out at 254, 300 and 350 nm and cleavage kinetic data obtained by HPLC/UV monitoring.

Results and Discussion

5,6-Benzocoumarinyl-neurotransmitter amino acids conjugates **1a-e** were obtained by cleavage of *N*-benzyloxycarbonyl or *N-tert*-butyloxycarbonyl groups under usual chemical deprotection conditions from the corresponding precursors with β-alanine, tyrosine, 3,4-dihydroxyphenylalanine and glutamic acid [9c] (Figure 1). The benzo-coumarinyl moiety will be designated in this report by a three-letter code (Bba) for simplicity of naming the various fluorescent conjugates, as indicated in Table 1.

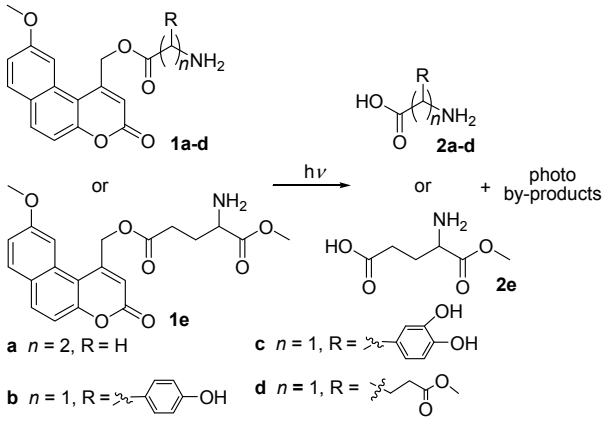

*Fig. 1. Photo-uncaging of neurotransmitter amino acids **2a-e** from the corresponding 5,6-benzocoumarinyl conjugates **1a-e**.*

The sensitivity of conjugates **1a-e** towards UV-visible irradiation was evaluated by exposing solutions of the mentioned compounds in ACN/HEPES buffer (80:20) solution in a Rayonet RPR-100 reactor at 254, 300 and 350 nm. The course of the photocleavage reaction was followed by reverse phase HPLC with UV detection. The plots of peak area (*A*) of the starting material *versus* irradiation time were obtained for each compound at the considered wavelengths. Peak areas were determined by HPLC, which revealed a gradual decrease with time, and were the average of three runs. The determined irradiation time represents the time necessary for the consumption of the starting materials until less than 5% of the initial area was detected (Table 1).

*Table 1. Irradiation times (t_{irr} in min) and rate constants ($\times 10^{-2}$ min^{-1}) for the photolysis of conjugates **1a-e** at different wavelengths in ACN/HEPES buffer (80:20) solution*

Compound	254 nm		300 nm		350 nm	
	t_{irr}	k	t_{irr}	k	t_{irr}	k
1a H-β-Ala-OBba	313	0.98	245	1.25	297	1.05
1b H-Tyr-OBba	155	1.89	78	3.76	201	1.55
1c H-DOPA-OBba	314	0.98	887	0.34	616	0.49
1d H-Glu(OMe)-OBba	277	1.10	372	0.80	394	0.78
1e H-Glu(OBba)-OMe	225	1.39	389	0.76	278	1.14

For each compound and based on HPLC data, the plot of ln *A versus* irradiation time showed a linear correlation for the disappearance of the starting material, which suggested a first order reaction, obtained by the linear least squares methodology for a straight line. The corresponding rate constants were calculated and are presented in Table 1.

Concerning the influence of the wavelength of irradiation on the rate of the photocleavage reactions of conjugates **1a-e** in ACN/HEPES buffer (80:20) solution, it was found that the shorter irradiation times were observed at 300 nm for conjugates **1a** and **1b** and at 254 nm for conjugates **1c-e**. By comparison of the results at 300 and 350 nm, it was noticeable that the release of β-alanine **2a**, tyrosine **2b** and glutamic acid **2d** was faster at 300 nm, contrary to the release of DOPA **2c** and glutamic acid **2e**, with shorter irradiation times at 350 nm. No significant difference in the release of glutamic acid methyl ester (**2d**,**e**) was seen in the cleavage of the conjugate's ester bond at its main (**1d**) or side chain (**1e**).

Furthermore, considering the influence of the structure of the neurotransmitter on the photocleavage rates, we could see that the DOPA conjugate **1c** had the longest irradiation times for all wavelengths. In contrast, the irradiation times for the cleavage of tyrosine conjugate **1b** were always shorter, the best result being at 300 nm (78 min).

Acknowledgments

Thanks are due to *Fundação para a Ciência e Tecnologia* (Portugal) for financial support through project PTDC/QUI/69607/2006 (FCOMP-01-0124-FEDER-007449) and a Ph.D. grant to M.J.G.F. (SFRH/BD/36695/2007).

References

1. Bochet, C.G. *J. Chem. Soc. Perkin Trans. 1*, 125-142 (2002).
2. Schade, B., Hagen, V., Schmidt, R., Herbrich, R., Krause, E., Eckardt, T., Bendig, J. *J. Org. Chem.* **64**, 9109-9117 (1999).
3. Cambridge, S.B., Geissler, E., Calegari, F., Anastassiadis, K., Hasan, M.T. *Nat. Methods* **6**, 527-531 (2009).
4. Furuta, T., Wang, S.S., Dantzker, J.L., Dore, T.M., Bybee, W.J., Callaway, E.M., Denk, W., Tsien, R.Y. *Proc. Natl. Acad. Sci. U.S.A.* **96**, 1193-1200 (1999).
5. Ando, H., Furuta, T., Tsien, R.Y., Okamoto, H. *Nat. Genet.* **28**, 317-325 (2001).
6. Hagen, V., Frings, S., Wiesner, B., Helm, S., Kaupp, U.B., Bendig, J. *ChemBioChem.* **4**, 434-442 (2003).
7. Fedoryak, O.D., Sui, J.Y., Haydon, P.G., Ellis-Davies, G.C.R. *Chem. Commun.* 3664-3666 (2005).
8. Mayer, G., Heckel, A. *Angew Chem. Int. Ed.* **45**, 4900-4921 (2006).
9. (a) Fernandes, M.J.G., Gonçalves, M.S.T., Costa, S.P.G. *Tetrahedron* **63**, 10133-10139 (2007);
   (b) Fernandes, M.J.G., Gonçalves, M.S.T., Costa, S.P.G. *Tetrahedron* **64**, 3032-3038 (2008);
   (c) Fernandes, M.J.G., Gonçalves, M.S.T., Costa, S.P.G. *Tetrahedron* **64**, 11175-11179 (2008).

Proceedings of the 31st European Peptide Symposium
Michal Lebl, Morten Meldal, Knud J. Jensen, Thomas Hoeg-Jensen (Editors)
European Peptide Society, 2010

What Could Be the Role of Quinacrine in Creutzfeldt-Jakob Disease Treatment?

Zbigniew Zawada[1,2], Jaroslav Šebestík[1], Martin Šafařík[1], Anna Krejčiříková[3], Anna Březinová[1], Jan Hlaváček[1], Ivan Stibor[1], Karel Holada[3], and Petr Bouř[1]

[1]Institute of Organic Chemistry and Biochemistry, Academy of Sciences CR, Flemingovo nám. 2, Prague 6, 166 10, Czech Republic; [2]Institute of Chemical Technology, Technická 5, 166 28 Prague 6, Czech Republic; [3]First Faculty of Medicine, Charles University in Prague, Kateřinská 32, Prague 2, Czech Republic

Introduction

A conversion from normal cellular form of prion protein (PrP^{C}) to a toxic one (PrP^{Sc}) is suspected to cause prion diseases [1] such as Kuru, Creutzfeldt-Jakob disease, mad cow disease, etc. This transformation can be prevented, at least *in vitro*, by quinacrine [2].

Quinacrine can react with primary amines [3] and thiols [4] to afford acridine analogs (Figure 1), what was utilized in our laboratory during the study of acridinylation reaction of free thiol groups of prion protein.

Results and Discussion

Since quinacrine prevents plaque formation *in vitro* [2] and it reacts with thiols, we suggested that the main action of quinacrine in prevention of plaque formation in cell is its reaction with thio groups of PrP cysteine residues. To find out the affinity of quinacrine towards PrP we started with affinity study of short fragments of PrP containing cysteine residue (Table 1).

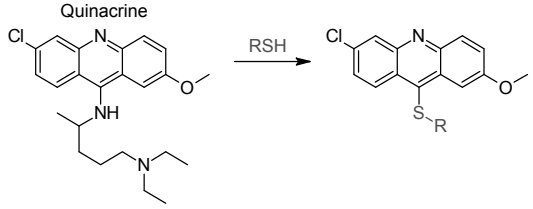

Fig. 1. Acridinylation reaction of primary thiol.

We were able to obtain two types of acridinylated peptides:

a) peptides where acridine moiety is attached just to the sulfur atom of cysteine (**1**, **2**, **3**, **4**, **5**, **6**, **7**, **8**), and

b) peptides where the acridine moiety is attached not only to the cysteine's sulfur atom, but also to the N-terminus amino group (**1**, **2**, **4**, **5**, **6**).

In the case of longer peptides **7** and **8** we were able to obtain just traces of bisacridinylated product, where both acridine moieties are attached to sulfur atom of cysteine residues. In these cases we were not able to observe any N-acridinylation. The most probable reason is poor solubility of both peptides under physiological conditions (phosphate buffer, pH=7.4, 37°C).

To prove that it is the N-terminus amino group that is acridinylated, and not histidine's imidazole ring, we prepared a set of three peptides **1**, **2** and **3** with almost the same sequence. Whereas we were not able to obtain any bisacridinylated N-acetylated peptide **3**, we were able to obtain bisacridinylated peptides **1** and **2**. It means that histidine is not necessary for the second acridinylation, but the N-terminus amino group is essential. We supported this hypothesis also by NMR spectra.

We found that it is possible to lead the reaction course toward almost pure cysteine S-acridinylation by lowering the pH value of reaction mixture, by using subequimolar amount of quinacrine and by shortening the reaction time. Bisacridinylated peptides can be obtained as a main product when huge excess of quinacrine is used in higher pH for longer reaction time.

Table 1. Peptides which were reacted with quinacrine

Compound	*Peptide*	*Length*	*Products*	
			Mono-acridinylated	*Bis-acridinylated*
1	H-Asp-Cys-Val-Asn-OH	4	+	+
2	H-His-Asp-Cys-Val-Asn-OH	5	+	+
3	Ac-His-Asp-Cys-Val-Asn-OH	5	+	-
4	H-Glu-Gln-Met-Cys-Ile-Thr-Asn-OH	7	+	+
5	H-Glu-Gln-Met-Cys-Val-Thr-Asn-OH	7	+	+
6	QMCVTQYQKESQAYY	15	+	+
7	H-Cys-MoPrP(179-212)-Cys-OH	36	[b]	[b]
8	Mouse PrP	235[a]	[b]	[b]

[a] *Recombinant mouse prion protein including anchor*

[b] *Only bisacridinylated products were obtained; both acridine moieties attached to sulfur atom of cysteine residue*

Since we proved that quinacrine reacts with prion protein free thio groups of both cysteine residues, we suggest that the most important interaction between quinacrine and prion protein is not a complexation of quinacrine by prion as was proposed by Vogtherr [5], but it is the covalent interaction – reaction of quinacrine with free thio group of prion protein. Furthermore we suggest that this reaction might be the key factor for prevention of plaque formation by quinacrine.

Acknowledgments
The work was supported by the Grant Agency of the Academy of Sciences (A400550702, M200550902, Z40550506) and the Czech Science Foundation (203/07/1517).

References

1. Prusiner, S.B. *PNAS* **95**, 13363-13383 (1998).
2. Doh-Ura, K., Iwaki, T., Caughey, B. *J. Virol.* **74**, 4894-4897 (2000).
3. Šebestík, J., Šafařík, M., Stibor, I., Hlaváček, J. *Biopolymers* **84**, 605-614 (2006).
4. Wild, F., Young, J.M. *J. Chem. Soc.* 7261-7274 (1965).
5. Vogtherr, M., Grimme, S., Elshorst, B., Jacobs, D.M., Fiebig, K., Griesinger, C., Zahn, R. *J. Med. Chem.* **46**, 3563-3564 (2003).

Proceedings of the 31st European Peptide Symposium
Michal Lebl, Morten Meldal, Knud J. Jensen, Thomas Hoeg-Jensen (Editors)
European Peptide Society, 2010

Synthetic Antifreeze Glycopeptide Analogs

Lilly Nagel[1], Carolin Plattner[1], Carsten Budke[2], Zsuzsa Majer[3], Thomas Koop[3], and Norbert Sewald[1]

[1]Bielefeld University, Bielefeld, 33615, Germany; [2]Department of Physical Chemistry, Bielefeld University, Bielefeld, 33615, Germany; [3]Eötvös Loránd University, Budapest, 1518, Hungary

Introduction

Antifreeze Glycopeptides (AFGP) are biological antifreezes in creatures living in polar and subpolar areas. These proteins decrease the freezing point of physiological fluids without changes in melting point by inhibiting the growth of large ice crystals and suppressing heterogeneous ice nucleation. Those polymers consist of iterative tripeptide units $(Ala\text{-}Ala\text{-}Thr)_n$ (n=4-56), where every threonine is linked to β-D-Galactosyl-(1→3)-α-*N*-acetyl-D-galactosamine (Figure 1), and adopt highly flexible threefold left-handed helices similar to the polyproline type II helix [1].

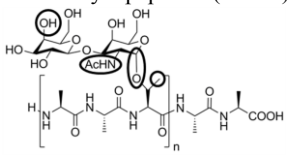

Fig. 1. Composition of AFGPs with important functionalities of anti-freeze activity.

Results and Discussion

Synthesis of the Building Block

Since AFGPs are not easily accessible from natural sources, the synthesis of such heavily glycosylated peptides is necessary. Therefore, the synthesis of glycosylated amino acid furnished either with a mono- or a disaccharide has to be developed first before the building blocks are introduced into peptide synthesis on solid phase. Both precursors of the T_N- and T-antigens (Figure 2) were obtained in a silver salts mediated glycosylation. The carbohydrate could be coupled to the sidechain of a Fmoc-protected threonine giving predominantly the α-anomeric product.

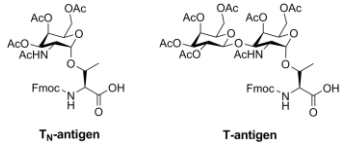

Fig. 2. T_N-antigen and T-antigen precursors for solid phase peptide synthesis.

Synthesis of Peptides

For the synthesis of these AFGP analogs, well-controlled and highly efficient coupling conditions during Fmoc-SPPS are essential. A semi-automated and microwave enhanced

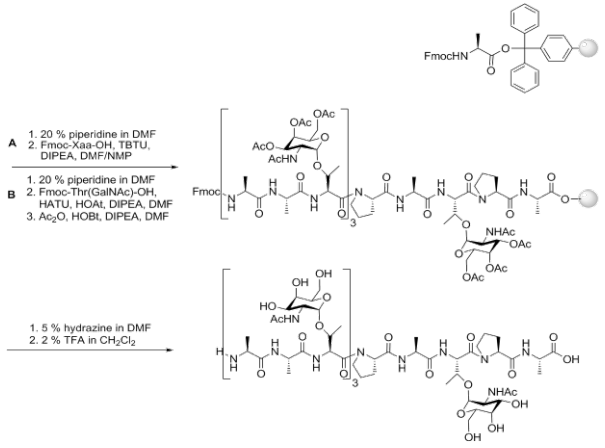

Fig. 3. Microwave-enhanced synthesis of proline containing AFGP analogs on solid phase.

synthesis on solid phase was employed (Figure 3). The synthesis was carried out on 2-chlorotrityl resin, which was preloaded with Fmoc-alanine. The glycosylated amino acid was added manually. The elongation was executed by sequential addition of the amino acids and the coupling reagent. In the case of unglycosylated residues the coupling reagent TBTU was used, while HATU and HOAt were employed for the coupling of the glycosylated amino acids. The entire synthesis of the glycopeptides was carried out at a maximum temperature of 40 °C to avoid cleavage of carbohydrate from the peptide backbone [2].

Structural Analysis

Proline containing glycopeptides and the corresponding backbones were synthesized to enforce a polyprolin type II helix:

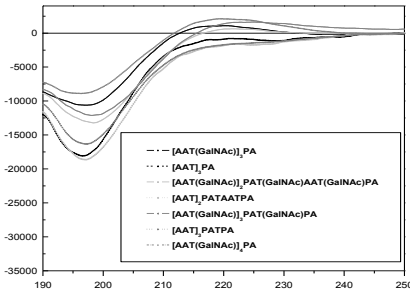

Fig. 4. CD analysis (c = 4 mg/mL, Millipore water, rt) of AFGP analogs.

Circular dichroism (CD) analysis (c = 4 mg/mL, Millipore water, rt) of AFGP analogs containing proline residues show a maximum at ~220 nm and a minimum at ~198 nm (Figure 4). The signature of polyproline II helical structure is significant, but with similarity to a random coil with high flexibility. Temperature-dependent spectra were measured, which show the existence of an isodichroic point indicating a local two-state population of e.g. polyproline II helix and random coil.

Furthermore it is obvious that the CD minima of the glycosylated peptides are less pronounced and a display of a slight red-shift in comparison to the corresponding aglycons is visible.

Microphysical Analysis

Optical microphotographs of ice crystals (Figure 5*)* show altered crystal habitus and no Ostwald ripening in the presence of AFGP analogs **b)** in comparison to the absence of any AFGPs **a)**. In detail the results indicate that larger ice crystals grow at the expense of smaller ones. Another implication is visible in an altered morphology of the ice crystals. In presence of AFGPs the faces of the ice crystals grow at a much slower rate with a hexagonal bipyramidal habitus [3].

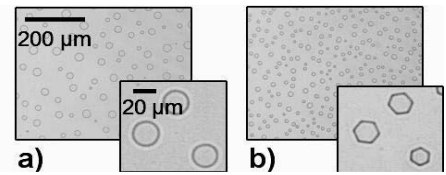

Fig. 5. Optical microphotographs of ice crystals (aq. 45 wt % sucrose solutions, -8 °C).

Acknowledgments

This work is supported by the DFG (SFB 613).

References

1. Tachibana, Y., Fletcher, G.L, Fujitani, N., Tsuda, S., Monde, K., Nishimura, S. *Angew. Chem.* **116**, 874-880 (2004); *Angew. Chem. Int. Ed.* **43**, 856-862 (2004).
2. Heggemann, C., Budke, C., Schomburg, B., Majer, Z., Wißbrock, M., Koop, T., Sewald, N. *Amino Acids* **38 (1)**, 213-222 (2010).
3. Budke, C., Heggemann, C., Koch, M., Sewald, N., Koop, T. *J. Phys. Chem. B* **113 (9)**, 2865-73 (2009).

Proceedings of the 31st European Peptide Symposium
Michal Lebl, Morten Meldal, Knud J. Jensen, Thomas Hoeg-Jensen (Editors)
European Peptide Society, 2010

Peptide Based Artificial Receptors for Carbohydrate Recognition

Predrag Cudic[1], Andreja Jakas[2], Nina Bionda[1], and Maré Cudic[1]
[1]Torrey Pine Institute for Molecular Studies, Port St. Lucie, 34987, FL, U.S.A.; [2]Division of Organic Chemistry and Biochemistry, Rudjer Boskovic Institute, Zagreb, 10000, Croatia

Introduction

Bacillus anthracis is a Gram-positive, rod-shaped, aerobic soil bacterium that causes anthrax in humans and other mammals. Recently it was found that one of the components of *B. anthracis* exosporium is a glycoprotein called BclA (*Bacillus* collagen-like protein of anthracis) whose carbohydrate portion is composed of tetrasaccharide β-Ant(1→3)α-L-Rhap(1→3) α-L-Rhap(1→2)L-Rhap [1]. The upstream terminal residue of this tetrasaccharide is a highly specific monosaccharide, named anthrose (4,6-dideoxy-4-[(3-hydroxy-3-methyl-1-oxobutyl)amino]-2-*O*-methyl-D-glucopyranose (Figure 1). Importantly, anthrose was not found in spores of either *Bacillus cereus* or *Bacillus thuringiensis*, two species that are the most phylogenetically similar to *B. anthracis*. Therefore, anthrose represents a promising target for the development of *B. anthracis* specific detection agents.

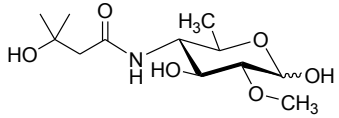

Fig. 1. B. antharacis specific monossacharide anthrose.

Carbohydrate binding protein mimicking molecules using the peptide based systems represent an attractive approach for the development of artificial receptors for specific carbohydrate binding. These receptors should possess the necessary three-dimensional structure, limited flexibility and lipophilic binding pocket where binding can occur through a combination of hydrophobic interaction and hydrogen bonds between receptor molecules and carbohydrate substrates.

Results and Discussion

As a model system for artificial receptors we have chosen a cyclic cationic decapeptide antibiotic polymyxin B, which is known to bind the lipid A moiety of LPS with a high affinity. Using a combinatorial chemistry approach we have prepared a soluble library of

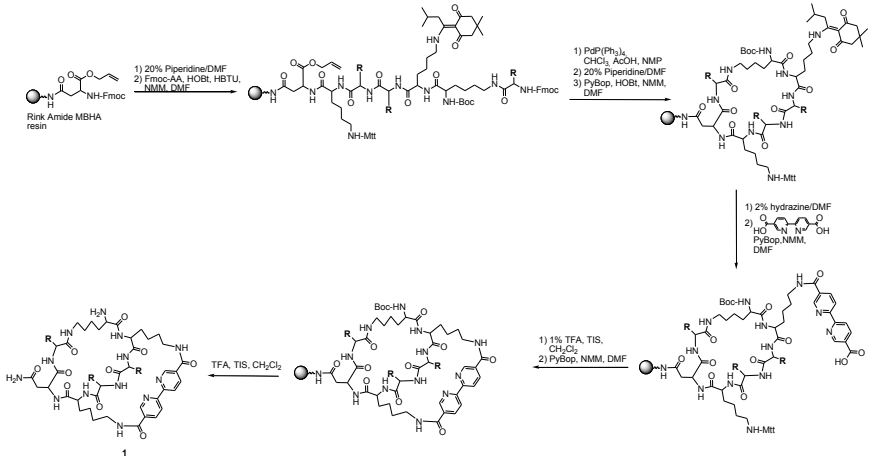

Fig. 2. Solid phase synthetic strategy.

polymyxin bicyclic peptide analogues bridged with a bipyridine group in order to introduce structural constraints pertaining to the stabilization of the peptide's binding conformation, and to incorporate additional hydrogen-bonding acceptor site.

Figure 2 shows a general scheme for synthesis of a library of bicyclic peptides with three amino acids positions available for randomization. The first amino acid Fmoc-Asp-OAllyl was anchored *via* side chain to the MBHA Rink Amide resin, followed by subsequential coupling of Fmoc-Lys(Mtt)-OH and one of amino acids. Standard Fmoc-coupling conditions including fourfold excess of amino acids and HOBt/HBTU/*N*-methylmorpholine was used throughout the synthesis of this tripeptide precursor. However, coupling of amino acids mixtures in order to randomize the remaining peptide sequence was shown to be more difficult. Due to the steric effects and different amino acids coupling kinetics, the standard solid-phase synthetic approach had to be optimized. A mixture of 19 L-amino acids (Cys was omitted due to the high possibility of an undesired disulfide bridge formation) was used in 10 fold excess compared to the resins loading capacity, and in mol percent ratios as was outlined in the paper of R. Houghten *et al.* [2]. Successful coupling was obtained by using an equimolar amount of HOBt/HBTU/*N*-methylmorpholine coupling reagents with the respect to the amount of amino acids in the mixture. Cyclization of a linear precursor was achieved by using 2 equivalents of PyBOP/HOBt/DIPEA in DMF, and vigorous mixing of the reaction mixture over night. Following the cyclization step, ivDde protecting group was removed from Lys side chain with 2% hydrazine in DMF, and coupling of 2,2'-bipyridine-5,5'-dicarboxylic acid to Lys side chain's amino group was achieved by PyBOP/HOBt/DIPEA. After removal of Mtt from the peptide, bicyclic compound was prepared using the same synthetic protocol. In all cases coupling efficacy was monitored by the Kaiser test. The final step included removal of the prepared bicyclic peptides from the resin. The outlined combinatorial chemistry approach allowed us to create a quite diverse library of bicyclic peptides for anthrose artificial receptor's binding optimization.

Lipidic derivative of anthrose was synthesized [3] as a model for *B. anthracis* exosporium, and lipidic derivative of glucose was synthesized as a control to evaluate specificity of bicyclic peptide receptor. Our further investigation will include binding assay development in a 384-well microplate format, and bicyclic peptide library screening for selective anthrose binding.

Acknowledgments

We gratefully acknowledge the financial support of the NATO Public Diplomacy Division, Science for Peace and Security Programme (SfP 983154) to P.C. and A.J.

References

1. Daubenspeck, J.M., Zeng, H., Chen, P., Dong, S., Steichen, C.T., Krishana, N.R., Prichard, D.G., Turnbough, C.L. *J. Biol. Chem.* **279**, 30945-30953 (2004).
2. Pinilla, C., Appel, J.R., Houghten, R.A. *Methods in Molecular Biology* **66**, 171-179 (1996).
3. Dhénin, S.G.Y., Moreau, V., Morel, N., Nevers, M.C., Volland, H., Créminon, C., Djedaïni-Pilard, F. *Carbohydr. Res.* **343**, 2101-2110 (2008).

Proceedings of the 31st European Peptide Symposium
Michal Lebl, Morten Meldal, Knud J. Jensen, Thomas Hoeg-Jensen (Editors)
European Peptide Society, 2010

Synthesis of Glycopeptides Potential Inhibitors of Human Rhinovirus 3C Protease

Dantcho L. Danalev[1,2], Nadège Lubin-Germain[2], Jacques Uziel[2], and Jacques Augé[2]

[1]University of Chemical Technology and Metallurgy, Department of Organic Chemistry, Sofia, Bulgaria, dancho_danalev@yahoo.com; [2]Université de Cergy-Pontoise, Cergy-Pontoise, France, Nadege.lubin-Germain@u-cergy.fr

Introduction

Recently, due to rapidly and dramatically changing climatic conditions, our environment is also varying quickly. Simultaneously, we are witnessing the emergence of several new and more resistant viruses such as HIV virus, AH1N1 influenza virus and an ever increasing resistance of viruses to applied drugs. In this global context, synthesis of completely new or modified antiviral agents and vaccines is of a great interest for medical practice.

Human rhinovirus (HRV) is a small picornavirus responsible for the common cold. Some enzymatic and structural proteins required for viral replication are generated by the viral encoded 3C Protease (3CP). The HRV 3CP is specific cysteine protease able to cleave P1-P1' Gln-Gly amide bond. Structurally, it closely resembles trypsin-like serine protease [1]. A tripeptide aldehyde Z-Leu-Phe-Gln-H is a well know inhibitor of human rhinovirus 3CP [2]. Several literature data reveal that P3 Leu residue is not important for antiviral activity and many groups could be tolerated at this place [3].

A lot of experiments connected with compounds possessing inhibitory activity against the cysteine-containing human rhinovirus 3C protease (3CP) revealed that some simple changes in the 3CP substrate H-His-Leu-Phe-Gln-Gly-Pro-OH could transform it into low molecular strong inhibitor Z-Leu-Phe-Gln-Michael acceptor [4].

A series of similar inhibitors have been synthesized and described in the literature in order to reveal the role of different parts of the molecule on the antiviral activity [4-7]. It was proven that Leu residue at P3 position is not necessary for the substrate-enzyme interaction [3]. Therefore, a wide variety of substitutes are tolerated at this position. Further studies showed that aldehyde group as a Michael acceptor is not acceptable because of their toxicity, lack of selectivity and stability [8].

Results and Discussion

Herein, we report a series of mimetics of this tripeptide by replacement of P3 Leu residue with Ser or Lys in order to make possible further glycopeptides synthesis. A linker of adipic acid was also incorporated between peptide and carbohydrate moieties (Figure 1).

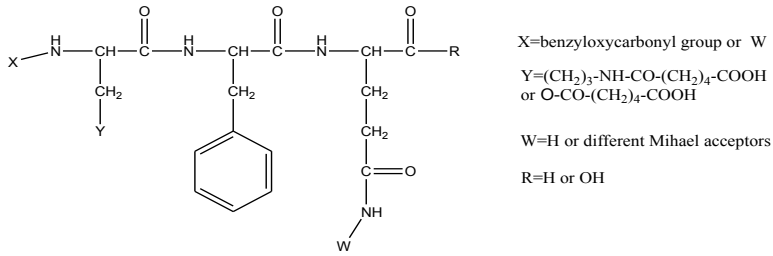

Fig. 1. General structure of aimed peptide mimetics.

Despite the large progress in peptide chemistry due to solid phase peptide synthesis (SPPS) discovered by Merrifield (1963), the synthesis of each new peptide sequence represents a major challenge and is often unpredictable, especially when obtaining peptides with high molecular weight and difficult sequences. The creation of new synthetic schemes for synthesis of peptides is facilitated both by the discovery of new methods for condensation and new protective groups (alone or in combination with already known ones) as well as

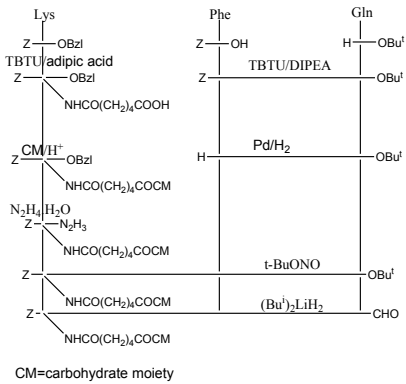

Fig. 2A. Synthesis of tripeptide mimetic with Lys at P3 position.

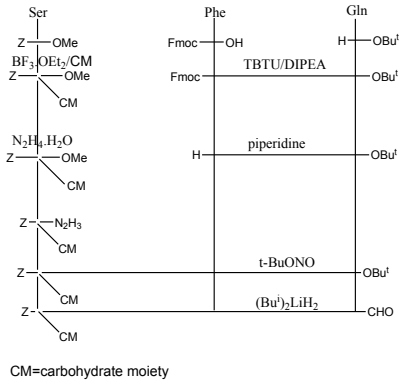

Fig. 2B. Synthesis of tripeptide mimetic with Ser at P3 position.

the possibilities to apply various strategies of realizing a peptide sequence using known condensation methods.

The target compounds were synthesized using conventional peptide synthesis in solution (Figure 2A and 2B). The structure of newly synthesized tripetide mimetics was proven by NMR. Further they were also synthesized using SPPS. In all syntheses allyl ester as a protection for δ-COOH function of Glu was used. This type of esters was advanced in the last 15 years due to their specific properties. First of all, they are more stable against acidic and alkaline hydrolysis than other ester groups such as OMe, OEt, OBzl and OBut, which allows its preservation during all reaction conditions for other protection group removal. Further, the –COO-All function can be successfully reduced to aldehyde group under the action of diisobutylaluminium hydride, or transformed to free COOH function using $Pd(PPh)_3/PhSiH_3$. So, this approach allows us to build the peptide chain using the specific features of OAll protection group either to its C- or N- terminus.

The main advantage of our strategy is that we use Glu as a first amino acid in place of the Gln residue in the target peptides needed to link the peptide moiety to the Rink amide resin. What is more important is that it was linked by its δ-COOH function. The unblocking of Glu using a standard "cocktail" of agents in the final stage of synthesis led to obtaining the required Gln residue [9].

Conclusions and Perspectives

A series of tripeptide mimetics with proven antiviral activity was synthesized using both standard synthesis in solution and SPPS. The synthesis of a series of carbohydrate moieties with proven antiviral activity is in progress. They will be further bonded to tripeptide mimetics already synthesized. The peptide moiety will be used to derivatise our carbohydrate molecules to increase its activity as well as cell penetrability.

Acknowledgments

We would like to thank to National Research Fund of Bulgaria for post-doctoral grant of Dr. Danalev. The work is supported by contract DOO2-296 of National Research Fund of Bulgaria.

References

1. Orr, D.C., Long, A.C., Kay, J., Dunn, B.M., Cameron, J.M. *J. Gen. Virol.* **70**, 2931-2942 (1989).
2. Webber, S., Okano K., Little T.L., et al. *J. Med. Chem.* **41**, 2786-2805 (1998).
3. Dragovich, P.S., Webber, S.E., Prins, T.J., et al. *Bioorg. Med. Chem. Lett.* **9**, 2189-2194 (1999).
4. Dragovich, P.S., Webber, S.E., Babine R.E., et al. *J. Med. Chem.* **41**, 2819-2834 (1998).
5. Dragovich, P.S. *Expert Opinion on Therapeutic Patents* **11**, 177-184 (2001).
6. Dragovich, P.S., Prins, T.J. *J. Med. Chem.* **46**, 4572-4585 (2003).
7. Wang, Q.M. *Prog. Drug. Res.* **52**, 197-219 (1999).
8. Dragovich, P.S., Zhou, R., Webber, S.E., et al. *Bioorg. Med. Chem. Lett.* **10**, 45-48 (2000).
9. Minchev, I., et al. *Int. J. Pept. Res. Ther.* **16 (4)**, 233 (2010).

Proceedings of the 31st European Peptide Symposium
Michal Lebl, Morten Meldal, Knud J. Jensen, Thomas Hoeg-Jensen (Editors)
European Peptide Society, 2010

Stereoselective Synthesis of Tetrahydro-β-carbolines via Pictet-Spengler Reaction

Saeed Balalaie, Vahid Dianati
Peptide Chemistry Research Center, K. N. Toosi University of Technology, Tehran, P.O. Box 15875-4416, Iran; balalaie@kntu.ac.ir

Introduction

The tetrahydro-β-carboline ring system is present in numerous biologically active indole alkaloids as well as synthetic compounds.The Pictet-Spengler reaction is a powerful way of accessing tetrahydro-β-carbolines by the condensation of tryptamine derivatives and aldehyde through acid catalysis reaction conditions.

The stereoselective synthesis of this new ring is an interesting subject for organic chemists. It was shown that the stereochemistry of the final product could affect the biological activity of the carboline structure. Bailey, et al. found that the existence of a chiral center could affect the stereoselectivity of the desired β-carboline structure [1]. In this regards, tryptophan is an interesting starting material, It was reported that tryptophan allyl esters reacted with benzaldehydes to give >95:5 cis:trans selectivity. It seems that the existence of a chiral center in the structure of starting material has an effective influence on the stereoselectivity of the products [2]. In continuation of our research work to find novel tandem reactions with ability of post-transformation, we wish to report herein stereo-selective synthesis of tetrahydro-β-carboline containing propargyl moiety.

Results and Discussion

In this research, reaction of propargyl ester of tryptophan and its reaction with aromatic aldehydes in the presence of TFA was investigated. The desired β-carboline product showed *cis* selectivity and the sole product was obtained as the *cis* isomer (Scheme 1).

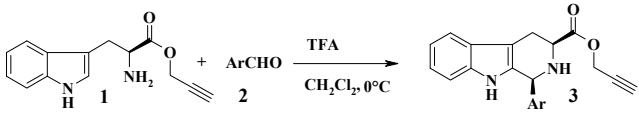

Scheme 1. Synthesis of tetrahydro-β-carbolines.

Meanwhile, the starting material was synthesized according to this reaction sequence: 1) formation of ester group using TBTU as coupling reagent, 2) Fmoc deprotection, 3) Boc deprotection (Scheme 2).

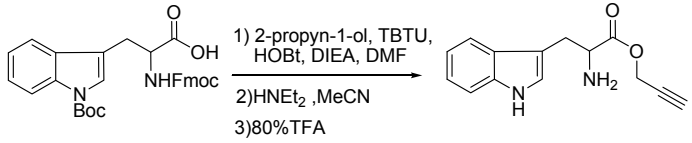

Scheme 2. Synthetic pathway to achieve starting material.

For investigation of diversity and scope of reaction, different aromatic aldehydes which contained electron-donating or electron-withdrawing groups were selected. We chose propargyl moiety to be able to carry out the click chemistry to form additional triazole ring.

The results of the synthesis of desired tetrahydro-β-carbolines with cis-selectivity are summarized in Table 1.

Table 1. Synthesis of tetrahydro-β-carbolines via Pictet-Spengler Reaction

Aldehyde	*Product*	*Yield (%)*	*Aldehyde*	*Product*	*Yield (%)*
	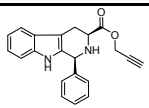	73	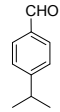	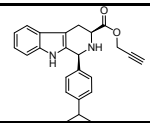	62
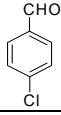	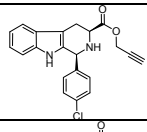	52	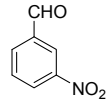	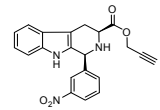	67
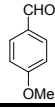	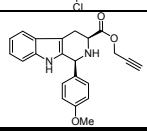	66	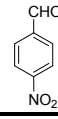	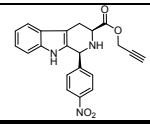	64

The distinguished peak for the stereo selective synthesis of product in ^{1}H- and ^{13}C-NMR spectra are related to the chemical shifts of H-1 and H-3 protons.

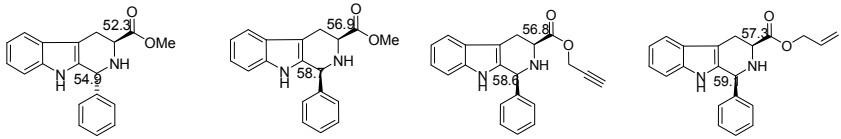

Scheme 3. Comparison of chemical shifts of the products with the synthetic cis- tetrahydro-β-carboline isomers.

The value of coupling constants and also chemical shifts could confirm the *cis* isomer as the final product.The yields of products were between 52-73%. The products have the suitable functional groups for carrying out the further reactions.

In summary, we have found that the Pictet-Spengler reaction of tryptophan propargyl esters with aromatic and heteroaromatic aldehydes generates *cis*-tetrahydro-*β*-carbolines with stereoselectivity.This reaction tolerates all substituted phenyl derivatives that we tried for aldehyde which means that this should be adaptable to a wide range of targets of medicinal synthetic interest.

References

1. Alberch, L., Bailey, P.D., Clingan, P.D., Mills, T.J., Price, R., Pritchard, R.G. *Eur. J. Org. Chem.* 1887 (2004).
2. Bailey, P.D., Beard, M.A., Phillips T.R. *Tetahedron Lett.* **50**, 3645-3648 (2009).
3. Sewgobind, N.V., Wanner, M.J., Ingemann, S., de Gelder, R., van Maarseveen, J.H., Hiemstra, H. *J. Org. Chem.* **73**, 6405-6408 (2008).

Proceedings of the 31st European Peptide Symposium
Michal Lebl, Morten Meldal, Knud J. Jensen, Thomas Hoeg-Jensen (Editors)
European Peptide Society, 2010

Synthesis of Aza-β³-Homoserine, Incorporation of This New Aza-β³-Amino Acid Into 26RFa(20-26) and Microwave-Assisted Deprotection of Its Side Chain

Olivier Tasseau[1], Patrick Bauchat[1], Cindy Neveu[2], Benjamin Lefranc[2], Jérôme Leprince[2], and Michèle Baudy-Floc'h[1]

[1]*UMR CNRS 6226, ICMV, University of Rennes 1, Rennes, France;*
[2]*INSERM U982, European Institute for Peptide Research, University of Rouen, Mont-Saint-Aignan, France*

Introduction

Aza-β³-peptides, mixing α- and aza-β³-amino acids (the aza analogs of β³-amino acids), represent an exciting type of peptidomimetics [1,2]. In particular, they show a stronger resistance to degradation by proteases *in vivo* and a better bioavailability in comparison with peptides. We have also shown that an aza-β³-amino acid induces a N-N turn or hydrazino turn, stabilized by an eight-membered-ring intramolecular hydrogen bond between the carbonyl acceptor group of the residue i-1 and the amide proton of the residue i+1. Interestingly, this N-N turn promotes different conformations such as γ and β turn [3]. On the other hand, 26RFa, a neuropeptide of the RFamide superfamily, exhibits high affinity for GPR103 and induces a potent orexigenic effect in mice [4]. 26RFa$_{(20-26)}$ (GGFSFRF-NH$_2$), whose sequence is strictly conserved across species, is about 75 times less potent than 26RFa to mobilize $[Ca^{2+}]_i$ in GPR103-transfected cells. In this study, aza-β³ moieties may become useful tools to increase interactions of 26RFa with his G-protein coupled receptor GPR103. In continuity of aza-β³ scan, we explore and develop procedures (a) to synthesize aza-β³ homo serine (aza-β³-Hse) protected derivatives (Figure 1); (b) to insert them in the 26RFa$_{(20-26)}$ sequence in position 23; and (c) to deprotect [aza-β³-Hse(R)]^{23}RFa$_{(20-26)}$ by selective R-group cleavage. During the synthesis of the monomer aza-β³-Hse, some problems occured as well as during its side chain deprotection. We will present in this paper the synthesis of Fmoc-aza-β³-Hse(R)-OH, the incorporation of this surrogate into the heptapeptide, and finally the side chain deprotection attempts, in particular the microwave-assisted strategy.

Results and Discussion

To prepare Fmoc-aza-β³-Hse(R)-OH we need to conveniently protect the hydroxy group of the diacetal otherwise side reactions can occur. As we are using the Fmoc strategy for the peptide synthesis, the hydroxy group was first protected as a methoxy ethyl ether using chloromethyl ethyl ether and sodium hydride. The protected diethyl acetal was then treated with aq. HCl in tetrahydrofuran (THF), to give protected aldehyde in low yield (5%, Table 1). So, different protections (Bn, All and Z) have been investigated to release protected aldehydes and to reach the desired hydrazones by condensation with the Fmoc hydrazine (Table1). Reduction of the crude mixture with sodium cyanoborohydride gave the required *N*,*N*'-disubstituted hydrazine (R = CH_2OEt, Bn, All, Z). Finally, reductive amination of glyoxilic acid leads to the final monomer Fmoc-aza-β³-Hse(R)-OH (R=CH_2OEt, Bn, All, Z).

The aim of this work consists to use the Fmoc-aza-β³-Hse(R)-OH analog in SPPS with the help of automatic microwave-assisted synthesizer. The Fmoc/*t*-butyl strategy on rink amide resin and the TBTU activation were implemented to prepare the aza-β³-peptide 26RFa$_{(20-26)}$ with aza-β³-Hse(R) insertion at position 23. Several methods were investigated to deprotect the hydroxyl derivative residues. First, different classical strategies were tested on aza-β³-peptidyl resin without success.

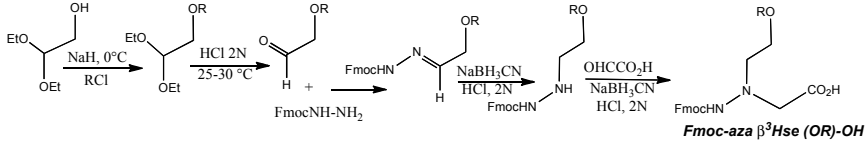

Fig. 1. Synthesis of Fmoc-azaβ^3Hse(R)-OH.

Table 1. Synthesis of Fmoc-aza-β³-Hse(R)-OH, step yields (%)

Protecting group R	*CH_2OEt*	*Bn*	*All*	*Z*
(i) OR - protection	89	70	90	53
(ii) acetal hydrolysis	5	73	79	88
(iii) condensation	85	60	80	82
(iv) reduction	53	89	81	70
(v) reductive amination	95	88	80	89

Then, the O-deprotection was performed after the peptidyl cleavage from the resin and removal of the guanido protecting group. The yields resulting from the Bn and All hydrogenolysis with Pd(C) or silane hydride under standard conditions were very low. The reaction carried out under microwave-assisted conditions (40W, 45min, 333K) led to a higher deprotection level (86% yield before purification) (Figure 2). Reaction effectiveness was evaluated by combining analytical HPLC and MALDI-TOF mass spectrometry. Subsequently, crude aza-β³-peptide was purified by reversed-phase HPLC in MeCN gradient elution. Collected fractions were characterized by MALDI-TOF MS to lead to the expected [aza-β³-Hse]²³26RFa$_{(20-26)}$ analog. Nevertheless, its binding affinity and its ability to increase the $[Ca^{2+}]_i$ on GPR103-transfected cells were, at least, twice lower than for 26RFa$_{(20-26)}$. However, this microwave-assisted specific efficiency retains our focus and opens perspectives to increase the reaction yield.

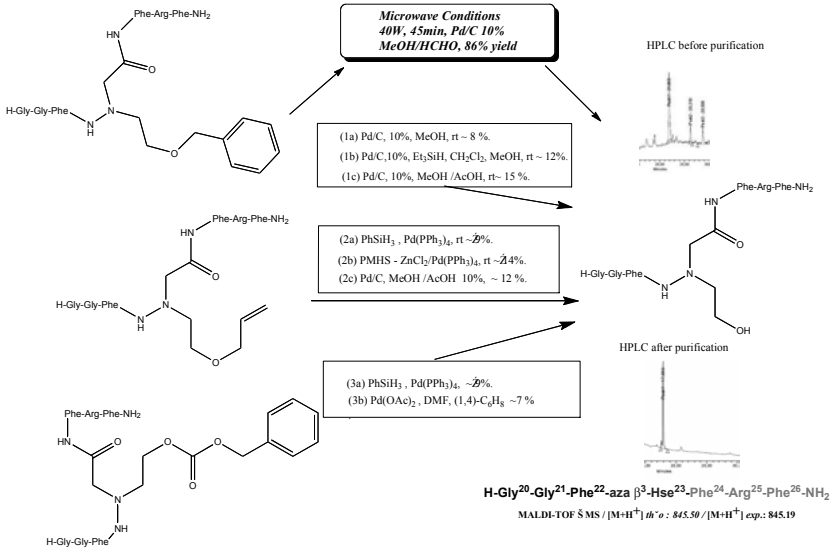

Fig. 2. A*za-β³Hse (OR)-protecting group cleavages by standard and microwave condition.*

References

1. Busnel, O., et al *J. Org. Chem.* **26**, 10701-10708 (2005).
2. Dali, H., et al. *Mol. Immunol.* **44**, 3024-3036 (2007).
3. Laurencin, M., Legrand, B., Duval, E., Zatylny-Gaudin, C., Bondon, A., Baudy-Floc'h, M. submitted.
4. Chartrel, N., et al. *Proc. Natl. Acad. Sci. U.S.A.* **100**, 15247- 15252 (2003).

Proceedings of the 31st European Peptide Symposium
Michal Lebl, Morten Meldal, Knud J. Jensen, Thomas Hoeg-Jensen (Editors)
European Peptide Society, 2010

Dimerization of the Immunosuppressory Decapeptide Ubiquitin Fragment

Marzena Cydzik[1], Monika Biernat[1], Alicja Kluczyk[1], Piotr Stefanowicz[1], Remigiusz Bąchor[1], Michał Zimecki[2], and Zbigniew Szewczuk[1]

[1]Faculty of Chemistry, Wroclaw University, Wroclaw, 50-383, Poland; [2]Institute of Immunology and Experimental Therapy, PAS, Wroclaw, 53-114, Poland

Introduction

Dimerization of the receptors is an essential step of various cellular signal transduction processes. Therefore, substances that are able to modulate the receptor dimerization may control such a process and affect biological activities. Properly designed analogs of dimeric ligands were found to enhance interactions between two neighboring receptors with parallel or anti-parallel orientation [1,2].

Ubiquitin is a highly conserved 76-amino acid polypeptide present in all eukaryotic cells. The polypeptide is involved in many key processes of cell biology. It has been postulated that ubiquitin originating cryptides could interfere in the ubiquitination process, affecting some ubiquitin activities [3]. Recently we found that ubiquitin fragments exhibit strong immunosuppressive activity, comparable to that of cyclosporine A [4,5]. Ubiquitin is known to exist in oligomeric form which can interact with various oligomeric receptors. However, the biological significance of some interactions of oligomeric ubiquitin still remains unknown. It may be concluded that the dimeric analogs of ubiquitin fragments are able to interact with the dimeric receptors, which may cause modulation of interaction of oligoubiquitin with the oligomeric receptors.

Results and Discussion

We designed and synthesized new dimeric analogs of the ubiquitin fragment, to probe whether the ubiquitin receptors may form oligomeric structures. Three dimerization strategies: N-terminus to N-terminus (compound 1), C-terminus to C-terminus (compound 2) and head to tail (compounds 3 and 4) (Figure 1) were used to synthesize the dimeric peptides on solid support. We selected polyethylene glycol derivatives as cross-linking reagents because of their flexibility, solubility and bioavailability. In the course of our research, we developed a new and straightforward procedure for the direct dimerization of the C-terminal residues of peptide by their side-chains on solid support using a polyethylene glycol spacer.

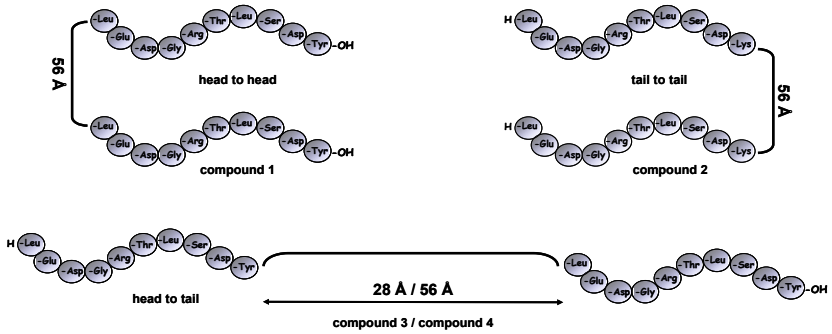

Fig. 1. Three ways of dimerization of the immunosuppressive ubiquitin fragment. Calculated length of the PEG-linker is given.

The effect of dimeric analogs on the immunomodulatory activity was examined in the AFC *in vitro* experiment. The immunological tests show that N- and C-terminal dimerization did not cause significant increase in the biological activity (compound 1 and compound 2). In contrast, the increase in immunological activity in case of the parallel dimers (compound 3 and compound 4) was observed. Compound 3, which contains a shorter linker, possesses higher immunosuppressory potency than its analog 4 with a longer linker.

Although mechanism of immunosuppressory action of ubiquitin fragments still remains unknown, they may interrupt the interactions of ubiquitin with its hypothetical receptors. Since ubiquitin is known to exist in oligomeric form, a possibility of interaction of oligoubiquitin with some oligomeric receptors cannot be excluded.

The enhanced immunosuppressory activity of the parallel dimers 3 and 4, as compared to their anti-parallel analogs (compounds 1 and 2), may suggest a parallel orientation of the molecules of the hypothetic ubiquitin receptors responsible for the immunomodulatory activity.

Acknowledgments

This work was supported in part by grant No. N N401 222734 from the Ministry of Science and Higher Education (Poland).

References

1. Szewczuk, Z., Biernat, M., Dyba, M., Zimecki, M. *Peptides* **25**, 207-215 (2004).
2. Biernat, M., Stefanowicz, P., Zimecki, M., Szewczuk, Z. *Bioconjugate Chem.* **17**, 1116-1124 (2006).
3. Pasikowski, P., Cydzik, M., Kluczyk, A., Stefanowicz, P., Szewczuk, Z. *BioMol. Concepts* **1**, 67-83 (2010).
4. Szewczuk, Z., Stefanowicz, P., Wilczyński, A., Staszewska, A., Siemion, I.Z., Zimecki, M., Wieczorek, Z. *Biopolymers* **74**, 352-362 (2004).
5. Jaremko, Ł., Jaremko, M., Pasikowski, P., Cebrat, M., Stefanowicz, P., Lisowski, M., Artym, J., Zimecki, M., Zhukov, I., Szewczuk, Z. *Biopolymer*s **91**, 423-431 (2009).

Proceedings of the 31st European Peptide Symposium
Michal Lebl, Morten Meldal, Knud J. Jensen, Thomas Hoeg-Jensen (Editors)
European Peptide Society, 2010

The Application of the New Tin(IV) Chloride Deprotection for the Preparation of Glycosylated Peptides

Orsolya Szolomájer-Csikós[1], Kinga Rákosi[1], Orsolya Hegyi[1], László Kalmár[2], János Kerékgyártó[2], and Gábor K. Tóth[1]

[1]Department of Medical Chemistry,Faculty of General Medicine, University of Szeged, 6720, Szeged, Hungary; [2]Department of Botany, Bio-organic Laboratory, University of Debrecen, Faculty of Sciences and Technology, Debrecen, 4032, Hungary

Introduction

Glycopeptides plays crucial roles in various biological functions, especially in biological recognition events, signal transduction, and immune response. The carbohydrate moieties are attached through the oxygen in the side-chain of serine/threonine in *O*-linked glycoproteins or through the carboxyamide nitrogen of asparagine in case of *N*-linked glycoproteins. The rational preparation of the glycosylated peptides is still one of the most challenging tasks of peptide chemistry especially of those having oligosaccharide moieties. There are two main strategies: the stepwise approach (normally proceeds through a protected glycosylated amino acid intermediate which usually serves as the building block for a solid-phase construction of a peptide sequence) and the convergent method (the required carbohydrate chain and peptide are each built independently, and the amide or ester linkage is created in the synthesis), both of them can be implemented in liquid or solid-phase. We describe here a mixed Fmoc/Boc solid-phase synthesis strategy for the preparation of glycopeptides by using a new, mild and selective Boc deprotecting agent.

Results and Discussion

According to literature the Fmoc-protected glycosylated asparagine and serine derivatives proved to be suitable building blocks for the solid-phase peptide synthesis. In some cases the preparation of Boc-protected glycosylated amino acid building blocks is more convenient than the Fmoc protected ones. For the incorporation of the Boc-protected glycosylated amino acid derivatives in the model peptides as selective Boc deprotecting agent-tin(IV) chloride was used [1]. The glycopeptides in this case were synthesised using the Fmoc chemistry on a TFA cleavable Rink-amide MBHA resin. According to our investigations other resins commonly used in Fmoc chemistry (Rink amide, 2-chlorotrityl resin, Wang resin) showed leakage of the peptide from the resin during cleavage with tin(IV) chloride, except the Rink-amide MBHA. As model peptides we used a shorter fragment of the Trp-cage miniprotein (Leu-Lys-Asn*-Gly-Gly-Pro) [2] and an aggrecan fragment, from the most glycosylated region of the protein (Gly-Val-Glu-Asp-Ile-Ser*-Gly-Leu-Pro-Ser-Gly), where * is site of glycosylation. As building blocks Nα-Boc-protected [GlcNAc(β1-N)]Asn, [GlcNAc(β1-4)GlcNAc(β1-N)]Asn, [Man(β1-4)GlcNAc(β1-4)GlcNAc(β1-N)]Asn and [Xil(Bz)$_3$(β1-O)]Ser were used (Figure 1).

The synthesis of Leu-Lys-[GlcNAc(β1-N)]Asn-Gly-Gly-Pro-NH_2,Leu-Lys-[GlcNAc(β1-4)GlcNAc (β1-N)]Asn-Gly-Gly-Pro-NH_2, Leu-Lys-[Man(β14)GlcNAc(β1-4)GlcNAc(β1-N)]Asn-Gly-Gly-Pro-NH_2 was carried out as follows:

Rink amide-MBHA PS resin (loading: 0.81 mM/g) was applied. The first 3 amino

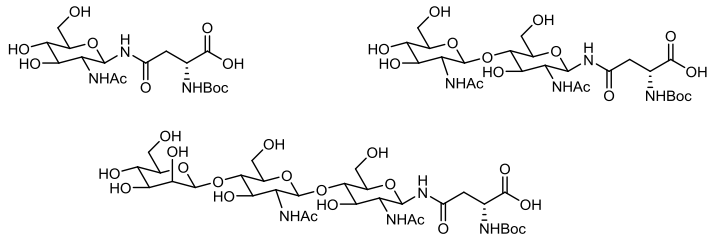

Fig. 1. Used building blocks.

acids were incorporated using the Fmoc/*t*Bu strategy with three equivalents of amino acid and three equivalents of *N*,*N*'-dicyclohexyl-carbodiimide in DMF for 3 hours. The coupling efficiency was monitored with the Kaiser test [3]. Fmoc-deprotection was made with 20% piperidine in DMF. Before coupling of Boc-protected glycosylated aspartic acid derivatives, the resin was pre-washed with dry DCM and then the resin was treated twice with 0.2 M $SnCl_4$ in dry DCM for 10 minutes, giving the resin a red colour due to complex formation with $SnCl_4$. Coupling of the last two amino acid was performed with the standard Fmoc-amino acids and *N*,*N*'-dicyclohexyl-carbodiimide. Cleavage of the peptides from the resin was performed by addition of a mixture containing TFA:H_2O (8:2) for 3 hours. After cleavage the peptides were precipitated onto the resin in ice cold diethyl ether and lyophilized after solubilization in H_2O. The synthesis strategy of H-Gly-Val-Glu-Asp-Ile-[Xil(β1-O)]Ser-Gly-Leu-Pro-Ser(Bzl)-Gly-NH_2 was the same as in case of N-glycopeptides with the exception that in this case the peptide contains a glycosylated serine derivative with three unprotected hydroxyl functional groups and several trifunctional amino acids, which side-chains must be protected during the synthesis. Based on our earlier research the Ser-Bzl, Ser(Xil)-Bz, Glu-, Asp-ODmab protecting group combination was suitable for the preparation of this glycopeptide. Dmab-deprotection was made with 2% hydrazine-hydrate/DMF, 10 min, on resin. Bz-deprotection was made in solution-phase with 20% hydrazine-hydrate/MeOH, 1h.

In summary we found a covenient solid-phase synthesis strategy for the preparation of the above glycosylated-hexapeptide conjugates. We have developed a strategy that combines the Fmoc and Boc SPPS approaches for the preparation of N-and O-glycopeptides in high purity and resonable yield, by making use of $SnCl_4$ for Boc deprotection, which leaves the acid sensitive glycosidic bonds intact (Figure 2).

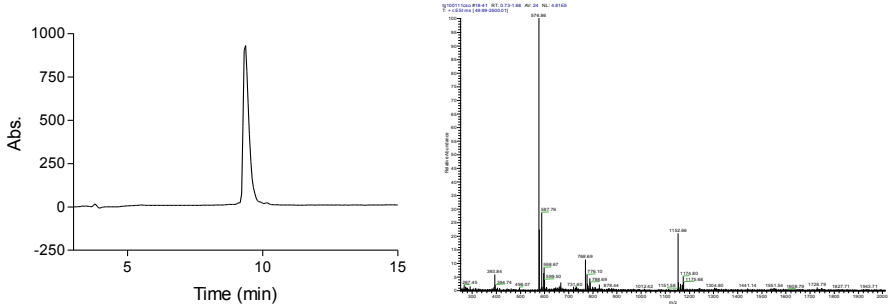

Fig. 2. Analytical HPLC (220 nm) chromatogram and ESI-MS spectrum of the purified peptide Leu-Lys-[Man(β14)GlcNAc(β1-4)GlcNAc(β1-N)]Asn-Gly-Gly-Pro-NH_2.

Acknowledgments

We are grateful for the grant from the Hungarian National Science Foundation (OTKA-71753) for the financial support.

References

1. Freeman, N.S., Gilon, C.H. *Synlett* **13,** 2097-2100 (2009).
2. Hudáky, P., Stráner, P., Farkas, V., Váradi, G.Y., Tóth, G., Perczel, A. *Biochemistry* **47**, 1007-1016 (2008).
3. Kaiser, E., Colescott, R.L., Bossinger, C.D., Cook, P.I. *Analytical Biochemistry* **34**, 595 (1970).

Proceedings of the 31st European Peptide Symposium
Michal Lebl, Morten Meldal, Knud J. Jensen, Thomas Hoeg-Jensen (Editors)
European Peptide Society, 2010

Efficient Microwave-Assisted Synthesis of Mitochondrial Signal Peptide Using Cltr-Cl and Wang Resin

Maria-Eleni Androutsou[1], Panagiotis Plotas[2], George Agelis[1], and John Matsoukas[1,2]

[1]*Department of Chemistry, University of Patras, Patras, 26500, Greece;*
[2]*Eldrug S.A., Patras Science Park, Rio, 26504, Greece*

Introduction

Mitochondrial targeting peptide plays an important role in transporting all the necessary information of proteins into mitochondria. A signal peptide is a short (3-60 amino acids long) peptide chain that directs the transport of a protein. The signal peptide that directs to the mitochondrial matrix has a sequence consisting of an alternating pattern (amphipathic helix) with a few hydrophobic amino acids and a few positively charged amino acids at the N terminus [1]. In this study the effect of two different resins (Cltr-Cl and Wang) was compared using microwave energy for the synthesis of a 18-mer signal peptide (H-Met-Leu-Ser-Leu-Arg-Gln-Ser-Ile-Arg-Phe-Phe-Lys-Pro-Ala-Thr-Arg-Thr-Leu-OH). Microwave energy represents a fast and efficient way to enhance both the deprotection and coupling reactions hindered by aggregation. In peptides, the *N*-terminal amine group and peptide backbone are polar, causing them to constantly try to align with the alternating electric field of the microwave. During peptide synthesis this can help break up the chain aggregation owing to intra and interchain association and allow for easier access to the solid phase reaction matrix [2].

Results and Discussion

1. Materials: The 18-mer signal peptide was synthesized by an automated microwave peptide synthesizer (Liberty, CEM) using Fmoc strategy. Cltr-Cl resin and protected amino acids were obtained from CBL Patras, Greece. Wang resin was obtained from Sigma-Aldrich. Purification of final products was performed with Waters Preparative HPLC (Waters Prep LC Controller) using SunFire Prep C18 column (50x100 mm) with 5 μm packing material. Purity was determined by Alliance HPLC of Waters 2695 Separation module equipped with Empower operating system using a Waters 2996 diode array UV/Vis detector and XBridge C18 column (4.6x150 mm) with 3.5 μm packing material. Identification was determined by Waters Acquity UPLC/MS System equipped with MassLynx operating system.

2. Esterification of Fmoc-Leu-OH on Cltr-Cl resin: 2-Chlorotritylchloride resin (0.36 g, 0.6 mmol Cl-/g of resin) was left to swell in dry DCM (5 mL) for 30 min, N-Fmoc-Leu-OH (0.338 g, 0.36 mmol), DIPEA (0.9 mmol) were added and stirred at RT. After 1 h, the suspension was filtered, washed successively with DCM/MeOH/DIPEA (17:2:1, v/v) (2 x

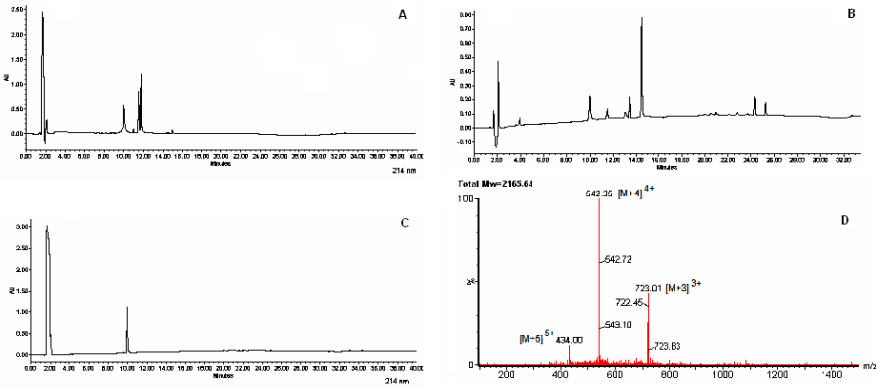

Fig. 1. Analytical RP-HPLC of final crude peptide using Cltr-Cl resin (A), Wang resin (B), final product (C) and ESI-MS of Mitochondrial Signal Peptide (D).

Table 1. Synthetic protocol in Liberty Peptide Synthesizer

Parameters	*Protocol in Microwave Peptide Synthesizer*	
	Time	*Conditions*
Coupling of Aminoacids	1 x 300sec	Reagents: HOBt/ DIC 30W, 75°C
Coupling of Fmoc-Arg(Pbf)-OH	2 x 300 sec	Reagents: HOBt/ DIC 25W, 60°C
Deprotection	1 x 30 sec 1 x 180 sec	Reagents: Pip/ DMF (1:5) Stage 1: 52W, 60°C Stage 2: 70W, 60°C

10 mL x 10 min), DMF (3 x 10 mL), i-Pro (2 x 10 mL), n-hexane (2 x 10 mL) and dried in vacuo for 24 h at RT. The loading of the amino acid/g of substituted resin was 0.7 mmol/g, calculated by weight and amino acid analysis. Removal of Fmoc group was achieved by the repetitive treatment with piperidine/DMF (1:4, 10 mL) for 10 and 20 min and the resin was thoroughly washed with DMF (3 x 10 mL), i-Pro (2 x 10 mL), n-hexane (2 x 10 mL) [3,4].
3. Esterification of Fmoc-Leu-OH on Wang resin: Wang resin (0.3 g, 0.6 mmol OH-/g of resin) was left to swell in dry DMF (5 ml) for 10 min. In a separate flask were dissolved N-Fmoc-Leu-OH (0.795 g, 2.25 mmol), HOBt (0.304 g, 2.25 mmol), DIC (0.35mL, 2.25 mmol) in the minimum amount of DMF. The solution was added to the resin. DMAP (0.11g, 0.9mmol) was dissolved in the minimum amount of DMF and was added to the resin. The mixture was stirred for 3 hours at room temperature. The solvent was removed by filtration under reduced pressure and then was added 15 mL solution acetic anhydride/pyridine/DCM (2:3:5) for 30 minutes [5]. The resin was filtered and washed 5 times with DMF, 3 times with DCM, and finally 3 times with methanol. After the final methanol wash, dry the resin was dried in vacuo. The substitution of the resin was estimated 0.7 mmol/g. Removal of Fmoc group was achieved by the repetitive treatment with piperidine/DMF (1:4, 10 mL) for 10 and 20 min and the resin was thoroughly washed with DMF (3 x 10 mL), i-Pro (2 x 10 mL), n-hexane (2 x 10 mL) [6].
4. Solid phase synthesis using microwave energy: The two different resins was transferred to Liberty Peptide Synthesizer and the two synthetic procedures were performed in the same conditions, on 0.25 mmol scale, using HOBt/DIC as coupling reagents (Table 1). The total synthesis was completed in 11 hours.
5. Cleavage from the resin: Cleavage from both resins were performed by treating the resin with 95/3/2 TFA/anisole/water for 2 hours in ambient temperature. Crude peptides were precipitated with diethyl ether, dissolved in DMSO or MeOH and analyzed in alliance HPLC (Figure 1). Separation was performed with stepped linear gradient from 5% (B) to 100% (B) in 30 min with a flow rate of 1 mL/min. [(A):TFA solution in H_2O 0,08%(v/v), (B):TFA solution in AcN 0,08%(v/v)]. Crude signal peptides were purified in Prep HPLC using a stepped linear gradient from 5% (B) to 60% (B) over 45 min at a flow rate of 12 mL/min. The identity of the peptide was verified using ESI mass spectroscopy.

This study was performed to determine the stability of two different resins using the same conditions and microwave energy. The present comparison of the two synthetic protocols showed that the results were quite similar. The synthetic protocols were pretty similar and both final crude products were of high purity. The yields for Cltr-Cl and Wang resin were 74% and 68% respectively. Also, compared to the traditional method the above synthetic protocols, using microwave energy, afforded cleaner peptides with higher yields.

Acknowledgments
This work was supported by Eldrug S.A..

References
1. Choo, K.H., et al. *BioMed Central* **6**, 249-257 (2005).
2. Friligou, I., et al. *J. Pept. Sci.* **14**, 90-93 (2008).
3. Androutsou, M.E., et al. *Amino Acids* **38**, 985-990 (2010).
4. Matsoukas, J., et al. *J. Med. Chem.* **48**, 1470-1480 (2005).
5. Jubilut, G.N., et al. *Chem. Pharm. Bull* **55**, 468-470 (2007).
6. Tselios, T., et al. *J. Med. Chem.* **45**, 275-283 (2002).

Proceedings of the 31st European Peptide Symposium
Michal Lebl, Morten Meldal, Knud J. Jensen, Thomas Hoeg-Jensen (Editors)
European Peptide Society, 2010

Electrochemical Reduction of β-Aryldehydroamino Acid Derivatives

Paula M.T. Ferreira[1], Luís S. Monteiro[1], Elisabete M.S. Castanheira[2], Goreti Pereira[1], and Carla Lopes[1]

[1]Chemistry Centre, [2]Centre of Physics, University of Minho, Gualtar, 4710-057, Braga, Portugal

Introduction

The reduction of an isolated double bond is not possible using electrochemical methods, however when the double bond is conjugated with an electron withdrawing group such as a carbonyl it becomes reducible in the accessible potential range [1]. For some years now we have been interested in the synthesis of dehydroamino acid derivatives and in using these compounds as substrates in several types of reactions [2]. As part of this work we have been studying the electrochemical behaviour of dehydroamino acid derivatives. Although there are many reports concerning the chemical reduction of α,β-dehydroamino acids, [3] to the best of our knowledge the electrochemical reduction of β,β-disubstituted dehydroamino acids has not yet been described. Since dehydroamino acids can be considered activated alkenes we decided to study the electrochemical reduction of β,β-diaryldehydroalanines and study the photophysical properties of some of the saturated amino acids prepared and compare them with those of the corresponding β,β-diaryldehydroalanines.

Results and Discussion

Several β,β-diaryldehydroalanines (compounds **1a-d**, Table 1) were prepared from a β,β-dibromoalanine derivative [4] and aryl boronic acids by a Suzuki-Miyaura coupling reaction [5]. The cathodic peak potentials of these compounds were measured by cyclic voltammetry and these were reduced to the corresponding alanine derivatives using controlled potential electrolysis.

Table 1. Cathodic peak potentials obtained by cyclic voltammetry[a] and results obtained in the controlled potential electrolysis[b] of β,β-diaryldehydroalanine derivatives

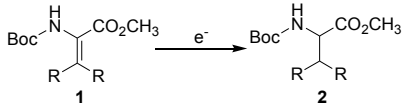

R=phenyl, **a**;
R=biphenyl, **b**;
R=naphthyl, **c**;
R=5-(1,2-dihydroacenaphthyl); **d**.

Reagent	*-Ep / (V vs SCE)*	*Product*	*Yield / %*
1a	1.81	2a	85
1b	1.75	2b	79
1c	1.80	2c	81
1d	1.76	2d	78

[a]Cathode: vitreous carbon. Solvent: dimethylformamide. Supp. electrolyte: Bu_4NBF_4 0.1 mol dm^{-3}. Substrate conc.: ≈0.005 mol dm^{-3}. [b]Solvent: acetonitrile. Supp. electrolyte:Et_4NCl (0.1 mol dm^{-3}); Proton donor:Et_3NHCl (0.04 mol.dm^{-3}).

From the cathodic peak potentials presented, it is possible to observe that all compounds studied have similar reduction potentials. Also when these potentials are compared with that of the methyl ester of *N-tert*-butoxycarbonyl-dehydrophenylalanine (Boc-ΔPhe-OMe, -1.84 V *vs* SCE [6]) it can be concluded that the presence of a second aryl moiety at the β-carbon atom does not significantly influence the reduction potential. Controlled potential electrolysis of compounds **1a-d** gave the corresponding β,β-diarylalanines in good to high yields (**2a-d**). This result is different from those reported for α,β-unsaturated ketones and *N,N*-diprotected dehydroalanines. In the case of α,β-unsaturated ketones the reduction products include the saturated ketone and a dimer [1,7]. *N,N*-Diprotected dehydroalanines give upon electrochemical reduction the corresponding diamino dicarboxylic acids [6]. The results obtained are consistent with the mechanism proposed for the reduction of

α,β-unsaturated ketones in protic media which involves the transfer of an electron to give a radical anion that rapidly protonates and tautomerizes to give an alkyl radical that is more easily reduced than the reagent and is converted into the β,β-diarylalanine [1].

The photophysical properties of compounds **2b** and **2c** were studied in three solvents of different polarity and compared with those of compounds **1b** and **1c** (Table 2).

*Table 2. Maximum absorption (λ_{abs}) and emission wavelengths (λ_{em}), molar absorption coefficients (ε) and fluorescence quantum yields (Φ_F) for compounds **1b**, **1c**, **2b** and **2c***

Solvent	λ_{abs} (nm) ($\varepsilon/10^4$ $M^{-1}cm^{-1}$)				λ_{em} (nm)				Φ_F[a]			
	1b	*1c*	*2b*	*2c*	*1b*	*1c*	*2b*	*2c*	*1b*	*1c*	*2b*	*2c*
Cyclohexane	283 (3.21) 203 (6.38)	298 (1.47) 216 (7.90)	260 (3.32) 206 (6.39)	296 (0.87) 285 (1.12) 274 (0.90) 222 (8.27)	368 382	363	318	328 339	0.067	0.086	0.37	0.13
Acetonitrile	281 (3.41) 204 (6.06)	297 (1.54) 216 (8.39)	262 (3.45) 203 (6.93)	295 (0.90) 285 (1.12) 275 (0.91) 220 (8.52)	368 385	367	318	328 339	0.025	0.044	0.32	0.15
Ethanol	281 (3.09) 201 (6.87)	298 (1.51) 216 (8.31)	261 (3.41) 205 (6.56)	295 (0.91) 285 (1.14) 275 (0.93) 220 (8.45)	369 387	365	319	327 339	0.043	0.035	0.40	0.23

[a] *Relative to anthracene in ethanol (Φ = 0.27 at 25 ºC) [8] for **1b** and **1c**; relative to naphthalene in cyclohexane (Φ_F = 0.23 at 25 ºC) [9].*

The results show that although the dehydroalanines show low quantum yields their reduction products show reasonably high fluorescent yields and could be useful as fluorescent markers.

Acknowledgments

Foundation for the Science and Technology (FCT) – Portugal and FEDER (Fundo Europeu de Desenvolvimento Regional) for support to Centro de Química (CQ-UM) and Centro de Física (CFUM) of U of Minho and through research project PTDC/QUI/81238/2006, cofinanced by FCT and program FEDER/COMPETE (FCOMP-01-0124-FEDER-007467). G.P. to FCT for a PhD grant SFRH/BD/38766/2007.

References

1. Grishaw, J., In *Electrochem. React. Mechan. Org. Chem.* Elsevier, The Netherlands, 2000, p.54-89.
2. Ferreira, P.M.T., Monteiro, L.S., In Attanasi, O.A, and Spinelli, D. (Eds.) *Targets in Heterocyclic Systems: Chemistry and Properties, Vol. 10,* Italian Society of Chemistry, Rome, 2007, p. 152-174.
3. a) Zhu, G., Zhang, X. *J. Org. Chem.* **63**, 3133-3138 (1998); b) Ohashi, A., Imamoto, T. *Org. Lett.* **3**, 373-375 (2001); c) Shultz, C.S., et al. *Org. Lett.* **7**, 3405-3408 (2005).
4. Silva, N.O., et al. *Tetrahedron Lett.* **44**, 3377-3379 (2003).
5. Pereira, G., et al. *Eur. J. Org. Chem.* 464-475 (2010).
6. Ferreira, P.M.T., Maia, H.L.S., Monteiro, L.S. *Tetrahedron Lett*. **44**, 2137-2139 (2003).
7. a) Zimmer, J.P., et al. *Anal. Chem.* **43**, 1000-1006 (1971); b) Annapoorna, S.R., Prasada, M. *J. Electroanal. Chem.* **490**, 93-97 (2000); c) Quintana-Espinoza, P., et al. *Electroanalysis* 521-525 (2006); d) Pastor, F.T., Drakulic B.J. *Tetrahedron Lett.* **51**, 734-738 (2010).
8. a) Melhuish, W.H. *J. Phys. Chem.* **65**, 229-235 (1961); b) Dawson, W.R., Windsor, M. W. *J. Phys. Chem.* **72**, 3251-3260 (1968).
9. Berlman, I.B., in *Hbk of Fluorescence Spectra of Aromatic Molecules,* Academic Press, London, 1971.

Proceedings of the 31st European Peptide Symposium
Michal Lebl, Morten Meldal, Knud J. Jensen, Thomas Hoeg-Jensen (Editors)
European Peptide Society, 2010

New Building Blocks for Solid-Phase Synthesis of Peptide Analogues: N^{β}-Fmoc-N^{β}-Methyl-aza-β^3-Amino Acids

Ksenija Kisselnova[1,2], Irène Nicolas[1], Patrick Bauchat[1], Jaak Järv[2], and Michèle Baudy-Floc'h[1]

[1]UMR CNRS 6226, ICMV, University of Rennes 1, Rennes, 35042, France; [2]Institute of Chemistry, University of Tartu, Ravila 14a, Tartu, 50411, Estonia

Introduction

N-Methylation is a precious tool to modify lipophilicity [1], proteolytic stability [2], and bioavailability [3] and to induce conformational rigidity to the peptide backbone [4]. However, multiple *N*-methylation has been seldom employed [5], probably due to the availability of *N*-methylated amino acids, as few *N*-methyl amino acids are commercially available, and their synthesis is tedious [6].

Unnatural aza-β^3-peptides are synthetic compounds designed to mimic peptides and increase their bioavailability [7]. They can have chemically diverse side chains, but they need to have amide bonds resistant to proteolysis. Yet, additional modifications are required to generate peptides with enhanced enzymatic stability and improved oral bioavailability.

Results and Discussion

We have previously reported a method to prepare N^{β}-Fmoc-aza-β^3-amino acids via reductive amination of glyoxylic acid and Fmoc-hydrazine [8]. Taking into account this previous method, we tried to reproduce the same reactions starting from methyl hydrazine instead of hydrazine. Thus the corresponding *N*-Fmoc-*N*-Me-hydrazine **2** was prepared using the enhanced nucleophilicity of the methylated *N*-atom of methylhydrazine **1**. Methylhydrazine was treated at -78°C with fluorenyl chloroformate in the presence of one equivalent of triethylamine. The monoacylation occurred on the substituted nitrogen in 92% yield, no acylation was observed on the unsubstituted nitrogen. Then we prepared the *N*-substituted Fmoc hydrazones by condensing fluoren-9-yl-methyl carbazate **2** with the appropriate aldehyde or ketone. Reduction of the hydrazone **3** with sodium cyanoborohydride afforded *N,N'*-trisubstituted hydrazine **4.** From the hydrazine **4** the reductive amination of glyoxylic acid lead to the N^{β}-Fmoc-N^{β}-Methyl-aza-β^3aa-OH **5** (R = CH_2R^1) (Figure 2 and Table 1).

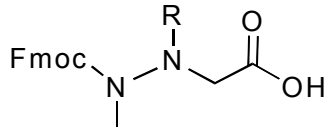

Fig. 1. N^{β}-Fmoc-N^{β}-Me-aza-β^3-aa.

For the monomer glycine a direct reductive amination of glyoxylic acid and fluoren-9-yl-methyl carbazate **2** with $NaBH_3CN$ and HCl 2N gives the corresponding N^{β}-Fmoc-N^{β}-Methyl aza-β^3-Gly-OH **5** R=H (Figure 2).

Nucleophilic substitution of the corresponding *t*-butyl bromo acetate with N^{β}-Fmoc-N^{β}-Methyl aza-β^3-Gly-OH **5** R=H would be an alternative to introduce the side chain for the aspartic analogue N^{β}-Fmoc-N^{β}-Methyl aza-β^3-Asp-OH **5** (R=CH_2CO_2t-Bu) (Figure 2).

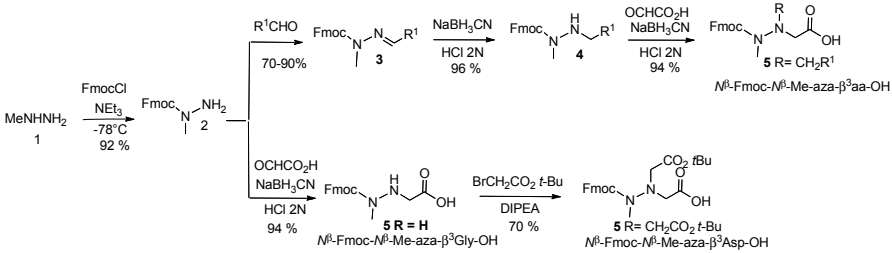

Fig. 2. Synthesis of N^{β}-Fmoc-N^{β}-Me-aza-β^3aa ***5.***

Table 1. Overall yield of N^{β}*-Fmoc-*N^{β}*-Me-aza-*β^3*-aa* ***5***

entry	N^{β}*-Fmoc-*N^{β}*-Me-aza-*β^3*-aa 5*	*R*	*yield (%)*
a	Fmoc-N^{β}-Me-aza-β^3-Gly-OH	H	83
b	Fmoc-N^{β}-Me-aza-β^3-Ala-OH	CH_3	28
c	Fmoc-N^{β}-Me-aza-β^3-Val-OH	$CH(CH_3)_2$	47
d	Fmoc-N^{β}-Me-aza-β^3-Leu-OH	$CH_2CH(CH_3)_2$	37
e	Fmoc-N^{β}-Me-aza-β^3-Phe-OH	CH_2Ph	89
f	Fmoc-N^{β}-Me-aza-β^3-Orn(Boc)-OH	$(CH_2)_3NHBoc$	34
g	Fmoc-N^{β}-Me-aza-β^3-Arg(Boc)$_2$-OH	$(CH_2)_3NHC(NHBoc)NBoc$	20
h	Fmoc-N^{β}-Me-aza-β^3-Asp(t-Bu)-OH	CH_2CO_2tBu	61

The analogue alanine was prepared in four step following the general procedure using formaldehyde in solution in water, but it could be obtained in two step starting from *N,N′*-dimethyl hydrazine **6** by nucleophilic substitution of fluorenyl chloroformate at -78°C in the presence of one equivalent of triethylamine. This reaction affords the monosubstitution in 39% yield after purification. The reductive amination then leads to **5** (R=CH_3).

Similarly to the synthesis of N^{β}-Fmoc-aza-β^3-Arg(Boc)-OH [9], N^{β}-Fmoc-N^{β}-Methyl-aza-β^3-Arg(Boc)-OH **5** (R = $(CH_2)_3NHC(NHBoc)NBoc$) was prepared from the N^{β}-Fmoc-N^{β}-Methyl-aza-β^3-Orn(Boc)-OBn. Condensation of 3-*t*-butoxy carbonyl aminopropanal with the *N*-Fmoc-*N*-Me hydrazine **2** and then reduction of the hydrazone with sodium cyanoborohydride affords *N,N′*-trisubstituted hydrazine **4** (R^1 = $(CH_2)_3NHBoc$). From this hydrazine the reductive amination of glyoxylic acid lead to the N^{β}-Fmoc-N^{β}-Methyl-aza-β^3-Orn(Boc)-OH **5** (R = $(CH_2)_3NHBoc$). In the other way, N^{β}-Fmoc-N^{β}-Methyl-aza-β^3-Orn(Boc)-OBn (R = $(CH_2)_3NHBoc$) was obtained by nucleophilic substitution of benzyl bromoacetate with hydrazine **4** (R = $(CH_2)_3NHBoc$). Selective deprotection with trifluoroacetic acid (TFA) gave N^{β}-Fmoc- N^{β}-Methyl-aza-β^3-Orn-OBn (R = $(CH_2)_3NH_2$) in 90% yield. The crude amine was guanidinylated with the Goodman reagent $(BocNH)_2NTf$ [10], and the protected analogue of arginine was obtained in 66% yield. Finally, deprotection of the benzyl protecting group with Pd/C (10 %) in ethanol gave the N^{β}-Fmoc-N^{β}-Methyl-aza-β^3-Arg(Boc)$_2$-OH **5** (R = $(CH_2)_3NHC(NHBoc)NBoc$) in 56% yield.

New building blocks corresponding to N^{β}-methylated-N^{β}-Fmoc-aza-β^3-aa-OH, can be conveniently prepared with various side chains. These new monomers, compatible with standard protocols of Fmoc/tBu SPPS, will facilitate preparation of modified peptides on solid-phase support. So, using these new monomers during the solid phase synthesis, four peptide analogs of RRASVA, known as the "minimal substrate" of the catalytic subunit of the cAMP-dependent protein kinase (PKA) have been prepared (H-R-N^{β}-Me-aza-β^3R-ASVA-OH, H-RR-N^{β}-Me-aza-β^3A-SVA-OH, H-RRAS-N^{β}-Me-aza-β^3V-A-OH, H-RRASV-N^{β}-Me-aza-β^3A-OH) and are under biological investigations.

References

1. Fairlie, D.P., Abbenante, G., March, D.R. *Curr. Med. Chem.* **2**, 654-686 (1995).
2. Cody, W.L., et al. *J. Med. Chem.* **40**, 2228-2240 (1997).
3. Barker, P.L., et al. *J. Med. Chem.* **35**, 2040-2048 (1992).
4. Chatterjee, J., Mierke, D, Kessler, H. *J. Am. Chem. Soc.* **128**, 15164-15172 (2006).
5. Holladay, M.W., et al. *J. Med. Chem.* **37**, 630- 635 (1994).
6. Rohrer, S.P., et al. *Science* **282**, 737-740 (1998).
7. Dali, H., Busnel, O., Hoebeke, J., Bi, L., Decker, P., Briand J.P., Baudy-Floc'h, M., Muller, S. *Mol. Immunol.* **44**, 3024-3036 (2007).
8. Busnel, O., Baudy-Floc'h, M. *Tetrahedron Lett.* **48**, 5767-5770 (2007).
9. Busnel, O., Bi, L., Dali, H., Cheguillaume, A., Chevance, S., Bondon, A., Muller, S., Baudy-Floc'h, M. *J. Org. Chem.* **70**, 10701-10708 (2005).
10. Planas, M., Bardaji, E., Jensen, K.J., Barany, G. *J. Org. Chem.* **64**, 7281 (1999).

Proceedings of the 31st European Peptide Symposium
Michal Lebl, Morten Meldal, Knud J. Jensen, Thomas Hoeg-Jensen (Editors)
European Peptide Society, 2010

Synthesis and Biological Studies of Cyclolinopeptide A Analogs Modified with 4-Substituted-Phenylalanine

K. Kierus[1], K. Ciupińska[1], M. Waśkiewicz[1], M. Grabowska[1], K. Kaczmarek[1], J. Olejnik[1], M. Zimecki[2], S. Jankowski[1], and J. Zabrocki[1,3]

[1]Institute of Organic Chemistry, Technical University of Łódź, 90-924 Lodz, Poland; [2]Institute of Immunology and Experimental Therapy, Polish Academy of Science, 53-114, Wrocław, Poland; [3]Peptaderm Inc., Krakowskie Przedmieście Str. 13, 00-071, Warsaw, Poland

Introduction

Immunosuppressors are used in the medical praxis to prevent graft rejection after organ transplantation and in the therapy of some autoimmune diseases. Cyclolinopeptide A (CLA) (**1**), a cyclic, hydrophobic nonapeptide isolated from linseed (Figure 1), possesses strong immunosuppressive and antimalarial activity [1]. It is postulated that both the Pro-Pro *cis*-amide bond [2] and an „edge-to-face' interaction between the aromatic rings of two adjacent Phe residues [3] are important for biological activity. Since the „edge-to-face' interaction can be modulated by electron withdrawing or electron donating substituent in aromatic rings, we present in this communication cyclic CLA analogues **2-9** in which phenylalanine residues in positions 3 and 4 have been replaced with *para*-nitro-phenylalanine **10**, *para*-amino-phenylalanine **11** and *para*-acetamido-phenylalanine **12** (Figure 2).

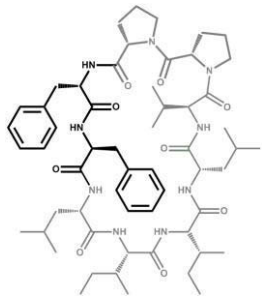

*Fig. 1. Cyclolinopeptide A (**1**).*

(**2**) c(P[1]-P[2]-(p-NO_2)F[3]-F[4]-L[5]-I[6]-I[7]-L[8]-V[9]-)
(**3**) c(P[1]-P[2]-F[3]-(p-NO_2)F[4]-L[5]-I[6]-I[7]-L[8]-V[9]-)
(**4**) c(P[1]-P[2]-(p-NO_2)F[3]-(p-NO_2)F[4]-L[5]-I[6]-I[7]-L[8]-V[9]-)
(**5**) c(P[1]-P[2]-(p-NH_2)F[3]-F[4]-L[5]-I[6]-I[7]-L[8]-V[9]-)
(**6**) c(P[1]-P[2]-F[3]-(p-NH_2)F[4]-L[5]-I[6]-I[7]-L[8]-V[9]-)
(**7**) c(P[1]-P[2]-(p-AcNH)F[3]-F[4]-L[5]-I[6]-I[7]-L[8]-V[9]-)
(**8**) c(P[1]-P[2]-F[3]-(p-AcNH)F[4]-L[5]-I[6]-I[7]-L[8]-V[9]-)
(**9**) c(P[1]-P[2]-(p-AcNH)F[3]-(p-AcNH)F[4]-L[5]-I[6]-I[7]-L[8]-V[9]-)

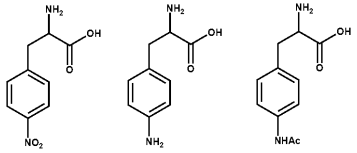

10 **11** **12**

*Fig. 2. Para-nitro-phenylalanine (**10**), para-amino-phenylalanine (**11**) and para-acetamido-phenylalanine (**12**).*

Results and Discussion

The linear analogs of peptides **2-4** and **7-9** were synthesized in 0.2 mmol scale by the manual solid-phase method using chloromethylated Merrifield resin as a solid support. Attachment of the first Boc-AA-OH (Boc-Phe-OH or Boc-(pNO2)Phe-OH or Boc-(pAcNH)Phe-OH) to the resin was performed according to cesium salt procedure [4]. The substitution level was determined around 0.60 mg/g. Standard N-Boc-protected amino acids and Boc-p-NO_2Phe-OH **13** were obtained from commercial sources. Another modified amino acid **14** (Boc-(pAcNH)Phe-OH) was obtained from Boc-(pNO_2)Phe-OH in two steps synthesis: the reduction using hydrogenolysis procedure and subsequent acylation with acetyl anhydride in presence of N-methyl-morpholine (Scheme 1).

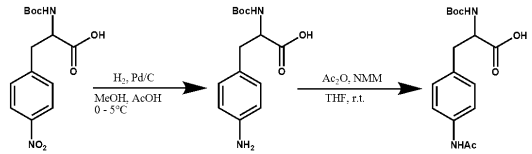

13 **14**

*Scheme 1. Synthesis of Boc protected para-acetamido-phenylalanine **12.***

The crude linear peptides were cyclized by means HOBt/EDC/ DIPEA in DCM at much lower

concentration (40 mg of the linear peptide in 600ml of DCM) than usually described for "head-to-tail" peptide cyclization reactions, to avoid the dimer formation [5,6]. The cyclic peptides **5** and **6** were obtained from the peptides **2** and **3** by one step catalytic hydrogenation (Scheme 2).

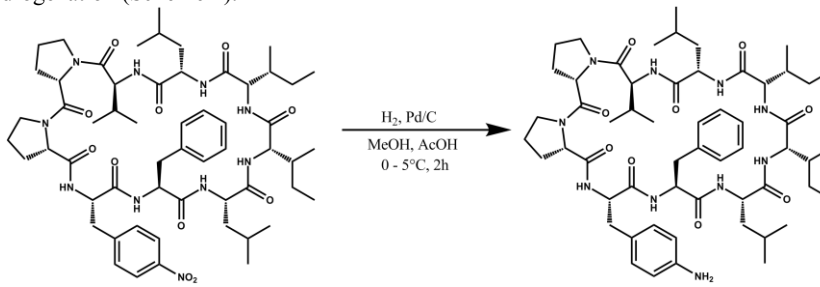

Scheme 2. Synthesis of CLA analog modified by para-amino-phenylalanine.

The compounds **2** - **9** at concentrations 1, 10 and 100 μg/ml were assayed in the proliferation test using human peripheral blood mononuclear cells (PBMC) and in the whole blood cell culture stimulated with lipopolysaccharide (determination of cytokine production). The rate of cell proliferation was determined using colorimetric MTT method [7].

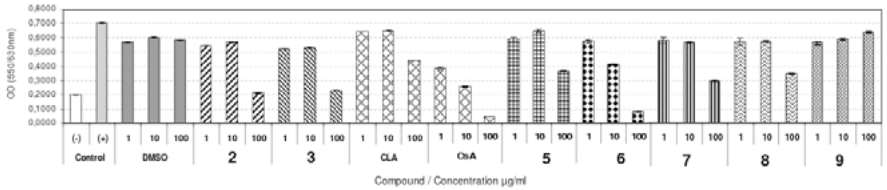

Fig. 3. Proliferation of human PBMC induced by PHA.

One can conclude that the antiproliferative and anti-inflammatory activities of the compounds **2** and **4** are comparable to unmodified CLA. Compound **3** and *para*-amino- and *para*-acetamido-phenylalanine analogues were less active (Figure 3). Compound **2** have pro-inflammatory activity.

Conformation of peptides **2** – **4** has been determined on the basis ^{1}H NMR spectra (1D, COSY, ROESY) recorded in $CDCl_3$ at -60 °C and 700 MHz. Orientation of phenyl rings relatively to ^{2}Pro ring is similar as in CLA. In spectra of **2** – **4** peptides one of proline γ protons signal is strongly shifted up-field and difference of γ protons shifts is about one ppm. The shielding effect of *para*-nitro-phenylalanine ring is weaker then the phenylalanine ring due to lower electron density of substituted aromatic ring. Analysis of ROE connectivities reveals proximity of **4** and CLA conformations. For nitro analogue **2** the lowest number of ROE signals was detected with almost no resemblance to CLA spectrum.

Acknowledgments
This work was partially supported by Technical University of Lodz grand no. DS./I-18/12/2010.

References

1. Wieczorek, Z., Bengtsson, B., Trojnar, J., Siemion, I.Z. *Peptide Res*. **4**, 275-283 (1991).
2. Kaczmarek, K., et al. *Biopolymers* **63**, 343-357 (2002).
3. Picur, B., Cebrat, M., Zabrocki, J., Siemion, I.Z. *J. Pept. Sci.* **12**, 569-574 (2006).
4. Gisin, B.F. *Helv. Chim. Acta* **56**, 1476 (1973).
5. Vojkovsky, T. *Pept.Res*. **8**, 236 (1995).
6. Li, P., Roller, P.P. *Curr. Top. Med. Chem.* **2**, 325 (2002).
7. Hansen, M.B., Nielsen, S.E., Berg, K. *J. Immunol. Methods* **119**, 203 (1989).

Proceedings of the 31st European Peptide Symposium
Michal Lebl, Morten Meldal, Knud J. Jensen, Thomas Hoeg-Jensen (Editors)
European Peptide Society, 2010

Synthesis and Folding of Kv1.3 Ion-Channel Blocking Peptides

G. Dello Iacono[1], T. Leedom[1], L. Wood[1], D. Tumelty[1], A. Bhat[1], G. Woodnutt[1], Curt Bradshaw[1], P. Morton[2], R. Numann[2], J. Ozer[2], G. Anderson[2], G. Weber[2], M. Schmidt[2], Z.-L. Mo[2], K. Keys[2], B. Koci[2], M. Williams[2], and J. Desharnais[1]

[1]*CovX; A Pfizer BTx Division, 9381 Judicial Drive, Suite 200, San Diego, CA, U.S.A.;*
[2]*Pfizer 700 Chesterfield Pkwy, Chesterfield, Saint Louis, MO, U.S.A.*

Introduction

T cell-mediated autoimmune diseases afflict millions of people worldwide and include disease such as multiple sclerosis (MS), rheumatoid arthritis (RA), psoriasis and others. Disease modifying immunotherapies have improved the management of autoimmune diseases, but these therapies induce a variety of unwanted side effects. Consequently, there remains an enormous unmet medical need for novel immunomodulators with different mechanisms of action and/or adverse-effect profiles from existing drugs. Preclinical and clinical evidence suggests that antagonizing Kv1.3 channels is effective in alleviating MS and RA syndromes. An example of such antagonists are the naturally-occurring toxin peptides produced by a variety of organisms, such as snakes, scorpions, spiders, bees, snails and sea anemones. In most cases, these toxin peptides have evolved as potent antagonists or inhibitors of ion-channels by binding to the channel pore and physically blocking the ion conduction pathway. Unfortunately due to their length (>35 aa) and complexity (most have multiple disulfide bridges), they are often overlooked at the research stage. Here we describe the synthesis and folding of a peptide found in the venom of the Asian scorpion *Orthochirus scrobiculosus* and reported to be a potent antagonist of the Kv1.3 ion-channel. We also briefly describe the conjugation of this peptide to the antibody CovX-2000 aimed to enhance its pharmacokinetic properties.

Results

Synthesis and Folding of OSK1 toxin

The peptide was assembled stepwise using Fmoc/tBu chemistry starting with Rink amide polystyrene resin. The Fmoc group was removed by a 20% piperidine/DMF solution. All the residues were double coupled using HBTU/HOBt/NMM in 1:1:4 ratio. The peptide was cleaved from the resin and simultaneously deprotected using theTFA/DTT/Phenol/ TIPS/Water, 85: 5: 5: 2.5: 2.5 cocktail for 2 hrs at room temperature. For the folding a 0.1M water solution of the peptide was made and a mix of Glutathione reduced/oxidized (GSH/GSSG 2:1 ratio) was added to a final concentration of 0.0005 M of each. The pH adjusted to around 8.3 using NH_4OH. After 12 hr, no further conversion to the oxidized form was observed. The cyclized peptide was estimated to be 75% by LC/MS analysis. (Figure 1).

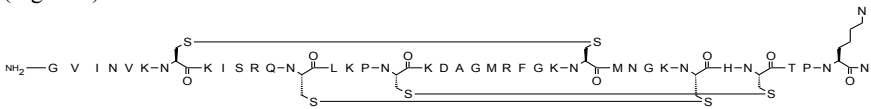

Fig.1. Folded peptide.

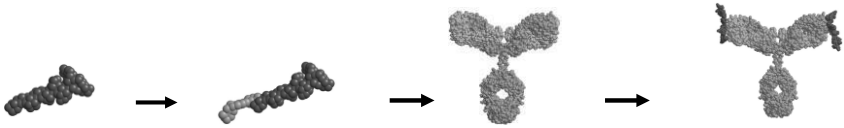

Fig. 2. The CovX-Body concept.

Fig. 3. Activity of CovX-Bodies in ^{125} IMgTX Competiton Binding Assay.

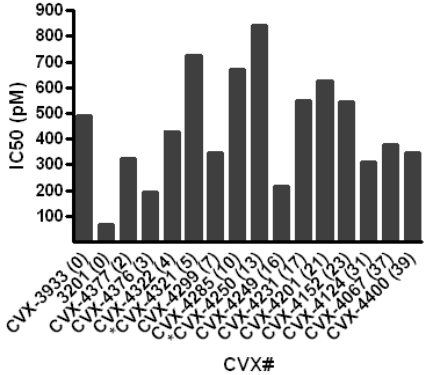

CovX Technology: *Tethering and conjugating the toxin peptide to the Antibody*
Peptides and monoclonal antibodies have emerged as important therapeutics, but each has limitations. Peptides are highly potent, but undergo rapid degradation in the body and require frequent administration. Traditional monoclonal antibodies have more favorable pharmacokinetics, but constrained by a challenging and lengthy development process. The CovX technology is based on a novel approach that addresses these limitations by combining the strengths of peptides and antibodies into a new molecule. This molecule, called a **CovX-Body**, is created by covalently joining, after appropriate tethering via proprietary linkers, a pharmacophore to the binding site of a specially designed antibody (**CVX-2000**); effectively reprogramming the antibody (see Figure 2). The conjugation of the toxin to the antibody was achieved by using a 2:1 molar ratio of the peptide with CVX-2000 Antibody (20 mg/ml, pH 6.5).

Binding affinity of CovX-Bodies for Kv1.3 was assessed by a I125-MgTx competition binding assay (Figure 3). Dilutions of test compound were incubated in presence of a constant amount I125 MgTx over membrane preparations made from a Kv1.3 overexpressing L929 cell line. After incubation, membrane preps were washed to remove unbound I125 MgTx and CovX-Body affinity of the Kv1.3 channel was determined by measuring residual I125-MgTx.

Conclusions
We described an efficient and simple way to achieve the synthesis and folding of complex peptides such as the toxin peptide containing a specific pattern of three disulfide bridges. At the same time we showed the conjugation of those peptides to the antibody CVX-2000 and reported preliminary activity data in binding the Kv1.3 ion channel. Further investigations are on the way to assess the stability and the pharmacokinetic of those compounds.

Proceedings of the 31st European Peptide Symposium
Michal Lebl, Morten Meldal, Knud J. Jensen, Thomas Hoeg-Jensen (Editors)
European Peptide Society, 2010

Synthesis of (Glyco)protein by Ligation Methods

Hironobu Hojo, Hidekazu Katayama, Akiharu Ueki, Yuko Nakahara, and Yoshiaki Nakahara

Department of Applied Biochemistry, Institute of Glycoscience, Tokai University, 4-1-1 Kitakaname, Hiratsuka, Kanagawa, 259-1292, Japan

Introduction

Proteins and glycoproteins have been mainly synthesized by the ligation methods, such as the native chemical ligation (NCL) [1] and the thioester method [2]. However, both methods still require further modifications to overcome their intrinsic drawbacks. In this paper, we report our recent approaches to overcome these problems.

Results and Discussion

NCL reaction at Xaa-Ser/Thr site

In the NCL method, the ligation site is limited to the Xaa-Cys site. As the natural abundance of cysteine in proteins is quite low, this problem severely limits the selection of the ligation site. We have developed an extended ligation reaction at the Xaa-Ser/Thr site, which is far more abundant in natural proteins than the Xaa-Cys site as shown in Scheme 1 [3]. In this method, a mercaptomethyl group on the hydroxyl group of Ser and Thr was used as a thiol auxiliary group. The advantage of this method is that this group is a labile thiohemiacetal and thus, an additional deprotection step for this auxiliary group is not required, as it is spontaneously hydrolyzed after the ligation. The efficiency of the method was demonstrated by the synthesis of glycopeptide, contulakin-G, and human calcitonin.

Fmoc-Ser/Thr(CH_2SSBu^t)-OH used for ligation were prepared in 5 steps starting from Fmoc-Ser/Thr-OBu^t. The obtained serine unit was used for the synthesis of contulakin-G **1** by NCL at Gly^6-Ser^7. N-terminal peptide thioester, pGlu-Ser-Glu-Glu-Gly-Gly-SPh **2**, was prepared by the solid-phase peptide synthesis (SPPS) using the *N*-alkylcysteine (NAC)-assisted thioesterification method [4]. C-Terminal glycopeptide, H-Ser(CH_2SSBu^t)-Asn-Ala-Thr(GalNAcBn)-Lys-Lys-Pro-Tyr-Ile-Leu-OH **3**, was prepared by the Fmoc method using thiol-free TFA cocktail for final cleavage. Then two peptides were ligated in sodium phosphate buffer pH 7.0 containing triscarboxyethylphosphine (TCEP). The thioester intermediate **4** was obtained in good yield within 10 min. After overnight, however, the desired product **6** was obtained in a yield of only 42%. As the *S*- to *N*-acyl shift in this ligation proceeds through 7-membered ring, the hydrolysis (Path B) significantly competed with the reaction. To avoid the hydrolysis, the reaction mixture was diluted with DMF containing 5% acetic acid after a 10 min ligation, when most of the starting peptides were converted to the thioester intermediate **4**. As a result, the desired product **6** was successfully

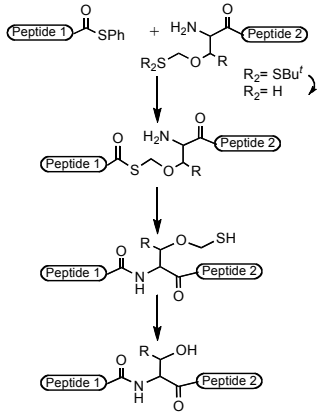

Scheme 1. Novel ligation at Xaa-Ser/Thr site.

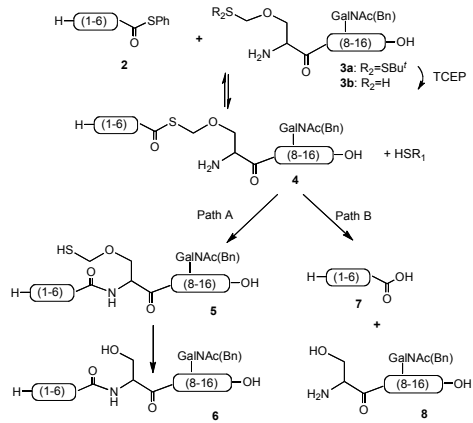

*Scheme 2. Pathway of the ligation for **6**.*

obtained in 80% yield (Scheme 2). The contulakin G **1** was easily obtained by the low-acidity TfOH treatment of glycopeptide **6**. In the same manner, human calcitonin was successfully prepared. These results demonstrates that this extended ligation method is useful, when cysteine residue does not exist at an appropriate position.

Azido group for use as an amino protecting group in the thioester method
Thioester method has the advantage that there is no restriction on the selection of the ligation site. Instead, the side chain amino and thiol groups have to be protected. To realize this, the Boc groups have to be reintroduced to the side chain amino groups, which were made free during the deprotection after SPPS. We examined the direct synthesis of the side chain-*N*-protected peptides by introducing azido-protected Fmoc-Lys during SPPS to overcome the inconvenience. The method was used for the synthesis of *N*- and *O*-glycosylated pro-opiomelanocortin (POMC) (1-74) **9** shown in Figure 1 [5]. The peptide chain was divided at Gly^{37}-Asn^{38} and both segments were prepared by the Fmoc strategy. To apply the NAC method for the synthesis of N-terminal thioester **10**, peptide chain was elongated starting from Fmoc-Gly-(Et)Cys(Trt)-$[Arg(Pbf)]_2$-NH-resin. Lys^{25} was introduced using Fmoc-Lys(N_3)-OH by DCC-HOBt method. After the completion of the chain assembly, peptide was deprotected by TFA and then thioesterified by 4-mercaptophenylacetic acid to obtain Fmoc-[$Cys(Acm)^{2,8,20,24}$, $Lys(N_3)^{25}$]-POMC(1-37)-$SC_6H_4CH_2COOH$ **10**. C-Terminal segment **11** was also prepared by the Fmoc strategy. For the introduction of Thr^{45}, Lys^{50}, Asn^{65}, Fmoc-Thr(3-*O*-benzyl-4,6-*O*-benzylidene-GalNAc)-OH, Fmoc-Lys(N_3)-OH, Fmoc-Asn($GlcNAcBn_3$)-OH, were used, respectively. After the protected-peptide resin was treated with Reagent K for 1 hr to deprotect the peptide portion, the obtained peptide was further treated with 20% thioanisole-TFA at 30 ºC for 14 h to remove benzyl groups to obtain the desired C-terminal glycopeptide [$Asn(GlcNAc)^{65}$, $Lys(N_3)^{50}$, $Thr(GalNAc)^{45}$]-POMC(38-74) **11**. Then the peptides **10** and **11** were condensed by the Ag^+-free thioester method in DMSO containing HOOBt and DIEA. After the Fmoc removal by piperidine, followed by the reduction of azido group with Zn in aq AcOH and by the removal of Acm groups by $AgNO_3$ treatment, the reduced form of the product **9** was obtained. Finally, disulfide bond was formed in the redox buffer composed of oxidized and reduced form of glutathione to successfully obtain the desired product **9** in 15% overall yield from peptide **10** and **11**. These results demonstrate that the use of azido group for amino group protection facilitates the peptide ligation by the thioester method.

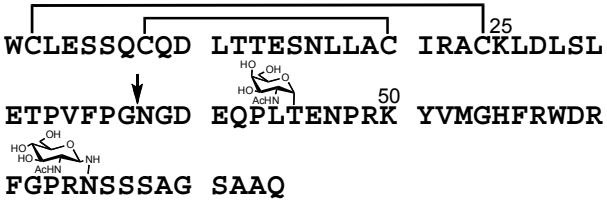

Fig. 1. Structure of POMC. An arrow indicates the site of segment coupling.

Acknowledgments
This work was partly supported by a Grant-in-Aid for Scientific Research from the Ministry of Education, Sport, Science and Technology of Japan. We thank Tokai University for a Grant-in-Aid for high-technology research.

References
1. Hojo, H., Aimoto, S. *Bull. Chem. Soc. Jpn*. **64**, 111-117 (1991).
2. Dawson, P.E., Muir, T.W., Clark-Lewis, I., Kent, S.B.H. *Science* **266**, 776-779 (1994).
3. Hojo, H., Ozawa, C., Katayama, H., Ueki, A., Nakahara, Y., Nakahara, Y. *Angew. Chem. Int. Ed*. **49**, 5318-5321 (2010).
4. Hojo, H., Onuma, Y., Akimoto, Y., Nakahara, Y., Nakahara, Y. *Tetrahedron Lett*. **48**, 25-28 (2007).
5. Katayama, H., Hojo, H., Shimizu, I., Nakahara, Y., Nakahara, Y. *Org. Biomol. Chem*. **8**, 1966- 1972 (2010).

Proceedings of the 31st European Peptide Symposium
Michal Lebl, Morten Meldal, Knud J. Jensen, Thomas Hoeg-Jensen (Editors)
European Peptide Society, 2010

S-Acyl Isopeptide Method: Preparation of Thioester-Containing Isopeptides by Fmoc-Based SPPS with Alloc Group

Taku Yoshiya, Yuka Hasegawa, Wakana Kawamura, Hiroyuki Kawashima, Youhei Sohma, Tooru Kimura, and Yoshiaki Kiso

Department of Medicinal Chemistry, Center for Frontier Research in Medicinal Science, Kyoto Pharmaceutical University, Kyoto, 607-8412, Japan

Introduction

We developed the *S*-acyl isopeptide method [1] for the synthesis of Cys-containing difficult peptides. In a study with a model peptide Ac-Val-Val-Cys-Val-Val-NH_2, its *S*-acyl isopeptide derivative had 1400-fold higher water-solubility than the native pentapeptide, and thus the isopeptide was readily purified by HPLC. The isopeptide could convert to the native peptide via an *S*-to-*N* intramolecular acyl migration reaction. Additionally, the synthesis of the isopeptide by Fmoc-based SPPS was improved when an allyl-type protective group was used. Side reactions at the thioester during base treatment for Fmoc deprotection (by aminolysis and/or diketopiperazine formation) were suppressed. We herein report the application of the *S*-acyl isopeptide method to diabetes-related amylin.

Results and Discussion

Amylin(1-12)-NH_2 (H–KCNTATCATQRL–NH_2 having a disulfide bond between

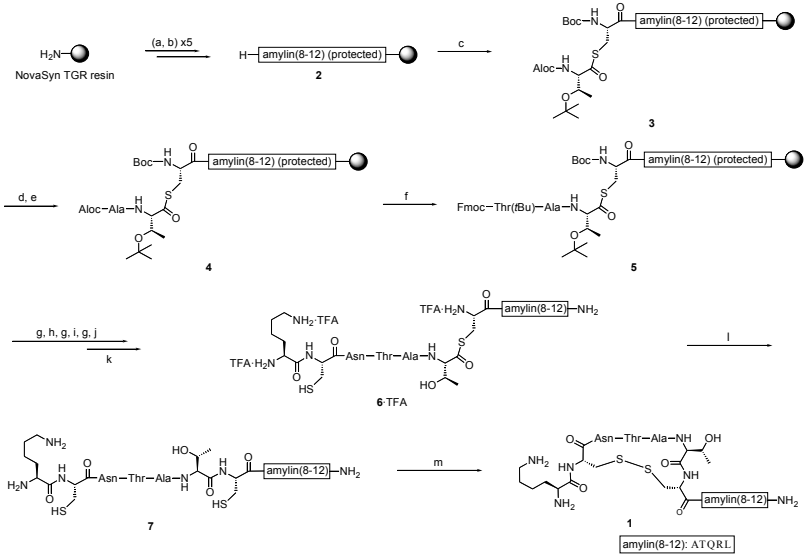

Scheme 1. Reagents and conditions: (a) Fmoc-Xaa-OH, DIPCDI, HOBt, DMF, 2 h; (b) 20% piperidine/DMF, 20 min; (c) Boc-Cys(Alloc-Thr(tBu))-OH, DIPCDI, HOAt, CH_2Cl_2, 3 h; (d) $Pd(PPh_3)_4$, $PhSiH_3$, 0.1% TFA, toluene, Ar, 20 min (3 times); (e) Alloc-Ala-OH, HCTU, DIPEA, DMF, 2 h; (f) $Pd(PPh_3)_4$, $PhSiH_3$, 0.1% TFA, toluene, Ar, 20 min; then, Fmoc-Thr(tBu)-OH, HCTU, DIPEA, DMF, 40 min (3 cycles); (g) 1-methylpyrrolidine (25 v/v%)–hexamethyleneimine (2 v/v%)–HOBt (3 w/v%) in NMP–DMSO (1:1) (also known as Reagent A [2]), 10 min; (h) Fmoc-Asn(Trt)-OH, DIPCDI, HOBt, DMF, 2 h; (i) Fmoc-Cys(Trt)-OH, DIPCDI, HOBt, DMF, 2 h; (j) Boc-Lys(Boc)-OH, DIPCDI, HOBt, DMF, 2 h; (k) TFA : ethanedithiol : H_2O : triisopropylsilane (94:2.5:2.5:1), 90 min; (l) pH 7.6 phosphate buffer, 10 min, 25°C; (m) then, addition of DMSO (for the concentration of 10%), 4 h.

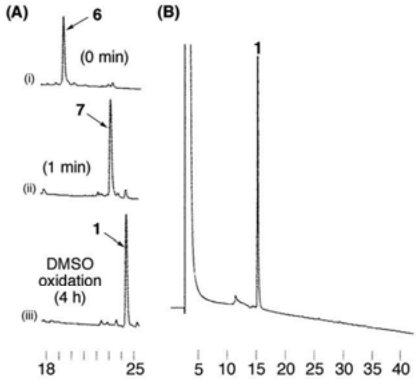

*Fig. 1. (A) Reduced-form amylin(1-12)-NH_2 (**7**) was released from the S-acyl isopeptide **6** in pH 7.6 phosphate buffer, and then oxidized to amylin(1-12)-NH_2 (**1**) by addition of DMSO to the migration buffer. Process was monitored by analytical RP-HPLC: (i) 0 s, (ii) 1 min and (iii) 4 h (after the addition of DMSO). (B) HPLC profile of purified **1**. Analytical HPLC was performed using a C18 reverse phase column (4.6 × 150 mm; YMC Pack ODS AM302) with binary solvent system: a linear gradient of CH_3CN ((A) 2%–32%/40 min, (B) 0–100%/40 min) in 0.1% aqueous TFA at a flow rate of 0.9 mL min^{-1} (40 ℃), detected at 230 nm.*

Cys^2-Cys^7, **1**), which is known as a difficult sequence, was synthesized by the optimized *S*-acyl isopeptide method (Scheme 1). Boc-Cys(Alloc-Thr(*t*Bu))-OH was coupled to **2** by the DIPCDI–HOAt method in CH_2Cl_2. After the Alloc group of resulting **3** was removed with Pd, Alloc-Ala-OH was coupled by the HCTU–DIPEA method to give **4**. Fmoc-Thr(*t*Bu)-OH was coupled after the deprotection of the Alloc group of **4**. Then, Fmoc-Asn(Trt)-OH was coupled after the removal of Fmoc group of **5** by a lower nucleophilic base cocktail (1-methylpyrrolidine (25 v/v%)–hexamethyleneimine (2 v/v%)–HOBt (3 w/v%) in NMP-DMSO (1:1), also known as Reagent A [2]). After following residues were coupled in a similar manner, isopeptide **6** was cleaved with TFA, and purified by RP-HPLC (Figure 1-A-i).

The purified isopeptide **6** was dissolved in phosphate buffer (pH 7.6) and the mixture was shaken at room temperature. After a 1 min reaction, quantitative *S*-to-*N* intramolecular acyl migration giving reduced amylin(1-12)-NH_2 (**7**) was observed (Figure 1-A-ii). Then, DMSO (final conc. 10%) was added to the solution, and the mixture was incubated at 37 ˚C for 4 h to form a disulfide bond at Cys^2–Cys^7 (Figure 1-A-iii). After final purification, the yield of amylin(1-12)-NH_2 (**1**) was 30% from resin-bound Arg residue (Figure 1-B) [3].

In this study, significant side reactions derived from thioester were not observed. Isopeptide **6** was rapidly and quantitatively converted to *N*-acyl peptide **7** in neutral buffer, and subsequent one-pot DMSO oxidation of **7** gave desired **1** cleanly. The total yield of amylin(1-12)-NH_2 (**1**) by the *S*-acyl isopeptide method was ~1.5-fold higher than that of conventional SPPS method (19%). Thus, the *S*-acyl isopeptide method would be a useful method to prepare the difficult sequence-containing peptides in the future.

Acknowledgments

This research was supported in part by the "Academic Frontier" Project for Private Universities: matching fund subsidy from MEXT (Ministry of Education, Culture, Sports, Science and Technology) of the Japanese Government, and the 21st Century COE Program from MEXT. We thank Dr. J-T. Nguyen for his English correction. We thank Ms W. Takagi for technical assistance.

References

1. Yoshiya, T., Ito, N., Kimura, T., Kiso, Y. *J. Pept. Sci.* **14**, 1203-1208 (2008).
2. Li, X., Kawakami, T., Aimoto, S. *Tetrahedron Lett.* **39**, 8669-8672 (1998).
3. Yoshiya, T., Hasegawa, Y., Kawamura, W., Kawashima, H., Sohma, Y., Kimura, T., Kiso, Y. *Biopolymers (Pept. Sci.)* in press.

Proceedings of the 31st European Peptide Symposium
Michal Lebl, Morten Meldal, Knud J. Jensen, Thomas Hoeg-Jensen (Editors)
European Peptide Society, 2010

Computational Study on Helical Structure of α,α-Disubstituted Oligopeptides Containing Chiral α-Amino Acids

Masaaki Kurihara[1], Yosuke Demizu[1], Yukiko Sato[1], Nanako Yamagata[1], Haruhiro Okuda[1], Masanobu Nagano[2], Mitsunobu Doi[3], Masakazu Tanaka[4], and Hiroshi Suemune[2]

[1]Division of Organic Chemistry, National Institute of Health Sciences, Tokyo, 158-8501, Japan, [2]Graduate School of Pharmaceutical Sciences, Kyushu University, Fukuoka, 812-8582, Japan, [3]Osaka University of Pharmaceutical Sciences, Osaka, 569-1094, Japan, [4]Graduate School of Biomedical Sciences, Nagasaki University, Nagasaki, 852-8521, Japan

Introduction

Computational simulation using conformational search calculations with AMBER* force field is most useful for conformational analysis of ligands in receptors or enzymes [1,2]. Prediction of the conformation of oligopeptides using computational simulation presents an interesting challenge to design of functionalized and bioactive peptides. We have shown the Monte Carlo conformational search method using *MacroModel* is useful to predict helical structures (α-helix, 3_{10}-helix) of oligopeptides prepared from α,α-disubstituted α-amino acids. Moreover, we have studied conformational analysis of oligopeptides containing chiral α,α-disubstituted α-amino acids to predict the helical screw sense of helical structures [3-9].

Results and Discussion

We calculated α,α-disubstituted peptides 1-6 (Figure 1) using MCMM conformational search with various force fields (AMBER*, MMFF, OPLS) and showed the results in Table 1. These calculations were performed with *MacroModel*. In the case of using AMBER* force field the results were in agreement with those of x-ray analysis and were most stable conformation evaluated by 3-21G level molecular orbital calculation. These results indicated that computational simulation using conformational search calculations with AMBER* force field is most useful for conformational analysis of oligopeptides containing α,α-disubstituted α-amino acids.

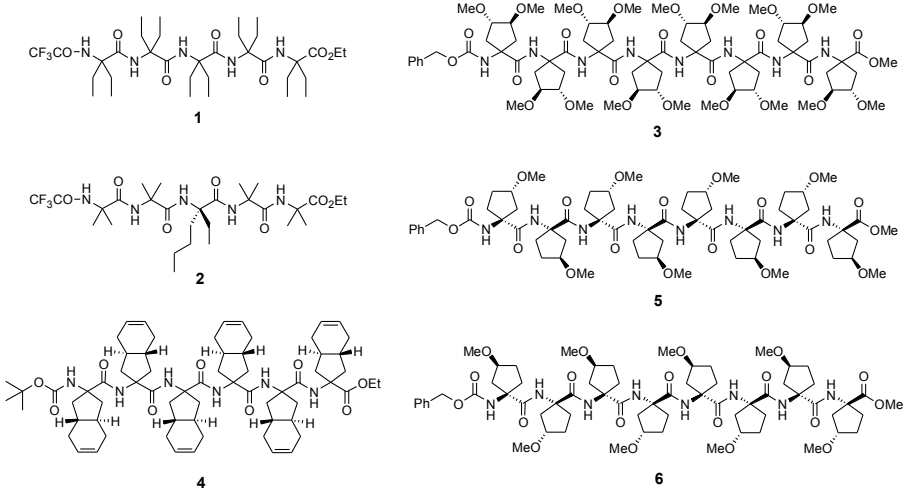

Fig. 1. Peptides 1-6.

Table1. Conformational search with various force fields

Peptide	*Global Minimum By MacroModel MCMM Conformational Search*			*X-ray*
	AMBER*	MMFF	OPLS	
1	3_{10}-helix	random coil	random coil	3_{10}-helix
		3-21G by *Spartan*		
	0 (kcal/mol)	+2.61	+14.24	
2	(*P*)-3_{10}-helix	random coil	random coil	(*P*)-3_{10}-helix
		3-21G by *Spartan*		
	0 (kcal/mol)	+14.09	+16.83	
3	(*M*)-α-helix	(*M*)-α,3_{10}-helix	(*M*)-α-helix	(*M*)-α-helix
		3-21G by *Spartan*		
	0 (kcal/mol)	+13.52	+9.32	
4	(*P*)-3_{10}-helix	(*P*)-α,3_{10}-helix	(*M*)-α-helix	(*P*),(*M*)-3_{10}-helix
		3-21G by *Spartan*		
	0 (*M*:+1.14)	+14.28	+20.67	
5	(*M*)-3_{10}-helix	(*M*)-α-helix	random coil	(*M*)-3_{10}-helix
		3-21G by *Spartan*		
	0 (kcal/mol)	+20.65	+20.96	
6	(P)-3_{10}-helix	(P)-α-helix	(P)-α-helix	(P)- 3_{10}-helix
		3-21G by Spartan		
	0 (kcal/mol)	+20.32	+7.62	

Acknowledgments
This work was supported in part by the Budget for Nuclear Research of the Ministry of Education, Culture, Sports, Science and Technology, based on the screening and counseling by the Atomic Energy Commission, by a Grant-in-Aid for Scientific Research (C) from the Japan Society for the Promotion of Science and by Health and Labour Science Research Grant from the Ministry of Health, Labour and Welfare of Japan.

References

1. Hakamata, W., et al. *Bioorg. Med. Chem. Lett.* **18**, 120-123 (2008).
2. Kurihara, M., et al. *Bioorg. Med. Chem. Lett*. **14**, 4131-4134 (2004).
3. Tanaka, M., et al. *Angew. Chem. Int. Ed*. **43**, 5360-5363 (2004).
4. Tanaka, M., et al. *J. Am. Chem. Soc*. **127**, 11570-11571 (2005).
5. Demizu, Y., et al. *Chem. Pharm. Bull*. **55**, 840-842 (2007).
6. Nagano, M., et al. *Org. Lett***. 11**, 1135-1137 (2009).
7. Demizu, Y., et al. *J. Pept. Sci.* **16**, 153-158 (2010).
8. Oba, M., et al. *Tetrahedron* **66**, 2293-2296 (2010).
9. Demizu, Y., et al. *J. Org. Chem*. **75**, 5234-5239 (2010).

Proceedings of the 31st European Peptide Symposium
Michal Lebl, Morten Meldal, Knud J. Jensen, Thomas Hoeg-Jensen (Editors)
European Peptide Society, 2010

En Route to Bicyclic Biaryl Peptides

Soledad Royo and Ernest Giralt
Institute for Research in Biomedicine, IRB Barcelona, Barcelona Science Park, Baldiri Reixac 10, Barcelona, 08028, Spain

Introduction

Natural cyclic peptides containing an aryl-aryl bond are abundant, diverse and constitute a heterogeneous group, including compounds which show antimicrobial or cytotoxic activities [1]. A common feature of all of them is the rigidity imposed by the presence of the biaryl bridge. The biaryl system also provides a site for aromatic-aromatic or π-cation interactions with the residues present on protein surfaces. This last structural feature has so far not been exploited in the design of peptide ligands for protein surface recognition. With this in mind, the scope of our project is to prepare cyclic peptide ligands which are further constrained by means of a biaryl bond. We envision this type of biaryl-containing bicyclic peptides as constrained scaffolds, which can be customized according to the corresponding target. The peptide ring is obtained by *head-to-tail* cyclization, while the synthesis of the biaryl bond is achieved through the Suzuki-Miyaura reaction [2]. A few examples have recently shown the applicability of this reaction to peptide modification [3-7]. We have focused our initial efforts on setting-up reaction conditions for the individual steps leading to the bicyclic systems. A model pentapeptide sequence containing two aromatic amino acids (Phe) and three aliphatic residues (Ala, ^{D}Pro) has been chosen for this purpose.

Results and Discussion

The precursor linear peptides have been assembled on resin using Fmoc/^{t}Bu chemistry. The Fmoc-protected borylated amino acid **1** was synthesized in solution, starting from the commercially available Boc-(4I)Phe-OH in four steps with good yields (Scheme 1). Given the instability of the Fmoc group under the basic conditions in which borylation proceeds, the reaction was carried out on the Boc-protected precursor and the protecting group was replaced subsequently.

Alternatively, on-resin borylation was achieved following a recently described methodology [7]. Due to the experimental conditions of this reaction, certain restrictions apply to the choice of both the resin and the protecting groups which can be used, in particular that of the α-amino functionality. As already mentioned, the Fmoc group is ruled out due to its instability under basic conditions. The Boc group, though compatible with the reaction conditions, cannot be used in combination with acid-labile resins, which we wish to use for our peptide synthesis, due to simultaneous cleavage from the resin during Boc removal. The *p*-nitrobenzyloxycarbonyl group (pNZ) was finally selected as the most suitable for on-resin borylation and subsequent peptide elongation. This protecting group is removed in nearly neutral conditions by treatment with a 6M $SnCl_2$, 1.6 mM HCl/dioxane solution in DMF [8], which makes it compatible with some acid-labile resins, such as Wang resin. Due to the tendency towards DKP formation shown by this sequence, tripeptide pNZ-Ala-(4I)Phe-^{D}Pro-Wang **2** was assembled through incorporation of the second residue also bearing the pNZ protecting group. Its deprotection under slightly acidic

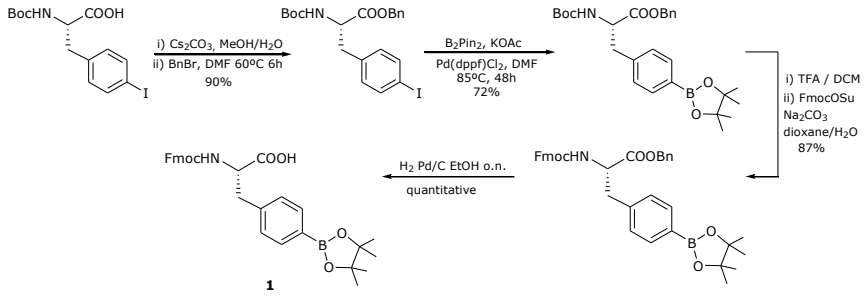

*Scheme 1. Solution-phase synthesis of Fmoc-protected borylated amino acid **1**.*

conditions and the subsequent coupling of the third amino acid with *in situ* neutralization (using PyBOP and DIEA) prevented this side reaction. Borylation of iodo peptide **2** proceeded satisfactorily under the described conditions [7]. Acidic cleavage of a sample of resin yielded boronopeptide **3** (Scheme 2).

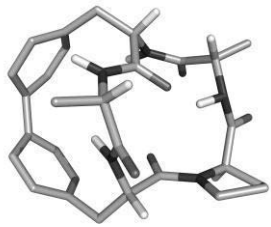

*Fig. 1. Biaryl bicyclic peptide **6**.*

Peptide elongation through stepwise coupling afforded Boc-Ala-(4I)Phe-Ala-(4Bpin)Phe-^{D}Pro-Wang (**4**). Additionally, Boc-Ala-(4Bpin)Phe-Ala-(4I)Phe-^{D}Pro-Wang (**5**) was synthesized by incorporation of the preformed borylated amino acid **1**. Both pentapeptides should yield the same biaryl bicyclic peptide when subjected to intramolecular head-to-tail cyclization and Suzuki-Miyaura reaction (Scheme 2). Resins **4** and **5** were initially treated with K_3PO_4 and $Pd(PPh_3)_4$ in DMF at 60 ºC during 48h, leading to the linear biaryl pentapeptide. Due to its low solubility in DMF, K_3PO_4 was replaced by Cs_2CO_3. The reaction could be scaled up successfully (until at least 400 mg resin). The linear biaryl pentapeptide was isolated after acidic cleavage and purification by RP-HPLC. Finally, *head-to-tail* cyclization was achieved by reaction with DPPA and $NaHCO_3$ in DMF for 24 h. A last purification step by RP-HPLC gave the desired biaryl bicyclic peptide **6** (Figure 1).

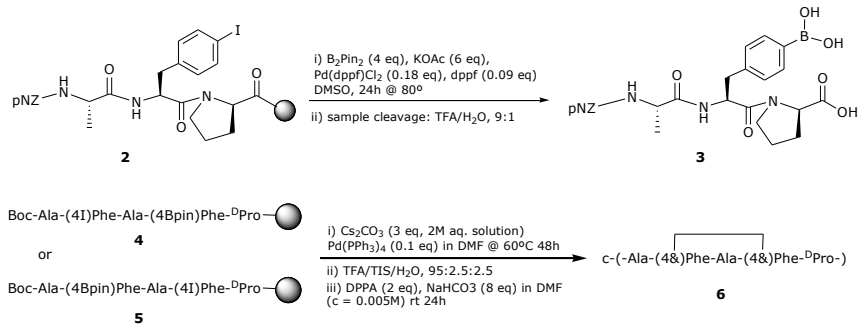

*Scheme 2. On-resin borylation of **2** (above); on-resin Suzuki-Miyaura and head-to-tail cyclization in solution leading to bicyclic peptide **6** (below).*

Acknowledgments

This research is financially supported by the Spanish Ministry of Science and Innovation (Bio2008-00799) and by the European Commission through a Marie Curie European reintegration grant (ERG-2009-248668) to S. R.

References

1. Feliú, L., Planas, M. *Int. J. Pept. Res. Ther.* **11**, 53-97 (2005).
2. Miyaura, N., Suzuki, A.J. *Chem. Rev.* **95**, 2457-2483 (1995).
3. Haug, B.E., Stensen, W., Svendsen, J.S. *Bioorg. Med. Chem. Lett.* **17**, 2361-2364 (2007).
4. Vilaró, M., Arsequell, G., Valencia, G., Ballesteros, A., Barluenga, J. *Org. Lett.* **10**, 3243-3245 (2008).
5. Cerezo, V., Amblard, M., Martinez, J., Verdie, P., Planas, M., Feliú, L. *Tetrahedron Lett.* **64**, 10538-10545 (2008).
6. Doan, N.D., Bourgault, S., Letourneau, M., Fournier, A. *J. Comb. Chem.* **10**, 44-51 (2008).
7. Afonso, A., Rosés, C., Planas, M., Feliú, L. *Eur. J. Org. Chem.* **2010**, 1461-1468 (2010).
8. Isidro-Llobet, A., Guasch-Camell, J., Álvarez, M., Albericio, F. *Eur. J. Org. Chem.* **2005**, 3031-3039 (2005).

Proceedings of the 31st European Peptide Symposium
Michal Lebl, Morten Meldal, Knud J. Jensen, Thomas Hoeg-Jensen (Editors)
European Peptide Society, 2010

Chemical Synthesis and Evaluation of a Backbone-Cyclized Minimized 2-Helix Z-Domain

Peter Järver, Cecilia Mikaelsson, and Amelie Eriksson Karlström
Royal Institute of Technology (KTH), School of Biotechnology, Division of Mol. Biotechnology, Stockholm, Sweden

Introduction

The Z-molecule is a small, engineered IgG-binding affinity protein derived from the immunoglobulin binding domain B of *Staphylococcus aureus* protein A (SpA). Z consists of 58 amino acids aligned in a well-defined antiparallel 3-helix structure. Two of the three helices are involved in ligand binding, while the third helix provides stability to the 3-helix bundle. By omitting the third stabilizing helix from the Z-domain and joining the N and C-termini by a native peptide bond, the affinity protein obtains the advantageous properties of a smaller scaffold, and in addition becomes resistant to exoproteases. We here demonstrate the synthesis and possible application of a novel cyclic 2-helix Z-domain, denoted Z_{min}. The protein sequence is based on the previously published 2-helix Z domain, $Z^{34}C$ [1]. The molecule has retained affinity for its target, is resistant to heat treatment, and lacks both free N-and C-termini (Figure 1).

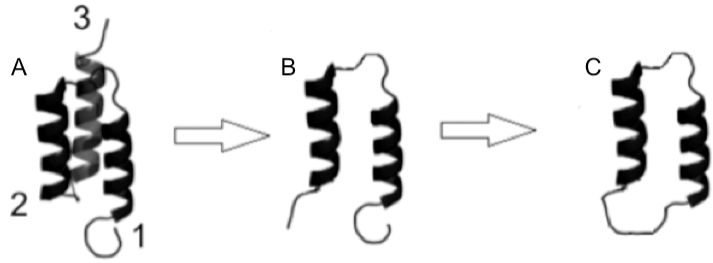

*Fig. 1. Strategy for developing a backbone cyclized 2-helix Z-molecule Z_{min}. **A)** 3-helix Z-molecule. Helixes numbered 1, 2, and 3. Removal of the third, stabilizing helix generates **B)** a 2-helix Z-domain (minimized Z-domain) **C)** The 2-helix domain is further stabilized through backbone ligation by native chemical ligation [2].*

Results and Discussion

The presented 2-helix Z_{min} domain is based on the previously reported sequence of $Z^{34}C$ [1]. $Z^{34}C$ was generated using structure-based design and phage display methods. In $Z^{34}C$, two cysteine residues were incorporated, resulting in a minimized two-helix structure stabilized by a disulfide bridge. In the Z_{min} sequence, a C-terminal thioester was instead introduced for backbone cyclization of the peptide.

Z_{min} was immobilized onto a sensor chip in order to study the interaction with hIgG in solution with hIgA used as a negative control. Z_{wt} and the engineered IgA-binding Z-variant Z_{IgA}, both with a C-terminal cysteine residue, were immobilized and utilized as positive and negative controls, respectively. Analysis of the binding kinetics shows that Z_{min} binds hIgG with comparable affinity to the positive control Z_{wt}. The dissociation constant K_D of the interaction between Z_{min} and hIgG was determined to be 15 nM, compared to 3 nM for Z_{wt} (Table 1) The determined dissociation constant are similar to those previously reported for the 3-helix and 2-helix Z-domains [1]. No interaction of hIgG with the negative control (Z_{IgA}) was observed.

Table 1. Molecular properties of Zwt and Zmin

Peptide	*Number of Helices*	*Approximated Size*	K_D
Z_{wt}	3	7kD	3nM
Z_{min}	2	4kD	15nM

When covalently immobilized onto a commercially available solid phase coupling gel (Sulfo Link® Pierce), Z_{min} was able to efficiently capture hIgG (data not shown). Covalent, site-specific immobilization was conveniently generated through the free thiol group on a single cysteine residue in the peptide. Elution of the bound protein was straightforward and a concentrated hIgG sample was easily obtained. These results show that the backbone-cyclized 2-helix domain Z_{min} can be employed for affinity purification of immunoglobulins, demonstrating a potential application for the minimized protein.

Acknowledgments
This study was supported by a grant in the SAMBIO program from VINNOVA.

References

1. Starovasnik, M.A., Braisted, A.C., Wells, J.A. *Proc. Natl. Acad. Sci. U.S.A.* **94**, 10080-10085 (1997).
2. Blanco-Canosa, J.B., Dawson, P.E. *Angew. Chem. Int. Ed. Engl.* **47**, 6851-6855 (2008).

Proceedings of the 31st European Peptide Symposium
Michal Lebl, Morten Meldal, Knud J. Jensen, Thomas Hoeg-Jensen (Editors)
European Peptide Society, 2010

Racemization-Free Synthesis of Cyclic Peptides by Use of the *O*-Acyl Isopeptide Method

Hiroyuki Kawashima, Taku Yoshiya, Yuka Hasegawa, Kazuhiro Okamoto, Tooru Kimura, Youhei Sohma, and Yoshiaki Kiso
Department of Medicinal Chemistry, Center for Frontier Research in Medicinal Science, Kyoto Pharmaceutical University, Kyoto, 607-8412, Japan

Introduction

Cyclic peptides generally possess higher biological activity and metabolic stability than their corresponding linear peptides due to conformational constraints. Despite the promises of the cyclic peptides in drug development, a head-to-tail cyclization reaction of the corresponding linear peptide is often accompanied by incomplete coupling and/or epimerization [1]. The epimerization occurs because peptides, in contrast to urethane-protected amino acids, easily form chirally labile oxazolones upon C-terminal carboxyl activation.

We previously reported a novel convergent method of peptide synthesis: racemization-free segment condensation methodology based on the *O*-acyl isopeptide method [2-5]. The idea was that an *N*-segment with a C-terminal *O*-acyl isopeptide structure at a Ser or Thr residue could be coupled to an amino group of the *C*-segment without epimerization, because the amino group of the C-terminal isopeptide is protected by a urethane-type protective group. Thus, formation of the racemization-inducible oxazolone was suppressed on the carboxyl group activation. Finally, the target peptide was generated from the *O*-acyl isopeptide via an *O*-to-*N* intramolecular acyl migration reaction.

If the racemization-free segment condensation strategy is applied to an intramolecular system, a linear peptide with a *C*-terminal *O*-acyl isopeptide could undergo epimerization-free cyclization due to the urethane-type protective group at the Ser or Thr residue, and following the *O*-to-*N* acyl migration of the cyclic *O*-acyl isopeptide, would give the target cyclic peptide [6,7].

Results and Discussion

The cyclization of protected linear *O*-acyl hexapeptide **1** Boc-Ser(H-Arg(Pmc)-Ala-Gly-Asn(Trt)-Ala)-OH was performed under three conditions (Table 1): HATU–collidine method in DMF (Entry 1), HATU–collidine method in CH_2Cl_2 (1% DMF contained, Entry

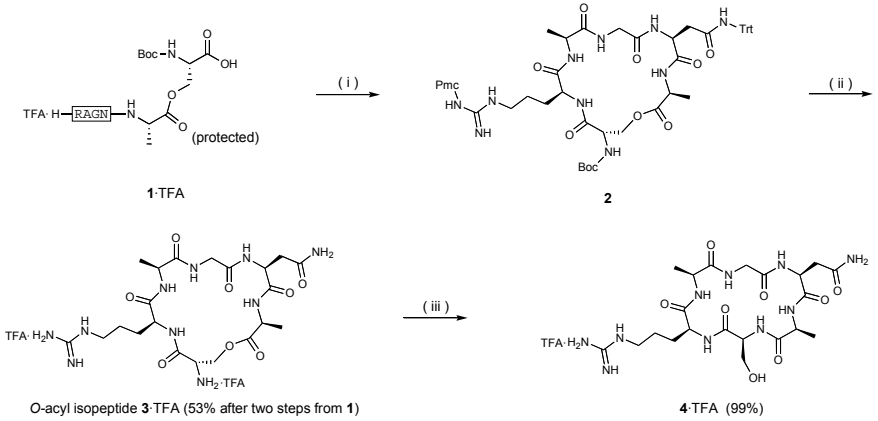

Scheme 1. Reagents and conditions: i) HATU (2 eq), 2,4,6-collidine (4 eq), CH_2Cl_2 (containing 6% DMF), final peptide conc: 1 mM, 3 h, rt; ii) TFA (92.5%)-m-cresol (2.5%)-thioanisole (2.5%)-H_2O (2.5%), 60 min, rt; iii) 3-(trimethylammonium)propyl-functionalized silica gel carbonate (2 eq), CH_3CN/H_2O (1:1), 3 h, rt, then treated with 0.1% aqueous TFA.

*Table 1. Cyclization of linear O-acyl isopeptide **1** to give the cyclic peptide **2***

Entry	Reagent	Solvent	Reaction (h)	HPLC Yield[b] (%)			
				1 : **2**	D-Ser-**2**[c]		des-Ser-**2**[d]
1	HATU (2 eq)-collidine (4 eq)	DMF	12	6 : 94	N.D.[e]		N.D.
2	HATU (2 eq)-collidine (4 eq)	CH_2Cl_2[f]	1	6 : 94	N.D.		N.D.
3	DPPA (3 eq)-$NaHCO_3$ (3 eq)	DMF	5 days	1 : 61	2		36

[a]peptide concentration = 1 mM; temp = rt; [b]Yields were estimated by the peak area in analytical HPLC; [c]Authentic D-Ser derivative was synthesized independently and used to determine the ratio of epimerization by RP-HPLC; [d]cyclo(RAGNA) + the [D-Ala] derivative; [e]N.D. = Not detected. (detection limit: 0.5%); [f]containing 1% DMF.

2) and DPPA (diphenylphosphoryl azide)–$NaHCO_3$ method in DMF (Entry 3). In Entry 1, the desired **2** (94%, HPLC yield) was obtained after 12 h reaction and the D-Ser derivative derived from epimerization was not detected in the crude sample. This result indicates that the [D-Ser] formation (39% in the cyclization of the corresponding native peptide by the conventional method) could be suppressed in the cyclization at the Boc-protected *O*-acyl isopeptide, suggesting that the ring-closing reaction did not involve the formation of the oxazolone. In Entry 2 with CH_2Cl_2 (1% DMF contained), 94% of **2** was formed after 1 h reaction without epimerization. In the cyclization with DPPA (Entry 3), the des-Ser byproduct (36%) was detected in addition to the desired **2**, and a few percent of a peak derived from the D-Ser derivative was detected. Finally, the isolated yield of cyclic *O*-acyl isopeptide **3**·TFA after two steps from **1** was 53% (Scheme 1).

In neutral phosphate buffer (pH 7.6), the isopeptide **3**·TFA was converted to the native cyclic peptide **4** via the *O*-to-*N* intramolecular acyl migration reaction within 1 min. Instead, when the isopeptide **3**·TFA was dissolved in water/CH_3CN (1:1) in the presence of two molar excess of 3-(trimethylammonium)propyl-functionalized silica gel carbonate, a quantitative *O*-to-*N* acyl migration was observed after 3 h reaction without any side reaction. The pure target peptide **4** was isolated after filtration followed by lyophilization of the filtrate.

Secondary structures of **3** and **4** were examined by CD spectrometry. (Figure 1) The *O*-acyl isopeptide **3** and cyclic peptide **4** adopted different secondary structures, suggesting that a well-known secondary structure disrupting effect by the introduced *O*-acyl isopeptide observed in many linear peptides [2,3] is also exerted in cyclic peptides.

In conclusion, the head-to-tail cyclization of the linear peptide with a C-terminal *O*-acyl isopeptide proceeded to give the cyclic *O*-acyl isopeptide without epimerization. Interestingly, the cyclic *O*-acyl isopeptide possessed a different secondary structure when compared to the native cyclic peptide. Finally, the isopeptide was efficiently converted to the desired cyclic peptide via the *O*-to-*N* acyl migration reaction.

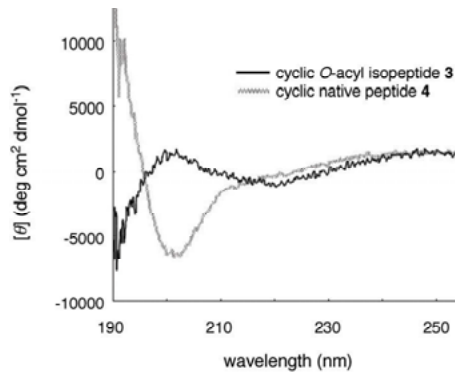

Fig. 1. CD spectra of cyclic peptides.

References

1. Davies, J.S. *J. Peptide Sci.* **9**, 471-501 (2003).
2. Sohma, Y., et al. *Chem. Commun*. 124-125 (2004).
3. Sohma, Y., et al. *Biopolymers (Pept. Sci.)* **88**, 253-262 (2007).
4. Yoshiya, T., et al. *Tetrahedron Lett.* **47**, 7905-7909 (2006).
5. Yoshiya, T., et al. *Org. Biomol. Chem.* **7**, 2894-2904 (2009).
6. Lécaillon, J., et al. *Tetrahedron Lett.* **49**, 4674-4676 (2008).
7. Yoshiya, T., Kawashima, H., et al. *J. Peptide Sci*. **16**, 437-442 (2010).

Proceedings of the 31st European Peptide Symposium
Michal Lebl, Morten Meldal, Knud J. Jensen, Thomas Hoeg-Jensen (Editors)
European Peptide Society, 2010

Traceless Chiral Triazine Based Coupling Reagent: A New Concept for Synthesis of Optically Peptides Products From Racemic Carboxylic Acids

Katarzyna Frankowska-Kasperowicz, Beata Kolesinska, and Zbigniew J. Kaminski
Institute of Organic Chemistry, Technical University of Lodz, 90-924, Lodz, Poland

Introduction

The rapid development of the methods of combinatorial chemistry in the systematic exploration of molecular diversity and in the search for improved activities and properties of a broad range of synthetic materials have resulted in a vigorously growing demand for numerous new chiral substrates with diversified structural features. In most cases, enantiomerically active substrates are needed only in tiny amounts. Therefore, an approach based on the enantiodifferentiating transformation of usually easily available racemic substrates would be valued as more advantageous than procedures involving racemate resolution or asymmetric synthesis. Such an approach would be considered the most convenient in the case of coupling chiral building blocks like amino acids used for the construction of more complex molecules. Classic enantioselective coupling reagents, due to the presence of three chiral centers (two or more in both condensed substrates and one in chiral reagent or catalyst) inevitably require selection of suitable auxiliary and optimization of reaction conditions for the given set of substrates. This makes this methodology unacceptable for the coupling of complex, expensive molecules such as peptides. To be accepted, the method of enantioselective synthesis of peptides from racemic amino acids should be predictable and controllable with respect to efficiency, configuration, enantiomeric enrichment in peptide syntheses in solution as well as in SPPS.

Results and Discussion

In order to remove the unpredictability of coupling results involving chiral components, enantioselective reagents with traceless chiral auxiliary were proposed, designed, and used in experiments of kinetic resolution of racemic carboxylic component. According to the concept, the traceless enantioselective coupling reagent **2** is a binary system consisting of a chiral auxiliary (L*) active only during the enantiodiscriminating activation of the carboxylic component and subsequently departing after the completion of the activation stage. Thus, the structure, reactivity, and properties of the activated carboxylic component **4** should be exactly the same as those obtained in a reaction involving a well-known, classic achiral reagent **3** with well-recognized scope and synthetic limitations (Figure 1).

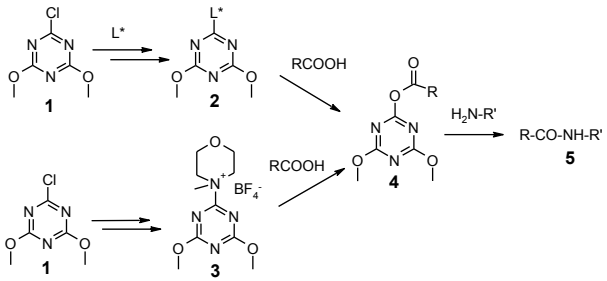

*Fig. 1. Activation of carboxylic group with chiral traceless enantioselective coupling reagent **2** yield the acylating intermediate **4** identical as the one formed with classic achiral reagent **3**.*

Moreover, due to the departure of the chiral auxiliary after activation, all further stages of the coupling procedure should remain free of the disturbances caused by the presence of the chiral auxiliary, and therefore the configuration and enantiomeric purity, once established during the activation, should remain essentially intact in all the syntheses involving this carboxylic component and reagent. Thus, for the every one racemic carboxylic component

all the final results of the syntheses could be predicted based on the simple model experiment. Until recently several chiral coupling reagents **2** were prepared using strychnine, brucine or other alkaloids as chiral auxiliary. Their effectiveness was proven in the synthesis of amides, esters and dipeptides with fully predictable configuration and ee reaching 86-99% [1]. Unresolved, however, remained access to both enantiomeric products of the condensation, because chiral auxiliaries used in the studies were accessible only in single enantiomeric form.

Herein both enantiomeric forms of the enantioselective coupling reagent **7R** and **7S** were prepared (Figure 2) in high yield by the treatment of tetrafluoroborates of methyl esters of R and/or S *N*-methylproline respectively with 2-chloro-4,6-disubstituted-1,3,5-triazine in the presence of sodium bicarbonate [2].

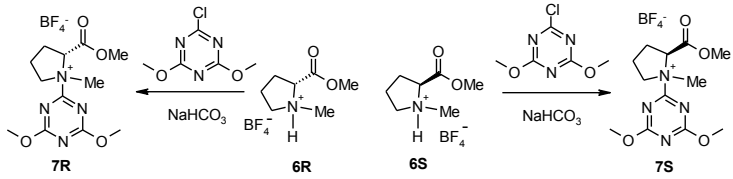

*Fig. 2. Synthesis of a pair of enantioselective coupling reagents **7S** and **7R**.*

Reagents **7R** and **7S** were found stable at room temperature. Both of them yielded with 4-methoxybenzoic acid appropriate active ester **4,** identical with a product obtained with N-methyl-N-(4,6-dimethoxy-1,3,5-triazin-2-yl)morpholinium tetrafluoroborate (**3**).

Table 1. Synthesis of Z-Ala-Gly-OMe from rac-Z-Ala-OH using enantioselective N-triazinylammonium salts derived from L and D proline

Entry	*coupling reagent*	*Yield [%]*	*configuration*	*D/L [%]*
1	**7S** (from L-Pro)	67	D	79/21
2	**7R** (from D-Pro)	65	L	25/75

It has been found that activation of *rac*-Z-Ala-OH with **7S** or **7R** followed by coupling with H-Gly-OMe gave enantiomerically enriched dipeptide Z-Ala-Gly-OMe (Table 1). Determination of enantiomeric excess and configuration of dipeptide by chromatographic method using standard procedure GC with capillary ChirasilVal column confirmed the opposite configurational preferences of both coupling reagents. It was found that reagent **7S** privileged activation of Z-D-Ala-OH, but in the presence of **7R** activation of Z-L-Ala-OH is favored.

Acknowledgments
This work was supported by Ministry of Science and Higher Education, Grant 6/PMPP/U/30-09.08/E-370/2009.

References

1. (a) Kolesinska, B., Kaminski, Z.J. *Org. Lett*. **11**, 765-768 (2009); (b) Kolesinska, B., Kasperowicz, K., Sochacki, M., Mazur, A., Jankowski, S., Kaminski, Z.J. *Tetrahedron Lett*. **51**, 20-22 (2010).
2. (a) Kolesinska, B., Kaminski, Z.J. *Polish Pat. Appl*. P-38476 from 04.02. 2008; (b) Kaminski, Z.J., Kolesinska, B. *Patent EPO* 09001796,3-1211, priority PL/04.02.08/ PLA 384377608. from 29.04.2009.

Proceedings of the 31st European Peptide Symposium
Michal Lebl, Morten Meldal, Knud J. Jensen, Thomas Hoeg-Jensen (Editors)
European Peptide Society, 2010

P-Triazinylphosphonium Sulphonates as Coupling Reagents for Peptide Synthesis in Solution

Beata Kolesinska, Olga Cieslak, Inga Relich, and Zbigniew J. Kaminski

Institute of Organic Chemistry, Technical University of Lodz, 90-924, Lodz, Zeromskiego 116, Poland

Introduction

N-Triazinylammonium tetrafluoroborates and sulphonates were found highly efficient coupling reagents useful in the peptide synthesis in solution and solid phase (SPPS) [1]. Herein, we attempted to expand the family of triazine based coupling reagents by including a new generation of coupling reagents based on *P*-triazinylphosphonium salts **5**.

Results and Discussion

P-Triazinylphosphonium sulfonates **5** were obtained by treatment of 2-chloro-4,6-dimethoxy-1,3,5-triazine with sulfonates of tertiary phosphine **3** in the presence of sodium bicarbonate (Figure 1).

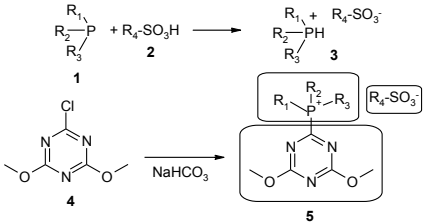

*Fig. 1. Synthesis of P-triazinylphosphonium sulfonates **5**.*

The modular structure of triazine condensing reagents made possible to create the library of *P*-triazinylphosphonium sulfonates **5a-i** (Figure 2). The library was prepared from salts of methanesulfonic acid, trifluoromethanesulfonic acid, camphorosulfonic acid, p-toluene-sulfonic acid with tributylphosphine and thiphenylphosphine.

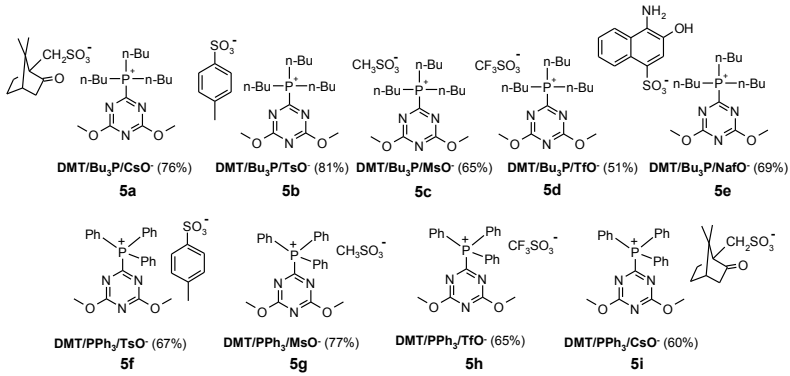

*Fig. 2. Library of P-triazinylphosphonium sulfonates **5a-i**.*

Peptide synthesis using **5a-i** as coupling reagents proceeded under mild conditions equivalent to those which were profitable in the case of *N*-triazinylammonium tetrafluoroborates and sulphonates [1]. Participation of triazine „superactive ester" **6** as active species has been documented in condensations mediated by **5a-i.** All *P*-triazinylphosphonium sulfonates were found useful as coupling reagents. The most versatile of them were found **5b** and **5f,** affording dipeptides in 78-89% yield (see Table 1).

According to HPLC, purity of the crude products isolated by extraction and standard washing procedure were found in the range 91-96%.

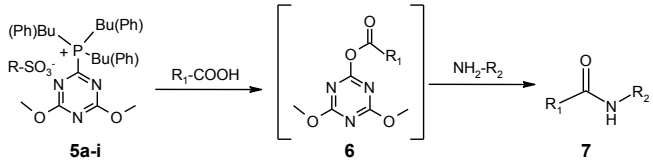

*Fig. 3. Synthesis of peptides by using **5**.*

*Table 1. Peptide synthesis using **5b** and **5f** as coupling reagents*

Coupling reagents	*Dipeptide*	*Activation time [min]*	*Yield [%]*
DMT/Bu_3P/TsO^- **(5b)**	Z-Ala-Phe-OMe	30	88
	Z-Ala-Gly-OMe		86
	Z-Ala-Aib-OMe		87
	Z-Ala-Tyr-OMe		82
	Z-Ala-Ser-OMe		85
	Fmoc-Ala-Leu-OMe		89
	Fmoc-Ala-Phe-OMe		88
	Fmoc-Phe-Ala-OMe		82
DMT/PPh_3/TsO^- **(5f)**	Z-Aib-Aib-OMe	45	81
	Z-Ala-Gly-OMe		84
	Z-Ala-Aib-OMe		83
	Z-Ala-Tyr-OMe		78
	Z-Ala-Phe-OMe		80
	Z-Phe-Aib-OMe		81
	Z-Ala-Ser-OMe		82
	Fmoc-Ala-Leu-OMe		83
	Fmoc-Ala-Phe-OMe		80
	Fmoc-Phe-Ala-OMe		79

Acknowledgments
This work was supported by Ministry of Science and Higher Education, under the Research Project: N N204 228734.

References

1. a) Kamiński, Z.J., Kolesińska, B., Kolesińska, J., Sabatino, G., Chelli, M., Rovero, P., Błaszczyk, M., Główka, M.L., Papini, A.M. *J. Am. Chem. Soc.* **127**, 16912-16920 (2005); b) Kolesińska, B., Frączyk, J., Papini, A.M., Kamiński, Z.J. *Chemistry Today* **25**, 26-29 (2007).

Proceedings of the 31st European Peptide Symposium
Michal Lebl, Morten Meldal, Knud J. Jensen, Thomas Hoeg-Jensen (Editors)
European Peptide Society, 2010

Triazine Condensing Agents for Synthesis of Peptide Bond in Aqueous Media

Krzysztof J. Zajac, Ireneusz Kaminski, Justyna Fraczyk, and Zbigniew J. Kaminski

Institute of Organic Chemistry, Technical University of Lodz, 90-924, Lodz, Poland

Introduction

Successful synthesis of the peptides bond in aqueous media still remains a challenge although several attempts have been made to resolve the problems [1]. To perform peptide synthesis in water, the coupling reagent must be water-soluble, maintain solubility and reactivity of intermediate products, preserve enantiomeric homogeneity of products in strongly polar environment and form conveniently removable waste (if any) in order to facilitate isolation of the main product. The pursuit for aqueous-compatible coupling reagent is promoted both by environmental problem of the safe disposal of large amounts of organic solvents required for SPPS, as well as by demand for efficient method useful for modification of complex molecules, incompatible with organic solvents, such as proteins and carbohydrates.

Results and Discussion

Coupling reagents were prepared in two subsequent stages by treatment 2,4-dichloro-6-methoxy-1,3,5-triazine (**1**) with aromatic and aliphatic aminosulphonic acids [2] in the presence of base, followed by quaternization of reactive intermediate in reaction with NMM and formation of zwitterionic final products **2a-f**. Activation of N-protected carboxylic components with **2a-f** proceeded in aqueous solution or in water miscible organic solvent affording water soluble intermediates **3a-f** due to the presence of sulphonic group (Figure 1).

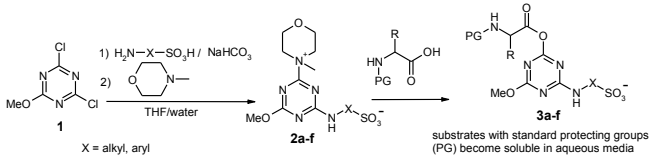

*Fig. 1. Synthesis of water-soluble coupling reagents **2a-f** and activation of N-protected carboxylic component.*

It has been observed that the structure of aminosulphonic acids have an effect on the efficiency of **2a-f** (see Figure 2). The most versatile as coupling reagent has been found **2a**, which was obtained from 4-aminobenzenesulphonic acid. Its structure was confirmed by X-ray analysis.

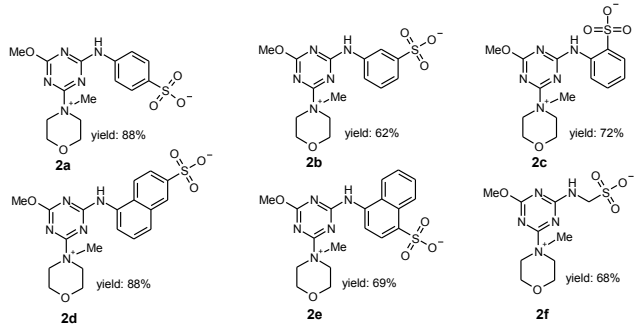

*Fig. 2. Coupling reagents **2a-f** for peptide synthesis in aqueous media.*

Synthesis of the peptide bond in aqueous solution using **2a** proceeded successfully with standard lipophilic Z and Boc protecting group without precipitation of activated intermediates, although in case of more hydrophobic Boc-Phe-Leu-OMe better yields were obtained in the presence of co-solvent such as DMF, THF or acetonitrile (compare Table 1, entry 4 and 5).

*Table 1. Synthesis of peptides using **2a** in aqueous solution*

Entry	*Carboxylic component*	*Amino component*	*Solvent*	*Yield [%]*
1	Z-Ala-OH	H_2N-Ala-OMe	water	83
2	Z-Ala-OH	H_2N-Phe-OMe	water	94
3	Boc-Gly-OH	H_2N-Ala-OMe	water	95
4	Boc-Phe-OH	H_2N-Leu-OMe	water	63
5	Boc-Phe-OH	H_2N-Leu-OMe	DMF/water	95
6	Boc-Gly-OH	H_2N-Phe-Leu-OMe	DMF/water	87
7	Boc-Gly-OH	H_2N-Gly-Phe-Leu-OMe	DMF/water	98
8	N-Boc-Tyr(Boc)-OH	H_2N-Gly-Gly-Phe-Leu-OMe	DMF/water	75

The presence of sulphonic group in **3a** and in appropriate side-products facilitated isolation of final product [3]. In most cases protected peptides precipitated almost quantitatively in the pure form the aqueous solution, but excess of acylating reagent and any impurities remained in solution. This advantageous procedure was found useful in the synthesis dipeptides and Leu-enkephalin in 75-98% yield.

Acknowledgments
Financial support of this studies by grant 9/PMPP/U/29-09.08/E-370/2009 donated by Ministry and Sciences and Higher Education (MNiSzW) is gratefully acknowledged.

References
1. Hojo, K., Maeda, M., Tanakamaru, N., Mochida, K., Kawasaki, K. *Protein Peptide Lett*. **13**, 189-192 (2006) and references cited therein.
2. Jung, R., Steinle, D., Anliker, R. *Food Chem. Toxicol*. **30**, 635-660 (1992).
3. Kaminski, Z.J., Zajac, K.J. *Acta Pharm. Poloniae*, in press.

Proceedings of the 31st European Peptide Symposium
Michal Lebl, Morten Meldal, Knud J. Jensen, Thomas Hoeg-Jensen (Editors)
European Peptide Society, 2010

Synthesis of Novel Non-Proteinogenic Amino Acids: *N*-Ethyldehydroamino Acids

Luís S. Monteiro, Joanna Kołomańska, and Ana C. Suarez
Chemistry Centre, University of Minho, Gualtar, 4710-057, Braga, Portugal

Introduction

Non-proteinogenic amino acids are an important class of organic compounds that can have intrinsic biological activity or can be found in peptides with antiviral, antitumor, anti-inflammatory or immunosuppressive activities. Among non-proteinogenic amino acids are *N*-alkylamino acids and α,β-dehydroamino acids which can be found in many biologically important peptides [1].

N-Alkylation of the peptide bond causes changes in the volume and conformation of peptides leading to reduced flexibility, increase of permeability for the membrane (increased lipophilicity) and prevention of cleavage by proteolytic enzymes [2]. Several *N*-alkylated peptides show antibiotic, anticancer or antiviral activity. For example *N*-methyl-leucine is found in cyclosporines [3]. Many methods of synthesis of *N*-alkylamino acids have been developed, most of them are *N*-methylations [2]. However, only a few methods for the synthesis of *N*-ethylated amino acids and their derivatives are available in the literature [4]. Recently, Liguori et al. proposed the use of a strong electron-withdrawing amine protecting group, 4-nitrobenzenesulfonyl (Nosyl), to enhance the low acidity of the α-amide hydrogen in order to accomplish alkylation using triethyloxonium tetrafluoroborate (Et_3OBF_4) as an alkylating agent [5].

Dehydroamino acids can be found in several yeasts and bacteria, in which they contribute with a catalytic role in the active sites of some enzymes, as well as in a variety of peptide antibiotics of bacterial origin that include the lantibiotics (nisin, epidermin, subtilin, gallidermin) [6]. In our laboratories we developed an efficient method for the synthesis of *N,N*-diacyl-α,β-dehydroamino acid derivatives from β-hydroxyamino acid derivatives by using 2 eq. of *tert*-butylpyrocarbonate (Boc_2O) and 4-dimethylaminopyridine (DMAP) as catalyst in dry acetonitrile [7]. In order to allow the synthesis of *N*-acyl-α,β-dehydroamino acid derivatives, a modification of this method was subsequently reported [8].

Herein, we report the use of a combination of the alkylation procedure reported by Liguori et al. [5] and the dehydration methodology developed by Ferreira et al. [7,8] to obtain new non-proteinogenic amino acids, namely, *N*-ethyl-α,β-dehydroamino acids.

Results and Discussion

The methodology proposed by Liguori for *N*-ethylation of *N*-Nosyl protected amino acid derivatives requires the use of side chain protection in the case of side chain functionalized amino acids [5]. To avoid the need for side chain protecting and subsequent deprotecting, our initial approach for the synthesis of *N*-ethyl-α,β-dehydroamino acid derivatives was a two step procedure in which the first step was dehydration followed by alkylation (Route A, Scheme 1). Thus, dehydration of the methyl esters of 4-nitrobenzenesulfonyl β-hydroxyamino acids (compounds **1a-c**, Scheme 1) was initially attempted by reaction with 1 eq. of Boc_2O using DMAP as catalyst, followed by treatment with *N,N,N',N'*-tetramethylguanidine (TMG) [8]. However, due to the high electron-withdrawing effect of the 4-nitrobenzenesulfonyl group, this method led to complex mixtures resulting from

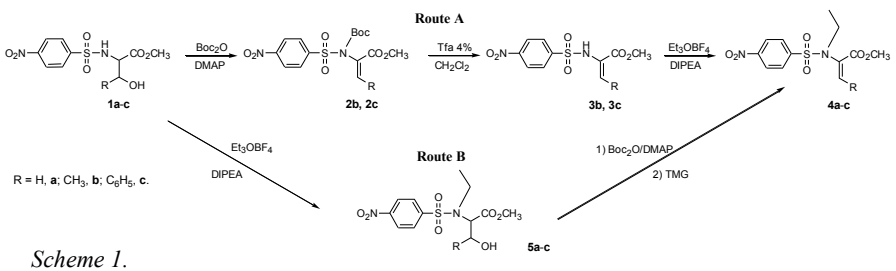

Scheme 1.

tert-butylcarbonylation of the hydroxyl group and also of the sulfonamide function. Thus, the alternative reaction with 2 eq. of Boc_2O was carried out [7]. In the case of reaction with compounds **1b** and **1c,** the corresponding *N*-Nosyl, *N*-Boc-dehydroamino acid derivatives were obtained (compounds **2b** and **2c**, 81% and 99% yield, respectively). In the case of reaction with coupound **1a**, the major product was the methyl ester of *N*-Boc, β-(4-nitrophenylsulfinyl)-α,β-dehydroserine [9]. The introduction of the *tert*-butyloxycarbonyl group makes necessary a deprotection step prior to alkylation, so compounds **2b** and **2c** were treated with a 4% solution of trifluoroacetic acid (Tfa) in dichloromethane to give compounds **3b** and **3c** in high yields (84% and 83%, respectively). These *N*-Nosyl-dehydroamino acid derivatives were subject to ethylation using the conditions proposed by Liguori [5] [2.5 eq. of Et_3OBF_4, 3.5 eq. of *N,N*-diisopropylethylamine (DIPEA) in dry dichloromethane] to give the corresponding *N*-Nosyl, *N*-ethyldehydroamino acid derivatives in good yields (compounds **4b** and **4c**, 70% and 78%, respectively).

In order to avoid the need for *tert*-butyloxycarbonyl group removal, an alternative strategy in which alkylation occurs prior to dehydration was attempted (Route B, Scheme 1). Thus, compounds **1a-c** were reacted directly without side chain protection with 1 eq. of Et_3OBF_4. Fortunately, the reaction was regioselective giving the corresponding *N*-Nosyl, *N*-ethyl-β-hydroxyamino acid derivative in high yields (compounds **5a-c**, 92-94%). These could now be dehydrated by reaction with 1 eq. of Boc_2O followed by treatment with TMG. In the case of reaction with compounds **5a** and **5c**, good yields in the corresponding *N*-Nosyl, *N*-ethyldehydroamino acid derivative were obtained (73% and 62%, respectively). Attempts in dehydration of compound **5b** resulted in long reaction times and complex mixtures which did not allow isolation of the product.

In conclusion, the route in which alkylation occurs prior to dehydration results in one step less, giving the *N*-ethyl derivatives of dehydroalanine and dehydrophenylalanine in overall yields of 67% and 57%, respectively. The dehydrophenylalanine derivative and the corresponding dehydroaminobutyric acid derivative could also be obtained by the alternative route (dehydration prior to alkylation) in overall yields of 64% and 48%, respectively. Thus, it was possible to obtain for the first time, new non-natural amino acids which incorporate both the *N*-alkyl and α,β-dehydro moieties. These can be interesting precursors of new peptides with potential pharmacological activity.

Acknowledgments

Foundation for Science and Technology (FCT) – Portugal and Fundo Europeu de Desenvolvimento Regional (FEDER) for financial support to Chemistry Centre of University of Minho. The NMR spectrometer Bruker Avance II™ 400 is part of the National NMR Network and was purchased in the framework of the National Programme for Scientific Re-equipment, contract REDE/1517/RMN/2005, with funds from POCI 2010, FEDER and FCT.

References

1. Goodman, T., Moroder, L., In Houben-Weyl (Eds.) *Synthesis of Peptides and Peptidomimetics*, Thieme, Stuttgart, Germany, 2003, vol. E22c, p. 215-271.
2. Aurelio, L., Brownlee, R.T.C., Hughes, A.B. *Chem. Rev.* **104**, 5823-5846 (2004) and references cited therein.
3. Wenger, R.M. *Angew. Chem., Int. Ed. Engl.* **24**, 77-85 (1985).
4. Ruckle, T., Dubray, B., Hubler, F., Mutter, M. *J. Pept. Sci.* **5**, 56-58 (1999).
5. Belsito, E.L., De Marco, R., Di Gioia, M.L., Liguori, A., Perri, F., Viscomi, M.C. *Eur. J. Org. Chem*. 4245-4252 (2010).
6. a) Palmer, D.E., Pattaroni, C., Nunami, K., Chadha, R.K., Goodman, M., Wakamiyia, T., Fukase, K., Horimoto, S., Kitazawa, M., Fujita, H., Kubo, A., Shiba, T. *J. Am. Chem. Soc*. **114**, 5634-5642 (1992); b) Jung, G. *Angew. Chem., Int. Ed. Engl.* **30**, 1051-1068 (1991); c) Chatterjee, C., Paul, M., Xie, L., Van Der Donk, W.A. *Chem. Rev.* **105**, 633-684 (2005).
7. Ferreira, P.M.T., Maia, H.L.S., Monteiro, L.S., Sacramento, J. *J. Chem. Soc., Perkin Trans.* **1** 3697-3703 (1999).
8. Ferreira, P.M.T., Monteiro, L.S., Pereira, G., Silva, L., Ribeiro, L., Sacramento, J. *Eur. J. Org. Chem*. 5934-5949 (2007).
9. Ferreira, P.M.T., Maia, H.L.S., Monteiro, L.S. *Eur. J. Org. Chem*. 2635-2644 (2003).

Proceedings of the 31st European Peptide Symposium
Michal Lebl, Morten Meldal, Knud J. Jensen, Thomas Hoeg-Jensen (Editors)
European Peptide Society, 2010

The Total Regioselective Control of Tartaric Acid

Jan Spengler[1,2], Ana I. Fernández-Llamazares[1,2], Javier Ruiz-Rodríguez[1,2], Klaus Burger[3], and Fernando Albericio[1,2,4]

[1]Institute for Research in Biomedicine, Barcelona Science Park, Baldiri Reixac 10, 08028, Barcelona, Spain; [2]CIBER-BBN, Networking Centre on Bioengineering, Biomaterials and Nanomedicine, Barcelona Science Park, Baldiri Reixac 10, 08028, Barcelona, Spain; [3]Institut für Organische Chemie, Universität Leipzig, Johannisallee 29, D-04103, Leipzig, Germany; [4]Department of Organic Chemistry, University of Barcelona, Martí i Franquès 1-11, 08028, Barcelona, Spain

Introduction

Tartaric acid is a structurally simple molecule which has found many applications in organic chemistry as a chiral pool compound. In peptide chemistry, it is a starting material for the total synthesis of natural and non-natural amino acid or hydroxy acids, and it serves as scaffold or core for (depsi) peptides [1].

The use of tartaric acid as a chiral building block often requires the appropriate differentiation between the functional groups present in its structure. The distinction between the two pairs of hydroxy and carboxy groups are easy to accomplish. These functionalities can be efficiently mono-derivatized by several methods. However, what still remains a challenge is the independent modification of the carboxy and the hydroxy group in a regioselective manner, which is crucial for the synthesis of certain products. The strategies reported to date require extensive preparative work, considerable study of reaction conditions, structural assignments, and sometimes cumbersome or impossible separations between regioisomers.

Results and Discussion

Herein we disclose an efficient strategy to synthesize tartaric acid derivatives bearing orthogonal sets of hydroxy and carboxy protecting groups. These 1-carboxy-2-hydroxy, and 1-carboxy-3-hydroxy protected building blocks can be prepared on a multi-gram scale (4-8 steps starting from L-tartaric acid or L-dimethyl tartrate, respectively, with overall yields between 38 – 56%).

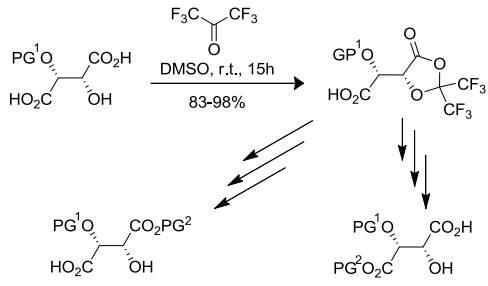

Fig. 1. PG[1]: Bzl, p-nitrobenzyl, p-methoxybenzyl; PG[2]: Me, allyl, tert-butyl.

Differentiation of all functional groups is achieved by the reaction of *O*-monobenzylated tartaric acid [2] with hexafluoroacetone (Figure 1). This reaction takes place with absolute selectivity exclusively affording the five-membered heterocycle. This dioxolanone is a key intermediate because each of the two carboxyl groups can be selectively derivatized, depending on the synthetic transformations that are carried out. In this way, all the four functional groups of tartaric acid can be modified without producing regioisomers [3].

These tartaric acid derivatives may contribute to significantly speed up the syntheses of products in which all four functional groups of tartaric acid have to be differentiated. Moreover, the use of these building blocks in some established synthetic routes should now make it possible to obtain products with additional points for structural modification.

Acknowledgments

This work was partially supported by CICYT (CTQ2009-07758 and CTQ2008-02856/BQU), the Generalitat de Catalunya (2009SGR 1024, 2009SGR-1472) and the IRB. We thank the Barcelona Science Park (Mass Spectrometry Core Facility, Nuclear Magnetic Resonance Laboratory) and the Universitat de Barcelona (Xavier Alcobé, Mercè Font, Unitat de Difracció de Raigs X Serveis Cientificotècnics) for the facilities.

References

1. Comprehensive reviews of applications in organic synthesis: (a) Coppola, G. M., Schuster, H.F. *Chiral α-Hydroxy Acids in Enantioselective Synthesis*, Wiley-VCH, Weinheim, 1997; (b) Gawronski, J., Gawronska, K. *Tartaric and Malic Acids in Synthesis: A Source Book of Building Blocks, Ligands, Auxiliaries, and Resolving Agents*, John Wiley, New York, 1999.
2. (a) Nagashima, N., Ohno, M. *Chem. Lett.* 141-144 (1987); (b) Nagashima, N., Ohno, M. *Chem. Pharm. Bull.* **39**, 1972-1982 (1991).
3. Spengler, J., Fernandez-Llamazares, A.I., Ruiz-Rodriguez, J., Burger, K., Albericio, F. *J. Org. Chem.* **75**, 5746-5749 (2010).

Proceedings of the 31st European Peptide Symposium
Michal Lebl, Morten Meldal, Knud J. Jensen, Thomas Hoeg-Jensen (Editors)
European Peptide Society, 2010

DTT Reacts with TFA to Form a Novel Bicyclic Dithioorthoester

Jan Pawlas[1], Stefan Hansen[1], Anne H. Sørensen[1], Gunnar Stærkær[1], Anette Møller[1], Neil Thompson[1], Thomas Pagano[2], Fangming Kong[2], Steve Koza[2], Mark Pozzo[3], Jari Finneman[3], and Patricia Droege[3]

[1]PolyPeptide Laboratories A/S, Herredsvejen 2, 3400, Hillerød, Denmark; [2]Pfizer Global Biologics, One Burtt Rd., Andover, MA, 01810, U.S.A.; [3]Pfizer Global Biologics, 700 Chesterfield Parkway West, St Louis, MO, 63017, U.S.A.

Introduction

Dithiothreitol (DTT, Cleland's reagent [1]) is a cheap, non-odorous reducing agent [2], which is produced by a safe and environmentally friendly process [3]. In fact, DTT was recently used as a scavenger during large scale preparation of the HIV fusion inhibitor Fuzeon [4]. We now report that DTT reacts with trifluoroacetic acid (TFA) to form a bicyclic dithioorthoester which can be difficult to detect by HPLC.

Results and Discussion

During a large scale production of a 37-mer peptide, we found that solutions of the peptide contained small amounts of an impurity, which were not easily detected by HPLC. At low peptide concentrations during purification, this impurity was virtually undetectable by HPLC. However, this material could be detected by ^{1}H NMR in highly concentrated samples of the peptide obtained after lyophilisation. Furthermore, we found that performing HPLC analyses with the UV detector set at 210 nm, this compound could be detected much easier than for example at 220 nm (see Figure 1). We set out to identify this compound and after some experimentation we were able to isolate a small quantity of this material from its mixture with the peptide. The bicyclic dithioorthoester **1** is fully consistent with the NMR and MS data for the isolated material, and we propose that this compound is formed via the dithianylium salt **2** (Figure 2). In fact, it is known that dithiols react with trifluoroacetic anhydride in the presence of strong acids to give dithianylium salts, which can be converted to α-trifluoromethyl substituted dithioorthoesters upon treatment with alcoholates [5].

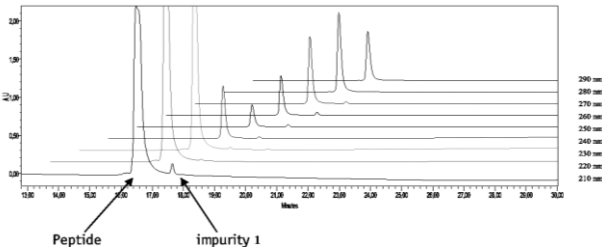

*Fig. 1. Overlay of chromatograms of a 37-mer peptide (ca 20 g/l) containing **1**.*

The peptide in which we detected dithioorthoester **1** was prepared by a standard Fmoc SPPS-cleavage-RP HPLC-lyophilisation process. Thus, the peptide resin was exposed to a DTT containing TFA cocktail and it is therefore conceivable that **1** was formed during the cleavage step of the process. In order to establish the precise conditions required for the formation of **1**, we allowed DTT to react with TFA in the presence of various additives common in cleavage cocktails. In all these experiments, DTT was fully consumed upon standing in TFA, and regardless of the presence of other reactants, **1** was formed as a major component of the reaction mixture. In fact, simply mixing DTT with TFA in the presence of triisopropylsilane (TIS) afforded **1** essentially quantitatively [6]. Finally, it is worth noting that DTT was completely stable when TFA (pK_a 0.30) was replaced by acetic acid (pK_a 4.76).

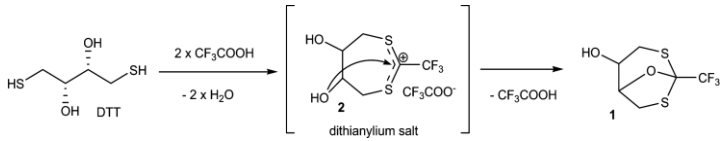

*Fig. 2. Proposed mechanism of formation of **1** via dithianylium salt **2**.*

We next sought practical conditions to remove **1** from the 37-mer peptide we had at hand. Extraction of **1** with toluene from an aqueous solution of the peptide did remove this non-peptide impurity completely. Nevertheless, on large scale it can be more convenient to purify peptides by chromatography and we set out to develop a process to remove **1** using RP HPLC. Towards this end, we examined several polymers as stationary phases and a range of mobile phases for their efficiency of removal of **1**.

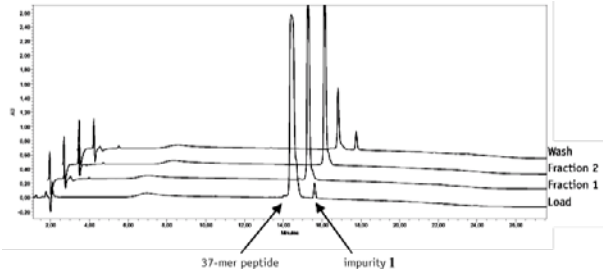

*Fig. 3. Removal of impurity **1** from a 37-mer peptide using RP HPLC [7].*

Interestingly, in all the purifications using silica C18 stationary phases, regardless of pH or the presence of various organic modifiers, the compound **1** (MW 232) coeluted with the peptide (MW > 4000). On the contrary, using polystyrene divinylbenzene (PS/DVB) based stationary phases, we were able to separate **1** from the peptide with every mobile phase system that we examined. An example of a purification using a PS/DVB resin is shown in Figure 3. Note that the main (peptide) peak contains some peptide related impurities as the test purification shown here was carried out using a batch of ca 90% pure 37-mer peptide. The purpose of this purification was solely to remove **1** and not to remove peptide related impurities.

In conclusion, we report that DTT in the presence of TFA forms a novel bicyclic dithioorthoester **1**. This compound can be difficult to detect by HPLC, especially with the UV detector set at 220 nm. The structural assignment that we propose is in full agreement with the spectral data and the formation of **1** can be explained by the mechanism shown in Figure 2. Although the choice of stationary phase was crucial for the removal of **1** from a 37-mer peptide using RP HPLC, a different set of conditions may be required for removal of **1** from another peptide.

Acknowledgments
We thank Ms. Sylvia Ritz for editorial assistance.

References

1. Cleland, W.W. *Biochemistry* **3**, 480 (1964).
2. Houghten, R.A., Li, C.H. *Anal. Biochem*. **98**, 36 (1979).
3. Bruckdorfer, T., Marder, O., Albericio, F. *Curr. Pharm. Biotechnol*. **5**, 29 (2004).
4. Zhang, H., Schneider, S.E., Bray, B.L., Friedrich, P.E., Tvermoes, N.A., Mader, C.J., Whight, S.H., Niemi, T.E., Silinski, P., Picking, T., Warren, M., Wring, S.A. *Org. Process Res. Dev*. **12,** 101 (2008).
5. Sevenard, D.V., Kirsch, P., Lork, E., Röschenthaler, G.-V. *Tetrahedron Lett*. **44**, 5995 (2003).
6. 1-(Trifluoromethyl)-8-oxa-2,7-dithia-bicyclo[3.2.1]octan-4-ol (1). At room temperature (rt) with stirring, neat TFA (30.0 ml, 403.8 mmol, 20.8 equiv) was added to DTT (3.0 g, 19.4 mmol, 1.0 equiv) and TIS (3.0 ml, 24.6 mmol, 1.3 equiv). The resulting solution was stirred at rt for 48 hours, after which DTT was fully consumed (HPLC) and the reaction was poured into 1.0 M aqueous HCl (200 ml). The suspension thus formed was extracted with ether (200 ml), the organic phase was dried ($MgSO_4$) and volatiles were removed in vacuo to afford the title compound (4.2 g, 93%) as an off-white solid. ^{1}H NMR (500 MHz, DMSO-d_6) δ 5.85 (d, *J*=5.0 Hz, 1H) 5.00 (bd, *J*=5.1 Hz, 1H), 3.86 (m, 1H), 3.61 (d, *J*=10.2 Hz, 1H), 3.33 (dd, *J*=10.2 Hz, 6.7Hz, 1H), 3.23 (dd, *J*=12.9 Hz, 10.7 Hz, 1H), 3.15 (dd, *J*=12.9 Hz, 5.1 Hz, 1H). ^{13}C NMR (100 MHz, DMSO-d_6) δ 122.8 (q), 99.1 (q), 84.5, 63.2, 32.8, 29.0. ^{19}F NMR (376 MHz, DMSO-d6) δ 73.7 HRMS *m/z* measured: 231.98351, calcd: 231.98395.
7. Stationary phase: Amberchrom XT20; mobile phase: A buffer - 1 mM HCl in water, B buffer – CH_3CN, recorded at 210 nm. Fractions 1 and 2 were obtained by eluting with 20-30% B, impurity 1 was eluted with >40% B (wash).

Proceedings of the 31st European Peptide Symposium
Michal Lebl, Morten Meldal, Knud J. Jensen, Thomas Hoeg-Jensen (Editors)
European Peptide Society, 2010

Solid Phase Synthesis of Structurally Diverse 1,2,5-Benzothiadiazepin-4-on-1,1-dioxides

Karel-Simon Slock, Jurgen Caroen, and Johan Van der Eycken
Laboratory of Organic and Bioorganic Synthesis, Department of Organic Chemistry, Ghent University, 9000, Gent, Belgium

Introduction

In modern drug research, a lot of attention goes out to so called "privileged structures". This term, introduced by Evans et al., was used to describe small molecules that show affinity for different therapeutic targets [1]. Using these molecules as a scaffold and decorating them with diverse side chains has proven to be a successful strategy in the finding of new drug candidates [2]. Therefore, our laboratory has shown a lot of interest in the search for new privileged structures.

A class of heterocyclic scaffolds currently under investigation are the 1,2,5-benzothiadiazepin-4-on-1,1-dioxides **1**, which are closely related to the well known 1,4-benzodiazepin-2,5-diones **2**. Although biological activity has already been reported with some benzothiadiazepines [3], these structures remain rather unexplored.

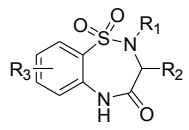

1

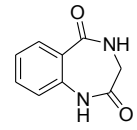

2

We would like to present a new solid phase synthesis of some structurally diverse 1,2,5-benzothiadiazepin-4-on-1,1-dioxides using commercial or easy to synthesize building blocks, as shown in the Figure 1.

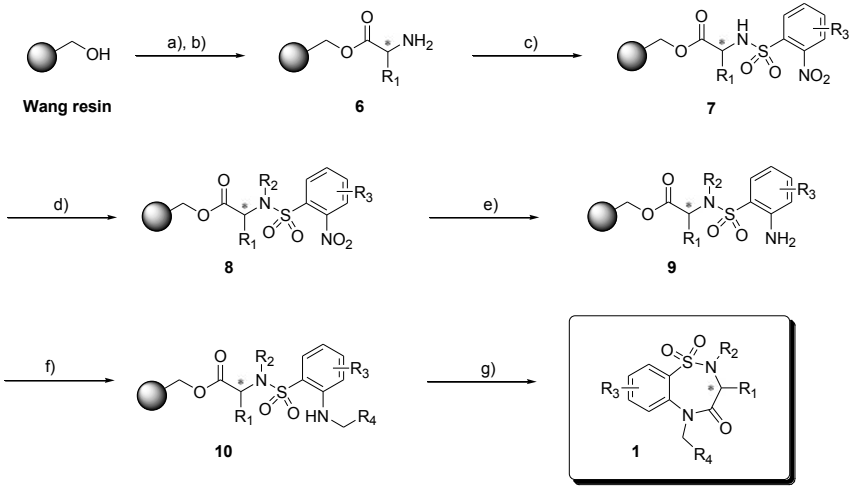

Fig. 1. a) Fmoc-AA-OH, DIC, DMAP, CH_2Cl_2, b) 20% 4 methylpiperidine in DMF, 2x10 min, c) ortho-nosylchloride, collidine, CH_2Cl_2, 2x1 hr, d) R_2-OH, DIAD, PPh_3, DCE, 2x1h, e) $CrCl_2$, DMF/MeOH 9/1, 2x1h, f) R_4-CHO, $NaBH(OAc)_3$, 1% AcOH in DCE, 2x24h, g) 1M LiOtBu in THF, 1h.

Table 1. Overview of the synthesized 1,2,5-benzothiadiazepin-4-on-1,1-dioxides. Yields are of purified material and are based upon the loading levels of the resin.

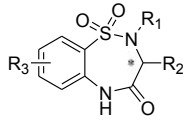

Product	R_1	R_2	R_3		Yield (%)
			7	8	
a	H	Bn	H	H	26
b	Me	Bn	H	H	38
c	$(CH_2)_2Ph$	Bn	H	H	54
d	i.Bu	Bn	H	H	41
e	$C_{10}H_{21}$	Bn	H	H	22
f	$(CH_2)_2N(CH_2CH_2)O$	Bn	H	H	33
g	H	H	H	H	39
h	Me	H	H	H	42
i	$(CH_2)_2Ph$	H	H	H	47
j	i.Bu	H	H	H	32
k	$C_{10}H_{21}$	H	H	H	10
l	$(CH_2)_2N(CH_2CH_2)O$	H	H	H	69
m	Me	iBu	H	H	48
n	Me	iBu	Cl	H	40
o	Me	$(CH_2)_4NHBoc$	H	H	54
p	Me	$CH_2Im(Trt)$	H	H	38
q	Me	CH_2indole(Boc)	H	H	57
r	Me	Bn	Cl	H	23
s	Me	Bn	Br	H	11
t	Me	Bn	H	F	24
u	Me	H	Cl	H	48
v	Me	H	Br	H	56
w	Me	H	H	F	61

Results and Discussion

In Table 1 a list of synthesized benzothiadiazepines is outlined. Diversification of the target heterocycles was achieved in three dimensions by using different amino acids (R_2), alcohols (R_1) and ortho-nosylchlorides (R_3).

Acknowledgments

We would like to thank the "IWT - Agency for Innovation by Science and Technology" and Ghent University for financial support.

References

1. Evans, B.E., et al. *J. Med. Chem.* **31**, 2235-2246 (1988).
2. a) Horton, D.E., Bourne, G.T., Smythe, M.L. *Chem. Rev.* **103**, 893-930 (2003); b) Costantino, L., Barlocco, D. *Curr. Med. Chem.* **13**, 65-85 (2006).
3. a) Ogawa, K., Matsushita, Y. *Chem. Pharm. Bull.* **40**, 2442-2447 (1992); b) Di Santo, R., Costi, R., Artico, M., Ragno, R., Lavecchia, A., Novellino, E., Gavuzzo, E., La Torre, F., Cirilli, R., Cancio, R., Maga, G. *Chem. Med. Chem.* **1**, 82-95 (2006).

Proceedings of the 31st European Peptide Symposium
Michal Lebl, Morten Meldal, Knud J. Jensen, Thomas Hoeg-Jensen (Editors)
European Peptide Society, 2010

Evaluation of Packing Materials Used for Preparative HPLC Purification of Peptide Derivatives

Kiyoshi Nokihara[1], Takafumi Ohyama[1], Noriko Ono[1], Kazuhiro Kitaori[2], and Tetsuyuki Saika[3]

[1]HiPep Laboratories, Nakatsukasa-cho 486-46, Kamigyo-ku, Kyoto, 602-8158, Japan;
[2]DAISO GmbH, Immermannstrasse 13, 40210, Duesseldorf, Germany;
[3]DAISO CO., LTD., Ohtakasu-cho 9, Amagasaki-shi, Hyogo, 660-0842, Japan

Introduction

With increasing demands for pharmaceutical peptides, selection and evaluation of packing materials for HPLC, especially silica-based reverse phase, are of great interest for the pharmaceutical industries. Focusing on preparative separation of peptides and their derivatives, several model peptides have been designed. These model peptides were used for separation-tests to compare the resolution of packing materials. The results were used as a feedback to find optimal derivatization procedures for the silica surface. In addition to efficient removal of by-products from the target peptide, recovery of desired products is also important for productivity. A GLP-1 analog, taspoglutide, consisting of 30 amino acid residues containing non-natural AAs, was chosen as a model peptide for the recovery test and for comparison of commercially available column packing materials.

H-**Aib**-EGTFTSDVSSYLEGQAAKEFIAWLVK-**Aib**-R-NH_2

Fig. 1. Taspoglutide (TAS; glucagon-like peptide-1, GLP-1; mwt : 3339.74).

Results and Discussion

By-product containing peptides are often deletion peptides, which are found for sequences containing sterically hindered amino acids, cis-trans isomers of Pro-, succinimidyl Asp-, Met(O)-residues or degradation compounds caused by cleavage of Trp residues. Model peptides containing these by-products (Table 1) have been synthesized using conventional Fmoc-SPPS with HBTU and HOBt on an automated peptide synthesizer with low-cost Wang-resin in DMF. Cleaved peptides were characterized with a high resolution reverse phase HPLC-column, HiPep-Cadenza (3 micron ODS, 3 i.d. X 150 mm), using on-line ion-trap MS to identify the desired peptide and by-products. These model peptides were then used for separation tests to compare the resolution, and results were used as a feedback to find optimal derivatization procedures for the silica surface.

Efficient removal of by-products from the target peptide on a large scale is indispensable and recovery of the desired products is important for productivity. A GLP-1 analog, taspoglutide (TAS), consisting of 30 amino acid residues containing two Aibs, non-natural amino acid, was chosen as a model peptide for the recovery test and for comparison of commercially available column packing materials. The synthesis of TAS (Figure 1) was carried out using an automated synthesizer (PSSM8, Shimadzu), with HBTU and HOBt as

Table 1. Design of model peptides containing by-products

	By-products	*Sequence of the target*	*Mol. wt*
1	Deletion Peptides	GQLKEALLDTG	1144.29
2	Cis-Trans isomer of Pro	SPTRRELQVWG	1328.49
3	Succinimide from Asp	LLDTGADDTVL	1132.23
4	Degradates of Trp generated by cleavage	PQITLWQRPLV	1350.63
5	Met(O)	KPKMIGGIGGF	1104.38

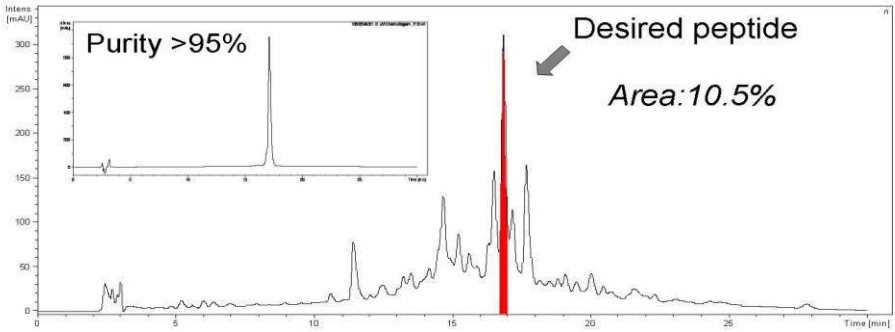

Fig. 2. Crude synthetic and preparative purified (inset) TAS. Gradient (B = 35 – 65 % in 30 min) A = 0.1% TFA, B = 0.1% TFA in 90% aq. ACN; Flow rate: 0.3 mL/min; Max. pressure: 69 kgf/cm^2.

coupling reagents (Aib was coupled with HATU) on TentaGel S RAM in DMF as a solvent. After cleavage the peptide was precipitated from ether to give the crude material (Figure 2). Several test columns (2 i.d. x 250 cm) were prepared and, for comparison, commercial ODS was also used. Based on the above tests a novel reverse phase silica for preparative separation has been developed and designated Daisogel®SP (octadecyl silica, 10 micrometer particles, 100 and 120 angstrom porosity) (Table 2). The recovery was calculated by the yield after re-chromatography. Both materials gave >65% recovery and the 100 angstrom material was slightly better than the 120 angstrom product for the model peptide. The homogeneity of the resulting purified peptides was confirmed by LCMS using the above HiPep-Cadenza (Figure 2 inset) to give >95% purity (calculated from peak area). These materials were packed in columns (5 i.d. x 50 cm) and several peptides were purified on a gram scale with flow rates of 35-50 mL/min.

Table 2. Yield from crude material and recovery in the re-chromatography. Freshly packed column was used for preparative purification and the same column was used as the second separation, re-chromatography of the purified material.

Packing material (10 micron)	*Yield from crude peptide*	*Recovery*
Daisogel®SP-100-ODS-P (100A)	14.3%	68.2%
Daisogel®SP-120-ODS-RPS (120A)	11.8%	66.4%
Commercially available 100A-C18 (from a leading company)	11.1%	32.5%

Proceedings of the 31st European Peptide Symposium
Michal Lebl, Morten Meldal, Knud J. Jensen, Thomas Hoeg-Jensen (Editors)
European Peptide Society, 2010

Structure-Activity Studies of Angiotensin IV Analogues Containing the Conformationally Constrained Aia Residue

Isabelle Van den Eynde[1], Aneta Lukaszuk[1], Koen Buysse[1], Heidi Demaegdt[2], Philippe Karoyan[3], Georges Vauquelin[2], Attila Keresztes[4], Geza Toth[4], Antal Péter[5], and Dirk Tourwé[1]

Vrije Universiteit Brussel, [1]Department of Organic Chemistry; [2]Department of Molecular and Biochemical Pharmacology, Pleinlaan 2, B-1050, Brussels, Belgium, [3]CNRS/UMR 7613, Université Pierre & Marie Curie, Place Jussieu 4, Paris, France, [4]Institute of Biochemistry, Biological Research Center, Hungarian Academy of Sciences, [5]University of Szeged, H-6701, Szeged, Hungary

Introduction

Angiotensin IV: H-Val-Tyr-Ile-His-Pro-Phe-OH (Ang IV) is a physiological active metabolite of Ang II in the renin-angiotensin system (RAS) [1]. At present it is clear that Ang IV and its analogues are effective at facilitating spatial learning [2], and have vascular and renal actions [3]. It was proposed that Ang IV may exert its effects through binding to AT4 receptors, also denoted as Insulin-Regulated Amino Peptidase (IRAP). We have reported earlier that the β-homo-amino acid containing analog H-β^{2}hVal-Tyr-Ile-His-Pro-β^{3}hPhe-OH (AL-11) is a potent, selective and stable Ang IV antagonist, in which the β^{2}hVal is responsible for stability and the β^{3}hPhe for selectivity [4]. We also reported an analogue (AL-40) in which the His^4-Pro^5 dipeptide residue is replaced by a constrained Trp residue, Aia-Gly (Figure 1).

AL-40 has improved potency compared to the previously reported Al-11 [5]. In this study we replaced Gly^5 in AL-40 by Ala, DAla, Pra, Nva or Gly^5 was deleted.

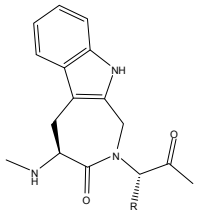

Fig. 1. The Aia-Gly (R=H) scaffold.

Results and Discussion

Synthesis of Boc-(R)- β^2-homo-Val:

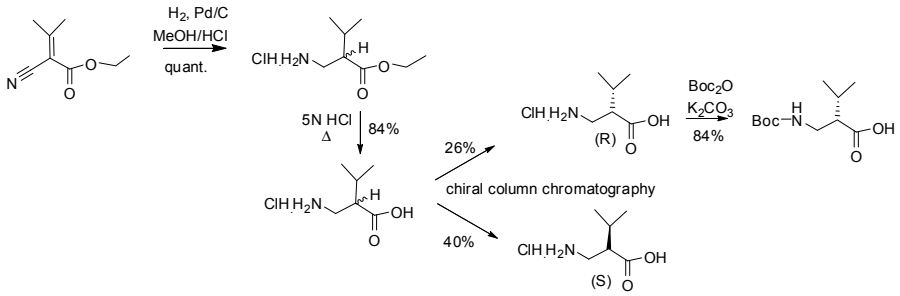

Scheme 1. Synthesis of Boc-(R) –β^2-homo-Val.

Ethyl-2-cyano-3-methylcrotonate was reduced by catalytic hydrogenation using 20wt% Pd/C (Johnson Mattey type 90) in MeOH/HCl in a Parr apparatus at 3.5 atm H_2 and 35°C. Ester hydrolysis was performed by refluxing overnight in 5N aqueous HCl. The obtained *rac*-β^2-homo-Val.HCl was resolved by semi preparative HPLC using a Chirobiotic Tag column with 0.1M TEAA/MeOH (30/70) as eluent (Scheme 1).

Peptide synthesis:

Peptide synthesis was performed on Merrifield resin, using Boc protected amino acids. The Aia structure was build on resin by reductive amination of Boc-2-formyl-L-Trp and the free

amine of the previous amino acid in presence of $NaCNBH_3$. After this reductive amination, a cyclisation was performed with TBTU/ DIEA to obtain the 4-amino-indolo[2,3-c]azepin-3-one structure [5]. After this, normal peptide synthesis was continued, followed by HF cleavage and by semi-prep reversed phase HPLC purification.

Enzyme assay:
Catalytic activity was measured by determining the rate of Leu-pNA cleavage in membrane homogenates of HEK293 cells transient transfected with human IRAP or AP-N in the presence of different concentrations of compound. [6] Results are reported in Table 1.

Table 1. Enzyme activity inhibited by Ang IV analogues in membranes of transfected HEK 293 cells

Code	*Compound*	*HEK 293 + IRAP pKi ± SD*	*HEK 293 +AP-N pKi ± SD*
Ang IV	H-Val-Tyr-Ile-His-Pro-Phe	7.25 ± 0.14	6.08 ± 0.02
AL11	H-(R)-β^2-hVal-Tyr-Ile-His-Pro-β^3-hPhe	7.56 ± 0.21	5.23 ± 0.04
AL40	H-(R)-β^2-hVal-Tyr-Ile-Aia-Gly-Phe	8.07 ± 0.05	6.10 ± 0.61
IVDE73	H-(R)-β^2-hVal-Tyr-Ile-Aia-Ala-Phe	7.56 ± 0.18	
IVDE74	H-(R)-β^2-hVal-Tyr-Ile-Aia-DAla-Phe	7.81 ± 0.18	
IVDE75	H-(R)-β^2-hVal-Tyr-Ile-Aia-Phe	7.37 ± 0.11	5.20 + 0.03
IVDE76	H-(R)-β^2-hVal-Tyr-Ile-Aia-Pra-Phe	7.59 ± 0.11	5.29 + 0.46
IVDE77	H-(R)-β^2-hVal-Tyr-Ile-Aia-Nva-Phe	5.80 + 0.24	

Enzyme stability study:
The stability of the peptides was tested in human plasma at 37±1°C and incubated for various time intervals. The reaction was stopped by addition to CH_3CN to precipitate the serum proteins. The supernatant was analyzed by RP-LC/MS.

AngIV is first metabolised between Val^1 and Tyr^2 and subsequently between Tyr^2 and Ile^3. The half-life time is 1h 40min. All Aia-containing analogues are stable to enzymatic degradation in these conditions.

Conclusions
A rapid synthesis using chiral HPLC resolution of (*R*)-β^2-h-Val was developed. Incorporation of the Aia constraint during solid phase synthesis provided AL-40 analogs without problems. All new analogues are in the same potency range as the previously synthesized AL-11 and AL-40, except IVDE77. Deletion of Gly (analog IVDE75) did not reduce potency. All analogues containing (*R*)-β^2-h-Val are stable in human plasma.

Acknowledgments
We thank the 'The Fund for Scientific Research – Flanders' (FWO, Vlaanderen) and the VUB for financial support.

References
1. Chai, S.Y., et al. *Cell Mol. Life Sci*. **61**, 2728-2737 (2004).
2. Wright, J.W., et al. *Prog. Neurobiol*. **84**, 157-181 (2008).
3. Wright, J.W., et al. *Fontiers in Neuroendocrinology* **16**, 23-52 (1995).
4. Lukaszuk, A., et al. *J. Med. Chem*. **51**, 2291-2296 (2008).
5. Feytens, D., et al. *J. Pept. Sci.* **15**, 16-22, (2009).
6. Lukaszuk, A., et al. *J. Med. Chem*. **52**, 6512-5618 (2009).

Proceedings of the 31st European Peptide Symposium
Michal Lebl, Morten Meldal, Knud J. Jensen, Thomas Hoeg-Jensen (Editors)
European Peptide Society, 2010

A Novel Method to Prepare Cyclic Peptides at Non-Cysteine Sites Using the Auxiliary Group, 4,5-Dimethoxy-2-Mercaptobenzyl (Dmmb)

Jane Spetzler
Novo Nordisk A/S, Novo Nordisk Park, 2760, Måløv, Copenhagen, Denmark

Introduction

Many cyclic peptides are of therapeutic interest but their preparation is challenging. This work presents a new general cyclization method [1] which applies the auxiliary group, 4,5-dimethoxy-2-mercaptobenzyl (Dmmb) to form end-to-end cyclic peptides in aqueous solution without protection of the side-chains. For native ligation [2] there are several examples known using Nα-(4,5-dimethoxy-2-mercaptobenzyl) (Dmmb) [3-5] peptide fragments to form longer peptides segments at X-Gly or X-Ala sites with C-terminal thioester peptides in the three following steps (1) transthioesterification (2) S to N acyl shift and (3) removal of the acyl transfer auxiliary group. This strategy has been applied for synthesis of a cyclic peptide. The peptide was prepared using standard Fmoc/tBu chemistry followed by the cyclization reaction. The aim of this study has been to use the strategy described above for the synthesis of cyclic peptides.

Results and Discussion

The auxiliary group 4, 5-dimethoxy-2-mercaptobenzylamine (Dmmb) which is similar to 1-pheny-2-mercaptoethyl has been extensively applied for native chemical ligation [3,4,6,7]. However, we have exploited the same strategy to form an end-to-end cyclic peptide from an unprotected linear peptide generated with Fmoc-chemistry as shown in Scheme 1. However, other research groups have utilized similar strategy to synthesize cyclic peptides [8-10].

The linear peptide precursor contains both Nα-(Dmmb)-Gly and Cα-thioester and was prepared in 2 steps (Scheme 1) by coupling the commercially available building block Boc-(Dmmb(Trt))-Gly-OH [5] to RGDSPA-2-chlorotrityl resin using DIC/HOAt. The protected peptide was cleaved from the resin with HOAc/TFE/DCM (1:1:8) and was not purified further. The peptide thioester 1 was obtained by the method of Von Eggelkraut-Gottanka et al. [11]. The yield of peptide thioester 1 in the second step was 31% and the correct mass was confirmed by LC-MS. The end-to-end cyclization reaction (Scheme 2) was performed in 6M guanidinium chloride at pH 7.5 in the presence of thiophenol and benzyl mercaptan (Scheme 2).

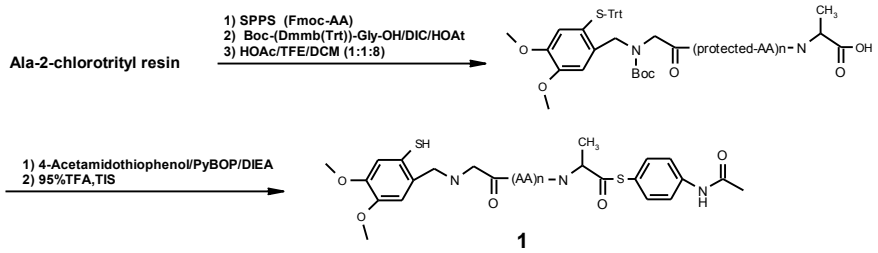

Scheme 1. Synthesis of the linear peptide thioester 1.

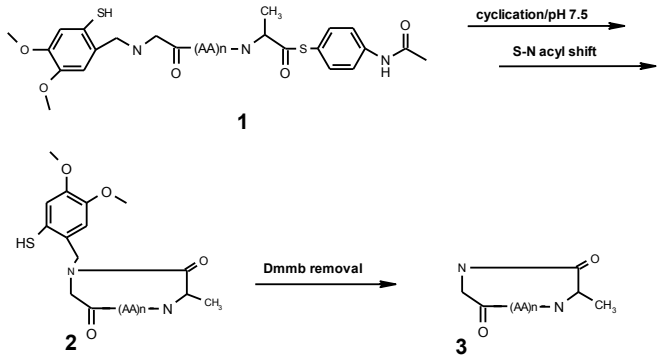

Scheme 2. End-to-end cyclization.

After 2 days at rt, the cyclic peptide 2 was observed by analytical UPLC and no byproducts were observed. The yield of the cyclization after purification of the peptide was 50%. The Dmmb group was then removed with 1M TFMSA and 1M thioanisol in TFA to give the target peptide 3 [12] and LC-MS confirmed the expected mass.

In conclusion, the auxiliary group Dmmb has been applied to form an end-to-end cyclic peptide at an Ala-Gly site and no polymerization was observed. The linear peptide precursor which contains both Nα-(Dmmb(Trt)-Gly and Cα-thioester was generated by standard Fmoc-chemistry.

References

1. Davies, J.S. *J. Pept. Sci*. **9**, 471-501 (2003).
2. Dawson, P.E., Muir, T.W., Clark-Lewis, I., Kent, S.B. *Science* **266**, 776-779 (1994).
3. Kawakami, T., Akaji, K., Aimoto, S. *Org. Lett*. **3**, 1403-1405 (2001).
4. Spetzler, J.C., Hoeg-Jensen, T. *Bioorg. Med. Chem*. **15**, 4700-4704 (2007).
5. Vizzavona, J., Dick, F., Vorherr, T. *Bioorg. Med. Chem. Lett*. **12**, 1963-1965 (2002).
6. Botti, P., Carrasco, M.R., Kent., S.B.H. *Tetrahedron Lett*. **42**, 1831-1833 (2001).
7. Marinzi, C., Offer, J., Longhi, R., Dawson, P.E. *Bioorg. Med. Chem*. **12**, 2749-2757 (2004).
8. Tchertchian, S., Hartley, O., Botti, P. *J. Org. Chem*. **69**, 9208-9214 (2004).
9. Shao, Y., Lu, W., Kent, S.B.H. *Tetrahedron Lett*. **39**, 3911-3914 (1998).
10. Zhang, L., Tam, J.P. *J. Am. Chem. Soc*. **119**, 2363-2370 (1997).
11. Von Eggelkraut-Gottanka, R., Klose, A., Beck-Sickinger, A., Beyermann M. *Tetrahedron Lett*. **44**, 3551-3554 (2003).
12. Mohri, H., Ohkubo,T. *Peptides* **14**, 861-865 (1993).

Proceedings of the 31st European Peptide Symposium
Michal Lebl, Morten Meldal, Knud J. Jensen, Thomas Hoeg-Jensen (Editors)
European Peptide Society, 2010

Synthesis and Oxidative Folding of Cyclic Cystine Knot Peptides: Towards Backbone Engineering

Teshome Leta Aboye[1], Richard J. Clark[2], Robert Burman[1], David J. Craik[2], and Ulf Göransson[1]

[1]Department of Medicinal Chemistry, Div. of Pharmacognosy, Uppsala University, Biomedical Centre, Box 574, SE-751 23, Uppsala, Sweden; [2]Institute for Molecular Bioscience, The University of Queensland, Brisbane, QLD 4072, Australia

Introduction

Cyclotides are a family of plant miniproteins with a range of biological activities of potential therapeutic interest, including antimicrobial, anti-HIV, antitumour and cardiotoxic activities [1]. They display a head-to-tail cyclized peptide backbone interconnected by three disulfide bonds (I-VI) forming a cyclic cystine knot (CCK) motif (Figure 1). The cystine knot in combination with the cyclic backbone appears to be a highly efficient motif for structure stabilization, resulting in exceptional conformational rigidity, together with stability against denaturing conditions, as well as against proteolytic degradation [2]. Möbius and bracelets are the two main subfamilies of cyclotides [1]. Bracelets display more sequence diversity, and higher potency in some assays, but has largely been intractable for chemical synthesis and oxidative folding.

Due to exceptional stability, there has been significant interest to exploit cyclotides as a scaffold in drug design; for example by grafting new bioactivities onto the CCK framework [3,4]. Using this kind of biomolecular engineering it may be possible to overcome the main deficiencies of peptide-based drugs' susceptibility to proteolytic degradation and poor bioavailability. However for this potential to be realized efficient synthetic and oxidative folding methods need to be developed.

Here we present a successful strategy for the cyclization and oxidative folding of bracelet cyclotides. In addition we present the first systematic quantification and comparison of heterogenous intermediates with different numbers and/or connectivities of disulfide bond(s) (1SS, 2SS, and 3SS) species in the process of oxidative refolding to native 3SS form (N) for selected subfamilies of cyclotides in four different buffers.

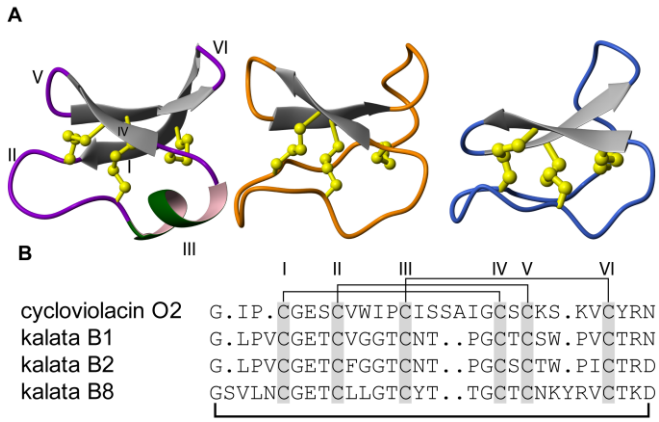

Fig. 1. Structures and sequences of selected cyclotides. Panel A. 3 D structures of three subfamilies: bracelet, cycloviolacin O2 (cyO2); hybrid, kalata B8 (KB8); and Möbius, kalata B1 (KB1) (from left to right). Panel B. shows the sequences of the four cyclotides used in the current study.

Results and Discussion

Linear cycloviolacin O2 (30 residues) was synthesized by manual solid phase peptide synthesis (SPPS) followed by cyclisation and oxidative folding [4]. Folding conditions were optimized to achieve maximum yield of correctly folded product (N). Concentrations of cosolvents, detergents, redox agents [5], salt, as well as the effects of temperature and duration of reaction, were examined. Under most conditions misfolded products, mainly non-native 3 SS species with I-II, III-IV and V-VI disulfide bridges, were predominant. However, using 35% DMSO as cosolvent gave a yield of ~40% N, which was further optimized with redox agents to ~52% N.

To have deeper understanding of the influence of various folding conditions on cyclotides, selected subfamilies (Möbius, hybrid and bracelet) were reduced and subjected to various oxidative refolding conditions. Samples were then collected at different time points, NEM alkylated, and relative quantities of heterogenous intermediates, i.e, 1SS, 2SS and 3SS species were determined by LC-MS. The result shows that some folding buffers favour non-native 3SS conformations that flip to the native fold directly or through partially oxidatively folded species depending on cyclotide subfamilies. Folding pathways of Möbius cyclotides to native species mainly dominated by 1SS/2SS while that of bracelet cyclotides dominated by non-native 3SS (usually without accumulating 1SS/2SS) (Figure 2).

These results are a significant step to the overall goal for biomolecular engineering on the cyclotide scaffold for utilization of their diversity and extraordinary structural stability and for the understanding of the major heterogeneous folding intermediates existing in oxidative folding pathways.

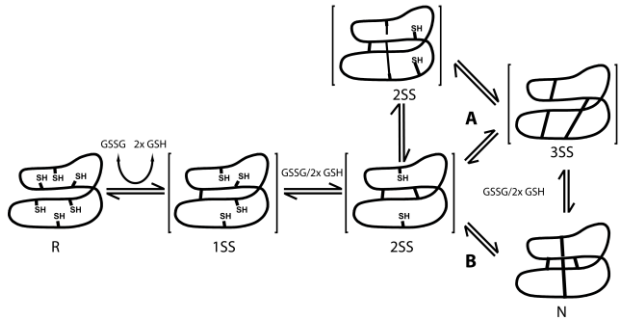

Fig. 2. Overview of folding pathways of cyclotides. Some folding buffers seem to favour non-native 3SS conformations that directly can flip to the native fold or go back through partly reduced species and then to the native structure. Path A is mainly and path B is partly favoured in the folding pathway of Möbius cyclotides, whereas path B (usually without accumulating 1SS and 2SS) is the dominant folding pathway in the folding of cyO2.

Acknowledgments

We thank Swedish International Development Cooperation Agency (SIDA), the Department for Research Cooperation (SAREC) (T.L.A. and U.G.), The Royal Swedish Academy of Sciences and the Disciplinary Domain of Medicine and Pharmacy, Uppsala University (U.G.). Work on cyclotides at the University of Queensland is supported by grants from the Australian Research Council and the National Health and Medical Research Council.

References

1. Craik, DJ., Cemazar, M., Daly, N.L. *Curr. Opin. Drug Discov. Devel*. **9,** 251-260 (2006).
2. Colgrave, M.L., Craik, D.J. *Biochemistry* **43**, 5965-5975 (2004).
3. Gunasekera, S, Foley, F.M., Clark, R.J., Sando, L., Fabri, L.J, Craik, D.J., Daly, N.L. *J. Med. Chem.* **51**, 7697-704 (2008).
4. Aboye, T.L., Clark, R.J., Craik, D.J., Göransson, U. *ChemBioChem* **9**, 103-113 (2008); Aboye, T. L., Clark, R.J., Burman, R, Craik, D.J., Göransson, U. *Antioxidants and redox signalling in press,* doi:10.1089/ars.2010.3112.
5. DeLa Cruz, R., Whitby, F.G., Buczek, O., Bulaj, G. *J. Pept. Res.* **61**, 202-212 (2003).

Proceedings of the 31st European Peptide Symposium
Michal Lebl, Morten Meldal, Knud J. Jensen, Thomas Hoeg-Jensen (Editors)
European Peptide Society, 2010

Synthesis and Structure Confirmation of the Cysteine Knotted Peptide Gurmarin by Selective Disulphide Formation

Rasmus Eliasen[1], Thomas Lars Andresen[2], and Kilian W. Conde-Frieboes[1]

[1]Novo Nordisk A/S, 2760, Måløv, Denmark; [2]Department of Micro- and Nanotechnology, Technical University of Denmark, 2800, Kgs. Lyngby, Denmark

Introduction

Gurmarin is a 35-residue peptide from the plant *Gymnema sylvestre* [1]. The peptide has been shown to function as a sweet taste inhibitor in mice [3]. The structure of Gurmarin (Figure 2) is defined by three disulphides in a common fold known as an inhibitor cysteine knot. Folding of such peptides is often achieved by equilibrium driven folding in a redox buffer [2]. In this study, the synthesis of Gurmarin was carried out in three different ways, where one of the three cysteine-pairs was trityl-protected, while the other two pairs were acetamidomethyl-protected. This allowed for selective formation of the first disulphide by air oxidation, followed by iodine oxidation of the last two disulphides. The structures of the peptides were confirmed by cleavage with thermolysin. In this way it was possible to determine the disulphide connection.

Results and Discussion

The peptides were synthesized by standard Fmoc chemistry on a CEM Liberty peptide synthesizer. HOBt was added to the piperidine deprotection to minimize aspartimide formation. The first disulphide was oxidized in 0.1 M Tris-HCl buffer (pH 7.8, 0.02mM peptide), 2 vol% DMSO with air bubbled through until complete oxidation was confirmed by UPLC. The final two disulphides were oxidized using 20 eq. iodine in 1:4 water:methanol (0.02 mM peptide) until complete oxidation was confirmed by MS. The peptides were cleaved with 1 mass eq. thermolysin in 0.2 M ammonium acetate (pH 6.5), 10 mM $CaCl_2$ 24h at 50°C.

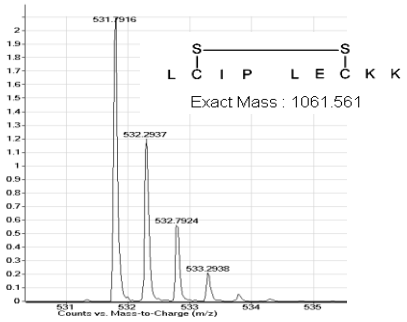

Fig. 1. Sequence and mass spectrum of a native disulphide fragment obtained by cleavage with thermolysin.

The synthesis of the peptide with trityl protected Cys-3 and Cys-18 produced a mixture of two products. One of these was identified as the native peptide by the fragment in Figure 1 and another fragment containing two native disulphides (second fragment, Table 1). In the latter fragment the disulphide between Cys-3 and Cys-18 was oxidized selectively first in the air oxidation of the trityl protected cysteines and consequently all three disulphides in this peptide are native.

The cleavage of the peptide synthesized with trityl protected Cys-10 and Cys-23 produced one fragment with the native disulphide between Cys-10 and Cys-23, as expected. However no other fragments containing native disulphides were found from this cleavage.

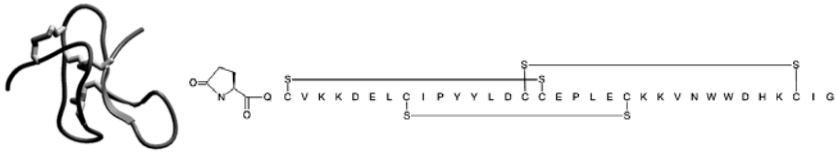

Fig. 2. The structure (PDB: 1C4E) of Gurmarin (left) and the primary sequence (right).

Table 1. Fragments obtained from cleavage with thermolysin of the three differently synthesized peptides. The three peptides are identified by the trityl protected cysteines in the first column. <E is pyroglutamate. Disulphides are indicated with lines.

Peptide	*Fragment*	*Theoretical mass*	*Observed mass*
1			
C3-C18	LCIP LECKK	531.78 ($M+2H^+$)	[a]531.79
Trityl	<EQC LDCCEP WDHKC	861.80 ($M+2H^+$)	[a]861.91
protected	<EDC LCIP LDCCEP	740.28 ($M+2H^+$)	740.29
	LECKK WDHKC	653.30 ($M+2H^+$)	653.31
2			
C10-C23	LCIP LECKK	531.78 ($M+2H^+$)	[a]531.79
Trityl	LDCCEP	677.22 ($M+1H^+$)	677.22
protected	<EQC WDHKC	523.69 ($M+2H^+$)	523.69
3			
C17-C33	<EQC LCIP	803.34 ($M+1H^+$)	803.35
Trityl	LDCCEP LECKK WDHKC	982.40 ($M+2H^+$)	982.42
protected			

[a]*The peptide fragment contains only native disulphides*

The third peptide was synthesized with trityl protected Cys-17 and Cys-33. The only native disulphide found in this cleavage was the selectively formed disulphide between Cys-17 and Cys-33. Only two other non-native disulphides were found.

In all three peptides non-natural disulphides were produced as the main product, when using the iodine oxidation. Disulphide formation between cysteines that are close in the primary sequence seems to be favoured. Despite the prevalence of non-native disulphide formation, it is possible to synthesize native Gurmarin with this synthesis route. The position of the protection groups are critical for the outcome of the disulphide oxidation, since only the synthesis route with trityl protected Cys-3 and Cys-18 produced native Gurmarin.

References

1. Imoto, T., et al. *Comp. Biochem. Phys. A.* **100(2)**, 309-314 (1991).
2. Moroder, L., et al. *Biopolymers* **40(2)**, 207-234 (1996).
3. Ninomiya, Y., Imoto, T. *Am. J. Physiol-Reg I.* **268(4)**, R1019-R1025 (1995).

Proceedings of the 31st European Peptide Symposium
Michal Lebl, Morten Meldal, Knud J. Jensen, Thomas Hoeg-Jensen (Editors)
European Peptide Society, 2010

Mimicking of Disulfide Bonds by Triazoles

Kai Holland-Nell[1,2] and Morten Meldal[1]
[1]Carlsberg Laboratory, Valby, 2500, Denmark; [2]Leibniz-Institute of Molecular Pharmacology, Berlin, 13125, Germany

Introduction

Disulfide bonds stabilize peptide and protein structures to maintain biological functions but presents rather unstable bonds and replacements with thioethers [1], amides [2] as well as carbon based bridges [3] and diselenides [4] have been investigated to overcome the problems associated with disulfides. We aimed at investigating the potential of triazoles as disulfide mimetics. Stability and formation by orthogonal *click chemistry* [5] favor triazoles as an improved disulfide substitute. The stabilitity of triazoles towards oxidative and reducing reagents is complemented by a remarkable biological stability. The triazole motif - usually not occurring in natural peptides and proteins - is not effected by any isomerases, hydrolases, and proteases. Reaction of azides to alkynes by CuAAC facilitates triazole formation under very mild conditions.

Results and Discussion

The approach has been applied to two model peptides: tachyplesin-I and conotoxin Xen2174. Tachyplesin-I is a 17 aa peptide isolated from the Japanese horseshoe crab *Tachypleus tridentatus*. It shows an interesting antimicrobial activity and antitumor activity has also been reported recently [6]. Conotoxin Xen2174 is an MrIA conotoxin analog, which selectively blocks the norepinephrine transporter and interferes with pain signaling in the human body [7]. This property made the peptide a promising analgesic drug candidate which is currently studied in clinical phase IIb. Both peptides exhibit a β-hairpin fold structure which is stabilized by two disulfide bridges. The focus of this work was placed on the substitution of the two disulfide bonds and the impact on the biological activity of those peptides.

In the first step, different tachyplesin and conotoxin analogs were synthesized by standard SPPS using Fmoc/^{t}Bu-strategy. Thereby, the four Cys in each peptide were replaced by appropriate alkyno and azido amino acids. Propargylglycine was selected as an alkyno component while β-azido-alanine, γ-azido-homoalanine, and δ-azido-norvaline all were investigated as azido components.

In the second step, the peptides were subjected to an on-resin cyclization on PEGA resin applying click chemistry conditions. Due to the high orthogonality of this reaction, the peptides can be cyclized in unprotected form. The hydroxymethyl-benzoic acid linker allowed the selective deprotection while maintaining resin attachment. Several cyclization conditions were evaluated. Neither CuI or CuBr in DMF nor $CuSO_4$/NaAsc in H_2O formed the desired products. Moreover, in the case of β-azido-alanine, a β-elimination of the azide to yield dehydro-alanine was observed. Finally, the formation of the triazoles and the cyclization of the peptides succeed with the application of $CuSO_4$/TCEP in water under argon. We took advantage of the excellent swelling properties of Versamatrix^{TM} $PEGA_{1900}$ resins in water.

The presence of two triazole moieties allowed the formation of two different reaction products: a globular and a correctly folded β-hairpin product. We observed the formation of two products exhibiting the same molecular weight but showing different HPLC retention time compared to the starting material. Ratios of 1:2 (tachyplesin) and 1:7 (conotoxin) in favor of the β-hairpin were observed. Notably, no linear or cyclic dimers were formed under these conditions. The reaction time could be reduced from 16h to 1h by applying microwave conditions. However, at the raised temperature most of the selectivity for formation of the correctly folded β-hairpin was lost.

Several experiments were performed in order to prove the cyclic nature of the products. Simple reduction experiments with dithiothreitol showed the absence of azido groups in the products and suggest the formation of triazoles. MS/MS-fragmentation patterns exhibited tremendous differences between the cyclic and linear peptides. Almost all fragments of the y- and b-series could be detected in case of the linear peptides. In contrast, the cyclic peptides showed only fragments of amino acids located outside the bicyclic peptide region.

NMR-analysis allowed full structural characterization of the cyclic products. In addition to signals from the assigned peptide amino acids signals were observed corresponding to the aromatic protons of the triazoles. Furthermore, NOESY-experiments revealed NOEs across these triazole bridges The NOEs allowed the determination of the spatial structure of the major isomer as a ribbon-like β-hairpin conformation and of the minor isomer as the globular product with the wrong triazole connectivity.

Lowest energy structures of both conformations were obtained by MD-calculations based on the NOEs. A comparison of the ribbon-like structure with that of the original peptides showed a high degree of similarity. Thereby, the triazole analogs perfectly mimic the natural β-hairpin fold of the backbone. Furthermore, almost all side chains were correctly positioned in analogy to the wild type peptides.

Encouraged by these results, the biological activity of the tachyplesin-I analogs was evaluated in an antimicrobial assay. Several bacteria strains (*E.coli, Staphylococcus epidermis, Salmonella typhimurium, Bacillus subtilis*) were grown with increased peptide concentrations and the minimal inhibitory concentrations (MIC) were determined. The linear and the globular peptides showed no activity, while the cyclic β-hairpin peptides significantly inhibited the bacterial growth. Remarkably, the triazole analogs performed similar or even better than the wild type tachyplesin.

The presented method of mimicking disulfide bonds by triazoles can be considered whenever orthogonality and higher stability is requested. The click chemistry approach opens a convenient route to achieve those triazole bridged analogs. The created peptide analogs show a high degree of structural similarity which is also reflected in related biological activity.

Acknowledgments
The German Research Foundation (DFG) has supported (KHN) the present work.

References

1. Bondebjerg, J., Grunnet, M., Jespersen, T., Meldal, M. *ChemBioChem* **4**, 186-194 (2003).
2. Hargittai, B., Sole, N.A., Groebe, D.R., Abramson, S.N., Barany, G. *J. Med. Chem.* **43**, 4787-4792 (2000).
3. Stymiest, J.L., Mitchell, B.F., Wong, S., Vederas, J.C. *Org. Lett.* **5**, 47-49 (2003).
4. Muttenthaler, M., et al. *J. Am. Chem. Soc.* **132**, 3514-3522 (2010).
5. Tornoe, C.W., Meldal, M. *Peptides, The wave of the future (Proceedings of the 17th American Peptide Symposium, San Diego)*, Springer 263-264 (2001); Meldal, M., Tornoe, C.W. *Chemical Reviews* **108**, 2952-3015 (2008).
6. Chen, J., et al. *Cancer Res.* **65**, 4614-4622 (2005); T. Nakamura, H. Furunaka, T. Miyata, F. Tokunaga, T. Muta, S. Iwanaga, M. Niwa, T. Takao, Y. Shimonishi, *J. Biol. Chem.* **263**, 16709-16713 (1988).
7. Brust, A., et al. *J. Med. Chem.* **52**, 6991-7002 (2009).

Proceedings of the 31st European Peptide Symposium
Michal Lebl, Morten Meldal, Knud J. Jensen, Thomas Hoeg-Jensen (Editors)
European Peptide Society, 2010

Identification of Sulphated Peptides Binding FGF1 Using a Micro Particle Matrix (MPM) Encoded Library

Manat Renil and Morten Meldal
Center for Solid-Phase Organic Combinatorial Chemistry (SPOCC),Department of Chemistry, Carlsberg Laboratory, Gamle Carlsberg Vej 10, DK-2500, Valby, Denmark

Introduction

Structure elucidation of highly active hits from a 'one bead one compound' combinatorial library has been a challenge ever since the introduction of 'on-bead' screening techniques. A relatively high concentration of 'on bead' ligands are required for the structural elucidation of active compounds by e.g. Edman's micro sequencing or mass spectrometric analysis frequently leading to false positives in 'on bead' screening analysis targeting interactions were nano-molar or even lower concentration of the bead bound ligand is desirable. Micro-Particle-Matrix (MPM) encoding of PEGA based beads has been recently introduced from our laboratory to circumvent this draw back [2]. Heparin mimetic sulphated peptide libraries [1] were used to identify sulphated peptides that binds to FGF1.

Results and Discussion

It has previously been shown that short *O*-sulphated peptides can inhibit heparin-FGF1/FGFR interaction using a combinatorial library approach [1]. In the previous library high concentration of on-bead peptide libraries were used in the screening to obtain several mM to μM inhibitors. In the present work we employed an MPM-encoded library [2,3] of 20.000 encoded beads where the peptide library structure was biased, based on a previously identified sulphated peptide ligand to FGF1. The library had a peptide concentration of only 1 μmol/mL to screen for activity and selectivity between ROX-labelled anti-thrombin and FGF1 binding. The ten amino acid residue library was synthesized by cycles of split/mix with code (image) recording during the splitting immediately prior to next coupling reaction. Hits were also recorded and codes were compared. Four amino acids (Table1) were coupled at each step i.e. with 5000 encoded beads per well.

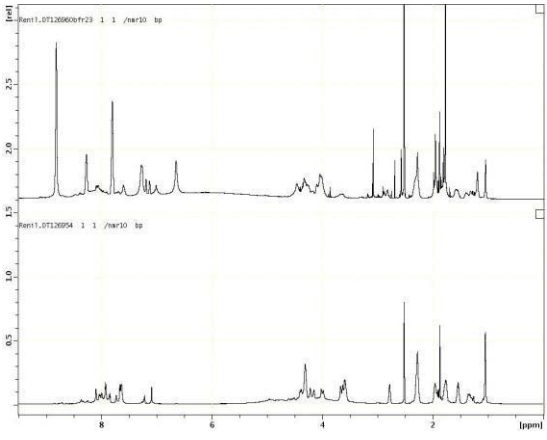

*Fig. 1. Ac-ETET*S*S*ES*ES*K-NH_2 - H^1 NMR of sulphated (above) and non-sulphated peptide (below).*

Progress of coupling reactions were monitored (Dhbt-OH). *O*-Sulphonation was performed at the end of synthesis on dry resin using sulphur trioxide pyridine (SO_3-Pyr) complex in DMF at 60°C. The library was incubated in BSA/PBS buffer at pH 7.5 with ROX labeled anti-thrombin. Beads with high fluorescence intensity were isolated and decoded. Of 20 beads 15 structures were determined and 5 determined partially.

*Table1. The amino acids used for library synthesis (*Post assembly sulphatation)*

R9	*R8*	*R7*	*R6*	*R5*	*R4*	*R3*	*R2*	*R1*	*R0*
Glu	Ser	Glu	Ser*	Ser*	Ser*	Glu	Ser*	Glu	Ser*
Asp	Thr	Asp	Thr*	Thr*	Thr*	Asp	Thr*	Asp	Thr*
Gln	Thr*	Gln	Hyp*	Hyp*	Hyp*	Gln	Hyp*	Gln	Hyp*
Asn	Ser*	Asn	Tyr*	Tyr*	Tyr*	Asn	Tyr*	Asn	Tyr*

Table 2. IC50 values for the binding inhibitions of FGF-1 binding to immobilised heparins. HPLC purified peptides characterized by H^1 NMR.

Peptide	*Structure: Ac-Peptide-K-NH_2*										*IC50*
A1	E	S*	N	S*	S*	#*	N	Y*	N	#*	>500μM
A2	Q	S*	Q	#*	S*	T*	D	S*	Q	#*	>500μM
A3	Q	T*	Q	Y*	S*	S*	N	Y*	Q	S*	>500μM
A4	Q	T*	N	#*	S*	S*	N	#*	E	#*	>500μM
A5	D	S*	Q	S*	Y*	S*	E	S*	Q	#*	400 μM
A6	E	T*	Q	S*	S*	T*	D	#*	Q	S*	325 μM
A7	Q	S*	Q	S*	S*	T*	Q	Y*	E	#*	150 μM
A8	E	T*	E	T*	S*	S*	E	S*	E	S*	4 μM
B	LMW heparin										188 nM

**Sulphated amino acids; # is Hyp*

Resynthesized structures are presented in Table 2. The peptides were purified on HPLC and characterized by H^1 NMR (Figure 1). By comparing the spectra with non-sulphated peptides there is a significant shift in the α-proton of amino acids after *O*-sulphatation.

To test the hits from the screening of the anti-thrombin binding, a competition assay of protein binding to immobilized heparin was carried out using surface plasma resonance (SPR). The binding of anti-thrombin to the immobilized heparin in presence of various sulphated peptides at different concentrations in solution was measured and only insignificant binding inhibition was observed indicating that on beads the protein takes advantage of more than one ligand. On the other hand, FGF1 showed significant interaction with some of the sulphated peptides, e.g. A7 identified against anti-thrombin. FGF1 binding inhibition (IC_{50}) of different sulphated peptides identified through antithrombin screening are shown in Table 2. The binding affinity is less than that of the original peptide A8 [1], and active structures show high similarity with A8 in the central region.

The results indicates that although binding to the arginine rich binding sites of heparin binding proteins are obtained, it is still a challenge to identify close mimics of heparin with short sulphated peptides. The affinity of sulphated peptides show significant sequence dependence and may be improved by screening of specifically designed targeted sulphated peptide libraries. Importantly, MPM encoded libraries of compounds, that otherwise are difficult to analyse structurally, can be applied for fast screening of protein - ligand interactions. Sulphated peptides can be conveniently synthesized using solid phase approach. In the present work H^1 NMR was used to fully characterize the structure of the sulphates peptides carrying numerous sulphate groups.

Acknowledgments
This work was supported by the Danish National Research Foundation. Technical assistance was by Pia Breddam (SPR) and Dana C. Tvermoes (SPS).

References

1. Vazquez-Campos, S., St.Hilaire, P.M., Damgaard, D., Meldal, M. *QSAR Comb. Sci*. **8**, 923-942 (2005).
2. Meldal, M., Christisen F.S. *Angew. Chem. Int. Ed.* **49**, 3473-3476 (2010).
3. Rasmussen, J.E., Christisen, F.S., Nørskov-Lauritsen, L., Meldal, M., Jensen, K.J., St.Hilaire, P.M. *Angew. Chem. Int. Ed.* **49**, 3477-3480 (2010).

Proceedings of the 31st European Peptide Symposium
Michal Lebl, Morten Meldal, Knud J. Jensen, Thomas Hoeg-Jensen (Editors)
European Peptide Society, 2010

Direct Synthesis of mTRAQ® Reagent Labeled Peptides Using the 433A Peptide Synthesizer

Stephan Rawer[1], Andrea Hartmann[2], and Matthias Glückmann[3]
[1]Life Technologies, Applied Biosystems Deutschland GmbH, D-64293, Darmstadt, Germany; [2]Sandoz GmbH, A-6259, Kundl, Austria; [3]AB SCIEX Germany GmbH, D-64293, Darmstadt, Germany

Introduction

Synthetic peptides are the major tools as quantitative markers for Protein Biomarker expression analysis. Relative quantification of low abundant proteins is very important to identify changes in the pathways of the cell status. In recent years the mTRAQ® reagent labeling technique has been established as a powerful method in proteomics. For quantitation in MS, purified synthetic peptides with mTRAQ® reagent labels are used as internal standard. Tryptic digestion leads to peptides with arginine and lysine at the C-terminus. The mTRAQ® reagent is chemically the N-succinimide ester of 4-Methyl-piperazine-1-yl acetic acid, which reacts with the amino groups of the peptides. Possible reacting candidates are the N-terminus and the ε-amino group of the lysine. After mTRAQ® reagent labeling, the peptides with arginine will have one and the peptides with a lysine will have two labels. The common strategy of labeling synthetic peptides in solution exhibits problems during labeling due to solubility, structural hindrance and side reactions. These problems will be addressed by direct synthesis of the mTRAQ® reagent labeled peptides (Figure 1).

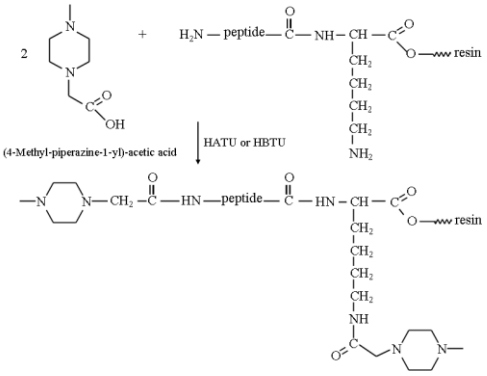

Fig. 1. Coupling of 4-Methyl-piperazine-1-yl acetic acid to a peptide with a Lysine at the C-terminus.

Results and Discussion

In contrast to the literature we found in our experiments that the removal of the ivDde group needs 8% hydrazine [1-3]. An advantage of this side chain protecting group is the possibility of monitoring at λ = 290 nm. The modified synthesis was successfully applied on a 433A peptide synthesizer with UV-monitoring (Figure 2). Additionally the deprotection of the ivDde-group could be detected at λ = 301 nm and optimized by the feedback mechanism. So there was no additional set up needed during synthesis. The synthesis described here can be applied in the same way to iTRAQ® reagent labelled peptides.

In this proof-of-principle study we have chosen the RNA polymerase multi-protein complex from *Bacillus subtilis* [4]. Because of its close relationship to important pathogens, e. g. *Staphylococcus aureus* or *Bacillus subtilis* it became an important paradigm for gram positive bacteria. The RNA polymerase multi-protein complex plays a crucial role during transcription of all classes of RNAs in bacteria and shows a high homology between prokaroytic and eukaryotic organisms.

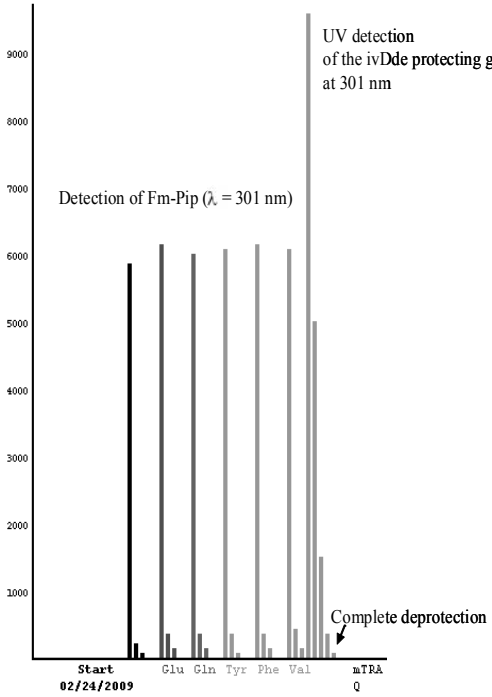

*Fig. 2. Monitoring trace of the synthesis of V*FYQEK*.*

For this purpose we established a quantification approach based on the absolute quantification of the RNA polymerase multi-protein complex partners using an adapted stable isotope dilution (SID) mass spectrometry method. Internal standard peptides carrying an mTRAQ® reagent label were specifically synthesized. Quantification was performed using a LC-MRM approach based on differentially mTRAQ® reagent labelled peptides.

The developed method was improved by synthesis of a set of mTRAQ® reagent labeled peptides. A set of 18 peptides were identified by MS and used for biomarker quantification.

Peptides of RNA polymerase multi-protein complex of *Bacillus subtilis* were used successfully for absolute quantitation in LCMS experiments. The known stoichiometry of the core enzyme RpoA:RpoB:RpoC 2:1:1 could be shown.

This method allows to synthesize specific mTRAQ® or iTRAQ® reagent labelled peptides for the quantitation of biomarkers with LCMS. This fits right into the strategy of discovery, verification and validation of candidate biomarkers using mTRAQ® or iTRAQ® reagent chemistry.

Acknowledgments

Jan Muntel, Sandra Maaß, Michael Hecker, Dörte Becher from the Institute for Microbiology, University Greifswald, Germany. This work was supported by the European Union (BaSysBio LSHG-CT-2006-037469).

References

1. Chhabra, S.R., et al. *Tetrahedron Letters* **39**, 1603-1606 (1998).
2. Rohwedder, B., et al. *Tetrahedron Letters* **39**, 1175-1178 (1998).
3. Wittmann, V., Seeberger, S. *Angew. Chem. Int. Ed. Engl*. **39**, 4348-4352 (2000).
4. Allison, L.A., et al. *Cell* **42***, 599-610.* (1985).

Proceedings of the 31st European Peptide Symposium
Michal Lebl, Morten Meldal, Knud J. Jensen, Thomas Hoeg-Jensen (Editors)
European Peptide Society, 2010

Synthetic Studies Toward the Mannopeptimycins

M. Morelle, K. Cariou, J. Thierry, and R. H. Dodd
Centre de Recherche de Gif-sur-Yvette, Institut de Chimie des Substances Naturelles UPR 2301, CNRS, Avenue de la terrasse, 91198, Gif-sur-Yvette, France

Introduction

The mannopeptimycins are a new family of five glycopeptide antibiotics characterized in 2002 by Wyeth laboratories [1]. Some of them exhibit high antibiotic activity against Gram-positive bacteria and more interestingly against MRSA and vancomycin-resistant enterococci *via* inhibition of cell wall synthesis. They are comprised of a peptidic core of five amino acids: a serine, a glycine, a β-methyl phenylalanine, a dimannosylated D-tyrosine and two enantiomeric non proteinogenic amino acids bearing a cyclic guanidine, one of which is *N*-mannosylated.

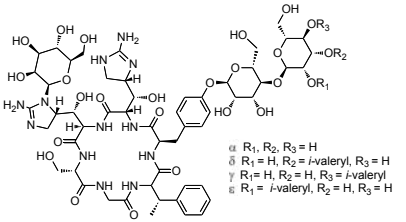

No total synthesis has been achieved so far although two papers describing the synthesis of derivatives of the non proteinogenic amino acids were recently published [2].

Three routes to the synthesis of these amino acids were designed, two of which rely on the intramolecular aziridination of an alkene *via* the addition of a nitrene generated from the oxidation of sulfamates in presence of transition metals [3]. The third one is a more classical and convergent approach for the synthesis of β-hydroxy α-amino acids using an aldol reaction between a glycine equivalent and an aldehyde bearing a cyclic guanidine.

Results and Discussion

Route 1: A [5.1.0] bicyclic aziridine could be obtained by the attack of a nitrene generated from the primary sulfamidate **A_1**. This sulfamate was prepared and reacted under conditions described previously [3]. The aziridination step gave the bicyclic compound **B_1** in a satisfactory yield in two cases with a major product having the desired configurations at C-2, C-3 and C-4. However, these compounds turned out to be very unstable making this approach inefficient to pursue the synthesis.

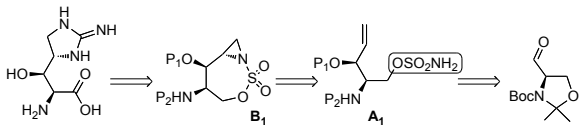

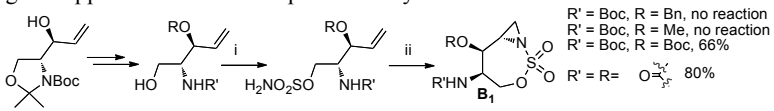

Reaction conditions : i : cf. ref. [3]; ii : $Rh_2(OAc)_4$ (5 mol%), PhIO (1.2 eq), 3 Å m.s., CH_3CN, -20°C,10h.

Route 2: A [3.1.0] bicyclic aziridine could be obtained by the attack of a nitrene generated from the secondary sulfamidate **A_2**. The aziridination step conducted with rhodium diacetate and iodosobenzene gave the bicyclic aziridine **B_2** in a 75% satisfactory yield. Moreover this bicyclic compound **B_2** showed good stability. The configurations of the stereogenic centers are still under investigation. The opening of **B_2** proceeded smoothly in 85% yield to give a mixture of azido compounds.

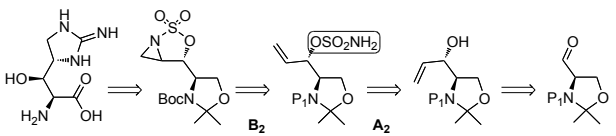

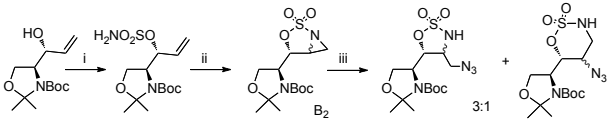

Reaction conditions: i: HCO_2H, $ClSO_2N{=}C{=}O$, 2,6-lutidine(5 eq), CH_3CN; ii: $Rh_2(OAc)_4$ (5 mol%), PhIO (1.2 eq), 3Å m.s., CH_3CN, -10°C, 10h; iii: TBAF cat., $TMSN_3$, THF, 10h, rt.

Route 3: The aldehyde C was prepared from (*S*)-glycidol in 7 steps in 53% overall yield. The primary alcohol was first protected. The epoxide ring was opened with sodium azide. Hydrogenolysis of this azide with 10% Pd/C gave quantitatively the amine which was reacted with Bis-*N,N'*-Boc methylisothiourea to yield the protected guanidine. The cyclic guanidine was obtained after activation of the secondary hydroxyl group followed by sodium hydride treatment. Deprotection of the acetal by acidolysis and oxidation of the alcohol gave the aldehyde C. All the reactions of this sequence gave quantitative yields except the oxidation step which performed poorly, the best yield (32%) being obtained with NMO/TPAP. The aldol reaction between C and Z-Gly-OEt was tested using various bases without success. However using lithium diisopropylamine and the Garner aldehyde, which is structurally similar to C, the desired condensation product was isolated in 58% yield.

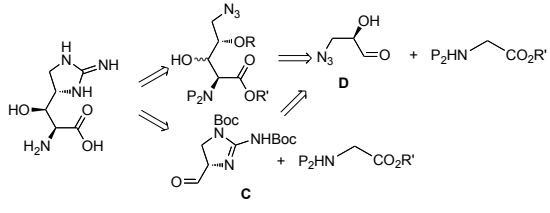

Assuming that the poor yields of the oxidation and aldol steps were due to the basicity

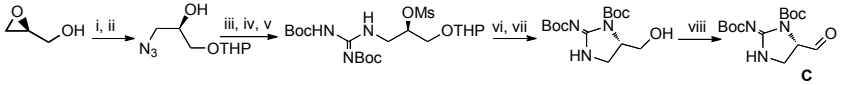

Reaction conditions : i : DHP (2 eq), APTS cat, CH_2Cl_2, 10h, rt; N_3Na (2 eq), NH_4Cl (2 eq), EtOH, H_2O (6/1), 3h, reflux; iii : 10% Pd/C, H_2, THF, 10h, rt; iv: BocN=(SMe)NHBoc (1.5 eq), CH_2Cl_2, 10h, rt; v : MsCl (1.1 eq), Et_3N (1.5 eq), 10h, rt; vi : NaH (1 eq), DMF, 10h, rt; vii : PTSA(1.1 eq), MeOH, rt; viii : NMO (2 eq), TPAP cat, CH_2Cl_2 10h, rt.

of the guanidine, we decided to perform the aldol reaction prior to the elaboration of the guanidino function. The aldehyde **D** was prepared from (*S*)-glycidol in 5 steps in a 74% overall yield.

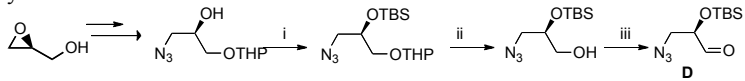

Reaction conditions: i : TBSOTf (2 eq), 2, 6-lutidine (2.5 eq), CH_2Cl_2, 10h, rt; ii: PPTS cat, MeOH, 2 days, rt; iii: IBX (1.2 eq), DMSO, 10h, rt.

The first attempt to run the aldol reaction with Z-Gly-OEt and **D** (1 eq) using LDA (2 eq) at -78°C gave the condensation product in 28% yield. Optimisation of the conditions of the aldol reaction is under progress as well as the elaboration of the guanidine ring.

This last approach seems to be the shortest and most promising way to obtain both enantiomers of the desired amino acid needed to perform the synthesis of the mannopeptimycin core.

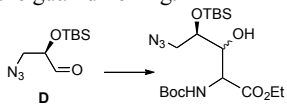

Acknowledgment

M. M. thanks ICSN-CNRS for a doctoral fellowship.

References

1. He, H., et al. *J. Am. Chem. Soc.* **124**, 9729-9736 (2002).
2. During the course of our studies two syntheses were published: Schwörer, C. J., Oberthür, M. *Eur. J. Org. Chem* 6129-6139 (2009); Olivier, K.S., Van Nieuwenhze, M.S. *Org. Lett.* **12**,1680-1683 (2010).
3. Dauban, P., Dodd, R.H. *Synlett* 1571-1586 (2003); Karila, D., Dodd, R.H. *Curr. Org. Chem* in press.

Proceedings of the 31st European Peptide Symposium
Michal Lebl, Morten Meldal, Knud J. Jensen, Thomas Hoeg-Jensen (Editors)
European Peptide Society, 2010

Design and Synthesis of β-Cyclodextrin/GnRH-Analogue Conjugation for the Treatment of Hormone Depended Cancer

Despina Laimou, Gerasimos Tsivgoulis, and Theodore Tselios
Department of Chemistry, Section of Organic Chemistry, Biochemistry and Natural Products, University of Patras, Patras, 265 00, Greece

Introduction

Cyclodextrins (CDs) are cyclic oligosaccharides consisting of α-D-glucoses. They are known for their ability to include into their hydrophobic cavity via host/guest complexation a variety of compounds [1]. Although more than one factor affects the above complexation, hydrophobic interactions are usually of main importance. This property has been extensively exploited to change the physicopharmaceutical properties of lipophilic drugs such as water-solubility, bioavailability, improved stability and effectiveness. Theoretically, almost any organic guest can be encapsulated by choosing cyclodextrin of appropriate size (α, β, γ) [2]. Thus, CDs have been extensively used in the construction of supramolecular systems and many examples where cyclodextrin derivatives have served as biomimetic systems in catalysis or/and transport have been already described [3]. Covalent linkage of bioactive peptides to cyclodextrins has also been proposed [4,5] to possibly take advantage of this complexation in terms of solubility and reduced catabolism.

Gonadotropin-Releasing Hormone [6] (GnRH, synonym for luteinizing-hormone-releasing hormone, LHRH), a linear decapeptide synthesized by gonadotropic cells of the hypothalamus, is the central regulator of the reproductive system. GnRH interacts with high affinity with the G-protein-coupled GnRH receptor (GnRHR) localized on anterior pituitary gland and cancer cells stimulating the biosynthesis and the releasing of luteinizing (LH) and follicle-stimulating (FSH) hormones. For the treatment of sex-hormone-dependent disorders, such as breast and prostate cancer, agonistic GnRH derivatives such as [DLeu^6]GnRH (Leuprolide [7]) or [DTrp^6]GnRH (Triptorelin), as well as antagonists such as the linear decapeptide Cetrorelix (Cetrotide) are clinically and therapeutic valuable.

The aim of the present work is to synthesize β-Cyclodextrin/GnRH-analogues conjugates as new therapeutic agents for hormone-depended cancer [8]. Permethylated β-Cyclodextrin will also be used based on its excellent lipophilic properties

Results and Discussion

β-Cyclodextrin bearing one amino group is an important intermediate in our synthesis. In such a modified cyclodextrin, attachment of various peptides (linear or cyclic ones) via the relatively stable peptide bond is possible.

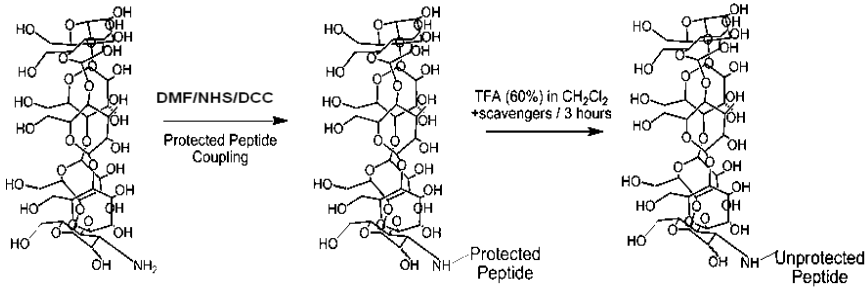

Fig. 1. Synthesis of the conjugate.

Solid phase synthesis is used for the preparation of the GnRH peptide [9]. This approach permits working in small scale while purification is easier. The analogue was purified by HPLC and characterized by ESI-MS spectroscopy.

Coupling between the mono-6-deoxy-β-cyclodextrin and the side chain-protected GnRH peptide analogue was performed with the NHS/DCC method in DMF were both reactants are soluble.

At the final step all the protected groups (*tert*-butyl, trityl and Pbf) were removed by triturating the final conjugate for 3h with 60% TFA/CH_2Cl_2 containing triethylsilane as scavenger as shown in the Figure 1.

A (GnRH analogue)– β-CD derivative has been successfully synthesized and characterized by ESI-MS. Future work will include, synthesis and identification of permethylated or not β-Cyclodextrin/GnRH analogues (linear and cyclic ones) using chromatographic and spectroscopic methods. Moreover, docking simulations of the synthesized conjugates into a homology modeling-derived structure of the human GnRH receptor will be performed in order to visualize the potential role of the cyclodextrin moiety in the ligand/receptor interaction. Finally, in vitro experiments will be carried out using several cancer lines in order to evaluate the stability and bioavailability of the conjugates compared to commercially available GnRH agonists or antagonists.

Acknowledgments

D. Laimou is financial supported by Karatheodoris Grant of University of Patras, Greece

References

1. Wenz, G. *Angew. Chem*. **106**, 851-870 (1994).
2. Bender, M.L., Komiyama, M. *"Cyclodextrin Chemistry", Springer-Verlag* **12***,* 311-337 (1978).
3. Breslow, R., Dong, S.D. *Chem. Rev*. **98**, 1997-2011 (1998**)**.
4. Albers, E., Muller, B.W. *Critical Reviews in Therapeutic Drug Carrier Systems* **12**, 311-37 (1995).
5. Parrot-Lopez, H., Djedaini, F., Perly, B., Coleman, A.W., Galons, H., Miocque, M. *Tetrahedron Lett*. **31**, 1999-2002 (1990).
6. Baba, Y., Matuso, H., Schally A.V. *Biochemic. Biophysic. Res. Commun.* **44**, 459-463 (1971).
7. Evans, R.M., Doelle, G.C., Alexander, A.N., Uderman H.D., Rabin, D. *J. Clin. Endoer. Metab.* **58**, 862-867 (1984).
8. Mantzourani, E., Laimou, D., Matsoukas, M., Tselios, T. *Anti-Inflammatory & Anti-Allergy Agents in Medicinal Chemistry* **13**, 294-306 (2008).
9. Laimou, D.K., Katsara, M., Matsoukas, M.I., Apostolopoulos, V., Troganis, A.N., Tselios, T.V. *Amino Acids* March **2010**, *In press*.

Proceedings of the 31st European Peptide Symposium
Michal Lebl, Morten Meldal, Knud J. Jensen, Thomas Hoeg-Jensen (Editors)
European Peptide Society, 2010

Novel Synthesis of Benzophenone Units for Photo-Affinity Labeling

Shirly Naveh[1], Carni Lipson[2], Michal Breker[3], Yftah Tal-Gan[1], Maya Schuldiner[3], Michal Sharon[2], and Chaim Gilon[1]

[1]Institute of Chemistry, The Hebrew University of Jerusalem, 91904, Jerusalem, Israel; [2]Department of Biological Chemistry, The Weizmann Institute of Science, 76100, Rehovot, Israel; [3]Department of Molecular Genetics, Weizmann Institute of Science, 76100, Rehovot, Israel

Introduction

Peptides are a common tool for the study of protein-protein interactions. Benzophenone (BP) is an attractive photo-affinity label which covalently binds to the inactive C-H bonds of the protein, upon exposure to UV irradiation [1]. In order to use BP for the study of protein interactions, a peptide-BP conjugate must be synthesized. The addition of BP to the target molecule has often proven to be a difficult synthetic step. Here we describe a one pot, two step synthesis of BP units that are compatible with standard solid phase peptide synthesis procedures. The proximity between the BP moiety and the peptide pharmacophores can affect both binding and activity, thus we developed BP units using spacers of varying lengths. In addition, the spacer has a dominant effect on the site at which the BP binds to the protein, and the use of various lengths enables more complete mapping of the binding site.

Results and Discussion

In order to mainstream the use of BP, we have developed a one pot, two steps synthesis of BP units suitable for standard solid phase peptide synthesis procedures. The synthesis is based on coupling between the carboxy group of Boc-amino-alkylene carboxylic acid and the amine of 2-amino-benzophenone, followed by Boc removal (Figure 1). Coupling was performed using phosgene as the coupling reagent. The product was treated with TFA to obtain the BP unit. Purification was performed on silica gel.

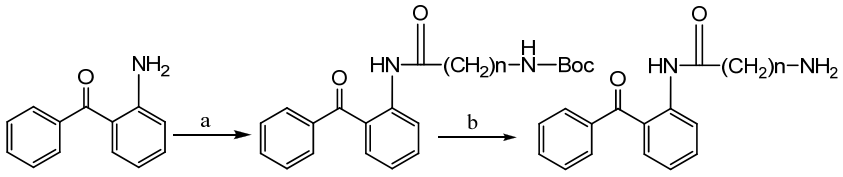

a) Boc-amino-alkylene carboxylic acid, phosgene, collidine. b) TFA n-2,3,5

Fig. 1. Synthesis of BP units.

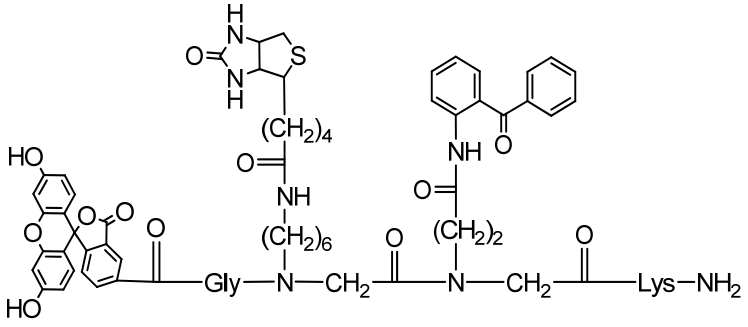

Fig. 2. Structure of SN1 containing photo-affinity label.

A

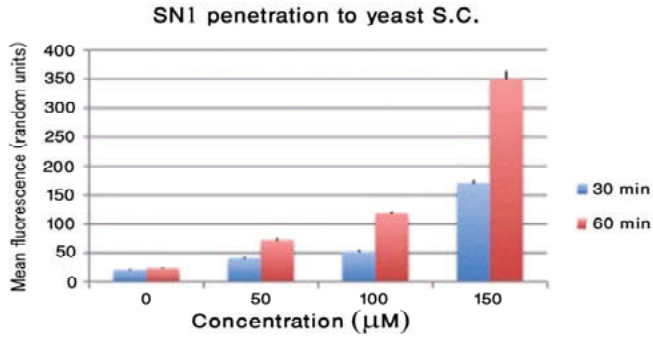

B

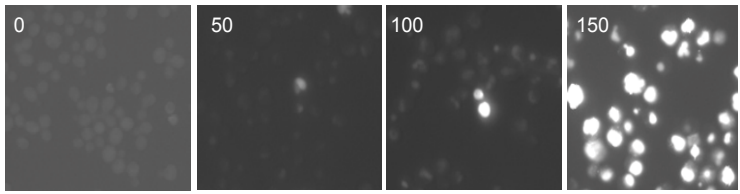

Fig. 3. Yeast cells were incubated with increasing concentrations of SN1 and were detected for fluorescence. (A) Columns chart describing the penetration level of SN1 over time to the yeast cells; (B) Fluorescence microscopy images of the penetrated cells.

To minimize proteolysis, we have designed the BP units so that their incorporation will form a stable peptomer sequence on solid support, using the "sub-monomer" procedure of Nuss, et al [2]. We used the BP units to synthesize a yeast permeable photo-affinity label, called SN1 (Figure 2). Fluorescein and biotin were incorporated into the structure of SN1, in addition to the BP unit, to enable additional validation techniques. Preliminary results indicate that SN1 penetrated into yeasts, as can be seen in Figure 3, and thus can be used to study protein-protein interactions in this system.

We are now constructing a new analog with an additional functional group that binds specifically to a target protein and plan to use it to investigate the role of the targeted protein in yeast proteomics.

References

1. Suva, L.J., Flannery, M.S., Caulfield, M.P., Findlay, D.M., Jüppner, H., Goldring, S.R., Rosenblatt, M., Chorev. M. *J. Pharmacol. Exp. Ther.* **283**, *876* (1997).
2. Nuss, J.M., Desai, M.C., Zuckermann, R.N., Singh, R., Renhowe, P.A., Goff, D.A., Chinn, J.P., Wang, L., Dorr, H., Brown, E.G., Subramanian, S. *Pure Appl. Chem.* **69**, 447 (1997).

Proceedings of the 31st European Peptide Symposium
Michal Lebl, Morten Meldal, Knud J. Jensen, Thomas Hoeg-Jensen (Editors)
European Peptide Society, 2010

The Chains of Insulin-Like Peptides Reveal Properties of Oxidoreductases

Kostas K. Barlos, Zoe Vasileiou, Vasso Chatziharalampous, Dimitrios Gatos, and Kleomenis Barlos
Department of Chemistry, University of Patras, 26500, Patras, Greece

Introduction

Various physiological and pathological conditions can lead to protein misfolding and cell stress. Protein misfolding is the originating factor of more than 60% of human diseases including aging, several cancer types, Alzheimer's disease and diabetes. Therefore, a better understanding of the principles that determine folding and unfolding of peptides and proteins could facilitate the development of artificial oxidoreductases and chaperones. We have recently found [1] that oxidized A-chain of the insulin like-peptide (INSL) human relaxin-2 (RLN2) reacts with the B-chain of human relaxin giving RLN2 with the native characteristic disulfide bond pattern and as a side product oxidized B-chain. It is believed that the chains of the INSL contain the structural information required for native folding in the sequence of their corresponding propeptides which fold correctly before the enzymatic cleavage, which results in the two chain native structure of the peptide. A question arises from the common disulfide bond pattern in INSL. Is folding determined by the individual sequences of the whole propeptide chains, the sequences of the A- and B-regions/chains or the distribution pattern of the sulphur atoms within the chains? In the latter case, folding of the A- and B-chains originating from different INSL could be also possible. If so, INSL could become easily accessible synthetically, as well as chimeric INSL.

Results and Discussion

The A and B-chains of the INSL (Figure 1) were synthesized by SPPS utilizing Fmoc-amino acids and 2-chlorotrityl resin. Chains containing Met were also synthesized as the corresponding Met-sulfoxide derivatives. The linear peptides were purified by preparative HPLC and the A-chains were oxidized with DMSO to the corresponding two disulfide bonds containing bicyclic derivatives. In all cases we obtained bicyclic A-chain as a mixture of the expected three bicyclic isomers with the remarkable exception of insulin where exclusively one bicyclic A-chain isomer is formed. Excess (1.05-4.00 mmolar) of bicyclic A-chain was then reacted with the linear B-chain of INSL [2]. The reactions were performed under denaturing conditions (Gnd.HCl) at pH = 10.6 (Na-glycinate) in the presence of the mild oxidant DMSO (5-50%). The proceeding of the reaction was followed by LC-MS.

A-chain

Relaxin 1	RPYVALFEK**CC**LI G**C**TKRSLAKY**C**
Relaxin 2	ZLYSALANK**CC**HVG**C**TKRSLARF**C**
Relaxin 3	DVLAGLSSS**CC**KWG**C**SKSEISSL**C**
Insulin	GIVEQ**CC**TSI **C**SLYQLENY**C**N
IGF-1	APQTGIVDE**CC**FRS**C**DLRRLEMY**C**A
IGF-2	RRSRGIVEE**CC**FRS**C**DLALLETL**C**A
INSL 3	AAATNPARY**CC**LSG**C**TQQDLLTL**C**PY
INSL 4	RSGRHRFDPF**CC**EVI **C**DDGTSVKL**C**
INSL 5	QDLQTL**CC**TDG**C**SMTDLSAL**C**
INSL 6	GYSEK**CC**LTG**C**TKEELSIA**C**

B-chain

Relaxin 1	KWKDDVIKL**CG**RELVRAQ IAI**CG**MSTWS
Relaxin 2	DSWMEEVIKL**CG**RELVRAQ IAI**CG**MSTWS
Relaxin 3	RAAPYGVRL**CG**REFIRAVI FT**CG**GRW
Insulin	VNQHL**CG**SHLVEALYLV**CG**ERGFFYTPKA
IGF-1	GPETL**CG**AELVDALQFV**CG**DRGFYFNKP
IGF-2	PSETL**CG**GELVDTLQFV**CG**DRGFYFSRP
INSL 3	PTPEMREKL**CG**HHFVRALVRV**CG**GPRWSTEA
INSL 4	ZSLAAELRG**CG**PRFGKHLLSY**CP**MPEKTFTTTP
INSL 5	SKESVRL**CG**LEY IRTV I Y I **CA**SSRW
INSL 6	SDISSARKL**CG**RYLVKE I EKL**CG**HANWSFR

CA-chain

IGF-1	GYGSSSRRAPQTAPQTGIVDE**CC**FRS**C**DLALLETL**CA**

Fig. 1. Sequences of INSL; with bold are indicated conserved or almost conserved residues.

In all cases mainly three products are obtained in various ratios. INSL, oxidized B-chain and dimeric chain-B. Linear chain-B is consumed in all cases almost quantitatively within 5 min at RT if the excess of bicyclic A-chain over linear B-chain is equal or exceeds the 2:1 ratio. Under these conditions B-chains were converted to INSL in 2-65% yield. Low yields were observed in the case of insulin (high yield of insulin is obtained if bicyclic A-chain and cyclic B-chain are equilibrated in the presence of a thiol catalyst) and RLN3. The highest yields were obtained in the case of RLN1, RLN2, INSL3 and

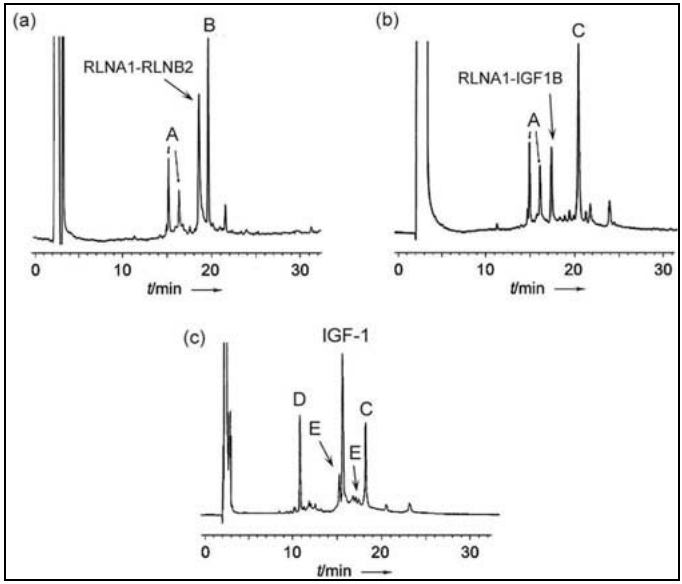

Fig. 2. Analytical HPLC of the product mixture obtained in 4h at RT during the folding at pH = 10.6 of (a) the bicyclic A-chain of RLN1 with the linear B-chain of RLN-2, (b) of bicyclic A-chain of RLN1 with the B-region of IGF-1 and (c) of bicyclic A-region of IGF-1 with its linear B-region. A = bicyclic A-chain of RLN1, B = oxidized B-chain of RLN2, C = oxidized B-region of IGF-1, D = bicyclic A-region of IGF-1 and E = isomers of two-chain IGF-1.

IGF-1. These results indicate strong oxidizing properties inherent in the bicyclic A-chains. In many cases, the bicyclic A-chains of one INSL react readily with the linear B-chain of the other, but not with the monocyclic A-chain. For example, the B-chain of IGF-1 folds readily with the bicyclic A-chains of RLN2 or INSL3. However, folding of IGF-1 A-chain with the B-chains of these peptides results in very low yields. Similarly, the formed monooxidized A-chain reacts in some cases readily with cyclic B-chains to yield the corresponding INSL (example IGF-1), while in other cases this reaction proceeds very slowly. It is remarkable that the folding reactions of the A-region of IGF-1 and those of the C-A-region of IGF-1 with the IGF-1 B-chain proceed almost identical. It is also of interest that IGF-1 folds similarly to the corresponding propeptide in mainly two isomers, but the opposite is observed for the chimeric peptides containing IGF B-chains which are obtained as one isomer (Figure 2).

In summary, bicyclic A-chains of INSL are powerful oxidizing peptides and fold with or oxidize readily B-chains of INSL independently of the individual chain. With the exception of IGF (similarly to the single chain IGF-1), the folding reactions proceed selectively giving exclusively the native INSL peptide, although a mixture of bicyclic A-chain isomers was applied in all cases, except of insulin. These oxidizing and reshuffling potencies of the A-chains observed in >100 folding reactions indicate strongly the oxidoreductase character of the A-chain of INSL. Furthermore, the A-region of IGF-1 seems to be responsible for the generation of the two isomers during the folding of the A or C-A-chain of IGF-1 with its B-chain.

Acknowledgments
We thank CBL Patras for financial support.

References

1. Barlos, K.K., et. al. *J. Peptide Sci.* **16**, 200-211 (2010).
2. U.S. Patent Application No. 12/783,223, Unpublished (K. Barlos, et al.).

Proceedings of the 31st European Peptide Symposium
Michal Lebl, Morten Meldal, Knud J. Jensen, Thomas Hoeg-Jensen (Editors)
European Peptide Society, 2010

Solid Phase and Ligation Approaches to Dendrimeric Immunogen Synthesis

Wioleta Kowalczyk, Marta Monsó, Beatriz G. de la Torre, and David Andreu

Department of Experimental and Health Sciences, Pompeu Fabra University, Barcelona Biomedical Research Park, Barcelona, Spain

Introduction

Dendrimeric immunogens such as multiple antigenic peptides (MAPs) were introduced by Tam some 25 years ago [1] and have found numerous applications in vaccine and diagnostics research. However, despite extensive and successful use, experimental reports on MAP and similar dendrimeric constructs are often lacking in chemical detail about their preparation and characterization.

MAPs can be synthetically approached by direct or indirect (convergent) methods. In the former approach the branched poly-lysine core and the epitopes displayed on it are entirely built by stepwise SPPS while the convergent approach relies on the chemical ligation (e.g. thioether) of properly functionalized peptide epitopes onto the poly-lysine core [2]. Theoretically, the use of pre-purified components in the ligation reactions can result in chemically more unambiguous materials than in stepwise methods, where minute but cumulative synthetic errors (deletions, truncations, etc.) become amplified by multimerization and may predictably lead to relatively heterogeneous immunogens.

In this study two methods of MAP preparation have been evaluated: fully stepwise SPPS and thioether ligation in solution. The pros and cons of both approaches have been investigated using a well-known epitope, the N-terminal ectodomain (M2e) of influenza type A virus M2 protein [3], a transmembrane tetrameric protein on the virus surface acting as an ion channel and consisting of three regions: the ectodomain, a transmembrane region and the cytoplasmic tail (Figure 1). The 24-residue M2e, a rather challenging sequence [4], and a shorter (12-residue, sM2e), more manageable version have been used as test epitopes.

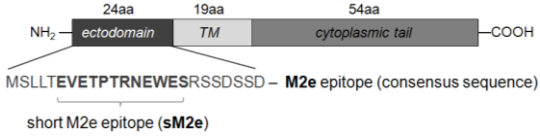

Fig. 1. Schematic structure of protein M2.

Results and Discussion

The all-SPPS (direct) approach was used to prepare two MAPs, each with four copies of sM2e. MAP **B** (Figure 2) only differed from **A** in the presence of 6-aminohexanoic acid (Ahx) spacer units at every branching point, a modification aimed at enhancing the overall flexibility of the construct. Both **A** and **B** were readily assembled on a Rink amide ChemMatrix resin using Fmoc chemistry and double couplings throughout the entire sM2e sequence. **A** was obtained in a 9% isolated yield and well characterized by MALDI-TOF MS ($C_{281}H_{432}N_{80}O_{102}S_1$, MW= 6595.05 Da, $[M+H^+]$ = 6596.28). A parallel process for **B** led to a more easily purifiable final product in significantly better yield (16.5%, $C_{317}H_{498}N_{86}O_{108}S_1$, MW = 7273.99Da, $[M+H^+]$ = 7274.34).

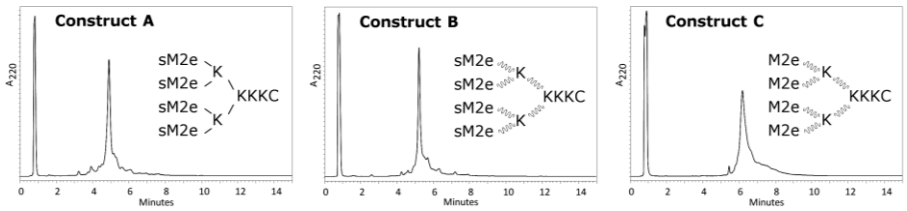

Fig. 2. Analytical HPLC of tetravalent MAP constructs (crude product) obtained by all-SPPS approach (wavy lines denote flexibilizing Ahx residues).

The canonic M2e epitope entailed considerable synthetic difficulties already as a simple monomer, which were substantially overcome by the use of ChemMatrix resin, systematic double couplings and, especially, pseudoproline dipeptide units at the two Ser-Ser pairs [4]. All these improvements, plus flexibilizing Ahx units at every branching point, were incorporated to the all-SPPS synthesis of tetravalent construct **C** (Figure 2), resulting in a clean, easily purifiable and satisfactorily characterized end product ($C_{517}H_{838}N_{146}O_{196}S_5$, MW = 12387.86 Da; $[M+H^+]$ = 12387.79; 4.8% yield).

To evaluate the convergent (chemical ligation) approach, constructs **D** and **E** (see Figure 3) were prepared [4]. For thioether ligations, a tetravalent core functionalized with chloroacetyl groups ($ClAc_4$-Lys core), and either the sM2e or the M2e monomers (for **D** and **E**, respectively; each C-terminally elongated with Cys) were prepared in highly pure form. Ligations were conducted in Tris·HCl, pH 7.6, 2 M guanidinium chloride, at 50 ºC, using 10-12-fold molar excess of peptide. Reaction progress was monitored by analytical HPLC and revealed in both cases rather complex processes (Figure 3) [4]. MALDI-TOF MS analysis showed MAP products containing different numbers of epitope copies, along with substantial amounts of the disulfide-bound dimers of the linear peptides. HPLC resolution of the reaction mixtures was challenging and did not allow efficient separation of the target tetravalent constructs from less substituted species. Additionally, in the ligation for **E**, an M2e tetramer, coeluting with the disulfide dimer and identified as a non-covalent double dimer, further complicated the situation [4].

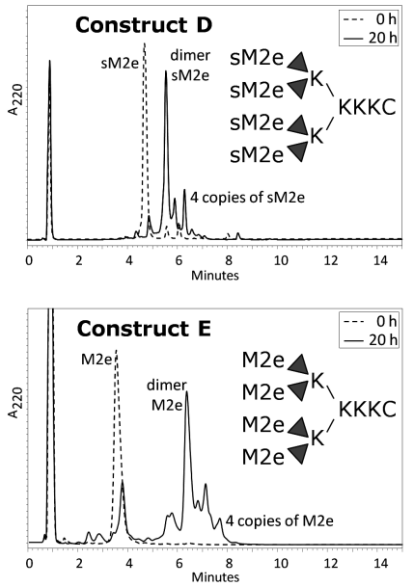

Fig. 3. Progress of thioether ligation monitored by HPLC (triangles indicate thioether linkage).

In view of these difficulties with the ligation approach, the all-SPPS route appears advantageous, particularly for epitopes such as M2e, where factors such as size (steric hindrance preventing access of the Cys thiol to unreacted ClAc groups), solubility and aggregation (both difficult to predict) can have severely limiting effects. Ligation is also more expensive and time-consuming than the all-SPPS approach, and in thiol-based chemistries tends to generate sizable amounts of disulfide dimer whose recycling back to the thiol form is costly in time and effort.

Regarding the all-SPPS approach, on the basis of the above results we would propose two recommendations: (i) incorporating flexibility-enhancing units (e.g., Ahx) at branching points can be synthetically beneficial; (ii) an exploratory synthesis of the linear epitope can identify trouble spots to be smoothed before the synthesis of the considerably more complicated MAP structures is undertaken.

Acknowledgments

Work supported by MICINN, the Spanish Ministry of Science and Innovation (grants BIO2005-07592-CO2-02 and BIO2008-04487-CO3-02 to D.A.), by the regional government of Catalonia (SGR2005-00494). W.K. is a fellow in the Juan de la Cierva Program of MICINN.

References

1. Tam, J.P. *Proc. Natl. Acad. Sci. U.S.A.* **85**, 5409-5413 (1988).
2. Tam, J.P., In Goodman M (Ed.) *Peptide Dendrimers and Protein Mimetics*, Thieme, Stuttgart, 2000, p. 129.
3. Cady, S.D., Luo, W., Hu, F., Hong, M. *Biochemistry* **48**, 7356-7364 (2009).
4. Kowalczyk, W., De la Torre, B.G., Andreu, D. *Bioconj. Chem.* **21**, 102-110 (2010).

Proceedings of the 31st European Peptide Symposium
Michal Lebl, Morten Meldal, Knud J. Jensen, Thomas Hoeg-Jensen (Editors)
European Peptide Society, 2010

Synthesis of the Thiolactone Derivative of *Enterococcus faecalis* Gelatinase Biosynthesis-Activating Pheromone Using the GyrA Mini-Intein

Koji Nagata[1], Yosuke Yamanaka[1], Shoichiro Horita[1], Hidekazu Katayama[2], Kou Hayakawa[1], Akihiro Yamamura[1], Mami Sato[3], Kenzo Nishiguchi[3], Kenji Sonomoto[3,4], Jiro Nakayama[3], and Masaru Tanokura[1]

[1]Graduate School of Agricultural and Life Sciences, The University of Tokyo, 1-1-1 Yayoi, Bunkyo-ku, Tokyo, 113-8657, Japan; [2]Institute of Glycoscience, Tokai University, 1117 Kitakaname, Hiratsuka, Kanagawa, 259-1292, Japan; [3]Faculty of Agriculture, Graduate School, [4]Bio-Architecture Center, Kyushu University, Fukuoka, 812-8581, Japan

Introduction

The expression of pathogenicity-related extracellular proteases in *Enterococcus faecalis* is positively regulated by the quorum sensing system mediated by an autoinducing peptide termed gelatinase biosynthesis-activating pheromone (GBAP) [1]. GBAP is an 11-residue cyclic peptide containing a lactone linkage formed by the side-chain hydroxyl group of Ser^3 and the main-chain carboxyl group of Met^{11} in the following amino-acid sequence, Gln-Asn-Ser-Pro-Asn-Ile-Phe-Gly-Gln-Trp-Met. Secreted GBAP binds to its membrane-bound receptor FsrC and triggers a two-component signal transduction cascade of FsrC and FsrA. We previously reported the chemical synthesis [2] and the solution structure determination of GBAP [3]. In order to analyze the intermolecular interaction of GBAP and FsrC by heteronuclear NMR, we need to establish a preparation method of isotopically labeled GBAP. Here, we describe a new method to synthesize the thiolactone derivative of GBAP, a GBAP agonist, from the fusion protein of [Cys^3]GBAP and *Mycobacterium xenopi* GyrA mini-intein [4]. With this method, we obtained 0.25 mg of ^{15}N-labeled GBAP thiolactone from 1 L of *Escherichia coli* culture, and measured its ^{1}H-^{15}N 2D HSQC.

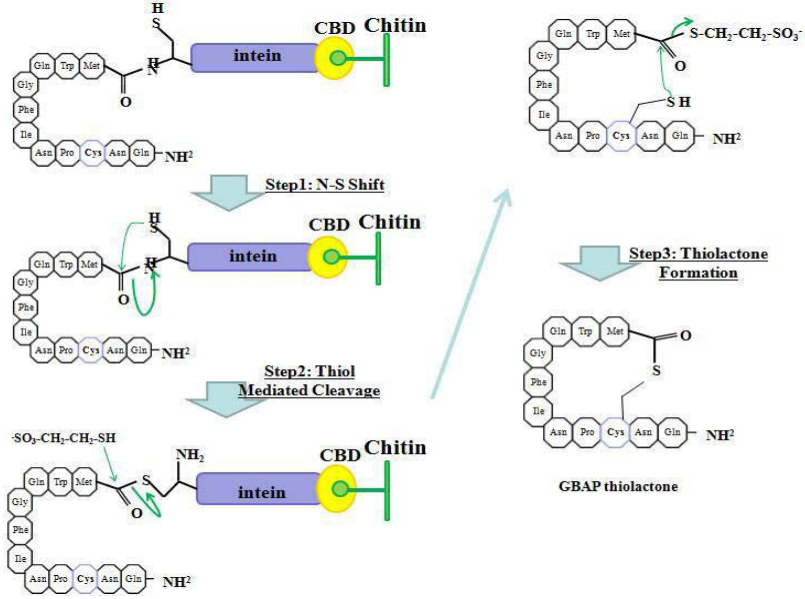

Fig. 1. Mechanism of GBAP thiolactone formation using GyrA mini-intein and MESNA.

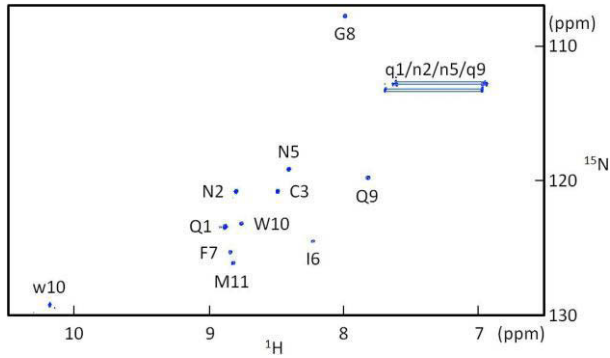

Fig. 2. ^{1}H-^{15}N HSQC spectra of ^{15}N-labeled GBAP thiolactone measured at 10°C. The backbone amide groups are labeled in capital letters; the side-chain amide and imide groups in lower-case letters. This peptide has an additional Met residue at the N-terminus.

Results and Discussion

The expression plasmid of the precursor protein of the thiolactone derivative of GBAP in which [Cys^{3}]GBAP was fused to the N-terminus of GyrA mini-intein was constructed using pTXB1 (New England Biolabs). The precursor protein, [Cys^{3}]GBAP-GyrA, was then expressed in *E. coli* Rosetta(DE3) (Novagen) and affinity-purified using chitin resin (New England Biolabs). The [Cys^{3}]GBAP was then cleaved from GyrA mini-intein by treating the fusion protein with 2-mercaptoethanesulfonic acid (MESNA) (Figure 1). The resultant [Cys^{3}]GBAP-thioester was autonomously converted to the thiolactone-derivative of GBAP, whose structure and activity were verified by MALDI-TOF-MS and the assay for GBAP activity, respectively. The activity of the GBAP thiolactone was slightly higher than the native form of GBAP (lactone). By this method, 0.70 mg and 0.25 mg of non-labeled and ^{15}N-labeled GBAP thiolactones (Figure 2) were purified from 1 L of *E. coli* culture in Terrific Broth and M9 minimal media, respectively. 1,4-Dithio-DL-threitol (DTT) was tested as an alternative reducing agent to MESNA to cleave [Cys^{3}]GBAP-GyrA, and three products were obtained in this case. Two of them were DTT-adducts to GBAP and the other was the linear form of [Cys^{3}]GBAP. The two different DTT-adducts to GBAP could be derived from the optical isomers of DTT. In contrast, no cleavage was observed when tris(2-carboxyethyl)phosphine (TCEP), a non-thiol-type reducing agent, was used.

A similar method was proposed to synthesize *Staphylococcus aureus* autoinducing peptides (AIPs) from the fusion protein in which each AIP was fused to the N-terminus of a mini-intein [5]. This method depends on the autonomously occurring *N-S* shift-mediated intein cleavage. However, this method was inefficient in synthesizing GBAP thiolactone due to low efficiency of autonomous intein cleavage. The intein cleavage in our method occurs more efficiently owing to the intermediate thioester formation by MESNA. Thus our method would be more widely applicable to the synthesis of various peptide thiolactones.

Acknowledgments

This work was supported in part by grants-in-aid for scientific research from the Ministry of Education, Culture, Sports, and Technology of Japan (grant 16087203 to K. Nagata), from the Japan Society for the Promotion of Science (grants 15580065, 17580068 and 40217930 to J. Nakayama), from the Kato Memorial Bioscience Foundation (to J. Nakayama), from the Waksman Foundation of Japan (to J. Nakayama), and by the Targeted Proteins Research Program (TPRP) of the Ministry of Education, Culture, Sports, Science and Technology of Japan (to M. Tanokura).

References

1. Nakayama, J., et al. *Mol. Microbiol.* **41**, 145-154 (2001).
2. Nakayama, J., et al. *Biosci. Biotechnol. Biochem.* **65**, 2322-2325 (2001).
3. Nishiguchi, K., et al. *J. Bacteriol.* **191**, 641-650 (2009).
4. Evans, T.C. Jr., et al. *Protein Sci.* **7**, 2256-2264 (1998).
5. Malone, C.L., et al. *Appl. Env. Microbiol.* **73**, 6036-6044 (2007).

Proceedings of the 31st European Peptide Symposium
Michal Lebl, Morten Meldal, Knud J. Jensen, Thomas Hoeg-Jensen (Editors)
European Peptide Society, 2010

Solvent-Free Synthesis of Peptides in a Ball-Mill

Valérie Declerck, Pierrick Nun, Jean Martinez, and Frédéric Lamaty
Institut des Biomolécules Max Mousseron (IBMM), UMR 5247 CNRS-UM1-UM2, Université Montpellier II, Place Eugène Bataillon, 34095, Montpellier Cedex 5, France

Introduction

The market for therapeutic bulk peptides is expected to rapidly grow in the next few years [1]. In spite of the well established procedures of peptide synthesis by chemical ways, i.e. stepwise synthesis in solution, solid phase peptide synthesis, one of the major problems related to peptide synthesis concerns the huge amount of solvent needed for their preparation, particularly on solid supports (2000 to 5000 kg for a large peptide). There is still a need for exploring efficient, convenient, and environmentally friendly methods for peptide synthesis, particularly when the time for scale-up of peptide production comes. A possible approach to solve this problem would be to carry out chemical reactions in the absence of solvent [2]. Techniques such as mixing, grinding or ball-milling have proved their efficiency in the field of organic chemistry in the solid state. We report herein a new strategy for the preparation of peptides in solvent-free conditions, using ball-milling technology [3].

Results and Discussion

The coupling of urethane-protected N-carboxyanhydride of aminoacids (UNCA's) **1** with aminoacids or aminoesters was studied, keeping in mind that all these compounds have to remain in their solid state under the ball-milling conditions (Scheme 1). UNCA's are activated forms of aminoacids which have proven to be useful in peptide and organic synthesis.

The various UNCA derivatives do not present the same reactivity profile. Boc-Val-NCA was quantitatively converted to the dipeptide while Fmoc-Val-NCA gave lower conversions. Very good yields were achieved with Boc-Phe-NCA except for the reaction of HCl·H-Phe-OMe. It is worth noting that better results were obtained with freshly prepared starting material, otherwise, the reaction was incomplete and hydrolysis of the UNCA occurred.

Scheme 1.

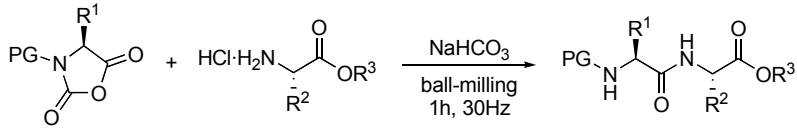

1

We also explored the possibility of preparing a tripeptide, from a dipeptide. Starting from HCl.Ala-Gly-OMe, it was possible to prepare the corresponding tripeptide after reaction with Boc-Val-NCA (Scheme 2). This is the first step towards the development of an iterative process to synthesize longer peptides, by successive reaction with urethane-protected N-carboxyanhydride of aminoacids. We also experimentally checked that this method does not lead to any epimerization of the peptide during its synthesis.

Scheme 2.

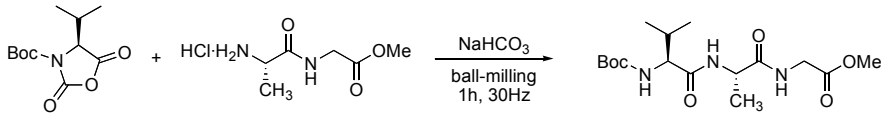

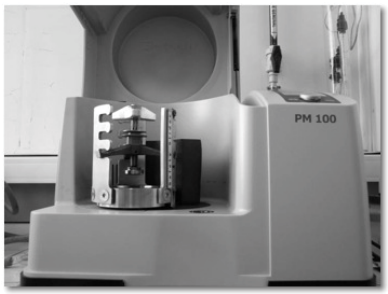

Fig. 1. Planetary ball-mill for the preparation of larger quantities of dipeptides.

The scale up of the reaction was also considered. Preliminary results are showing that the results can be translated to about 5 g of dipeptide. For this purpose, the reaction was performed in a planetary ball-mill.

We investigated also the kinetics of the reaction. Interestingly, and for each vibration speed, the profile (Figure 2) showed apparent zero-order kinetics in agreement with solid-solid state reaction mechanism. This means that the reaction rate does not depend on the concentration of the reactants.

In conclusion, this solvent-free method represents a new paradigm in the preparation of peptides.

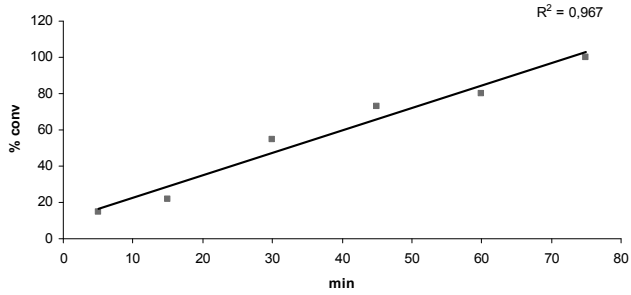

Fig. 2. Kinetics profile of the reaction of Boc–Phe–NCA with HCl·H–Ala–OMe in the presence of $NaHCO_3$ at a frequency of 30 Hz.

Acknowledgments
We thank the Fondation d'Entreprise EADS, the MENRT and the CNRS (Programme "Chimie pour le développement durable") for financial support.

References

1. Vlieghe, P., Lisowski, V., Martinez, J., Khrestchatisky, M. *Drug Discovery Today* **15**, 40-56 (2010).
2. Tanaka, K., Toda, F. *Chem. Rev.* **100**, 1025-1074 (2000).
3. Declerck, V., Nun, P., Martinez, J., Lamaty, F. *Angew. Chem. Int. Ed.* **48**, 9318-9321 (2009).

Proceedings of the 31st European Peptide Symposium
Michal Lebl, Morten Meldal, Knud J. Jensen, Thomas Hoeg-Jensen (Editors)
European Peptide Society, 2010

A Study to Assess the Cross-Reactivity of Cellulose Membrane Bound Peptides with Detection Systems: An Analysis at the Amino Acid Level

Carsten C. Mahrenholz, Victor Tapia, and Rudolf Volkmer
Institute of Medical Immunology, Charité Medical School, Berlin, Germany
Contact: rve@charite.de

Introduction

The growing demand for binding assays to study protein-protein interaction can be addressed by peptide array-based methods [1]. The SPOT technique is a widespread peptide-array technology, which is able to distinguish semi-quantitatively the binding affinities of peptides to defined protein targets within one array. The quality of an assay system used for probing peptide arrays depends on the well-balanced combination of screening and read-out methods. The former address the steady-state of analyte capture, whereas the latter provide the means of detecting captured analyte. In all cases, however, false positive results can occur when challenging a peptide array with analyte or detecting captured analyte with label conjugates. Little is known about the cross-reactivity of peptides with the detection agents. Here we describe at the amino acid level the potential of 5-(and 6)-carboxytetramethylrhodamine [5(6)-TAMRA] to cross-react with individual amino acids in a peptide sequence. Peptides with different amino acid cores were synthesized and tested for interaction with common dyes and detection systems. Further studies including random peptide libraries and other influential factors, as well as additional detection systems (fluoresceinisothiocyanate [FITC], and biotin/streptavidin) can be found in our corresponding manuscript [2].

Experimental Setup

To investigate the potential interaction of this detection system with individual amino acids, 20 peptides of the sequence GGG$[B]_5$GGG were designed. Herein, $[B]_5$ denotes five repeats of one of the 20 amino acids (for a schematic overview see Figure 1). Glycine was used to create nonreactive regions flanking the functional core at the N- and C-termini. This approach generates peptides of reasonable length for the homogeneous display of the defined cores. The peptides were prepared via SPOT synthesis [3], with each GGG$[B]_5$GGG sequence repeated three times in columns on the peptide array.

As soluble interaction partner, a peptide of the sequence Gly-Gly-Gly was synthesized, N-terminally modified with TAMRA (label-GGG), and finally purified by HPLC. This tripeptide was used to better meet the assay conditions, because labels are usually chemically coupled to an analyte or a detection antibody.

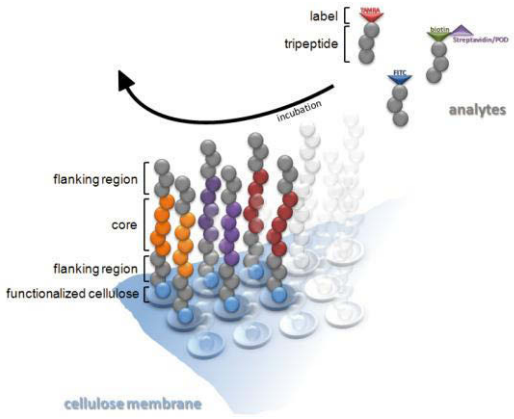

Fig. 1. Peptide and analyte composition.

Peptide arrays containing the core-motifs were incubated *in situ* with a label-GGG and evaluated using optical and fluorescent methods. Strict conditions including short incubation periods and long-time washing procedures were applied to ensure stringency of binding. Binding experiments resulted in measurable spot signal intensities signifying directly or indirectly captured label conjugate.

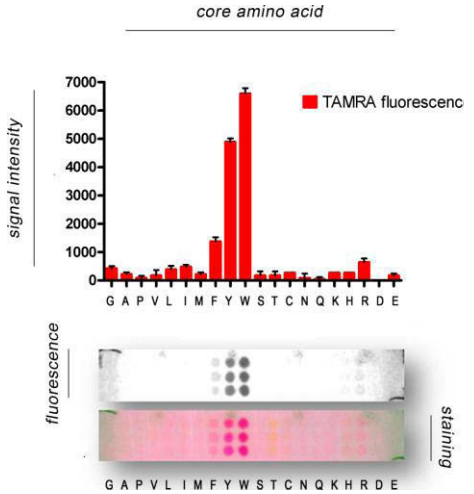

*Fig. 2. TAMRA cross-reaction. (**A**) Fluorescence emission of each corresponding spot measured at 645 nm is calculated from a circular region around the spot center detected in the image. All signals below an SI of 500 are at the background level and should therefore not be considered interactions between the amino acid core and the detection system. (**B**) Fluorescent and (**C**) densitometric read-out. Each spot represents a cellulose membrane-bound peptide of the sequence GGG[B]$_5$GGG, where [B]$_5$ denotes five repeats of one of the 20 amino acids. Contrast was adjusted to ensure better visibility. The negative control without analyte shows no signal. Error bars represent the standard deviation of three spots.*

Results and Discussion

The results draw a clear picture of the cross-reactivity of amino acid cores with the peptide TAMRA-GGG. As shown in Figure 2, significant spot signal intensities at 645 nm were observed for Phe, Tyr, and Trp cores. The strength of cross-reactivity between these amino acids and TAMRA follows the order Phe < Tyr < Trp. Additionally, densitometry was used to read the capturing of TAMRA-GGG via staining. As shown in Figure 2B and 2C, the results are in accordance with the fluorescence read-out approach. The aromatic TAMRA moiety interacts exclusively with aromatic amino acid cores (Figure 2A). Therefore, aromatic stacking is most likely the common driving force for the interaction between amino acid and TAMRA. Stacking is a widespread mechanism for stabilizing organic moieties. It is accomplished by the favorable interaction of π-electrons of aromatic systems [4]. In this case, the π-electron systems of TAMRA and the side group of Trp may interact in an energetically favorable manner via stacking interactions, which the smaller aromatic systems of Tyr and Phe possibly cannot provide to the same extent.

Further studies including random peptide libraries and other influential factors, as well as additional detection systems (fluoresceinisothiocyanate [FITC], and biotin/streptavidin) can be found in our corresponding manuscript [2].

One has to bear in mind that a method is always limited by the effectiveness and validity of the read-out system. To prevent or identify false positives, factoring in these results is highly recommended when analyzing measurements. Taking these new results into consideration will, in future, strengthen the reliability of the analysis of SPOT-synthesis-generated data.

Acknowledgments

This work was generously funded by the Manchot Foundation (Henkel KGaA) and supported by scholar- and fellowships from the Federation of the Societies of Biochemistry and Molecular Biology, the Charité Medical School, and GlaxoSmithKline.

References

1. Andresen, H., et al. *Proteomics* **6**(5), 1376-1384 (2006).
2. Mahrenholz, C.C., et al. *J. Pep. Sci.* **16**, 297-302 (2010).
3. Frank, R. *J. Immunol. Methods* **267**(1), 13-26 (2002).
4. Sygula, A., et al. *J. Am. Chem. Soc.* **129**(13), 3842-3843 (2007).

Proceedings of the 31st European Peptide Symposium
Michal Lebl, Morten Meldal, Knud J. Jensen, Thomas Hoeg-Jensen (Editors)
European Peptide Society, 2010

The Microwave Revolution: Recent Advances in Microwave Assisted Peptide Synthesis

Sandeep K. Singh, Alicia D. Douglas, Eric J. Williamson, and Grace S. Vanier*
CEM Corporation, Bioscience Division, PO Box 200, 3100 Smith Farm Road, Matthews, NC, 28106, U.S.A.

Introduction

In solid phase peptide synthesis (SPPS), while certain peptide sequences are synthesized relatively easily, some sequences are much more difficult. Efficient couplings occur within a fully solvated peptide-polymer matrix, where reagent penetration is rapid and unhindered. Sudden decreases in reaction rates and incomplete couplings have been attributed to peptide aggregation resulting in poor salvation [1]. Microwave energy represents a fast and efficient way to enhance both the deprotection and coupling reactions hindered by aggregation. The *N*-terminal amino group and peptide backbone are polar and they may constantly try to align with the alternating electric field of the microwave, and assist in breaking up the chain aggregation. The application of microwave energy has proved to be a major enabling tool for enhancing slow and difficult chemical reactions [2]. Unlike conventional heating, microwave energy could selectively activate any molecule with a dipole moment and thereby allow for rapid heating at the molecular level. Microwave assisted SPPS has been successfully applied to and shown useful for the synthesis of a range of difficult peptides [3]. Microwave peptide synthesis routinely shows substantial improvements in crude purity with reduced synthesis time compared to conventional SPPS. Previous studies have investigated the effects of microwave on aspartimide formation and epimerization, and offered optimized conditions for susceptible sequences to these well-known side reactions [4]. We now report our recent results on the development of microwave assisted *N*-terminal modifications and head-to-tail on-resin cyclization.

Results and Discussion

N-terminal modifications. Fatty acid acylation on the *N*-terminus of a peptide increases its cell permeability and affinity, and is a common post-translational modification for a wide variety of viral, bacterial and eukaryotic proteins and peptides [5]. Biotin labeled peptides have numerous biochemical and microbiological applications [6]. Under conventional conditions, these modifications often require coupling reactions of 24 h or more due to poor solubility and reactivity of the fatty acid or biotinylating reagents. We envisaged that sluggish reaction kinetics in these couplings could be overcome by the application of microwave irradiation.

The acyl carrier protein, ACP-(65-74) sequence (Val-Gln-Ala-Ala-Ile-Asp-Tyr-Ile-Asn-Gly) was selected as the test peptide for the present study. ACP-(65-74) was synthesized on Fmoc-Gly Wang resin (0.61 mmol/g) in less than 5 h using the CEM Liberty automated microwave peptide synthesizer. Fmoc deprotection with 20% piperidine in DMF for 0.5 min and 3 min at 75 ^{o}C and coupling with Fmoc-AA-OH/HBTU/DIEA for 5 min at 75 ^{o}C gave the ACP-(65-74) with a crude purity of more than 95% (Figure 1a). Double coupling of *n*-hexanoic acid to ACP for 5 min at 75 ^{o}C using HCTU/DIEA activation gave the *N*-capped peptide in 80% crude purity (Figure 1b). Similarly, microwave coupling of biotin-LC to ACP using HATU/DIEA for 5 min at 75 ^{o}C gave the biotin labeled peptide in 93% crude purity (Figure 1c). Thus, *N*-terminal modifications with a fatty acid or biotin were completed in

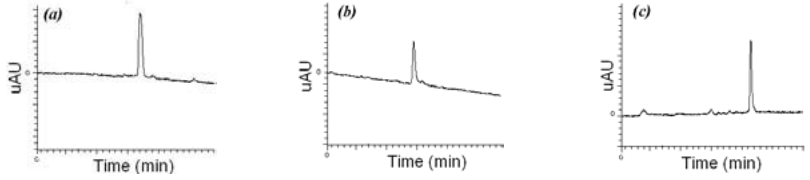

Fig. 1. HPLC crude chromatograms of (a) ACP-(65-74), (b) n-Hexanoic-ACP-(65-74), (c) Biotin-LC- ACP-(65-74).

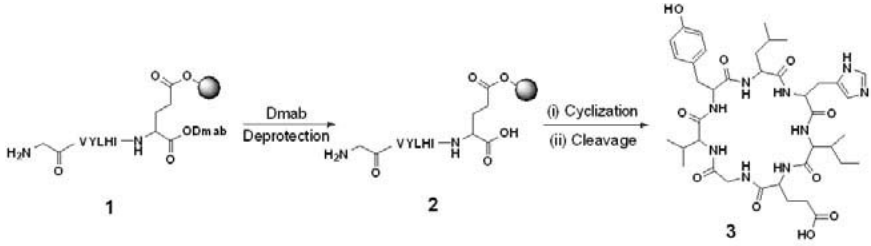

Scheme 1. On-resin peptide cyclization.

excellent yields in less than 15 min using microwave.

Head-to-tail on-resin cyclization. Introduction of a conformational restraint in peptides through cyclization increases their receptor affinity. Cyclic peptides exhibit improved metabolic stability, and increased potency and bioavailability as compared to their linear counterparts [7]. Head-to-tail on-resin cyclization strategy is an important tool in SPPS that takes advantage of the resin induced pseudo-dilution effects. However, such cyclizations often require long reaction times under conventional conditions and result in a low crude purity of the cyclized peptide.

The present work describes optimized microwave reaction conditions for each step in the head-to-tail on-resin cyclization method (Scheme 1). All of the synthesis steps were carried out in a fully automated fashion using the CEM Liberty microwave peptide synthesizer. The test sequence (Gly-Val-Tyr-Leu-His-Ile-Glu) for the cyclization studies was synthesized on Fmoc-Glu(Wang resin)-ODmab (0.32 mmol/g) in which the side chain γ-carboxyl group is anchored to the resin and the α-carboxyl is protected by Dmab orthogonal protecting group. A small amount of peptidyl resin was cleaved at the end of each step to assess the purity. Thus, Fmoc deprotection with 20% piperidine in DMF for 0.5 min and 3 min at 75 ^{o}C and coupling with Fmoc-AA-OH/HBTU/DIEA for 5 min at 75 ^{o}C assembled the backbone **1** in 91% crude purity (Scheme 1). Selective on-resin removal of Dmab protection was effected by treatment with 5% hydrazine in DMF (2 x 3 min at 75 ^{o}C) to give the linear precursor **2** in 91% crude purity. Head-to-tail cyclization of resin bound peptide **2** was accomplished using DIC/HOBt (3 x 10 min at 75 ^{o}C); cleavage of the cyclic peptide **3** from the resin followed by LC-MS analysis of the crude product indicated 77% purity.

In summary, we have developed efficient microwave assisted methods for the *N*-terminal modifications and head-to-tail on-resin cyclization of peptides. Microwave synthesis allows the completion of these transformations in high yields and purities in a fraction of the time compared to conventional peptide synthesis.

Acknowledgments
We thank the Bioscience Division of CEM Corporation for providing the research facilities.

References

1. Quibell, M., Johnson, T. *In Fmoc Solid Phase Peptide Synthesis. A Practical Approach*; Chan, W.C., White, P.D., (Eds.), Oxford University Press, New York, 2000.
2. Loupy, A. *Microwaves in Organic Synthesis* Wiley-VCH, Weinheim, 2002.
3. (a) Yu, H.-M., et al. *J. Org. Chem*. **57**, 4781-4784 (1992); (b) Erdelyi, M., Gogoll, A. *Synthesis* **11**, 1592-1596 (2002); (c) Collins, J.M., et al. *Poster Presentation at the 18th American Peptide Symposium, Boston, MA.* (2003); (d) Matsushita, T., et al. *Org. Lett.* **7**, 877-880 (2005); (e) Bacsa, B., et al. *J. Pept. Sci.* **12,** 633-638 (2006); (f) Fara, M.A., et al. *Tetrahedron Lett.* **47**, 1011-1014 (2006); (g) Tantry, S.J., et al. *ARKIVOC* **I**, 21-30 (2006); (h) Grieco, P., et al. *J. Med. Chem.* **51**, 2701-2707 (2008); (i) Santagada, V., et al. *Mini Rev. Med. Chem.* **9**, 340-358 (2009); (j) Galanis, A.S., et al. *Biopolymers* **92**, 23-34 (2009).
4. Palasek, S.A., Cox, Z.J., Collins, J.M. *J. Pept. Sci.***13**, 143-148 (2007).
5. Chicharro, C., et al. *Antimicrob. Agents Chemother.* **43**, 1267-1269 (1999).
6. Winkler, D.F.H., McGeer, P.L. *Proteomics* **8**, 961-967 (2008).
7. Rovero, P. In *Solid Phase Synthesis. A Practical Guide;* Kates, S.A., Albericio, F., (Eds.), Marcel Dekker, New York, 2000.

Proceedings of the 31st European Peptide Symposium
Michal Lebl, Morten Meldal, Knud J. Jensen, Thomas Hoeg-Jensen (Editors)
European Peptide Society, 2010

Microwave-Assisted Solid-Phase Peptide Synthesis of the 60-110 Domain of Human Pleiotrophin (hPTN) on CLTR-Cl Resin

Irene Friligou[1], Evangelia Papadimitriou[2], Dimitrios Gatos[1], John Matsoukas[1], and Theodore Tselios[1]

[1]Department of Chemistry, University of Patras, GR-265 04, Patras, Greece;
[2]Laboratory of Molecular Pharmacology, Department of Pharmacy, University of Patras, GR-265 04, Patras, Greece

Introduction

Human pleiotrophin (hPTN) is a heparin-binding growth factor with diverse biological activities, the most studied being those related to the nervous system, tumor growth and angiogenesis. It is interesting to determine which regions of hPTN are responsible for its diverse functions, in order to identify the molecular mechanisms involved and to identify possible therapeutic targets or/and agents. The binding of hPTN to heparin is mediated by the two central regions that are homologous to the thrombospondin type I repeat (TSR-1), with the carboxyl terminal TSR-1 domain (60-110) being the main heparin-binding site of PTN [1,2]. Here we report the Microwave Enhanced Solid Phase Peptide Synthesis (MW-SPPS) of the C-terminal 60-110 domain of hPTN composed of 51 amino acids using the Fmoc/tBu methodology [3,4].

Results and Discussion

The linear protected peptide was synthesized using the Liberty™ Microwave Peptide Synthesizer (CEM) on 2-chlorotrityl chloride resin (CLTR-Cl) [3]. Fmoc deprotection was achieved with 20% piperidine in DMF, while for the coupling reactions HOBt/DIC in DMF were used (Figure 1). Moreover, this domain is supposed to contain two disulfide bonds, one between 67-99 residues and one between 77-109 residues [2]. In order to achieve selective formation of these disulfide bonds, the Cys(Trt) at 77, 109 positions and Cys(Acm) at 67, 99 positions were used. After cleavage of the protected peptide from the resin and removal of the side chain protecting groups [except for Cys(Acm)^{67} and Cys(Acm)^{99}], the first disulfide bond was formed by dimethyl sulfoxide (DMSO) [4]. The second disulfide bridge was formed simultaneously with the Acm group removal using iodine. The desired linear peptide was obtained in only 30h of total processing time and in 60% crude yield [4]. The products were checked for their purity by analytical HPLC (Waters Alliance 2695 Separations Module combined with Waters 2996 photodiode array detector) using a C-8 Purospher column (5 μm, 250 × 4 mm) at 214 nm and 254 nm, separation was achieved by gradient elution of 5% to 100% solvent B (solvent A=0.08% TFA in H_2O; solvent B=0.08% TFA in ACN) over 30 min at a flow rate of 1ml/min (Figure 2), and they were identified by ESI-MS [4]. In this report, we demonstrated that microwave energy can also be applied in the case of the solid-phase synthesis of large peptides utilizing the acid sensitive CLTR-Cl resin.

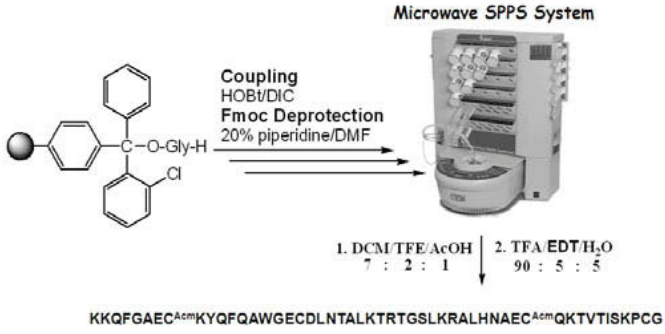

Fig. 1. Synthetic procedure of [Cys(Acm)^{67,99}]-hPTN$_{60-110}$.

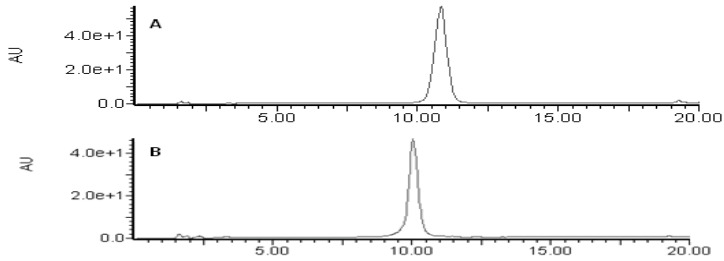

Fig. 2. Analytical RP-HPLC of ***(A)*** *purified linear [Cys(Acm)$^{67-99}$]-hPTN$_{60-110}$ and* ***(B)*** *bicyclic hPTN60-110.*

Acknowledgments

This work was supported by the E.U.-European Social Fund (75%) and the Greek Ministry of Development-GSRT (25%) (Grant PENED2003, 036Δ560). Special thanks to Eldrug SA for providing access to CEM Liberty automated microwave peptide synthesizer.

References

1. Papadimitriou, E., et al. *Eur. Cytokine Netw.* **20**, 180-190 (2009).
2. Mikelis, C., et al. *Recent Patents on Anti-Cancer Drug Discovery* **2**, 175-186 (2007).
3. Barlos, K., et al. *Angew. Chem. Int. Ed. Engl.* **30**, 590-593 (1991).
4. Friligou, I., et al. *Amino Acids* DOI 10.1007/s00726-010-0753-6 (2010).

Proceedings of the 31st European Peptide Symposium
Michal Lebl, Morten Meldal, Knud J. Jensen, Thomas Hoeg-Jensen (Editors)
European Peptide Society, 2010

Solid-Phase Synthesis of the Lipopeptide Myr-HBVpreS/2-78; A Hepatitis B Virus Entry Inhibitor

Alexa Schieck[1], Thomas Müller[1], Uwe Haberkorn[1], Stephan Urban[2], and Walter Mier[1]

[1]Department of Nuclear Medicine, University Hospital Heidelberg, Heidelberg, 69120, Germany; [2]Department of Infectious Diseases, Molecular Virology, University Hospital Heidelberg, Heidelberg, 69120, Germany

Introduction

Chronic HBV infection is the leading cause of liver cirrhosis and hepatocellular carcinoma (HCC). Synthetic peptides derived from the Hepatitis B Virus envelope, have been shown to efficiently inhibit an HBV infection *in vitro* [1] and *in vivo* [2]. Myr-HBVpreS/2-78 is the parent compound of these lipopeptides. It is a 77 amino acid peptide representing the *N*-terminal part of the viral L-protein. As the region 3-77 of the L-protein is required for HBV infectivity in primary human hepatocytes [3,4], the corresponding peptide is expected to address a cellular receptor on hepatocytes to block the HBV entry.

Constituting a novel class of anti HBV drugs an efficient synthesis of this peptide is required. The solid phase synthesis of the *N*-terminal 77 amino acids of the viral L-protein was studied in detail [5]. Difficult sequence regions were identified by using a software based on the Chou and Fasman secondary structure prediction algorithm. Based on the identification of difficult synthetic sections, the aim was to optimize the synthesis through the use of pseudoproline dipeptides, additional coupling steps (double couple), and the use of elevated temperature during the solid phase synthesis.

Results and Discussion

The analysis of the aggregation potential revealed that the sequence is prone to be difficult from position 43 to 47 of the peptide sequence (Figure 1B). The changes of the Fmoc cleavage signal are in perfect agreement with the predicted structured properties and provide an indicator for significant aggregations of the growing peptide (Figure 2A). Mass spectrometric analysis of the crude peptide products showed a number of terminated peptide by-products all blocked with a N_{α}-acetyl group (Figure 2, grey chromatogram). These acetylated by-products arise in the regions identified to have a higher aggregation potential.

Different strategies were pursued to overcome the difficulties within the synthesis. It was tried to increase the coupling yield by double coupling of the corresponding amino acid and using HATU instead of HBTU. To avoid a truncation of the peptide chain at position 35, the pseudoproline dipeptide Fmoc-Asp(OtBu)-Thr(ΨMe,Mepro)-OH was inserted at position 40 of the peptide sequence. Analytical RP-HPLC and mass

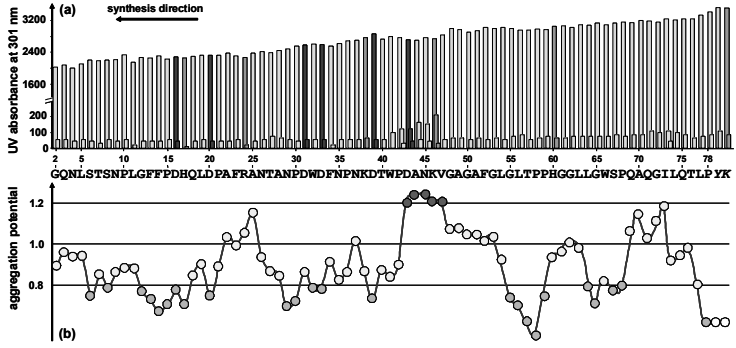

Fig. 1. (a) UV measurement of the peptide synthesizer (FMOC cleavage) and (b) prediction of the difficult sequences according to the aggregation potential (software Peptide Companion).

Table 1. Integration results of RP-HPLC chromatograms obtained after solid phase peptide synthesis of HBVpreS/2-78

Peptide sequence	*Area [%]*	
	Room temp.	*50 °C*
2-80	23.8	31.2
25-80^{Ac}	6.2	3.9
36-80^{Ac}	7.9	4.9
42-80^{Ac}	4.5	2.6
46-80^{Ac}	3.3	2.5

spectrometric analysis of the crude peptide after solid phase synthesis showed that none of these strategies could enhance the efficiency of the peptide synthesis – an almost identical pattern of side products was detected.

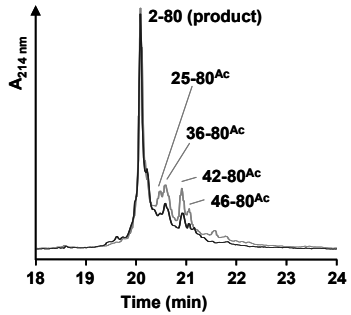

Fig. 2. RP-HPLC of the crude peptide after solid phase synthesis at room temperature (grey) and at elevated temperature (black).

By comparing the crude product obtained after heating (50 °C) with the synthesis at room temperature, it could be demonstrated that the formation of almost all side products was decreased (Table 1, Figure 2). After purification the HPLC chromatogram consists of a single product peak. The analysis of the synthesized peptide by LC-MS confirmed formation of the desired product. The resulting purity of Myr-HBVpreS/2-78 defined after RP-HPLC analysis was found to be ≥98%. The overall yield was 7.3%.

Although the classical stepwise chain assembly of large peptides is complicated, we showed that the solid phase peptide synthesis described provides a suitable access to the 77-mer lipopeptide Myr-HBVpreS/2-78. The preliminary identification and assessment of difficult regions within the peptide chain by a predictive method helped to consider individual solutions. Attempts were undertaken to optimize the synthesis by heating, double coupling or the use of pseudoproline dipeptides. The efficiency of the synthesis could be increased best by applying elevated temperature resulting in a higher purity of the crude product after solid phase synthesis.

Acknowledgments
This work was funded by the Bundesministerium für Bildung und Forschung (BMBF), Innovative Therapieverfahren, Grant Number 01GU0702.

References

1. Gripon, P., Cannie, I., Urban, S. *Journal of Virology* **79**, 1613-1622 (2005).
2. Petersen, J., Dandri, M., Mier, W., Lutgehetmann, M., Volz, T., von Weizsacker, F., Haberkorn, U., Fischer, L., Pollock, J.M., Erbes, B., Seitz, S., Urban, S., Braun, W., Wider, G., Lee, K.H., Wüthrich, K. *Nature Biotechnology* **26**, 335-341 (2008).
3. Gripon, P, Rumin, S., Urban, S., Le Seyec, J., Glaise, D., Cannie, I., Guyomard, C., Lucas, J., Trepo, C., Guguen-Guillouzo, C. *PNAS* **99**, 15655-15660 (2002).
4. Le Seyec, J., Chouteau, P., Cannie, I., Guguen-Guillouzo, C., Gripon, P. *Journal of Virology* **73**, 2052-2057 (1999).
5. Schieck, A., Müller, T., Schulze, A., Haberkorn, U., Urban, S., Mier, W. *Molecules* **15**, 4773-4783 (2010).

Proceedings of the 31st European Peptide Symposium
Michal Lebl, Morten Meldal, Knud J. Jensen, Thomas Hoeg-Jensen (Editors)
European Peptide Society, 2010

Automated Microwave-Assisted Peptide Synthesis with a Novel Robotic Synthesizer: Synthesis of Difficult Sequences

Søren L. Pedersen[1], Amit Mehrotra[2], and Knud J. Jensen[1]*
[1]University of Copenhagen, Faculty of Life Sciences, IGM, DK-1871, Frederiksberg C, Denmark, E-mail: kjj@life.ku.dk; [2]Biotage AB, SE-753 18, Uppsala, Sweden

Introduction

Solid-phase peptide synthesis (SPPS) is still often faced with challenges in the assembly of long and 'difficult' sequences, *e.g.* due to aggregation and steric hindrance giving rise to incomplete reactions. These problems have only partly been solved by new coupling reagents and solid supports. Precise microwave heating has emerged as one new parameter for SPPS, in addition to coupling reagents, resins, solvents, etc. [1-5].

Fig. 1. The Biotage Syro Wave™.

Recently the first X-Y robotic microwave-assisted peptide synthesizer was introduced to the peptide community. The synthesizer is built around a Biotage Initiator and a MultiSynTech Syro I, which means that the instrument has the capability to perform a single reaction in the microwave cavity or conventional room temperature (RT) peptide synthesis on the parallel reactor block (Figure 1) [4]. The reactor vessel is placed in the microwave cavity for the duration of the synthesis and mixing is achieved by vortexing.

Results and Discussion

The synthesis of peptides with successive *N*-methylated amino acids - especially if they also are β-branched - can be challenging and often needs strong coupling reagents such as PyBOP [6] or triphosgene [7,8] for high coupling yields. As a model peptide, sequence **1** was chosen [9]. Here the coupling of the last *N*-methylated alanine residue onto the peptidyl bound *N*-methylated Ile proved to be the major challenge.

H-MeAla-MeIle-MeGly-NH_2 (**1**)

Using coupling times of 60 min at RT we were only able to synthesize peptide **1** in very low purities, even when using coupling reagents such as HATU/HOAt and COMU. Prolonging the coupling time to 24 h using DIC/HOAt led to moderate peptide purity of 39% (Table 1) and as predicted the major deletion product was the H-MeIle-MeGly-NH_2 dipeptide. Elevating the temperature to 75°C using the Syro *Wave*™ for 20 min or 2×10 min, during the HATU or DIC activated coupling reactions gave the desired tri-peptide in high crude purity >75% (Table 1, Figure 2). Interestingly, DIC/HOAt and HATU/HOAt outperformed COMU which only led to moderate peptide purity.

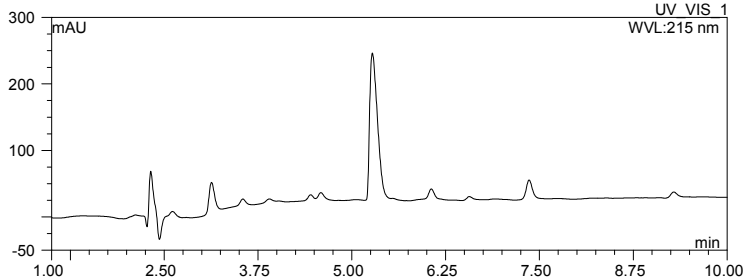

Fig. 2. HPLC chromatogram of crude H-MeAla-MeIle-MeGly-NH_2 at 5.3 min (Table 1, Entry 8).

*Table 1. Coupling conditions for the synthesis of peptide **1***

Entry	*Coupling Time, Temp.*[a]	*Coupling reagent*	*Equiv.*	*Purity (HPLC)*
1	60 min, RT	DIC/HOAt	3	<5%
2	60 min, RT	HATU/HOAt	3	<5%
3	60 min, RT	COMU	3	<5%
4	24 h, RT	DIC/HOAt	3	39%
5	20 min, 75°C	DIC/HOAt	3	76%
6	20 min, 75°C	HATU/HOAt	3	75%
7	20 min, 75°C	COMU	3	59%
8	2×10 min, 75°C	DIC/HOAt	3	83%

[a] *N^{α}-deprotection: 3 min piperidine-NMP (2:3), then 10 min with piperidine-NMP (1:4),*

ACP65-74 has in the past been known to be a difficult sequence, however the introduction of state-of-the-art resins and coupling reagents has solved previous problems associated with its synthesis. Replacing the two sequential Ala residues, which are positioned *N*-terminally to the Ile residue, with the sterically hindered α-methylated amino acid Aib, re-introduces substantial challenges in the synthesis. Thus peptide **2** was chosen as an additional model sequence.

H-Val-Gln-**Aib-Aib**-Ile-Asp-Tyr-Ile-Asn-Gly-NH_2 (**2**)

Several tests using the Syro *Wave*™ demonstrated that the optimal coupling condition for the difficult couplings (residues 66-68) was 3×10 min at 75°C and 2 min at 75°C for the residual couplings (residues 65+69-74). In comparison, coupling at RT (3×90 min for residues 66-68 and 45 min for the residual amino acids) gave the desired peptide in only 37% crude purity. All the couplings were performed using DIC/HOAt as coupling reagents.

We have shown that microwave irradiation can overcome the challenges of coupling amino acids onto sterically hindered resin bound peptides. Using the microwave methodology we can decrease coupling times and increase the crude purity significantly compared to RT. The Syro *Wave*™ has proven to be a very stable and efficient synthesizer, and has shown to be a very flexible instrument for SPPS due to its ability to perform either single microwave reactions or conventional parallel synthesis at RT.

Acknowledgments
We gratefully acknowledge Biotage for the peptide synthesis research collaboration with University of Copenhagen. We acknowledge Dr. Udo Treffer from MultiSynTech for his valuable support.

References

1. Brandt, M., Gammeltoft, S., Jensen, K.J. *Int. J. Pept. Res. Therap.* **12**, 349-357 (2006).
2. Palasek, S.A., Cox, Z.J., Collins, J.M. *J. Pept. Sci.* **13**, 143-148 (2007).
3. Bacsa, B., Horvati, K., Bosze, S., Andreae, F., Kappe, C.O. *J. Org. Chem.* **73**, 7532-7542 (2008).
4. Malik, L., Tofteng, A.P., Pedersen, S.L., Sørensen, K.K., Jensen, K.J. *J. Pept. Sci.* **16**, 506-512 (2010).
5. Pedersen, S.L., Sørensen, K.., Jensen, K.J. *Biopolymers - Pept. Sci*. **94**, 206-212 (2010).
6. Teixidó ¸M., Albericio, F., Giralt, E. *J. Pept. Res.* **65**, 153-166 (2005).
7. Angell, Y.M., Garcia-Echeverria, C., Rich, D.H. *Tetrahedron Lett.* **35**, 5981-5984 (1994).
8. Carpino, L.A., Elfaham, A., Albericio, F. *J. Org.Chem.* **60**, 3561-3564 (1995).
9. Rodríguez, H., Suarez, M., Albericio, F. *J. Pept. Sci.* **16**, 136-140 (2010).

Proceedings of the 31st European Peptide Symposium
Michal Lebl, Morten Meldal, Knud J. Jensen, Thomas Hoeg-Jensen (Editors)
European Peptide Society, 2010

The Oxime-Based Family of Coupling Reagents

Ramon Subirós-Funosas[1,2], Ayman El-Faham[1,3], and Fernando Albericio[1,2,4]

[1]Institute for Research in Biomedicine, Barcelona Science Park, Baldiri Reixac 10, Barcelona, 08028, Spain; [2]CIBER-BBN, Networking Centre on Bioengineering, Biomaterials and Nanomedicine, Barcelona Science Park, Baldiri Reixac 10, Barcelona, 08028, Spain; [3]Department of Chemistry, Faculty of Science, Alexandria University, Ibrahimia, 21321, Egypt; [4]Department of Organic Chemistry, University of Barcelona, Martí i Franquès 1-11, Barcelona, 08028, Spain

Introduction

HOBt and other parent benzotriazoles show explosive properties, a feature that is increasingly limiting their commercial availability. Consequently, alternative scaffolds are required for safe and efficient amide bond formation. A few decades ago, several stable and acidic ketoximes were proposed as additives, although with little success because of the lack of relevant data [1,2]. Recently, exhaustive studies on ethyl 2-cyano-2-(hydroxyimino) acetate (Oxyma, **1**), and the derived uronium salt, bearing a dimethylmorpholino carbocation skeleton (COMU, **2**), have proved that oximes are indeed a reliable choice as coupling reagents (Figure 1) [3,4]. Thus, here we further studied the potential of oxime-based compounds by testing new reactive phosphonium and uronium salts, along with novel Fmoc- and Alloc-oxime carbonates.

Results and Discussion

Two tris(pyrrolidino)phosphonium salts of Oxyma were easily obtained in 75-80% yield in a one-pot fashion by reaction of its potassium salt with a bromotris(pyrrolidino) phosphonium salt, obtaining either the hexafluorophosphate (PyOxP, **3**) or tetrafluoroborate (PyOxB, **4**) versions (Figure 2, left) [5]. The higher stability of PyOxP (commercially known as PyOxyme) than PyOxB confers the reagent greater suitability in the assembly of peptide fragments or cyclizations. PyOxyme also combined impressive solubility with high stability, compared with known benzotriazole-based PyAOP, PyBOP and PyClock. In addition, PyOxyme induced outstanding control of optical purity and shows high efficiency in the assembly of sterically demanding linear sequences. Last but not least, PyOxyme afforded the highest percentage of target peptide during cyclization studies, exceeding the performance of PyAOP (Table 1).

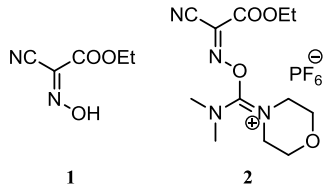

1 **2**

Fig. 1. Structure of Oxyma and COMU.

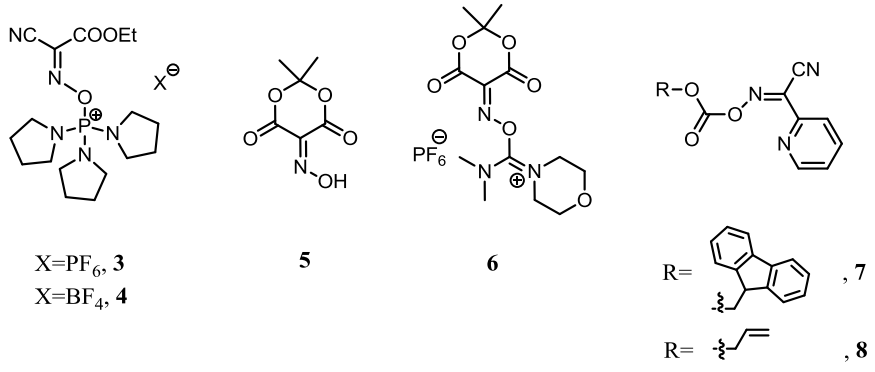

X=PF_6, **3**
X=BF_4, **4**

5 **6**

R= , **7**

R= , **8**

Fig. 2. Structure of oxime-based coupling and alkyloxycarbonyl-introducing reagents.

Table 1.Cyclization of H-Ala-Ala-MeAla-Ala-Ala-OH

Coupling Reagent	*Cyclic penta (%)*	*Linear penta (%)*	*Linear dimer (%)*
PyAOP	54	10	36
PyBOP	43	28	29
PyClock	61	15	24
PyOxyme	70	10	20
PyOxB	47	15	38

Other oxime scaffolds have been evaluated, like that derived from Meldrum's acid (HONM, **5**, Figure 2 center). This additive can be readily prepared in nearly 70% yield by nitrosation followed by acidification [6]. The corresponding uronium salts, bearing various carbocation skeletons, are obtained directly in 3 steps from dimethylcarbamoyl chloride and a secondary amine, in high yield and purities. Unfortunately, the high reactivity of HONM (**5**) causes the appearance of side reactions, thereby compromising its application as peptide additive. However, the parent uronium salts have proved to be useful reagents for the acylation of poor nucleophiles, such as anilines, probably as a result of the presence of a neighboring group effect. In agreement with previous studies, the dimethylmorpholino-derivative HMMU (**6**, Figure 2 center) performed better than the tetramethyl and dimethylpyrrolidino counterparts and thus represent a reliable alternative for peptide bond formation by ensuring low racemizations and high coupling extentions.

With the aim of improving traditional strategies for the introduction of Fmoc and Alloc urethane-type protecting groups, we have synthesized several oxime carbonates from the corresponding chloroformates in >80% yield and high purities [7]. These carbonates, formed by the inclusion of oximes with electron-withdrawing substituents, such as dicyano, diethylcarboxylate or cyano ethyl carboxylate (Oxyma), were tested in the *N*-α protection of H-Gly-OH, the most prone amino acid to dipeptide formation, conducted in the presence of sodium carbonate at pH=8 in a few hours. The *N*-Hydroxypicolinimidoyl cyanide derivatives (**7** and **8**, Figure 2 right) were found to efficiently protect the *N*-terminus (>99.5% purity) and simultaneously prevent the increase of side-products, such as dipeptides (0.01% for Fmoc-Gly-OH, 0.02% for Alloc-Gly-OH), as confirmed by coinjection with pure samples.

Acknowledgments

This work was partially supported by *Centro de Investigación Científica y Tecnológica* (CICYT) (CTQ2009-07758), the *Generalitat de Catalunya* (2009SGR 1024), Luxembourg Bio Technologies, Ltd. (Rehovot), the Institute for Research in Biomedicine and the Barcelona Science Park. RS-F thanks the *Ministerio de Educación y Ciencia* for a FPU PhD fellowship. Suzhou Highfine Biotech Co., Ltd. is thanked for a sample of the Fmoc-oxime.

References

1. Itoh, M. *Bull. Chem. Soc. Japan* **46**, 2219-2221 (1973).
2. Izdebski, J. *Pol. J. Chem.* **53**, 1049-1057 (1979).
3. Subirós-Funosas, R., Prohens, R., Barbas, R., El-Faham, A., Albericio, F. *Chem. Eur. J.* **15**, 9394-9403 (2009).
4. El-Faham, A., Subiros-Funosas, R., Prohens, R., Albericio, F. *Chem. Eur. J.* **15**, 9404-9416 (2009).
5. Subiros-Funosas, R., El-Faham, A., Albericio, F. *Org. Biomol. Chem.* **8**, 3665-3673 (2010).
6. El-Faham, A., Subiros-Funosas, R., Albericio, F. *Eur. J. Org. Chem.* 3641-3649 (2010).
7. Khattab, S.N., Subiros-Funosas, R., El-Faham, A., Albericio, F. *Eur. J. Org. Chem.* 3275-3280 (2010).

Proceedings of the 31st European Peptide Symposium
Michal Lebl, Morten Meldal, Knud J. Jensen, Thomas Hoeg-Jensen (Editors)
European Peptide Society, 2010

Engineering of Amyloid-β-Binding Affibody Molecules for Improved Chemical Synthesis and Higher Binding Affinity

Joel Lindgren[1], Lars Abrahmsén[2], Sebastian Wärmländer[3], and Amelie Eriksson Karlström[1]

[1]Royal Institute of Technology (KTH), School of Biotechnology, Division of Molecular Biotechnology, AlbaNova University Centre, SE – 106 91, Stockholm, Sweden; [2]Affibody AB, Lindhagensgatan 133, SE – 112 51, Stockholm, Sweden; [3]Department of Biochemistry and Biophysics, The Arrhenius Laboratories for Natural Sciences, Stockholm University, SE – 106 91, Stockholm, Sweden

Introduction

Affibody molecules, based on the engineered domain Z, are a class of affinity proteins with several advantageous properties, such as small size (58 aa) and rapid and reversible folding.

An Affibody molecule ($Z_{A\beta3}$) previously selected by phage display has been shown to bind Amyloid-β (Aβ) peptides with nanomolar affinity and to inhibit Aβ peptide aggregation [1,2]. The oligomerization and aggregation of Aβ peptides are generally considered to be one of the most important contributors to the onset and progression of Alzheimer's disease (AD). Proteins binding Aβ peptides with high affinity and selectivity are therefore important tools to better understand the aggregation process and could possibly be used for diagnosis and treatment of AD.

Structure analysis of the Aβ peptide binding Affibody molecule showed that $Z_{A\beta3}$ binds as a disulfide-linked homodimer, and that the original three-helix bundle structure of the Z domain is lost in the $Z_{A\beta3}$ Affibody molecule (Figure 1). Instead, the first α-helix of the parental protein is found unstructured in the free form of $Z_{A\beta3}$, and upon binding to the Aβ peptide, residues 15-19 adopt a β-strand conformation [3]. We here describe the design, synthesis and evaluation of six N-terminally truncated variants, together with a full-length version of the $Z_{A\beta3}$ Affibody molecule [4].

Results and Discussion

Six truncated variants of the $Z_{A\beta3}$ Affibody molecule (Figure 1), together with a full length variant, were successfully synthesized using standard Fmoc SPPS. All variants were found to be soluble during the purification, workup and analysis of the molecules. The synthetic yields of $Z_{A\beta3}$(18-58), $Z_{A\beta3}$(15-58) and $Z_{A\beta3}$(12-58) were 35%, 30% and 29%, respectively, while the yield of the full-length protein, $Z_{A\beta3}$(1-58), was only 8% using the same reaction conditions.

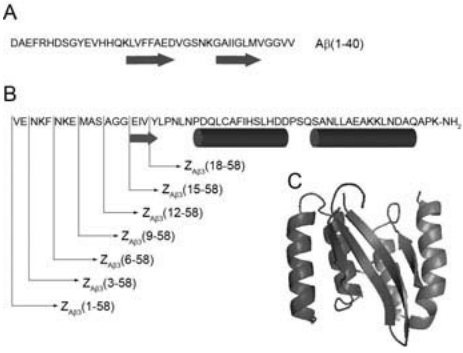

Fig. 1. The amino acid sequences of the Aβ(1-40) peptide (A) and the ZAβ3(1-58) Affibody molecule (B). The arrows indicate the sites of truncation giving rise to the seven different variants produced by SPPS. (C) show the previously solved solution structure of the Aβ/ ZAβ3 complex. [3] Block arrows indicate α-strands, while the cylinders indicate α-helical structure, as determined in the structure analysis of the complex done by Hoyer et al. [3] Figure adopted from [4].

The dissociation constant (K_D) of the full-length control Affibody molecule $Z_{A\beta3}$(1-58) was determined to to 9.5 nM. No binding to the Aβ(1-40) peptide could be detected for the shortest variant, $Z_{A\beta3}$(18-58). On the other hand, both $Z_{A\beta3}$(12-58) and $Z_{A\beta3}$(15-58) showed high binding affinities with K_D values of respectively 0.69 nM and 0.48 nM. The main contributor to the higher affinities of both $Z_{A\beta3}$(12-58) and $Z_{A\beta3}$(15-58) are faster on-rates for the truncated variants compared to the full-length molecule $Z_{A\beta3}$(1-58) (Table 1).

CD-melting profiles were used to investigate the effect on the stability of the Affibody dimers of addition of

Table 1. Thermodynamic and kinetic data for $Z_{A\beta3}$(1-58), $Z_{A\beta3}$(12-58), $Z_{A\beta3}$(15-58) and $Z_{A\beta3}$(18-58) binding to the Aβ(1-40) peptide, obtained from CD and SPR measurements. Table adopted from [4]

Affibody	*Tm free Affibody (°C)*[b]	*Tm Affibody in complex with Aβ-peptide (°C)*[b]	*ΔTm (°C)*	k_a $(M^{-1}s^{-1})$[a]	k_d (s^{-1})[a]	K_D (nM)[a]	χ^2
ZAβ3(1-58)	50.5	58.1	7.6	4.1×10^4	3.9×10^{-4}	9.5	0.8
ZAβ3(12-58)	46.2	62.6	16.4	4.5×10^5	3.1×10^{-4}	0.7	0.5
ZAβ3(15-58)	49.1	63.8	14.7	6.3×10^5	3.0×10^{-4}	0.5	1
ZAβ3(18-58)	37.9	40.7	2.8	n/a	n/a	n/a	n/a

[a]*Determined by SPR measurements*

[b]*Determined by CD spectroscopy melting profiles at 220 nm*

Aβ(1-40) peptide. An increased Tm indicates binding and stabilization of the complex. The T_m of $Z_{A\beta3}$(12-58) and $Z_{A\beta3}$(15-58) are both higher than of the full length variant in presence of Aβ(1-40), indicating a stronger binding to the Aβ(1-40) peptide (Table 1).

The four Affibody variants displayed different transformations of their secondary structure upon titration with Aβ(1-40). The titration of Aβ(1-40) to $Z_{A\beta3}$(18-58) showed no indication of change in the secondary structure of $Z_{A\beta3}$(18-58). For $Z_{A\beta3}$(1-58), the CD signal decreases rather uniformly upon addition of Aβ(1-40), indicating loss of helical structure. For $Z_{A\beta3}$(12-58), the CD signal indicates both a loss of helical content and increased β-strand structure in the Affibody/Aβ complex upon addition of Aβ(1-40). Finally, for $Z_{A\beta3}$(15-58), the CD signal only indicates an increased β-strand content in the system when Aβ(1-40) is added. The CD signal of the free Aβ(1-40) peptide was found to be negligible compared to the signal of the Affibody molecules. This reflects the unstructured nature of free Aβ(1-40), which is characterized by a weak CD signal. However, Aβ(1-40) displays a secondary structure when bound to an Affibody molecule dimer.

To conclude, removal of the first 11 and 14 amino acids of $Z_{A\beta3}$ yields truncated Affibody molecules $Z_{A\beta3}$(12-58) and $Z_{A\beta3}$(15-58), respectively, with higher binding affinity to the Aβ (1-40) peptide than the full-length $Z_{A\beta3}$(1-58), where the higher on-rate for the N-terminally truncated Affibody variants is the main reason for the higher affinity. This is probably related to the free full-length Affibody dimer having a partially helical N-terminus, which must unfold prior to binding the Aβ peptide. Correspondingly to $Z_{A\beta3}$, the truncated versions lock the Aβ peptide in a biologically relevant β-hairpin conformation. The shorter Affibody molecules can be produced in significantly higher yields than the full-length molecule by standard SPPS. This higher yield is an important advantage, since chemical production expands the possibilities of making different conjugates and heterodimeric molecules for further studies of the Affibody molecule/Aβ peptide complex.

Acknowledgments

This study was supported by grants from the Swedish Natural Science Research Council, the Knut & Alice Wallenberg Foundation, and the SAMBIO program from VINNOVA.

References

1. Gronwall, C., et al. *J. Biotechnol*. **128**, 162-83 (2007).
2. Luheshi, L.M., et al. *PLoS. Biol.* **8**, e1000334 (2010).
3. Hoyer, W., et al. *Proc Natl. Acad. Sci. U.S.A.* **105**, 5099-104 (2008).
4. Lindgren, J., et al. *Protein Sci.* In press.

Proceedings of the 31st European Peptide Symposium
Michal Lebl, Morten Meldal, Knud J. Jensen, Thomas Hoeg-Jensen (Editors)
European Peptide Society, 2010

Chemical Synthesis of Fluorescent-Labeled Affibody Molecules for Use in Cancer Diagnostics

Anna Perols and Amelie Eriksson Karlström
Royal Institute of Technology (KTH), School of Biotechnology, Division of Molecular Biotechnology, 106 91, Stockholm, Sweden

Introduction

Affibody molecules are a class of affinity proteins, which is based on the non-immunoglobulin Z domain, derived from staphylococcal protein A. The Z domain is a three-helix bundle protein, where 13 residues in helices 1 and 2 have been randomized to generate a combinatorial Affibody molecule library, from which binders to a variety of different target proteins have been selected by phage display (Figure 1). The proteins are only 58 amino acid residues, making it suitable for production by solid phase peptide synthesis. Since the proteins lack cysteine residues, a unique thiol can be introduced for site-specific labeling.

Results and Discussion

In the present study, two Affibody molecules targeting known cancer biomarkers, EGFR [1] and HER2 [2], have been synthesized. Both targets belong to the epidermal growth factor receptor (ErbB) family, which is involved in signal pathways regulating processes such as cell proliferation and differentiation. High expression of HER2 has been associated with different types of cancer, such as breast, ovary and bladder cancer. Similar findings have been reported for EGFR, which is up-regulated in many different human cancers. EGFR and HER2 are both membrane bound receptors which are activated through dimerization, which could either occur with the same receptor or with another member from the ErbB family.

The Affibody molecules were synthesized in high yield on solid phase by Fmoc/tBu chemistry with a C-terminal Cys-Gly dipeptide extension to enable site-specific labeling with fluorophores in solution by maleimide chemistry. Variants were purified by RP-HPLC prior to conjugation and synthesis yield was determined. The Affibody molecules were then conjugated to three fluorophores, which have high fluorescence quantum yield and high photo-stability; ATTO 488, ATTO 594 and ATTO 647N (ATTO-TEC Gmbh, Siegen) using maleimide conjugation strategy. Labeled variants were further purified by RP-HPLC and the correct products were verified using ESI-Q-TOF. A summary of synthesis yield and labeling efficiency as well as determined molecular weights could be seen in Table 1.

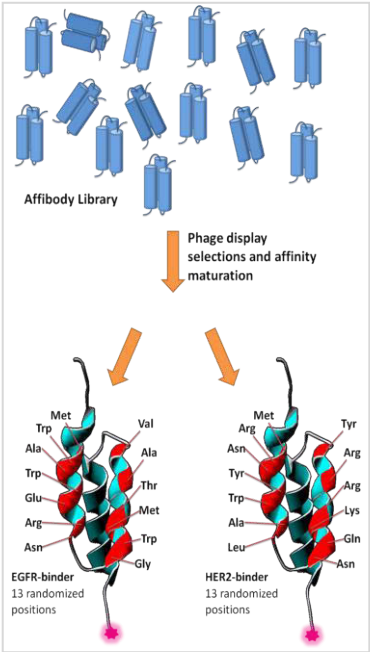

Fig. 1. The Affibody molecule comprised of three helices where 13 amino acid substitutions in helices 1 and 2 have generated a specific binding surface. Labeling is performed with maleimide chemistry on the cysteine in the C-terminal tail region that has been incorporated for the purpose.

Table 1. A summary of synthesis yield and labeling efficiency

Affibody Variant	*Synthetic yield*	*ATTO-tec Dye*	*Labeling Yield*	*Theoretical Mw (Da)*	*Experimental Mw(Da)*
Z_{HER2}	10.6%	488	70%	7491.7	7492.6
		594	100%*	7707.7	7708.9
		647N	100%*	7547.7	7548.8
Z_{EGFR}	21.6%	488	72%	7331.4	7331.0
		594	100%*	7546.4	7547.8
		647N	100%*	7387.4	7387.5

**No unlabeled product was detected*

The fluorescent-labeled Affibody molecules are currently used in fluorescence microscopy to study the relative expression and spatial distribution of the EGFR and HER2 proteins in human breast cancer cell lines with the aim of identifying differences that can be of diagnostic or prognostic value in the analysis of patient samples. These labeled binders will also be used for ultrahigh resolution microscopy (STED = Stimulated emission depletion).

Conclusions

To conclude, a protocol for chemical synthesis of Affibody molecules binding EGFR or HER2 has successfully been established. In addition, a protocol for in solution labeling has been optimized for ATTO-TEC fluorophores enabling high yield conjugation.

Affibody molecules have many advantages compared to antibodies in molecular imaging:

- Site specific labeling – Affibody molecules provide well defined, homogeneous affinity reagents
- High stability – The excellent refolding properties of Affibody molecules enables for high resolution purification using RP-HPLC
- Small size – Great value in high resolution optical methods where the reagent size is becoming the limiting factor

Acknowledgments

The research leading to these results has received funding from the European Community's Seventh Framework Programme FP7/2007-2011 under grant agreement no. 201837.

References

1. Friedman, M., et al. *J. Mol. Biol.* **376**, 1388-402 (2008).
2. Orlova, A., et al. *Cancer Res.* **66**, 4339-4348 (2006).

Proceedings of the 31st European Peptide Symposium
Michal Lebl, Morten Meldal, Knud J. Jensen, Thomas Hoeg-Jensen (Editors)
European Peptide Society, 2010

Oxyfold: A New Solid Supported Reagent for the Simple and Effective Formation of Disulfide Bond in Peptides

L. Ronga[1], P. Verdié[2], M. Cristau[2], M. Amblard[2], S. Cantel[2], C. Enjalbal[2], K. Puget[1], G. Subra[2], and J. Martinez[2]

[1]Genepep, St Clément de Rivière, 34980, France, [2]Institut des Biomolécules Max Mousseron (IBMM), Montpellier, 34093, France

Introduction

The importance of disulfide bridges in peptide conformation and activity make their formation a fundamental step of peptide synthesis. Formation of disulfide bond is probably one of the most challenging steps to achieve regarding the formation of unwanted by-products and oligomerization. In order to minimize the latter phenomenon, disulfide bridge cyclizations are performed under high diluted conditions which require time consuming removal of solvent at the end of the reaction. Dimethyl sulfoxide (DMSO) is one of the oxidizing reactants most commonly used [1]. One of its major drawbacks is its elimination from the reaction medium, which requires evaporation under strong vacuum or repeated lyophilizations. Furthermore, the dimethyl sulfide generated during the reaction is volatile and toxic. On the other hand, supported reactants are particularly advantageous for promoting intramolecular reactions. In fact, they are known to cause a phenomenon of "pseudodilution" which makes it possible to minimize oligomerization and to use much smaller amounts of solvents [2]. Here we present the synthesis and the use of novel solid supported oxidation reactants for disulfide bond formation. This family of supported reagents consists in a series of oxidized methionines grafted onto a solid support. We demonstrate the efficiency and easiness of these supported reagents for the formation of disulfide bridges in peptides.

Results and Discussion

Three different solid supported methionine sulfoxides were synthesized by anchoring a Fmoc-protected Met on different matrices: Amino PEGA, Amino PEG-PS and aminomethyl polystyrene. After Fmoc deprotection and acetylation, methionine oxidation was performed by treatment of the resin with H_2O_2. The ability of these supported methionine sulfoxides to promote disulfide bond formation of crustacean cardioactive peptide CCAP (PFCNAFTGC-NH_2) [3] was explored at pH=6.1 (ammonium acetate buffer) and pH=7.5 (phosphate buffer). Under the same conditions, the CCAP oxidation promoted by Ellman's reagent prepared on amino PEGA resin and 10% DMSO solution was investigated. Our results (Figure 1) show that Oxyfold is more effective than DMSO and supported Ellman's reagent. Among the compared resins, amino PEGA resin gives the best results of CCAP oxidation. Moreover, pH=7.5 seems the ideal pH for Oxyfold-promoted oxidation.

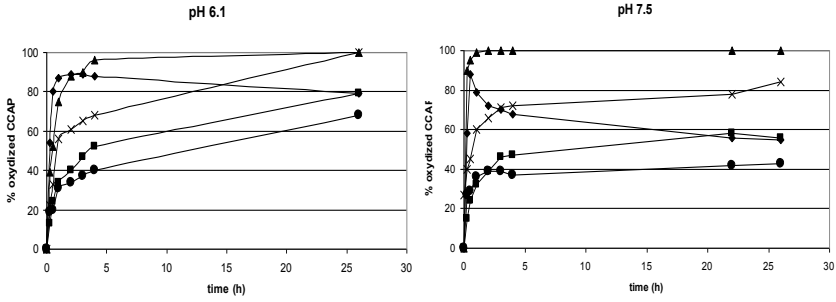

Fig. 1. CCAP oxidation: ■ 10% DMSO,▲ Ac-Met[O]-PEGA,● Ac-Met[O]-PS, ♦ Ellman's reagent-PEGA,× Ac-Met[O]-PEG-PS.

In order to minimize the volume of resin to be used for disulfide bond formation, we decided to increase the number of methionine oxide motifs on the resin. To this aim, as alternative to the stepwise synthesis of Oxyfold, we explored another strategy of synthesis based on the on-support oligomerization of methionine N-carboxy anhydride (NCA) followed by oxidation (Figure 2). This method allows the preparation of resins with a number of Met[O] between 3 and 18 and it opens the way of large scale economic preparation of supported reactant to promote disulfide bond in peptides.

Further oxidation experiments have demonstrated that using the same number of eq of Met[O] we obtain comparable result with different poly Met oxide chain length (n=1,3,5 and 7). Moreover, we have proved that Oxyfold prepared by Met NCA is as effective as Oxyfold with the same number of Met (n=7) prepared by stepwise solid phase synthesis. Overall, all the described characteristics make the use of Oxyfold a fast, cheap, effective, facile and green procedure for disulfide bridge formation.

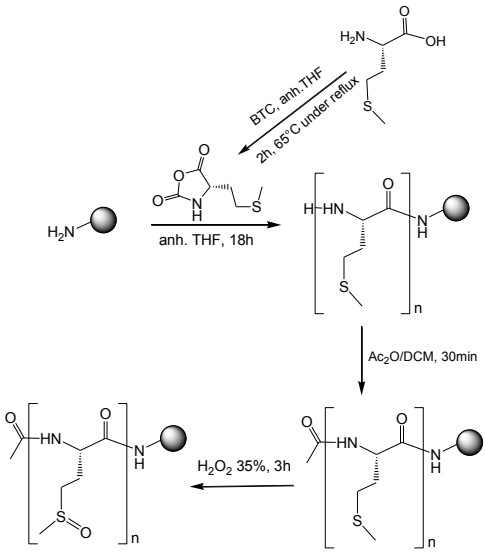

Fig. 2. Oxyfold synthesis: oligomerization of Met NCA on solid support.

Acknowledgments
The authors acknowledge financial support from "La Région Languedoc Roussillon" and "FEDER".

References

1. Tam, J.P., Wu, C.-R., Liu,W., Zhang, J.-W. *J. Am. Chem. Soc.* **113**, 6657-6662 (1991).
2. Shi, R., Wang, F., Yan, B. *Int. J. Pept. Res. Ther.* **13**, 213-219 (2006).
3. Nicholls, R., Kaminski, S., Walling, E., Zornik, E. *Peptides* **20**, 1153-1158 (1999).

Proceedings of the 31st European Peptide Symposium
Michal Lebl, Morten Meldal, Knud J. Jensen, Thomas Hoeg-Jensen (Editors)
European Peptide Society, 2010

An Efficient MW-Assisted Synthesis of Dicarba-Analogues

G. Cane, A. Di Cianni, M. Lumini, AM. Papini, and M. Ginanneschi
Laboratory of Peptide & Protein Chemistry & Biology, University of Florence, Polo Scientifico e Tecnologico, Sesto Fiorentino (Fi), I-50019, Italy, and Department of Chemistry "Ugo Schiff", Via della Lastruccia 3/13, University of Florence, Polo Scientifico e Tecnologico, Sesto Fiorentino (Fi), I-50019, Italy

Introduction

A frequent structural motif found in natural peptides and proteins is constituted of the cystine (S-S) group which forms intra- and intermolecular bridges of fundamental importance for biomolecules structure and hence their biological activity [1]. Octreotide **1** is a cyclic octapeptide somatostatin agonist, showing higher affinity and specificity toward the somatostatin receptor subtype sst2 and a better resistance to enzymatic degradation compared to the native somatostatin. It is the first analogue mainly a carrier for radionuclides used in clinical protocols for cancer diagnostics and therapy [2]. It is well-known that the disulfide bridge is prone to be attacked by endogenous reducing enzymes or by nucleophilic and basic agents [3]. Therefore, we replaced the cystine bond by the dicarba isostere **2** to increase its metabolic stability. The substitution of the disulfide group in peptides and proteins by the isosteric, stable, dicarba-bond was easier accessible after the discovery of the Ru-catalysed mediated Ring-Closing Metathesis (RCM) reaction proposed by Grubbs [4,5]. The difficulty in this synthetic strategy applied to peptides let us to investigate the use of microwave (MW) technology. In fact, more and more interesting results are reporting the use of MW irradiation in organic and also in solid-phase peptide synthesis. In that case, it is noteworthy that MWs could be useful in reducing peptide aggregation, leading to proper peptide construction and higher crude purity [8,9].

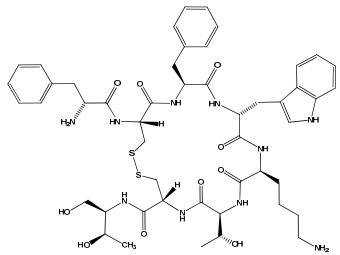

1

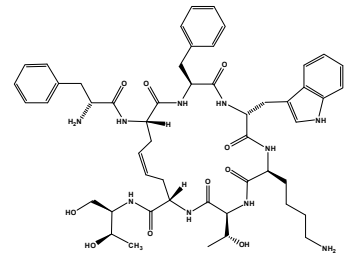

2

Results and Discussion

The key reaction to achieve the target compounds is the ring-closing metathesis (RCM) catalyzed by ruthenium complexes on the linear peptide containing suitably placed, non-proteinogenic L-allylglycine (Hag) residues. The RCM was applied directly on linear hexa- and octapeptides linked to chlorotrityl resin (3) and Rink amide resin (8) respectively, using both microwaves and normal heating. The reaction was firstly performed in an oil bath at 50 °C with second generation Grubb's catalyst under controlled experimental conditions, i.e. anhydrous argon atmosphere and long reaction times [6,7]. Subsequently we employed a microwave-assisted strategy (MW) that emerged in increasing yield in 6-membered-ring formation of Somatostatin dicarba-analogues (**4-6**), as well as in shortening reaction times (Scheme 1) [8,9]. This prompted us to evaluate

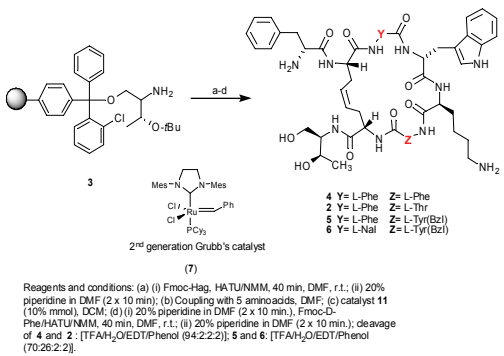

Scheme 1. Synthesis of 6-membered ring Somatostatin dicarba-analogues.

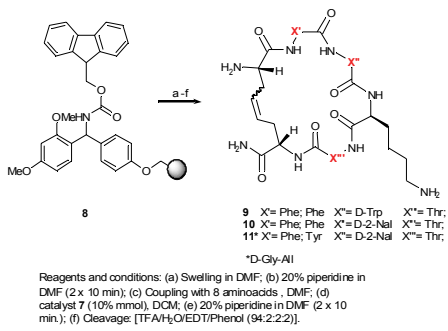

Scheme 2. Synthesis of 8-membered ring Somatostatin dicarba-analogues.

the efficacy of the MW technique for obtaining cyclooctapeptides dicarba-analogues (**9-11**) (Scheme 2) impossible to be obtained with normal heating methods (data not shown).

We applied different MW methods in order to clarify which parameters (MW power, time, and temperature) could influence RCM reaction. Differences among the available methods are due to the possibility of setting temperature and power as a function one of each other, while pressure had a fixed upper limit threshold. Its value was correlated to temperature and power. We succeded to complete the RCM cyclization step for almost all the linear peptides in 1 h (instead of 24-48 h required with conventional heating) applying 300 W, 100 °C and 70-90 psi pressure (main parameter for obtianing the cyclization reaction). Reaction time extended to 2 h increased yield in RCM. There is evidence that different amino acids configuration (L/D) in the sequence can favour or disfavour the RCM, even under MW irradiation.

Table 1. Comparison in cyclic/linear yield and reaction time (h) between conventional heating (50 °C) and microwave assisted irradiation (100 °C, 300 W, 70-90 psi) for the synthesis of Somatostatin dicarba-analogues

Dicarba analogue	*Heating method*	*Time (hours)*	*Yield (HPLC cyclic/linear ratio)*
4	Oil bath	48	90:10
4	MW	1	86:14
2	Oil bath	48	50:50
2	MW	1	84:16
5	Oil bath	24	90:10
5	MW	1	75:25
6	Oil bath	24	90:10
9	Oil bath	48	5:95
9	MW	1	75:25
10	Oil bath	48	5:95
10	MW	1	70:30
11	Oil bath	48	5:95
11	MW	2	98:2

Acknowledgments
Supported by Ente Cassa di Risparmio di Firenze and Advanced Accelerator Applications S. p. a..

References

1. Maemoto, A., et al. *J. Biol. Chem.* **279**, 44188-44196 (2004).
2. Weckbecker, G., Lewis I., Albert, R., et al. *Nat. Rev. Drug Discovery* **2**, 999-1018 (2003).
3. Williams, R.M., Liu, J. *J. Org. Chem.* **63**, 2130-2132 (1998).
4. Miller, S.J., et al. *J. Am. Chem. Soc*. **118**, 9606-9614 (1996).
5. Grubbs, R.H. *Tetrahedron* **60**, 7117-7140 (2004).
6. Carotenuto, A., et al. *Lett. Org. Chem*. **2**, 274-279 (2005).
7. D'Addona, D., et al. *J. Med. Chem.* **51**, 512-520 (2008).
8. Rizzolo, F., et al. *Int. J. Pept. Res. Ther.* **13**, 203-208 (2007).
9. Kappe, C.O. *Angew. Chem. Int. Ed. Engl*. **43**, 6250-6284 (2004).

Proceedings of the 31st European Peptide Symposium
Michal Lebl, Morten Meldal, Knud J. Jensen, Thomas Hoeg-Jensen (Editors)
European Peptide Society, 2010

Microwave-Assisted Solid Phase Synthesis of [Asn^{641}(Glc)]FAN(635-655): A New Case Study for Optimisation of Glycopeptide Synthesis

Fabio Rizzolo[1,2], Francesca Nuti[1,2], Shashank Pandey[1,2], Mario Chelli[1,2], Paolo Rovero[1,3], and Anna Maria Papini[1,2]

[1]Laboratory of Peptide & Protein Chemistry & Biology, University of Florence, Polo Scientifico e Tecnologico, Sesto Fiorentino (Fi), I-50019, Italy; [2]Department of Chemistry ''Ugo Schiff'' and CNR-ICCOM, Via della Lastruccia 3/13, University of Florence, Polo Scientifico e Tecnologico, Sesto Fiorentino (Fi), I-50019, Italy; [3]Department of Pharmaceutical Sciences, Via Ugo Schiff 6, University of Florence, Polo Scientifico e Tecnologico, Sesto Fiorentino (Fi), I-50019, Italy

Introduction

Factor associated with neutral sphingomyelinase activation (FAN) represents a member of the WD-repeat family of proteins that includes mainly regulatory proteins [1]. A preliminary bioinformatic study revealed high sequence homology of the fragment 635-655 of this protein with CSF114(Glc), the synthetic glycopeptide developed to detect antibodies in Multiple Sclerosis (MS) patients' sera [2]. As FAN(635-655) is characterized by the minimum consensus pattern for *N*-glycosylation of asparagine residues (Asn-Xaa-Ser/Thr, where Xaa is any amino acid except Pro), we investigated a possible involvement of this peptide as linear natural epitope of antibodies in MS.

The bottleneck of this study was to obtain by Solid-Phase Peptide Synthesis (SPPS) [Asn^{641}(Glc)]FAN(635-655) in high purity and good yield to be tested in immuneenzymatic assays on sera. In fact conventional SPPS protocol failed during the coupling of the sterically hindered building block Asn^{641}(GlcOAc$_4$) and of other bulky amino acid residues. Finally we succeeded in the synthesis of this glycopeptide using microwave irradiations [3].

Results and Discussion

The main difficulty associated with high-throughput glycopeptide synthesis resides in the extremely low coupling efficiency of sterically hindered, sugar-bound amino acid derivatives.

Solid-Phase Glycopeptides Synthesis (SPGS) could be improved by employing a large excess of Fmoc-Asn(GlcOAc$_4$)-OH, but considering the non trivial protocol to achieve this product, it is important to optimize glycopeptides synthetic strategy in order to obtain them in high yield and purity.

[Asn^{641}(Glc)]FAN(635-655) sequence is the following: H-Gly-Ile-Thr-Val-Ser-Arg-Asn(Glc)-Gly-Ser-Ser-Val-Phe-Thr-Thr-Ser-Gln-Asp-Ser-Thr-Leu-Lys-OH.

The glycopeptide synthesis was performed on Liberty™ Microwave Peptide Synthesizer (CEM), a monomode microwave system, starting from a Fmoc-Lys(Boc)-Wang resin (0.67 mmol/g, 0.150 g) using the following protocols: N$^{\alpha}$-Fmoc deprotection with a 20% piperidine solution in DMF; coupling reactions using a 0.2 M solution of amino acid in DMF (5 eq), 0.5 M solution of TBTU in DMF (5 eq) and a 2 M solution of DIEA in NMP (10 eq); building block coupling reaction with a 0.25M solution of HOBt/DIPCDI in DMF (3 eq) and 0.1 M solution of Fmoc-Asn(GlcOAc$_4$)-OH in NMP (3 eq).

MW-SPPS cycle consists in two deprotection steps performed at 75 °C using 35 W for 30 sec and 60 W for 180 sec respectively. Coupling steps were performed at 75 °C, using 30 W for 300 sec, while Fmoc-Asn(GlcOAc$_4$)OH coupling was performed at 55°C, 15 W for 900 sec**.** The synthesis ongoing was monitored by microwave-assisted micro-cleavages using TFA/water/TIS solution (95:2.5:2.5 v/v/v). Final cleavage of the peptide from the resin and side-chain deprotections were performed with *ad hoc* cleavage cocktail TFA/water/TIS solution (95:2.5:2.5 v/v/v), in 3 hours at room temperature.

The application of microwaves to SPGS allowed us to synthesize glycopeptides containing sterically hindered building blocks, which are not easily accessible by conventional synthetic methods. In order to facilitate the coupling reactions and deprotections, we successfully used microwave irradiation to synthesize [Asn^{641}(Glc)]FAN(635-655). Microwaves were also applied to perform micro-cleavages of peptide fragments to monitor the elongation of the chain, and in particular, during the Fmoc-Asn(GlcOAc$_4$)-OH coupling.

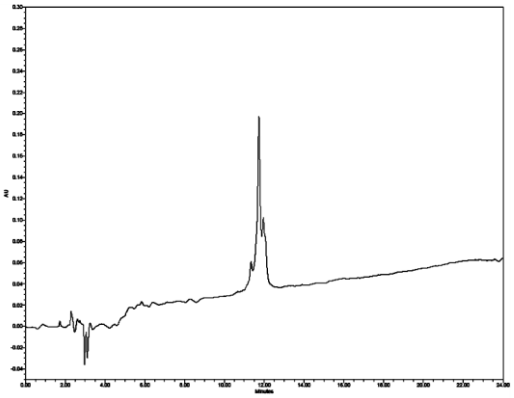

Fig. 1. HPLC of crude [Asn^{641}(Glc)]FAN(635-655) synthesized by MW-assisted strategy. HPLC method: 10-60% MeCN in water (+0.1% TFA) over 20 min.

The HPLC of final crude [Asn^{641}(Glc)]FAN(635-655) synthesized using microwaves showed a 60% purity (Figure 1).

Our work reports that once again the use of microwaves is efficient for SPGS as a rapid method to synthesize glycopeptides [4]. In particular, the microwave-assisted strategy allowed us to obtain [Asn^{641}(Glc)]FAN(635-655) in good purity, optimising coupling and deprotection times. We couldn't obtain the same glycopeptides by a conventional room temperature protocol. Moreover by microwave-assisted micro-cleavages we monitored in a fast and reliable way the progress of the synthesis. In conclusion, we consider the application of microwave energy a very interesting and useful strategy to improve the SPGS of non trivial peptide sequences containing hindered glycosylated building blocks.

Acknowledgments
Ente Cassa Risparmio di Firenze and ANR Chaire d'Excellence 2009-2013 PepKit (France) are gratefully acknowledged.

References

1. Adam-Klages, S., Adam, D., Wiegmann, K., Struve, S., Kolanus. W. *Cell* **86**, 937-947 (1996).
2. Lolli, F., et al. *Proc. Natl. Acad. Sci. U.S.A.* **102**, 10273-10278 (2005).
3. Matsushita, T., Hinou, H., Kurogochi, M., Shimizu, H., Nishimura, S-I. *Org. Lett*. **7**, 877-880 (2005).
4. Rizzolo, F., Sabatino, G., Chelli, M., Rovero, P., Papini, A.M. *Int. J. Pept. Res. Ther*. **13**, 203-208 (2007).

Proceedings of the 31st European Peptide Symposium
Michal Lebl, Morten Meldal, Knud J. Jensen, Thomas Hoeg-Jensen (Editors)
European Peptide Society, 2010

Conventional and Microwave-Assisted SPPS Approach: A Comparative Study of PTHrP(1-34)NH_2 Synthesis

Fabio Rizzolo[1,2], Chiara Testa[1,2,3], Michael Chorev[4,5], Mario Chelli[1,2], Paolo Rovero[1,6], and Anna Maria Papini[1,2,3]

[1]Laboratory of Peptide & Protein Chemistry & Biology, University of Florence, Polo Scientifico e Tecnologico, Sesto Fiorentino (Fi) I-50019, Italy; [2]Department of Chemistry "Ugo Schiff", Via della Lastruccia 3/13, University of Florence, Polo Scientifico e Tecnologico, Sesto Fiorentino (Fi) I-50019, Italy; [3]Laboratoire SOSCO – EA4505 Université de Cergy-Pontoise, 5 mail Gay-Lussac, Neuville-sur-Oise, Cergy-Pontoise 95031, France; [4]Laboratory for Translational Research, Harvard Medical School, Cambridge, MA, 02139, U.S.A; [5]Department of Medicine, Brigham and Women's Hospital, Boston, MA, 02115, U.S.A.; [6]Department of Pharmaceutical Science, Via Ugo Schiff 6, University of Florence, Polo Scientifico e Tecnologico, Sesto Fiorentino (Fi), I-50019, Italy

Introduction

Parathyroid hormone-related peptide (PTHrP) is an autocrine/paracrine regulator of endochondral bone development and involved in excessive osteoclastic bone resorption associated with humoral hypercalcaemia of malignancy (HHM) [1]. PTHrP is a 139 to 173-amino acid protein having the first thirteen N-terminal amino acids in common with parathyroid hormone (PTH). Like PTH, PTHrP releases calcium from bone and increases secretion of calcium and phosphate in the distal tubule [2].

Similar to PTH the calcium metabolism-related activities are located in the first 34 N-terminal residues. Consequently, our synthetic efforts focused on this bioactive sequence that was the subject of numerous structure-activity-conformation relationship studies [3].

Considering the presence of clusters of arginines, sterically hindered and hydrophobic amino acid residues in the 19-28 sequence of PTHrP and the considerable length of the peptide, the synthesis of PTHrP(1-34)NH_2 is quite challenging. We therefore undertook the synthesis comparing the conventional (room temperature) Solid-Phase Peptide Synthesis (SPPS) vs. the MicroWave-assisted SPPS [4].

Results and Discussion

PTHrP(1-34)NH_2 sequence is: H-Ala[1]-Val-Ser-Glu-His-Gln-Leu-Leu-His-Asp[10]-Lys-Gly-Lys-Ser-Ile-Gln-Asp-Leu-Arg-Arg[20]-Arg-Phe-Phe-Leu-His-His-Leu-Ile-Ala-Glu[30]-Ile-His-Thr-Ala-NH_2. The peptide was synthesized by SPPS, following Fmoc/tBu strategy, at room temperature and by microwave irradiation, using in both cases Liberty peptide synthesizer (CEM) and the same reagents concentration. The synthesis was monitored by LC-MS using MW-assisted mini-cleavages of the intermediate fragments using Discover single mode microwave system (CEM).

The SPPS was performed using the NovaSyn TGR (500 mg, 0.2 mmol/g), 0.2 M solution of amino acids in DMF (5 equiv.), 0.5 M solution of TBTU in DMF (5 equiv.), 2 M solution of DIPEA in NMP (10 equiv.). Final cleavage of the peptide from the resin and side-chain deprotections were performed with *ad hoc* cleavage cocktail TFA/water/TIS solution (95:2.5:2.5 v/v/v) for 3 hours at room temperature.

The room temperature-SPPS cycle (Liberty, CEM) consisted of two deprotection steps (5 and 10 min respectively) and 20 min for the coupling steps. The MW-SPPS cycle (Liberty, CEM), the deprotection steps were performed at 75 °C using 35 W for 30 sec for the first one and 60 W for 180 sec for the second one, while the coupling steps were performed at 75 °C, using 30 W for 300 sec.

MW-assisted mini-cleavage cycles (Discover, CEM) were carried out at 45 °C, using 15 W for 15 min with external cooling of the reaction vessel.

In this comparative study of PTHrP(1-34)NH_2 SPPS, using the same instrumentation and the same reagents concentration, MW-assisted strategy gave an increased purity of the crude peptide as compared with the conventional approach. RP-HPLC purification of the crude peptide was evaluated by LC-MS (ACQUITY UPLC™ System coupled with Micromass® Quattro micro API Mass Spectrometer, Waters) yielded 27 mg and 18 mg of >95% pure PTHrP(1-34)NH_2 from the MW-assisted synthesis and SPPS at room temperature, respectively (Table 1).

Table 1. Room temperature- vs MW-assisted synthetic approach

SPPS strategy	*Purity of crude peptide (%)*	*% Yield of pure >95% peptide (mg)*
Room temperature	35	4.4 (18 mg)
MW-assisted	77	6.3 (27 mg)

In conclusion, microwave technology has improved SPPS of particularly difficult sequences as compared with the conventional room temperature method. This improvement is attributed to prevention of peptide backbone aggregation and acceleration of deprotection and coupling steps.

In general, MW-assisted SPPS is proposed as a reliable strategy to overcome some limitations encountered in conventional SPPS. In our case, although the application of microwaves in SPPS led only to moderate improvement in final yield it allowed us to obtain a crude PTHrP(1-34)NH_2 of higher quality and enabled the development of a fast micro-cleavages as an alternative method for monitoring SPPS.

Therefore, based on our experience, the advantages of MW-assisted SPPS vs RT-SPPS can be summarized as follow: 1) shortening reaction time, 2) shortening micro-cleavage time, 3) crude peptides of higher quality facilitating the subsequent purification steps.

Acknowledgments
Ente Cassa Risparmio di Firenze and ANR Chaire d'Excellence 2009-2013 PepKit (France) are gratefully acknowledged.

References

1. Stewart, A.F. *N. Engl. J. Med.* **352**, 373-379 (2005).
2. Wysolmerski, J.J., Stewart, A.F. *Annu. Rev. Physiol.* **60**, 431-460 (1998).
3. Horiuchi, N., et al. *Science* **238**, 1566-1568 (1987).
4. Sabatino, G., Papini, A.M. *Curr. Opin. Drug Discov. Devel.* **11**, 762-770 (2008).

Proceedings of the 31st European Peptide Symposium
Michal Lebl, Morten Meldal, Knud J. Jensen, Thomas Hoeg-Jensen (Editors)
European Peptide Society, 2010

Microwave-Assisted Total Synthesis of Macrocyclic Cystine Knot Miniproteins

S. Park, S. Gunasekera, T. Aboye Teshome, and U. Göransson
Div. of Pharmacognosy, Dept. of Medicinal Chemistry, Uppsala University, BMC Box 574, SE-751 23, Uppsala, Sweden

Introduction

Cyclotides are mini-proteins of approximately 30 amino acids residues that have a unique structure consisting of a head-to-tail cyclic backbone with a knotted arrangement of three disulfide bonds [1] (Figure 1). This unique structure provides exceptional stability to chemical, enzymatic and thermal treatments [2] and has been implicated as an ideal drug scaffold for the development into agricultural and biotechnological agents [3]. We developed the first method for microwave assisted Fmoc-SPPS of cyclotides [4]. We overcame the difficulties that previous studies [5-7] encountered for synthesis of cyclic peptides which involves numerous and time consuming reaction steps.

Results and Discussion

The protocol adopts a strategy that combines the optimized microwave assisted chemical reactions for Fmoc-SPPS of peptide backbone synthesis, thioesterification of the C-terminal carboxylic acid of the peptide and a one pot reaction that promotes cyclisation through native chemical ligation and oxidative folding (Figure 1). The application of this protocol was exemplified for the synthesis of three prototypic cyclotides; kalata B1, MCoTI-II and cycloviolacin O2.

By utilization of current protocol, the results are as follows. For peptide chain elongation, microwave assisted coupling reaction showed the yield higher than 99.3%. With microwave application, the cleavage time was effectively shortened from 3 hours at room temperature into 45 minutes. Thioester was efficiently introduced at C-terminal protected peptide; LC-MS analysis confirmed full conversion into thioester with PyBOP/*p*-acetamidothiophenol/DIPEA (5/5/10 equiv) in DMF under microwave radiation.

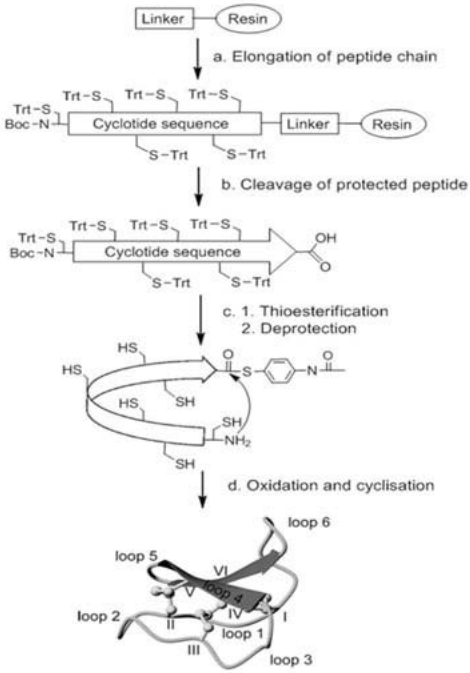

Fig. 1. Synthetic strategy for synthesis of cyclotides. (a) Assembly of the protected peptide backbone by MW assisted Fmoc SPPS (coupling reaction for non-Cys: 5 min, 35W, 75°C for Cys: 7min, 30W, 55°C); (b) AcOH/TFE/DCM (1/1/8) under microwave radiation (45 min, 10W, 40°C); (c) (1) PyBOP/p-acetamido-thiophenol /DIPEA (5/5/10 equiv) in DMF under microwave radiation (5 min, 35W, 75°C), (2) TFA/TIPS/ water (95/2.5/2.5), rt, 2 hr; (d) 1:1 (v/v) mixture of 0.25 M Tris buffer (pH 8.0) and isopropanol, containing reduced and oxidised glutathione (8 respective 2 mM), rt, 24 hr.

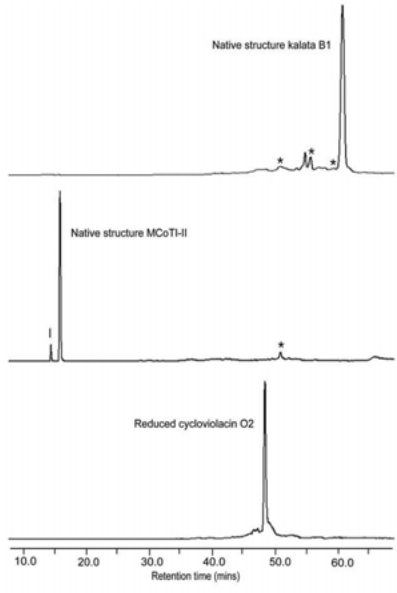

Fig. 2. LC-MS analyses of final products using microwave LC-MS chromatograms showing native folded kalata B1 and MCoTI-II, and reduced cycloviolacin O2. The misfolded cyclotides are marked with asterisks on the corresponding peaks, and the β-aspartyl isomer of MCoTI-II is marked with the letter I on the corresponding peak. The α-aspartyl isomer of MCoTI-II was the main product.

As a result of one pot reaction, kalata B1 and MCoTI-II thioesters were converted to the native structures in high yields (>95%) as shown in Figure 2.

The current protocol provides strong advantages in key steps of cyclic peptide synthesis using Fmoc-chemistry; that is, peptide assembly, thioesterification and cyclization/oxidative folding. Firstly, it does not need nucleophilic base labile linkers prior to peptide chain elongation. This prevents low yield of resulting peptide. In addition, different thiols can potentially be used in combination with this method. The p-acetamidothiophenol used in the current study has the advantage of being a good leaving group; thus, it does not need further chemical conversion steps for native chemical ligation. It has low toxic profile, and is conveniently odorless when used at elevated temperatures in the microwave reactor. Lastly, the lack of intermediate purification steps in the protocol maximizes the yields and minimizes the time for the total synthesis of cyclotides.

In summary, we demonstrated that microwave irradiation can successfully assist the chemical reactions (i.e. peptide assembly, mild cleavage and thioester formation) needed for Fmoc-SPPS based total synthesis of cyclic cysteine-rich peptides. Using optimized microwave assisted chemical reactions, we attempted for the first time to reduce the number of reaction/purification steps in cyclotide chemical synthesis. We omitted intermediate purification steps - the crude thioester peptide mixture was directly incubated in the 'one pot' buffer to yield the desired product. As a result, the method developed in the current work has maximized the yields and minimized the time for the total synthesis of cyclotides. This protocol may be readily applicable in disulfide-rich cyclic peptide synthesis but also in the synthesis of long peptide chains via native chemical ligation.

Acknowledgments

UG is supported by the Swedish Research Council and the Swedish Foundation for Strategic Research. TLA is supported by a grant from the Swedish International Development Cooperation Agency / The Department for Research Cooperation.

References

1. Craik, D.J., Daly, N.L., Bond, T., Waine, C. *J. Mol. Biol.* **5**, 1327-1336 (1999).
2. Dutton, J.L., Renda, R.F., Craik, D.J., et al. *J. Biol. Chem.* **279**, 46858-46867 (2004).
3. Gunasekera, S., Daly, N.L., Anderson, M.A., Craik, D.J. *IUBMB Life* **58**, 515-524 (2006).
4. Park, S., Gunasekera, S., Aboye, T., Göransson, U. *Int. J. Pept. Res. Ther.* **6**, 167-176 (2010).
5. Camarero, J.A., Hackel, B.J., De Yoreo, J.J., Mitchell, A.R. *J. Org. Chem*. **69**, 4145-4151 (2004).
6. Clippingdale, A.B., Barrow, C.J., Wade, J.D. *J. Pept. Sci.* **6**, 225-234 (2000).
7. Ingenito, R., Bianchi, E., Fattori, D., Pessi, A. *J. Am. Chem. Soc*. **121**, 11369-11374 (1999).

Proceedings of the 31st European Peptide Symposium
Michal Lebl, Morten Meldal, Knud J. Jensen, Thomas Hoeg-Jensen (Editors)
European Peptide Society, 2010

Racemization in Automated Solid Phase Synthesis

Krzysztof Darlak, Miroslawa Darlak, and Thomas E. Hopkins
Creosalus Inc., Louisville, KY, 40228, U.S.A.

Introduction

Automated peptide synthesis allows for preparation of a large number of peptide sequences in a fairly straightforward manner. Currently, the most widely applied methodologies utilize Fmoc-protection in combination with uronium/phosphonium activating agents for synthesis of peptides. The racemization process has been extensively studied with these activating agents on solid support [1,2]. Most experiments were carried out via manual protocols. Automated peptide synthesis adds another limitation affecting racemization process. Our recently presented studies covering the two most racemization-prone amino acids, cysteine and histidine, pointed out optimal conditions for their incorporation to a peptide chain using an automated peptide synthesis [3]. We have expanded the current work to the following commonly used amino acids: Asp, Leu, Ser and Tyr. In order to obtain a baseline resolution of the studied isomers we have applied in our experiments the previously published model peptide H-Gly-Xxx-Phe-NH_2 [4]. Herein we reevaluate the degree of racemization of Asp, Leu, Ser and Tyr using several popular activating agents applied to a typical automated peptide synthesis using an in-situ activation method.

Experimental

Model peptides H-Gly-Xxx-Phe-NH_2, Xxx=Asp, Leu, Ser and Tyr, were prepared on Fmoc-Phe-Rink-MBHA resin using the Tetras (Thuramed) multiple peptide synthesizer with *in situ* activation. Reagents used in the studies were: 0.6 M solution in NMP (BOP, PyBOP®, HCTU, HATU, COMU), 0.4 M solution in NMP (HBTU, PyClock®), 0.9 M DIEA solution in NMP, 1.0 M solution in NMP (DIC, HOBt, 6-Cl-HOBt, Oxyma Pure). Coupling conditions for uronium/phosphonium reagents (order of addition to the 150 mg of resin, 0.6 meq/g, no preactivation): Fmoc-amino acid 0.5 mmole, amine 0.9 mmole, reagent 0.5 mmole, mixing for 120 min; with DIC/additive: additive 0.5 mmole, Fmoc-amino acid 0.5 mmole, DIC 0.5 mmole, mixing for 120 min. Target peptides were cleaved from the resin with the mixture of TFA : water : phenol : TIPS (87.5:5:5:2.5) for 2 hours at RT. The resin was filtered off and TFA was evaporated under reduced pressure. The product was precipitated by addition of cold diethyl ether, centrifuged and dried. Chromatographic analysis of the obtained products was performed on Waters Alliance HPLC system using a Vydac C_{18} column (4.6x250 mm, 218TP54) with the linear gradients: 1-21% B in 30 min for H-Gly-Asp-Phe-NH_2 and H-Gly-Ser-Phe-NH_2, 10-30 % B in 30 min for H-Gly-Leu-Phe-NH_2, 5-35% B in 30 min for H-Gly-Tyr-Phe-NH_2. Buffers used for the analysis where A: 0.1% TFA in Water: MeCN 98:2 (v/v) and B: 0.1% TFA in MeCN: Water 98:2 (v/v) with flow of 1ml/min and detection at 220 nm. The content of LDL isomer was calculated as relative peak areas (Absorbance) from HPLC as: A (LDL isomer)/[A (LDL isomer + A (LLL isomer)] x 100. Results of the analysis are presented in Table 1.

Results and Discussion

We have used listed above peptides as targets to evaluate the degree of racemization during incorporation of Fmoc-Asp(OBut)-OH, Fmoc-Leu-OH, Fmoc-Ser(But)-OH and Fmoc-Tyr(But)-OH to the solid support utilizing a Tetras (Thuramed) automated peptide synthesizer with *in situ* activation. Selected reagents are presented in Table 1, including recently introduced reagents: COMU [3,4], PyClock [5] and Oxyma Pure [3,4,6,7]. During routine peptide synthesis the same activating method is used to prepare an entire peptide sequence. This approach is necessary due to the limitation of instrumentation (lack of sufficient number of reagents precisely delivered on board of synthesizer) or the user's choice. Our previous studies indicated that use of DIC with various additives was found to be a method of choice for introduction of cysteine and histidine residues using an automated peptide synthesis. Presented results in Table 1 show clearly, that in all studied cases (Asp, Leu, Ser, and Tyr) the level of racemization was found below 1%. The majority of the examples implementing DIC mediated activation with various additives gave lower racemization than uronium/phosphonium reagents. Changing the amount of base to one

Table 1. Racemization during SPPS of model peptides (% LDL isomers)

Reagent	*H-Gly-Xxx-Phe-NH_2*			*Z-Ile-Xxx-Pro-OH*		
	Asp	*Leu*	*Ser*	*Tyr*	*Cys(Trt)*	*His*
BOP	0.71	0.11	0.32	0.22	5.1	1.1
COMU	0.80	0.12	0.34	0.27	1.5	14.9
COMU 1/2B	0.66	0.13	0.34	0.20	-	-
HATU	0.62	0.09	0.25	0.22	2.9	0.7
HBTU	0.44	0.23	0.35	0.17	4.4	2.0
HCTU	0.51	0.10	0.37	0.25	6.5	2.8
PyBOP	0.42	0.11	0.53	0.20	5.0	1.3
Pyclock	0.51	0.17	0.25	0.27	7.5	4.1
DIC/Cl-HOBt	0.72	0.15	0.06	0.19	0.6	0.7
DIC/HOAt	0.44	0.14	0.21	0.19	-	-
DIC/HOBt	0.40	0.08	0.07	0.22	0.6	2.3
DIC/OXYMA	0.70	0.09	0.06	0.16	0.1	2.2

equivalent in COMU mediated coupling did not reduce significantly racemization as reported earlier [8]. Use of traditional activating reagents such as DIC in combination with racemization suppressants especially Oxyma Pure as HOBt replacement are good alternatives to minimize epimerization of amino acids including cysteine and histidine residues during activation in solid phase peptide synthesis. This strategy can be a universal activation protocol during automated peptide synthesis for most amino acids.

References

1. Goodman, M. *Synthesis of Peptides and Peptidomimetics. Houben-Weyl, Methods of Organic Chemistry*, **Vol. E22**, Thieme, Stuttgart-New York, 2002.
2. Fenza, A., Rovero, P. *Lett. Pept. Sci.* **9**, 125 (2002).
3. El-Fahan, A., Subiros-Funosas, R., Albericio, F., *J. Pept. Sci. Suppl.* **14**, 57 (2008).
4. El-Fahan, A., Albericio, F. *Chem. J. Pept. Sci.* **16,** 6 (2009).
5. Moreno, J.A., Bayo-Puxan, N., Tulla-Puche, J., Luxemburg, Y., Philosof-Oppenheimer, R., Shvo, Y., Evenson, A., Albericio, F. *poster presentation, 29th European Peptide Symposium*, Gdansk, Poland, 2006.
6. Itoh, M. *Bull Chem. Soc. Japan* **46**, 2219 (1973).
7. Izdebski, J. *Pol. J. Chem.* **53**, 1049 (1979).
8. El-Fahan, A., Subiros-Funosas, R., Prohens, R., Albericio, F. *Chem. Eur. J.* **15**, 9404 (2009).

Proceedings of the 31st European Peptide Symposium
Michal Lebl, Morten Meldal, Knud J. Jensen, Thomas Hoeg-Jensen (Editors)
European Peptide Society, 2010

Octapeptide Ligands with Affinity for Recombinant Erythropoietin Derived From the Screening of Combinatorial Libraries

María C. Martínez-Ceron[1], Mariela M. Marani[1], Marta Taulés[2], Marina Etcheverrigaray[3], Fernando Albericio[4], Osvaldo Cascone[1], and Silvia A. Camperi[1]

[1]Cátedra de Microbiología Industrial y Biotecnología, Facultad de Farmacia y Bioquímica, Universidad de Buenos Aires, Junin 956, Bs. As., 1113, Argentina;[2]Serveis Cientificotècnics, Universitat de Barcelona, Barcelona, 08028, Spain; [3]Laboratorio de Cultivos Celulares, Facultad de Bioquímica y Ciencias Biológicas, UNL. Ciudad Universitaria, Santa Fe, 3000, Argentina; [4]IRB Barcelona and CIBER-BBN, Parc Científic de Barcelona, Barcelona, 08028, Spain

Introduction

Erythropoietin (Epo), glycoprotein hormone produced in mammalian kidney and liver, is the main inducer and regulator of red cell proliferation and differentiation in bone marrow. Recombinant erythropoietin (rhEpo) is used for therapeutics of anemia associated with chronic renal disease, AZT-induced anemia of AIDS and for the treatment of cancer patients on chemotherapy and surgical patients to avoid the need for a red blood cell transfusion [1]. Affinity Chromatography (AC) is ideally suited for the purification of therapeutic proteins as it is the most effective method for the direct isolation and purification of biomolecules from complex mixtures. Its good selectivity minimizes contamination and yields samples of high purity in a single step [2]. Successful separation by AC requires the availability of a ligand with satisfactory affinity and selectivity. Small peptides consisting of a few amino acids represent promising affinity ligand candidates for industrial separations. Peptide ligands are much more physically and chemically stable than antibody ligands and are very resistant to proteolytic cleavage. They can be readily synthesized in bulk amounts at a lower cost under good manufacturing practices (GMP) by standard chemistry. Also, peptides can be easily modified by chemical methods to facilitate product elution under mild conditions. Furthermore, peptides allow site-directed immobilization and high ligand density and the matrices are more robust during elution and regeneration than protein-based affinity matrices such as monoclonal antibodies. Moreover, in the case of leakage into the product, peptides have low toxicity and generate low immune responses compared with proteins, dyes and transition metal ion ligands [3]. When leakage does occur, small peptide molecules can be easily removed from a macromolecular product. The combinatorial synthesis of peptide libraries allows the production of millions of peptides, thus greatly facilitating the discovery of suitable ligands for a given protein of interest. The preparation of combinatorial libraries by the divide–couple–recombine (DCR) or mix and split solid-phase method assures a theoretically even representation of the library members and a one-bead-one-compound distribution [4,5].

In previous studies, we developed a rapid and inexpensive strategy for the identification of peptides contained on positive beads, using matrix-assisted laser desorption/ionization time-of-flight mass spectrometry (MALDI-TOF-MS), and 4-hydroxymethylbenzoic acid (HMBA) immobilized in ChemMatrix resin [6-8].

The aim of this study was to apply that strategy for the identification of peptide ligands with affinity for rhEpo and to attach these peptides to agarose in order to purify rhEPO by AC.

Results and Discussion

By the screening of a one-bead-one peptide library composed of 132,000 tetrapeptides with the combination of all the natural amino acids except Cys, we obtained low-affinity tetrapeptide ligands for rhEpo. Cys was omitted in order to prevent disulfide bridge formation. Afterward, a one-bead-one peptide combinatorial library containing 100,000 octapeptides XXXFXXAG where X=A, D, E, F, H, L, N, P, S or T was synthesized on HMBA-ChemMatrix resin by the DCR method using Fmoc chemistry. Side-chain deprotection was carried out with TFA. For the library screening, the rhEpo was coupled

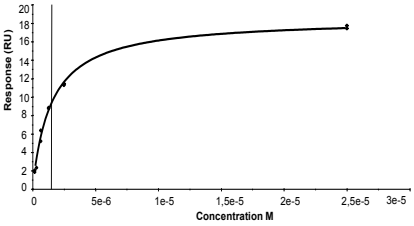

Fig. 1. A representative affinity analysis with Biacore T100 of rhEPO with a positive peptide.

with either Texas Red or biotin, as described previously by Marani et al. [6,7]. Fluorescent beads or beads showing a positive reaction with streptavidin-peroxidase were isolated. Fifty beads showed a positive reaction. Peptides were cleaved from each bead with NH_4OH, eluted with AcOH/MeCN/H_2O (3/4/3) and sequenced by tandem MALDI-TOF-MS. Those sequences showing greater consensus were synthesized and their affinity to rhEpo was evaluated using a plasma resonance biosensor (Biacore T100). Kd values between 10^{-5}-10^{-6} M were obtained (Figure 1). Peptides with the highest affinity were immobilized on NHS-agarose. All peptide-agarose matrices showed affinity for rhEpo (Figure 2A). Also, the affinity of the peptide-agarose matrices for bovine seroalbumin (BSA) - usually present in the culture supernatants - was assessed (Figure 2B). Those peptides with the highest selectivity between rhEpo and BSA were chosen for future development of a chromatographic matrix for rhEPO purification.

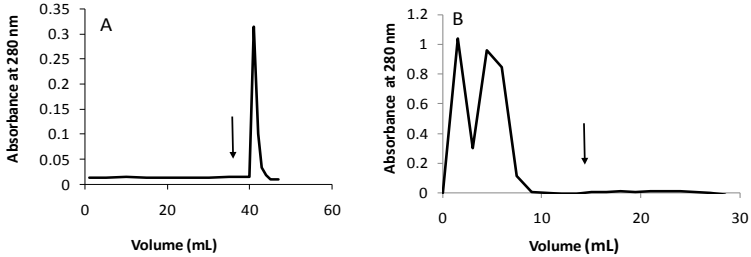

Fig. 2. Agarose-positive peptide column chromatogram of A) rhEpo and B) SAB. After applying the protein solution, the column was washed with the equilibrating buffer (20 mM sodium phosphate, pH 4.0). Elution was performed with 100 mM sodium acetate buffer, pH 3.0, 0.5 M NaCl. The rhEpo was adsorbed while the SAB pass through without interaction with the column. The arrow indicates the buffer change.

Acknowledgements
This study was partially supported by the Consejo Nacional de Investigaciones Científicas y Técnicas (CONICET: PIP 00230, PIP 00052), the University of Buenos Aires (UBA: B 043), the Agencia Nacional de Promoción Científica y Tecnológica de la República Argentina (ANPCyT: PICT 32309), CICYT (CTQ2006-03794/BQU, CTQ2008-00177), and the Generalitat de Catalunya (2005SGR 00662). M.M.M, M. E., O.C. and S.A.C. are researchers of the CONICET. We thank Simon Côté from Matrix Innovation Inc. for kindly donating HMBA-ChemMatrix.

References

1. Jelkmann, W. *Br. J. Haematol*. **141**, 287-297 (2008).
2. Roque, A.C., Lowe, C.R. *Meth. Mol. Biol.* **421**, 1-21 (2008).
3. Tozzi, C., Anfossi, L., Giraudi, G. *J. Chromatogr. B* **797**, 289-304 (2003).
4. Lam, K.S., Salmon, S.E., Hersh, E.M., Hruby, V.J., Kazmierski, W.M. *Nature* **354**, 82-84 (1991).
5. Furka, A., Sebestyen, F., Asgedom, M., Dibo, G. *Int. J. Peptide Protein Res.* **37**, 487-493 (1991).
6. Marani, M.M., de Oliveira, E., Côte, S., Camperi, S.A., Albericio, F., Cascone, O. *Anal. Biochem*. **370**, 215-222 (2007).
7. Marani, M.M., Martínez Ceron, M.C., Giudicessi, S.L., de Oliveira, E., Côté, S., Erra-Balsells, R., Albericio, F., Cascone, O., Camperi, S.A. *J. Comb. Chem.* **11**, 146-150 (2009).
8. Martínez-Ceron, M.C., Giudicessi, S.L., Marani, M.M., Albericio, F., Cascone, O., Erra-Balsells, R., Camperi, S.A. *Anal. Biochem*. **400**, 295-297 (2010).

Proceedings of the 31st European Peptide Symposium
Michal Lebl, Morten Meldal, Knud J. Jensen, Thomas Hoeg-Jensen (Editors)
European Peptide Society, 2010

Post-Synthesis Modification of *p*-Iodo-Phenylalanine-Containing Peptides on Solid-Phase via the Palladium-Catalyzed Sonogashira Reaction

Ngoc-Duc Doan, David Chatenet, and Alain Fournier
Institut National de la Recherche Scientifique-Institut Armand-Frappier, Université du Québec, 531 boulevard des Prairies, Ville de Laval, Qc, H7V 1B7, Canada; Laboratoire International Associé Samuel de Champlain (INSERM – INRS)

Introduction

Peptides are active regulators and transmitters of key biological functions thus making them particularly appealing for drug discovery [1]. As a matter of fact, their high biological activity is often associated with low toxicity and high specificity for their targets. However, due to inherent limitations such as low stability and oral bioavailability, difficult delivery, as well as costly synthesis, the development of peptide-based drugs remains relatively uncommon. The quest for novel molecular structures with improved biological activity profiles led to the development of potent small molecules that possess unique properties and the ability to modify the activities of larger molecules. Hence, to improve key pharmacological characteristics, structure-activity relationship studies generating libraries of peptide analogs proved to be very helpful to identify new therapeutic peptides. In fact, to improve the therapeutic potential of peptides, several modifications including lactamization, "stapling" of peptides, incorporation of non natural amino acids, and pegylation were applied and showed frequently a significant improvement of the pharmacological properties of peptides [2]. In this line of view, we developed an effective method, based on the Sonogashira reaction, to modify on solid phase p-iodo-phenylalanine-containing peptides.

Results and Discussion

Initially, the Sonogashira cross-coupling reaction was attempted in solution with Boc-*p*-iodo-L-phenylalanine and phenylacetylene, in the presence of the palladium-catalyst $PdCl_2(PPh_3)_2$, copper (I) bromide, triethylamine (TEA) and a phosphine ligand (PCy_3), in methylene chloride (DCM). In this condition, Boc-*p*-phenylacetylenyl-L-phenylalanine (Boc-Pep-OH) was obtained in good yield (85%) after purification on silica gel (EtOAc:*n*-heptane 1:1). Our attention was next turned towards the direct modification of *p*-iodo-phenylalanine-containing peptides on solid support. In this regard, [$Ala^{1,2,3}$, Leu^8]Enk (AAAYGGFL) was used as a peptide model to evaluate the feasability of the Sonogashira reaction in solid-phase peptide chemistry.

All peptide-resins were synthesized using standard Fmoc chemistry with the N-terminal amino acid being introduced as a Boc derivative. Prior to the Sonogashira reaction, a small amount of peptide was cleaved and analyzed by analytical RP-HPLC and MALDI-TOF MS to ensure the homogeneity and molecular mass of the starting material. The methodology for the Sonogashira solid-phase peptide modification was then optimized through the study of the influence of temperature, base, catalyst, solvent and reaction time on the reaction yield. It was found that the best results were obtained with $PdCl_2(PPh_3)_2$ as catalyst, TEA as base, dimethylformamide (DMF):DCM mixture as solvent and temperature of 40°C, overnight.

Previous studies suggested that the presence of unprotected amino groups ($-NH_2$) can interact with Pd and retard the catalytic cycle of metal-catalyzed reaction [3]. The stability of Fmoc and Boc protecting groups was assessed and results suggested that both protecting groups were stable in the optimized reaction conditions, even after 24 hrs; however, longer reaction time (4 days) caused a slight cleavage of the Fmoc moiety. We also observed that linkers, such as Wang and Rink Amide, were stable under Sonogashira reaction.

Since the conversion of N-α-Boc-[$Ala^{1,2,3}$, Phe(*p*I)^4, Leu^8]Enk to N-α-Boc-[$Ala^{1,2,3}$, Pep^4, Leu^8]Enk was successfully achieved using the optimized conditions of the Sonogashira reaction described above, we then performed the same modification with more complex peptides containing sensitive amino acids such as cysteine, histidine, and tryptophan. Conversion of these iodinated peptides ([Phe(*p*-I)^{13}]ET(9-21) (KECVF(*p*-I)FCHLDIIW) and Ac-[Phe(*p*-I)^6, Nle^{17}]PACAP27 (Ac-HSDGIF(*p*-I)TDSYSRYRKQ*Nle*-

Table 1. Sonogashira cross-coupling reaction of para-iodo-phenylalanine-containing peptides with phenylacetylene

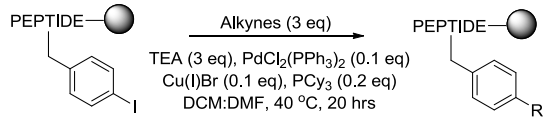

No	*Peptides*	*Alkynes*	*R*	*Yield (%)*[a]
1	[Ala[1,2,3], Phe(p-I)[4], Leu[8]]Enk	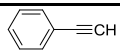	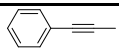	91
2	[Phe(p-I)[13]]ET(9-21)	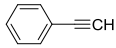	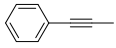	77
3	Ac-[Phe(p-I)[6], Nle[17]]PACAP27	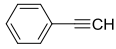	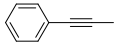	86
4	Ac-[Phe(p-I)[6], Nle[17]]PACAP27	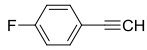	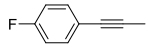	94
5	Ac-[Phe(p-I)[6], Nle[17]]PACAP27	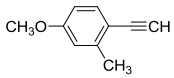	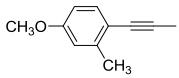	< 10
6	Ac-[Phe(p-I)[6], Nle[17]]PACAP27	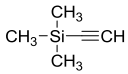		91
8	Ac-[Phe(p-I)[6], Nle[17]]PACAP27	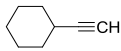	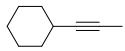	74

[a] *The reaction yield was determined using analytical RP-HPLC (λ = 212 nm) as previously described [4]*

AVKKYLAAVL) was achieved in good yield (Table 1) and no side-reaction was observed. Then, using optimal conditions, we generated a small library of PACAP27 analogs modified at position Phe[6]. Electron-withdrawing substrates such as 4-fluorophenylacetylene appeared to be more reactive than electron-donating derivatives, *i.e.* 2-methyl-4-methoxyphenylacetylene (Table 1) probably by facilitating the formation of the organo-copper complex. The coupling of PACAP derivative with cyclohexylacetylene or trimethyl-silyl-acetylene also gave good yields. These PACAP analogs were then pharmacologically characterized using CHO cells co-expressing the human PAC1 receptor and a mitochondrial apo-aequorin protein. Preliminary results showed that these analogs potently bind and activate the PACAP related receptor.

Acknowledgments

The authors thank Myriam Létourneau and Vanessa Laflamme for technical support. This study was supported by the Canadian Institutes of Health Research. N-D.D. is the recipient of a doctoral research award from the Heart and Stroke Foundation of Canada and an excellence award from the Foundation Armand-Frappier.

References

1. Sewald, N., Jakubke, H.D. *Peptides: Chemistry and Biology*; Wiley-VCH: Weinheim, Germany, (2002).
2. Gauthier, M.A., Klok, H.A. *Chem. Commun*. **23**, 2591-611 (2008).
3. Chinchilla, R., Nájera, C. *Chem. Rev*. **107** (3), 874-922 (2007).
4. Doan, N.D., Bourgault, S., Letourneau, M., Fournier, A. *J. Comb. Chem*. **10,** 44-51 (2008).

Proceedings of the 31st European Peptide Symposium
Michal Lebl, Morten Meldal, Knud J. Jensen, Thomas Hoeg-Jensen (Editors)
European Peptide Society, 2010

Specific Substrates and Inhibitors of Human Furin

Adam Lesner, Magdalena Wysocka, Anna Łęgowska, and Krzysztof Rolka

University of Gdansk, Faculty of Chemistry, Sobieskiego 18, 80-952, Gdansk, Poland

Introduction

Proprotein convertases (PCs) are calcium-dependent serine proteases of the subtilisin family which are known to generate the important biologically active peptides by the specific cleavage of peptide bond at the C-terminal fragments R-X-(K/R)-R of their precursors. Such groups of enzymes are initially synthesized as inactive proenzyme forms that undergo activation under physiological conditions. Furin, one of the seven endoproteases that belong to the PC family, is ubiquitously expressed in mammalian cells processing and activating a wide variety of proprotein substrates. The endogenous substrates of furin are receptors such as insulin proreceptor, plasma proteins, growth factors and hormones as well as proteases such as matrix metalloproteinases – like membrane type 1-matrix metalloproteinase (MT1-MMP). Increased activity of furin was identified in head and breast tumors, neck tumors, and also in lung cancer. Recent reports have indicated that furin is a target of hypoxia-inducible factor 1 (HIF-1) and that hypoxia induces elevated levels of furin, leading to more aggressive tumors. Therefore PC inhibitors may constitute new promising antitumor agents. The aim of this study is to select, using combinatorial chemistry methods, specific furin substrates that will display FRET and chromogenic properties. The general formula of the peptide library synthesized is as follows:

$$ABZ\text{-}X_4\text{-}X_3\text{-}X_2\text{-}Arg\text{-}ANB\text{-}NH_2,$$

where:

ABZ = 2-aminobenzoic acid (donor of fluorescence);

$ANB\text{-}NH_2$ = amide of 5-amino-2–nitrobenzoic acid (acceptor of fluorescence);

$X_2 – X_4$ = nonproteinogenic basic amino acids (D-Arg, Amf, Gnf, Har, Orn, Dab, βlys) along with Arg and Ala (used as reference amino acids) were introduced and their chemical structure are displayed on Figure 1.

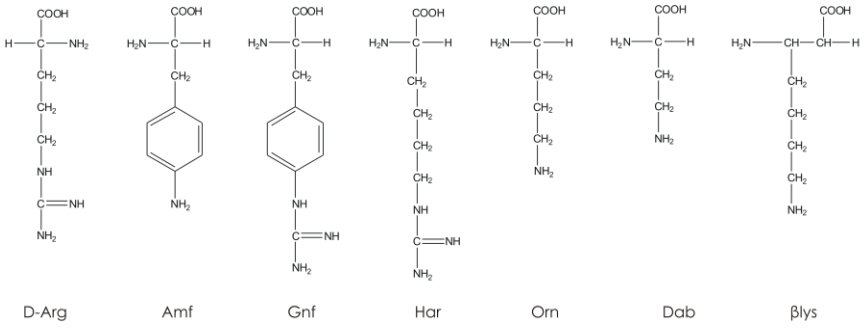

Fig. 1. Chemical formulas of nonproteinogenic basic amino acids used to construct the peptide library.

Results and Discussion

Iterative method was applied for selection process of the most efficiently hydrolyzed substrates. Among non proteinogenic basic charged residues present in the library X_3 position which corresponds to the substrate P_4 position, the most efficient fluorescence was

observed for few residues including Arg, Har, Gnf and for βLys. No significant proteolysis was detected for Orn, Dab and Amf. In position P_3 human furin was able to hydrolyzed almost all residues except Dab. The highest fluorescent intensity was recorded for Arg and βLys. A slightly lower response was observed for Gnf. Substrate preferences in position P_2 was similar as in position P_4. Arg and βLys followed by Gnf and Har were hydrolyzed with the highest rate. Low fluorescence was observed for the remaining amino acids. All peptides that undergoes proteolysis were characterized and their kinetic parameters (k_{cat} and K_M) are presented in Table 1.

Based on the selected substrate ABZ-Gnf-Gnf-βLys-Arg-ANB-NH_2, a set of aldehyde inhibitors were designed. FRET substrates were converted into corresponding peptide aldehydes. Simply, ANB-NH_2 present at the *C*-terminus of peptide was replaced by aldehyde group yielding the peptide aldehyde. The solid support was used to synthesize

Table 1. Physicochemical characteristic and kinetic parameters of human furin substrates

Substrate	t_R *[min]*	*MW calc. (determ)*	k_{cat} $[s^{-1}]$	K_M $[\mu M]$	k_{cat}/K_M $[s^{-1}\times M^{-1}]$
ABZ-Gnf-Gnf-βLys-Arg-ANB-NH_2	12.8	1007.1 (1007.3)	7.8±0.4	12.5±1.2	645.4×10^3
ABZ-Gnf-Gnf-Har-Arg-ANB-NH_2	10.2	1028.1 (1028.4)	4.2±0.2	39.4±2.7	106.7×10^3
ABZ-Gnf-Gnf-Gnf-Arg-ANB-NH_2	14.3	1069.2 (1069.3)	4.9±0.4	11.8±2.1	415.1×10^3
ABZ-Gnf-Gnf-Arg-Arg-ANB-NH_2	9.8	1014.3 (1014.3)	7.2±0.8	15.4±1.3	467.2×10^3

such peptide derivative. A set of peptide aldehydes (ABZ-Gnf-Gnf-βLys-X-H) modified in position X by amino acid residues used for library construction (Figure 1) was synthesized. The preliminary activity test of obtained compounds indicate that the activity of human furin is diminished when incubated with ABZ-Gnf-Gnf-βLys-Gnf-H, and ABZ-Gnf-Gnf-βLys-Har-H. Peptide aldehydes with Arg, D-Arg, Orn and Amf displayed lower inhibitor potency. The lowest PC inhibition was observed for βLys, Dab and Ala.

In summary we would like to conclude that human furin is able to recognize and hydrolyze peptide with non proteinogenic amino acid within its sequence. Among them the highest value of the specificity constant was obtained for ABZ-Gnf-Gnf-βLys-Arg-ANB-NH_2 ($k_{cat}/K_M = 645\times10^3\ M^{-1}\times s^{-1}$).The peptide aldehydes that sequence was based on selected FRET substrate were able to inhibit human furin activity with values of inhibiton constants at nanomolar range.

Acknowledgments
This work was supported by Polish Ministry of Science and Higher Education under grant 1600/B/H03/2009/36.

References

1. Mollay, S.S., Bresnhahan, P.A., Leppla, S.H., Klimpel, K.R., Thomas, G. *J. Biol. Chem.* **267**, 16396-16402 (1992).
2. Steiner, D.F. *Curr. Opin. Chem. Biol.* **2**, 31-39 (1998).
3. Wysocka, M., Kwiatkowska, B., Rzadkiewicz, M., Lesner, A., Rolka, K. *Comb. Chem. High Through S.* **3**, 171-180 (2007).
4. Furka, A., Sebestyn, F., Asgedom, M., Dib, G. *Int. J. Peptide Prot. Res.* **37**, 487-494 (1991).

Proceedings of the 31st European Peptide Symposium
Michal Lebl, Morten Meldal, Knud J. Jensen, Thomas Hoeg-Jensen (Editors)
European Peptide Society, 2010

Novel Peptide Conjugates: Heterocyclic Modifications of the Immunomodulatory Ubiquitin Fragment

Alicja Kluczyk[1], Malgorzata Ratajska[1*], Anna Staszewska[1], Marek Cebrat[1], Hubert Bartosz-Bechowski[1], Piotr Stefanowicz[1], Michal Zimecki[2], and Zbigniew Szewczuk[1]

[1]Faculty of Chemistry, University of Wroclaw, 50-383 Wroclaw, Poland; [2]Institute of Immunology and Experimental Therapy PAS, 53-114 Wroclaw, Poland;
**current address: The Kostrzyca Forest Gene Bank, 58-535 Milkow, Poland*

Introduction

Ubiquitin, a 76-amino acid polypeptide, is one of the pivotal factors in cellular physiology as a post-translational addition to proteins that targets them for degradation by the proteasome [1]. In addition to protein degradation, ubiquitin is known to activate cell signals in several pathways: tolerance to DNA damage, inflammatory response, protein trafficking, and ribosomal protein synthesis. The immunomodulatory properties of ubiquitin were discussed by us recently [2]. We discovered that the peptide **I** Asp-Gly-Arg-Thr-Leu (52-56) is the shortest active fragment of the immunosuppressory (50-59) loop of ubiquitin [3] and we analyzed the structure of this fragment [4], as well as the activity of dimeric peptides containing the (50-59) Leu-Glu-Asp-Gly-Arg-Thr-Leu-Ser-Asp-Tyr sequence.

Results and Discussion

A series of analogues of peptide **I**, with the N-terminal Asp residue replaced by novel aromatic nonproteinaceous amino acid residues (Figure 1), were synthesized to investigate their physicochemical properties, metal ion affinity and immunosuppressory activity. A special derivative of phenylalanine, Fmoc-β-(4-amino-3-nitrophenyl)-alanine, was used as a substrate to obtain 2-substituted 1*H*-benzimidazol-5-yl alanine [5] or 2,3-disubstituted quinoxalin-6-yl alanine [6] analogues of **I**. The heterocyclic motifs were formed on-resin after solid phase peptide assembly; the purity and identity of conjugates was confirmed using HPLC, mass spectrometry and NMR.

The interactions with metal ions were investigated in respect to Cu(II) using ESI-MS, circular dichroism and NMR. High resolution mass spectra (Figure 2) reveal formation of several coordination compounds varying in peptide-metal ratio, dimer formation was also observed. The collision induced dissociation experiments suggest that the presence of copper ion changes the fragmentation pathway of the conjugate as a result of radical

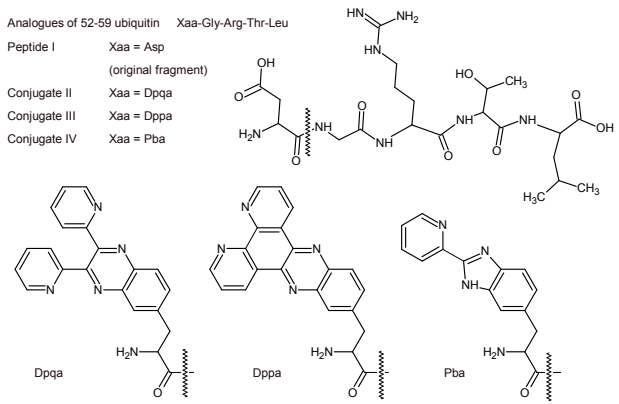

Fig. 1. Peptide conjugates, analogues of 52-59 fragment of ubiquitin, containing substituted quinoxaline and benzimidazole heterocyclic motifs.

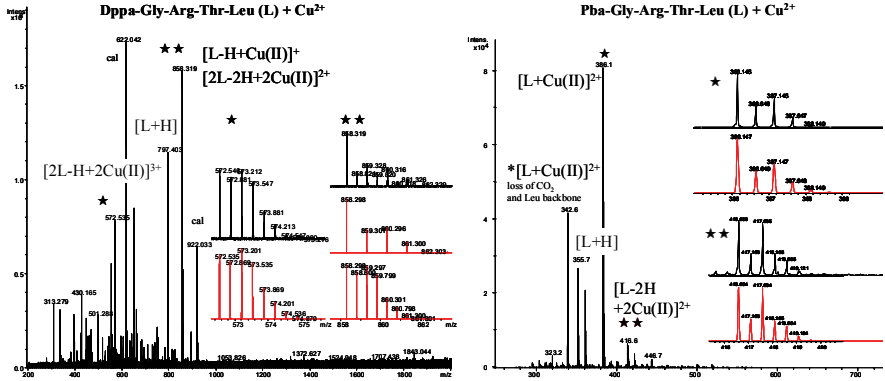

Fig. 2. High resolution mass spectra of Cu(II) complexes of selected heterocyclic peptide conjugates. Isotopic patterns simulated for proposed complex formulas in red (gray). Cal – internal calibration was used to increase m/z precision.

formation. The observed fragments result from deterioration of peptide chain and, according to isotopic pattern analysis, all contain the copper ion, suggesting the relative stability of the complex and localization of metal ion in heterocyclic part of the conjugate. The results of CD and NMR experiments imply that the interactions with Cu(II) ion affect the structure of peptide conjugate with a shift to a more ordered conformation. The primary interaction site is located in the bipyridyl-like motif of the heterocyclic moiety.

The immunomodulatory activity of the investigated conjugates and their complexes was examined *in vitro* in the mouse model of secondary humoral immune response to sheep erythrocytes (SRBC) using the antibody forming cells (AFC) test. The effect of the heterocyclic motif was established after comparison with the original ubiquitin sequence (peptide I, 83% immunosuppression at the dose of 100 μg/ml), whereas the sequence involvement was examined in relation to respective dipeptides (Xaa-Gly). The unusually high immunostimulatory effect of conjugate III, containing a rigid phenazine skeleton (280% stimulation of immune response), seems to be unique for this combination of heterocycle and peptide sequence, as a respective dipeptide Dppa-Gly was a strong immunosuppressor (87% at the highest dose). All copper complexes of investigated conjugates evoked significant immunosuppression (77 – 90% at the highest dose).

Conclusions

The combination of the immunomodulatory fragment DGRTL of the 50-59 loop of ubiquitin with heterocyclic motifs resulted in peptides with significant metal ion affinity and interesting biological properties. The MS experiments and NMR analysis indicate the coordination of metal ion mostly by the heterocyclic component of the conjugate. Introducing the heterocyclic modifications to bioactive peptides may result in novel bioactive compounds - targeted metal carriers.

Acknowledgments

This work was supported in part by grant No. N N401 222734 from the Ministry of Science and Higher Education (Poland).

References

1. Hershko, A., Ciechanover, A. *Annu. Rev. Biochem.* **67**, 425-479 (1998).
2. Pasikowski, P., Cydzik, M., Kluczyk, A., Stefanowicz, P., Szewczuk Z. *Biomolecular Concepts* **1**, 67-84 (2010).
3. Szewczuk, Z., Stefanowicz, P., Wilczynski, A., Staszewska, A., Siemion, I.Z., Zimecki, M., Wieczorek, Z. *Biopolymers* **74**, 352-362 (2004).
4. Jaremko, L., Jaremko, M., Pasikowski, P., Cebrat, M., Stefanowicz, P., Lisowski, M., Artym, J., Zimecki, M., Zhukov, I., Szewczuk, Z. *Biopolymers* **91**, 423-431 (2009).
5. Staszewska, A., Stefanowicz, P., Szewczuk, Z. *Tetrahedron Lett.* **46**, 5525-5528 (2005).
6. Koprowska-Ratajska, M., et al. *Amino Acids* **36**, 309-315 (2009).

Proceedings of the 31st European Peptide Symposium
Michal Lebl, Morten Meldal, Knud J. Jensen, Thomas Hoeg-Jensen (Editors)
European Peptide Society, 2010

The Characterization of Staphopains Enzyme Family from *Staphylococcus aureus* Using Combinatorial Chemistry Methods

Adam Lesner[1], Magdalena Wysocka[1], Marcelina Jaros[1], Anna Łęgowska[1], Katarzyna Guzow[1], Grzegorz Dubin[2], Benedykt Władyka[2], Wiesław Wiczk[1], and Krzysztof Rolka[1]

[1]Gdansk University, Faculty of Chemistry, Gdansk, 80-952, Poland; [2]Jagiellonian University, Faculty of Biochemistry, Biophysics and Biotechnology, Cracow, 30-357, Poland

Introduction

Staphylococcus aureus is a main cause of nosocomial infections of all kinds. It colonizes and infects virtually every tissue of the body. To encounter the environmental diversity faced, the bacteria is well equipped with a broad spectrum of secreted proteins. Three different catalytic classes, including metallo-, serine- and cysteine proteases are found among the secreted staphylococcal proteins. A variety of different functions including, but not limited to, tissue degradation [1], defense against host immune response [2], interception of host enzymes and bacterial adhesion regulation [3] have been attributed to these proteins. Staphopains A, B and C are the major secreted cysteine proteases of *S. aureus*. The literature contains evidence both for and against their role as virulence factors. All three proteases are members of the papain superfamily of enzymes and are encoded on the genome as preproenzymes. Staphopain A and B shared 47% of amino acid homology. The structure of mature staphopain A is known. It shows that staphopains are remote members of the papain superfamily of enzymes with cathepsin B as their closest structural neighbor among the eukaryotic enzymes. Proteolytical activity of those enzymes are strictly controlled by the endogenous inhibitors called staphostatines [4].

The main goal of this research was to obtain detailed information about specificity of those three enzymes in substrate segment comprised positions $P_4 – P_1$. To do so, we applied combinatorial chemistry methods to synthesize the library of peptides with the general formula:

$$ABZ\text{-}X_4\text{-}X_3\text{-}X_2\text{-}X_1\text{-}ANB\text{-}NH_2$$

where:
ABZ – 2-aminobenzoic acid (donor of fluorescence),
$ANB\text{-}NH_2$ – amide of 5-amino-2-nitrobenzoic acid (acceptor of fluorescence),
X_4, X_3, X_2 and X_1 = all proteinogenic amino acid residues were present.
The presence of ABZ and $ANB\text{-}NH_2$ in peptides synthesized indicates that the library was designed to contain fluorogenic substrates of the investigated proteases.

Results and Discussion

The library synthesized was screened in solution against three members of cystein protease family (staphopain A (StpA), staphopain B (StpB) and staphopain C (StpC)) using iterative method of deconvolution. All enzymes displayed the highest activity measured as increase of the fluorescence in time when in position X_4 (equivalent to the substrate P_4 position) of the library the hydrophobic residues were present. StpA prefers the aromatic Phe followed by Ile and Leu since for StpB and StpC this trend was reversed; Ile predominates over Phe and Tyr. The charged residues present in discussed position significantly reduced the hydrolysis rate of the library for all three proteinases. In position P_3 of the library, all enzymes reveal broad specificity. StpA prefers library with Gly followed by Ala and Met. Asp and Pro in this position reduced the rate of proteolysis. StpB rapidly hydrolyzed peptide library when Ala or Gly were present in discussed position. This was not true for Trp and low fluorescence readout was observed. A quite similar picture was observed in the case of StpC. Ala followed by Ile, Gly and Arg(!) present in the position P_3 reveal the highest hydrolysis rate. Again Trp and Pro introduced in the discussed position yielded inactive peptides.

In position P_2, for two enzymes (StpA and StpB) the most intense fluorescence was detected for Ala. All other amino acids displayed at least twice lower hydrolysis rate. In the case of StpC, sub-libraries with Lys in position P_2 followed by Gly, Arg and Glu were the

ones most susceptible for proteolysis. No enzyme activity was observed for library with Pro in discussed position.

StpA and StpB displayed broad specificity in position P_1. They were able to hydrolyze with almost the same rate substrates with Lys, Leu, Asp (StpA) and Gly, Lys and Pro (StpB) in this position. This is not the case for StpC which very efficiently hydrolyzed only one peptide with Asp in position P_1. Fluorescence of all other peptides is several times lower.

Based on the performed kinetic investigations, several FRET peptides that could serve as efficient substrates of *Staphylococcal aureus* cystein proteinases were selected. For StpA the best substrate sequence is ABZ-Phe-Gly-Ala-Lys-ANB-NH_2, StpB: ABZ-Ile-Ala-Ala-Gly-ANB-NH_2 and StpC ABZ-Ile-Ala-Lys-Asp-ANB-NH_2. Their determined kinetic parameters are listed in Table 1.

Table 1. Kinetic characteristic of fluorescent substrates

Substrate	*Enzyme*	k_{cat} $[s^{-1}]\times10^{1}$	K_M $[M]\times10^{6}$	k_{cat}/K_M $[s^{-1}\times M^{1}]\times10^{-3}$
	StpA	**$7.16\pm8.26\times10^{-2}$**	**5.6±0.4**	**127.8±7.4**
ABZ-Phe-Gly-Ala-Lys-ANB-NH_2	StpB	$1.12\pm0.47\times10^{-2}$	154.6±15.5	0.7±0.1
	StpC	$0.23\pm0.03\times10^{-2}$	385.3±20.4	below 0.1
	StpA	$0.56\pm0.03\times10^{-2}$	163.9±12.2	3.4±0.2
ABZ-Ile-Ala-Ala-Gly-ANB-NH_2	**StpB**	**$8.86\pm6.02\times10^{-2}$**	**7.6±1.1**	**118.0±12.2**
	StpC	$0.02\pm0.01\times10^{-2}$	271.4±10.2	below 0.1
	StpA	$0.32\pm0.11\times10^{-2}$	587.1±48.1	below 0.1
ABZ-Ile-Ala-Lys-Asp-ANB-NH_2	StpB	$0.12\pm0.07\times10^{-2}$	612.9±52. 7	below 0.1
	StpC	**$8.91\pm5.86\times10^{-3}$**	**14.3±1.35**	**62.4±3.1**

Primary specificity of enzymes studied are in good agreement with crystallographic data provided by Filipek and coworkers [5] for staphopain B – staphostatin B (inhibitor) complex. In position P_1 they observed specific conformation of the peptide chain that could be adopted only by Gly residue. It's worth emphasizing that staphostatin is a large polypeptide consisted of more than 100 amino acid residues with defined structure. Since the library used in this study are tetrapeptides that display much broader flexibility within its peptide chain, there is no surprise that we observed more than one rapidly hydrolyzed sequence.

We would like to emphasize that to our knowledge this is the first comparative report that describes the substrate specificity of three cysteine proteases originated from *Staphylococcus aureus.*

Acknowledgments
This work was supported by Ministry of Science and Higher Education under grant 1600/B/H03/2009/36.

References

1. Potempa, J., Dubin, A., Korzus, G., Travis, J. *J. Biol. Chem*. **263**, 2664-2667 (1988).
2. Arvidson, S., Fischetti, V.A., Novick, R.P., Ferretti, J.J., Potrnoy, D.A., Rood, J.I. (Eds.) *Gram-positive pathogens.* American Society for Microbiology, Washington D.C, 2000, p.379.
3. Maeda, H., Yamamoto, T. *Biol. Chem. Hoppe-Seyler* **377**, 217-226 (1996).
4. Dubin, G. *Acta Biochim. Pol.* **50**, 715-724 (2003).
5. Filipek, R., Rzychon, M., Oleksy, A., Gruca, M., Dubin, A., Potempa, J., Bochtler, M. *J. Biol. Chem.* **278**, 40959-40966 (2008).

Proceedings of the 31st European Peptide Symposium
Michal Lebl, Morten Meldal, Knud J. Jensen, Thomas Hoeg-Jensen (Editors)
European Peptide Society, 2010

Convergent Syntheses of HuPrP106-126 (Difficult Sequence) Using Native Chemical Ligation and Desulfurization/Deselenization

Jaroslav Šebestík, Martin Šafařík, Zbigniew Zawada, and Jan Hlaváček*
Institute of Organic Chemistry and Biochemistry, vvi, Academy of Sciences, CR, Flemingovo n. 2, 166 10, Prague, Czech Republic

Introduction

Prion proteins are causative agents of neurodegenerative diseases such as scrapie, CJD, mad-cow disease (nvCJD), GSS, etc. [1]. The Prion-derived peptide HuPrP106-126 was found as a difficult sequence for the Fmoc approach [2]. We have described its synthesis using a divergent approach in 9% yield [3]. In order to improve the yield of this peptide by Fmoc approach, we employed 2- and 3-segment convergent approaches using a native chemical ligation with subsequent desulfurization/deselenization [4] of peptide precursors.

Results and Discussion

Two splitting places of the difficult sequence of HuPrP106-126 were designed. The first one between Gly^{114}-Ala^{115} residues and the second one between Gly^{119}-Ala^{120}. This choice demanded the syntheses of peptide thioesters with C-terminal Gly residue and thus avoided racemization. Retro syntheticaly functional group introduction was applied on N-terminal alanine residue i.e. Ala to Cys transformation was carried out. Syntheses of segments with 12 and 14 residues were non-competitive to divergent solid phase approach (comparison of items 4, 6, 8, 10, and 12 at Table 1 with item 2). Competitive could be solely synthesis of selenocysteine (U) derivative (item 3), and synthesis of peptide thioester by Beck-Sickinger's [5] method (item 11). Limited availability of difficult peptide segments led us to the synthesis of HuPrP106-126 using Kent's modular approach [6]. Here, we used both spliting sites in one synthetic scheme. The middle part of peptide was prepared by Beck-Sickinger's [5] method with protection of N-terminal Cys as 4-thiazolidine carboxylic acid. This method provided two peptides (items 13 and 14) in very competitive yields to divergent peptide synthesis (item 2). When the HuPrP106-126 was prepared by consecutive chemical ligation from the peptides (item 3, 11, and 14) the yield limiting step was the synthesis of N-terminal peptide thioester (item 3).

Methods

A: Synthesis of peptides on Wang polystyrene resin by Fmoc/tBu strategy. Cleavage of peptides was achived by TFA/TIS/H_2O/EDT mixture (90:2.5:2.5:5).
B: Synthesis of peptides on Wang polystyrene resin by Fmoc/tBu strategy. Cleavage by Hilvert's method [7] with $AlMe_3$/EtSH, followed by TFA/TIS/H_2O/EDT mixture (90:2.5:2.5:5). Unfortunatelly, Asn residues were converted to aspartimide (Table 1, underlined).
C: Synthesis of peptides on Ellman's sulfonamide resin [8]. The resin was activated with TMS-CHN_2 and cleaved with Mpa-OnBu/DMF (55 ^oC, several days). The side protection groups were removed with TFA/TIS/H_2O/EDT mixture (90:2.5:2.5:5).
D: Syntheses of protected peptides on chlorotritylchloride resin [5]. Protected peptide was cleaved with HFIP/DCM (1:3) 5 min, and coupling with DIC/DMAP/EtSH followed. Protected peptide thioester was deprotected with TFA/TIS/H_2O/EDT mixture (90:2.5:2.5:5).

Table 1. Yields of peptide segments achieved by various methods

Item	*Peptide*	*Yield*	*Method*
1	HuPrP106-126	< 0.1% [2]	[2]
2	HuPrP106-126	9% [3]	[3]
	C-terminal part		
3	UVVGGLG	65%	A
4	UAAAGAVVGGLG	10%	A
5	CVVGGLG	16%	A
6	CAAAGAVVGGLG	13%	A
	N-terminal part		
7	KTNMKHMAG-**SEt**	9%	B
8	KTNMKHMAGAAAAG-**SEt**	11%	B
9	KTNMKHMAG-**Mpa-OnBu**	6%	C
10	KTNMKHMAGAAAAG-**Mpa-OnBu**	2%	C
11	KTNMKHMAG-**SEt**	30%	D
12	KTNMKHMAGAAAAG-**SEt**	6%	D
	Middle part		
13	CAAAG-**SEt**	54%	D
14	**Thz**-AAAG-**SEt**	52%	D

Acknowledgments
This work was supported by grant of Czech Science Foundation (GA CR) No. 203/07/1517 and Research Project Z40550506.

References
1. Prusiner, S.B. *PNAS U.S.A.* **95**, 13363-13383 (1998).
2. Jobling, M., Barrow, C., White, A., Masters, C., Collins, S., Cappai, R. *Lett. Pept. Sci*. **6**, 129-134 (1999).
3. Sebestik, J., Hlavacek, J., Stibor, I. *Biopolymers* **84**, 400-407 (2006).
4. Wan, Q., Danishefsky, S.J. *Angew. Chem. Int. Ed.* **46**, 9248-9252 (2007).
5. von Eggelkraut-Gottanka, R., Klose, A., Beck-Sickinger, A.G., Beyermann, M. *Tetrahedron Lett.* **44**, 3551-3554 (2003).
6. Bang, D., Kent, S.B.H. *Angew. Chem. Int. Ed.* **43**, 2534-2538 (2004).
7. Sewing, A., Hilvert, D. *Angew. Chem. Int. Ed.* **40**, 3395-3396 (2001).
8. Backes, B.J., Ellman, J.A. *J. Org. Chem.* **64**, 2322-2330 (1999).

Proceedings of the 31st European Peptide Symposium
Michal Lebl, Morten Meldal, Knud J. Jensen, Thomas Hoeg-Jensen (Editors)
European Peptide Society, 2010

Functionalized PNA Backbone Building Blocks Eligible for Diels-Alder Click Chemistry in Molecular Imaging

Rüdiger Pipkorn, Manfred Wießler, Waldemar Waldeck, Mario Koch, and Klaus Braun

German Cancer Research Center, INF 280, D-69120, Heidelberg, Germany

Introduction

Therapies of cancer via "old fashioned" chemotherapeutics normally lead to undesired adverse reactions followed by abortion of the therapy. Modern chemotherapeutics are marked by their cell specific interaction with DNA without harming the surrounding healthy tissue. This progress in chemotherapeutic development led to molecular therapies demanding molecular diagnostics [1-3]. The open questions concerning the transport of imaging components in blood circulation, the differentiation between tumor and surrounding healthy tissue, and the local enrichment within target tissue and target cells can be answered as follows: Development and design of the needed molecules led to modularly built, functional molecules which require not only synthesis and quality insurance, but also attributes like fast, specific, quantitative and irreversible ligation of these single modules[4]. Numerous approaches for improving the ligation of components finally led to our special "click chemistry". Furthermore, a combination of several selectable different ligation compounds, either diagnostic compounds or therapeutic agents in one multistep reaction is possible by the Diels-Alder reaction with inverse electron demand (DAR_{inv}).

Results and Discussion

The synthesis of the functionalized PNA backbone for the DAR_{inv} was carried out in the steps as described here. The commonly used synthesis of the desired PNA building blocks is shown in Figure 1. The chemical synthesis of the "Reppe anhydride"-PNA building block tetracyclo-[5.4.2^{1,7}.O^{2,6}.O^{8,11}]3,5-dioxo-4-aza-9,12-tridecadiene, Fmoc protected, is shown in Figure 2.

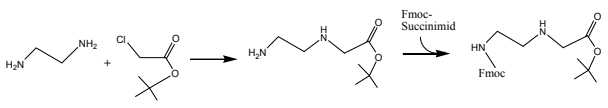

Fig. 1. Synthesis of the Fmoc protected PNA backbone module.

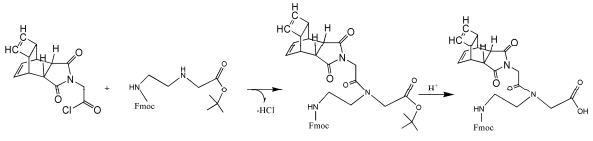

Fig. 2. Synthesis of PNA monomer functionalized with Reppe anhydride.

Using the solid phase synthesis (SPPS) we can prepare functional modular PNA-backbone polymers for coupling different active agents or imaging molecules in order to reach local concentrations at the desired target site until now unachievable. Using the SPPS we prepared a pentamer (shown in Figure 3) harboring a PNA's amide backbone with an additional cysteine attached to the amino terminus, which in turn will be coupled later to the cysteine of a cell membrane transport facilitating peptide (CPP) permitting an efficient cellular uptake imperative for biochemical studies.

This pentamer represents the corresponding reacting partner (a dienophile compound) for the DAR_{inv} mediated ligation to pharmacologically active substances or molecules for imaging in diagnostics harbouring the diene groups. After attachment of the pentamer loaded with the functional molecules to the CPP, which facilitates the passage across biological membranes the modular conjugate forms a "BioShuttle" transporter variant as exemplified in Figure 4.

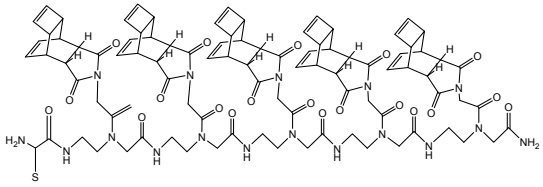

Fig. 3. Structure of the pentamer functionalized with the dienophile compound "Reppe anhydride".

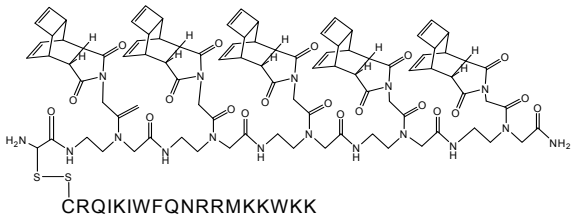

Fig. 4. "Reppe anhydride" pentamer connected via a disulfide bridge with the CPP.

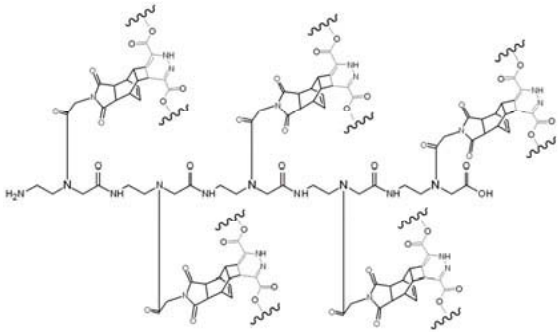

Fig. 5. Ligation product of the pentamer after the complete DAR_{inv} reaction with the diene compound derivatized with the fluorescence marker dansyl chloride.

Figure 5 shows the complex molecule after the complete ligation by the DAR_{inv} (shortened to the reaction site). The steps of the chemical reaction are documented in detail by Wiessler [2].

Figure 5 also shows the reaction product of DAR_{inv}-mediated ligation of the Reppe anhydride pentamer with the diaryl-1,2,4,5-tetrazine-3,6-dicarboxylate functionalized with two dansyl chloride dyes.

Here we demonstrated the design of PNA backbone building blocks suitable for a multi-faced spectrum of ligation reactions. The DAR_{inv} is chemically favourable [2, 5, 6].

For future applications the rapid and selective ligation must also fulfill strict requirements - e.g. 1) stable educts, and 2) proper intermediates and products. To meet these demands, the PNA's amide backbone can be considered as an appropriate candidate. The physico-chemical properties warrant the intensive development of amide backbone based molecules with all new functions qualified for ligation reactions in the field of the "Click chemistry".

References

1. Waldeck, W., et al. *Int. J. Med. Sci.* **5**, 273 (2008).
2. Wiessler, M., Waldeck, W., Kliem, C., Pipkorn, R., Braun, K. *Int. J. Med. Sci.* **7**, 19 (2009).
3. Braun, K., et al. *Int. J. Med. Sci.* **7**, 136 (2010).
4. Wiessler, M., et al. *Int. J. Med. Sci.* **7**, 213 (2010).
5. Pipkorn, R., et al. *J. Pept. Sci.* **15**, 235 (2009).
6. Pipkorn, R., Wiessler, M., Waldeck, W., Braun, K. *Biopolymers* **92**, 350 (2009).

Proceedings of the 31st European Peptide Symposium
Michal Lebl, Morten Meldal, Knud J. Jensen, Thomas Hoeg-Jensen (Editors)
European Peptide Society, 2010

Fmoc Solid Phase Synthesis of Peptide Thioesters for Native Chemical Ligations Employing a *tert*-butyl Thiol Linker

Richard Raz[2,3] and Jörg Rademann[1,2]

[1]*Medicinal Chemistry, Department of Pharmacy, Leipzig University, Leipzig, 01403, Germany;* [2]*Leibniz Institute of Molecular Pharmacology (FMP) Berlin, 13125, Germany;* [3]*Institute for Chemistry and Biochemistry Free University Berlin, Berlin, 14195, Germany*

Introduction

Peptide thioesters are key molecules in the chemical and biochemical synthesis of peptides and proteins, for example as starting materials for native chemical ligation (NCL) [1]. Thioesters are generally known to be base labile, which has previously precluded their use as linkers in Fmoc-based SPPS. *Tert*-butyl thioesters, however, are special and distinct from other thioesters: While being stable under alkaline conditions they are easily cleaved under only slightly basic conditions by primary thiolates [2]. In some examples they resisted treatment with nucleophilic base or with strong acid in the presence of a cleaved acetate ester in the very same molecule [3].

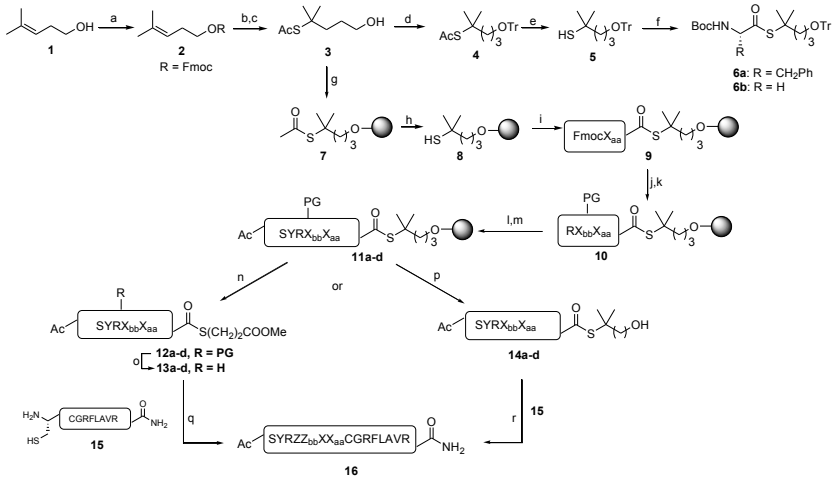

Fig. 1. Synthesis of the 4-mercapto-4-methylpentan-1-ol linker. a) Fmoc-Cl, pyridine, 1 h; b) CH_3COSH, $InCl_3$ (15 mol %), DCE, 14 h, 80 °C; c) Et_3N, pyridine, 2 h; d) Tr-Cl, DMAP, 18 h; e) NaSMe, MeOH, 1h; f) tBoc-Phe-OH, DCC, DMAP, DCM, 18 h; g) 2-Cl-tritylchloride resin, pyridine, 3d; h) H_2N-NH_2·Ac, DMF, 90 min.; i) Fmoc-X_{aa}-F, DIPEA, DMF, 1x2h, 1x18 h j) 20% piperidine/DMF; k) Fmoc-Arg-X_{bb}, HATU, HOAt, DIPEA, THF; l) Fmoc-SPPS, DIC, HOBt, DMF; m) Ac_2O, DIPEA, DMF; n) NaSPh, 15-crown-5, $HS(CH_2)_2COOMe$, THF, 4h; o) Reagent B (88% TFA, 5% H_2O, 2.5% TIS, 5% Phenol), 2.5 h; p) 94% TFA, 1% TIS, 2.5% water, 2.5% EDT, 2.5 h; q) NaSPh,15-crown-5, 10 equiv ***15****, r.t., 24 h; r) 0.1 M NaPi (pH = 7.4), thiophenol,* ***15****, r.t., 18 h.*

Results and Discussion

In order to validate this strategy, the stability of various thioesters was investigated under Fmoc-cleavage conditions (20% piperidine in DMF) by HPLC-MS at 220 nm. The following stability pattern was discovered: *tert*-butyl > *iso*-propyl > trityl > ethyl > benzyl. This finding confirms that beyond steric hinderance, the electronic properties of the thioester residue R determine the stability of thioesters. The *tert*-butyl thioester of Boc-phenylalanine displayed a half life of 6.5 days which strongly supported the feasibility of a *tert*-butyl linker system allowing for the direct synthesis and cleavage of peptide thioesters on solid support employing Fmoc chemistry.

Table 1. Yields of selected crude peptide thioesters

Entry	*Peptide thioester*	*Yield[a] (%)*
1	Ac-SYRGF-S$(CH_2)_2$COOMe **(13a)**	69/89[b]
2	Ac-SYRGW-S$(CH_2)_2$COOMe **(13b)**	78[b]
3	Ac-SYRGQ-S$(CH_2)_2$COOMe **(13c)**	86
4	Ac-SYRPV-S$(CH_2)_2$COOMe **(13d)**	67
5	Ac-SYRGF-MMP **(14a)**	54/83[b]
6	Ac-SYRGW-MMP **(14b)**	90[b]
7	Ac-SYRGQ-MMP **(14c)**	53
8	Ac-SYRGF-MMP **(14d)**	88

[a]*The yields were determined based on weight from the resulting peptide based on the first amino acid coupling. Purities of products were determined via HPLC at 220 nm with UV/Vis spectroscopy to be >90 % pure.* [b]*This peptide yield was attained with the coupling of a dipeptide to the initial amino acid.*

For investigating the stability of this linker on trityl resin, acetyl-protected 4-mercapto 4-methylpentanol (MMP) **3** was designed as a linker precursor, and model compound **6a** was synthesized (Figure 1). Thioester **6a** possessed a half-life of more than 9 days in the presence of 20% piperidine in DMF. In contrast to the Boc-Phe thioester **6a**, the corresponding thioester of Boc-glycine **6b** was synthesized and treated with 20% piperidine in DMF. The stability of **6b** in the presence of piperidine was reduced in comparison with **6a** displaying a half-life of approximately 7.5 hours.

Optimized acylation of the thiolinker resin **8** was accomplished with double couplings of Fmoc-amino acid fluorides delivering yields of **9** of up to 90% under racemization-free conditions. Diketopiperazine (DKP) formation after the second deblocking step led to only moderate loss of yield depending on the peptide sequence. This could be fully avoided by coupling of dipeptides to the first resin bound amino acid using HATU/HOAt.

For a detailed validation of the linker concept and the sequence-dependent comparison of reactions, a number of N-acetylated pentapeptides of generic structure Ac-SYR$X_{bb}X_{aa}$ **11** were synthesized and cleaved off the resin using various conditions. Nucleophilic cleavage gave protected peptides **12a-d** and subsequent treatment with TFA furnished peptidyl thioesters **13a-d** in high purity and excellent yields (Table 1). Acidic cleavage of resin-bound thioester peptides **11a-d** with TFA furnished **14a-d** also in high purity and good yields (Table 1). No cleavage of the MMP-linker was observed in any of these products, no truncated products or failed sequences were detected. NMR analysis of thioester **14a** showed conservation of the thioester carbonyl after TFA cleavage and thus excluded an S → O transesterification of the peptide C-terminus.

We have presented, to our knowledge, the first direct synthesis of peptide thioesters using common Fmoc-based methodology. The MMP-linker can be obtained quickly from well accessible starting materials and can be applied for the preparation of protected and unprotected peptide thioesters displaying a broad range of sequences. The products can be directly used in native chemical ligations and possibly in other reactions of peptidyl thioesters.

Acknowledgments
We thank André Horatscheck and Dr. Peter Schmieder for technical support, and Dr. Valentin Wittmann for helpful discussions. We gratefully acknowledge the DFG (RA895/2, FOR 806 and SFB 765) and the Fonds der Chemischen Industrie for continuous support.

References

1. a) Wieland, T., Bokelmann, E., Bauer, L., Lang, H.U., Lau, H. *Justus Liebigs Ann. Chem.* **583**, 129-149 (1953); b) Dawson, P.E., Muir, T.W., Clark-Lewis, I., Kent, S.B. *Science* **266**, 776-779 (1994); c) Raz, R. Rademann, J. submitted for publication.
2. Morse, B.K., Tarbell, D.S. *J. Am. Chem. Soc.* **74**, 416-419 (1952).
3. Mohrig, J.R., et al. *J. Org. Chem.* **72**, 793-798 (2007); c) Wallace, O.B., Springer, D.M. *Tetrahedron Lett.* **39,** 2693-2694 (1998).

Proceedings of the 31st European Peptide Symposium
Michal Lebl, Morten Meldal, Knud J. Jensen, Thomas Hoeg-Jensen (Editors)
European Peptide Society, 2010

Assembly and Stimulatory Activity of Backbone to Side Chain Cyclic Octapeptide-Ligands for the N-terminal SH2-domain of the Protein-tyrosine-phosphatase SHP-1

Mohammad S. Zoda[1], Martin Zacharias[2], Franziska Mussbach[1,3], Buerk Schaefer[3], and Siegmund Reissmann[1,3*]

[1]Friedrich-Schiller-University Jena, Institute of Biochemistry and Biophysics, Philoso-phenweg 12, D-07743, Jena, Germany; [2]Technische Universität München, Physik-Department (T38), James Franck-Str. 1, D-85748, Garching, Germany; [3]Jena-Bioscience GmbH, Loebstedter Str. 80, D-07749, Jena, Germany

Introduction

The cytosolic protein-tyrosine phosphatase SHP-1 plays an important role in processing of immune cells, in prevention of cancer genesis, and in cell adhesion and proliferation. In the non-stimulated form the catalytic domain it is shielded by the N-terminal SH2-domain. Activation by phosphotyrosine peptides occurs mainly through binding to this N-terminal SH2-domain [1,2]. As activating peptides would require a specific steric display of the phosphotyrosine side chain and backbone structure, a basic conformation was designed using a docking model [3,4]. The purpose of our study was to stabilize such spatial arrangement by a specific backbone to side chain cyclization, containing N-functionalized phosphotyrosine.

Results and Discussion

Assembly: The amino acid sequence was derived from the activating physiological Ros-kinase sequence: Glu-Gly-Leu Asn-pTyr-Met-Asp-Leu. To reduce the synthetic difficulties, Asn at position 4 was replaced by the isosteric α-amino-butyric acid (Abu) and Met at position 6 by Nle. Based on these concept peptides of the following general structure were synthesized:

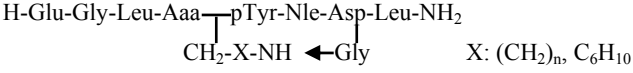

Optimizing the synthesis of the designed phosphotyrosine containing cyclic peptides we studied the preparation of N-functionalized tyrosine derivatives, coupling of the next amino acid to the N-alkylated tyrosine derivatives, and the assembly of the octapeptides [5].

Activities: Table 1 shows the stimulating activities of linear and cyclic octapeptides on highly purified SHP-1, free of any Tag. All linear and cyclic octapeptides stimulated the phosphatase activity of SHP-1. No reduction of the basal activity could be detected, indicating that no particular ligand has any inhibitory activity. Selected octapeptides (**2,7,9**) had no effect on the catalytic domain, even in high concentrations (250 μM). The stimulatory activity seems to depend on ring size, flexibility and hydrophobicity of the lactam bridges. Obviously the cycles force the peptides to form a folded conformation and bind to the deep and hydrophobic pocket of the SH2-domain. The reduced activity of some cyclic (**4**,**5**,**6**) compared to the linear analogs (**1**,**2**) results from a missing H-bond to the SH2-domain as the N-alkylated residues are not able to form a H-bond. In contrast to the N-alkyl amide group, the reduced amide bond in the cyclic octapeptide **9** is not only more flexible but also able to form H-bonds. Thus this compound shows the highest stimulating activity and furthermore represents an easier to synthesize structure. The found activities agree well with the docking model. By cyclization of the peptide ligands we achieved both, stabilization of bioactive conformation and stabilization against proteolytic degradation (cell homogenate, chymotrypsin and even proteinase K), respectively. Beside biological activity this proteolytic stability remains an essential prerequisite for developing orally applicable drugs.

To check the intracellular stimulation of SHP-1 we internalized certain octapeptide-ligands into transfected NIH 3T3-cells [1] using JBS-Proteoducin (a cocktail of cell penetrating peptides). In contrast to their stimulatory activity on isolated SHP-1 the tested

peptides (**2**,**7**,**9)** were unable to reduce the NGF-triggered cell aggregation through dephosphorylation of functional proteins and of adhesion molecules. We believe that this unexpected finding results from interaction with other functional proteins than SHP-1. Their activation can occur because the 120 (115) sequence-types of SH2-domains in the human genome are distributed in over more than 1000 functional proteins. Thus, each type of SH2-ligands can statistically activate about 10 different proteins. This fact and the found promiscuity of SH2-domains require developing of bi- or multivalent ligands [6] for signal transduction therapy and methods for local administration.

Table 1. Stimulation of recombinant human SHP-1 by linear and cyclic octapeptides

	Structure	*Activity*	*Ringsize*
	Basal activity of the SHP-1	28	
1	H-Gly-Glu-Leu-Asn-**p**Tyr-Nle-Asp-Leu-NH_2	260	0
2	H-Gly-Glu-Leu-Abu-**p**Tyr-Nle-Asp-Leu-NH_2	210	0
3	H-Glu-Gly-Leu-Abu-Tyr-Nle-Asp-Leu-NH_2	125	0
4	H-Glu-Gly-Leu-Asnψ[CO-N]**p**Tyr-Nle-Asp-Leu-NH_2 $(CH_2)_3$-NH ← Gly	140	17
5	H-Glu-Gly-Leu-Abuψ [CO-N]**p**Tyr-Nle-Asp-Leu-NH_2 $(CH_2)_3$-NH ← Gly	45	17
6	H-Glu-Gly-Leu-Abuψ [CO-N]**p**Tyr-Nle-Asp-Leu-NH_2 $(CH_2)_4$-NH ← Gly	105	18
7	H-Glu-Gly-Leu-Abuψ [CO-N]**p**Tyr-Nle-Asp-Leu-NH_2 $(CH_2)_5$-NH ← Gly	160	19
8	H-Glu-Gly-Leu-AbuΨ[CO-N]**p**Tyr-Nle-Asp-Leu-NH_2 Gly CH_2-C_6H_{10}-CH_2-NH	390	20
9	H-Glu-Gly-Glu-Abuψ [CH_2-NH]**p**Tyr-Nle-Lys-Leu- NH_2	420	21

Activity: nmolPi/min, released from p-nitrophenylphosphate

Acknowledgements
Financial support by the Deutsche Forschungsgemeinschaft (Re 853/10-1) is gratefully acknowledged. We thank Dr. Andrea Perner for performing ESI-MS analyses, Dr. Wolfgang Guenther for measurement of ^{1}H- and ^{13}C-NMR spectra and Manuela Flad for estimation of SHP-1 stimulation. Stabile transformed NIH3T3-cells are a generous gift from Prof. F. Boehmer.

References

1. Keilhack, H., Müller, M., Böhmer, S.-A., Frank, C., Weidner, K.M., Birchmeier, W., Ligensa, T., Berndt, A., Kosmehl, H., Günther B., Müller, T., Birchmeier, C., Böhmer, F.D. *J. Cell Biol.* **152**, 325-334 (2001).
2. Yang, J., Liang, X., Niu, T., Meng, W., Zhao, Z., Zhou, G.W. *J. Biol. Chem.* **273**, 28199-28207 (1998).
3. Imhof, D., Wieligmann, K., Hampel, K., Nothmann, D., Zoda, M.S., Schmidt-Arras, D., Böhmer, F., Reissmann, S. *J. Med. Chem.* **48**, 1528-1539 (2005).
4. Wieligmann, K., Castro, L.F., Zacharias, M. *In Silico Biology* **2**, 305-311 (2002).
5. Zoda, M.S., Zacharias, M., Reissmann, S. *J. Peptide Sci.* **16,** 403-413 (2010).
6. Teichmann, K., Kühl, T., König, I., Wieligmann, K., Zacharias, M., Imhof, D. *Biopolymers* **93,** 102-112 (2010).

Proceedings of the 31st European Peptide Symposium
Michal Lebl, Morten Meldal, Knud J. Jensen, Thomas Hoeg-Jensen (Editors)
European Peptide Society, 2010

Synthesis of Neuropeptide Y Analogues as PET Imaging Agents

Simon J. Mountford[1], Lei Zhang[2], Herbert Herzog[2], Bim Graham[1], and Philip E. Thompson[1]

[1]Medicinal Chemistry and Drug Action, Monash Institute of Pharmaceutical Sciences, Parkville, VIC, 3052, Australia; [2]Neuroscience Research Program, Garvan Institute of Medical Research, St Vincent's Hospital, Darlinghurst, NSW, 2010

Introduction

Neuropeptide Y is a 36-amino acid peptide that belongs to a family of structurally related peptides including pancreatic polypeptide (PP) and peptide YY (PYY). NPY is a peptide neurotransmitter mediating effects at the central nervous system [1] (e.g. stimulation of feeding behaviour and inhibition of anxiety) and the peripheral nervous system [2] (e.g. vasoconstriction, insulin release, renal secretion, gastrointestinal secretion). These central and peripheral activities are mediated by at least six G-protein coupled receptor subtypes (Y1, Y2, Y3, Y4, Y5, and y6) [3]. Over-expression of receptor subtype Y1 occurs in human tumours such as breast cancer [4] and therefore selective Y1-receptor peptide conjugates with the appropriate pharmacokinetic properties may be suitable for imaging and/or delivery of radiotherapy. However, the inclusion of auxiliary imaging groups on to peptides can dramatically change the potency and selectivity of the resultant conjugate. Incorporation of labels must not compromise the molecular recognition of the ligand by the receptor and retain the selectivity for the Y1-receptor. We are pursuing analogues of a variety of Y1 ligands, including novel amino acids whereby the side chain is modified to allow attachment of radiolabels or other imaging agents *via* click chemistry. In this paper we report on the synthetic approaches to such compounds.

Results and Discussion

We have developed syntheses of three reported Y1 ligands, [5,6] that can be adapted for inclusion of imaging agents. Included among these, are efficient synthesis of the cyclic disulfide-bridged peptide **1,** (Figure 1), and the cyclic lactam bridged dimer, GR231118, **2**. Peptides were synthesized using Fmoc-based solid phase peptide synthesis on a Protein Technologies PS3, automated peptide synthesizer on Rink Amide resin (0.7 meq). Couplings were performed using 3-fold excess of Fmoc-protected amino acid and HCTU/DIPEA for activation. After cleavage (Reagent K, 2h) peptides were purified by RP-HPLC. Oxidation to produce **1** was performed with 25mM NH_4HCO_3 (aq), 18h at RT. Synthesis of the dimeric peptide, **2,** was achieved by treatment of the Fmoc-protected linear precursor Ile-Glu-Pro-Dap-Tyr-Arg-Leu-Arg-Tyr-NH_2, with PyBOP at RT followed by Fmoc-deprotection with piperidine/DMF.

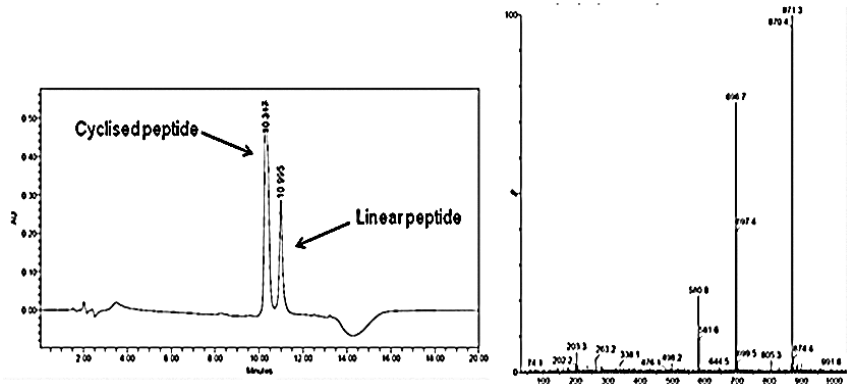

*Fig. 1. HPLC trace of disulfide bridged peptide **1,** spiked with linear precursor. ESI-MS of purified product.*

Table 1. Summary of peptide synthesis and receptor binding assay results

	Peptide	*Mol. Wt.*	*IC_{50}*	*Ref.*
1	Des-AA11-18,Cys7,21,D-Lys(Ac)9, D-His26, Pro34]-NPY	3480.0	0.16 nM	Mullins et al.
2	1992U91 (GR231118)	2352.7	0.084 nM	Daniels et al.
3	1911U90 (BVD15)	1206.4	16 nM	Daniels et al.
4	DOTA(Cu)-Lys4-BVD15	1669.4	7.9 nM	Guerin et al.
5	Fluorophore-triazole-(2)	2623.0	31 nM	
6	Fluorophore-A-triazole-(1)	3621.1	3.2 nM	
7	Fluorophore-B-triazole-(1)	3783.3	9.1 nM	

Utilizing brain tissue homogenates from Y2,Y4-receptor knockout mice, each of these peptides has been assayed as Y1 receptor ligands in competition binding assays versus ^{125}I-PYY (25 pM). The IC_{50} values obtained were in accord with previously reported data from other cell types.

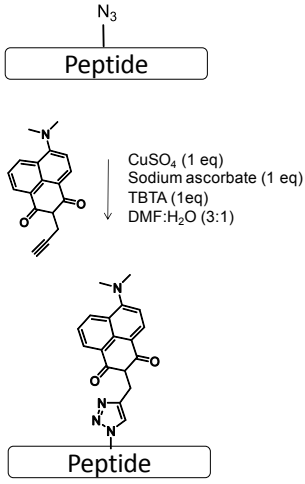

Fig. 2. Attachment of a fluorophore via the click reaction.

With these peptides in hand we have been preparing and assessing a range of conjugates possessing potential imaging moieties. We have been investigating the DOTA-style chelating groups and found that incorporation into the BVD15 structure, as described by Guerin, [7] is well tolerated by the receptor.

Our other synthetic focus has been to utilize click chemistry to allow a variety of peptide ligands and imaging moieties to be interchanged readily. We have synthesized known and novel alkyne and azide amino acids, and incorporated them efficiently into synthetic peptides. For click coupling, we have been utilizing a range of potential fluorophores as exemplified in Figure 2. Though successful, the incorporation of a fluorophore (not shown) into GR231118, resulted in a peptide **5** that is approximately 370-fold less potent at the Y1 receptor. Introduction of fluorophores into peptide **1,** has been more successful with product **6** only 20-fold less potent than the parent peptide.

A number of other highly potent peptide conjugates have been identified in this process that also reveal novel structure-activity relationships for Y1 receptor ligands. Further studies on the selectivity and metabolic stability of these peptides is currently underway.

Acknowledgments
We thank Oscar Liu for technical support. Supported by the Co-operative Research Centre for Biomedical Imaging and Development.

References

1. Wettstein, J.G., et al. *Pharmacol. Ther.* **65**, 397-414 (1995).
2. Sheikh, S.P. *Am. J. Physiol*. **261**, G701-715 (1991).
3. Michel, M.C., et al. *Pharmacol. Rev*. **50**, 143-150 (1998).
4. Reubi, J.C., et al. *Cancer Res*. **61**, 4636-4641 (2001).
5. Daniels, A.J., et al. *PNAS* **92**, 9067-9071 (1995).
6. Mullins, D., et al. *Mol. Pharmacol*. **60**, 534-540 (2001).
7. Guérin, B., et al. *Bioorg. Med. Chem. Lett.* **20**, 950-953 (2010).

Proceedings of the 31st European Peptide Symposium
Michal Lebl, Morten Meldal, Knud J. Jensen, Thomas Hoeg-Jensen (Editors)
European Peptide Society, 2010

3TS: Thiazolidine-Triggered Thioester Synthesis

Julien Dheur, Nathalie Ollivier, Annick Blanpain, and Oleg Melnyk
CNRS UMR 8161, Univ Lille Nord de France, Institut Pasteur de Lille, IFR 142, Institut de Biologie de Lille, 1 rue du Pr. Calmette, 59021, Lille, France; CSB platform (http://csb.ibl.fr)

Introduction

Nowadays, chemical synthesis of moderate size proteins is principally achieved by use of Native Chemical Ligation (NCL) developed by Dawson et al. in the middle of the 90's [1]. The principal constraint on NCL widespread application is the chemical synthesis of unprotected α-thioester fragments by the widely used Fmoc-Solid Phase Peptide Synthesis (Fmoc-SPPS) method. Based on both well-known *N* to *S*-acyl shift [2] and thiazolidine chemistry, we describe herein the efficient synthesis of C-term thioester peptides by combining supported and solution peptide chemistry. First, Fmoc / *t*-Bu SPPS is used to obtain highly stable amide peptides derivatives, featuring a *bis*-β-amino thiol arm at the C-terminus. In acidic medium, these peptides undergo a *N* to *S*-acyl-transfer-mediated step and the presence of an aldehyde such as glyoxylic acid affords the 3-(2-sulfanylethyl)-thiazolidine-2-carboxylic acid (SETCA) functionality in good yields.

Results and Discussion

Racemization-free synthesis of peptides (**1-4a**) featuring a *bis*-β-aminothiol arm at the C-terminus was achieved by Fmoc/*t*-Bu SPPS based on an innovative solid support compatible with classical elongation/deprotection/cleavage conditions (Figure 1). Reduction of **(1-4a)** disulfide bridge induced a pH dependent *N,S* acyl shift equilibrium between peptide amide (**1-4b**) and peptide thioester (**1-4c**). The later form was the major specie at pH below 2.8 (Figure 1).

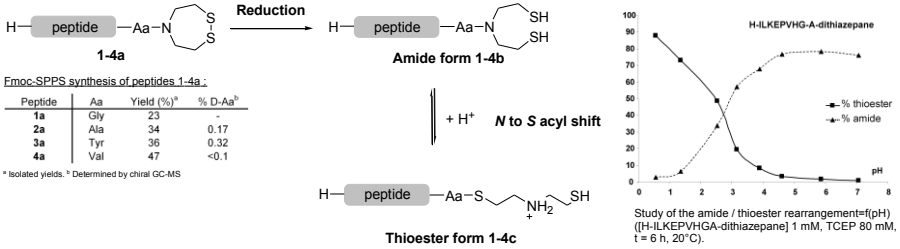

*Fig. 1. Study of the N,S acyl shift for peptides **(1-4b)**.*

To displace the amide / thioester equilibrium toward peptide thioesters, we investigated the usefulness of the widespread thiazolidine chemistry. Indeed, the intramolecular rearrangement of the *bis*-β-aminothiol leads to a free aminothiol moiety which could be engaged in the formation of a thiazolidine ring with an external aldehyde functionality. For this, dithiazepane peptides **(1-4a)** were first reduced with 5 equivalents of zinc dust in acidic medium (1% TFA aqueous solution) to afford quantitatively and rapidly the desired peptides **1-4b** [3]. Then, excess zinc was removed by centrifugation and the supernatant was recovered and engaged without further treatment in the thiazolidine formation step. SETCA-peptides formation took place efficiently in the 1% TFA solution (pH ~ 1) used for peptide **(1-4a)** reduction. Five equivalents of glyoxylic acid at 37°C led to the efficient formation of SETCA-peptides within 24 h, except for bulky amino acids like Valine which required longer reaction times. SETCA-peptides appeared to be very stable to RP-HPLC purification conditions and compounds were isolated with good yields (Figure 2).

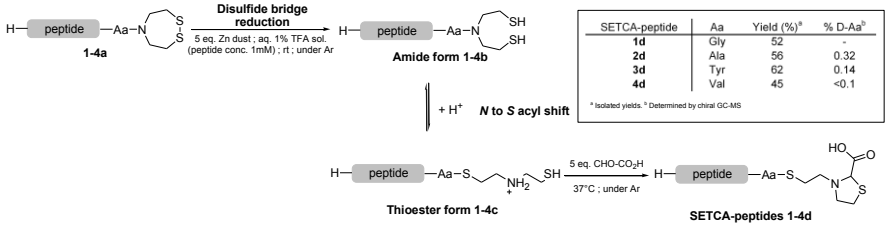

SETCA-peptide	Aa	Yield (%)[a]	% D-Aa[b]
1d	Gly	52	-
2d	Ala	56	0.32
3d	Tyr	62	0.14
4d	Val	45	<0.1

[a] Isolated yields. [b] Determined by chiral GC-MS

Fig. 2. Synthesis of SETCA-peptides. Peptides (1-4a) were reduced with zinc in acidic medium (1% aqueous TFA) and reacted with glyoxylic acid to afford thiazolidines (1-4d).

In order to evaluate their usefulness in NCL, SETCA-peptides were reacted with cysteinyl-peptide (Figure 3). Classical conditions were employed and ligated peptides were obtained in high isolated yields

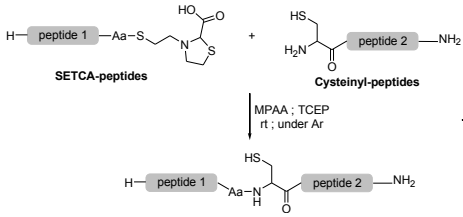

SETCA-peptide	Cys-peptide	Yield (%)[a]
H-ILKEPVHGY-SETCA	H-CILKEPVHGV-NH2	62
H-ILKEPVHGV-SETCA	H-CILKEPVHGV-NH2	47

[a] Isolated yields

Fig. 3. SETCA-peptides are useful thioesters for NCL.

Acknowledgments

We thank financial support from CNRS, Région Nord-Pas-de-Calais, Institut Pasteur de Lille and Cancéropôle Nord-Ouest. We acknowledge CSB platform (http://csb.ibl.fr) for technical support.

References

1. Dawson, P.E., Muir, T.W., Clark-Lewis, I., Kent, S.B.H. *Science* **266**, 776 (1994).
2. (a) Ollivier, N., Behr, J.-B, El-Mahdi, O., Blanpain, A., Melnyk, O. *Org. Lett.* **7**, 2647 (2005); (b) Nakamura, K., Mori, H., Kawakami, T., Hojo, H., Nakahara, Y.; Aimoto, S. *Int. J. Pep. Res. Therap.* **13**, 191 (2007); (c) Tsuda, S., Shigenaga, A., Bando, K., Otaka, A. *Org. Lett.* **11**, 823 (2009); (d) Kawakami, T., Aimoto, S. *Tetrahedron* **65**, 3871 (2009).
3. Erlandsson, M., Hällbrink, M. *Int. J. Pept. Res. Ther.* **11**, 261 (2005).

Proceedings of the 31st European Peptide Symposium
Michal Lebl, Morten Meldal, Knud J. Jensen, Thomas Hoeg-Jensen (Editors)
European Peptide Society, 2010

Convenient Synthesis of C-Terminal Glycopeptide Conjugates *via* Click Chemistry

Jean-Philippe Ebran, Nabil Dendane, and Oleg Melnyk*
CNRS UMR 8161, University of Lille Nord de France, Institut Pasteur de Lille, IFR 142, Institut de Biologie de Lille, 1 rue du Pr. Calmette, 59021, Lille, France ; http://csb.ibl.fr

Introduction

Glycoproteins are involved in many biological processes such as immune defense, cell growth or inflammation. Access to natural glycoproteins and glycopeptides are usually achieved by recombinant techniques or, by total or semisynthetic chemical ligation strategies. Another approach relies on the assembly of glycopeptides mimetics containing unnatural linkages between the peptide and oligosaccharide moieties using chemical ligation. To that purpose, the regioselective Cu-Catalyzed Azide-Alkyne Cycloaddition (CuAAC) developed independently by Meldal [1] and Sharpless [2] proved to be a very efficient and versatile tool. Indeed the chemoselective 1,3-dipolar cycloaddition between an organic azide and a terminal alkyne lead to the 1,4-disubstituted triazole linkage. Previous works [3,4] have reported the CuAAC ligation of unprotected azide carbohydrates and alkyne side chain peptides. Recently our research focused on the design of a novel access to unprotected C-terminal azide linker peptides and their application to copper catalyzed cycloaddition with oligosaccharide-based acetylenes.

Results and Discussion

A new reliable and efficient approach regarding the synthesis of 3-azidopropyl-amine [5] salts is depicted herein (Figure 1). A two steps synthesis from phtalimide bromide derivative, *via* an azide phtalimide intermediate, afforded the expected hydrochloride or tosylate salts with 82 and 85% overall yield, respectively. Fmoc/*t*Bu solid phase peptide synthesis (SPPS) was carried on 4-Fmoc hydrazino-benzoyl AM resin. The aminolysis cleavage [6] from the solid support was achieved by oxidation with Cu(II) in aerobic media using azidopropylamine as nucleophilic amine. The released peptides were deprotected by trifluoroacetic acid treatment giving the corresponding C-terminal azide linker peptides with yields from 12 to 29% (Figure 2). Copper oxidative cleavage was found to be the suitable method since low yield (<10%) was obtained using NBS oxidative cleavage.

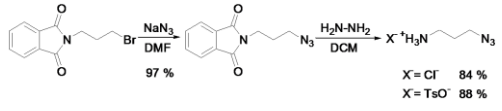

Fig. 1. Synthesis of amine-azide salts.

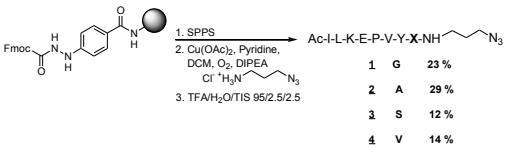

Fig. 2. Synthesis of C-terminal azide linker peptides.

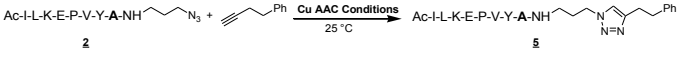

Entry	Catalyst	Solvent	Time	Conversion[b]
1	10 mol % CuI 5 eq DIPEA	DMF	20 h	< 5%
2	10 mol % $CuSO_4$-$5H_2O$ 100 mol % NaAsc	CH_3CN/H_2O 1:1	20 h	< 1%
3	10 mol % $CuSO_4$-$5H_2O$ 100 mol % NaAsc	*t*BuOH/H_2O 1:1	4 h	99% (89 %)[c]
4	5 mol % $CuSO_4$-$5H_2O$ 50 mol % NaAsc	*t*BuOH/H_2O 1:1	20 h	93 %
5	10 mol % $CuSO_4$-$5H_2O$ 100 mol % Cu(0)	*t*BuOH/H_2O 1:1	20 h	14 %
6	10 mol % $CuSO_4$-$5H_2O$ 100 mol % NaAsc	H_2O	20 h	< 5%

[a] Reactions were performed on 3 mM concentration of peptide with a ratio Azide to Alkyne of 1:2. [b] Conversion determined by HPLC integration on azide consumption. [c] Isolated yield

Fig. 3. Cu(I)-catalyzed cycloaddition optimization.

With alanine peptide **2** in hand, attention was turned to Cu(I)-catalysed cycloaddition optimisation using 4-phenyl-1-butyne as model alkyne. A

number of conditions were screened at room temperature in which both solvent and catalyst were varied (Figure 3). CuI/DIPEA system in DMF did not turn out to be suitable for the reaction (entry 1). $CuSO_4$-$5H_2O$ proved to be adequate catalyst yielding 1,3-triazole with 99% conversion in 4 h using *t*BuOH/H_2O (1:1) as solvent (entry 3) instead of CH_3CN/H_2O (1:1).

Decreasing catalyst loading to 5 mol % afforded the cycloadduct in 93% conversion but reaction time needed to be extended to 20 h (entry 4). *t*BuOH as cosolvent proved to be mandatory for the reaction to occur (entry 6). Optimized reaction conditions corresponded to 10 mol % $CuSO_4$-$5H_2O$ with 100 mol % sodium ascorbate (NaAsc) in *t*BuOH/H_2O (1:1). Encouraged by these results, a series of alkyne carbohydrates were examined along with various C-terminal azide linker peptides (Figure 4). Cu(I)-catalyzed cycloaddition of shikimic[7] (entry 1) or quinic [7] (entry 4) *N*-propargyl amide derivatives with peptides **1** and **3** afforded expected C-terminal glycopeptides respectively with 79 and 72% yields. Peptides **2** and **4** can also react efficiently with *O*-alkyne carbohydrates, such as α-glucose (entry 2) or β-*N*Ac glucosamine (entry 3) compounds, to yield the triazole cycloadducts with excellent conversions.

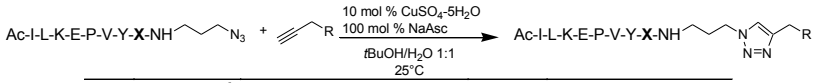

Entry	Azide peptide[a] (X)	Alkyne	Time	Conversion[b] (Yield)[c]
1	**G**	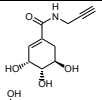	4 h	100 % (79 %)
2	**A**	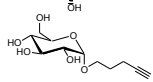	4 h	> 93 %
3	**V**	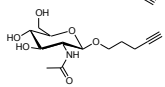	4 h	> 96 % (78 %)
4	**S**	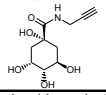	4 h	> 99 % (72 %)

[a] Reactions performed on 5 mM scale with a ratio Azide to Alkyne of 1:2. [b] Conversion determined by HPLC integration on azide consumption. [c] Isolated yield.

Fig. 4. C-Terminal glycopeptides synthesis.

In summary, an efficient and reliable two steps synthesis of amine-azide salts has been described. Cu(II) oxidative aminolysis has been applied to the synthesis of C-terminal azide linker peptides. Finally Cu(I)-catalysed cycloaddition can be carried out on unprotected C-terminal azide linker peptides with various carbohydrate derivatives and analogues with high yields leading to C-terminal glycopeptide conjugates.

Acknowledgments

We thank financial support from CNRS, Région Nord-Pas-de-Calais, Institut Pasteur de Lille and Endotis Pharma Inc. We acknowledge CSB platform (http://csb.ibl.fr) for technical support.

References

1. Tornøe, C.W., Christensen, C., Meldal, M. *J. Org. Chem.* 67, 3057-3064 (2002).
2. Rostovtsev, V.V., et al. *Angew. Chem. Int. Ed.* **41**, 2596-2599 (2002).
3. Lin, H., Walsh, C.T. *J. Am. Chem. Soc.* **126**, 13998-14003 (2004).
4. Wan, Q., Chen, J., Chen, G., Danishefsky, S.J. *J. Org. Chem.* **71**, 8244-8246 (2006).
5. a) Carboni, B., Benalil, A., Vaultier, M. *J. Org. Chem.* **58**, 3736-3741 (1993); b) Tamanini, S., Rigby, E.J., Motevalli, M., Todd, M.H., Watkinson, M. *Chem. Eur. J.* **15**, 3720-3728 (2009).
6. Brunsveld, L., et al. *Chem. Eur. J.* **11**, 2756-2772 (2005).
7. a) Grandjean, C., Gras-Masse, H., Melnyk, O. *Chem. Eur. J.* **7**, 230-239 (2001); b) Angyalosi, G., et al. *Bioorg. Med. Chem. Lett.* **12**, 2723-2727 (2002).

Proceedings of the 31st European Peptide Symposium
Michal Lebl, Morten Meldal, Knud J. Jensen, Thomas Hoeg-Jensen (Editors)
European Peptide Society, 2010

Preparation of Thioacid-Containing Amino Acids and Peptides and Their Application in Ligation Reactions

Katja Rohmer, Odin Keiper, Jamsad Mannuthodikayil, and Valentin Wittmann*
Fachbereich Chemie, Universität Konstanz, 78457, Konstanz, Germany

Introduction

Ligation reactions have emerged as an important tool for the chemoselective conjugation of large and complex molecules. One recent example is the reaction of thiocarboxylic acids (thioacids) with electron-deficient organic azides, such as sulfonyl azides [1]. This reaction proceeds at room temperature in different solvents and leads to *N*-acylsulfonamides in excellent yields. In the peptide field, this ligation reaction has been applied for the synthesis of neoglycopeptides [2], peptide mimetics [3], C-terminal labeling of peptide thioacids [4], and labeling of sulfonyl azide-modified peptides [5]. Here we present the preparation of hitherto unknown amino acids and peptides with protected side chain thioacids and their application in ligation reactions with sulfonyl azide-substituted carbohydrates.

Results and Discussion

Sulfonyl azide-modified carbohydrates **4** and **5** were obtained by Lewis acid-promoted glycosylation of 2-hydroxyethanesulfonyl azide **3** with peracetylated β-D-gluco- (**1**) and β-D-galactopyranose (**2**) (Scheme 1).

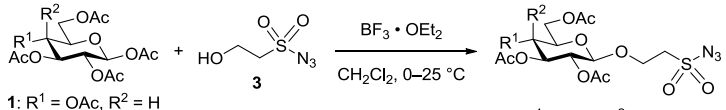

Scheme 1. Preparation of sulfonyl azide-modified carbohydrates.

For the synthesis of thioacid-containing amino acids, we initially reacted Boc-Asp(OSu)-OBn **6** and Boc-Glu(OSu)-OBn **7**, respectively, with sodium hydrogen sulfide to yield the thioacids Boc-Asp(SH)-OBn **8** and Boc-Glu(SH)-OBn **9**, respectively (Scheme 2). These products, however, were accompanied by small amounts (up to 20%) of diacyl disulfides **10** and **11**, respectively, due to oxidation. Fmoc-Asp(SH)-OBn was obtained following an analogous route. The thioacid/diacyl disulfide mixtures could, after work-up, be directly employed in subsequent ligation reactions with sulfonyl azides **4** and **5** giving access to the corresponding *N*-acylsulfonamides in yields between 83% and 94%.

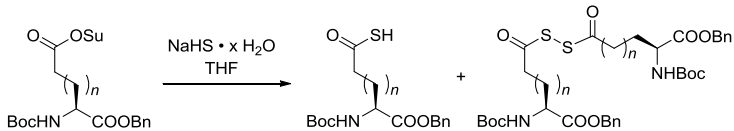

Scheme 2. Synthesis of thioacid-containing amino acids. Su = succinimidyl.

Improved yields of thioacids were obtained from trityl thioesters by treatment with 5% TFA in CH_2Cl_2. As depicted in Scheme 3, Fmoc-Asp-OBn **12** was converted to Fmoc-Asp(STrt)-OBn **13** by activation with DCC/DMAP. Thioacid Fmoc-Asp(SH)-OBn was generated by TFA treatment and, after evaporation, reacted with sulfonyl azide **4** to give ligation product **14** in 94% yield. It is worth mentioning that, under these conditions, the formation of diacyl disulfides was not observed.

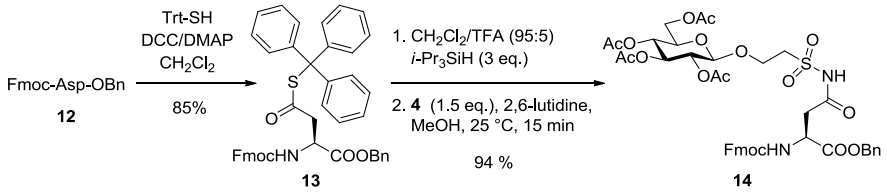

*Scheme 3. Synthesis of thioacid from trityl thioester and subsequent ligation reaction with sulfonyl azide-modified glucose **4**. Trt = trityl.*

Scheme 4 shows the preparation of a thioacid-containing dipeptide and its ligation to sulfonyl azide-modified glucose **4**. Fmoc-Asp(OBn)-OH **15** and H-Val-O*t*Bu **16** were coupled to give dipeptide **17**. After side chain deprotection, trityl thioester **18** was obtained via DCC/DMAP activation and reaction with triphenylmethanethiol. Employing the same reaction conditions described in Scheme 3, neoglycopeptide **19** was obtained in 83% yield after purification by RP-HPLC.

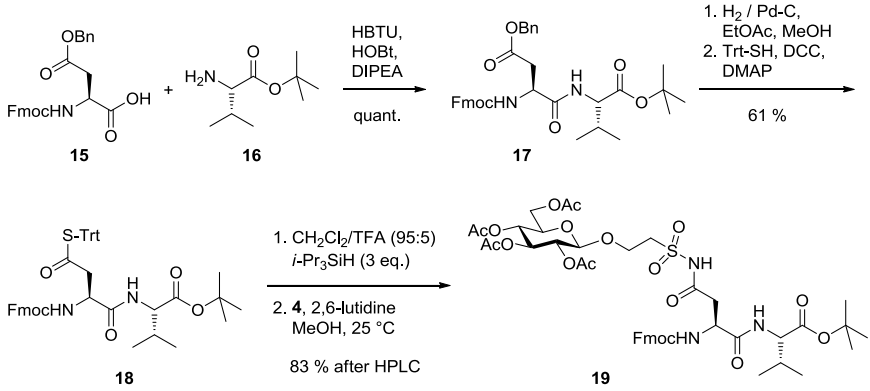

*Scheme 4. Synthesis of a thioacid-containing dipeptide and subsequent ligation with sulfonyl azide-modified glucose **4**.*

In summary, we have shown that the thioacid/sulfonyl azide ligation can be efficiently used for the conjugation of sulfonyl azide-modified carbohydrates to amino acids and peptides. Trityl thioesters turned out to be excellent precursors for the preparation of thioacids without concurrent formation of diacyl disulfides. Importantly, the modification of peptides containing thioacid derivatives of aspartic acid occurred without concurrent aspartimide formation.

Acknowledgments
Financial support by the Konstanz Research School Chemical Biology (PhD fellowship to J. M.) is gratefully acknowledged.

References

1. a) Shangguan, N., Katukojvala, S., Greenberg, R., Williams, L.J. *J. Am. Chem. Soc.* **125**, 7754-7755 (2003); b) Kolakowski, R.V., Shangguan, N., Sauers, R.R., Williams, L.J. *J. Am. Chem. Soc.* **128**, 5695-5702 (2006).
2. Zhu, X., Pachamuthu, K., Schmidt, R.R. *Org. Lett.* **6**, 1083-1085 (2004).
3. Merkx, R., Brouwer, A.J., Rijkers, D.T.S., Liskamp, R.M.J. *Org. Lett.* **7**, 1125-1128 (2005).
4. Zhang, X., Li, F., Lu, X.-W., Liu, C.-F. *Bioconjugate Chem.* **20**, 197-200 (2009).
5. Rijkers, D.T.S., Merkx, R., Yim, C.-B., Brouwer, A.J., Liskamp, R.M.J. *J. Pept. Sci.* **16**, 1-5 (2010).

Proceedings of the 31st European Peptide Symposium
Michal Lebl, Morten Meldal, Knud J. Jensen, Thomas Hoeg-Jensen (Editors)
European Peptide Society, 2010

Molecular Dynamics Calculation and NMR Conformational Studies of Heterodetic Triazolyl Cyclo-Nonapeptides: A Comparative Study

Mario Scrima[1], Anna Maria Papini[2], Michael Chorev[3], and Anna Maria D'Ursi[1]*

[1]Department of Pharmaceutical Sciences, University of Salerno, I-84084 Fisciano, Italy; [2]Laboratory of Peptide & Protein Chemistry & Biology, Dipartimento di Scienze Farmaceutiche, University of Firenze, I-50019, Italy; [3]Laboratory for Translational Research, Harvard Medical School, Cambridge, MA, 02139, U.S.A.; Department of Medicine, Brigham and Women's Hospital, Boston, MA, 02115, U.S.A.

Introduction

A solid phase assembly of model peptides derived from human parathyroid hormone-related protein (11-19) containing w-azido- and w-yl-α-amino acid residues in positions i and i+4 was cyclised in solution. These series of heterodetic cyclo-nonapeptides varied in the size of the disubstituted-[1,2,3]triazolyl-containing bridge, the location and the orientation of the [1,2,3]triazolyl moiety within the bridge (Scheme 1). We have recently reported a comprehensive conformational analysis employing CD, NMR and molecular dynamics in H_2O/HFA (1:1, v/v)[1]. Our data showed that all heterodetic cyclo-nonapeptides in which the [1,2,3]triazolyl is flanked by a total of 5 or 6 methylenes nicely accommodate α-helical structures.

Here we present an extensive unconstrained molecular dynamic calculation on the mentioned series of heterodetic cyclo-nonapeptides. The results of MD studies were compared to the experimental NMR data obtained in DMSO/water and in HFA/water solvents. MD trajectories confirm NMR structural data. MD data allow us to assess the role of the triazolyl moiety, the size of the methylene bridge, and the side chain specificity on the stabilization of the cyclo-peptide regular secondary structures.

Results and Discussion

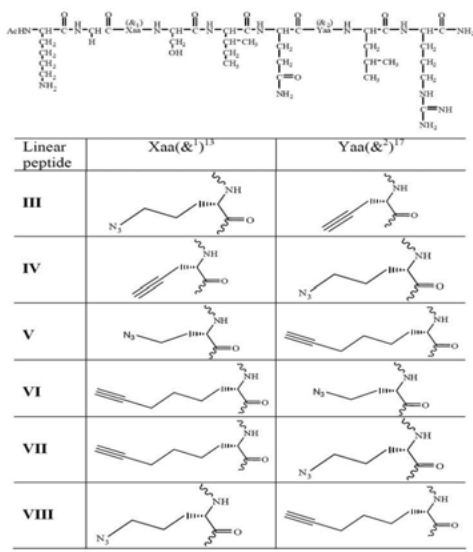

Scheme 1. 1,4-[1,2,3]triazolyl-containing cyclo-peptide (CuI-catalyzed 1,3-dipolar cycloaddition from the linear precursors).

NMR spectra were acquired in DMSO/water (80:20, v/v). Chemical shift assignments of the proton spectra of cyclopeptides **I-VIII** were achieved via the standard systematic application of DQF-COSY, TOCSY and NOESY experiments, using SPARKY software package according to the procedure of Wüthrich. The summary of NOE data for triazolyl containing cyclopeptides **I-VIII** are shown in Figure 1. Diagnostic sequential a-N(i,i+1) and NH-NH(i,i+1) NOE effects, as well as medium range a-N(i,i+2), NH-NH(i,i+2), NH-NH(i,i+3) NOE effects, define patterns which are diagnostic of specific secondary structures.

Analysis of NMR structure bundles using PROMOTIF shows that compounds **I** and **II** present γ-turn in the cyclic 3-5 portion. Compound **V** shows γ-turn and type I β-turn conformations in the 2-4 and 3-6 segments respectively. Compounds **VI** prevalently assumes γ-turn structure on the 5-7 residues. Compounds **VII** and **VIII** show type I β-turn and type VIII β-turn on the 3-6 and 3-9 residues respectively.

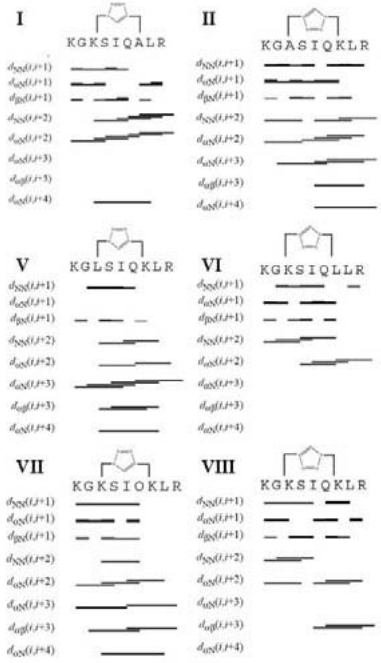

Fig. 1. Short and medium range connectivities of compounds ***I-VIII,*** *in DMSO/water (80:20, v/v).*

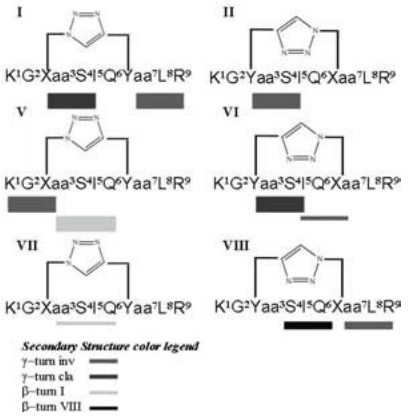

Fig. 2. Secondary structure of heterodetic triazolyl cyclo-nonapeptides in DMSO/H2O 80:20 v/v obatined by molecular dynamics studies. The intensity of bars is proportional to the number of obtained conformers.

MD studies were carried out in explicit solvent (DMSO/H2O 80:20 v/v) at room temperature for 10ns using NMR low energy structures as starting point. The MD results (Figure 2) confirm the conformational stability of selected NMR structures for all cyclopeptides during the simulations. The MD results confirm the conformational stability of selected NMR structures for all cyclopeptides during the simulations. The obtained data show that cyclopeptides V and VII are stabilized in the favourite conformation for the target interaction but only compound V preserve this correct stabilization during all simulation time.

To understand if the triazole was a coauthor in the correct conformational stabilization of cycloeptides V and VII, radial distribution function (RDF) analysis were carried out (data not shown). The interactions of triazole ring with Ser4 and Gln6 respectively were evaluated. The RDf results show that the interaction between Ser4 side chain and triazole is favourite when the triazole nitrogens are oriented toward the C-term segment (compounds II VI and VIII). This interaction gives an unfavourable contribution to the stabilization of the cyclopeptides II, VI, VII secondary structure. The RDf analysis shows that the interaction between Gln6 sidechain and triazole ring is favourite in cyclopeptides V and VII, where the triazole nitrogens are oriented toward the N-terminal region of cyclopeptides This interaction gives a favourable contribution to the stabilization of the cyclopeptides V and VII in bturn I secondary structure.

As previously mentioned we have recently reported a comprehensive conformational analysis employing CD, NMR and molecular dynamics of cyclopeptides I, II, V, VI, VII [1]. We compared the data presently reported, derived from NMR and MD analysis in DMSO/water, with the data in HFA/water. Interestingly all the data agree that that cyclo-nonapeptides (III-VI) in which the [1,2,3]triazolyl is flanked by a total of 5 or 6 methylenes nicely accommodate a-helical structures and reproduce very closely the helical structure stabilized by the analogous cyclo-nonapeptide in which Lys13 and Asp17 are bridged by the isosteric lactam.

The agreement between data in HFA/water and DMSO/water as well as the conformational stability in the dynamic calculation constitute strong evidence that the conformational preferences of tryazolil containing cyclopeptides are not affected by the solvent, but derive from intrinsic chemical-physical properties of the cyclopeptides characterized by different size of the disubstituted-[1,2,3]triazolyl-containing bridge, the location and the orientation of the [1,2,3]triazolyl moiety within the bridge.

References

1. Scrima, M., et al. *Eur. J. Org. Chem.* **3**, 446-457 (2010).

Proceedings of the 31st European Peptide Symposium
Michal Lebl, Morten Meldal, Knud J. Jensen, Thomas Hoeg-Jensen (Editors)
European Peptide Society, 2010

Reverse Thioether Ligation Approach to Dendrimeric Peptide Platforms: Solution and Solid Phase Studies

Marta Monsó, Beatriz G. de la Torre, Wioleta Kowalczyk, and David Andreu

Department of Experimental and Health Sciences, Pompeu Fabra University, Barcelona Biomedical Research Park, Barcelona, Spain

Introduction

Multimerization is recognized as one of the most effective tools for enhancing peptide immunogenicity. MAPs (multiple antigenic peptides) [1] are the most popular type of multimeric immunogen, based on a core of Lys dendrites onto which a number of peptide epitopes are attached. MAPs were first prepared by standard SPPS methods and later through various forms of solution ligation that allegedly improved on the all-SPPS approach. The most frequent solution approach uses a poly-Lys platform functionalized with α- and ε-chloroacetyl (ClAc) groups to which peptide epitopes (with a C-terminal Cys and N-terminally acylated) are then linked via thioether bonds. We have explored the reverse approach, namely a thiol-functionalized platform to which ClAc-modified peptide epitopes are linked (Figure 1).

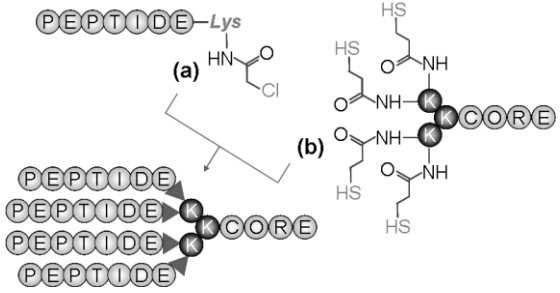

Fig. 1. Scheme of the reverse approach: (a) chloroacetylated epitope; (b) tetrathiol core (triangle denotes –Lys-CO-CH_2-S-CH_2-CH_2-CO-).

Results and Discussion

The starting components of the reverse ligation (Figure 1) were made by SPPS. The epitope (Figure 1, a) was C-terminally elongated with Fmoc-Lys(Mmt), which can be selectively side chain-deprotected and chloroacetylated on-resin. For the tetrathiol platform, Trt-protected mercaptopropionic acid (Mpa) was coupled via DIPCDI to a tetravalent MAP core.

One significant advantage of the reverse thioether ligation approach described here derives from the possibility of adding TCEP to the reaction mixture. The TCEP amounts are sufficient to maintain the thiol platform continuously reactive at the pH 7.5 of the experiment, so that the risk of disulfide cross-linking between core thiol groups is readily averted. In standard thioether ligations, epitope dimerization is a significant shortcoming

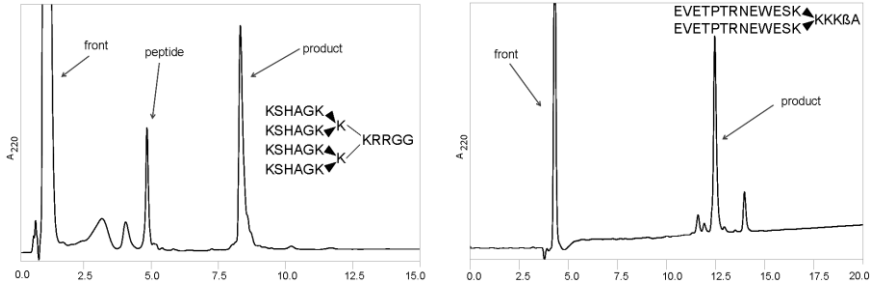

Fig. 2. Analytical HPLC of reverse thioether ligation in solution: (a) tetravalent construct, (b) bivalent construct (triangle denotes –CO-CH_2-S-CH_2-CH_2-CO-).

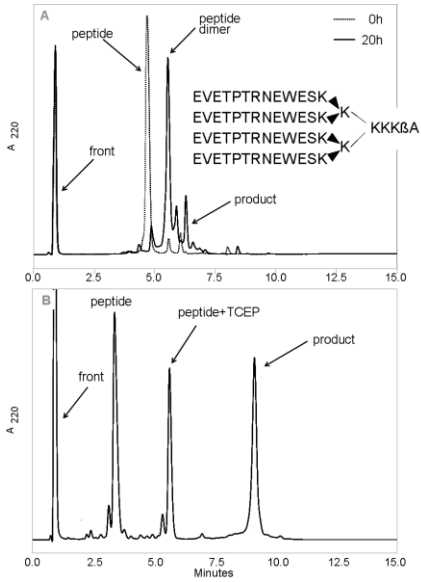

Fig. 3. Comparison of conventional (A) and reverse (B) thioether ligation approaches (triangle denotes thioether linkage).

(Figure 3B) [2], compounded by the high excess of thiol-functionalized epitope required, and the problem cannot be solved by TCEP *in situ* reduction, since exposure to high amounts of phosphine blocks reactive sites in the ClAc-functionalized core. In contrast, in the reverse format, TCEP amounts are low enough to pose minimal damage to ClAc groups of the peptide epitope. Another benefit of *in situ* TCEP reduction is that it allows employing much less peptide. Thus, a standard ligation using a tetravalent ClAc core typically requires at least 16 equiv of thiol-functionalized peptide (4 equiv / branch), of which a great deal becomes lost to dimerization. In contrast, the reverse format needs only 2 equiv / branch of ClAc peptide. All this ensures that ligations can be efficiently driven to quantitative replacement at all thiol sites, vs. the partial replacement levels inevitably encountered in standard thioether ligations. As a result, the end products are more homogeneous and easier to purify (Figures 2 and 3B).

Given the well-known advantages of solid phase vs. solution chemistry, we have also explored the feasibility of reverse thioether ligations in the solid phase. Among the anticipated advantages of such an approach are not only efficiency and cleanliness, with minimal purification required, but more importantly the possibility of (1) using water-compatible resins (e.g. ChemMatrix), and (2) driving ligations to completion by submitting the resin-bound thiol core to repeated alkylation (ClAc epitope) and reduction (TCEP) cycles, with intermediate washing steps. The resin-bound version of the polythiol core b (Figure 1) is not achievable by Mpa acylation of a standard poly-Lys core-resin, because complete on-resin removal of the S-Trt group is difficult. As an alternative, we have used acylation with dithiodipropionic acid followed by quantitative TCEP treatment. Thus prepared, the resin-bound polythiol platform can be efficiently used in reverse thioether ligation reactions similar to the ones described above.

Acknowledgements

W.K. is a fellow in the Juan de la Cierva Program of the Spanish Ministry of Science and Innovation (MICINN). Work supported by grants BIO2008-04487-CO3-02 from MICINN, and SGR2005-00494 and SGR2009-00494 from Generalitat de Catalunya.

References

1. Tam, J.P. *Proc. Natl. Acad. Sci. U.S.A.* **85**, 5409-5413 (1988).
2. Kowalczyk, W., De la Torre, B.G., Andreu, D. *Bioconj. Chem*. **21**, 102-110 (2010).

Proceedings of the 31st European Peptide Symposium
Michal Lebl, Morten Meldal, Knud J. Jensen, Thomas Hoeg-Jensen (Editors)
European Peptide Society, 2010

A Double Heteroatom Mitsunobu Coupling with Amino Hydroxybenzoic Acids on Solid Phase: A Novel Application of the Mitsunobu Reaction to Form Dendron Building Blocks

Tzachi Shalit[1,2], Amnon Albeck[2], and Gary Gellerman[1*]
[1]*Department of Biological Chemistry, Ariel University Center of Samaria, Ariel, Israel;*
[2]*Department of Chemistry, Bar-Ilan University, Ramat Gan, Israel*

Introduction

A new highly efficient double heteroatom Mitsunobu coupling with amino hydroxybenzoic acids on solid phase is described. We previously reported the synthesis of two types of bi-functional dendron building blocks (BB) from phenolic templates via double Mitsunobu reaction for convergent dendrimer growth on solid support [1]. This work is a novel and extended aspect of double heteroatom Mitsunobu coupling on solid phase for forming dendron building blocks containing an aminohydroxybenzoic acid core. The synthetic routes reported in this work are general and applicable for the preparation of diverse building blocks, controlling protection, arm length, chirality and peripheral functional groups. These novel units can form unusual dendritic architectures by solid phase chemistry, which may be incorporated into specific complex structures expanding the scope of dendrimer science.

Results and Discussion

Dendrimers are polymeric molecules with many arms emanating radially from a central core. A high degree of structural symmetry and a defined number of terminal groups rendering at the surface are important features of the dendritic architecture. Depending on their generation or order, dendrons not only have an impact on the backbone conformation and flexibility but also introduce a large number of functional groups at the periphery. The combination of these features creates an environment within the dendrimer molecule, which facilitates new discoveries in many important research areas such as Material and Biomedical Sciences [2]. However, most dendronized polymers known today are constructed from symmetrical dendron building blocks and carry only one kind of functional group, usually either amine or hydroxyl [3], which limits the choices for "surface" engineering. For increasing the options for surface chemical derivatization and branching capabilities, and therefore of dendrimers, we decided to develop a short synthesis for novel heteroatom dendron building blocks "around" a benzoic acid core. Coupling sites other than classical hydroxyl group can provide dendrons with extended tunable physico-chemical properties of the dendrimers. We did not find in the literature any direct Mitsunobu coupling to the amine group, most probably due to its insufficient acidity, although Iranpoor et al. reported facile *N*-alkylation of aromatic amines with 1° and 2° alcohols using triphenylphosphine (PPh_3) and 2,3-dichloro-5,6-dicyanobenzoquinone (DDQ) [4]. Our key hypothesis is based on the possible sufficient acidity of amine protons on the aminobenzoic acid core to enable Mitsunobu coupling, due to the presence of electron withdrawing (EW) carboxyester group on the benzene ring. Solid phase synthesis was chosen as our synthetic method, being advantageous over solution chemistry, mostly because of higher yields and avoiding problems associated with purification. Initially we have reacted Alloc protected 3-aminopropanol with preloaded 4-aminobenzoic acid **1** on acid sensitive Cl-Trt resin (Scheme 1), to examine whether the

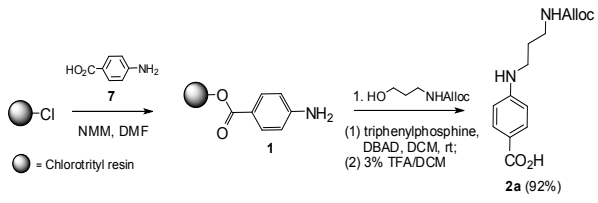

*Scheme 1. Mono-Mitsunobu solid phase synthesis of 4-aminobenzoic acid **2a**.*

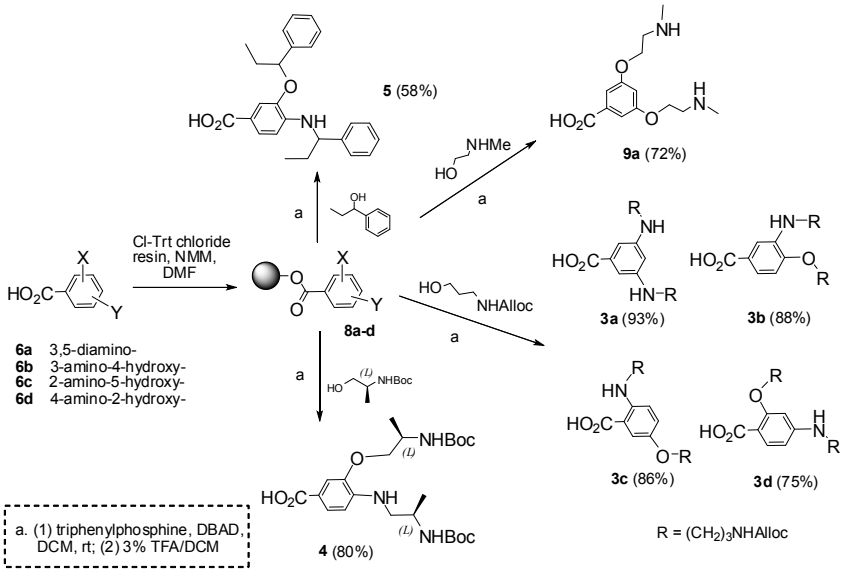

*Scheme 2. Double hetero-Mitsunobu solid phase synthesis of BBs **3a-d, 4, 5, 9a.***

corresponding aromatic amine can undergo Mitsunobu reaction. The Mitsunobu product **2a** was indeed obtained in good yields without further purification. Encouraged by this result, we proceeded to the double heteroatom Mitsunobu reaction with a variety of commercially available disubstituted amino- and hydroxybenzoic acids **6a-d.**

Subsequently, in same manner as for **7** but with larger excess of reagents, the preloaded **8a-d** were submitted to the series of heteroatom couplings with functionalized alcohols, yielding a unique collection of double armed dendron BBs **3a-d, 4, 5** and **9a** (Scheme 2). These BBs vary by nature of the alkylated atom (oxygen or amine), arm positioning on the benzene ring, length, peripheral functional groups, protection and chirality (BBs **4, 5**), demonstrating extended chiral diversification capabilities of amino and hydroxybenzoic acids from easily accessible protected amino alcohols. We also examined the tolerance of the Mitsunobu coupling reaction of alcohol synthons bearing unprotected aliphatic primary and secondary amines. Peripheral polyamines play an important role in medicinal dendrimer science due to their solubility, ion salvation properties, delivery and membrane permeability (PAMAM) [5]. Only an unprotected secondary amine was compatible with these conditions yielding unprotected **9a.** Attempts to optimize the reaction conditions, including microwave assisted chemistry, as well as implementation of our dendron building blocks in convergent dendrimer evolution on solid support are in progress.

Acknowledgments

We wish to thank Dr. Hugo Gotlib from Bar Ilan University for analytical assistance.

References

1. Gellerman, G., Shitrit, S., Shalit, T., Ganot, O., Albeck, A. *Tetrahedron* **66**, 878-886 (2010).
2. Swamy, K.K.C., Kumar, B.N.N, Pavan Kumar, K.V.P. *Chem. Rev*. **109**, 2551-2651 (2009).
3. Mitsunobu, O. *Synthesis* 1-28 (1981).
4. Iranpoor, N., Firouzabadi, H., Khalili, H. *Tetrahedron* **65**, 3893-3899 (2009).
5. Majoros, I.J., Myc, A., Baker, J.R., Jr. *Biomacromolecules* **7**, 572-579 (2006).

Proceedings of the 31st European Peptide Symposium
Michal Lebl, Morten Meldal, Knud J. Jensen, Thomas Hoeg-Jensen (Editors)
European Peptide Society, 2010

Peptidomimetic PKB/Akt Inhibitors as Anti-Cancer Drug Leads

Yftah Tal-Gan[1], Shoshana Klein[2], Alexander Levitzki[2], and Chaim Gilon[1]

[1]*Institute of Chemistry, The Hebrew University of Jerusalem, Jerusalem, 91904, Israel*
[2]*Unit of Cellular Signaling, Dept of Biological Chemistry, The Alexander Silberman Institute of Life Sciences, The Hebrew University of Jerusalem, Jerusalem, 91904, Israel*

Introduction

Protein Kinase B (PKB/Akt), a member of the Ser/Thr kinase family, is involved in cell proliferation and suppresses cell death (apoptosis). Persistently activated PKB/Akt is associated with many types of human cancer, such as breast, colon, ovary, pancreas, head and neck, and prostate cancer. Inhibition of PKB/Akt is therefore an attractive strategy for targeted cancer therapy. Screening of small molecules as enzyme inhibitors is very common. However, in the case of ATP-mimetic kinase inhibitors, the resulting small molecular weight inhibitors usually exhibit low selectivity towards the desired kinase, because kinase ATP-binding sites are strongly conserved. Substrate-based inhibitors, especially those based on the peptidic nature of the substrate, are more likely to be selective, because the substrate-binding site on each kinase is specific.

Recently, a series of peptides derived from a PKB/Akt substrate – the protein Glycogen Synthase Kinase 3 (GSK-3) – was developed and their interactions with PKB/Akt were studied [1]. The peptide Arg-Pro-Arg-Nva-Tyr-Dap-Hol (PTR6154), based on the GSK-3 substrate peptide Arg-Pro-Arg-Thr-Ser-Ser-Phe, was found to be a selective PKB/Akt inhibitor [1]. PTR6154 was used as a parent compound for this study. A library of peptomer derivatives of PTR6154 was produced and tested for inhibition of PKB/Akt.

Results and Discussion

The peptomers were named according to the modified residue (e.g. Peptomer 1 means modification on Arg 1). There are two synthetic pathways for solid phase peptomer synthesis: The first is based on reductive alkylation of glycine with the appropriate aldehyde or ketone to obtain the desired N^{α}-alkylated glycine derivative (Scheme 1a) [2]. The second method is based on coupling of bromo-acetic acid to the free amine of the growing peptide, followed by the introduction of a primary amine bearing the appropriate alkyl side chain residue to obtain the desired N^{α}-alkylated glycine derivative (Scheme 1b), and is often referred to as the "sub-monomer" method [3]. Peptomers 4a, 5a and 7a (Table 1) were synthesized, using readily available aldehydes and amines, by both methods for comparison. No significant differences were detected between the two methods, either in yield or in product purity. In Peptomer 7a, a racemic HoIle peptomer building unit was incorporated instead of a Hol peptomer building unit, for reasons of starting material availability. In order to synthesize Peptomers 1a and 3a (Table 1), we used the microwave assisted reductive alkylation procedure of Park, et al. [4].

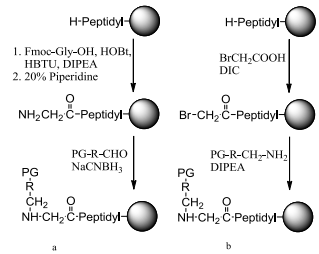

Scheme 1. Synthetic pathways for N^{α}-alkylated glycine derivative: a) using reductive alkylation. b) using the "sub-monomer" method. R – side chain, PG – protecting group.

The peptomer library was screened for inhibition of PKB/Akt in a cell-free radioactive assay, and compared with PTR6154 [5]. The peptomer modification that was introduced led to a dramatic decrease in potency (Table 1). All of the peptomer analogs had negligible potency, and the "best" peptomers were still 10-fold less active than PTR6154. These results suggest that the local constraints induced by the N^{α}-alkylated glycine derivative, or the inability of the backbone to produce the same number of hydrogen bonds as the parent PTR6154, reduced PKB/Akt inhibition.

Our results indicate that the hydrogen bonds formed by the backbone have important roles in site recognition and affinity to the enzyme. These results further suggest that

Table 1. Inhibitory activity of the peptoid library

Name	*Structure*	*% Inhibition (100 μM)*	*% Inhibition (5 μM)*
PTR6154	H-Arg-Pro-Arg-Nva-Tyr-Dap-Hol-NH_2	99 ± 1	87 ± 2
Peptomer 1a	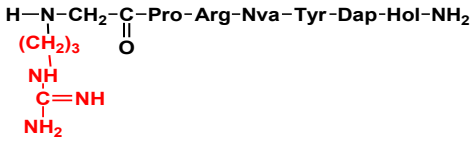	95 ± 1	32 ± 4
Peptomer 3a	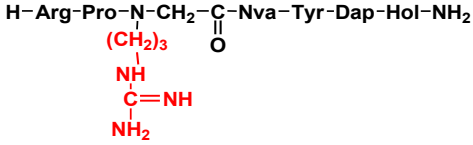	30 ± 4	N.D.
Peptomer 4a	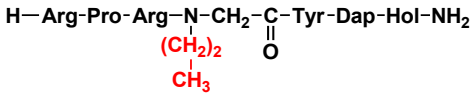	16 ± 4	N.D.
Peptomer 5a	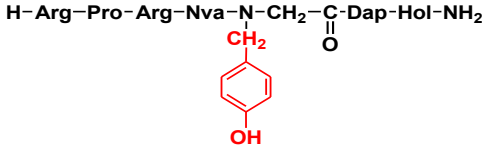	85 ± 5	23 ± 4
Peptomer 7a[#]	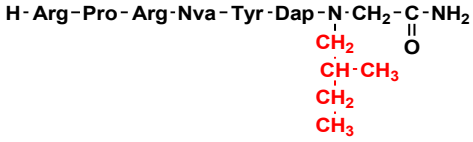	39 ± 1	N.D.

PKB/Akt inhibition was determined according to radioactive kinase assay. Inhibition at the concentration of inhibitor indicated in parenthesis is shown as the percent of reduction in PKB/Akt activity (0% inhibition = activity in the absence of inhibitor). % inhibition at 5 μM was determined only for inhibitors that showed over 80% inhibition at 100 μM. N.I. = no inhibition. N.D. = not determined. [#] A HoIle peptomer building unit was prepared instead of a Hol peptomer building unit.

conformational freedom is vital for proper substrate-enzyme complementarity fit and therefore, any local constraints induced by steric effects reduce efficacy significantly.

Acknowledgments
A.L. was supported by grants from The European Commission (Prokinase Consortium), the Prostate Cancer Foundation (USA) and the Goldhirsh Foundation (USA).

References

1. Litman, P., et al. *Biochemistry* **46**, 4716-4724 (2007).
2. Meyer, J.P., Davis, P., et al. *J. Med. Chem.* **38**, 3462 (1995).
3. Nuss, J.M., et al. *Pure Appl. Chem.* **69**, 447 (1997).
4. Park, M.-S., Oh, H.-S., Cho, H., Lee, K.-H. *Tetrahedron Lett.* **48**, 1053 (2007).
5. Tal-Gan, Y., Freeman, N.S., Klein, S., Levitzki, A., Gilon, C. *Bioorg. Med. Chem.* **18**, 2976-2985 (2010).

Proceedings of the 31st European Peptide Symposium
Michal Lebl, Morten Meldal, Knud J. Jensen, Thomas Hoeg-Jensen (Editors)
European Peptide Society, 2010

Application of Fragment Based Drug Design for the Discovery of Peptidomimetic as Inhibitors of Cyclophilins

Lionel Colliandre[1], Abdelhakim Ahmed-Belkacem[2], Jean-Michel Pawlotsly[2], and Jean-François Guichou[1]
[1]Centre de Biochimie Structurale, UMR5048, UM1, CNRS, Inserm, 34090, Montpellier, France; [2]IMRB, Inserm U955, Equipe 18, Hôpital Henri Mondor, 94010, Créteil, France

Introduction

Ongoing Hepatitis C virus (HCV) is a major causative agent of chronic hepatitis, cirrhosis, and hepatocellular carcinoma. Approximately 200 million individuals are infected worldwide and HCV infection causes approximately 280,000 deaths per year. The current standard treatment for chronic hepatitis C is based on the use of pegylated interferon (IFN-α) in combination with ribavirin for up to one year. However, only up to 50% of patient with HCV genotype 1 infection can eradicate infection upon therapy. Moreover, both IFN-α and ribavirin are associated with adverse effects. Therefore, more efficient and better tolerated therapies are needed for hepatitis C. Current HCV "Drug Discovery" efforts focus primarily on developing molecules that specifically inhibit the function of two viral enzymes: the NS3-4A serine protease and the NS5B RNA-dependant polymerase, both of which are essential for viral replication. However, due to the high genetic variability of the virus, amino acid substitutions that confer drug resistance are likely to emerge during treatment with specific inhibitors of the HCV protease or polymerase. Viruses depend on host-derived factors that are required for viral replication and may be less prone to the development of drug resistance. Cyclophilins are cellular factors that were initially identified as having high affinity for cyclosporine A (CsA), an immunosuppressive agent. Cyclophilins form a family of peptidyl-prolyl isomerases that catalyze the cis-trans interconversion of amino-terminal peptide bonds to proline residues, facilitating changes in protein conformation. Some authors have recently reported the involvement of CypA and B in HCV genome replication and proposed a model for the molecular mechanism, where Cyp's would interact with NS5B and promote its RNA binding affinity. The Cyp's represents an interesting target for the development of new antiviral strategies targeting HCV replication without targeting viral enzymes. The application of Fragment Based Drug Design to Cyclophilins for the design and synthesis of peptidomimetic as inhibitors for these enzymes was performed.

Results and Discussion

Several rounds of virtual screening were used to focus on fragments to be screened by NMR and X-Ray crystallography against CypD. Virtual screening was performed on filtered lists from the ZINC Database. Examples of the properties used for filtering were molecular weight (<250), clogP (<3), and restriction to the chemical supplier Sigma-Aldrich, Acros, Chembridge, ChemDiv and Maybridge. For example, we were keen to find other molecules capable of forming the hydrogen bond interactions in the Abu pocket. The starting format of the compounds was in 2D SDFiles and 3D coordinates were generated using CORINA. Docking studies were performed using the program interface LEA3D based on the docking program FlexX. The X-ray coordinates of CypD PDB-ID 2bit were used to dock the fragments. The site for docking was defined to cover the entire active site with the two pockets (hydrophobic and Abu pocket). No water molecules were included in the binding site. After docking, the top 10 percent poses of the docking were manually inspected and compounds which formed good hydrogen bonds or made lipophilic contact with CypD were selected. The virtual screening set consisting of 102 compounds was then used in the NMR or X-crystallography experiment. We first produced ^{15}N labelled CypD and made the attribution of the ^{15}N HSQC spectrum for CypD in presence or absence of 20% DMSO-*d6*. A set of 50 fragments were selected from virtual screening and used to screening by NMR experiment. The ability of compounds to interact with CypD was determined by 2D HSQC spectrum NMR measurements using 100 μM protein sample and mixtures of 10 fragments per sample (10 mM each in buffer or in 20% DMSO depending on solubility). For each mark of the HSQC ^{1}H-^{15}N spectra, we measured the variation of the chemical shifts in absence and in presence of the compounds. The variation is considered as

significant when it is greater or equal to twice of the standard deviation for all the chemical shifts variations of the spectra. Compounds that cause a significant variation of marks that correspond to active site residues are considered as NMR hit. Compound mixtures producing significant chemical shift variations were subsequently deconvoluted (10 hits). The NMR hits were used to select another set of fragment (52 compounds). We produced a large number of CypD crystals which are suitable for soaking [1]. The soaking conditions were demonstrated to be robust for use with a variety of fragments. CypD crystals were soaked with 52 compounds, and the X-ray structures for the crystals were obtained. Coot was used to fit into the Fo-Fc electron density maps that were calculated after initial refinement against an unliganded CypD structure (2BIT.pdb). Protein-ligand structures of bound fragments were subjected to further refinement steps. Multiple low affinity fragment hits were identified that bind the hydrophobic pocket, the Abu pocket, and some were found to be multibinders. The output from this fragment screening process was a set of experimentally determined binding modes for several fragments bound to CypD (14 hits, Figure 1).

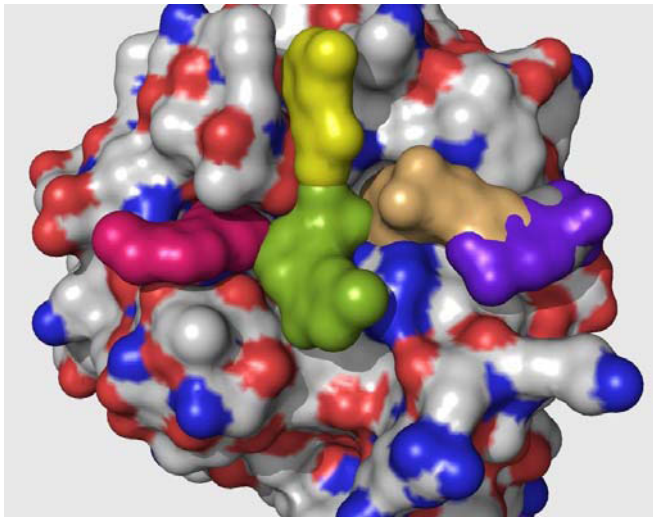

Fig. 1. Examples of complexes of CypD with 5 fragments (superposition): the protein and the ligands are represented by their surface.

This information was used to design different ligands which are composed of the different fragments connected by different linker. We were able to find some molecules (peptidomimetics) with inhibition around 500 nM against the Cyp's peptidyl-prolyl isomerase activity [2] and with a micromolar activity against the HCV virus. The process to develop nanomolar compounds is ongoing and it should afford new chemical tools to treat patients with an HCV infection.

Acknowledgments
Supported by grant ANR Jeune Chercheur "Fragscreens", ANRS (2009-139) and Région Languedoc-Roussillon "Chercheur d'Avenir" (Source of Money).

References

1. Schlatter, D., Thoma, R., Küng, E., Stihle, M., Müller, F., Borroni, E., Cesura, A., Hennig, M. *Acta Crystallographica* Section D, **D61**, 513-519 (2005).
2. Kofron, J.L., Kuzmic, P., Kishore, V., Colon-Bonilla, E., Rich, D.H. *Biochemistry* **30**, 6127-6134 (1991).

Proceedings of the 31st European Peptide Symposium
Michal Lebl, Morten Meldal, Knud J. Jensen, Thomas Hoeg-Jensen (Editors)
European Peptide Society, 2010

SPOS Route to Novel 9-Anilinoacridine Derivatives: Biological Evaluation

Gary Gellerman[1*], Tamara Brider[1], Arie Budovsky[2], and Stella Aronov[2]

[1]Department of Biological Chemistry, Ariel University Center of Samaria, Ariel, 40700, Israel; [2]Department of Molecular Biology, Ariel University Center of Samaria, Ariel, 40700, Israel

Introduction

A highly efficient derivatization of medicinally-important 9-aminoacridine (9-AA) at the amine position using S_NAr reaction on solid phase is described. The resulting 9-anilino-acridines (9-AnA), bis-9-anilinoacridines and their peptidyl derivatives are easily obtained in good yields from accessible starting materials, rapidly generating novel potential DNA intercalators with variable spacer lengths and charged, polar or hydrophobic residues at desired positions, which can increase binding affinity, conformation stability, intracellular transport and/or biological activity. The synthetic routes reported in this work are generally applicable and significantly expanding the scope of potential 9-AA anticancer hits. *In vitro* anticancer activity of representative compounds has been evaluated.

Results and Discussion

The 9-aminoacridine (9-AA) core fragment is a structure of interest to medicinal chemists and appears in many biologically active compounds, mostly with anticancer and anti-malaria applications. In the field of antitumor DNA-intercalating agents, 9-anilinoacridine derivatives play an important role due to their antiproliferative properties [1]. Several cancer chemotherapeutics based on the 9-aminoacridine scaffold, such as Amsacrine and Ledakrin, have been developed. So far, 9-AA analogs have been prepared through several step synthesis involving harsh conditions and laborious purification of intermediates and

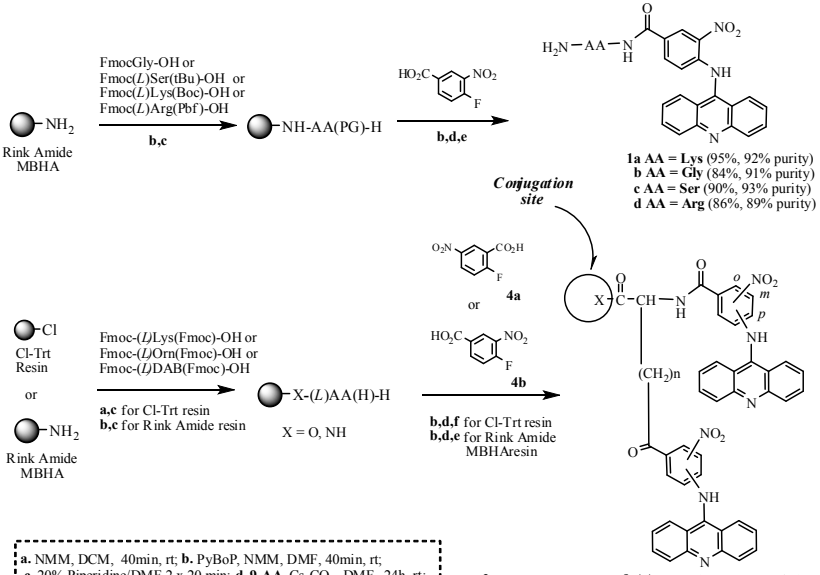

*Scheme 1. SPOS of mono and bispeptidyl-9-anilinoacridine derivatives **1** and **2** by S_NAr.*

Table 1. IC_{50} in μmol; Cell lines: HT29-Colon carcinoma, MDA-MB-A31-renal, NCI-ADR-MDR ovarian, OVCAR8-ovarian, MCF7-breast, H1299-lung carcinoma; na-not active

Compound	*HT29*	*MDA-MB A31*	*NCI-ADR*	*OVCAR8*	*MCF7*	*H1299*
9-AA	2.9	1.1	1.8	5.2	1.5	8.5
1a	2.6	1.6	2.4	5.1	2.4	1.04
1b	6.6	2.7	na	1.2	2.4	na
1c	2.8	na	50	9.8	2.4	na
1d	1.8	11.7	na	na	6.3	na
2a	15	13	7.2	4.7	1.2	na
2b	0.9	0.6	0.2	0.4	0.7	0.6
2c	0.8	0.4	50	2.5	0.3	0.9
2d	1	1.2	0.8	3.7	0.8	2.6
Amsacrine	0.7	0.6	1.5	50	0.6	3

final compounds. Thus, finding short and efficient solid phase organic synthesis (SPOS) methods for the rapid generation of new 9-AA core based compounds will greatly enhance their availability for examination in biological systems. We have previously demonstrated a new, highly-efficient, one-pot derivatization in solution of 9-AA at the 9-amine position by simple reductive amination and S_NAr reactions yielding series of novel substituted *N*(9)-benzylaminoacridines and *N*(9)-anilinoacridines correspondingly [2]. This unique method allows formation of aniline, and benzyl tethers with electron withdrawing (EW) groups on 9-AA core. This is a difficult task to accomplish using traditional nucleophilic substitution of the deactivated amines on 9-chloroacridines [3]. Recently, we developed a SPOS approach to novel 9-AA derivatives and various mono- and bis-9-anilinoacridine peptidyl substances [4] using Fmoc chemistry compatible protocol. Such synthetic strategy rapidly generates 9-AAs with variable spacer lengths and charged, polar or hydrophobic residues at desired positions like in **1** and **2** (Scheme 1), which can increase binding affinity, conformation stability and/or biological activity. Notably, the CO_2H on **2a** after cleavage from acid sensitive resin (Cl-Trt resin) can act as an anchor for possible conjugation to the carrier. The preliminary screening of representative **1** and **2** on several cancer cell lines (Table 1) exhibits an antiproliferative activity for all compounds in μmolar to sub-μmolar concentrations, as compared to 9AA itself and Amsacrine. The differences in the sensitivity to the tested compounds were observed between these cell lines. This observation can be explained in terms of SAR centered on the substitution pattern on the aniline moiety. Interestingly, our peptidyl 9-AnAs are significantly more stable in human plasma ($t_{1/2}$ = 12h-36h) than Amsacrine ($t_{1/2}$ = 0.5h) and AHMA ($t_{1/2}$ = 1.5h) [5], pointing on possible reduced toxicity than parent 9-AA drugs. Encouraged by this feasibility experiment, we proceeded to the massive rational drug design program based on our synthetic tools and assisted by extensively reported modeling data on 9-AAs and their peptidyl derivatives [6]. Our current research is focused on the optimization and the mechanism of action studies of the recently discovered most promising sub-μmolar leads against lung carcinoma (H1299), relatively insensitive to chemotherapy.

Acknowledgments
We wish to thank Dr. Hugo Gotlib from Bar Ilan University for analytical assistance.

References

1. Sebestik, J., et al. *Curr. Prot. Pept. Sci*. **8**, 471-483 (2007).
2. Gellerman, G., Gaisin, V., Brider, T. *Tet. Lett.* **51**, 836-839 (2010).
3. Guetzoyan, L., Ramiandrasoa, F., Perree-Fauvet, M. *Bioorg. Med. Chem*. **15**, 3278-3289 (2007).
4. He, Z., et al. *Bioorg. Med. Chem*. **16**, 4390-4400 (2008).
5. Tsann-Long, Su *Cur. Med. Chem.* **9**, 1677-1688 (2002).
6. Caffrey, C.R., et al. *Antimicrobial Agents and Chemotherapy* **51**, 2164-2172 (2007).

Proceedings of the 31st European Peptide Symposium
Michal Lebl, Morten Meldal, Knud J. Jensen, Thomas Hoeg-Jensen (Editors)
European Peptide Society, 2010

Hepatitis C Virus NS3 Protease Inhibitors Based on a 2(1*H*)-Pyrazinone-Glycine Scaffold

Anna Karin Belfrage[1], Johan Gising[1], Pernilla Örtqvist[1], Aparna Vema[1], Sofia Svahn Gustafsson[2], Mats Larhed[1], U. Helena Danielson[2], and Anja Sandström[1]

[1]Department of Medicinal Chemistry, Organic Pharmaceutical Chemistry, BMC, Uppsala University, Box 574, SE-751 23, Uppsala, Sweden; [2]Department of Biochemistry and Organic Chemistry, BMC, Uppsala University, Box 596, SE-751 24, Uppsala, Sweden

Introduction

Hepatitis C virus (HCV) infection is a serious and growing threat to public health. An estimated 170 million of the global population are infected and at risk of developing cirrhosis or cancer [1]. The current standard treatment, associated with severe adverse effects, involves a combination of pegylated interferon-α and ribavirin. The efficacy is dependent on the genotype of the virus with sustained virological response in only 40-50% of genotype 1 infected patients [2]. Viral resistance is one of the major issues in future development of HCV therapies. To combat the mutated virus there is a need for novel inhibitors based on structural motifs different from those of known anti-HCV clinical candidates. Substituted pyrazinones can act as β-strand inducers in protease inhibitors. Consequently, this heterocyclic system is interesting from a medicinal chemistry point of view. We have previously reported a rapid microwave method for synthesis of *N*-1, C-6-disubstituted 3,5-dichloro-2-(1*H*)-pyrazinones [3] and its promising incorporation in small HCV NS3 protease inhibitors. We herein present our further optimization of these lead compounds (A, B) (Figure 1) [4].

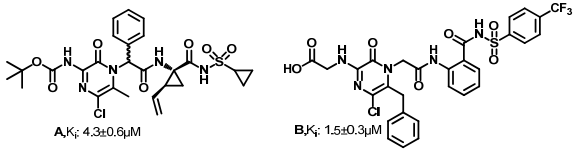

Fig. 1. Lead compounds A and B.

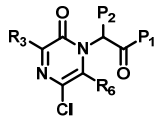

Fig. 2. Protease inhibitors.

Results and Discussion

Molecular modelling of HCV NS3 protease inhibitors, of the type shown in Figure 2, suggested that the space occupied by the P2 side chain could be reached by the substituent in position six on the P3-pyrazinone [4]. Based on these results we hypothesized that a

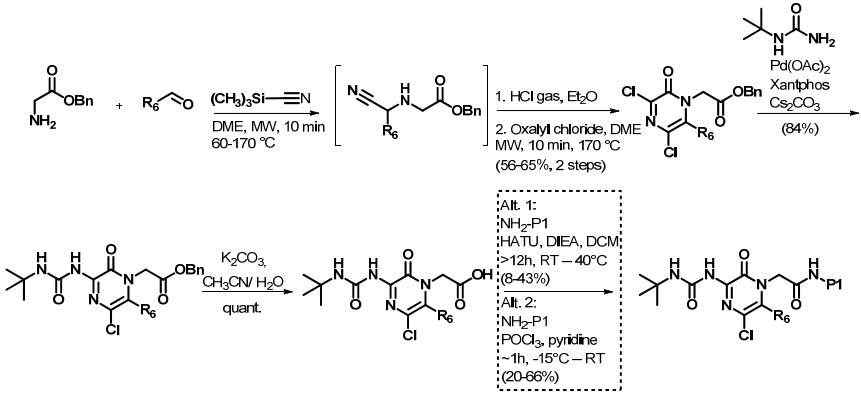

Scheme 1.

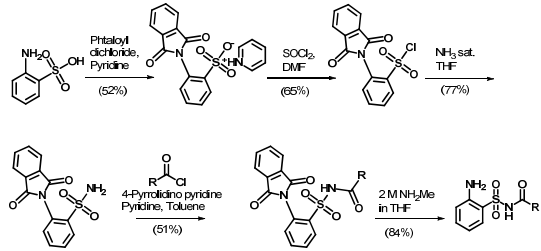

Scheme 2.

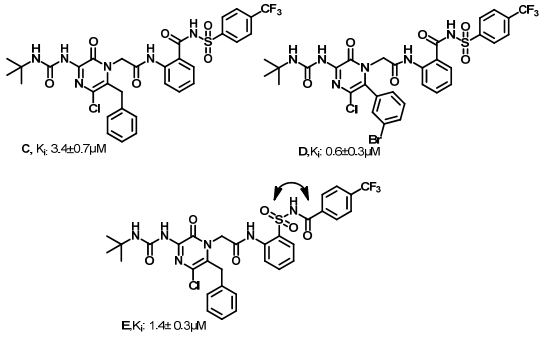

Fig. 3. Three representative compounds.

meta-substituent on a phenyl in this position could gain potency by filling the S2 pocket more efficiently. In order to synthesize more stable compounds we decided to introduce a urea functionality at the R3 position, instead of the previously used carbamate group. Different R6 aryls in combination with an unsubstituted P2 (glycine analogue) were introduced in the development of a structure activity relationship around this position. Also, we decided to investigate the effect on inhibitory potency by using a reversed acyl sulfonamide group as a P1 substituent (Figure 2). The synthesis is outlined in Scheme 1 and starts with a two step generation of the pyrazinone building block [3] followed by introduction of the urea group via a palladium catalyzed, Buchwald-type, N-arylation reaction. After hydrolysis of the benzylester the aromatic P1 group was introduced. The weak nucleophile (aniline) makes this coupling reaction slow and low yielding. A change from HATU as the coupling reagent to activation of the acid with phosphorus oxychloride in pyridine increased the yield and shortened the reaction time considerably (Scheme 1). The reversed sulfonamide was prepared as outlined in Scheme 2. This protocol enables introduction of a wide range of acid chlorides and hence a variation of suitable aromatic P1 substituents. The phtaloyl protecting group withstands the reaction conditions and is easily removed in the last step.

Evaluation of three representative compounds (C-E, Figure 3) shows a promise in the above mentioned design. Introduction of a urea function in position R6 (compound C) produced more stable inhibitors with potencies comparable to compounds A and B. A *meta*-bromo phenyl group in position R3 gave compound D with much improved inhibitory potency.

The aromatic reversed acyl sulfonamide substituent in P1 was very well tolerated as shown by compound E being more potent than compound C. Further work on this type of compounds is in progress.

Acknowledgments

We gratefully acknowledge financial support from Medivir AB. The Swedish Academy of Pharmaceutical Sciences and Anna-Maria Lundins Foundation for supporting the participation in ACS Fall 2010 and the 31st EPS 2010.

References

1. Shepard, C.W., et al. *Lancet Infect. Dis*. **5**, 558-567 (2005).
2. Webster, D.P., et al. *Lancet Infect. Dis.* **9**, 108-117 (2009).
3. Gising, J., et al. O*rg. Biomol. Chem.* **7**, 2809-2815 (2009).
4. Örtqvist, P., et al. *Bioorg. Med. Chem.* **18**, 6512-6525 (2010).

Proceedings of the 31st European Peptide Symposium
Michal Lebl, Morten Meldal, Knud J. Jensen, Thomas Hoeg-Jensen (Editors)
European Peptide Society, 2010

Peptide Nucleic Acids with Chiral Backbone – Synthesis and Properties

Tatyana Dzimbova and Tamara Pajpanova
Institute of Molecular Biology, BAS, Sofia, 1113, Bulgaria

Introduction

Peptide nucleic acids (PNAs) are new completely artificial DNA/RNA analogues in which the backbone is replaced by pseudopeptide. There are many applications of PNAs. Originally conceived as agents for double-stranded DNA binding, the unique properties of PNAs as DNA mimics were first exploited for gene therapy drug design. Now PNAs are used in different fields as anti-gene and antisense agents, as delivery agents, in PCR and Q-PNA PCR, nucleic acid capture, solid-phase hybridization techniques.

We present here the synthesis of new PNAs with a chiral backbone, containing unnatural amino acids. Amino acid analogues were based on the natural amino acids Arg, Orn and Lys.

Results and Discussion

All amino acid analogues were prepared by previously described procedures by our team [1,2] and their purity was checked by analytical HPLC (Conditions of HPLC: ZIC® - HILIC column (100 x 4,6 mm; 5 µm); 50% 0,05 M CH_3COONH_4 (pH=6,8) : 50% CH_3CN). Structures of all analogues were presented in Figure 1.

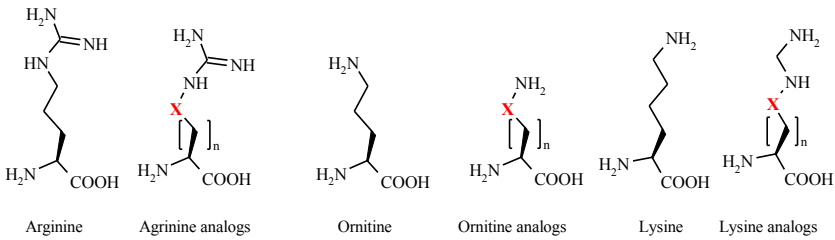

Fig. 1. Unnatural amino acid analogues. X=O, SO_2, n=1-3.

Originally PNAs are based on a pseudopeptide (polyamide) backbone made of N-(2-aminoethyl) glycine units and they are neutral and achiral [3] (Figure 2 aegPNA). We present here analogues of PNA with the pseudopeptide chiral backbone (Figure 2 lysPNA and xPNA).

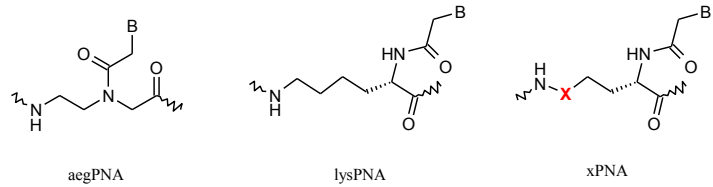

Fig. 2. PNA structures.

For the synthesis of PNA oligomers we used the L-enantiomer of each analogue. PNAs were synthesized by SPPS according to the proposed scheme (Figure 3). The appropriate resin for our purpose is Merrifield resin. The attachment is stable at all stages of the synthetic scheme as well as in the case of microwave-assisted (MWA) synthesis. First we built the pseudopeptide backbone using well known coupling reaction protocols (TBTU, DIPEA). After the backbone was built, the PNA analogue was prepared in reaction with the base. In our case the base was thymine, which was converted to thymin-1-ylacetic acid [4].

Coupling was done by the TBTU method. The final step of the synthesis of PNA analogues was cleavage from the resin.

SPPS was performed both conventionally and by using microwave irradiation (MARS-X). Some of the steps of SPPS were performed using both techniques. One of the reasons for using MWA-SPPS was the shorter reaction time. It was several times shorter than conventional SPPS. And because of the shorter time the possibility for racemization is less pronounced. For instance, the synthesis of $(NCan)_3$ pseudopeptide backbone by conventional SPPS took about 11 hours, but in MWA-SPPS the time was about 1 hour and 15 minutes. Even in the second case not all steps of the scheme were performed in conditions of microwave irradiation. The process could be optimized to be faster and to prevent racemization of unnatural amino acid analogues.

Our purpose was to synthesize chiral PNA oligonucleotide analogues and we monitored their purity at each step of the synthetic scheme.

In conclusion we could say that new classes of chiral PNAs were synthesized. Synthesis was made by both conventional and microwave-assisted methods. Reaction time is many times shorter in microwave-assisted synthesis than in conventional synthesis.

Acknowledgments

We are grateful to the European Social Fund and the Bulgarian Ministry of Education and Science (Contract BG051PO001-3.3.04/58 – 2009) and NFSR of Bulgaria (Contract MY-FS-13-07).

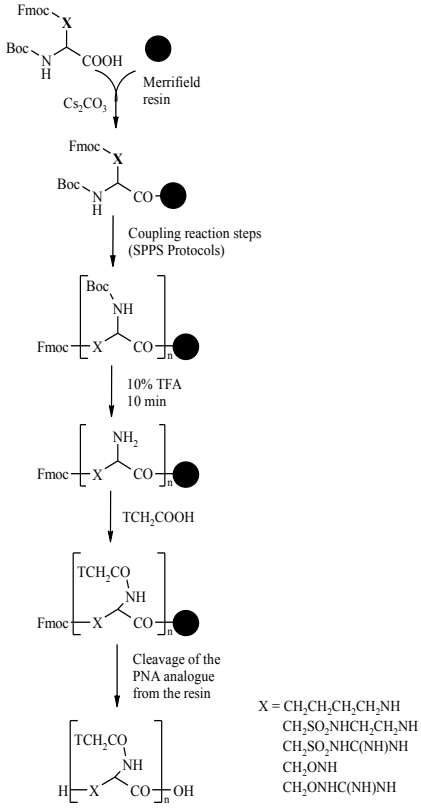

Fig. 3. Scheme of PNA synthesis.

References

1. Dzimbova, T., Pajpanova, T., Golovinsky, E. *Collect. Czech. Chem. Commun.* **6**, 12-14 (2003).
2. Dzimbova, T., Pajpanova, T., Tabacova, S., Golovinsky, E. In: *5th Hellenic Forum on Bioactive Peptides*, TYPORAMA, Greece, Cordopatis P. (Ed.), 223-227(2007).
3. Nielsen, P.E., Egholm, M., Berg, R.H., Buchardt, O. *Science* **254,** 1497-1500 (1991).
4. Dueholm, K.L., Egholm, M., Behrens, C., Christensen, L., Hansen, H.F., Vulpius, T., Petersen, K.H., Berg, R.H., Nielsen, P.E, Buchardt, O. *J. Org. Chem.* **59**, 5767-5773 (1994).

Proceedings of the 31st European Peptide Symposium
Michal Lebl, Morten Meldal, Knud J. Jensen, Thomas Hoeg-Jensen (Editors)
European Peptide Society, 2010

A New Synthetic Strategy for Novel Antibacterial Hybrid Drug-Like Molecules

I. Lapidot[1,2], G. Zats[1,2], A. Albeck[2], G. Gellerman[1], and S. Shatzmiller[1]
[1]Department of Biological Chemistry, Ariel, 40700, Ariel University Center of Samaria, Israel; [2]Department of Chemistry, Ramat-Gan, 52900, Bar-Ilan University, Israel

Introduction

The phenomenon of antibiotic resistant bacteria is a global problem which is hard to deal with and is getting worse. Therefore, it is necessary to discover new antibiotics. Antibacterial peptides (AMPs) are the effector molecules of innate immunity. Generally they contain 15–45 amino acid residues. Most antibacterial peptides share several common features i.e.: positive charge domains (i.e. contain lysines and arginines), hydrophobic amino acids (i.e. contain valine and phenyl alanine) and amphipathic structures. Furthermore, most native antimicrobial peptides have no cytolytic activity against normal mammalian cells at their minimal antimicrobial inhibitory concentration (MIC) [1].

Various known and novel scaffolds are, among others, 1, 4-Dihydropyridines [2,3] and Benzodiazepines [4,5]. They are abundant source of molecules with proven biological activity. The present research refers to the phenomenon of pharmacokinetics as well as pharmacodynamics in pharmacologic activity, namely the modification that extends use of existing medicines. In particular, the changes of the medications which are known and usable. For medicines known, this change is achieved by combining them with peptide sequences (based on Dermaseptine fragments [6,7]), in order to produce hybrid drug like molecules with better desired potential therapeutic features.

Results and Discussion

The advantage of the AMPs over conventional antibiotics is their operating mechanism, which refers to the interaction between the bacteria's membrane and the peptide. This fact makes it much more difficult for the microorganisms to develop resistancy to AMPs. Bacteria's ability to become resistant to antibiotics presents an urgent need to develop various tools to supplement the current available antibiotic treatments. However, the pharmaceutical industry shows interest in Synthetic Antimicrobial Peptidomimetics (SAMPs) and not in AMPs. The reason for that preference is probably because of the high molecular weight of the natural polypeptides, low stability in the blood serum, low selectivity and the high cost [8,9].

We have identified in the amino-acids sequence of the antibacterial polypeptide from frog skins, Dermaseptin-S1 (Figure 1) a short sequence of 5 amino-acids (via the Linear epitope system) present in the natural product, namely KTMLK (**[1a]** Lys-Thr-Met-Leu-Lys). This was found to have bactericidal activity, i.e. killing Gram negative as well as Gram positive bacteria. Linear epitopes based on **[1a]** were prepared in which the amino-acids T and M as well as L were replaced by other hydrophobic amino acids. All show the same biological activity.

S4=ALLGAAADTISQGTQWMTLLKKVL**KAAAK**ALNAVLVGANA
S1=ALW**KTMLK**KLGTMALHAGKAA

Fig. 1. Dermaseptine sequence amino-acids (S1 & S4).

As a result of all these facts we designed novel peptidomimetics compounds that contain 1,4-Dihydropyridines (**IL**) and Benzodiazepines (**GZ**) (scaffolds- Figure 2) bound to AMPs sequence that derived from the Dermaseptine skin – all this unit together constitute Hybrid drug-like molecule.

There are many suggestions for mechanisms explaining the bactericidal nature of these more than 800 isolated natural antimicrobial peptides [8-10]. However, one of these mechanisms is based on the idea that positively charged amino acids like Lysine, Arginine present in the antimicrobial peptides in large abundance can replace metal cations attached to phospholipids – lipopolysacchrides [11] and peptide-glycans – Teichoic acid [12] layers forming the essential supra-molecular structures based on coordination with metal cations

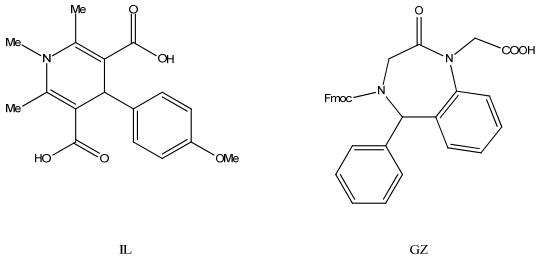

Fig. 2. The Scaffolds- IL and GZ.

present in cell walls of Gram negative and Gram positive bacteria respectively. This replacement can bring about a catastrophic chain of events leading to the collapse of the cell wall, forming thereby pores in it leading to the destruction of the cell and the death of the microorganism.

In this work we tested the compounds **1-4** (Table 1). Since the red blood cells membranes are built differently from bacteria cells, for example, we tested our compound for hemolytic damage but they do not cause cleavage in red blood cells preparations (<7 %).

The penetration of the bactericide to the inside of the microorganism cell might not be needed for the main process of killing [13]. Provided the death of the microbe is caused by altering the cationic distribution – chelating to Mg^{++} or Ca^{++} ions for example - on the surface of the cell wall leading to disintegration of the pathogenic cell wall [14].

Table 1. Biological activities of the hybrid drug-like molecules

Compound Number	*Peptidomimetic compound Sequence*	*MW (g/mole)*	*MIC Results (μM)*	
			E.Coli	*S. Aureus*
1	Leu-Lys-**IL**-Lys-Leu	800	95	100
2	Lys-Pro-**IL**-Pro-Lys	767.91	36	45
3	Cys-Lys-**GZ**-Lys	654	38	19
4	Leu-Lys-**GZ**-Lys	664	200	200

Future Directions

These mimetic compounds will be incorporated to a unique fluorescent probe in order to test them for their capacity to bind CBRs/ PBRs and DHPR receptors in aim to assay their biological activities on rats' brain.

References

1. Reddy, K.V.R., Yedery, R.D., Aranha, C. *Int. J. Antimicro. Ag.* **24**, 536-547 (2004).
2. Li, M., Zuo, Z., Wen, L., Wang, S. *J. Comb. Chem*. **10**, 436-441(2008).
3. Lipinsky, C., Hopkins, A. *Nature* **432**, 855-861, (2004).
4. Herrero, S., Teresa, M. *J. Org. Chem*. **68**, 4582-4585 (2003).
5. Patchett, A., Nargund, A. *Ann. Rep. Med. Chem*. **35**, 289 (2000).
6. Krugliak, M., Feder, R., et al. *Antimicrob. Agents. Chemother*. **44**, 2442-2451 (2000).
7. Lorin, C., Saidi, H., et al. *Virology* **334**, 264-275 (2005).
8. Svenson, J., Stensen, W., et al. *Biochemistry* **47**, 3777-3788 (2008).
9. Staubitz, P., Peschel, A., et al. *J. Pep. Sci*. **7**, 552-564 (2001).
10. a) Oren, Z., Hong, J., Shai Y. *J. Biol. Chem* . **272**, 14643-14649 (1997); b) Makovitzki, A., Avrahami, D., Shai, Y. *Proc. Natl. Acad. Sci.***103**, 15997-16002 (2006).
11. Svenson, J., Karstad, R., et al. *Mol. Pharmaceutics* **6**, 996-1005 (2009).
12. Wickham, J.R., Halye, J.L., et al. *J. Phys. Chem. B.* **113**, 2177-2183 (2009).
13. Wade, D., Boman, A., et al. *Proc. Nat. Acad. Sci.* **87**, 4761-4765 (1990).
14. a) Friedrich, C.L., et al. *Antimicrob. Agents. Chemother*. **44**, 2086-2092 (2000); b) Toke, O. *Biopolymers (Peptide Science)* **80**, 717-735 (2005).

Proceedings of the 31st European Peptide Symposium
Michal Lebl, Morten Meldal, Knud J. Jensen, Thomas Hoeg-Jensen (Editors)
European Peptide Society, 2010

Design and Synthesis of Protein-Protein Interaction Mimics as Plasmodium Falciparum Cysteine Protease Falcipain-2 Inhibitors

Luca Rizzi[1], Srividhya Sundararaman[2], Katarina Cendic[1], Nadia Vaiana[1], Reshma Korde[2], Dipto Sinha[2], Asif Mohommed[2], Pawan Malhotra[2], and Sergio Romeo[1]

[1]Dipartimento di Scienze Farmaceutiche "Pietro Pratesi", Università degli Studi di Milano, Via L. Mangiagalli 25, 20133, Milan, Italy; [2]International Centre for Genetic Engineering and Biotechnology, Aruna Asaf Ali Marg, NewDelhi, 110067, India

Introduction

Cysteine proteases play a significant role in the growth and the development of several human parasites such as *Plasmodium, Leishmania*, and *Trypanosoma* which affect more than 3.5 billion people worldwide. Falcipain-2 (FP-2) is an important cysteine protease of the human malaria parasite, *P. falciparum* (Pf), and is one of the most promising targets for the development of new Pf inhibitors [1]. FP-2 plays roles in haemoglobin degradation and merozoites egression at the asexual blood stages of *Plasmodium* development.

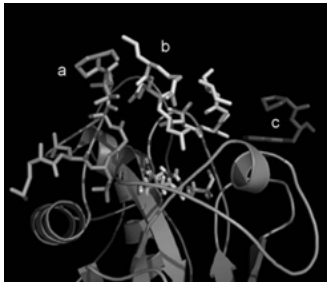

Fig. 1. Interacting domains of CEWC.

Cystatins are endogenous proteinaceous cysteine protease inhibitors that have been described in a number of eukaryotic systems, but the high molecular weight and the peptidic structure raise difficulties in their exploitation in drug design [2]. Small molecules mimicking the interaction between FP-2 and Cystatin could be a starting point for the development of a new class of anti-malarial.

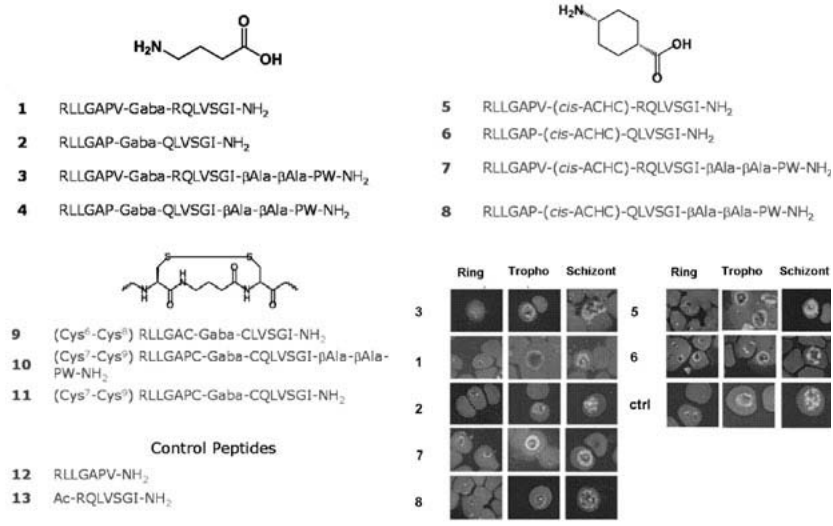

Fig. 2. Synthesized peptides and their effect on P. falciparum morphology.

*Table 1. Inhibition of FP-2 (%) at a given concentration by compounds **1-13***

	Peptides												
	1	*2*	*3*	*4*	*5*	*6*	*7*	*8*	*9*	*10*	*11*	*12*	*13*
50 μM	64	56	64	60	72	60	73	70	58	56	57	50	40
25 μM	61	53	63	52	69	60	71	70	55	53	57	41	28
10 μM	60	50	59	47	68	49	68	65	52	49	45	15	15
5 μM	57	44	49	32	63	50	60	57	50	39	47	5	10

Results and Discussion

The crystal structure of FP-2 in complex with chicken egg white cystatin (CEWC) shows three regions of CEWC interacting with the active site of FP-2: the N-terminal sequence (^{6}RLLGAPV^{12} - Figure 1a) and a β-hairpin loop (^{52}RQLVSGI^{58} - Figure 1b) are in close contact with the active site of FP-2, while a second β-hairpin loop (^{103}PW^{104} - Figure 1c) is situated at a greater distance [3]. Since the distance between the N-terminal sequence and the first β-hairpin loop is about 4-5 Å, we reasoned that the cystatin protein scaffold could be replaced by an appropriate linker joining the interacting domains.

Cystatin/FP-2 interaction mimics were designed linking the neighboring amino acidic pairs of the N-terminal sequence (^{6}RLLGAPV^{12}) and the β-hairpin loop (^{52}RQLVSGI^{58}) with cyclic and acyclic amino acids selected based on docking studies. Pro^{11}-Gln^{53} and Val^{12}-Arg^{52} were therefore joined with γ-aminobutyric acid (GABA) and cis-4-aminocyclohexanecarboxylic acid (ACHC) (**1**, **2**, **5** and **6**).

Compounds **3**, **4**, **7**, **8** are analogous of compounds **1**, **2**, **5** and **6** in which the dipeptide Pro-Trp has been added to the carboxyl terminus in order to evaluate the importance of the second loop and two β-alanines have been introduced to fill up the distance between the loops. In a third series of compounds (**9-11**) the conformational freedom of GABA was reduced by replacing the amino acids bound to GABA with two cysteines and a disulphide bridge was then build. Finally the N-terminal (^{6}RLLGAPV^{12}) and the loop (^{52}RQLVSGI^{58}) sequences were synthesized as control peptides (**12**, **13**).

Inhibition of FP-2 has been determined and peptides **5-8** containing the cis-ACHC linker were the most potent inhibitors, while most of the peptides containing the GABA linker and the disulphide bridge (**1-4**, **9-11**) were less potent, with the exception of peptide **1** that showed 57% inhibition at 5 μM. Compounds **1**, **3**, **5**, **7** having two additional amino acids were always more active. Insertion of the Pro-Trp dipeptide (**3**, **4**, **7**, **8**) did not have significant effect on FP-2 inhibition. Control peptides (**12-13**) showed only weak inhibitory activities (Table 1).

Treatment of parasites in in vitro culture at late ring stage with cystatin mimics resulted in phenotype similar to that seen in parasite treated with other cysteine protease inhibitors such as E-64/leupeptin [4,5]: food vacuole at early trophozoite stage was swollen and in some cases it also showed clumps of malarial pigment (Figure 2).

Acknowledgments

This publication was generated in the context of the AntiMal project, funded under the 6th Framework Programme of the European Community (contract no.IP-018834). LR was funded by "Compagnia San Paolo" in the context of the Italian Malaria Network.

References

1. Rosenthal, P.J. *Int. J. Parasitol.* **34**, 1489-1499 (2004).
2. Stubbs, M.T., et al. *EMBO J.* **9**, 1939-1947 (1990).
3. Wang, S.X., et al. *Proc. Natl. Acad. Sci. U.S.A.* **103**, 11503-11508 (2006).
4. Sijwali, P.S., et al. *Proc. Natl. Acad. Sci. U.S.A.* **101**, 4384-4389 (2004).
5. Rosenthal, P. *J. Exp. Parasitol.* **80**, 272-281 (1995).

Proceedings of the 31st European Peptide Symposium
Michal Lebl, Morten Meldal, Knud J. Jensen, Thomas Hoeg-Jensen (Editors)
European Peptide Society, 2010

Structural Features of Antimicrobial Aza-β³-peptides

Baptiste Legrand[1], Mathieu Laurencin[2], Céline Zatylny-Gaudin[3], Joel Henry[3], Arnaud Bondon[1], and Michèle Baudy Floc'h[2]

[1]Université de Rennes 1, RMN-ILP, UMR CNRS 6026, Campus de Villejean, 35043, Rennes cedex, France; [2]Université de Rennes 1. ICMV, UMR CNRS 6226 Sciences Chimiques de Rennes, 263 Avenue du Général Leclerc, 35042, Rennes Cedex, France; [3]Université de Caen Basse Normandie, LBBM, UMR IFREMER, 14032, Caen Cedex, France

Introduction

Designing antimicrobial molecules based on pseudopeptides to increase the activity, selectivity and bioavailability of natural peptides is now widespread. Recently, numerous peptidomimetics have been developed for biological applications including azapeptides, β-peptides, peptoids, and oligoureas. In this context, aza-β³-amino acids were used as new blocks to compose antimicrobial peptide sequences.

From a natural antimicrobial peptide, H-ALSGDAFLRF-NH_2 (AD), depending on the aza-β³-residue insertions, the modifications can result either in inactive pseudopeptides, or in a drastic enhancement of the antimicrobial activity without cytotoxicity. We present here the first NMR solution structures of peptides containing aza-β³-amino acids to study their structure-activity relationship.

Results and Discussion

In SDS micelles, the global fold of AD and AK displays disordered N-terminal regions and well-defined amphipatic helical C-terminal moieties (5-10) (Figure 1). The Aβ3K peptide is based on AK, substituting the lysine in position 5 by an aza-β³-lysine (Aβ³K). Its global fold is very different from the two previous peptides and do not exhibit a helical C-terminal part. A typical aza-β³ residues hydrazino turn, previously described in crystals, can be also observed in solution [1-3]. Despite the two possible conformations of the aza-β³ lysine nitrogen stereocenter, only one set of signals is observable on the NMR spectra and the NOESY spectrum have numerous NOEs. The configuration of the stereocenter of the aza-β³-Lys5 was not defined in the CNS topology and parameter files, and two sets of conformations can be obtained from the NMR restraints according to the configuration R or S of the N_α stereocenter. Based on the NMR spectra, one cannot discriminate if only one conformation is present in solution, or if two configurations are in fast exchange.

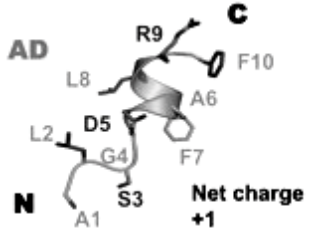

Fig. 1. AD natural cuttlefish peptide NMR structure.

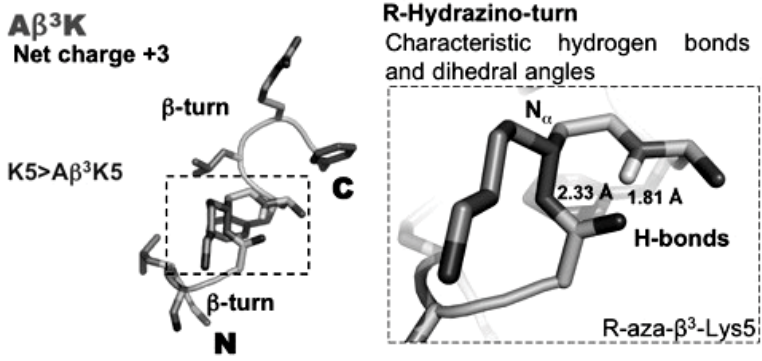

Fig. 2. Aβ³K peptide NMR structure.

Table 1. Sequences and MIC activity of the natural peptide and of five synthetic analogues (MIC: Minimum Inhibitory Concentration in μM; na: not active; nd: not determined)

Name	*Primary sequence*	*S. aureus*	*E. coli*
AD	H-ALSGDAFLRF-NH_2	na	584
AK	H-ALSG**K**AFLRF-NH_2	262	65
Aβ ^{3}K	H-ALSG-**aza-β^{3}K**-AFLRF-NH_2	na	na
K2Nal7	H-ALSGKA-**aza-β^3-1Nal**-LRF-NH_2	nd	268
K-1Nal	H-ALSGKA-aza-β^3-1Nal-LR-aza-β^3-Nal-NH_2	15	30
K-2Nal	H-ALSGKA-aza-β^3-2Nal-LR-aza-β^3-Nal-NH_2	30	118

Two new peptides, named K2Nal7 and K2Nal, were designed with subsequent substitution of the phenylalanine by aza-β^3-naphtylalanine amino acids (aza-β^{3}Nal). As AD and AK, only their C-terminal moeities are ordered but not folded in helix. They share a similar turn which approaches the two hydrophobic aromatic residues in position 7 and 10. Nevertheless, in each case, they are too far to pack each other (~9 Å) and no NOEs can be detected between the residues 7 and 10 aromatic protons. The K2Nal7 and K2Nal dominant structures do not have a hydrazino-turn, indeed the hydrazino-turn NOEs marker previously noticed on the Aβ^{3}K NOESY spectrum cannot be detected for these peptides.

The incorporation of aza-β^3 residues broke the helical structures to induce different peptide folds. The Aβ^{3}K structure is quite rigid and shows a hydrazino-turn surrounded by two β-turn (Figure 2). However, despite the presence of aza-β^3 amino-acids, the K2Nal7 and K2Nal appear to be quite flexible, their structures do not have a stable hydrazino-turn and only the C-terminal part is well defined.

Structural parameters, such as peptide helicity, hydrophobicity, hydrophobic moment, peptide charge and the size of the hydrophobic/hydrophilic domain, could increase the antibacterial activity and improve the prokaryotic selectivity of natural peptides and analogues.

Acknowledgments
We thank SERB Laboratories and the "Région Bretagne" for their financial support.

References

1. Cheguillaume, A., et al. *J. Org. Chem.* **66**, 4923-4929 (2001).
2. Salaün, A., Potel, M., Gall, P., Le Grel, P. *J. Org. Chem.* **70**, 6499-6502 (2005).
3. Le Grel, P., Salaün, A., Potel, M., Le Grel, B., Lassagne, F. *J. Org. Chem.* **71**, 5638-5645 (2006).

Proceedings of the 31st European Peptide Symposium
Michal Lebl, Morten Meldal, Knud J. Jensen, Thomas Hoeg-Jensen (Editors)
European Peptide Society, 2010

Synthesis of Peptidomimetics by the Pictet-Spengler Reaction

Marta Slupska[1], Karolina Pulka[1], Malgorzata Przygodzka[1], and Aleksandra Misicka[1,2]

[1]Faculty of Chemistry, Warsaw University, Warsaw, 02-093, Poland; [2]Medical Research Center, Polish Academy of Science, Warsaw, 02-106, Poland

Introduction

Tryptophan is often a key pharmacophore which determines the affinity of peptide ligands for their receptors. Therefore cyclic analogues of tryptophan which introduce local constraints, reduce the flexibility of the peptide chain and stabilize the bioactive conformation are valuable tool in peptidomimetic research. The Pictet-Spengler [1] reaction has been one of the possibilities to prepare analogues containing 1,2,3,4-tetrahydro-β-carboline skeleton which introduce local constraints and reduce the flexibility of the indole moiety of tryptophan. The heterocyclic skeleton of 1,2,3,4-tetrahydro-β-carbolines possesses multiple sites for functionalization, therefore it is an ideal choice for the design potent and selective ligands to biological target receptors. The use of chiral carbonyl components (e.g. α-aminoaldehydes) in Pictet-Spengler reaction influence the configuration of the newly created in this reaction stereogenic center [2].

We now report the diastereoselectivity studies of Pictet-Spengler condensation of L- and D-α-aminoaldehydes as carbonyl components with N-terminal α-Trp, β^2- or β^3-*homo*-Trp dipeptides as arylethylamine substrates.

Results and Discussion

The synthesis of L-β^3-*homo*-tryptophan was accomplished by Arndt-Eistert homologation of L-α-tryptophan [3]. Optically active L-β^2-*homo*-tryptophan was synthesized with the use of (+)-2,10-camphorsultam as chiral auxiliary [4].

The Pictet-Spengler cyclizations of different tryptophan derivatives with L- and D-α-aminoaldehydes were performed in the presence of TFA and at low temperature (-40°C) to avoid racemization of chiral aminoaldehydes (Figure 1).

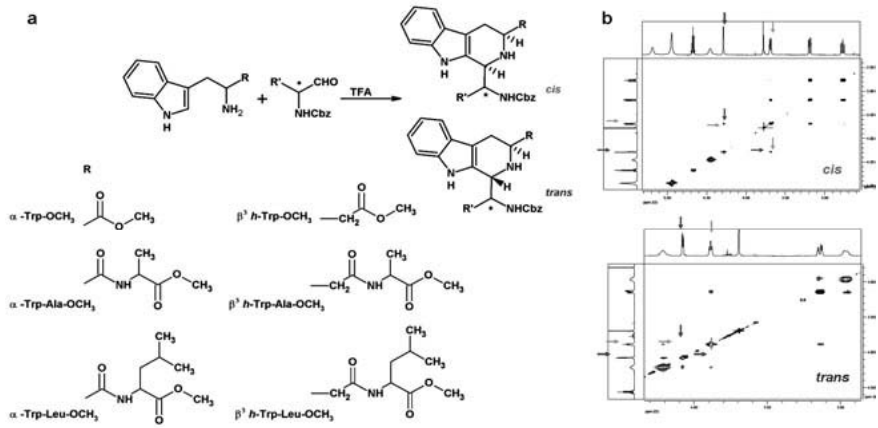

Fig. 1. a) Synthesis of tetrahydro-β-carbolines, b) 2D NMR ROESY spectra of cis/trans products of Pictet-Spengler condensations of L-α-Trp-OCH$_3$ with Cbz-L-Ala-H.

Table 1. Diastereoselectivity studies of the Pictet-Spengler reaction

Aminoaldehyde / *Arylethylamine*	*Cbz-L-Ala-H* *cis/trans ratio [%]*	*Cbz-L-Ile-H* *cis/ trans ratio [%]*	*Cbz-D-Ala-H* *cis/trans ratio [%]*	*Cbz-D-Leu-H* *cis/trans ratio [%]*
α-Trp-OCH_3	35/65	0/100	100/0	100/0
α-Trp-Ala-OCH_3	26/74	0/100	100/0	100/0
α-Trp-Leu-OCH_3	28/72	0/100	100/0	100/0
β^{3}-h-Trp-OCH_3	60/40	0/100	100/0	100/0
β^{3}-h-Trp-Ala-OCH_3	46/54	0/100	100/0	100/0
β^{3}-h-Trp-Leu-OCH_3	32/68	0/100	100/0	100/0

Pictet-Spengler condensation of L- and D-α-aminoaldehydes as carbonyl components with methyl ester and N-terminal α-Trp or β^3-*homo*-Trp dipeptides as arylethylamine substrates led to 1,3-disubstituted 1,2,3,4-tetrahydro-β-carbolines. During the Pictet-Spengler reaction a new stereogenic center was created and the mixture of *cis/trans* products was obtained. It was confirmed by 1H and 2D NMR (COSY, ROESY) spectra. The results of reactions are summarized in Table 1. The ratio of *cis/trans* diastereomers depended on the stereogenic centre of used aminoaldehyde. For β^3-*homo*-Trp-OCH_3 reaction with Cbz-L-Ala-H led to the opposite stereoselectivity in comparison to α-Trp-OCH_3 and *cis* isomer was the main product. The stereoselectivity in the reaction of β^3*h*-Trp-OCH_3 with Cbz-L-Ile-H and D-aminoaldehydes was the same as for α-Trp-OCH_3. In the reaction with Cbz-L-Ile-H only *trans* isomer was obtained. The reactions with D-aminoaldehydes were totally selective and only *cis* diastereomer was formed.

The conformation of newly created 6-membered ring in 1,3-disubstituted 1,2,3,4-tetrahydro-β-carbolines was determined by 2D NMR ROESY spectra. It depended on the size of substituents. In the case of *trans* isomers small substituents (ester moiety) were axially located, big ones (peptide moieties) were equatorially located. *Cis* isomers adopted the conformation with both substituents equatorially located [5].

During the Pictet-Spengler reaction with the use of L-β^2-*homo*-Trp-OCH_3 a new 7-membered ring was created (Figure 2). Two different diastereoisomers were produced as a result of reaction with L-aminoaldehyde and D-aminoaldehyde. Chemical shifts of -OCH_3 signal in 1H NMR spectra confirmed that obtained compounds were different diastereoisomers. The stereoselectivity of these reactions is under investigation.

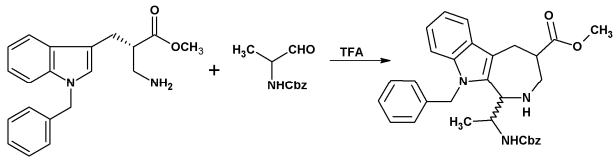

Fig. 2. Pictet-Spengler reaction of β^2-hTrp-OCH_3.

References

1. Pictet, A., Spengler, T. *Ber. Dtsch. Chem. Ges*. **44**, 2030-2036 (1911).
2. Pulka,, K., Kulis P., Tymecka, D., Frankiewicz, L., Wilczek, M., Kozminski, W., Misicka, A., *Tetrahedron* **64**, 1506-1514 (2008).
3. Koch, K., Podlech, J. *Synthetic Communications* **35**, 2789-2794 (2005).
4. Moumne, R., Larregola, M., Boutadla,, Y., Lavielle, S., Karoyan, P. *Tetrahedron Letters* **49**, 4704-4707 (2008).
5. Pulka, K., Slupska, M., Misiak, M., Lipkowska, Z., Kozminski, W., Misicka, A., *1,3-Disubstituted 1,2,3,4-tetrahydro-β-carbolines as peptidomimetics of tryptophan: synthesis and conformational analysis (Poster in the 30th European Peptide Symposium)*, Helsinki, Finland, 2008.

Proceedings of the 31st European Peptide Symposium
Michal Lebl, Morten Meldal, Knud J. Jensen, Thomas Hoeg-Jensen (Editors)
European Peptide Society, 2010

From Peptides to Non Peptide Mimetics: The Examples of Angiotensin II and Myelin

Amalia Resvani[1], George Agelis[1], Maria-Eleni Androutsou[1], Dimitra Kalavrizioti[2], Konstantinos Kelaidonis[1], Maria Katsara[3], George Deraos[1], Irene Friligou[1], Panagiotis Plotas[2], Vasso Apostolopoulou[3], and John Matsoukas[2,4]

[1]Department of Chemistry, University of Patras, Patras, 26500, Greece; [2]Department of Medicine, University of Patras, Patras, 26500, Greece; [3]Immunology and Vaccine Laboratory, Austin Campus, Victoria, 3084, Australia; [4]ELDRUG S.A. Patras Science Park, Rio, 26504, Greece

Introduction

In our laboratory in Patras, research is focused mainly towards design and synthesis of AT1 receptor antagonists for treating hypertension as well as of Myelin epitope linear and cyclic analogues in the immunotherapy of Multiple Sclerosis. Losartan was the first non peptide Angiotensin II (Ang II) receptor antagonist, by Dupont [1] followed by a series of other Ang II antagonists now on the market. Previous Ang II peptide antagonists such as Sarilesin and Saralasin [2,3] failed to become drugs due to their peptide nature rendering them susceptible to proteolytic enzymes. Reversion of butyl and hydroxymethyl groups at the 2- and 5-positions of the imidazole ring in Losartan resulted in potent AT1 Ang II receptor antagonist [4,5].

On the other hand, Immunodominant Epitopes MBP 83-99, PLP 139-151, MOG 35-55 of human proteins MBP, PLP, MOG [6] of myelin sheath are implicated in Multiple Sclerosis (MS). These epitopes have been the tools in our laboratories for the Design, Synthesis and Preclinical Evaluation of linear and cyclic analogues conjugated to reduced or oxidized mannan via [Lys-Gly] bridge. In the light of these results in our research, the main immunodominant peptides MOG 35-55, PLP 139-151 and MBP 83-99 and their head to tail cyclic counterparts alone or conjugated to reduced mannan have been selected to constitute a mixture cocktail drug for preclinical investigation in preparation of New Drug Application (NDA) for Clinical Phase I and II studies in the Immunotherapy of Multiple Sclerosis.

Results and Discussion

Research work on AT1 receptor antagonists: This research has focused on the design and synthesis of the analogue 5-butyl-2-hydroxymethyl-1-[[2´-(2H-tetrazol-5-yl)biphenyl-4-yl]methyl]imidazole (V8) that differs in the substitution pattern around the imidazole ring compared to Losartan [4] (Figure 1). Thus, the alkyl chain and hydroxymethyl group possess different topographical position in an attempt to optimize the mimicry of lipophilic superimposition of the butyl chain with isopropyl group of Ile5 in Ang II and to probe the significance of the position of hydroxymethyl group. A general alkylation protocol has been developed in this research which facilitates the synthesis of a 1,5 disubstituted imidazole derivative by selective alkylation of *N*-3 nitrogen of 4(5)-butyl-imidazole with biphenyl tetrazole moiety where the *N*-1 nitrogen is temporarily protected by the trityl group.

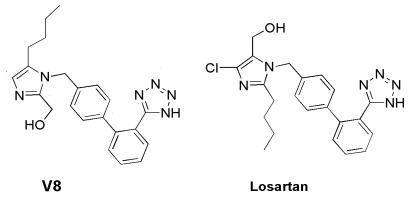

V8 **Losartan**

*Fig. 1. Synthesized analogue **V8** and Losartan.*

In vitro antihypertensive activity of **V8** showed similar affinity for the AT_1 receptor, indicating that the reorientation of butyl and hydroxymethyl groups on the imidazole template of losartan retained high binding to the AT_1 receptor. The docking studies are confirmed by binding assay results which clearly show comparable binding score of the designed compound **V8** to Losartan.

Research work on Myelin: In our studies, we demonstrated that linear peptide MBP_{83-99} (P1) [7], linear peptide MBP_{87-99} (P2) [8], the mutated $MBP_{87-99}[A^{91}, A^{96}]$ (P3) and its rationally designed cyclic counterpart cyclo(87-99) $MBP_{87-99}[A^{91}, A^{96}]$ (P4) [9] binds to HLA-DR4 which is consistent with our previous findings that cyclic peptides bind to HLA-DR4 and induces Th1 cytokines (IFN-γ, IL-2,). Furthermore, we demonstrated that mannosylation with reduced mannan of linear peptides P1 and P2 diverts immune responses from Th1 to Th2 in SJL/J mice. This switch taken together with HLA binding data of mutated peptides P2, P3 render conjugated P4 as possible candidates for MS therapy. Wild type P2 and linear mutant P3 and P4 with substitution at positions 91,96 critical for TCR contact were evaluated for their effects on the cytokine secretion by PBMC culture derived from 13 MS patients and their ability to induce Th1 / Th2 pathways. In particular, linear P1 in preliminary bioassays induced experimental allergic encephalo-myelitis (EAE) while mutant linear P2 and cyclic P3 peptides suppressed disease. Previous studies [8] in SJL/J mice have shown that conjugation of P1, P2, P3 to reduced mannan diverted immune responses to Th2 and generated antibodies which did not cross react with native MBP protein. A recent successful clinical trial phase III, with linear sequence MBP 82-98 (Dirucotide) [10] showed delay of disease progression in an HLA Class II on patients with progressive multiple sclerosis. These results and ours overwhelmingly justify our studies with cyclic MBP analogues and may open the avenues for more effective, more stable therapeutics in treating disease.

Acknowledgments
We thank ELDRUG S. A., Patras Science Park, Greece as well as VIANEX **P**harmaceutical **C**ompany for financial support.

References

1. Carini, D.J., et al. *J. Med. Chem*. **34**, 2525-2546 (1991).
2. Matsoukas, J.M., et al. *J. Med. Chem.* **36**, 904-911 (1993).
3. Matsoukas, J.M., et al. *Peptides* **11**, 367-374 (1990).
4. Agelis, G., et al. *J. Comput.-Aided Mol. Des.* **24**, 749-758 (2010).
5. Agelis, G., et al. *Amino Acids* 2010 In press.
6. Katsara, M., et al. *Cur. Med. Chem.* **13**, 2221-2232 (2006).
7. Matsoukas, J., et al. *J. Med. Chem.* **48**, 1470-80, **(**2005).
8. Katsara, M., et al. *J. Med. Chem*. **51**, 3971-3978 (2008).
9. Katsara, M., et al. *J. Med. Chem*. **52,** 214-218 (2009).
10. Krantz, M., et al. *Eur. J. Neurol.* **13**, 887-95 (2006*)*.

Proceedings of the 31st European Peptide Symposium
Michal Lebl, Morten Meldal, Knud J. Jensen, Thomas Hoeg-Jensen (Editors)
European Peptide Society, 2010

Efficient Synthesis and Biological Evaluation of Imidazole AT1 Ang II Receptor Antagonists Based on 4(5)-Butylimidazole

George Agelis[1], Amalia Resvani[1], Tereza Tůmová[2], Jiřina Slaninová[2], and John Matsoukas[3]

[1]Department of Chemistry, University of Patras, Patras, 26500, Greece; [2]Institute of Organic Chemistry and Biochemistry, AS CR, Prague 6, 16610, Czech Republic; [3]ELDRUG S.A., Patras Science Park, Rio, 26504, Greece

Introduction

The Renin-Angiotensin System (RAS) is known to play an important role in blood pressure regulation and electrolyte homeostasis. Angiotensin II (Ang II), the biologically active peptide of the RAS, is a potent vasoconstrictor agent which also stimulates aldosterone secretion and is therefore regarded as a major mediator of hypertensive disorders. The discovery of the first orally active Ang II antagonist, losartan, by DuPont [1], opened a new phase of research for the development of other antagonists [2-4]. Nearly all of them contain an alkyl-substituted imidazole ring linked to a biphenylmethyltetrazole moiety. Furthermore, the necessity of a ring cluster and of an acidic function ortho substituted to the distal phenyl ring have been demonstrated for high binding affinity [5,6]. Additionally, the presence of hydroxymethyl group enhances biological activity as well as a bulky lipophilic, electron-withdrawing substitutent, such as a halogen atom seems to favor activity. In this study, we present an efficient synthesis of imidazole biphenyltetrazole derivatives with reversion of butyl and hydroxymethyl groups at the 2- and 5-positions of the imidazole ring in comparison to losartan as potent AT1 Ang II receptor antagonists.

Results and Discussion

This research has focused on the synthesis of analogues that differ in the substitution pattern around the imidazole ring compared to losartan (Figure 1). In particular, we have elaborated an efficient synthesis of AT1 Ang II receptor antagonists based on 4(5)-butylimidazole in which the hydroxymethyl and butyl groups attached to the imidazole ring present different topographical positions in comparison to losartan [7-9]. The synthesis was regioselective, facile and high yielding, rendering it an efficient process. The preparation of the target compounds **20** and **24-26** was accomplished starting from the synthesis of the alkylating agent **7** (Figure 2).

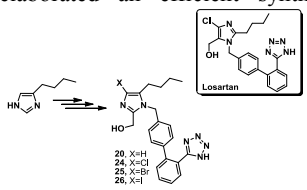

Fig. 1. Synthesized analogues based on 4(5)-butylimidazole.

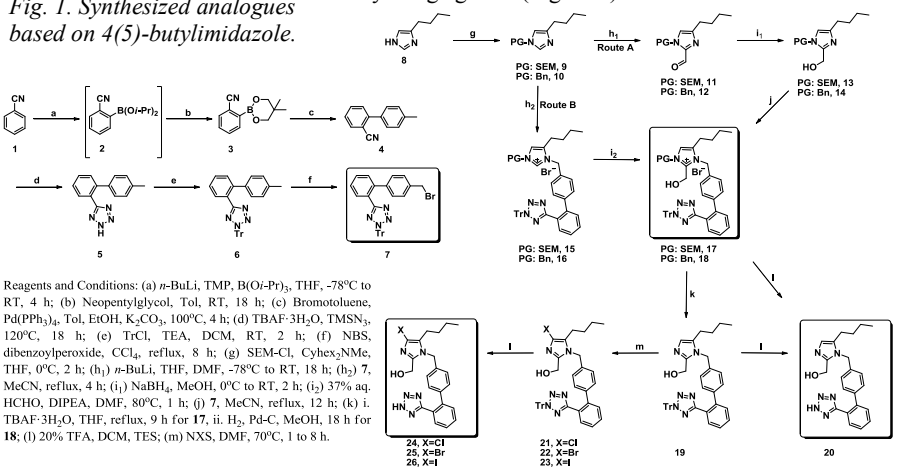

Reagents and Conditions: (a) *n*-BuLi, TMP, $B(O\text{-}i\text{-}Pr)_3$, THF, -78°C to RT, 4 h; (b) Neopentylglycol, Tol, RT, 18 h; (c) Bromotoluene, $Pd(PPh_3)_4$, Tol, EtOH, K_2CO_3, 100°C, 4 h; (d) TBAF·$3H_2O$, $TMSN_3$, 120°C, 18 h; (e) TrCl, TEA, DCM, RT, 2 h; (f) NBS, dibenzoylperoxide, CCl_4, reflux, 8 h; (g) SEM-Cl, $Cyhex_2NMe$, THF, 0°C, 2 h; (i_1) *n*-BuLi, THF, DMF, -78°C to RT, 18 h; (h_2) **7**, MeCN, reflux, 4 h; (i_1) $NaBH_4$, MeOH, 0°C to RT, 2 h; (i_2) 37% aq. HCHO, DIPEA, DMF, 80°C, 1 h; (j) **7**, MeCN, reflux, 12 h; (k) i. TBAF·$3H_2O$, THF, reflux, 9 h for **17**, ii. H_2, Pd-C, MeOH, 18 h for **18**; (l) 20% TFA, DCM, TES; (m) NXS, DMF, 70°C, 1 to 8 h.

*Fig. 2. Synthetic routes for the alkylating agent **7** and the target compounds **20**, **24-26**.*

*Table 1. In vitro antihypertensive activity of analogues **20**, **24-26** in rat uterus assay*

Compound	pA_2
Losartan	8.33±0.13
20	7.97±0.07
24	6.98±0.19
25	7.58±0.15
26	7.35±0.24

The synthesis included the conversion of the commercially available benzonitrile **1** to the stable ortho arylboronic ester **3** by *in situ* trapping of unstable lithio intermediate using 2,2,6,6-tetramethylpiperidine (TMP)/ triisopropylborate in anhydrous THF at -78°C, followed by transesterification with neopentylglycol [10]. The boronic ester **3** was readily converted to the biphenyl compound **4** by Suzuki cross-coupling reaction using bromotoluene in Tol / EtOH in the presence of catalyst $Pd(PPh_3)_4$ and K_2CO_3 as base. The resulting nitrile **4** was converted to the alkylating agent **7** according to an established procedure [11].

The synthetic procedure described in Figure 2 was employed to synthesize the target compounds **20**, **24-26** based on 4(5)-butylimidazole. The key intermediates **17** and **18** were prepared by two synthetic routes A and B which included the protection of the N-1 of the imidazole ring using appropriate protective groups such as [2-(trimethylsilyl)ethoxy]methyl (SEM) and benzyl (Bn) groups, compatible with the reaction conditions. The regioselectivity of the N-1 protection was confirmed by 1D NOE experiment. Thus, the former route included formylation at the 2-position of imidazole ring by treatment with *n*-BuLi in THF at -78°C, followed by addition of dry DMF. Reduction of the resulting aldehydes followed by selective alkylation at the 3-position of imidazole ring with the alkylating agent **7**, furnished the key intermediates **17** and **18**. On the other hand, the latter route included similarly alkylation at the 3-position followed by direct hydroxymethylation at the 2-position in the presence of formalin in a sealed tube, affording analogues **17** and **18**. Deprotection of SEM and Bn groups using $TBAF{\cdot}3H_2O$ under reflux and hydrogenolysis in the presence of Pd-C, respectively, led to the analogue **19**. Halogenation of **19** in the presence of appropriate succinimide NXS (X=Cl, Br, I) at the 4-position of imidazole ring and removal of the trityl group furnished the final analogues **20** and **24-26**.

As illustrated in Table 1, the final compounds were evaluated for their antagonist activity (pA_2) in rat uterus assay. The analogue **20** as well as the brominated analogue **25** showed high antihypertensive activity (pA_2=7.97, 7.58, respectively) close to losartan (pA_2=8.33). It indicates that reorientation of butyl and hydroxymethyl groups on imidazole template retained anti-Ang II activity. However, the chlorine atom is not an optimal substitution in this case.

Acknowledgments
We thank ELDRUG S. A., Patras Science Park, Greece as well as VIANEX Pharmaceutical Company for financial support. The work was also supported by the research project No Z40550506 of the Institute of Organic Chemistry and Biochemistry, AS CR.

References

1. Carini, D.J., et al. *J. Med. Chem*. **34**, 2525-2546 (1991).
2. Matsoukas, J., et al. *J. Biol. Chem*. **269**, 5303-5311 (1994).
3. Matsoukas, J., et al. *J. Med. Chem.* **37**, 2958-2969 (1994).
4. Aulakh, G.K., et al. *Life Sci*. **81**, 615-639 (2004).
5. Matsoukas, J., et al. *J. Med. Chem*. **38**, 4660-4669 (1995).
6. Wahhab, A., et al. *Drug Res.* **43**, 1157-1168 (1993).
7. Agelis, G., et al. *J. Comput.-Aided Mol. Des.* **24**, 749-758 (2010).
8. Agelis, G. *Amino Acids* (2010) In press.
9. Resvani, A., et al. *J. Pept. Sci.* **16** (2010).
10. Kristensen, J., et al. *Org. Lett.* **3**, 1435-1437 (2001).
11. Duncia, J.V., et al. *J. Org. Chem*. **56**, 2395-2400 (1991).

Proceedings of the 31st European Peptide Symposium
Michal Lebl, Morten Meldal, Knud J. Jensen, Thomas Hoeg-Jensen (Editors)
European Peptide Society, 2010

Synthesis and Biological Evaluation of 1-Biphenylmethyl Substituted Imidazole AT1 ANG II Receptor Antagonists

Konstantinos Kelaidonis[1,4], George Agelis[1,4], Dimitra Kalavrizioti[2,4], Amalia Resvani[1,4], John Mikroyiannidis[1], Panagiotis Plotas[2,4], Dimitrios Vlahakos[3], and John Matsoukas[1,4]

[1]Department of Chemistry, University of Patras, Patras, 26 500, Greece; [2]Department of Medicine, University of Patras, Patras, 26 500, Greece; [3]Department of Internal Medicine, "ATTIKON" University Hospital, Athens; [4]ELDRUG S.A., Patras Science Park, Patras, Greece

Introduction

Angiotensin II (ANG II) is the octapeptide produced by the Renin-Angiotensin System (RAS) which plays a central role in blood pressure regulation and electrolyte homeostasis. Inactivation of RAS has stimulated many researchers to design drugs either by inhibiting Renin or the ACE or by blocking the ANG II receptors. The DuPont group was the first to develop Losartan (DuP 753) [1], an orally effective Angiotensin receptor blocker, which is metabolized *in vivo* to the more potent full antagonist EXP 3174 [2]. On the base of Structure-Activity Relationships (SAR) of the Losartan type AT1 antagonists we report an efficient synthesis of 1-biphenylmethyl substituted AT1 ANG II receptor antagonists based on Urocanic acid [3].

Results and Discussion

We report herein on the preparation of *E*-urocanic acid based analogues, focusing our attention on the structural modifications on the imidazole ring which would possibly enhance potency. Consequently, we have designed and synthesized a series of urocanic acid derivatives bearing a biphenylmethyl tetrazole moiety at 1-position and a bulky lipophilic and electron-withdrawing group such as bromide or iodide, at 5-position of the imidazole ring. Thus, the acrylic acid of *E*-urocanic acid at 4-position can align with the C-terminal carboxyl group of ANG II. Additionally, the rigid acrylic or saturated acid side chain was lengthened by esterification, resulting in the methyl ester or the bulky ester group (5-methyl-2-oxo-1,3-dioxol-4-yl)methyl of Olmesartan Medoxomil [4] (Figure 1), which is *in vivo* metabolized to the carboxyl moiety and may provide an effective structural element, emerging to compounds with improved activity. *In vitro* biological evaluation of the target compounds showed moderate binding affinity to the AT1 receptor.

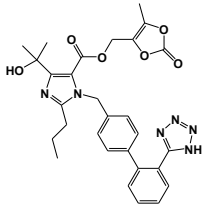

Fig. 1. Olmesartan Medoxomil, the prodrug of the carboxylic acid Olmesartan, a potent AT1 ANG II Receptor Antagonist.

This work has been the result of SAR and NMR studies on Angiotensin towards non-peptide mimetics as drugs for treating hypertension and cardiovascular diseases [5-10]. Biphenyl tetrazole derivative **4** was prepared as shown in Figure 2. In Figure 3 demonstrates the synthesis of the biphenyl tetrazole derivatives. Urocanic acid **5** was converted to the corresponding methyl ester **6** by esterification in dry methanol (MeOH). Alkylation of the methyl ester **6** at the N-1 position of the imidazole ring with the biphenyl

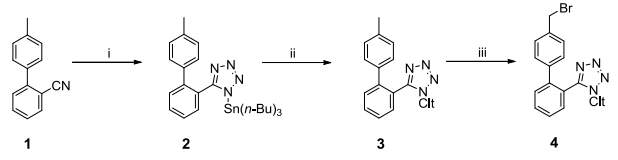

Fig. 2. Reagents and Conditions. (i) Sn(n-Bu)$_3$Cl, NaN$_3$, Tol; (ii) HCl in THF/H$_2$O, then Clt-Cl, TEA, DCM; (iii) NBS, DBP, CCl$_4$, reflux.

alkylating agent **4**, in the presence of sodium hydride (NaH) in *N,N*-dimethylformamide (DMF) provided the derivative **7**. Catalytic hydrogenation of the alkylated intermediate **7** in the presence of 10% Pd-C as catalyst in ethyl acetate (EtOAc)**,** afforded **8**. Halogenation of **8** with *N*-bromosuccinimide (NBS) and *N*-iodosuccinimide (NIS) in DMF afforded the bromo and iodo derivatives **9a**,**b**, respectively. Alkaline hydrolysis of the methyl esters **7**, **8**, **9a**,**b** under mild conditions using a solution of KOH in MeOH/H_2O/dioxane gave **13c**, **15c**, **17ac**,**bc**. Treatment of these acids with 4-chloromethyl-5-methyl-2-oxo-1,3-dioxole in *N,N*-dimethylacetamide (DMA) furnished the derivatives **13d**, **15d, 18ad,bd**.

Finally, removal of the 2-chlorotrityl protecting group with trifluoroacetic acid (TFA) in dichloromethane (DCM), in the presence of triethylsilane (TES) provided the target compounds **10**, **11**, **12a**,**b, 14c**,**d**, **16c**,**d**, **19ac,bc** and **20ad**,**bd**, respectively.

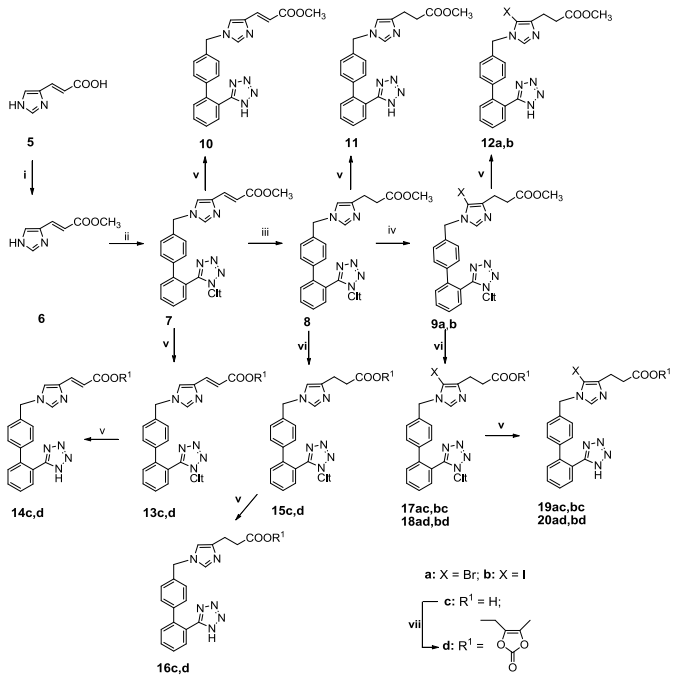

*Fig. 3. Reagents and conditions. (i) MeOH, conc. H_2SO_4, reflux; (ii) NaH, DMF, **4**; (iii) H_2/Pd-C, EtOAc; (iv) NXS, DMF, X = Br, I; (v) TFA/DCM/TES; (vi) KOH, H_2O/MeOH/Dioxan; (vii) K_2CO_3, DMA, 4-chloromethyl-5-methyl-2-oxo-1,3-dioxole.*

Acknowledgments

This research project was supported by ELDRUG S.A., Patras Science Park, Greece.

References

1. Carini, D.J., et al. *J. Med. Chem*. **34**, 2525-2547 (1991).
2. Christ, D.D., et al. *J. Pharmacol. Exp. Ther.* **268**, 1199-1205 (1994).
3. Agelis, G., et al. *Aminoacids* (2010) in press.
4. Yanagisawa, H., et al. *J. Med. Chem*. **39**, 323-338 (1996).
5. Agelis, G., et al. *J. Comput.-Aided Mol. Des.* **24**, 749-758 (2010).
6. Matsoukas, J., et al. *Biophys. Biochem. Res. Commun.* **122**, 434-438 (1984).
7. Matsoukas, J., et al. *J. Med. Chem.* **28**, 780-783 (1985).
8. Matsoukas, J., et al. *J. Biol. Chem.* **269**, 5303-5311 (1994).
9. Matsoukas, J., et al. *J. Med. Chem.* **37**, 2958-2969 (1994).
10. Matsoukas, J., et al. *J. Med. Chem.* **38**, 4660-4669 (1995).

Proceedings of the 31st European Peptide Symposium
Michal Lebl, Morten Meldal, Knud J. Jensen, Thomas Hoeg-Jensen (Editors)
European Peptide Society, 2010

Three Disulfide Bridged μ-Conopeptoids and Their Minimized Disulfide-Depleted Selenopeptide Derivatives

Aleksandra Walewska[1], Tiffany S. Han[2], Min-Min Zhang[2], Doju Yoshikami[2], Baldomero M. Olivera[2], Grzegorz Bulaj[3], and Krzysztof Rolka[1]

[1]Faculty of Chemistry, University of Gdańsk, Poland; [2]Department of Biology and [3]Medicinal Chemistry, University of Utah, Salt Lake City, UT, U.S.A.

Introduction

Peptide neurotoxins from cone snails continue to provide compounds with a therapeutic potential. The analgesic μ-conotoxin KIIIA is a three disulfide bridged peptide inhibitor of voltage-gated sodium channels, but more SAR studies are needed to optimize its subtype selectivity. Recent studies suggested that Lys[7] in KIIIA might be an attractive target for engineering selectivity in μ-conotoxins toward neuronal sodium channel subtypes [1,2]. Furthermore, converting this three disulfide bridged peptide into a one-disulfide-containing disulfide-depleted selenopeptide analogue did not significantly affect its bioactivity, but dramatically simplified oxidative folding [2]. Here, we report chemical synthesis, oxidative folding and bioactivity of two series of μ-conopeptoid analogues of KIIIA in which we replaced Lys[7] with peptoid monomers of increasing side-chain size: N-methylglycine (Sar), N-butylglycine (Nnle) and N-octylglycine (Noct). Each of the μ-conopeptoid analogues from the first series contained three disulfide bridges. To simplify oxidative folding, the second series of peptide-peptoid hybrid (peptomeric) analogues was introduced in the context of disulfide-depleted selenoconopeptides (Figure 1).

Fig. 1. Primary structure of disulfide-depleted selenoconopeptomeric analogues, where in position X= Sar, Nnle, or Noct.

Results and Discussion

The μ-conopeptoid analogues were synthesized using the Fmoc protocols. *N*-Substituted glycine derivatives (peptoids) were introduced into the peptide chain by the submonomeric approach [3]. In the series of disulfide-depleted selenoconopeptoid analogues, the cysteine thiols were protected with trityl (Trt) groups, whereas the selenocysteine (Sec) residues were protected with 4-methoxybenzyl (Mob) groups. The protected groups were removed during the cleavage of the peptides from the resin with an enriched reagent K and the Mob groups came off easily with 2,2'-dithiobis-(5-nitropyridine) (DTNP). The presence of DTNP in the cleavage mixture was critical for the removal of the p-methoxybenzyl groups and a simultaneous formation of a diselenide bridge. The oxidative folding was carried out in buffered solution (0.1 M Tris-HCl, pH 7.5) containing 1 mM reduced and 1 mM oxidized glutathione, followed by HPLC separation using reversed-phase C18 columns. The identity of each of the folded species was confirmed by MALDI-TOF or ESI mass spectrometry**.**

Electrophysiological experiments demonstrated that all μ-KIIIA analogues retained activity in blocking $Na_v1.2$, a neuronal subtype of sodium channel expressed in oocytes. Table 1 summarizes on- and off-rates of the block of $Na_v1.2$ as well as the percent block of the sodium currents by 10 μM peptide. Two analogues [Noct[7]]KIIIA and [Ala[1,9], Sec[2,15], Noct[7]]KIIIA, with the long side-chain size of Noct, turned out to be the most potent peptides.

These results prove that the peptoid strategy can be effectively applied to conotoxins containing three disulfide bridges.

Table 1. Kinetic parameters of KIIIA analogues (10 μM) in blocking Na_v 1.2

Analogue	*Block [%]*	k_{on} *[min^{-1}]*	k_{off} *[min^{-1}]*
[Sar^{7}]KIIIA	75	0.1	0.005
[Nnle^{7}]KIIIA	80	0.06	0.008
[Noct^{7}]KIIIA]	90	0.01	Double Exp.
[Ala^{1,9}, Sec^{2,15}, Sar^{7}]KIIIA	70	0.34	0.35
[Ala^{1,9}, Sec^{2,15}, Nnle^{7}]KIIIA	81	0.42	0.21
[Ala^{1,9}, Sec^{2,15}, Noct^{7}]KIIIA	85	0.17	0.23

Acknowledgments
This work was supported by University of Gdansk grant no BW/8290-5-462-0, and also in part by NIH grant GM-49677. T.S.H. acknowledges support from the US Student Fulbright Program.

References
1. Zhang, M.M., Green, B.R., Catlin, P., Fiedler, B., Azam, L., Chadwick, A., Terlau H., McArthur, J.R., French, R.J., Gulyas, J., Rivier, J.E., Smith, B.J., Norton, R.S., Olivera, B.M., Yoshikami, D., Bulaj G. *J. Biol. Chem*. **282**, 30699-30706 (2007).
2. Han, T.S., Zhang, M.M., Gowd, K.H., Walewska, A., Yoshikami, D., Olivera, B.M., Bulaj, G. *ACS Med. Chem. Lett*. **1**, 140-144 (2010).
3. Zuckermann, R.N., Kerr, J.M., Kent, S.B.H., Moos, W.H. *J. Am. Chem. Soc*. **114**, 10646-10647 (1992).

Proceedings of the 31st European Peptide Symposium
Michal Lebl, Morten Meldal, Knud J. Jensen, Thomas Hoeg-Jensen (Editors)
European Peptide Society, 2010

Conformational Analysis of Aliskiren, a Potent Renin Inhibitor, in Solution using Nuclear Magnetic Resonance (NMR) and Molecular Dynamics (MD)

Minos–Timotheos Matsoukas[1], Panagiotis Zoumpoulakis[2], and Theodore Tselios[1]

[1]University of Patras, Department of Chemistry, Patras, GR-26500, Greece; [2]Laboratory of Molecular Analysis, Institute of Organic and Pharmaceutical Chemistry, National Hellenic Research Foundation, Athens, GR - 11635, Greece

Introduction

Aliskiren [1] is a non-peptidic molecule that specifically and potently inhibits human renin (Figure 1). It has been newly introduced to the pharmaceutical industry as a standalone antihypertensive drug with various effects, especially blockade of the renin receptor. In previous studies, 1D NMR experiments have been performed on aliskiren [2], but no structural data is available in terms of its structural characteristics in solution. In this report, the conformational behavior of aliskiren is studied in water (H_2O) and N,N-dimethyl-formamide (DMF) solutions, through High Resolution 600MHz NMR spectroscopy, by means of 2D-NMR spectroscopy [3] and molecular modeling techniques. Data extracted on the interatomic distances between distant protons of the molecule's functional groups are combined with molecular dynamics simulations for inspection and evaluation of the drug's molecular properties.

Results and Discussion

NMR spectra were recorded on a Varian 600 MHz spectrometer (Figure 2). The sample concentration was kept *ca*. 10 mM dissolved in D_2O and DMF-d_7. Interatomic proton-proton distances were calculated using the two-spin approximation, and the integrated cross peaks intensity of a pair of adjacent aromatic protons was assumed to have a distance of 2.46 Å. The resulting distances were corrected for the frequency offset effects to be eliminated. Upper and lower limit values of constraints were allowed (10% of toleration).

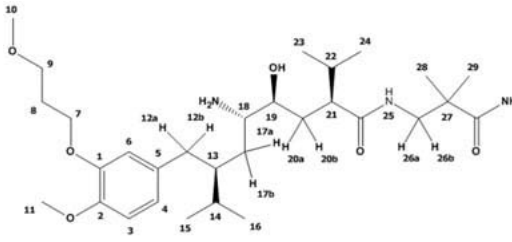

Fig. 1. Chemical structure of Aliskiren.

The conformational space of aliskiren was explored using

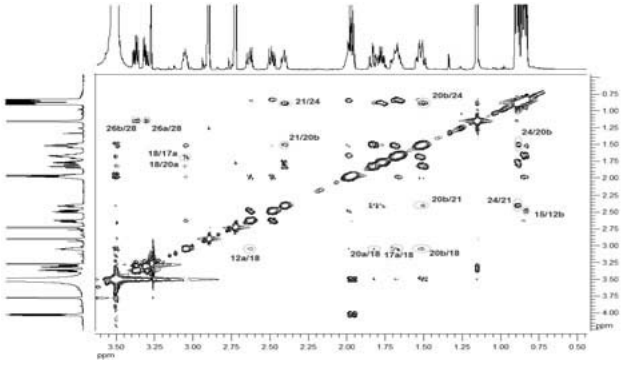

Fig. 2. 2D ROESY spectrum with interproton distances highlighted, obtained in DMF at 25 °C (region 0-4.0 ppm).

random sampling algorithms. The starting conformation was sketched in 2D and was subjected to an unconstrained conformational search on Discovery Studio with the Generate Conformations protocol and the BEST method which includes random conformation search and torsion search algorithms and ensures the best coverage of conformational space. The Generalized Born with a Simple SWitching (GBSW) implicit solvent model was applied, which is a molecular surface approximation that uses a van der Waals based surface with a smooth dielectric boundary, was used. The SHAKE algorithm was also implemented to satisfy bond geometry constraints and keep fixed bond lengths during all simulations. The dielectric constant (ε) was set to 81 (H_2O) and 37 (DMF) respectively in order to simulate in the most approximate way the environment of the different solvents used in the NMR studies. Among the 1000 conformers extracted for each solvent environment, the ones that satisfied the critical ROE data were chosen. These conformers were assigned as the starting ones for the molecular dynamics simulations under constraints.

Distance constraints from ROESY experiments were set prior to all further MD simulations. The procedure included an initial minimization stage for 200 steps, a second minimization stage for 200 steps, using the Adopted Basis Newton algorithm, a heating stage from 0^oK to 300^oK gradually, followed by an equilibration stage at 300^oK with a time step of 0.002 ps for 0.2 ns and finally a production stage for 30 ns. 500 minimization steps with each of the SD and ABNR algorithms respectively were applied, to relax the generated conformations and remove steric overlaps.

Parameters on saving result frequencies were set in such a way in order to extract 1000 conformations for each molecule. The same implicit solvent model was used, as for the generation of the initial conformations, with the dielectric constant (ε) set to $\varepsilon = 81$ for the D_20 and $\varepsilon = 37$ for the DMF environments. All minimizations had the limit of an RMSD of 0.01 Å as an energy convergence criterion. Five energy local minimum conformations were extracted from the MD run according to their Potential Energy.

When visualising results, it is clear that the most representative conformations of aliskiren in H_2O and DMF solutions are by far different in terms of situation of the pharmacophore groups compared to the conformation of the X-ray crystallography of aliskiren bounded to the recombinant glycosylated human renin receptor.

Apart from the significantly "curved" structures of this antihypertensive agent in H_2O and DMF, the essential structural difference is the position of the "backbone" of the molecule. In general the two different solvents impose a "curved" structure in both cases but a different orientation to the pharmacophoric groups. Overall, both are very different from the crystal structure indicating the flexibility of the compound and that in a dynamic receptor – ligand interaction, the molecule might undergo simple but essential structural changes in order to approach and fit the binding site.

Acknowledgments

We gratefully acknowledge the support of ELDRUG SA, Patras Science Park, Greece. We also thank Prof. Leonardo Pardo (Universitat Autònoma de Barcelona) for computer facilities and software use.

References

1. Hanessian, S., Guesne, S., Chenard, E. *Org. Lett.* **12**, 1816-1819 (2010).
2. Rahuel, J., Rasetti, V., Maibaum, J., Rüeger, H., Göschke, R., Cohen, N.C., Stutz, S., Cumin, F., Fuhrer, W., Wood, J.M., Grütter, M.G. *Chem. Biol.* **7**, 493-504 (2000).
3. Matsoukas, J., Agelis, G., Hondrelis, J., Yamdagni, R., Wu, Q., Ganter, R., Moore, D., Moore, G.J. *J. Med. Chem.* **36**, 904-911, (1993).

Proceedings of the 31st European Peptide Symposium
Michal Lebl, Morten Meldal, Knud J. Jensen, Thomas Hoeg-Jensen (Editors)
European Peptide Society, 2010

Development of a Protease-Resistant Bicyclic Peptide Targeting Human Plasma Kallikrein

Elise Bernard, David Loakes, and Gregory Winter
Laboratory of Molecular Biology, Medical Research Council, Hills Road, Cambridge, CB2 0QH, United Kingdom

Introduction

Many kallikreins are involved in carcinogenesis making them interesting potential biomarkers for cancer. Human plasma kallikrein is a serine protease involved in hereditary angioedema but only subcutaneous treatment is commercially available at the moment. We have been creating constrained bicyclic peptides; by constraining the peptide and engaging the target with two loops we aim to improve their binding affinities over linear peptides. The constrained loops are also more difficult to cleave with proteases; however to get the bicyclic peptides through the proteases of the gut we need to make further improvements. We focused our research on modifying the sequence of a bicyclic kallikrein inhibitor to obtain a good resistance to proteases.

Results and Discussion

We obtain bicyclic peptides by nucleophilic substitution of linear sequences around a benzenic core. The three Cys residues substitute to trisbromomethylbenzene [1,2] to form the constrained peptide. Our lead peptide, PK15 or ACSDRFRNCPADEALCG, is a consensus sequence obtained by cloning and targeting human plasma kallikrein [3]. We selected it for its excellent binding affinity of 4 nM. When cyclised, both loops are six amino acids long.

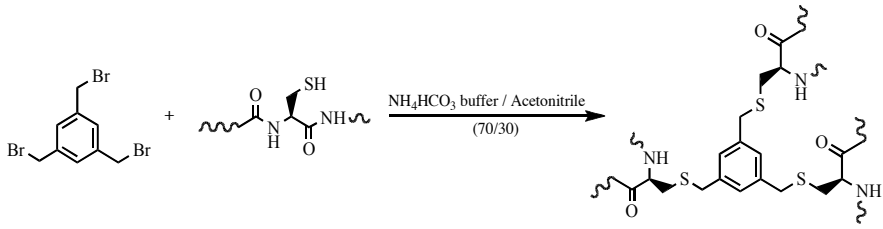

Fig. 1. Synthesis of bicyclic peptides.

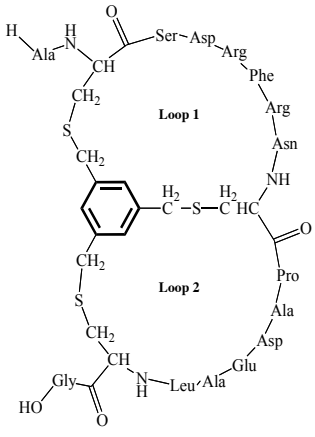

Fig. 2. Bicyclic PK15.

We focused our research on the modification of loop 1 of bicyclic PK15. This loop was shown to have a greater importance than the second loop as a truncated PK15 containing only the first loop is 20 times more potent than a truncated PK15 containing the second loop. Loop 1 was highly conserved in clones selected with human plasma kallikrein [3].

We designed two classes of peptidomimetics to find some better protease resistant structures that could resist a journey through the digestive system. Alteration of the side chain was investigated with peptides containing D-Phe, and where the Arg residues were replaced by homoarginine known for introducing a resistance to trypsin [4]. Alteration of the backbone was investigated with peptides containing *N*Me-Arg residues [5] and also with peptides having a reduced bond between Phe6 and Arg7 [6]. This modification was obtained by reacting Fmoc-phenylalaninal with the free amine of the peptide supported on the resin and reducing the resulting imine bond with $NaBH_4$/AcOH overnight [7].

Binding assays and digestion assays are in progress to determine how we can improve PK15 sequence to obtain a structure resistant to trypsin. The best compound could be a good candidate for further development of therapeutic agents.

References

1. Meloen, R., Timmerman, P., Langedijk, H. *Molecular Diversity* **8**, 57-59 (2004).
2. Timmerman, P., Puijk, W.C., Meloen, R.H. *J. Mol. Recogn.* **20**, 283-299 (2007).
3. Heinis, C., Rutherford, T., Freund, S., Winter, G. *Nature Chem. Biol.* **5**, 502-507 (2009).
4. Izdebski, J., Witkowska, E., Kunce, D., Orlowska, A., Baranowska, B., Radzikowska, M., Smoluch, M. *J. Pept. Sci.* **8**, 289-296 (2002).
5. Haviv, F., et al. *J. Med. Chem.* **36**, 363-369 (1993).
6. Coy, D., Hocart, S.J., Sasaki, Y. *Tetrahedron* **44**, 835-841 (1988).
7. Douat, C., Heitz, A., Martinez, J., Fehrentz, J.-A. *Tetrahedron Lett.* **41**, 37-40 (2000).

Proceedings of the 31st European Peptide Symposium
Michal Lebl, Morten Meldal, Knud J. Jensen, Thomas Hoeg-Jensen (Editors)
European Peptide Society, 2010

Structure-Activity Relationship Study of an Interleukin-1 Receptor Negative Modulator by α-Amino γ-Lactam Scanning

Luisa Ronga[1], Kim Beauregard[1], Andrew G. Jamieson[1], Daniel St-Cyr[1], Christiane Quiniou[2], Sylvain Chemtob[2], and William D. Lubell[1]

[1]Départment de Chimie, Universitè de Montréal, Montreal (Quebec), H3C 3J7, Canada; [2]St.-Justine Hospital Research Centre, Université de Montréal, Montreal (Quebec), H3T 1C5, Canada

Introduction

Agl (α-amino γ-lactam) residues in peptides have stabilized β-turn structures and enhanced potency and receptor selectivity [1], underlining their importance as synthetic tools in conformational analysis and drug discovery. The single and multiple insertion of Agl into a peptide sequence has been performed on solid support using a six-member cyclic sulfamidate derived from homoserine to install the amino lactam residue onto the peptide chain [2,3]. Moreover, the introduction into a peptide sequence of a beta-hydroxy-gamma-lactam (Hgl, a constrained Ser/Thr mimic) was recently achieved by employing N-(Fmoc)oxiranylglycine as a bis-electrophile in TFE to sequentially alkylate and acylate the growing peptide on solid support [4]. These methods have provided access to several analogs of the allosteric negative modulator of the interleukin-1 receptor 101.10 (D-Arg-D-Tyr-D-Thr-D-Val-D-Glu-D-Leu-D-Ala: rytvela) [5]. With the goal to better understand the conformational preferences responsible for the biological activity of 101.10, a library of (*R*)- and (*S*)-Agl analogs of rytvela was produced, including analogs possessing two Agl residues. Analogs of rytvela were also synthesized by replacing the D-Thr residue with Hgl residues of different stereochemistry. The efficacy of these lactam analogs was ascertained by measuring their influence on IL-1-induced human thymocyte TF-1 proliferation. Certain analogs retained activity and some exhibited improved properties relative to those of the parent peptide. Moreover, the conformational preferences of the Agl analogs of rytvela were examined by circular dichroism (CD) spectroscopy. Compared to the parent peptide, which is characterized by a disordered structure, the lactam analogs often exhibited spectra indicative of turn-like conformation.

Results and Discussion

The assessment of efficacy in inhibiting IL-1 induced TF-1 cell proliferation demonstrated that replacement of the *N*-terminal D-Arg[1] residue by (*R*)-Agl, in rytvela analog (*R*)-Agl**1**, led to a 2.2 fold increase in efficacy (44%) compared to the parent peptide. Moreover, replacement of D-Val[4] by (*R*)-Agl gave the rytvela analog (*R*)-Agl**4**, which exhibited similar activity (78%) as the parent peptide.

In light of the improved activity of (*R*)-Agl**1** and the maintained potency of (*R*)-Agl**4**, the combination of two (*R*)-Agl residues at positions 1 and 4 in rytvela was explored. In the assay for IL-1-induced proliferation of human thymocytes, (*R*)-Agl**1**-(*R*)-Agl**4** maintained a similar inhibitory effect (79%) as the parent peptide. At first assessment, the results suggest that the side chains of both D-Arg**1** and D-Val**4** may not be necessary for activity.

The CD spectrum of rytvela in water was compared to those of the Agl analogs. Enantiomeric D-peptides, such as rytvela and its lactam analogs, exhibit inverted curve shapes indicative of mirror image secondary structures to those formed by L-peptides [6].

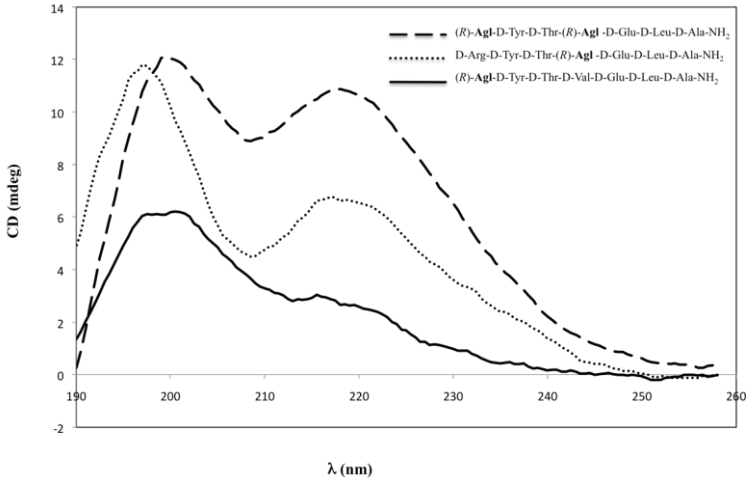

*Fig. 1. Far UV CD spectra in water at 20 µM of mono-lactam analogs (R)-Agl**1** and (R)-Agl**4** as well as bis-lactam analog (R)-Agl**1**-(R)-Agl**4**.*

The insertion of (*R*)-Agl motifs into the rytvela sequence influenced the shape of the CD spectra. The CD spectrum of rytvela exhibits a curve shape characteristic of a disordered structure [3]. On the other hand, the spectra of the mono Agl analogs ((*R*)-Agl-**1** and (*R*)-Agl-**4**) and the bis-Agl analog ((*R*)-Agl**1**, (*R*)-Agl**4**) showed two maxima around 198 nm and 220 nm, suggesting that these peptides adopt a helical conformation [6]. The better-defined maximum around 200 nm in the spectrum of the bis-Agl analog suggests that the insertion of the second Agl motif increases helical-like character relative to the mono-Agl analogs. Overall, the CD characterization has demonstrated that lactam analogs of rytvela exhibited spectra indicative of helical conformation. Examination of the biological activity of rytvela analogs by lactam scanning has thus been useful for enhancing peptide potency and for studying conformation-activity requirements.

Acknowledgments

The authors acknowledge financial support from the Natural Sciences and Engineering Research Council of Canada (NSERC), the Université de Montréal, the Canadian Institutes of Health Research (CIP-79848) CIHR-Team in GPCR allosteric regulation (CTiGAR), the Fonds Québecois de la Recherché sur la Nature et les Technologies (FQRNT), and equipment made possible from the Canadian Foundation for Innovation. L.R. thanks the Foreign Affairs and International Trade office of Canada (DFAIT) and the Fonds de la recherché en santé Québec for the post-doctoral research fellowships.

References

1. Freidinger, R.M. *J. Med. Chem*. **46**, 5553-5566 (2003) and references within.
2. Jamieson, A.G., Boutard, N., Beauregard, K., Bodas, M.S., Ong, H., Quiniou, C., Chemtob, S., Lubell, W.D. *J. Am. Chem. Soc.* **131**, 7917-7927 (2009).
3. Ronga, L., Jamieson, A.G., Beauregard, K., Quiniou, C., Chemtob, S., Lubell, W.D. *Biopolymers Peptide Science* **94**, 183-191 (2010).
4. St-Cyr, D.J., Jamieson, A.G., Lubell, W.D. *Org. Lett.* **12**, 1652-1655 (2010).
5. Quiniou, C., Przemyslaw, S., Lahaie, I., Hou, X., Brault, S., Beauchamp, M., Leduc, M., Rihakova, L., Joyal, J.-S., Nadeau, S., Heveker, N., Lubell, W.D., Sennlaub, F., Gobeil, Jr. F., Miller, G., Pshezhtsky, A.V., Chemtob, S. *J. Immunol.* **180**, 6977-6987 (2008).
6. Sakurai, K., Chung, S.H., Kahne, D. *J. Am. Chem. Soc.* **126**, 16288-16289 (2004).

Proceedings of the 31st European Peptide Symposium
Michal Lebl, Morten Meldal, Knud J. Jensen, Thomas Hoeg-Jensen (Editors)
European Peptide Society, 2010

The Synthesis of Peptide DualAG

Zhiguo Liu, Shengwu Wang, Qian Qiu, Shawn Lee, and Xiaohe Tong
CPC Scientific Inc., 1245 Reamwood Ave., Sunnyvale, CA, 94089, U.S.A.

Introduction

Recently, it was reported that peptide DualAG, H-s-QGTFTSDYSKYLDSRRAQDFVQW-LMNTKRNRNNIAC(CH_2CO-PEG4-Cholesterol), exhibits superior weight loss, lipid lowering activity, and antihyperglycemic efficacy [1]. The preparation and conjugation of cholesterol with PEG_4 linker to the C-terminus of native oxyntomodulin via a Cys sidechain improve pharmacokinetics and are also key steps for synthesis of peptide DualAG which incorporate a D-Ser^2 substitution that confers resistance to dipeptidyl peptidase 4(DPP-4). Here we report the synthesis of DualAG with Fmoc solid phase synthesis to obtain peptide precursors and solution phase work to make and react cholest-5-en-3-yl 1-iodo-2-oxo-6,9,12,15-tetraoxa-3-azaoctadecan-18-oate(**3**) with the free thiol-containing peptide to obtain peptide DualAG.

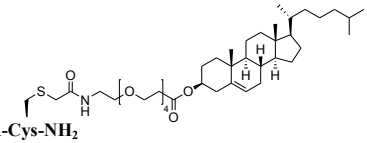

H-s-QGTFTSDYSKYLDSRRAQDFVQWLMNTKRNRNNIA-Cys-NH_2

Fig. 1. The structure of DualAG.

Results and Discussion

Cholesterol (**1**) was reacted with Fmoc-PEG_4-OH in dry DCM solution containing DIC and DMAP to give the Fmoc-PEG_4-cholesterol with 85% yield. The Fmoc-PEG_4-cholesterol was treated with diethylamine in THF and the reaction mixture was purified by silica gel to obtain the NH_2-PEG_4-cholesterol (**2**) with 45% yield. The NH_2-PEG_4–cholesterol (**2**) was iodoacetylated with iodoacetic anhydride in anhydrous DCM and the reaction mixture was purified by silica gel to give a key intermediate cholest-5-en-3-yl 1-iodo-2-oxo-6,9,12,15-tetraoxa-3-azaoctadecan-18-oate(**3**) with 90% yield.

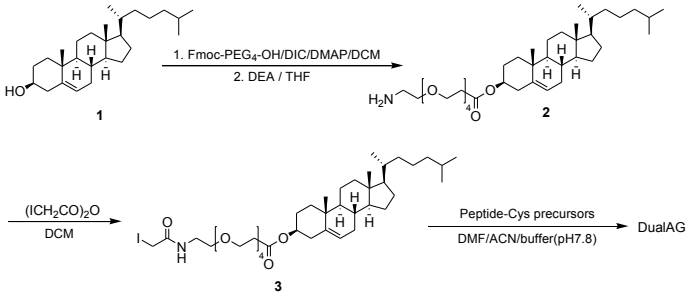

Fig. 2. Synthesis of DualAG.

The free thiol-containing peptide precursor of DualAG, H-s-QGTFTSDYSKYLDSRRA-QDFVQWLMNTKRNRNNIAC, was synthesized by standard solid-phase peptide synthesis using Fmoc/t-Bu chemistry and purified by RP HPLC using water/acetonitrile (0.1% TFA) gradients with >95% purity. Cholesterol-peptide conjugate (DualAG) was synthesized by reaction of the free thiol-containing peptide precursors with 3 in mixture solvent of DMF/acetonitrile/PBS buffer (pH 7.8) at room temperature. After the reaction was completed, the peptide conjugates was purified by RP HPLC using water/acetonitrile (0.1% TFA) gradients. Purified DualAG was characterized by electrospray MS.

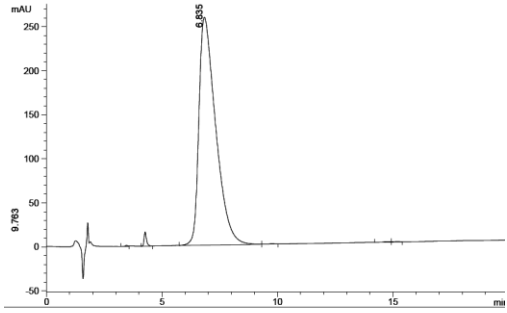

Fig. 3. RP-HPLC of DualAG, A: 0.1%TFA in water, B: 0.1%TFA in (80% ACN + 20% water), linear gradient 68-78% B in 20 min, flow 1 ml/min.

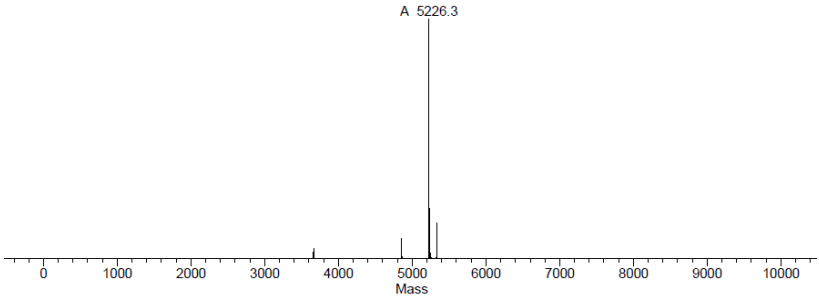

Fig. 4. Electrospray MS of DualAG. Theoretical $M+H^+$ 5226.0.

References

1. Alessandro, P., et al. *Diabetes* **58**, 2258-2266 (2009).

Proceedings of the 31st European Peptide Symposium
Michal Lebl, Morten Meldal, Knud J. Jensen, Thomas Hoeg-Jensen (Editors)
European Peptide Society, 2010

Structure–Activity Relationship Studies for Cystapep 1 and Its Analogues

Aneta Pogorzelska[1], Sylwia Rodziewicz-Motowidło[1], Maria Smużyńska[1], Zet Freiburghaus[2], Anders Grubb[2], and Franciszek Kasprzykowski[1]

[1]Department of Medicinal Chemistry, University of Gdansk, Gdansk, 80-952, Poland;
[2]Department of Clinical Chemistry, University Hospital, Lund, SE-221 85, Sweden

Introduction

In 1989, a group of potential antimicrobial compounds structurally based upon the amino-terminal inhibitory centre of human cystatin C was described. Peptidyl diazomethanes were found to inhibit growth of *Streptococcus pyogenes*. Because of their origin it was thought that this sequence inhibits cysteine protease produced by bacteria, but subsequent analysis of a number of similar compounds showed that their antimicrobial effect does not include protease inhibition. The search for both linear and cyclic analogues found that one of the compounds, called later **Cystapep 1** (CpV) (Figure 1), has comparatively low MIC and MBC values for *S. pyogenes* and *S. aureus*. Cystapep 1 is also effective against antibiotic resistant staphylococci and streptococci, as well as against susceptible strains of these species [1,2].

Results and Discussion

Calorimetric traces of interaction between CpV analogues and POPG LUVs were measured by ITC experiments. Binding parameters were defined on the assumption that all surface of LUVs is available for interaction and to disregard the electrostatic attraction. In the case of inactive analogues A-89 and A-92 the research showed that they do not interact with POPG LUVs. Among others, compounds A-134 and CpV are active against gram-positive bacteria whilst A-141 does not inhibit growth of tested pathogens, however, the exothermic binding reactions are observed for these peptidomimetics. Under the condition used, the peptidomimetics are completely bound to the lipid vesicles. In the case of Cystapep 1 complicated titration pattern is observed. The heat of reaction did not decrease smoothly with each injection but showed an inflection point. This behaviour was observed previously for some surfactant and was explained by a process which could be identified as a micelle formation ↔ demicellization equilibrium of the phospholipid / surfactant mixture [3].

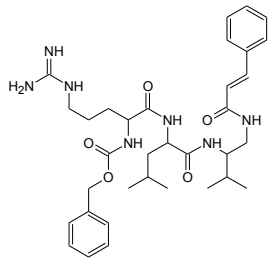

Fig. 1. Cystapep 1 structure.

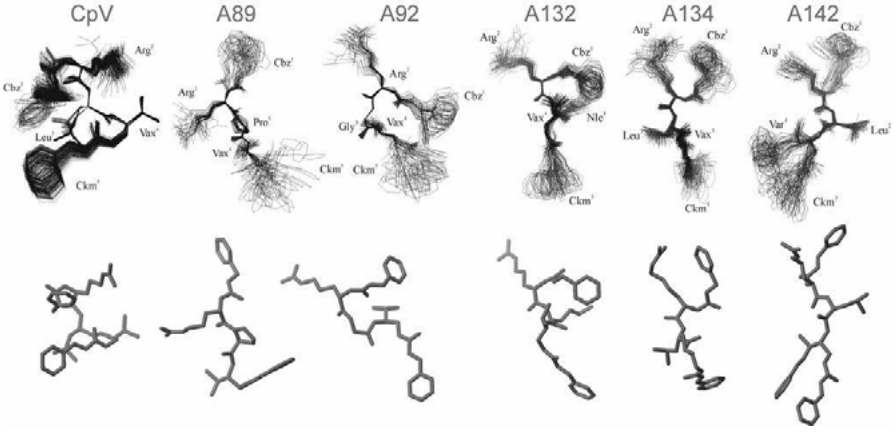

Fig. 2. Superimposed conformations of studied peptidyl derivatives.

Interaction between positively charged peptides or peptidomimetics and negatively charged POPG membranes can be divided into at least two steps. The first step is an electrostatic adsorption process which leads to an increased peptide concentration above the plane of membrane. The second step is a hydrophobic adsorption which is characterized by penetration of the molecule into the lipid bilayer. However, in these studies the electrostatic attraction was omitted in calculation. Assumption, that only hydrophobic effects are important in the interaction, is based on the fact that Cystapep 1 analogues are highly hydrophobic molecules. Moreover, the positive charge of molecules is low and it comes from the guanidinium group which possesses special hydrogen bond properties [5]. The lack of interactions between POPG LUVs and A-89 or A-92 may also indicate that electrostatic attraction for the membrane surface does not play important role in the case of CpV analogues.

POPG LUVs constitute the model of bacterial cell membrane. POPG is potential cell-surface target for the tested peptidomimetics. However, ITC research showed that interaction with POPG LUVs is not strongly depend on antibacterial activity of tested compounds. The most active peptidomimetic from among derivatives tested by ITC studies A-134 has the lowest value of binding constant. ITC results suggest that the membrane disruption is not a significant mode of action for Cystapep 1 analogs in bacterial system. Probably these peptidomimetics interact with intracellular site of bacteria.

We have also performed some experiments using Cvp analogues and POPC LUVs. Research of interaction between this kind of liposomes and peptidomimetics may give some information about compounds ability to interact with eukaryotic cells. These studies showed that none of tested analogues can interact with model of cell membrane of advanced organisms. Toxicity studies showed that Cystapep 1 analogues are not toxic against eukaryotic cells.

The NMR spectra of all investigated molecules show two or more sets of proton resonances. In the NOESY or ROESY spectra it is possible to observe the close contacts between Cbz1 and Ckm5 residues for CpV molecule (see Figure 2). For A-92 NOE effects are observed between Cbz1 and Vax4 residues, but for A-89, A-132, A-134 and for A-142 no medium- or long-range contacts are found.

Based on the integration of non-overlapping signals in 1D spectra a ratio of major and minor conformations at 303 K was determined. The proportion of minor conformations was estimated to about 20% for Cystapep 1, 30-40% for A-92, A-132, A-134 and for A-142 peptidomimetics. For A-89 it is difficult to measure.

The antibacterial investigations show that positions 2, 3 and 4 in the studied compounds are very sensitive to replacements. The replacement of very hydrophobic Leu residue in CpV by less hydrophobic Gly or Pro residues in A-89 and A-92, respectively lead to the loss of the biological activity. Replacement of position 2, 3 or 4 in CpV by homoarginine, by norleucine or by benzyloxy group in A-134, A-132 and A-142, respectively lead to the better biological activity.

The major and two or more minor conformations in NMR spectra characterize all studied compounds. It suggests high flexibility of studied peptidomimetics, where very high flexibility could be responsible for very low biological activity. The lower flexibility, with *cis-trans* isomerization of Arg2-Leu3 peptide bond in A-132, A-134 and in A-142 compounds could be responsible for very high antibacterial activity.

The structural studies of all peptidomimetics show that close contact between guanidyl group of Arg2 or Har2 and aromatic ring of Cbz1 and existence of the compact hydrophobic part in the molecules could be responsible for the high antibacterial activity.

Acknowledgments

The work was supported by Ministry of Science and Higher Education, Grant No.0235/B/H03/2008/35 and NN204 023535 and European Social Fund. The calculations were carried out in the TASK in Gdansk, Poland.

References

1. Jasir, A., Kasprzykowski, F., Lindström, V., Schalèn, Grubb, A. *Indian J. Med. Res*. **119**, 74 (2004).
2. Jasir, A., et al. *APMIS* **111**, 1004 (2003).
3. Wenk, M.R., Seelig, J. *J. Phys. Chem. B*, **101**, 5224 (1997).
4. Wenk, M.R., Seelig, J. *Biochemistry* **37**, 3909 (1998).
5. Gonçalves, E., Kitas, E., Seelig, J. *Biochemistry* **44**, 2692 (2005).

Proceedings of the 31st European Peptide Symposium
Michal Lebl, Morten Meldal, Knud J. Jensen, Thomas Hoeg-Jensen (Editors)
European Peptide Society, 2010

Anticancer Activity of Short Cationic Beta-Peptidomimetics

Veronika Tørfoss[1], Dominik Ausbacher[1], Terkel Hansen[1], Martina Havelkova[1], and Morten B. Strøm[1]

[1]*Institute of Pharmacy, Department of Health Sciences, University of Tromsø, Tromsø, N-9037, Norway*

Introduction

Current anticancer chemotherapy is based on alkylating agents, antimetabolites and different natural products. However, these compounds show poor selectivity for tumor cells and cause severe side-effects, resulting in troublesome therapeutic regimes and low patient compliance [1]. Tumor cells are also notorious for developing resistance to current therapies by evolving efflux pumps that transport the chemotherapeutics out of the tumor cells, or by other mutations that prevent efficient drug-target interactions [2,3]. There is therefore an urgent demand for developing anticancer drugs with new targets and modes of action to improve anticancer selectivity, diminish induction of resistance, and improve patient compliance.

In the search for new types of anticancer drugs there is an increasing interest for cationic antimicrobial peptides (AMPs), or host defense peptides belonging to the innate immunity of mammals, amphibians and insects [4-8]. Cationic AMPs that display anticancer activity show a unique mode of action by targeting the cell membrane of tumor cells. The AMPs can destabilize the cytoplasmic membrane to cause lysis or translocate across the cell membrane and attack the mitochondria, inducing apoptosis [9]. The selectivity of cationic AMPs for cancer cells compared to non-malignant cells is thought to reside in a small excess of phosphatidylserine (PS) and other anionic cell membrane constituents on the tumor surface, which are not present on the outer leaflet of the cell membrane of healthy cells, giving the tumor cells a slightly more negative membrane surface than healthy cells [10-14].

We have in the present study synthesized and tested the toxicity and antitumoral potency of eight cationic beta-peptidomimetics that were designed to mimic the amphipathic properties of Lactoferricin B (LfcinB). LfcinB is a well-known antitumoral peptide, and the basis of its antitumoral properties is assumed to reside in its content of aromatic residues, a net positive charge, and an overall strong amphipathic structure. The beta-peptidomimetics were designed to mimic the structural properties of LfcinB by introducing a bulky, lipophilic beta-amino acid into a palindromic model heptameric peptide (H-Lys-Lys-Trp-'beta-amino acid'-Trp-Lys-Lys-NH_2). By changing the bulkiness and lipophilicity of the substituents of the beta-amino acids, we have investigated how the bulk of the beta-amino acid could influence the antitumoral potency and toxicity of the beta-peptidomimetics.

Results and Discussion

The beta-peptidomimetics displayed high anticancer potency against RAMOS cells (human Burkit´s lymphoma) and the murine A20 cancer cell line, with IC_{50} values from 8-24 microMolar for the three most potent compounds. The beta-peptidomimetics displayed furthermore up to 6-fold selectivity for cancer cells compared to non-malignant human MRC-5 fibroblasts, and were basically non-hemolytic.

Using retention times on a C_{18}-RP-HPLC column as a measurement of overall lipophilicity, and correlating the retention times with biological data, we were able to visualize important trends in our results (Figure 1).

In general, the anticancer potency increased with increasing retention time, and thereby increasing lipophilicity of the beta-peptidomimetics. However, when considering the selectivity of the different beta-peptidomimetics, there was no apparent linear correlation with the retention times. But as we looked at the distribution of the beta-peptidomimetics with respect to retention times, three clusters of compounds were evident (Figure 1). Since the only difference between the beta-peptidomimetics was the substituent of the beta-amino acid, and since the retention times did not correlate with the calculated logPs of the compounds, this clustering might reflect different types of structural conformations of the peptide chains. The selectivity for A20 over MRC-5 was highest for

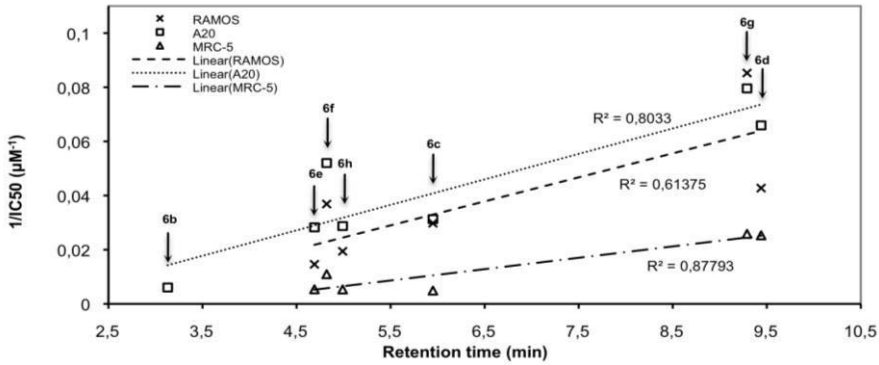

Fig. 1. Antitumor activity against the A20 and RAMOS cell lines and toxicity against the MRC-5 cell line of compounds 6a-h correlated to retention time on a C_{18}-RP-HPLC column. Linear regression is displayed for the three different cell lines, as well as the coefficients of determination (R^2).

compounds with retention times between 4.5 and 6 min, while it was low, or not measurable, for compounds with the longest and shortest retention times. This might imply that the selectivity for cancer cells was more dependent on structural differences, and not on overall lipophilicity, as opposed to the anticancer potency of the beta-peptidomimetics.

Conclusion

We have designed and synthezised a total of eight higly potent and selective beta-peptidomimetics resembeling AMPs, and their antitumoral activity correlated well with their retention times on a RP-HPLC column. At the same time the selectivity of the compounds did not correlate with the retention times in the same way, but seemed to be more dependent on structureal differences. Further studies are in progress to elucidate a pharmacophore model for short anticancer beta-peptidomimetics.

Acknowledgments

The project was supported by KOSK II grant 185141/V30 (Norwegian Research Council).

References

1. Smith, L.L., et al. *Critical Reviews in Toxicology* **30**, 571-594 (2000).
2. Pérez-Tomás, R. *Current Medicinal Chemistry* **13**, 1859-1865 (2006).
3. Ellis, L.M., Hicklin, D.J. *Clin. Cancer Res.* **15**, 7471-7478 (2009).
4. Hoskin, D.W., Ramamoorthy, A. *Biochimica et Biophysica Acta (BBA) – Biomembranes* **1778**, 357-375 (2008).
5. Leuschner, C., Hansel, W. *Current Pharmaceutical Design* **10**, 2299-2310 (2004).
6. Papo, N., Shai, Y. *Cellular and Molecular Life Sciences* **62**, 784-790 (2005).
7. Mader, J.S., Hoskin, D.W. *Expert Opin. Investig. Drugs* **15**, 933-946 (2006).
8. Schweizer, F. *European Journal of Pharmacology* **625**, 190-194 (2009).
9. Eliassen L.T., et al. *International Journal of Cancer* **119**, 493-500 (2006).
10. Kim, Y., Varki, A. *Glycoconjugate Journal* **14**, 569-576 (1997).
11. Utsugi, T., et al. *Cancer Res.* **51**, 3063-3066 (1991).
12. Schröder-Borm, H., Bakalova, R., Andrä, J. *FEBS Letters* **579**, 6128-6134 (2005).
13. Dobrzynska, I., et al. *Molecular and Cellular Biochemistry* **276**, 113-119 (2005).
14. Iwasaki, T., et al. *Peptides* **30**, 660-668 (2009).

Proceedings of the 31st European Peptide Symposium
Michal Lebl, Morten Meldal, Knud J. Jensen, Thomas Hoeg-Jensen (Editors)
European Peptide Society, 2010

Bactericidal Activity of Small Beta-Peptidomimetics

Terkel Hansen, Dominik Ausbacher, Martina Havelkova, and Morten B. Strøm*

*Department of Pharmacy, Faculty of Health Sciences, University of Tromsø, 9018, Tromsø, Norway; *Corresponding author, e-mail: morten.strom@uit.no*

Introduction

The number of causalities reported in the US by methicillin resistant *Staphylococcus aureus* (MRSA) infections is currently higher than the number of both HIV/AIDS and tuberculosis together; hence the need for novel antimicrobial agents is urgent [1,2]. Cationic antimicrobial peptides (AMP's) have since their discovery during the 1980's been heavily investigated for their antimicrobial properties. AMP's show a unique mode of action by targeting the bacterial cytoplasmic membrane in a non-receptor specific manner, and thereby have a much lower risk of inducing resistance compared to conventional antimicrobial drugs [3-5].

A pharmacophore model for short AMP's was reported in 2003. In this model activity against both *E. coli* and *S. aureus* necessitates an amphipathic peptide with a net positive charge of +2 [6]. To obtain antimicrobial activity against the Gram-negative bacterium *E. coli* three bulky/lipophilic groups is also a necessity, whereas for activity against the Gram-positive bacteria *Staphylococcus aureus*, MRSA and methicillin resistant *Staphylococcus epidermidis* (MRSE), only two bulky/lipophilic groups are needed [6].

The objective of the current project was to investigate if a scaffold based on an achiral lipophilic 3-amino-2,2-disubstituted propionic acid (beta^{2,2}-amino acid) coupled to a C-terminal amidated L-arginine residue could confine all the elements of the pharmacophore model for *anti-staphylococcal* activity. The minimal inhibitory concentration (MIC) of the compounds was determined against *S. aureus*, MRSA, MRSE and *E. coli*. A toxicity assessment was performed using human erythrocytes by measuring the hemolytic activity of the beta-peptidomimetics. Plating of treated bacterium suspensions at different time intervals and at different concentrations was used to investigate if the main mechanism of action was bactericidal or bacteriostatic.

Results and Discussion

Synthesis:

The beta-peptidomimetics were prepared in a seven-step synthesis in which only the three intermediates shown in Scheme 1 were isolated, as previously reported by our group [7]. The total yields for synthesis of the crude Boc-beta^{2,2}-amino acids (**3a-n**) ranged therefore from 30-71%, depending on the bulkiness of the lipophilic side-chains. For details regarding structures and synthesis, see Hansen, et al [7].

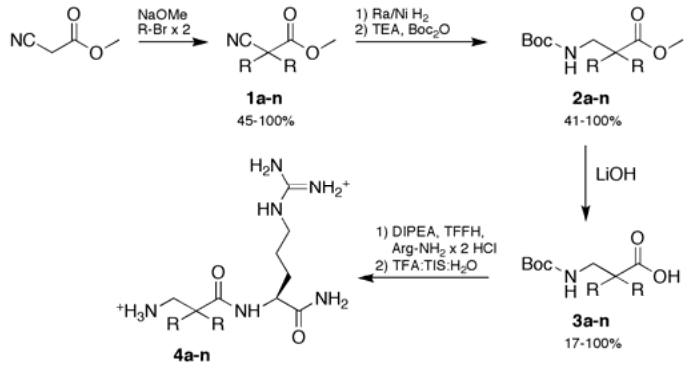

Scheme 1. Overview of synthesis.

Biological results:
By varying the lipophilic side-chains of the beta^{2,2}-amino acids, we obtained a series of highly potent beta-peptidomimetics with MIC values of 2.1-7.2 μM against MRSA, MRSE, *S. aureus* and *E. coli* [7]. The results from screening of antimicrobial activity showed furthermore that the beta-peptidomimetics were in general more potent against the Gram-positive bacteria than against *E. coli*. There was also a strong correlation between antimicrobial potency of the compounds and overall lipophilicity measured on a RP-HPLC system [7]. The beta-peptidomimetics displayed very low hemolytic activity, with EC_{20} values well above their MIC values. Plating of treated bacterium suspensions showed that the beta-peptidomimetics were bactericidal. The bactericidal effect correlated with both increased concentration and increased time of treatment.

Conclusion
In the current study we chose to investigate a scaffold that would fulfill the pharmacophore model of short AMP's. The resulting peptidomimetics were bioisosteres of di-peptides but having the side-chain functionalities of tri-peptides due to the beta^{2,2}-amino acid derivatives. The small size of the beta-peptidomimetics may provide solutions to many common problems associated with developing AMP's into novel antimicrobial agents. The study has demonstrated that small beta-peptidomimetics can be used to mimic the antimicrobial potency and selectivity of much larger AMP's, and that such small amphipathic scaffolds may be promising drug-candidates for treatment of serious bacterial infections.

References
1. Projan, S.J. *Drug Discov. Today* **13**, 279-280 (2008).
2. Boucher, H.W., et al. *Clinical Infectious Diseases* **48**, 1-12 (2009).
3. Hancock, R.E. *Microbiology* **149**, 3343-3345 (2003).
4. Giuliani, A., et al. *Central Eur. J. Biol.* **2**, 1-33 (2007).
5. Boman, H.G. *J. Intern. Med.* **254**, 197-215 (2003).
6. Strøm, M.B., et al. *J. Med. Chem.* **46**, 1567-1570 (2003).
7. Hansen, T., et al. *J. Med. Chem.* **53**, 595-606 (2010).

Proceedings of the 31st European Peptide Symposium
Michal Lebl, Morten Meldal, Knud J. Jensen, Thomas Hoeg-Jensen (Editors)
European Peptide Society, 2010

Synthesis of Peptidomimetics Mimicking the Hormone Binding Domain of the Estrogen Receptor

Rosa Romeralo Tapia, Fréderique Backaert, Jan Goeman, and Johan Van der Eycken

Laboratory for Organic and Bioorganic Synthesis, Department of Organic Chemistry, Ghent University, Krijgslaan 281 (S4), B-9000, Ghent, Belgium

Introduction

Endocrine disrupting chemicals (EDC's) are an important class of pollutants, which have in common that they show affinity for the hormone-binding domain of the estrogen receptor (HBD-ER), thus disturbing the endocrinal system. Detection in wastewater has not been successful due to their low concentration. Therefore, new sensitive screening methods are highly demanded. A possible solution is to preconcentrate them using estrogen receptor mimics for solid phase extraction. To this end, a dipodal peptidomimetic of the HBD-ER will be attached on a solid support. Amino acids known to be important for the estrogen-receptor interaction will be preferably incorporated [1] onto the aromatic scaffold: 3,5-diamino benzoic acid.

Results and Discussion

The first peptide mimic was built using standard solid phase Fmoc-linear peptide chemistry. Fmoc-Gly-OH was introduced as the first residue. Coupling of non-polar amino acids (Ala, Leu and Phe) and Glu *via* amide bond formation was optimized. Finally, the peptidomimic, **1** was purified by RP-HPLC.

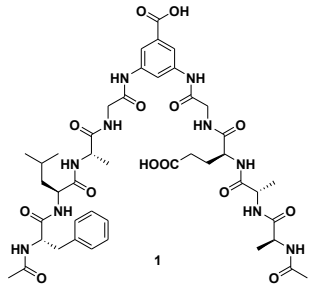

1

NMR characterization was performed in order to confirm the amino acid sequence and to get information about the three dimensional arrangement, like possible chain interactions and H bonding. Chemical shifts of every residue were assigned in 2D TOCSY and the sequence was confirmed by NOE contacts between adjacent amino acids leading to the verification of the two peptidic arms in N to C direction: Ala-Ala-Glu-Gly and Phe-Leu-Ala-Gly. To analyze the possible H bonding between chains or nonadjacent residues, the decay of amide proton signal intensities due to hydrogen exchange spectra was analyzed. The most evident result is found in the amide proton from the phenylalanine residue where the signal disappears when the solvent was changed from H_2O to deuterated water. From this experiment we can conclude that these protons are not involved in H bondings, making the H easily accessible for the exchange with the solvent. The less intense decay is observed for the amide protons of the leucine and the alanine. On the other hand, all amide protons from the second synthesized strand, Gly-Glu-Ala-Ala, showed decay after solvent was changed to D_2O.

Secondly, a convergent route based on click chemistry [2] was explored for an easier coupling of the amino acid on the electron-poor amine of this scaffold. First, the synthesis of azido peptides was performed using 2-chlorotrityl chloride resin as solid support. After the synthesis of the peptides, azidoacetic acid was coupled in the last amino position. Coupling yields were followed by measurements of UV absorption of the dibenzofulvene adduct of aliquots taken from the resin. The crude cleaved azido peptides were clicked onto

the scaffold, sequentially modified by 4-pentynoic acid using CuI and ascorbic acid [3]. Synthesis of azido peptides was later improved by the solid phase diazotransfer reaction using the reagent developed by Goddard-Borger and Stick [4].

Subsequently, a second $N_3CH_2COLeuPhe$-OH moiety was introduced after Fmoc removal and 4-pentynoic acid coupling. The product was cleaved and the crude material was purified using reversed phase HPLC, yielding the dipodal peptide, **2**, in 82% purity and an overall yield of 27%. This methodology demonstrates to us that it is possible to introduce two different peptide chains in the future. Doing so, a library of potential estrogen receptor mimics can be created.

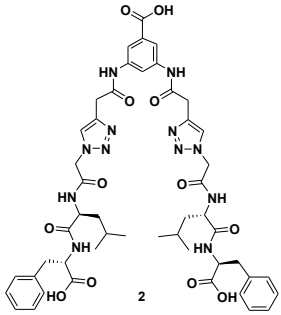

2

Peptide mimic **2** is completely symmetric, and thus an identical set of signals are found for the leucine and for the phenylalanine residues from each of the two strands by NMR. Identification of each proton signal was not difficult due to the high purity of the compound. Different chemical shifts for the δ protons from leucine can be explained, as the delta protons from each methyl group are inequivalent. From the NOE contact between an amide proton from leucine and the aromatic protons from the phenylalanine side chain, it could be proposed that these protons are involved in H bondings between chains due to the sterical hindrance between protons from the same chain. The hydrophobic cavity of **2** is probably narrower than the cavity formed in **1.**

Acknowledgments

This research project is supported by a Marie Curie Early Stage training Fellowship of the European Community´s Sixth Framework Programme under contract number MEST-CT-2005-020643 and by Ghent University. Katelijne Gheysen and prof. J. Martins from the NMR and Structural Analysis Group (UGent) are gratefully acknowledged for their scientific support.

References

1. a) Brzozowski, A.M., Pike, A.C.W, Dauter, Z., Hubbard, R.E., Bonn, T., Engström, O., Lars, O., Greene, G.L. *Nature* **389***,* 753-758 (1997); b) Tannenbaum, D.M., Wang, Y., Shawn, P.W., Sigler, P.B. *Proc. Natl. Acad. Sci.* **95***,* 5998-6003 (1998).
2. a) Rostovtsev, V.V., Green, L.G., Fokin, V.V., Sharpless, K.B. *Angew Chem. Int. Ed.* **41** 2596-2599 (2002); b) Tornoe, C.W., Christensen, C., Meldal, M. *J. Org. Chem.* **67,** 3057-3064 (2002).
3. Zhang, Z.S., Fan, E. *Tetrahedron Letters* **47**, 665-669 (2006).
4. Goddard-Borger, E.D., Stick, R.V. *Org. Lett.* **9**, 3793-3800 (2007).

Proceedings of the 31st European Peptide Symposium
Michal Lebl, Morten Meldal, Knud J. Jensen, Thomas Hoeg-Jensen (Editors)
European Peptide Society, 2010

Pyrrolo[3,2-e][1,4]diazepin-2-one γ-Turn Mimic Synthesis on TAP Soluble Support

Nicolas Boutard, Julien Dufour-Gallant, and William D. Lubell
Département de Chimie, Université de Montréal, C.P. 6128 Succursale Centre-Ville, Montréal, Québec, H3C 3J7, Canada

Introduction

1,4-Aryldiazepin-2-ones are privileged structures, which display a wide range of biological activities, including antagonism at G-protein coupled receptors, enzyme inhibition and antibiotic activity. Moreover, the diazepin-2-one ring can mimic an inverse γ-turn peptide conformation (Figure 1) [1,2]. We have developed a modular solution-phase method for accessing pyrrolo[3,2-e][1,4]diazepin-2-one scaffold **1** from *N*-(PhF)-4-hydroxyproline **3** (Scheme 1) employing a diastereoselective Pictet-Spengler reaction [1]. Tetraaryl-phosphonium (TAP) salts have emerged as solubility control groups (SCGs) for applications as soluble supports of reagents and for the preparation of small molecules and peptides [3-5]. These SCGs are soluble in polar solvent systems and precipitated in low polarity solvents. In the context of a study directed towards the development of a supported synthesis of γ-turn mimics, we now present our results concerning the preparation of heterocyclic scaffold **1** on TAP soluble support.

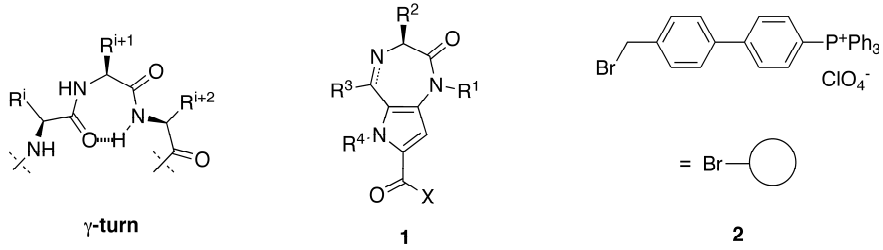

*Fig. 1. γ-Turn, pyrrolo[3,2-e][1,4]diazepin-2-one scaffold (**1**) and "Merrifield TAP" (**2**).*

Results and Discussion

Soluble supports offer practical advantages for organic synthesis such as the oppourtunity to perform reactions under homogenous conditions. Protocols used for the synthesis of **1** in solution [1] were adopted using "Merrifield resin-like" (4'-(bromomethyl)-[1,1'-biphenyl]-4-yl)triphenylphosphonium support **2** as its perchlorate salt [5] (Figure 1), because of its stability to acidic conditions used in the TFA-catalyzed Pictet-Spengler reaction and its ease of precipitation in Et_2O. All reactions were monitored by TLC ($MeOH/CH_2Cl_2$ eluents) and RP-HPLC-MS. Work-ups were followed by a saturated aqueous $LiClO_4$ wash, to ensure the presence of the ClO_4^- counteranion, a dionized water wash, drying over sodium sulfate and concentration. The resulting residue was disolved in a minimum volume of CH_2Cl_2 and precipitated upon addition of a 5-fold volume of Et_2O.

(2*S*,4*R*)-4-Hydroxy-*N*-(PhF)proline **3** was prepared according to the previously described procedure [6] and converted to the corresponding cesium salt, **4**, by treatment with 20% Cs_2CO_3 until pH 7, and dried under vacuum. "Merrifield-TAP"-bound 4-hydroxy-*N*-(PhF)proline **5** was obtained by reacting cesium salt **4** (10 mol% excess) and **2** with a catalytic amount of potassium iodide in DMF at 60°C for 3 h as indicated by TLC (Scheme 1) [7]. The alcohol was oxidized with oxalyl chloride, DMSO and DIEA in DCM at low temperature to give 4-oxoproline **6** in high conversion, albeit as an unstable intermiediate which was immediately used in the following step. Ketone **6** was quantitatively converted to pyrrole **7** by reaction with *N*-benzylamine and a catalytic amount of *p*-TsOH at room temperature in CH_3CN, because TAP salts have limited solubility in THF [8]. Amine acylation of **7** was accomplished using Fmoc-Phe activated with bis(trichloromethyl)carbonate (BTC) and 2,4,6-collidine in a DCM/THF 8:2 mixture to allow solubility of all species [9]. The Fmoc group of the aminoacylpyrrole **8** was removed by treatment with a piperidine/DCM 1:1 mixture for 10 min. The key

Pictet-Spengler reaction with *p*-nitrobenzaldehyde was shortened from 48 h [1] to 3 h by performing the reaction under microwave irradiation in a 1% TFA solution of 1,2-dichloroethane, instead of toluene. The *cis* relative stereochemistry of **10** was assigned based on previous results [1]. Sodium methoxide mediated cleavage from the TAP support occurred with concomitant dehydrogenation at positions 4 and 5 of the diazepinone ring, leading to ester **11** in 17% overall yield after isolation by chromatography on silica gel.

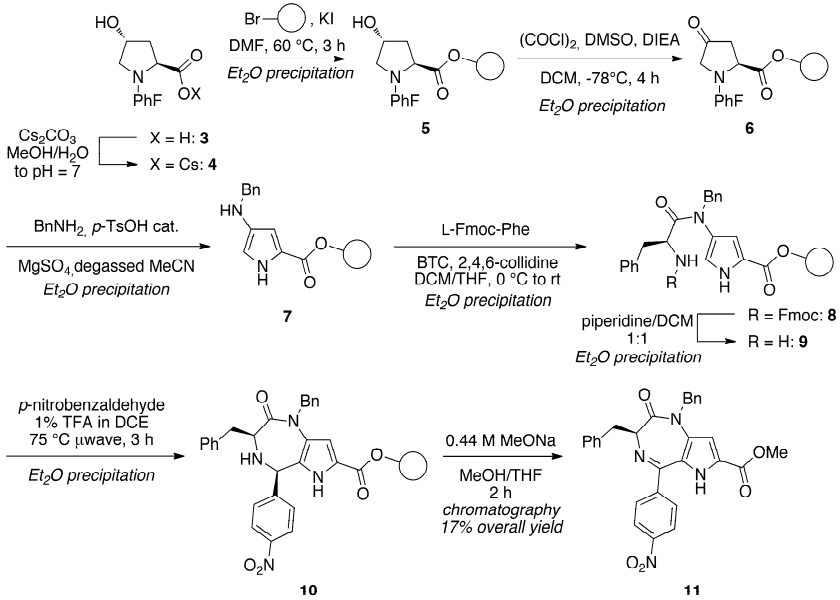

*Scheme 1. Synthesis of pyrrolo[3,2-e][1,4]diazepin-2-one **11** on "Merrifield TAP" **2**.*

Effective synthesis of pyrrolodiazepinone **11** was achieved using "Merrifield TAP" **2** as soluble support. This strategy permited straightforward isolation of intermediates and direct following of reactions by TLC and HPLC-MS. Only one purification of the final ester by silica gel column chromatography was performed after seven steps. Work is underway to improve the cleavage step and to explore other supports for the combinatorial synthesis of pyrrolo[3,2-e][1,4]diazepin-2-ones.

Acknowledgments

We acknowledge financial support from NSERC, CIHR, CIHR-Team in GPCR allosteric regulation (CTiGAR), FQRNT. We thank Marie-Noelle Roy of Soluphase Inc. (Montreal, Canada) for fruitful discussions.

References

1. Deaudelin, P., Lubell, W.D. *Org. Lett.* **10**, 2841-2844 (2008).
2. Iden, H.S., Lubell, W.D. *Org. Lett.* **8**, 3425-3428 (2006).
3. Poupon, J.C., Boezio, A.A., Charette, A.B. *Angew. Chem., Int. Ed.* **45**, 1415-1420 (2006).
4. Roy, M.N., Poupon, J.C., Charette, A.B. *J. Org. Chem.* **74**, 8510-8515 (2009).
5. Stazi, F., Marcoux, D., Poupon, J.C., Latassa, D., Charette, A.B. *Angew. Chem., Int. Ed.* **46**, 5011-5014 (2007).
6. Brouillette, Y., Rombouts, F.J.R., Lubell, W.D. *J. Comb. Chem.* **8**, 117-126 (2006).
7. Gisin, B. *Helv. Chim. Acta* **56**, 1476-1482 (1973).
8. Marcotte, F.-A., Lubell, W.D. *Org. Lett.* **4**, 2601-2603 (2002).
9. Falb, E., Yechezkel, T., Salitra, Y., Gilon, C. *J. Pept. Res.* **53**, 507-517 (1999).

Proceedings of the 31st European Peptide Symposium
Michal Lebl, Morten Meldal, Knud J. Jensen, Thomas Hoeg-Jensen (Editors)
European Peptide Society, 2010

Cellular Binding and Internalization by Water-Soluble Aromatic Amide Foldamers

Jone Iriondo-Alberdi[1], Katta Laxmi-Reddy[1], Aissa Bouguerne[1], Cathy Staedel[2], and Ivan Huc[1]

[1]Université de Bordeaux – CNRS UMR5248, Institut Européen de Chimie et Biologie, 2 rue Robert Escarpit, Pessac, 33607, France; [2]Affiliation Université de Bordeaux – INSERM U869, 16 rue Léo Saignat, Bordeaux, 33076, France

Introduction

Aromatic foldamers constitute a new subclass of non-natural oligomers that possess great advantages over their natural counterparts [1], such as their stability, robustness, the predictability of their conformation and the diversity of precursor monomers. Additionally, even though they display linear or helical structures that are considerably different to those of α-peptides [2], several aromatic foldamers have been shown to exhibit peptide-like biological activity (e.g. antimicrobial activity [3] and an ability to inhibit protein-protein interactions [4]).

We report here the synthesis of three fluorescein-tagged oligomers of 8-amino-2-quinolinecarboxylic acid (Figure 1) and their cellular uptake in HeLa, Jurkat lymphocyte and Huh-7 hepatocyte cells. These studies were designed to assess the effect of structural features such as oligomer length (and therefore the number of charges) on the ability of these compounds to cross the cell membrane [5].

Results and Discussion

The synthesis of the aromatic amide foldamers was carried out *via* a segment-doubling strategy [5], where a dimer was obtained from two monomers, a tetramer from two dimers, the hexamer from a tetramer and a dimer, and so on. The introduction of the water-solubilizing aminopropoxy side-chain was achieved *via* a Mitsunobu reaction at an early stage in the route, whereas the fluorescent probe was attached to the foldamers in the last step of the synthesis.

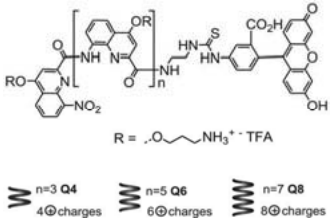

Fig. 1. Water soluble aromatic foldamers. Q8= octamer, Q6= hexamer, Q4= tetramer.

Foldamer toxicity was evaluated by means of the MTS assay, and the results indicated that the longest oligomer Q8 led to a 80% decrease in the cell viability only at the highest dose of 200 mg/mL, whereas Q4 and Q6 remained non-toxic up to this concentration. Such an increase in the relative toxicity of the longer oligomer is expected to result from the higher number of charges in the molecule [6].

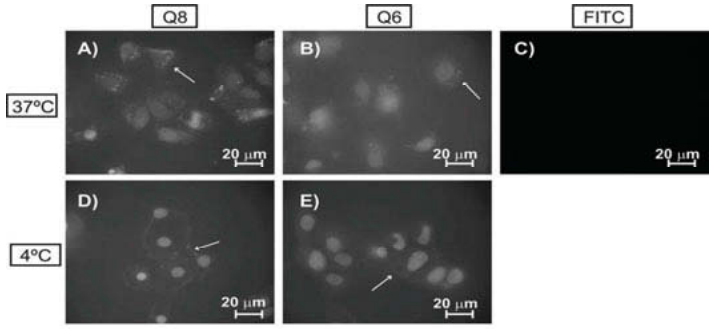

Fig. 2. Fluorescence microscopy images of Huh-7 cells incubated for 1 h with Q6, Q8 and FITC at 100 µM concentration at 37 ºC (A and D) and 0 ºC (B and E).

The cell translocation ability of Q4, Q6 and Q8 was quantified by means of flow cytometry with HeLa, human hepatic Huh-7 cells and human T-lymphocyte Jurkat cells. The results indicated that the uptake efficiency remarkably increased with the oligomer size, and while octamer Q8 labelled 100% of cells in all cell lines, the affinity of Q4 for all cell lines was insignificant. The cellular uptake of Q6 ranged from 26 to 64%, depending on the nature of the cell. The higher affinity of the longer oligomers might point to the role of the number of positive charges carried by them, as observed in other studies on the cell penetration ability of cationic peptides and peptoids. The excellent penetration abilities of foldamers Q6 and Q8 was verified by fluorescence microscopy (Figure 2). The punctuated fluorescence pattern observed in the images indicated that the foldamers accumulated in vesicles, suggesting that they follow an endocytic pathway for internalization.

In order to investigate the mechanism of translocation, the process was investigated at a low temperature (4 ºC) in Huh-7 cells. At low concentrations (10 and 30 μM), lowering the temperature substantially reduced the percentage of labeled cells. Intriguingly, at 100 μM, 45% and 95% of the cells were still labeled for Q6 and Q8, respectively. However, microscopy fluorescence images showed that the helices appeared to bind strongly to the external surface of the plasma membrane, indicating that the high percentage of labeled cells obtained by flow cytometry did not in fact reflect penetration. Such a strong cell membrane association of the longer helices at a low temperature suggests that the translocation is dependent on non-specific, electrostatic interactions of the oligomers with the membrane. A higher number of positive charges would promote this initial attachment, leading to a more efficient translocation.

In conclusion, as part of our investigations on the potential use of aromatic oligoamide foldamers as drug delivery carriers, we have studied the effect of altering structural features, such as length and number of charges, on the cell translocation ability of foldamers. The results suggest that a minimum length and number of positive charges is necessary for efficient cell translocation, with the octamer exhibiting extraordinary penetration abilities in HeLa, Huh-7 and (more importantly) in the often hard-to-transfect Jurkat cell lines. We have also proved that these compounds display practical advantages, including good water solubility and non-toxicity, up to high concentrations. The experiments carried out at lower temperatures have provided an insight into the mechanism of the internalization process, suggesting that the uptake of foldamers follows an energy dependent pathway. These results have been obtained with non-optimised foldamers. Chemical modification at the side-chain position provides a ready source of diversity and the possibility to optimise the ability of aromatic foldamers to translocate the plasma membrane. Further efforts will focus on studying the feasibility of these compounds to deliver bioactive cargo molecules into cells.

Acknowledgments

This work was supported by ANR contract PCV07_185434, by the European Union (Marie Curie IEF-2009-236605, post-doctoral fellowship to J. I.-A.), by the Government of the Basque Country, and by ARC (Post-Doctoral fellowship to K. L.-R.).

References

1. Hecht, S., Huc, I. *Foldamers: Structure, Properties and Applications,* Wiley-VCH, Weinheim, 2007.
2. a) Huc, I. *Eur. J. Org. Chem.* **1**, 17-29 (2004); b) Li, Z.-T., Hou, J.-L., Li, C. *Acc. Chem. Res.* **41**, 1343-1353 (2008); c) Gong, B. *Acc. Chem. Res.* **41**, 1376-1386 (2008).
3. a) Liu, D., Choi, S., Chen, B., Doerksen, R.J., Clements, D.J., Winkler, J.D., Klein, M.L., DeGrado, W.F. *Angew. Chem. Int. Ed.* **43**, 1158-1162 (2004); b) Tew, G.N., Liu, D., Chen, B., Doerksen, R. J., Kaplan, J., Carroll, P.J., Klein, M.L., DeGrado, W.F. *Proc. Natl. Acad. Sci. U.S.A.* **99**, 5110-5114 (2002).
4. a) Saraogi, I., Hebda, J.A., Becerril, J., Estroff, L.A., Miranker, A.D., Hamilton, A.D. *Angew. Chem. Int. Ed.* **49**, 736-739 (2010); b) Wilson, A.J. *Chem. Soc. Rev.* **38**, 3289-3300 (2009).
5. Iriondo-Alberdi, J., Laxmi-Reddy, K., Bouguerne, B., Staedel, C., Huc, I. *ChemBioChem* **11**, 1679-1685 (2010).
6. a) Lv, H., Zhang, S., Wang, B., Cui, S., Yan, J. *J. Controlled Release* **114**, 100-109 (2006).

Proceedings of the 31st European Peptide Symposium
Michal Lebl, Morten Meldal, Knud J. Jensen, Thomas Hoeg-Jensen (Editors)
European Peptide Society, 2010

Detection of the Apo-B,E-binding Site of Low Density Lipoprotein Receptor

Irina V. Shutova and Vladimir P. Golubovich
Institute of Bioorganic Chemistry of the National Academy of Sciences of Belarus, Minsk, Kuprevich str. 5/2, 220141, Belarus; e-mail: shutova2001@mail.ru

Introduction

Apolipoproteins Apo-E and Apo-B100 play an important role in the development of the cardiovascular diseases. Their selective elimination from patient's serum is one of the methods of the treatment and prophylaxis of cardiovascular disease such as myocardial infarction, stroke and atherosclerosis. These proteins bind with one receptor – low density lipoprotein receptor (LDLR). Detection of the Apo-B,E-binding site of LDLR and designing its low-molecular analogs can result in the making of new medical adsorbents and therapeutic agents.

Low density lipoprotein receptor is a protein with known 3D structure and consists of several independent domains. Ligand-binding domain of LDLR is placed in N-terminal of molecule and consists of 7 repeats with 50% homology. Apo-E binds with repeat 5 of LDLR. Apo-B100 has two binding regions: one of them binds with repeat 4 of LDLR and another binds with repeat 5 of LDLR and has high homology with receptor-binding region of Apo-E. Repeat 5 of LDLR presumably has one Apo-B,E-binding site and both Apo-E and Apo-B100 competitively bind with it [1]. The aim of our study was to detect the Apo-B,E-binding site of LDLR.

Results and Discussion

Detection of the Apo-B,E-binding site of LDLR was carried out by a program designed by us. As is known, the specific protein binding sites usually are placed in the cavities or convexities on protein surfaces [2]. Therefore, the detection of the structural features of protein surfaces – cavities and convexities, is often the first stage of the functional analysis of proteins. The next step is the investigation of the detected structural features. Most widely used methods are those in which the cavities are ranked by area and/or by volume. In this case the cavities with rank one refer to potential binding sites [3-5]. It is known that the binding sites of proteins usually form charged regions or have well-marked hydrophobic nature [2]. So for the detection of potential binding sites of proteins we consider it expedient to investigate the hydrophobic properties and charge distribution in the cavities and on protein surfaces.

We have designed the program for prediction of potential binding sites of proteins (Figure 1). This program consists of three modules which allow us to build the molecular protein surfaces (module 1); to detect and to rank the cavities – structural features of protein surfaces (module 2); and to carry out the analysis of hydrophobic areas and charge distribution on protein surfaces (module 3).

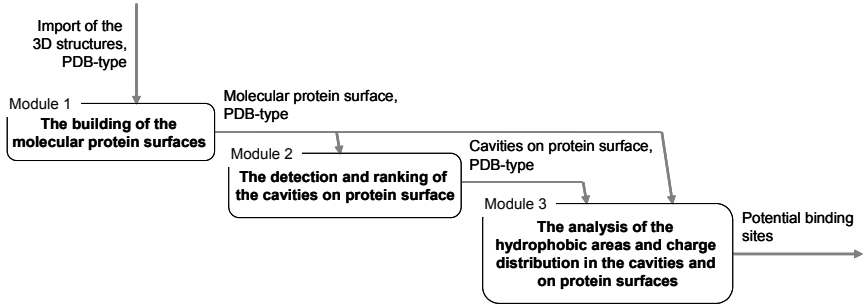

Fig. 1. Scheme of the program.

We have developed these modules in the VC++ language. For building protein surfaces (module 1) we have chosen the Connolly algorithm of presentation of the surface by points. For detection of cavities on protein surfaces (module 2) we have chosen the SurfNet algorithm as a basis and modified it. Modifications designed by us decrease the number of alpha and beta errors; it rejects pseudo-cavities and defines cavities with the non-conical shape of a surface. Module 3 allows one to detect hydrophobic clusters on protein surfaces; to view charge distribution in the chosen cavities and, in this way, to predict potential protein binding sites. The protein atom coordinates imported from PDB-files are the input data for all program modules. The output data of module 1 (protein surfaces) and module 2 (cavities) also are saved in the *PDB* format and can serve as the input data for the following modules. Potential binding sites of the protein (output data of module 3) are saved as a list of their amino acid residues in the *txt* format.

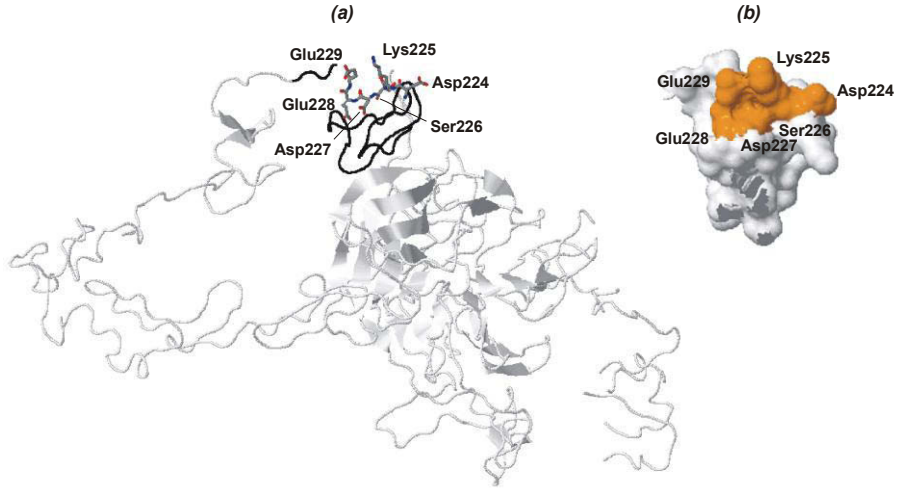

Fig. 2. Low density lipoprotein receptor (PDB ID 1N7D) and its detected cavity with rank one. (a) All receptor domains. Repeat 5 of the ligand-binding domain is marked by black bold line. (b) Surface of repeat 5 of the ligand-binding domain of LDLR. Detected cavity with rank one is marked by dark color. Note: The residues numbers are given according to their numbers in the primary sequence of LDLR imported from database UniProt (ID P01130 [6]). In 1N7D these residues correspond to residues Asp203, Lys204, Ser205, Asp206, Glu207 and Glu208.

For the detection of the Apo-B,E-binding site of low density lipoprotein receptor at the first step we imported from ProteinDataBank (PDB; http://www.rcsb.org/pdb/) the 3D structures of LDLR (PDB ID 1N7D), repeat 5 of LDLR (PDB ID 1AJJ) and Apo-E (PDB ID 1GS9). Then using our program we built surfaces and defined in the repeat 5 of LDLR cavity with rank one which form highly charged region. This cavity is formed by residues Asp224, Lys225, Ser226, Asp227, Glu228 and Glu229 (Figure_2).

We think that the region 224-229 of LDLR form its Apo-B,E-binding site and is perspective to investigate its peptide's analogues on their ability to Apo-E and Apo-B100 binding.

References

1. Boren, J., et al. *J. Clin. Invest*. **101(5)**, 1084-1093 (1998).
2. Laurie, A.T.R., Jackson, R.M. *Current Protein and Peptide Science* **7**, 395-406 (2006).
3. Laskowski, R.A., et al. *Protein Sci.* **5**, 2438-2452 (1996).
4. Laskowski, R.A. *J. Mol. Graph.* **13**, 323-328 (1995).
5. Peters, K.P., Fauck, J., Frommel, C. *J. Mol. Biol.* **256**, 201-213 (1996).
6. http://www.uniprot.org/uniprot/P01130

Proceedings of the 31st European Peptide Symposium
Michal Lebl, Morten Meldal, Knud J. Jensen, Thomas Hoeg-Jensen (Editors)
European Peptide Society, 2010

Silver Nanoparticle Influence on *Staphylococcus aureus* Peptidoglycan Cell Wall

Fateme Mirzajani*, Alireza Ghassempour, Atousa Aliahmad, and Mohammad Ali Esmaeili

Medicinal Plants and Drugs Research Institute, Shahid Beheshti University, G.C. Evin, Tehran, Iran

Introduction

Colloidal silver nanoparticles (AgNPs) with sizes smaller than 100 nm in at least one dimension, have recently received a lot of attention and concern due to their anti-microbial activity [1]. It is obvious that silver, whether in the ionic or nanoparticle form, has interactions with the bacterial cell wall [2]. The peptidoglycan (PGN) is a specific and essential structural element in the cell wall of almost all bacteria. Its main structural features are linear glycan strands cross-linked by short peptides. The glycan strands are made up of alternating N-acetylglucosamine and N-acetylmuramic acid (MA) residues linked by β-1→4 bonds [3], and the peptide is composed of L-alanine, D-glutamine, L-lysine, and D-alanine in the case of *Staphylococcus aureus*.

Results and Discussion

As can be seen from the UV spectra in Figure 1a, the λ_{max} of colloidal AgNPs was 426 nm. The DLS analysis (Figure 1b) of synthesized AgNPs demonstrates that their size, volume mean diameter (VMD), and surface mean diameter (SMD) were 18.34 nm (X_{99}), 4.10 nm, and 2.26 nm, respectively. Anti-Staphylococcal properties of AGNPs were confirmed by the macro-broth dilution susceptibility tests (MIC = 2 μg/ml and MBC = 4 μg/ml).

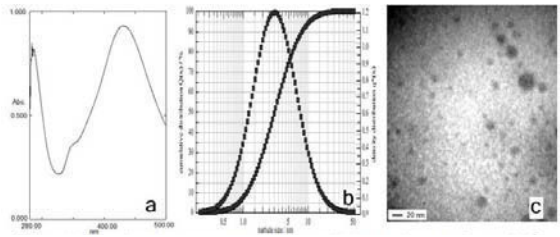

Fig. 1. (a) UV absorbance spectra, (b) DSL, (c) TEM image of Ag colloids.

To evaluate the influence of AgNPs on the bacterial PGN cell wall and specifically its peptide part, their CD spectra were recorded in DMSO. Figure 2a demonstrates the CD spectra in the peptide-bond absorption region (200–260 nm) of irradiated PGNs. In the region of 210-220 nm, a noticeable change can be observed. In view of the fact that this region involves the characteristic wavelengths of the hydrogen bond and α-helix as well as the peptide secondary structure, it can be concluded that AgNPs mostly affected the peptide hydrogen bonds.

The electron density images of the treated *S. aureus* are illustrated in Figure 2b and 2c. The dark and light areas show where the sample had a high and low electron density, respectively. The images of the samples treated with AgNPs were greatly different from those of the untreated cells (Figure 2b). The PGNs' fragmentation after treatment (Figure 2c) proves their interaction with AgNPs, which caused the cell wall destruction in *S. aureus*.

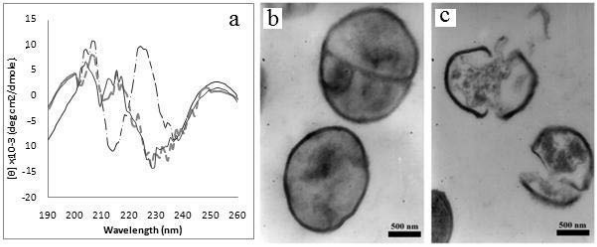

Fig. 2. (a) CD spectra of PGN (.-), PGN treated with AGNP after 30 min. (..) and 3 h. (-). Transmission electron microscopy images of S. aureus before (b) and after 24 h (c) AGNP treatment.

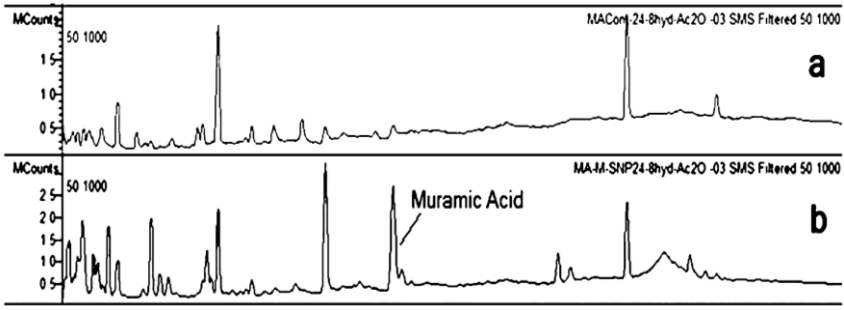

Fig. 3. GC-MS^n analysis of culture media (a) without treatment, (b) AgNPs treated.

To specifically monitor effects of AgNPs on cell wall PGN glycan strands, the amount of Muramic acid (MA), released into the culture media was studied. For this purpose, GC-MS^n was carried out before and after treatment. It can be seen from Figure 3b that AgNPs treatment caused an increase in MA concentration in the culture medium.
Studies demonstrated that PGNs should be digested for HPLC analysis.

We hypothesized that, as PGNs structure were broken by AgNPs treatment, the produced fragments can be monitored using HPLC/MS^n analyses. Increase of the low molecular weight fractions on the HPLC chromatogram after AgNPs treatment will approve our hypothesis, that they caused PGN breakage. The MS^n analysis of them has been performed using mass spectrometry. It can be seen from the PGN standard solution sample (Figure 4a) the fragments higher than 2500 m/z. On the other hand the treatment of AgNPs caused some breakage of PGNs structure, which is shown on part Figure 4b. From that treatment more fragmentation on PGN with low molecular weight, (fragments lower than 2800 m/z) were obtained. These results indicate that the reaction with AgNPs affects the peptide primary structure and increasing the number of degradation products after these PGNs treatment.

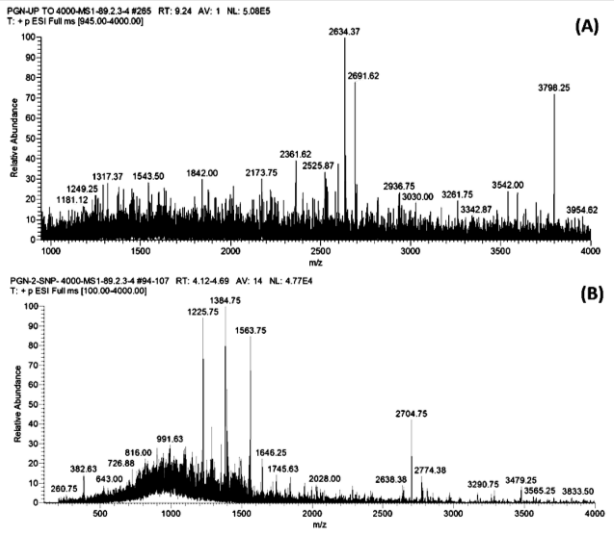

Fig. 4. Mass Spectrometry analysis of the PGN standard solution sample (a), and after the AgNPs treatment (b) of PGNs, using Finigan LCQ deca ion trap instrumentation.

References

1. Shrivastava, S., et al. *Nanotechnology* **18**, 225103 (2007).
2. Dibrov, P., et al. *Antimicrob. Agents Chemother.* **46**, 2668-2670 (2002).
3. Vollmer, W., Blanot, D., de Pedro, M.A. *FEMS. Microbiol. Rev.* **32**, 149-167 (2008).

Proceedings of the 31st European Peptide Symposium
Michal Lebl, Morten Meldal, Knud J. Jensen, Thomas Hoeg-Jensen (Editors)
European Peptide Society, 2010

Peptidomic Analysis of Human Blood Serum for Specific Disease Markers

Rustam H. Ziganshin, Georgii P. Arapidi, Igor V. Azarkin, Vadim M. Govorun, and Vadim T. Ivanov

Department of Proteomics, Shemyakin-Ovchinnikov Institute of Bioorganic Chemistry, Russian Academy of Sciences, Moscow, 117997, Russia

Introduction

Blood and its derivatives (plasma and serum) is very attractive for a biomarker studies due to the unique properties of this liquid connective tissue, which comes into contact with practically all cells in the organism absorbing some traces of their metabolic activity, including markers of disease-induced metabolic change [1]. Albumin, immunoglobulins, and other proteins that are present in blood in very high concentrations are known to bind to and transport various low-molecular compounds, including small proteins and peptides [2]. As a result, these compounds are protected from removal from the bloodstream by kidneys and can be accumulated in blood in considerable amounts. It has been suggested that this peptidome may serve as an important source of clinical diagnostic information [3].

Results and Discussion

A simple and reproducible method of peptide desorption from abundant blood proteins was developed. This method increases the quantity of peptides detected in serum samples by MALDI-TOF MS and improves the quality and reproducibility of the recorded MS profiles. Blood serum samples obtained from 39 patients with ovarian cancer, 42 patients with colorectal cancer, 72 patients with syphilis and 200 healthy donors were fractionated using a profiling kit containing MB-WCX surface-functionalized magnetic beads (Bruker Daltonics, Germany) according to the manufacturer's protocols, with small modifications. MALDI-TOF MS data of fractionated serum samples (Figure 1) were acquired automatically in a linear mode using ultraflex™ mass spectrometer (Bruker Daltonics, Germany). MS data analyses, classification models generation and validation were made using software for biomarker detection and evaluation – ClinProTools 2.1 (Bruker

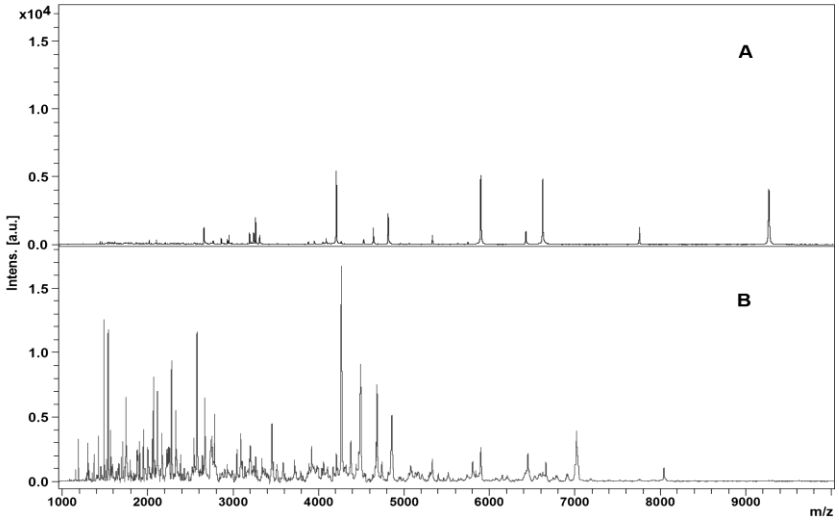

Fig. 1. MALDI-TOF MS profiles of the same serum sample fractionated on MB-WCX magnetic beads before (A) and after (B) heating. The spectrum intensity and m/z values (Da) are plotted along the Y-axis and X-axis, respectively.

Table 1. The quantity of identified proteins and peptides for each group of samples

Experimental groups	*Number of identified proteins*	*Number of identified peptides*
Healthy donors	290	656
Ovarian cancer	178	462
Colorectal cancer	137	354
Syphilis	158	452

Daltonics, Germany). The best generated classification models demonstrated the following values of sensitivity and specificity for the detection of studied diseases: ovarian cancer – 100% and 100%; colorectal cancer – 100% and 100%; syphilis – 92% and 100% (for sensitivity and specificity, respectively).

Serum samples of all experimental groups were subjected to consecutive separation by WCX and SAX chromatography followed by RP-LC-MS/MS analyses using the Agilent 1200 HPLC-Chip/MS Interface coupled with the Agilent 6520 Accurate-Mass Q-TOF. As a result of MS/MS identification of peptides that was performed by PhenyxServer (Geneva Bioinformatics S.A.) using databank Uniprot-SwissProt 1087 unique peptides representing 487 proteins were reliably identified (see Table 1) (validation of peptide identifications was made by searching MS/MS data against the reversed version of Uniprot-SwissProt).

LC-MS/MS analysis of serum samples revealed significant discrepancy between identified peptides and proteins in various experimental groups that contradict visual similarity of MALDI-TOF MS profiles between the same groups. Resolution of linear mode of MALDI-TOF mass spectrometers is too low for detail analyses of such complex peptide mixture as serum is, while a reflector mode is difficult to use because of its lower sensitivity. From the obtained results it is also obvious that it is impossible to correlate the data of LC-MS/MS identifications with MS peaks of potential biomarkers revealed from MALDI-TOF MS profiling of serum samples. We believe that high-throughput comparative MALDI-TOF MS profiling of serum samples can be used for preliminary estimation of differences between peptide profiles of tested groups, with following detection of peptide biomarkers using label-free quantitative LC-MS approach and their further identification by LC-MS/MS.

Acknowledgments
This work is supported by Russian Foundation for Basic Research (09-04-12085).

References

1. Anderson, N.L., Anderson, N.G. *Mol. Cell. Proteomics* **1**, 845-867 (2002).
2. Mehta, A.I., Ross, S., Lowenthal, M.S., Fusaro, V., Fishman, D.A., Petricoin, E.F., 3rd, Liotta, L.A. *Dis. Markers* **19**, 1-10 (2003).
3. Geho, D.H., Liotta, L.A., Petricoin, E.F., Zhao, W., Araujo, R.P. *Curr. Opin. Chem. Biol.* **10**, 50-55 (2006).

Proceedings of the 31st European Peptide Symposium
Michal Lebl, Morten Meldal, Knud J. Jensen, Thomas Hoeg-Jensen (Editors)
European Peptide Society, 2010

The Top-Down Analysis of Chemical Modification of Ubiquitin by ECD Method

Piotr Stefanowicz, Karolina Kowalewska, Monika Kijewska, Alicja Kluczyk, Marek Cebrat, and Zbigniew Szewczuk
University of Wrocław, Wrocław, 50-137, Poland

Introduction

The ECD (electron-capture dissociation) is a method of choice for top-down analysis of proteins and large polypeptides. In contrast to CID (collision-induced dissociation) fragmentation method, ECD preserves labile posttranslational modifications. We investigated the nonspecific chemical modification of ubiquitin by ECD method. The protein was subjected for glycation [1] and N-phosphorylation [2]. Although these modifications are unstable in gas phase during CID experiments, the ECD fragmentation of glycated and N-phosphorylated peptides provided high sequence coverage. The reactivity of ubiquitin toward glucose [3] and phosphoramidate [2] was investigated. The glycation level of lysine moieties as well as N-phosphorylation of histidine residues in ubiquitin was investigated on the intact, chemically modified protein.

Results and Discussion

The high temperature glycation of ubiquitin was performed according to procedure published recently by us [3]. The N-phosphorylation of ubiquitin was performed using a

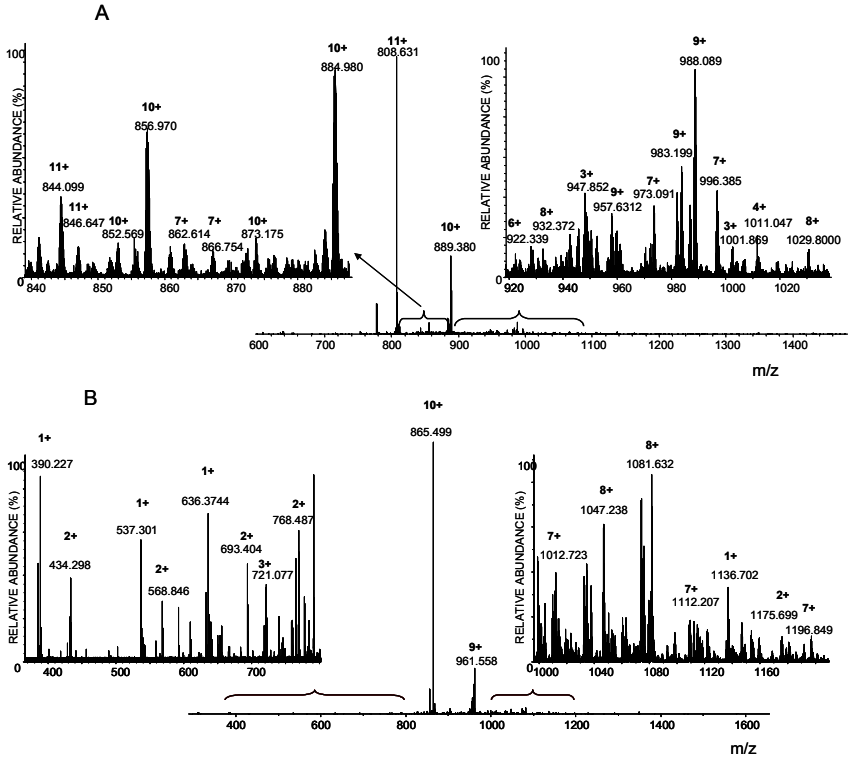

Fig. 1. ECD spectra of chemically modified ubiquitin. A - diglycated protein, B - monophosphorylated protein.

protocol previously described [2]. The protein and monopotassium phosphoramidate were used at the ratio 1:100 (w:w).

All mass spectrometric experiments were performed on an Apex-Qe Ultra 7T instrument (Bruker Daltonics, Bremen, Germany) equipped with a dual ESI source. All mass spectrometric experiments were performed on an Apex-Qe Ultra 7T and a heated hollow cathode dispenser. The precursor ions were selected on the quadrupole and directed to the ICR cell where they were fragmented. The parameters were set as 150 ms for the ECD pulse length and ECD bias was 0.8 V. Analysis of the obtained spectra was carried out with the Biotools (Bruker) software. Obtained ECD spectra (Figure 1) allows the identification of the numerous fragments of c_n and $(z+1)_n$. The number of identified fragments for diglycated and phosphorylated protein was 90 and 189 respectively what indicate the high sequence coverage. The data analysis reveled that only one residue (His 68) undergoes phosphorylation. On the other hand the glycation reaction was less specific and all (or majority) lysine residues undergoes glycation.

The ECD method was found useful for the localization of chemical modification sites in glycated and phosphorylated ubiquitin. Its main advantage is a significant reduction of the neutral losses related to aminofructose (Fru) or phosphoramidate moiety (P).

Acknowledgments
Supported by Grant No. N N401 222734 from the MSHE (Poland).

References

1. Stefanowicz, P., Boratyński, J., Kanska, U., Petry, I., Szewczuk, Z. *Acta Biochim. Pol*. **48**, 1137-1141 (2001).
2. Kowalewska, K., Stefanowicz, P., Ruman, T., Fraczyk, T., Rode, W.K., Szewczuk, Z. *Bioscience Reports* in press, doi:10.1042.
3. Stefanowicz, P., Kijewska, M., Szewczuk, Z. *J. Mass Spectrom*. **44**, 1047-1052 (2009).

Proceedings of the 31st European Peptide Symposium
Michal Lebl, Morten Meldal, Knud J. Jensen, Thomas Hoeg-Jensen (Editors)
European Peptide Society, 2010

Effect of Point Mutation in the Hinge Region on a Structure of an Amyloidogenic Protein - Human Cystatin C

Marta Orlikowska[1], Elzbieta Jankowska[1], Dominika Borek[2], Robert Kołodziejczyk[3], Zbyszek Otwinowski[2], Mariusz Jaskólski[3,4], and Aneta Szymańska[1]

[1]Department of Medicinal Chemistry, Faculty of Chemistry, University of Gdańsk, Gdańsk, Poland; [2]Department of Biochemistry, UT Southwestern Medical Center, Dallas, TX, U.S.A. [3]Department of Crystallography, Faculty of Chemistry, A. Mickiewicz University, Poznań, Poland; [4]Center for Biocrystallographic Research, Institute of Bioorganic Chemistry, Polish Academy of Sciences, Poznań, Poland

Introduction

Cystatins are natural inhibitors of cysteine proteases – enzymes widely distributed in animals, plants and microorganisms. At physiological conditions hCC wt is a monomeric protein, but it was also found to be a component of massive amyloid deposits formed in a brain of patients suffering from a lethal disease called amyloid angiopathy [1]. Physiologically monomeric, under crystallization conditions hCC formed the domain swapped dimer [2]. The dimerization process is probably facilitated by the presence in the hCC structure of a flexible loop L1 (55-59, QIVAG) connecting protein subdomains undergoing the exchange process. This loop is the only part of hCC which undergoes significant structural changes during the dimerization process which, according to the experimental [3,4] and theoretical [5,6] studies, are driven by the conformational constraints attributed to the located near the top of the loop Val residue (Val57). Values of the ψ angles for this residue are not optimal and that can account to propensity of the protein to undergo the domain swapping. With the aim to check implications of greater or decreased stability of this loop on dimerization propensity of human cystatin C and its impact on the overall structure of the protein, we designed and obtained hCC L1 variants with Val57 residue replaced by Asp, Asn (β-turn stabilization) or Pro (turn broadening). All proteins were subjected to dimerization studies and their structure was determined by means of crystallography.

Results and Discussion

Protein state in solution was examined by gel-filtration on Superdex 75 column (GE Healthcare) (Figure1). The retention times of the aspartic acid and asparagine mutants were similar to that of the wild type protein whereas the proline mutant eluted from the column as two peaks (monomer/dimer equilibrium). *In vitro* dimerization experiments showed that, unlike the wild type protein, two of the studied variants of hCC (V57D and V57N) did not undergo dimerization induced by growing concentration of destabilizing agents, *e.g* guanidinum chloride whereas for the predominantly dimeric proline variant the fraction of the dimer further increased with incubation time [7]. These results confirmed predicted stabilizing effect of V57N and V57D mutations and destabilizing effect of the proline substitution.

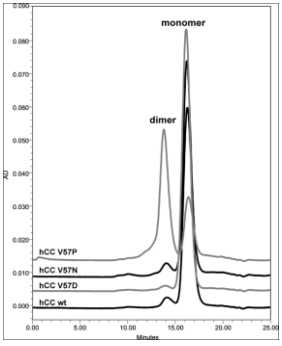

Fig. 1. Gel filtration chromatograms of wt hCC and its variant.

The crystal structures of V57D, V57N and V57P variants at the resolution 3.0, 2.04 and 2.25Å respectively, reveal the typical cystatin fold with a five-stranded antiparallel β-sheet wrapped around an α-helix (Figure 2). Crystallization of V57N resulted in the monomeric structure [8]. This result is very interesting considering the limited scope of the structural intervention in this mutant. The single point mutation stabilizing the L1 loop was sufficient to preserve human cystatin C molecule in a monomeric form. Mutant V57D under crystallization conditions (0.1 M Imidazole

(pH=6.5) and 1.0 M sodium acetate) forms the domain swapped dimer. Most of V57P crystals did not diffract well (resolution above 5 Å). Data indexing resulted in a high symmetry space group P622 with enormous cell parameter (a=246 Å, b=246 Å and c=375 Å). It indicates presence of more than 45 copies of the molecule in the asymmetric unit and presumably oligomeric state in the crystal. We were able to get good quality data only for crystals grown in 0.1 M Imidazole (pH=6.5) and 1.0 M Sodium acetate. This form has the domain swapped dimer in the asymmetric unit.

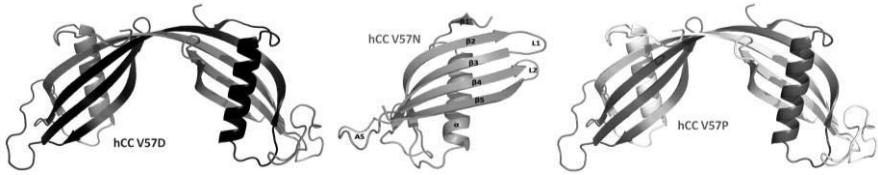

Fig. 2. Crystal structures of hCC mutants.

The secondary structure of the presented hCC mutants can be summarized as follows: (N)-β1-α-β2-L1-β3-(AS)- β4-L2-β5-(C). Similar to other proteins belonging to the cystatin family, for which the crystal structure was determined (chicken cystatin, dimeric wt hCC), no electron density was observed for the N-terminal region comprising the first eleven residues, probably because of its flexibility.

The experimental structure of human cystatin C V57N mutant illustrates the fold of monomeric cystatin C and defines conformation of loop L1, which is essential for the inhibition of papain-like cysteine proteases. In hCCV57N the electron density in the L1 area of molecules A and B is of very good quality (Figure 3), allowing modeling of the backbone and side chain conformations without ambiguity.

In summary, by applying rational mutagenesis approach we were able to obtain hCC variants stable in the monomeric form both in solution and in the crystal (V57N), monomeric in solution but dimeric in the crystal (V57D) and dimeric in solution and presumably oligomeric in the crystal (V57P).

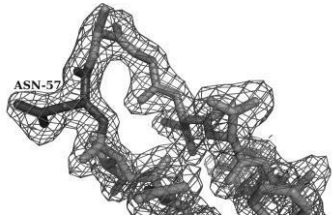

Fig. 3. Conformation of loop L1.

Acknowledgments
This work was supported by a grant of Polish Ministry of Science and Higher Education No 2739/B/H03/2010/38 and DS/8440-4-0172-0.

References

1. Olafsson, I., Grubb, A. *Amyloid Int. J. Exp. Clin. Invest*. **7**, 70-79 (2000).
2. Janowski, R., Kozak, M., Jankowska, E., Grzonka, Z., Grubb, A., Abrahamson, M., Jaskólski, M. *Nat. Struct. Biol*. **8**, 316-320 (2001).
3. Engh, R.A., Dieckmann, T., Bode, W., Aueswald, E.A., Turk, V., Huber, R., Oschkinat, H. *J. Mol. Biol*. **234**, 1060-1069, (1993).
4. Martin, J.R., Craven, C.J., Jerala, R., Kroonzitko, L., Żerovnik, E., Turk, V., Waltho, J.P. *J. Mol. Biol*. **246**, 331-343 (1995).
5. Ding, F., Prutzman, K.C., Campbell, S.L., Dokholyan, N.V. *Structure* **14**, 5-14 (2006).
6. Rodziewicz-Motowidło, S., Iwaszkiewicz, J., Sosnowska, R., Czaplewska, P., Sobolewski, E., Szymańska, A., Stachowiak, K., Liwo, A. *Biopolymers* **91**,373-83 (2009).
7. Szymańska, A., Radulska, A., Czaplewska, P., Grubb, A., Grzonka, Z., Rodziewicz-Motowidło, S. *Acta Biochim. Pol.* **56**, 455-463 (2009).
8. Orlikowska, M., Jankowska, E., Kołodziejczyk, R., Jaskólski, M., Szymańska, A., sent to *J. Struct. Biol.*

Proceedings of the 31st European Peptide Symposium
Michal Lebl, Morten Meldal, Knud J. Jensen, Thomas Hoeg-Jensen (Editors)
European Peptide Society, 2010

Crystal Structure of L68V Mutant of Human Cystatin C, an Amyloidogenic Protein

Marta Orlikowska[1], Elzbieta Jankowska[1], Dominika Borek[2], Zbyszek Otwinowski[2], and Aneta Szymańska[1]

[1]Department of Medicinal Chemistry, Faculty of Chemistry, University of Gdańsk, Gdańsk, Poland; [2]Department of Biochemistry, UT Southwestern Medical Center, Dallas, TX, U.S.A.

Introduction

Human cystatin C (hCC) is a low molecular mass protein that belongs to a family of single-chain reversible inhibitors of papain-like (C1 family) and legumain-related (C13 family) cysteine proteases [1]. At physiological conditions hCC wt is a monomeric protein but under crystallization conditions formed the domain swapped dimer [2]. Besides its inhibitory function, hCC plays a causal role in development of one of neuropathological diseases – an amyloid angiopathy. In brain arteries of elderly individuals suffering from this disease cystatin C forms massive amyloid deposits leading to cerebral hemorrhages and finally death of patients [3]. The naturally occurring single point mutant of human cystatin C - L68Q hCC - is implicated in hereditary cystatin C amyloid angiopathy, also known as hereditary cerebral hemorrhage with amyloidosis, Icelandic type. L68Q variant oligomerizes much more easily than its wild-type analog, even at physiological temperature. Deposition of L68Q aggregates in cerebral and spinal arteries and arterioles leads to recurrent hemorrhagic strokes causing serious brain damage and death of young, less than 40 years old, adults [4]. The increased propensity of the L68Q hCC variant for oligomerization can be connected with its decreased conformational stability caused by an introduction of a bulky and polar residue into the hydrophobic interior of the protein [5]. To get deeper insight into the possible mechanism of hCC oligomerization and assess the impact of modifications introduced into position 68 on this process we designed and constructed hCC variants with Leu68 residue replaced isosteric but polar Asn residue and hydrophobic but smaller in the van der Waals radius valine.

Results and Discussion

L68N mutation resulted in strong destabilization of the protein comparable with the one caused by glutamine residue. Isolation of this protein using cold osmotic shock protocol, which is suitable for soluble recombinant proteins exported to periplasmic space [6], was not successful and most of the protein remained in the insoluble fraction. It suggests that over expression results in the formation of inclusion bodies composed of insoluble aggregates of the expressed protein. Purification of hCC L68N from inclusion bodies led to massive precipitation during refolding step what confirms low conformational stability and high tendency for aggregation of this protein.

L68V mutant turned out to be more stable and could be expressed and purified in good yield as a monomeric protein, but it shows increased propensity for dimerization in *in vitro* tests [Szymanska A, unpublished data]. It dimerizes slowly during incubation at physiological conditions (PBS, 37 ^{o}C, Figure 1c). Addition of guanidine hydrochloride, necessary to induce dimerization of the wild type hCC, has much pronounced effect on the mutant that on the wt protein since it shifts the equilibrium towards the dimeric form regardless the GdnHCl concentration (Figure 1a, b).

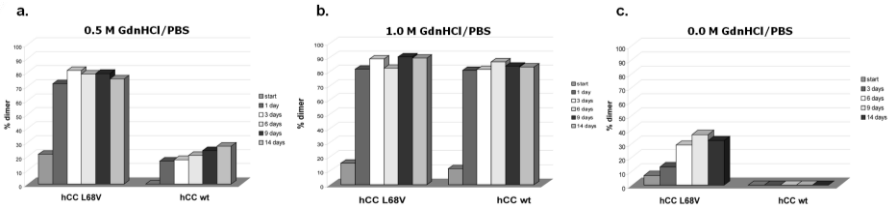

Fig. 1. Results of the dimerization experiments performed in PBS containing 0.5 M or 1.0 M guanidine hydrochloride (Gdn·HCl) at 37°C with the protein at 0.5 mg/ml concentration.

Replacement of residue Leu68 by hydrophobic but smaller in the van der Waals radius valine residue does not change the overall fold of the protein. Under crystallization conditions (0.18 M tri-sodium citrate, 0.1 M Tris-HCl pH=8.0, 30% PEG 400 and 0.1 M sodium acetate pH=4.6, 8% PEG 4000) it forms the domain swapped dimer, similar to the wild type protein (Figure 2a).

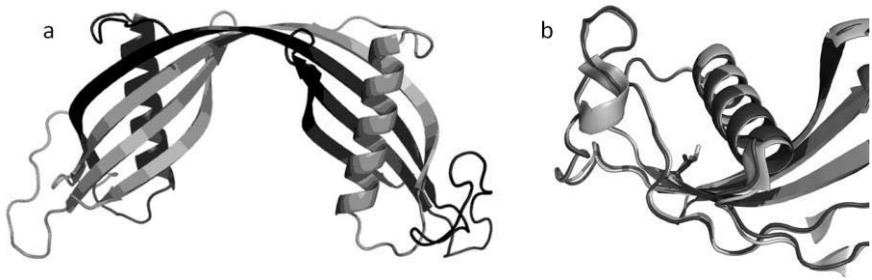

Fig. 2. Assumed biological molecule of hCCL68V (a). Superposition of hCC wt (black) and hCC L68V (grey) (b).

Superposition of both molecules do not reveal significant differences between the dimeric structure obtained for the reference wild type and the variant of hCC (rmsd=0.414). Closer examinations of the surroundings of the substituted position 68 (Figure 2b) also shows that the distance between an α-helix and the β-sheet part is the same in the case of both dimers. Therefore, lowered stability of the hCC variant in the monomeric form cannot be attributed to changes in the secondary or tertiary structure of the studied protein. Increased dimerization susceptibility of hCC L68V the most likely arises from the disruption of the network of hydrophobic interactions surrounding the native leucine residue.

Acknowledgments
This work was supported by a grant of Polish Ministry of Science and Higher Education No 2739/B/H03/2010/38 and DS/8440-4-0172-0.

References
1. Grubb, A. *Adv. Clin. Chem*. **35**, 63-99 (2000).
2. Janowski, R., Kozak, M., Jankowska, E., Grzonka, Z., Grubb, A., Abrahamson, M., Jaskólski, M. *Nat. Struct. Biol*. **8**, 316-320 (2001).
3. Olafsson, I., Grubb, A. *Amyloid Int. J. Exp. Clin. Invest*. **7**, 70-79 (2000).
4. Gudmundsson, G., Hallgrimsson, J., Jonasson, T.A., Bjarnason, O. *Brain* **95**, 387-404 (1972).
5. Szymańska, A., Radulska, A., Czaplewska, P., Grubb, A., Grzonka, Z., Rodziewicz-Motowidło, S. *Acta Biochim. Pol*. **56**, 455-463 (2009).
6. Neu, H.C., Heppel, L.A. *J. Biol Chem*. **249**, 3685-3692 (1965).

Proceedings of the 31st European Peptide Symposium
Michal Lebl, Morten Meldal, Knud J. Jensen, Thomas Hoeg-Jensen (Editors)
European Peptide Society, 2010

Mutants of an Amyloidogenic Human Cystatin C in Pressure-Induced Denaturation Studies Using Hydrogen Exchange Mass Spectrometry

Elzbieta Jankowska[1], Marta Orlikowska[1], Marta Sosnowska[1], Aneta Szymanska[1], Piotr Stefanowicz[2], Karolina Kowalewska[2], and Zbigniew Szewczuk[2]

[1]*Faculty of Chemistry, University of Gdansk, Sobieskiego 18, 80-952, Gdansk, Poland*
[2]*Faculty of Chemistry, University of Wroclaw, Joliot-Curie 14, 50-383, Wroclaw, Poland*

Introduction

Human cystatin C (hCC) is a 120 amino acids containing protein, ubiquitous in all body fluids. Its main physiological function is regulation of activity of cysteine proteases, either released from damaged or dying lysosomes or originated from microbial invasion. Besides its inhibitory function, hCC plays a role in development of a neurodegenerative disease called amyloid angiopathy, caused by pathological aggregation of the wild-type protein or its naturally occurring L68Q variant [1]. The mechanism of cystatin C amyloid formation has not been elucidated till now. It is postulated, however, that aggregation and fibrilization proceed through propagated 3D domain-swapping process, which was evidenced as a mechanism of hCC dimerization [2]. The dimer reconstructs in duplicate the general fold of the monomeric protein with the exception of the hinge region encompassing residues $Q^{55}IVAG^{59}$, which links the swapped subdomain to the rest of the molecule. With the aim to check implications of greater or decreased stability of this region for dimerization and aggregation propensity of human cystatin C, we designed and constructed hCC mutants with Val57 residue replaced by Asp, Asn or Pro, respectively. The obtained proteins were subsequently the subject of hydrogen exchange mass spectrometry analysis combined with high pressure-induced denaturation to monitor stability and an unfolding/refolding process of the mutants in comparison to the wild-type human cystatin C.

Results and Discussion

HCC variants, obtained by protein engineering methods [3], were dissolved in a deuterated buffer and incubated under elevated pressure. After 30 min of incubation during which the protein underwent unfolding and deuteration, each sample was decompressed and diluted with a non-deuterated buffer, what initialized the deuterium-hydrogen (D/H) back exchange. Following this process by mass spectrometry we were able to gain some knowledge about stability of different variants of hCC and their refolding process.

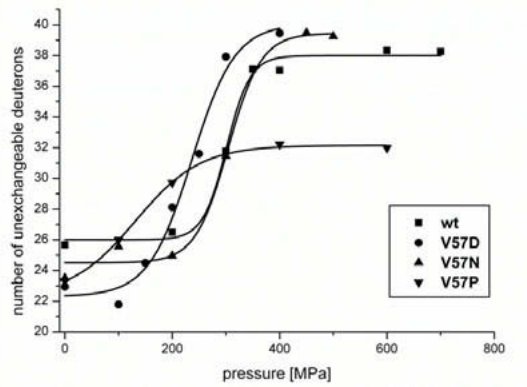

Fig. 1. Number of unexchangeable deuterons in hCC variants depicted as a function of the applied pressure.

Human cystatin C as a protein containing eight Pro residues possesses 111 amide protons potentially available for the hydrogen-deuterium exchange (in V57P mutant this number is reduced to 110, due to additional Pro residue in the sequence). Besides the backbone amide protons, also protons from the amino acid side chain functionalities containing O-H and N-H bonds can be substituted by deuterons, overall 107 protons in the wild-type hCC, 109 in V57N and 108 in V57D mutant. To the group of labile protons belong also the protons from the terminal amine and carboxylic functions in each protein. Summarizing, the total number of the exchangeable protons amounts to 218 in case of the wild-type cystatin C, 217 in V57P mutant, and 219 and 220, respectively, for V57D and V57N hCC variants.

Application of increasing pressure forced the unfolding of hCC molecules, gradually exposing more and more buried protons to the solvent and allowing their exchange into deuterons. Because pressure denaturation is a reversible process, after decompression the proteins started to refold. Subsequent dilution of the samples in a non-deuterated solvent caused substitution of the available deuterons by protons, however, the deuterons which were captured inside the refolded protein were protected against the back-exchange and stayed at their positions. Figure 1 depicts dependence of a number of unexchangeable deuterons upon the applied pressure for the equilibrium point (60 min after decompression and dilution) and reflects differences between the wild-type and mutated cystatin C in regard to their structural stability. The pressure-induced changes in the wild-type protein and V57N mutant began above 200 MPa, at 400 MPa both proteins adopted stable unfolded conformation and further pressure increase did not cause any additional perturbations in their structure. In the case of V57D mutant, the unfolding process started earlier – at about 150 MPa, but complete unfolding took place at the same moment as for the wild-type hCC – at a pressure of 400 MPa. Lack of any plateau in the first part of the denaturation curve of V57P clearly indicates that the unfolding of this protein started at the very beginning of the denaturation process, and points out the proline mutant as the least stable hCC variant, without any resistance to the applied pressure. Simultaneously, V57P mutant occurred to attain the final unfolded conformation at lower pressure (300MPa) than the other studied proteins.

Only 32 deuterons were trapped in the molecule of V57P mutant after its recovery from the completely unfolded structure whereas V57N, V57D and the wild-type hCC in the identical experiments captured from 6 to 8 deuterons more (Figure 1). These results suggest that V57P did not refold with the same rate as the rest of the studied proteins or was even unable to refold correctly. Its structure was penetrable by solvent molecules for an extended period of time allowing free re-exchange of the incorporated deuterons into protons. Delayed establishing of the equilibrium of the D/H back-exchange process, resulting in a lower number of the trapped deuterons, indicated evidently that proline residue at the hinge region made the protein structure more flexible and dynamic, and prolonged its existence in a kind of an 'open' state. Flexibility of the hCC V57P mutant may be interpreted as a result of the reported broadening of the hinge loop L1 caused by V→P substitution and the preference of Pro residue to adopt the dihedral angles characteristic for an extended structure [4]. Quite easy achievable and apparently fairly stable 'open' conformation probably allows V57P molecule to exist in this form in solution for the time long enough to meet another 'open' molecule and swap domains with it, giving rise to the dimeric structure. Enhanced stability of the 'open' conformation explains the observation that V57P dimerizes the most eagerly among all hCC mutants [3].

Acknowledgments
The work was supported by grants BW/8000-5-0253-9 and 1264/B/H03/2009/37.

References

1. Olafsson, I., Grubb, A. *Amyloid* **7**, 70-79 (2000).
2. Janowski, R., Kozak, M., Jankowska, E., Grzonka Z., Grubb, A., Abrahamson, M., Jaskólski M. *Nature Struct. Biol*. **8**, 316-320 (2001).
3. Szymanska, A., Radulska, A., Czaplewska, P., Grubb, A., Grzonka, Z., Rodziewicz-Motowidło, S. *Acta Biochim. Pol.* **56**, 455-463 (2009).
4. Rodziewicz-Motowidło, S., Iwaszkiewicz, J., Sosnowska, R., Czaplewska, P., Sobolewski, E., Szymanska, A., Stachowiak, K., Liwo, A. *Biopolymers* **91**, 373-383 (2009).

Proceedings of the 31st European Peptide Symposium
Michal Lebl, Morten Meldal, Knud J. Jensen, Thomas Hoeg-Jensen (Editors)
European Peptide Society, 2010

Characteristics of a Human Cystatin C – Antibody Complex

Anna Sladewska[1], Aneta Szymanska[1], Aleksandra Kolodziejczyk[1], Anders Grubb[2], and Paulina Czaplewska[1]

[1]Faculty of Chemistry,University of Gdansk, Gdansk; [2]Department of Clinical Chemistry, University Hospital, Lund, Sweden

Introduction

The immune system plays a major role in the defense of organisms against infections. Nowadays scientists are working on the use of antibodies in a search of inhibitors for many kinds of amyloidogenic diseases. The great potential of this concept is hidden in monoclonal antibodies (mAb), which recognize only one epitope of the antigen and are highly specific to this particular antigen. Grubb and coworkers described the influence of monoclonal antibodies on the dimerization process of human cystatin C (hCC). It was found that even catalytical amounts of monoclonal antibodies visibly diminished the process [1]. This clearly showed that the mAb can be considered as potential therapeutic agent in amyloidosis caused by aggregation of hCC and its L68Q mutant. Therefore, it is necessary to develop sensitive analytical methods that enable to clarify details of the interactions between amyloidogenic molecules. Recent developments show that selective proteolytic excision combined with mass spectrometric peptide mapping (Epitope-Excision-MS) present high potential for the determination of epitopes for antigen-epitope mapping and for the identification of antibody paratope sequences [2].

Results and Discussion

In this work we present preliminary results of studies on the influence of the monoclonal antibody Cyst-13 on the dimerization process of human cystatin C and the identification of the epitope of this antibody with the use of mass spectrometric epitope extraction and excision methods. The studies were carried out using a molecular affinity mass spectrometry approach. The method uses the resistance of the epitope sequence against enzymatic digestions due to the shielding of the protein-antibody interaction site. Analysis of the MS spectra obtained in the proteolytic excision/extraction procedure enabled us to identify and locate the epitope. The results of digestions by using different enzymes and the analysis of the MS spectra obtained at successive steps of the extraction/excision procedures revealed that the epitope for mAb Cyst-13 comprises the residues 107-114 of human cystatin C (QGTMTLSK). The sequence was obtained after an epitope excision experiment on cystatin C–mAb

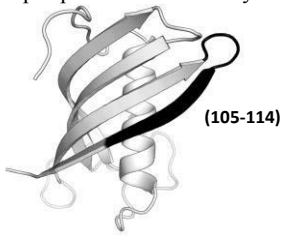

Fig. 1. Location of binding site for complex of hCC with monoclonal antibodies Cyst-13.

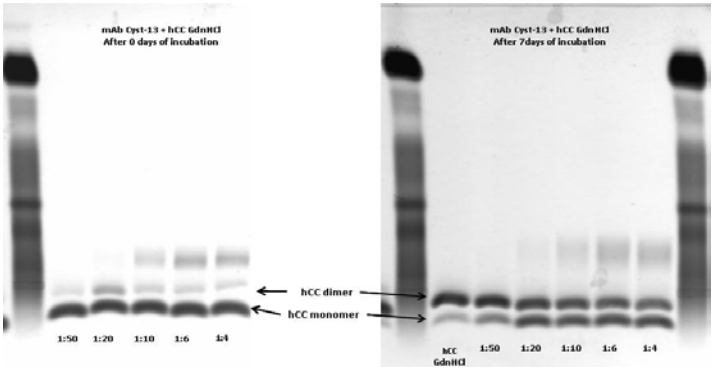

Fig. 2. Influence of Cyst13 mAb on hCC dimerization.

Cyst-13 complex. Literature data suggest that an epitope is generally composed of five to seven core amino acids and up to 10 contact residues. Our results correspond to these data, as we identified eight amino acid residues as the direct epitope, but in an affinity experiment with the synthetic peptide epitope, the octapeptide was not binding to the antibody. Prolongation of the epitope from the N-terminus by two residues resulted in the decapeptide PWQGTMTLSK showing much higher binding ability in affinity experiments. It was proved that prolongation of the epitope sequence by two residues stabilizes the complex and ensures the specificity of the molecular recognition. The determined epitope sequence is located in the C-terminal region of cystatin C which is exposed to the environment, therefore there is no steric hindrance which can impede interactions between hCC and the antibody. The epitope sequence (hCC 107-114) is located within the L2-β5 strand (Figure 1).

The identification of the binding site may be of high importance for dimerization/oligomerization and fibrillization studies of hCC. Gel electrophoresis proved the direct influence of mAb Cyst-13 on the dimerization of hCC. The incubation of hCC with mAb Cyst-13 showed the suppression of the dimerization process for all mAb/hCC molar ratios applied. Even the lowest amount of the antibody slightly suppressed the dimer formation in comparison with the dimerization of the native protein (Figure 2). It is of further interest to investigate how blocking of the C-terminal part by interaction with the antibody can influence the dimerization process.

The production of specific antibodies in the human organism is an important regulatory mechanism for different processes. Thanks to the use of the epitope extraction- and excision-mass spectrometry method we were able to identify successfully the epitope for the monoclonal antibody Cyst-13 raised against human cystatin C. The epitope identification offer a possibility to use a more defined active immunization with a partial sequence of hCC conjugated to a carrier protein. This approach may yield a strong antibody response to a definite region of cystatin C and is therefore promising in combating pathological conditions related to hCC amyloidogenity (HCCAA).

Acknowledgments
The work was supported by Ministry of Science and Higher Education, Grant No. 1264/H03/2009/37.

References

1. Nilsson, M.X. Wang, Rodziewicz-Motowidło, S., Jankowski, R., Lindstrom, V., Onnerfjord, P., Westermark, G., Grzonka, Z., Jaskólski, M., Grubb, A. *J. Biol. Chem*. **279**(23), 24236-45 (2004).
2. Stefanescu, R., Iacob, R.E., Damoc, E.N., Marquardt, A., Amstalden, E., et al. *Eur. J. Mass. Spectrom. (Chichester, Eng.)* **13**, 69-75 (2007).

Proceedings of the 31st European Peptide Symposium
Michal Lebl, Morten Meldal, Knud J. Jensen, Thomas Hoeg-Jensen (Editors)
European Peptide Society, 2010

Characterization of Human Cystatin C – Serum Amyloid A Complex

Marta Spodzieja[1], Aneta Szymańska[1], Anna Śladewska[1], Piotr Stefanowicz[2], Zbigniew Szewczuk[2], Zbigniew Grzonka[1], Claudia Cozma[3], Michael Przybylski[3], Aleksandra Kołodziejczyk[1], and Paulina Czaplewska[1]

[1]University of Gdansk, Faculty of Chemistry, Gdansk, 80-952, Poland; [2]University of Wroclaw, Faculty of Chemistry, Wroclaw, 50-383, Poland; [3]University of Konstanz, Konstanz, 78457, Germany

Introduction

Cystatin C (hCC) is the most abundant human extracellular inhibitor of cysteine proteinases. This single-chain protein dimerizes through 3D domain swapping mechanism. HCC in its native, physiological state is monomeric while in pathological conditions is present as a dimer [1,2]. Serum amyloid A (SAA) plays a major, but a relatively uncharacterized role in the acute phase response and it is an important component of the human immune systems. Analysis of the primary structure of SAA suggests that approximately 80% of the molecule consists of a helical structure while the remaining *C*-terminal part is disordered [3]. *In vitro* and *in vivo* experiments revealed that cystatin C can form a complex with SAA [4]. In this work we present identification of the binding sites between human cystatin C and serum amyloid A. The extraction/excision mass spectrometry method was previously used for identification of hCC-Aβ complex [5]. In this work we established that the binding sites of SAA-hCC complex are located in the *C*-terminal part of both proteins. The identification of the binding site in hCC should be very important for its oligomerization studies and new oligomerization inhibitors may be designed based on SAA binding fragment.

Results and Discussion

Proteolytic excision- and extraction-mass spectrometry method was used for the hCC-SAA binding site identification. Its principle is that one of the complex components (SAA) is attached to a solid matrix that simplifies the workout of the immune complex and allows efficient removal of the unbound protein (hCC) or its fragments. Mass spectrometry analysis applied for the epitope identification gives the possibility of using a minimal amount of proteins and enzymes, making the whole procedure simple and cheap. In the analysis all kinds of proteolytic enzymes can be used. The protocol consists of two complementary variants: epitope-excision and digestion, while the epitope extraction procedure starts with digestion of the protein (hCC) in a solution. Further procedure is identical for both procedures – washing, elution of bound fragments and MS analysis. Results are presented in Table 1.

All digestion experiments of hCC in the complex with SAA (SAA attached to the matrix) revealed that C-terminal part of cystatin C is responsible for the interaction with serum amyloid A. Further studies with pronase (unspecific protease digesting a protein to its component amino acids) showed more definite fragment, namely hCC(96-102). The binding experiment with C-terminal part of hCC (residues 93-120) and the repeated excision experiment with pronase confirmed previously identified binding site as hCC(96-102).

Studies in the reversed system – hCC on the matrix and the digestion of serum amyloid A – were performed analogically to the previous ones. Extraction and excision experiments showed that for SAA also C-terminal part is responsible for interactions with cystatin. In this case after digestion of the complex with pronase a set of short SAA fragments binding to hCC was identified. All short peptides were interacting with hCC in binding experiments. ELISA performed with all of them confirmed the interaction but the affinity of the SAA fragment to hCC decreased with the peptide length.

Table 1. Results of extraction/excision and affinity experiments for A) serum amyloid A bound to cystatin C (on solid matrix); B) human cystatin C and SAA (on the solid matrix)

A

Experiment	Fraction	$M_{theoretical}$	$M_{experimental}$	SAA fragment	Sequence
Affinity experiment with SAA(70-92)	Supernatant	2437.52	2438.0	70-92	FGRGAEDSLADQAANEWGRSGKD
	Last wash	-	-	-	-
	Elution	-	-	-	-
Affinity experiment with SAA(87-105)	Supernatant	2126.37	2126.9	87-105	GRSGKDPNHFRPAGLPEKY
	Last wash	-	-	-	-
	Elution	2126.37	2126.2	87-105	GRSGKDPNHFRPAGLPEKY
Affinity experiment with SAA(88-98)	Supernatant	1309.66	1309.7	88-98	RSGKDPNHFRP
	Last wash	-	-	-	-
	Elution	1309.66	1309.7	88-98	RSGKDPNHFRP
Affinity experiment with SAA(91-103)	Supernatant	1476.75	1476.4	91-103	KDPNHFRPAGLPE
	Last wash	-	-	-	-
	Elution	1476.75	1476.8	91-103	KDPNHFRPAGLP E

B

Experiment	Fraction	$M_{theoretical}$	$M_{experimental}$	hCC fragment	Sequence
Epitope excision with pronaze	Elution	906.39	906.5	96-102	FCSFQIY
		1227.5	1227.1	91-100	LKRKAFCSFQ
		1646.89	1646.3	96-109	FCSFQIYAVPWQGT
		3168.67	3168.9	93-120	RKAFCSFQIYAVPWQGTMTLSKSTCQDA
		3338.92	3338.1	91-119	LKRKAFCSFQIYAVPWQGTMTLSKSTCQD
Affinity experiment with hCC(93-120)	Supernatant	3168.67	3168.9	93-120	RKAFCSFQIYAVPWQGTMTLSKSTCQDA
	Last wash	-	-	-	-
	Elution	3168.67	3169.0	93-120	RKAFCSFQIYAVPWQGTMTLSKSTCQDA
Affinity experiment with hCC(96-102)	Supernatant	906.39	906.8	96-102	FCSFQIY
	Last wash	-	-	-	-
	Elution	906.39	906.5	96-102	FCSFQIY

The complex formation between C-terminal fragments of hCC and SAA was confirmed with MS experiments. First, we obtained high resolution spectra of the complex (Figure 1A) and then the complex signal was studied by MS/MS analysis (Figure 1B).

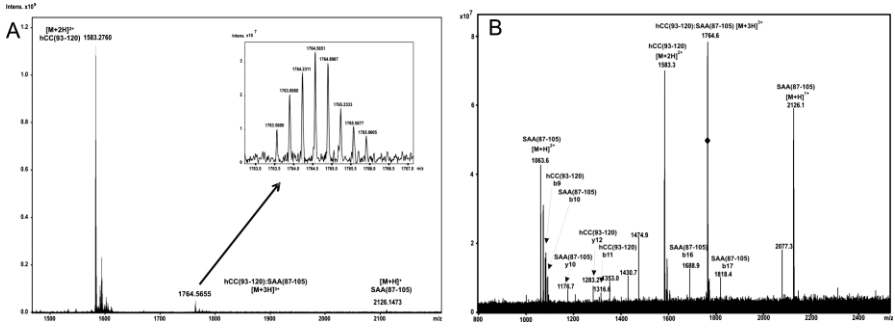

Fig. 1. ESI-FTICR MS spectrum of complex formed between fragments of hCC(93-120) and SAA(87-105). A) MS spectra of complex in solution; B) MS/MS analysis of complex signal.

Our further studies will show which resides are important for interaction of the protein and reveal whole structure of it.

Acknowledgments

This work is supported by Polish Ministry of Science and Higher Education, grant 1264/H03/2009/37 to Dr. Paulina Czaplewska.

References

1. Grzonka, Z., et al. *Acta Biochim Pol.* **48,** 1-20 (2001).
2. Janowski, R., et al. *Nat. Struct. Biol.* **8**, 316-320 (2001).
3. Stevens, F.J. *Protein Folding Disord.* **11**, 71-80 (2004).
4. Bokarewa, M., et al. *J. Rheumatol*. **34**, 1293-1301 (2007).
5. Macht, M., Fiedler, W., Kurzinger, K., Przybylski, M. *Biochemistry* **35**, 15633-15639 (1996).

Proceedings of the 31st European Peptide Symposium
Michal Lebl, Morten Meldal, Knud J. Jensen, Thomas Hoeg-Jensen (Editors)
European Peptide Society, 2010

Recognition of Cytoskeletal Proteins Monoclonal IgGs by CSF114(Glc), the Synthetic Probe of Multiple Sclerosis

Shashank Pandey[1,2], Duccio Lambardi[1,3], Feliciana Real-Fernández[1,2], Maria Claudia Alcaro[4], Elisa Peroni[1,5], Mario Chelli[1,2], Anna M Papini[1,2,5], Francesco Lolli[1,6], and Paolo Rovero[1,3,4]

[1]Laboratory of Peptide & Protein Chemistry & Biology, Polo Scientifico e Tecnologico, University of Florence, Sesto Fiorentino (FI), Italy; [2]Department of Chemistry and CNR ICCOM, Via della Lastruccia 3/13, University of Florence, I-50019, Sesto Fiorentino (FI), Italy; [3]Department of Pharmaceutical Sciences Via Ugo Schiff 6, University of Florence, I-50019, Sesto Fiorentino (FI), Italy; [4]Toscana Biomarkers Srl, via Fiorentina 1, I-53100, Siena, Italy; [5]Laboratoire SOSCO-EA4505, Universitè de Cergy-Pontoise, Neuville-sur-Oise, F-95031, Cergy-Pontoise, France; [6]Department of Neurological Sciences & Azienda Ospedaliera Careggi, Viale Morgagni 34, University of Florence, I-50134, Firenze, Italy

Introduction

Multiple sclerosis (MS) is an inflammatory demyelinating disease of the central nervous system (CNS), the pathogenesis of the disease has not been yet elucidated. In our previous study, we demonstrated for the first time that CSF114(Glc) (Figure 1) is able to recognize the presence of specific autoantibodies (94%) in the sera of a statistically significant number of Multiple Sclerosis patients with high specificity. No false positive data were obtained with sera from patients affected by other autoimmune diseases or other neurological diseases. Therefore, CSF114(Glc) is a simple, reliable, and efficient tool, which clearly shows that an aberrant N-glucosylation is involved in autoantibody recognition in Multiple Sclerosis [1-5].

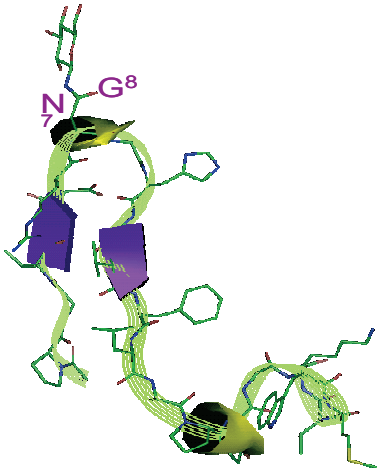

Fig. 1. Ribbon diagram of the lowest energy conformer of 200 calculated structures of CSF114(Glc) derived from NMR data.

We report herein for the first time the recognition of specific cytoskeletal proteins monoclonal IgGs antibodies and its crossreactivity with the artificially N-glucosylated peptide sequence.

Results and Discussion

Frozen rat brain was homogenized and solubilized in tritonX-100. Solubilized fractions were analysed in 12% SDS-PAGE.

Extracted proteins were transferred onto Nitrocellulose membrane and western blots were performed using affinity purified anti-CSF114(Glc) IgGs from Multiple Sclerosis patients' sera and normal blood donors as controls. We constantly found in Multiple Sclerosis three positive bands recognizing affinity purified anti-CSF114(Glc) IgGs and corresponding to 130kDa, 98kDa, and 47kDa. On the contrary, normal blood donors' sera displayed no relevant recognition.

Bands of interest from SDS-PAGE were excised and trypsin digested. Digested samples were analyzed by MALDI-TOF followed by MS/MS analysis. We succeeded in identifying 2',3'-Cyclic-Nucleotide 3' Phosphodiesterase, Creatine kinase BB, Alpha actinin, and Alpha fodrin corresponding to positions 47kDa, 98Da, and 130kDa respectively (Table 1).

Table 1. Proteins identified by MALDI-TOF and further confirmed by MS/MS analysis

SDS-WB band (kDa)	*Protein identified*	*ID*	*score (thld)*	*sig.*
47kDa [1]	2',3'-Cyclic-Nucleotide 3-Phosphodiesterase (Rat)	I56577	94(63)	4.4e-05
47kDa [2]	Creatine kinase (Rat)	Q499P7_rat	90(63)	1.2e-04
98kDa	Brain specific alpha actinin (Rat)	Q6T487_rat	83(63)	5.7e-04
130kDa	Spectrin alpha chain or Alpha fodrin (Rat)	AAC33127	133(63)	6.1e-09

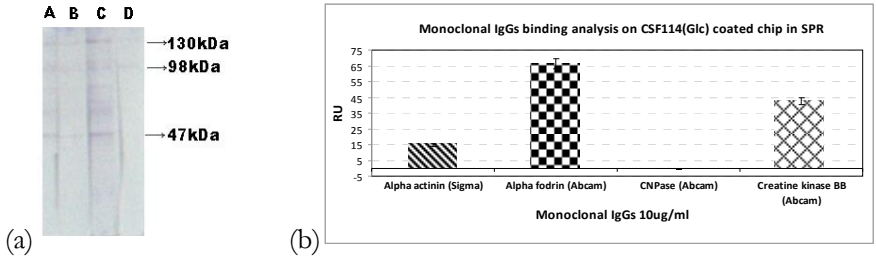

Fig. 2. (a) Western blot of rat brain proteins with affinity purified anti-CSF114(Glc) IgGs from Multiple Sclerosis patients' sera (lane A, B, C) and anti-CSF114(Glc) IgGs from one representative normal blood donor (lane D). (b) Surface Plasmon Resonance of identified cytoskeletal proteins monoclonal IgGs (Sigma, Abcam) on CSF114(Glc)-coated chip.

Further confirmation was obtained using commercially available monoclonal antibodies to Alpha fodrin, Creatine kinase BB, and CNPase (*Abcam*), and Alpha actinin (*Sigma*). All the monoclonal IgGs were used in Surface Plasmon Resonance (BIAcore T100^{TM}) for binding analysis with CSF114(Glc)-coated chips. Interestingly, we found that anti-Alpha fodrin, anti-Creatine kinase BB, and anti-Alpha actinin monoclonal IgGs were able to bind with CSF114(Glc). Differently anti-CNPase IgGs did not display any binding at the same concentration (Figure 2).

In conclusion, we characterized for the first time that the artificially designed CSF114(Glc) specifically recognizes anti-Alpha fodrin and anti-Alpha actinin monoclonal IgGs, belonging to the same family of cytoskeletal proteins.

The question arising now: are the proteins Alpha fodrin, Creatine kinase BB, and Alpha actinin real native antigens involved in triggering autoantibody-mediated Multiple Sclerosis?

Acknowledgments
Italian government scholarship for biotechnology 2008 (India) and MIUR scholarship 2009 (Italy) to S.P., Ente Cassa Risparmio di Firenze (Italy) as well as Chaire d'Excellence 2009-2013 (France) to A.M.P. are gratefully acknowledged for financial support.

References

1. Papini, A.M., et al. *Granted U.S.A. Patent & PCT WO 03/000733 A2*.
2. Papini, A.M. *Simple test for multiple sclerosis*. *Nat. Med*. **11**, 13 (2005).
3. Carotenuto, A., et al. *J. Med. Chem*. **51**, 5304-5309 (2008).
4. Lolli, F., et al. *P.N.A.S.* **102**, 10273 (2005).
5. Lolli, F., et al. *J. Neuroimmunol.* **167**, 131 (2005).

Proceedings of the 31st European Peptide Symposium
Michal Lebl, Morten Meldal, Knud J. Jensen, Thomas Hoeg-Jensen (Editors)
European Peptide Society, 2010

Role of Triple Hyp→Pro Substitution on Conformation and Bioactivity of Integramide A

Marta De Zotti[1], Wim De Borggraeve[2], Bernard Kaptein[3], Quirinus B. Broxterman[3], Sheo B. Singh[4], Peter J. Felock[5], Daria J. Hazuda[5], Fernando Formaggio[1], and Claudio Toniolo[1]

[1]ICB, Padova Unit, CNR, Department of Chemistry, University of Padova, Padova, 35131, Italy; [2]Department of Chemistry, Catholic University Leuven, Leuven, 3001, Belgium; [3]DSM Innovative Synthesis BV, Geleen, 6160 MD, The Netherlands; [4]Medicinal Chemistry, Merck Research Laboratories, West Point, 19486, PA, U.S.A.; [5]Medicinal Chemistry, Merck Research Laboratories, Rahway, 07065, NJ, U.S.A.

Introduction

AIDS is produced by HIV-induced infections. HIV integrase is an important enzyme as it is critical for the integration of HIV genome into that of the host cell. Because this complex process is exclusively brought about by the virus, the enzyme, not found in the host cell, represents a safe target for the development of a single or a combined anti-HIV therapy. Integramide A is a 16-mer long, effective peptaib inhibitor of HIV-1 integrase. Its primary structure is: Ac-D-Iva-L-Hyp-L-Iva-L-Leu-Aib-Aib-Aib-L-Hyp-L-Iva-D-Iva-Gly-OH (Ac, acetyl; Aib, α-aminoisobutyric acid; Hyp, (4*R*)-hydroxyproline; Iva, isovaline) [1].

Results and Discussion

We have recently described a versatile synthetic strategy in solution to afford this natural compound and its diastereomer at positions 14 and 15, and found that both peptides display a significant inhibitory activity [2]. In this study, we present our data on the synthesis in solution, in-depth FT-IR absorption, CD and 2D-NMR conformational analysis (Figure 1), and biological activity against HIV-integrase (Table 1) of the analogues of the two above mentioned peptides in which all of the three (2*S*,4*R*)-Hyp residues at positions 2, 9, and 13 are replaced by L-Pro.

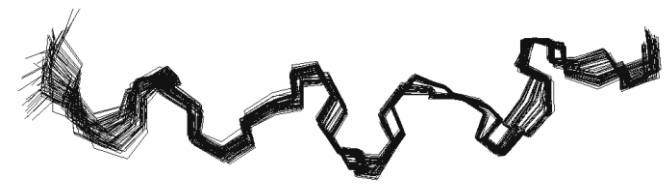

I

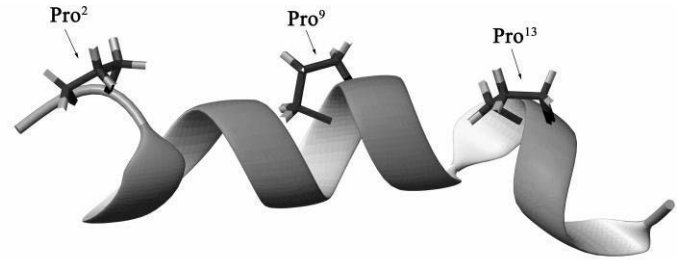

II

Fig. 1. (I) Superposition of the 22 lowest-energy backbone, mixed α-/3$_{10}$- helical 3D-structures (energy < 129 Kcal/mol) for the integramide A analogue containing the -L-Iva^{14}-D-Iva^{15}- sequence consistent with the 2D-NMR derived distances and dihedral angle restraints. (II) Ribbon representation of the lowest-energy 3D-structure obtained for the same peptide. The three L-Pro residues are labeled.

Table 1. Evaluation of the inhibition activity against HIV-1 integrase in both coupled and strand transfer reactions of the two integramide A analogues and the natural compound

Peptide	*IC_{50} for strand transfer reaction*	*IC_{50} for coupled reaction*
natural and synthetic integramide A	30-34 μM	7-10 μM
[D-Iva^{14}-L-Iva^{15}] integramide A	55 μM	8 μM
[L-Pro^{2,9,13}] integramide A	60 μM	19 μM
[L-Pro^{2,9,13}, D-Iva^{14}-L-Iva^{15}] integramide A	21 μM	10 μM

From the results shown in Table 1, we can safely conclude that in general the two L-Pro-containing integramide A analogues are only slightly less active than natural (or synthetic) integramide A itself in inhibiting HIV-1 integrase.

This study definitely confirms that the mixed α-/3_{10}- helical conformation of natural integramide A plays a key role in its mechanism of inhibition. Moreover, our data provide evidence that the amphipathic character of this helical structure is not required for the activity of integramide A against HIV-1 integrase. These observations will hopefully be useful to further clarify the precise mechanism of inhibition of this interesting peptaib and to identify shorter peptide sequences active against HIV-1 integrase.

References

1. Singh, S.B., Hereth, K., Guan, Z., Zink, D.L., Dombrowski, A.W., Polishook, J.D., Silverman, K.C., Lingham, R.B., Felock, P.J., Hazuda, D.J. *Org. Lett.* **4**, 1431-1434 (2002).
2. De Zotti, M., Damato, F., Formaggio, F., Crisma, M., Schievano, E., Mammi, S., Kaptein, B., Broxterman, Q.B., Felock, P.J., Hazuda, D.J., Singh, S.B., Kirschbaum J., Brückner, H., Toniolo, C. *Chem. Eur. J.* **16**, 316-327 (2010).

Proceedings of the 31st European Peptide Symposium
Michal Lebl, Morten Meldal, Knud J. Jensen, Thomas Hoeg-Jensen (Editors)
European Peptide Society, 2010

Angiotensin I Converting (ACE) Inhibitory Peptides – A Bioinformatic-Assisted Idea of Research

Anna Iwaniak
Chair of Food Biochemistry, University of Warmia and Mazury, Olsztyn, 10-712, Poland

Introduction

Angiotensin I converting enzyme (ACE) inhibitory peptides are known as vasodilators. These peptides are encrypted in many food-derived bioactive proteins and due to their special properties they are found as the valuable food components that can be regarded as health-promoting ingredients [1].

Much information concerning ACE inhibitory sequences is available in the literature and computer databases. Specially designed mathematical and statistical algorithms along with some bioinformatic and cheminformatic tools are helpful for the understanding the biological processes which take place in the living organisms [2]. Application of above mentioned tools in defining bioactive peptides in protein is consistent with the idea of food peptidomics which covers the research concerning both the composition, changes of the pool of peptides and the methods applied in the studying of these groups of molecules [3].

The aim of the work was to elaborate the idea of research of ACE inhibitors (214 di- and tripeptides in total) derived from major groups of proteins by means of bio- and cheminformatic tools. To achieve it, the BIOPEP database (http://www.uwm.edu.pl/biochemia) was mostly applied. This strategy involved the use of qualitative and quantitative criteria to evaluate protein as the source of ACE inhibitors as well as the prediction of their release due to the action of digestive enzymes. The prediction of products potentially released by selected endopeptidase(s) was performed by means of one of the BIOPEP functions called "Enzymes action".

Results and Discussion

The correlation coefficients illustrating experimental versus theoretical values of activity, were relatively low (*e.g.* R^2=0.234 for tripeptides) and their calculation was based on the quantum chemistry descriptors. Thus principal component analysis (PCA) was applied to find some structural similarities of ACE inhibitors which would decide about their activity. The main characteristic feature in most of the peptides analyzed was the presence of proline (C-end) or aliphatic/aromatic/cyclic amino acid at the N-end (and/or second position in tripeptides). Referring the results to the variables affecting the peptides' bioactivity, the hydrophobicity, the size of a molecule and electronic properties had the influence on their activity. The above-mentioned structural similarities between peptides as well as physicochemical properties of the individual amino acids forming peptides were consistent with results obtained by other scientific groups [4].

The ACE inhibitors possessing the indicated features were used as "standards" to find them in the protein sequences representing major groups of food. It was enabled by means of one of the BIOPEP functions *i.e.* profile of ACE inhibitory activity of a protein. This analysis revealed that milk and plant proteins can be considered as the material for proteolytic processes design. *In silico* proteolysis specified that β-casein and globulins from oat and soybean should be qualified for an *in vitro* experiment. Milk is widely known as the source of ACE inhibitors and thus was eliminated from the experimental part of the research. The oat globulin was firstly taken for the further studies. Some of potentially released peptides were not defined by BIOPEP as "bioactive". However, their sequences revealed contained three amino acid residue fragments with *in vivo* confirmed activity (see BIOPEP database). It covers the idea of fragmentomics, according to which the relatively small and active substances are the fragments of larger structures [5].

Depending on the enzymes combination used, eighteen peptides could be potentially released. Experimental verification of results revealed, that oat protein hydrolysates showed the ACE inhibitory effect. IC_{50} values calculated for the hydrolysates of pepsin as well as the combination of pepsin with trypsin/chymotrypsin were: 0.43, 0.015 and 0.33mg/ml, respectively.

Identification of peptides by LC-MS and LC-ESI MS/MS revealed that five out of eighteen peptides obtained *via* computer simulation of hydrolysis (BIOPEP) were detected.

They were the sequences: RCTGVSVIRRVIEPQGL, VIEPQGL, TNPNSMVSHIAGK and VQVVNNNGQTVF (depending on the combination of enzymes applied). The peptide with the sequence RCTGVSVIRRVIEPQGL found in pepsin and pepsin+chymotrypsin hydrolysate is so-called proteotypic peptide *i.e.* peptide which can be identified at least in a half of the experiments with the same analyte [6].

To conclude, the idea of research based on chemo- and bioinformatic tools in combination with laboratory analysis is a suitable and modern trend of studying the bioactive peptides derived from food proteins. However, it should be noted, that results obtained in this way should be verified *in vitro* before introducing new food bioactive compounds on the market.

Acknowledgments
Supported by grant 529-0712-915 (Ministry of Science and Higher Education).

References

1. Iwaniak, A., Dziuba, J. *Food Technol. Biotechnol.* **47 (4)**, 441-449 (2009).
2. Blythe, M.J., Doytchinova, I.A., Flower, D.R. *Bioinformatics* **18, 3**, 434-439 (2007).
3. Minkiewicz, P., et al. *Food Technol. Biotechnol.* **4**, 1-10 (2008).
4. Pripp, A.H., et al. *J. Agric. Food Chem.* **16 (11),** 484-494 (2005).
5. Zamyatnin, A.A. *Biochemistry (Moscow)* **74,** 1575-1585 (2009).
6. Mallick, P., et al. *Natur. Biotechnol.* **25**, 125-131 (2007).

Proceedings of the 31st European Peptide Symposium
Michal Lebl, Morten Meldal, Knud J. Jensen, Thomas Hoeg-Jensen (Editors)
European Peptide Society, 2010

A Method for Screening Peptides Bound to EGFR by Using Multiple Fluorescent Amino Acids as Fluorescent Tags

Mizuki Kitamatsu, Takahiro Yamamoto, and Masahiko Sisido
Department of Medical and Bioengineering, Graduate School of Natural Science and Technology, Okayama University, 3-1-1 Tsushimanaka, Okayama, 700-0082, Japan

Introduction

A peptide library is generally used for screening peptides bound to a target protein. The phage display method [1] and the one-bead–one-compound method [2,3] are widely used methods for screening with a peptide library. However, the methods have a drawback in the case of screening for short peptides because of the need to fix the short peptides on large carriers like phages and beads. The carriers often interact with targets nonspecifically. To overcome this drawback, we have developed a new screening method without large carriers [4]. In this method, a peptide library is labeled with multiple fluorescent amino acids. The peptides binding to targets are detected quantitatively by specific fluorescence from the fluorescent amino acids labeling on peptides. In this study, we screened 8-mer peptides bound to epidermal growth factor receptor (EGFR) by this method. EGFR is a receptor tyrosine kinase over-expressed on surface of many human cancers. Therefore, an EGFR-binding peptide can be regarded as a significant target of tumor and it is an attractive medical tool.

Results and Discussion

Two hundred twenty-five peptides were prepared by solid-phase peptide synthesis. The sequence is shown in Figure 1. Y_1 and Y_2 indicate 15 D-amino acids other than Cys, Gly, Leu, Glu and Gln. X indicates equimolar mixture of these amino acids. Fl indicates a fluorescent amino acid. Fifteen fluorescent amino acids were used in this study (Figure 1).

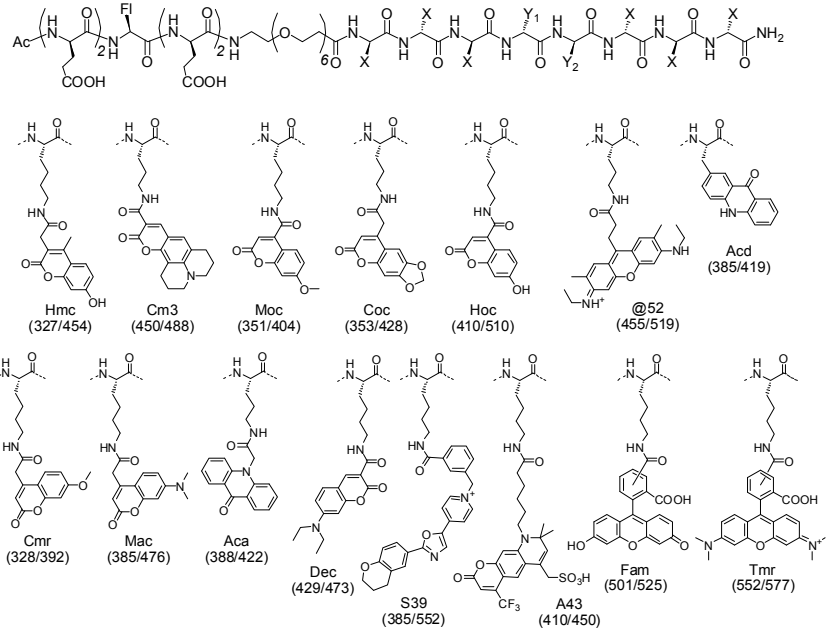

Fig. 1. Chemical structure of the peptide modified with a fluorescent amino acid and chemical structures of fluorescent amino acids. Values in a parenthesis indicate maximum excitation/emission wavelengths obtained from the 2D-FL spectrum of each fluorescent amino acid in 70 mM HEPES buffer (pH 7.4)/methanol (1/1 (v/v)) at room temperature.

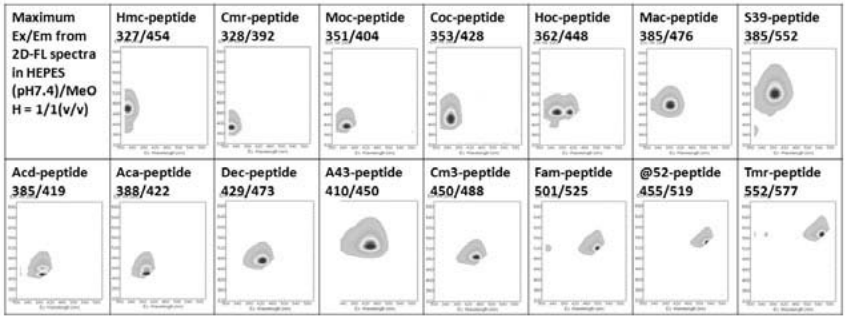

Fig. 2. 2D-FL spectra of the fifteen peptides modified with fluorescent amino acids.

Peptides binding to the EGFR were selected and quantified by the method using these fluorescent peptides. In this study, the water-soluble ErbB1 (sErbB1; the extracellular domain of human EGFR) was used as an EGFR. Fifteen fluorescent peptides were incubated with the EGFR in 70 mM HEPES-NaOH buffer (pH 7.4, 150 mM NaCl) at 4 ˚C for 2 h. Each final concentration of the peptides was 190 μM (4.5 nmol) and the concentration of EGFR was 8.6 μM (0.36 nmol). The fluorescent peptides binding to EGFR were recovered by gel filtration chromatography (Superdex^{TM} 75 prep grade was purchased from GE Healthcare.). Then the amounts of fluorescent peptides binding to the EGFR were determined with 2D-FL spectroscopy in 70 mM HEPES-NaOH buffer (pH 7.4, 150 mM NaCl)/methanol (1/1 (v/v)). The binding of each fluorescent peptide to EGFR was quantified by least-squares analysis from the 2D-FL spectrum of each fluorescent peptide (Figure 2). We repeated the aforementioned protocols for 15 sets of fifteen fluorescent peptides.

These fluorescent peptides were successfully estimated by this method, and it was shown that the amount of the peptide binding to the EGFR depends on a dipeptide unit, Y_1-Y_2, in the 8-mer peptide library. Many fluorescent peptides did not bind to the EGFR, but binding of some of the peptide to the EGFR could be detected. Of 225 fluorescent peptides, Ac-EE-Fam-EE-Sp6-XXX-Y-F-XXX-NH_2 was found to show the strongest binding to the EGFR. The binding amount of the peptide was 41 pmol. The reverse sequence, F-Y, showed weak binding to the EGFR (9 pmol). It was clarified that the sequence is important for binding to the EGFR. Dipeptide units containing amino acids carrying an aromatic ring (F, Y and W) and a hydrophobic group (I and V) seemed to bind to the EGFR strongly.

In summary, we synthesized 225 peptides modified with a fluorescent amino acid as fluorescent tags for screening EGFR-binding peptides. Binding amounts of peptides to the EGFR were successfully quantified by this method. The 8-mer peptide containing a dipeptide unit, Y-F, was the strongest binding peptide to the EGFR. Determination of an 8-mer peptide sequence that binds to the EGFR by this method is currently underway.

Acknowledgments

This work was supported by Iketani Science and Technology Foundation. This work was also supported by a Grant-in-Aid for Scientific Research from the Ministry of Education, Culture, Sports, Sciences, and Technology, Japan (No. 21750172).

References

1. Scott, J.P., Smith, G.P. *Science* **249**, 386-390 (1990).
2. Lam, K.S., Salmon, S.E., Hersh, E.M., Hruby, V.J., Kazmierski, W.M., Knapp, R.J. *Nature* **354**, 82-84 (1991).
3. Lam, K.S., Lebl, M., Krchnak, V. *Chem. Rev.* **97**, 411-448 (1997).
4. Kitamatsu, M., Kuroiwa, H., Sakata, D., Yamamoto, T., Inoue, K., Kishimoto, Y., Futami, M. and Sisido, M., In Lankinen, H., Vallivirta, J., Strandin, T., Hepojoki, J. (Eds.) *Peptides 2008: (Proceedings of the 30th European Peptide Symposium),* The Finnish Peptide Society and the European Peptide Society, 2010, pp. 540-541.

Proceedings of the 31st European Peptide Symposium
Michal Lebl, Morten Meldal, Knud J. Jensen, Thomas Hoeg-Jensen (Editors)
European Peptide Society, 2010

Improving Peptide Therapeutics for HIV and Other Viral Diseases

Antonello Pessi[1], Matteo Porotto[2], Christine Yokoyama[2], Laura M. Palermo[2], Aparna Talekar[2], Ilaria DeVito[2], Barry Rockx[3], Heinz Feldmann[3], Riccardo Cortese[4], and Anne Moscona[2]

[1]PeptiPharma, 00040, Pomezia (RM), Italy; [2]Weill Medical College of Cornell University, NY, 10021, U.S.A.; [3]Laboratory of Virology, NIAID, NIH, Hamilton, MT, U.S.A.; [4]CEINGE, Via Comunale Margherita 482, Naples, Italy

Introduction

Fusion of enveloped viruses with the host cell is driven by specialized proteins. The "Class I" fusion proteins harbor two heptad-repeat (HR) regions, central to the conformational changes leading to fusion: HR1, adjacent to the fusion peptide, and HR2, immediately preceding the transmembrane domain [1]. Fusion is inhibited by HR2-derived peptides like, for HIV, C34 and T20: the latter is in clinical use with the name enfuvirtide.

We have devised a general method to increase the potency of fusion inhibitors, by pre-concentrating the peptide in the membrane raft microdomains where viral fusion occurs. The method is based on the addition of a cholesterol group to the peptide ("cholesterol-tagging"). We have previously described that for HIV, cholesterol-tagging of C34 led to a dramatic increase in antiviral potency, yielding the most potent HIV fusion inhibitor known to date [2]. We apply here cholesterol-tagging to another family of enveloped viruses, the *paramixoviridae*. In particular, we show that cholesterol tagging is highly effective for inhibition of the paramyxoviruses parainfluenza virus type 3 (HPIV3), a major cause of lower respiratory diseases in infants, and Nipah virus (NiV), an emerging zoonotic virus causing lethal central nervous system diseases.

Results and Discussion

It is already known that peptides from the HR2 region of a number of paramyxoviruses can inhibit viral infectivity [3]. For the HR2 peptide derived from HPIV3, we have shown the ability of inhibiting, in addition to the homologous HPIV3 virus, also NiV virus [4]. When we applied cholesterol tagging to the HPIV3 HR2 peptide, we found considerably increased

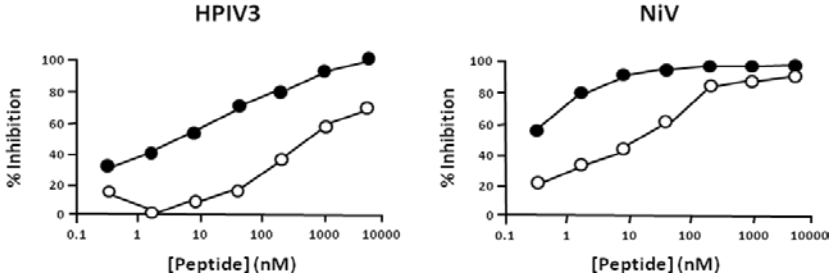

Fig. 1. Inhibiton of viral infection by cholesterol-tagged HPIV3 peptide. (Left) CV1 cell monolayers were infected with wild-type HPIV3 at a multiplicity of infection (MOI) of $6.7x10^{-4}$ in the presence of increasing concentrations of cholesterol-tagged (filled circles) or untagged (empty circles) HPIV3 peptide. After 90 min cells were overlaid with methylcellulose, and plaques were stained and counted after 18 h. (Right) 293T cell monolayers were infected with NiV pseudotyped virus at an MOI of 0.25 in the presence of increasing concentrations of tagged or untagged HPIV3 peptide. After 24 h, cells were collected and fixed for FACS analysis. The sequence of the peptide is VALDPIDISIVLNKAKSDLEESKEWIRRSNQKLDSI, corresponding to residues 449-484 of the fusogenic F protein, with the mutation Glu459→Val [4].

antiviral activity against both viruses, as shown in Figure 1 [5].

Further improvement of the HR2 HPIV3 peptide against both viruses was achieved by mutating three residues: Ala463→Ile, Gln479→Lys, and Lys480→Ile. The resulting cholesterol-tagged peptide was extremely potent against NiV, with an IC_{50} of 20 pM in the pseudotype infection assay.

Nipah virus (NiV) is an important zoonotic paramyxovirus, for which neither an antiviral therapy nor a vaccine are available. It causes seasonal outbreaks of encephalitis in Asia, with fatality of up to 70% of cases. In addition to acute infection, it may cause late onset disease years after initial infection, and persistent neurological sequelae [6].

We took advantage of the existence of a validated small animal model of NiV encephalitis to test the efficacy of our HPIV3-derived inhibitor in vivo. As shown in Figure 2, prophylactic treatment with a low subcutaneous dose of the cholesterol-tagged peptide, initiated 2 days before infection with a lethal dose of virus, could completely protect golden hamsters. Because of plasma protein binding, cholesterol-tagging extends the circulatory half-life [2] and accordingly, the HPIV3 peptide could be dosed only once daily. Experiments are ongoing to test its protective efficacy when given post infection. The

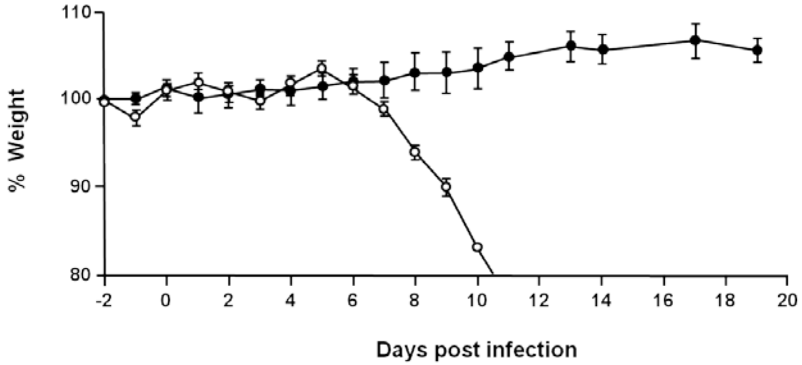

Fig. 2. Cholesterol-tagged HPIV3 peptide protects from lethal infection in vivo. Golden hamsters (5/group) were injected subcutaneously with peptide (2 mg/kg) (filled circles) or vehicle (empty circles) 2 days before infection, and then every day for 14 days post infection. The hamsters were infected by intraperitoneal inoculation of NiV, using 100x LD_{50}. At day 10, there were no survivors in the control group. The sequence of the peptide is VALDPIDISIVLNKI KSDLEESKEWIRRSNKILDSI.

findings described here further validate the concept that targeting inhibitors to lipid rafts where fusion occurs, via cholesterol-tagging, is a simple, yet effective way of increasing their potency and their pharmacological properties. Work is ongoing on other viral families.

Acknowledgments

We are grateful to E. Bianchi, A. Langella, A. Santoprete, M. Finotto, E. Capitò, F. Rech, G. Ciliberto, A. Kutcher, and J. Ledecky. This work was supported by a March of Dimes grant, Public Health Service grants AI076335 and AI31971 from NIAID, and NIH/NIAID Northeast Center of Excellence for Bio-defense and Emerging Infectious Disease Research grant U54AI057158, to A.M. and M.P.

References

1. Eckert, D.M., Kim, P.S. *Annu. Rev. Biochem*. **70**, 777-810 (2001).
2. Ingallinella, P., et al. *Proc. Natl. Acad. Sci. U.S.A*. **106**, 5801-5806 (2009).
3. Lambert, D.M., et al. *Proc. Natl. Acad. Sci. U.S.A*. **93**, 2186-91 (1996).
4. Porotto, M., et al. *J. Virol*. **81**, 10567-10574 (2007).
5. Porotto, M., et al. *J. Virol*. **84**, 6770-6778 (2010).
6. Eaton, B.T., et al. *Nat. Rev. Microbiol*. **4**, 23-35 (2006).

Proceedings of the 31st European Peptide Symposium
Michal Lebl, Morten Meldal, Knud J. Jensen, Thomas Hoeg-Jensen (Editors)
European Peptide Society, 2010

De Novo Designed Cyclic Decapeptides with Anticancer Activity

Lidia Feliu[1], Glòria Oliveras[2], Anna D. Cirac[1], Cristina Rosés[1], Ramon Colomer[3], Eduard Bardají[1], Marta Planas[1], and Teresa Puig[2]
[1]LIPPSO, University of Girona, Girona, 17071, Spain; [2]Catalan Institute of Oncology-Girona Biomedical Research Institute, Girona, 17001, Spain; [3]MD Anderson España, Madrid, Spain

Introduction

Antimicrobial peptides are known to exhibit anticancer activity. Particularly those with low hemolytic activity can be considered as good candidates for the development of new anticancer agents [1-3]. We have recently designed and synthesized a library of cyclic decapeptides with general structure c(X_5-Phe-X_3-Gln) where X is Lys or Leu that displays high antibacterial activity and low hemolysis [4]. In the present study, we tested the anticancer activity of these peptides on five human carcinoma cell lines, and their effects on apoptosis and cell signaling proteins in cultured human cervical carcinoma cells. For the peptide with the optimal biological profile, we also evaluated its ability to synergize with cisplatin in HeLa cells.

Results and Discussion

The library comprised 66 cyclic decapeptides which incorporated a Phe and a Gln residue at positions 6 and 10, respectively, and alternating Lys and Leu at the other positions. Among them, 50 peptides incorporated all combinations of three Leu and five Lys, and 16 cyclopeptides consisted of the substructure $Lys^5PheLysLysLeuGln^{10}$ and all possible combinations of Leu and Lys at positions 1 to 4.

The anticancer activity of the full cyclic decapeptide library was first screened in MDA-MB-231 human breast adenocarcinoma cells by determining the growth inhibition percentage at a peptide concentration of 40 μM by an MTT assay. Eight sequences caused ≥ 50% inhibition, indicating that these peptides exhibit a potential anticancer effect. All these peptides (BPC88, BPC94, BPC96, BPC98, BPC184, BPC194, BPC198, and BPC202) have the substructure $Lys^5PheLysLysLeuGln^{10}$ as common structural feature. The IC_{50} of these sequences was determined against five human carcinoma cell lines (Table 1). Peptides were active at the concentrations tested against all cell lines with IC_{50} values ranging from 18.5 to 57.5 μM, except for BPC198 in HepG2. HeLa cells were the most sensitive cell line to the peptides: except for BPC202 (IC_{50} of 54 μM) and BPC98 (IC_{50} of 38.5 μM), the other peptides exhibited an $IC_{50} \leq 35$ μM.

The hemolytic activity of the cyclic peptides was evaluated at 375 μM (Table 1). Two of the eight selected peptides, BPC94 and BPC184, showed significant hemolysis (73 and 89%, respectively). In contrast, the other peptides exhibited a low hemolytic activity, ranging from 2 to 36%.

The activity on non-malignant human cells (fibroblasts N1) was assessed for peptides that displayed high cytotoxic activity against HeLa cells and also low hemolysis (Table 1). Interestingly, the IC_{50} values of BPC88, BPC96, BPC98 and BPC194 in non-malignant fibroblasts were up to two fold their IC_{50} values in malignant HeLa cells. This trend is particularly important for BPC96, which only caused a lethality of 13% in non-malignant cells at its IC_{50} value in HeLa cells (24.5 μM).

Apoptosis and induction of caspase activity were checked by western blotting analysis. Treatment of HeLa cells with peptides at 20 μM for 12 h induced a marked increase on the levels of the poly-ADP-ribose polymerase (PARP) cleavage product (89 kDa band) that, compared to untreated cells, ranged between 32 (BPC88) and 684-fold (BPC194). Treatment of HeLa cells with BPC98, BPC194 and BPC198 at 20 μM for 12 h had little effect on the cellular protein levels of the tumor suppressor factor p53. In contrast, incubation of cells with BPC88 and BPC96 at 20 μM for 12 h noticeably increased the protein levels of p53 compared to untreated cells (1.8 and 1.5-fold, respectively). Concerning ERK1/2-related pathway, incubation of cells with BPC88, BPC96, and BPC198 at 20 μM for 12 and 24 h substantially blocked this survival pathway based on the decrease in the activated form of ERK1/2 (p-ERK1/2) compared to untreated cells.

Table 1. Cytotoxicity (IC_{50})[a] of selected cyclic decapeptides against a panel of human carcinoma cells and non-malignant fibroblasts (N1), and hemolytic activity

Code	*MDA-MB-231*	*HeLa*	*HepG2*	*A431*	*Panc-1*	*Hemolysis*[b]	*N1*
BPC88	31.2	22.5	32.5	28.0	32.5	33	42.0
BPC94	22.0	23.0	20.5	21.5	18.5	73	nd[c]
BPC96	40.0	24.5	34.5	35.0	51.0	32	39.0
BPC98	40.7	38.5	44.0	47.5	44.5	36	58.5
BPC184	32.2	30.5	42.2	24.5	41.5	89	nd
BPC194	32.5	29.5	46.0	50.0	40.0	17	56.5
BPC198	53.2	35.0	>60	49.5	57.5	14	7.5
BPC202	40.5	54.0	46.0	35.5	43.5	2	nd

[a]*Cells were treated for 48 h. Cytotoxicity (μM) was determined using the MTT assay*
[b]*Percentage of erythrocytes hemolysis at 375 μM*
[c]*Not determined*

Peptide BPC96 was selected to study its ability to synergize with cisplatin in HeLa cells. These cells were co-treated for 48 h with different concentrations of BPC96 (5-30 μM) along with a fixed cisplatin dose (1.5, 2.5, 4.5, and 6.5 μM). A strong synergistic cytotoxicity in all cisplatin concentrations assayed was observed. Interestingly, this synergistic effect was even significant when the lowest BPC96 concentration tested (5 μM) was combined with the lowest cisplatin dose assayed (1.5 μM). The lethality of HeLa cells treated with 5 μM BPC96 or with 1.5 μM cisplatin was 8% and 5%, respectively, while lethality of HeLa cells co-treated with 1.5 μM cisplatin plus 5 μM BPC96 increased to 25%. Analysis by the isobole method showed a median interaction index value of 0.74, indicating a marked synergistic interaction.

Acknowledgments
Financial support was provided by grant from the University of Girona (Grant for R+D Projects on Health Sciences). We are also grateful to the Serveis Tècnics de Recerca of the University of Girona for their support with the mass spectrometry analysis. We acknowledge the Banc de Sang i Teixits of Josep Trueta Hospital of Girona for supplying us the human serum and to Girona Division of Catalan Institute of Oncology Hospital Pharmacy for providing us the cisplatin.

References

1. Hoskin, D.W., Ramamoorthy, A. *Biochim. Biophys. Acta* **1778**, 357-357 (2008).
2. Leuschner, C., Hansel, W. *Curr. Pharm. Design* **10**, 2299-2310 (2004).
3. Mader, J.S., Hoskin, D.W. *Expert Opin. Investig. Drugs* **15**, 933-946 (2006).
4. Monroc, S., Badosa, E., Besalú, E., Planas, M., Bardají, E., Montesinos, E., Feliu, L. *Peptides* **27**, 2575-2584 (2006).

Proceedings of the 31st European Peptide Symposium
Michal Lebl, Morten Meldal, Knud J. Jensen, Thomas Hoeg-Jensen (Editors)
European Peptide Society, 2010

Synthesis of Tacrine Analogues Comprising a Peptide Moiety

Dantcho L. Danalev[1], Lyubomir T. Vezenkov[1], and Nikolay Vassilev[2]
[1]University of Chemical Technology and Metallurgy, Department of Organic Chemistry, Sofia, Bulgaria, dancho_danalev@yahoo.com; [2]Institute of Organic Chemistry, Bulgarian Academy of Sciences, Sofia, Bulgaria

Introduction

Alzheimer's disease (AD) is a neurodegenerative illness, which affects millions of people worldwide. According to World Health Organization around 26.6 million people worldwide had AD in 2006. As of September 2009, this number is reported to be 35 million-plus worldwide. Following the dynamic development of the disease this number may quadruple by 2050.

AD is characterized by progressive dementia, loss of memory, intellectual, speech and brain disturbances and inevitably leads to complete personality decay and a lethal outcome. The cause and progression of AD are not well understood. In recent years research has been focused on AD to clarify the mechanisms of development of the disease and to establish the reasons for its occurrence. Designating neuropathological lesions associated with all forms of AD are senile plaques (SPs), and amyloid angiopathy as well as neurofibril tangles (NFTs).

Today a most useful approach for the treatment of AD in a medical practice is to restore the level of acetylcholine by inhibiting AChE with reversible inhibitors [1]. Few of these inhibitors may pass into the brain and remain effective without serious side effects [2]. There are significant differences in the mechanisms of action of various cholinesterase inhibitors [3]. As of 2008, the cholinesterase inhibitors approved for the management of AD symptoms are donepezil (brand name Aricept), galantamine (Razadyne), and rivastigmine (branded as Exelon and Exelon Patch).

Clinical trials have shown that acetylcholinesterase inhibitors as tacrine (1,2,3,4-tetrahydro-9-akridinamin) and physostigmine ((3aS-cis)-1,2,3,3a,8,8a-hexahydro-1,3a,8-trimetilpirolo[2,3-b]indole-5-ol methylcarbamate (ester)) effectively improve the memory of some patients [1,2]. Tacrine, although weaker than physostigmine, is more useful in the treatment of AD. Its uses lead to improvement in orientation, the total assessment for learning and testing, but just like physostigmine it causes side effects [2]. Unfortunately, the use of tacrine is limited by poor oral bioavailability, the necessity for four-times daily dosing, and considerable adverse drug reactions (including nausea, diarrhea, urinary incontinence and hepatotoxicity) such that few patients could tolerate therapeutic doses [4].

Results and Discussion

Herein, we report for the synthesis of a series of hybrid analogs of tacrine molecule and peptide fragments (Figure 1). This is aimed at obtaining the hybrid molecules with combined pharmacological effect, acetylcholinesterase inhibitory activity due to the molecule of tacrine and γ-secretase inhibitory activity due to the peptide fragment. Additionally, we tried to reduce the high toxicity of some tacrine analogues, well known from the literature, using peptide fragments. Moreover, a series of analogues containing a "spacer" of 6-aminohexanoic acid between two active parts of hybrid molecules was synthesized.

Taking into account our previous experience with the synthesis of hybrid analogues of the acetylcholinesterase inhibitor, based on galanthamine molecule [5], we used peptide analogues of 3,5-dichlorophenylalanine with proven γ-secretase inhibitory activity [6] (Figure 2).

In addition, for the purposes of our study, a residue of 6-aminohexanoic acid methyl ester was linked to peptide derivatives of *N*-(3,5-dichlorophenyl)-D, L-alanine, the resulting esters were hydrolyzed using 2N NaOH to corresponding free acids with the general formula presented in Figure 3. The structure of final hybrid molecules comprising linker of 6-aminohexanoic acid is presented in Figure 4.

All compound structures were proven with ^{1}H, ^{13}C and 2D NMR recorded on Avance AV II+ spectrometer at 600.13 MHz for ^{1}H and $CDCl_3$ as solvent. The reaction progress was monitored on TLC using the following systems 3:1:1 (n-BuOH:AcOH:H_2O) for esters and 8:2 or 1:1 (ethylacetate:hexane) for all other compounds. The reactions of hydrolysis of

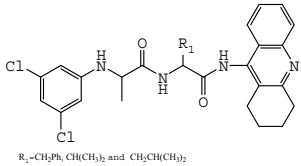

Fig. 1. Structure of peptide fragment linked to tacrine molecule.

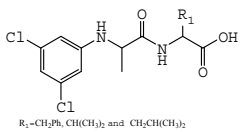

Fig. 2. Structure of peptide fragment synthesized.

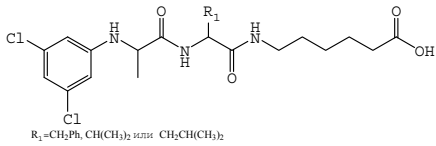

Fig. 3. Structure of peptide fragments linked to 6-aminohexanoic acid.

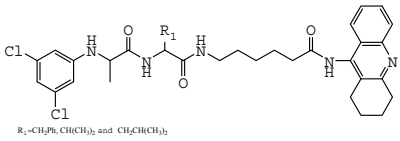

Fig. 4. Hybrid structures comprising 6-aminohexanoic acid linker.

methyl esters of 6-aminohexanoic acid linkers were monitored by means of IR spectroscopy (KBr pills, FT-IR sPerkin-Elmer 1600 Series spectrophotometer). All final compounds were purified using silica gel flash chromatography using the same systems as those applied for TLC monitoring.

A series of coupling reagents (TCTU, TBTU, DCC and *N*-cyclohexyl-*N*-[β-(*N*-methylmorpholino)-ethyl-]carbodiimide) were studied in order to obtain the best results according to yields and purity of final products. Commensurate and best results were obtained using TCTU and *N*-cyclohexyl-*N*-[β-(*N*-methylmorpholino)-ethyl-]carbodiimide.

A kinetic investigations according to AChE et BuChE and biological trials are in progress.

Acknowledgments

We would like to thank for a financial support of National Research Fund of Bulgaria, Contract MU-FS-03.

References

1. Mary, A., Renko, D.Z., Guillou, C., Thal, C. *Bioorg. Med. Chem.* **6**, 1835 (1998).
2. Han, S.Y., Sweeney, J.E., Bachman, E.S., Schweiger, E.J., Forloni, G., Coyle, J.T., Davis, B.M., Joullie, M.M. *Eur. J. Med. Chem.* **27**, 673 (1992).
3. Carroll, P., Furst, G.T., Han, S.Y., Joullie, M.M. *Bull. Soc. Chim. Fr.* **127**, 769 (1990).
4. Sweetman, S., Martindale, (Eds.) *The complete drug reference*, 34th ed. London: Pharmaceutical Press, 2004.
5. Vezenkov, L., Georgieva, M., Danalev, D., Ivanov, Tch., Ivanova, G. *Protein & Peptide Lett.* **16**, 1024-1028 (2009).
6. Dovey, H.F., et al. *J. Neurochem.* **76**, 173-181 (2001).

Proceedings of the 31st European Peptide Symposium
Michal Lebl, Morten Meldal, Knud J. Jensen, Thomas Hoeg-Jensen (Editors)
European Peptide Society, 2010

Inhibition of Amyloid Formation in Model Peptides

Enrico Brandenburg[1], Hans v. Berlepsch[2], and Beate Koksch[1]
[1]Organische Chemie, Institut für Chemie und Biochemie, Freie Universität Berlin, Takustraße 3, 14195, Berlin, Germany; [2]Forschungszentrum für Elektronenmikroskopie, Institut für Chemie und Biochemie, Freie Universität Berlin, Fabeckstraße 36a, 14195, Berlin, Germany

Introduction

Many neurodegenerative diseases such as Alzheimer's disease, type II diabetes, Parkinson's disease and Creutzfeldt-Jacob disease, are associated with failure of a peptide or protein to adopt, or remain in, its functional conformational state. Often, these undergo a conformational change from the native and mainly unfolded or particularly helically folded state into β-sheet rich, insoluble and fibrillar assemblies, that have a characteristic cross-β structure.

We present the inhibition of amyloid formation in two *de novo* designed model peptides by a third *de novo* designed α-helical ideal coiled coil peptide. The design of all three peptides is based on the naturally occurring coiled coil folding motif in which a 26 residue primary sequence is characterized by a periodicity of seven residues (heptad repeat), commonly denoted *a* to *g* [1,2].

Results and Discussion

By introducing only a few changes to the primary sequence of an ideal coiled-coil model peptide we were able to access a subset of model peptides having dramatically different behaviours. Peptide A forms a stable coiled coil with itself at neutral pH and works as an inhibitor of conformational change. The incorporation of three valine residues as β-sheet inducing features leads to peptide B which undergoes a conformational change at neutral pH from an α-helical coiled coil to a β-sheet rich amyloid-like fibril with a twisted ribbon-like morphology. In contrast, the additional presence of lysine residues in peptide C results in a large positively charged domain which destabilizes the α-helical coiled coil. This

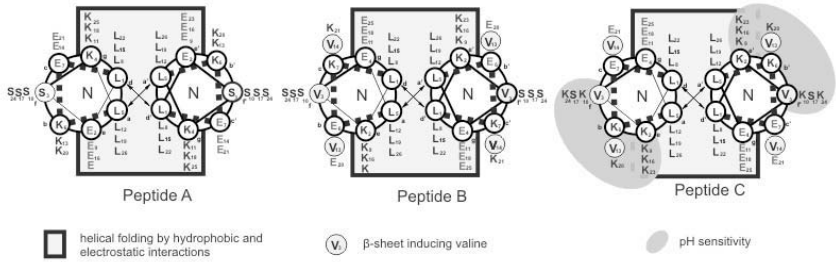

Fig. 1. Helical wheel diagram of the model peptides A, B and C.

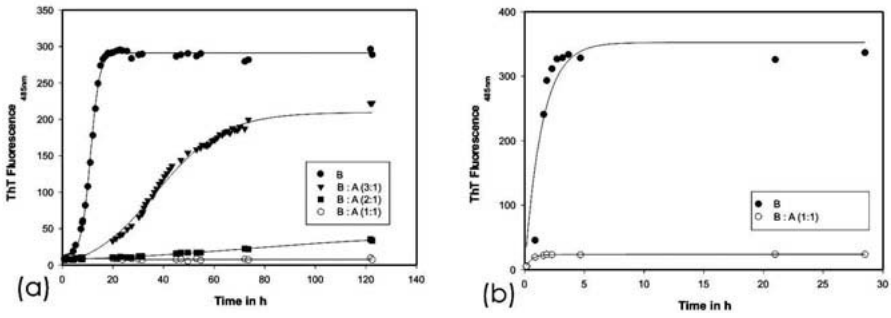

Fig. 2. (a) ThT assay of non-seeded peptide B and (b) seeded peptide B at pH 7.4 after different incubation times and for different equivalents of A (100μM B, 10μM ThT).

peptide also undergoes a conformational change at acidic pH from random coil to β-sheet rich amyloid-like fibrils with ribbon-like and tubular morphology [3] (Figure 1).

Conformational change and fibril formation of the pure peptides B and C, as well as the inhibition of amyloid formation in the presence of model peptide A, were studied by circular dichroism (CD) spectroscopy, time-dependent fluorescence of Thioflavin T (ThT) (Figure 2) or NIAD-4 (Figure 3), transmission-electron microscopy (TEM) and wide-angle X-ray scattering (WAXS), analytical ultracentrifugation (AUC) and size-exclusion chromatography (SEC). The data show a nucleus-dependent growth of amyloid-like fibrils for both pure amyloid forming model peptides and a clear inhibition of fibril formation in both amyloid forming model peptides in the presence of the inhibitor peptide through the formation of soluble α-helical structures in case of peptide B and helical fibers in case of peptide C.

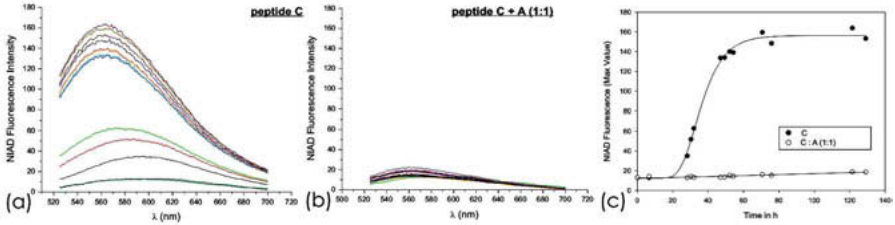

Fig. 3. (a) NIAD-4 assay of peptide C at pH 4 after different incubation times,(b) in the presence of one equivalent of A (100μM) and (c) maximum fluorescence intensities as a function of time (100μM A, 20μM NIAD-4, 10mM acetate buffer, pH 4).

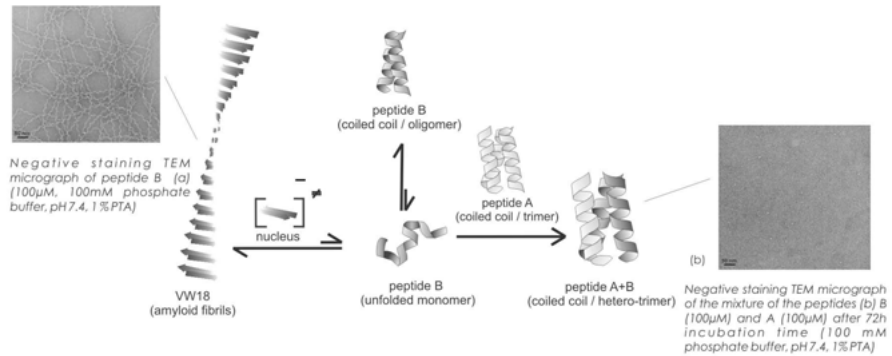

Fig. 4. Concept of the inhibitory effect of the ideal coiled coil peptide.

These results support the conclusion that the inhibition of amyloid fibril formation in peptides B and C is due to the formation of heteromeric coiled coil oligomers [4]. Evidently, the amyloidogenic target peptide becomes engaged in a stable helical arrangement when the ideal helical coiled coil peptide A is present during structure formation. Moreover, the ideal coiled coil model peptide is able to disassemble amyloid-like fibrils once they have already formed (data not shown). Hence, the present studies suggest that stabilization of the helical conformation through the formation of stable coassemblies could be a promising approach to preventing an amyloidogenic peptide from converting into the potentially cytotoxic state.

References

1. Pagel, K., et al. *J. Am. Chem. Soc*. 2196-2197 (2006).
2. Pagel, K., Koksch, B. *Curr. Opin. Chem. Biol.* **12**, 730-739 (2008).
3. Pagel, K., et al. *Chem. Eur. J.* 11442-11451 (2008).
4. Pagel, K., Vagt, T., Koksch, B. *Org. Biomol. Chem.* 3843-3850 (2005).

Proceedings of the 31st European Peptide Symposium
Michal Lebl, Morten Meldal, Knud J. Jensen, Thomas Hoeg-Jensen (Editors)
European Peptide Society, 2010

Synthesis and *in vitro* Characterization of New, Potent and Selective Oxytocin Receptor Agonists

Kazimierz Wiśniewski, Robert Galyean, Claudio D. Schteingart, Hiroe Tariga, Glenn Croston, Sudarkodi Alagarsamy, and Pierre J.-M. Rivière

Ferring Research Institute Inc., 4245 Sorrento Valley Boulevard, San Diego, CA, 92121, U.S.A.

Introduction

Oxytocin (OT, **1**) exerts its numerous biological functions by interacting with oxytocin receptors (OTR) located in the periphery (uterine contractions, milk ejection) and in the CNS (social and maternal behavior) [1]. OT is widely used as a labor-inducing agent [2] and, in a few markets, for lactation support in term mothers. Substantial research has been focused on identifying OTR antagonists suitable for treatment of premature labor [3], while efforts to design new OTR agonists have been relatively sparse. Side effects associated with the intravenous or intranasal administration of OT are well described in the literature and are attributed to lack of selectivity versus related receptors such as the V_2R, which may result in hyponatremia [4]. Therefore, the identification of oxytocin agonists that selectively activate the OTR could be therapeutically useful and free of these dose-limiting side effects.

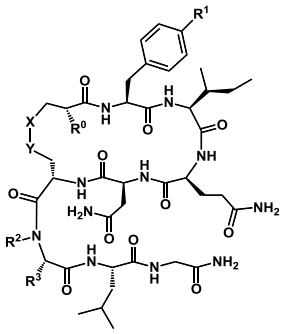

Fig. 1. Structure of OT analogues synthesized in this study.

The biological activity of the OT molecule has been shown to be very sensitive to changes in position 7. OT analogs with Gly^7 or Sar^7 have shown an improved selectivity profile versus the related vasopressin receptors [5] whereas other modifications in position 7 [6] resulted in compounds with different degrees of antagonistic activity.

Here we report the synthesis and *in vitro* evaluation of a series of OT agonists with N-alkylglycine residues ($-NR^2-CH_2-CO-$) in position 7 as the key modification (Figure 1). All new compounds were prepared as desamino analogs (R^0 = H) containing either an unaltered disulfide bridge or its monocarba modifications, and some compounds were also modified in position 2 with Phe.

Results and Discussion

The linear peptides were synthesized by standard SPPS methods using the Fmoc strategy. The N-alkylglycine residues in position 7 were introduced by a two step procedure comprising the acylation of the resin-bound C-terminal dipeptide with bromoacetic acid followed by a treatment with an appropriate primary amine. Several Fmoc-N-alkylglycines were also prepared separately by a modified literature procedure [7] and used in SPPS. The linear peptides were cleaved from the resin and cyclized in solution and purified by preparative HPLC.

The compounds were tested in *in vitro* functional assays for their agonistic potency and efficacy at the OTR and for the selectivity versus the related vasopressin receptors (Table 1). While the natural ligand OT (**1**) lacks OTR specificity, carbetocin (carba-1-[$Tyr(Me)^2$]dOT) **2**, clinically used for prevention of postpartum bleeding [8], is fairly selective versus both the hV_2R (selectivity ratio of 240) and the $V_{1a}R$. To improve the selectivity profile of **2**, a substituent in position 4 of the pyrrolidine ring of the Pro^7 residue was introduced. The modification led to compound **3** with selectivity versus hV_2R of 700. Analogue **4** in which the Pro residue was replaced with Gly (R^2 = R^3 = H) showed further improvement in V_2R selectivity as compared to **2**. That result prompted us to investigate the position 7 open ring analogues in which the Pro^7 residue was replaced with a variety of N-alkylglycines. Compounds **5-22** were prepared with the disulfide bridge or its monocarba modification. The Tyr^2 analogues **8** (R^2 = 3-MeBzl), **12** (R^2 = 4-FBzl) and **22** (R^2 = 3-

Table 1. Structure and in vitro profile of analogues 1-22

Analogue	Structure[a]					In vitro potency, EC_{50} (nM) at a receptor			Selectivity vs. receptor[b]	
	R^1	R^2	R^3	X	Y	hOT	hV_2	hV_{1a}	hV_2	hV_{1a}
1	OH	-$(CH_2)_3$-		S	S	2.3	7.3	10	3	4
2	OMe	-$(CH_2)_3$-		CH_2	S	0.70	170	41[c]	240	58[c]
3	OMe	-CH_2-CH(OMe)-CH_2-		CH_2	S	0.98	690	>10000[d]	700	>10000
4	OMe	H	H	CH_2	S	0.37	450	>1000[e]	1200	>2700
5	OH	n-Bu	H	S	S	0.06	35	>10000[d]	580	>160000
6	OH	n-Bu	H	CH_2	S	0.12	73	>10000[d]	600	>83000
7	H	n-Bu	H	CH_2	S	0.23	2000	>10000[d]	8600	>43000
8	OH	3-MeBzl	H	S	S	0.01	30	>10000[d]	3000	>1000000
9	OH	3-MeBzl	H	CH_2	S	0.08	210	>10000[d]	2600	>120000
10	OH	3-MeBzl	H	S	CH_2	0.02	55	71	2700	3500
11	H	3-MeBzl	H	S	CH_2	0.56	1600	>10000[d]	2800	>17000
12	OH	4-FBzl	H	S	S	0.01	82	>10000[d]	8200	>1000000
13	OH	4-FBzl	H	CH_2	S	0.08	330	>10000[d]	4100	>120000
14	OH	4-FBzl	H	S	CH_2	0.04	140	>10000[d]	3500	>250000
15	H	4-FBzl	H	S	CH_2	0.23	1400	>10000[d]	6000	>43000
16	OH	2-MeOEt	H	S	S	0.03	80	>10000[d]	2600	>330000
17	OH	2-MeOEt	H	CH_2	S	0.11	70	>10000[d]	630	>90000
18	H	2-MeOEt	H	CH_2	S	0.96	1100	>10000[d]	1100	>10000
19	H	2-MeOEt	H	S	CH_2	0.85	1300	>10000[d]	1500	>11000
20	OH	Bzl	H	CH_2	S	0.04	140	>10000[d]	3500	>250000
21	OH	2-PhEt	H	CH_2	S	0.04	160	>10000[d]	4000	>250000
22	OH	3-HOPr	H	CH_2	S	0.01	500	>10000[d]	50000	>1000000

*[a] For compound **1** R^0 is NH_2 and for all other compounds is H; [b] Selectivity ratios are rounded down to the nearest values with two significant figures; [c] partial agonist at the $hV_{1a}R$; [d] highest concentration tested 10000 – nM; [e] highest concentration tested- 1000 nM*

HOPr) showed a 70-fold gain in *in vitro* potency as compared to **2**. The analogues where R^2 was an arylalkyl (**8-14, 20, 21**) or hydroxyalkyl (**22**) displayed much desired improvement in selectivity versus the hV_2R. The Phe^2 compounds **7**, **11**, **15**, **18**, **19** (R^1 = H) turned out to be less potent as OT agonists and showed lower potencies at the hV_2R than their Tyr^2 counterparts thus resulting in similar selectivity profiles of the two series. All compounds **3-22** displayed excellent selectivity versus hV_{1a} and hV_{1b} (data not shown) receptors with selectivity ratios exceeding 1000. The alterations to the disulfide bridge did not have a significant impact on the overall *in vitro* pharmacological profile of these analogs.

Based on overall favorable properties, compound **13**, carba-1-[4-FBzlGly^7]dOT, has been selected as a clinical candidate for use in peripheral indications including lactation. In addition, recent reports of CNS activities of oxytocin and oxytocin analogues, suggest that compound **13** could also be used to treat multiple central disorders.

References

1. Gimpl, G., Fahrenholtz, F. *Physiol. Rev*. **81**, 629-683 (2001).
2. Smith, J.G., Merrill, D.C. *Clin. Obstet. Gynecol.* **49**, 594-608 (2006).
3. Allen, M.J., Livermore, D.G.H., Mordaunt, J.E. *Prog. Med. Chem.* **44**, 331-373 (2006).
4. Morgan, D.B., et al. *Br. J. Obstet. Gynaecol.* **84**, 6-12 (1977).
5. Grzonka, Z., et al. *J. Med. Chem.* **26**, 555-559 (1983).
6. Fragiadaki, M., et al. *Eur. J. Med. Chem.* **42**, 799-806 (2007).
7. Weber, D., et al. *J. Med. Chem.* **46**, 1918-1930 (2003).
8. Peters, N.C., Duvekot, J. *J. Obstet. Gynecol. Surv.* **64**, 129-135 (2009).

Proceedings of the 31st European Peptide Symposium
Michal Lebl, Morten Meldal, Knud J. Jensen, Thomas Hoeg-Jensen (Editors)
European Peptide Society, 2010

Amidine Neighbouring-Group Effect on the Stability of B9870, a Highly Potent Anti-Cancer Bradykinin B1/B2 Antagonist Peptide Dimer

Lajos Gera[1,3], Richard Duke[2,3], Daniel C. Chan[2,3], Paul A. Bunn, Jr.[2,3], Robert S. Hodges[1], John M. Stewart[1,3], and James Blodgett[4]

[1]Department of Biochemistry and Molecular Genetics, University of Colorado Denver, Aurora, CO, 80045, U.S.A.; [2]Cancer Center, University of Colorado Denver, Aurora, CO, 80045, U.S.A.; [3]ApopLogic Pharmaceuticals, Inc., Aurora, CO, 80010, U.S.A.; [4]Indianapolis, IN, 46236, U.S.A.

Introduction

Bradykinin (BK) is a biologically active nonapeptide that plays an important role in many physiological processes, such as cardiovascular diseases, septic shock, pain, chronic and acute inflammation, and cancer. The first full-chain, highly enzyme-resistant BK antagonist which showed high affinity at both B1 and B2 receptors, B9430 (DArg-Arg-Pro-Hyp-Gly-Igl-Ser-DIgl-Oic-Arg, where Hyp is *trans*-4-hydroxyproline, Igl is α-(2-indanyl)glycine and Oic is octahydroindole-2-carboxylic acid), was developed more than a decade ago [1]. Since BK is an autocrine growth factor for many types of cancer, notably of lung and prostate, it was logical to try the potent BK antagonist B9430 as a growth inhibitor for cancer. Disappointingly, the B9430 potent BK antagonist peptide monomer was almost ineffective against cancer but the N-terminal suberimidyl-crosslinked B9430 dimer, known as B9870 (later also named B201, CU201, NSC 710295, and Breceptin), was found to be an extremely potent anti-cancer agent. The synthesis, stability, and the anti-cancer activity of B9870 will be discussed in this article.

Results and Discussion

The synthesis of the monomer peptide B9430 was accomplished *via* standard solid-phase methodology on Merrifield resin using Boc-chemistry. The dimerization of B9430 was independently conceived and carried out by Dr. Gera [2] (notwithstanding other claims [3]) and involved the formation of the amidine-structure dimer with dimethyl suberimidate. This approach to the dimerization was based on Gera's previous work involving amidine chemistry [4]. The dimerization of B9430 with thio-suberimidates increases the yield significantly (Gera, et al., unpublished results). B10346 [Sub-$(B9430)_2$, Sub: suberyl), the bis-amide analog of dimer B9870, was prepared with the dimerization on the resin with suberyl dichloride. The peptides were purified by preparative RP-HPLC and characterized by analytical RP-HPLC, TLC, mass spectroscopy and amino acid analysis. BOP-HOBt was used for the coupling of amino acids. The stability study was carried out by RP-HPLC and the degradation products were characterized by LC/MS. The stability of B9870 (CU201) has also been studied at the National Cancer Institute [5]. The bis-amidine dimer, B9870 is highly stable when stored frozen as a dry powder. It is also highly stable when reconstituted in physiological saline and stored in the refrigerator (4ºC; 5% loss at 4 weeks). The compound undergoes degradation in saline solution buffered with phosphate (pH 7.4) to B10660 (DArg-Suim-B9430, Suim: suberimidyl; an alternative, isomeric ring-opened product is also possible but B10660 appears more likely) and B9598 (des-$DArg^0$-B9430) *via* amidine group participation according to the proposed mechanism (Figure 1). Other degradation products also observed were the hemi-amide dimer (B10658), bis-amide dimer (B10346) and 7-mer monomer peptide (B9924, Hyp-Gly-Igl-Ser-DIgl-Oic-Arg), the latter possibly formed *via* N-terminal diketopiperazine formation from B9598 by a mechanism for which precedents exist in the literature [6]. B10346 bis-amide peptide is stable under physiological conditions, where B9870 undergoes degradation. Our potent BK antagonists were routinely screened [7] for anti-cancer activity. The compounds, including the metabolism-resistant, highly potent BK antagonist B9430, blocked Ca^{2+} mobilization by bradykinin *in vitro* but did not show significant growth inhibition of lung or prostate cancer cells (Table 1). However, B9870, the suberimidyl dimer of B9430 monomer BK antagonist was found to have high anti-cancer activity *in vitro* and *in vivo* in nude mouse xenografts [8]. Concerning the pH-sensitive N-terminal amidine structure, its inclusion in B9870 was

Table1. Structures and activities of selected BK antagonist peptides

Number	*Structure*	*Biological activity*				
		GPI[a] *pA_2*	*SCLC*[b] *in vitro*	*SHP-77*[c] *in vivo (%)*	*A-549*[c,d] *in vivo (%)*	*PC3*[c,e] *in vivo (%)*
B9430		8.2	120	15	42	Not active
B9870	Suim-(B9430)2	8.4	0.15	65	58	78
B10346	Sub-(B9430)2	--	6	--	40	--

[a]*Bradykinin antagonist activity (pA_2) on isolated guinea pig ileum (GPI)*
[b]*IC_{50} (μM) for cytotoxicity by MTT test for small cell lung cancer (SCLC) in vitro with cell line SHP-77*
[c]*Per cent inhibition of growth of xenografts in nude mice. Compounds were injected i.p. at 5 mg/kg/day*
[d]*Non-small cell lung cancer (NSCLC) cell line A-549*
[e]*Prostate cancer (PC3)*

intended to create a potential anti-cancer bradykinin-antagonist peptide dimer prodrug. Prodrugs of bioactive amidine compounds have been investigated and some have advanced into human clinical studies [9]. The stable bis-amide dimer, B10346, shows lower anti-cancer potency than B9870. It is not clear whether this is the result of the inability of the bis-amide to undergo the degradation reactions of B9870. Whether due to its prodrug nature, i.e., the degradation process producing active derivatives, or otherwise, B9870 is a potent anti-cancer agent. The precise role of the degradation process in this context is under investigation.

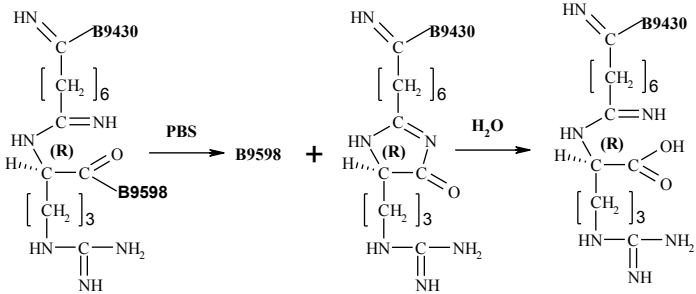

B9870 B10660

An IND application to test B9870 in small cell lung cancer was recently approved by the FDA and therefore the clinical trial can now proceed.

References

1. Gera, L., Stewart, J.M. *Immunopharmacol.* **33**, 174-177 (1996).
2. Gera, L., et al. *Immunopharmacol.* **33**, 178-182 (1996).
3. Chan, D.C., et al. *Drug Resist. Updates* **1**, 377-388 (1998).
4. Bernath, G., Toth, G., Fulop, F., Gondos, G., Gera, L. *J.C.S. Perkin1* 1765-1769 (1979).
5. Wang, J., et al. *J. Pharm. Biomed. Anal.* **51**, 824-833 (2010).
6. Straub, J.A., Akiyama, A., Parmar, P., Musso, G.F. *Pharmaceut. Res.* **12**, 305-308 (1995).
7. Chan, D.C., Gera, L., et al. *Immunopharmacol.* **33**, 201-204 (1996).
8. Chan, D.C., Gera, L., et al. *Clin. Cancer Res.* **8**, 1280-1287 (2002).
9. Maryanoff, B.E., et al. *Chem. Biol. Drug Des.* **68**, 29-36 (2006).

Proceedings of the 31st European Peptide Symposium
Michal Lebl, Morten Meldal, Knud J. Jensen, Thomas Hoeg-Jensen (Editors)
European Peptide Society, 2010

Synthesis and Biological Evaluation of Cytotoxic Peptide Conjugates Containing 5-Fluorouracil

Sergey V. Burov, Tatyana V. Yablokova, Maria V. Leko, Anton Yu. Alenko, and Marina Yu. Dorosh
Institute of Macromolecular Compounds, Russian Academy of Sciences, St. Petersburg, 199004, Russia

Introduction

The efficiency of conventional cancer chemotherapy is limited by the lack of drug selectivity and significant toxicity to normal cells. Conjugation of cytotoxic drugs to receptor-binding peptides is one of the promising approaches for their targeted delivery to cancer cells. 5-Fluorouracil (5-FU) is widely applied for the treatment of solid tumors, such as breast, colorectal, and gastric cancers. However, apart from well-known side effects, 5-FU undergoes rapid clearance in blood plasma and can not destroy the large number of malignant cells.

There are many 5-FU derivatives, described in the literature and protocols useful for its attachment to macromolecular carriers, including a very elegant approach, suggested by D.A. Putnam [1]. However, their practical utility for the synthesis of cytotoxic peptide analogues is still limited due to the insufficient stability or complexity of synthetic procedure.

Results and Discussion

As a promising candidate for attachment of cytotoxic agent to peptide carrier we have chosen 5-fluorouracil-1-acetic acid or 1-carboxymethyl-5-fluorouracil (CMFU), synthesized by M. Tada in 1975 as a result of 5-FU alkylation by chloroacetic acid [2]. This stable derivative possessed cytotoxic properties and now is widely applied for the conjugation with different natural compounds in order to improve its anticancer activity and selectivity of action.

In 1990 we described truncated GnRH analogues containing CMFU moiety [3]. Corresponding peptides were synthesized using CMFU-ONP derivative possessed very high activity in amino group acylation reaction. However, biological experiments revealed that antitumor action of tested analogues in vivo is relatively low due to the strong influence of cytotoxic moiety on their hormonal activity and binding to GnRH receptors.

Considering these data we synthesized a set of GnRH analogues (I)-(VIII) which differ by presence or absence of CMFU moiety, N-terminal modification and the structure of linker between peptide and cytotoxic agent (Figure 1).

Ac-Pro-D-Phe-Pro-Ser-Tyr-D-Lys-Leu-Arg-Pro-Gly-NH_2 (I)
Ac-Pro-D-Phe-Pro-Ser-Tyr-D-Lys(CMFU)-Leu-Arg-Pro-Gly-NH_2 (II)
Pam-Pro-D-Phe-Pro-Ser-Tyr-D-Lys-Leu-Arg-Pro-Gly-NH_2 (III)
Pam-Pro-D-Phe-Pro-Ser-Tyr-D-Lys(CMFU)-Leu-Arg-Pro-Gly-NH_2 (IV)
CMFU-Pro-D-Phe-Pro-Ser-Tyr-D-Lys(CMFU)-Leu-Arg-Pro-Gly-NH_2 (V)
pGlu-His-Trp-Ser-Tyr-D-Lys-Leu-Arg-Pro-Gly-NH_2 (VI)
pGlu-His-Trp-Ser-Tyr-D-Lys(CMFU)-Leu-Arg-Pro-Gly-NH_2 (VII)
pGlu-His-Trp-Ser-Tyr-D-Lys(X-CMFU)-Leu-Arg-Pro-Gly-NH_2 (VIII)
Lev-Arg-Gly-Asp-Phe-OH (IX)
Pyv-Arg-Gly-Asp-Phe-OH (X)
CMFU-X-Arg-Gly-Asp-Phe-OH (XI)

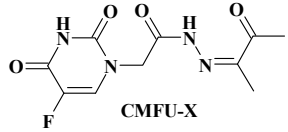

CMFU-X

Fig. 1. Synthesized GnRH analogs and model RGD peptides.

Table 1. Antitumor activity in vivo (prostate cancer model, ACI rats)

Peptide	*Dose (μg/kg)*	*Inhibition of tumor growth (%)*[a]
II	100	9
IV	10	67
V	10	45
Buserelin	100	63

[a] *29th day of treatment*

For the synthesis of cytotoxic peptide conjugates we applied both stable amide bond formation by means of CMFU-ONp derivative and hydrazone ligation using CMFU hydrazide. In the first case solid-phase conjugation was the method of choice for histidine containing peptides due to the side reaction of Ser and Tyr O-acylation, observed during the synthesis in solution.

In order to optimize the hydrazone formation conditions we prepared model RGD analogues containing reactive keto groups (Figure 1). Peptides (IX) and (X) were obtained as a result of N-terminal acylation by levulinic or pyruvic acid. In accordance with literature data it was shown that presence of ethanedithiol at the stage of final deprotection lead to the formation of dithioketal as the main side product. Triisopropylsilane should also be excluded from the cleavage cocktail due to its ability to reduce the carbonyl group. In the case of pyruvoyl peptide X RP-HPLC analysis of final product gave a broad peak due to the equilibrium between keto- and hydrate- forms [4].

At the stage of hydrazone formation, surprisingly, levuloyl peptide IX did not interact with CMFU hydrazide at all, both in water solution at different pH and in MeOH with catalytic amount of TFA. In contrast, for pyruvoyl derivative X under the same conditions, reaction was completed in 24 hr. Investigation of stability towards acid hydrolysis unexpectedly revealed that analog XI is completely stable at pH 5 and substantially hydrolyzed only at pH 3. Thus hydrazone bond should be intact at acidic endosomal pH and the only chance of CMFU release is enzymatic cleavage.

By using different 5-FU attachment technique we synthesised two GnRH analogues VII and VIII and investigated their cytotoxic activity *in vitro*. The biological experiments were done on GnRH receptor-positive human HepG2 cells. The comparison of cytotoxic properties revealed that peptide VII has at least the same activity as free CMFU, while compound VIII is slightly less active. Considering the number of synthetic stages and surprisingly high stability of corresponding hydrazone it seems that application of CMFU hydrazide has no evident advantages.

Biological experiments in vivo on prostate cancer model (Table 1) showed that cytotoxic GnRH conjugates significantly suppress tumor growth as compared to control group and parent compounds. Moreover, peptides V and VI were efficient at the dose of 10 μg/kg, while clinically applied anticancer GnRH analog buserelin has a similar effect only at the dose of 100 μg/kg. These data suggested the possibility of CMFU application for the synthesis of cytotoxic peptide conjugates useful for the suppression of tumor growth *in vivo*.

References

1. Putnam, D.A., Shiah, J.G., Kopecek, J. *Biochem. Pharmacol.* **52**, 957-962 (1996).
2. Tada, M. *Bull. Chem. Soc. Jpn.* **48,** 3427-3428 (1975).
3. Vlasov, G.P., Burov, S.V., Semko, T.V., Veselkina, O.S., Sepetov, N.F., Makusheva, V.P. *Peptides 1990* (*Proceedings of the 21th European Peptide Symposium)*, Escom, Leiden, 1991, p. 682.
4. Katayama, H., et al. *Tetrahedron Lett.* **50**, 818-821 (2009).

Proceedings of the 31st European Peptide Symposium
Michal Lebl, Morten Meldal, Knud J. Jensen, Thomas Hoeg-Jensen (Editors)
European Peptide Society, 2010

IMMUNOPEPdb - A Novel Immunomodulatory Peptides Database

Osmar N. SIlva[1,2], William F. Porto[1], Diego G. Gomes[1], Simoni S. Dias[1] and Octávio L. Franco[1,2]

[1]Centro de Analises Proteômicas e Bioquímicas, Universidade Católica de Brasília, Brasília, Brazil; [2]Programa de Pós-graduação em Ciências Biológicas (Imunologia/Genética e Biotecnologia), Universidade Federal de Juiz de Fora, Juiz de Fora, Minas Gerais, Brazil

Introduction

Immunomodulatory peptides are known for two common main effects: immunostimulants or immunosuppressants. The understanding of the mechanisms of action, their cognate

Figure 1. An overview of the organization of website.

properties and further adaptation for clinical use is a real challenge, once that literature in this specific field is recent and widely scarce. In order to support and improve the knowledge of immunomodulatory peptides, a novel and original IMMUNOPEPdb immunomodulatory peptide database was developed and here presented.

Methodology

To ensure the accuracy of the data deposits, all sequences were carefully analyzed such as the correct function assigned in databank, the presence of signal peptide in a Signal Peptide Database (SPdb) and also redundancy degree. IMMUNOPEPdb was developed with PHP (Hypertext Preprocessor) and relational database management system (RDBMS), MySQL, based on SQL (Structured Query Language). Database is monthly update by a semi-automatic procedure.

Results and Discussion

In Figure 1 can be viewed website organization. At date, host information detailed of 117 entries in which (Table 1).

Table 1. Major groups of organisms with sequences of peptides deposited in immunomodulatory peptide database.

Organisms	Number of peptides
Mammalian	74
Arthropoda	19
Amphibian	9
Fungi	6
Others	9
Total:	117

Information about peptides may be obtained by using keywords such as peptide name and molecular weight or by submission of a sequence previously determined as an immuno-modulatory peptide in common databanks. Due to the capability of these peptides in modulating innate immunity, IMMUNOPEPdb can be a powerful tool to development of a new therapeutic strategy combating infectious diseases and autoimmune disorders.

Due to the capability of these peptides in modulating innate immunity, IMMUNOPEPdb can be a powerful tool to development of a new therapeutic strategy in combating infectious diseases and autoimmune disorders.

Acknowledgments

We thank CAPES (Brazilian Council for Graduate Studies), CNPq (Brazilian Council for Science and Technology), and Catholic University of Brasília, Federal University of Juiz de Fora.

Proceedings of the 31st European Peptide Symposium
Michal Lebl, Morten Meldal, Knud J. Jensen, Thomas Hoeg-Jensen (Editors)
European Peptide Society, 2010

Delta-Sleep Inducing Peptide (DSIP) and Its Analogues: Studies On Their Therapeutic Potency

Inessa I. Mikhaleva[1*], Igor A. Prudchenko[1], Eugeniy S. Efremov[1], Ludmila V. Onoprienko[1], Leonid D. Chikin[1], Raisa I. Yakubovskaya[2], Elena P. Nemtsova[2], and Olga A. Bezborodova[2]

[1]Shemyakin-Ovchinnikov Institute of Bioorganic Chemistry, Russian Academy of Sciences, Moscow, 117997, Russia; [2]Gertsen Scientific-Research Cancer Institute, Moscow, 125284, Russia

Introduction

At present, one of the topical lines of development of the modern oncology is a search for ways to significant improvement of selectivity of therapeutic anti-tumor agents and decrease in toxicity of the anti-tumor therapy. In this connection we have undertaken the studies of delta-sleep inducing peptide (DSIP) [1] and its analogues as potent agents capable to mitigate some adverse effects of widely used cytostatic drugs. We have studied structure-functional peculiarities, biological properties, and mechanism of action of DSIP over a long period of time. As a result, pronounced stress-protective activity of this regulatory factor was revealed, and biochemical mechanisms of its realization are investigated [2-4]. Previously, we have detected the ability of DSIP to increase the anti-tumor resistance of animals under the conditions of inoculation of tumor cells under the background of stress and to inhibit dissemination (metastasis) of Lewis carcinoma after its surgical removal [5]. The DSIP was found capable to limit the spontaneous carcinogenesis and mutagenesis [6]. Results of the previous studies demonstrate that some of DSIP-related compounds might be promising for oncological practice, in particular, for possible inhibition of metastasis, decrease in the toxic effects of a cytostatic, and limitation of disorders of neuroendocrine status.

Results and Discussion

Detoxifying effects of DSIP and a number of its analogues were examined on models of toxicosis induced by cytostatic agents cisplatin and cyclophosphan. The animals (the BDF1 female mice) were intravenously injected one time with cisplatin or cyclophosphan at doses of 15 mg/kg or 450 mg/kg, respectively. The animal death from the acute cisplatin-induced toxicity was observed. The tested peptides (P1-P10 and DSIP) were intravenously administered at single doses of 50 and 250 μg/kg respectively during four days (the course doses of 200 and 1000 μg/kg, respectively) after the cisplatin injection. The animal death from the acute cisplatin-induced toxicity was observed, and hematolytic and biochemical parameters of blood of the survived animals were evaluated. DSIP and its P1, P2, P5 and P7 analogues facilitated a decrease in the cisplatin toxicity, in particular, they decreased the animal mortality in 1,5 times (Figure 1). The P1 peptide exhibited the most positive effect; its four-times administration at a course dose of 200 μg/kg 24 h after the cisplatin introduction resulted in the significant (up to 17%) decrease in the mortality, whereas the animal death in the control group was as high as 50-67%. DSIP was active as P1 only at course dose 1000 μg/kg.

Administration of the peptide facilitated the remarkable decrease in hepatotoxicity and nephrotoxicity of the cytostatic. Combinational administration of cisplatin with DSIP or its P1 analogue to the animals with transplanted Lewis lung carcinoma (LLC) did not abandon the therapeutic effect of cisplatin, but did not cause its increase as well. Only biologically insignificant decrease in the animal death from the acute toxicity of the cytostatic was observed on the model of toxicosis that was induced by the toxic dose of cyclophosphan.

Investigation of the influence of the peptides on the growth of the primary tumor and processes of metastasis of the Lewis lung carcinoma demonstrated that the peptides at the studied doses and chosen limited experimental protocol had no stimulating or inhibiting effect on the growth of the primary tumor and processes of metastasis (without the removal of the primary focus). Peptides were nontoxic towards organisms of the tumor-bearing animals. We have detected the dependence of these peptides protective effects on a type of

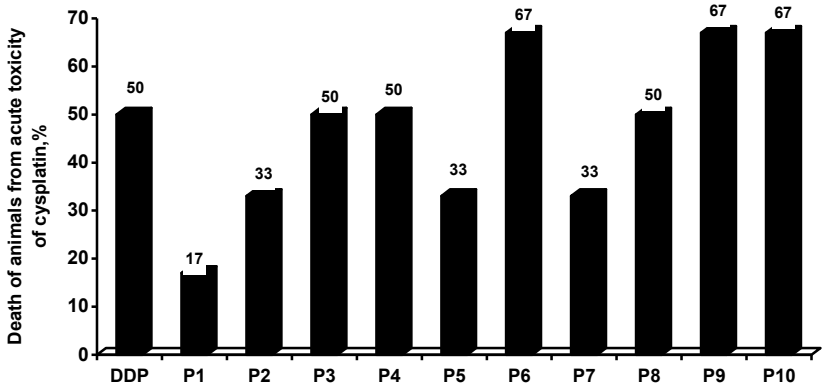

Fig. 1. Effect of DSIP analogues P 1-10 on the toxic action of cisplatin (DDP) at LD_{50} dose, n=6.

tested experimental protocol under varying the course doses of peptides, duration of treating, time intervals.

So, we have found that administration of DSIP and its active derivatives resulted in significant decrease in mortality of the animals after introduction of cisplatin in LD_{50} dose due to a decrease in hepatotoxicity and nephrotoxicity caused by cytostatic. The search for the most promising peptide and optimal exprimental scheme of its application is in progress.

Acknowledgments:
This study was supported by the Moscow City Government.

References

1. Graf, M., Kastin, A. *Peptides* **7**, 1165-1187 (1986).
2. Shustanova, T., Bondarenko, T., Milyutina, N., Mikhaleva, I. *Biokhimiya (Rus)* **66**, 632-639 (2001).
3. Khvatova, E., Samartzev, V., Zagoskin, P., Prudchenko, I., Mikhaleva, I. *Peptides* **24**, 307-311 (2003).
4. Koplik, E., et al. *Neuroscience and Behavioral Physiology* **38**, 953-957 (2008).
5. Shmal'ko, Iu., Mikhaleva, I. *Exp. Onkol*. **10**, 57-60 (1988).
6. Popovich, I., et al. *Mech. Ageing Dev.* **124**, 721-731 (2003).

Proceedings of the 31st European Peptide Symposium
Michal Lebl, Morten Meldal, Knud J. Jensen, Thomas Hoeg-Jensen (Editors)
European Peptide Society, 2010

Dual μ-/δ-Opioid Antagonist, H-Dmt-Tic-Lys-NH-CH_2-Ph: Potential Candidate for Management of Obesity, Diabetes and Osteoporosis

Lawrence H. Lazarus[1], Gianfranco Balboni[2], Severo Salvadori[3], and Ewa D. Marczak[1]

[1]National Institute of Environmental Health Sciences, Research Triangle Park, NC, 27709, U.S.A., [2]Department of Toxicology and Pharmacology, University of Cagliari, Cagliari, I-09124, Italy, [3]Department of Pharmaceutical Science and Biotechnology Center, University of Ferrara, Ferrara, I-44100, Italy

Introduction

Opioid antagonists represent an important class of synthetic drugs affecting neural reward- and homeostatic mechanisms. Reward mechanisms include craving, addiction and compulsive behaviors, such as excessive consumption of high caloric foods leading to obesity, and entail interaction with the μ-opioid receptor [1]. The potential amelioration of obesity by selective opioid antagonists could be a relevant approach to curtail these major public health issues. Whereas obesity exerts an economic toll and severe medical and social consequences, prevention remains limited; many treatments are merely palliative and rates of recidivism are high. While osteoporosis affects >90% of postmenopausal women worldwide, patients taking anti-pain medication, particularly opiate-derivatives, have symptoms of osteoporosis and exhibit increased risk of bone fractures due to loss of bone mass [2,3]. This effect is related to a direct interaction of opioid agonists on osteoblasts to regulate bone mineral density (BMD). Therefore, an opioid antagonist that has the potential to simultaneously enhance osteoporosis and treat obesity exists.

We described the synthesis and pharmacological profile of a potent dual acting μ-/δ-antagonist (MZ-2, Figure 1) [4] that inhibited morphine antinociception, development of morphine tolerance [5], and decreased obese-related factors in ob/ob mice [6] and diet-induced obesity (DIO) mice [7]. MZ-2 portends to be a potential clinical candidate for management of obesity and related diseases, and the amelioration of osteoporosis.

Results and Discussion

Genetically obese mice (ob/ob) and wt lean controls were treated daily for 3 weeks with MZ-2 (po, 10 mg/kg), followed by recovery for 2 weeks; control groups consisting of ob/ob and wt animals received saline [6]. DIO mice were fed a high fat diet for 32 weeks before treating with saline or MZ-2 (10mg/kg/day via implanted mini-pumps) for 12 weeks [7]. During treatment, mice were kept in either sedentary or with access to exercise wheels. Voluntary exercise was recorded for the duration of the experiment by magnetic switches connected to the Vital View 3000 data acquisition system (Mini Mitter, Bend, OR, U.S.A.). Bone mineral density (BMD) and body fat content were assessed before treatment and at the end of experiment using PIXImus2 Mouse Densitometer (GE Medical Systems, Madison, WI, U.S.A.).

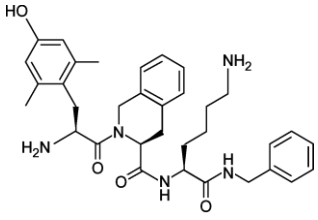

Fig. 1. Structure of MZ-2.

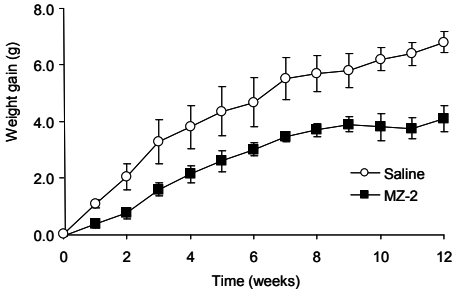

Fig. 2. Effect of MZ-2 or saline on body weight gain in sedentary DIO mice.

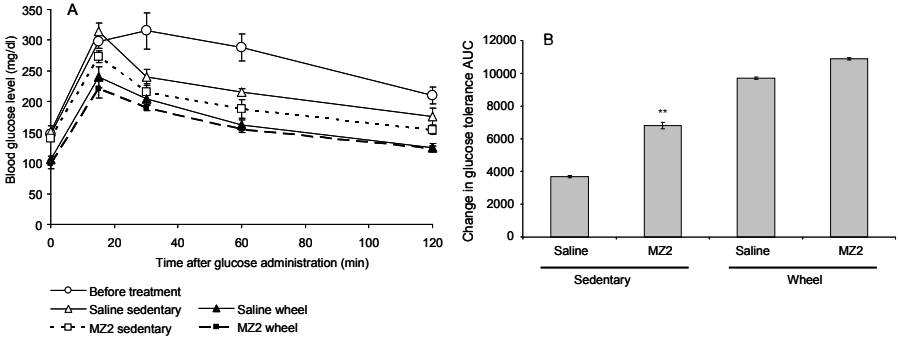

Fig. 3. Glucose tolerance in DIO mice before and after a 12-week treatment with MZ-2 or saline. (A) Blood glucose levels after oral administration of glucose (2 g/kg); (B) Change in glucose tolerance after 12 weeks of treatment.

Blood chemistry was determined at the end of the experiment in both animal models, while an oral glucose tolerance test was performed in DIO mice before and after treatment.

MZ-2 reduced body weight gain in sedentary ob/ob [6] and DIO mice (Figure 2) while it had no any effect on body weight gain in exercising mice [6,7]. MZ-2 decreased body fat content, insulin and glucose serum levels, and elevated the HDL/LDL ratio 70% in both obese animal models [6,7]. While saline treatment decreased glucose tolerance AUC in DIO mice, MZ-2 treatment resulted in a significant decrease ($P < 0.01$) (Figure 3). Exercise significantly decreased glucose tolerance AUC in comparison to sedentary mice treated with MZ-2 or saline. Although the difference was not statistically significant in comparison to saline, MZ-2 had an additive effect on decreasing glucose tolerance AUC (Figure 3). MZ-2 significantly decreased consumption of high fat diet in DIO mice and the standard diet in sedentary ob/ob mice [6]. MZ-2 stimulated voluntary running on activity wheels in both lean and obese (ob/ob, DIO) mice by 65-69% during the 12 hr dark period, which corresponds to their peak physical activity.

MZ-2 enhanced BMD *in vivo* and *in vitro* in lean and obese (ob/ob, DIO) animals [6,7]. In cell cultures of human osteoblast-like cells (MG-63), MZ-2 significantly elevated mineral nodule formation (31%). This was nearly twice as effective as the non-selective opiate antagonist naltrexone (17%), while the quintessential μ-agonist morphine inhibited mineral nodule formation (17%) [6]. Since patients taking opiates for pain medication exhibit an elevated risk of bone fractures due to loss of bone mass [2,3], the enhancement of BMD in ob/ob, DIO and lean mice with MZ-2 appears to be a direct effect of opioids on bone formation.

In summary, we provide experimental evidence that MZ-2, a potent dual μ-/δ-opioid antagonist, has a potential application in the clinical management of obesity, diabetes and osteoporosis.

Acknowledgments
These studies were supported in part by the University of Cagliari and the University of Ferrara, and in part by the Intramural Research Program by the NIH and NIEHS.

References
1. Bodnar, R.J. *Peptides* **30**, 2432-79 (2009).
2. Reid, I.R. *An. Endocrinol*. **67**, 125-129 (2006).
3. Greco, E.A., et al. *Int. J. Clin. Prac*. **64**, 817-820 (2010).
4. Balboni, G., et al. *J. Med. Chem*. **49**, 5610-5617 (2006).
5. Jinsmaa, Y., et al. *Pharmacol. Biochem. Behav*. **90**, 651-657 (2008).
6. Marczak, E.D., et al. *Eur. J. Pharmacol*. **616**, 115-121 (2009).
7. Marczak, E.D., et al. *in preparation*.

Proceedings of the 31st European Peptide Symposium
Michal Lebl, Morten Meldal, Knud J. Jensen, Thomas Hoeg-Jensen (Editors)
European Peptide Society, 2010

Molecular Modeling of the Interactions Between μ-Conotoxin SmIIIA and the Pore of Voltage-Gated Sodium Channel Subtypes $Na_V1.2$ and $Na_V1.4$

Pawel Gruszczynski[1,2,3], Doju Yoshikami[3], Rajmund Kazmierkiewicz[1], Min-Min Zhang[3], Baldomero M. Olivera[3], Grzegorz Bulaj[4], and Thomas E. Cheatham[4]

[1]Intercollegiate Faculty of Biotechnology, University of Gdansk and Medical University of Gdansk, Gdansk, 80-822, Poland; [2]Faculty of Chemistry, University of Gdansk, Gdansk, 80-952, Poland; [3]Departments of Biology; [4]Medicinal Chemistry, University of Utah, Salt Lake City, 84112, UT, U.S.A.

Introduction

μ-Conotoxin SmIIIA is a conopeptide derived from the venom of a marine snail *Conus stercusmuscarum*. This peptide was initially found to preferentially and irreversibly block TTX-resistant sodium currents in amphibian dorsal root ganglion neurons [1]. The combination of NMR and biochemical studies suggested that the last two intercystine loops were critical for the peptide's ability to block TTX-resistant sodium channels [2]. Recent experiments show that SmIIIA targets mammalian sodium channels, including two subtypes $Na_V1.2$ (neuronal subtype) and $Na_V1.4$ (skeletal muscle subtype) (Zhang, M.M., et al. manuscript in preparation). The block of these two subtypes by SmIIIA is significantly more potent, as compared to that for other two similar μ-conotoxins, namely SIIIA and KIIIA. Since all three peptides, SmIIIA, SIIIA and KIIIA share structural similarities of the last two intercystine, the functional differences provided an opportunity and rationale to explore how SmIIIA may interact with both isoforms of sodium channels. No modeling studies have been reported to-date on the molecular interactions between μ-conotoxins and neuronal subtypes of sodium channels.

The molecular structures of sodium channels, including $Na_V1.2$ and $Na_V1.4$, are still unknown, although several structural models have been proposed [3,4-9]. To characterize molecular interactions between SmIIIA and sodium channels, we employed a model of $Na_V1.4$ proposed by Lipkind and Fozzard [6] as a template to build a new model of $Na_V1.2$ using homology modeling method. Previously published studies on the docking skeletal muscle specific μ-conotoxin GIIIA into $Na_V1.4$ facilitated our efforts to evaluate toxin-channel complexes. Specific docking models were chosen based on known interactions of GIIIA [3,9-14], energy and clustering. Surprisingly, our molecular modeling and docking results suggest multiple binding modes of μ-conotoxin SmIIIA with $Na_V1.2$ and $Na_V1.4$. Our work provides a hypothesis that diverse modes of the molecular interactions between μ-conotoxins and the pore of the sodium channels subtypes may be present.

Results and Discussion

We present a series of structural binding models of μ-conotoxin SmIIIA into two channel subtypes $Na_V1.2$ and $Na_V1.4$. We also show three different types of binding modes for GIIIA docked to Nav1.4 channel. It is postulated that there are more than one binding mode for both of the conopeptides, but some of them are more preferred than the other. Our models might be useful to explain some difficult-to-interpret experimental data on the interactions between GIIIA and Nav1.4 and ravel that there is more than one binding model of the GIIIA with $Na_V1.4$, similarly to what we observed for the interactions between SmIIIA and each of the channels subtypes, $Na_V1.2$ and $Na_V1.4$.

There is no available experimental data, where mutant analysis was employed for exploring interactions between SmIIIA and both $Na_V1.2$ and $Na_V1.4$ sodium channels. Therefore our work provides a basis for such mutational studies. Here, we propose the residues that can be mutated in the SmIIIA μ-conotoxin to verify our models. Within each of our models, we find Arg13 as the key residue that block the sodium channel filter.

We hypothesize, that our results can be transferred to other μ-conotoxins. For example, in KIIIA Ala-walk experiment [15] shown that substitution of the key-residue

Lys7 by alanine residue did not affect the affinity of the KIIIA[K7A] to $Na_V1.2$. Surprisingly in the same experiment [15] the biggest effect from the mutation of the charged residues had R14A on both subtypes of examined sodium channels $Na_V1.2$ and $Na_V1.4$. The residue R14 is an analogical residue to R19 of GIIIA and R20 of SmIIIA. The binding modes of R19 and R20 were indicated for GIIIA and SmIIIA, respectively.

Acknowledgments
This work was supported in part by the NIH grants: R21 NS055845(GB), Program Project GM 48677 (BMO), and University of Gdansk fund DS/M021-4-0162-0.

References

1. West, P.J., et al. *Biochemistry* **41**, 15388-15393 (2002).
2. Keizer, D.W., et al. *J. Biol. Chem.* **278**, 46805-46813 (2003).
3. Tikhonov, D.B., et al. *Biophys. J.* **88**, 184-197 (2005).
4. Guy, H.R., Durrell, S.R. *Soc. of Gen. Phys.* **50**, 1-16 (1995).
5. Guy, H.R., Durell, S.R. *Ion Channels* **4**, 1-40 (1996).
6. Lipkind, G.M., Fozzard, H.A. *Biochemistry* **39**, 8161-8170 (2000).
7. Li, R.A., et al. *J. Biol. Chem.* **276**, 11072-11077 (2001).
8. Penzotti, L.J., et al. *Biophys. J.* **75**, 2647-2657 (2006).
9. Scheib, H., et al. *J. Mol. Model* **12**, 813-822 (2006).
10. Dudley, S.C., et al. *J. Gen. Physiol.* **116**, 679-690 (2000).
11. Hui, K., Lipkind, G., Fozzard, H.A., French, R.J. *J. Gen. Physiol.* **119**, 45-54 (2002).
12. Li, R.A., et al. *FEBS Lett.* **511**, 159-164 (2002).
13. Xue, T., Ennis, I.L., Sato K., French, R.J., Li, R.A. *Biophys. J.* **85**, 2299-2310 (2003).
14. Choudhary, G., et al. *Channels (Austin)* **1**, 344-352 (2007).
15. Zhang, M.M., et al. *J. Biol. Chem.* **282**, 30699-30706 (2007).

Proceedings of the 31st European Peptide Symposium
Michal Lebl, Morten Meldal, Knud J. Jensen, Thomas Hoeg-Jensen (Editors)
European Peptide Society, 2010

Bradykinin Analogues Acylated on Their N-Terminus

Małgorzata Śleszyńska[1], Dariusz Sobolewski[1], Tomasz H. Wierzba[2], Jiřina Slaninová[3], and Adam Prahl[1]

[1]Department of Chemistry, University of Gdańsk, 80-952, Gdańsk, Poland; [2]Department of Physiology, Medical Uniwersity of Gdańsk, 80-211, Gdańsk, Poland; [3]Institute of Organic Chemistry and Biochemistry, Academy of Sciences of the Czech Republic, Prague, Czech Republic

Introduction

Two receptors, B_1 and B_2, mediate biological activities of BK. These receptors belong to a G-protein-coupled family and their activation stimulates smooth muscle cells, sensory nerve endings, causes vasodilation and microvascular leakage and modulates the response of immunocompetent cells. There is also considerable evidence that BK contributes to the inflammatory responses [1,2]. Moreover, after injection to the skin, BK produces all of the basic signs of inflammation. Due to its ability to lower blood pressure, BK has been implicated in the pathogenesis of several shock syndromes. The classical B_2 receptors are of high affinity and they seem to require the full bradykinin sequence for effective activation. Accumulated evidence indicates that most of the clinically relevant effects of bradykinin are functions of B_2 receptors and this is the reason why research on their antagonists is a topic of great interest.

Our previous studies suggested that acylation of the *N*-terminus of several known B_2 antagonists with various kinds of bulky acyl groups consistently improved their antagonistic potency in rat blood pressure assay. On the other hand, our earlier observations also seemed to suggest that the effects of acylation on the contractility of isolated rat uterus depended substantially on the chemical character of the acyl group, as we observed that this modification might either change the range of antagonism or even transform it into agonism.

In some recent work we placed two of the previously used groups (9-acridine-carboxylic acid and 9-anthracenecarboxylic acid) in the *N*-terminus of the BK molecule [3]. Proposed modification transformed activity of analogues from agonistic to weak antagonistic in the rat blood pressure test and depressed its agonistic activity in the interaction with rat uterine receptors. It should be pointed out that these were the first reported B_2 blockers without any changes in main peptide chain.

Results and Discussion

In the current work we present some pharmacological properties of ten new analogues of bradykinin modified in the N-terminal part of the molecule (Arg-Pro-Pro-Gly-Phe-Ser-Pro-Phe-Arg) with a variety of acyl substituents. Of the many acylating agents, tested previously on B_2 receptor antagonists, the following residues were used: 1-adamantane-acetic acid (Aaa, ***1***), 1-adamantane-carboxylic acid (Aca, ***2***), 4-tert-butylbenzoic acid (t-Bba, ***4***), 4-aminobenzoic acid (Aba, ***3***), 12-aminododeca-noic acid (Adc, ***10***), succinic acid (Sua, ***8***), 4-hydroxybenzoic acid (***6***), 4-hydroxy-3-methoxy-benzoic acid (***5***), 3-(4-hydroxyphe-nyl)propionic acid (***9***) and 6-hydroxy-2-naphthoic acid (***7***) (Figure 1). All the peptides were obtained by the solid-phase method on a Symphony Multiple Peptide Synthesizer (Protein Technologies Inc., U.S.A.) using the Fmoc-strategy and starting from Fmoc-Arg(Pbf)-Wang resin (capacity 0.4 mmol/g, 25 μmol scale). The crude peptides were desalted on a Sephadex G-15 column, and purified by RP-HPLC. The purity of the peptides was checked using analytical HPLC. MALDI TOF mass spectrometry (molecular ion) was used to confirm the identity of the pure products. Biological activity of the compounds was assessed in the *in vitro* rat uterus test [4] and the *in vivo* rat blood pressure test [5]. Pharmacological data of analogues **I-X**

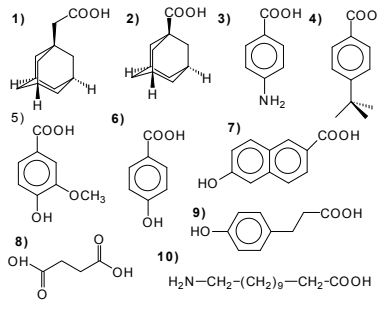

Fig. 1. Structures of acids used.

Table 1. Pharmacological properties of the new BK analogues

Analogue	Vasodepressor potency[a]			Uterotonic potency: % of activity of BK or pA_2[c]
	ED_{20} [μg/min]	ED_{50} [μg/min]	ED_{90} [μg/min]	
I	0.57±0.28	8.49±3.03	13.57±4.88	25%
II	4.37±1.99	336.95±132.14[b]	855.93±339.66[b]	2.4%
III	1.67±0.39	94.21±33.48	238.44±85.12	0.4%
IV	11.30±3.13	1041.71±310.00[b]	2648.05±794.33[b]	1%
V	1.55±0.35	23.71±10.63	56.26±23.85	43%
VI	6.02±1.50	364.06±87.29[b]	722.20±374.92[b]	0.5%
VII	2.52±1.18	80.47±21.01	201.98±52.47	2.8%
VIII	24.63±8.74	1896.96±883.13[b]	4815.70±2258.54[b]	3.8%
IX	1.79±0.52	48.85±15.75	122.21±40.25	24.5%
X	6.22±2.28	368.69±160.27[b]	933.81±409.19[b]	13.2%
[d]	0.43±0.03	3.19±0.33	52.60±10.59	pA_2 = 7.7±0.13

[a]ED_{20}, ED_{50} and ED_{90} represent doses of BK antagonist (μg/min) that inhibit the vasodepressor response to 250 ng of BK by 20, 50 and 90%, respectively; [b]Values ED_{50} or ED_{90} extrapolated from the dose-response curve; [c]Agonistic activity was calculated as percentage of the BK activity (set to 100%); antagonistic activity was calculated as pA_2 (negative common logarithm of analogue concentration shifting the log dose-response curve for BK by a factor of 0.3 to the right: the calculations were made from the linear portions of the curves); [d]Stewart's antagonist

together with those of Stewart's antagonist (used as a positive control) and some related peptides are summarized in Table 1.

In the rat blood pressure test compounds **I-X** displayed antagonistic activity, however the dimension of this effect was variable, starting from very low potency (peptide **IV** and **VIII**), through moderate (peptide **II**, **III**, **V**, **VI**, **VII** and **IX**) and ending on the model one (peptide **I**). In the rat uterus test all the analogues turned out to be agonists. In case of peptide **I**, **V**, **IX** and **X** BK agonistic activity was reduced to 25%, 43%, 24% and 13% respectively. Compound **II**, **VII** and **VIII** exhibited very weak agonistic properties. Analogues **III**, **IV** and **VI** were practically inactive.

Interestingly all the new compounds inhibited the vasodepressor response in the rat blood pressure test (antagonistic activity) and at the same time they caused the contraction of the uterine tissue in the rat uterus test (agonistic activity). This would support the idea of the presence of different types of BK receptor in the rat uterus and blood vessels. Although (up to the present) there is no evidence for more than one gene for B_2 receptor within a single species and B_2 receptor gene knockout mouse has lost all responses to exogenous BK, alternative splicing of a single gene transcript cannot be ruled out. The pharmacological discrepancies observed with BK and its antagonists may be explained by their interaction with orphan G-protein-coupled receptors for which ligands are not known (for example GPCR 100 [6]) or with B_2 receptor existing in one of the few possible conformations that results in stimulating the specific intracellular effector. Undoubtedly, further studies are needed to confirm these hypotheses.

Acknowledgments
This work was supported by the University of Gdańsk (**DS**/8453-4-0169-0).

References

1. Bhoola, K.D., Figueroa, C.D., Worthy, K. *Pharmacol. Rev.* **44,** 1-78 (1992).
2. Regoli, D., Barabe, J. *Pharmacol. Rev.* **32**, 1-46 (1980).
3. Prahl, A. *J. Pept. Sci.* **13,** 206-210 (2007).
4. Holton, P. *Br. J. Pharmacol.* **3**, 328-334 (1948).
5. Labudda, O., et al. *Acta Biochim. Pol.* **54**, 193-197 (2007).
6. Boels, K., Schaller, H.C. *Br. J. Pharmacol.* **140**, 932-938 (2003).

Proceedings of the 31st European Peptide Symposium
Michal Lebl, Morten Meldal, Knud J. Jensen, Thomas Hoeg-Jensen (Editors)
European Peptide Society, 2010

Synthesis and Biological Activity of Quercetin Derivatives of Endogenous Opioid Peptides Leu- and Met-enkephalin

Andreja Jakas[1], Nina Bjeliš[1], Ivo Piantanida[1], and Marijeta Kralj[2]
[1]Rudjer Boskovic Institute, Division of Organic Chemistry and Biochemistry, 10000, Zagreb, Croatia; [2]Rudjer Boskovic Institute, Division of Molecular Medicine, 10000, Zagreb, Croatia

Introduction

Quercetin, 3,3',4',5,7-pentahydroxyflavone is well-known flavonoid distributed ubiquitously as a glycoside in fruits, vegetables and herbs (apples, onions, Ginkgo biloba) and related products, specially in red wine [1]. In plants, flavonoids are involved in energy production and exhibit strong anti-oxidant properties, possibly protecting plants against harmful ultraviolet rays. Quercetin has become a subject of many investigations because of strong anti-cancer, anti-inflammatory, anti-oxidative and other therapeutic activities of significant potency such as cardioprotective, bacteriostatic and nevertheless its systemic toxicity is quite low.

On the other hand, it is known that the endogenous opioid peptides Leu- and Met enkephalin (Tyr-Gly-Gly-Phe-Leu/Met) acting as a cell growing factors have a role in anticancer activity as an inhibitor of cell division in a receptor-mediated fashion [2].

Results and Discussion

The goal of this study was to design and generate novel enkephalin analogs and to evaluate their anticancer activity. Taking in consideration that quercetin also has anticancer activity [3] prompted us to combine in the same molecule both quercetin and enkephalin in order to investigate their antitumor activity. Thus in the first stage, we carried out and determined the synthesis of coupling products between quercetin and Leu/Met-enkephalin as model system.

Figure 1 shows the pathway of derivatization of quercetin with protected Leu- and Met-enkephalin. Different protecting groups were used in the reaction in order to see the effects on reactivity and selectivity in the formation of mono-, di- or penta-substituted quercetine compound. Two condensation reagents, BOP and isobutylchloroformate, were used, for preparation of the protected compounds.

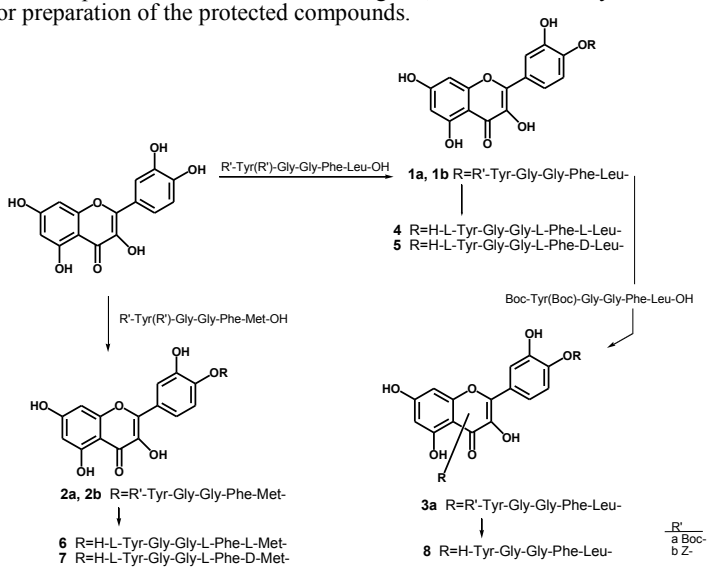

Fig. 1. Pathway of derivatization of quercetin with protected Leu-and Met–enkephalin.

Table 1. GI_{50} values (in μM) for quercetin derivatives 4-7

Compound	GI_{50}[a] (μM)		
	Cell lines		
	HCT 116	*SW 620*	*MCF-7*
4	>100	>100	>100
5	≥100	>100	≥100
6	≥100	>100	>100
7	78±16	>100	73±14

[a]*GI_{50}; the concentration that causes 50% growth inhibition*

While BOP method was good for the preparation of compound **1b**, in general for the preparation of enkephalin derivatives of quercetin isobutylchloroformate was the better choice. The yields of protected compounds of quercetin with Leu/Met-enkephalin **1-3** were between 50-70%. Yields of the deprotected compounds were between 60-85%.

According to the MS and NMR analysis position of the substitution in compounds **4-7** was defined while in the case of compound **3a** and **8** the position of second peptide is unknown, but MS analysis for compound **8** confirms that second peptide was bonded (HRMS MALDI [M+H]+; m/z=1377,56). Racemization of the activated amino acid in the reactions with isobutylchloroformate was between 9-18%, and in the reactions with BOP ~52%.

Interactions with ct-DNA of prepared compounds **4-7** were investigated using UV/VIS, flurescence, and CD measurements, but no interactions were observed. Table 1 shows results of the evaluation of antitumor activity on MCF-7 (brest carcinoma), SW 620 (colon carcionoma), HCT 116 (colon carcinoma). Compound **7** shows modest antiproliferative activity, at highest tested concentration. Prepared compounds do not exhibit interactions with ct-DNA and do not have significant antitumor activity in spite of our expectation based on starting compounds. Further investigation concerning anti-oxidative and anti-bacterial activities will be conducted.

Acknowledgments
We gratefully acknowledge the financial support of the Croatian Ministry of Science, Education and Sports, Grants No. 098-0982933-2936, 098-0982914-2918 and 098-0982464-2514.

References

1. El, Gharras *Int. J. Food Sci. Technol.* **40,** 2512-2518 (2010).
2. Cheng, F., McLaughlin, P.J., Verderame, M.F., Zagon, I.S. *Mol. Cancer* **7**, 5-16 (2008).
3. Chen, D., Dou, Q.P. *Int. J. Mol. Sci.* **9**, 1196-1206 (2008).

Proceedings of the 31st European Peptide Symposium
Michal Lebl, Morten Meldal, Knud J. Jensen, Thomas Hoeg-Jensen (Editors)
European Peptide Society, 2010

Cryptophycins – Synthesis of Potent Functionalized New Antitumor Agents

Benedikt Sammet and Norbert Sewald
Bielefeld University, Organic and Bioorganic Chemistry, Bielefeld, 33615, Germany

Introduction

Cryptophycins are a family of macrocyclic depsipeptides with high cytotoxicity. The bioactivity of cryptophycins is based on their ability to interact with tubulin, which leads to a strong suppression of the microtubule dynamics. Cryptophycin-1 was isolated from a culture of *Nostoc sp. ATCC 53789* in 1990 and many more synthetic derivatives followed. Cryptophycin-52 (**1**) has been the pharmacologically most important representative, so far (Figure 1). However, clinical phase I and phase II trials were discontinued due to neurotoxic side-effects and lack of efficacy *in vivo* [1].

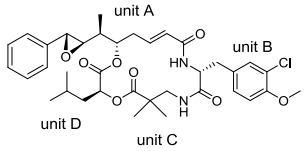

*Fig. 1. Structure of cryptophycin-52 (**1**) comprising of four units.*

Results and Discussion

In the course of our cryptophycin research a target was to alter the stereochemistry at the epoxide to give rise to the cryptophycin-39 (**2**) unit A fragment with a *cis*-epoxide (Figure 2). No total synthetic approach to cryptophycin-39 had been published so far. The basis for the synthetic strategy was lactone **4** (Scheme 1). Years ago, a synthesis of **rac-4** was published in high yields using potassium peroxomonosulfate (Oxone®) and *trans*-styrylacetic acid (**3**) [2]. Due to the similarity of the Shi-epoxidation reaction conditions to the racemic lactone synthesis it was possible to apply a Shi-epoxidation to obtain lactone **4** in high enantiomeric excess on a multi-gram scale. The following steps were similar to a unit A cryptophycin synthesis recently published [3]. With only five steps to allyl alcohol **8** it is currently the shortest synthesis of a cryptophycin unit A building block in literature [4].

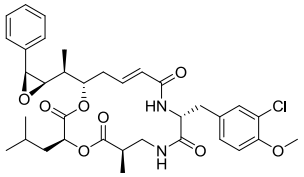

*Fig. 2. Structure of cryptophycin-39 (**2**).*

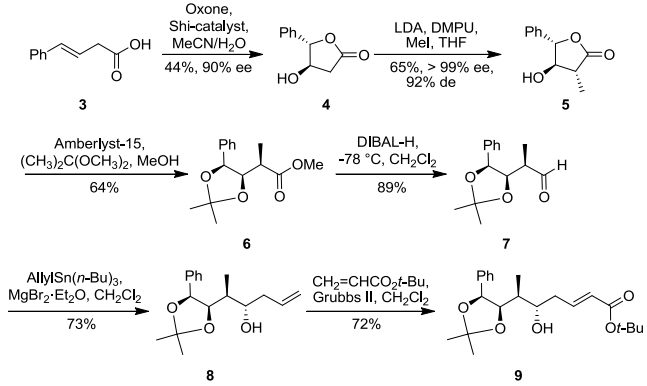

*Scheme 1. Synthesis of cryptophycin-39 unit A building blocks **8** and **9** [4].*

We also developed a very convenient synthesis of cryptophycin analogs containing an ester or a free carboxylic acid for bioconjugations [5]. After analysis of possible protective group strategies, a novel unit D allyl ester precursor was synthesized from (*S*)-aspartate in three steps (see [5] for details). In addition, a novel synthesis of known unit AB precursor **12** was based on the recently published allyl alcohol **11** (Scheme 2) [3].

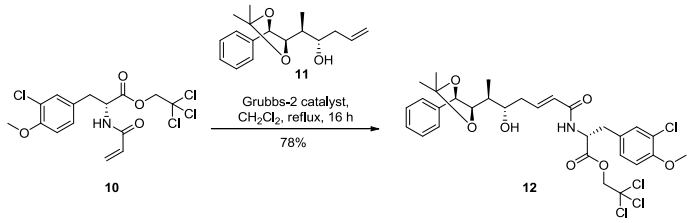

*Scheme 2. Novel metathesis approach to unit AB precursor **12** [5].*

The trichloroethyl ester protection group in **12** enabled an elegant macrolactamization [6] and the overall synthetic route allowed a very convergent cryptophycin synthesis. Moreover, the novel one-pot Staudinger reduction/cyclization procedure to macrocycle **14** significantly reduced the number of protective group operations in the synthesis (Scheme 3).

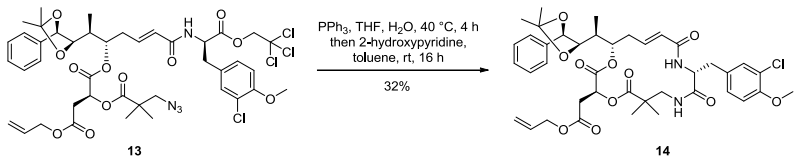

*Scheme 3. Staudinger reduction/cyclization procedure to macrocycle **14** [5].*

In the course of the acetonide to epoxide conversion a modified hydrolysis procedure for fragile cryptophycin bromohydrin formyl esters was developed (see [5] for details). Eventually, the final deprotection of the allyl ester **15** to carboxylic acid **16** made use of standard deprotection conditions (Scheme 4). The IC_{50} values of both cryptophycin derivatives **15** and **16** are below 100 pM against KB-3-1 cells [5].

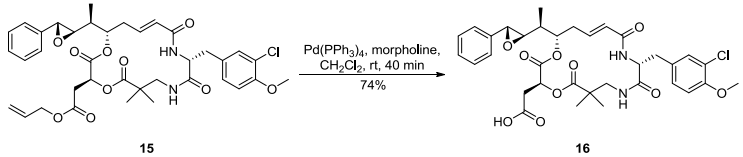

*Scheme 4. Deprotection of allyl ester **15** to carboxylic acid **16** [5].*

Acknowledgments
This work has been supported by the DFG (German Research Foundation) and the German National Academic Foundation (Studienstiftung des deutschen Volkes).

References

1. Eissler, S., Stoncius, A., Nahrwold, M., Sewald, N. *Synthesis* **22**, 3747-3789 (2006).
2. van Horn, J.D., Burrows, C.J. *Tetrahedron Lett.* **40**, 2069-2070 (1999).
3. Eissler, S., et al. *Org. Lett.* **9**, 817-819 (2007).
4. Sammet, B., et al. *Synlett.* **3**, 417-420 (2009).
5. Sammet, B., et al. *J. Org. Chem.* published online (2010).
6. Fray, A.H. *Tetrahedron: Asymmetry* **9**, 2777-2781 (1998).

Proceedings of the 31st European Peptide Symposium
Michal Lebl, Morten Meldal, Knud J. Jensen, Thomas Hoeg-Jensen (Editors)
European Peptide Society, 2010

Efficient Synthesis of Fertirelin Acetate as a Reproductive Control Drug: A GnRH Hormone Analogue

Vahid Dianati, Armin Arabanian, and Saeed Balalaie

Peptide Chemistry Research Group, K. N. Toosi University of Technology, Tehran, P.O. Box 15875-4416, Iran, balalaie@kntu.ac.ir

Introduction

Fertirelin acetate is an analogue for Gonadotropin Hormone Releasing Hormone (GnRH), also known as Luteinizing-hormone releasing hormone (LHRH). GnRH is a tropic peptide hormone responsible for the release of FSH and LH from the anterior pituitary which are synthesized and released from neurons within the hypothalamus. Fertirelin acetate (**1**) is a LHRH agonist intended for the treatment of ovarian follicular cysts in mammals and for the improvement of conception rates. It induces ovulation in mammals, and it is used as a drug for cows.

Nowadays, Pfizer Company produces this drug [1-4]. In continuation of our research in the synthesis of GnRH analogues, herein we wish to report the synthesis of Fertirelin acetate. It was shown that the 100- and 200µg doses of fertirelin acetate increase pregnancy rates in virgin heifers and tended to improve pregnancy rates in suckled cows when injected during the midluteal phase after insemination.

Results and Discussion

Fertirelin acetate as a GnRH analogue was syntheiszed via a combination of solid and solution phase peptide synthesis manually on the 2-chlorotrityl chloride resin using the standard Fmoc strategy. Cleavage of peptide off the surface of 2-chlorotrityl resin needs a mild acidic condition. Meanwhile, the ethylamidation of produced N-terminal nonapeptide was done using ethylammonium hydrochloride in the presence of NMM (N-methyl morpholine) in NMP as solvent. The product was purified using preparative HPLC and structure was confirmed by the MALDI-Mass spectrometry data. Orthogonality has an important role in selection of the type of resin, and strategy of synthesis.

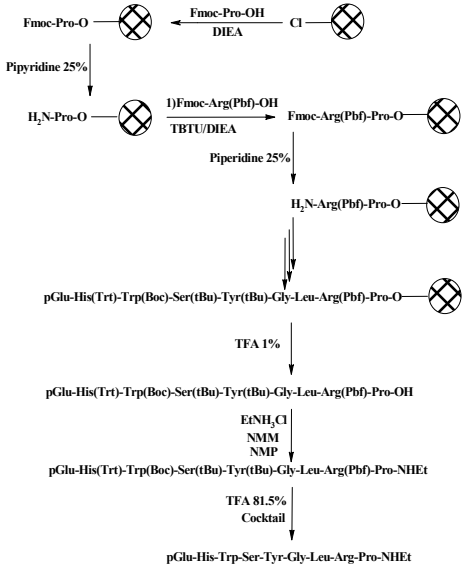

Scheme 1. Synthetic procedure for the synthesis of fertirelin acetate.

Fertirelin acetate is an amidated C-terminal peptide. There are different methods for the synthesis of *C*-terminal amidated peptides such as; a) enzymatic amidation, [4] b) the combination of rDNA technology with chemical modification of the *C*-terminus, c) using of amide resins in SPPS, d) using carboxypeptidase in the presence of ammonia, e) conversion of the *C*-terminus of peptides to the methylester and addition of ammonia at low temperature.

All of the reported methods have some drawbacks such as: a) laborious reaction conditions, b) high price of enzymes and limitation of solubility parameters, c) using of ammonia or alkylamines as gas and performing the reaction at low temperature, d) the use of HF for the cleavage of the peptide from the surface of the resin. Separation and purification of enzymes need more time and energy [6]. According to these drawbacks, we used ethylammonium hydrochloride in solution phase for the synthesis of ethylamidated form of C-terminal peptides.

The final deprotection of the protected peptides was performed by reacting with *reagent K* (20ml/g peptide) for 2 h at room temperature. The crude product was in general of good purity as shown by analytical HPLC analysis.

Synthesis was carried out using 2-chlorotrityl chloride resin (1.0 mmol/g) following standard Fmoc strategy. Fmoc-Pro-OH (3.54 g, 10 mmol) was attached to the 2-CTC resin (5.0 g) with DIPEA (6.85 ml, 40 mmol) in anhydrous DCM:DMF (50 ml, 1:1) at room temperature for 2 h. After filtration, the remaining trityl chloride groups were capped by a solution of DCM:MeOH:DIPEA (17:2:1, 120 ml) for 30 min. The resin was filtered and washed thoroughly with DCM (1×20 ml), DMF (4×20 ml) and MeOH (5×20 ml). The loading capacity was determined by weight after drying the resin under vacuum and was 1.0. The resin-bound Fmoc-amino acid was washed with DMF (3×20 ml) and treated with 25% piperidine in DMF (65 ml) for 30 min. and the resin was washed with DMF (3× 20 ml). Then a solution of Fmoc-AA-OH (7.5 mmol), TBTU (2.40 g, 7.5 mmol), DIPEA (3.0 ml, 17.5 mmol) in 30 ml DMF was added to the resin-bound free amine and shaken for 1 h at room temperature. After completion of coupling, resin was washed with DMF (4×20 ml) and DCM (1×20 ml). The coupling was repeated as the same methods for other amino acids of their sequences. In all cases for the presence or absence of free primary amino groups, Kaiser Test was used. Fmoc determination was done using UV spectroscopy method.

In conclusion, fertirelin acetate was synthesized using Fmoc strategy and novel amidation method using ethyl ammonium hydrochloride in solution phase, in good yield.

Acknowledgments

We are grateful Kimia Exir Company for Chemicals donation. A part of this research work was supported by research council of K.N. Toosi University of Technology which is gratefully acknowledged. We also thank Tofigh Daru Research & Engineering Co. for kind cooperation.

References

1. Sasaki, K., et al. *Nature* **257**, 751-757 (1975).
2. Shinigawa, S., Fujino, M. *Chem. Pharm. Bull*. **23**, 229-232 (1975).
3. Yamada, K., Nakao, T., Nakada, K., Matsuda, G. *Animal Reproduction Science* **74**, 27-34 (2002).
4. Inaba, T., Tani, H., Gonda, M., Nakagawa, A., Tamada H., Sawada, T. *Theriogenology* **49**, 975-982 (1998).
5. Rettmer, I., Stevenson, J.S., Corah, L.R. *J. Anim. Sci.* **70**, 7-12(1992).
6. a) Bui, C.T., Bray, A.M., Nguyen, T., Ercole, F., Maeji, N.J. *J. Peptide Sci*. **6**, 243 (2000); b) Kappel, J.C., Barany, G. *J. Peptide Sci*. **11**, 525 (2005); c) Stathopoulos, P., Papas, S., Tsikaris, V. *J. Peptide Sci.***12**, 227 (2006); d) Maeda, D.Y., Ishmael, J.E., Murray, T.F., Aldrich, J.V. *J. Med. Chem*. **43**, 3941 (2000); e) Deeks, T., Crooks, P.A., Waigh, R.D. *J. Med. Chem*. **26**, 762 (1983).

Proceedings of the 31st European Peptide Symposium
Michal Lebl, Morten Meldal, Knud J. Jensen, Thomas Hoeg-Jensen (Editors)
European Peptide Society, 2010

Synthesis, Characterization and Activity of Antamanide and its Analogues as Inhibitors of the Mitochondrial Permeability Transition Pore

Andrea Calderan[1], Nicola Antolini[1], Luca Azzolin[2], Paolo Bernardi[2], Andrea Rasola[2], Paolo Ruzza[1], and Stefano Mammi[1]

[1]Institute of Biomolecular Chemistry of CNR, Padova Unit and Department of Chemical Sciences, University of Padova, Padova, 35131, Italy;[2]Department of Biomedical Sciences, University of Padova, Padova, 35121, Italy

Introduction

Antamanide (AA) is a non-toxic cyclic decapeptide which has the following amino acid sequence: c(Val-Pro-Pro-Ala-Phe-Phe-Pro-Pro-Phe-Phe). It was isolated in 1968 from the fungus *Amanita phalloides*. AA acts as an antidote in poisoning by this fungus, preventing the cellular accumulation of toxins, such as Phalloidin. It was also reported that AA inhibits tumor cell growth in vitro [1], displays an antitumor action in an animal model [2], and attenuates IL-2-induced multisystem organ edema [3]. Like Cyclosporin A (CsA) and Cyclolinopeptide A, it has a powerful immunosuppressant activity [4]. Moreover, as CsA and Cyclolinopeptide A, it interacts favorably with Cyclophilin-D (Cyp-D). Cyp-D is a mitochondrial protein that has a high sequence homology and essentially identical folding with other Cyclophilins. Cyp-D plays a key role in regulating the mitochondrial permeability transition pore (PTP), but it is not a component of the pore. The fact that the administration of CsA or the genetic ablation of Cyp-D leads to inhibition of PTP opening suggested Cyp-D as a potential pharmacological target for the treatment of diseases caused by dysregulation of the pore, such as muscular dystrophy [5]. Studies on mice showed that ablation of Cyp-D protects the animal from cerebral ischemia and reperfusion injury and promotes recovery in diseases such as muscular dystrophy, autoimmune encephalomyelitis, and Alzheimer's disease. All these factors suggest that inhibiting Cyp-D can be a valuable therapeutic strategy [6]. To assess its affinity for Cyp-D and to obtain valuable information about the structure-activity relationships, we synthesized AA and several of its mono-substituted derivatives and studied their effect on the PTP on isolated mitochondria or in whole cells.

Results and Discussion

Peptides (Table 1) were synthesized by classical solution methodology. The synthetic route was based on the preparation of three different fragments corresponding to the sequences 1-4 (containing *ab initio* a C-terminal *tert*-butyloxycarbonyl-protected hydrazide moiety), 5-6 and 7-10. These fragments were subsequently assembled by the azide method following the Rudinger procedure obtaining the linear 5-4 sequence of AA. The same method was used for the cyclization reaction exploiting the possibility to separate the activation from the condensation, which was carried out at concentrations not exceeding 10^{-3} M in the presence of an inorganic base (K_2HPO_4).

Table 1. Sequences of Antamanide and its derivatives (substitutions are underlined)

Antamanide (AA)	c(Val-Pro-Pro-Ala-Phe-Phe-Pro-Pro-Phe-Phe)
AAGly^{6}	c(Val-Pro-Pro-Ala-Phe-<u>Gly</u>-Pro-Pro-Phe-Phe)
AAGly^{9}	c(Val-Pro-Pro-Ala-Phe-Phe-Pro-Pro-<u>Gly</u>-Phe)
AATyr^{6}	c(Val-Pro-Pro-Ala-Phe-<u>Tyr</u>-Pro-Pro-Phe-Phe)
AATyr^{9}	c(Val-Pro-Pro-Ala-Phe-Phe-Pro-Pro-<u>Tyr</u>-Phe)
desPhe^{5,6}AAGly^{9}	c(Val-Pro-Pro-Ala-<u>des</u>-<u>des</u>-Pro-Pro-<u>Gly</u>-Phe)
desPhe^{5,6}AATyr^{9}	c(Val-Pro-Pro-Ala-<u>des</u>-<u>des</u>-Pro-Pro-<u>Tyr</u>-Phe)

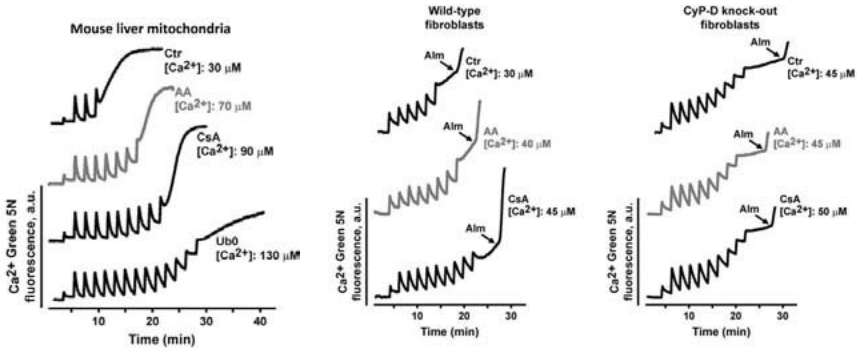

Fig. 1. Effect of AA on PTP opening in isolated mouse liver mitochondria (left) and in mitochondria of wild-type or CyP-D knock-out mouse fibroblasts (right).

The CRC (Calcium Retention Capacity) assay was used to assess PTP opening following trains of Ca^{2+} pulses and measured fluorimetrically at 25 °C in the presence of the Ca^{2+} indicator Calcium Green-5N. Experiments were performed either on isolated mitochondria or on whole cells (Figure 1). The data obtained show that AA induces opening of the pore and this effect is due to its interaction with Cyp-D, as it was absent in cells derived from Cyp-D knock-out animals. All AA derivatives tested proved to be ineffective.

Tests were also conducted to evaluate the effect of AA on mitochondrial depolarization and cell death induced by clotrimazole or hexokinase II N-terminal peptide (data not shown). The results show a protective action on both events. Mitochondrial depolarization was tested by measuring the fluorescence of TMRM, a probe that accumulates in polarized mitochondria. Cell death was instead tested by measuring the fluorescence of propidium iodide, which is unable to cross membranes and, therefore, a signal arising from this probe means an irreversible damage of the membrane after the death of the cell.

In conclusion, we demonstrated that AA desensitizes the PTP, a central effector of cell death induction, by targeting the PTP regulator CyP-D. Indeed, pore inhibition by AA is not additive with the effect of the CyP-D-binding drug CsA, and AA is ineffective on mitochondria or cells derived from CyP-D knock-out animals. Pore desensitization by AA needs two critical residues in the peptide ring, Phe^6 and Phe^9, and is additive with ubiquinone 0 (Ub0), which acts on the PTP in a CyP-D-independent way. AA also abrogates mitochondrial depolarization and the resulting cell death caused by two well-characterized PTP inducers, clotrimazole or a hexokinase II N-terminal peptide. Conversely, the reported AA inhibition of the toxic effects of the phallotoxin Phalloidin is independent of PTP modulation. Our findings have implications for the comprehension of CyP-D activity on the pore and for the development of novel PTP-targeting drugs usable as cell death inhibitors.

References

1. Ruzza, P., et al. *J. Pept. Res.* **53**, 442-452 (1999).
2. Nielsen, O. *Acta Pharmacol. Toxicol. (Copenh)* **59**, 249-251 (1986).
3. Welbourn, R., et al. *J. Appl. Physiol.* **70**, 1364-1368 (1991).
4. Benedetti, E., Pedone, C. *J. Pept. Sci.* **11**, 268-272 (2005).
5. Waldmeier P., et al. *Curr. Med. Chem.* **10**, 1485-1506 (2003).
6. Yang, Y.,et al. *Biochem. Biophys. Res. Commun.* **363**, 1013-1019 (2007).

Proceedings of the 31st European Peptide Symposium
Michal Lebl, Morten Meldal, Knud J. Jensen, Thomas Hoeg-Jensen (Editors)
European Peptide Society, 2010

"Clicktophycin-52": A Bioactive Cryptophycin-52 Triazole Analogue

Tobias Bogner, Markus Nahrwold, and Norbert Sewald
Bielefeld University, Organic and Bioorganic Chemistry, Bielefeld, 33615, Germany

Introduction

Cryptophycins are a family of cytotoxic, 16-membered macrocyclic depsipeptides. The name is based on their high toxicity against yeasts of the genus *cryptococcus*. Researchers at Merck isolated the first cryptophycin, cryptophycin-1 (Figure 1), from cyanobacteria *Nostoc* sp. (ATCC 53789) in 1990. Many different cryptophycins were later discovered in cyanobacteria, but also in marine sponges. Because of their high cytotoxicity cryptophycins were investigated as potential anti-cancer drugs. However, cryptophycin-52 (**1**), a synthetic analogue of cryptophycin-1, failed in clinical phase II studies due to high neurotoxicity and lack of efficacy [2].

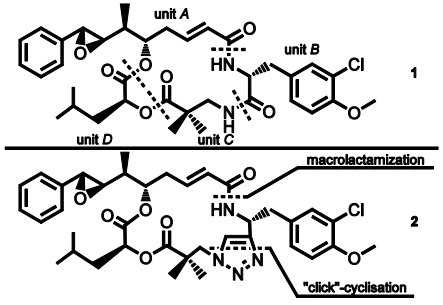

Fig. 1. Cryptophycin-52, "clicktophycin-52".

Retrosynthetically, cryptophycins can be divided into four building blocks (units *A*-*D*). Units *A* and *D* are hydroxy acids and units *B* and *C* are amino acids. These units are connected via two ester bonds and two amide bonds. The link between units A and *B* is a *cis*-amide bond. We envisioned to replace the *trans*-amide bond between units *B* and *C* by a 1,4-disubstituted triazole ring to study the effect of the substitution on the biological activity [1]. It is known that these triazoles can be used as *trans*-amide mimetics, despite their larger size and dipole moment.

Results and Discussion

We used two different coupling strategies: Either, ring closure via macrolactamization (Figure 2), wherein the click reaction is used to connect units *B* and *C*, or ring closure via click reaction (Figure 3). The key intermediate in both synthetic routes to "clicktophycin-52" is the unit *B*-alkyne building block **5**.

Azidopivalic acid **8** and the unit *D* precursor **7** were condensed to give the *CD* segment **9**. Then alkyne **5** was coupled via Cu(I)-catalysed cycloaddition to the *CD* segment **9,** yielding compound **10**. After hydrogenolytic cleavage of the benzyl ester the

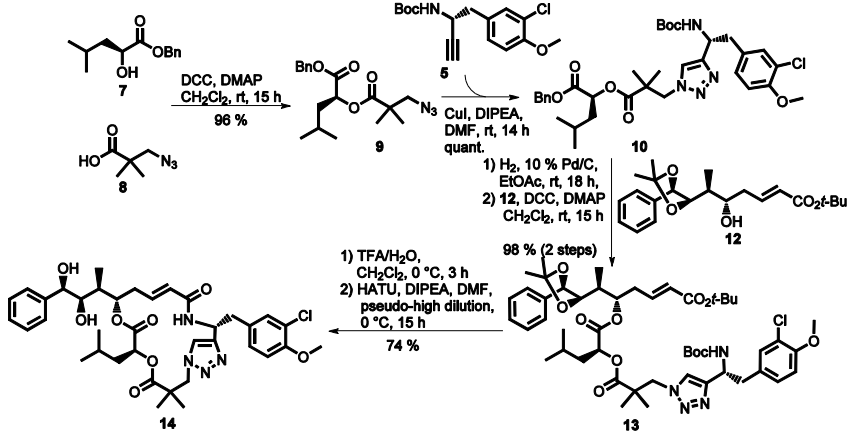

Fig. 2. Coupling strategy 1: ring closure by macrolactamization.

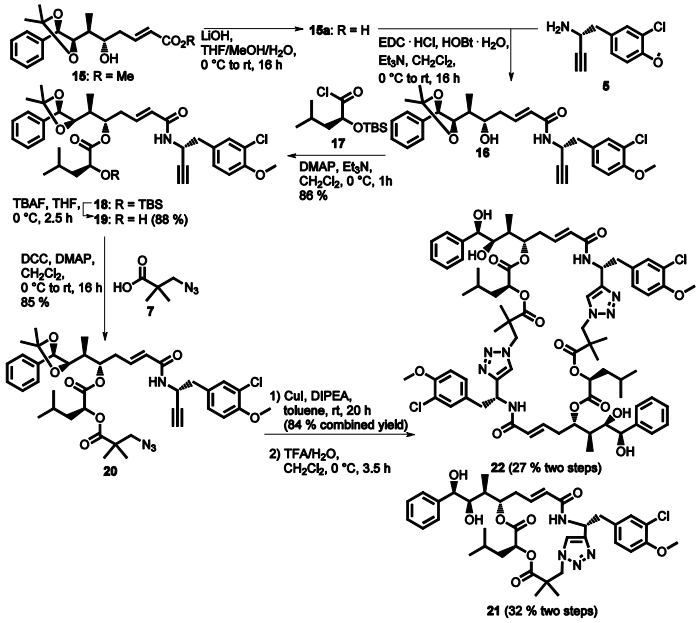

Fig. 3. Coupling strategy 2: ring closure by click reaction.

resulting segment *BCD* was coupled to unit *A* **12** using DCC/DMAP in DCM. Macrolactamization of the *seco*-compound **13** was conducted under pseudo-high dilution condition by activation with HATU, affording the macrocyclus **14** in 74% yield. Conversion of **14** via diol-epoxide transformation lead to "clicktophycin-52" (**2**).

The macrocyclization by click reaction starts with alkyne **5**, which was coupled with unit *A* building block **15a** using EDC·HCl and HOBt·H_2O to afford the *AB* segment **16**. This segment was subsequently condensed with unit *D* precursor **17**. The resulting *DAB* segment **19** was esterified with azidopivalic acid to yield the *seco*-*CDAB* segment **20**. We used the Cu^I catalyzed [3+2] cycloaddition for the ring closure. Besides the desired product the corresponding cyclodimer was formed. After acidic cleavage of the acetonides to the free diols, cyclomonomer **21** and cyclodimer **22** were separated. The cyclomonomer was obtained in 32% yield and the dimer in 27% yield. The *syn*-diol **21** was finally converted to "clicktophycin-52" (**2**) via diol epoxide transformation, whereas the larger macrocycle **22** was opened under similar reaction conditions.

The biological activity of **2** was measured using a resazurin assay. IC_{50} values were determined for the human cervix carcinoma cell line KB-3-1 and the multidrug resistant subclone KB-V1. "Clicktophycin-52" is an active cryptophycin analogue, even though it is less active than cryptophycin-52. The IC_{50} value against KB-3-1 is 1 nM, compared to 0.016 nM for cryptophycin-52. As expected the IC_{50} value is higher for the multidrug resistant cell line (13 nM "clicktophycin"; 0.261 nM cryptophycin-52). The loss of activity against the multidrug resistant cell line is relatively low and comparable to the loss of activity of cryptophycin-52, which is known to be highly active against multi drug resistant cell lines. In summary, the exchange of the *trans*-amide by a triazole ring affords a new and active cryptophycin-52 analogue.

Acknowledgments

We thank C. Michalek for helpful technical assistance. This work has been supported by the DFG (German Research Foundation).

References

1. Nahrwold, M., Bogner, T., Eissler, S., Verma, S., Sewald, N. *Org. Lett.* **12**, 1064-1067 (2010).
2. Eissler, S., Stoncius, A., Nahrwold, M, Sewald, N. *Synthesis* **22**, 3747-3789 (2002).

Proceedings of the 31st European Peptide Symposium
Michal Lebl, Morten Meldal, Knud J. Jensen, Thomas Hoeg-Jensen (Editors)
European Peptide Society, 2010

CD and Fluorescence Screening of α-Synuclein-Peptide Interactions

Anna Marchiani[1], Giada Massalongo[1], Stefano Mammi[1], Isabella Tessari[2], Luigi Bubacco[2], Andrea Calderan[1], and Paolo Ruzza[1]

[1]Institute of Biomolecular Chemistry of CNR, Padova Unit, and Department of Chemical Sciences, University of Padova, Padova, 35131, Italy;[2]Department of Biology, University of Padova, Padova, 35131, Italy

Introduction

α-Synuclein (AS) is the major component of the intracellular protein-aggregates found in the dopaminergic neurons of Parkinson's disease patients.

A critical step in the aggregation of AS is the production of oligomers, which are more cytotoxic than the amyloid-like fibrils. Aggregation inhibitors are expected to reduce AS cytotoxicity by preventing oligomer formation; on the other hand, an aggregation accelerator has recently been reported to reduce AS cytotoxicity [1], likely by causing oligomer precipitation. Therefore, ligands that modulate amyloid aggregation may have a therapeutic potential. For this purpose, we synthesized two peptides [2,3], named BB1 and BB2, respectively, and their all-D amino acid analogues as potential amyloid aggregation modulating ligands. In addition, a rotamer-scan of the Phe4 residue into the BB1 peptide was performed with the aim to evaluate the influence of the topography of this residue in the binding process.

Constraint-producing amino acid substitutions are typically used as modifier of the peptide/residue topography. The Tic residue is characterized by only two allowed side-chain orientations, the *g(-)* or *g(+)* conformations (Figure 1). The preferred conformation of the D-Tic residue into peptide chain is *g(-),* which corresponds to *g(+)* for an L-residue in the same position [4].

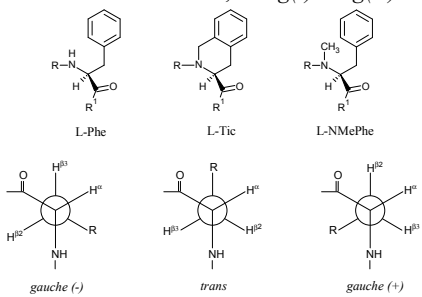

Fig. 1. Structure of constrained analogues of Phe and staggered side-chain conformers.

For the L-NMePhe residue, all three side-chain conformations are possible in principle, but mostly the *t* and *g(-)* conformations are observed in peptides (Figure 1) [5]. The presence of a methyl group on the nitrogen constrains the ψ angle of the preceding residue to a large value typical of those found in extended or β-structures.

In addition to providing topography restrictions, constraint residues can impart other properties to peptides, such as increased resistance to proteolysis.

Results and Discussion

Peptides were synthesized by manual SPPS on Rink-amide resin. HBTU/HOBt activation employed a three-fold molar excess of Fmoc-amino acids in DMF solution for each coupling cycle. Coupling to the secondary amino group of constrained residues was performed using HATU as the coupling reagent. Deprotection was performed with 20% piperidine. Cleavage from the resin and deprotection were performed by treatment with TFA-anisole-TIS-H_2O (95:2.5:2.0:0.5 v/v). Peptides were purified by preparative RP-HPLC and the molecular weights were checked by ESI-MS.

Binding of BB1-peptides to AS was monitored by changes in Trp fluorescence emission (Figure 2A). Peptides (1.5 μM) in 20 mM phosphate buffer, pH 6.8, at 25 °C were titrated with small aliquots of AS (65.9 μM) with minimal dilution. Peptide fluorescence emissions were recorded using an excitation wavelength of 295 nm. Binding constants were estimated from the titration data using a nonlinear least-squares computer fit to the equation based on 1:1 binding stoichiometry [6].

Far-UV CD analysis was used both to determine the binding of BB2-peptides to AS and to evaluate the influence of peptide interactions on AS conformation (Figure 2B).

Table 1. Peptide sequences and corresponding K_d values

Peptide	*Sequence*	*K_d (μM)*
BB1	H-Arg-Lys-Val-Phe-Tyr-Thr-Trp-NH_2	2.43±0.21
BB1-D	H-arg-lys-val-phe-tyr-thr-trp-NH_2	2.12±0.39
BB1-MP	H-Arg-Lys-Val-NMePhe-Tyr-Thr-Trp-NH_2	2.94±0.36
BB1-DMP	H-Arg-Lys-Val-NMephe-Tyr-Thr-Trp-NH_2	3.38±0.52
BB1-Tic	H-Arg-Lys-Val-Tic-Tyr-Thr-Trp-NH_2	4.68±0.59
BB1-DTic	H-Arg-Lys-Val-tic-Tyr-Thr-Trp-NH_2	5.59±1.20
BB1-Ala	H-Arg-Lys-Val-Ala-Tyr-Thr-Trp-NH_2	1.04±0.13
BB2	H-Arg-Gly-Ala-Val-Val-Thr-Gly-Arg-NH_2	0.50±0.10[a]
BB2-D	H-arg-Gly-ala-val-val-thr-Gly-arg-NH_2	0.35±0.08[a]

[a]*Determined by CD measurements*

For this purpose, AS (4 μM) in 20 mM phosphate buffer, pH 6.8, at 25 °C was titrated with small aliquots of each peptide (200 μM) with minimal dilution. Each CD spectrum was subtracted of the solvent and peptide contribution, and corrected for dilution. Binding constants (Table 1) were estimated from the titration data using a nonlinear least-squares computer fit to the equation based on 1:1 binding stoichiometry [7].

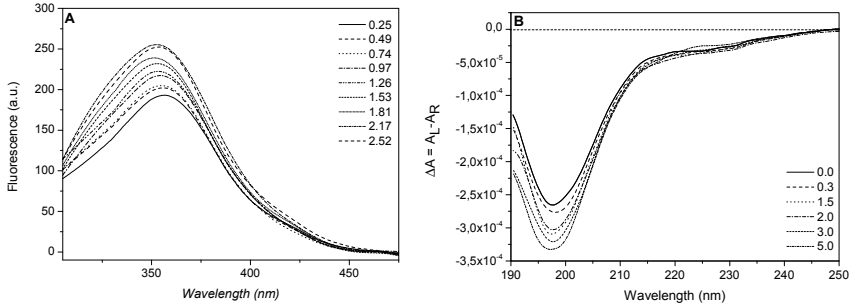

Fig. 2. (A) Fluorescence titration of BB1-Ala peptide by AS, (B) far-UV CD titration of AS by BB2 peptide. Peptide-AS molar ratios are reported inside each figure.

CD spectra showed that AS conformation was strongly influenced by the interaction with designed peptides. While the interaction with BB1 and BB2 induced an increase of the negative band at 198 nm, suggesting a corresponding increase of the unordered conformation of AS, other peptides caused a decrease of this band indicative of a reduction of the random coil conformation. The absence of an ordered CD spectrum suggests that these conformational changes are localized in small portions of AS. Surprisingly, both BB1-MP and BB1-Tic did not affect the far-UV CD spectrum of AS.

References

1. Bodner, R.A., et al. *Proc. Natl. Acad. Sci. U.S.A.* **103**, 4246-4251 (2006).
2. Kokkoni, N., et al. *Biochemistry* **45**, 9906-9918 (2006).
3. Palelogou, K.E., Irvine, G.B., El-Agnaf, O.M.A. *Biochem. Soc. Trans.* **33**, 1106-1110 (2005).
4. Valle, G., et al. *Int. J. Pept. Protein Res.* **40**, 222-232 (1992).
5. Schiller, P.W., et al. *Proc. Natl. Acad. Sci. U.S.A* **89**, 11871-11875 (1992).
6. Fan, T.C., et al. *J. Biol. Chem.* **283**, 25468-25474 (2008).
7. Siligardi, G., et al. *J. Biol. Chem.* **277**, 20151-20159 (2002).

Proceedings of the 31st European Peptide Symposium
Michal Lebl, Morten Meldal, Knud J. Jensen, Thomas Hoeg-Jensen (Editors)
European Peptide Society, 2010

Antidepressive Action of Short Human Urocortin III Fragments and Analogues

Kinga Rákosi[1], Masaru Tanaka[2], Gyula Telegdy[2], and Gábor K. Tóth[1]
[1]*University of Szeged, Department of Medical Chemistry, Szeged, 6720, Hungary;*
[2]*University of Szeged, Department of Pathophysiology, Szeged, 6720, Hungary*

Introduction

Depressive disorder is one of the most prevalent psychiatric diseases and there is no good antidepressive drug available uniformly appropriate for the treatment of it. In the activation of stress mechanism the corticotropin-releasing factor (CRF) is important. The action is elicited via CRF1 receptor, stimulating the ACTH-adrenal system and increasing the corticosteroid secretion of the adrenal cortex, and it is responsible for the anxiety related stress activation [1]. Discovery of the CRF family peptides led to urocortin III, which is present in highest concentration in the hypothalamus and amygdala, and it is a specific ligand of CRF2 receptor. The urocortin III-CRF2 receptor stimulates serotonin release from the basolateral amygdala and strengthens the antidepressive action in depression tests [2]. Urocortin III, consisting of 38 amino acids, its shorter fragments and their analogues, obtained with deletion or replacement of amino acids from the original human urocortin III sequence, were synthesized and tested for treatment of depression and anxiety.

Results and Discussion

In order to find out the biologically active center of the molecule, urocortin fragments were tested for antidepressant action in forced swimming test (FST) and anxiolytic action in elevated plus maze (EPM) test. Several shorter fragments were found to preserve the antidepressive and anxiolytic action of the longer sequence, but we especially focused on the C-terminal alanyl-glutaminyl-isoleucine tripeptide of urocortin III and its analogues [3].

Urocortin III and its shorter fragments and analogues (compounds **1-10**) were manually synthesized on 4-methylbenzhydryl resin (1.02 mM/g) (Table 1). The amino acids were incorporated using the Boc/Bzl strategy. Cleavage from the resin was made using a mixture containing 20 ml HF, 0.4 ml anisole, 1.6 ml dimethyl-sulfide, 0.4 ml p-cresole and 0.3 g DTT for 45 minutes at -5°C. After cleavage, the peptide was precipitated onto the resin in ice cold diethyl ether and lyophilized after solubilization in 10 ml 50% acetic acid and 100 ml H_2O. The crude peptides were analysed by RP-HPLC using (A) 0.1% TFA and (B) 80% MeCN, 0.1% TFA as eluents. Elution was conducted at a flow rate of 1.2 ml/min and detection was performed at 220 nm.

For compound **7, a**fter the final Boc-deprotection the resin was treated twice with 10 ml 30% (v/v) Ac_2OH/DCM (1x 5 min, 1x 25 min).The acetylation efficiency was verified with the Kaiser test.

Table 1. Prepared peptides

No.	*Ucn(36-38) analogues*
1	H-Ala-Asn-Ile-NH_2
2	H-Ala-Gln-Leu-NH_2
3	H-Ala-Gln-Val-NH_2
4	H-Gly-Gln-Ile-NH_2
5	H-Ala-Gln-Ile-OH
6	H-Ala-Cit-Ile-NH_2
7	Ac-Gln-Ile-NH_2
8	H-*D*-Ala-*D*-Gln-*D*-Ile-NH_2
9	H-*D*-Ile-D-Gln-*D*-Ala-NH_2
10	H-Ala-*D*-Gln-Ile-NH_2
11	Boc-*D*-Gln-iBu amide
12	Ac-*D*-Gln-iBu amide
13	Ac-Gln-iBu amide

For compounds **11-13** we used as starting material Boc-*D*-Gln-OH or Boc-*L*-Gln-OH and for the coupling with isobutyl amine the mixed anhydride method was used, treating the carboxy-terminus with isobutyl chloroformate and *N,N*-diisopropylethylamine. After TFA-cleavage of the Boc group, acetylation was made by treatment with acetic acid anhydride.

Ureas represent a class of peptidomimetics that have improved pharmacokinetic (bio-availability and metabolic stability) properties compared to peptides.

An efficient „one-pot" solid phase urea synthesis [4] was used for compounds **14 a-e** (Figure 1). The direct activation of Fmoc-protected amino acids to their isocyanates was accomplished by treatment with $MeSiCl_3$ and Et_3N in DCM at room temperature. The resin-bound isocyanates that were formed *in situ* were

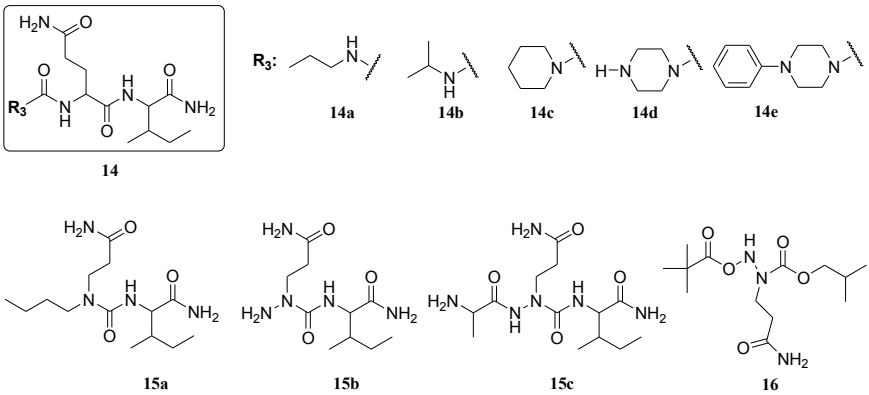

Fig. 1. Structures of urea derivatives and azapeptides.

treated with amines to produce, upon cleavage, the desired ureas in high HPLC purities.

Azapeptides are peptide analogues in which the α-CH of one or more amino acid residue has been substituted by a nitrogen, bearing an appropriate side chain. The aza-carbonyl bond is much more stable to hydrolysis (both chemical and enzymatic) than a natural peptide bond.

For compounds **15 a-c** and **16** preparation of the azaglutamine side-chain containing building block was needed. For this tert-butyl carbazate, n-butylamine and Fmoc-amino acid hydrazides underwent a Michael addition with acrylamide to give substituted carbazates having the side-chain of glutamine on nitrogen [5]. Reacting these aza-Gln precursors with the 2,4-dinitrophenyl carbonate (2,4-DNPC) activated amino group [6] of the isoleucine, immobilized on a solid support (Rink amide resin, loading 0.72 mM/g), gave the azaglutamine-containing Ucn3 analogues. 2,4-DNPC was prepared by the nitration of diphenyl carbonate with conc. HNO_3 and H_2SO_4 [7]. We have found that the AQI short fragment conserves the above mentioned biological action of the longer urocortin III.

For improved pharmacokinetic properties we designed and synthesized several ureas and azapeptides by modification of the peptide backbone via formation of a resin bound isocyanate or activated carbamate intermediate, followed by nucleophilic attack with an amine or an amino acid acyl hydrazide. We have found that many of these shorter fragments and analogues show similar or improved antidepressive and anxiolytic action, some of them even on oral administration.

References

1. Bale, T.L., et al. *Nat. Genet*. **24,** 410-414 (2000).
2. Tanaka, M., Telegdy, G. *Brain Res. Bulletin* **75,** 509-512 (2008).
3. Telegdy, G., Tóth, G.K., Rákosi, K., Tanaka, M. *Patent* **WO 2010/020825**.
4. Chong, P.Y., Petillo, P.A. *Tetrahedron Letters* **40,** 4501-4504 (1999).
5. Gray, C.J., Quibell,M., Jiang, K.-L., Baggett, N. *Synthesis* **Febr**., 141-146 (1991).
6. Gray, C.J., Quibell, M., Baggett, N., Hammerle, T. *Int. J. Peptide Protein Res*. **40**, 351-362 (1992).
7. Gray, C.J., Ireson, J.C., Parker, R.C. *Tetrahedron* **33,** 739-743 (1977).

Proceedings of the 31st European Peptide Symposium
Michal Lebl, Morten Meldal, Knud J. Jensen, Thomas Hoeg-Jensen (Editors)
European Peptide Society, 2010

Design, Synthesis and RNase Activity of Novel Peptidomimetics Against Influenza Viruses

L.S. Koroleva[1,2], O.V. Morozova[1,3], E.I. Isaeva[3], L.M. Rustamova[4], V.M. Sabynin[4], N.P. Schmeleva[4], N.V. Gribkova[4], and V.N. Silnikov[1]

[1]Institute of Chemical Biology and Fundamental Medicine, Novosibirsk, Russia; [2]Novosibirsk State University, Novosibirsk, Russia; [3]Ivanovskiy Institute of Virology, Moscow, Russia; [4]Research Institute for Epidemiology and Microbiology, Minsk, Republic of Belarus

Introduction

Influenza virus remains one of the major causes of respiratory diseases. Vaccination efficacy is limited because of high mutation rate of the influenza virus genome RNA. Therapy of influenza is currently based on blocking of the ion channels formed by M2 virus protein (drugs of the adamantane groups: amantadine and rimantadine) and neuraminidase inhibitors (zanamivir and ozeltamivir) and search of new antivirals is in progress. The aim: design and synthesis of novel peptidomimetic: Xaa-diamine-Xaa, where Xaa - Lys, Glu, Ser, His, Pro, Thr, Trp, Leu, as well as analysis of their cytotoxicity and inhibition of influenza virus A and B.

Results and Discussion

Recently a number of artificial peptide ribonucleases modeling known catalytic centers of natural RNases have been described [1-3]. RNA cleavage was shown to be more efficient in the presence of aliphatic hydrophobic fragment. However, a potential role of alkyl chain in the structure of the artificial RNases remains unclear. Interaction of hydrophobic residues in peptides was suggested to result in structurization of RNase mimetics in solutions thus enhancing their ribonuclease activity. To prove this suggestion, symmetric aliphatic diamides containing natural amino acid residues have been synthesized. The compounds were shown to possess high ribonuclease activity with model oligoribonucleotides and HIV-1 recombinant RNA fragment of 96 nucleotides long. Peptidomimetics were synthesized using method of activated esters and Boc-strategy. The general scheme is shown in Figure 1. The purity of the intermediates and the products of the reactions were monitored by TLC. The structures of the target compounds were confirmed by ^{1}H NMR spectroscopy and MALDI-TOF mass-spectrometry. The peptidomimetics have high solubility in water and DMSO, all solutions are stable and retain their activity after storage at +4°C for 12 months.

Peptidomimetics were dissolved in water and added to culture medium of MDCK cells permissive to influenza, adeno- and adeno-associated viruses without a serum at concentrations 50, 25, 12.5, 6.25 and 3.125 μg/ml before or simultaneously with infection with influenza viruses A and B. Then the cellular monolayers were observed for 3 days.

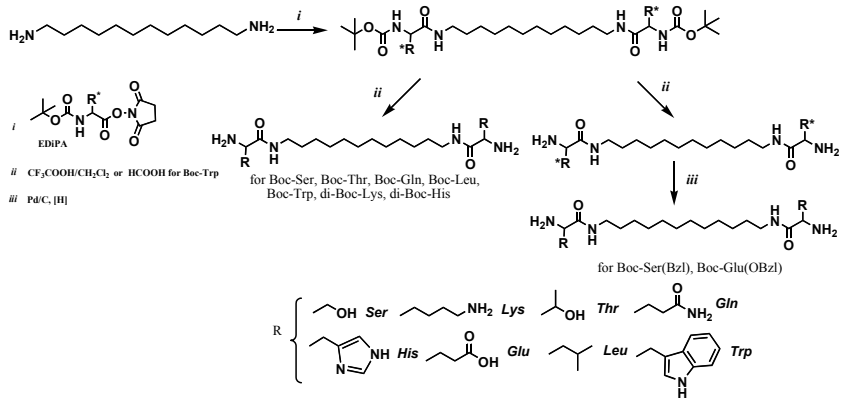

Fig. 1. General scheme of synthesis of artificial ribonucleases.

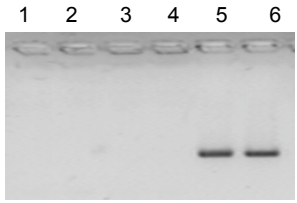

Lanes:
1 – negative control of RT-PCR
2-4 – viral RNA after incubation of influenza virus A with 25 μM solution of K-L_1-K (lane 2), K-L_2-K (lane 3) and E-L_2-E (lane 4) for 1 hour at 37^{0}C
5 – influenza A virus RNA
6 – positive control of RT-PCR

Fig. 2. Results of electrophoresis in 1.5% agarose gel of RT-PCR products.

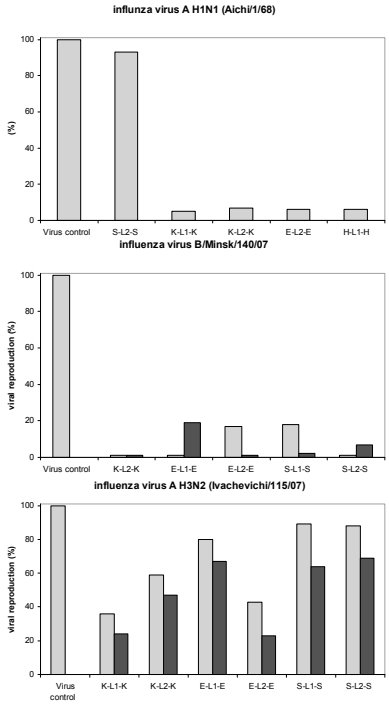

Fig. 3. Results of ELISA of the influenza virus A and B antigens after treatment of infected MDCK cells with peptidomimetics. Viral reproduction (%) = (OD in the presence of the artificial RNases/ OD of viral control)x100%. (Top) ELISA of influenza virus A H1N1 antigen after treatment with 25 μg/ml artificial RNases; (Middle) ELISA of influenza virus B antigen after treatment with 3.125 μg/ml artificial RNases; (Bottom) ELISA of influenza virus A H3N2 antigen after treatment with 3.125 μg/ml artificial RNases. Simultaneous infection and addition of artificial RNases (gray columns) or treatment of MDCK cells with artificial RNases in 60 min before infection (black column).

Inhibition of influenza virus A (H1N1 (strain Aichi 1/68) and H3N2 (strain Ivachevichi/ 115/07)) and B (strain Minsk/140/07) was estimated in hemagglutination (HA), enzyme-linked immunosorbent assay (ELISA) and reverse transcription (RT) with subsequent PCR. Treatment of extracellular virions of both influenza virus A and B with peptido-mimetics (3.125-25 μg/ml) for periods from 30 min to 18 hours resulted in negative HA and ELISA (Figure 3) in 1-3 days post infection. RT-PCR revealed complete cleavage of the influenza virus RNA before infection (Figure 2).

One should note that HA and ELISA titers corresponding to the virus antigen amounts remained the same before infection. Additions of peptidomimetics in culture media of infected MDCK cells in a few hours post infection did not cause essential viral RNA degradation, inhibition of HA and ELISA, as well as infectivity reduction. Taken together, the data proved RNase activity of new artificial RNases, absence of influenza virus surface antigens (HA and neuraminidase) modifications and penetration of peptidomimetics into extracellular virions but not within infected cells.

Acknowledgments
This work was supported by RFBR-09-04-01483, Integration grant of SB RAS-83, Integration grant of SB RAS-88.

References
1. Koroleva, L., et al. *Russ. Chem. Bull.* **54**, 2682-2691 (2005).
2. Konevetz, D., et al. *Russ. J. Bioorg. Chem.* **28**, 331-341 (2002).
3. Kuznetsova, I., et al. *Russ. Chem. Bull.* **53**, 455-462 (2004).

Proceedings of the 31st European Peptide Symposium
Michal Lebl, Morten Meldal, Knud J. Jensen, Thomas Hoeg-Jensen (Editors)
European Peptide Society, 2010

Solid Phase Synthesis and In Depth Analysis of the Tumour Targeting Peptide DOTATOC for Clinical Applications

Susanne Krämer[1], Carl von Gall[1], William Edmund Hull[2], Michael Eisenhut[3], Uwe Haberkorn[1], and Walter Mier[1]

[1]Department of Nuclear Medicine, University Hospital Heidelberg, Heidelberg, 69120, Germany; [2]Deutsches Krebsforschungszentrum, Core Facility: Molecular Structure Analysis, Heidelberg, Germany, [3]Deutsches Krebsforschungszentrum, Division of Radiochemistry and Radiopharmacology, Heidelberg, Germany

Introduction

Peptides are useful tools for the targeted delivery of radionuclides and/or chemotherapeutic drugs to their site of action within an organism. Due to its excellent performance the peptide derivative (1,4,7,10-tetraazacyclododecane-N,N',N'',N'''-tetraacetic acid)-Tyr^3-octreotide DOTATOC is the gold standard of peptide radiopharmaceuticals. DOTATOC binds to somatostatin receptors (receptor subtypes SSTR2 and SSTR5) and can be used for the diagnosis and therapy of tumours expressing these receptors. Somatostatin receptors are expressed on neuroendocrine tumours, including carcinoid tumours, pituitary adenoma, pheochromocytoma, and medullary thyroid carcinoma. Somatostatin receptors are also positive on the cell surfaces of other types of tumours, such as small cell lung carcinoma, meningioma, astrocytoma, and neuroblastoma. When labelled with ^{68}Ga DOTATOC allows the diagnosis by positron emission tomography (PET), ^{90}Y labelled DOTATOC has been proven to be effective for endoradiotherapy. The basis for the clinical application of this peptide is an efficient solid phase synthesis.

Results and Discussion

Even though Tyr^3-octreotide contains only eight residues, the synthesis is complicated by several structural features. The conjugation of the chelator sets further hurdles to obtain a product with essentially no side products. Here we describe a synthetic protocol which allows the solid phase formation and purification of DOTATOC at pharmaceutical quality. The product is characterized in detail by high resolution LC/MS using orbitrap technology and a complete assignment of its ^{1}H and ^{13}C NMR spectra. In addition conformational features of the peptide were evaluated using 1D and 2D NMR experiments. DOTATOC was prepared by solid-phase synthesis on a resin loaded with Fmoc-Thr(tBu)-Ol as shown in Figure 1.

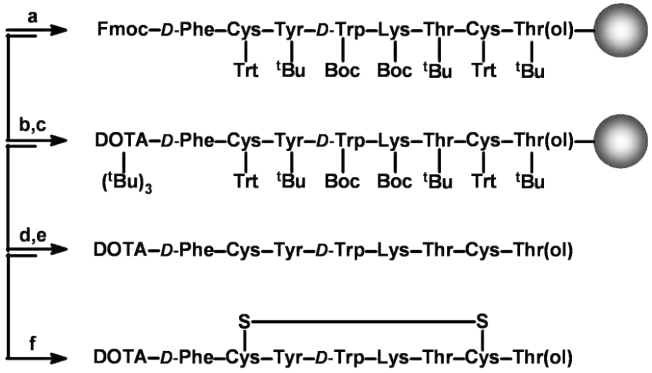

Fig. 1. DOTATOC solid-phase synthesis strategy using O-tBu-threoninol 2-chlorotrityl resin (grey spheres). Key: (a) stepwise elongation, (b) piperidine, (c) tris(tBu)DOTA, HATU, DIPEA, (d) TFA, H_2O, phenol, TIS, (e) TFA (f) air oxidation.

In order to prevent racemisation, Cys was introduced using Fmoc-Cys(Trt)-PFP. DOTA was introduced using tris(tBu)-DOTA. The peptide was cleaved from the resin, and the disulfide bridge was subsequently formed by air oxidation. During the oxidation process, the reduced and oxidized forms of DOTATOC cannot be distinguished by HPLC, and the mixture of the two forms yields one sharp peak. High-resolution LC-MS clearly shows peaks with m/z values corresponding to the two species. However, MS of the final reaction product gave the correct molecular mass for the oxidized species and showed that no reduced peptide remained. The crude product was isolated by preparative HPLC using water/acetonitrile gradients containing acetic acid. In order to conclusively exclude the formation of diastereomeric side products due to racemisation of Cys, (D-Cys7)-DOTATOC and (D-Cys2)-DOTATOC, the two possible products containing one D-Cys were synthesized using pure Fmoc-D-Cys(Trt)-OH. HPLC of a mixture containing DOTATOC and the two D-Cys diastereomers demonstrated that all three forms can be resolved with significantly different retention times (Figure 2). Finally, the purified DOTATOC was analyzed by 1H and 13C NMR spectroscopy at 9.4 T (400 MHz for 1H) at 52 °C in D2O solution. The 1D spectra confirmed the expected non-exchangeable proton and carbon counts. Complete 1H and 13C signal assignments were made using a combination of standard 2D NMR experiments (COSY, cROESY, HSQC, HMBC), which confirmed the amino acid residues present, their sequence, the disulfide bridge, and the attachment of DOTA with a purity of >95 percent.

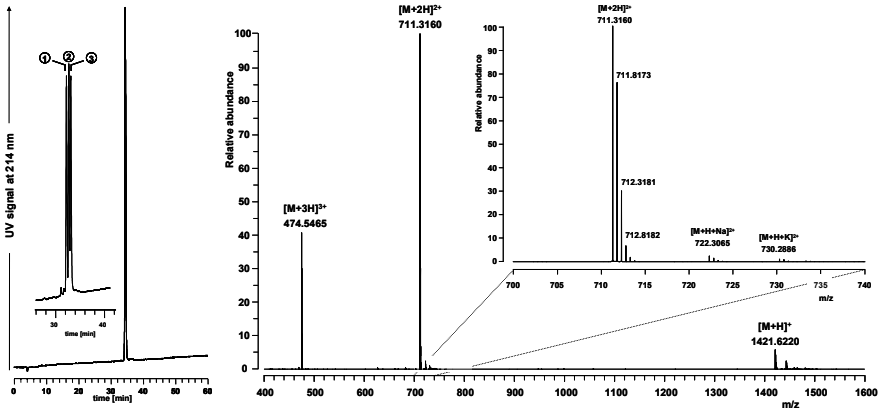

Fig. 2. Left: HPLC analysis of purified DOTATOC using a linear gradient of 0 - 50% solvent B over 60 min, flow rate 0.5 mL/min, at 60 °C (solvent A = 0.1% TFA in water, B = 0.1% TFA in acetonitrile). Insert: HPLC of the DOTATOC isomers (D-Cys7)-DOTATOC (1), DOTATOC (2) and (D-Cys2)-DOTATOC (3). Right: LC-MS analysis of DOTATOC. Positive-ion ESI-MS displays signals corresponding to $[M+3H]^{3+}$, $[M+2H]^{2+}$, $[M+H]^{+}$ as well as sodium and potassium adducts. The most abundant peak at m/z = 711.3160 corresponds to $[M+2H]^{2+}$ (calc. 711.3150) for DOTATOC with the disulfide bridge: $C_{65}H_{92}N_{14}O_{18}S_2$ (exact mass M = 1420.6155).

Conclusion

In contrast to small-molecule drugs, peptides can exhibit complex conformational properties which complicate the analysis (e.g. DOTATOC in DMSO could not be analyzed by NMR). Therefore, the repertoire of methods for peptide analysis is limited, typically employing a combination of RP-HPLC (to determine the homogeneity) and mass spectrometry (to determine the identity). It could be shown that DOTATOC can be synthesized with high purity by solid-phase methods, provided that specific synthesis protocols are applied.

Proceedings of the 31st European Peptide Symposium
Michal Lebl, Morten Meldal, Knud J. Jensen, Thomas Hoeg-Jensen (Editors)
European Peptide Society, 2010

Solid-Phase Synthesis and Analytical Characterization of Myrcludex B: A Potent New Entry Inhibitor for the Treatment of HBV Infections

Alexa Schieck[1], Thomas Müller[1], Uwe Haberkorn[1], Stephan Urban[2], and Walter Mier[1]

[1]Department of Nuclear Medicine, University Hospital Heidelberg, Heidelberg, 69120, Germany; [2]Department of Infectious Diseases, Molecular Virology, University Hospital Heidelberg, Heidelberg, 69120, Germany

Introduction

Chronic HBV infection is the leading cause of liver cirrhosis and HCC. Synthetic peptides derived from the N-terminus of the large HBV envelope protein, have been shown to efficiently block HBV entry *in vitro* [1] and *in vivo* [2]. The inhibition of viral HBV infection by preventing the virus entry into hepatocytes constitutes a new therapeutic strategy. Myrcludex B is a first-in-class HBV entry inhibitor currently progressing to clinical application. It consists of the 47 N-terminal amino acids of the viral surface protein and is myristoylated at the N-terminus (Figure 1). For the industrial production according to GMP standards an efficient and cost-effective synthesis of this peptide is required.

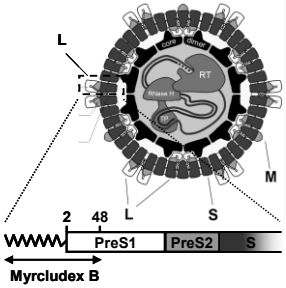

Fig. 1. Hepatitis B Virus patrticle with its surface proteins S, M and L.

Consequently, the solid phase synthesis of Myrcludex B was studied in detail. For characterization, the Fmoc cleavage pattern (UV monitoring) of the peptide synthesizer, RP-HPLC and LC-MS measurements were employed. Samples of the crude and purified Myrcludex B were characterized to identify arising side products during SPPS. In addition, the purified peptide was enzymatically degraded. Degradation products were analyzed by LC-MS to localize the positions of missing or problematic amino acids within the peptide sequence.

Results and Discussion

Although Myrcludex B consists of almost 50 amino acids, the Fmoc cleavage pattern of the peptide synthesizer and RP-HPLC analysis of the crude product after solid phase synthesis show a very efficient synthesis. Integration results of the HPLC chromatogram reveal that the main peak corresponding to the desired peptide sequence represents ~60%. Side products are failure sequences lacking one amino acid or truncated, acetylated peptide sequences. After the coupling of the myristic acid to the N-terminus all acetylated by-products remain at the starting position facilitating the preparative purification step.

Nevertheless, it became obvious that some impurities were impossible to separate by the use of standard preparative RP-HPLC protocols. LC-MS analyses show impurities below the purified peptide peak (Figure 2B). Failure sequences lacking the amino acid asparagine and water (mainly due to aspartimide formation) were considered to be the main impurities.

The attempt to avoid failure sequences lacking the amino acids Asn, Pro and Gly by double coupling could not minimize the formation of these impurities. Enzyme degradation protocols generating the fragments 2-11^{myr}, 2-38^{myr}, 12-48 and 39-46 could show an identical impurity pattern indicating that the failure amino acids are missing at more than only one specific sequence position. The composition of the peptide sequence (8 asparagines, 5 aspartic acids, 7 prolines, etc.) complicates the analysis by enzymatic degradation even more. The exchange of Asp to Glu at position 31 of the peptide sequence could decrease the amount of side products with [M-H_2O] showing that this aspartic acid (beside the four others) plays a critical role in aspartimide formation.

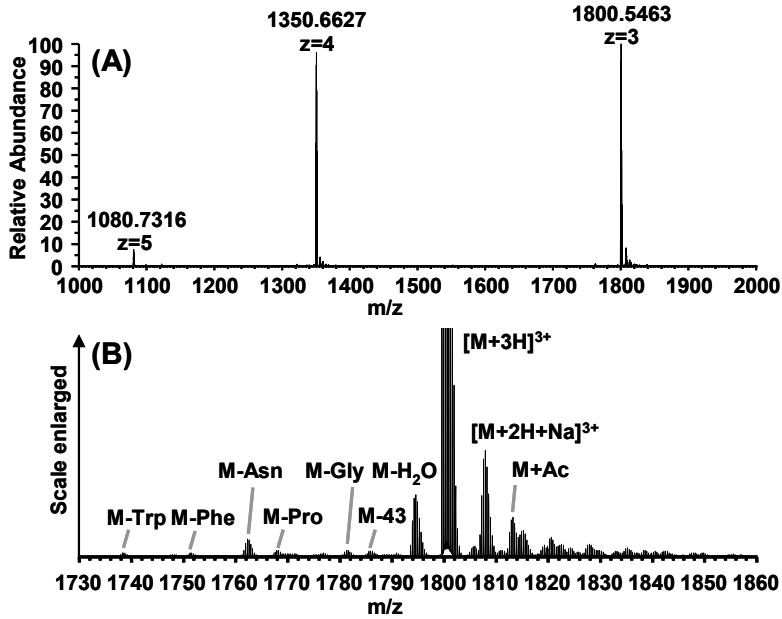

Fig. 2. LC-MS analysis of the purified lipopeptide Myrcludex B. (A) Mass spectrum. (B) Expanded mass spectrum of the 3-fold charged mass peak. Identified impurities are demonstrated.

Considering that the peptide sequence contains almost 50 amino acids the crude product after solid phase synthesis shows already a very good purity profile. Only when using optimized HPLC conditions some remaining impurities were detected (≤ 3%). By-products like truncated sequences due to acetylation were prevented by the use of purified Fmoc-amino acids. Thereby the overall yield could be further increased. Aspartimide formation at position 31 of the peptide sequence could be reduced by the exchange of Asp to Glu. To reduce this side reaction in the original peptide sequence and to enhance the overall purity, we aim at using Hmb-protected amino acids.

By critical observation of the solid phase synthesis of Myrcludex B and localizing the main difficulties within the synthesis, it was possible to obtain the peptide described in high yields and purity.

Acknowledgments

The authors gratefully acknowledge Stefan Seitz for providing the figure of the HBV particle. This work was funded by the Bundesministerium für Bildung und Forschung (BMBF), Innovative Therapieverfahren, Grant Number 01GU0702.

References

1. Gripon, P., Cannie, I., Urban, S. *Journal of Virology* **79**, 1613-1622 (2005).
2. Petersen, J., Dandri, M., Mier, W., Lutgehetmann, M., Volz, T., von Weizsacker, F., Haberkorn, U., Fischer, L., Pollock, J.M., Erbes, B., Seitz, S., Urban, S. Braun, W., Wider, G., Lee, K.H., Wüthrich, K. *Nature Biotechnology* **26**, 335-341 (2008).

Proceedings of the 31st European Peptide Symposium
Michal Lebl, Morten Meldal, Knud J. Jensen, Thomas Hoeg-Jensen (Editors)
European Peptide Society, 2010

Binding of Hemopressin Peptide with Cannabinoid CB1 Receptor: A Structural Study

Mario Scrima[1], Sara Di Marino[1], Manuela Grimaldi[1], Ettore Novellino[2], Maurizio Bifulco[1], and Anna Maria D'Ursi[1*]

[1]*Department of Pharmaceutical Sciences, University of Salerno, I-84084, Fisciano, Italy;*
[2]*Department of Pharmaceutical and Toxicological Chemistry, University of Naples Federico II, I-80131, Naples, Italy*

Introduction

Hemopressin (PVNFKFLSH), a bioactive nonapeptide derived from the α1-chain of hemoglobin, was recently shown to possess selective antagonist activity at cannabinoid CB_1 receptor [1]. CB_1 receptor antagonists have been extensively studied for their possible therapeutic use in the treatment of obesity, drug abuse and heroin addiction.

Using circular dichroism and nuclear magnetic resonance spectroscopy, the present work reports the conformational analysis of hemopressin and its truncated, biologically active fragment hemopressin(1-6). The binding modes of both hemopressin and hemopressin(1-6) are investigated by molecular docking calculations.

Results and Discussion

CD Spectroscopy. The quantitative evaluation of the CD curves, indicated that hemopressin and hemopressin(1-6) in a water solution at pH 5.4 assume random coil conformations with minimal amounts of turn and strand structures. In mixed DPC/SDS micelles, hemopressin and hemopressin(1-6) prevalently assume α-helical and β-turn (negative ellipticity value at 218 nm), with small amounts of random coil conformations.

NMR Spectroscopy. An entire set of 1D and 2D proton spectra (COSY, TOCSY and NOESY) of hemopressin and hemopressin(1-6) (peptide concentration range of 0.5-15 mM) were recorded in water and in DPC/SDS (90/10 M:M) mixed micelles. Analysis of hemopressin structure bundles according to the PROMOTIF procedure points to the presence of regular type I β-turn structures on residues Phe4-Leu7, Lys5-Ser8, and Phe6-His9. H-bonds between C=O (Phe4) and HN (Leu7) as well as C=O (Phe6) and HN (His9) stabilize the β-turn structures. Analysis of hemopressin(1-6) structure bundles following the procedure reported for hemopressin indicates that this shorter fragment assumes γ-turn structures centered on residues Phe4-Phe6.

Homology modeling. CB1 receptor shares 21% identity with visual rhodopsin (code PDB: 1GZM) [2]. Based on previously performed alignment studies [3,4], we built a molecular model of the CB1 receptor using MODELLER software. (Figure 1). The stereochemical quality of the CB1 model was assessed using PROCHECK software. The final results showed 94.8% of residues in the most favored regions, 4% in additional allowed regions, 0.4% in generously allowed regions and 0.8% in disallowed regions; the residues in disallowed regions were not located in the binding pocket.

*Molecular docking***.** Molecular docking calculations of hemopressin at the CB1 binding site were conducted starting from the low-energy hemopressin NMR structure using Autodock 4.0 software. The binding of hemopressin and hemopressin (1-6) at the CB1 binding site are shown in Figure 2 and 3, respectively.

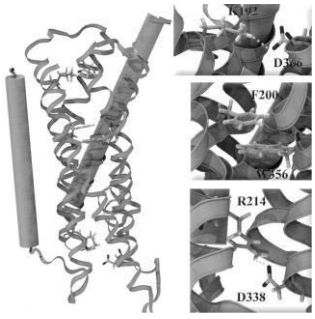

Fig. 1. Molecular model of CB1 receptor in the inactive state as predicted by Homology Modeling. On the right residues crucial to stabilize the receptor three-dimensional structure.

The binding of hemopressin at the CB1 binding site was stabilized by essential hydrogen bonds involving Asn3 C=O (hemopressin)-LYS192 $N\zeta$ (CB1) and Lys5 $N\zeta$ (hemopressin)-ASP366 C=O (CB1). The phenyl rings of residues Phe4 and Phe6 of hemopressin were involved in hydrophobic interactions with CB1 receptor residues PHE189, TRP255, and LEU190, and PHE368, and MET363, respectively. Pro1 and Val2 hemopressin were involved in hydrophobic interactions with PHE180, HIS181, and ILE375. Ser8 and His9 hemopressin interacted with residues neighboring those of the binding site. Interaction of hemopressin(1-6) at the binding site was stabilized by hydrogen bonds between Asn3 C=O (hemopressin(1-6)-LYS192 $N\zeta$ (CB1) and Lys5 $N\zeta$ (hemopressin(1-6)-ASP366 C=O (CB1). The phenyl rings of Phe4 and Phe6 were involved in hydrophobic contacts with LEU193 and PHE189, and PHE368, VAL367, and GLY369, respectively. Hemopressin(1-6) Pro1 and Val2 participated in the binding thorough Van der Waals interactions with PHE177, PHE180, HIS181, ARG182.

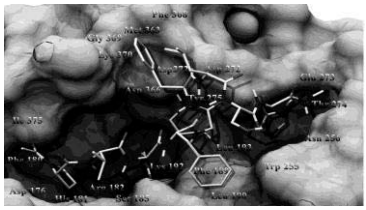

Fig. 2. Binding conformation of hemopressin at the CB1 receptor binding site.

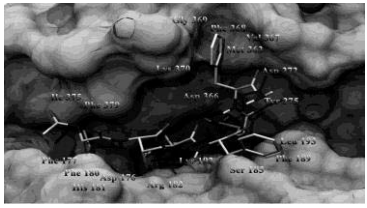

Fig. 3. Binding conformation of hemopressin (1-6) at the CB1 receptor binding site.

Hemopressin vs rimonabant: comparison of binding modes. Molecular docking calculation of rimonabant at the CB1 binding site were carried out for internal references. Analysis of rimonabant binding shows that rimonabant's interactions are consistent with those reported in the quoted studies [5,6]. In particular, the carboxamide oxygen of rimonabant formed hydrogen bonds with LYS192 Nζ and ASP366 C=O. The 2,4-dichlorophenyl and 4-chlorophenyl rings of rimonabant produce aromatic stacking interactions with TRP279/PHE200/TYR275 and TRP356 [5,6]. The lipophilic piperidinyl moiety was involved in hydrophobic interactions with VAL196, MET363, MET384, LEU387, and PHE379. Rimonabant, characterized by a smaller molecular size in comparison to hemopressin peptides, penetrates a deep cavity within the CB1 binding pocket with its aromatic rings; this region is not accessible by hemopressin and hemopressin(1-6), whose Phe rings are confined in a more external CB1 binding site region. The hydrogen bond involving LYS192 and ASP366 of the CB1 binding site is an essential interaction common to hemopressin and rimonabant (Figure 4). This interaction is crucial to stabilize the inactive state of the receptor and thus provides a structural basis to explain the activity of hemopressin peptides as inverse agonists. Hemopressin and hemopressin(1-6) N-terminal residues interact with a region of the CB1 binding pocket that also reached by the rimonabant piperidyl ring, that provides a structural basis to explain the biological data on the importance of N-terminal residues for hemopressin CB1 antagonist activity.

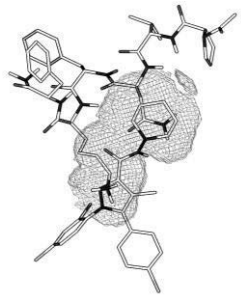

Fig. 4. Superimposition of binding poses of hemopressin(1-6) and rimonabant. Van der Waals volume intersection of rimonabant and hemopressin(1-6) binding poses is shown.

References

1. Heimann, A., et al. *PNAS* **104**, 20588-20593 (2007).
2. Baldwin, J.M., et al. *J. Mol. Biol.* **272**, 144-164 (1997).
3. Salo, O.M., et al. *J. Med. Chem.* **47**, 3048-3057 (2004).
4. Shim, J.Y., et al. *Biopolymers* **71**, 169-189 (2003).
5. Hurst, D.P., et al. *Mol. Pharmacol.* **62**, 1274-1287 (2002).
6. McAllister, S.D., et al. *J. Biol. Chem.* **279**, 48024-48037 (2004).

Proceedings of the 31st European Peptide Symposium
Michal Lebl, Morten Meldal, Knud J. Jensen, Thomas Hoeg-Jensen (Editors)
European Peptide Society, 2010

Synthesis of a PEG Conjugated HIV Gp41 MPER Fragment: A New Gp41 Helix Bundle Mimic

Manuela Grimaldi[1], Antonia Mastrogiacomo[1], Daniela Eletto[1], Mario Scrima[1], Simone Giannecchini[2], Fabio Rizzolo[3,4], Paolo Rovero[3,4], and Anna M. D'Ursi[1]

[1]Department of Pharmaceutical Science, University of Salerno, Fisciano, I- 84084, Italy; [2]Department of Public Health, Firenze, I-50134, Italy; [3]Department of Pharmaceutical Science, University of Firenze, Sesto Fiorentino, I-50019, Italy; [4]Laboratory of Peptide & Protein Chemistry & Biology, Univeristy of Firenze, I-50019, Sesto Fiorentino, Italy

Introduction

Human Immunodeficiency Virus (HIV), responsible for acquired immunodeficiency syndrome (AIDS), perform cell entry via a molecular mechanism involving viral Env glycoproteins with the final fusion mediated by the surface glycoproteins Gp41. The global architecture of Gp41 consists of a transmembrane (TM) region separating the cytoplasmic domain from the ectodomain enclosing the membrane-proximal external regions (MPER) directly involved in the virus cell fusion. In particular the fusion mechanism occurs through conformational changes of three Gp41 with the interaction of three Gp41 N-terminal helices forming a highly stable six helix bundle and the MPER effecting the events that occur after merging of the viral and cell membrane. Peptides deriving from MPER in the ectodomain of TM glycoprotein are able to prevent HIV cell membrane fusion [1], and one of these, formerly peptide T-20, is clinically used as anti HIV fusion inhibitors [2]. It was recently shown that polyethylene glycol (PEG) conjugated dimeric and trimeric fusion inhibitors, selected from a combinatorial peptide database, to mimic the Gp41 trimeric helix bundle, were characterized by a significant increased in antiviral potency [3]. We recently synthesized and tested for antiviral activity, EPK249 a Trp rich peptide corresponding to residues 666-681 of Gp41 MPER. EPK249 displayed weak *in vitro* antiviral activity.

Here we present the synthesis of PEG conjugated dimers and trimers of EPK249 designed in the attempt to achieve, according to the previous reported strategy, an improvement in the antiviral, fusion inhibitory activity.

Results and Discussion

According to the approach experimented by Welch [3], we first used the following synthetic strategy (Scheme 1):

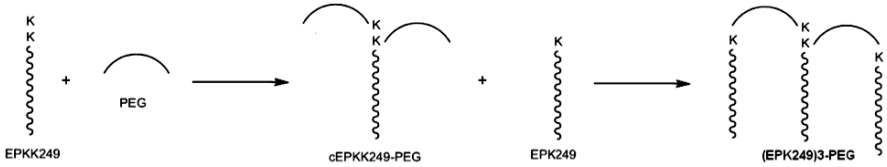

Scheme 1. Synthesis strategy of Welch.

The synthetic procedure was repeated several times by slightly changing the experimental conditions. The different experiments showed that the major obstacle to the success of the reaction was the hydrophobicity of EPK249 sequence. Therefore we designed a synthetic scheme that did not start by the central peptide (EPKK249), but starting by EPK249-PEG (see Scheme 3). This synthetic strategy allowed the obtaining of dimer (Scheme 2) and trimer (Scheme 4) EPK249 with a high purity.

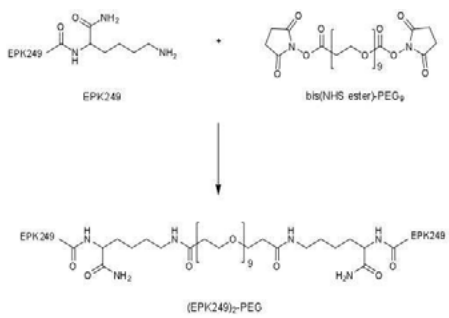

Scheme 2. Synthetic strategy for the dimer.

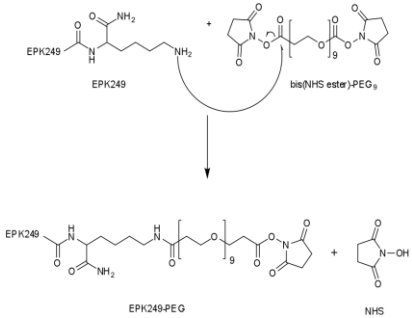

Scheme 3. Strategy for EPK249-PEG.

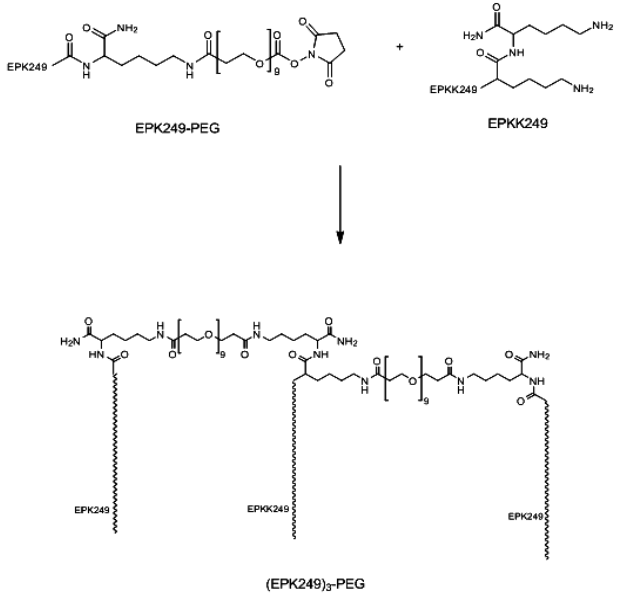

Scheme 4. Synthetic strategy for $(EPK249)_3$-PEG.

In conclusion we have demonstrated that the synthesis of helix bundles employing PEG can be performed by following different synthetic approaches that should be designed according to the specific peptide sequence.

References

1. Jin, B., Jin, S., Ryu, R., Ahn, K., Yu, Y.G. *AIDS Res. Hum. Retroviruses* **16**, 1797-1804 (2000).
2. Kilby, J.M., Lalezari, J.P., Eron, J.J., Carlson, M., Cohen, C., Arduino, R.C., Goodgame, J.C., Gallant, J.E., Volberding, P., Murphy, R.L., Valentine, F., Saag, Nelson, E.L., Sista, P.R., Dusek, A. *AIDS Res. Hum. Retroviruses* **18(10)**, 685-693 (2002).
3. Welch, B.D., VanDemark, A.P., Heroux, A., Hill, C.P., Kay, M.S. *Proc. Natl. Acad. Sci.* **104(43)**, 16828-16833 (2007).

Proceedings of the 31st European Peptide Symposium
Michal Lebl, Morten Meldal, Knud J. Jensen, Thomas Hoeg-Jensen (Editors)
European Peptide Society, 2010

Investigation on the Inhibition of the Two Active Sites of Angiotensin I Converting (ACE) Enzyme by Modified Prolyl Peptides

Boryana K. Yakimova[1], Bozhidarka Pandova[2], Stanislav G.Yanev[2], Bozhidar B. Tchorbanov[1], and Ivanka B. Stoineva[1]

[1]Institute of Organic Chemistry with Centre of Phytochemistry; [2]Dept.Drug Toxicology, Institute of Neurobiology, Bulgarian Academy of Sciences, Sofia, 1113, Bulgaria

Introduction

Many bioactive peptides derived from food proteins or artificial synthetic products inhibit Angiotensin I converting enzyme (ACE) in the cardiovascular system and contribute to the prevention and treatment of hypertension. Angiotensin I converting enzyme (ACE) belongs to the class of zinc proteases and has two distinct active catalytic sites, called the N- and C-domains. The relative potencies of competitive artificial inhibitors are different for the C domain (Lisinopril > Enalapril > Captopril) and the N domain (Captopril > Enalapril > Lisinopril) [1]. In this study we investigate the inhibitory potency of prolyl peptides in comparison with Lisinopril which prefer to bind to the C domain.

Results and Discussion

Three different proline peptides derivatives, two-, three- and tetra-peptides and three aminoacyl carbohydrates were tested for their inhibitory potency compared with the well known ACE inhibitor - Lisinopril (pyrrolidine derivative which is not metabolized and is excreted unchanged in the urine). An original HPLC method was applied for ACE activity determination. Rabbit serum was used as enzyme source. Serum aliquot was incubated in buffered medium with the ACE substrate analogue Hippuryl-Histidyl-Leucine (HHL). The IC_{50} values were determined by non-linear regression analysis of enzyme activity/inhibitor concentration curves using software package GraphPad Prism 5.0.

From the six compounds studied, the highest inhibitory potency possessed H-Val-Pro-Pro-OH with IC_{50} around 26 μM, followed by H-Val-Pro-Pro-Pro-OH (IC_{50} around 0.51 mM), and H-Val-Pro-OH (IC_{50} around 0.9 mM) (Figure 1). Sucrose-O-Pro, Glucose-O-Pro and Sucrose-O-Pro-NBoc were ineffective up to 1 mM concentration. The inhibitory effect of Lisinopril was much greater than that of H-Val-Pro-Pro-OH. The enzyme activity was 100% inhibited after 0.8 μM.

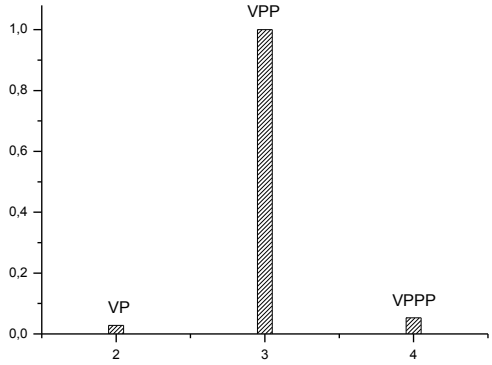

Fig. 1. Relative inhibitory potency of prolyl peptides.

Using the mapping of subside structures based on Lisinopril binding to tACE [2], where the tripeptide interacted with Ala354, His353, His513, Lys511 and Tyr520 and basing on our theoretical calculations [3], it is possible to conclude that the structures of the tripeptides Val-Pro-Pro with highest inhibitory potency allow only the NH_2…O=C and C=O…HO interactions with Ala354 and Tyr520 in the cavity of the enzyme (Figure 2).

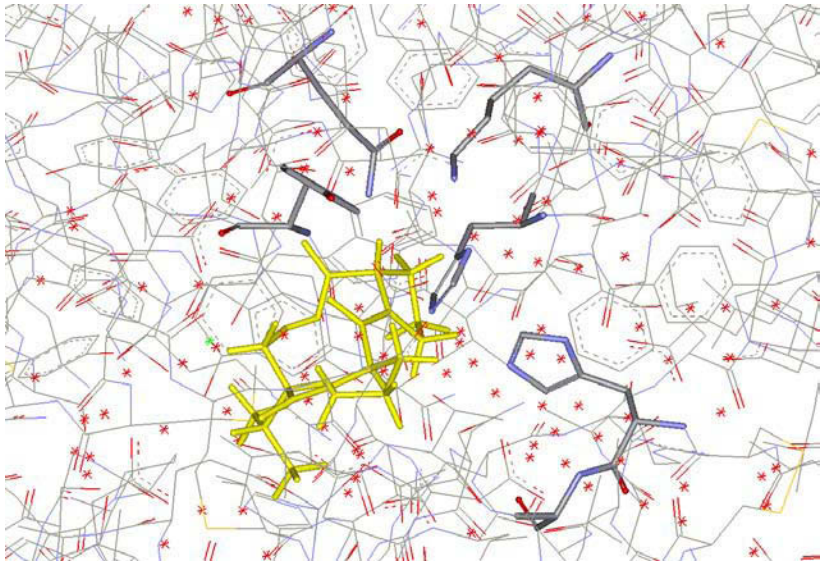

Fig. 2. Supposed binding of Val-Pro-Pro to the active site of tACE.

Each technique - spectrophotometric, fluorometric, HPLC, has its own limitation when following the hydrolysis of synthetic substrates used for assaying ACE activity. Therefore, sensitive and specific substrates are required for the determination of functional differences of the two domains of ACE, as well as ACE activity in biological fluids and tissues. For that reason we synthesized internal molecularly quenched fluorogenic peptide substrates as Ant-Gly-Phe(NO_2)-Pro-OH and Ant-Ser-Asp-Phe(NO_2)-Pro-OH. Kinetic *in vitro* measurements of these substrates with rabbit ACE are in progress now.

The significant inhibition of ACE activity by some prolyl peptides derivatives is probably due to the specific interaction with the C-domain. It is a good base for further design of new pro-drugs with greater inhibitory potency. Using highly sensitive fluorogenic substrates would shed light on the selectivity of ACE inhibitors on N- or C- domains. That would improve their pharmacological profile in terms of stability, duration of action and selectivity in the treatment of cardiovascular and renal diseases.

Acknowledgments

The work was supported by Bulgarian National Fund for Scientific Research (contracts X-1603 and X-1608).

References

1. Wei, L., et al. *J. Biol. Chem.* **267**, 13398-13405 (1992).
2. Sturrock, E.D., Natesh, R., van Rooyen, J.M., Acharya, K.R. *CMLS, Cell. Mol. Life. Sci.* **61**, 2677-2686 (2004).
3. Kolev, Ts., et al. *Protein Pept. Lett*. **16**, 112-115 (2009).

Proceedings of the 31st European Peptide Symposium
Michal Lebl, Morten Meldal, Knud J. Jensen, Thomas Hoeg-Jensen (Editors)
European Peptide Society, 2010

Protection Against Heat Stress Injury of Deuterohemin Peptide in *C. elegans*

Guan Wang, Pengfei Li, Shuwen Guan, Changrun Guo, Limin Zhu Hongkuan Fan, and Liping Wang*
College of Life Science, Jilin University, Changchun, 130012, P.R. China

Introduction

Heat stress will have a profound impact on *Caenorhabditis elegans* (*C.elegans*. Mild heat stimulation can cause hormesis and lead to extend the longevity. On the other hand continued heat stress would cause reduced life expectancy [1]. In this experiment *C.elegans* was kept at 30 ^{o}C and 35 ^{o}C after adult to establish the sustained heat stress model. A deuterohemin peptide called DhHP-6, which have already been proved that it can extend the lifespan of *C.elegans* [2], can raise the survival rate of *C.elegans* cultured in the environment of 30 ^{o}C and extend the longevity in the 35 ^{o}C. There have been the similar results in the daf-16 or sir-2.1 mutation strain indicating that DhHP-6 can protect *C.elegans* form the heat stress in a sir-2.1 and daf-16 independent way. The subsequent experiment used real time-PCR to investigate the differences in gene expression before and after heat shock. The results show that DhHP-6 can significantly increase the expression of heat shock protein HSP-16.1 and decrease the expression of sir-2.1, msh-2 and xpa-1 after heat shock. Combining with other gene data suggest a possible explanation for the protective effect of DhHP-6 on the *C.elegans* : the presence of DhHP-6 can decrease the high oxidation level caused by heat shock and accelerate the main response to stress by shortening the time for HSP's up-regulation.

Results and Discussion

DhHP-6, as a kind of peroxidase simulation, can help *C.elegans* to prolong the lifespan and increase the survival rate under a model of heat environment established in this experiment. Experiment proved that whether at 30 ^{o}C or 35 ^{o}C DhHP-6 have a protective effect on the wild type of *C.elegans* under the heat stress. DhHP-6 still have obvious protect effect to two kinds of mutations worm, CF1038 (*daf-16* [3] mutations) and VC199 (*sir-2.1* [4] mutations), which of the mutation gene are the key factor in the two most important of signaling pathways of stress resistance in the two heat stress conditions. The mutation of *daf-16* and *sir-2.1* does not effect the protection of DhHP-6 to worm under heat stress implying DhHP-6 heat protective effect has no *daf-16* and *sir-2.1* dependency. Another notable result is comparison with wild type loss of *daf-16* or *sir-2.1* seen to lead to decrease the tolerance of heat for *C.elegans*.

To further explore which pathway the DhHP-6 of the heat protective effect for *C.elegans* may be adopted. This study examines the effect of DhHP-6 to gene expression for *C.elegans* under heat stress. The results can show that the gene expression of the *ctl-1* one of cytoplasmic catalase in *C.elegans* [5] displays a certain reduction after given DhHP-6 in the wild type suggesting that the DhHP-6 can reduce oxidative pressure of *C.elegans*. The result after heat shock shows that the heat stress protective effect of DhHP-6 in *C.elegans* is likely to be achieved by effect on the level of intracellular oxidation. As for gene *sir-2.1*, both in wild-type and the *daf-16* mutant strain have shown a reduction of the expression after given DhHP-6. The result may be due to DhHP-6 that can reduce the level of oxidative stress in *C.elegans*. The down regulation of *sir-2.1* after heat shock also reflects the heat stress resistance of DhHP-6 to the early life of *C.elegans* is not dependent on *sir-2.1* gene pathway, which is consistent with the results that DhHP-6 heat protective effect have not *sir-2.1* dependency. After that we examined *hsp-16.1,* an important HSP in *C.elegans* [6]. The results show that the expression of *hsp-16.1* was significantly increased in the presence of DhHP-6 with further increase after heat shock. But the expression of *hsp-16.1* wasn't increased in the absence of DhHP-6 after heat shock that may be due to the short time interval between heat shock and extraction of total RNA so that there's not enough time to change the expression and the existence of DhHP-6 can shorten the time for stress resistance. These results also indicated that the DhHP-6 protects *C. elegans* reducing heat damage from heat environment by up-regulation *hsp-16.1*. It is notable that there are similar results in the *daf-16* mutant strain indicating that the up-regulation effect to *hsp-*

16.1 of DhHP-6 has not *daf-16* dependency again. Then we examined *xpa-1* which is part of nucleotide excision repair [7], *msh-2* involved in mismatch repair [8] and *hus-1* one of the cell cycle checkpoint gene in *C. elegans* [9] to focus on DNA repair signaling pathway. The results show that the expression of three genes were all decreased after given DhHP-6 in wild-type indicating that the DhHP-6 can reduce the mistake in DNA replication. Under the heat stress the heat shock-dependent up-regulation of *hus-1* and the down-regulation of two genes involved gene repair as well as the results for *hsp-16.1* above suggest a possible regulation to resistance to the heat stress in *C. elegans*: heat shock makes an increase of intracellular oxidative stress and causes an increase of DNA replication mistakes leading to increase the expression of cell checkpoint gene subsequently and regulate the protection of the protein as the main resistant pathway for stress, when the DNA repair as the secondary. On the one hand the presence of DhHP-6 can decrease the oxidation levels, on the other hand DhHP-6 can speed up the rate of the up-regulation for HSP and thus protect the biological functions in *C. elegans*. Finally we detected *cep-1* the homologous of p53 in *C. elegans* to investigate the influence of heat stress and DhHP-6 to apoptosis. The results show that the expression of *cep-1* is significantly decreased in the presence of DhHP-6 in wild type but independent heat shock indicating that DhHP-6 can reduce the apoptosis *in vivo* and short-term heat shock has little effect on apoptosis. The change trend of *cep-1* was similar in *daf-16* mutant and wild-type worm suggesting the effect has no *daf-16* dependency.

In conclusion DhHP-6 can protect *C.elegans* from the heat stress in a *sir-2.1* and *daf-16* independent way and the possible mechanism is that the presence of DhHP-6 can decrease the high oxidation level caused by heat shock and accelerate the main response to stress by shortening the time for hsp's up-regulation.

Acknowledgments

We would like to thank the Product Quality Supervision Inspection of Jilin for providing the real time PCR used in this research. We would like to thank the Caenorhabditis Genetics Center for providing strains used in this research.

References

1. Wu, D., Cupser, J.R., Yashin, A.L., Johnson, T.E. *J. of Gerontology* **63**(7), 660-668 (2008).
2. Guan, S., Li, P., Luo, J., Li, Y., Huang, L., Wang, G., Zhu, L., Fan, H., Li, W., Wang, L. *Free Radic Res.* **44**(7), 813-820 (2010).
3. Lin, K., Hsinh, Libina, N., Kenyon, C. *Nat. Genet.* **28**(2), 139-145 (2001).
4. Berdichevsky, A., Guarente, L. *Cell Cycle*. **5**(22), 2588-2591 (2006).
5. Taub, J., Lau, J.F., Ma, C., Hahn, J.H., Hoque, R., Rothblatt, J., Chalfie, M. *Nature.* **399**(6732), 162-166 (1999).
6. Candido, E.P., Jones, D., Dixon, D.K., Graham, R.W., Russnak, R.H., Kay, R.J. *Genome*. **31**(2):690-697 (1989).
7. Park, H.K., Yook, J.S., Koo, H.S., Choi, I.S., Ahn, B. *Mol. Cells* **14**(1), 50-55 (2002).
8. Tijsterman, M., Pothof, J., Plasterk, R.H. *Genetics* **161**(2), 651-660 (2002).
9. Hofmann, E.R., Milstein, S., Boulton, S.J., Ye, M., Hofmann, J.J., Stergiou, L., Gartner, A., Vidal, M., Hengartner, M.O. *Curr. Biol.* **12**(22), 1908-1918 (2002).
10. Schumacher, B., Hofmann, K., Boulton, S., Gartner, A. *Curr. Biol.* **11**(21), 1722-1727 (2001).

Proceedings of the 31st European Peptide Symposium
Michal Lebl, Morten Meldal, Knud J. Jensen, Thomas Hoeg-Jensen (Editors)
European Peptide Society, 2010

Mechanism in Inhibition of Histone Deacetylase by Cyclic Tetrapeptides with Various Functional Groups

Md. Shahidul Islam[1], Md. Nurul Islam[1], Nsiama Tienabe[1], Naoto Oishi[1], Tamaki Kato[1], Norikazu Nishino[1], Akihiro Ito[2], and Minoru Yoshida[2]

[1]Graduate School of Life Science and Systems Engineering, Kyushu Institute of Technology, Wakamatsu, Kitakyushu, 808-0196, Japan; [2]RIKEN, Saitama, 351-0198, Japan

Introduction

Class 1 and 2 histone deacetylases (HDACs) involve zinc atom at the active centre to employ metalloprotease-like mechanism in cleavage of acetyl group. As natural inhibitors of these HDAC enzymes, two different types of metabolites have been known. One group includes tricostatin A, which bears hydroxamic acid functional moiety at the end of the molecule. Cyclic tetrapeptides in another group have typically epoxyketone moiety as a part of quite unusual amino acid in the cyclic peptides. Having epoxyketone is not necessary to function as the natural inhibitors. Simple ketone and hydroxymethylketones are also found as HDAC inhibitors so far. In the last decade, a number of HDAC inhibitors have been reported in literature and patented as the possible candidate of cancer drug. However, they have randomly different type of so-called zinc ligand which is expected to bind to the enzyme strongly at the active site. The functional groups are, for instance, hydroxamic acid, retro-hydroxamic acid, o-aminoanilide, ketone, trifluoromethylketone, hydroxymethylketone, methoxymethylketone, mercaptan, disulfide, thioether, thioacetate, borate, phosphate and so on. In order to evaluate such functional groups in the same molecular condition as HDAC inhibitory activity, we introduced new (azide, click product, acryloyl and carboxyl) and known functional groups to the chlamydocin framework, cyclo(-L-AA-Aib-L-Phe-D-Pro-), (where AA bears different possible zinc ligands at the end of side chain) as standard of comparison.

Results and Discussion

Finnin, et al. [1] proposed a first explanation of the catalytic activity of these enzymes. The enzyme contains a zinc ion at the bottom of the active site, and the active center consists of a tyrosine, two aspartic acids, and three histidines. In this mechanism, the carbonyl oxygen of the substrate binds the zinc ion and is located adjacent to a water molecule. The electrophilicity of the carbonyl carbon is increased by coordination to the zinc ion, and so the carbonyl carbon is attacked by the water molecule activated by His 140 and His 141. This nucleophilic attack results in a tetrahedral transition state, which is stabilized by a zinc-oxygen interaction and by hydrogen bonds with Tyr 303 and His 140.

In the final step, proton transfer from His 141 to the nitrogen of the intermediate triggers scission of the carbon-nitrogen bond to afford the acetate and lysine products. The naturally occurring cyclic tetrapeptide chlamydocin is a very potent inhibitor of cell proliferation [2]. It has also been reported as a highly potent HDAC inhibitor. In our

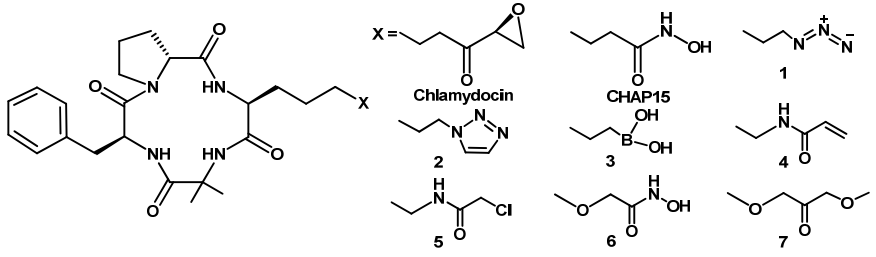

Fig. 1. Structures of the reported and synthesized compounds.

Table 1. HDAC inhibitory activity and p21 promoter assay data

Compound	*IC_{50} (μM)*			*p21 promoter assay EC_{1000} (μM)*
	HDAC1	*HDAC4*	*HDAC6*	
Chlamydocin	0.00015	-	1.100	-
[a]CHAP15	0.00044	-	0.038	-
1	>100	>100	>100	>250
2	65	52	>100	86
3	2.1	0.15	21	3.6
4	15	19	>100	>25
5	13	18	>100	>25
6	0.65	0.77	14	6.6
7	0.31	0.20	>100	0.47

[a]CHAP, cyclic hydroxamic-acid-containing peptide; IC_{50} half maximal inhibitory concentration; EC_{1000}, Effective concentration (10 fold)

designing, we focused on the proposed deacetylation mechanism. We selected chlamydocin scaffold as the carrier of functional group and synthesized seven cyclic tetrapeptides in which the epoxyketone moiety of chlamydocin was replaced by seven different functional groups or zinc ligands. The functional groups or zinc ligands are azide, triazole, borate, acrylamide, chloroacetamide, oxyacetic hydroxamate and dioxyacetone. The optimal ligand from these compounds can be utilized as the preferred ligand for other HDAC inhibitors. To compare the effectiveness of azide, triazole and borate versus epoxyketone, compounds in which these groups and the epoxyketone are in the same position were synthesized (Figure 1, compounds **1-3**). We next synthesized compounds **4-7** in which the carbonyl groups of the functional groups were in the same position as in chlamydocin. All the compounds were characterized by high resolution FAB-MS. The synthesized compounds were subjected to HDAC inhibitory activity using HDAC1, HDAC4, HDAC6 and p21 promoter assay, the results of which are shown in Table 1. All the compounds were less potent than chlamydocin which reveals that the extent of zinc binding affinities for these ligands in mechanism of HDAC inhibition is less than that of chlamydocin.

In conclusion, our aim was to find potent zinc ligands/functional groups, which may have enhanced binding affinities for zinc in HDAC inhibition mechanism. We have introduced new and known functional groups to the chlamydocin scaffold and evaluated these functional groups in the same molecular condition as HDAC inhibitory activity and compared with the reported compounds, CHAP15 and chlamydocin [3].

References

1. Finnin, M.S., Donigian, J.R., Cohen, A., Richon, V.M., Rifkind, R.A., Marks, P.A., Breslow, R., Pavletich, N.P. *Nature* **401**, 188-193 (1999).
2. De Schepper, S., Bruwiere, H., Verhulst, T., Steller, U., Andries, L., Wouters, W., Janicot, M., Arts, J., Van Heusden, J. *J. Pharmacol. Exp. Ther.* **304**, 881-888 (2003).
3. Furumai, R., Komatsu, Y., Nishino, N., Khochbin, S., Yoshida, M., Horinouchi, S. *Proc. Natl.Acad. Sci. U.S.A.* **98**, 87-92 (2001).

Proceedings of the 31st European Peptide Symposium
Michal Lebl, Morten Meldal, Knud J. Jensen, Thomas Hoeg-Jensen (Editors)
European Peptide Society, 2010

Anti-Plasmodium Effects of Angiotensin II Analogues

Vani X. Oliveira Jr.[1], Mayra Chamlian[1], Ceres Maciel[2], Margareth L. Capurro[2], and Antonio Miranda[3]

[1]Universidade Federal do ABC, Santo André, 09210-170, Brazil; [2]Universidade de São Paulo, São Paulo, 05508-000, Brazil; [3]Universidade Federal de São Paulo, São Paulo, 04023-900, Brazil

Introduction

Malaria is a major parasitic disease affecting around 300-500 million people in the world. The efforts to control this disease are hampered by drug resistance in parasites, insecticide resistance in mosquitoes, and the lack of an effective vaccine. Recently, we performed a study, which showed that Angiotensin II (AII) and some analogues are highly active against immature and mature sporozoites of *Plasmodium gallinaceum* [1]. In an attempt to increase the biological activity, we have scanned the whole AII sequence with i-(i+2) and i-(i+3) lactam bridge, consisting of the Asp-$(X)_n$-Lys scaffold. The biological results indicated cell damage, after 60 minutes incubation with cyclic analogues VC-5, VC-17 and VC-19, which present the introduction of the side-chain to side-chain bridging element in the N-terminal portion, and with the linear peptides VC-12, VC-26 and VC-28, that present the insertion of Asp and Lys residues in the C-terminal portion. These results suggest that the lactam bridge position in the sequence is important for the association of the molecule with the sporozoite membrane; and that biological effect could be increased with the addition of charged amino acid residues. This kind of approach may offer the basis for development the new drugs for malaria prevention and chemotherapy.

Results and Discussion

The peptides were synthesized by solid-phase methodology, using *t*-Boc strategy on a chloromethylated resin [2]. Solid phase side-chain to side-chain cyclization of the peptides on the resin was performed by BOP/DIEA [3]. Peptides were cleaved from the resin using anhydrous HF, purified by RP-HPLC and characterized by RP-HPLC, capillary zone electrophoresis, amino acid analysis and mass spectrometry [4].

In the bioassays, the sporozoites were incubated with 40 μM digitonin, 60 μM AII analogues or PBS, for 60 minutes at 37°C. Cell membrane integrity was then monitored by fluorescence microscopy, adding 1 μl of propidium iodide. The biological results are presented in the Figure 1.

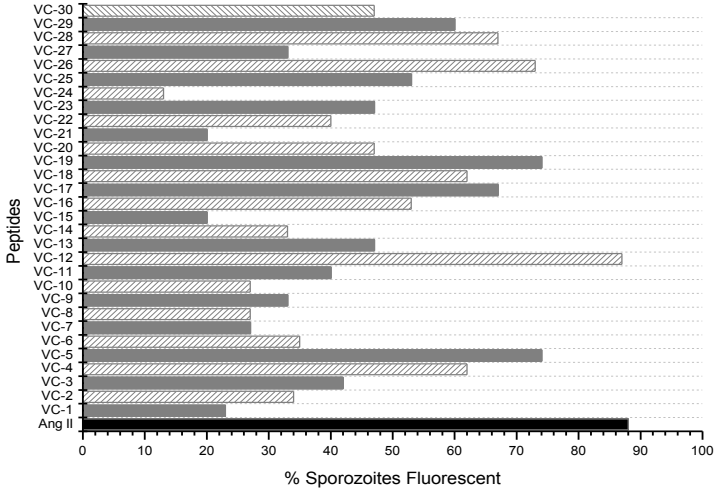

Fig. 1. Effects on membrane permeability of mature sporozoites when incubated with AII and VC peptides.

These peptides were engineered successfully to abolish their agonist functions, while retaining parasiticidal activity. The analogues presented low response in the bioassays performed on cytosensor microphysiometer [5], using AT_1-receptor transfected cells suspension, when compared to those caused by AII at 10^{-7} M [4].

In the antimalarial assays, we observed that analogues 1 to 30, designed with i-(i+2) and i-(i+3) lactam bridge, presented low biological activity in comparison with Angiotensin II, with the exception of some analogues: a) cyclic analogues VC-5, VC-17 and VC-19, that showed to be equipotent (Table 1). These analogues presented lactam bridge position among the amino acid residues Asp, Arg and Val, suggesting that the N-terminal portion is more susceptible to insertion of lactam bridge then the rest of the molecule; and b) linear analogues VC-12, VC-26 and VC-28 which showed biological activity nearly equal with Angiotensin II, around 75%. We observed that the potency could be increased with the introduction of charged amino acids (e.g. aspartic acid and lysine residues) at C-terminal position of the AII molecule.

We have demonstrated that these peptides disrupt selectively the *P. gallinaceum* cell membrane, although the mechanism of action is not completely understood.

Table 1. Primary sequences of the most active AII analogues

Nº	*Sequences*	*Percentage of Spz Fluorescent*
AII	Asp-Arg-Val-Tyr-Ile-His-Pro-Phe	88%
VC-5	Asp-Asp-Lys-Arg-Val-Tyr-Ile-His-Pro-Phe	76%
VC-12	Asp-Arg-Val-Tyr-Ile-**Asp**-His-**Lys**-Pro-Phe	87%
VC-17	**Asp**-Asp-Arg-**Lys**-Val-Tyr-Ile-His-Pro-Phe	67%
VC-19	Asp-**Asp**-Arg-Val-**Lys**-Tyr-Ile-His-Pro-Phe	74%
VC-26	Asp-Arg-Val-Tyr-**Asp**-Ile-His-**Lys**-Pro-Phe	73%
VC-28	Asp-Arg-Val-Tyr-Ile-**Asp**-His-Pro-**Lys**-Phe	67%

Acknowledgments

This research was supported by Fundação de Amparo à Pesquisa do Estado de São Paulo/FAPESP, Conselho Nacional de Desenvolvimento Científico e Tecnológico/CNPq and Coordenação de Aperfeiçoamento de Pessoal de Nível Superior/CAPES.

References

1. Maciel, C., et al. *Plos One.* **3**, e3296 (2008).
2. Cipriano, T.C., et al. *J. Mater. Sci.* **45**, 5101-5108 (2010).
3. Miranda, A., et al. *J. Med. Chem*. **37**, 1450-1459 (1994).
4. Oliveira, V.X., et al. *Biopolymers* **71**, (3) 372-372 (2003).
5. Oliveira, V.X., et al. *J. Peptide Sci.* **14**, (5) 617-625 (2008).

Proceedings of the 31st European Peptide Symposium
Michal Lebl, Morten Meldal, Knud J. Jensen, Thomas Hoeg-Jensen (Editors)
European Peptide Society, 2010

Targeted Platinum Peptide Complexes Holding Diamino and Dicarboxylic Coordination Modes

Agnieszka M. Glowinska[1], Anna Lesniak[2], Marzena Lazarczyk[2], Ewa Matyja[2], Andrzej W. Lipkowski[2], and Aleksandra Misicka[1]
[1]Faculty of Chemistry Warsaw University, Warsaw, 02-093, Poland; [2]Medical Research Centre Polish Academy of Science, Warsaw, 02-106, Poland

Introduction

Applying biologically active carrier ligands into platinated drug moieties generates a promising tool in anticancer therapy. Previously presented outcome [1] based on the opioid receptors' overexpression at cancer cells [2], indicated a potential for selective drug delivery, targeting malignant cells. Our idea was to reduce cisplatin drawbacks by use of hybride-molecules combining two fragments. One part of the molecule contains the opioid pharmacophore and the other fragment is designed to form a complex with platinum ion [3]. As a result such molecule can serve not only as carrier for platinum but also give a strong analgesic effect with potential anticancer activity.

Results and Discussion

Selective delivery of platinum moiety built into a multivalent complex was based on bifunctional structure design consisting of vector ligand and anticancer drug fragments linked by specific spacers (Figure 1). Promising antiproliferative properies (the proliferation T98G cells measured on the 4th day is 50% lower, compared to the control) and opioid receptor binding results (affinity at the opioid receptors in the nM range), obtained for the pioneer molecule (Table 1, compound 1) and demonstrated our structures as potential model for anticancer drug design. Recently, we have focused on improving compound solubility and the separation distance of active fragments. Hydrophilic linkers (1-amino-4,7,10-trioxa-13-tridecaamide and 4,7,10-trioxa-1,13-tridecanediamine succinic acid monoamide [4]) were chosen to result in solubility enhancement. In addition, lipophilic spacer (1,3-propanediamine succinic acid monoamide) was selected to induce membrane permeability. Ligands responsible for platinum ion coordination were divided into groups involving diamino (DAP, DAB), dicarboxylic (Glu) or mixed amino-carboxylic type (His). Diamino ligand type with chloro ions as leaving groups, were reported to be responsible for effective DNA structure distortions defining carcinoma cell's death. [5] On the other hand, decreased reactivity of carboxylate ions as leaving groups has been proved to diminish such interactions what resulted in reduced drug toxicity effect. We decided to implement both modes of platinum ion chelation types in our bifunctional systems and verify how introduction of disparate ligand's lability, platinum coordination type and linker character may influence compound physical properties and bioactivity.

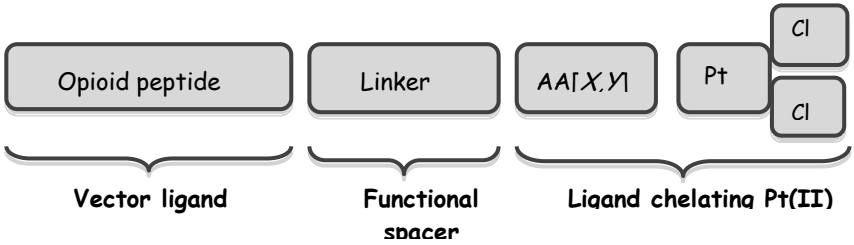

Fig. 1. Multivalent complex components.

Table 1. Binding affinity to opioid receptors of selected platinum peptide complexes

	Structure	Binding affinity results (nM)	
		IC_{50} (δ)[a]	IC_{50} (μ)[b]
1	Tyr-D-Ala-Gly-Phe-NHNH-Phe-Cys[*N,S*]$PtCl_2$	78	7.9
2	Tyr-D-Ala-Gly-Phe-NHNH-Phe-DAP[*N,N'*]$PtCl_2$	1,26	20
3	Tyr-Pro-Phe-Phe-TOTA-DAP[*N,N'*]$PtCl_2$	>1000	316
4	Tyr-D-Ala-Phe-Phe-NHNH-Phe-DAB[*N,N'*]$PtCl_2$	-	5.6
5	Tyr-D-Ala-Gly-Phe-Pdas-His[*N,O*]$PtCl_2$	251	63
6	Tyr-D-Ala-Gly-Phe-Pdas -Glu[*O,O'*]$PtCl_2$	>1000	>1000
7	Tyr-D-Ala-Gly-Phe-Ttds-Glu[*O,O'*]Pt[*N,N'*]Bpy	>1000	>1000

[a]*δ-ligand: [^{3}H] deltorphin,* [b]*μ-ligand: [^{3}H] DAMGO*
TOTA:1-amino-4,7,10-trioxa-13-tridecaamide;
Ttds: 4,7,10-trioxa-1,13-tridecanediamine succinic acid monoamide
Pdas: 1,3-propanediamine succinic acid monoamide

Impact of implemented structure modifications on compounds' binding affinity to opioid receptors is presented in the Table 1. Estimated diverse structure modifications provided changes in affinity at opioid receptor types. In comparison to previously referred bioactivity obtained for pioneer compound (1), modifications incorporating dicarboxylic Pt(II) coordination deteriorated binding results. For all synthesized analogues it was observed that the presence of Glu[*O,O'*]Pt coordination mode (compound 6 and 7) results in reduced receptors binding affinity. However, as expected, this type of Pt ion chelation dramatically increased molecules water solubility. The same effects were observed for monocarboxylic coordination of platinum ion (compound 5). Presumably lower binding activity is generated through steric hindrance of Pt ligands size disturbing opioid pharmacophore binding. Nevertheless providing second coordination type, consisting of diamino chelation [*N,N'*]Pt (compounds 2, 3, 4), retained opioid receptors' binding affinity. Biological activity was moreover determined towards different spacer type introduction. Presence of hydrophilic linkers (compound 3, 7) improved products' water solubility. However, obtained parameters were not as good as in the case of dicarboxylic coordination group properties. As expected, introduction of 1-amino-4,7,10-trioxa-13-tridecaamide spacer (compound 3) displayed better solubility in water system than 4,7,10-trioxa-1,13-tridecanediamine-succinic acid monoamide (compound 7) containing terminal aliphatic chain residue, with retention of opioid receptors' good binding affinity. The best opioid receptor binding affinities were obtained for compounds (compounds 2, 4) consisting of hydrazide bridged structures possessing diamino (DAP, DAB) platinum ion coordination.

Prepared derivatives are undergoing biological investigations regarding cancer cells antiproliferative activity properties.

Acknowledgements
Project supported by EU grant Normolife (LSHC-CT-2006-037733).

References

1. Głowińska, A., Tomczyszyn, A., Kosson, P., Matalińska, J., Lipkowski, A.W., Misicka A., *Proceedings 30th EPS*, 2-21-197, 404, (2008).
2. Hatzoglou, A., et al. *J. Clin. Endocrinol. Metab.* **80**, 418-423, (1995).
3. Misicka, A., Lipkowski, A.W., Głowińska, A., International Patent Application: PCT/PL2008/000068; Publication: WO/2009/04/18441.
4. Bartos, A., Uray, K., Hudecz, F. *Peptide Science* **92**, 2, 110-115 (2009).
5. Zhang, J., Li, Y., Sun, J. *Eur. J. Med. Chem.* **44**, 2758-2762 (2009).

Proceedings of the 31st European Peptide Symposium
Michal Lebl, Morten Meldal, Knud J. Jensen, Thomas Hoeg-Jensen (Editors)
European Peptide Society, 2010

Preclinical Pharmacokinetics of Myrcludex B, a Novel Entry Inhibitor for the Treatment of HBV Infections

A. Schieck[1], A. Meier[2], T. Müller[1], U. Haberkorn[1], S. Urban[2], and W. Mier[1]

[1]Department of Nuclear Medicine, University Hospital Heidelberg, Germany, [2]Department of Infectious Diseases, Molecular Virology, University Hospital Heidelberg, Germany

Introduction

About 360 million people are living with a chronic HBV infection. Currently approved therapies either block reverse transcription of the HBV-pregenomic RNA in infected hepatocytes or aim at stimulating the immune system with IFNα/pegIFNα. Both strategies show limitations as they are non-curative and in the case of nucleoside analogues, drug-resistant virus strains are likely to arise during treatment. On the search for new antiviral strategies, we have recently demonstrated that HBV L-protein derived lipopeptides block the HBV infection *in vitro* [1] and *in vivo* [2]. The inhibition of viral HBV infection by preventing virus entry into hepatocytes constitutes a new therapeutic strategy. Myrcludex B is a first-in-class HBV entry inhibitor currently progressing to clinical application. It consists of 47 N-terminal amino acids of the viral HBV L-protein and is myristoylated at the N-terminus. The lipopeptide specifically binds to and inactivates an essential HBV-receptor expressed on differentiated human hepatocytes. For the development of Myrcludex B as a new drug, pharmacodynamic and pharmacokinetic analyses are indispensable. To predict the pharmacokinetic behaviour of Myrcludex B in humans, the lipopeptide was radioactively labelled and the organ distribution was investigated in different species.

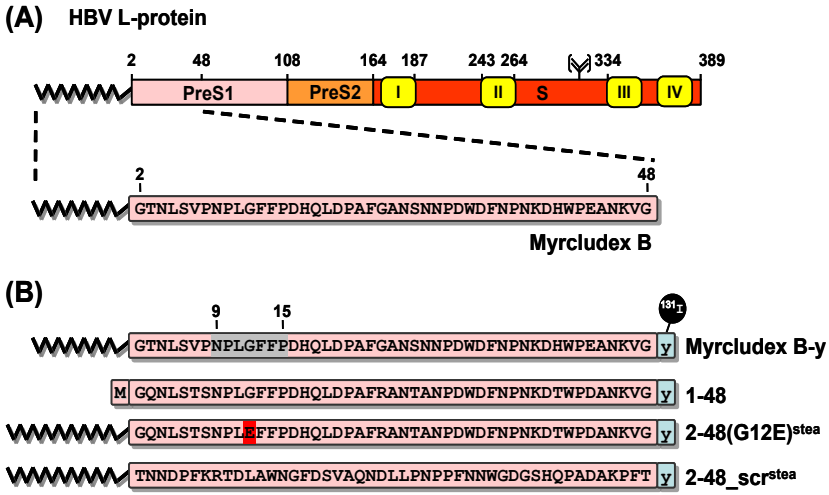

Fig. 1. A) Domain structure of the large HBV surface protein and the entry inhibitor Myrcludex B. The surface of the hepatitis B virion consists of three different envelope proteins (L, M and S). The L-protein consists of three subdomains, the preS1-domain (108 aa), the preS2-domain (55 aa) and the S-domain (226 aa), which contains four trans-membrane regions (I-IV). The L-protein is N-terminally myristoylated at position 2 of the peptide sequence. (B) HBVpreS-derived peptide sequences. For radioactive labeling with iodine D-tyrosine was added to the C-terminal end of the peptides. The sequence motif aa. 9-15 directs the peptide to the liver and is mandatory for the inhibitory activity of the preS-derived peptides. The point mutation of the peptide 2-48(G12E)^{stea} is accentuated in grey.

Results and Discussion

In vivo studies in mice, rats and dogs revealed a rapid and exclusive accumulation of the radiolabeled Myrcludex B-y in the liver. The integrity of Myrcludex B-y in the liver was characterized by radioactive RP-HPLC and HPLC-MS/MS measurements of liver homogenates. Up to 24 h p.i. the full length peptide could be detected. Surprisingly, cynomolgus monkeys did not show a preferencial uptake of the radiolabeled peptide in the liver. It was uniformly distributed and rapidly excreted via the kidneys. In this animal model, Myrcludex B behaved in a similar way to peptides with mutational changes within the essential sequence motif 9-NPLGFFP-15 in mice. *In vitro* experiments using FACS analyses confirmed this behavior. Highly specific binding of Myrcludex B to hepatocytes from mouse, rat, dog and human could be demonstrated whereas cynomolgous and rhesus monkey hepatocytes did not show binding.

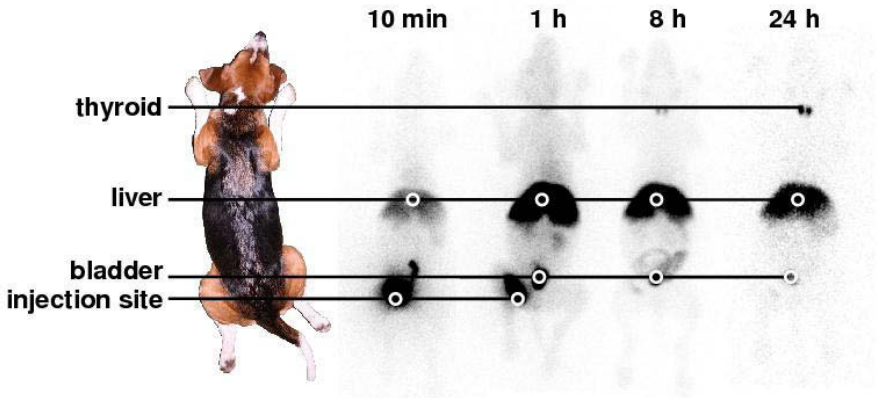

Fig. 2. Planar imaging of Myrcludex B-y-^{123}I in a beagle dog. Scintigraphies were performed 10 min, 1 h, 8 h and 24 h after subcutaneous injection. As demonstrated before in rats and mice, Myrcludex B shows a liver specific uptake in beagle dogs. Peak values were reached after 4 h. 24 h post injection it was still possible to detect the labeled compound in the liver. Significant amounts of radioactivity could be also seen in the areas corresponding to the urinary bladder, abdominal cavity and the thyroid.

Conclusion

Myrcludex B is a new antiviral drug that targets human hepatocytes and inhibits the HBV-preS1-specific virus entry. As human hepatocytes show strong binding of Myrcludex B and since the *in vivo* and *in vitro* data of the different species is coherent, we assume a rapid and exclusive accumulation of Myrcludex B in the human liver. The excellent pharmacokinetic properties, the extraordinary stability in human serum and the liver, its high potency to block a HBV infection, and its low toxicity, make Myrcludex B a promising therapeutic for the treatment of acute and chronic HBV infection.

References

1. Gripon, et al. *J. Virol.* **79**, 1613-1622 (2005).
2. Petersen, et al. *Nature Biotech.* **26**, 335-341 (2008).

Proceedings of the 31st European Peptide Symposium
Michal Lebl, Morten Meldal, Knud J. Jensen, Thomas Hoeg-Jensen (Editors)
European Peptide Society, 2010

Chemical Modification of Natural Immunomodulators Tuftsin and Muramyl Dipeptide Significantly Influence Their Biological Activity

Anna Wardowska[2], Krystyna Dzierzbicka[1], Małgorzata Rogalska[2], and Piotr Trzonkowski [2]

[1]Department of Organic Chemistry, Faculty of Chemistry, Technical University of Gdansk, Poland; [2]Laboratory of Clinical Immunology and Transplantology, Department of Immunology, Medical University of Gdansk, Poland

Introduction

Tuftsin and muramyl dipeptide (MDP) are well known particles displaying various immunomodulatory properities [1]. In this study, we are continuing our program of syntheses of muramyl dipeptide (MDP) and nor-muramyl dipeptide (nor-MDP) conjugates as potential immunomodulators [2-4]. We designed novel conjugates of MDP or nor-MDP with tuftsin and retro-tuftsin derivatives containing isopeptide bond (Figure 1).

Results and Discussion

The aim of this study was to asses the influence of the synthesized compounds on the viability of white blood cells: either heterogenous population of peripheral blood mononuclear cells (PBMC) or peripheral blood leukocytes (PBL) and isolated monocytes. The next step was to asses the observed influence on immune cells by determining the cytokine profile stimulated by the examined compounds. We analyzed three cytokines: two proinflammatory (IL-6, TNFα), as well as anti-inflammatory (IL-10).

Viability tests: PBMC – the viability of those cells was higher after incubation with the following conjugates: **10**, **11**, **12** and **13**; PBL – isolated leukocytes were most viable in presence of the above mentioned compounds (**10**-**13**) as well as conjugates **2** and **6**; monocytes – only conjugates **5**, **12** and **14** had promising impact on the viability of this phagocytes. The examined conjugates had little impact on TNFα production by PBMC, only compounds **7** and **14** slightly induces the secretion of this cytokine. The other analysed proinflammatory cytokine – IL-6 – was secreted on higher levels in presence of several conjugates: **2**, **5** and **13**, but the most active in this filed were **7** and **14**. Examined conjugates merely influenced anti-inflammatory cytokine production – IL-10.

We assume that the analysis of the cytokine profile will confirm our assumption that examined conjugates of tuftsin and MDP are capable of activating antibacterial mechanisms by switching on Th1 immune response.

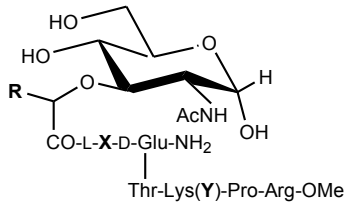

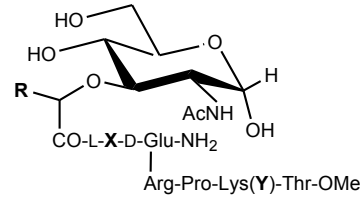

Comp.	R	X	Y
1	H	Ala	Ala
2	H	Ala	Val
3	H	Val	Ala
4	H	Val	Val
5	CH_3	Ala	Ala
6	CH_3	Ala	Val
7	CH_3	Val	Val
8	CH_3	Pro	Ala
9	CH_3	Pro	Val

Comp.	R	X	Y
10	H	Pro	Ala
11	H	Pro	Gly
12	CH_3	Pro	Val
13	H	Ala	Gly
14	H	Val	Gly

Fig. 1. Examined conjugates.

Acknowledgments
This work was supported by the Polish State Committee for Scientific Research (Grant No. N N405 181135).

References

1. Dzierzbicka, K., Kołodziejczyk, A.M. *Pol. J. Chem.* **77**, 373-395 (2003).
2. Dzierzbicka, K., Trzonkowski, P., Sewerynek, P., et al. *J. Pept. Sci.* **11**, 123-135 (2005).
3. Wardowska, A., Dzierzbicka, K., Trzonkowski, P., et al. *Int. Immunopharmacol*. **6**, 1560-1568 (2006).
4. Wardowska, A., Dzierzbicka, K., Szaryńska, M., et al. *Vaccine* **27**, 369-374 (2009).

Proceedings of the 31st European Peptide Symposium
Michal Lebl, Morten Meldal, Knud J. Jensen, Thomas Hoeg-Jensen (Editors)
European Peptide Society, 2010

Synthesis and Antimicrobial Evaluation of Temporin L Analogues Containing D-Amino Acids

Alfonso Carotenuto[1], Maria Luisa Mangoni[2], Ludovica Marcellini Hercolani Gaddi[2], Maria Rosaria Saviello[1], Salvatore Di Maro[1], Pietro Campiglia[3], Isabel Monterrey-Gomez[1], Luigia Auriemma[1], Ettore Novellino[1], and Paolo Grieco[1]

[1]Dept, Chimica Farmaceutica e Toss., University of Naples, "Federico II", Napoli, 80131, Italy; [2]Dept. Biochemical Science, University of Rome, "La Sapienza", Rome, 00185, Italy; [3]Dept. Pharmaceutical Science, University of Salerno, Fisciano, 84084, Italy

Introduction

Temporins A and L are antimicrobial peptides isolated from the skin of Red European frog *"Rana temporaria"*. Actually, they are the smallest natural antimicrobial amide-peptides characterized by short sequence (10-14 residues) with a net positive charge at neutral pH value. Temporins are active against a broad spectrum of microorganism: Temporin A (TA) (FLPLIGRVLSGIL-NH_2) is preferentially active against Gram-positive bacterial strains; Temporin L (TL) (FVQWFSKFLGRIL-NH_2) has the highest activity among all temporins against fungi, and bacteria, including resistant Gram-negative strains, but it shows hemolytic activity too. They have the ability to bind and permeate both artificial and biological membranes. We have recently investigated two members of this AMP family Temporin L and Temporin A [1-3]. At the same time, we developed new analogues of these peptides, among which Pro3TL (FVPWFSKFLGRILNH_2) exhibiting a higher antimicrobial activity and a lower hemolytic activity than the native peptide TL. To elucidate the molecular basis of the interaction of the native TL with bacterial membrane and to develop new potent analogues with improved activity, but without haemolytic activity, we synthesized new analogues of Pro3TL, where C-terminal residues were replaced one-by-one by D-amino acid. Here we report the preliminary results of this study.

Results and Discussion

The temporin L and their analogues were synthesized in solid phase by the classical strategy via Fmoc using Rink-Amide resin. Finally, the peptide chains were cleaved from the resin using TFA 95% TIS 2.5% H_2O 2.5% mixture. The purification was achieved using a semipreparative RP-HPLC C-18 bonded silica column (Vydac 218TP1010). The purified peptides were 98% pure as determined by analytical RP-HPLC. The correct molecular weight of the peptide was confirmed by mass spectrometry. The structures of synthesized peptides are showed in Table 1 [4]. In Figure 1, we report the NMR structures in DPC of Pro^3-Temporin L and Pro^3-$dLeu^9$-Temporin. In particular, main differences are localized in the C-terminal region of the peptides, where the TL-D3 is missing of helical character observed in Pro^3-Temporin L. This behaviour could be responsible of a reduction of hemolytic activity of peptide TL-D3, without significant difference in anti-microbial activity. The antimicrobial activity of these peptides was evaluated as the ability to inhibit the growth of Gram-positive, Gram-negative and fungi strains, using the microdilution broth method. Antimicrobial activities were expressed as the minimal inhibitory concentration (MIC), the concentration of peptide at which 100% inhibition of microbial growth is observed after 18–20 h of incubation. The results are shown in Table 2.

Table 1. Peptides synthesized

Temporin L	FVQWFSKFLGRIL-NH_2
TL-D1	FVPWFS*dK*FLGRIL-NH_2
TL-D2	FVQWFSK*dF*LGRIL-NH_2
TL-D3	FVPWFSKF*dL*GRIL-NH_2
TL-D4	FVPWFSKFLG*dR*IL-NH_2
TL-D5	FVPWFSKFLGR*dI*L-NH_2
TL-D6	FVPWFSKFLGRI*dL*-NH_2
TL-D7	FVPWFSKFL*dP*RIL-NH_2

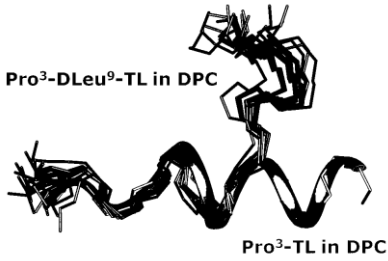

Fig. 1. Structures of Pro^3-TL and Pro^3-dLeu^9-TL.

Table 2. Antimicrobial activities of Temporin L analogues (MIC mM)

STRAINS	TL	TL-D1	TL-D2	TL-D3	TL-D4	TL-D5	TL-D6	TL-D7
Bacillus megaterium Bm11	1.6	3.0	3.0	1.6	1.6	3.0	3.0	3.0
Candida albicans ATCC 10231	12.5	12.5	12.5	6.0	6.0	12.5	12.5	25.0
Enterobacter faecalis ATCC15692	6.0	>50	50.0	25.0	25.0	25.0	25.0	50.0
Eschericia Coli D21	12.5	50.0	25.0	12.5	12.5	12.5	12.5	50.0
Pseudomonas aeruginosa ATCC 15692	25.0	>50	>50	>50	>50	50.0	50.0	>50
Staphylococcus aureus ATCC 25923	3.0	25.0	6.0	6.0	6.0	12.5	12.5	50.0
Staphylococcus aureus Cowan I	3.0	12.5	6.0	6.0	6.0	12.5	6.0	25.0
Yersinia pseudotubercolosis YPIII	3.0	12.5	6.0	6.0	6.0	12.5	6.0	25.0
Staphylococcus capiti 1	1.6	12.5	6.0	6.0	6.0	12.5	6.0	25.0
P. syringae pv tobaci1918NCPPB	6.0	>50	12.5	25.0	25.0	12.5	12.5	>50
Saccharomyces cerevisiae	6.0	12.5	12.5	6.0	6.0	6.0	12.5	12.5
Streptococcus pyogens ATCC 21547	6.0	12.5	6.0	6.0	6.0	12.5	12.5	25.0
Pseudomonas aeruginosa ATCC 27853	>50	>50	50.0	>50	>50	>50	>50	>50
Acinetobacter baumani ATCC 19606	6.0	25.0	12.5	12.5	12.5	12.5	25.0	50.0

Conclusion

This preliminarily study has highlighted that the amino acids Lys7, Gly10, and Ile12 could be important for antimicrobial and hemolytic activity. In fact, the peptides TL-D1, TL-D6, and TL-D7 showed to have a reduced biological activity in respect to the native peptide. Further biological studies are under investigation to evaluate the ability of these peptides to inhibit the growth of further Gram-positive, Gram-negative and yeast species and to evaluate their hemolytic activity**.**

Acknowledgments

The LC-MS and NMR spectral data were provided by Centro di Ricerca Interdipartimentale di Analisi Strumentale, Università degli Studi di Napoli "Federico II". The assistance of the staff is gratefully appreciated.

References

1 Shai, Y. *Biopolymers* **66**, 236-248 (2002).
2 Mangoni, M.L., Rinaldi, A.C., Di Giulio, A., Mignogna, G., Bozzi, A., Barra, D., Simmaco, M. *Eur. J. Biochem.* **267**, 1447-1454 (2000).
3 Carotenuto, A., Malfi, S., Saviello, M.R., Campiglia, P., Gomez-Monterrey, M.I., et.al. *J. Med. Chem.* **51**, 2354-2362 (2008).
4 Saviello, M.R., Malfi, S., Campiglia, P., Cavalli, A., Grieco, P., Novellino, E., Carotenuto, A. *Biochemistry* **49**, 1477-1485 (2010).

Proceedings of the 31st European Peptide Symposium
Michal Lebl, Morten Meldal, Knud J. Jensen, Thomas Hoeg-Jensen (Editors)
European Peptide Society, 2010

Conjugates of Tuftsin and Muramyl Dipeptide as Stimulators of Monocyte-Derived Dendritic Cells

Anna Wardowska[2], Krystyna Dzierzbicka[1], Agnieszka Menderska[2], and Piotr Trzonkowski[2]

[1]Department of Organic Chemistry, Faculty of Chemistry, Technical University of Gdansk, Poland; [2]Laboratory of Clinical Immunology and Transplantology, Department of Immunology, Medical University of Gdansk, Poland

Introduction

Dendritic cells, as professional APC (antigen presenting cells) play a role of a linkage between innate and adaptive immune response. Those cells have been widely and extensively studied as potential tools in therapy of several severe diseases. It has been already proven that muramyl dipeptide (MDP) and its analogues can accelerate maturation and activation of dendritic cells. But we were curious whether conjugates of muramyl dipeptide and retro-tuftsin synthesized in our laboratory (Figure 1) can be more powerful in modulating activity of that APC population [1-3].

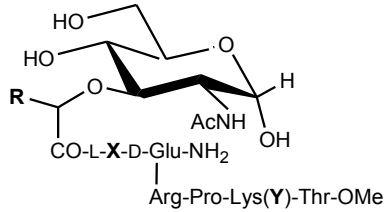

Comp.	R	X	Y
1	H	Pro	Ala
2	H	Pro	Gly
3	CH_3	Pro	Val
4	H	Ala	Gly

Fig. 1. Examined conjugates.

Results and Discussion

The maturity and activity of monocyte-derived dendritic cells was assessed by the flow cytometry analysis of the expression of two important cell markers: DC8O and HLA-DR. The obtained results of DC activity were strictly dependent on the very compound used to stimulation. MDP and LPS (positive control in all performed tests) are extremely strong stimulators of maturation and activation of DC – induced increased expression of DC8O and HLA-DR on the surface of the examined cells (Figure 2). Tuftsin and conjugate **3** could stimulate higher expression of mature DC markers, but to lesser extend than MDP and LPS. Moreover, tuftsin proved to be rather a poor inducer of DC activity. Conjugates **1**, **2** and **4** turned out to have the weakest impact on maturation and activation of DC, as they lowered the activation level in comparison to MDP. The examined conjugates of muramyl dipeptide and retro-tuftsin, seem to keep balance between the activity of both native immunomodulators.

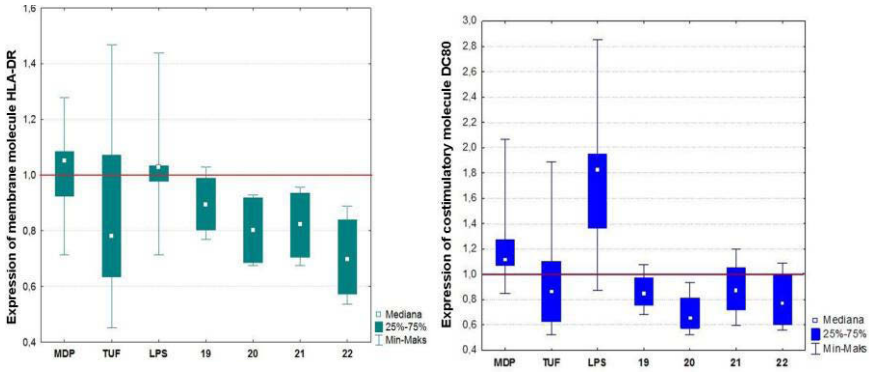

Fig. 2. The level of expression of molecule HLA-DR and DC80. Comparison of the stimulation levels between the negative control and test.

Acknowledgments

This work was supported by the Polish State Committee for Scientific Research (Grant No. N N405 181135).

References

1. Dzierzbicka, K., Trzonkowski, P., Sewerynek, P., et al. *J. Pept. Sci.* **11**, 123-135 (2005).
2. Wardowska, A., Dzierzbicka, K., Trzonkowski, P., et al. *Int. Immunopharmacol*. **6**, 1560-1568 (2006).
3. Wardowska, A., Dzierzbicka, K., Szaryńska, M., et al. *Vaccine* **27**, 369-374 (2009).

Proceedings of the 31st European Peptide Symposium
Michal Lebl, Morten Meldal, Knud J. Jensen, Thomas Hoeg-Jensen (Editors)
European Peptide Society, 2010

Synthesis of Peptide Analogs of the A2 Subunit (Sequence 558-565) of the Factor FVIIa of Blood Coagulation

Charis Anastasopoulos, Yiannis Sarigiannis, and George Stavropoulos*
Department of Chemistry, University of Patras, 26500, Patras, Greece

Introduction

It is known that platelets aggregation causes clotting in the blood vessels during the blood circulation due to several reasons. The clots formation is prevented by using anticoagulant drugs. On the other hand the coagulation of blood is important for maintaining vascular integrity and thus the precaution of an organism from bleedings and takes place through a process of thrombin production. The glycoprotein factor VIII (FVIII) is a key component of the fluid phase of the blood coagulation and is comprised of a heavy (A1-A2-B) and a light (A3-C1-C2) peptide chain, which are efficiently cleaved by proteases at three sites, two within the heavy and one within the light chain, resulting in alteration of its covalent structure and conformation [1,2]. This proteolytic cleavage is caused by thrombin or by factor Xa. Thrombin production is depended on FIXa, which plays a crucial role in curtailing of thrombin generation and accordingly on the additional activation of platelets. Peptides which are expected to inhibit selectively the maximization of thrombin production are based on the regions in which FVIII interacts with FIX. These both factors are essential for normal coagulation and deficiency of either is associated with the bleeding diathesis [3].

Results and Discussion

Based upon the acceptance that the sequence loop 558-565:

Ser^{558}-Val^{559}-Asp^{560}-Gln^{561}-Arg^{562}-Gly^{563}-Asn^{564}-Gln^{565}

of the A2 subunit domain of FVIIIa interacts with FIXa, our research efforts focus on the synthesis of linear and cyclic head to tail peptides and peptidomimetics, analogs of this sequence, aiming at the inhibition of interaction between FVIIIa and FIXa, in order to suspend the platelets adhesion and furthermore the thrombin production [4]. All the synthesized analogs are purified (RP-HPLC) and identified (ESI-MS). We have synthesized linear (No 1-3) and cyclic head to tail (No 4) peptides incorporating Asn or Asp (No 3). In addition, the analog (No 5) and smaller segments of the same sequence of the A2 subunit have been synthesized by replacement the Gly^{563} with NPhe (No 6-8).

The synthesized peptide analogs were investigated for their inhibitory activity and tested for clotting deficiency by measuring their activated partial thromboplastin time (APTT) and the reduction of the % value of the FVIIIa that they generate in samples containing recombinant FVIIIa, *in vitro* [5,6].

In the first biological assay, control A is poor platelet plasma (PPP) diluted with buffer Owren-Koller in propotion 1:1. In the second one, control A is pure recombinant factor VIIIa and control B is recombinant factor VIIIa diluted with buffer Owren-Koller in propotion 1:1. The results (Table 1) show clearly that the natural linear peptides (No 1, 2, 3) are the most active in the first biological assay. Also No 1 and the cyclic one as well as the peptidomimetics show increased inhibition of the FVIIIa activity. Specifically the No 5 shows activity similar to the natural No 1 in the time delay of APTT.

Table 1. Biological assays of the synthesized analogs

Analogs of the Peptide Sequence Ser^{558}–Gln^{565}	*APTT*	*% Value FVIIIa*
Control A	39.2	49.0
Control B		24.9
1. Ser^{558}–Val^{559}–Asp^{560}–Gln^{561}–Arg^{562}–Gly^{563}–Asn^{564}–Gln^{565}-OH	45.0	7.4
2. Ser^{558}–Val^{559}–Asp^{560}–Gln^{561}–Arg^{562}–Gly^{563}–Asn^{564}–Gln^{565}–$\mathbf{NH_2}$	44.3	15.7
3. Ser^{558}–Val^{559}–Asp^{560}–Gln^{561}–Arg^{562}–Gly^{563}–$\mathbf{Asp^{564}}$–Gln^{565}–OH	44.2	8.9
4. Cyclo[-Ser^{558}–Val^{559}–Asp^{560}–Gln^{561}–Arg^{562}–Gly^{563}–Asn^{564}–Gln^{565}]	40.1	7.5
5. Ser^{558}–Val^{559}–Asp^{560}–Gln^{561}–Arg^{562}–$\mathbf{NPhe^{563}}$–Asn^{564}–Gln^{565}–OH	44.5	5.4
6. Gln^{561}–Arg^{562}–$\mathbf{NPhe^{563}}$–Asn^{564}–Gln^{565}–OH	43.1	7.3
7. Arg^{562}–$\mathbf{NPhe^{563}}$–Asn^{564}–Gln^{565}–OH	42.4	13.1
8. $\mathbf{NPhe^{563}}$–Asn^{564}–Gln^{565}–OH	41.1	5.5

Acknowledgements
This Research Project is co-financed: 80% by European Union – European Social Fund and 20% by General Secretary of Research & Technology (PENED 03ED569). Also, we thank the pharmaceutical company SANOFI-AVENTIS for the financial fund.

References

1. Fay, P., Jenkins, V. *Blood Reviews* **19**, 15-27 (2005).
2. Obergfell, A., Sturm, A., Speer, C., et al. *Platelets* **17**, 448- 453 (2006).
3. Shen, B.W., Spiegel, P.C., Chang, C.H., et al. *Blood* **111**, 1240-1247 (2008).
4. Anastasopoulos, Ch., et al. In H. Lankinen (Ed), *Peptides 2008 (Proceedings of the 30th EPS)*, Helsinki, Finland, (2009), 416-417.
5. Minors, D. *Anaesthesia and Intensive Care Medicine* **8**, 214-216 (2007).
6. Barrowcliffe, T.W., Raut, S., et al. *Seminars in Thrombosis and Hemostasis* **28**, 247-255 (2002).

Proceedings of the 31st European Peptide Symposium
Michal Lebl, Morten Meldal, Knud J. Jensen, Thomas Hoeg-Jensen (Editors)
European Peptide Society, 2010

Peptides versus Nonpeptides as Therapeutics: An Exciting Challenge for Big Pharma

Maurice Manning, Stoytcho Stoev, and Krzysztof Bankowski
University of Toledo, College of Medicine, Toledo, Ohio, U.S.A.

Introduction

Peptides were abandoned by Big Pharma in favor of small molecule approaches to drug discovery, almost two decades ago [1,2]. During this period, the peptide field has been under constant siege by the illusionary promise of nonpeptides (see for example [3,4]), despite the striking reemergence of peptides as therapeutic agents [5,6,8]. Using examples from the vasopressin/oxytocin field and from the CRF field, we illustrate that despite impressive advances in the discovery of nonpeptide vasopressin and oxytocin antagonists, to date, only one nonpeptide vasopressin V_2/V_1 antagonist and one nonpeptide vasopressin V_2 antagonist have been approved by the FDA for clinical use [1,2] (Tables 1-4; adapted from 1,2). To date, no nonpeptide CRF antagonists have been approved for clinical use.

Results and Discussion

Table 1. Some nonpeptide vasopressin V_{1a} and V_{1b} antagonists

No.	*Company*	*Code*	*Name*	*Status*
1	Otsuka	OPC-21268	none	Phase II
2	Sanofi-Synthelabo	SR49059	Relcovaptan	**stopped**
3	Azevan	SRX251	none	Phase I
4	Sanofi*	SSR149415	Nelivaptan	**stopped**
5	Organon*	ORG52186	none	Pre-clinical

**V_{1b} antagonists*

Summary: No nonpeptide V_{1a} or V_{1b} vasopressin antagonists have been approved by the FDA [1,2].

Table 2. Nonpeptide oxytocin agonist

No.	*Company*	*Code*	*Name*	*Status*
1	Wyeth-Ayerst	WAY-267464	None	**failed**

Summary: No nonpeptide oxytocin agonist has been approved for clinical use [1].

Table 3. Some nonpeptide vasopressin V_2 and V_2/V_{1a} antagonists

		Receptor type: V_2		
No.	*Company*	*Code*	*Name*	*Status*
1	Otsuka	OPC-31260	Mozavaptan	**Failed**
2	Otsuka	OPC-41061	**Tolvaptan**	**FDA approved 2009**
3	Sanofi	SR121463(B)	Satavaptan	Phase III, **marketing Suspended**
4	Wyeth-Ayrest	VPA-985	Lixivaptan	Phase III
5	Astellas	YM-087	**Conivaptan**$^+$	FDA approved 2005, i.v. use only

$^+$*V_2/V_{1a} antagonist*

Summary:
•One nonpeptide vasopressin antagonist: (Tolvaptan) has received FDA approval [1].
•One nonpeptide vasopressin V_2/V_{1a} antagonist: (Conivaptan) has received FDA approval for i.v. use in hospitals [1,2].

Table 4. Some nonpeptide oxytocin antagonists

No.	*Company*	*Code*	*Name*	*Status*
1	Merck	L-368,899	none	Phase II, **discontinued**
2	Merck	L-371,257	none	**Discontinued**
3	Merck	L-372,257	none	Phase II, **discontinued**
4	GlaxoSmith-Kline	GSK2211149A	Retosiban	Phase II

Summary: No nonpeptide oxytocin antagonist has been approved for clinical use [2].

Perpetuating the Nonpeptide Myth-2010

The following two statements (A and B) from a recent highly influential publication [3] by Dr. Tom Insel – Director of the NIMH and a pioneer in studies on the behavioral effects of oxtocin and vasopressin in animals, illustrate this problematic phenomenon:

"Nonpeptide antagonists [7] and agonists [4], currently in development could transform the field" [3]. (B)"*...with the advent of nonpeptide oxytocin agonists [4] and expanded clinical trial ... there may soon be an opportunity to develop new pharmacological agents tailored to social deficits."*

Rebuttal of Nonpeptide Myth-2010

•The development of the Merck nonpeptide oxytocin antagonists (Table 4) was discontinued many years ago [2].

•The development of the nonpeptide oxytocin agonist WAY-267464 (Table 2) [4] developed by Wyeth (now Pfizer) was recently discontinued [1].

•The nonpeptide approach to a long acting oxytocin agonist [4] has been abandoned by Pfizer (personal communication to M. Manning during recent visit to Pfizer). Pfizer is now actually exploring the design of a long-acting, peptide based, oxytocin agonist for the treatment of ASD (Autism Spectrum Disorders).

Conclusions

Two decades of development and millions of dollars of investments by Big Pharma in the nonpeptide approach have resulted in only two therapeutic agents in the oxytocin/vasopressin field (Tolvaptan and Conivaptan), and no therapeutic drugs in the CRF field. By contrast, striking advances in the development of peptides as therapeutic agents have been made during this period [5,6,8]. Clearly it is time for Big Pharma to embrace the challenge offered by the enormous re-emerging therapeutic potential of peptides. Furthermore, granting agencies and Study Sections need to be made aware of:

i. the failure of nonpeptides in the clinic [1,2].
ii. the extraordinary successes of peptides as effective therapeutic agents [5,6,8].

Acknowledgement

We thank Ms. Anna Chlebowski for her expert assistance in the preparation of this manuscript and Dr. Rao Makineni for his financial support.

References

1. Manning, M., In Cordopatis, P. (Ed.) *Peptides versus Non-Peptides, European Peptide Society Newsletter*, 2010, p. 14.
2. Manning, M., et al., In Newmann, I.D. and Landgraf, R. (Eds.) *Peptide and non-peptide agonists and antagonists for the vasopressin and oxytocin V1a, V1b, V2 and OT receptors: research tools and potential therapeutic agents*, *Prog. Brain. Res*. **170**, 437-512 (2008).
3. Insel, T.R. *Neuron* **65**, 768-779 (2010).
4. Ring, R.H., et al. *Neuropharmacology* **58**, 69-77 (2010).
5. Vlieghe, P., et al. *Drug Discovery Today* **15**, 40-56 (2010).
6. Nestor, J. *Current Medicinal Chemistry* **16**, 4399-4418 (2009).
7. Pettibone, D.J., et al. *J. Pharmacol. Exp. Ther*. **264**, 308-312 (1993).
8. Reichert, J. *Development Trends for Peptide Therapeutics, Peptide Therapeutics Foundation*, 2010 Report.

Proceedings of the 31st European Peptide Symposium
Michal Lebl, Morten Meldal, Knud J. Jensen, Thomas Hoeg-Jensen (Editors)
European Peptide Society, 2010

Fluctuations and the Rate-Limiting Step of Peptide-Induced Membrane Leakage

Claudia Mazzuca[1], Barbara Orioni[1], Massimiliano Coletta[2], Fernando Formaggio[3], Claudio Toniolo[3], Giuseppe Maulucci[4], Marco De Spirito[4], Basilio Pispisa[1], Mariano Venanzi[1], and Lorenzo Stella[1]

[1]Dipartimento di Scienze e Tecnologie Chimiche, Università di Roma "Tor Vergata", Rome, 00133, Italy; [1]Dipartimento di Medicina Sperimentale e Scienze Biochimiche, Università di Roma "Tor Vergata", Rome, 00133, Italy; [3]Dipartimento di Scienze Chimiche, Università di Padova, Padova, 35131, Italy; [4]Istituto di Fisica, Università Cattolica del Sacro Cuore, Rome, 00168, Italy

Introduction

Peptide-induced vesicle leakage is a common experimental test for the membrane-perturbing activity of antimicrobial peptides. Obviously, a quantitative analysis of the peptide-induced leakage kinetics can potentially provide several insights into the mechanism of pore formation. The release curves determined in these experiments in most cases share two peculiar characteristics: they are usually very slow, requiring minutes to hours for complete release of vesicle contents, and exhibit a biphasic behavior (Figure 1). In this work, we systematically evaluate all of the possibilities for the rate-limiting step, by taking as an example a very well characterized peptide, *i.e.* the peptaibol trichogin GA IV [1-4], and provide a stochastic model of the leakage process based on the discrete nature of a vesicle suspension.

Results and Discussion

Stopped-flow kinetic experiments show that peptide-membrane binding, peptide translocation to the inner leaflet of the membrane and peptide aggregation in the bilayer are completed in a few seconds. Direct observation of peptide-induced GUV leakage indicates that, once a pore is formed, liposomes empty very quickly. Therefore, all these processes can be ruled out as the rate-limiting step of the vesicle leakage process, which is much slower. On the other hand, our data show that vesicle leakage rate increases with vesicle radius, and peptides are continuously and rapidly exchanging among vesicles. This led us to propose a simple stochastic model: a vesicle (or cell) suspension is obviously a discrete system, and the release of the contents of each vesicle is not influenced by the other liposomes in the sample. Furthermore, a liposome is a nanoscopic system, and the number

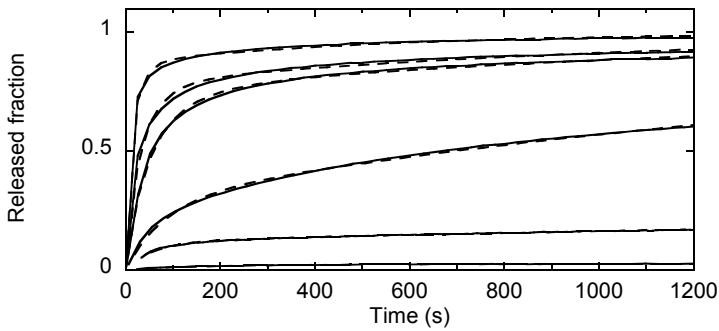

Fig. 1. Kinetics of carboxyfluorescein release after addition of the trichogin GA IV analogue F10 [1] to a LUV suspension. [Lipid]=0.2mM and [F10]=1.2 μM; 2.3 μM; 3.7 μM; 4.7 μM; 6.9 μM; 10.8 μM; (from bottom to top). The dashed lines are the best fit to the data with the model described in the present paper.

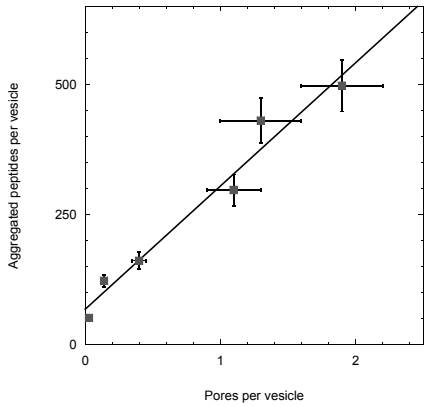

Fig. 2. Correlation between the average number of pores in a single vesicle, obtained from the fit to the leakage kinetics, and the number of membrane-bound peptide molecules participating in aggregates, determined from time-resolved fluorescence experiments at equilibrium. ePC/cholesterol LUVs, [lipid]=0.2 mM, vesicle radius 50 nm.

of peptides or the number of pores in each vesicle can be rather small, well below the thermodynamic limit. Therefore, peptide exchange among vesicles produces significant fluctuations over time in the number of peptide molecules bound to each vesicle, and in the formation of pores.

According to this model, the fast initial leakage is caused by those vesicles which, after the random distribution of peptides among liposomes, already contain at least one pore, while the slower release is associated to the time needed in an intact vesicle to occasionally reach the critical number of bound peptides necessary for pore formation. Fluctuations due to peptide exchange among vesicles represent therefore the rate-limiting step of such a slow mechanism. Such a model can be described quantitatively by the following equation:

$$R(t) = 1 - e^{-\bar{n}[1-\exp(-t/\varphi)]} e^{-\bar{n}t/\tau}$$

where R is the fraction of vesicles' contents released, ϕ and τ are characteristic times for vesicle emptying through a formed pore, and for peptide exchange among vesicles, respectively, $\bar{n}$ is the average number of pores per vesicle, and t is time.

Figure 1 reports the best fit of the leakage data to this equation as dotted lines. The most important result of this analysis is that it provides an estimate of $\bar{n}$, which in this case could be compared with the concentration of membrane-bound peptides participating in aggregates, determined independently from time-resolved experiments [1]. The strong correlation between the two datasets (Figure 2) provides strong support both to the kinetic model and to the hypothesis that aggregates of membrane-bound peptides constitute the pores.

Acknowledgments
This work was supported by grant PRIN 2008 (Italian Ministry of Education, University and Research, MIUR).

References

1. Stella, L., et al. *Biophys. J.* **86**, 936-945 (2004).
2. Mazzuca, C., et al. *Biophys. J.* **88**, 3411-3421 (2005).
3. Gatto, E. et al. *J. Phys. Chem. B* **110**, 22813-22818 (2006).
4. Bocchinfuso, G. et al. *J. Pept. Sci.* **15**, 550-558 (2009).

Proceedings of the 31st European Peptide Symposium
Michal Lebl, Morten Meldal, Knud J. Jensen, Thomas Hoeg-Jensen (Editors)
European Peptide Society, 2010

Effect of Helix Kink on the Activity and Selectivity of an Antimicrobial Peptide

Sara Bobone[1], Gianfranco Bocchinfuso[1], Antonio Palleschi[1], Jin Young Kim[2], Yoonkyung Park[2], Kyung-Soo Hahm[2,3], and Lorenzo Stella[1]

[1]Dipartimento di Scienze e Tecnologie Chimiche, Università di Roma Tor Vergata, Rome, 00133, Italy; [2]Research Center for Proteineous Materials (RCPM), Chosun University, 375 Seosuk-Dong, Dong-Ku, South Korea; [3]Department of Cellular Molecular Medicine, Chosun University, 375 Seosuk-Dong, Dong-Ku, South Korea

Introduction

Antimicrobial peptides (AMPs) are oligopeptides (usually less than 40 residues long) with a strong antibacterial activity, linked to their ability to perturb the permeability of bacterial cell membranes. For this reason, they are promising compounds for the development of new antibiotic drugs, but a deep understanding of the structural features required for activity is necessary to design new molecules with improved pharmaceutical properties. AMPs often show an amphiphilic helical structure and a cationic character. Furthermore, many helical peptides have a kink or a hinge in the middle of their structure, caused by a Pro or Gly residue. In order to understand the role of this kink in peptide activity and selectivity we designed a series of analogues of the amphipathic, helical and cationic peptide P5 [1,2], in which the central Pro was moved along the peptide sequence, or removed altogether. Cytotoxicity and hemolicity studies were carried out with the different analogues; the activity was also studied on model membranes of different compositions, mimicking bacterial or eukaryotic cell membranes.

Results and Discussion

The peptides' activity against bacteria was only influenced marginally by Pro position. On the other hand, the hemolytic activity of the analogues increased significantly and systematically as the Pro residue was moved towards the termini, with P5F (the peptide lacking the Pro) being the most toxic against red blood cells, even at very low concentrations (Figure 1).

Studies with model membranes showed that the petides exhibit similar differences in selectivity also with liposomes with a lipid composition mimicking that of eukaryotic or bacterial membranes, as indicated by vesicle leakage experiments and studies on the peptides' effects on membrane order. Peptide-membrane binding experiments performed by exploiting the intrinsic fluorescence due to the presence of a single Trp residue in the

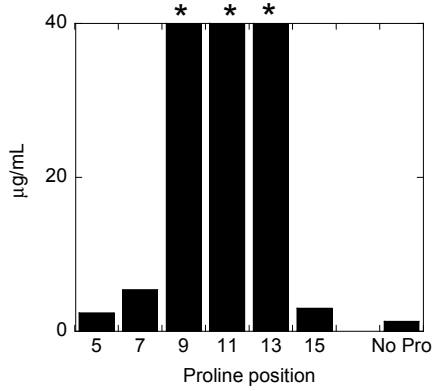

Fig. 1. Analogue concentration causing 5% hemolyticity. The maximal concentration tested was 40 μg/mL. Analogues indicated by an asterisk did not cause hemolysis at all concentrations tested.

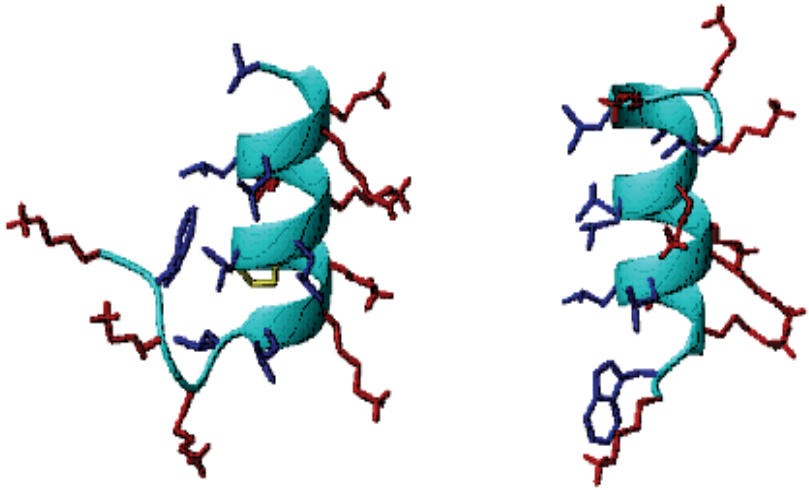

Fig. 2. Structures of P5 (left) and P5F (right) in water, as obtained from the MD simulations. Hydrophobic and charged sidechains are shown in blue (darker grey) and red (lighter grey), respectively.

sequence of the analogues showed that the different activities of the peptides correlate with their affinity for lipid bilayers of different composition: the kinked P5 peptide, which exhibits the highest selectivity for bacterial cells, has a dramatically higher affinity for negatively charged vesicles (mimicking the composition of bacterial membranes) than for neutral liposomes (which are similar to mammalian cells). On the other hand, analogue P5F, lacking the central Pro residue, exhibits comparable affinities for anionic and neutral membranes. The P5E analogue, with the Proline in position 15, shows an intermediate behavior.

Fluorescence quenching studies with the water-soluble quencher acrylamide suggested that all analogues bind on the membrane surface, at a very shallow depth. CD experiments and molecular dynamics (MD) simulations (Figure 2) indicated that all analogues are largely helical when associated to membranes or to micelles, so that their differences in water-membrane partition are probably due to their behaviour in the water phase.

In water the fraction of helical structure is significantly reduced for P5, while P5F maintains its helical conformation. HPLC retention times and theoretical calculations indicate that in water the helix-breaking Pro residue allows P5 to attain a closed conformation, in which its hydrophobic residues are partially shielded from the solvent. This is also confirmed by time-resolved fluorescence experiments, in which the Trp residue of P5F was more accessible to a quencher than that of P5. This property might explain the low affinity of P5 towards neutral bilayers, since in this case the hydrophobic effect is the main driving force of peptide-membrane association.

The observed differences in the biological and biophysical properties of the analogues highlight the role of the central Pro-induced kink in the selectivity of AMPs, and provide hints for the design of new, highly selective compounds.

Acknowledgments

This project was supported by the Italian Foreign Affair Ministry and by the Korea Foundation for International Cooperation of Science & Technology (KIKOS). Computational resources were kindly made available by the Fermi and CASPUR Research Centers (Rome).

References

1. Park, Y., et al. *Biotech. Lett.* **25**, 1305-1310 (2003).
2. Park, Y., et al. *Biochim. Biophys. Acta* **1764**, 24-32 (2006).

Proceedings of the 31st European Peptide Symposium
Michal Lebl, Morten Meldal, Knud J. Jensen, Thomas Hoeg-Jensen (Editors)
European Peptide Society, 2010

Membrane Insertion of *para*-Cyanophenylalanine Labeled Alamethicin Analogues. Correlation of Fluorescence and Infrared Absorption Data

Sara Bobone[1], Marta De Zotti[2], Annalisa Bortolotti[1], Gema Ballano[2], Fernando Formaggio[2], Claudio Toniolo[2], and Lorenzo Stella[1]

[1]Department of Chemical Sciences and Technologies, University of Rome "Tor Vergata", Rome, 00133, Italy; [2]ICB, Padova Unit, CNR, Department of Chemistry, University of Padova, Padova, 35131, Italy

Introduction

Different classes of peptides, such as antimicrobial, cell penetrating, and fusogenic peptides, exert their bioactivities by interacting with cellular membranes. Therefore, the determination of their position and orientation inside a lipid bilayer is a fundamental step in the characterization of their mechanism of action. In this respect, the α-amino acid *para*-cyanophenylalanine (*p*CNPhe) is a very promising probe, since it can be employed both in fluorescence and in IR absorption experiments [1,2]. Its fluorescence quantum yield is significant (0.11, as compared to 0.025 for Phe), and the C≡N stretching vibrational transition is located around 2230 cm^{-1} (*i.e.*, far from the water background absorption) and is sensitive to the medium polarity.

Results and Discussion

In this study, we exploited the peculiar properties of *p*CNPhe to investigate the membrane interaction of the [Glu(OMe)^{7,18,19}] alamethicin analogue by synthesizing three mono-labeled peptides in which Ala^4 (AL4), Val^9 (AL9) or Val^{15} (AL15) are substituted by *p*CNPhe. Liposome leakage kinetics data indicated that the label does not perturb significantly the peptide activity. Furthermore, the *p*CNPhe fluorescence (Figure 1) is sensitive to the fluorophore environment, allowing a characterization of peptide aggregation and water-membrane partition. These experiments showed a very similar behavior for all analogues.

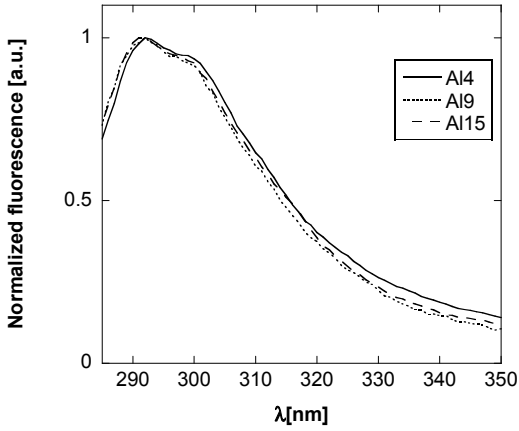

Fig. 1. Fluorescence spectra of the three alamethicin analogues AL4, AL9 and AL15 in phosphate buffer, 140 mM NaCl, 0.1 mM EDTA, pH=7.4., exhibiting the characteristic emission bands of the pCNPhe chromophore.

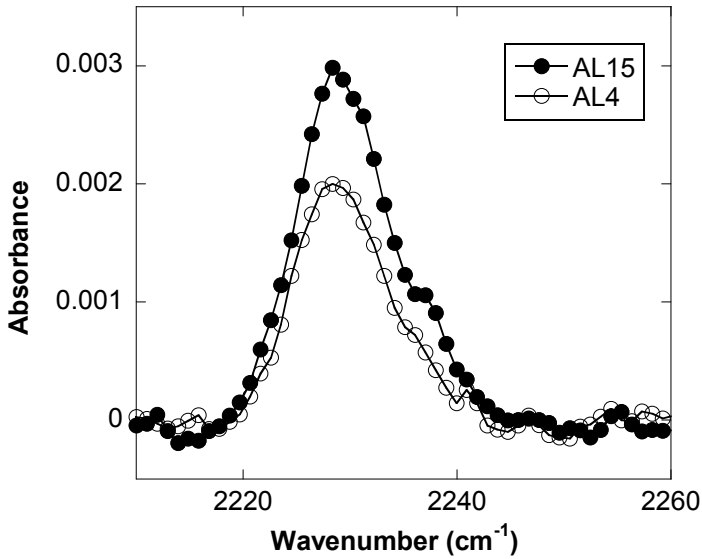

Fig. 2. ATR-FTIR spectra of the alamethicin analogues AL4 and AL15 associated to POPC phospholipid bilayers. The band near 2230 cm^{-1} is typical of the pCNPhe moiety.

The position of the fluorophore in the membrane was determined by fluorescence, depth-dependent quenching experiments, performed using vesicles containing lipids labeled with a doxyl group at different positions. These data showed that the *p*CNPhe probe in AL4 was quenched only by lipids labeled on their headgroup, while the probe in AL15 was not significantly quenched, irrespective of the quencher position. These finding indicated that the N-terminus of alamethicin is associated to the membrane, although in a very superficial position, while the C-terminus remains in the aqueous phase. ATR-FTIR experiments on AL4 and Al15 associated to POPC phospholipid bilayers showed that for both analogues the absorption band of Phe_{CN} was centered at about 2230 cm^{-1} (Figure 2), suggesting a similar probe environment for the two peptides. This finding confirmed a location of the peptide at the membrane surface, parallel to it. Overall, these data offer a picture of alamethicin interaction with the membrane and confirm that *p*CNPhe is an extremely useful probe in fluorescence and IR absorption studies of peptide-membrane interactions.

Acknowledgments
This work was supported by grant PRIN 2008 (Italian Ministry of Education, University and Research, MIUR).

References
1. Tucker, M.J., Oyola, R., Gai, F. *J. Phys. Chem.* **B109**, 4788-4795 (2005).
2. Marek, P., Mukherjee, S., Zanni, M.T., Raleigh, D.P. *J. Mol. Biol.* **400**, 878-888 (2010).

Proceedings of the 31st European Peptide Symposium
Michal Lebl, Morten Meldal, Knud J. Jensen, Thomas Hoeg-Jensen (Editors)
European Peptide Society, 2010

Cell-Penetrating Peptides as Adenovirus Vector Carrier

Shinya Kida[1], Yusuke Eto[2], Yasuo Yoshioka[2], Shinsaku Nakagawa[2], Keiko Hojo[1], Mitsuko Maeda[1], and Koichi Kawasaki[1]

[1]Life Science Center, Faculty of Pharmaceutical Sciences, Kobe Gakuin University, 1-1, Minatojima, Chuo-ku, Kobe 650-8586, Japan; [2]Graduate School of Pharmaceutical Sciences, Osaka University, 1-6, Yamadaoka, Suita, Osaka, 565-0871, Japan

Introduction

Application of gene therapy is expected for the treatment of not only genetic disease but also other intractable diseases such as cancer. A key aspect of gene therapy lies in the vector used for transgenesis. Adenovirus (Ad) with appropriate gene-transduction and gene-expression properties is widely used in gene therapy studies; however, for routine clinical procedures, more efficient transfer vectors must be developed. We aimed to modify the viable virus, Ad, with peptide transporters for preparation of a peptide-Ad hybrid as shown in Figure 1.

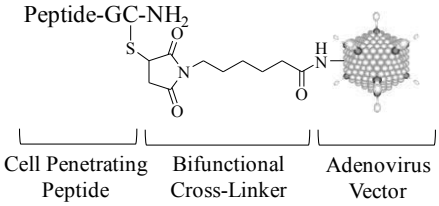

Fig. 1. Structure of cell penetrating peptide-Ad hybrid.

Results and Discussion

We reported that Asp-Gly-Arg (RGD)-peptide conjugate of Ad can transfer genes efficiently through integrin-mediated endocytosis. Although Ad also transfers genes through its receptor, coxsackie-adenovirus receptor (CAR), the RGD-conjugated Ad exhibits efficient gene transfer activity even in a CAR-negative cell line, B16BL6 [1]. We also reported that Tat(48-60,GRKKRRQRRRPPQ) conjugated Ad exhibited excellent gene transfer efficiency in B16BL6 cells [2]. Following the Tat-related peptide hybrid of Ad, Pro-rich peptide derivative and octaarginine-related peptide hybrids of Ad were prepared and examined for cell-penetrating ability. A Pro-rich peptide, $(Val\text{-}Arg\text{-}Leu\text{-}Pro\text{-}Pro\text{-}Pro)_3$, derived from the *N*-terminal domain of maize γ-zein, was reported as a new family of potential carriers, which have cell internalization property with no toxicity[3,4]. The octaarginine peptide contains eight arginine residues optimal for efficient translocation of Arg-rich peptides, as proposed by Futaki, et al. [5]. The Pro-rich peptide derivative[(acetyl-$(VRLPPP)_3$-GC-amide, ProrGC] and the octaarginine derivative (acetyl-RRRRRRRR-GC-amide, R8GC) were prepared by the solid phase method. Each synthetic peptide was coupled with the heterobifunctional cross-linking reagent, 6-maleimidohexanoic acid *N*-hydroxysuccinimide ester (MHSu) and then conjugated to the Ad vector containing luciferase gene. Each peptide-modified Ad was examined for gene transfer activity in B16BL6 cells and A549 cells.

The gene transduction efficiency of each novel conjugate was compared with that of WT-Ad in cells with and without Car, which transports Ad across the plasma membrane: A549 (CAR-positive) and B16BL6 (CAR-negative) cells. The gene transduction efficiency, or luciferase activity, of R8GC-Ad and ProrGC-Ad is given in Tables 2 and 3, respectively. R8GC-Ad and ProrGC-Ad exhibited lower luciferase activity in A549 cells. Modification of Ad might disturb the binding between Ad and its receptor, CAR. On the other hand, both R8GC-Ad and ProrGC-Ad exhibited higher luciferase activity than WT-Ad in B16BL6 cells: the activity was about 30 and 20 times, respectively, as high as WT-Ad. These results suggest that cell-penetrating peptide conjugation to Ad enhances Ad infection in the absence of CAR, where gene transduction was difficult for Wt-Ad. It suggests that Ad modified with cell-penetrating peptides has a wide CAR-independent infection area. The

chemically-modified functional Ad hybrid is thus expected to be an efficient tool for the development of gene transfer therapy.

Table 1. Transduction efficiency of R8GC-Ad and WT-Ad into A549 and B16BL6 cells

	Luciferase activity (RLU/well)	
	B16BL6 (CAR-negative)	*A549 (CAR-positive)*
WT-Ad	7.8×10^5	3.6×10^8
R8-GC-Ad	2.4×10^7	8.2×10^7

Table 2. Transduction efficiency of ProrGC-Ad and WT-Ad into A549 and B16BL6 cells

	Luciferase activity (RLU/well)	
	B16BL6 (CAR-negative)	*A549 (CAR-positive)*
WT-Ad	3.0×10^5	3.6×10^8
Pro-pep-GC-Ad	6.1×10^6	1.4×10^6

In summary, we prepared peptides (R8-GC-NH_2 and Pro-pep-GC-NH_2) that can serve as efficient Ad transporters into CAR-negative cells (B16BL6). The chemically modified Ads, R8-GC-Ad and Pro-pep-GC-Ad, are promising tools for the development of gene transfer therapy. The modification of a viable virus with a synthetic peptide is a new field of peptide chemistry and will be a potent new resource for developing virus function.

Acknowledgments
This work was supported in part by Grant-in-Aid for Scientific Research and by "Academic Frontier" Project for Private Universities matching fund subsidy from the Japanese Ministry of Education, Culture, Sports, Science and Technology, 2006-2010.

References

1. Maeda, M., Kida. S., Hojo, K., Eto, Y., Gao, J-Q., Kurachi, S., Sekiguchi, F., Mizuguchi, H., Hayakawa, T., Mayumi, T., Nakagawa, S., Kawasaki, K. *Bioog. Med. Chem. Lett.* **15**, 621-624 (2005).
2. Kida, S., Maeda, M., Hojo, K., Eto, Y., Gao, J-Q., Kurachi, S., Mizuguchi, H., Hayakawa, T., Mayumi, T., Nakagawa, S., Kawasaki, K. *Bioorg. Med. Chem. Lett.* **16**, 743-745(2006).
3. Fernandez-Carneado, J., Kogan, M.J., Castel, S., Giralt, E. *Angew. Chem. Int. Ed. Engl.* **43**, 1811-1814 (2004).
4. Fernandez-Carneado, J., Kogan, M.J., Pujals, S., Lopez-Iglesias, C., Heitz, F., Giralt, E., *J. Peptide Res*. **65**, 580-590 (2005).
5. Futaki, S., Suzuki, T., Ohashi, W., Yagami, T., Tanaka, S., Ueda, K., Sugiura, Y. *J. Biol. Chem.* **276**, 5836-5840 (2001).

Proceedings of the 31st European Peptide Symposium
Michal Lebl, Morten Meldal, Knud J. Jensen, Thomas Hoeg-Jensen (Editors)
European Peptide Society, 2010

Jelleine-I Analogues with Improved Antibacterial Activity

Paul R. Hansen
IGM-Bioorganic Chemistry, Faculty of Life Sciences, University of Copenhagen, Denmark

Introduction

Jelleine-I (Figure 1) is an octapeptide amide, H-PFKLSLHL-NH_2 (**1**) isolated from Royal Jelly of honeybees (*Apis mellifera*) [1]. The peptide is active against Gram-positive and Gram-negative bacteria. However, Jelleine-I is also hemolytic towards human erythrocytes. In the present paper, we report the synthesis and antibacterial activity of 21 analogues of Jelleine I including an Ala-scan and single residue substitutions.

Results and Discussion

The peptides were synthesized using standard Fmoc chemistry, on a TentaGel RAM resin (50 mg, loading 0.24 mmol/g). Activation of the Fmoc amino acids and formation of peptide bonds were carried out using DIC and HOBt. All Fmoc amino acids and coupling reagents were used in fourfold excess. Fmoc deprotection was accomplished by treatment with 20% piperidine in NMP (1 x 3 min and 1 x 7 minutes). The peptides were cleaved from the solid support along with the permanent side chain protection groups using TFA/H_2O/TIS/thioanisole (90:5:2.5:2.5: v/v). The crude peptides were purified by preparative HPLC and characterized by MALDI-TOF-MS. A stock peptide solution in 1% DMSO was prepared and the concentration was determined by amino acid analysis. The peptides were tested against the American Type Culture Collection (ATCC) *S. aureus* ATCC 25923 and *E. coli* ATCC 25922. The MIC of each peptide was determined using a microtitre broth dilution assay modified from the method of Hancock [2]. Briefly, serial twofold dilutions of the peptides were made in solutions of 0.2% bovine serum albumin and 0.01% acetic acid in 96-well polypropylene microtiter plates in volumes of 50 µL.

To each well was added 50 µL of the test organism in Mueller Hinton Broth to a final concentration of approximately 2×10^5 CFU/mL. The plates were incubated overnight at 37°C and the MIC of each peptide was read as the lowest concentration of peptide that inhibited visible growth of the organism. All MIC determinations were performed in duplicate, and are the average of three independent determinations.

Freshly drawn human erythrocytes in citrate-dextrose-phosphate (CDP) buffer, from Copenhagen University Hospital were used to determine the hemolytic activity as described by Ryge and Hansen [3].

Alanine positional scanning showed restrictions on 6 out of the 8 residues (data not shown), and a moderate drop in MIC-activity for the [Ala^1] and [Ala^5] Jelleine-I analogues (Table 1).

Based on the above results, two series of analogues were designed and tested. Pro^1 was replaced with either Ala or 3-(2 naphthyl)-L-alanine (X) and Ser^5 was replaced with Asn or one of the more hydrophobic amino acids Val, Leu, Ile, Trp, Phe. The MICs obtained for the Jelleine-I analogues are listed in Table 1.

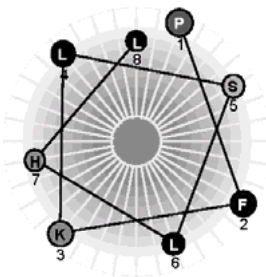

Fig. 1. Helical wheel of Jelleine-I.

Table 1. MIC (μM) and hemolytic activity (50 μM) of the Jelleine-I analogues

	Peptide	*S.aureus*	*E.coli*	*% Hemolysis*
1	H-PFKLSLHL-NH_2	6.25-12.5	1.56	27
2	H-AFKLSLHL-NH_2	25	3.125	9
3	H-PFKLALHL-NH_2	25-50	12.5	8
4	H-AFKLVLHL-NH_2	25	6.25	0
5	H-AFKLLLHL-NH_2	12.5	25	1
6	H-AFKLILHL-NH_2	1.56	1.56	0
7	H-AFKLFLHL-NH_2	12.5	3.125	1
8	H-AFKLNLHL-NH_2	100	6.25	3
9	H-AFKLWLHL-NH_2	3.125	6.25	36
10	H-XFKLVLHL-NH_2	25	100	0
11	H-XFKLLLHL-NH_2	12.5	100	3
12	H-XFKLILHL-NH_2	100	>100	0
13	H-XFKLFLHL-NH_2	6.25	100	0
14	H-XFKLNLHL-NH_2	6.25	1.56	44
15	H-XFKLWLHL-NH_2	25	-	1
16	H-XFKLKLHL-NH_2	-	3.125	7

Our most promising candidate was [Ala^1, Ile^5] Jelleine-I which displayed improved MIC-activities towards *S. aureus* and *E. coli* (1.56 μM both strains) as compared with Jelleine-I, which showed 6.25-12.5 μM and 1.56 μM against *S. aureus* and *E. coli*, respectively. Furthermore, [Ala^1, Ile^5] Jelleine-I showed no hemolytic activity.

Acknowledgements
Jette Petersen and Sophie Andresen are thanked for skilled technical assistance. This work was supported by the Danish Council for Strategic Research, the Augustinus Foundation, the Frimodt–Heineke Foundation, the Family Hede Nielsen Foundation, the JS Foundation and the Aase & Ejnar Danielsens Foundation.

References
1. Fontana, R., et al. *Peptides* **25**, 919-928 (2004).
2. http://www.cmdr.ubc.ca/bobh/methods.htm.
3. Ryge,T.S., Hansen, P.R. *J. Peptide Science* **11**,727-734 (2005).

Proceedings of the 31st European Peptide Symposium
Michal Lebl, Morten Meldal, Knud J. Jensen, Thomas Hoeg-Jensen (Editors)
European Peptide Society, 2010

Antimicrobial Activity of Small 3-(2-Naphthyl)-L-Alanine Containing Peptides

Paul R. Hansen[1,3] and Niels-Frimodt Møller[2,3]

[1]IGM-Bioorganic Chemistry, Faculty of Life Sciences, University of Copenhagen, Denmark; [2]National Center for Antimicrobials and Infection Control, SSI, Denmark; [3]Danish National Center for Antibiotic Research and Development, Denmark

Introduction

Antibiotic-resistant pathogens have become a very serious problem world-wide. Most alarming is the discovery of Gram-negative Enterobacteriaceae containing New Delhi metallo-β-lactamase 1 (NDM-1) which are highly resistant to many antibiotic classes, including β-lactams, fluoroquinolones, and aminoglycosides—the main antibiotic classes for the treatment of Gram-negative infections [1].

Antimicrobial peptides (AMPs) are a part of the innate immunity in all multicellular organisms and are promising lead structures for developing new antimicrobial agents [2]. However, AMPs often display undesirable pharmaceutical properties, such as susceptibility to proteolytic breakdown. This may be circumvented by incorporation of non-standard amino acids into the peptide, such as 3-(2-naphthyl)-L-alanine.

In the present study, we investigated the antimicrobial activities of 6 peptides containing 3-(2-naphthyl)-L-alanine: H-XFXLKKK-NH_2 (**1**), H-FXLKKK-NH_2 (**2**), H-XFLKKK-NH_2 (**3**), H-XKFKXKLKK-NH_2 (**4**), H-KFKXKLKK-NH_2 (**5**), H-XKFKKLKK-NH_2 (**6**), X being the non-proteinogenic amino acid.

Results and Discussion

The peptides were synthesized using standard Fmoc chemistry, on a TentaGel RAM resin (50 mg, loading 0.24 mmol/g). Activation of the Fmoc amino acids and formation of peptide bonds were carried out using DIC and HOBt. All Fmoc amino acids and coupling reagents were used in fourfold excess. Fmoc deprotection was accomplished by treatment with 20% piperidine in NMP (1 x 3 min and 1 x 7 minutes). The peptides were cleaved from the solid support along with the permanent side chain protection groups using TFA/H_2O/TIS/thioanisole (90:5:2.5:2.5: v/v).

The crude peptides were purified by preparative HPLC and characterized by MALDI-TOF-MS. A stock peptide solution in 1% DMSO was prepared and the concentration was determined by amino acid analysis. The peptides were tested against clinically relevant bacteria and fungi as described previously [3].

The MIC of each peptide was determined using a microtitre broth dilution assay modified from the method of Hancock [4]. Briefly, serial twofold dilutions of the peptides were made in solutions of 0.2% bovine serum albumin and 0.01% acetic acid in 96-well polypropylene microtiter plates in volumes of 50 µL. To each well was added 50 µL of the test organism in Mueller Hinton Broth to a final concentration of approximately 2×10^5 CFU/mL. The plates were incubated overnight at 37°C (two days for the fungi) and the MIC of each peptide was read as the lowest concentration of peptide that inhibited visible growth of the organism. All MIC determinations were performed in duplicate, and are the average of three independent determinations.

Freshly drawn human erythrocytes in citrate-dextrose-phosphate (CDP) buffer, from Copenhagen University Hospital were used to determine the hemolytic activity as described by Ryge and Hansen [5].

Table 1. MIC (μM) and hemolytic activity (50 μM) of the analogues

	MRSA	*VISA*	*VREVanA*	*E. coli*	*Ps. aeruginosa*	*C. neoformans*	*C. albicans*	*% HA*
1	≤12.5	12.5	≤1.25	25	25-50	50	50	19
2	100	100	100	100	100	100	100	5
3	100	100	100	100	100	100	100	1
4	3.12	6.25	≤1.25	≤1.25	3.12	25	12.5	91
5	100	100	25	6.25	100	50	25	2
6	100	100	50-100	100	100	100	50	3

HA:Hemolytic activity at 50μM peptide

The most active was compound **4**, which displayed excellent activity against the Gram-positive bacteria methicillin-resistant *S. aureus* (3.12 μM); vancomycin intermediate *S. aureus* (6.25μM), vancomycin resistant *E. faecium* VRE (≤1.25 μM), the Gram-negative bacteria *E.coli* (≤1.25 μM), *P. aeruginosa* (3.12 μM) and the fungi amphotericin B resistant *C. albicans* (12.5 μM) and *C. neoformans* (25 μM). However, compound **4**, was also hemolytic towards red blood cells (91%).

In conclusion, the results presented here suggest that small 3-(2-naphthyl)-L-alanine containing peptides are promising lead structures for developing future antibacterial agents.

Acknowledgements
We thank Jette Petersen and Frank Hansen for excellent technical assistance. This work was supported by the Danish Council for Strategic Research, the Augustinus Foundation, the Frimodt–Heineke Foundation, the Family Hede Nielsen Foundation, the JS Foundation and the Aase & Ejnar Danielsens Foundation.

References

1. Kumarasamy, K., et al. *Lancet Infect. Dis*. **10**, 597-602 (2010).
2. Matzusaki, K. *Biochimica et Biophysica Acta* **1788**, 1687-169 (2009).
3. Ryge T.S., Frimodt-Møller, N., Hansen, P.R. *Chemotherapy* **54**, 152-156 (2008).
4. http://www.cmdr.ubc.ca/bobh/methods.htm
5. Ryge, T.S., Hansen, P.R. *J. Peptide Science* **11**, 727-734 (2005).

Proceedings of the 31st European Peptide Symposium
Michal Lebl, Morten Meldal, Knud J. Jensen, Thomas Hoeg-Jensen (Editors)
European Peptide Society, 2010

Antimicrobial Peptides Containing D-Amino Acids with *In Vivo* Activity against Plant Pathogenic Bacteria

Imma Güell[1], Esther Badosa[2], Montse Talleda[1], Rafael Ferre[1], Jordi Cabrefiga[2], Emili Montesinos[2], Eduard Bardají[1], Lidia Feliu[1], and Marta Planas[1]

[1]LIPPSO, Department of Chemistry; [2]Laboratory of Plant Pathology, Institute of Food and Agricultural Technology-CIDSAV-XaRTA, University of Girona, Girona, 17071, Spain

Introduction

Phytopathogenic bacteria are responsible for a wide range of plant diseases causing large economic losses in fruit and vegetable crops. Their control by chemical pesticides is hampered by environmental concerns and the emergence of antibiotic-resistant strains [1]. In recent years, antimicrobial peptides have been described to be effective against plant pathogens.

Up to now, we have identified linear undecapeptides with high in vitro activity against the plant pathogenic bacteria *Erwinia amylovora*, *Pseudomonas syringae* and *Xanthomonas vesicatoria* [2]. The best peptide, KKLFKKILKYL-NH2 (BP100), was also effective in vivo to prevent infections of *E. amylovora* in flowers. However, the in vivo dose was 20 to 40-fold higher than the MIC. This loss of activity could be attributed to peptide degradation by plant proteases. One strategy used to protect peptides against enzymatic hydrolysis is the incorporation of D-amino acids in the sequence. In the present study, we designed and synthesized BP100 analogues containing D-amino acids [3].

Results and Discussion

Peptides were designed based on the amino acid sequence of BP100 (KKLFKKILKYL-NH_2) (Table 1). We investigated the influence of incorporating D-amino acids at various positions on the biological activity of this peptide: (i) one D-amino acid (BP138-BP148); (ii) two or three D-amino acids (BP149-BP152, BP154); (iii) four to ten D-amino acids at the C-terminus (BP155-BP161) and at the N-terminus (BP162-BP168); and (iv) all D-amino acids (BP153).

Peptides were screened for their *in vitro* growth inhibition of the above bacteria (Table 1). Single D-amino acid replacement had a pronounced effect on the peptide activity against *X. vesicatoria* and *E. amylovora*. In contrast, for *P. syringae* seven sequences retained BP100 activity. BP143, BP145 and BP147 were the most active against the three bacteria with MIC values ranging from 2.5 to 7.5 μM. Double- or triple-D-amino acid replacements led to peptides generally less active than BP100. For peptides incorporating four to ten D-amino acids at the C-terminus, activity increased with the number of D-residues. In contrast, a decrease of activity was generally observed when five to eight D-amino acids were incorporated at the N-terminus, but peptides incorporating four, nine or ten D-amino acids were more active than BP100. The all D-isomer was more active than the parent peptide against the three pathogens.

The toxicity to eukaryotic cells of the most active peptides was tested by their ability to lyse human red blood cells (Table 1). Eighteen sequences displayed a hemolysis <10% at 250 μM. Among the most active peptides, BP143, BP157, BP162, BP167 and BP168 showed low hemolytic activity (3-21%).

Peptide susceptibility to proteolysis was studied by exposure to proteinase K and degradation was monitored by HPLC over time (Table 1). Stability of peptides BP156 and BP162-BP168 could not be analyzed by HPLC and was qualitatively evaluated by MALDI-TOF. All peptides were more stable than BP100. Sixteen sequences displayed a degradation < 20% after 1 h.

Peptides BP143 and BP145 were tested *in vivo* by evaluating their preventive effect in inhibiting infections caused by the above bacteria, and compared to BP100 and streptomycin. All the tested peptides significantly reduced the infection severity caused by the three bacteria. The effect of BP143 and BP145 against *E. amylovora* and *X. vesicatoria* was comparable to BP100 and streptomycin. BP143 was more effective against *P. syringae* than BP100 and not significantly different from streptomycin.

Table 1. Antibacterial activity (MIC), cytotoxicity and stability to protease degradation

Peptide	*Sequence*[a]	*MIC (μM)*			*Hemolysis*[b] *(%)*	*Digestion*[d] *(%)*
		Xv[c]	*Ps*[c]	*Ea*[c]		
BP100	KKLFKKILKYL	5 – 7.5	2.5 – 5	2.5 – 5	54 ± 0.1	75
BP138	KKLFKKILK**Y**L	>7.5	>7.5	>7.5	7 ± 0.1	53
BP139	KKLFKKILKY**L**	>7.5	>7.5	>7.5	23 ± 0.9	6
BP140	KKLFKKIL**K**YL	>7.5	5 – 7.5	>7.5	0 ± 0	1
BP141	KKLFKKI**L**KYL	>7.5	2.5 – 5	2.5 – 5	4 ± 0.3	1
BP142	KKLF**K**KILKYL	>7.5	2.5 – 5	5 – 7.5	3 ± 0.6	35
BP143	KKL**F**KKILKYL	5 – 7.5	2.5 – 5	2.5 – 5	5 ± 0.8	18
BP144	KK**L**FKKILKYL	>7.5	2.5 – 5	>7.5	7 ± 0.4	50
BP145	K**K**LFKKILKYL	5 – 7.5	2.5 – 5	2.5 – 5	51 ± 0.5	61
BP146	KKLFK**K**ILKYL	>7.5	2.5 – 5	>7.5	53 ± 1.1	24
BP147	**K**KLFKKILKYL	2.5 – 5	2.5 – 5	2.5 – 5	71 ± 0.4	47
BP148	KKLFKK**I**LKYL	>7.5	>7.5	>7.5	0 ± 0	0
BP149	KK**L**FKKIL**K**YL	>7.5	>7.5	>7.5	0 ± 0	6
BP150	KKLFKKI**LK**YL	2.5 – 5	>7.5	>7.5	1 ± 0.1	0
BP151	KK**L**FK**K**IL**K**YL	5 – 7.5	5 – 7.5	>7.5	1 ± 0.3	0
BP152	KKLFKK**ILK**YL	5 – 7.5	>7.5	>7.5	5 ± 1.6	1
BP154	**KK**L**F**KKILKYL	5 – 7.5	2.5 – 5	5 – 7.5	41 ± 6.2	37
BP155	KKLFKKI**LKYL**	>7.5	>7.5	>7.5	3 ± 0.1	6
BP156	KKLFKK**ILKYL**	5 – 7.5	2.5 – 5	>7.5	49 ± 1.2	-[e]
BP157	KKLFK**KILKYL**	1.25 – 2.5	2.5 – 5	1.25 – 2.5	3 ± 1.0	0
BP158	KKLF**KKILKYL**	2.5 – 5	1.25 – 2.5	2.5 – 5	28 ± 2.1	0
BP159	KKL**FKKILKYL**	2.5 – 5	1.25 – 2.5	2.5 – 5	58 ± 5.7	12
BP160	KK**LFKKILKYL**	1.25 – 2.5	1.25 – 2.5	2.5 – 5	65 ± 1.9	0
BP161	K**KLFKKILKYL**	1.25 – 2.5	1.25 – 2.5	1.25 – 2.5	66 ± 2.9	1
BP162	**KKLF**KKILKYL	2.5 – 5	1.25 – 2.5	1.25 – 2.5	17 ± 0.7	-
BP163	**KKLFK**KILKYL	5 – 7.5	>7.5	2.5 – 5	8 ± 5.0	-
BP164	**KKLFKK**ILKYL	>7.5	2.5 – 5	>7.5	0 ± 0	-
BP165	**KKLFKKI**LKYL	>7.5	1.25 – 2.5	>7.5	6 ± 0.2	-
BP166	**KKLFKKIL**KYL	>7.5	2.5 – 5	>7.5	1 ± 0.2	-
BP167	**KKLFKKILK**YL	2.5 – 5	2.5 – 5	2.5 – 5	21 ± 7.4	-
BP168	**KKLFKKILKY**L	5 – 7.5	1.25 – 2.5	2.5 – 5	3 ± 2.7	-
BP153	**KKLFKKILKYL**	0.6 – 1.25	1.25 – 2.5	1.25 – 2.5	50 ± 2.1	5

[a]D-Amino acids are in bold and underlined. All peptides are C-terminal amides. [b]Percent hemolysis at 250 μM plus confidence interval (α = 0.05). [c]Xv, Xanthomonas vesicatoria; Ps, Pseudomonas syringae; Ea, Erwinia amylovora. [d]Percentage of degraded peptide calculated by HPLC. [e]Degradation was monitored by MALDI-TOF.

Acknowledgments

I. G. was recipient of a predoctoral fellowship from the Generalitat de Catalunya. This work was supported by grants AGL2004-07799-C03-01 and AGL2006-13564/AGR from MICIN of Spain, and CIRIT 2005SGR00835 and 2005SGR00275 from the Catalonian Government.

References

1. Montesinos, E., Vilardell, P. *Eur. J. Plant Pathol*. **107,** 787-794 (2001).
2. Badosa, E., et al. *Peptides* **28**, 2276-2885 (2007).
3. Badosa, E., et al. Péptidos lineales antimicrobianos con aminoácidos de la serie D, P200930538.

Proceedings of the 31st European Peptide Symposium
Michal Lebl, Morten Meldal, Knud J. Jensen, Thomas Hoeg-Jensen (Editors)
European Peptide Society, 2010

Synthesis and Preliminary Conformational Analysis of TOAC Spin-Labelled Analogues of the Medium-Length Peptaibiotic Tylopeptin B

Marina Gobbo[1,2], Barbara Biondi[2], Marta De Zotti[1], Fernando Formaggio[1,2], and Claudio Toniolo[1,2]

[1]Department of Chemical Sciences, University of Padova, Padova, 35131, Italy; [2]CNR Institute of Biomolecular Chemistry - Padova Unit, Padova, 35131, Italy

Introduction

The achiral tetrasubstituted α-amino acid 4-amino-1-oxyl-2,2,6,6,-tetramethylpiperidine-4-carboxylic acid (TOAC) has been used as a paramagnetic probe to study, by electron spin resonance (ESR), the mode by which peptides insert into a membrane. In particular, detailed information about the location, orientation and aggregation of membrane-active peptides in the phospholipid bilayer has been obtained for the TOAC-labeled peptaibiotics alamethicin F50/5 [1,2] and trichogin GA IV [3], in which one or two α-aminoisobutyric acid (Aib) residues in the sequence were replaced by the free radical-containing amino acid. Considering that the detailed mechanism of membrane permeabilization by medium-length peptaibiotics, e.g. tylopeptin B, is largely unknown, we have planned to synthesize a series of analogues in which the TOAC amino acid replaces the Aib residue at one of the three positions (4, 8 or 13) throughout the 14-mer tylopeptin sequence (Figure 1), and to investigate their interaction with model membranes by a combination of ESR techniques.

Results and Discussion

We have recently reported the solid-phase synthesis of tylopeptin B based on the Fmoc/*t*But strategy and the acid sensitive 2-chlorotrityl resin [4]. For the synthesis of the TOAC-containing analogues we decided to avoid any harsh acidic treatment that can destroy the free radical character of the TOAC residue [5], thereby loosing the paramagnetic probe. Consequently, the Gln and Trp residues were introduced without side-chain protecting groups and as preformed active esters, and the alcoholic function of the Ser residue was protected by the nucleofile sensitive *tert*-butyldimethylsilyl (TBDMS) group. After assembly of peptides on the solid support, the TBDMS group was removed by a 5 min treatment with 0.1 M tetrabutylammonium fluoride in DMF and the peptides were cleaved from the resin upon repeated treatment with 50% hexafluoroisopropanol in DCM. Yields of the TOAC containing analogues of tylopeptin B were in the range 10-65%, depending on the position of the TOAC residue in the peptide sequence. In particular the TOAC residue was difficult to introduce at position 3 or 4. In the course of these syntheses we observed the formation of several by-products, exceeding those corresponding to the truncated sequences. After HPLC purification the products were characterized by analytical HPLC and ESI-MS.

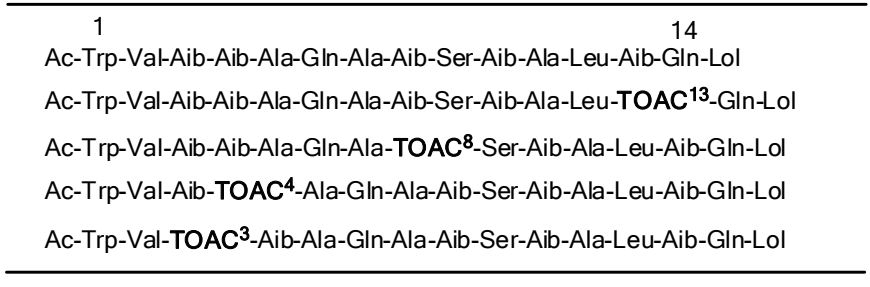

Fig. 1. Amino acid sequences of tylopeptin B and the synthesized TOAC-containing analogues (Lol corresponds to the 1,2-amino alcohol leucinol).

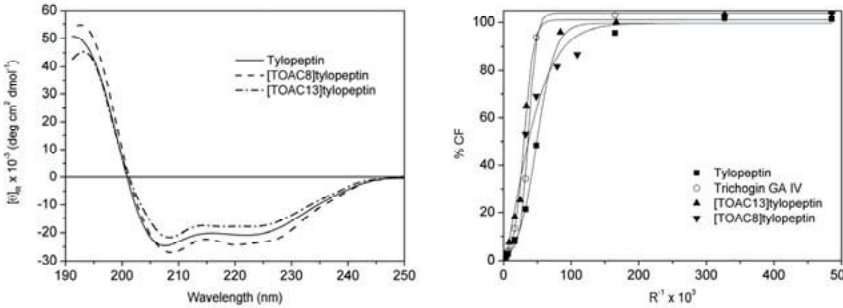

Fig. 2. Left: CD spectra in methanol of tylopeptin B and the TOAC-containing analogues (peptide concentration 10^{-4}M). Right: Peptide-induced carboxyfluorescein (CF) leakage from egg phosphatidylcholine /cholesterol (7:3) SUV for different [peptide]/[lipid] ratios (R^{-1}).

The TOAC spin-labelled analogues of tylopeptin B were submitted to a preliminary conformational analysis by circular dichroism (CD) in different solvents. Recently, we have shown that tylopeptin B is largely helical in solution, with a preference for the α- or the 3_{10}-helix type, depending upon the nature of the solvent [4]. The CD spectra of the spin-labelled analogues (Figure 2, left, shows two representative examples) in methanol, 2,2,2-trifluoroethanol and 30 mM sodium dodecylsulphate closely resemble those of the parent peptide, showing that in membrane-mimicking enviroments these peptides adopt an amphiphilic secondary structure.

The membrane-modifying properties of these tylopeptin analogues were compared to those of the parent peptide and trichogin GA IV (our standard membrane-active peptaibiotic) by measuring the induced leakage of CF entrapped in small unilamellar vesicles (SUV). As shown in Figure 2 (right), [TOAC^{13}]tylopeptin and [TOAC^{8}]tylopeptin exhibited a very high activity in this membrane permeabilization assay that is comparable to or even slightly higher than that of the natural peptide.

In summary, TOAC spin-labelled analogues of tylopeptin B can be considered good models to investigate the detailed mechanism of membrane permeabilization by medium-length peptaibiotics, using a combination of ESR techniques.

Acknowledgments
This work was supported by Italian Ministry of Education, University and Research (PRIN 2008).

References

1. Marsh, D., Jost, M., Peggion, C., Toniolo, C. *Biophys. J.* **92**, 473-481 (2007).
2. Milov, A.D., Samoilova, M.I., Tsvetskov, J., Jost, M., Peggion, C., Formaggio, F., Crisma, M., Toniolo, C., Handgraaf, J.-W., Rapp, J. *Chem. Biodivers*. **4**, 1275-1297 (2007).
3. Monaco, V., Formaggio, F., Crisma, M., Toniolo, C., Hanson, P., Milllhauser, G.L. *Biopolymers* **50**, 239-253 (1999).
4. Gobbo, M., Poloni, C., De Zotti, M., Peggion, C., Biondi, B., Ballano, G., Formaggio, F., Toniolo, C. *Chem. Biol. Drug Des.* **75**, 169-181 (2010).
5. Formaggio, F., Broxterman, Q.B., Toniolo, C. In Goodman, M., Felix, A., Moroder, L., Toniolo, C. (Eds.) *Houben-Weyl: Methods of Organic Chemistry, Synthesis of Peptides and Peptidomimetics,* Vol E22c, Thieme, Stuttgart, 2003, p. 292.

Proceedings of the 31st European Peptide Symposium
Michal Lebl, Morten Meldal, Knud J. Jensen, Thomas Hoeg-Jensen (Editors)
European Peptide Society, 2010

Porphyrin-Antimicrobial Peptide Conjugates: Synthesis, Conformational Studies and Preliminary Light Activated Biocidal Activity

Cristiano Tampieri[1], Barbara Biondi[2], Sandro Campestrini[1], Ryan Dosselli[3], Elena Reddi[3], and Marina Gobbo[1,2]

[1]Department of Chemical Sciences, University of Padova, Padova, 35131, Italy; [2]CNR Institute of Biomolecular Chemistry, Padova, 35131, Italy; [3]Department of Biology, University of Padova, Padova, 35131, Italy

Introduction

Photodynamic therapy (PDT) is a very promising approach for killing bacteria [1]. It is well established that singlet oxygen is produced as the main species responsible for cell death. During PDT multiple cellular targets are damaged and this strongly reduces the probability of developing the resistance phenomena, which frequently occur after repeated antibiotic treatments. Porphyrins are commonly used as photosensitizers, that can generate reactive oxygen species upon exposure to light in the presence of oxygen. Short cationic antimicrobial peptides (CAMP) are components of the innate defense of many organisms [2]. Their overall positive charge ensures accumulation at the poly-anionic microbial cell surfaces. Beyond the presence of several cationic amino acids, a substantial proportion of hydrophobic amino acid residues permit most of CAMP to fold into an amphipathic structure, that allows them to insert into the phospholipid bilayer. After insertion, antimicrobial peptides act by either disrupting the physical integrity of the membrane or translocating across the membrane to hit bacterial internal targets. By conjugating a porphyrin to an antimicrobial peptide we can expect to direct the photosensitizer against specific bacterial targets and increase the efficacy of PDT. Here, we present the synthesis of two conjugates in which a 5(4'-carboxyphenyl)-10,15,20-triphenylporphyrin (TPP-OH, Figure 1) has been covalently linked to the N-terminal end of two antimicrobial peptides: apidaecin 1b (GNNRPVYIPQPRPPHPRL) and magainin 2 (GIGKFLHSAKKFGKAFVGEIMNS).

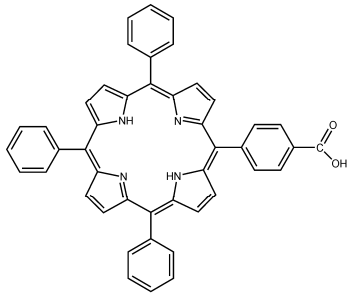

Fig. 1. Chemical structure of the TPP-OH photosensitizer.

Results and Discussion

The synthesis of the photosensitizer, opportunely functionalized for the covalent binding to the peptide, was carried out according to the Lindsey's procedure, starting from pyrrole, benzaldehyde and 4-formylbenzoic acid methyl ester [3]. After purification on silica gel, the 5(4'-methoxycarbonylphenyl)-10,15,20-triphenylporphyrin was isolated from the mixture of different isomers in 38% yield and, after ester hydrolysis, the photosensitizer (TPP-OH) was characterized by ^{1}H-NMR, UV-vis and ESI-MS.

Peptides were automatically synthesized on solid phase by the standard Fmoc/HBTU protocol and, after removal of the N-terminal amino protecting group, TPP-OH (2.5 eq) was directly coupled to the peptide chain using diisopropylcarbodiimide/HOBt as activating agents. TPP-apidaecin was obtained in very good yield (over 75%), whereas the reaction with magainin yielded only about 13% of the corresponding conjugate. Notably, the porphyrin induced also extensive oxidation of the methionine residue in magainin, as detected by MS analysis. To evade this side-reaction, TPP-OH was reacted with a magainin analogue in which the Met residue was replaced by Leu, and the TPP-[Leu^{21}]magainin conjugate was obtained in 35% yield. After HPLC purification, both TPP-peptide conjugates were characterized by analytical HPLC, ESI-MS and UV-vis spectroscopy.

The conformational preferences of TPP-apidaecin and TPP-[Leu^{21}]magainin were preliminarily investigated by circular dicroism (CD) and compared to those of the parent peptides. Magainin and apidaecin belong to different structural classes of antimicrobial

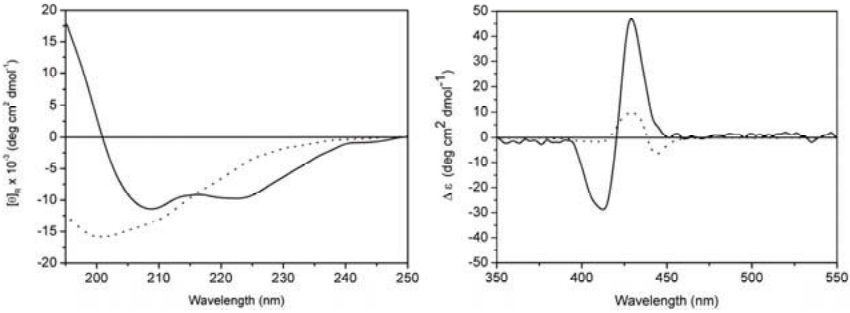

Fig. 2. CD spectra in water of (·····) TPP-apidaecin (10^{-4}M) and (——) TPP-[Leu^{21}] magainin (10^{-5}M) in the absorption regions of the amide bond (left) and the Soret band (right).

peptides: magainin presents a disordered conformation in aqueous environment but assumes a prevalently amphipathic helical structure in organic solvents; apidaecin, because of the abundance of Pro residues, adopts a prevalently extend conformation in different environments. In the far-UV region (Figure 2, left), the CD spectrum of TPP-apidaecin in water is similar to that of the parent peptide and it is characterized by a broad negative minimum around 200 nm, indicative of extended and prevalently disordered structures. On the contrary, in the same solvent, the spectrum of the TPP-[Leu^{21}]magainin differs substantially from that of the peptide and exhibits a positive maximum around 190 nm and two negative minima near 208 and 222 nm. This pattern, typical of peptides which adopt an α-helical structure, suggests that the porphyrin system induces the peptide backbone to fold, at least partially, into an amphiphatic α-helix. Moreover, split Cotton effects appear in the porphyrin Soret band region (Figure 2, right) and they could indicate the appearance of aggregation phenomena, in particular in the case of TPP-[Leu^{21}]magainin.

The bactericidal activity under light activation of the porphyrin-peptide conjugates was preliminarily tested for TPP-apidaecin [4]. At low concentration (1.5 – 15 μM) the conjugate was able to reduce the survival of *E. coli* cells by 3-4 $\log_{10}$ and it remained photoactive also against hard-to-treat *P. aeruginosa* bacteria, although at higher concentration (60 μM). Under similar condition, the photosensitizer alone was only photoactive against *S. aureus,* but at higher concentration than the conjugate. In conclusion, the antibacterial activity of the conjugate was higher than that of the individual components and TPP-apidaecin exhibited a broader spectrum activity.

Acknowledgments
This work was supported by the University of Padova (PRAT 2009).

References

1. Hamblin, M.R., Hasan, T. *Photochem. Photobiol. Sci.* **3,** 436-450 (2004).
2. Hancock, R.W., Sahl, H.-G. *Nature Biotechnology* **24**, 1551-1557 (2006).
3. Lindsey, J.S., Schreiman, I.C., Hsu, H.C., Kearney, P.C., Marguerettaz, A.M. *J. Org. Chem.* **52**, 827-836 (1987).
4. Dosselli, R., Gobbo, M., Bolognini, E., Campestrini, S., Reddi, E. *ACS Med. Chem. Lett.* **1**, 35-38 (2010).

Proceedings of the 31st European Peptide Symposium
Michal Lebl, Morten Meldal, Knud J. Jensen, Thomas Hoeg-Jensen (Editors)
European Peptide Society, 2010

Sequences of the Polypeptide Antibiotics (Peptaibiotics) Acretocins

Hans Brückner and Jochen Kirschbaum
Research Center for BioSystems, Land Use and Nutrition (IFZ), Department of Food Sciences, University of Giessen, Giessen, 35392, Germany

Introduction

Peptaibiotics are a constantly growing family of fungal peptides characterized by a high proportion of the α-dialkylated α-amino acid Aib (α-aminoisobutryric acid, 2-methylalanine). They display a multitude of biological activities. We have developed rapid and reliable methods to screen fungi for the production of peptaibiotics which are based on the detection of the marker amino acid Aib by GC-MS or HPLC. Solid-phase extraction of peptides and subsequent online LC-ESI-MS^n (**'peptaibiomics'**) are used to determine the entirety of peptaibiotics (the **'peptaibiome'**) [1-3]. We have already reported on the production and sequences of a mixture of 16-residue peptaibiotics named acretocins (ACRs) by *Acremonium crotocinigenum* CBS 217.70. However, at that time we could not assign a mass fragment of Δ142 Da (Gly + 83 Da) in MS/MS experiments [4]. Here, we show that it represents the sequence Gly^8-Acc^9 (Acc, 1-aminocyclopropane-1-carboxylic acid) present in all acretocin homologues.

Results and Discussion

The mold *A. crotocinigenum* CBS 217.70 [3] was grown in submerged culture using a malt extract medium. Acretocins (ACRs) were isolated and purified by XAD and LH-20 chromatography as described previously [4]. The analytical HPLC elution profile of ACRs in comparison to the related peptaibiotics tolypin [5] and efrapeptin [6] are shown in Figure 1. The peptide mixture was fractioned by semi-preparative RP-HPLC, and the individual peptides were analyzed by direct infusion ESI-MS and online HPLC-ESI-MS^n. An aliquot of ACRs (0.2 mg) was hydrolyzed in 6M HCl (110°C/24 h). The amino acids released were converted into their *N*-trifluoroacetyl-2-propyl esters. The derivatives were analyzed by GC-SIM-MS and GC-TIC-MS using a Chirasil-L-Val© capillary column. The presence of the previously undetected Acc (Figure 1) as well as other constituents was determined.

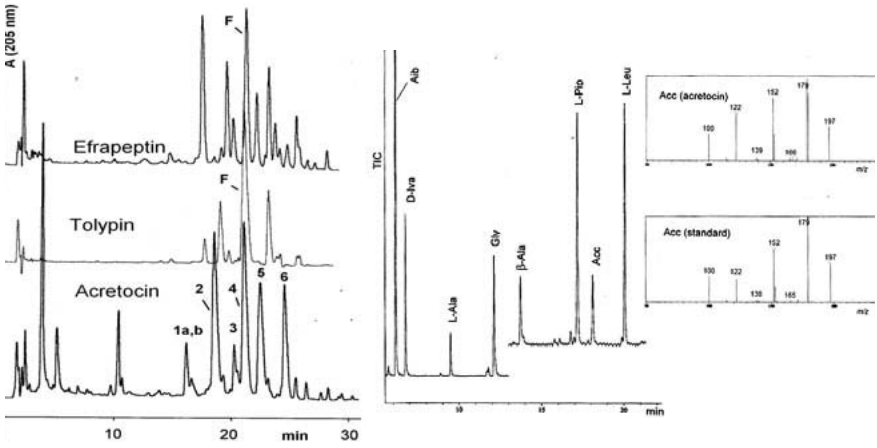

Fig. 1. HPLC elution profiles (left side) of acretocins [4] in comparison to tolypins [5] and efrapeptins [6]. GC-MS (right side) of TFA-amino acid-2-propyl esters of a total hydrolysate of acretocins on Chirasil-L-Val; EI-MS of Acc from acretocins (insert above) and from a standard of Acc (insert below).

These methods provided the complete chiral sequences of ACRs and established the positions Gly[8]-Acc[9] in all peptides (Figure 2). The *C*-terminal heterocyclic residue PIHPPE in all ACRs was concluded by comparison of the ESI-MS data with those resulting from efrapeptin-F and tolypin-F (from *Tolypocladium* spp.) serving as standards. Components 'F' of the latter have identical sequences [5,6] but do not contain Acc. ACRs are closely related to the Acc-containing neoefrapeptins from *Geotrichum candidum* SID 22780 [7].

	1	2	3	4	5	6	7	8	9	10	11	12	13	14	15	16
(A)																
1a	Ac	Pip	Aib	Pip	D-Iva	Aib	Leu	β-Ala	Gly	Acc	Aib	Pip	Aib	Gly	Leu	Aib	Y
1b	Ac	Pip	Aib	Pip	Aib	Aib	Leu	β-Ala	Gly	Acc	Aib	Pip	Aib	Gly	Leu	D-Iva	Y
2	Ac	Pip	Aib	Pip	D-Iva	D-Iva	Leu	β-Ala	Gly	Acc	Aib	Pip	Aib	Gly	Leu	Aib	Y
3	Ac	Pip	Aib	Pip	D-Iva	Aib	Leu	β-Ala	Gly	Acc	Aib	Pip	Aib	Gly	Leu	D-Iva	Y
4	Ac	Pip	Aib	Pip	D-Iva	D-Iva	Leu	β-Ala	Gly	Acc	Aib	Pip	Aib	Gly	Leu	D-Iva	Y
5	Ac	Pip	Aib	Pip	D-Iva	Aib	Leu	β-Ala	Gly	Acc	Aib	Pip	Aib	Ala	Leu	D-Iva	Y
6	Ac	Pip	Aib	Pip	D-Iva	D-Iva	Leu	β-Ala	Gly	Acc	Aib	Pip	Aib	Ala	Leu	D-Iva	Y
(B)	Ac	Pip	Aib	Pip	L-Iva	Aib	Leu	β-Ala	Gly	Acc	Aib	Pip	Aib	Gly	Leu	L-Iva	Y
(C)	Ac	Pip	Aib	Pip	Aib	Aib	Leu	β-Ala	Gly	Aib	Aib	Pip	Aib	Ala	Leu	L-Iva	Y

Fig. 2. Sequences of acretocins 1a,b – 6 ***(A)*** *in comparison to neoefrapeptin-A* ***(B)*** *and efrapeptin-F* ***(C).*** *The latter corresponds to tolypin-F. Abbreviations of constituents: Ac, acetyl; Pip, L-pipecolic acid; Iva, L- or D- isovaline (2-ethylalanine); Leu, L-leucine; β-Ala, β-alanine; Acc, 1-aminoacyclopropane-1-carboxylic acid; Y, N-**p**eptido-1-**i**sobutyl-2-(2,3,4,6,7,8-**h**exahydro-1-**p**yrrolo-[1,2-α]-**p**yrimidino)**e**thylamine (PIHPPE).*

References

1. Krause, C., Kirschbaum, J., Brückner, H. *Amino Acids* **30**, 435-443 (2006).
2. Degenkolb, T., Brückner, H. *Chem. Biodivers.* **5**, 1817-1843 (2008).
3. Brückner, H., Becker, D., Gams, W., Degenkolb, T. *Chem. Biodivers*. **6**, 38-56 (2009).
4. Kirschbaum, J., Slavíčková, M., and Brückner, H., In Flegel, M., Fridkin, M., Gilon, C., and Slaninová J. (Eds.) *Peptides: Bridges Between Disciplines (Proceedings of the 28th European Peptide Symposium)*, Keenes International, Geneva, 2005, p. 415-416.
5. Maťha, V., Jegorov, A., Kieß, M., Brückner, H. *Tissue Cell* **24**, 559-564 (1992).
6. (a) Gupta, S., Krasnoff, S.B., Roberts, D.W., Renwick, J.A.A., Brinen, L.S., Clardy, J. *J. Am. Chem. Soc*. **113**,707-709 (1991); (b) Gupta, S., Krasnoff, S.B., Roberts, D.W., Renwick, J.A.A., Brinen, L.S., Clardy, J. *J. Org. Chem*. **57**, 2306-2313 (1992).
7. Fredenhagen, A., Molleyres, L.-P., Böhlendorf, B., Laue, G. *J. Antibiot*. **59**, 267-280 (2006).

Proceedings of the 31st European Peptide Symposium
Michal Lebl, Morten Meldal, Knud J. Jensen, Thomas Hoeg-Jensen (Editors)
European Peptide Society, 2010

Conformational Studies of Toac-Analogues from New Cytolytic Peptide Isolated from *Hypsiboas Albopunctatus*

Eduardo F. Vicente[1], Graziely F. Cespedes[1], Edson Crusca Jr[1], Mariana S. Castro[2], Maria José S. Mendes-Giannini[1], Luís Guilherme M. Basso[3], Antonio J. Costa-Filho[3], Reinaldo Marchetto[1], and Eduardo M. Cilli[1]

[1]UNESP – Univ Estadual Paulista, Araraquara, Brazil; [2]UnB – University of Brasília, Brasília, Brazil; [3]USP – Universidade de São Paulo, São Paulo, Brazil

Introduction

Antibiotic resistant bacterial strains represent a global health problem with a strong social and economic impact. Thus, there is an urgent need for the development of antibiotics with novel mechanisms of action. Castro's group isolated and determined from the skin secretion of the frog *Hypsiboas albopunctatus* the new antimicrobial peptide called Hylin (*hy* - GWLDVAKKIGKAAFNVAKNFI/L). The sequence analysis of this peptide (http://ca.expasy.org/tools/blast/) revealed identity with ceratoxin – extracted from the female reproductive accessory glands of the dipteran insect *Ceratitis capitata*. The aim of the present work was to evaluate three analogues containing TOAC to supply information about the topology of this peptide in mimetic membrane and the pore formation mechanism. These analogues contain Ile in C-terminus and addition of TOAC (4-amino-4-carboxy-2,2,6,6-tetramethyl-piperidine-1-oxyl; [1,2]) in position 0 or replacing Trp^2 and Ala^{13}. These modifications allowed studying the conformational properties and its interaction with membrane models by EPR.

Results and Discussion

The peptides were synthesized manually according to the standard SPPS-N^{α}-Fmoc (9-fluorenylmethyloxycarbonyl) protecting group strategy. The cleavage reaction was performed with anhydrous TFA (trifluoroacetic acid), TIS (triisopropylsilane) and water (9:0.5:0.5). The crude spin-labeled peptides were submitted to alkaline treatment (pH 10, 4 h) for complete reversion (monitored by analytical HPLC) of the N-O protonation that occurs during the TFA reaction [3,4]. The peptides were purified by preparative HPLC at pH 5.0. The synthesis and purification of peptides by HPLC was efficient and a high purity level (≥ 96%) was obtained. The biological activity [5] of these peptides was determined. All synthetic peptides exhibited hemolytic, antimicrobial and antifungal activity. The hemolytic activities of analogues $TOAC^0$-*hy* (3 μmol L^{-1}) and $TOAC^{13}$-*hy* (1 μmol L^{-1}) were bigger than wild type (WT-*hy*) synthetic peptide (7 μmol L^{-1}), except by $TOAC^2$-*hy* (19 μmol L^{-1}). Most peptides showed similar antimicrobial activity from WT-*hy*, except $TOAC^0$-*hy* that showed high value of MIC (minimal inhibitory concentrations). To obtain more information about the difference among the peptides permeabilization, studies in vesicles containing DPPC:DPPA:SM and DPPC:DPPA:DPPE (80:5:15; w:w:w) were performed (Figure 1). The data showed that $TOAC^2$-*hy* has the lowest activity, followed by $TOAC^0$-*hy*, $TOAC^{13}$-*hy* and WT-*hy*. To understand the difference between the biological activities, the secondary structure was evaluated by CD spectroscopy in aqueous solution (at 25ºC and pH 7.0), presence of trifluoroethanol 60% (v/v) and vesicles. The CD studies demonstrated that peptides in water had a random coil structure, except by $TOAC^{13}$-*hy*, which had an α-helix structure. This is in accordance with the TOAC properties, which exhibits a tendency to strongly promote helical conformations. In the presence of TFE or mimetic

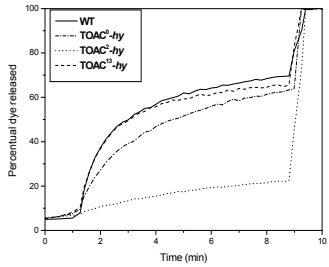

Fig. 1. Membrane permeabilization of DPPE/DPPA/DPPC vesicles induced by 2 mmol L^{-1} of synthetic peptides.

membrane, all peptides acquired a high amount of α-helix. The order of α-helix content was TOAC^{13}-*hy* ≈ wild type peptide > TOAC^{0}-*hy* ≥ TOAC^{2}-*hy*.

EPR assays in vesicles (Figure 2) showed that TOAC^{13}-*hy* had the highest interaction with both vesicle models described above. Apparently, TOAC^{0}-*hy* had no interaction, locating outside these systems; TOAC^{2}-*hy* is located in the interface between the vesicles and the aqueous solution and, finally, TOAC^{13}-*hy* is fully immersed in the membrane. These findings allowed the description of the peptide topology in the membrane, where the N-terminal region is not immersed; the position 2 is in the interface, and 13 is fully inserted. The NLLS (Non-Linear Least-Squares simulations) in LPC indicate that, in this mimetic system interface, the TOAC^{0} N-terminus has two different components. These results suggest a mode of action where the N-terminal region is responsible for starting the pore formation (Figure 2B). This conclusion is in accordance with the model of pore formation to monolayer proposed by Lopes et al. [6] in *Saccharomyces cerevisiae*. In this model, the disordered peptide is attracted to the negative charged phospholipids, promoting the formation of one amphipathic α-helix. Afterwards, the peptide remains associated with the vesicle surface and, at the same time, the N-terminal residues are inserted among the acyl chain of the phospholipids promoting its disruption.

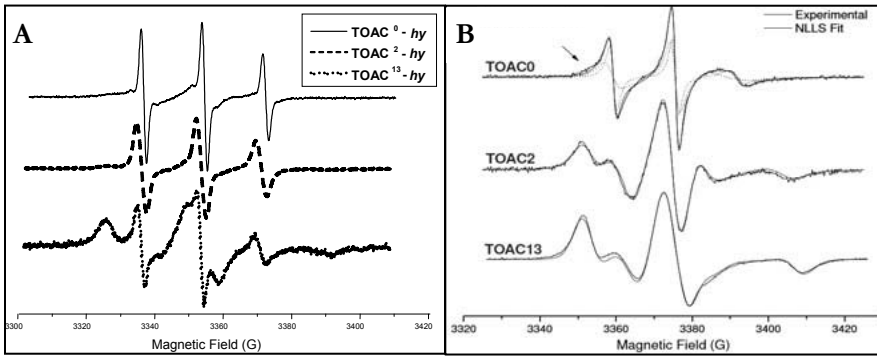

Fig. 2. A) EPR spectra of synthetic peptides in DPPC:DPPA:DPPE (80:5:15; w:w:w); B) NLLS (Non-linear least-squares simulations) fits of the peptides in the LPC micelles. The noisy lines indicate the experimental results and the smoothed lines, the total NLLS fits. In TOAC^{0}, the dotted lines indicate the first and second components of the system.

Acknowledgments

This work was supported by: FAPESP, CNPq and FUNDUNESP.

References

1. Nakaie, C.R., Schreier, S., Paiva, A.C.M. *Biochimica et Biophysica Acta* **742**, 63-71 (1983).
2. Marchetto, R., Schreier, S., Nakaie, C.R. *J. Amer. Chem. Soc.* **115**, 11042-11043 (1993).
3. Oliveira, E., Cilli, E.M., Miranda, A., Jubilut, G.N., Albericio, F., Andreu, D., Paiva, A.C.M., Schreier, S., Tominaga, M., Nakaie, C.R. *European Journal of Organic Chemistry* **21**, 3686-3694 (2002).
4. Toniolo, C., Crisma, M., Formaggio, F. *Biopolymers* **47**, 153-158 (1998).
5. Castro, M.S., Ferreira, T.C.G., Cilli, E.M., Crusca, E., Jr., Mendes-Giannini, M.J.S., Sebben, A., Ricart, C.A.O., Souza, M.V., Fontes, W. *Peptide Science* **30**, 291-296 (2009).
6. Lopes, J.L.S., Nobre, T.M., Siano, A., Humpola, V., Bossolan, N.R.S., Zaniquelli, M.E.D., Tonarelli, G., Beltramini, L.M. *Biochimica et Biophysica Acta* **1788**, 2252-2258 (2009).

Proceedings of the 31st European Peptide Symposium
Michal Lebl, Morten Meldal, Knud J. Jensen, Thomas Hoeg-Jensen (Editors)
European Peptide Society, 2010

Increasing Amphiphilicity in Peptaibiotics: Gly to Lys Replacements in Trichogin GA IV

Marta De Zotti[1], Barbara Biondi[1], Cristina Peggion[1], Fernando Formaggio[1], Yoonkyung Park[2,3], Kyung-Soo Hahm[3,4], and Claudio Toniolo[1]

[1]ICB, Padova Unit, CNR, Department of Chemistry, University of Padova, Padova, 35131, Italy;[2]Department of Biotechnology, Chosun University, Gwangju, 501-759, Korea; [3]Department of Biomaterials, Chosun University, Gwangju, 501-759, Korea; [4]Department of Cellular and Molecular Medicine, Chosun University, Gwangju, 501-759, Korea

Introduction

Trichogin GA IV, isolated from the fungus *Trichoderma longibrachiatum* [1], is the prototype of lipopeptaibols [2], the sub-class of short-length peptaibiotics exhibiting membrane-modifying properties. The primary structure of the 10-amino acid peptide trichogin GA IV is as follows:

1-Oct-Aib-Gly-Leu-Aib-Gly-Gly-Leu-Aib-Gly-Ile-Lol

(1-Oct, 1-octanoyl; Aib, α-aminoisobutyric acid; Lol, leucinol). In previous papers we have shown, using a variety of physico-chemical techniques including X-ray diffraction, that this peptaibol is predominantly folded in a mixed 3_{10}-/α- helical conformation with a clear, albeit modest, amphiphilic character [3].

Results and Discussion

In this work we synthesized by the solid-phase methodology, purified, and fully characterized (Figure 1) a set of trichogin GA IV analogues in which the four Gly residues at positions 2, 5, 6, 9, lying on the poorly hydrophilic face of the helical structure, are substituted by one (position 2 or 9), two (positions 5 and 6), three (positions 2, 5, and 9), or four (positions 2, 5, 6, and 9) Lys residues. The analogue with the triple Lys replacement was additionally modified by the incorporation of a helix-inducing Aib residue at position 6.

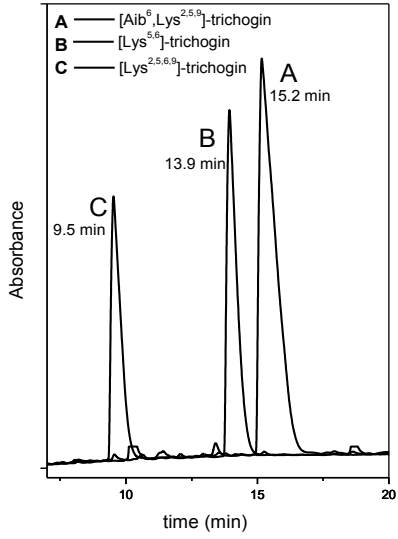

*Fig. 1. RP-HPLC chromatograms obtained for the trichogin analogues containing two (**B**), three (**A**) and four (**C**) Lys residues. Column: Vydac C_{18}; gradient: 50-90% B in 25min; eluants: A: H_2O+0.1 %TFA, B: CH_3CN/H_2O 9:1+0.1 % TFA.*

The conformational preferences of selected Lys-containing analogues were assessed by CD and 2D-NMR techniques in aqueous, organic, and membrane-mimetic environments. These compounds were found to be mostly helical under the different experimental conditions examined. The role played in the analogues by the markedly increased amphiphilicity (one face is, partially or totally, positively charged) was further tested by fluorescence leakage experiments in model membranes, protease resistance, antibacterial and antifungal activities, cytotoxicity, and hemolysis (Figure 2).

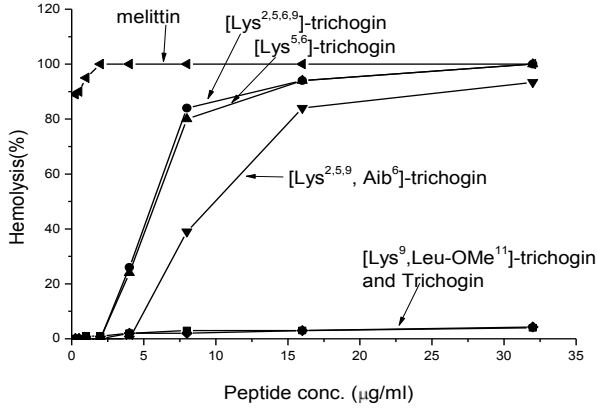

Fig. 2. Hemolytic activities of the Lys-containing trichogin analogues.

References

1. Auvin-Guette, C., Rebuffat, S., Prigent, Y., Bodo, B. *J. Am. Chem. Soc.* **114**, 2170-2174 (1992).
2. Toniolo, C., Crisma, M., Formaggio, F., Peggion, C., Epand, R.F., Epand, R.M. *Cell. Mol. Life Sci.* **58**, 1179-1188 (2001).
3. Peggion, C., Crisma, M., Epand, R.F., Epand, R.M., Toniolo, C. *J. Pept. Sci.* **9**, 679-689 (2003).

Proceedings of the 31st European Peptide Symposium
Michal Lebl, Morten Meldal, Knud J. Jensen, Thomas Hoeg-Jensen (Editors)
European Peptide Society, 2010

Synthesis, Preferred Conformation, and Membrane Activity of Heptaibin, a Medium-Length Peptaibiotic

Marta De Zotti, Barbara Biondi, Cristina Peggion, Marco Crisma, Fernando Formaggio, and Claudio Toniolo
ICB, Padova Unit, CNR, Department of Chemistry, University of Padova, Padova, 35131, Italy

Introduction

The medium-length peptaibiotics [1] are characterized by a primary structure of 13-15 amino acid residues and include *inter alia* some samarosporins, stilbellins, bergofungins, and emerimicins. Despite the interesting antibiotic and antifungal properties exhibited by these membrane-active peptides, their exact mechanism of action is still unknown. Our current aim is to investigate the relationships between their conformational properties and bioactivity.

Results and Discussion

Here, we present our results on heptaibin, a 14-amino acid residue peptaibiotic, extracted from the culture of *Emericellopsis sp.* BAUA8289 and chemically characterized by Ishiyama *et al.* ten years ago [2]. The heptaibin primary structure is as follows:

Ac-Phe-$(Aib)_3$-Val-Gly-Leu-$(Aib)_2$-Hyp-Gln-Aib-Hyp-Aib-Phol

(Ac, acetyl; Aib, α-aminoisobutyric acid; Hyp, 4(*R*)-hydroxy-(*S*)-proline; Phol, the 1,2-aminoalcohol (*S*)-phenylalaninol). The solid-phase synthesis of bergofungin D, the sequence of which is similar to that of heptaibin, has been recently reported [3].

Our solid-phase synthesis of heptaibin involved the Fmoc-protection/HATU C-activation methodology. Special attention was devoted to prevent 2,5-dioxopiperazine formation, particularly when the N-terminal sequence of the growing chain is the H-Aib-Hyp- dipeptide. The final product was purified (Figure 1) and fully characterized. A detailed conformational analysis was performed by use of FT-IR absorption, CD, 2D-NMR combined with molecular dynamics (MD) calculations, and X-ray crystallography (the latter technique on an N-terminal segment). Being rich (>50%) of the non-coded C^{α}-tetrasubstituted Aib residue, heptaibin is mostly helical under different experimental conditions (Figure 2) and it is stable against the pronase E proteolytic attack. Fluorescence leakage experiments revealed that heptaibin is a membrane-permeabilizing compound.

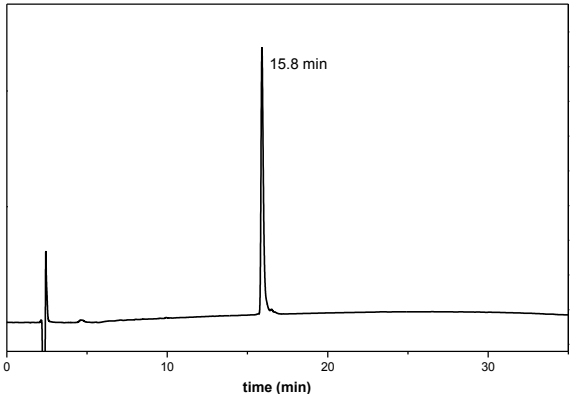

Fig. 1. RP-HPLC profile obtained for heptaibin. Column: Vydac C_{18}; gradient: 50-100% B in 25min; eluants: A: H_2O+0.1% TFA, B: CH_3CN/H_2O 9:1+0.1% TFA.

Fig. 2. 3D-Representation of the 54 structures with energy < 147 kcal/mole resulting from the MD calculations of heptaibin ($2 \cdot 10^{-3}$ M, 600 MHz, 313K, 100mM SDS-d_{25} in 9:1 H_2O/D_2O) with the backbone atoms superimposed. The Hyp^{10} kink residue is highlighted. Average kink angle: 25.2° (+/- 3°).

References

1. Toniolo, C., Brückner, H. *Peptaibiotics: Fungal Peptides Containing α-Dialkyl α Amino-Acids*, Verlag Helvetica Chimica Acta, Zürich, Switzerland, and Wiley-VCH, Weinheim, Germany, 2009.
2. Ishiyama, D., Satou, T., Senda, H., Fujimaki, T., Honda, R., Kanazawa, S. *J. Antibiot. (Tokyo)* **53**, 728-732 (2000).
3. Hjørringgaard, C.U., Pedersen, J.M., Vosegaard, T., Nielsen, N.C., Skrydstrup, T. *J. Org. Chem.* **74**, 1329-1332 (2009).

Proceedings of the 31st European Peptide Symposium
Michal Lebl, Morten Meldal, Knud J. Jensen, Thomas Hoeg-Jensen (Editors)
European Peptide Society, 2010

Synthesis, Characterization and Cytostatic Effect of New Pemetrexed-Peptide Conjugates

Erika Orbán[1], Zsanett Miklán[1], Zoltán Bánóczi[1], and Ferenc Hudecz[1,2]

[1]Research Group of Peptide Chemistry, Hungarian Academy of Sciences, Eötvös Loránd University, Budapest, H-1117, Hungary; [2]Department of Organic Chemistry, Eötvös Loránd University, 1518, Budapest, 112 POB 32, H-1518, Hungary

Introduction

Pemetrexed is used as a folate-antimetabolite in the treatment of pleural mesothelioma and non-small cell lung carcinoma. This drug inhibits at least three enzymes (thymidylate synthase, dihydrofolate reductase and glycinamide-ribonucleotide formyl transferase) involved in purine- and pyrimidine synthesis. Pemetrexed (Pem) treatment could be accompanied by various side-effects like nausea, vomiting, diarrhea, etc. Conjugation of anticancer drug (e.g. daunomycin, methothrexate) with peptide carrier could decrease or even eliminate side effects [1,2]. Oligoarginines are *de novo* designed cell penetrating peptides capable to translocate covalently attached cargoes [2]. Oligoarginine and other oligopeptides were conjugated with Pem in our group earlier [3]. It was observed that peptide IELLQAR used as selective inhibitor could inhibit the attachment of E-selectin to the cell surface-carbohydrates and thus limit the risk of metastases formation [4].

Results and Discussion

In this study we report on the synthesis and characterization of novel Pem – peptide conjugates containing cell-penetrating octaarginine and/or E-selectin binding IELLQAR peptide and thioether bond between the moieties. The conjugates were characterized by RP-HPLC and ESI MS. The cytostatic effect of Pem derivatives and conjugates was studied on NCI-H358 non-small cell lung carcinoma and on HL-60 human leukemia cell lines.

For the synthesis of these conjugates, we first prepared Pem dimethylester by the reaction between Pem disodium salt and thionyl chloride in methanol, based on published procedure [5]. Pure $Pem(OMe)_2$ was obtained by crystallization from ethanol. In the next step $ClAc\text{-}Pem(OMe)_2$ was synthesized by the reaction of chloroacetic acid anhydride and $Pem(OMe)_2$ in the presence of DIEA in DMF.

C-terminally modified octaarginine and peptide IELLQAR as well as the conjugate peptide, $IELLQARGGCGGR_8$ was prepared on solid phase by Fmoc-strategy using *in situ* active ester coupling strategy. Cysteine amino acid was incorporated into the sequence to provide an appropriate site for thioether bond formation with the chloroacetyl group of pemetrexed.

Peptide conjugates of $Pem(OMe)_2$ were prepared by the reaction between chloroacetyl group of $Pem(OMe)_2$ and thiol group of Cys, present in the peptide sequence, under alkaline conditions (pH 8). Finally, peptide conjugates of Pem were prepared by removing the methylester protecting groups from the carboxylic groups of Pem. Removal of the protecting groups is indispensable because these carboxylic groups are essential for the biological activity of Pem, as demonstrated in *in vitro* experiments (Table 1). To remove the protecting groups three times molar excess of 0.1 M NaOH and acetone (1:1, v/v) was used as cleavage mixture at 5°C for 60-90 min. The progress of the reaction was monitored by analytical RP-HPLC and terminated by adding of 0. 1M HCl solution to the mixture.

Table 1. Chemical characteristics and cytostatic effect of Pem- derivatives

Compound	MS [M][a]		R_t (min)[b]	IC_{50} (μM)[c]	
	Calculated	Measured		NCI-H358	HL-60
IELLQARGGC[Pem]-amide	1525.7	1525.8	28.7	3.53	2.17
RRRRRRRRGGC[Pem]-amide	1951.2	1951.5	24.4	7.70	6.24
IELLQARGGC[Pem]-GGRRRRRRRR-amide	2889.3	2890.3	33.3	1.93	2.64
Pem	427.1	427.3	32.2	1.05	0.55
$Pem(OMe)_2$	455.2	455.3	29.0	87.34	9.44

[a]ESI-MS; [b]HPLC retention time, SupelcosilTM LC-18-DB (C18, 120 Å, 5μm, 4.6 × 250 mm; Bellefonte, PA., U.S.A.) column, gradient elution: 0-5 min 5% B eluent, 5-50 min 95% B eluent, where eluent A: 0.1% TFA in water, eluent B: 0.1% TFA in ACN : water (80 : 20, v/v); [c]IC_{50} values of compounds in μM on NCI-H358 and HL-60 cells.

Compounds were purified with semipreparative RP-HPLC and chemically characterized by analytical RP-HPLC and ESI-MS. For the analytical RP-HPLC SupelcosilTM LC-18-DB (C18, 120 Å, 5μm, 4.6 × 250 mm; Bellefonte, PA, U.S.A.) column was used, gradient: 0-5 min 5% B eluent, 5-50 min 95% B eluent, where eluent A: 0.1% TFA in water, eluent B: 0.1% TFA in ACN : water (80 : 20, v/v). Cytostatic effect was determined by MTT-assay [6] on HL-60 human leukemia and NCI-H358 human non-small cell lung carcinoma cell lines. Table 1 shows the calculated and measured molecular mass, retention time and IC_{50} values of studied compounds.

We found that attachment of Pem to three oligopeptides studied (IELLQARGGC, RRRRRRRRGGC, and IELLQARGGC-GGRRRRRRRR) only slightly decreased the cytostatic effect of free Pem in both cell lines (IC_{50} changed from 1.05 to 7.7 in case of NCI-H358 cell and from 0.55 to 6.24 in case of HL-60 cells). It is interesting to note that there was no significant difference between the cytostatic effect of Pem-conjugates on NCI-H358 and on HL-60 cells, $Pem(OMe)_2$ was not as effective as Pem with free carboxylic groups.

Acknowledgments
These studies were supported by grants from Hungarian Research Fund (OTKA, No. K68285), Hungarian Ministry of Education (NKFP 1A005/04, Medichem 2), and grants from the National Office for Research and Technology, Hungary (3.2.1 – 2004-04-0005/3.0 and 3.2.1-2004-04-0352/3.0).

References

1. Hudecz, F., Reményi, J., Szabó, R., Kóczán, Gy., Mező, G., Kovács, P., Gaál, D. *J. Mol. Recognition* **16**, 288-298 (2003).
2. Miklán, Zs., Orbán, E., Csík, G., Schlosser, G., Magyar, A., Hudecz, F. *Biopolymers Peptide Science* **92**, 489-501 (2009).
3. Miklán, Zs., Szabó, R., Schlosser, G., Andreu, D., Hudecz, F., In Rolka, K., Rekowski, P. and Silberring, J. (Eds.) *Peptides 2006: (Proceedings of the 29th European Peptide Symposium)*, Kenes International, Switzerland, 2007, p. 538-539.
4. Hudecz, F., Bánóczi, Z., Csík, G. *Medicinal Research Reviews* **25**, 679-786 (2005).
5. Fukuda, M., et al. *Cancer Research* **60**, 450-456 (2000).
6. Slater, T.F., Sawyer, B., Strauli, U. *Biochimica Biophysica Acta*, **77**, 383-393 (1963).

Proceedings of the 31st European Peptide Symposium
Michal Lebl, Morten Meldal, Knud J. Jensen, Thomas Hoeg-Jensen (Editors)
European Peptide Society, 2010

Towards Lasso Peptide Engineering: Insights into the Maturation Mechanism of Microcin J25

Kok-Phen Yan, Séverine Zirah, Yanyan Li, Christophe Goulard, and Sylvie Rebuffat

Muséum National d'Histoire Naturelle, Centre National de la Recherche Scientifique, Laboratoire Molécules de Communication et Adaptation des Microorganismes, FRE 3206 CNRS-MNHN, 75005, Paris, France

Introduction

Lasso peptides are knotted structures of bacterial origin, consisting of 16-21 residues, where an N-terminal macrolactam ring (resulting from the condensation of the N-terminal amine with a side chain carboxylate at position 8-9) traps the C-terminal tail of the peptide within it [1]. These peptides are remarkably resistant to proteases and denaturing agents and show diverse biological activities such as receptor antagonists or enzyme inhibitors, resulting for some of them in antimicrobial activities. Such properties thus confer lasso peptides a high biotechnological interest. It is therefore essential to understand the mechanisms of their biosynthesis. Lasso peptides are biosynthesized from a gene-encoded precursor that is processed by two maturation enzymes [2,3]. In this study, we used microcin J25 (MccJ25) [4,5] as a model peptide to unveil the mechanisms underlying the biosynthesis of lasso peptides. MccJ25 is synthesized as a linear 58 amino acid precursor (McjA) containing a leader region in its N-terminal part, which is processed by two maturation enzymes (McjB and McjC) (Figure 1A). In a previous study, we were able to synthesize mature MccJ25 *in vitro* upon incubation of McjA with McjB and McjC in the presence of ATP and Mg^{2+} [2]. McjB shows weak similarities to putative transglutaminases that belong to the cysteine protease family. McjC is homologous to proteins involved in the formation of amide bonds (asparagine synthetases and β-lactam synthetases). We therefore hypothesized that McjB could be responsible for the cleavage of the precursor McjA and that McjC could be involved in the formation of the macrolactam ring. In order to examine this hypothesis, we used a site-directed mutagenesis approach in order to study the role of the McjA leader peptide and to confirm the respective roles of McjB and McjC.

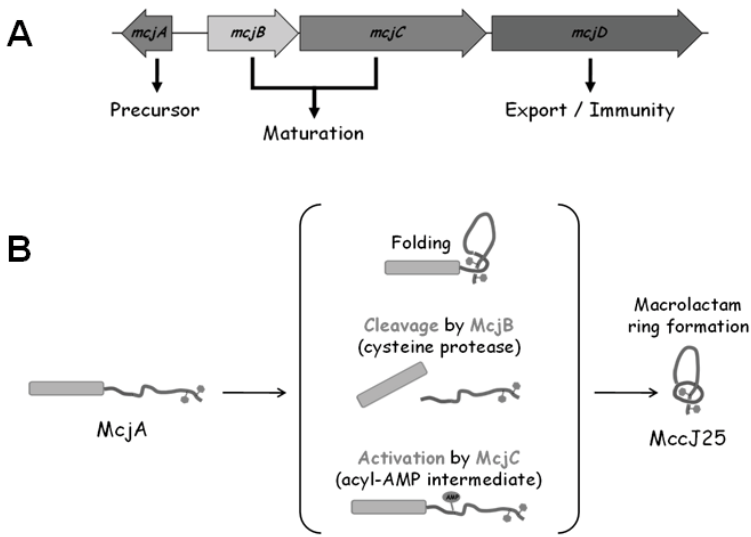

Fig. 1. A. Genetic system encoding MccJ25; B. Schematic view of MccJ25 maturation (the order of the 3 steps in brackets remains to be determined).

Results and Discussion

Site-directed mutagenesis was performed on the pTUC202 plasmid (containing the MccJ25 biosynthesis cluster) by using the QuickChange XL Site-Directed Mutagenesis Kit (Agilent Technologies). The plasmid carrying mutations was transformed into a producing strain, which was then cultured in M63 medium to assess the production of mature MccJ25 in the culture supernatant by LC-MS detection.

Sequence analysis of McjB enabled to hypothesize that McjB could be a protease responsible for the cleavage of the precursor McjA [2]. Site-directed mutagenesis allowed to show that McjB is actually a cysteine protease, where Cys150, His182 and Glu186 are crucial residues for its activity, probably constituting a catalytic triad. The involvement of Cys150 of McjB in the maturation process has been confirmed *in vitro* by analyzing the production of MccJ25 from recombinant McjA in the presence of either recombinant McjB or McjB[C150A], and recombinant McjC, ATP and Mg^{2+}.

The homologue of McjC, the asparagine synthetase, catalyses the activation of the carboxyl group via an acyl-AMP intermediate and subsequent formation of the amide bond. Sequence analysis of McjC revealed conserved residues involved in the binding of ATP and Mg^{2+} [2]. Site-directed mutagenesis of these residues (Ser199, Asp203 and Asp302) confirmed that they are crucial for McjC activity. It thus provides evidence that McjC is responsible for the activation of the side chain of Glu8 of MccJ25, which is a pre-required step for the macrolactam ring formation.

Therefore, the study shows that the biosynthesis of MccJ25 requires the involvement of two enzymes: one is a cysteine protease (McjB), which cleaves the precursor McjA, while the other (McjC) activates the substrate possibly by formation of an acyl-AMP intermediate. Prior to the macrolactam ring closure, the folding of the precursor must occur so that the C-terminal tail can be properly trapped within it (Figure 1B). However the order of these different steps remains to be determined.

Our work provides insights into the biosynthesis of lasso peptides. Such knowledge would probably have important biotechnological impacts, as the lasso structure in combination with its maturation enzymes could be used to generate peptides endowed with novel bioactivities. The understanding of the mechanisms underlying the formation of the lasso structure is therefore a major step towards the engineering of lasso peptides.

Acknowledgments

This work was supported by the ANR project n BLAN-NT09-692063. We acknowledge the mass spectrometry platform at the MNHN for access to the ESI-Qq-TOF spectrometer as well as the bacteriology facility.

References

1. Rebuffat, S., Blond, A., Destoumieux-Garzón, D., Goulard, C., Peduzzi, J. *Curr. Protein Pept. Sci.* **5**, 383-391 (2004).
2. Duquesne, S., Destoumieux-Garzón, D., Zirah, S., Goulard, C., Peduzzi, J., Rebuffat, S. *Chem. Biol.* **14**, 793-803 (2007).
3. Knappe, T.A., Linne, U., Zirah, S., Rebuffat, S., Xie, X., Marahiel, M.A. *J. Am. Chem. Soc.* **130**, 11446-11454 (2008).
4. Salomón, R.A., Farías, R.N. *J. Bacteriol.* **174**, 7428-7435 (1992).
5. Rosengren, K.J., Clark, R.J., Daly, N.L., Goransson, U., Jones, A., Craik, D.J. *J. Am. Chem. Soc.* **125**, 12464-12474 (2003).

Proceedings of the 31st European Peptide Symposium
Michal Lebl, Morten Meldal, Knud J. Jensen, Thomas Hoeg-Jensen (Editors)
European Peptide Society, 2010

Enterocins L50A and L50B from *Enterococcus durans* A5-11: Conformational and Antibacterial Studies

Séverine Zirah[1], Christophe Goulard[1], Rémi Ducasse[1], Michèle Dalgalarrondo[2], Jean Peduzzi[1], Jean-Marc Chobert[2], Thomas Haertlé[2], and Sylvie Rebuffat[1]

[1]Muséum National d'Histoire Naturelle, Centre National de la Recherche Scientifique, Laboratoire Molécules de Communication et Adaptation des Microorganismes, FRE 3206 CNRS-MNHN, 75005 Paris, France. [2]Institut National de la Recherche Agronomique, UR 1268, Biopolymères Interactions Assemblages, équipe Fonctions et Interactions des Protéines Laitières, Nantes, France

Introduction

Bacteriocins produced by lactic acid bacteria are ribosomally-synthesized peptides that show potent antibacterial activity against certain Gram-positive bacteria and in particular food pathogens such as *Listeria*. They present a strong interest as potential food preservatives. Class IIb bacteriocins consist of two different unmodified peptides for which optimal antibacterial activity requires the presence of both peptides in about equal amounts [1,2], while class IId includes leaderless peptides (class II2 in the enterocin classification) [3], synthesized without an N-terminal leader sequence.

Two antibacterial peptides secreted by *Enterococcus durans* A5-11 isolated from Mongolian airag (traditional fermented mare's milk) [4] were purified from culture supernatants and characterized in terms of amino-acid sequences, conformations, antibacterial activities, and potential synergy.

Results and Discussion

Isolation. *Enterococcus durans* A5-11 isolated from Mongolian airag was grown in M17 medium at 37°C overnight. The supernatant was subjected to SP-Sepharose cation-exchange chromatography. The active fraction (elution in 0.6 M NaCl) was salted out by solid-phase extraction on a C_{18} cartridge. Enterocins were further purified by reversed-phase high-performance liquid chromatography on an Uptisphere C_4 column.

Peptide sequences. The purified peptides were identified as enterocins L50A and L50B isolated previously from *Enterococcus faecium* [5]. Despite 72% of sequence identity, the two peptides showed different sensibility to proteases, L50A and L50B being resistant and sensible to trypsin, respectively.

L50A: `f-MGAIAKLVAK FGMPIVKKYY KQIMQFIGEG WAINKIIEWI KKHI`
L50B: `f-MGAIAKLVTK FGMPLIKKFY KQIMQFIGQG WTIDQIEKWL KRH`

Table 1. Minimal inhibitory concentrations of L50A and L50B

	MIC (nM)				
	EntL50A	*EntL50B*	*EntL50 A/B*		
			75/25	50/50	25/75
Lactobacillus brevis F1.114	156	312	156	156	312
Enterococcus faecium	156	312	nd	156	nd
Lactobacillus sakei sp.*sakei*	500	>500	nd	250	nd
Listeria ivanovii sp. *ivanovii* N29	312	625	312	312	625
Lactobacillius plantarum	625	312	nd	625	nd

Antibacterial activities. Each isolated peptide exhibited potent activity on a variety of Gram-positive bacteria. L50A was in most cases twice more active than L50B. A weak synergy effect of EntL50A/EntL50B combination was observed on the *Lactobacillus sakei* sp. *sakei* strain, exclusively.

Conformational studies

The CD spectra revealed a helical conformation for L50A and L50B peptides in phosphate buffer at pH 7.0, both in the absence and in the presence of SDS micelles. The helix content increased in the presence of micelles only in the case of L50B.

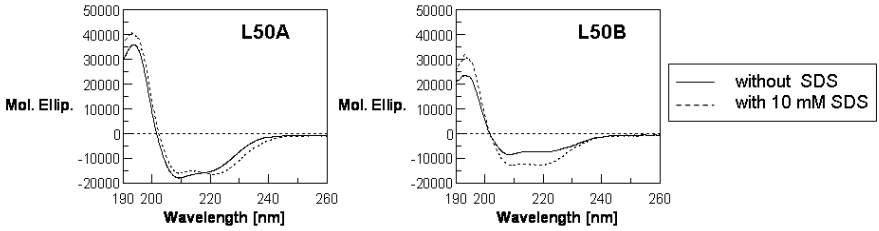

Fig. 1. Circular dichroism spectra of L50A and L50B, 100 µM in 10 mM phosphate buffer, pH 7.

Conclusion

Enterococcus durans A5-11 produces the two leaderless peptides - enterocins L50A and L50B, what confers to this strain interest as a biopreservative or a probiotic. Enterocins L50A and L50B are well structured in aqueous media and exhibit individual and weak synergistic activities, two characteristics that differ from those shared by two-peptide bacteriocins from class IIb.

The different properties observed for L50A and L50B in spite of high sequence similarities paves the way for studies of structure/activity relationships.

Acknowledgments

We acknowledge the mass spectrometry facility of the MNHN for access to the ESI-Qq-TOF spectrometer.

References

1. Oppegård, C., Rogne, P., Emanuelsen, L., Kristiansen, P.E., Fimland, G., Nissen-Meyer, J. *J. Mol. Microbiol. Biotechnol.* **13**, 210-219 (2007).
2. Nissen-Meyer, J., Oppegård, C., Rogne, P., Haugen, H.S., Kristiansen, P.E. *Probiotics Antimicrob. Proteins* **2**, 52-60 (2010).
3. Franz, C.M.A., Belkum, M.J., Holzapfel, W.H., Abriouel, H., Gálvez, A. *FEMS Microbiol. Rev.* **31,** 293-310 (2007).
4. Batdorj, B., Dalgalarrondo, M., Choiset, Y., Pedroche, J., Métro, F., Prévost, H., Chobert, J.-M., Haertlé, T. *J. Appl. Microbiol.* **101**, 837-848 (2006).
5. Cintas, L,M., Casaus, P., Holo, H., Hernandez, P.E., Nes, I.F., Havarstein, L.S. *J. Bacteriol.* **180**, 1988-1994 (1998).

Proceedings of the 31st European Peptide Symposium
Michal Lebl, Morten Meldal, Knud J. Jensen, Thomas Hoeg-Jensen (Editors)
European Peptide Society, 2010

Revealing the Lytic Mechanism of the Antimicrobial Peptide Gomesin by Optical Microscopy of Giant Unilamellar Vesicles and Isothermal Titration Calorimetry

Tatiana M. Domingues[1], Joachim Seelig[2], Karin A. Riske[1], and Antonio Miranda[1]

[1]Department of Biophysics, Federal University of São Paulo, São Paulo, 04044-020, Brazil; [2]Department of Biophysical Chemistry, Biocenter of the University of Basel, 4051, Basel, Switzerland

Introduction

Gomesin (Gm) is a potent cationic antimicrobial peptide from a Brazilian spider [1,2]. Here we use optical and fluorescence microscopy to study the interaction of Gm, its low active linear analogue, [Ser^{2,6,11,15}]-Gm (GmL), and a fluorescent labeled analogue, Gm-Rh, with giant unilamellar vesicles (GUVs, 10 μm) composed of mixtures of the neutral lipid POPC with the negatively charged lipid POPG or cholesterol, so as to mimic bacterial and mammalian cell membranes, respectively. We observed the effect of injecting a peptide solution with a micropipette close to GUVs. As a result of peptide-lipid interaction, GUVs burst suddenly. Stable pores, which result in leaky vesicles, were not observed. These facts lead us to conclude that Gm and GmL disrupt the membrane via the carpet model [3]. GmL exhibited lower lytic activity as compared to Gm, but this difference vanished at high POPG molar fraction. Additionally, the interaction of Gm and GmL with large unilamellar vesicles (LUVs, 100 nm) of various POPC:POPG ratios was investigated with isothermal titration calorimetry (ITC). Binding of GmL to negatively charged vesicles is an exothermic process for all POPC:POPG ratios investigated. On the other hand, the binding of Gm entails an exothermic and an endothermic component; the latter is more pronounced at low POPG ratio and vanishes for 50 mol% POPG.

Results and Discussion

Different experimental setups were used to study the interaction between the antimicrobial peptides and the vesicles (GUVs and LUVs). First we observed the effect of injecting

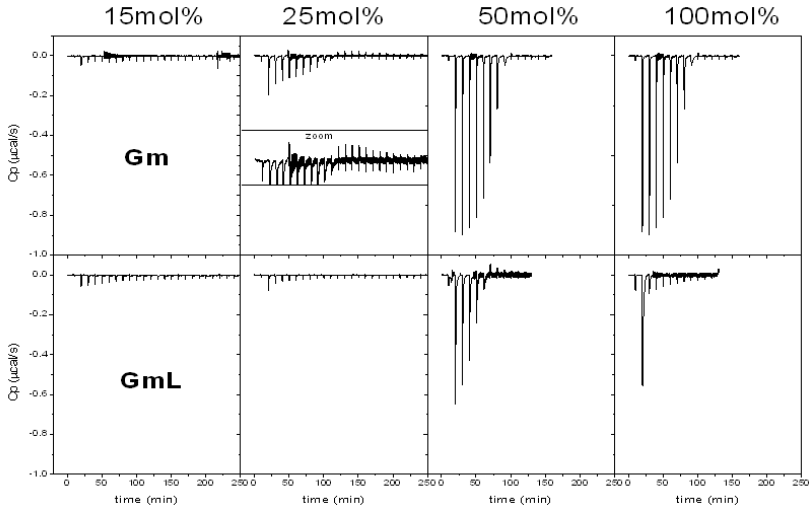

Fig. 1. Heat flow vs. time measured with ITC. The syringe was loaded with 6 mM lipid and the cell was filled with 10 μM peptide in all experiments. T = 25 °C, 10 mM Phosphate buffer, pH 7.4

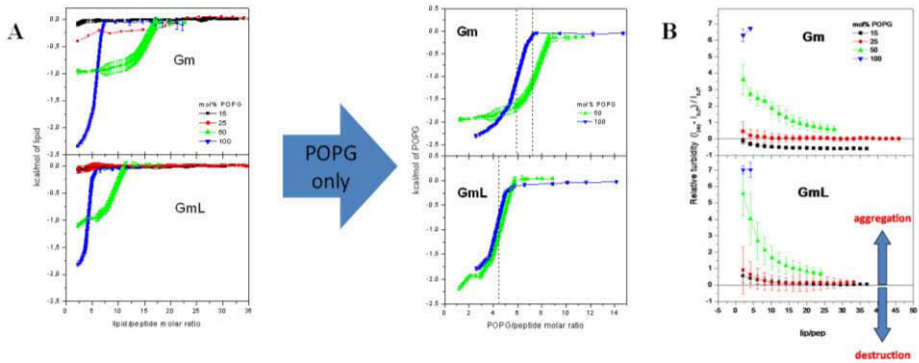

Fig. 2. (A) Integrated heat per injection normalized with respect to the number of moles of lipids (all, left or POPG only, right). (B) Relative intensity of 90º light scattering.

fluorescently labeled Gm (Gm with a rhodamine group attached to the N^{ε}-amino group of the lysine residue; denoted Gm-Rh) by a micropipette placed at the vicinities of a GUV by optical microscopy (data not shown). Generally, we observed that Gm-Rh first binds to the vesicle surface, then accumulates at certain points (small high-contrast regions).

Afterwards, the vesicles suddenly burst through the opening of a large hole, and the membrane rearranges into an interconnected tubular structure. As control, in the absence of peptide, the GUVs were never spontaneously disrupted [3].

Still using the optical microscopy, GUV solutions of different composition were mixed with increasing concentrations of Gm or [$Ser^{2,6,11,15}$]-Gm (data not shown). The number of GUVs as a function of time was used to quantify the lytic activity of the peptides. The measurements were done for different compositions of GUVs and concentrations of Gm and [$Ser^{2,6,11,15}$]-Gm. In the other setup, we tested the interaction between these peptides (Gm and GmL) and LUVs by using ITC. As shown in Figure 1, the magnitude of ΔH increased with the mol% of POPG. Besides that, the interaction of Gm with one bilayer composition was always stronger than its linear analogue interaction [4]. The sigmoidal curves obtained at high mol% POPG fall close to a mastercurve when the data is shown relative to the mol% POPG only (Figure 2A). In our last experiment, the 90º light scattering (λ = 400 nm) of dispersions of LUVs with peptides was measured in the same conditions as in the ITC experiments. The data, Figure 2B, are shown as relative intensities: positive values indicate aggregation of LUVs driven by the peptides and negative values indicate destruction of LUVs induced by peptide action. High binding affinity (both peptides against 50 and 100 mol% POPG) is accompanied by extensive vesicle aggregation. The interaction of both Gm and GmL with POPC/POPG is mainly an enthalpy-driven process ($\Delta H < 0$), which seems to happen with POPG lipids only. An endothermic component appears under some conditions.

Acknowledgments
This work was supported by FAPESP, CNPq, and CAPES.

References

1. Silva Jr., P.I., et al. *J. Biol. Chem.* **275**, 33464-33470 (2000).
2. Fazio, M.A., et al. *Biopolymers* **84**, 205-218 (2006).
3. Domingues, T.M., et al. *Langmuir*. **26**, 11077-11084 (2010).
4. Seelig, J. *Biochim. Biophys. Acta.* **1331**, 103-116 (1997).

Proceedings of the 31st European Peptide Symposium
Michal Lebl, Morten Meldal, Knud J. Jensen, Thomas Hoeg-Jensen (Editors)
European Peptide Society, 2010

Study of a New Maurocalcine CPP Analogue Devoid of Pharmacological Activity

Cathy Poillot and Michel De Waard
Grenoble Institute of Neuroscience, Inserm U836, Laboratory "Calcium Channels, Functions and Pathologies", University Joseph Fourier, 38043, Grenoble, France

Introduction

Maurocalcine (MCa) is a peptide isolated from the venom of a Tunisian scorpion *Scorpio maurus palmatus*. The 3D solution structure of MCa was defined by 1H-NMR. The peptide displays an inhibitor cystine knot motif [1] containing three β-strands. β-Strands 2 and 3 form an antiparallel sheet. The folded/oxidized peptide contains three disulfide bridges arranged according to the pattern: Cys3-Cys17, Cys10-Cys21 and Cys16-Cys32 [2]. MCa could be classified in the growing list of cell penetrating peptides (CPP) due to its ability to efficiently cross the plasma membrane, alone or coupled to various cargoes. However, MCa was initially studied for its pharmacological properties. It interacts with an intracellular calcium channel, the ryanodine receptor (RyR) inducing Ca2+ release from intracellular stores. Here, our study aimed at producing a MCa analogue that no longer recognizes the RyR, avoiding the associated Ca2+ release from the endoplasmic reticulum, but keeping intact the cell penetration properties of the peptide. We achieved this goal by producing D-MCa, a folded analogue in which all L-amino acids were replaced by D-amino acids.

Methods

D-MCa was chemically synthesized by a solid-phase method [3] using an automated peptide synthesizer (CEM© Liberty). N-α-Fmoc-D-aminoacids, Wang-Tentagel resin and reagents used for synthesis were purchased from Iris Biotech. Peptide chain was assembled on a Fmoc-D-Arg(Pbf)-Wang-Tentagel resin using a N-α-fluorenylmethyloxycarbonyl (Fmoc) D-amino-acid derivatives. The protecting groups for the side chain were: tert-butyloxycarbonyl for lysine, Pbf for arginine, trityl for cysteine and asparagines and tert-butyl for serine, threonine, glutamate and aspartate. When the peptide chain was assembled, the resin was treated for 4 hrs at room temperature with a mix of trifluoroacetic acid/water/triisopropylsilane/dithiothreitol and then filtered. The filtrate was then precipitated by addition of cold t-butylmethyl ether. The reduced peptide was dissolved in a Tris-HCl buffer and stirred for 72 hrs at room temperature for oxidation and folding. D-MCa was then purified by HPLC, and the purified fraction was analyzed by MALDI-TOF mass spectrometry. The pure D-MCa was then labeled by 5(6)-carboxyfluorescein (FAM).

Results and Discussion

MCa has been the first demonstrated animal toxin acting as a cell penetrating peptide. It is unique in the sense that its natural molecular target, RyR, is localized inside cells at the endoplasmic reticulum membrane. The binding site of MCa onto RyR is localized at the cytosolic face of the channel indicating that MCa has to cross the plasma membrane in order to reach its target [4]. To avoid these pharmacological properties, it was necessary to develop new MCa analogues that would only keep the cell penetration properties of the original molecule. Several strategies had been used in the past, including point mutated analogues of MCa [5], and an MCa peptide devoid of disulfide bridges [6]. These two strategies, while efficiently working, produced analogues whose cell penetrating properties were slightly less efficient than the native molecule. Here (Figure 1) we illustrate the result of a novel strategy in which all L-amino acids were replaced by D-amino acids during peptide synthesis. Remarkably, the peptide folded/oxidized particularly well, presenting the same disulfide bridge pattern and β-strand structures than L-MCa. D-MCa preserves the characteristic basic face, presumed to be essential for cell penetration of the peptide. The anisotropy of charge is thus perfectly maintained and D-MCa is the mirror image of L-MCa. Ligand / receptor recognition is sensitive to the

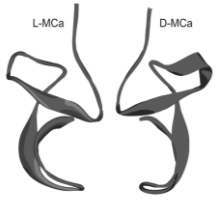

Fig. 1. Ribbon representation of L-MCa and D-MCa.

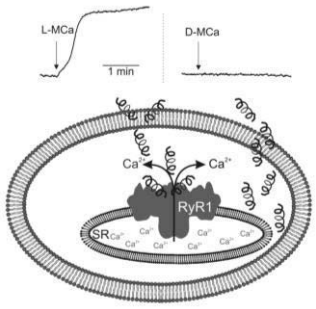

Fig. 2. Effect of L-MCa and D-MCa on Ca^{2+} release through RyR.

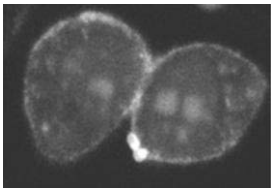

Fig. 3. Cell penetration of D-MCa-FAM in CHO cells.

enantiomeric form of the ligand. D-MCa should no longer bind onto RyR and thus ineffectively trigger Ca^{2+} release from the endoplasmic reticulum (Figure 2). This was indeed observed as published earlier [7]. As expected from a peptide synthesized with D amino acids, D-MCa is fully protease resistant (to trypsin and chymotrypsin), even after 24 hrs of incubation, at times and concentrations where L-MCa is fully degraded. The objective of the study was to develop an analogue that preserved cell penetration properties. Earlier studies on CPPs had demonstrated that D-Tat or D-penetratin kept normal cell penetration properties. A similar behavior was expected for D-MCa. This conserved property can be explained by intact interaction with glycoaminoglycans (GAGs) and negatively charged lipids [8]. D-MCa was labeled on its N-terminus with 5,6-carboxyfluorescein first. Dose-response curves for cell penetration of FAM-D-MCa, as assessed by flow cytometry, demonstrate that FAM-D-MCa penetrates with a similar dose-dependent relationship than FAM-L-MCa [7]. Also, cell penetration was evidenced by confocal microscopy and images reflected either diffuse staining (likely by a process of membrane translocation), indicating a predominant cytoplasmic localization, or more punctuate staining (indicating a form of endocytosis), that is reminiscent of late endosomes (Figure 3). An earlier study had pointed out that depending on the nature of the cargo, L-MCa could preferentially choose between membrane translocation [9] and macropinocytosis [8] for cell entry. This question was sorted out by applying inhibitors of macropinocytosis and quantifying by FACS the amount of cell entry of FAM-D-MCa. We found out that endocytosis represents only a minor fraction of D-MCa entry, suggesting that D-MCa would be an excellent vector for the delivery of compounds within the cytoplasm.

Concluding remarks

We were able to produce a D-analogue of L-MCa that folded remarkably well and preserved the original disulfide pattern of L-MCa. The resulting peptide shows a total lack of pharmacological activity since it no longer recognizes RyR or produces Ca^{2+} release from the endoplasmic reticulum. The data demonstrate however that D-MCa is as efficient as L-MCa for cell penetration and cargo delivery. It has the added benefit to be protease-resistant. For all these reasons, we predict that it has a bright future for the cell delivery of compounds *in vivo* for applications where the half-life of the vector / cargo couple matters.

Acknowledgments

This work was supported by grants from technology pour la santé (Program TIMOMA2 of the Commissariat à l'Energie Atomique) and from ANR PNANO (SYNERGIE and NanoFret programs).

References

1. Mosbah, A., et al. *Proteins* **40** (3), 436-442 (2000).
2. Fajloun, Z., et al. *FEBS Lett*. **469**(2-3), 179-185 (2000).
3. Merrifield, R.B. *Mol. Biol.* **32**, 221-296 (1969).
4. Altafaj, X., et al. *J. Biol. Chem*. **280**(6), 4013-4016 (2005).
5. Mabrouk, K., et al. *Biochim Biophys Acta* **1768**(10), 2528-2540 (2007).
6. Ram, N., et al. *J. Biol. Chem.* **283**(40), 27048-270056 (2008).
7. Poillot, C., et al. *J. Biol. Chem*. in press (2010).
8. Ram, N., et al. *J. Biol. Chem*. **283**(35), 24274-24284(2008).
9. Aroui, S., et al. *Pharm. Res*. **26**(4), 836-845(2009).

Proceedings of the 31st European Peptide Symposium
Michal Lebl, Morten Meldal, Knud J. Jensen, Thomas Hoeg-Jensen (Editors)
European Peptide Society, 2010

Comparison of the Mechanism of Action of Antimicrobial Peptides on Giant Unilamellar Vesicles via Optical Microscopy

Marta N.C. Martins, Tatiana M. Domingues, Karin A. Riske, and Antonio Miranda

Department of Biophysics, Federal University of São Paulo, São Paulo, SP, 04044-020, Brazil

Introduction

Antimicrobial peptides (AMPs) are important components of the innate defense system of plants and animals against microorganisms, such as bacteria and fungi. Most AMPs are cationic and amphipathic, features which are essential for their interaction with the lipid phase. Initially, the cationic aspect of AMPs ensures an accumulation at the membrane surface of the microorganisms, rich in negatively charged lipids. Subsequently, the amphiphilic character of the AMPs facilitates their insertion into lipid bilayers, with formation of pores and/or disruption of membranes. Due to its broad antibacterial and antifungal activity spectrum AMPs are a potential target for the development of alternative therapeutic applications. In order to understand the mechanism of lytic action we used optical microscopy to compare the interaction of different AMPs (Table 1) with giant unilamellar vesicles (GUVs) composed of mixtures of the neutral lipid palmitoyl-oleoyl phosphatidylcholine (POPC) with the negatively charged lipid palmitoyl-oleoyl-phosphatidyl-glycerol (POPG) (1:1) so as to mimic bacterial cell membrane.

Results and Discussion

Peptides were synthesized by SPPS, purified by preparative RP-HPLC and characterized by AAA and LC-MS [1]. GUVs were grown by the electroformation method [2,3] in 0.2 M sucrose and later diluted into 0.2M glucose. This created a sugar asymmetry which enhanced the optical contrast with phase contrast microscopy. The GUVs were then placed in an observation chamber. A solution of peptide was injected and a population of vesicles was followed with time in order to evaluate the lytic activity of the different AMPs studied (Table 1). Our results (Figure 1) indicated that gomesin [4], polyphemusin II [5] and tachyplesin I [6] induced sudden burst of GUVs, with accompanying fast release of the entrapped volume. Stable pores, which result in leaky vesicles, were not observed. On the other hand, magainin II [7] and protegrin I [8] were able to induce the opening of stable pores through which the initial sucrose/glucose asymmetry of the GUVs was lost.

Table 1. Antimicrobial peptides employed in this study.

Name	*Sequence*[a]
gomesin	Z-C-R-R-L-C-Y-K-Q-R-C-V-T-Y-C-R-G-R-NH_2
polyphemusin II	R-R-W-C-F-R-V-C-Y-K-G-F-C-Y-R-K-C-R-NH_2
tachyplesin I	K-W-C-F-R-V-C-Y-R-G-I-C-Y-R-R-C-R-NH_2
magainin II	G-I-G-K-F-L-H-S-A-K-K-F-G-K-A-F-V-G-E-I-M-N-S-NH_2
protegrin I	R-G-G-R-L-C-Y-C-R-R-R-F-C-V-C-V-G-R-NH_2

[a] *Z = pyroglutamic acid*

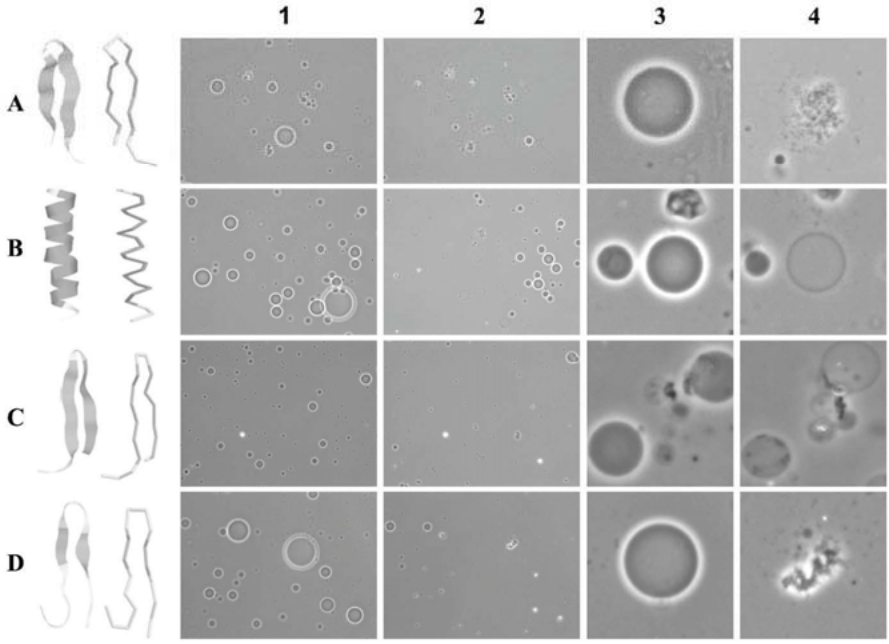

Fig. 1. Phase contrast images of GUVs composed by POPG/POPC (1:1) in the presence of (A) gomesin (A4) after t.480 s; (B) magainin II,(B4) after t.675 s; (C) protegrin I, (C4) after t.973 s; (D) polyphemusin II, (D4) after t.835 s; (E) tachyplesin I, (E4) after t.778 s. The snapshots in columns 1 and 2 were taken with a 20x objective and those in columns 3 and 4 were taken with a 63x objective.

Although magainin II and protegrin I strongly interacted with phospholipid vesicles and induced leakage, their mechanism of action was different and could be discerned with optical microscopy of giant vesicles. We conclude that gomesin, polyphemusin II and tachyplesin I act via the carpet model, whereas magainin II and protegrin I form toroidal or barrel pores. Consequently, studies with GUVs provide an easy way of testing the potential antimicrobial activities of several lead compounds.

Acknowledgments
The work was supported by FADA-UNIFESP, FAPESP, CNPq and CAPES.

References

1. Miranda, A., et al. *J. Med. Chem.* **37**, 1450-1459 (1994).
2. Angelova, M.I., et al. *Faraday Discuss.* **81**, 303-311 (1986).
3. Domingues, T.M., et al. *Langmuir* **26,** 11077-11084 (2010).
4. Silva, P.I., et al. *J. Biol. Chem.* **275**, 33464-33470 (2000).
5. Powers, J.P., et al. *Biochim Biophys Acta* **1698**, 239-250 (2004).
6. Kawano, K., et al. *J. Biol. Chem.* **265**, 15365-15367 (1990).
7. Zasloff, M., et al. *Proc. Natl. Acad. Sci.* **84**, 5449-5453 (1987).
8. Aumelas, A., et al. *Eur. J. Biochem.* **237**, 575-583 (1996).

Proceedings of the 31st European Peptide Symposium
Michal Lebl, Morten Meldal, Knud J. Jensen, Thomas Hoeg-Jensen (Editors)
European Peptide Society, 2010

Lasiocepsin: Novel Antimicrobial Peptide from the Venom of Eusocial Bee *Lasioglossum laticeps*

Lenka Monincová, Jiřina Slaninová, Vladimír Fučík, Oldřich Hovorka, Zdeněk Voburka, Lucie Bednárová, Petr Maloň, and Václav Čeřovský

Institute of Organic Chemistry and Biochemistry, Academy of Sciences of the Czech Republic, Flemingovo nám. 2, Prague 6, 166 10, Czech Republic

Introduction

We have already shown that the venom of wild bees is a rich source of pharmacologically interesting antimicrobial peptides (AMPs). As an example, three linear α-helical AMPs named lasioglossins (LL-I, LL-II and LL-III) were identified by us in the venom of the wild eusocial bee *Lasioglossum laticeps* [1]. Further detailed inspection of the venom extract revealed the presence of other interesting AMPs. One of those, which we named lasiocepsin (LAS), is a 27 amino acid residue peptide containing two intramolecular disulfide bridges (Figure 1). Here we describe its isolation, synthesis, structure characterization and biological activities.

Results and Discussion

Bee specimens of *Lasioglossum laticeps* were collected in front of our institute in Prague in June 2009. The venom reservoirs of 10 individuals were removed by dissection and their contents extracted with a mixture (25 µl) of acetonitrile/water (1:1) containing 0.5% TFA. The extract was fractioned by RP-HPLC (Figure 2). The components of the peaks detected at 220 nm were analyzed by mass spectrometry and tested for the presence of antimicrobial activity against *Micrococcus luteus* (Figure 2, inset). The anti-*M. luteus* active peptides were subjected to Edman degradation. Three peaks (24, 28 and 29) corresponded to the recently identified lasioglossins (LL-I, LL-II and LL-III) [1]. Two peptides (20, 23), showed sequence and structure similarities to lasioglossins (LL-IV and LL-V). The peptide of the peak numbered 22 showed a significantly different sequence. We named this peptide lasiocepsin (LAS) and it became the object of our study.

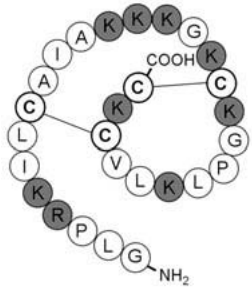

Fig. 1. Primary sequence of Lasiocepsin.

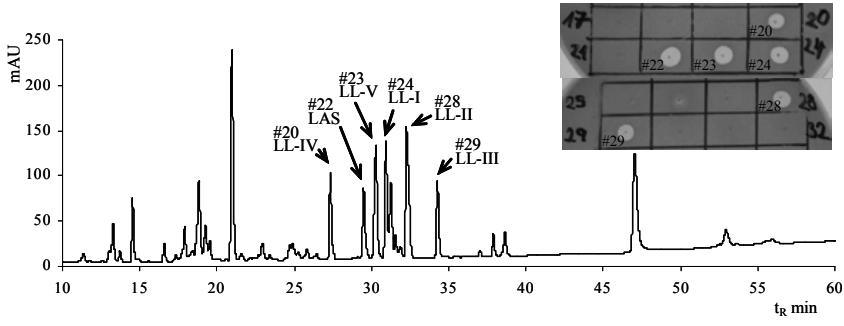

Fig. 2. RP-HPLC profile of Lasioglossum laticeps venom extract at 220 nm on Vydac C-18 column (205 x 4.6 mm). An elution gradient of solvent from 5% to 70% of acetonitrile/water/0.1% TFA was applied for 60 min at 1 ml/min flow rate. Inset: Anti-M. luteus activity (clear zones in the drop diffusion test) of individual fractions delineated in the profile.

Table 1. Antimicrobial and hemolytic activity of lasiocepsin (LAS) and its two analogous side products differing in the pattern of disulfide bridges (LAS 8-27,17-25 and LAS 8-17,25-27) compared to other antimicrobial compounds

Peptide	*Mw [Da]*	*Antimicrobial activity MIC [μM][a]*				*Hemolytic activity*
		B.s.	*E.c.*	*S.a.*	*P.a.*	*LC_{50} [μM]*
LAS	2891.7	0.4	8.6	93	15	> 200
LAS 8-27,17-25	2891.7	0.8	41.7	> 100	> 80	> 200
LAS 8-17,25-27	2891.7	6.0	> 25	> 100	> 25	> 200
LL-I	1722.1	0.8	1.7	14.3	15.8	> 200
Indolicidin	1906.3	1.0	> 100	13.0	> 100	> 200
Tetracycline	444.4	12.5	0.4	1.5	75.7	> 200

[a]*B.s., Bacillus subtilis; E.c., Escherichia coli; S.a., Staphylococcus aureus; P.a., Pseudomonas aeruginosa*

Lasiocepsin primary sequence determined by Edman degradation and pattern of disulfide bridges (Cys8-Cys25, Cys17-Cys27) determined by MS analysis of the fragments resulting from trypsin digestion of the peptide, is shown on Figure 1.

The linear peptide was synthesized manually using a solid-phase method in a 5 mL polypropylene syringe with a bottom Teflon filter. The synthesis was done using standard protocol of N^{α}-Fmoc chemistry on 2-chlorotrityl chloride resin. All Cys side chains were protected with trityl groups. The crude peptide showing HPLC profile dominated by the peak of required product was purified by HPLC. The purified linear peptide was then oxidized by stirring the peptide in the 0.1 M ammonium acetate buffer pH 7.8 in the open air. This oxidative folding resulted however in the mixture of three peptides differing in the pattern of disulfide bridges. The amount of lasiocepsin in the mixture represented roughly half of the distribution. Synthetic lasiocepsin (LAS) showed potent antimicrobial activity against both Gram-positive and -negative bacteria. Especially interesting is its high potency against *Pseudomonas aeruginosa* and no hemolytic activity against rat and human erythrocytes. Lasiocepsin also possess antifungal activity against *Candida albicans*. CD spectra of lasiocepsin and of its analog having wrong pattern of disulfide bridges both showed significant portion of α-helical structure (35% for the natural LAS, lower – 26% proportion for the non natural analog LAS 8-27,17-25). Upon addition of 2,2,2-trifluoroethanol as a helix promoting solvent both peptides adopted similar conformation containing about 40% of α-helical structure although dynamics of this change was faster for the natural LAS. This conformational behavior correlates with differences in antibacterial activity and supports the idea of the significance of α-helical conformation as a part of the lasiocepsin molecule for the biological process.

Acknowledgments

This work was supported by the Czech Science Foundation, grant No. 203/08/0536 and the research project No. Z40550506 of the Institute of Organic Chemistry and Biochemistry, Academy of Sciences of the Czech Republic.

References

1. Čeřovský, V., et al. *ChemBioChem* **10**, 2089-2099 (2009).

Proceedings of the 31st European Peptide Symposium
Michal Lebl, Morten Meldal, Knud J. Jensen, Thomas Hoeg-Jensen (Editors)
European Peptide Society, 2010

Selective Membrane Interactions of Nucleolar-Targeting Peptides

Margarida Rodrigues[1], Gandhi Rádis-Baptista[2,3], Beatriz G. de la Torre[2], Miguel Castanho[1], David Andreu[2], and Nuno C. Santos[1]

[1]Instituto de Medicina Molecular, Faculdade de Medicina da Universidade de Lisboa, 1649-028, Portugal; [2]Departament de Ciències Experimentals I de la Salut, Universitat Pompeu Fabra, Barcelona, E-08003, Spain; [3]Laboratório de Bioquímica e Biotecnologia, Instituto de Ciências do Mar, Universidade Federal do Ceará, Fortaleza, 60165-081, Brazil

Introduction

Crotamine is one of the major components of the venom of *Crotalus durissus terrificus*, a rattlesnake from South America. This toxin, when present at high (mM) concentrations, leads to the spastic paralysis of the hind limbs [1]. However, when present at (μM) concentrations, it can selectively translocate into actively proliferating cells [2], both *in vivo* and *in vitro* and localize to the nucleus. Moreover, it was observed that crotamine is able to deliver specific cargoes into the interior of the cell [2,3]. These characteristics allowed its classification as cell-penetrating peptide (CPP). Nucleolar-targeting peptides (NrTP) were designed by structural dissection of crotamine and, at μM concentration, they were also able to penetrate different cell types and exhibit exquisite nucleolar localization [4]. This new family of peptides was, therefore, classified as novel CPP. The peptides used throughout this work were: NrTP1 (YKQCHKKGGKKGSG), NrTP2 (YKQCHKKGG-Ahx-KKGSG), NrTP5 (ykqchkkGGkkGsG) and NrTP6 (KQSHKKGGKKGSG). Fluorescent derivatives of all peptides were also produced using rhodamine B as the fluorescent probe. The aim of this work was to pursue the study of NrTP molecular mechanism for translocation into cells, as well as to determine the ability of NrTP to deliver large molecules into cells.

Results and Discussion

The biophysical characterization was done by fluorescence spectroscopy using tyrosine intrinsic fluorescence as well as rhodamine B labeled NrTP. The work included quenching studies, quantification of partition into membrane model systems and translocation experiments. Quenching experiments with acrylamide showed a linear dependence on the acrylamide concentration. This result indicates that Tyr residues are exposed to acrylamide and that there is no peptide aggregation in solution. The Stern-Volmer constant (K_{SV}) for NrTP1 is 9.7 ± 0.2 M^{-1}, for NrTP2 12.1 ± 0.3 M^{-1} and for free Tyr 28.1 ± 0.2 M^{-1}. In the presence of lipid vesicles, the K_{SV} has a three-fold decrease except for free Tyr. This can be interpreted as a reduction of Tyr residues exposure to acrylamide. NrTP1 and NrTP2 interact with lipid membranes; consequently, they become less accessible to the quencher. NrTP1 and NrTP2 (Table 1) showed higher partition coefficients (for review see [5]) for POPC (zwitterionic) and POPG (anionic), both liquid state phospholipids, than for POPC:cholesterol (raft-like mixture on the liquid ordered state).

For the translocation experiments, rhodamine B labeled NrTP were used and tested with giant multilamellar, NBD-labeled vesicles. The co-localization of fluorescence spikes from NBD and rhodamine B (NrTP1-RhB) (Figure 1-A) indicates successful peptide translocation once it represents the presence of peptide in the inner membranes that appear inside some of the lipid vesicles. Despite the fact that the peptide fluorescence intensity is much lower than the one from NBD labeled vesicles, it is significantly different from the background, which thus, validates the conclusions. On the other hand, the translocation in cells is clearly more efficient

Table 1. Partition coefficient (K_p) for NrTP1 and NrTP2 in POPC, POPC:Chol and POPG LUV

Lipid	*NrTP1*	*NrTP2*
	$K_p(x\ 10^5) \pm SE$	$K_p(x\ 10^5) \pm SE$
POPC	2.7 ± 1.1	3.1 ± 0.8
POPC:Chol (2:1)	1.2 ± 0.2	0.7 ± 0.1
POPG	2.9 ± 0.6	2.5 ± 0.3

(Figure 1–B). Both lymphocyte cell lines (Bv173 and MOLT4) and peripheral blood mononuclear cells (PBMC) showed very high levels of peptide entry. These experiments were done using both NrTP1-RhB and NrTP5-RhB, and the results are very similar both for the profile in multilamellar giant vesicles and cells.

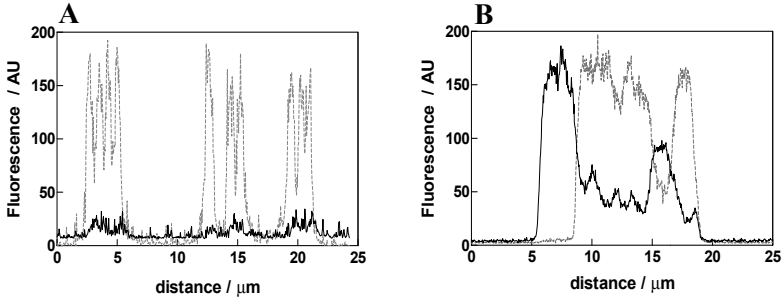

*Fig. 1. Translocation of NrTP1-RhB into giant multilamellar vesicles (POPC + DPPE-NBD 1%) and Bv173 (pre-B cell leukemia) cell line. Graphs represent fluorescence intensity along a longitudinal line drawn on the vesicle or cell, respectively. Panel **A** shows the co-localization of NBD (---) (488 nm laser) with NrTP1-RhB 15 mM (—) (561 nm laser). Each spike of NBD fluorescence corresponds to a lipid bilayer. Panel **B** shows the co-localization of the nuclear dye Hoeschst (---) (405 nm laser) with NrTP1-RhB 15 mM (—), (561nm laser).*

Finally, a conjugate of NrTP (NrTP6-C) bound to β–galactosidase (from *E. coli*) was prepared by chemical synthesis. This conjugate maintains enzymatic activity and is stable at 4ºC for several days, retaining its activity after -20ºC storage. Internalization studies for the delivery of β-galactosidase into HeLa cells were conducted with the above mentioned conjugate. Efficient translocation of the enzyme was detected in a cell free extract fluorescence based assay (Figure 2).

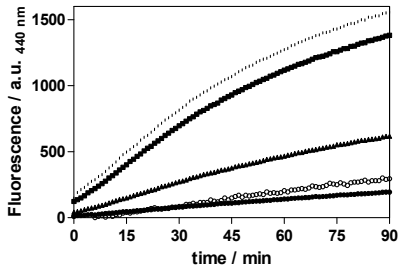

Fig. 2. Progression curves of β-galactosidase enzymatic activity. Fluorescence intensity is measured at 440 nm upon addition of enzyme to 0.5 mM of MUG. The plot represents the in vitro activity of the conjugate (NrTP6-C-β-galactosidase) when it is present at 0.5 nM (●), 2 nM (■), 5 nM (▲) and 7 nM (▏).The progression curve of a cell free extract resulting from the incubation of 0.3 mM of conjugate with HeLa cells (○).

The work done so far with this new family of CPP has revealed strong interaction and translocation with lipid model systems. Moreover, and as a proof of concept that these cell-penetrating peptides are good carriers for the delivery of large molecules into the cell interior, we have successfully observed that NrTP can translocate β-galactosidase into cells.

Acknowledgments

Partial funding and M.R. PhD grant (SFRH/BD/37432/2007) by Portuguese Ministry of Science (FCT-MCTES) and by Spanish Ministry of Science and Innovation (MICINN, grant BIO2008-04487–CO3) are acknowledged.

References

1. Nicastro, G. *Eur. J. Biochem.* **270**, 1969-1979 (2003).
2. Kerkis, A., et al. *FASEB J.* **18**, 1407-1409 (2004).
3. Nascimento, F.D., et al. *J. Biol. Chem.* **282**, 21349-21360 (2007).
4. Rádis-Baptista, G., et al. *J. Med. Chem.* **51**, 7041-7044 (2008).
5. Santos, N.C., et al. *Biochim. Biophys. Acta*. **1612**, 123-135 (2003).

Proceedings of the 31st European Peptide Symposium
Michal Lebl, Morten Meldal, Knud J. Jensen, Thomas Hoeg-Jensen (Editors)
European Peptide Society, 2010

Interactions of Cell-Penetrating Peptides in the Model of Giant Plasma Membrane Vesicles

Pille Säälik[1,2], Aira Niinep[1], Mats Hansen[3], Ülo Langel[3,4], and Margus Pooga[1,2]

[1]Institute of Molecular and Cell Biology, University of Tartu, Tartu, Estonia; [2]Estonian Biocentre, Tartu, Estonia; [3]Department of Neurochemistry, Stockholm University, Sweden; [4]Institute of Technology, University of Tartu, Estonia

Introduction

The cellular uptake mechanism of cell-penetrating peptides (CPP) is still a matter of debate in spite of the remarkable development in the area. Both endocytosis and direct membrane translocation are shown to be involved in the process. However, the exact mechanism and determinants of the translocation process have remained elusive.

We have exploited the model of giant plasma membrane vesicles (GPMV) [1] from rat basophilic leukaemia cells (RBL) to study the membrane interactions of six most well-known cell-penetrating peptides. Since GPMVs are derived from the cell's plasma membrane, their composition is very close to this organelle, being thus more native model system for CPP studies compared to artificial vesicles consisting of just a small number of varying lipids. The membrane of GPMVs segregates into liquid-ordered (L_o) and liquid-disordered (L_d) lipid phases domains at low temperature, which can be visualized with fluorescently labeled cholera toxin B subunit and annexin V, respectively. Therefore, GPMVs have been used earlier to study the lipid phase dynamics and the phase preference of different plasma membrane proteins [2,3]. We aimed to use these vesicles to elucidate the involvement of membrane domains with different organization in the cellular uptake of six CPPs - Tat peptide (pTat), nonaarginine (R_9), model amphipathic peptide (MAP), Penetratin (pAntp), Transportan (TP), and its shorter analogue Transportan10 (TP10).

Results and discussion

In parallel with the results that the primary and secondary amphipathic CPPs [4] - TP, TP10, pAntp and MAP, clearly preferred the L_d phase when interacting with plasma membrane components, we also detected the translocation and accumulation of all the tested CPPs into GPMVs at two temperatures below physiological (Figure 1). This corroborates the ability of CPPs to cross the biological membrane without using endocytic processes [5,6]. The result that the control peptide, a slightly negative (general charge -1) 18-mer peptide from the C-terminal part of rat adrenergic receptor β1 either didn't internalize or entered the GPMVs in a very low extent suggested that the property of accumulation into GPMVs is characteristic only to peptides with penetration ability.

The preference of all the membrane-affine CPPs, TP, TP10, pAntp and MAP, for the L_d phase in GPMVs suggests that in live cell, these peptides might also interact favorably with the membrane areas of more dynamic and less densely packed nature. Our suggestion that the L_d phase is a preferred portal for CPPs when translocating into GPMVs is also supported by the fact that the vesicles showing preferentially only CtxB-staining, i.e. containing mainly L_o phase, were sometimes devoid of CPPs. Furthermore, GPMVs depleted of cholesterol by methyl-β-cyclodextrin treatment revealed more uniform uptake of all tested CPPs, confirming that the presence of densely packed membrane areas acts rather as a barrier than a contributor of CPP uptake.

The accumulation of all the tested CPPs into the giant plasma membrane vesicles was the highest for pTat and R_9, as detected by flow cytometry analysis. The continuous accumulation of these CPPs into vesicles took place during one hour. On the contrary to pTat and R_9, Transportan rapidly interacted with GPMVs and reached a plateau, revealing the fast and stable interaction with the membrane components.

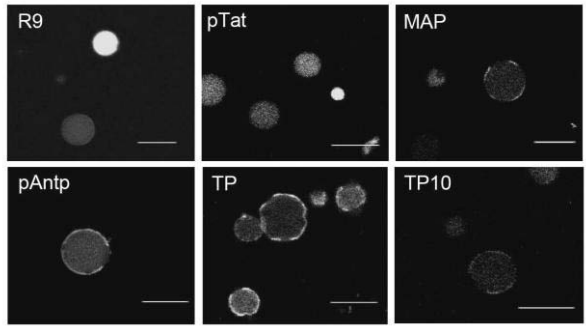

Fig. 1. GPMVs from RBL-2H3 cells were incubated with 1 μM fluorescein- (R9, pTat, MAP, pAntp, TP10) or Oregon-green 488-labeled (TP) CPPs at low temperature. All images were recorded in 40-60 minutes after the start of the incubation.

Based on our results, we propose that the uneven uptake of tested CPPs into the lumen of GMPVs depends on the balance between the general positive charge and hydrophobicity of the peptide, two parameters by which CPPs are divided to classes of primary, secondary and non-amphipathic CPPs [4]. In addition, inside GPMVs the cellular RNA and DNA might act like attractants for R_9 and pTat. As the presence of nucleic acids in GPMVs has been demonstrated before [7], and while R_9 and pTat are known to reveal affinity towards nucleic acids [8], it is feasible that the presence of these compounds in the lumen of GPMVs and the respective chemical gradient drive the accumulation of cationic compounds like nucleic acid-binding dyes or highly positively charged CPPs, especially pTat and R_9 into vesicles.

Acknowledgements
The authors would like to thank A. Florén for the β1 peptide. The study was supported by grants from the Estonian Science Foundation (ESF 7058) and the Estonian Ministry of Education and Research (0182691s05 and 0180027s08).

References

1. Scott, R.E. *Science* **194**, 743-745 (1976).
2. Baumgart, T., Hammond, A.T., Sengupta, P., Hess, S.T., Holowka, D.A., Baird, B.A., Webb, W.W. *Proc. Natl. Acad. Sci. U.S.A.* **104**, 3165-3170 (2007).
3. Johnson, S.A., Stinson, B.M., Go, M., Carmona, L.M., Reminick, J.I., Fang, X., Baumgart, T. *Biochim. Biophys Acta* **1798**, 1427-1435 (2010).
4. Ziegler, A. *Adv. Drug Deliv. Rev.* **60**, 580-597 (2008).
5. Duchardt, F., Fotin-Mleczek, M., Schwarz, H., Fischer, R., Brock, R. *Traffic* **8**, 848-866 (2007).
6. Fretz, M.M., Penning, N.A., Al-Taei, S., Futaki, S., Takeuchi, T., Nakase, I., Storm, G., Jones, A.T. *Biochem. J.* **403**, 335-342 (2007).
7. Reich, C.F., 3rd, Pisetsky, D.S. *Exp. Cell. Res.* **315**, 760-768 (2009).
8. Ziegler, A., Seelig, J. *Biochemistry* **46**, 8138-8145 (2007).

Proceedings of the 31st European Peptide Symposium
Michal Lebl, Morten Meldal, Knud J. Jensen, Thomas Hoeg-Jensen (Editors)
European Peptide Society, 2010

Antimicrobial Oligopeptides and Rapid Alkalinization Factors in Chilean Grape

Alexander A. Zamyatnin[1,2] and Olga L. Voronina[2]
[1]Universidad Técnica Federico Santa Maria, Departamento de Informática, El Centro Cientifico Tecnologico de Valparaiso, Valparaiso, 1680, Chile; [2]A.N.Bach Institute of Biochemistry, Russian Academy of Sciences, Moscow, 119071, Russian Federation

Introduction

Regulatory oligopeptides generally do not exceed ~50 amino acid residues [1], and they differ substantially from larger polypeptides (proteins) in their physicochemical and biological properties. The primary structure of more than 10,000 oligopeptides from more than 1700 different living organisms representing all the biological kingdoms have been identified today [2]. Now ~600 new natural oligopeptides emerge annually. Most of the information on the structure and function of endogenous oligopeptide molecules is contained in different databases. Their primary structure is determined either directly or by translation from nucleotide sequences. Both ways are experimental and laborious.

From the other hand there are a lot of unknown oligopeptide sequences. e.g., only one grape (*Vitis vinifera*) oligopeptide primary structure was extracted and characterized before among more than 1000 known plant oligopeptide regulators [2] whereas information on numerous grape uncharacterized proteins has to be found in different protein databases.

Since antimicrobial peptides play important role in the innate defense system of plants and represent a relatively unexplored source of antimicrobial peptides of biotechnological potential, it is necessary to obtain more information on their structures and functions.

Rapid alkalinization factor (RALF) possessing new functional property was discovered in common tobacco [3]. It consisted of 49 amino acid residues and induced a rapid alkalinization of the culture medium of tobacco suspension-cultured cells and a concomitant activation of an intracellular mitogen-activated protein kinase. A family of oligopeptides inducing rapid pH alkalinization was isolated later from several plant species, but not from grape. Thereupon we have carried out a theoretical structure–function analysis of uncharacterized grape protein amino acid residue sequences in order to identify new primary structures of oligopeptides possessing antimicrobial and RALF activities.

Results and Discussion

The data of DEGECHIVID database [6] containing primary structures of unrecognized grape proteins (more than 300,000 sequences) were used as an object of investigation. Their sequences were compared with EROP-Moscow database containing information on structure and functions of plant regulatory oligopeptides [2] using specially created computer programs [4,5].

This method permitted to reveal 10 grape protein structure sites homologues to known regulatory oligopeptides elucidated from other plant species. Six potentially active antimicrobial oligopeptide sequences (Figure 1) have been identified among them. They consisted of from 49 amino acid residues and their similarity with known grape primary structure Vv-AMP1 [7] was from 66.0 to 100.0%. All these primary structures contained eight Cys residues forming potentially four disulfide bridges. One structure was the same as Vv-AMP1 but had the difference in pre-pro-peptide region of oligopeptide precursor. Primary structures of several AMPs were found by us earlier [4]. However AMP3 and AMP4 had unique amino acid residue sequences not described before.

This method revealed also four structures of potentially active rapid alkalinization factors (Figure 2). They consisted of from 49 to 57 amino acid residues and their similarity with common tobacco RALF primary structure [3] was from 57.1 to 89.8%. All of them were also characterized by a conserved sequences but containing four cysteine residues forming potentially two disulfide bridges. Primary structures of these RALF1-RALF4 found in other databases were described by us before [8].

Vv-AMP1	...vaear**RTCESQSHRFKGTCVRQSNCAAVCQTEGFHGGNCRGFRRRCFCTKHC**	100,0%
Vv-AMP1	...mvaea**RTCESQSHRFKGTCVRQSNCAAVCQTEGFHGGNCRGFRRRCFCTKHC**	100,0%
Vv-AMP2	...mvaea**R**P**CESQS**P**RFKGTCVRQSNCAAVCQTEGFHGGNCRGFRRRCFCTKHC**	95,7%
Vv-AMP3	...mvaeaK**TCESQSHRFKGTCVR**H**SNCAAVCQTEGFHGGNCRGFRRRCFCTKHC**	95,7%
Vv-AMP4	...meaea**RTC**D**SQSHRFKGTCV**THI**NCAAVC**H**T**DGFHG**R**NCRGFRR**P**CFCTKHC**	83,0%
Vv-AMP5	...qetea**R**L**CESQSH**W**FR**G**V**CV**SNH**NCA**V**VC**R**N**EH**F**VGG**R**CRGFRRRCFCT**R**N**C**	68,1%
Vv-AMP6	...vpsea**R**V**CESQSH**K**FEGAC**MGDH**NCA**L**VC**R**N**EGF**S**GG**K**CKGL**RRRCFCTK**L**C**	66,0%

Fig. 1. Sequence alignment of DEGECHIVID uncharacterized proteins and known grape antimicrobial oligopeptide Vv-AMP1 (capital letters). Small letters show a part of outside oligopeptide sequence.

Nt-RALF	...rril**ATKKYISYGALQKNSVPCSRRGASYYNCKPGAQANPYSRGCSAITRCRS**	100,0%
Vv-RALF1	...rril**AT**S**KYISYGALQ**R**NSVPCSRRGASYYNC**Q**P**GAQANPY**N**RGCS**T**ITRCRS**	89,8%
Vv-RALF2	...rril**AS**K**RYISYGAL**SR**NSVPCSRRGASYYNC**R**P**GAQANPY**T**RGCSAITRCR**R	85,7%
Vv-RALF3	...rrslAQRRR**YISYGAL**RR**N**Q**VPC**N**RRG**R**SYYNC**RR**G**GR**ANPY**R**RGCS**V**IT**K**C**H**RFTD	63,3%
Vv-RALF4	...rrvlVMQ**KKYISY**ET**LK**KDMI**PC**A**R**P**GASYYNC**RASGE**ANPY**N**RGC**EV**IT**G**CARGVRDINS	57,1%

Fig. 2. Sequence alignment of DEGECHIVID uncharacterized proteins and known tobacco (Nicotiana tabacum) RALF primary structure. RRXL motif is underlined in outside oligopeptide sequence.

It has been pointed out that the mature tobacco RALF oligopeptide was released from its precursor by proteolysis [3] because there were specific subtilase site [9] with a dibasic amino acid residue motif RRXL in pro-peptide region of precursor. This motif was found in all our primary structures. We did not know exactly where precursors of putative oligopeptides might be split. However, some evidences of predicted sequences exist. The same position of dibasic amino acid motif RRXL and oligopeptide in protein and in known precursors of plant oligopeptides at the C terminus were these proofs. Nevertheless, the problem of existence of predicted oligopeptides might be finally solved after their direct extraction from the grape followed by sequencing.

Functional type of the predicted oligopeptide is usually postulated to be the same type as of known homologs. However, Figure 2 demonstrates that RALF oligopeptides contain many positively charged residues K or R. This feature is common to a wide variety of antimicrobial oligopeptides. Such similarity indicates that RALF molecules can potentially participate in other plant regulatory processes, i.e., to be the polyfunctional regulators.

Acknowledgements
Our thanks to H. Peña-Cortes for kindly providing access to DEGECHIVID data. This study was supported by Chilean National Science and Technology Research Fund FONDECYT, Grant No. 1080504.

References

1. Zamyatnin, A.A. *Protein Seq. and Data Anal.* **4**, 49-52 (1991).
2. Zamyatnin, A.A., Borchikov, A.S., et al. *Nucl. Acids Res*. **34**, 261-266 (2006).
3. Pearce, G., Morua, D.S., et al. *Proc. Natl. Acad Sci.* U.S.A. **98**, 12843-12847 (2001).
4. Zamyatnin, A.A. *J. Health Sci*. **2**, 179-183 (2009).
5. Zamyatnin, A.A., Voronina, O.L. *Biochem. (Moscow)* **75**, 214-223 (2010).
6. Peña-Cortes, H., Cuadros, A., et al. *Abstr. Plant & Animal Genomes IV Conf*. W166 (2006).
7. de Beer, A., Vivier, M.A. *BioMed Central Plant Biol.* **8**, 75 (2008).
8. Zamyatnin. A.A. *Recent Adv. Biol. Biophys. Bioeng. Comput. Chem*. **5**, 33-38 (2009).
9. Siezen, R.J., Leunisson, J.A. *Protein Sci*. **6**, 501-523 (1997).

Proceedings of the 31st European Peptide Symposium
Michal Lebl, Morten Meldal, Knud J. Jensen, Thomas Hoeg-Jensen (Editors)
European Peptide Society, 2010

Glycine and Histidine-rich Antifungal Peptides: On the Way to the Mode of Action of Shepherin I

César Remuzgo[1*], Thiago R. S. Lopes[1], Thaís S. Oewel[1], Gláucia M. Machado-Santelli[2], Sirlei Daffre[3], and M. Terêsa Machini Miranda[1]

[1]Department of Biochemistry, Institute of Chemistry; Departments of [2]Cell and Developmental Biology and of [3]Parasitology, Institute of Biomedical Sciences; 05508-000, University of São Paulo, São Paulo, Brazil
**Present address: Special Laboratory of Pain and Signalling, Butantan Institute, São Paulo, Brazil*

Introduction

The emergence of microorganisms resistant to the commercial antibiotics has become a worldwide problem due to the lack of new drugs for the treatment of infectious diseases. Thus, the investigation of novel antimicrobial molecules has been considered critical for the development of a new generation of antibiotics [1].

Shepherin I (Shep I) is a 28-mer peptide isolated from the roots of the *Capsella bursa-pastoris* plant that is characterized by its almost exclusive glycine (67.9%) and histidine (28.6%) contents, presence of six tandem repeats of the motif Gly-Gly-His and expression of antimicrobial activity against yeast phase-fungi and mycelial fungi [2].

With the aim of studying this glycine- and histidine-rich antimicrobial peptide, we synthesized truncated, amidated, fluorescently labeled and/or tryptophan-containing analogues, tested them against some *Candida* strains and *Saccharomyces cerevisiae* at low and high salt concentration in absence or presence of Zn^{2+} ions and evaluated its toxicity on human erythrocytes. Also, we determined the killing kinetics of Shep Ia against *C. albicans* MDM8 and investigated its internalization into these cells.

Results and Discussion

Stepwise solid-phase peptide syntheses were performed manually at 60°C using conventional heating and customized protocols [3,4]. The crude peptides were characterized by LC-ESI/MS and purified by RP-HPLC. The overall purities of final peptides, evaluated by RP-HPLC and confirmed by LC-ESI/MS, were higher than 95%. Their peptide contents were obtained by full hydrolysis followed by amino acid analysis of the hydrolyzates. Their anticandidal, anticandidacidal and hemolytic activity were measured as earlier described [5,6]. The internalization of the fluorescently labeled analogues into the yeast cells was also verified by confocal microscopy and FACS analysis.

Shep Ia, Shep I (3-28)a and Shep I (6-28)a were as active as Shep I against *C. albicans* strains, *C. tropicalis* Squibb 1600, *C. parapsilosis* ATCC 22019 and *S. cerevisiae* ATCC 2601, indicating that Shep I (6-28)a may be the minimal fully active portion of Shep Ia. Shep Ia was more active (4-8 fold) than Shep I against *C. krusei* ATCC 6258. The effect of salt concentration on the anticandidal activity was less pronounced for Shep Ia, Shep I (3-28)a and Shep I (6-28)a than for the corresponding carboxyl-free analogues. On the other hand, the activity of Shep I and amidated analogues were significantly enhanced in the presence of the Zn^{2+} ion (Table 1). Shep Ia killed *C. albicans* MDM8 cells at 62.5 μM in 30 min (Figure 1), caused low hemolysis in human erythrocytes in isotonic glucose

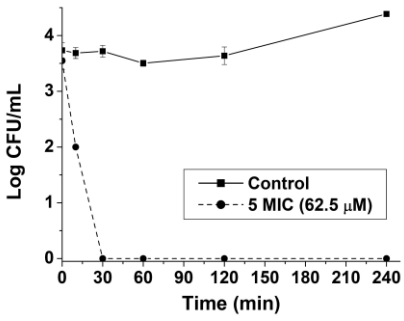

Fig. 1. Killing kinetics of Shep Ia against C. albicans MDM8.

phosphate buffer (IGP) and was not hemolytic in phosphate buffered saline (PBS).

The amidated fluorescently labeled analogues Fluo-Shep Ia, Fluo-Shep I (3-28)a and Fluo-Shep I (6-28)a were (i) more active against *C. albicans* ATCC 90028 than their respective unlabeled-analogues and (ii) rapidly internalized into *C. albicans* in an energy-and temperature-dependent manner (Figure 2) that suggest internalization by endocytic process.

Except for the [Trp^3]-Shep I (3-28)a analogue, all amidated Trp-containing analogues were 2-fold more active than Shep Ia against *C. albicans* ATCC 90028. All of them were equally or 2-fold less active than Shep Ia against *C. parapsilosis* ATCC 22019 and equally or 2-fold more active against *C. krusei* ATCC 6258. None of them was hemolytic in IGP or PBS.

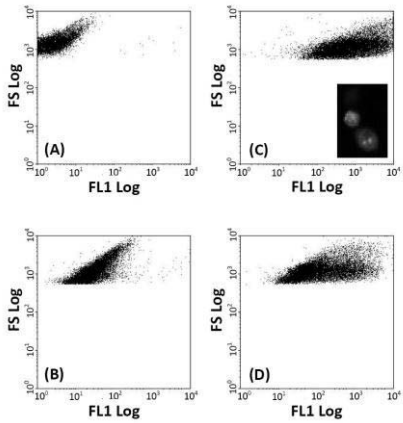

Fig. 2. Effect of the temperature and sodium azide (NaN_3) on internalization of Fluo-Shep Ia (insert of C). (A) control, (B) 0.05% NaN_3 at 37°C, (C) 37°C and (D) 0°C.

Altogether, these results indicate that: (i) amidated Trp-containing analogues of Shep I can act as anticandidal drugs; (ii) [Trp^6]-Shep I (6-28)a is the best analogue obtained so far; (iii) the fluorescently labeled analogues have the potential to act as vectors for the delivery of macromolecules and/or drugs into cells.

Table 1. Effect of the Zn^{2+} ion on the MICs (μM) of Shep I and some analogues

Peptide	*C. albicans MDM8*		*C. albicans ATCC 90028*		*C. albicans HU 168*		*C. tropicalis Squibb 1600*	
	No Zn^{2+}	Zn^{2+}	No Zn^{2+}	Zn^{2+}	No Zn^{2+}	Zn^{2+}	No Zn^{2+}	Zn^{2+}
Shep I	12.5	3.13	>100	>100	25	6.25	1.56	n.d.
Shep Ia	12.5	1.56	>100	6.25	25	3.13	1.56	0.39
Shep I (3-28)a	12.5	3.13	>100	25	25	6.25	1.56	1.56
Shep I (6-28)a	12.5	3.13	>100	>100	50	12.5	1.56	1.56

Acknowledgments

Supported by grant 2008/11695-1 (FAPESP) and 142022/2003-9 (CNPq/doctoral fellowship for CR). We thank Dr. N. Lincopan (*C. albicans* ATCC 90028 and HU 168 strains), Dr. S.R. Almeida (*C. krusei* ATCC 6258 *and C. parapsilosis* ATCC 22019), A.Y. Matzukuma and R.C. Modia (help with FACS and confocal microscopy, respectively).

References

1. Planta, M.D. *J. Am. Board Fam. Med.* **20,** 533-539 (2007).
2. Park, C.J., et al. *Plant Mol. Biol.* **44**, 187-197 (2000).
3. Remuzgo, C., et al. *Biopolymers* **92**, 65-75 (2009).
4. Souza, M.P., et al. *Tetrahedron* **60**, 4671-4681 (2004).
5. Fehlbaum, P., et al. *J. Biol. Chem.* **269**, 33159-33163 (1994).
6. Machado, A., et al. *Biopolymers* **88**, 413-426 (2007).

Proceedings of the 31st European Peptide Symposium
Michal Lebl, Morten Meldal, Knud J. Jensen, Thomas Hoeg-Jensen (Editors)
European Peptide Society, 2010

Targeting the Nuclear Pore Complex with Proteomimetic Cell Penetrating Peptides

Sarah Jones and John Howl
Research Institute in Healthcare Science, University of Wolverhampton, Wolverhampton, WV1 1LY, UK

Introduction

The past decade has witnessed a resurgent interest in the therapeutic utilizations of cell penetrating peptides (CPPs). Accordingly, CPP technologies have successfully been employed for the modulation of intracellular signal transduction. Moreover, CPPs with intrinsic signal transduction modulatory properties offer a novel strategy for the modulation of intracellular biological events [1-3]. QSAR analysis was employed to identify putative CPP sequences within human Cytochrome *c* [4]. Two such sequences located within the C-terminal helix, Cyt $c^{77\text{-}101}$ and Cyt $c^{86\text{-}101}$ induced apoptosis of malignant astrocytoma when exogenously applied, thus mimicking the well-documented role(s) of Cyt *c* as a key regulator of programmed cell death [1]. Whilst Cyt $c^{86\text{-}101}$ preferentially demonstrated a nuclear localization [1], Cyt $c^{77\text{-}101}$ proved to be an extremely efficient CPP and was thus selected for modification to incorporate additional bioactive peptide sequences.

Results and Discussion

N-terminal extension of Cyt $c^{77\text{-}101}$, via a flexible aminohexanoic acid linker, with a target mimetic of FxFG nucleoporins (Nup153$^{980\text{-}987}$, *CH_3CO*-NFKFGLSS) yielded a chimeric peptide (*Ac*-Nup153-Cyt *c*) that displayed a significantly enhanced apoptogenic potency (LD_{50} = 0.73 μM) compared to Cyt $c^{77\text{-}101}$ alone and a scrambled chimeric analogue, (*Ac*-*Scr*Nup153-Cyt *c*) (Table 1). Significantly, the apoptogenic potency of *Ac*-Nup153-Cyt *c* (0.73 μM) would also indicate *in vivo* applicability. The detection of intra-nucleosomal DNA fragmentation by *in situ* TUNEL analysis and a specific activation of caspase-3 confirmed that apoptosis was indeed the mechanism of cell death employed by *Ac*-Nup153-Cyt *c* in the U373MG astrocytoma model cell line.

To gain insight into the possible mechanisms employed by this novel chimeric construct, Nup153$^{980\text{-}987}$ was translocated into U373MG cells as a fluorescein-labelled disulphide-linked cargo, using the inert CPP M918. Following a subsequent intracellular reduction of cysteine, liberated *Fluo*-Nup153$^{980\text{-}987}$ assumed a preferential co-localization with the nuclear pore complex (NPC). To refine these results, U373MG cells were treated with the rhodamine-labelled chimera *Rho*-Nup153-Cyt *c* (3μM) and scrambled analogue for 1 hour. Whilst the scrambled chimera demonstrated a diffuse and generalised cytoplasmic distribution, *Rho*-Nup153-Cyt *c* strongly co-localised with the nuclear pore protein nucleoporin 153 (Table 1). Moreover, after 4 hours of treatment, exogenous application of *Ac*-Nup153-Cyt *c* (3μM) further facilitated the dramatic redistribution of immuno-labelled NPC proteins into the nucleoplasm and cytoplasm, a phenomenon that was not a downstream consequence of caspase activation since this redistribution event also occurred in the presence of the pan-caspase inhibitor Q-VD-Oph (20 μM).

Studies with scrambled peptides confirmed that the observed apotogenic action was both translocation- and sequence-dependent. Notably, translocation efficacies of both chimeras, *Rho*-Nup153-Cyt *c* and *Rho*-*Scr*Nup153-Cyt *c*, were significantly enhanced (408.5 $\pm$ 15.8 fold and 412.5 $\pm$ 5.20 fold, respectively) compared to that of Cyt $c^{77\text{-}101}$ alone (105.9 $\pm$ 0.42 fold) and thus indicates a sequence-dependent specificity of action for the *Ac*-Nup153-Cyt *c* chimera. We conclude that *Ac*-Nup153-Cyt *c* demonstrates therapeutic potential as a potent inducer of apoptosis, whilst propounding the nuclear pore complex as an accessible, and therefore druggable, intracellular target.

Table 1. Apoptogenic and translocation profiles

Peptide	Sequence	Apoptogenic Potency (LD_{50})[a]	Translocation Efficacy[b]	Intracellular Target (co-localization coefficient)[c]
Cyt $c^{77\text{-}101}$	*H*-GTKMIFVGIKKKEERADLIAYLKKA *NH_2*	80.63 μM	105.9 ± 0.42	Endoplasmic Reticulum (0.996 ± 0.02)
Ac-Nup153-Cyt *c*	*CH_3CO*-NFKFGLSS(Ahx)GTKMIFVGIKKKEERADLIAYLKKA *NH_2*	0.73 μM	408.5 ± 15.8	Nucleoporin 153 (0.931 ± 0.02)
Ac-*Scr*Nup153-Cyt *c*	*CH_3CO*-GFSNSFKLN(Ahx)GTKMIFVGIKKKEERADLIAYLKKA *NH_2*	Not toxic	412.5 ± 5.20	Cytoplasmic

[a]*LD_{50} values indicate the peptide concentration required to reduce U373MG cell viability by 50%. Values were obtained using the MTT conversion assay [5] and % viability expressed as a % of those cells treated with medium alone. Cells were exposed to peptides for 24 hours and LD_{50} values were calculated from 3 independent experiments performed in sextruplicate.*

[b]*Translocation efficacies were measured using rhodamine-labelled peptides. U373MG cells were incubated with peptides (5μM) for 1 hour. Thereafter, cell lysates were analyzed using fluorescence spectroscopy and results expressed as fold uptake compared to untreated cells. Data are from 3 independent experiments performed in triplicate.*

[c]*Intracellular co-localization analysis was carried out using live confocal cell imaging of U3773MG cells treated with rhodamine-labelled peptides (3 μM) for 1 hour. Co-localization coefficients were calculated using the Carl Zeiss quantitative co-localization analysis software. Coefficient values (overlap coefficient after Manders) are between 0 and 1, where a value of 1 indicates that all pixels are co-localized, whilst a value of 0 denotes no co-localization.*

Acknowledgments

We would like to thank Imre Mäger at the Laboratory of Molecular Biotechnology, Institute of Technology, Tartu University, Estonia and Professor Ülo Langel at the Department of Neurochemistry, Stockholm University, Sweden for their assistance in the synthesis of *Fluo*-Nup153-M918.

References

1. Howl, J., Jones, S. *Int. J. Pept. Res. Ther*. **14**, 359-366 (2008).
2. Johansson, H.J., et al. *Mol. Ther*. **16**, 115-123 (2008).
3. Östlund, P., et al. *Int. J. Pept. Res. Ther.* **11**, 237-247 (2005).
4. Hällbrink, M. *Int. J. Pept. Res. Ther.* **11**, 249-259 (2005).
5. Carmichael, J., et al. *Cancer Research* **47**, 936-942 (1987).

Proceedings of the 31st European Peptide Symposium
Michal Lebl, Morten Meldal, Knud J. Jensen, Thomas Hoeg-Jensen (Editors)
European Peptide Society, 2010

AntiMicrobial Protein Analyzer (AMPA): A Computational Tool to Screen Antimicrobial Domains in Proteins and Peptides

Marc Torrent and David Andreu
Department of Experimental and Health Sciences, Pompeu Fabra University, Barcelona Biomedical Research Park, 08003, Barcelona, Spain

Introduction

Host defense antimicrobial peptides (AMPs) or proteins are important effectors of the innate immune system and play a vital role in the prevention of bacterial infections. Computational algorithms are useful tools for predicting active fragments in proteins and peptides that can potentially be developed as therapeutic agents to combat bacterial infections. Automated systems for prediction of short AMP sequences have been developed, but a methodology for full protein scanning is not available. Here we present AMPA, a new algorithm that can identify antimicrobial proteins and successfully locate their active regions. AMPA is able to perform a fast screening analysis over large protein sets in order to identify potentially active AMPs derived from large protein molecules.

Results and Discussion

The AMPA algorithm uses an antimicrobial propensity scale to generate an antimicrobial profile by means of a sliding window system. The propensity scale has been derived using high-throughput screening results from the AMP bactenecin 2A, a 12-residue peptide for which antimicrobial IC_{50} values for all amino acid replacements at each position have been determined [1]. From the IC_{50} for each substitution, propensity values (PV) for individual residues can be calculated (Table 1) that provide a fair assessment of the tendency of such amino acid to be found within an AMP sequence. As low IC_{50} values correspond to high activity, amino acids with a low PV are the most favoured to be part of an AMP. Cationic (R, K) residues, necessary to direct AMPs to negatively charged bacterial surfaces, are especially favoured. Some hydrophobic residues (W, Y, I, V), needed to destabilize lipid bilayers and eventually cause cell death, also display low PVs. Anionic residues, as expected, are unfavoured and thus have high PVs.

The prediction algorithm was applied to a training set of 100 proteins (50 bactericidal and 50 non-bactericidal) including representative members of the main antimicrobial protein families in the literature. A 7-residue sliding window was chosen for the screening. To improve accuracy, 3 predictive lengths (10, 12 and 14 residues) were evaluated and, for each length, the optimal number of allowed gaps (2, 3 or 4) was determined. For each length/gap combination, a receiver-operating curve (ROC) was then constructed, and the accuracy, sensitivity and selectivity evaluated in order to identify the best parameters. Optimal results were obtained using a predictive length of 12 amino acids, with 2 gaps allowed. For these parameters, the average propensity value (avPV) ensuring the best predictive accuracy was 0.225; residues with avPV<0.225 were considered favourable whereas residues with avPV>0.225 were considered unfavourable.

Table 1. Antimicrobial propensity values (PV) of amino acid residues

Residue	*Arg*	*Lys*	*Cys*	*Trp*	*Tyr*	*Ile*	*Val*
PV	0.106	0.111	0.165	0.172	0.185	0.198	0.200
Residue	*His*	*Asn*	*Thr*	*Phe*	*Leu*	*Gln*	*Gly*
PV	0.202	0.240	0.242	0.246	0.246	0.248	0.265
Residue	*Met*	*Ser*	*Ala*	*Pro*	*Glu*	*Asp*	
PV	0.265	0.281	0.307	0.327	0.449	0.479	

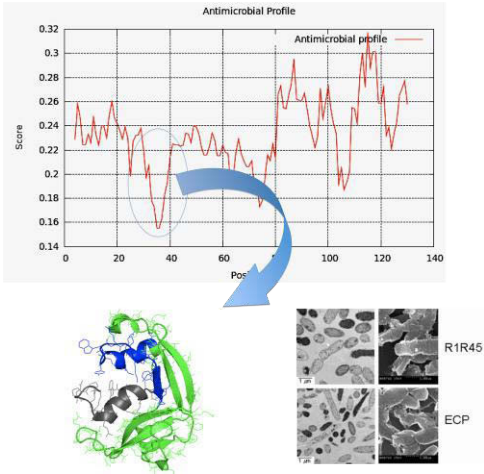

Fig. 1. The AMPA profile of eosinophile cationic protein identifies the N-terminal (1-45) region as antimicrobial. For experimental corroboration and further details, see ref. [2].

The results of the AMPA screen were compared with available data. Most of the proteins with known antimicrobial activity in the training set were correctly identified and their antimicrobial domains, whenever sufficient information on them was available, accurately predicted. In addition, several *de novo* AMPA-identified sequences in proteins with hitherto unknown or poorly defined antimicrobial determinants were experimentally validated by means of synthetic versions of the AMPA-defined regions. A case in point is eosinophile cationic protein, for which a strong antimicrobial motif was identified in the N-terminal region [2,3] (Figure 1).

Taken together, the results of applying the AMPA algorithm to the training set were judged to be quite satisfactory: high sensitivity (90%) and specificity (80%), with 85% average accuracy. To probe further its reliability, AMPA was also applied to a positive testing set of 20 antimicrobial proteins, of which 90% were accurately predicted. A negative testing set was also screened, and 81% of the proteins were again correctly identified as non-antimicrobial. These results are in good agreement with those observed for the training data set. In conclusion, AMPA is a useful, straightforward tool for detecting regions conferring antimicrobial properties to proteins. AMPA-selected regions may thus become starting points for the development of new AMP-derived drugs.

Acknowledgments

MT is the recipient of a postdoctoral grant from Alianza Cuatro Universidades (Spain). This work was supported by grants BIO2008-04487-CO3-02 from the Spanish Ministry of Science and Innovation, SGR2005-00494 and SGR2009-00494 from Generalitat de Catalunya, and HEALTH-F3-2008-223414 (Leishdrug) from the European Union.

References

1. Hilpert, K., Volkmer-Engert, R., Walter, T., Hancock, R.E. *Nat. Biotech.* **23**, 1008-1012 (2005).
2. Torrent, M., de la Torre, B.G., Nogués, M.V., Andreu, D., Boix, E. *Biochem. J.* **421**, 425-434 (2009).
3. Torrent, M., Nogués, M.V., Boix, E. *BMC Bioinf.* **10**, 373-382 (2009).

Proceedings of the 31st European Peptide Symposium
Michal Lebl, Morten Meldal, Knud J. Jensen, Thomas Hoeg-Jensen (Editors)
European Peptide Society, 2010

Analogs of Contulakin-G, an Analgetically Active Glycopeptide from Conus Geographus

Samson Afewerki[1], Ola Blixt[2], Henrik Clausen[2], and Thomas Norberg[1]
[1]Department of Biochemistry and Organic Chemistry, Uppsala University, PO Box 576, 751 23, Uppsala, Sweden; [2]Department of Cellular and Molecular Medicine, Faculty of Health Sciences, University of Copenhagen, 2200, Copenhagen N, Denmark

Introduction

Cone snails are marine predators who use immobilizing venoms for catching prey. Chemical analysis of the venoms has revealed a variety of biologically active small and intermediate size peptides rich in post-translational modifications (modified amino acids, glycosylation). Contulakin-G (structure, see **2** in Scheme 1) is a potent analgesic from *Conus geographus* venom. The *in vivo* activity of synthetic Contulakin-G was previously found [1] to be significantly higher compared to that of a peptide lacking the glycan. These observations touch on the general question of the function of glycans of glycopeptides and glycoproteins in Nature. We believe that *Conus* glycopeptides are among the best model compounds available to address this question, since they are comparatively small molecules which can be readily prepared and modified by chemical synthesis. In order to further investigate the importance of the glycan of Contulakin-G, we have now synthesized glycopeptide analogs where the glycan chain has been altered. The glycopeptides were prepared by a combination of solid-phase peptide synthesis and enzymatic synthesis.

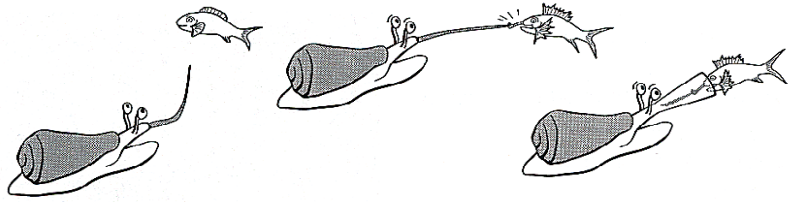

Fig. 1. A typical cone snail hunting session.

Results and Discussion

The glycopeptide **1** (see Scheme 1) was prepared by Fmoc-type solid-phase peptide synthesis on Fmoc-Leu-NovaSyn TGA resin using commercial Fmoc-protected amino acid derivatives and in-house prepared [2] N-Fmoc-O-(3,4,6-tri-O-acetyl-2-acetamido-2-deoxy-β-D-galactopyranosyl)-L-threonine. After resin cleavage and de-O-acetylation with methanolic sodium methoxide the glycan was enzymatically elongated, first with 1,3-GalT/UDP-Gal to produce **2** (native Contulakin-G) and then with 2,3-ST/CMP-NeuAc to produce glycopeptide **3**, which was purified with HPLC and characterized by MALDI-TOF mass spectrometry. To our knowledge, this is the first time that a cone snail glycopeptide with a sialic acid residue has been prepared. Evaluations of biological activity of **1**, **2** and **3** will be carried out in various test systems.

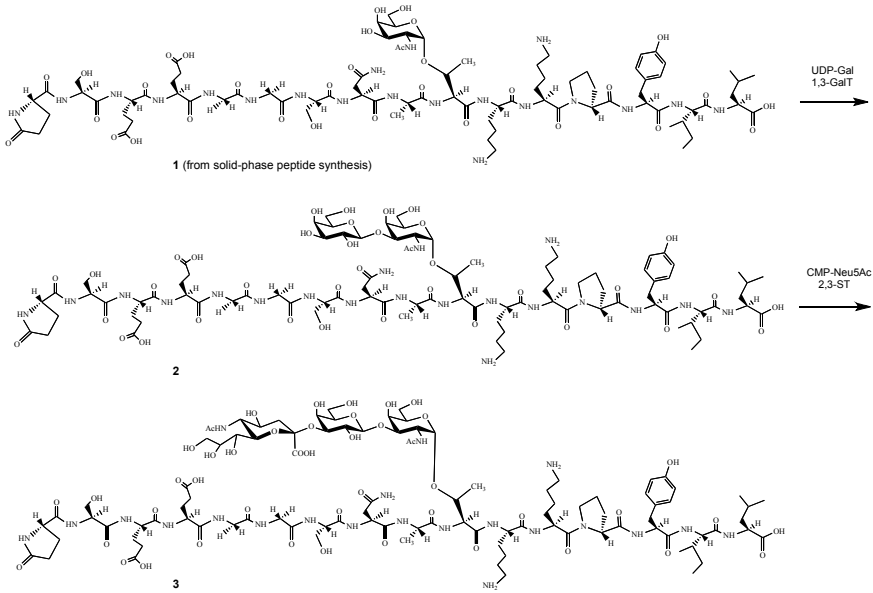

*Scheme 1. Enzymatic synthesis of glycopeptide **3**.*

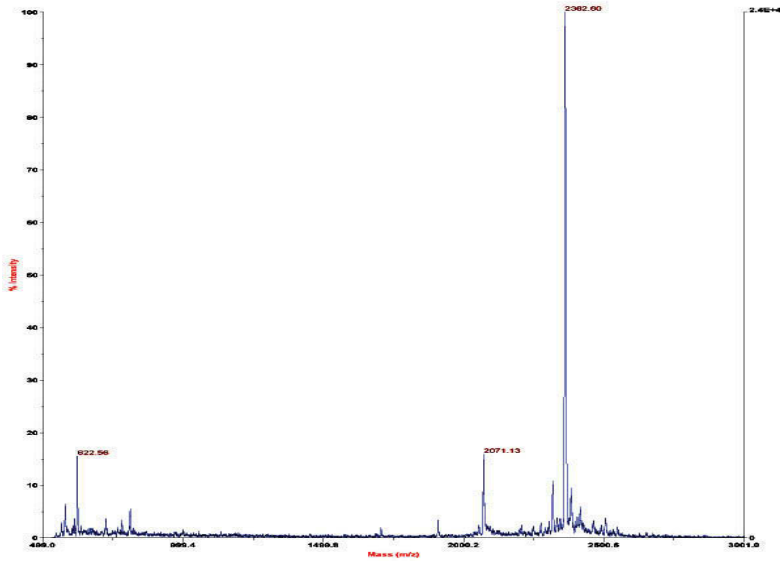

*Fig. 1. MALDI-MS of glycopeptide **3**.*

References

1. Craig, A.G., Norberg, T., Griffin, D., Hoeger, C., Akhtar, M., Schmidt, K., Low, W., Dykert, J., Richelson, E., Hillyard, D., Imperial, L., Cruz, L.J., Olivera, B.M. *J. Biol. Chem.* **274**, 13752-13759 (1999).
2. Lüning, B, Norberg, T. *Glycoconjugate J.* **6**, 5-19 (1989).

Proceedings of the 31st European Peptide Symposium
Michal Lebl, Morten Meldal, Knud J. Jensen, Thomas Hoeg-Jensen (Editors)
European Peptide Society, 2010

Active Peptidomimetic Insect Kinin Analogs with Type VI Turn Motif 4-Aminopyroglutamate Lack Native Peptide Bonds

Krzysztof J. Kaczmarek[1,2], Geoffrey M. Coast[1,3], Janusz Zabrocki[1,2], and Ronald J. Nachman[1*]

[1]Areawide Pest Management Research Unit, Southern Plains Agricultural Research Center, U.S. Department of Agriculture, College Station, TX, 77845, U.S.A.; [2]Institute of Organic Chemistry, Technical Universtiy of Lodz, 90-924, Poland; [3]School of Biological and Chemical Sciences, Birkbeck College, London, WC1E 7HX, U.K

Introduction

Insect neuropeptides of the insect kinin class share a common C-terminal pentapeptide sequence Phe[1]-Xaa[2]-Xbb[3]-Trp[4]-Gly[5]-NH_2 (Xaa[2] = Asn, His, Phe, Ser or Tyr; Xbb[3] = Pro, Ser or Ala) and has been isolated from various insects [1,2]. It has been reported that these peptides regulate such critical physiological processes as water and ion balance, hindgut motility, and digestive enzyme release [1]. The C-terminal sequence is all that is required to elicit a physiological response in hindgut myotropic and cricket Malpighian tubule secretion assays [1]. The active core sequence Phe[1]-Tyr[2]-Pro[3]-Trp[4]-Gly[5]-NH_2 is equipotent with the parent nonapeptide (SGADFYPWGa) in these two assays. Conformational studies suggest that the active conformation adopted by the C-terminal pentapeptide active core of the insect kinins at the cricket Malpighian tubule receptor site is the *cis*-Pro type VI β-turn over residues 1-4 [1-3]. Analogs incorporating the tetrazole and 4-aminopyroglutamate (APy) motifs, mimics of a *cis*-peptide bond and a type VI β-turn (Figure 1), elicited significant diuretic activity and provided evidence for this preference in active conformation [1-3]. An evaluation of all four stereochemical variants of the APy motif in the insect kinin core sequence in the cricket Malpighian tubule secretion assay revealed that the analog ***(2R,4S)-APy*** (EC_{50} = 7 x 10^{-9} M) was an order of magnitude more potent than the other three analogs, including the parent analog ***(2S,4S)-APy*** (EC_{50} = 1.4 x 10^{-7} M)[3].

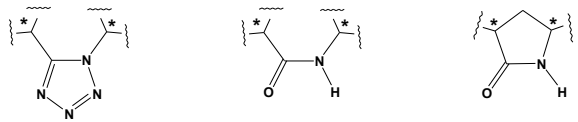

Fig 1. Comparison of structures of the tetrazole and 4-aminopyroglutamate (APy) motifs, mimics of a cis-peptide bond.

Unfortunately, insect kinin peptides are unsuitable as pest control agents and/or research tools for insect neuroendocrinologists due to susceptibility to degradation by both exo- and endo-peptidases in the hemolymph (blood) and gut, as well as an inability to efficiently penetrate the outside cuticular layer of the insect. Two susceptible hydrolysis sites in insect kinins [4] have been reported. The primary site is between the Pro[3] and Trp[4] residues and the secondary site is N-terminal to the Phe[1] residue in natural, extended insect kinin sequences. In this study, we synthesized simplified mimetic analogs of the insect kinin C-terminal pentapeptide core that incorporate the ***(2R,4S)-APy (Apy)*** and ***(2S,4S)-APy (APy)*** motifs, a reduced peptide bond linkage ([**r**]) between residues Trp[4]-Gly[5], and feature a hydrocinnamyl (**Hca**) group as a replacement and mimic of the Phe[1] residue. The two analogs (**Hca-APy**-Trp[**r**]Gly-NH_2 [**1796**] and **Hca-Apy**-Trp[**r**]Gly-NH_2 [**1797**]) were evaluated on the cricket Malpighian tubule fluid secretion assay. The biostable, mimetic analogs contain no native peptide bonds that would be susceptible to degradation by internal peptidases.

Results and Discussion

Following synthesis of the two stereochemical variant insect kinin mimetic analogs **1796** and **1797** containing ***(2S,4S)-APy (APy)*** and ***(2R,4S)-APy (Apy)***, respectively, they were evaluated on isolated Malpighian tubules of the house cricket *Acheta domesticus* to

determine if they could retain the fluid secretion stimulatory effects of the natural insect kinins and parent APy analogs. Despite the major structural modifications present in these mimetic analogs in comparison with the natural insect kinins and even the parent APy analogs, the two biostable analogs retained significant diuretic activity on the cricket Malpighian tubule fluid secretion assay. Both retained activity at a threshold concentration between 1 and 10 μM; and while the activity of **1797** appeared to be somewhat greater than that of **1796**, this difference was not statistically significant under these experimental conditions. For comparison, native achetakinin I (AK-I) at 1 μM is also included in Figure 2. The maximal response (efficacy) of the two analogs and the natural AK-I are statistically equivalent.

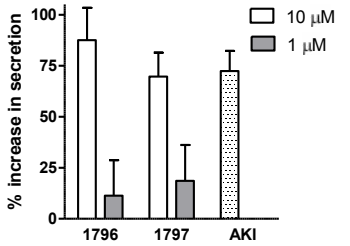

*Fig. 2. Diuretic activity of mimetic insect kinin analog **1796** and **1797** compared with native AK-I.*

The two peptidomimetic APy analogs of the insect kinin C-terminal pentapeptide active core feature major structural modifications in comparison with the natural sequence, including subsititution of the Phe[1] residue with Hca, replacement of the peptide linkage between the C-terminal Trp[4]-Gly[5] residue block with an isosteric reduced bond and a cyclic APy linkage as a replacement for the Xaa[2]-Pro[3] dipeptide block. As a consequence, the analogs contain no native peptide linkages that would be expected to render them susceptible to hydrolysis by either exo- or endo-peptidases in the hemolymph (blood) or tissues of pest insects. A diuretic agonist that the target insect is unable to inactivate *via* normal proteolytic pathways offers the potential to disrupt the water balance critical for insect survival. Previous reports indicate that while other insect kinin analogs with enhanced biostability show potency levels that are several orders of magnitude less than native peptides in *in vitro* Malpighian tubule secretion assays they nonetheless match the potency of the native peptides in an *in vivo* housefly diuretic assay [1-3]. Interestingly, biostable insect kinin analogs containing Aib residues have recently been reported to demonstrate potent oral aphicidal effects [4].

The active biostable insect kinin analogs described in this study and/or 2nd generation analogs, either in isolation or in combination with biostable analogs of other neuropeptide classes that also regulate aspects of diuretic, antidiuretic, digestive, reproductive and/or developmental processes, represent potential leads in the development of selective, environmentally friendly pest insect control agents capable of disrupting those critical processes.

Acknowledgments

We thank Allison Strey and Nan Pryor for technical assistance. We acknowledge financial assistance from the North Atlantic Treaty Organization (NATO) Collaborative Research Grant (#LST.CLG.979226) and the USDA/DOD DWFP Research Initiative (#00500-32000-001-01R).

References

1. Nachman, R.J., Zabrocki, J., Olczak, J., Williams, H.J., Moyna, G., Scott, A.I., Coast, G.M. *Peptides* **23**, 709-745 (2002).
2. Nachman, R.J., Kaczmarek, K., Williams, H.J., Coast, G.M., Zabrocki, J. *Biopolymers* **75**, 412-419 (2004).
3. Kaczmarek, K., Williams, H.J., Coast, G.M., Scott, A.I., Zabroki, J., Nachman, R.J. *Peptide Science* **88**, 1-7 (2006).
4. Smagghe, G., Mahdian, K., Zubrzak, P., Nachman, R.J. *Peptides* **31**, 498-505 (2010).

Proceedings of the 31st European Peptide Symposium
Michal Lebl, Morten Meldal, Knud J. Jensen, Thomas Hoeg-Jensen (Editors)
European Peptide Society, 2010

Synthesis and Bioactivity Studies on the C-Terminally Expressed Heptapeptide Orthologues of Various Proenkephalin A Sequences

Fruzsina Babos[1,3], Engin Bojnik[2], Sándor Benyhe[2], and Anna Magyar[3]
[1]Department of Organic Chemistry, Eötvös Lorand University, Budapest, Hungary; [2]Institute of Biochemistry, Biological Research Centre, Hungarian Academy of Sciences, Szeged, Hungary; [3]Research Group of Peptide Chemistry, Hungarian Academy of Sciences, Eötvös Lorand University, Budapest, Hungary

Introduction

Since the isolation of enkephalins a number of other opioid peptides have been discovered, including heptapeptide with the sequence of Tyr-Gly-Gly-Phe-Met-Arg-Phe (Met-enkephalin-Arg6-Phe7, YGGFMRF or MERF). The heptapeptide MERF is a potent opioid cleft from the sequence of proenkephalin A (PENK), the common precursor of Met- (ME) and Leu-enkephalin (LE).

Our bioinformatic analysis exposed chemical biodiversity at the heptapeptide region of PENK among 56 animals [1]. Four novel orthologoues sequences were found, such as YGGFMGY (Zebrafish), YGGFMRY (Newt), YGGFMKF (Hedgehog tenrek) and YGGFMRI (Mudpuppy).

Each novel heptapeptides were subjected to functionality studies, using receptor binding and G-protein activation assays. The relative affinities of the heptapeptides reveal rather mu-receptor preference over the delta-receptors. [^{35}S]GTPgS assay has demonstrated that these novel heptapeptides are also potent in stimulating the regulatory G-proteins.

Results and Discussion

The peptides were synthesized by automated SPPS (SYRO, Multisyntech), using Fmoc/tBu strategy on 2-chloro-trityl resin with double-coupling protocol. The crude products were purified by HPLC. The structure of the peptides was proved by electron spray ionization (ESI) mass spectrometry.

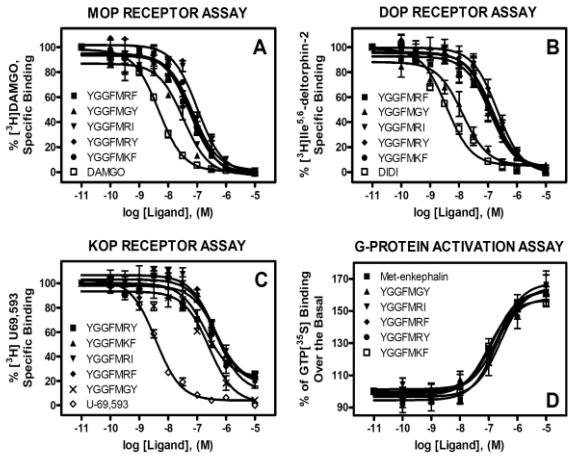

Fig. 1. Receptor binding and G-Protein activation assays.

All binding assays were performed at 25°C for 30 minutes in 50 mM Tris–HCl buffer (pH 7.4) in a final volume of 1 ml, containing 1 mg BSA and 0.2–0.4 mg/ml membrane protein.

Rat brain membrane fractions (~10 μg of protein/ sample) were incubated at 30°C for 60 min in Tris–EGTA buffer (50 mM Tris–HCl, 1 mM EGTA, 3 mM $MgCl_2$, 100 mM NaCl, pH 7.4) containing [^{35}S]GTPγS (0.05 nM) and increasing (10^{-9} to 10^{-5} M) concentrations of the compounds tested in the presence of 30 μM GDP in a final volume of 1 ml. Total binding was measured in the in the presence of 10 μM unlabeled GTPγS and subtracted from total binding to calculate the specific binding. All data are expressed as means ± standard error of the mean of n experiments. Curve fitting was performed using PRISM 4.0 (GraphPad Software Inc., San Diego, U.S.A.).

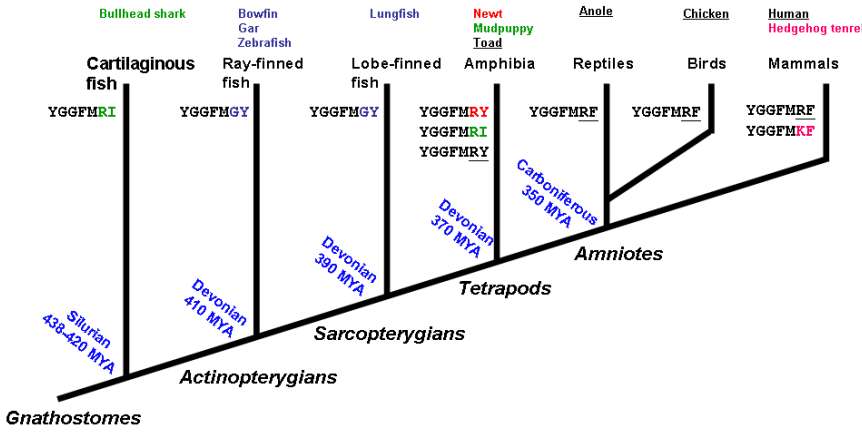

Fig. 2. Evolutionary diversity of proenkephalin-derived heptapeptides (the vertebrate evolutionary chart is adapted from [2]).

Each novel heptapeptide was subjected to functionality studies, using receptor binding and G-protein activation assays. The relative affinities of the heptapeptides reveal rather mu-receptor preference over the delta-receptors (Figure 1/A,B,C). [^{35}S]GTPgS assay has demonstrated that these novel hepta-peptides are also potent in stimulating the regulatory G-proteins (Figure 1/D).

The overall binding and signaling profile of the novel heptapeptides revealed moderate opioid agonist activities and a rank order of potencies for the mu>delta>>>kappa receptor binding sites. Importantly, these new endogenous sequences represent further illustration of the chemical biodiversity observed within the opioid peptide family. One significance of these mutationally variable sequences is that they represent a natural "combinatorial" peptide library emerged by the evolution and offer template sequences for structure-activity relationship studies (Figure 2). Opioid peptide variability is a good example for the chemical biodiversity.

Acknowledgments

This work was supported by grants from the National Office for Research and Technology, Hungary (OTKA-NKTH CK-78566) and by the "Foundation for Hungarian Peptide- and Protein Research", Budapest, Hungary.

References

1. Bojnik, E., Babos, F., Magyar, A., Borsodi, A., Benyhe, S. *Neuroscience* **165(2)**, 542-552 (2010).
2. Dores, R.M., Lecaude, S., Bauer, D., Danielson, P.B. *Mass Spectrom. Rev.* **21**, 21-24 (2002).

Proceedings of the 31st European Peptide Symposium
Michal Lebl, Morten Meldal, Knud J. Jensen, Thomas Hoeg-Jensen (Editors)
European Peptide Society, 2010

Substitution of Various *p*-*N*-Alkylcarboxamidophenylalanine Analogues for Tyr[1] in TIPP Opioid Peptides

Irena Berezowska, Carole Lemieux, Nga N. Chung, and Peter W. Schiller

Laboratory of Chemical Biology and Peptide Research, Clinical Research Institute of Montreal, Montreal, Quebec, H2W 1R7, Canada

Introduction

Replacement of the Tyr[1] residue in the cyclic enkephalin analogue H-Tyr-c[D-Cys-Gly-Phe(*p*NO2)-D-Cys]NH_2 with 4'-[*N*-((4'-phenyl)-phenethyl)carboxamido]phenylalanine (Bcp) resulted in a highly potent, μ-selective opioid agonist [1]. Unexpectedly, an analogue of the δ opioid antagonist peptide TIPP (H-Tyr-Tic-Phe-Phe-OH); Tic = 1,2,3,4-tetrahydroisoquinoline-3-carboxylic acid) [2] containing Bcp in place of Tyr[1] showed potent δ opioid *agonist* activity [3]. To further explore structure-activity relationships of TIPP at the N-terminal amino acid residue, derivatives of 4'-carboxamidophenylalanine (Cpa) containing various alkyl substituents at the 4'-carboxamido group were synthesized and substituted for Tyr[1]. These include 4'-[*N*-(hexyl)carboxamido]phenylalanine (Hcp), 4'-[*N*-(decyl)carboxamido]phenylalanine (Dcap), 4'-[*N*-(diethyleneglycol)carboxamido]-phenylalanine (Dgcp) and 4'-[*N*-(methoxypolyethyleneglycol)carboxamido]phenylalanine (Mgcp) (Figure 1).

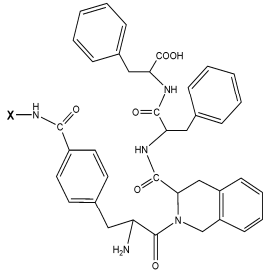

X=H	H-Cpa-Tic-Phe-Phe-OH
X=CH_3-$(CH_2)_5$-	H-Hcp-Tic-Phe-Phe-OH
X=CH_3-$(CH_2)_9$-	H-Dacp-Tic-Phe-Phe-OH
X=HO-$(CH_2)_2$-O-$(CH_2)_2$-	H-Dgcp-Tic-Phe-Phe-OH
X=CH_3O-$(CH_2$-CH_2-$O)_n$-$(CH_2)_2$-	H-Mgcp-Tic-Phe-Phe-OH

Fig. 1. Structure of TIPP analogs.

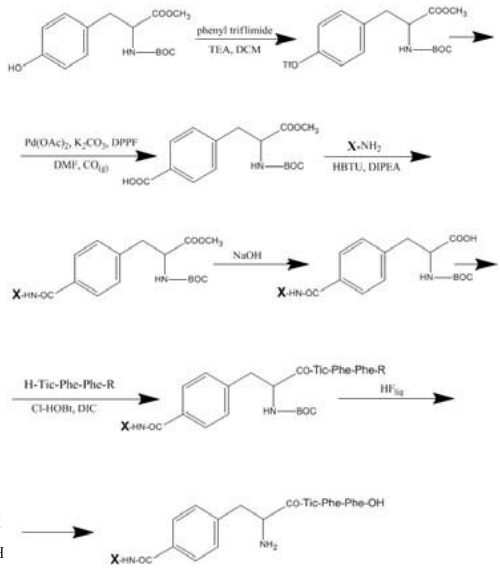

Fig. 2. Synthetic scheme.

Materials and Methods

Boc-Phe(4`-COOH)-OMe was synthesized by activating the hydroxyl group of Boc-Tyr-OMe as the triflate, followed by carbonylation with carbon monoxide in the presence of potassium acetate, DPPF and palladium (II) acetate, as described by Wang et al. [4]. Subsequent reactions with ammonium chloride, hexylamine, decylamine, diethylene glycolamine or methoxypolyethylene glycol amine using HBTU as coupling agent, followed by ester hydrolysis with 2N NaOH yielded the target compounds (Figure 2). Peptides were synthesized on solid-phase. μ, δ and κ opioid receptor affinities were measured in binding assays based on displacement of μ-, δ- and κ-selective radioligands

Table 1. GPI and MVD assay of TIPP analogues

Compound	GPI		MVD	
	IC_{50} (nM)	K_e (nM)	IC_{50} (nM)	K_e (nM)
[Cpa[1]]TIPP		6030		18.3
[Hcp[1]]TIPP	875 (IC_{30})[a]		0.392 (IC_{30})[a]	
[Dcap[1]]TIPP	> 1000		8.26	
[Dgcp[1]]TIPP		4870		411
[Mgcp[1]]TIPP	*inactive*		*inactive*	

[a]*Partial agonist (maximal inhibition of contractions = 60 %)*

from rat or guinea pig brain membrane binding sites, and agonist or antagonist activities were determined in the guinea pig ileum (GPI) and mouse vas deferens (MVD) bioassays.

Results and Discussion

The parent peptide [Cpa[1]]TIPP is a potent δ opioid receptor antagonist with subnanomolar δ receptor binding affinity (Tables 1 and 2). It displays high δ vs. μ receptor selectivity, as determined in both the binding assays and in the functional MVD and GPI assays. Interestingly, [Hcp[1]]TIPP showed subnanomolar δ partial agonist activity and δ receptor binding affinity, and retained high δ receptor selectivity. The analogue containing a further extended alkyl chain, [Dcap[1]]TIPP, displayed 4-fold lower δ receptor binding affinity than [Hcp[1]]TIPP and turned out to be a full δ agonist. Surprisingly, the ethyleneglycol-containing analogue [Dgcp[1]]TIPP was a weak δ opioid antagonist. Finally, the analogue carrying the methoxypolyethyleneglycol moiety on the side chain at the 1-position, [Mgcp[1]]TIPP, was found to be inactive at concentrations up to 10 μM. These results indicate that both the δ opioid receptor binding affinity and the intrinsic efficacy at the δ receptor are highly dependent on the length and the polarity of the carboxamide substituent at the 1-position residue in these TIPP analogues.

Table 2. Opioid receptor binding affinities of TIPP analogues

Compound	K_i^{μ} [nM]	K_i^{δ} [nM]	K_i^{μ} / K_i^{δ}
[Cpa[1]]TIPP	2190	0.978	2240
[Hcp[1]]TIPP	507	0.369	1370
[Dcap[1]]TIPP	174	1.54	113
[Dgcp[1]]TIPP	> 5000	380	-
[Mgcp[1]]TIPP	> 10000	> 10000	-

Acknowledgments

This work was supported by grants from the CIHR (MOP-89716) and NIH (DA-004443).

References

1. Weltrowska, G., Nguyen, T.M.-D., Lemieux, C., Chung, N.N., Schiller, P.W. *Chem. Biol. Drug Design* **72**, 337-340 (2008).
2. Schiller, P.W., Nguyen, T.M.-D., Weltrowska, G., Wilkes, B.C., Marsden, B.J., Lemieux, C., Chung, N.N. *Proc. Natl. Acad. Sci. U.S.A.* **89**, 11871-11875 (1992).
3. Berezowska, I., Chung, N.N., Lemieux, C., Wilkes, B.C., Schiller, P.W. *J. Med. Chem.* **52**, 6941-6945 (2009).
4. Wang, W., Obeyesekere, N.U., McMurray, J.S. *Tetrahedron Lett.* **37**, 6661-6664 (1996).

Proceedings of the 31st European Peptide Symposium
Michal Lebl, Morten Meldal, Knud J. Jensen, Thomas Hoeg-Jensen (Editors)
European Peptide Society, 2010

NMR Studies of Vasopressin Analogues Modified with Indoline-2-carboxylic Acid in Position 2 in Dodecylphosphocholine Micelle

Emilia Lubecka, Emilia Sikorska, Anna Kwiatkowska, and Jerzy Ciarkowski
Faculty of Chemistry, University of Gdańsk, 80-952, Gdańsk, Poland

Introduction

We used NMR spectroscopy and molecular modeling methods to find dominant conformations of two vasopressin analogues: [Mpa^1,L-Ica^2]AVP (**I**) and [Mpa^1,L-Ica^2,D-Arg^8]VP (**II**) (Mpa=3-mercaptopropionic acid; Ica=indoline-2-carboxylic acid). The NMR spectra were recorded in the mixture of phosphate buffer, pH=7.4 and DMSO-d_6 (1:1) in the presence of dodecylphosphocholine (DPC) micelle. The current model for peptide hormone interactions with their receptors suggests that the bioactive conformation of the peptide is induced upon association with the cell membrane followed by a two-dimensional diffusion process, whereby the peptide is recognized and then interacts with the receptor [1]. Therefore, exploring the conformational and dynamic properties of a ligand in a membrane-mimicking environment can contribute to better understanding of the molecular features involved in their interactions with the target receptor. Dodecylphosphocholine (DPC) micelle is considered to be a good model of eukaryotic cell membrane [1].

Pharmocological studies have shown that **II** is a moderate oxytocin antagonists, whereas **I** is a very weak agonist. Both compounds exhibit only negligible antidiuretic activity and are devoid of the pressor potency. Analogue **II** reveals also significantly higher affinity to the OT receptors than **I** (unpublished).

*Table 1. Structural statistics for the set of the last 100 conformations of [Mpa^1,L-Ica^2]AVP (**I**) and [Mpa^1,L-Ica^2,D-Arg^8]VP (**II**)*

Peptide / *Statistic*	*[Mpa^1,L-Ica^2]AVP (**I**)*		*[Mpa^1,L-Ica^2,D-Arg^8]VP (**II**)*			
The clusters	I	II	I	II	III	IV
The numbers of conformations	20	80	23	50	9	18
Atomic r.m.s. differences (Å):						
Backbone atoms 1-6	0.263	0.422	0.473	0.629	0.460	0.343
Heavy atoms 1-6	1.098	1.190	1.118	1.524	1.136	0.904
Conformational properties: Dominant reverse structures	2,3β I/IV 3,4β I',III'/IV	2,3β I/IV 4,5β I,I'/II'	7,8β II	2,3β[a,b] 3,4β I,IV/VII 4,5β IV[b] 5,6β IV[b] 7,8β II/IV	2,3β[a] 4,5β[a] 7,8β II	2,3β I' 3,4β IV/VII 7,8β II/IV
Most popular hydrogen bonds	HN^3-CO^1 HN^5-CO^1	HN^3-CO^1 HN^4-CO^1	HN^9-CO^6	HN^4-CO^1 HN^6-CO^4 HN^9-CO^6	-	HN^4-CO^2

[a]*different types of β-turns;* [b]*occurs in approximately 50% of the conformation*

Results and Discussion

The three-dimensional structures of both analogues studied were determined in AMBER 9.0 [2] force field using ensemble-averaged molecular dynamics with the locally enhanced sampling (LES) option. The calculations were performed in an *explicit* DPC micelle. The obtained conformational ensembles of both peptides were clustered into families with an rms deviation cut-off of 1.8 Å over the 1-6 Cα atoms (Table 1 and Figure 1).

The common feature of **I** and **II** are β-turns at positions 2,3; 3,4 and/or 4,5. The existence of β-turns in cyclic part of molecules is in good agreement with experimental data. The C-terminus of **II** is additionally involved in β-turn in Cys^6-Gly^9 fragment, which is a consequence of replacement of L-Arg with its enatiomer D. It is worth to highlight, that this simple modification changes a very weak oxytocin agonist (analogue **I**) into moderate antagonists (analogue **II**). Nevertheless, various pharmacological profile of peptides is rather a result of different mutual arrangement of aromatic residues in positions 2 and 3 than the changes of Arg^8 configuration from L to D, most of all that the Arg is believed to be crucial for interactions with vasopressin receptors and not with oxytocin one [3]. In the case of **I**, the positively charged guanidine group of Arg^8 displays tendency to be directed to aromatic side chain of Ica^2, which may result in cation-π interactions [4]. This type of interactions may have influence on orientation of Ica^2 side chain of **I** and indirectly may be a reason of different activity.

The analysis of interactions of both peptides with DPC micelle shows that **I** is more deeply immersed into the micelle core than **II**. The differences are primarily observed for C-terminal part of molecules.

Our results offer new information about structure-activity relationship of AVP analogues and may be profitably used for the design of new analogues with better pharmacological profiles.

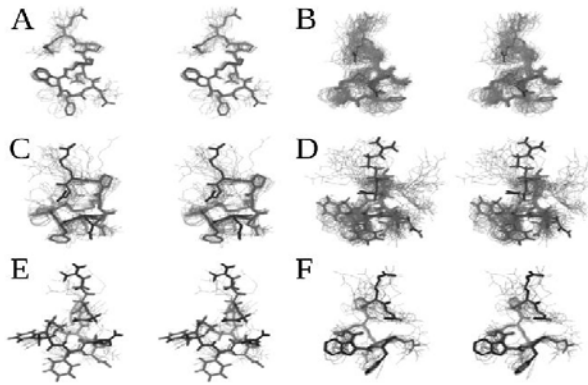

*Fig. 1. Stereoviews of the conformational ensembles of [Mpa^1,L-Ica^2]AVP (**I**): cluster I (A) and cluster II (B), and [Mpa^1,L-Ica^2,D-Arg^8]VP (**II**): cluster I (C), cluster II (D), cluster III (E) and cluster IV (F). $RMSD_{1-6}$= 0.272, 0.451, 0.507, 0.658, 0.471 and 0.385 Å for C_α atoms, respectively.*

Acknowledgments

This work was supported by the Polish Scientific Research Committee Grant No. N N204 181736 grant and the University of Gdańsk, DS. 8453-4-0169-0 and BW. 8372-5-0648-0. The calculations were carried out in the Academic Computer Centre (TASK) in Gdańsk, Poland.

References

1. Wymore, T., Gao, X., Wong, T. *J. Mol. Struct.* **485**, 195-206 (1999).
2. Case, D., Darden, T., Cheatham, T., Simmerling, C., Wang, J., Duke, R., Luo, R., Merz, K., Pearlman, D., Crowley, M., Walker, R. *AMBER 9*, University of California, San Francisco (2006).
3. Postina, R., Kojro, E., Fahrenholz, F. *J. Biol. Chem.* **271**, 31593-31601 (1996).
4. Shi, Z., Olson, C.A., Kallenbach, N.R. *JACS* **124**, 3284-3291 (2002).

Proceedings of the 31st European Peptide Symposium
Michal Lebl, Morten Meldal, Knud J. Jensen, Thomas Hoeg-Jensen (Editors)
European Peptide Society, 2010

Synthesis of New lGnRH-III Analogues and Studies on Prostate Cancer Cell Proliferation

Paul Cordopatis[1], Eleni V. Pappa[1], Aikaterini A. Zompra[1], Zinovia Spyranti[1], Zoi Diamantopoulou[2], Fotini N. Lamari[1], Panagiotis Katsoris[2], and Georgios A. Spyroulias[1]

[1]Department of Pharmacy, University of Patras, Patra, 26504, Greece;
[2]Department of Biology, University of Patras, Patra, 26500, Greece

Introduction

Lamprey Gonadotropin-releasing hormone (pGlu-His-Trp-Ser-His-Asp-Trp-Lys-Pro-Gly-NH_2, lGnRH-III), is a variant of the hypothalamic neurohormone GnRH that has been isolated from the brain of the sea lamprey (Petromyzon marinus). The ability of lGnRH-III to inhibit proliferation of cancer cells combined with the absence of endocrine activity at the concentrations effective against growth of cancer cells makes it an excellent starting compound for the development of constrained peptide analogues with increased and potentially selective anticancer activity [1,2].

In order to study the structure-activity relationship of lGnRH-III on prostate cancer cell proliferation, we synthesized twenty-two new peptide analogues of lGnRH-III with modifications in several positions [3,4]. Asp in position 6 of lGnRH-III was substituted by Asn, Asp(OMe), Glu and Gln (Group A). Trp3,7 were replaced by DTrp or DTic (Group B). pGlu1 was replaced by Glu or Ac-Glu and His5 and Lys8 switched places (Group C). Cyclopeptides are of great pharmaceutical and chemical importance since they often exhibit increased biological activity and selectivity. Furthermore, they are more stable in metabolism than the parent linear molecules. Taking into consideration of these potentials we synthesized four cyclic peptides (Group C) and studied their effect on prostate cancer cell proliferation. Conformational studies of lGnRH-III were also performed through NMR spectroscopy and a well characterized structural model is given for the first time.

Results and Discussion

NMR spectroscopy revealed that the solution structures of lGnRH-III and GnRH-I are significantly different. lGnRH-III has no secondary conformational characteristics while GnRH-I has a well defined β-turn conformation (Figure 1).

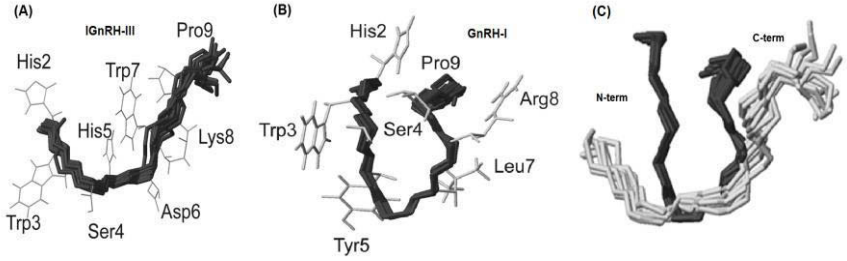

Fig. 1. A) Backbone representation of the family of 20 energy-minimized DYANA models for lGnRH-III. Side chains are illustrated in grey color. (B) Backbone representation of the family of 20 energy-minimized DYANA models for GnRH-I. Side chains are illustrated in grey color. (C) Superimposition of the lGnRH-III (grey) and GnRH-I (black) backbone.

GnRH-III and analogue IV with Gln^6 had significant antiproliferative effect only on LNCaP cell proliferation while, analogue II with Asp(OMe) in position 6 significantly inhibited the proliferation of LNCaP and PC3 cells (Figure 2). *C*-terminal modification of analogue VIII resulted in higher antiproliferative effect (analogue IX). Furthermore, replacement of Trp in positions 3 and 7 by DTrp or DTic resulted in two analogues (XII and XIII) with significant antiproliferative effect. Cyclic analogues XV, XVI and analogue

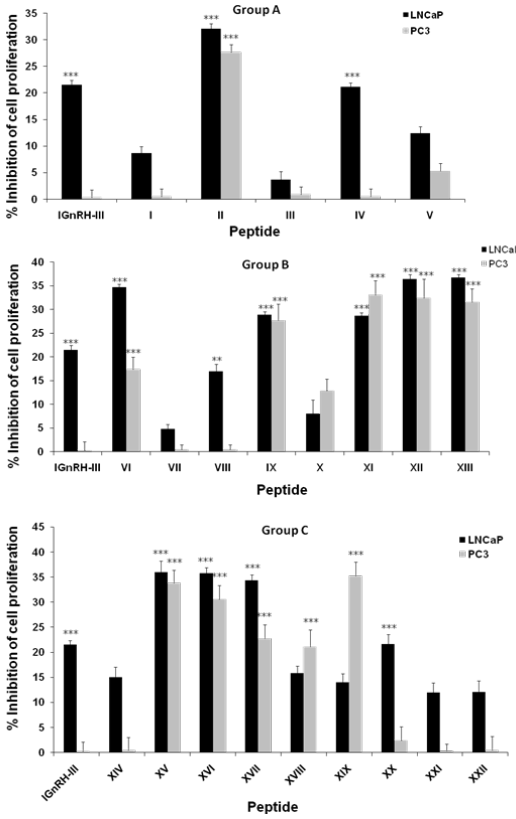

Group A	
No	Peptide
I	[Asn^6]- lGnRH-III
II	[Asp^6(OMe)]- lGnRH-III
III	[Glu^6]- lGnRH-III
IV	[Gln^6]- lGnRH-III
V	[Aib^6]- lGnRH-III

Group B	
No	Peptide
VI	[DTrp^3]- lGnRH-III
VII	[DTrp^7]- lGnRH-III
VIII	[DTrp^3, DTrp^7]- lGnRH-III
IX	[DTrp^3, DTrp^7]- lGnRH-III-NHEt
X	[Tic^3, Tic^7]- lGnRH-III
XI	[DTic^3, DTic^7]- lGnRH-III
XII	[DTrp^3, DTic^7]- lGnRH-III
XIII	[DTic^3, DTrp^7]- lGnRH-III

Group C	
No	Peptide
XIV	[NMeGlu^1]- lGnRH-III
XV	[cyclo(Glu^1, Lys^8)]- lGnRH-III
XVI	[cyclo(Ac-Glu^1, Lys^8)]- lGnRH-III
XVII	[ε-*N*-Ac-Lys^8]- lGnRH-III
XVIII	[Glu^1, ε-*N*-Ac-Lys^8]- lGnRH-III
XIX	[Ac-Glu^1, ε-*N*-Ac-Lys^8]- lGnRH-III
XX	[Lys^5, His^8]- lGnRH-III
XXI	[cyclo(Glu^1, Lys^5), His^8]- lGnRH-III
XXII	[cyclo(Ac-Glu^1, Lys^5), His^8]- lGnRH-III

Fig. 2. Effect of lGnRH-III, and lGnRH-III analogues on LNCaP and PC3 prostate cancer cell proliferation. Two asterisks (**) indicate significant difference from control at the level of P<0.01 and three asterisks (***) at the level of P<0.001.

with ε-*N*-Ac-Lys^8 (XVII) had significant antiproliferative effect on both cancer cell lines while, switching places between amino acids in position 5 and 8 resulted in peptides with similar or lower antiproliferative effect then that of the parent hormone.

In conclusion, in this study a well characterized structural model of lGnRH-III is given for the first time. lGnRH-III has no secondary conformational characteristics thus, the solution structure of that form of GnRH is significantly different than GnRH-I. The majority of the new analogues of lGnRH-III seem to have antiproliferative effect higher than the parent hormone. Interestingly, while lGnRH-III had no antiproliferative activity on PC3 cancer cells, eleven analogues had significant effect on the proliferation on both cancer cell lines.

References

1. Kovács, M., Vincze, B., Horváth, J.E., Seprödi, J. *Peptides* **28**, 821-829 (2007).
2. Mezö, I., Lovas, S., Pályi, I., Vincze, B., Kálnay, A., Turi, G., et al. *J. Med. Chem.* **40**, 3353-3358 (1997).
3. Herédi-Szabó, K., Lubke, J., Toth, G., Murphy, R.F., Lovas, S. *Peptides* **26**, 419-422 (2005).
4. Pappa, E.V., Zompra, A.A., Spyranti, Z., Diamantopoulou, Z., Pairas, G., Lamari, F.N., Katsoris, P., Spyroulias, G.A., Cordopatis, P. *Biopolymers,* in press (2010).

Proceedings of the 31st European Peptide Symposium
Michal Lebl, Morten Meldal, Knud J. Jensen, Thomas Hoeg-Jensen (Editors)
European Peptide Society, 2010

New Analogues of Arginine Vasopressin and Its Selected Agonists Modified at Position 2 with (*S*)-2-(1-Adamantyl)glycine

Bernard Lammek[1], Anna Kwiatkowska[1], Dariusz Sobolewski[1], Lenka Borovičková[2], Jiřina Slaninová[2], and Adam Prahl[1]
[1]Faculty of Chemistry, University of Gdańsk, Gdańsk, Poland; [2]Institute of Organic Chemistry and Biochemistry, Academy of Sciences of the Czech Republic, Prague, Czech Republic

Introduction

About 55 years ago du Vigneaud and his co-workers elucidated the primary structure of AVP and also worked out its synthesis [1]. Since then, analogues of AVP have attracted considerable attention and have been investigated from many points of view [2-4]. A number of highly interesting studies have been undertaken in an attempt to determine the structure-activity relationship. The data obtained from pharmacological evaluation of hundreds of AVP analogues provided a fairly good understanding of this correlation.

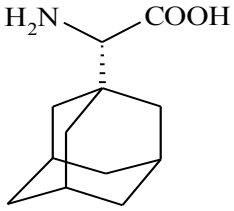

Fig. 1. Strucure of (S)-2-(1-adamantyl)glycine.

It is generally accepted that conformation of the N-terminal part of neurohypophyseal hormone analogues is important for their pharmacological activity. In this study we present the synthesis and some pharmacological activities of five new analogues of AVP, [Mpa[1]]AVP (Mpa = 3-mercaptopropionic acid), [Val[4]]AVP, [D-Arg[8]]VP and [Mpa[1], D-Arg[8]]VP, carrying at position 2 a conformationally constrained non-proteinogenic alpha-amino acid, (S)-1-adamantyl-glycine (Adg) (Figure 1). It should be noticed that the modification, apart from reducing the flexibility, also changed the character of the molecule from aromatic to aliphatic.

Results and Discussion

The five new analogues of AVP (**I**-**V**) were synthesized by Fmoc strategy, purified and characterized. The values of the molecular ions were as expected and the purity was higher than 98%. The activities of the new analogues were determined in the *in vitro* rat uterotonic test in the absence of magnesium ions, the rat pressor test, and in the antidiuretic assay on conscious rats (for details concerning all tests, see ref. [5]). The results of pharmacological evaluation of peptides **I**-**V**, together with relevant data for AVP and some related peptides, are presented in Table 1. None of these new analogues exhibited either pressor or antivasopressor activity. Peptides **I** and **III**-**V** modified at position 2 with Adg showed weak oxytocic agonism (values ranging from 0.20 to 1.90 IU/mg), whereas compound **II** was a weak oxytocic antagonist. As regards antidiuretic activity, peptides **I**-**III** and **V** are weak agonists, with the exception of analogue **IV** which possesses moderate antidiuretic properties.

It is hypothesized that the bulky planar side chain of the modified molecule together with its aliphatic character are responsible for an almost complete loss of activity of the analogues. On the basis of these results, we are now undertaking further SAR studies using NMR and theoretical molecular modelling methodology.

Table 1. Pharmacological properties of the new AVP analogues (IU/mg or pA_2)

Analogue		*Activity*		
		Uterotonic in vitro no Mg^{2+}	*Pressor*	*Antidiuretic 60 min. (200 min.)*
AVP[a]		17	412	465
[Mpa[1]]AVP[a]		27-63	346-370	1300-1745
[D-Arg[8]]VP[a]		0.4	4.1	114-257
[Mpa[1],D-Arg[8]]VP[a]		1.5-5.1	~0.39	800-50 000[b]
[Val[4]]AVP[a]		-	32	738[c]
[Adg[2]]AVP	**I**	1.90	0	<0.45 (<0.45)
[Mpa[1],Adg[2]]AVP	**II**	pA_2~6.64	0	<0.45 (~45)
[Adg[2],D-Arg[8]]VP	**III**	0.20	0	<0.45 (<0.45)
[Mpa[1],Adg[2],D-Arg[8]]VP	**IV**	1.0	0	~45 (~400)
[Adg[2],Val[4]]AVP	**V**	0.46	0	<0.45 (<0.45)

[a]*Values taken from ref 2.* [b]*The antidiuretic activity from antidiuretic test on anaesthetized rats.* [c]*Values taken from ref 6.*

Acknowledgments
Partial funding for this work was provided by Polish Ministry of Science and Higher Education under grant No. 0230/B/H03/2008/35 and by research project No. Z4055905 of the Academy of Sciences of the Czech Republic.

References

1. Du Vigneaud, V., Gash, D.T, Katsoyannis, P.G. *J. Am. Chem. Soc.* **76**, 4751-4752 (1954).
2. Lebl, M., Jošt, K., Brtník, F., In Jošt, K., Lebl, M., Brtník, F. (Eds.) *Handbook of Neurohypophyseal Hormone Analogs, Vol II, Part 2: Tables of Analogues*, CRC Press, Boca Raton, 1987, p. 127.
3. Manning, M., Sawyer, W.H. *J. Receptor Res.* **13**, 195-214 (1993).
4. Hruby, V.J., Smith, C.W. In Undenfriend, S., Meienhofer, J. (Eds.) *The Peptides, Vol 8: Structure - Activity Relationship of Neurohypophysial Peptides*, Academic Press, Orlando, 1987, p. 77.
5. Kowalczyk, W., Prahl, A., Derdowska, I., Dawidowska, O., Slaninová, J., Lammek, B. *J. Med. Chem.* **47**, 6020-6024 (2004).
6. Slaninová, J., In Jošt, K., Lebl, M., Brtník, F. (Eds.) *Handbook of Neurohypophyseal Hormone Analogs, Vol I, Part 2: Fundamental Biological Evaluation*, CRC Press, Boca Raton, 1987, p. 83.

Proceedings of the 31st European Peptide Symposium
Michal Lebl, Morten Meldal, Knud J. Jensen, Thomas Hoeg-Jensen (Editors)
European Peptide Society, 2010

Interaction of Curcumin with α-Synuclein and Its Relationship to Curcumin's Ability to Inhibit Fibril Deposit

Anna Marchiani[1], Stefano Mammi[1], Isabella Tessari[2], Luigi Bubacco[2], Sandra Monti[3], Francesco Manoli[3], and Paolo Ruzza[1]

[1]Institute of Biomolecular Chemistry of CNR, Padova Unit, and Department of Chemical Sciences, University of Padova, Padova, 35131, Italy; [2]Department of Biology, University of Padova, Padova, 35131, Italy; [3]Institute of Organic Synthesis and Photoreactivity (ISOF) of CNR, Bologna, 40129, Italy

Introduction

Lewy bodies and Lewy neurites in the brain constitute the main histopathological features of Parkinson's disease (PD), and are composed of amyloid-like fibrils that contain mainly a small protein named α-synuclein (AS). The aggregation of AS in the brain has been implicated as a critical step in the development of the disease. Therefore, the current search for disease-modifying drugs is focused on molecules that can act on the process of AS deposition in the brain.

Curcumin, a constituent of the Indian spice Turmeric, has been demonstrated to bind Aβ amyloid and prevent oligomerization of Aβ monomers onto amyloid β-sheets in Alzheimer's disease (AD) [1].

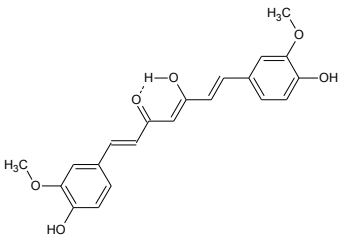

Fig. 1. Chemical structure of the keto-enol form of curcumin.

Reasoning that oligomerization kinetics and mechanism of amyloid formation seems to be similar in PD and AD, we evaluated the use of curcumin to prevent AS aggregation and/or to reduce AS fibril formation.

Curcumin has low solubility in aqueous solution and its soluble portion undergoes rapid degradation at physiological pH. Recently, the use of serum albumin as carrier for curcumin has been reported, implying that this protein has the ability to stabilize curcumin [2].

Results and Discussion

The kinetics of curcumin degradation were investigated analyzing the change in the absorption around 420 nm in different environments. Results confirm the degradation of curcumin in buffer solution, while the decay in the presence of either BSA or AS is negligible. These results clearly highlight the ability of AS to interact with and stabilize curcumin.

The curcumin binding to AS was evaluated by the quenching of tyrosine fluorescence. AS (1 μM in 20 mM phosphate buffer, pH 6.8) was titrated with aliquots of curcumin (0.8 mM in ethanol). The binding constant ($K_a = 6.34\times10^4$ M^{-1}) and the number of binding sites ($n = 0.95$) for curcumin on AS were determined from the following equation [3]

$$\log\frac{F_0 - F}{F} = \log K_a + n\log[curc]$$

where F_0 and F represent the initial and observed fluorescence values, respectively.

A K_a value of $1.30\pm0.32\times10^5$ M^{-1} was calculated using a nonlinear least-squares computer fit to the equation based on 1:1 binding stoichiometry [4],

$$F = \frac{(F_S - 100)}{2K_aP}[(K_aP + K_aL + 1) - \sqrt{(K_aP + K_aL + 1) - 4K_a^2PL}] + 100$$

where F and F_s represent the observed and saturation fluorescence values, respectively, and P and L the total AS and curcumin concentrations, respectively.

AS emission lifetimes were measured by TCSPC (Time Correlated Single Photon Counting) in a 15 μM solution in phosphate buffer at pH 6.8 in the absence and presence of curcumin at various concentrations. The protein decay was biexponential with $\tau_1 = 0.85$ ns and $\tau_2 = 2.2$ ns. The biexponential decay was not affected by the addition of 2 eq. ($\tau_1 = 0.85$ ns, $\tau_2 = 2.1$ ns) or 5 eq. ($\tau_1 = 0.78$ ns, $\tau_2 = 2.05$ ns) of curcumin.

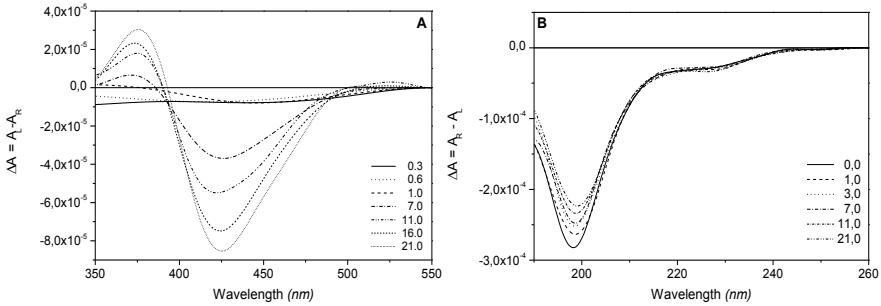

Fig. 2. (A) UV-visible CD spectra of curcumin and (B) far-UV CD spectra of AS, at different curcumin/AS molar ratios as indicated inside each figure.

Curcumin is not optically active and exhibits induced CD bands at 425 nm (negative) and at 374 nm (positive) upon binding to AS (Figure 2A). The Cotton bands observed in the presence of AS are of opposite sign to that reported for the curcumin-human albumin complex [5], suggesting that curcumin adopts an opposite chirality in the complex with AS.

The far-UV CD spectra of AS (4.0 μM) at different curcumin-to-protein molar ratios are characterized by a decrease in the intensity of the negative band at about 198 nm, indicative of a reduction of the random coil conformation (Figure 2B). The absence of an ordered CD spectrum suggests that curcumin-induced structural changes are localized in small portions of AS. The binding constant estimated from the far-UV CD data using a nonlinear least-squares computer fit to the equation based on 1:1 binding stoichiometry [6] was $1.0\pm0.3\times10^5$ M^{-1}, in agreement with that determined by fluorescence titration.

Chemical shift perturbation mapping was used to identify the curcumin binding interface of AS. The experiment consists of a stepwise addition of ligand (56 mM in acetone-d_6) to an ^{15}N-labelled AS sample (0.3 mM), monitoring the chemical shifts of the backbone amide resonances of the protein. Backbone amide resonances of free AS in 20 mM phosphate buffer, pH 6.8, assigned using 2D-^{15}N-HSQC-TOCSY, and 2D-^{15}N-HSQC-NOESY experiments, were in agreement with those reported in the literature [7]. Control HSQC experiments were performed to evaluate the effect of acetone on the amide resonances of AS.

Residues which directly interact with curcumin are likely to display the biggest chemical shift changes. It is possible that ligand-induced conformational restrictions may affect also amide resonances of residues involved in long-range interactions [8]. Residues involved in the interaction with curcumin are G41, K45, V52, A56, I88, A90, A91, T92, G93, V95, L113, M116, M127, Q134, D135 and A140.

Our data shows that curcumin binds to the AS monomer in a 1:1 stoichiometry ($K_d = 10\pm3$ μM) and this interaction prevents curcumin degradation in aqueous solution. This result, in addition to literature data, supports the possible application of curcumin as modulator of AS aggregation. Further studies will be performed to analyze the capability of curcumin to disaggregate AS fibrils.

References

1. Pandey, N., et al. *Acta Neuropathol.* **115**, 479-489 (2008).
2. Leung, M.H.M., Kee, T.W. *Langmuir* **25**, 5773-5777 (2009).
3. Min, J., et al. *J. Mol. Struct.* **692**, 71-80 (2004).
4. Fan, T.C., et al. *J. Biol. Chem.* **283**, 25468-25474 (2008).
5. Pulla Reddy, et al. *Lipids* **34**, 1025-1029 (1999).
6. Siligardi, G., et al. *J. Biol. Chem.* **277**, 20151-20159 (2002).
7. Bodner, C.R., et al. *Biochemistry* **49**, 862-871 (2010).
8. Dedmon, M.M., et al. *J. Am. Chem. Soc.* **127**, 476-477 (2005).

Proceedings of the 31st European Peptide Symposium
Michal Lebl, Morten Meldal, Knud J. Jensen, Thomas Hoeg-Jensen (Editors)
European Peptide Society, 2010

Synthesis, Antiproliferative Activity on Prostate Cancer Cells, Enzymatic Stability and Conformational Studies of New GnRH Analogues

Fotini N. Lamari[1], Eleni V. Pappa[1], Zinovia Spyranti[1], Aikaterini A. Zompra[1], Zoi Diamantopoulou[2], Panagiotis Katsoris[2], G. Liapakis[3], Georgios A. Spyroulias[1], and Paul Cordopatis[1]

[1]Department of Pharmacy, University of Patras, Patra, 26504, Greece; [2]Department of Biology, University of Patras, Patra, 26500, Greece; [3]Department of Medicine, University of Crete, Crete, 71003, Greece

Introduction

GnRH (pGlu[1]-His[2]-Trp[3]-Ser[4]-Tyr[5]-Gly[6]-Leu[7]-Arg[8]-Pro[9]-Gly[10]-NH_2) analogues have been used in oncology to induce reversible chemical castration. In addition to the classic hypophysiotropic action of GnRH, it has been shown that many malignant cells, such as prostate cancer cells, secrete GnRH and express the GnRH receptor/s [1-3].

Leuprolide ([DLeu[6], *des*Gly[10])-GnRH-NHEt]) is a commercially available GnRH agonists but despite its long record of use, issues concerning its conformation have not yet been resolved. In order to further study the structure-activity relationships we synthesized eleven new leuprolide analogues with multiple amino acid changes in positions 4 and 6 (Table 1) and studied their effect on prostate cancer cell proliferation (PC3 and LNCaP cell lines) [4,5]. To improve enzymatic stability, NMeSer was incorporated in position 4 and the rate of hydrolysis by α-chymotrypsin and subtilisin was investigated. DLeu[6] of Leuprolide was substituted by DLys [alone or modified by conjugation of Gly, Ala, Sar, αMeVal, NMeVal or Gly(tBu)], D-or L-Glu and Ser[4] by NMeSer.

Conformational studies of leuprolide and three more analogues (IX, X, XI) have been performed in an attempt to elucidate structural changes occurring upon substitution of native residues and to study structure-activity relationship for these analogues.

Results and Discussion

After 72 h treatment the peptides slightly inhibited the proliferation of PC3 and LNCaP cells. Leuprolide and analogues V, VI and X had a comparable effect on PC3 cell proliferation while, there was no significant difference between the effect of analogues with

Table 1. New analogues of GnRH

Peptide	*GnRH Analogues*
GnRH	pGlu[1]-His[2]-Trp[3]-Ser[4]-Tyr[5]-Gly[6]-Leu[7]-Arg[8]-Pro[9]-Gly[10]-NH_2
Leuprolide	[DLeu[6], *des*Gly[10]]-GnRH-NHEt
I	[NMeSer[4],DLys[6], *des*Gly[10]]-GnRH-NHEt
II	[NMeSer[4],DLys[6](Sar), *des*Gly[10]]-GnRH-NHEt
III	[NMeSer[4],DLys[6](Ala), *des*Gly[10]]-GnRH-NHEt
IV	[NMeSer[4],DLys[6](Gly), *des*Gly[10]]-GnRH-NHEt
V	{DLys[6][Gly(tBu), *des*Gly[10]]}-GnRH-NHEt
VI	{NMeSer[4],DLys[6][Gly(tBu), *des*Gly[10]]}-GnRH-NHEt
VII	[NMeSer[4],DLys[6](αMeVal), *des*Gly[10]]-GnRH-NHEt
VIII	[NMeSer[4],DLys[6](NMeVal), *des*Gly[10]]-GnRH-NHEt
IX	[Glu[6], *des*Gly[10]]-GnRH-NHEt
X	[DGlu[6], *des*Gly[10]]-GnRH-NHEt
XI	[NMeSer[4],DGlu[6], *des*Gly[10]]-GnRH-NHEt

NMeSer[4] and their counterparts. Besides that, inhibition of cell proliferation, on hormone-sensitive LNCaP cells was in general higher than that on PC3 cells under the same experimental conditions.

Concerning treatment of the three analogues with NMeSer in position 4 (II, IV and VII) with α-chymotrypsin (Figure 1), peptide VII with DGlu in position 6 remained intact in the reaction mixture for the longest period (33% after 12 h) followed by analogue II with DLys[6](Sar) (9% after 12 h), while analogue IV with DLys[6][Gly(tBu)] was completely digested in 6 h. Analogous results were obtained by incubation of peptides with subtilisin. However, degradation rate was much slower and 56% of peptide [NMeSer[4], DGlu[6],

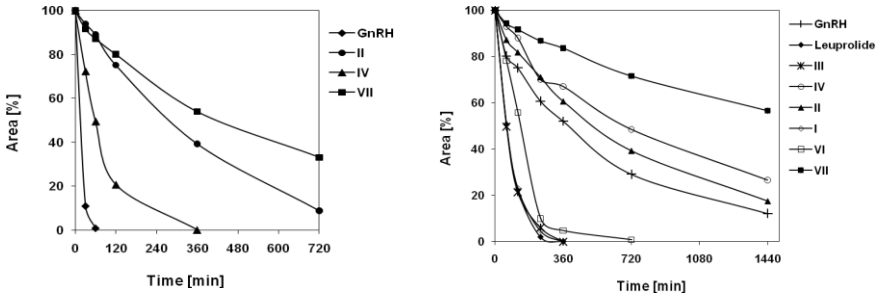

Fig. 1. Peptide degradation rates upon incubation with (left) α-chymotrypsin and (right) Subtilisin.

*des*Gly[10]]-GnRH-NHEt (analogue VII) remained in the reaction mixture even after 24 h.

In general, all four peptide solution structures exhibit a common fold to a U-type conformation (Figure 2). This conformation brings the N-terminal close to C-terminal residues and the type of N-to-C interaction depends on the different NOE interactions observed in each peptide. Long range proton-proton interactions have been observed in the NOESY spectra between Ser[4] and Arg[8] in the analogues V and VI suggesting that L/D amino acids have the same effect on the turn formation of the GnRH backbone. Despite the fact that such a long range NOE is totally absent in the [NMeSer[4], DGlu[6],*des*Gly[10]]-GnRH-NHEt analogue, the β-turn structure of Ser[4]-Arg[8] fragment remained intact in all conformers of the ensemble, demonstrating that the calculation of the β-turn structure spanning residues Ser[4]-Arg[8] is based exclusively on NOE constraints of the above residues. The conformational characteristics and the increased stability against proteolysis of NMeSer[4]- containing analogs are promising and might provide new options in GnRH drug development but further *in vivo* characterization of pharmacokinetic properties and activity studies are necessary.

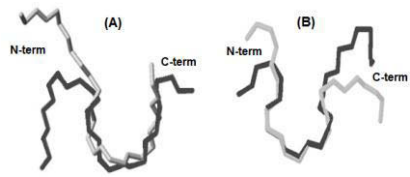

Fig. 2. Superimposition of the backbone of the four analogues in pairs.(A) leuprolide (grey) and [NMeSer[4], DGlu[6],desGly[10]]-GnRH-NHEt (black)(B) [Glu[6], desGly[10]]-GnRH-NHEt (grey) and [DGlu[6], desGly[10]]-GnRH-NHEt (black).

References

1. Dondi, D., Festuccia, C., Piccolella, M., Bologna, M., Motta, M. *Oncol. Rep.* **15**, 393 (2006).
2. Kraus, S., Naor, Z., Seger, R. *Cancer Lett.* **234**, 109 (2006).
3. Naor, Z. *Front. Neuroendocrinol.* **30**, 10 (2009).
4. Zompra, A.A., Magafa, V., Lamari, F.N., Nikolopoulou, A., Nock, B., Maina, Th., Spyroulias, G.A., Karamanos, N.K., Cordopatis, P. *J. Pept. Res.* **66**, 57 (2005).
5. Pappa, E.V, Zompra, A.A., Spyranti, Z., Diamantopoulou, Z., Pairas, G., Lamari, F.N., Katsoris, P., Spyroulias, G.A., Cordopatis, P. *Biopolymers,* in press (2010).

Proceedings of the 31st European Peptide Symposium
Michal Lebl, Morten Meldal, Knud J. Jensen, Thomas Hoeg-Jensen (Editors)
European Peptide Society, 2010

Analogues of Neurohypophyseal Hormones, Oxytocin and Arginine Vasopressin, Conformationally Restricted and Acylated in the N-terminal Part of the Molecule

Dariusz Sobolewski[1], Anna Kwiatkowska[1], Lenka Borovičková[2], Jiřina Slaninová[2], and Adam Prahl[1]

[1]Faculty of Chemistry, University of Gdańsk, Gdańsk, Poland; [2]Institute of Organic Chemistry and Biochemistry, Academy of Sciences of the Czech Republic, Prague, Czech Republic

Introduction

The most straightforward approach for subtle peptide modifications is introduction of changes into the side chains of amino acids at predetermined positions. By incorporation of non-proteinogenic amino acid residues, it is possible to introduce either bulky groups or sterically restricted substituents to restrict conformational flexibility of certain part of the peptide chain. Conformational restrictions may increase receptor binding selectivity, metabolic stability, or intrinsic activity and lead to highly potent agonists or antagonists.

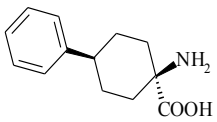

Fig.1. Structure of cis-1-amino-4-phenylcyclo-hexane-1-carboxylic acid (cis-Apc).

In this work, we decided to investigate how the substitution of position 2 with bulky *cis*-1-amino-4-phenyl-cyclohexane-1-carboxylic acid (*cis*-Apc, Figure 1) would alter pharmacological properties of oxytocin (OT), [Mpa^1]OT and [Cpa^1]OT (analogues **I-III**; Mpa = 3-mercaptopropionic acid; Cpa = 1-mercaptocyclohexaneacetic acid). Moreover, we decided to learn how acylation of the N-terminus of [*cis*-Apc^2,Val^4]AVP with different acyl groups would affect biological potency of the new analogues. The [*cis*-Apc^2,Val^4]AVP peptide was chosen as a reference compound owing to its interesting pharmacological profile. This analogue turned out to be a potent oxytocin antagonist (pA_2 = 8.22), weak pressor antagonist (pA_2 = 6.85), while its antidiuretic potency was lower than that of AVP but with significantly prolonged action [1]. The new analogues were obtained by acylation of the N-terminus of the peptide with 1-adamantane carboxylic acid (Aca) (**IV**), 4-*tert*-butylbenzoic acid (t-Bba) (**V**), 4-hydroxybenzoic acid (Hba) (**VI**) and 4-aminobenzoic acid (Aba) (**VII**) (Figure 2).

Results and Discussion

The seven new analogues of OT and AVP (**I-VII**) were synthesized by Boc or Fmoc strategy, purified and characterized. The values of the molecular ions were as expected and the purity was higher than 98%. The activities of the new analogues were determined in the *in vitro* rat uterotonic test in the absence of magnesium ions, the rat pressor test, and in the antidiuretic assay using conscious rats (for details concerning all tests, see ref. [2]). The results of pharmacological evaluation of peptides **I-VII,** together with relevant data for OT, AVP and some related peptides, are presented in Table 1. Peptides **I-IV**, **VI** and **VII** exhibited different antioxytocic activities ranging from pA_2 = 5.70 to 8.11, while compound **V** was a weak agonist (10.1 ± 3.8 IU/mg). Regarding the pressor test, three analogues (**I**, **II** and **V**) showed weak antagonism, whereas compounds **IV**, **V** and **VII** were inactive. All the new peptides did not virtually interact with the V_2 receptor.

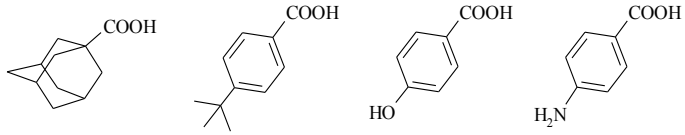

Fig. 2. Structures of 1-adamantane carboxylic acid (Aca), 4-tert-butylbenzoic acid (t-Bba), 4-hydroxybenzoic acid (Hba) and 4-aminobenzoic acid (Aba).

Table 1. Pharmacological properties of the new OT and AVP analogues (IU/mg or pA_2)

Analogue		*Activity*		
		Uterotonic in vitro no Mg^{2+}	*Pressor*	*Antidiuretic 60 min (200 min)*
OT[a]		450	5	5
[Mpa[1]]OT[a]		803	1.44	19
[Cpa[1]]OT[a]		pA_2=7.61	–	–
[cis-Apc[2]]OT	**I**	pA_2=7.89±0.07	pA_2=5.75	0
[Mpa[1], cis-Apc[2]]OT	**II**	pA_2=8.11±0.18	pA_2=6.0	0
[Cpa[1], cis-Apc[2]]OT	**III**	pA_2=7.97±0.24	-	0
AVP[a]		17	412	465
[Val[4]]AVP[a]		-	32	738[b]
[cis-Apc[2], Val[4]]AVP[c]		pA_2=8.22±0.11	pA_2=6.85	~15 (~2000)
Aca-[cis-Apc[2], Val[4]]AVP	**IV**	pA_2=5.7	0	<0.01 (<0.5)
t-Bba-[cis-Apc[2], Val[4]]AVP	**V**	10.1±3.8 IU/mg	0	<0.01 (<0.5)
Hba-[cis-Apc[2], Val[4]]AVP	**VI**	pA_2=7.61	pA_2=6.4	<0.01 (<0.5)
Aba-[cis-Apc[2], Val[4]]AVP	**VII**	pA_2=7.26±0.40	0	0

[a]*Values taken from ref 3.* [b]*Values taken from ref 4.* [c]*Values taken from ref 1.*

Summing up, our studies resulted in several analogues with interesting pharmacological properties that can contribute to mapping the receptor binding sites. We believe that even more important is the fact that we could once more demonstrate that the modification of the N-terminal part of the molecule, especially the reduction of conformational freedom, has a dramatic impact on the pharmacological activities, which in turn opens new possibilities for designing new analogues of AVP and OT with desired activities.

Acknowledgments
Partial funding for this work was provided by Polish Ministry of Science and Higher Education under grant No. 0230/B/H03/2008/35 and by research project No. Z4055905 of the Academy of Sciences of the Czech Republic.

References

1. Prahl, A., Kwiatkowska, A., Śleszyńska, M., Derdowska, I., Sobolewski, D., Borovičková, L., Slaninová, J., Lammek, B., In Lankinen, H. (Eds.) *Peptides 2008: Chemistry of Peptides in Life Science, Technology and Medicine (Proceedings of the 30th European Peptide Symposium)*, Helsinki, Finland, 2008, p. 294.
2. Kowalczyk, W., Prahl, A., Derdowska, I., Dawidowska, O., Slaninová, J., Lammek, B. *J. Med. Chem.* **47**, 6020-6024 (2004).
3. Lebl, M., Jošt, K., Brtník, F., In Jošt, K., Lebl, M. and Brtník, F. (Eds.) *Handbook of Neurohypophyseal Hormone Analogs, Vol II, Part 2: Tables of Analogues*, CRC Press, Boca Raton, 1987, p. 127.
4. Slaninová, J., In Jošt, K., Lebl, M., Brtník, F. (Eds.) *Handbook of Neurohypophyseal Hormone Analogs, Vol I, Part 2: Fundamental Biological Evaluation*, CRC Press, Boca Raton, 1987, p. 83.

Proceedings of the 31st European Peptide Symposium
Michal Lebl, Morten Meldal, Knud J. Jensen, Thomas Hoeg-Jensen (Editors)
European Peptide Society, 2010

Side-Chain to Side-Chain Cyclization of Opioid Peptides Enhances Proteolytic Stability of Their Exocyclic Peptide Bonds

Marek Cebrat[1], Piotr Stefanowicz[1], Alicja Kluczyk[1], Zbigniew Szewczuk[1], Katarzyna Filip[2], Małgorzata Ciszewska[2], and Jan Izdebski[2]

[1] *Faculty of Chemistry, University of Wrocław, Wrocław, 50-383, Poland*
[2] *Department of Chemistry, Warsaw University, Warsaw, 02-093, Poland*

Introduction

Side-chain to side-chain cyclization can significantly affect proteolytic stability, which is an important factor in designing the peptide-based drugs [1,2].

Previously we described the synthesis and biological activity of deltorphin and enkephalin analogs restricted by cyclization *via* the urea bridge. The analogs contained a carbonyl bridge which linked two side-chain amino groups to form an ureido moiety. Several of these compounds showed a very high δ-receptor agonist potency [3].

The goal of our present work was to analyze proteolytic stability of the cyclic peptides **1-9** incubated in the presence of chymotrypsin and pepsin and to identify degradation products of the peptides by electrospray mass spectrometry (ESI-MS).

Results and Discussion

We studied the proteolytic stability of peptides in the presence of chymotrypsin and pepsin by analysis of ESI-MS spectra of the reaction mixture obtained after various incubation times, as shown on the example of peptide 1 (Figure 1).

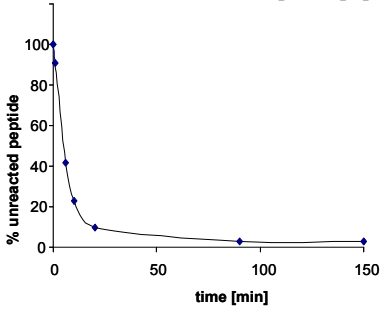

Fig. 1. The percentage of peptide 1 hydrolyzed by chymotrypsin estimated from the peak areas in the ESI-MS spectra.

Identification of the degradation products was based on the analysis of the high resolution mass spectra (HR-MS) and tandem mass spectrometry (MS/MS) of the main digestion products.

Cyclization *via* the urea bridge increased the resistance of the peptides incubated with pepsin and chymotrypsin to proteolytic digestion.

The observed stability depends not only on the ring size but also on localization of the urea bridge within the ring. One of the intriguing observations is the proteolytic stability of a potent opioid peptide 2, whereas its isomer 1 hydrolyzed rapidly in the presence of chymotrypsin (Figure 2).

Our studies indicate that the cyclization *via* the urea bridge formation influences not only the potency and selectivity of the peptide but also its enzymatic stability. A high stability against proteolytic enzymes was detected for peptide 3 which also showed a high activity as the δ-receptor agonist [3]. The combination of the high stability, potency, and selectivity of this compound makes it an attractive lead compound for the design of new analgetic drugs.

Presented results indicate the usefulness of mass spectrometric procedure for the fast screening of the proteolytic stability of bioactive peptides. The advantage of the presented approach is its speed as well as the possibility of the simultaneous identification of proteolytic fragments by MS/MS method.

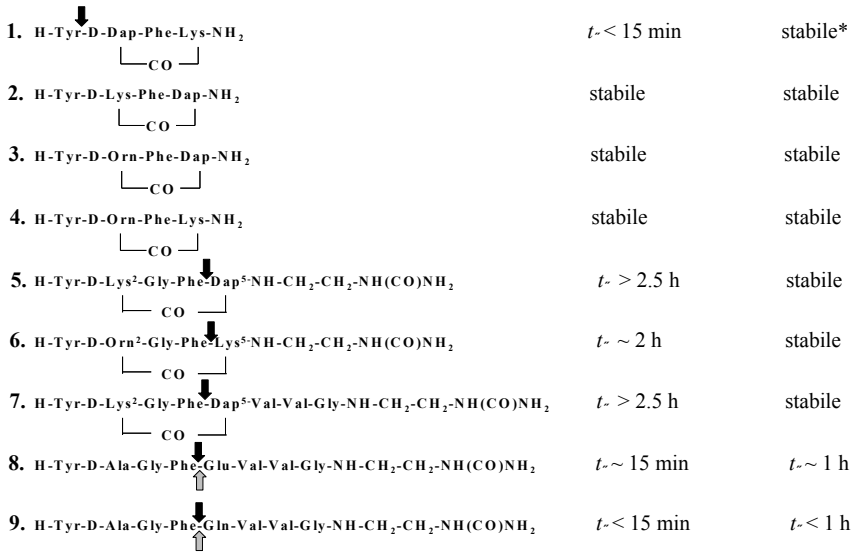

*Fig. 2. Proteolytic stability of peptides 1-9 and localization of the peptide bonds hydrolyzed by chymotrypsin and pepsin. The peptide bonds hydrolyzed by chymotrypsin and pepsin are indicated by black and gray arrows, respectively; *"stable"(stabile) means that no degradation products were observed even after 2.5 h of incubation with the protease; t values mean* $t_{1/2}$.

References

1. Szewczuk, Z., Gibbs, B.F., Yue, S-Y., Purisima, E.O., Konishi, Y. *Biochemistry* **31**, 9132-9140 (1992).
2. Szewczuk, Z., Wilczyński, A., Dyba, M., Petry, I., Siemion, I.Z., Wieczorek, Z. *Peptides* **21**, 1849-1858 (2000).
3. Filip, K., Oleszczuk, M., Pawlak, D., Wojcik, J., Chung, N.N., Schiller, P.W., Izdebski, J. *J. Peptide Sci.* **9**, 649-657 (2003).

Proceedings of the 31st European Peptide Symposium
Michal Lebl, Morten Meldal, Knud J. Jensen, Thomas Hoeg-Jensen (Editors)
European Peptide Society, 2010

VCD Spectroscopic Analysis of μ-Opioid Peptides

Attila Borics[1], Géza Tóth[1], and Sándor Lovas[2]
[1]Institute of Biochemistry, Biological Research Center of the Hungarian Academy of Sciences, Szeged, H-6726, Hungary; [2]Department of Biomedical Sciences, Creighton University Medical Center, Omaha, NE, 68178, U.S.A.

Introduction

The determination of structural requirements of binding to the μ-opioid receptor is a key aspect of the development of novel analgesics. Many natural and synthetic peptides and peptidomimetics bind to the μ-opioid receptor with high affinity and selectivity, but there is no consensus about what is the structural requirement for such biological activity [1,2]. Previously, ten μ-opioid receptor ligands (Table 1), including β-amino acid [3] or β-turn inducing pseudo-dipeptide [4] containing endomorphin-1 and 2 (EM-1, EM-2) analogues, possessing different affinity and selectivity were examined using molecular dynamics (MD) in aqueous and dimethyl sulfoxide (DMSO) environment. Four structural parameters were found to correlate with receptor binding data [5]. In the present study, IR and VCD spectroscopies were applied to determine the solution structure of these molecules. Theoretical simulation of the vibrational spectra of EM-1, utilizing quantum chemical calculations, was carried out using conformational data obtained from a previous MD simulation. In this approach the theoretical spectra is built from spectra calculated for the representative structures of dominant conformational families. The effect of explicitly included solvent molecules on the quantum chemical spectrum calculations was investigated as well.

Table 1. μ-Opioid receptor ligands addressed in this study

	Sequence	*Receptor affinity* (K_i^{μ} / *nM*)	*μ/δ selectivity* (K_i^{δ}/K_i^{μ})
1	H-Tyr-Pro-Trp-Phe-NH_2	0-10	>1000
2	H-Tyr-Pro-Phe-Phe-NH_2	0-10	>1000
3	H-Tyr-D-Ala-Gly-*N*-Me-Phe-Gly-ol	0-10	1000-100
4	H-Tyr-(1*S*2*R*)-ACHC-Phe-Phe-NH_2	0-10	1000-100
5	H-Tyr-Pro-Trp-Gly-NH_2	10-100	1000-100
6	H-Tyr-(*R*)-spiro-Aba-Gly-Phe-NH_2	10-100	>1000
7	H-Tyr-Pro-Phe-Pro-NH_2	10-100	1000-100
8	H-Tyr-(1*R*2*R*)-ACPC-Trp-Phe-NH_2	10-100	100-10
9	H-Tyr-(1*R*2*S*)-ACHC-Phe-Phe-NH_2	100-1000	>1000
10	H-Tyr-(*R*)-spiro-Aba-Gly-Phe-NH_2	100-1000	<10

Results and Discussion

IR and VCD spectra were recorded in D_2O, DMSO-d_6, 50% (v/v) TFE-D_2O mixture and 80 mM SDS in D_2O. Two main components were apparent in the amide I' band of IR spectra of all peptides which were most distinguishable in spectra recorded in DMSO-d_6. The ratio of components varied depending on peptide and solvent. In general, a negative couplet-type signal is observed in the amide I' region of VCD spectra, indicative of various turn and random meander structures [6,7]. In the case of peptide **5,** this signal was found to be a

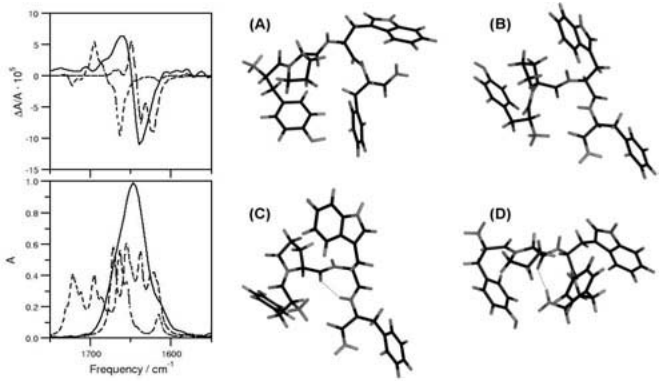

*Fig. 1. Average IR and VCD spectra of structures shown on the side, calculated in vacuum (short dashed) and in explicit D_2O (long dashed), and experimental spectra of peptide **1** recorded in D_2O (continuous line).*

simple negative lobe in 50% (v/v) TFE-D_2O mixture and strongly negatively biased in other solvents. Such simple negative amide I' VCD signal was obtained for **9** in all solvents. For peptide **3,** more complex, markedly different VCD spectra were measured in the amide I' region. Furthermore, VCD spectra of this peptide demonstrated strong dependence on the solvent environment. This may be attributed to the high diversity of the solution conformational ensemble of this peptide as indicated by previous MD simulations. In summary, no striking spectral characteristics were found which could be correlated to a special structural component and hence μ-opioid activity. This suggests that such components could only be determined via the deconvolution of VCD spectra. The IR and VCD spectra of 37 representative structures of peptide **1,** identified by previous MD simulations, was computed on the B3LYP/6-31G(d) level of theory. Inspection of the resultant prototypical spectra revealed that the following structures result in IR and VCD spectra similar to the ones observed experimentally: random meander, bent structure with no specific hydrogen bond or backbone dihedral angle values to define a β-turn, classic γ-turn around Trp^3 and C-terminal β-turn (Figure 1 A, B, C and D, respectively). A simple average of spectra computed for these structures in both vacuum and explicit D_2O molecules is shown on Figure 1 together with the experimental spectra. Clearly, constructs of spectra calculated in solvent environment show better agreement with experimental results. However, much better results could be obtained if the exact contribution of each component were known. Despite the fair agreement between theoretical and experimental spectra, the determination of the exact contribution of each conformational state remains a challenge. It is most likely, that the improvement of theoretical conformational analysis would facilitate the achievement of such accuracy and yield a powerful method for solution conformational analysis of short peptides, which could help to identify correlation between structure and biological activity.

Acknowledgments
This work was supported by Hungarian OTKA PD-73081 (A. Borics) and NIH-INBRE P20 RR016469 (S. Lovas) grants.

References

1. Leitgeb, B. *Chem. Biodivers.* **4**, 2703-2724 (2007).
2. Keresztes, A., et al. *Chem. Med. Chem.* **5**, 1176-1196 (2010).
3. Keresztes, A., et al. *J. Med. Chem.* **51**, 4270-4279 (2008).
4. Tömböly, Cs., et al. *J. Med. Chem.* **51**, 173-177 (2008).
5. Borics, A., et al. *J. Mol. Graph Model* **28**, 495-505 (2010).
6. Dukor, R.K., et al. *Biopolymers* **31**, 1747-1761 (1991).
7. Borics, A., et al. *Protein Pept. Lett.* **14**, 353-359 (2007).

Proceedings of the 31st European Peptide Symposium
Michal Lebl, Morten Meldal, Knud J. Jensen, Thomas Hoeg-Jensen (Editors)
European Peptide Society, 2010

Synthesis, Evaluation and Conformational Solution Studies of Cysteine-based $\alpha_4\beta_1$ Integrin Ligands

George K. Daletos[1], Margarita Lamprou[1], Panagiotis Zoumpoulakis[2], Maria Zervou[2], Nikos L. Assimomytis[3], Athina Geronikaki[4], Evangelia Papadimitriou[1], Vassiliki Magafa[1], and Paul Cordopatis[1]

[1]Department of Pharmacy, University of Patras, GR-26500, Patras, Greece; [2]Laboratory of Molecular Analysis, Institute of Organic and Pharmaceutical Chemistry, NHRF, 48 Vas. Constantinou Ave, GR-11635, Athens, Greece; [3]Department of Mechanical Engineering, TEI of Patras, 1 M. Alexandrou str, Koukouli, GR-26334, Patras, Greece; [4]Department of Pharmacy, University of Thessaloniki, GR-54006, Thessaloniki, Greece

Introduction

Integrins are transmembrane receptors consisting of one a and one β subunit. Until now, scientists have found 18 a and 8 β subunits which form 24 different integrins [1]. These receptors, as their name indicates, "integrate" the extracellular matrix with the intracellular cytoskeleton. By creating focal adhesion complexes with different kinases and adaptor proteins, integrins activate intracellular signalling pathways which regulate the migration, proliferation, survival and apoptosis of the cells, functions of vital importance for the organism. One integrin with particular interest is $\alpha4\beta1$ (VLA-4, very late activating antigen-4). The role of $\alpha4\beta1$ to promote inflammation is well known, while recent studies indicate also the importance of this integrin in angiogenesis [2]. The aim of this research is the development of $\alpha_4\beta_1$ cyclic peptide ligands and their study as inflammation and tumor angiogenesis inhibitors. The synthesized analogues have the basic cyclic sequence X_1-X_2-cyclo(Cys-Asp-Pro-Cys)-COY, where X_1=L-/D-Tyrosine, D-Tyrosine(OEthyl) [D-Tyr(Et)], Salicylic acid (Sal), 2-Naphtylalanine (2-Nal), L-β-(2-thienyl)-alanine [Thi], X_2=L- or D-Arginine, Tryptophan, β-alanine and Y=OH or NH_2.

Results and Discussion

For the synthesis of the peptide analogues we used Fmoc/Bu^t solid phase peptide synthesis methodology [3], utilizing 2-chlorotrityl chloride resin [4] and Rink Amide MBHA resin [5] to provide peptides with *C*-terminal carboxylic acid or amide respectively. The creation of the disulphide bond was performed in DMSO/H_2O (10:90 v/v) solution for 24-48 h [6] and the cyclisation was controlled with Ellman's test [7]. All analogues were purified by gel filtration chromatography on Sephadex G-15 using 15% acetic acid as the eluent. Final purification was achieved by semi-preparative HPLC on reversed-phase support C-18 with a linear gradient from 5 to 85% acetonitrile (0.1% TFA) for 30 min at a flow rate of 1.5 ml/min and UV detection at 220 and 254 nm. ESI mass spectrometry revealed that the purified peptides were the expected products and their purity, determined by analytical HPLC, was higher than 98%. The physicochemical properties of the new analogues are summarized in Table 1.

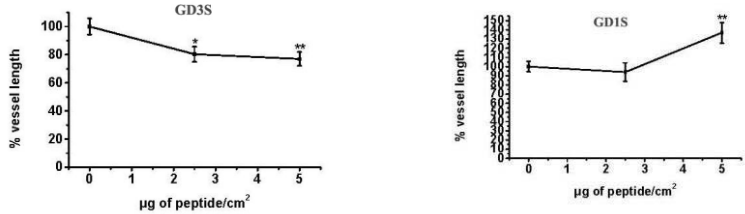

A: Analogue GD3S

B: Analogue GD1S

**P<0.01

Fig. 1. % vessel length in CAM vs the concentrations of the added substances.

Table 1. Physicochemical properties of the synthesized analogues

Code	Analogues	HPLC t_R (min)	TLC[α] R_{fA}	TLC[α] R_{fB}
GD1S	Tyr-Arg-c(Cys-Asp-Pro-Cys)-$CONH_2$	10.25	0.21	0.18
GD2S	Tyr-Arg-c(Cys-Asp-Pro-Cys)-OH	8.24	0.12	0.09
GD3S	Sal-Arg-c(Cys-Asp-Pro-Cys)-OH	13.38	0.34	0.31
GD4S	Tyr-Trp-c(Cys-Asp-Pro-Cys)-OH	13.10	0.27	0.28
GD5S	2-Nal-Arg-c(Cys-Asp-Pro-Cys)-OH	9.10	0.15	0.17
GD6S	Sal-Tyr-Arg-c(Cys-Asp-Pro-Cys)-OH	14.22	0.35	0.32
GD7S	Tyr-D-Arg-c(Cys-Asp-Pro-Cys)-OH	12.90	0.27	0.18
GD8S	D-Tyr-Arg-c(Cys-Asp-Pro-Cys)-OH	9.11	0.15	0.11
GD9S	D-Tyr(Et)-Arg-c(Cys-Asp-Pro-Cys)-OH	10.40	0.23	0.14
GD10S	Thi-Arg-c(Cys-Asp-Pro-Cys)-OH	6.93	0.08	0.08
GD11S	Tyr-β-Ala-c(Cys-Asp-Pro-Cys)-OH	10.05	0.20	0.14

[α] *A) butan-1-ol/water/acetic acid/pyridine (4/1/1/2, v/v); B) butan-1-ol/water/acetic acid (4/5/1 v/v, upper phase)*

The analogues were studied, under *in vivo* conditions, for their potentiality as inhibitors of angiogenesis in chicken embryo chorioallantoic membrane (CAM), as previously described [8]. All the compounds tested in this study, except analogue **GD1S** and **GD3S**, had no significant activity on angiogenesis in CAM model. In particular, analogue **GD3S** showed important inhibition of angiogenesis at dose-dependent manner (Figure 1A). On the other hand, peptide **GD1S** promoted angiogenesis at the higher concentration, but showed slight inhibition at the lower one (Figure 1B). A series of NMR spectra including ^{1}H, 2D TOCSY and 2D NOESY were recorded on a Varian 600MHz spectrometer for the analogues **GD1S, GD2S**, **GD3S** and **GD6S**. All peptides were dissolved in DMSO-d_6 solvent. The mixing time for the TOCSY was set to 80ms and for the NOESY 75ms. For the assignment of the proton peaks, standard procedures were followed based on the 2D spectra. NOE constrains have also provided crucial information regarding the conformation of the peptides in solution. Molecular modelling techniques are currently performed in order to study the conformational properties of the peptides, as well as similarities and differences between them. Finally, experiments are going to be held for the study of these analogues as anti-inflammatory agents.

References

1. Heckman, D., Kessler, H. *Methods in Enzymology* **426**, 463-495 (2007).
2. Avraamides, C.J., Garmcy-Susini, B., Varner, J.A. *Nat. Rev. Cancer* **8**, 604-617 (2008).
3. Fields, B.G., Noble, L.R. *Int. J. Pept. Prot. Res*. **35,** 161-214 (1990).
4. Barlos, K., Chatzi, O., Gatos, D., Stavropoulos, G. *Int. J. Pept. Prot. Res*. **37**, 513-520 (1991).
5. Rink, H. *Tetrahedron Lett.* **28**, 3787-3790 (1987).
6. Tam, J.P., Wu, C.R., Liu, W., Zhang, J.W. *J. Am. Chem. Soc.* **13**, 6657-6662 (1991).
7. Ellmam, G. *Arch. Biochem. Biophys.* **82**, 70-77 (1959).
8. Papadimitriou, E., Polykratis, A., Courty, J., Koolwilk, P., Heroult, M., Katsoris, P. *Biochem. Biophys. Res. Commun.* **282**, 306-313 (2001).

Proceedings of the 31st European Peptide Symposium
Michal Lebl, Morten Meldal, Knud J. Jensen, Thomas Hoeg-Jensen (Editors)
European Peptide Society, 2010

Synthesis and Biological Evaluation of New Linear and Cyclic Analogues of Neurotensin

Revekka Exarchakou[1], Vassiliki Magafa[1], Evy Manessi-Zoupa[2], Nikos L. Assimomytis[3], Maria Georgiadou[4], Maria Venihaki[5], George Varvounis[6], George Liapakis[4], and Paul Cordopatis[1]

[1]Department of Pharmacy, University of Patras, GR-26500, Patras, Greece; [2]Department of Chemistry, University of Patras, GR-26500, Patras, Greece; [3]Department of Mechanical Engineering, TEI of Patras, 1 M. Alexandrou str, Koukouli, GR-26334, Patras, Greece; [4]Department of Pharmacology, [5]Department of Clinical Chemistry, Faculty of Medicine, University of Crete, GR-71003, Heraklion, Crete, Greece; [6]Department of Chemistry, University of Ioannina, GR-45110, Ioannina, Greece

Introduction

Neurotensin [(pGlu-Leu-Tyr-Glu-Asn-Lys-Pro-Arg-Arg-Pro-Tyr-Ile-Leu), NT] is a tridecapeptide originally isolated from bovine hypothalamus and later from intestines. NT displays a wide spectrum of biological actions both in the central and peripheral nervous systems of different mammalian species [1]. The physiological and biochemical actions of NT are mediated through binding to NT receptors (NTS1, NTS2 & NTS3) [2]. All three receptors recognize the same *C*-terminal hexapeptide fragment of NT [NT(8-13)]. Although NT(8-13) possesses high receptor binding affinity, it is rapidly degraded by peptidase action. Therefore, it is important to synthesize analogues with stabilized bonds against metabolic deactivation which do not lose binding affinity. Based on these findings, we herein report the synthesis of new linear and cyclic analogues of NT(8-13) with modifications in the basic structure needed for high affinity binding in order to improve the metabolic stability. The analogues contain D-Tyrosine(Ethyl) [D-Tyr(Et)] in position 11, D-Arginine in position 8 or 9, L-Lysine in position 8 or 9 and 1-[2-(aminophenyl)-2-oxoethyl]-1*H*-pyrrole-2-carboxylic acid (AOPC) in position 8 or 7. AOPC is an unnatural amino acid with promise in applications as a building block for the synthesis of peptidomimetic compounds.

Results and Discussion

All analogues shown in Table 1 were synthesized by the Fmoc/Bu^t solid phase methodology [3] utilizing 2-chlorotrityl chloride resin [4]. Stepwise synthesis of a peptide analogue was achieved with diisopropylcarbodiimide/1-hydroxybenzotriazole (DIC/HOBt) as coupling agents in dimethylformamide (DMF) [5,6] in 2.0 (Fmoc-amino acid), 2.2 (DIC) and 3.0 (HOBt) molar excess for 2 h at room temperature. AOPC was synthesized in four steps from 1-(2-nitrophenyl)ethanone (Scheme 1). The coupling of the carboxylic acid *C*-terminus of AOPC with the *N*-terminus of the peptides took place with 2-(1*H*-benzotriazole 1-*yl*)-1,1,3,3-tetramethyluronium tetrafluoroborate (TBTU), 1-hydroxy benzotriazole (HOBt) and diisopropyl ethylamine (DIEA) in DMF [7] without protection of the AOPC amino group. The overall yield of the syntheses of the NT analogues was in the

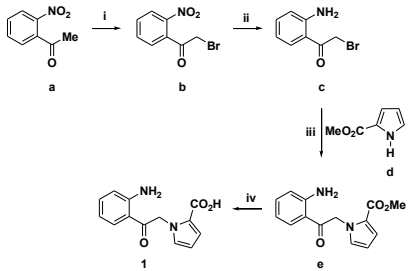

Scheme 1. Synthesis of 1-[2-(aminophenyl)-2-oxoethyl]-1H-pyrrole-2-carboxylic acid (AOPC). Reagents and conditions: (i) Br_2, chloroform, 83%, (ii) Cu, H_2SO_4, 57%, (iii) K_2CO_3, DMF, 66%, (iv) (a) NaOH, H_2O, MeOH, 60 ^oC, (b) 2 N HCl, 87%.

Table 1. Physicochemical properties of the synthesized NT analogues

Code	Analogues	Yield (%)	HPLC	TLC[a]	
			t_R(min)	R_{fA}	R_{fB}
I.	NT (1-13)	88	10.39	0.28	0.37
II.	[Lys-Pro-Arg-Arg-Pro-Tyr-Ile-Leu] NT(6-13)	92	9.01	0.31	0.40
III.	[Arg-Arg-Pro-Tyr-Ile-Leu] NT(8-13)	95	9.19	0.39	0.45
1.	[D-Arg^8, Lys^9, D-Tyr(Et)^{11}] NT(8-13)	93	12.49	0.42	0.48
2.	[Lys^8, D-Arg^9, D-Tyr(Et)^{11}] NT(8-13)	91	11.62	0.44	0.50
3.	cyclo[D-Arg^8, Lys^9, D-Tyr(Et)^{11}] NT(8-13)	70	11.97	0.56	0.63
4.	[AOPC^8, D-Tyr(Et)^{11}] NT(8-13)	81	15.17	0.72	0.78
5.	[AOPC^8, Lys^9, D-Tyr(Et)^{11}] NT(8-13)	83	14.61	0.71	0.79
6.	[AOPC^8, D-Arg^9, D-Tyr(Et)^{11}] NT(8-13)	79	14.91	0.63	0.70
7.	[AOPC^7, D-Arg^8, Lys^9, D-Tyr(Et)^{11}] NT(8-13)	77	13.64	0.65	0.73
8.	[AOPC^7, Lys^8, D-Arg^9, D-Tyr(Et)^{11}] NT(8-13)	80	13.63	0.57	0.65
9.	cyclo[Lys^8, D-Arg^9, D-Tyr(Et)^{11}] NT(8-13)	72	11.13	0.54	0.67
10.	[Lys^8, D-Arg^9, D-Tyr(Et)^{11}] NT(8-13)	86	12.46	0.55	0.61

[a] *A) butan-1-ol/water/acetic acid/pyridine (4/1/1/2, v/v); B) butan-1-ol/water/acetic acid (4/5/1 v/v, upper phase)*

range 70-95% (calculated on the amount of linker initially coupled to the resin). ESI mass spectrometry revealed that the purified peptides were the expected products and their purity, determined by analytical HPLC, was higher than 98%.

Competition binding studies were performed in membrane homogenates from HT-29 cells endogenously expressing Neurotensin receptors on their membranes [8]. Aliquots of membrane suspension (50 μl) were incubated either with **NT(1-13)** or NT-related peptides (synthesized in this study) at the single concentration of 100 nM (screening experiments) or with increasing concentrations of these peptides (competition binding experiments) in the presence of ~5 nM of [^{3}H]-Neurotensin (98.6 Ci/mmol, Perkin Elmer) in a final volume of 0.1 ml. Data for competition binding were analyzed by nonlinear regression analysis, using GraphPad Prism 4.0 (GraphPad Software, San Diego, CA). IC_{50} values were obtained by fitting the data from competition studies to a one-site competition model. In agreement with previous studies [2] Neurotensin is bound to HT-29 cells with a high affinity (~0.2 nM). All compounds tested in this study, except **NT(6-13)** and **NT(8-13)**, did not cause inhibition more than 50% of [^{3}H]-Neurotensin specific binding to HT-29 cells. These results suggest that analogues **1-10** tested in this study were bound to NT receptors endogenously expressed in HT-29 cells, with an affinity more than 100 nM.

References

1. Carraway, R., Leeman, E.S. *J. Biol. Chem.* **248**, 6854-6861 (1973).
2. Vincent, J.P., Mazella, P., Kitabgi, P. *Trends Pharmacol. Sci.* **20**, 302-309 (1999).
3. Fields, B.G., Noble, L.R. *Int. J. Pept. Prot Res.* **35**, 161-214 (1990).
4. Barlos, K., Chatzi, O., Gatos, D., Stavropoulos, G. *Int. J. Pept. Prot. Res.* **37**, 513-520 (1991).
5. Sarantakis, D., Teichnan, J., Lien, E.L., Fenichel, R.L. *Biochem. Biophys. Res. Commun.* **73**, 336-342 (1976).
6. König, W., Geiger, R. *Chem. Ber.* **103**, 788-798 (1970).
7. Knorr, R., Trzeciak, A., Bannwarth, W., Gillessen, D. *Tetrahedron Lett.* **30**, 1927-1930 (1989).
8. Morinville, A., Martin, S., Lavallée, M., Vincent, J.P, Beaudet, A., Mazella, J. *Int. J. Bioch. & Cell Biol.* **36**, 2153-2168 (2004).

Proceedings of the 31st European Peptide Symposium
Michal Lebl, Morten Meldal, Knud J. Jensen, Thomas Hoeg-Jensen (Editors)
European Peptide Society, 2010

Influence of Non-Natural Amino Acids at Position 3 of [Mpa[1], D-Tyr(Et)[2]] or [Mpa[1], D-1-Nal[2]] Oxytocin on Their Pharmacological Properties

Vassiliki Magafa[1], Nikos L. Assimomytis[2], George Pairas[1], Revekka Exarchakou[1], George K. Daletos[1], Lenka Borovičková[3], Jiřina Slaninová[3], and Paul Cordopatis[1]

[1]Department of Pharmacy, University of Patras, Patras, GR-26500, Greece; [2]Department of Mechanical Engineering, TEI of Patras, Koukouli, Patras, GR-26334, Greece; [3]Department of Antimicrobial Peptides, Institute of Organic Chemistry and Biochemistry, Academy of Sciences of Czech Republic, Prague 6, CZ-16610, Czech Republic

Introduction

Oxytocin (OT) is a cyclic nonapeptide [cyclo(Cys-Tyr-Ile-Gln-Asn-Cys)-Pro-Leu-Gly-NH_2] hormone synthesized in hypothalamus and released into the general circulation from the posterior lobe of the pituitary gland. Its major physiological roles are: a) to induce uterine contractions and b) milk injection. Beside these actions, OT is involved in several other processes, such as vascular and cardiac regulation and sexual, maternal and social behavior [1,2]. The role of OT in preterm labor led to the search for and design of synthetic peptide antagonists as potential tocolytic agents [3]. Moreover, in view of the widespread OT-related actions, OT antagonists may not only be studied as promising inhibitors of preterm labor but may also prove useful in the treatment of dysmenorrhea, benign prostatic hyperplasia and psychiatric illnesses such as anxiety, sexual dysfunctions, eating disorders etc. [4]. In this study we synthesized 8 new analogues of [Mpa[1], D-Tyr(Et)[2]]OT or [Mpa[1], D-1-Nal[2]]OT containing L-/D-1-naphtylalanine [1-Nal] or L-/D-allylglycine [allylGly] in position 3. We also studied the effect of modified *C*-terminal amide on biological potency of 2 new OT analogues containing L-*β*-(2-thienyl)-alanine [Thi] and L-allylglycine in position 3.

Results and Discussion

The new analogues were synthesized by Fmoc solid phase methology [5] utilizing a Rink Amide MBHA and [3-((Ethyl-Fmoc-amino)-methyl)-1-indol-1-yl]acetyl AM resins as solid support and diisopropylcarbodiimide/1-hydroxybenzotriazole (DIC/HOBt) as coupling reagents. The cyclization was performed in DMSO/H_2O (1:4, v/v) for 24-48h [6] or alternatively in AcCN/CCl_4 using tetrabutylammonium fluoride (TBAF) [7]. The analogues were tested for their potency in two pharmacological assays: a) uterotonic *in vitro* test in the absence of Mg^{2+} on an isolated strip of rat uterus [8] and b) in the pressor test on phenoxybenzamine treated male rats [9]. In parallel, determination of binding affinity of the analogues to cloned human OTR using crude HEK OTR cell membrane preparation was performed [10]. The biological evaluation of the new analogues is summarized in Table 1. For comparison purposes the activities of the analogues [Mpa[1], D-Tyr(Et)[2]]OT (**I**), [Mpa[1], D-1-Nal[2]]OT (**II**) and [Mpa[1], D-1-Nal[2], Thi[3]]OT (**III**) [11] are also presented in Table 1. As can be seen from Table 1, replacement of Ile[3] by the L- or D-form of the non natural amino acids combined with D-Tyr(Et)[2] or D-1-Nal[2] and Mpa[1] modifications influenced biological activities very differently. Analogues having in position 3 residue L-1-Nal, which has more compact side chain than Ile, exhibited no substantial change in the antagonistic potency in comparison to analogues **I** and **II** having no change in position 3. On the other hand, the introduction in position 3 of a residue with less bulky aliphatic side chain than Ile, such as allylGly, had an inconsistent effect; analogue **3** having combined substitutions in position 1 (Mpa), in position 2 [D-Tyr(Et)] and in position 3 allylGly exhibited slightly improved antagonistic potency in comparison to analogue **I**, while analogue **7** having combined substitutions in position 1 (Mpa), in position 2 (D-1-Nal) and in position 3 allylGly showed oxytocin antagonistic potency slightly decreased in comparison to analogue **II**.

Table 1. Biological activities of oxytocin analogues

Code	Analogues	Activity		
		Anti-Uterotonic in vitro (pA_2)	*Anti-Pressor (pA_2)*	*Binding Affinity IC_{50} (nM)[a]*
I.	[Mpa^1, D-Tyr(Et)^2]OT	7.82±0.07	0	148±26
1.	[Mpa^1, D-Tyr(Et)^2, L-1-Nal^3]OT	7.70±0.10	0	356±55
2.	[Mpa^1, D-Tyr(Et)^2, D-1-Nal^3]OT	0	0	9 858±341
3.	[Mpa^1, D-Tyr(Et)^2, L-allylGly^3]OT	8.30±0.14	<6.0	8.0±2.8
4.	[Mpa^1, D-Tyr(Et)^2, D-allylGly^3]OT	6.20±0.01	0	3 443±513
II.	[Mpa^1, D-1-Nal^2]OT	7.92±0.21	0	34.6±2.9
5.	[Mpa^1, D-1-Nal^2, L-1-Nal^3]OT	8.00±0.23	0	42.7±6.8
6.	[Mpa^1, D-1-Nal^2, D-1-Nal^3]OT	0	0	>10 000
7.	[Mpa^1, D-1-Nal^2, L-allylGly^3]OT	7.44±0.18	0	156±2.0
8.	[Mpa^1, D-1-Nal^2, D-allylGly^3]OT	0	0	>10 000
9.	[Mpa^1, D-1-Nal^2, L-allylGly^3]-NHEt OT	7.69±0.05	0	88±17
10.	[Mpa^1, D-1-Nal^2, Thi^3]-NHEt OT	8.25±0.13	<6.0	3.0±0.2
III.	[Mpa^1, D-1-Nal^2, Thi^3]OT	8.50±0.24	6.1	5.2±0.7

[a]*The value for oxytocin is 2.7±0.2 nM*

D-diastereoisomers of the tested nonproteinogenic amino acids (analogues **2**, **4**, **6** and **8**) showed no inhibitory potency or lower one than the L-counterparts (analogues **1**, **3**, **5** and **7**). Ethyl substitution of the amide in position 9 (analogues **9** and **10**) influenced the activity negligibly. Furthermore, most of the analogues were selective, showing no pressor activity. The binding affinities to human OTR more or less mirror the biological activities. Analogues with L-stereoisomers of 1-Nal or allylGly in position 3 exhibit higher binding affinity than the D-counterparts. Analogues with D-1-Nal^2 modification generally show higher binding affinity in comparison to the D-Tyr(Et)^2 substituted analogues.

Acknowledgments
The work was supported by the research project No. Z40550506 of the Institute of Organic Chemistry and Biochemistry, AS CR.

References

1. Gimpl, G., Fahrenholz, F. *Physiol Rev* **81**, 629-683 (2001).
2. Lippert, T.H., Mueck A.O., Seeger, H., Plaff, A. *Horm. Res*. **60**, 262-271 (2003).
3. Manning, M., Stoev, S., Chini, B., Durroux, T., Mouillac, B., Guillon, G. *Prog. Brain Res.* **170**, 473-512 (2008).
4. Moutquin, J.M., Fisk, N.M., MacLennan, A.H., Maršál,K., Rabinovici, J. *Br. J. Obstet. Gynaecol.* **108**, 133-142 (2001).
5. Fields, B.G., Noble, L.R. *Int. J. Pept. Prot. Res.* **35**, 161-214 (1990).
6. Tam, J.P., Wu, C.R., Liu, W., Zhang, J.W. *J. Am. Chem. Soc.* **113**, 6657-6662 (1991).
7. Maruyama, T., Ikeo, T., Ueki, M. *Tetrahedron Lett.* **40**, 5031-5034 (1999).
8. Slaninová, J., in Lebl, M., Jost, K., Brtnik, F., (Eds.). *Handbook of Neurohypophyseal Hormone Analogs*, CRC Press, Boca Raton, Vol. I, pp. 83-107 (1987).
9. Dekanski, J. *Br. J. Pharmacol*. **7**, 567-572 (1952).
10. Fahrenholz, F., Boer, R., Crause, P., Fritzsch, G., Grzonka, Z. *Eur. J. Pharmacol*. **100**, 47-58 (1984).
11. Petraki, S., Magafa, V., Borovičkova, L., Slaninová, J. and Cordopatis, P., In Rolka, K., Rekowski, P. and Silberring, J. (Eds.), *Peptides (Proceedings of the 29thEuropean Peptide Symposium)* Kenes International, Gdansk, Poland, 2007, p. 580.

Proceedings of the 31st European Peptide Symposium
Michal Lebl, Morten Meldal, Knud J. Jensen, Thomas Hoeg-Jensen (Editors)
European Peptide Society, 2010

Conformational Behaviour of Vasopressin-like Peptides in the Membrane-Mimetic Environment

Emilia Sikorska and Anna Kwiatkowska
Faculty of Chemistry, University of Gdańsk, Sobieskiego 18, 80-952, Gdańsk, Poland

Introduction

It is believed that lipids are implicated in interaction of peptide hormones with their membrane receptors. This interaction, through the change of peptide conformation, is likely to facilitate the entry of the hormone into the microenvironment of the receptor [1]. In the present study, we used a combined experimental and computational approach to learn how vasopressin-like peptides interact with a dodecylphosphocholine (DPC) micelle. The micelle simulates eukaryotic cell membranes that are generally rich in zwitterionic phospholipids. We use NMR spectroscopy and molecular modelling to examine two vasopressin analogues, Aca[*cis*-Apc^2,Val^4]AVP (**I**) and [Nmp^2,D-Arg^8]VP (**II**) (Aca: 1-adamantanecarboxylic acid; *cis*-Apc: *cis*-1-amino-4-phenyl-cyclohexanecarboxylic acid and Nmp: (2S,4R)-4-(naphthalene-2-ylmethyl)pyrrolidine-2-carboxylic acid) embedded in the dodecylphosphocholine (DPC) micelle. Both analogues exhibit antioxytocic activity. With [Nmp^2,D-Arg^8]VP (**II**), a weak antipressor activity has also been reported (unpublished).

Previous studies have shown that Cα-Cα cyclized residues, such as *cis*-Apc, imparts considerable stereochemical rigidity to peptide backbones and are constrained to adopt conformations in the 3_{10}/α-helical regions of the ϕ and ψ spaces. They can be accommodated at either the *i+1* position of type βIII (III')-turns or at the *i+2* position of type βII (II')-turns. Furthermore, they display the tendency to induce γ- or inverse γ-turns (C7-conformation) [2-4]. In turn, the proline ring of Nmp has significant effect on the ϕ and ψ dihedral angles. The former should be relatively fixed at about -60°, whereas the later may reach two minima, 40° and 150° [5]. Consequently, Nmp, similar to proline, is likely to exhibit a strong preference for the *i+1* position of β-turn. Moreover, in the case of peptides containing proline-like residues the *cis/trans* isomerization of peptide bond can take place. The differences in conformational behaviour arising from *cis/trans* isomerization are crucial for biological profile of peptides.

Results and Discussion

The three-dimensional structures of both analogues studied were determined by time-averaged molecular dynamics in an *explicit* DPC micelle with the parm99 force field in AMBER11.0 [6] package. The NMR spectra of peptide **II** indicate a *cis* Cys^1-Nmp^2 peptide bond, which was included during MD simulations. The *cis* peptide bond between residues at positions 1 and 2 was also found for native vasopressin in SDS micelle [7].

The analogue **I** adopts βI' or III' β-turns at positions 2,3 and 3,4. The former is stabilized by HN^4-CO^1 hydrogen bond, whilst the later is not tight enough and is not hydrogen bonded. In turn, analogue **II** reveals the tendency to create the βIII'- or βII-turns at positions 4,5 and 7,8 respectively. The β-turn at position 7,8 is closed by HN^9-CO^6 hydrogen bond. Moreover, the side chains of Gln^4 and Asn^5 of analogue **II** are involved in hydrogen bonds with oxygen atoms of Cys^1 and Gly^9, respectively.

The average radii of gyration (Rg) calculated with all of the heavy atoms for both analogue (7.1 and 6.9 Å for analogues **I** and **II**, respectively) indicate similar sizes of the molecules, despite the fact that analogue **I** is additionally acylated with Aca at its N-terminus.

It is believed that mutual arrangement of the aromatic side chains of a ligand is likely to play a crucial role in specific receptor affinity. Therefore, the relationship between the flat angle between the planes of aromatic rings ($F_{X\text{-}Phe}$) and dihedral angle between two planes, where the former is determined by the centre of mass of aromatic part of *cis*-Apc/Nmp^2, Cα of *cis*-Apc/Nmp^2 and Cα of Phe^3, whereas the latter by Cα of *cis*-Apc/Nmp^2, Cα of Phe^3 and the centre of mass of aromatic ring of Phe^3 ($D_{X\text{-}Phe}$) was established. The dihedral angle values, $D_{X\text{-}Phe}$, are clustered about horizontal lines, $D_{X\text{-}Phe}$= -50° for both peptides. In turn, the average values of the flat angle, $F_{X\text{-}Phe}$, are 50° and 125°,

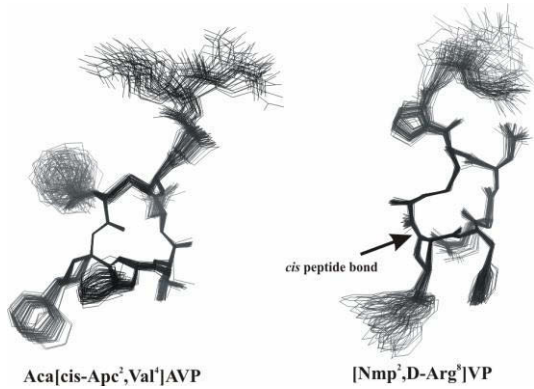

*Fig. 1. The 50 last conformations of both analogues obtained using MD with TAV. RMSD=0.136 and 0.147 Å for Ca of the cyclic part of Aca[cis-Apc^2,Val^4]AVP (**I**) and [Nmp^2,D-Arg^8]VP (**II**), respectively.*

for analogue **I** and **II**, respectively, were calculated. The differences arise from different orientation of the Phe^3 side chain.

The addition of 1-adamantanecarboxylic acid (Aca) to the N-terminus and replacement of the polar Gln residue with hydrophobic Val one enhanced the hydrophobic properties of analogue **I**. Consequently, peptide **I** strongly interacts with the hydrophobic part of the DPC micelle, which is particularly evident in its N-terminus. The Arg^8 side chain of analogue **I** shows the tendency to be associated with negatively charged phosphate groups of the DPC micelle and at the same time, it is located near the hydrophobic part of the micelle. In turn, the change of Arg^8 configuration from L to D alters the side chain orientation. Consequently, the D-Arg^8 side chain of analogue **II** is exposed to the aqueous phase.

In summary, the specific orientation of the side chains at positions 2 and 3 is important for antagonistic properties. The conformation or/and orientation of the Arg side chain seems to be crucial for interactions with V_{1a} receptors.

Acknowledgments

This work was supported by the Polish Scientific Research Committee Grant No. N N204 181736 grant and the University of Gdańsk, DS. 8453-4-0169-0. The calculations were carried out in the Academic Computer Centre (TASK) in Gdańsk, Poland.

References

1. Schwayzer, R.J. *Mol. Recog.* **8**, 3-8 (1995).
2. Toniolo, C., Benedetti, E. *Macromolecules* **24**, 4004-4009 (1994).
3. Paul, P.K.C., Sukumar, M., Bardi, R., Piazzesi, A.M., Valle, G., Toniolo, C., Balaram, P. *J. Am. Chem. Soc.* **108**, 6363-6370 (1986).
4. Paradisi, M., Torrini, I., Zecchini, G.P., Luente, G., Gauvuzzo, E., Mazza, F., Pochetti, G. *Tetrahedron* **51**, 2379-2386 (1995).
5. Wiliamson, M.P. *Biochem J.* **297**, 249-260 (1994).
6. Case, D.A., Darden, T.A., Cheatham, III T.E., Simmerling, C.L., Wang, J., Duke, R.E., Luo, R., Walker, R.C, Zhang, W., Merz, K.M., Roberts, B., Wang, B., Hayik, S., Roitberg, A., Seabra, G., Kolossváry, I., Wong, K.F., Paesani, F., Vanicek, J., Wu, X., Brozell, S.R., Steinbrecher, T., Gohlke, H., Cai, Q., Ye, X., Wang, J., Hsieh, M.J., Cui, G., Roe, D.R., Mathews, D.H., Seetin, M.G., Sagui, C., Babin, V., Luchko, T., Gusarov, S., Kovalenko, A., Kollman, P.A. *AMBER 11*, University of California, San Francisco, 2010.
7. Rodziewicz-Motowidło, S., Sikorska, E., Oleszczuk, M., Czaplewski, C. *J. Pept. Sci.* **14**, 85-96, 2008.

Proceedings of the 31st European Peptide Symposium
Michal Lebl, Morten Meldal, Knud J. Jensen, Thomas Hoeg-Jensen (Editors)
European Peptide Society, 2010

M1154 – A Novel Galanin Ligand to Delineate the Galaninergic System

Johan Runesson[1], Indrek Saar[1,2], Rannar Sillard[1], and Ülo Langel[1,2]
[1]Department of Neurochemistry, Arrhenius Laboratories for Natural Sciences, Stockholm University, Stockholm, SE-10691, Sweden; [2]Laboratory of Molecular Biotechnology, Institute of Technology, University of Tartu, Tartu, 50411, Estonia

Introduction

Galanin was isolated from porcine intestine by Professor Viktor Mutt and colleagues in 1983 [1] at the Karolinska Institute in Stockholm. Galanin is a 29 amino acid (30 amino acid in human) neuropeptide distributed broadly in the brain, spinal cord and gut that has been ascribed involvement in a diversity of physiological actions [2]. Galanin conducts its effects via three members (GalR1-3) of the G-protein-coupled receptor (GPCR) superfamily. The receptors have distinct distribution patterns and signaling pathways. GalR1 and GalR3 predominantly signal via Gi/o, leading to reduced cAMP-levels, whereas GalR2 mainly signal via Gq/11, leading to inositol phosphate accumulation and an increase in intracellular [Ca^{2+}] (see Figure 1). The galanin-peptide family consists of galanin, galanin message-associated peptide (GMAP), galanin-like peptide (GALP) and alarin. To distinguish between the three receptor subtypes, GalR1-3, in biological experiments, selective ligands are of great importance, particularly since subtype specific antibodies are not available [3]. We published in 2009 a novel galanin receptor type 2 (GalR2) selective chimeric peptide, M1145 [$(RG)_2$-N-galanin(2-13)-VL-$(P)_3$-$(AL)_2$-A-amide]. The M1145 peptide showed a more than 90-fold higher affinity for GalR2 over GalR1 and a 76-fold higher affinity over GalR3 [4]. Here we present preliminary data on receptor binding and the functional response for a novel galanin receptor selective peptide.

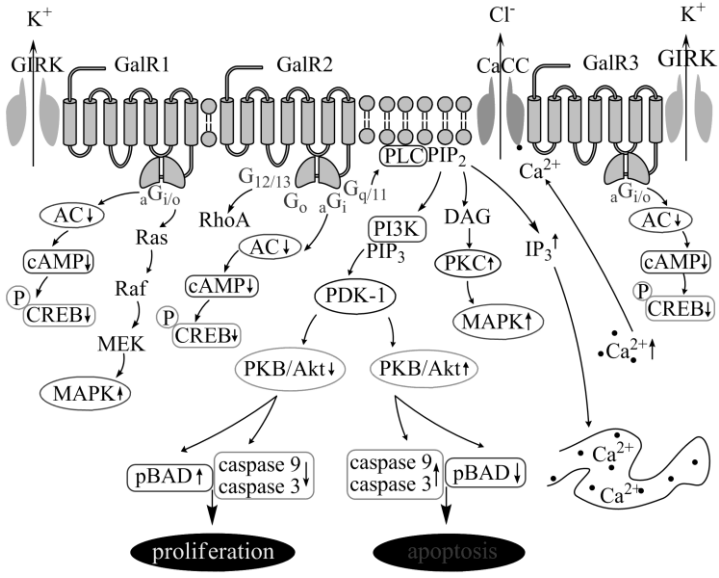

Fig. 1. Signaling induced by activation of GalR1-3.

Results and Discussion

The M1154 was designed to eliminate a biological response from the GalR3, as a mixed GalR1/GalR2 ligand has been implicated as a putative therapeutic for its potential effects, such as analgesic, anxiolytic and anticonvulsant effects (for a review see Mitsukawa et al., 2008 [5]). The peptide M1154 retains high affinity binding to GalR2, although two fold lower than the published M1145 (Ki 6.55 nM). M1154 binds with similar affinity to GalR1, disparate with the loss of affinity towards GalR1 seen for M1145 (Ki 587 nM). When tested on GalR3 M1154 showed no binding at the highest tested concentration, 10000 nM (Figure 2). These results reveal that M1154 is selective for GalR1 and GalR2 and the difference towards GalR3 is greater than 1000 times; manuscript in preparation.

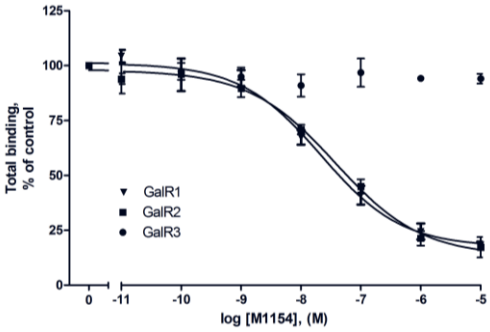

Fig. 2. Displacement curve for M1145 at hGalR1-3 (n=3).

Acknowledgments

We thank Kathryn A. Jones and Tiina P. Iismaa, Neurobiology Program, Garvan Institue of Medical Research, Sydney, Australia for Chinese Hamster Ovary cells stably transfected with Galanin Receptor 2 and Silvia Gatti-McArthur and Monique Dellenbach, F. Hoffmann-La Roche AG, Basel, Switzerland for Flp-In T-REx 293 cell line stably transfected with the human GalR3. This work was supported by grants from the Swedish Research Council (VR-MED), the Swedish Center for Biomembrane Reseach, the Knut and Alice Wallenberg Foundation, Stiftelsen Olle Engkvist Byggmästare (JR) and ARCHIMEDES Foundation (IS).

References

1. Tatemoto, K., Rökaeus, A., Jörnvall, H., McDonald, T.J., Mutt, V. *FEBS Lett.* **164(1)**, 124-128 (1983).
2. Runesson, J., Robinson, J.K., Sollenberg, U.E., Langel, Ü. (2009). Twenty-five Years of Galanin Research, in *Bioactive Peptides* Howl, J., Ed. CRC Press.
3. Lu, X., Bartfai, T. *Naunyn Schmiedbergs Arch. Pharmacol.* **379(4)**, 417-420 (2009).
4. Runesson, J., Saar, I., Lundström, L., Järv, J., Langel, Ü. *Neuropeptides* **43**, 187-192 (2009).
5. Mitsukawa, K., Lu, X., Bartfai, T. *Cell. Mol. Life Sci.* **65**, 1796-805 (2008).

Proceedings of the 31st European Peptide Symposium
Michal Lebl, Morten Meldal, Knud J. Jensen, Thomas Hoeg-Jensen (Editors)
European Peptide Society, 2010

Design, Synthesis and Biological Evaluation of Novel Endomorphins with Multiple Structural Modifications

Géza Tóth[1], Jayapal Reddy Mallareddy[1], Attila Borics[1], Katalin E. Kövér[2], and Attila Keresztes[1]

[1]*Biological Research Centre of Hungarian Academy of Sciences, Szeged, Hungary;* [2]*Department of Inorganic and Analytical Chemistry, University of Debrecen, Debrecen, Hungary*

Introduction

Two endogenous opioid peptides, endomorphin-1 (Tyr-Pro-Trp-Phe-NH_2) and endomorphin-2 (Tyr-Pro-Phe-Phe-NH_2) were isolated from the bovine and subsequently the human CNS [1]. Structure-activity studies have demonstrated that Tyr^1, Phe^3/Trp^3 and the C-terminal amidated Phe are essential pharmacophore elements, required for the for μ-opioid receptor recognition. Our earlier structure-activity studies of endomorphins resulted in very promising analogues using dimethyltyrosine (Dmt), alicyclic β-amino acids (2-aminocyclopentanecarboxylic acid (ACPC), 2-aminocyclohexanecarboxylic acid (ACHC)), para halogenated Phe-s or βMePhe isomers. In all cases one amino acid substitution was used [2,3]. In this presentation, we report on the synthesis and structure-activity study of new endomorphin analogues, which were obtained as a result of systematic substitutions of natural amino acids with Dmt, *cis*-(1*S*,2*R*)ACHC/*cis*-(1*R*,2*S*)ACHC, (2*R*,3*R*)βMePhe/ (2*S*,3*S*)βMePhe and pFPhe in endomorphins (EMs). Two or three unnatural amino acids were used for substitution in the new analogues. The proteolytic stability of the new analogs was investigated in rat brain homogenate [4]. Structure activity studies were done using NMR spectroscopy.

Results and Discussion

The synthesis of 14 new peptide analogues was performed by manual solid phase technique using Boc-protected amino acids and MBHA resin to obtain C-terminal amides. Racemic Boc-*cis*(1*S*,2*R*)ACHC/(1*R*,2*S*)ACHC in the position 2, and Boc-(2S,3S)βMePhe/ (2R,3R)βMePhe (*erythro*-βMePhe) in position 4 were incorporated into the diastereomeric peptides. The peptides were purified by column chromatography and RP-HPLC. Dmt and pFPhe were also introduced in the positions 1 and 4, respectively. The purified peptides were hydrolyzed to obtain amino acid mixtures and the configurations of the ACHC and βMePhe were determined by chiral TLC. The biological potencies of these peptide analogues were evaluated in radioligand binding assays in rat brain membrane homogenate (Table 1), followed by the determination of agonist/antagonist properties using ligand stimulated [^{35}S]GTPγS functional assays. Substitution of Tyr with Dmt in the opioid peptides gave more potent but less selective analogues compared to the parent peptides. Endomorphins containing Dmt in position 1 are more lipophilic compounds, on the other hand the phenolic group in the Dmt is less acidic. (1S2R) ACHC was used as a proline mimetic. Unnatural Phe analogues (βMePhe or pFPhe) in position 4 yielded compounds with higher potencies compared to the parent peptides. The half-life of peptide analogues was investigated *in vitro* in rat brain homogenate and the incorporation of *cis*-(1S, 2R) ACHC in the EMs resulted in compounds which are very stable against proteolytic enzymes. Combined application of Dmt^1, *cis*-(1*S*, 2R) $ACHC^2$ and $pFPhe^4$ resulted in the most potent analogue (Dmt-(1S, 2R) ACHC-Phe-pFPhe-NH_2). Furthermore, this compound was found to be very active in the [^{35}S] GTPγS functional binding assays and its stability is high in rat brain preparation (half life: >20 hours). These modifications were designed to diminish *cis/trans* isomerisation of the amide bond between Tyr and (1S, 2R) ACHC. The population of χ_1 rotamers (gauche-, trans and gauche+) of the aromatic side chains was calculated from the measured $^3J_{H\alpha\text{-}H\beta}$ and $^3J_{H\alpha C\gamma}$ coupling constants and were found to be in perfect agreement with a recently proposed possible bioactive structure model of μ-opioid peptides [5].

Table 1. Opioid receptor binding affinities and selectivities of endomorphin analogues, measured in rat brain membrane preparation

Peptide	*Inhibitory constants*		*Selectivity*
	K_i^{μ} *(nM)*[a]	K_i^{δ} *(nM)*[b]	K_i^{δ}/K^{μ}
Tyr-Pro-Trp-Phe-NH_2	1.6 ± 0.3	4169 ± 881	2605
Tyr-(1*S*,2*R*)ACHC-Trp-(2*S*,3*S*)βMePhe-NH_2	4.2 ± 0.9	1444 ±182	343
Tyr-(1*S*,2*R*)ACHC-Trp-(2*R*,3*R*)βMePhe-NH_2	34.6 ± 3.5	3364 ± 1093	97
Dmt-(1*S*,2*R*)ACHC-Trp-(2*S*,3*S*)βMePhe-NH_2	0.93 ± 0.07	123 ± 17	132
Dmt-(1*S*,2*R*)ACHC-Trp-(2*R*,3*R*)βMePhe-NH_2	4.11 ± 0.7	287 ± 55	69
Tyr-(1*S*,2*R*)ACHC-Trp-pFPhe-NH_2	3.2 ± 0.5	571 ± 92	178
Tyr-(1*R*,2*S*)ACHC-Trp-pFPhe-NH_2	143.1 ± 5.9	7823 ± 1039	54
Dmt-(1*S*,2*R*)ACHC-Trp-pFPhe-NH_2	11.1 ± 2.0	2636 ± 670	237
Tyr-Pro-Phe-Phe-NH_2	1.35 ± 0.2	8771 ± 1316	6497
Tyr-(1*S*,2*R*)ACHC-Phe-(2*S*,3*S*)βMePhe-NH_2	0.82 ± 0.2	661 ± 43	816
Tyr-(1*S*,2*R*)ACHC-Phe-(2*R*,3*R*)βMePhe-NH_2	33.9 ± 6.0	1268 ± 33	37
Dmt-(1*S*,2*R*)ACHC-Phe-(2*S*,3*S*)βMePhe-NH_2	0.47 ± 0.06	142 ± 8	302
Dmt-(1*S*,2*R*)ACHC-Phe-(2*R*,3*R*)βMePhe-NH_2	9.7 ± 1.3	198 ± 48	20
Tyr-(1*S*,2*R*)ACHC-Phe-pFPhe-NH_2	1.5 ± 0.3	366 ± 61	244
Tyr-(1*R*,2*S*)ACHC-Phe-pFPhe-NH_2	2.8 ± 0.5	689 ± 98	246
Dmt-(1*S*,2*R*)ACHC-Phe-pFPhe-NH_2	0.13 ± 0.02	96 ±9	738

Acknowledgments
This work was supported by Hungarian OTKA-73081 and European FP6 (LSHS-CT-2006-037733) grants.

References

1. Zadina, J.E., Hackler, L., Ge, L.J., Kastin, A.J. *Nature* **386**, 499-502 (1997).
2. Keresztes, A., Szücs, M., Borics, A., et al. *J. Med. Chem.* **51**, 4270-4279 (2008).
3. Keresztes, A., Borics, A., Tóth, G. *ChemMedChem* **5,** 1176-1196 (2010).
4. Tömböly, C., Péter, A., Tóth, G. *Peptides* **23,** 1573-1580 (2002).
5. Borics, A, Tóth, G. *J. Mol. Graph. Mod.* **28**, 495-505 (2010).

Proceedings of the 31st European Peptide Symposium
Michal Lebl, Morten Meldal, Knud J. Jensen, Thomas Hoeg-Jensen (Editors)
European Peptide Society, 2010

A Neuropeptidomics Study of the Bovine Hypothalamus Reveals Novel Endogenous Peptides and Processing Pathways

Michelle L. Colgrave[1]*, Li Xi[1,2], Sigrid Lehnert[1], Traute Flatscher-Bader[3,4], Henrik Wadensten[5], Anna Nilsson[5], Per E. Andren[5], and Gene Wijffels[1]

[1]CSIRO Livestock Industries, 306 Carmody Rd, St Lucia, QLD 4067, Australia; [2]College of Veterinary Medicine, Northwest A&F University, Xi'an, 712100, China; [3]CRC for Beef Genetic Technologies, C.J. Hawkins Homestead, University of New England, Armidale, New South Wales, 2351, Australia; [4]The University of Queensland, School of Animals Studies, Gatton, QLD 4343, Australia; [5]Department of Pharmaceutical Biosciences, Medical Mass Spectrometry, Biomedical Centre, P.O. Box 583, Uppsala University, SE-75123, Uppsala, Sweden

Introduction

Mass spectrometry (MS) has been adopted for neuropeptide research because of its ability to rapidly and sensitively detect, characterize and quantify neuropeptides. Peptidomics is the term coined to describe the field that deals with the comprehensive qualitative and quantitative analysis of peptides in biological samples [1]. While peptidomic studies hold considerable promise for the discovery of new bioactive molecules and the elucidation of biochemical regulatory networks, there are a number of challenges that remain to be resolved. The low concentration at which many endogenous peptides exist and are active is compounded by the vast array of proteins present in biological samples at much higher concentrations. Furthermore, neuropeptide processing *in vivo* begins with cleavage by prohormone convertases at dibasic sites and subsequent trimming of the basic residues by carboxypeptidase D/E. The end result is peptides of small size that lack basic residues. These peptides may be difficult to ionize and/or display lower charge states in the mass spectrometer. In the current study, we have evaluated a range of data acquisition strategies in the investigation of snap-frozen bovine hypothalamus samples.

Results and Discussion

In order to maximize the number of peptide identifications, we employed six parallel acquisition strategies. These are detailed in Table 1 as Strategies A-F. Not surprisingly, the highest number of identifications was achieved when twice the amount of sample was loaded onto the HPLC column (Strategy F: 104 peptides).

The use of the "Smart Exit" software feature has recently found utility in typical proteomics experiments [2,3]. This feature works by monitoring the quality of the MS/MS spectra "on-the-fly" and, upon fulfilling the criteria for a "good" spectrum, exits its acquisition thus shortening the information-dependent acquisition (IDA) cycle time and enabling more spectra to be acquired in the LC-MS timeframe. We used the SmartExit software feature that enabled the acquisition of MS/MS spectra of varying quality – in effect we achieved greater signal-to-noise (S/N) ratios for the fragment ions giving rise to higher scoring peptide matches, but at the detriment of cycle time. The method utilizing the SmartExit software functionality in which the SmartExit setting was increased to the maximum value (20) to obtain the highest quality data for each MS/MS spectrum gave the next highest number of peptide identifications (Strategy E: 74 peptides). In comparison, the number of identifications from the acquisition strategy using a 'normal' SmartExit setting (Strategy A: SmartExit 2) was lower (63 peptides). Surprisingly, the use of a medium setting (6) resulted in a decreased number of identifications (53 peptides). This can be explained by the lower number of precursors selected for MS/MS (25% less). These data indicated that the advantage of increasing spectral quality, through use of the SmartExit functionality, was only justified when using the highest setting.

We also employed the dynamic background subtraction (DBS) software feature, which enables the selection of relatively minor precursor ions in the presence of high background conditions. In a typical LC-MS/MS analysis, there are a large number of potential candidate ions at any given point in time. In a standard IDA experiment, the most intense ions are selected for MS/MS. Despite being abundant in nature, these ions might be from the

Table 1. Identification of neuropeptides using six acquisition strategies. The conditions used for data analysis are shown in the top half of the table, while the results obtained are detailed in the bottom half of the table. A total of 118 neuropeptides were identified in the stabilized samples. DBS refers to the Dynamic Background Subtraction software feature and SmartExit refers to the quality of the MS/MS spectra obtained where the value may be 1-20.

Strategy	*A*	*B*	*C*	*D*	*E*	*F*
Injection volume (µl)	5	5	5	5	5	10
Precursor *z*	2-5	2-5	2-5	1-3	2-5	2-5
DBS	Off	Off	On	On	Off	Off
SmartExit	2	6	2	2	20	6
No. neuropeptide ID's	63	53	53	54	74	104
% of total (118)	53	45	45	45	62	87
No. spectra acquired	973	742	423	877	900	1210
% spectra identified	57	55	68	36	68	76

background, i.e., present for the duration of the LC-MS analysis, or they may be from a peptide derived from a highly abundant protein. Many of the less intense ions may avoid selection for MS/MS acquisition. The DBS software feature measures the intensity of each ion over several scans and triggers MS/MS acquisition based at the point in time at which they are rising most quickly in intensity. The use of the Dynamic Background Subtraction (DBS) feature resulted in a decreased number of peptide identifications (Strategy B: 53 for precursors with charge state 2-5; 54 for precursors with charge state 1-3). The DBS-triggered datasets of multiply charged precursors showed a much lower number of precursors selected for MS/MS (approximately half of the number selected in non-DBS runs). For the DBS-triggered datasets in which singly charged precursors were included (Strategy D), the number of MS/MS spectra acquired was roughly equivalent to that obtained by Strategies A and E, but the percentage of identified spectra dramatically decreased.

The acquisition strategy used, specifically focusing on acquisition of MS/MS spectra of singly to triply charged precursors rather than precursors of charge +2 to +5 (as is used in our traditional proteomic workflows) did not lead to a significant increase in the number of neuropeptide identifications despite the increased number of spectra acquired. Manual inspection of the spectra provided by Strategy D proved that the vast majority of singly charged precursors selected were not peptidic in nature and/or yielded poor MS/MS spectra.

In conclusion, the optimization of the acquisition conditions and the database searching strategy resulted in increases in the number of neuropeptides identified (up to 2-fold increase) with >75% of spectra identified.

Acknowledgments

We thank Alun Jones and the Molecular and Cellular Proteomics Facility at the University of Queensland Institute for Molecular Bioscience for access to mass spectrometry instrumentation. We thank the Cooperative Research Centre for Beef Genetic Technologies for making tissue samples available to this project, and the Kilcoy Pastoral Company for their cooperation in sample collections. Professor Michael D'Occhio developed the bovine hypothalamus sampling protocol and Dr. Ainu Suhaimi was involved in bovine hypothalamus sample collection.

References

1. Schulz-Knappe, P., et al. *Comb. Chem. High Throughput Screen.* **4**, 207-217 (2001).
2. Zhu, M., et al. *J. of Proteomics* **73**, 790-805 (2010).
3. Dwivedi, R.C., et al. *J. Proteome Res.* **9**, 1144-1149 (2010).

Proceedings of the 31st European Peptide Symposium
Michal Lebl, Morten Meldal, Knud J. Jensen, Thomas Hoeg-Jensen (Editors)
European Peptide Society, 2010

Synthesis, Conformational Analysis, and Biological Activity of [Aza-3-indoylgly^4] GHRP-6 as an Aza-Tryptophan Analog of Growth Hormone Releasing Peptide-6

Caroline Proulx[1], David Sabatino[1], Petra Pohankova[2], Huy Ong[2], and William D. Lubell[1]

[1]Département de Chimie, Université de Montréal, C.P. 6128, Succursale Centre-Ville, Montréal, Québec, H3C 3J7, Canada; [2]Faculté de Pharmacie, Université de Montréal, C.P. 6128, Succursale Centre-Ville, Montréal, Québec, H3C 3J7, Canada

Introduction

Peptide mimics in which the alpha-carbon of one or more amino acid residues has been substituted by a nitrogen atom are called azapeptides [1]. The carbon to nitrogen exchange may induce β-turn formation by constraining both the phi (ϕ) and psi (ψ) dihedral angles, as respective consequences of the lone pair-lone pair repulsion between the two adjacent nitrogen atoms and replacement of an amide bond by urea functionality [2]. The aza-phenylalanine^4 analog of growth hormone releasing peptide-6 (GHRP-6, His-D-Trp-Ala-Trp-D-Phe-Lys-NH_2) has shown selectivity for the CD36 over the GHS-R1a receptor. In an effort towards better mimicking the Trp^4 residue while preserving the conformational bias induced by the aza-amino acid, the syntheses of [azaTrp^4]- and [aza-3-indoylgly^4]GHRP-6 were pursued [3,4].

Results and Discussion

Attempts to synthesize azaTrp-containing peptide met with loss of the indolylmethyl moiety upon treating the resin with TFA during resin cleavage [4]. On the other hand, [azaPhe^4]GHRP-6 was stable and displayed a circular dichroism (CD) signature in water, which was characteristic of a β turn, in contrast to the random coil CD curve displayed by the parent sequence (Figure 1) [5]. Moreover, relative to GHRP-6, [azaPhe^4]GHRP-6 maintained affinity to the CD36 receptor, with a 1000 fold loss of affinity towards the GHS-R1a receptor. The synthesis of [aza-3-indoylgly^4]GHRP-6 (6) was accomplished by submonomer azapeptide synthesis [5], featuring regioselective *N*-arylation of resin-bound semicarbazone 3 with *N*-Boc-3-iodoindole (Scheme 1) [3]. Tolerant to the acidic conditions used for resin cleavage, the aza-3-indoylglycine residue may serve as a stable azaTrp surrogate.

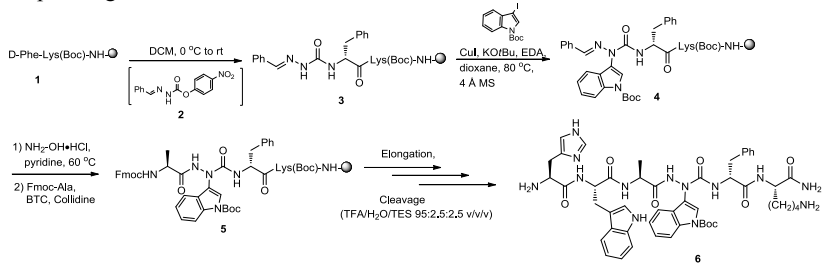

Scheme 1. Synthesis of [aza-3-indoylgly^4]GHRP-6.

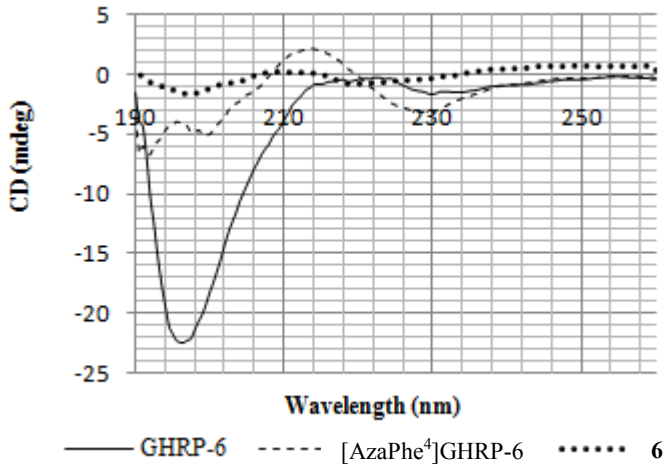

*Fig. 1. Circular dichroism spectra of [azaPhe^4]GHRP-6, [aza-3-indoylgly^4]GHRP-6 (**6**), and GHRP-6 in water.*

The evaluation of the biological activity of azapeptide **6** revealed a 10 fold loss of binding affinity towards the CD36 receptor, in spite of exhibiting a CD signature suggestive of a β turn, with negative maxima at 230 and 190 nm and a positive maximum at 215 nm. Although the indolyl side chain of the Trp^4 residue of the GHRP-6 sequence was maintained in [aza-3-indoylgly^4]GHRP-6, the spacial alignment and conformational constraints imposed by this aza-arylglycine residue appear to disfavor binding to the CD36 receptor.

Acknowledgments
The authors thank the Natural Sciences and Engineering Research Council of Canada and Boehringer Ingelheim for financial support.

References

1. Gante, J. *Synthesis* 405 (1989).
2. (a) André, F., Boussard, G., Bayeul, D., Didierjean, C., Aubry, A., Marraud, M. *J. Peptide Res.* **49**, 556-562 (1997); (b) André, F., Vicherat, A., Boussard, G., Aubry, A., Marraud, M. *J. Peptide Res.* **50**, 372-381 (1997).
3. Proulx, C., Lubell, W.D. *Org. Lett.* **12**, 2916-2919 (2010).
4. Boeglin, D., Lubell, W.D. *J. Comb. Chem.* **7**, 864-878 (2005).
5. Sabatino, D., Proulx, C., Klocek, S., Bourguet, C.B., Boeglin, D., Ong, H., Lubell, W.D. *Org. Lett.* **11**, 3650 (2009).

Proceedings of the 31st European Peptide Symposium
Michal Lebl, Morten Meldal, Knud J. Jensen, Thomas Hoeg-Jensen (Editors)
European Peptide Society, 2010

N^{α}-Linked Homodimers of the Kinin B1 Receptor Antagonist R-715

Witold A. Neugebauer[1], Martin Savard[1], Klaus Klarskov, and Fernand Gobeil Jr

Department of Pharmacology, Université de Sherbrooke, Sherbrooke, J1H 5N4, Québec, Canada; E-mail: witold.neugebauer@usherbrooke.ca (WN); fernand.gobeil@usherbrooke.ca (FG); [1]These authors contributed equally to this work

Introduction

The kinin B1 receptor (B1R) may play an important role in pathological conditions. We previously developed a highly potent and selective kinin B1R antagonist, R-715 (Ac-Lys-[D-βNal[7], Ile[8]]desArg[9]-bradykinin) [1,2]. However, R-715 is only partially resistant against enzyme degradation, which may explain its relatively short half life in vivo. It is contemplated that covalent peptide dimers may improve stability [3-7], circulating half-life and make more potent therapeutics than monomers. With this in mind, we 1) designed and synthesized on solid phase *N*α-linked homodimers of R-715 comprising linkers with different acyl-chain lengths such as 6 (adipoyl) (NG2049), 8 (suberyl) (NG2035), 10 (sebacoyl) (NG2050) and 12 carbons (dodecanedioyl) (NG2051) and 2) determined their antagonistic potencies (pA_2 value) using rabbit aortic strip contraction assays.

Material and Methods

Peptide synthesis: Peptides (Figure 1) were synthesized using Boc chemistry on ABI/Applied Biosystems 430A Peptide Synthesizer starting with Boc-Ile-Merrifield resin. Step by step coupling of Boc amino acids were performed in DCM/1-methyl-2-pyrolidinone using DCC/HOBT as coupling agents. Boc deprotection was performed with 64% TFA in DCM. TFA salts were neutralized with DIPEA in DCM. At the last step, peptides were bridged at their Nα-Lys[1] amino-terminal function with diacid dichlorides (adipoyl-, suberyl-, sebacoyl- and dodecanedioyl-) in DCM in presence of DIPEA. Final peptides and protective group cleavage were performed by liquefied anhydrous HF treatment. Peptides salts (with resin) were precipitated in anhydrous ethyl ether, filtered, dissolved in 25% Acetic acid and lyophilized. The crude peptides were finally purified by C18 column chromatography in acetonitrile gradient in water with 0.1% TFA. Peptide identities were confirmed by MALDI mass spectrometry (see Table 1) and their chromatographic purity verified by analytical HPLC.

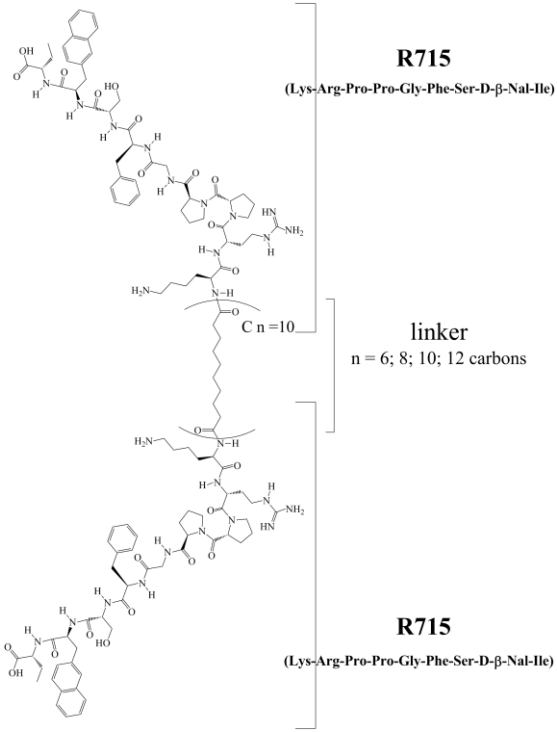

Fig. 1. Structures of B1R antagonist R-715 homodimers.

Organ bath: Rabbit aortas from male New Zealand rabbits (1.5-2.0 kg) were used. Tissue preparation and experimental

Table 1. Analytical data and antagonistic activities of dimer derivatives of R-715

Compound	*Linker (n of Carbons)*	*Calculated m.w. (Da)*	*Mass found in MALDI-MS (m / z)*	*Bioassay* RbA pA_2*
R-715	none	1140.29	1140.48	8.42 ± 0.12
NG2049	Adipoyl (n = 6)	2306.70	2307.86	8.43 ± 0.17
NG2035	Suberyl (n = 8)	2334.76	2335.83	8.66 ± 0.19
NG2050	Sebacoyl (n = 10)	2362.81	2362.97	7.69 ± 0.14
NG2051	Dodecanedioyl (n = 12)	2390.86	2390.61	7.75 ± 0.12

**Values are means ± S.E.M of 3-4 experiments. Inhibition of the contraction of the rabbit aorta (RbA) induced by the kinin B1R agonist desArg^9-bradykinin (0.5 μM)*

protocol for vascular contractility bioassays were performed as described [1,2]. The apparent affinity of each antagonist was evaluated and expressed in terms of pA_2 (the negative log of the molar concentration of an antagonist that makes it necessary to double the concentration of the agonist desArg^9-bradykinin needed to elicit the original submaximal response).

Results and Discussion

Our results showed that all dimeric analogues of R-715 (Figure 1) were capable of blocking the contractile responses to the kinin B1R agonist desArg^9-bradykinin in rabbit aortic strips, although not to the same extent (Table 1). In comparison with the parent monomer antagonist R-715 (pA_2: 8.40±0.12), the peptide NG2049 (pA_2: 8.43±0.17) and NG2035 (pA_2: 8.66±0.19) maintained similar inhibitory effects while peptides NG2050 (pA2: 7.69±0.14) and NG2051 (pA_2: 7.75±0.12) showed reduced potencies. We concluded that the optimum length of spacer arms of *N*-terminal dimeric R-715 analogues for B1R antagonism is with acyl chains of 6 and 8 carbons, which corresponds to a maximal length of 7.5 and 9.8 Å. Further studies are needed to test whether the strategy of R-715 dimerization translates to greater potency and long-lasting in vivo activity.

Acknowledgments

M. Savard is a former recipient of a fellowship award from the Fonds de la recherche en santé du Québec (FRSQ). F. Gobeil is a recipient of a Junior 2 scholarship from the FRSQ, a researcher of the Canada Foundation for Innovation, and a member of the FRSQ-funded Centre de recherche clinique Étienne-Le Bel. Research reported in this study was supported by Institutional funds and a grant from the Canadian Institute of Health Research (CIHR).

References

1. Gobeil, F. jr., et al. *Hypertension* **28**, 833-839 (1996).
2. Gobeil, F. jr., et al. *Hypertension* **33**, 823-829 (1999).
3. Cheronis, J.C., et al. *J. Med. Chem.* **35**, 1563-1572 (1992).
4. Cheronis, J.C., et al. *J. Med. Chem.* **37**, 348-355 (1994).
5. Gera, L., et al. *Immunopharmacology* **33**, 178-182 (1996).
6. Howl, J., et al. *FASEB J.* **11**, 582-590 (1997).
7. Daffix, I., et al. *J. Peptide Res.* **52**, 1-14 (1998).

Proceedings of the 31st European Peptide Symposium
Michal Lebl, Morten Meldal, Knud J. Jensen, Thomas Hoeg-Jensen (Editors)
European Peptide Society, 2010

Identification of a New Citrullinated Epitope on Filaggrin for the Early Diagnosis of Rheumatoid Arthritis

Fruzsina Babos[1,2], Eszter Szarka[1], Ádám Bartos[2], György Nagy[3], Gabriella Sármay[1,4], Anna Magyar[2], and Ferenc Hudecz[1,2]

[1]Department of Immunology, Eötvös Loránd University, Budapest, Hungary; [2]HAS-ELTE Research Group of Peptide Chemistry, Budapest, Hungary; [3]Buda Hospital of Hospitaller Brothers of St. John, Budapest, Hungary; [4]Immunology Research Group of the Hungarian Academy of Sciences at ELTE, Budapest, Hungary

Introduction

Anti-citrullinated protein antibodies (ACPA) are sensitive and specific markers for diagnosis and prognosis in Rheumatoid Arthritis (RA). Citrullination is a post-translational modification of arginine by deimination, induced by peptidylarginine deiminase (PAD). It is a physiologically occurring phenomenon during apoptosis, inflammation or keratinization. Citrullination has been observed in different synovial proteins, including fibrinogen, vimentin [1] and collagen. Antibodies specific for cyclic citrullinated filaggrin [2] peptide (CCP1) were detected in RA sera and anti-CCP positivity is widely used for diagnostic purposes. However, to determine the ACPA-reacting epitopes on vimentin and new epitopes on filaggrin would be useful in the diagnosis of anti-CCP3 seronegative patients. Our aim was to develop new tools for the detection of ACPA and thus for the early diagnosis of RA by the use of clearly defined epitopes on filaggrin and vimentin.

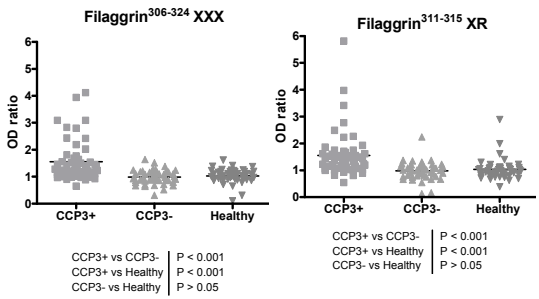

Fig. 1. Multipin ELISA, measuring IgG plus IgM.

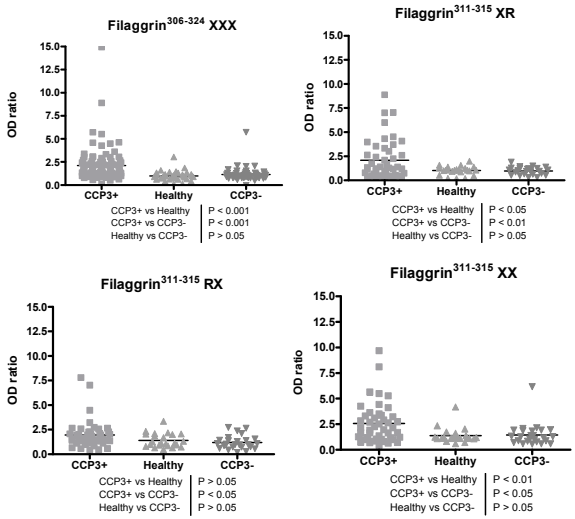

Fig. 2. Multipin ELISA, measuring IgG.

Results and Discussion

First, we used conventional solid-phase peptide synthesis, carried out on „MULTIPIN NCP" non-cleavable kit (Mimetopes, Australia). Citrulline containing peptides and the unmodified counterparts containing arginine were synthesized on the pins in order to compare their respective reactivities. We used these peptides-on-pins in an indirect ELISA and ACPAs were determined in the sera of RA and non-RA patients using anti-IgG plus IgM secondary antibodies (Figure 1) and later IgG

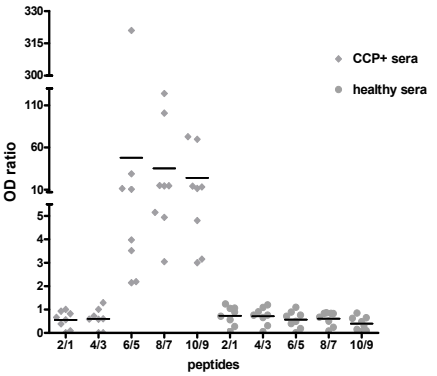

Fig. 3. Indirect ELISA with biotinylated peptides, pre-coated with NeutrAvidin.

specific secondary antibodies (Figure 2).

Comparing the short sequences of filaggrin and vimentin, we have found that the 5-mer filaggrin-peptide was recognized by the RA sera with sensitivity and specificity comparable with the currently used tests.

We detected lower sensitivity and specificity than in our first test. However, OD ratios of all peptides have shown a significant correlation with the MCV (mutated citrullinated vimentin) titer, which is associated with activity of disease. On the other hand, OD ratios did not show correlation with the CCP3 titer. These data suggest that the short citrulline containing filaggrin peptide (Filaggrin$^{311\text{-}315}$ XX) might be a useful biomarker for RA.

Selected peptides (Table 1) were synthesised manually by SPPS, according to Fmoc/^{t}Bu strategy using Rink-Amide MBHA or MBHA resin. For the coupling Fmoc-amino acid : HOBt : DIC = 2 : 2 : 2 activation was used. C- or N-terminally biotinylated forms were made using biotin, biotinyl-6-aminohexanoic acid and 4,7,10-trioxa-1,13-tridecanediamino succinic acid linker (Ttds) [3]. The ratio of the coupling reagents was biotin : HOBt : PyBOP : DIEA = 3 : 3 : 3 : 6. We coupled the Fmoc-Ttds as a protected amino acid. The crude products were purified by reversed-phase chromatography. The structure of the peptides was proved by electron spray ionization (ESI) mass spectrometry. We have used these peptides in an indirect ELISA, on NeutrAvidin pre-coated plates, the reaction was detected by anti IgG-HRP (Figure 3).

The CCP3+ serum samples specifically recognized the C terminally biotinylated 5-mer filaggrin peptide, while showed no reaction with the N-terminally biotinylated ones.

Table 1. Structures of studied peptides

1	biotin-6-amino-hexanoyl- Filaggrin$^{311\text{-}315}$ RR -NH_2
2	biotin-6-amino-hexanoyl- Filaggrin$^{311\text{-}315}$ XR -NH_2
3	biotinyl- Filaggrin$^{311\text{-}315}$ RR -NH_2
4	biotinyl- Filaggrin$^{311\text{-}315}$ XR -NH_2
5	Ac- Filaggrin$^{311\text{-}315}$ RR -K(biotin-6-amino-hexanoyl)-NH_2
6	Ac- Filaggrin$^{311\text{-}315}$ XR -K(biotin-6-amino-hexanoyl)-NH_2
7	Ac- Filaggrin$^{311\text{-}315}$ RR -K(Ttds-biotin)-NH_2
8	Ac- Filaggrin$^{311\text{-}315}$ XR -K(Ttds-biotin)-NH_2
9	Ac- Filaggrin$^{311\text{-}315}$ RR -Ttds-K(biotin-6-amino-hexanoyl)-NH_2
10	Ac- Filaggrin$^{311\text{-}315}$ XR -Ttds-K(biotin-6-amino-hexanoyl)-NH_2

As a conclusion we can say that the short Filaggrin$^{311\text{-}315}$ XX peptide and Multipin ELISA may be a useful addition to the array of diagnostic tools of early RA. Our results were validated by conventional indirect ELISA, also showing that only the C-terminal biotinylation can be applied for the 5-mer filaggrin-peptide.

Acknowledgments

We thank to EPS for travel grant. This work was supported by National Office for Research and Technology (RET-06/2006, GVOP-3.1.1.-2004-05-0183/3.0, OTKA-NKTH CK_80689), Hungary.

References

1. Vossenaar, E.R., Despres, N., Lapointe, E., van der Heijden, A., Lora, M., Senshu, T., Van Venrooij, W.J., Menard, H.A. *Arthritis Res. Ther*. **6**(2), 86-89 (2004).
2. Schellekens, G.A., de Jong, B.A.W., van den Hoogen, F.H.J., van de Putte, L.B.A., Van Venrooij, W.J. *J. Clin. Invest.* **101**, 273-281 (1998).
3. Bartos, Á., Uray, K., Hudecz, F. *Peptide Science* **92,** 110-115 (2009).

Proceedings of the 31st European Peptide Symposium
Michal Lebl, Morten Meldal, Knud J. Jensen, Thomas Hoeg-Jensen (Editors)
European Peptide Society, 2010

4-Methylpseudoproline Analogues of Cyclolinopeptide A: Synthesis, Conformation and Biology

J. Katarzyńska[1], S. Jankowski[1], K. Huben[1], M. Zimecki[2], and J. Zabrocki[1,3]

[1]Institute of Organic Chemistry, Technical University of Lodz, Łódź, 90-924, Poland; [2]Institute of Immunology and Experimental Therapy, Polish Academy of Sciences, R. Weigla 12, Wrocław, 53-114, Poland; [3]Peptaderm Inc., Krakowskie Przedmieście 13, Warszawa, 00-071, Poland

Introduction

Pseudoprolines (ψpro), 1,3-oxazolidines and 1,3-thiazolidines derived from Ser, Thr or Cys, have been introduced by Mutter and coworkers [1]. They have been applied as a versatile tool in structure-activity relationship studies due to enhanced rate of *cis/trans* isomerisation, depending on stereochemistry and degree of substitution at the C-2 atom position of the proline ring.

4-Alkylpseudoprolines derived from α-alkyl-α-hydroxymethyl amino acids can be transformed into suitable pseudoproline (oxazolidine) unit [2]. The presence of alkyl substituent at the C-4 atom of the ring changes their chemical and conformational properties in comparison to pseudoprolines derived from serine or threonine.

Results and Discussion

Synthesis and conformational analysis of the short peptides containing (*R*)- and (*S*)-4-metylpsudoproline were reported previously [3]. Now we present synthesis, conformation and biological activity of new analogues of cyclolinopeptide A (CLA), containing 4-methylpseudoproline instead of proline residues in position 6 or 7. It is known that immunosuppressive activity of CLA, comparable with cyclosporine A, is connected to the presence of the tetrapeptide Pro-Pro-Phe-Phe fragment containing Pro-Pro *cis* amide bond [3].

Leu^1 - Val^2 - (*R*)-MeSer(ψpro)^3 - Pro^4 - Phe^5 - Phe^6 - Leu^7 - Ile^8 - Ile^9
Leu^1 - Val^2 - Pro^3- (*R*)-MeSer(ψpro)^4 - Phe^5 - Phe^6 - Leu^7 - Ile^8 - Ile^9
cyclo - (Leu^1 - Val^2 - (*R*)-MeSer(ψpro)^3 - Pro^4 - Phe^5 - Phe^6 - Leu^7 - Ile^8 - Ile^9) **7R**
cyclo - (Leu^1 - Val^2 - Pro^3 - (*R*)-MeSer(ψpro)^4 - Phe^5 - Phe^6 - Leu^7 - Ile^8 - Ile^9) **6R**
Leu^1 - Val^2 - (*S*)-MeSer(ψpro)^3 - Pro^4 - Phe^5 - Phe^6 - Leu^7 - Ile^8 - Ile^9
Leu^1 - Val^2 - Pro^3- (*S*)-MeSer(ψpro)^4 - Phe^5 - Phe^6 - Leu^7 - Ile^8 - Ile^9
cyclo - (Leu^1 - Val^2 - (*S*)-MeSer(ψpro)^3 - Pro^4 - Phe^5 - Phe^6 - Leu^7 - Ile^8 - Ile^9) **7S**
cyclo - (Leu^1 - Val^2 - Pro^3 - (*S*)-MeSer(ψpro)^4 - Phe^5 - Phe^6 - Leu^7 - Ile^8 - Ile^9) **6S**

The linear precursors of modified CLA analogues were prepared manually by standard solid-phase procedure "step by step" on Wang resin, using Fmoc group for N^{α}-amino protection and TBTU as a coupling reagent. *N*-9-Fluorenylmethyloxycarbonyl derivatives of 4-methylpseudoproline were obtained in good yield (~70%) by one pot cyclocondensation of the corresponding α-methylserine with formaldehyde and N-(9-fluorenylmethoxycarbonyloxy)succinimide in alkaline solution. The NH-group in 4-methylpseudoproline residue was acylated ("difficult coupling") by using BTC (*bis*-(trichlomethyl)carbonate) in the presence of collidine. The cyclization of linear precursors has been achieved in solution using EDC/HOBt as coupling reagents. Structures of all compounds were characterized by MS and NMR spectroscopy.

NMR-studies

The replacement of one or both Pro residues by 4-methylpseudoproline changed significantly the ^{1}H NMR spectra of **6R** and **7R** in comparison to that recorded for the unmodified CLA in $CDCl_3$ at 298 K and 700 MHz. All signals except signals of methyl groups are broad and unresolved. The presence of MeSer(ψpro) residue decreased the rate of the chemical exchange among conformers of similar energy, characteristic for CLA.

Broad NH signals spread within the region of 1.2 ppm could not be applied for the assignment based on COSY/TOCSY spectra.

Biology
The synthesized compounds were tested for their potential effects on mitogen - induced T- and B-cell proliferation in the mouse model with cyclosporine A (CsA) as a reference drug.

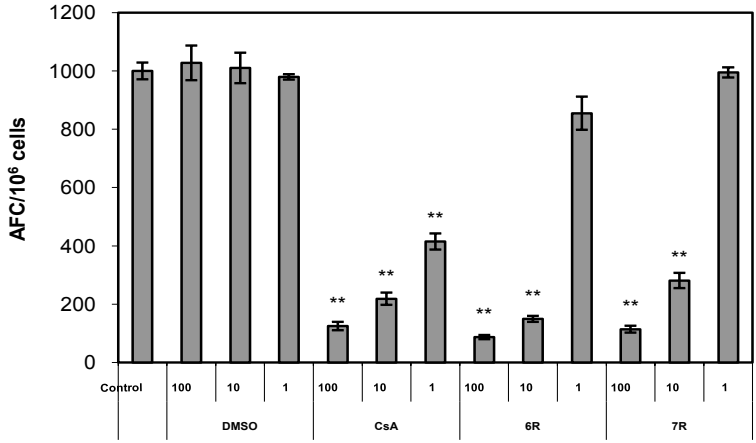

Fig.1. Effects of the peptides on the secondary, humoral immune response of mouse splenocytes to SRBC in vitro.

The results revealed strong, dose dependent inhibitory effects of both **6R** and **7R** compounds on the proliferation of splenocytes which were more pronounced in the case of **6R** and comparable at 10 and 100 μg/mL concentrations to these of CsA (data not shown). The inhibitory actions of the **6R** and **7R** compounds on PWM-induced cell proliferation followed the same pattern as described above for ConA-induced proliferation. The compounds were tested for their ability to suppress the humoral immune response *in vitro* at 1-100 μg/mL concentrations. The results shown in Figure 1 demonstrated that both peptides strongly inhibited the number of antibody-forming cells at concentrations of 10 and 100 μg/mL and these effects were comparable to the inhibitory action of CsA at this concentration range.

Activity of the **6S** and **7S** in comparison to **6R** and **7R** was smaller in similar tests (data not shown). Interestingly, the cytotoxic effect of all peptides with regard to mononuclear cells from human blood was comparable to that of CLA. The statistically significant inhibition of cell viability was observed only at 100-25 μg/mL concentration for **6R**.

Acknowledgments
Supported by Technical University of Lodz, grant DS-I18/12/2010.

References
1. Tuchscherer, G., Mutter, M. *Chimia* **55**, 306-313 (2001).
2. Katarzyńska, J., Jankowski, S., Huben, K., Leplawy, M.T., Zabrocki, J. In Benedetti, E., Pedone, C. (Eds) *Peptides 2002 (Proceedings of the 27th European Peptide Symposium)*, Italy, Napoli, 2002, p.160-161.
3. a) Siemion, I.Z., Pędyczak, A., Strug, I., Wieczorek, Z. *Arch. Immunol. Ther. Exp.* **42**, 459-465 (1994); b) Gaymes, T.J., Cebrat, M., Siemion, I.Z., Kay, J.E. *FEBS Lett.* **418**, 224-227 (1997); c) Benedetti, E., Padone, C. *J. Pept. Sci.* **11**, 268-272 (2005); d) Picur, B., Cebrat, M., Zabrocki, J., Siemion, I.Z. *J. Pept. Sci.* **12**, 569-574 (2006).

Proceedings of the 31st European Peptide Symposium
Michal Lebl, Morten Meldal, Knud J. Jensen, Thomas Hoeg-Jensen (Editors)
European Peptide Society, 2010

Design, Synthesis and Stability Studies of Potent Inhibitors of Pro-Protein Convertases (PCs)

Anna Kwiatkowska[1], Nicholas Chevalier[2], Roxane Desjardins[2], Frédéric Couture[2], François D'Anjou[2], Sophie Routhier[2], Christine Levesque[2], Yves Dory[2], Witold Neugebauer[2], and Robert Day[2]

[1]Faculty of Chemistry, University of Gdańsk, Sobieskiego 18, 80-952, Gdańsk, Poland;
[2]Institut de Pharmacologie de Sherbrooke, Faculté de médecine et des sciences de la santé 3001, 12e Avenue Nord Sherbrooke, Qc, J1H 5N4, Canada

Introduction

Pro-protein convertases (PCs) are a mammalian family of serine endoproteases responsible for post-translational processing of inactive precursors of many regulatory proteins. Seven structurally related PCs, known as furin, PACE4, PC1/3, PC2, PC4, PC5/6 and PC7 cleave various precursors at the motif (K/R)-$(X)_n$-(K/R)↓ [1]. Several important pathologies have been linked with PC-like activity such as cancer and viral and bacterial, infections. We have previously developed a relatively specific inhibitor of PACE4, PC5/6 and PC7 (Figure 1) [2]. The introduction of multi-Leu residues in the P8-P5 positions made the peptide more selective for these enzymes in comparison to Furin and PC2. This inhibitor has potent effects on cell proliferation and tumor progression, especially in cell models of prostate cancer [2]. However further stabilization of the structure is necessary for potential *in vivo* use.

Ac-**Leu-Leu-Leu-Leu-**Arg-Val-Lys-Arg-NH_2

Fig. 1. Structure of multi-Leu inhibitor.

Objectives

The aim of this work was to introduce a series of chemical modifications in the multi-Leu part of our potent PC inhibitor. Several approaches including the use of D-amino acids (D-Leu), unusual amino acids (Nle), and click chemistry have been used to improve the pharmacokinetic properties of the model peptide (Figure 2).

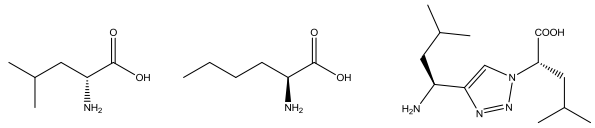

D-Leu Nle Leu1,4[1,2,3(triazole)]Leu

Fig. 2. Modifications of multi-Leu inhibitor.

We synthesized 14 new analogues of multi-Leu inhibitor: Ac-[D-Leu^1]LLLRVKR-NH_2 (**I**), Ac-L[D-Leu^2]LLRVKR-NH_2 (**II**), Ac-LL[D-Leu^3]LRVKR-NH_2 (**III**), Ac-LLL[D-Leu^4]RVKR-NH_2(**IV**), Ac-[D-Leu^1,D-Leu^2,D-Leu^3,D-Leu^4]RVKR-NH_2 (**V**), Ac-[Nle^1]LLLRVKRNH$_2$ (**VI**), Ac-L[Nle^2]LLRVKR-NH_2 (**VII**), Ac-LL[Nle^3]LRVKR-NH_2 (**VIII**), Ac-LLL[Nle^4]RVKR-NH_2(**IX**), Ac-[Nle^1,Nle^2,Nle^3,Nle^4]RVKR-NH_2 (**X**), Ac-L1,4[1,2,3(triazole)]LLLRVKR-NH_2 (**XI**), Ac-LL1,4[1,2,3(triazoil)]LLRVKR-NH_2 (**XII**), Ac-LLL1,4[1,2,3(triazoil)]LRVKR-NH_2 (**XIII**), Ac-L1,4[1,2,3(triazole)]LL1,4[1,2,3(triazole)]LRVKR-NH_2 (**XIV**) and determined their inhibitory potency against PCs. Furthermore, we characterized the stability and bioavailability of selected compounds.

Results and Discussion

Peptides were synthesized using standard Fmoc/tBu solid phase procedures. The analysis of inhibition was done in duplicate and is presented as the mean of three or more independent experiments (Figure 3). Quantitative data analysis was done using four-parameter logistic and real inhibition constants (K_i) were determined using the method and K_m values described previously [3].

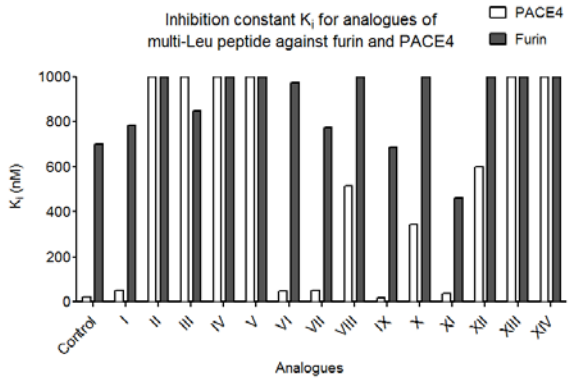

Fig. 3. Inhibition constants of multi-Leu analogues against furin and PACE4.

The proteolytic stability of peptides in absence or presence of prostate carcinoma cells (6000 DU145 cells) was determined by RP-HPLC analysis (Figure 4).

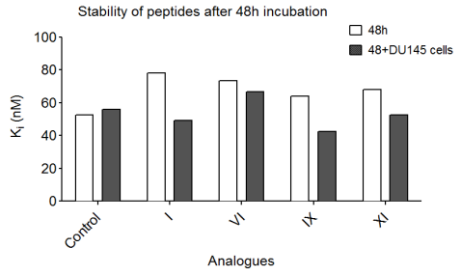

Fig. 4. Proteolytic stability of selected multi-Leu analogues.

Conclusion

Our results showed that position P6 (Leu^3) of inhibitors based on Ac-LLLLRVKR-NH_2 sequence is crucial for their activity. Modification of this position by D-Leu, Nle resulted in suppression of inhibitory potency. On the other hand, substitution of position P8 or introduction of triazole ring between P8 and P7 (Leu^1-Leu^2) did not affect peptide activity. On the other hand, replacement of the Leu^1 residue by D-Leu or Nle, Nle^4 substitution or introduction of triazole ring increase proteolytic stability of resulting peptides (in absence of prostate carcinoma cells), as compared to control multi-Leu peptide. In regard to cell penetration properties of two derivatives of multi-Leu, the FACS analysis showed that replacement of β-Ala by PEG8 fragment greatly decrease penetration properties of resulting peptide (FITC-PEG8-ML). It is worth it to emphasize, that results obtained from MTT analysis showed that the antiproliferative effect of PEG8-ML on DU145 is significantly lower than ML peptide suggesting a role of intracellular PACE4 in tumor proliferation.

Acknowledgments

This work is supported by research grants to RD from the Canadian Institutes of Health Research (CIHR) and the Ministère du Développement Économique, de l'Innovation et de l'Exportation (MDEIE) du Québec.

References

1. Fugère, M., Day, R. *Trends Pharmacol. Sci*. **26**, 294-301 (2005).
2. Day, R., Fugère, M., Neugebauer, W.A. *International patent application no. PCT/CA2009/000935*; Jan 14, 2010.
3. Fugère, M., Limperis, P.C., Beaulieu-Audy, V., et al. *J. Biol. Chem.* **277**, 7648-7656 (2002).

Proceedings of the 31st European Peptide Symposium
Michal Lebl, Morten Meldal, Knud J. Jensen, Thomas Hoeg-Jensen (Editors)
European Peptide Society, 2010

A New Class of Somatostatin Analogues with Antiproliferative Activity in Human Cancer Cells

Yuko Tsuda[1,2], Anna Miyazaki[1], Emiko Okuno[1], Isoko Kuriyama[3], Yoshiyuki Mizushina[2,3], and Hiromi Yoshida[2,3]

[1]Faculty of Pharmaceutical Sciences, Kobe Gakuin University, [2]Life Science Center for Cooperative Research, Kobe Gakuin University, Chuo-ku, Kobe, 650-8586, Japan; [3]Faculty of Nutrition, Kobe Gakuin University, Kobe, 651-2180, Japan

Introduction

Somatostatin [SS-14: H-Ala-Gly-c(Cys-Lys-Asn-Phe-Phe-Trp-Lys-Thr-Phe-Thr-Ser-Cys)-OH] suppresses growth of cancer cells. This lead to efforts to develop antitumor drugs based on SS-14. Despite efforts, difficulties exist on separating two specific functions: namely, the inhibitory action on tumor cell growth, and the regulatory effect on endocrine and exocrine systems. A derivative of SS-14, TT-232 [H-D-Phe-c(Cys-Tyr-D-Trp-Lys-Cys)-Thr-NH_2] [1], had potent antiproliferative activity in human cancer cells without antisecretory action mediated SS-14 receptors (SSTRs). Toward this goal, we prepared small peptides (YO-82-92, Figure 1) related to TT-232 and screened for their biological activities.

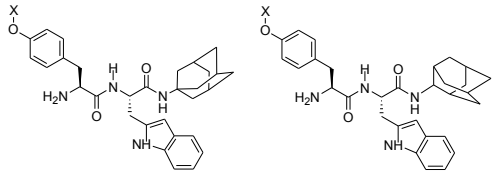

Fig. 1. Investigated system. *YO-84 X=BrZ* *YO-85 X=BrZ* *YO-89 X=Bzl* *YO-90 X=Bzl* *YO-91 X=Pic(Picolyl)* *YO-92 X=Pic(Picolyl)*

Results and Discussion

Protected peptides were synthesized by a solution method using Boc-chemistry. Final products were identified by MALDI-TOF mass spectrometry and elemental analyses. The SS-14 receptors binding activity was assessed using [^{125}I]Tyr^{11}-SS-14 and recombinant cells expressing SSTR1-SSTR5. Antiproliferative activity in human cancer cells and *in vitro* DNA polymerase inhibition by the compounds were evaluated by the MTT test and the dTTP incorporation to DNA template-primer such as poly(dA)oligo(dT), respectively. The effect of compounds on the cell cycle of HCT116 cells was analyzed by flow cytometry.

All compounds exhibited 1000-fold less binding activity toward SSTR1-SSTR5 than SS-14 (K_D = 0.034-0.9 nM). However, they suppressed the growth of human colon carcinoma cells (HCT116) (Figure 1). They showed stronger inhibition of cell growth in this cancer cell line than YO-13 and -14 [2]. Among the analogues tested, YO-85, in which hydroxyl group was masked with 2-bromobenzyloxycarbonyl (BrZ), had the most potent antiproliferative activity (<5% viability at 100 μM). The fraction of HCT116 cells in a specific cell cycle was measured after treatment with YO-85 (10 μM) for 24 h. The results were as follows: a 1.3-fold increase in cells in the S phase (22.8% to 30.0%), a 1.15-fold decrease in the population in the G1 phase, and the ratio of G2/M phase was nearly unchanged (26.6% to 25.7%). These data suggest that YO-85 induced cell cycle arrest at the S phase in human cancer. Furthermore, YO-85 inhibited rat DNA polymerase β (>95% inhibition at 100 μM). These findings suggested that small peptides related TT232 including YO-85 are a new class of somatostatin analogues exhibiting antiproliferative activity lacking interaction with SSTRs.

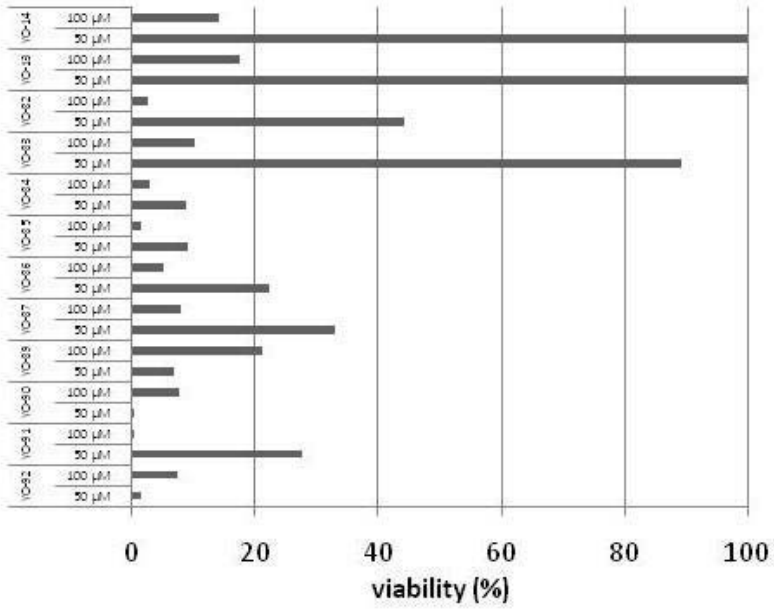

Fig. 1. Antiproliferative activity of YO-85-92 in HCT116 cells.

Acknowledgments
This work was supported by NEST "Academic Frontier" Project (2006) and a Grand-in-Aid for Scientific research (C) (No. 22590111) from NEXT.

References
1. Keri, G., et al. *Proc. Natl. Acad. Sci. U.S.A.* **93**, 12513-12518 (1996).
2. Miyazaki, A., et al. *J. Med. Chem.* **51**, 5121-5124 (2008).

Proceedings of the 31st European Peptide Symposium
Michal Lebl, Morten Meldal, Knud J. Jensen, Thomas Hoeg-Jensen (Editors)
European Peptide Society, 2010

Analogues of Trypsin Inhibitor SFTI-1 Modified in Absolutely Conserved P1' Position by Synthetic or Non-Proteinogenic Amino Acids

Rafał Łukajtis, Anna Łęgowska, Dawid Dębowski, Magdalena Wysocka, Adam Lesner, and Krzysztof Rolka
Faculty of Chemistry, University of Gdansk, Sobieskiego 18, Gdansk, 80-952, Poland

Introduction

The inhibitors of Bowman-Birk family are canonical inhibitors found in various plant sources. One of the most studied inhibitor of this family is trypsin inhibitor SFTI-1 isolated from sunflower seeds [1]. The amino acid sequences of BBIs indicate that Ser at P1′ and *cis*-Pro at P3′ are absolutely conserved in this family of inhibitors. In the case of SFTI-1, these amino acid residues are located in the positions 6 and 8, respectively (see Figure 1). There are several reports that substitution of Ser located in the P1′ position by Ala preserved trypsin inhibitory activity. On the other hand, according to Mc Bride, et al. [2], the interaction between Ser6 and Thr4 appears to be instrumental in projecting the P_1 side chain outwards for the interaction with the enzyme S_1 pocket. Bearing in mind the results of our previous studies on peptomeric SFTI-1 analogues and the limited experimental evidence supporting the statement about the role played by the inhibitor's P1′ position, we decided to focus our attention on the role of hydroxyl group of Ser6 in the inhibitor – enzyme interaction.

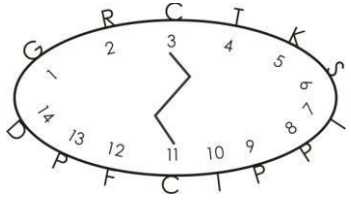

Fig. 1. Primary structure of SFTI-1.

Herein we report chemical synthesis and determination of α-chymotrypsin and trypsin inhibitory activity of a series of linear and monocyclic analogues of SFTI-1 modified in the P1′ position by Ala, Sar, Pro, Hyp, Hpr (L-homoproline), Hse (L-homoserine) and Nhse *(N*-(2-hydroxyethyl)glycine), Aze (L-azetidine-2-carboxylic acit) and Oic (L-octahydro-indole-2-carboxylic acid). Consequently, either Phe, Nphe or Lys were introduced in the substrate specificity P_1 position.

Results and Discussion

All 21 SFTI-1 analogues were synthesized by the solid phase method. Association equilibrium constants (K_a) of analogues synthesized with bovine β-trypsin and bovine α-chymotrypsin as well as their proteolytic stability were also determined. Details of synthetic methods and kinetic investigations were described in our previous work [3].

The Ka values determined for most active analogues modified in discussed position (Table 1) proved that absolutely conserved in BBI Ser residue located in the P1' position is not essential for inhibitory activity. Analogues with Ala, Hse, Pro, Hyp and Aze additionally modified in substrate specificity P1' position are able to inhibit both of experimental enzymes. On the other hand, the introduction of Hpr residue in discussed position decreased the Ka values of such modified analogues by at least three orders of magnitude whereas Oic yielded inactive analogues. Interestingly enough, introduction of the peptoid monomer Nhse in position P1' produced analogues 3 and 5 that were almost equipotent with that containing in this position naturally occurring Ser. This is the first evidence that the absolutely conserved Ser present in the BBI inhibitor's P1' position can be successfully replaced by a synthetic derivative. Studies on proteolytic resistance on these active monocyclic analogues of SFTI-1 displayed full proteolytic resistance of analogues 4 and 5 whereas other like 2, 3 and 13 with Phe5 and the non-proteinogenic Hse, Nhse and Aze in position 6 were slowly hydrolyzed by the cognate enzyme. It should be emphasized that linear analogues containing aforementioned modifications were inactive due to their high proteolytic susceptibility.

Table 1. Association equilibrium constants (K_a) with bovine α-chymotrypsin and bovine β-trypsin of SFTI-1 analogues modified in the P1 or/and P1′ position

Analogue	$K_a [M^{-1}]$	
	trypsin	*chymotrypsin*
SFTI-1 wild	$(1.1\pm0.2)\times10^{10}$	$(5.2\pm1.6)\times10^{6}$
SFTI-1	$(9.9\pm1.1)\times10^{9}$	$(4.9\pm1.4)\times10^{6}$
[Phe^5]SFTI-1		$(2.0\pm0.2)\times10^{9}$
[Nphe^5]SFTI-1		$(3.9\pm0.3)\times10^{8}$
[Phe^5,Ala^6]SFTI-1(**1**)		$(1.4\pm0.1)\times10^{8}$
[Phe^5,Hse^6]SFTI-1 (**2**)		$(2.1\pm0.2)\times10^{8}$
[Phe^5,Nhse^6]SFTI-1 (**3**)		$(3.4\pm0.6)\times10^{9}$
[Nphe^5,Hse^6]SFTI-1 **(4)**		$(4.0\pm0.4)\times10^{7}$
[Nphe^5,Nhse^6]SFTI-1 **(5)**		$(1.1\pm0.1)\times10^{8}$
[Pro^6]SFTI-1 **(6)**	$(9.3\pm0.5)\times10^{7}$	
[Phe^5,Pro^6]SFTI-1 **(7)**		$(5.4\pm0.6)\times10^{7}$
[Hyp^6]SFTI-1 **(8)**	$(6.4\pm0.2)\times10^{7}$	
[Phe^5,Hyp^6]SFTI-1 **(9)**		$(9.5\pm0.3)\times10^{7}$
[Hpr^6]SFTI-1 **(10)**	$(9.8\pm0.8)\times10^{4}$	
[Phe^5,Hpr^6]SFTI-1 **(11)**		$(7.9\pm0.3)\times10^{4}$
[Aze^6]SFTI-1 **(12)**	$(8.4\pm0.3)\times10^{7}$	
[Phe^5,Aze^6]SFTI-1 **(13)**		$(1.5\pm0.1)\times10^{8}$

Acknowledgments
This work was supported by Ministry of Science and Higher Education (Grant No. 2889/H03/2008/34).

References
1. Luckett, S., et al. *J. Biol. Chem.* **290**, 525-533 (1999).
2. McBride, J.D., et al. *Biopolymers* **66**, 79-92 (2002).
3 Łęgowska, A., et al. *Bioorg. Med. Chem*. **17**, 3302-3307 (2009).

Proceedings of the 31st European Peptide Symposium
Michal Lebl, Morten Meldal, Knud J. Jensen, Thomas Hoeg-Jensen (Editors)
European Peptide Society, 2010

The Influence of Disulfide Bridge of Trypsin Inhibitor SFTI-1 for Enzyme – Inhibitor Interaction

Anna Łęgowska, Dawid Dębowski, Magdalena Wysocka, Adam Lesner, and Krzysztof Rolka
Faculty of Chemistry, University of Gdansk, Sobieskiego 18, Gdansk, 80-952, Poland

Introduction

The trypsin inhibitor SFTI-1 isolated in 1999 from the sunflower seeds by Luckett, et al. [1] is currently the smallest naturally occurring peptidic proteinase inhibitor. This peptide displays the strongest trypsin inhibitory activity among the Bowman-Birk family of inhibitors. Owing to its small size (14 amino acid residues) and the well-defined structure (stabilized by head-to-tail cyclization and disulfide bridge), SFTI-1 has been chosen by several research teams to be a lead structure in the design of new inhibitors of serine proteinases. In order to investigate in detail the role of disulfide bridge in inhibitory activity, two series of SFTI-1 analogues were synthesized. In the first series of monocyclic SFTI-1 analogues, the disulfide bridge was formed by combination of Cys, Hcy, Pen and Nhcy (*N*-sulfanylethylglycine) introduced at positions 3 and/or 11, originally occupied by the Cys residues. In addition, in the substrate specificity P_1 position, peptoid monomers Nlys and Nphe, resembling proteinogenic Lys and Phe, respectively were introduced instead of Lys5. We have already proved [2] that both peptoid monomers are accommodated well in the substrate pockets of trypsin and chymotrypsin, respectively. In the second series of monocyclic SFTI-1 analogues, a ring formation was achieved *via* a ureido group incorporating the side-chain amino groups of L-2,3-diaminopropionic acid (Dap), L-2,4-diaminobutyric acid (Dab), Orn and Lys placed in positions originally occupied by Cys residues (Figure 1). The objective of the introduction of the set of dibasic amino acid residues starting with Dap (one CH_2 group) up to Lys (four CH_2 groups) in the positions 3 and 11 was the determination of the optimal size of the SFTI-1 cycle/ring for the inhibitor – trypsin interaction. In addition, unlike disulfide bridge, *N*-(ureidoethyl)-amide moieties are redox stable. This is a very important factor in case of introducing such peptides into the biological system.

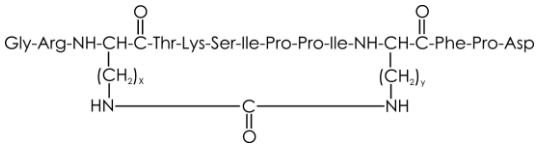

Fig. 1 Chemical structure of SFTI-1 analogues with carbonyl bridge, (x, y = 1 for Dap, 2 for Dab, 3 for Orn and 4 for Lys).

Results and Discussion

All SFTI-1 analogues were synthesized by the solid phase method. Peptoid monomers (Nphe, Nlys(Boc) and Nhcy(Trt)) were introduced into the peptide chain by the submonomeric approach [3]. The carbonyl bridge was introduced in two step procedure. Dde and *iv*Dde protecting groups were removed from side-chain amino functions of Orn, Lys, Dab and Dap, followed by reaction of bis(4-nitrophenyl) carbonate with free side-chain amino groups of peptidyl-resin [4]. Association equilibrium constants (K_a) of synthesized analogues with bovine β-trypsin and bovine α-chymotrypsin as well as their proteolytic stability were determined. Details on synthetic methods and kinetic investigations were described in our previous work [5].

The results presented in Table 1 clearly indicated that Pen and Nhcy were not acceptable at the position 3, yielding inactive analogues, whereas another residue (Cys11) could be substituted without any significant impact on the affinity towards both of experimental enzymes. On the other hand, elongation of the Cys3 side chain by

Table 1. Inhibitory activity of SFTI-1 analogues

Analogue	K_a [M^{-1}]	
	trypsin	*chymotrypsin*
SFTI-1 wild	$(1.1\pm0.2)\times10^{10}$	$(5.2\pm1.6)\times10^{6}$
SFTI-1	$(9.9\pm1.1)\times10^{9}$	$(4.9\pm1.4)\times10^{6}$
[Phe^{5}]SFTI-1		$(2.0\pm0.2)\times10^{9}$
[$Nlys^{5}$]SFTI-1	$(1.4\pm0.7)\times10^{8}$	
[$Nphe^{5}$]SFTI-1		$(3.9\pm0.3)\times10^{8}$
[$Nlys^{5}$,Pen^{3}]SFTI-1 (**1**)	$(8.37\pm0.16)\times10^{3}$	
[$Nlys^{5}$,Pen^{11}]SFTI-1 (**2**)	$(3.64\pm0.35)\times10^{8}$	
[$Nlys^{5}$,$Pen^{3,11}$]SFTI-1 (**3**)	$(1.04\pm0.03)\times10^{4}$	
[$Nphe^{5}$,Pen^{3}]SFTI-1 (**4**)		$(1.15\pm0.03)\times10^{5}$
[$Nphe^{5}$,Pen^{11}]SFTI-1 (**5**)		$(1.40\pm0.13)\times10^{8}$
[$Nphe^{5}$,$Pen^{3,11}$]SFTI-1 (**6**)		$(3.11\pm0.09)\times10^{5}$
[$Hcy^{3,11}$]SFTI-1 (**7**)	$(7.24\pm1.18)\times10^{9}$	
[Phe^{5},$Hcy^{3,11}$]SFTI-1 (**8**)		$(7.56\pm1.79)\times10^{9}$
[$Nhcy^{3,11}$]SFTI-1 (**9**)	NA	
[$Nlys^{5}$,$Nhcy^{3,11}$]SFTI-1 (**10**)	NA	
[Phe^{5},$Nhcy^{3,11}$]SFTI-1 (**11**)		NA
[$Nphe^{5}$,$Nhcy^{3,11}$]SFTI-1 (**12**)		NA
[Phe^{5},$Nhcy^{3}$]SFTI-1 (**13**)		NA
[Phe^{5},$Nhcy^{11}$]SFTI-1 (**14**)		$(4.79\pm0.54)\times10^{8}$

NA - not active

introduction of Hcy did not affect inhibitory activity and analogues **7** and **8** with the Hcy – Hcy disulfide bridge were among the most potent inhibitors of trypsin and chymotrypsin, respectively. It's worth emphasizing that all active analogues appeared to be resistant to proteolysis.

All eight SFTI-1 analogues (not shown in the Table) containing different-sized carbonyl ring (between 6 – 11 chemical bonds in the side-chain ring) displayed strong trypsin inhibitory activity with the K_a values ranging from $(3.46\pm0.27)\times10^{8}$ M^{-1} for [$Dap^{3,11}$]SFTI-1 to $(3.80\pm0.71)\times10^{9}$ M^{-1} determined for [Lys^{3},Dap^{11}]SFTI-1. This clearly showed that such redox-stable modification of naturally occurring cyclic element of SFTI-1 is well tolerated in the structure of the inhibitor and therefore can be beneficial for a design of peptidomimetic inhibitors of this family of enzymes.

Acknowledgments
This work was supported by Ministry of Science and Higher Education (grant no. 2889/H03/2008/34).

References
1. Luckett, S., et al. *J. Biol. Chem.* **290**, 525-533 (1999).
2. Stawikowski, M., et al. *ChemBioChem.* **6**, 1057-1061 (2005).
3. Zuckermann, .R.N., et al. *J. Am. Chem. Soc.* **114**, 10646-10647 (1992).
4. Filip, K., et al. *J. Pept. Sci.* **9**, 649-657 (2003).
5. Łęgowska, A., et al. *Bioorg. Med. Chem*. **17**, 3302-3307 (2009).

Proceedings of the 31st European Peptide Symposium
Michal Lebl, Morten Meldal, Knud J. Jensen, Thomas Hoeg-Jensen (Editors)
European Peptide Society, 2010

B-Cell Epitope Mapping of Immunodominant Proteins in Pemphigus Vulgaris: Prediction, Synthesis, and Immunoserological Evaluation

Hajnalka Szabados[1], Szilvia Bősze[1], Antal Blazsek[2], Pálma Silló[2], Sarolta Kárpáti[2], Ferenc Hudecz[1,3], and Katalin Uray[1]

[1]Research Group of Peptide Chemistry, Hungarian Academy of Sciences, Eötvös Loránd University, Budapest, H-1117, Hungary; [2]Department of Dermato-Venereology and Skin Oncology, Semmelweis University, Budapest, Hungary; [3]Institute of Chemistry, Eötvös Loránd University, Budapest, H-1117, Hungary

Introduction

Pemphigus vulgaris (PV) is an autoimmune, intraepithelial, blistering disease affecting the skin and mucous membranes and is mediated by circulating and tissue-bound IgG1 and IgG4 autoantibodies directed against keratinocyte cell surfaces. PV induced autoantibodies bind to the extracellular domains of the desmosomal proteins desmoglein 1 (Dsg1) and desmoglein 3 (Dsg3). Dsg1 and Dsg3 proteins are transmembranous components of desmosomes, that are adhesion units specialized in conferring epidermal keratinocyte cohesion and linked to intercellular molecules of the desmosomal plaque. The binding of antibody to Dsg1 and Dsg3 may have a direct effect on desmosomal adherents or may trigger a cellular process that results in acantholysis [1].

Results and Discussion

As antibody epitopes are located on the hydrophilic surface of proteins, and many of them at or near β-turn structures, we have predicted β-turns within the sequences of proteins Dsg1 [2] and Dsg3 [3] using the Chou-Fasman secondary structure prediction method [4] and performed hydrophobicity predictions by Eisenberg et al. [5]. Segments with low probability of β-turn secondary structure (P_{β}-turn<1) and high probability of hydrophobicity ($P_{hydrophobicity}$>0) were dropped. We have reinforced our results using the PredictProtein website [6]. According to these results pentadecapeptides overlapping in five amino acid residues were synthesized in duplicates on hydroxypropylmethacrylate pins with Fmoc/tBu chemistry [7] covering large parts of the extracellular domains of proteins Dsg1 and Dsg3. The side chain protecting groups were removed with trifluoroacetic acid in the presence of scavengers, but the peptides remained covalently attached to the pins. To detect the interaction between the autoantibodies and the synthetic peptides ELISAs (Enzyme Linked Immunosorbent Assay) were performed with the pin-attached peptides using sera obtained from five PV patients (previously diagnosed as Dsg1 or Dsg3 positive) and a healthy control.

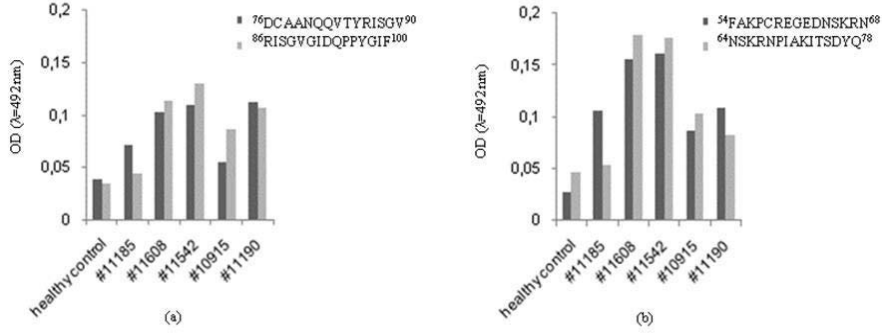

Fig. 1. Serum autoantibody binding to the pin-attached peptides within region 76-100 of protein Dsg1 (a) and within region 54-78 of protein Dsg3 (b).

Table 1. Antibody recognition of regions (represented by overlapping pin-attached 15-mer peptides) corresponding to the sequence of proteins Dsg1 and Dsg3 by PV patients

protein	sequential position of amino acids	#11185, 49y, ♂, Dsg1 positive	#11608, 51y, ♀, Dsg1,3 positive	#11542, 64y, ♂, Dsg1 positive	#10915, 74y, ♀, Dsg3 positive	#11190, 22y, ♀, Dsg1 positive
Dsg1	76-100	-	+	+	-	+
	146-160	-	+	+	-	+
	186-220	-	+	+	-	+
	446-450	-	+	+	-	+
	476-500	-	+	+	-	+
Dsg3	54-78	+	+	+	+	+
	340-354	-	+	+	-	+
	375-389	-	+	+	-	+
	601-615	-	+	+	+	-

Criteria for peptide recognition to identify possible epitopic regions of proteins Dsg1 and Dsg3:
PV patients' measured OD ≥ mean OD + 7× sd value of control (Dsg1 related pin-attached peptides)
PV patients' measured OD ≥ mean OD + 5× sd value of control (Dsg3 related pin-attached peptides)

In summary, five regions within the sequence of the protein Dsg1 (75-100 (Figure 1a), 145-160, 185-220, 445-450, 476-500) and four regions within the sequence of the protein Dsg3 (52-78 (Figure 1b), 340-355, 375-390, 600-615) have been determined with positive serum antibody recognition by three out of five patients (Table 1).

Acknowledgments
These studies were supported by grants of Hungarian Research Fund (OTKA K 61518), GVOP (GVOP-3.2.1 – 2004 – 04 -0352/3.0, 3.2.1 – 2004-04-0005/3.0). Number of ethical permission: TUKEB 74-75/1998.

References

1. Waschke, J. *Histochem. Cell Biol*. **130**, 21-54 (2008).
2. Wheeler, G.N., Parker, A.E., Thomas, C.L., Ataliotis, P., Poynter, D., Arnemann, J., Rutman, A.J., Pidsley, S.C., Watt, F.M., Rees, D.A., Buxton, R.S., Magee, A.I. *Proc. Natl. Acad. Sci.* U.S.A. **88**, 4796-4800 (1991).
3. Amagai, M., Klaus-Kovtun, V., Stanley, J.R. *Cell.* **67**, 869-877 (1991).
4. Chou, P.Y., Fasman, G.D. *Biochem.* **13**, 222-45 (1974).
5. Eisenberg, D., Wesson, M., Wilcox, W. In Fasman, G.D. (Eds.), *Prediction of protein structure and the principles of protein conformation.* Plenum Press, New York, 1989, p. 635.
6. Rost, B., Yachdav, G., Liu, J. *Nucleic Acids Research* **32**, W321-W326 (2004).
7. Geysen, H.M., Meloen, R.H., Barteling, S.J. *Proc. Natl. Acad. Sci. U.S.A*. **81**, 3998-4002 (1984).

Proceedings of the 31st European Peptide Symposium
Michal Lebl, Morten Meldal, Knud J. Jensen, Thomas Hoeg-Jensen (Editors)
European Peptide Society, 2010

T-Cell Epitopes in Autoimmune Bullous Skin Disorders

Katalin Uray[1], Márta Marschalkó[2], Hajnalka Szabados[1], Antal Blazsek[2], Ferenc Hudecz[1,3], Sarolta Kárpáti[2], and Szilvia Bősze[1]

[1]Research Group of Peptide Chemistry, Hungarian Academy of Sciences, Eötvös Loránd University, Budapest, H-1117, Hungary; [2]Department of Dermato-Venereology and Skin Oncology, Semmelweis University, Budapest, H-1085, Hungary; [3]Department of Organic Chemistry, Eötvös Loránd University, Budapest, H-1117, Hungary

Introduction

Autoimmune bullous skin diseases, such as bullosus pemphigoid (BP) and pemphigus vulgaris (PV), are rare, severe, sometimes life-threatening skin disorders. Serologically they are characterized by autoreactive serum antibodies directed against different adhesion molecules of the epidermis and the dermoepidermal basement zone [1]. The antibody binding affects the adhesive function of these molecules resulting in detachment of the cells and subsequent blister formation [2,3].

In the pathogenesis of both pemphigus and pemphigoid, autoreactive T-cell response plays a crucial role, because initiation and perpetuation of B-cell response needs the recognition of T-cell epitopes. In both types of diseases the T-cells recognize epitopes from the extracellular domain of desmoglein 3 (Dsg3) [4-6] or NC16a domain of collagen XVII (BP180) proteins [3,6], producing different cytokines, e.g. interferon-γ (IFN-γ).

We have selected potential T-cell epitope regions within the proteins BP180 (502-515) and Dsg3 (96-112). The synthetic peptides were used to stimulate the peripheral blood monomorphonuclear cells (PBMC) of patients and healthy controls, and the amount of produced IFN-γ was determined by ELISA.

Results and Discussion

Peptides were synthesized by solid phase peptide synthesis method using standard Fmoc/tBu chemistry on Rink-amide MBHA resin. The peptides were RP-HPLC purified, then characterized by ESI-MS and amino acid analysis, showing the expected composition (Table 1).

PBMC from the peripheral blood of healthy donors (D1, ♂30y, D2, ♀ 34y) and patients diagnosed with pemphigus vulgaris (D3, ♂74y, D4, ♀30y) were isolated as described [7]. PBMC were cultured at 1.5-1.8 x 10^5/well in 96-well U-bottom plates. Dsg3 and BP180 peptides were added at concentrations 0.05 and 0.025 mM [8]. As nonspecific positive control, phytohaemagglutinin (PHA-P) and Enterotoxin B, Staphylococcal (SEB) were used at c = 5 μg/mL. After 20 or 90 h of incubation, supernatants were harvested. IFN-γ content was measured by sandwich ELISA. As capture antibody human anti-IFN-γ (BD 551221) was used. The INF-γ level of PBMC supernatant was determined using biotinylated mouse anti-IFN-γ (BD 554550) as detection antibody.

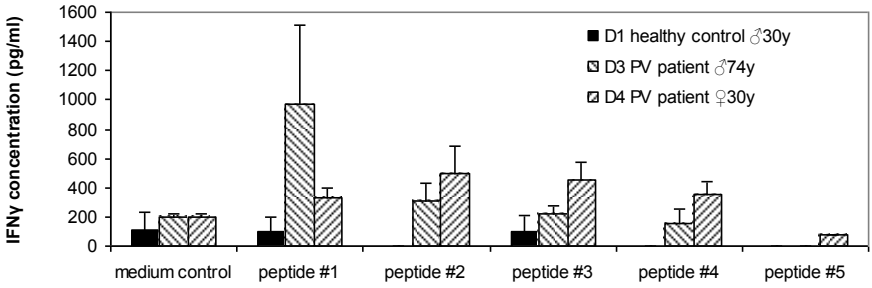

Fig. 1. IFN-γ level of supernatants obtained from PBMC of donors after 20 hrs incubation with 0.025mM peptide, determined by ELISA.

Table 1. Analytical characterization of synthetic peptides derived from Dsg3 and BP180

	Sequence	*M(av) $_{calc}$*	*M(av)$_{meas}$[a]*	*R_t/min[b]*
	Dsg3 peptides			
#1	^{96}PFGIFVVDK^{104}	1020.2	1020.2	23.0
#2	^{100}FVVDKNTGD^{108}	993.1	993.1	13.3
#3	^{104}KNTGDINIT^{112}	974.1	974.5	14.9
	BP180 peptides			
#4	^{502}LERIRRSILPYGDS^{515}	1673.9	1674.2	18.6
#5	^{504}RIRRSILPYGDS^{515}	1431.6	1431.7	24.2

[a]*ESI-MS, Bruker Esquire 3000+*
[b]*RP-HPLC, Knauer, Phenomenex Jupiter C18, 250x5mm, 5µm column, λ=214nm, gradient: 10-75 B% in 35 min. Eluent A: H_2O+0.1 v/v% TFA, eluent B: AcN: H_2O =80:20 (v/v) +0.1 v/v% TFA.*

The culture medium induced IFN-γ production was considered as negative control. As positive control, PHA and SEB were used (data not shown). After 20 or 90 hrs of incubation with peptides, PBMC of healthy donors showed no significant IFN-γ production (Figure 1). (Data of donor 2 are not shown.)

Our results suggested that 0.025 mM peptide concentration was sufficient to induce IFN-γ release on PBMC. According to our results, 0.05 mM peptide concentration, in case of some peptides and some patients, proved cytotoxic to the isolated PBMC (data not shown).

The Dsg 3 derived peptides caused increased IFN-γ release on the PBMC of both PV patients to a different extent (Figure 1). After 90 hrs of incubation similar data were obtained for donor D3, but in case of donor D4 IFN-γ release was undetectable from the supernatant (data not shown).

Out of the two BP-180 derived peptides only the 14-mer peptide ^{502}LERIRRSILPYGDS^{515} induced IFN-γ production on one patients' PBMC.

Synthetic peptides at 0.025 mM and 20 hrs of incubation proved to be efficient to distinguish between IFN-γ production of PBMC obtained from healthy controls and PV patients using ELISA. Further and fine T-cell epitope structure analysis with carefully selected synthetic peptides could be considered in the development of synthetic antigens for the early detection of PV with optimized T-cell response provoking capacity.

Acknowledgments
These studies were supported by OTKA K61518, NKTH-OTKA 68358, GVOP-3.2.1-2004-04-0005/3.0 and GVOP-3.2.1-2004- 04-0352/3.0. Number of ethical permission: TUKEB 74-75/1998.

References

1. Wick, G., Beutner, E.H. *Immunology* **16**, 149-156 (1969).
2. Hertl, M. *Int. Arch. Allergy Immunol*. **122**, 91-100 (2000).
3. Hertl, M., Eming, R., Veldman, C. *J. Clin. Invest*. **116**, 1159-1166 (2006).
4. Amagai, M., Klaus-Kovtun, V., Stanley, J.R. *Cell* **67**, 869-877 (1991).
5. Kárpáti, S., Amagai, M., Prussick, R., Cehrs, K., Stanley, J.R. *J. Cell Biol*. **122**, 409-15 (1993).
6. Veldman, C.M., Gebhard, K.L., Uter , W., Wassmuth, R., Grötzinger, J., Schultz, E., Hertl, M. *J. Immunol*. **172**, 3883-3892 (2004).
7. Jurcevic, S., Hills, A., Pasvol, G., Davidson, R.N., Ivanyi, J., Wilkinson, R.J. *Clin. Exp. Immunol*. **105**, 416-421 (1996).
8. Bősze, Sz., Caccamo, N., Majer, Zs., Mező, G., Dieli, F., Hudecz, F. *Biopolymers (Peptide Science)* **76**, 467-476 (2004).

Proceedings of the 31st European Peptide Symposium
Michal Lebl, Morten Meldal, Knud J. Jensen, Thomas Hoeg-Jensen (Editors)
European Peptide Society, 2010

The Transcriptional Activator PhoB: Chemical Synthesis of Epitopes and Functional Studies

Markus Ritzefeld[1], Katrin Wollschläger[1], André Körnig[2], Michael Birlo[2], Robert Ros[2], Dario Anselmetti[2], and Norbert Sewald[1]
[1]*Organic and Bioorganic Chemistry, Bielefeld University, Bielefeld, 33615, Germany;*
[2]*Experimental Biophysics and Applied Nanosciences, Bielefeld University, Bielefeld, 33615, Germany*

Introduction

DNA-protein interactions are a key element in the regulation of cellular processes. As a model system, the transcription factor PhoB from *E. coli* is investigated on peptide and on protein level using surface plasmon resonance (SPR) and atomic force spectroscopy (AFM). PhoB belongs to the family of winged helix-turn-helix proteins. After phosphorylation of the transactivation domain (amino acids 1-127), two PhoB DNA binding domains (amino acids 127-229) bind in a head to tail arrangement to specific DNA sequences (pho box) containing two TGTCA consensus sequences and two AT-rich minor grooves [1].

Results and Discussion

To elucidate the specific DNA binding of the transcription factor, epitopes representing parts of the DNA binding domain were chemically synthesized by microwave assisted solid phase peptide synthesis (PhoB(190-209)). Moreover, the complete DNA binding domain was synthesized and purified using intein mediated protein splicing (PhoB(127-229)).

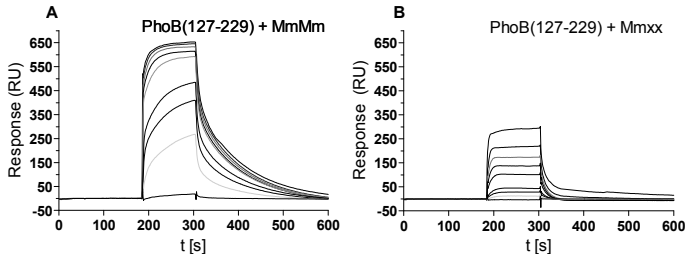

*Fig. 1. Surface Plasmon Resonance Results. **A,B**: Sensograms at different analyte concentrations. PhoB(127-229)WT was used as analyte and the oligonucleotide duplexes as ligands.*

In order to investigate the binding mechanism of PhoB the specific recognition of different oligonucleotides based on the pho box sequence of the *pstS*-regulon were analyzed (Figure 1) using PhoB(127-229). The results indicate equal affinities of PhoB for both binding sites in position 5' and 3'. In addition all findings reveal that two proteins are able to bind to the complete pho box simultaneously. This trimeric complex (Table 1, entry 1) exhibits a significantly reduced K_D in comparison to the 1:1 complexes (Table 1, entries 2,3) due to extensive protein-protein interactions.

Table 1: Equilibrium dissociation constants of the investigated PhoB(127-229)-DNA complexes. CI = 95% confidence interval.

Entry	*Sequence*	*K_D [μM]*	*CI*
1	C**TGTCA***TAAAA*C**TGTCA***TATTC*CT	1.4	0.0-1.8
2	CGAGGC*TAAAA*C**TGTCA***TATTC*CT	14.5	6.9-21.9
3	C**TGTCA***TAAAA*CGAGGCAGCATCT	21.9	10.3-33.4
4	CGAGGC*TAAAA*C**TGTCA**AGCATCT	---	---

In case of an oligonucleotide containing only an AT-rich minor groove in position 5' and a TGTCA-motif in position 3' no binding was observed (Table 1, entry 4). This result indicates that both binding sites (the TGTCA motif and the AT-rich minor groove) are essential for the binding process.

Table 2. AFM dynamic force spectroscopy of PhoB peptides and proteins using pho box DNA [2,3]. k_{off}=dissociation rate constant for peptide/protein DNA complexes. $\tau=1/k_{off}$

Name	k_{off} [s^{-1}] peptide PhoB(190-209)	τ [s]	k_{off} [s^{-1}] protein PhoB(127-229)	τ [s]
WT (wildtype)	3.1 ± 2.1	0.32	1.4	400
R193A	0.071 ± 0.053	14	14.5	83
H198A	49.5 ± 21.2	0.020	21.9	1
R203A	---	---	---	---

Single molecule force spectroscopy experiments were performed to determine the kinetic *off*-rates of peptide and protein epitopes (Table 1). DNA molecules were covalently bound to the AFM tip and the PhoB epitopes to the surface. To elucidate the binding contributions of certain amino acids, the corresponding residues were substituted by alanine [2,3]. All results are comparable for the protein and the peptide mutants. DNA-protein/peptide binding could be observed for R193A and H198A whereas mutant R203A did not bind to DNA (Table 2). Taking into consideration that the arginine at position 203 is conserved within the PhoB family, these results emphasize the relevance of this residues for DNA binding [2,3].

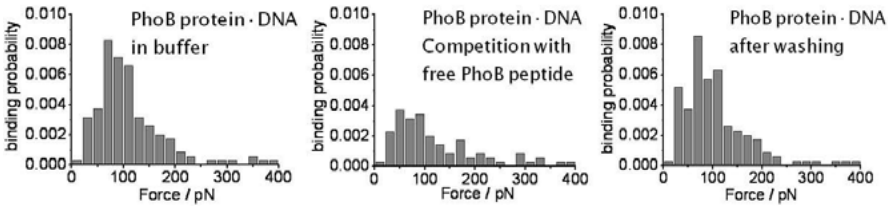

Fig. 2. AFM competition experiments using PhoB(127-229)WT, Pho box DNA and PhoB(190-209)WT as competitor [2,3].

To prove the sequence specific DNA-binding of both, peptides and proteins, competition experiments were accomplished (Figure 2) [2,3]. Therefore force spectroscopy experiments of PhoB(127-229)WT with pho box DNA were performed. Addition of the competitor PhoB(190-209)WT resulted in an overall decrease of binding. The washing step could restore binding. These results implicate that the recognition process is specific in both cases [2,3].

Acknowledgments
This work was supported by the DFG (SFB 613) and the German National Academic Foundation (Studienstiftung des Deutschen Volkes (PhD scholarship to Markus Ritzefeld)).

References

1. Makino, K., et al. *Mol. Biol.* **259**, 15-26 (1996).
2. Wollschläger, K., et al. *Small* **5**, 484-495 (2008).
3. Eckel, R., et al. *Angew. Chem.* **117**, 3989-2933 (2005); *Angew. Chem. Int. Ed.* **44**, 3921-3924 (2005).

Proceedings of the 31st European Peptide Symposium
Michal Lebl, Morten Meldal, Knud J. Jensen, Thomas Hoeg-Jensen (Editors)
European Peptide Society, 2010

Assay of Histone Methyltransferases Using Ac-Peptidyl-MCA as Substrates

Norikazu Nishino[1], Tienabe K. Nsiama[1], Hongfang Chi[1], Yasushi Takemoto[2], Akihiro Ito[2], and Minoru Yoshida[2]
[1]Kyushu Institute of Technology, Kitakyushu, Japan; [2]RIKEN, Wako, Japan

Introduction

The methylation of lysine side chain is often found at the *N*-terminal peptide segment (histone tail) of histone octamer as the post-translational modification [1]. The methylation is mediated by various histone methyltransferases (HMTs) such as G9a, Set9, and others [2,3]. Since the importance of modification of histone tails and other proteins by methylation is recognized, the discovery of HMT inhibitors has been extensively challenging, though the screening method is limited by the conventional radioisotope (RI) detection and ELISA. In the present study, we successfully developed a high-throughput screening procedure using fluorescent substrate of trypsin. The lysine residue in peptidyl MCA (4-methylcoumarine-7-amide) can be methylated by HMT and then lose the susceptibility toward tryptic activity. These actions of enzymes have been combined into a system for convenient detection of HMT activity.

Results and Discussion

At the earliest stage, we prepared Boc-L-Lys(Me)$_n$-MCA, where n = 1, 2, and 3, and subjected to the action of trypsin and lysyl endopeptidase (LEP) to confirm the very poor susceptibilities of Lys(Me)$_n$ toward these enzymes (Figure 1). In order to measure the activity of HMTs, we used the fluorescent intensity of AMC (7-amino-4-methylcoumarin, ex. 390 nm, em. 460 nm) as an index. Boc-L-Lys-MCA was methylated by the action of HMTs for an appropriate interval, then trypsin was added to hydrolyze the remaining substrate resulting into the release of AMC. Thus we could detect the HMT activity by the decrease of fluorescence intensity.

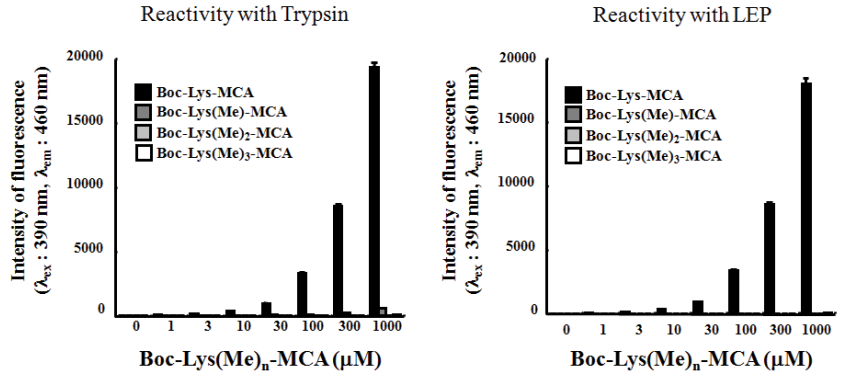

Fig. 1. Hydrolytic susceptibility of Boc-Lys(Me)$_n$-MCA toward trypsin and LEP.

In the next stage, we synthesized various Ac-peptidyl-MCA with Lys at the C-termini learning from the amino acid sequences of histone tail peptide and some proteins which are known as HMT substrates (Table 1). Since histone H3K4 and H3K9 are known as the methylation sites of Set9 and G9a, respectively, we examined the sequence specificity of HMTs by employing these Ac-peptidyl-MCA. As a result we discovered that Ac-ARTKQTARK-MCA, the longest peptide is the most specific and susceptible substrate of G9a. However, Set9 methylated moderately histone tail-related Ac-peptidyl-MCA, but showed higher activity to p53 and Estrogen Receptor α-sequences; Ac-KRSK-MCA from ERα was the best substrate of Set9 (data not shown). Thus, we confirmed the substrate specificities of HMTs regarding the aminoacid sequences. This assay system could be applied for further understanding of various HMTs.

Table 1. Ac-peptidyl-MCA as substrates of histone methyltransferases

Ac-peptidyl-MCA	*Amino acid sequence*
Boc-Lys-MCA	Boc-K-MCA
Ac-histone H3 (1-4)-MCA	Ac-ARTK-MCA
Ac-histone H3 (5-9)-MCA	Ac-QTARK-MCA
Ac-histone H3 (1-9)-MCA	Ac-ARTKQTARK-MCA
Ac-histone H3 (7-9 / 25-27)-MCA	Ac-ARK-MCA
Ac-histone H3 (23-27)-MCA	Ac-KAARK-MCA
Ac-histone H3 (19-27)-MCA	Ac-QLATKAARK-MCA
Ac-p53 (369-372)-MCA	Ac-LKSK-MCA
Ac-p53 (367-372)-MCA	Ac-SHLKSK-MCA
Ac-ERα (299-302)-MCA	Ac-KRSK-MCA
Ac-ERα (297-302)-MCA	Ac-MIKRSK-MCA
Ac-AR (630-633)-MCA	Ac-RKLK-MCA
Ac-AR (628-633)-MCA	Ac-GARKLK-MCA
Ac-GR (491-494)-MCA	Ac-RKTK-MCA
Ac-GR (489-494)-MCA	Ac-EARKTK-MCA

ERα: estrogen receptor α; AR: androgen receptor;
GR: glucocorticoid receptor

In addition, we carried out the evaluation of gliotoxin, a known G9a inhibitor by new assay procedure using Ac-ARTKQTARK-MCA and obtained 2.8 μM as K_i value, close to the reported value. When Ac-LKSK-MCA was used to examine the Set9 inhibition by gliotoxin, this compound showed no inhibitory activity (>100 μM) suggesting specific inhibition of G9a.

Since it is also known that S-(5'-adenosyl)-L-homocystein (SAH), another product of methylation reaction, is an inhibitor of HMTs as negative feedback, we determined its inhibitory activity by this assay procedure. The IC_{50} of 0.49 mM was obtained for G9a.

In conclusion, we have established a convenient assay system for HMTs by employing fluorogenic peptide substrates. This system is useful for screening the HMT inhibitors. The discovery of Set9 inhibitors from the chemical library is being challenged at present by our group.

References

1. Lachner, M., Jenuwein, T. *Curr. Opin. Cell Biol.* **14**, 286-298 (2002).
2. Jenuwein, T. *Trends Cell Biol.* **11**, 266-273 (2001).
3. Tachibana, M., Sugimoto, K., Fukushima, T., Shinkai, Y. *J. Biol. Chem.* **276**, 25309-25317 (2001).

Proceedings of the 31st European Peptide Symposium
Michal Lebl, Morten Meldal, Knud J. Jensen, Thomas Hoeg-Jensen (Editors)
European Peptide Society, 2010

Molecular Modeling, Design and Structural Studies of a New Class of Peptide Inhibitors of Bacterial Topoisomerases

Luiz Carlos B. Barbosa, Saulo S. Garrido, Davi B. Delfino, Anderson Garcia, and Reinaldo Marchetto

Institute of Chemistry, UNESP – Univ Estadual Paulista, Department of Biochemistry and Chemistry Technology, Araraquara, SP, 14.800-900, Brazil

Introduction

The ParD-ParE is a bacterial toxin-antitoxin system that contributes to plasmid stability by a mechanism that relies on the differential stability of toxin and antitoxin proteins. ParE (a 12.1 kDa protein) is the toxic component of this system which targets the intracellular DNA gyrase [1], unique type IIA topoisomerase able to introduce negative supercoils into bacterial DNA. The scarce information about its structure, its interactions with the antitoxin and with its intracellular target, led us consider the ParD-ParE system as a model of study for the design of new peptide inhibitors of bacterial topoisomerases.

Results and Discussion

Unlike others members of the RelE/ParE superfamily that inhibit the translation by inducing cleavage of mRNAs, ParE acts blocking the DNA gyrase activity [1]. Recently, we built a 3D Model for *E. coli* ParE toxin [2]. Structural prediction from ParE primary structure using PSIPRED server showed the β-α-α-β-β-β-α sequence as secondary structure, as inferred in the proposed 3D Model (Figure 1). As an approach for structure-function studies and based on proposed Model, we have designed and synthesized by solid-phase methodology a series of linear peptides and studied their activity by supercoiling and relaxation assays. Recent studies have shown that residues at the extreme C-terminus of ParE are necessary for protein stability and toxicity [3]. In this context, for the peptides design, initially we considered the residues P80 to S105 that contain the predicted C-terminal β-sheet and α-helix structures. After, we also included other nineteen residues (L61 to A79) in the peptide design. So, from the natural ParE, ten peptide sequences were obtained and the predicted C-terminal secondary structures were confirmed by FTIR analyses (Figure 2). The ability of the peptides to inhibit the supercoiling reaction of DNA gyrase and the relaxation reaction of topoisomerase IV (Topo IV) was investigated by gel electrophoresis with an initial screening at 37°C and 100 μmol.L^{-1} of synthetic peptides. EcParE3 (P80-R100), EcParE8 (L61-S105) and EcParE10 (L61-F87) were selected as good inhibitors for both DNA gyrase and Topo IV enzymes.

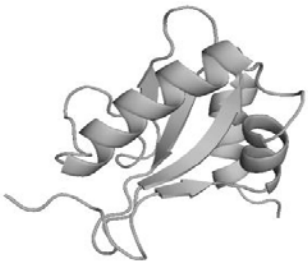

Fig. 1. Predicted 3-D Structure of Escherichia coli ParE toxin.

EcParE1	**********	**********	**********	***LMARLSER	******
EcParE2	**********	**********	********FHER	MDLMARLSER	******
EcParE3	**********	**********P	ALVVAIFHER	MDLMARLSER	******
EcParE4	**********	**********	**********	***LMARLSER	LNIES
EcParE5	**********	**********	********FHER	MDLMARLSER	LNIES
EcParE6	**********	**********P	ALVVAIFHER	MDLMARLSER	LNIES
EcParE7	**********HY	VFCLPHGSAP	ALVVAIFHER	MDLMARLSER	LNIES
EcParE8	LRMIHCEHHY	VFCLPHGSAP	ALVVAIFHER	MDLMARLSER	LNIES
EcParE9	**********HY	VFCLPHGSAP	ALVVAIF****	**********	******
EcParE10	LRMIHCEHHY	VFCLPHGSAP	ALVVAIF****	**********	******

Fig. 2. Primary structure of synthetic peptides from natural ParE protein.

The selected peptides were assayed for determination of the minimum concentration that produced complete inhibition of supercoiling and relaxation activities (termed IC_{100}). In standard supercoiling assays at 37°C with 3.4 nmol.L^{-1} of gyrase, a relaxed DNA (500 ng) substrate is completely negatively supercoiled in 1h [4]. EcParE3, EcParE8 and EcParE10 inhibited this reaction (Figure 3A) with IC_{100} values of 25, 50 and 25 µmol.L^{-1} respectively.

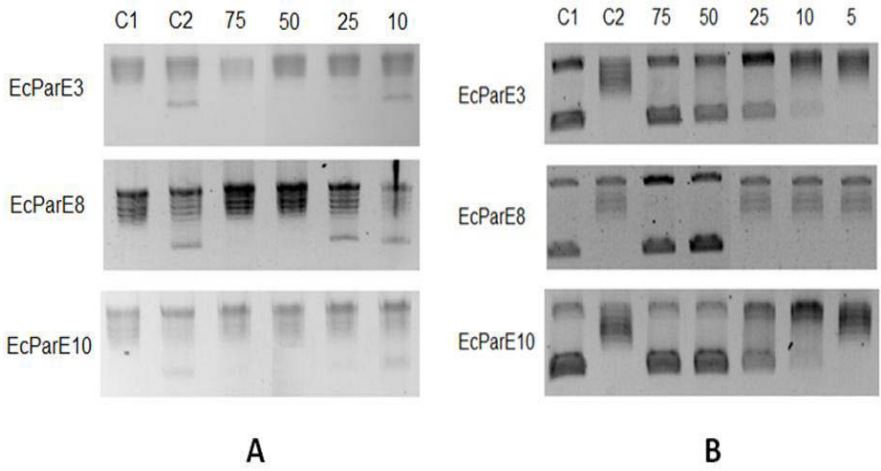

Fig. 3. EcParE peptides-mediated inhibition of (A) DNA supercoiling reactions of DNA gyrase and (B) DNA relaxation reactions of Topo IV. Controls: C1: negative (absence of peptide and enzyme); C2: positive (absence of peptide); The numbers in the lanes represents the concentration of the peptides in µmol.L^{-1}.

In addition, EcParE3, EcParE8 and EcParE10 inhibited the ATP-dependent relaxation reaction of Topo IV, in standard assays (37°C, 5 nmol.L^{-1} of enzyme and 400 ng of supercoiled DNA) with IC_{100} values of 5, 25 and 10 µmol.L^{-1} (Figure 3B). For both, there is no evidence of cleavage complex. From these results it is possible to speculate about of the requirement of the C-terminal LNIES sequence in a probable structure-activity relationship of the peptides synthesized. Comparatively EcParE3 and EcParE10, the best inhibitors of both Gyrase and Topo IV, do not include this sequence in its primary structure. Probably peptides with this sequence do not have the adequate molecular adjustments for the formation of an inactive complex with the enzymes. Our preliminary findings revealed a new class of peptide inhibitors of bacterial topoisomerases and suggest that DNA gyrase as well as Topo IV may be effective targets of the natural ParE toxin.

Acknowledgments
This work was supported by FAPESP in the form of grant (10/07841-2) and by CNPq in the Ph.D fellowship form (L.C.B. Barbosa) R. Marchetto is the recipient of research fellowship from CNPq.

References

1. Jiang, Y., Pogliano, J., Helinski, D.R., Konieczny, I. *Mol. Microbiol.* **44**, 971-979 (2002).
2. Barbosa, L.C.B., Garrido, S.S., Garcia, A., Delfino, D.B., Marchetto, R. *Bioinformation* **4**, 438-440 (2010).
3. Fiebig, A., Rojas, C.M.C., Siegal-Gaskins, D., Crosson, S. *Mol. Microbiol*. **77**, 236-251 (2010).
4. Trovatti, E., Cotrim, C.A., Garrido, S.S., Barros, R., Marchetto, R. *Bioorg. Med. Chem. Lett.* **18**, 6161-6164 (2008).

Proceedings of the 31st European Peptide Symposium
Michal Lebl, Morten Meldal, Knud J. Jensen, Thomas Hoeg-Jensen (Editors)
European Peptide Society, 2010

Structural Aspects and Biological Evaluation of New Mannose Derived Immunomodulating Adamantyltripeptides

Rosana Ribić[1], Lidija Habjanec[2], Branka Vranešić[2], Ruža Frkanec[2], and Srđanka Tomić-Pisarović[1]

[1]Department of Chemistry, Faculty of Science, University of Zagreb, Horvatovac 102a, Zagreb, 10000, Croatia; [2]Institute of Immunology Inc., Rockefellerova 10, Zagreb, 10000, Croatia

Introduction

The aim of this work was to compare the immunomodulating activity of adamantyltripeptides D/L-(adamant-1-yl)Gly-L-Ala-D-*iso*Gln (Ad_1TP1 and Ad_1TP2) and D/L-(adamant-2-yl)Gly-L-Ala-D-*iso*Gln (Ad_2TP1 and Ad_2TP2) and their mannosyl derivatives. Structure-activity relationship was studied with respect to the absolute configuration of mannose molecule, chiral spacer and adamantyltripeptides molecules. Adjuvant activity was assessed for these novel compounds and compared to the previously known activity of peptidoglycan monomer (PGM, β-D-GlcNAc-(1→4)-D-MurNAc-L-Ala-D-*iso*Gln-*meso*DAP(εNH_2)-D-Ala-D-Ala) [1]. We have demonstrated in our previous investigations that the adamantyltripeptides (Ad_2TP1 and Ad_2TP2), structurally related to bacterial peptidoglycans, have different biological activity, especially adjuvanticity [1,2].

Results and Discussion

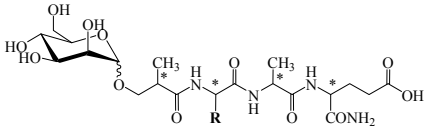

R = Adamant-1-yl ; Adamant-2-yl

Fig. 1. Mannosyl derivatives of adamantyltripeptides; α-D-Man-(R/S)-$OCH_2CH(CH_3)$CO-D/L-(adamant-1-yl)Gly-L-Ala-D-isoGln and α-D-Man-(R/S)-$OCH_2CH(CH_3)$CO-D/L-(ada mant-2-yl)Gly-L-Ala-D-isoGln.

α-D-Mannose was coupled to D/L-(adamant-1-yl)Gly-L-Ala-D-*iso*Gln (Ad_1TP1 and Ad_1TP2) and D/L-(adamant-2-yl)Gly-L-Ala-D-*iso*Gln (Ad_2TP1 and Ad_2TP2) via chiral linker ($HOCH_2CH(CH_3)COOCH_3$, *linker*) (Figure 1) as previously described for PGM [3]. All tested compounds were characterized by NMR and their purity was tested by HPLC. All examined compounds are water-soluble, non-toxic and non-pyrogenic substances. The adjuvant effect of prepared diastereoisomers was tested on CBA mice with ovalbumin (OVA) as a model antigen and compared to the adjuvant effect of PGM

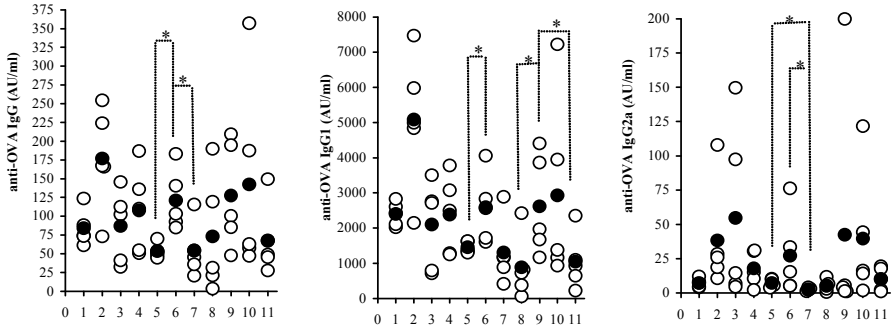

*Fig. 2. The effect of examined compounds on the production of total anti-OVA IgG (a - left) and its subtypes IgG1 (b - middle) and IgG2a (c - right) after second booster. Experimental groups (X-axis) 1. OVA;2. OVA + PGM ; 3. OVA + Ad_1TP1;4. OVA + α-D-Man-R-linker-Ad_1TP1; 5. OVA + Ad_1TP2; 6. OVA + α-D-Man-R-linker-Ad_1TP2; 7. OVA + α-D- Man-S-linker-Ad_1TP2; 8. OVA + Ad_2TP1; 9. OVA + Ad_2TP2; 10. OVA + α-D-Man-R-linker-Ad_2TP2; 11. OVA + α-D-Man-S-linker-Ad_2TP2. • denotes group mean value, **o** denotes each serum separately. * $p<0.05$ for the groups connected with dashed line.*

Table 1. The ratio of anti-OVA IgG1 and anti-OVA IgG2a (IgG1/IgG2a) antibodies developed in CBA mice. For each mouse serum, obtained after second booster, log_{10} IgG1/IgG2a was calculated and the result for each experimental group (n=5) is presented as average ± standard deviation (SD).

Experimental groups	*Average of log_{10} IgG1/IgG2a ± SD*
1. OVA	2.55 ± 0.2
2. OVA + PGM	2.23 ± 0.4
3. OVA + Ad_1TP1	1.87 ± 1.0
4. OVA + α-D-Man-*R-linker*-Ad_1TP1	2.23 ± 0.3
5. OVA + Ad_1TP2	2.33 ± 0.2*
6. OVA + α-D-Man-*R-linker*-Ad_1TP2	2.17 ± 0.4*
7. OVA + α-D-Man-*S-linker*-Ad_1TP2	2.66 ± 0.1
8. OVA + Ad_2TP1	2.12 ± 0.2
9. OVA + Ad_2TP2	2.59 ± 0.7
10. OVA + α-D-Man-*R-linker*-Ad_2TP2	2.05 ± 0.6
11. OVA + α-D-Man-*S-linker*-Ad_2TP2	2.06 ± 0.8

$p<0.05$ in comparison to the exp. group 7

as a standard. Experimental groups of five mice were immunized and boosted two times subcutaneously into the tail base at 21-days intervals. Mice were anesthetized prior to blood collection on 7th day after each booster. Sera were collected, decomplemented at 56 °C for 30 minutes and stored at -20 °C until tested. The dose of OVA was 10 μg per mouse. The dose of PGM and adamantyltripeptides was 200 μg per mouse. OVA and tested substances were dissolved in saline and the injection volume in all experimental groups was 0.1 mL per mouse.

Mannosylated adamantyltripeptides did not stimulate stronger adjuvant activity compared to PGM, but they demonstrated immunomodulatory activity. The results revealed that the immunomodulating activity of examined mannosylated compounds was slightly changed in comparison to the parent adamantyltripeptide molecules in favor of *R* absolute configuration of the applied linker (Figure 2). Mannosylated **Ad_1TP1** (Figure 2a-3) did not demonstrated any significant difference in induction of total specific IgG antibodies in comparison to the parent molecule. Mannosylation of **Ad_1TP2** revealed the difference in total IgG antibodies content between the tested compounds regarding the *R* (Figure 2a-6) and *S* (Figure 2a-7) absolute configuration of the linker molecule, in favor of *R* isomer. Mannosylated **Ad_2TP2** showed, as well, the difference in adjuvant activity regarding the absolute configuration of the linker, again in favor of the *R* isomer.

The effect of tested compounds on IgG1 induction was basically the same as the one observed for total specific IgG. Regarding IgG2a, the significant difference was found between mannosylated adamantyltripeptides coupled via *R* and *S* linker, respectively, again in favor of *R* isomer. Only **mannose-Ad_1TP2** with *S* linker had impact on switching the immune response towards more pronounced Th2 type, specific for OVA (Table 1).

Acknowledgment

We wish to thank the Ministry of Science, Education and Sports of the Republic of Croatia for support of this work (Research Projects 021-0212432-2431 and 119-1191344-3121).

References

1. Tomašić, J., et al. *Vaccine* **18**, 1236-1243 (2000).
2. Vranešić, B., et al. *Helv. Chim. Act.* **76**, 1752-1757 (1993).
3. Ribić, R., et al. *Bioorg. & Med. Chem.* **17**, 6096-6105 (2009).

Proceedings of the 31st European Peptide Symposium
Michal Lebl, Morten Meldal, Knud J. Jensen, Thomas Hoeg-Jensen (Editors)
European Peptide Society, 2010

N/OFQ(1-13)NH_2 Analogues with Aminophosphonate Moiety: Synthesis and Analgesic Activity

Emilia D. Naydenova[1], Petar T. Todorov[1], Nikola D. Pavlov[1], Elena B. Dzhambazova[2], and Adriana I. Bocheva[3]

[1]Department of Organic Chemistry, University of Chemical Technologies and Metallurgy, 1756, Sofia, Bulgaria; [2]Department Physiology and Clinical Physiology, Sofia University St. Kl. Ohridski, Faculty of Medicine, 1407, Sofia, Bulgaria; [3]Department of Pathophysiology, Medical University, 1431, Sofia, Bulgaria

Introduction

Nociceptin/orphanin FQ is a neuropeptide (heptadecapeptide: Phe-Gly-Gly-Phe-Thr-Gly-Ala-Arg-Lys-Ser-Ala-Arg-Lys-Leu-Ala-Asn-Gln) that selectively interacts with the opioid-like receptor (ORL_1 or NOP), a novel member of the opioid receptor family. It has been reported that the nociceptin-NOP system modulates several biological functions, including pain transmission, stress and anxiety, learning and memory, locomotor activity, food intake [1]. N/OFQ(1-13)NH_2 is the minimal sequence maintaining the same activity as the natural peptide nociceptin. Structure-activity studies demonstrated that N- and C-terminal modifications of nociceptin/orphanin FQ generate highly potent NOP receptor ligands**.**

Pain is a frequently observed symptom of various diseases. Some of the greatest achievements in medicine in theoretical and in clinical aspect are connected with the research on pain and especially on the development of analgesic drugs. α-Amino-phosphonic acids and aminophosphonates have reached position of eminence in the research works intending to discover, to understand and to modify physiological processes in the living organisms. They are also a potential source of medicinal lead compounds [2].

Results and Discussion

Aiming to develop ligands for the NOP that possess stronger analgesic activity, a new series of N-modified analogues of the N/OFQ(1-13)NH_2 with aminophosphonate moiety were prepared and tested for the nociceptive effects. The new analogues (Figure 1) have been synthesized including cyclic α-aminophosphonates at position 1, using SPPS by Fmoc (9-fluorenylmethoxy-carbonyl) chemistry. The 1-[(dimethoxyphosphono) methylamino]-cycloalkanecarboxylic acids were previously prepared by our group following Kabachnik-Fields reaction [2,3].

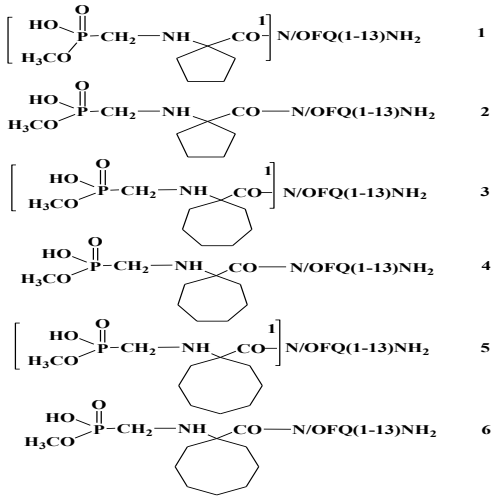

Fig. 1. N-modified analogues of N/OFQ(1-13)NH_2 with aminophosphonate moiety.

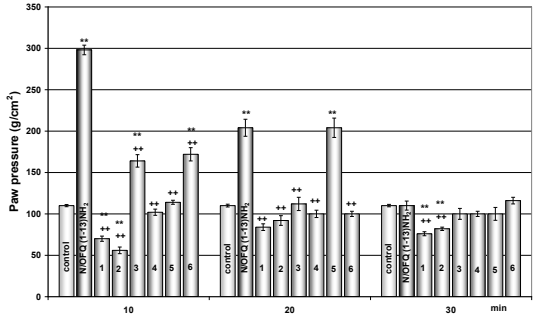

*Fig. 2. Effects of N/OFQ(1-13)NH_2 analogues on nociception measured with paw pressure test. Mean values ± S.E.M. are presented. **P<0.01 vs. control, $^{++}$P<0.01 vs. nociceptin.*

Analgesic activity was examined by two nociceptive tests - paw-pressure (PP) and hot-plate (HP). All compounds were injected intraperitoneally (i.p.) in male Wistar rats at a dose of 10 μg/kg. The biological investigations started 10 min after injection of peptides.

Our previous results showed that in PP test N/OFQ(1-13)NH_2 (10 μg/kg, i.p.) administered alone in intact animals has significant well pronounced and time dependent analgesic effect versus control group [4].

All newly synthesized analogues decreased significantly the pain threshold compared to N/OFQ(1-13)NH_2 during the whole investigated period with exception of analogue 5 on 20th min. Only analogues 3 and 6 on the 10th min and analogue 5 on 20th min showed statistically significant ($p<0.01$) and short lasting analgesic effect compared to the control (Figure 2).

In HP test N/OFQ(1-13)NH_2 and all its analogues significantly decreased HP latency during the whole investigated period, more pronounced for the analogues where the effects were hypo- to hyperalgesic (not shown in the figure).

Conclusions

Incorporation of 1-[(methoxyphosphono)methylamino]cycloalkanecarboxylic acid in position 1 of N/OFQ molecule decreases the analgesic activity of the newly synthesized peptide analogues. Among the newly synthesized peptide analogues only compounds 3, 5 and 6 significantly increased pain threshold in PP test compared to control group of intact animals. Different involvement of mechanical, thermal receptors leads to different analgesic effects of newly synthesized N/OFQ analogues. The results also suggest participation of two types of receptors - opioid and nociceptin (ORL_1 or NOP).

Further studies involving the antagonists of these receptors are needed to clarify the mechanisms of their action.

Acknowledgments

The research was supported by Grant No. 845 (DTK 02/61) of the National Research Fund, Sofia, Bulgaria.

References

1. Mogil, J.S., Pasternak, W. *Pharmacol. Rev*. **53**(3), 381-415 (2001).
2. Naydenova, E., Todorov, P., Troev, K. *Amino Acids* **38**(1), 23-30 (2010).
3. Naydenova, E., et al. *Eur. J. Med. Chem.* **43**(6), 1199-1205 (2008).
4. Dzambazova, E., Nocheva, H., Bocheva, A. *Pharmacy* **55**(1-4), 30-34 (2008).

Proceedings of the 31st European Peptide Symposium
Michal Lebl, Morten Meldal, Knud J. Jensen, Thomas Hoeg-Jensen (Editors)
European Peptide Society, 2010

Fluorescent and Luminescent Fusion Proteins for Detection of Amyloid Beta Peptide Localization and Aggregation

Kenji Usui[1,2,3], Masayasu Mie[3], Takashi Andou[3], Naoki Sugimoto[1,2], Hisakazu Mihara[3], and Eiry Kobatake[3]

[1]Faculty of Frontiers of Innovative Research in Science and Technology (FIRST), Konan University, Kobe, 650-0047, Japan; [2]Frontier Institute for Biomolecular Engineering Research (FIBER), Konan University, Kobe, 650-0047, Japan; [3]Graduate School of Bioscience and Biotechnology, Tokyo Institute of Technology, Yokohama, 226-8501, Japan

Introduction

In Alzheimer's disease (AD), the amyloid beta peptide (Aβ) forms fibrillar aggregates known as amyloid fibrils. This amyloid fibril is the principal component of extracellular deposits which are regarded as causative agents. However, how Aβ can aggregate *in vivo* and how the generated aggregates affect the disease development, are still in question. Since recent studies have implicated Aβ and its ability to self-assemble as key factors in the pathogenesis of AD [1], understanding the behaviors of Aβ *in vivo*, such as where Aβ can accumulate and what structure (monomers, oligomers or fibrils) Aβ adopts at each localized point, is a promising clue to these mysteries. From this point of view, development of molecules that can bind to Aβ and can provide some output signals depending on Aβ structural states would be required. In this study, the fusion protein, consisting of Aβ sequence, and fluorescent and luminescent proteins was constructed to analyze Aβ localization and aggregation in internal and external cells.

Results and Discussion

First of all, the fusion protein, Y-Aβ-L (Figure 1), consisting of Aβ sequence, and fluorescent and luminescent proteins (EYFP; enhanced yellow fluorescent protein, and hRluc; humanized *Renilla* luciferase) at both termini of the Aβ sequence was designed. The Aβ sequence in the fusion protein was employed to give some affinities and co-aggregations with Aβ. Fusion of EYFP and hRluc with the Aβ sequence was applied to allow detecting Aβ localization and monitoring conformational changes. According to recent papers [2,3], it was expected that EYFP fluorescence and/or hRluc luminescence could be increased or decreased when the conformation of the fusion protein was varied.

Then, expression vectors for the fusion proteins were constructed and the protein was expressed in *E. coli* and was purified. Using the protein, we conducted co-aggregation experiments by monitoring fluorescent and luminescent changes during incubation with Aβ. After the 20 hr incubation, Y-Aβ-L with Aβ showed that its luminescence was significantly decreased but that there were little changes in fluorescence. This implied that the detection system for Aβ localization and aggregation could be achieved with luminescence giving Aβ conformational information and with fluorescence contributing Aβ localization information. In addition, Y-Aβ-L alone gave no fluorescence and no luminescence after the incubation and dynamic light scattering data showed that hydrodynamic radius of Y-Aβ-L alone was increased with the incubation. TEM images also supported that Y-Aβ-L alone aggregated to amorphous form. These results implied that Y-Aβ-L alone could aggregate by itself and that this aggregation seemed more intense than wild type Aβs. This might reduce the background fluorescence of Y-Aβ-L alone in the detection of Aβ localization.

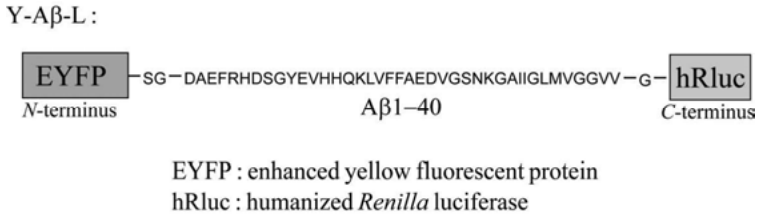

Fig. 1. Structure of the fusion protein.

Furthermore, expression vectors for the fusion proteins were constructed and transfected into HeLa cells. Using the protein-overexpressed HeLa cell lysate, fluorescent and luminescent changes during incubation with Aβ were monitored. As the samples were incubated for 50 hr, Y-Aβ-L luminescence intensity with Aβ1-42 was significantly more decreased than that without Aβ1-42 (ca. 2 times), whereas there were little changes in Y-Aβ-L fluorescence both with/without Aβ1-42. It was additionally found that fluorescence intensities of thioflavin T with Aβ1-42 in cell lysate were increased depending on the incubation time in the thioflavin T assay. These results indicated that the decrement of Y-Aβ-L luminescence denoted Aβ aggregation. Additionally, intra- or extracellular localization of aggregated Aβ was analyzed using the protein.

Throughout these experiments, the detection system for Aβ localization and aggregation was achieved with luminescence changes providing Aβ conformational information (Aβ aggregation information) and with fluorescence changes giving Aβ localization information. With more improvements, this system would be one of the powerful tools for the study of amyloidogenic protein behaviors and localization in internal and external cells.

Acknowledgments

This study was in part supported by the Grants-in-Aid for Scientific Research, the "Core research" project (2009-2014) from the Ministry of Education, Culture, Sports, Science and Technology (MEXT). K.U. is grateful to Grant-in-Aid for Research Activity Start-up from MEXT. T.A. is grateful for Research Fellowships of the Japan Society for the Promotion of Science (JSPS) for Young Scientists.

References

1. Usui, K., Hulleman, J.D., Paulsson, J.F., Siegel, S.J., Powers, E.T., Kelly, J.W. *Proc. Natl. Acad. Sci. U.S.A.* **106**, 18563-18568 (2009).
2. Wurth, C., Guimard, N.K., Hecht, M.H. *J. Mol. Biol.* **319**, 1279-1290 (2002).
3. Kim, W., Hecht, M.H. *Proc. Natl. Acad. Sci. U.S.A.* **103**, 15824-15829 (2006).

Proceedings of the 31st European Peptide Symposium
Michal Lebl, Morten Meldal, Knud J. Jensen, Thomas Hoeg-Jensen (Editors)
European Peptide Society, 2010

Phakellistatins: Are They True Active Natural Products?

Marta Pelay-Gimeno[1,2*], Judit Tulla-Puche[1,2], Andrés M. Francesch[3], Carmen Cuevas[3], and Fernando Albericio[1,2,4]

[1]Institute for Research in Biomedicine (IRB Barcelona), Barcelona Science Park, Baldiri Reixac 10, 08028, Barcelona, Spain; [2]CIBER-BBN, Networking Centre on Bioengineering, Biomaterials and Nanomedicine, Barcelona Science Park, Baldiri Reixac 10, 08028, Barcelona, Spain; [3]Pharma Mar S.A., Avda de los Reyes 1, E-28770, Colmenar Viejo, Madrid, Spain; [4]Department of Organic Chemistry, University of Barcelona, Martí i Franqués 1-11, 08028, Barcelona, Spain

Introduction

Phakellistatins [1] are members of a family of proline-rich cyclic peptides isolated from marine sponges of the genus *Phakellia* displaying interesting biological activities, such as cytotoxic and antiproliferative effects, when isolated from the natural extracts. Surprisingly, although they proved to be chemically identical to their natural counterparts, the majority of the synthesized cyclopeptides showed significantly different biological properties [2,3]. Conformational differences [4] or a highly bioactive contaminant [5] retained in very small amounts in phakellistatins samples would account for this unexpected behavior.

Results and Discussion

The synthetic approach for phakellistatin 19 follows a Fmoc/tBu strategy with chlorotrityl chloride resin (CTC), which minimizes the formation of DKPs and allows retention of the protecting groups after cleavage, which is crucial for the head-to-tail solution-phase cyclization step (Figure 2). Once the synthesis was well established, chemical equivalence between the synthetic and the natural cyclopeptide was validated by co-elution in a reverse-phase C18 column with a linear gradient over 30 minutes of 0.036% TFA in ACN and 0.045% TFA in H_2O from 35:65 to 55:45.

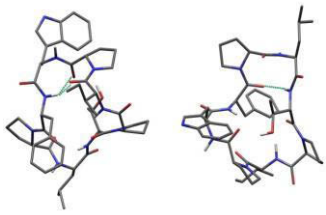

Fig. 1. Low energy structure of phakellistatin 19 obtained using restrained SA.

A detailed NMR analysis was performed. Complete ^{1}H and ^{13}C assignment in DMSO-d_6 was achieved by using 1D and homo- and heteronuclear 2D experiments. The ROESY spectrum cross-peaks Phe^{2}-Hα/Pro^{1}-Hδ, Ile^{5}-Hα/Pro^{4}-Hδ and Thr^{7}-Hα/Pro^{6}-Hδ provided evidence of the *trans* geometry of all the Xaa-Pro^{x} amide bonds, also supported by the small difference between β and γ ^{13}C NMR chemical shifts of prolines. Finally, the hydrogen bonding pattern in DMSO-d_6 was studied by calculating the temperature coefficients of the amide protons. The low values found for HN-Phe^{2} (2.18 ppb/K) and HN-Thr^{7} (0.20 ppb/K) strongly suggest its participation in two intramolecular hydrogen bonds. This would be consistent with the existence of two β-turns, one involving Pro^{1}-Leu^{8} and the other Pro^{4}-Trp^{3}.

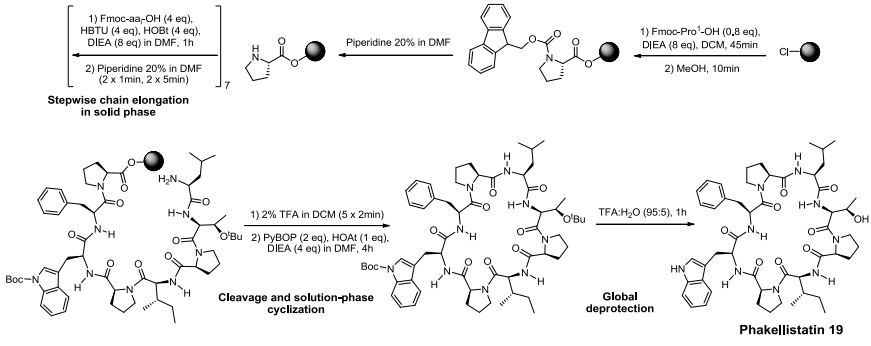

Fig. 2. Synthetic strategy for phakellistatin 19.

Table 1. Biological evaluation of natural and synthetic phakellistatin 19

Phakellistatin 19	*GI_{50} (M) MDA-MB-231*	*GI_{50} (M) A549*	*GI_{50} (M) HT29*
Natural	5.15×10^{-7}	4.62×10^{-7}	4.41×10^{-7}
Synthetic	n.d.	n.d.	n.d.

n.d. Not detected

A low energy structure for phakellistatin 19 was obtained performing a standard protocol of restrained simulated annealing (SA) using ROESY data (Figure 1). As it can be seen in the resulting structure, the presence of a β-turn involving Pro^1-Leu^8 is confirmed. On the other hand, as suggested by monodimensional NMR, a second intramolecular hydrogen bond stabilizes a γ-turn involving the residues Phe^2-Trp^3-Pro^4 and leaving the indole moiety of the tryptophan completely solvent-exposed.

Some hypotheses that may explain the surprising biological behavior shown by phakellistatin 19 (Table 1) were investigated.

- An epimer that co-elutes with synthetic phakellistatin 19 or that corresponds with one of the extra peaks detected in the chromatogram of the natural cyclopeptide could be responsible of the biological activity.

The ten epimers, including those replacing L-Ile and L-Thr with L-*allo*-Ile and L-*allo*-Thr respectively, were synthesized. None of the ten epimers displayed a GI_{50} below 10^{-6} M in biological assays, allowing us to rule out the first hypothesis.

- The presence of several proline residues capable of *cis-trans* isomerism in a constrained macrocycle provides structures with a complex conformational profile. Individual conformers at proline linkages bearing different biological properties could be stabilized in different conditions (i.e. solvents).

A detailed NMR analysis of *cis-trans* isomerism was therefore carried out. Synthetic phakellistatin 19 was studied by NMR in three different deuterated solvents: DMSO-d_6, CD_3OD and $CDCl_3$. A spectrally comparable and H_2O-soluble analogue obtained by replacement of Leu^8 with Orn^8 was also studied in DMSO-d_6, H_2O:D_2O (9:1), pH = 5.95 and H_2O:D_2O (9:1), pH = 8.12. *Trans* geometry was detected for all the Xaa-Pro^x amide bonds in all the solvents. Only when working with CD_3OD and $CDCl_3$ other conformers (10% approx.) were detected. No assignment of Pro linkages geometry was achieved for the minor conformers.

- Preparations of natural phakellistatins could contain a spectrally undetectable amount of highly potent cytotoxic agents.

Due to the impossibility of working on the last hypothesis, the synthesis and biological evaluation of the seven possible *cis-trans* conformers of phakellistatin 19 using proline derivatives capable of fixing *cis*-configuration at proline linkages, could eventually shed some light on the unexpected biological behavior of phakellistatins family.

Acknowledgments
This work was funded by CICYT (Grant CTQ2009-07758), Generalitat de Catalunya (2009SGR 1024), Pharma Mar S.A., the Institute for Research in Biomedicine and Barcelona Science Park. M.P.G thanks Ministerio de Educación y Ciencia for a FPU PhD fellowship.

References

1. Pettit, G.R., Cichacz, Z., Barkoczy, J., Dorsaz, A.C., Herald, D.L., Schmidt, J.M., Tackett, L.P., Brune, D.C. *J. Nat. Prod.* **56**, 260-267 (1993).
2. Pettit, G.R., Rhodes, M.R., Tan, R. *J. Nat. Prod.* **62**, 409-414 (1999).
3. Napolitano, A., Bruno, I., Riccio, R., Gomez-Paloma, L. *Tetrahedron* **61**, 6808-6815 (2005).
4. Tabudravu, J.N., Jaspars, M., Morris, L., Al, Kettenes-van den Bosch, J.J., Smith, N. *J. Org. Chem.* **67**, 8593-8601 (2002).
5. Pettit, G.R., Lippert III, J.W., Taylor, S.R., Tan, R., Williams, M.D. *J. Nat. Prod.* **64**, 883-891 (2001).

Proceedings of the 31st European Peptide Symposium
Michal Lebl, Morten Meldal, Knud J. Jensen, Thomas Hoeg-Jensen (Editors)
European Peptide Society, 2010

Celiac Disease: Synthesis of Overlapping Linear Peptide Epitopes of tTG[Aa(1-230)]

Margherita Di Pisa[1,2], Giuseppina Sabatino[1,3], Mario Chelli[1,2], Paolo Rovero[1,5], Claudio Tiberti[6], and Anna Maria Papini[1,2,4]

[1]Laboratory of Peptide & Protein Chemistry & Biology, University of Florence, I-50019, Sesto Fiorentino, Italy; [2]Department of Chemistry "Ugo Schiff" and CNR-ICCOM, University of Florence, I-50019, Sesto Fiorentino, Italy; [3]Espikem Srl, I-59100, Prato, Italy; [4]Laboratoire SOSCO – EA4505 Université de Cergy-Pontoise, Neuville-sur-Oise, F-95031, Cergy-Pontoise, France; [5]Department of Pharmaceutical Sciences, University of Florence, I-50019, Sesto Fiorentino, Italy; [6]Department of Clinical Sciences, Policlinico Umberto I, Sapienza, University of Rome, Italy

Introduction

Celiac Disease (CD) is considered an autoimmune disease characterized by villous atrophy and inflammatory cell infiltration of the lamina propria triggered by the gliadin fraction of wheat gluten and similar alcohol soluble proteins called prolamines. CD has a complex and multifactorial aetiology and occurs in genetically susceptible individuals in association with environmental factors (gliadin), leading to a chronic inflammatory condition [1]. The gluten intake leads to a complex immune response, both T cell mediated and humoral response leading to the secretion of autoantibodies. The endomysial protein tissual Transglutaminase (tTG) is considered the main autoantigen in CD playing a key role in the pathogenesis [2]. Untreated CD patients have high levels of circulating IgA and IgG directed to different autoantigens, i.e. tTG, gliadin, and endomysium that are directly involved in mucosal injury [3]. Up to now the "gold standard" for the diagnosis of CD is the bowel biopsy even though simple serological tests could have a high impact as non invasive diagnostic tools. Reliable assays are necessary not only for an early diagnosis but also for monitoring the disease activity evaluating antibodies as specific biomarkers [4]. The improvement of the sensitivity of serological tests could be obtained by substituting extracted or recombinant antigens with synthetic probes based on peptide epitopes [5]. The screening of overlapping peptides libraries is an excellent strategy to identify the minimal epitope recognised as an antigen [6]. Therefore, the characterization of tTG antigenic domains is a crucial step in understanding onset and developement of CD. Sera from patients with CD at first diagnosis were demonstrated to have high levels of auto-antibodies recognising distinct tTG' functional domains. In particular, Tiberti *et al*. showed that there is an evidence of a specific epitope loss of anti-transglutaminase immunoreactivity in gluten free diet celiac sera (6 and 24 months after the diagnosis), which is supposed to be only against protein N-terminal portion [7]. Our aim was to characterize linear autoantigenic epitopes by testing in celiac patients' sera the reactivity of different overlapping synthetic peptide fragments of tTG [aa(1-230)]. We performed an epitope mapping based on the "Chemical Reverse Approach", synthesizing 23 overlapping peptides of tTG(1-230) by SPPS. The penta-decapeptides will be useful for RIA, ELISA, and SPR to evaluate the IgA response against tTG specific epitopes in gluten free diet celiac patients' sera.

Results and Discussion

The activity of peptide fragments of tTG(1-230) (Table1) was qualitatively and quantitatively evaluated in inhibition experiments of the ^{35}S tTG-antibody binding in patients' sera. The gluten free diet patients' sera used in the assay were selected because they recognise in RIA antibodies to full length tTG protein but not of the protein fragments tTG(227-687) and tTG(473-687).

Table 1. Overlapping peptides of tTG(1-230) tested in RIA (underlined residues indicate common fragments)

Peptide	*tTG fragment*	*Sequence*
I	tTG(1-25)	MAEELVLERCDLELETNGRDHHTAD
II	tTG(16-40)	TNGRDHHTADLCREKLVVRRGQPFW
III	tTG(31-55)	LVVRRGQPFWLTLHFEGRNYEASVD
IV	tTG(46-60)	ENGRYEASVDSLTFS
V	tTG(56-70)	SLTFSVVTGPAPSQE
VI	tTG(66-80)	APSQEAGTKARFPLR
VII	tTG(76-90)	RFPLRDAVEEGDWTA
VIII	tTG(106-120)	TPANAPIGLYRLSLE
IX	tTG(116-130)	RLSLEASTGYQGSSF

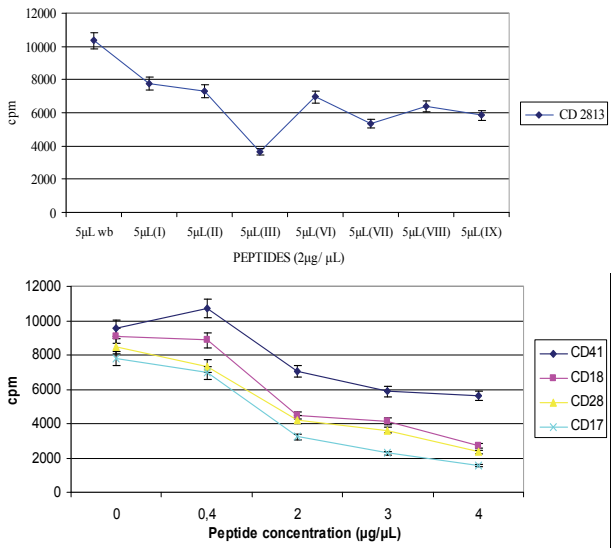

Peptide fragments reported in Table 1 were tested in RIA. They showed that tTG (31-55) is able to inhibit anti tTG-Ab binding to the radio-labelled protein (Fig. 1) with a dose - response pattern. Moreover tTG(31-55) induced a remarkable decrease of the cpm measured at the β-counter in all the sera tested. On the basis of these findings we can assume that the tTG (31-55) fragment is able to inhibit the tTG-Ab binding to the radio-labelled protein.

Fig. 1. Upper: RIA Screening of the peptides reported in Table1 for a representative patient'serum; Lower: dose-response curve of tTG(31-55).

Acknowledgments
This work is supported by Ente Cassa di Risparmio di Firenze and the ANR Chaire d'Excellence PepKit 2009-2013 (France).

References
1. Sollid, LM. *Nat Rev. Immunol* **2**, 647-655 (2002).
2. Dieterich, W., et al. *Nat. Med.* **3**, 797-801 (1997).
3. Halttunen, T., Mäki, M. *Gastroenterology* **116**, 566-572 (1999).
4. Baker, M. *Nature Biotech.* **23**, 297-304 (2005).
5. Alcaro, M.C., et al. *Chemistry Today* **27**(2), 36-39 (2009).
6. Lolli, F., et al. *Expert Rev. Neurotherapeutics* **6**(5), 781-794 (2006).
7. Tiberti, C., et al. *Clinical Immunology* **121**, 40-46 (2006).

Proceedings of the 31st European Peptide Symposium
Michal Lebl, Morten Meldal, Knud J. Jensen, Thomas Hoeg-Jensen (Editors)
European Peptide Society, 2010

Celiac Disease: Characterization of Amino Acids and Short Peptides Finger Print for a Fast I.V.D.

Margherita Di Pisa[1,2], Giuseppina Sabatino[1,3], Mario Chelli[1,2], Paolo Rovero[1,5], Claudio Tiberti[6], and Anna Maria Papini[1,2,4]

[1]Laboratory of Peptide & Protein Chemistry & Biology, University of Florence, I-50019, Sesto Fiorentino, Italy; [2]Department of Chemistry "Ugo Schiff" and CNR-ICCOM, University of Florence, I-50019, Sesto Fiorentino, Italy; [3]Espikem Srl, I-59100, Prato, Italy; [4] Laboratoire SOSCO – EA4505 Université de Cergy-Pontoise, Neuville-sur-Oise, F-95031, Cergy-Pontoise, France; [5]Department of Pharmaceutical Sciences, University of Florence, I-50019, Sesto Fiorentino, Italy; [6]Department of Clinical Sciences, Policlinico Umberto I, Sapienza, University of Rome, Italy

Introduction

Celiac Disease (CD) is an autoimmune disease characterized by villous atrophy and inflammatory cell infiltration of the lamina propria caused by the gliadin fraction of wheat gluten. The endomysial protein tissue Transglutaminase (tTG) is the main autoantigen in CD playing a key role in the pathogenesis [1]. tTG catalyzes deamidation of Gln residues or protein cross-linking through the formation of isopeptide bonds between Gln and Lys residues in gliadin peptides that are rich in proline and glutamine and thus very resistant to proteolysis [2]. CD is characterized by the presence of specific antibodies recognizing gliadin, food proteins, and the endomysial autoantigen tissue Transglutaminase. Amino acids and short peptides are important targets for metabolic profiling in many areas, including clinical diagnostics for evaluating disease conditions [3,4]. Total amino acids content in plasma and urine is expected to reflect the nutritional/metabolic status, i.e. confirming or ruling out the suspected aminoacidopathies. In order to achieve a better understanding of this multifactorial disease, we are evaluating the free amino acids and short peptides profile in serum of newly diagnosed celiac patients compared to healthy subjects by a quantitative AccQ•Tag Ultra UPLC analysis (Waters). Protocol analysis is rather fast and includes a precolumn derivatization, which converts both primary and secondary amino acids into exceptionally stable, fluorescent derivatives as suitable analytes for UV-absorbance, fluorescence, electrochemical, and MS detection. Celiac patients' sera, previously treated with sulfosalicilic acid to induce protein precipitation, were derivatized with a standard solution of 6-aminoquinolyl-N-hydroxysuccinimidyl carbamate (AQC reagent) (Figure 1).

Results and discussion

Quantification of individual amino acids has a relevant importance in monitoring the therapeutic intervention by dietary manipulations and/or vitamin supplement therapy.

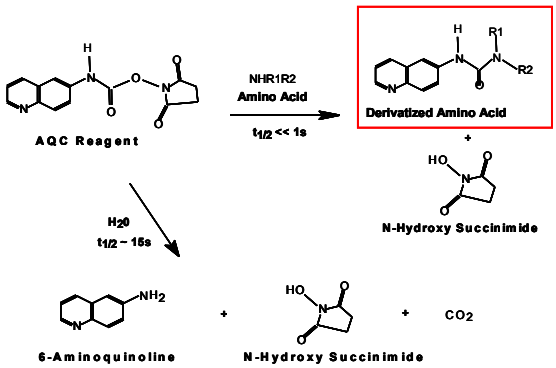

Fig.1. Sample derivatization using AQC reagent.

A comparative evaluation of 15 healthy subjects and 21 celiac patients at the diagnosis was performed to try to identify the presence of significant differences between these groups (age 7-15) in free amino acids serum levels. We found 14 residues (from a total of 43 amino acids investigated) showing remarkably different values between healthy and celiac populations (Figure 2). Applying a statistical analysis we realized that only 12 values were comparable. A larger cohort of patients is under evaluation. This comparative

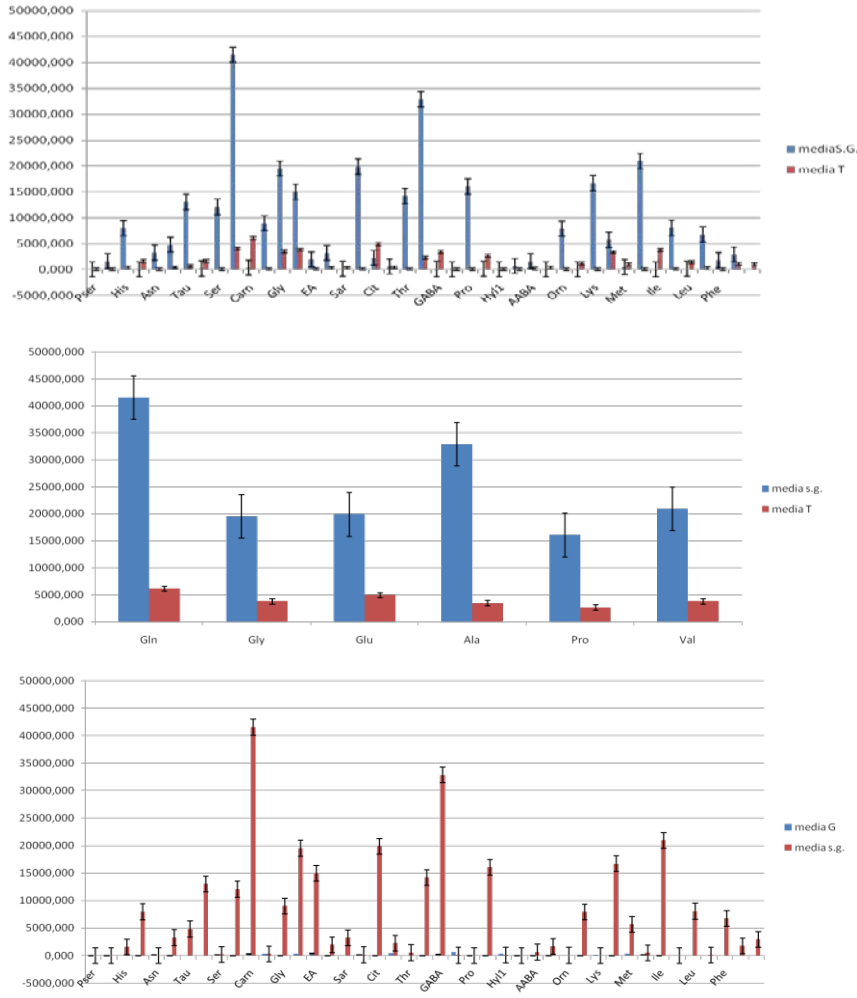

Fig. 2. From top to bottom. Comparison (mmol/mL) of amino acids in CD patients before gluten free diet (T) and after diet (s.g.). Six representative amino acids values are reported. Comparison (mmol/mL) of 42 amino acids in CD patients after gluten free diet (S.G.) and healthy controls (G).

study between healthy and celiac subjects let us to hypothesize that amino acids profile in celiac disease can have a diagnostic and/or prognostic value, and that celiac patients can display a different amino acids profile compared to healthy ones even if they are following a gluten free diet. This observation could assume a peculiar importance in the case of earlier identification of different autoimmune diseases in celiac patients.

Acknowledgments
This work is supported by Ente Cassa di Risparmio di Firenze and the ANR Chaire d'Excellence PepKit 2009-2013 (France).

References
1. Dieterich, W., et al. *Nat. Med*. **3**, *725-726* (1997).
2. Stenberg, P., et al. *Eur. J. of Medicine* **19**(2), 83-91 (2008).
3. Suresh Babu, S.V., et al. *Ind. J. of Clin. Biochem.* **17** (2), 7-26 (2002).
4. Huub, W.A., Waterval, W.A.H., et al. *Clin. Chim Acta* **407**, 36-42(2009).

Proceedings of the 31st European Peptide Symposium
Michal Lebl, Morten Meldal, Knud J. Jensen, Thomas Hoeg-Jensen (Editors)
European Peptide Society, 2010

Search for Inhibitors or Activators of Human Proteasome

R. Rostankowski[1,2], E. Jankowska[1], M. Gaczyńska[3], P.A. Osmulski[3], S. Madabhushi[3], and F. Kasprzykowski[1]

[1]Faculty of Chemistry, University of Gdansk, Sobieskiego 18, 80-952, Gdansk, Poland; [2]Department of Biochemistry, University of Texas Southwestern Medical Center, 5323 Harry Hines Blvd, Dallas, 75309, TX, U.S.A.; [3]Institute of Biotechnology, University of Texas Health Science Center, 15355 Lambda Dr, San Antonio, 78245, TX, U.S.A.

Introduction

Cell metabolism is strictly dependent on number and activity of many different proteins, which are regulated by transcription, translation and post-translative modification, as well as their irreversible proteolysis effectivity. One of the degradation systems, present in eukaryotic cells, is ATP-dependent ubiquitin-proteasome pathway [1]. Proteasome is multicatalytic protein complex responsible for intracellular protein degradation. The proteasome is made up of two subcomplexes: a catalytic core particle (CP; also known as the 20S proteasome) and one or two terminal 19S regulatory particles (RP) that serves as a proteasome activator with a molecular mass of approximately 700 kDa (called PA700). The 19S RP binds to one or both ends of the latent 20S proteasome to form an enzymatically active proteasome 26S. The eukaryotic proteasome is a multicatalytic protease characterized by three activities with distinct specificities against short synthetic peptides: a "chymotryptic-like" activity with preference for tyrosine or phenylalanine at the P1 position; a "tryptic-like"activity with preference for arginine or lysine at the P1 position; and a "postglutamyl" hydrolyzing activity with a preference for glutamate or other acidic residues at the P1 position. [2]. Proteasome activity has a major role in homeostasis of the whole organism. Disturbance of regular functioning of proteasome is observed in many diseases, for example neurodegenerative illnesses such as Parkinson, Alzheimer or Huntington [3]. An increase of proteasome activity is also observed in case of immunological and pulmonary illnesses like mucoviscidosis [4]. Due to its function nowadays researchers of the world try to find new regulators of proteasome activity.

Results and Discussion

Yeast culturing: Saccharomyces cerev, strain MHY501 (kindly provided by Mark Hochstrasser, Yale University) was inoculated in YPD medium (yeast extract, peptone, D-Glucose). After culturing, yeast cells were harvested and processed using microfluidizer and homogeniztion grinder respectively. Isolated protein was purified in three steps: anion exchange chromatography, hydroxyapatite chromatography and gel filtration as a last step.

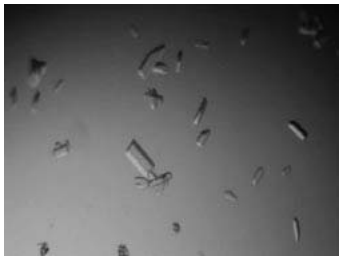

Fig. 1. Proteasome crystals.

Purification: Anion exchange chromatography purification used following protocol: equilibration of column, direct load, column buffer, 250mM NaCl, 400mM NaCl, 1M NaCl with 5-10 min at 4°C, 500 rpm spinning in every step

Hydroxyapatite purification: Purification used following protocol: 10mM sodium phosphate buffer, 100mM, 200mM, 300mM, 400mM and 500mM buffer with 5 min at 4°C , 200 g spinning in every step.

Gel filtration: Purification proceeded as follows: isocratic separation against gel filtration buffer containing: 50 mM Tris-Cl pH 7.0 and 10% glycerol on Superose 6 column. Flow rate 0.4 ml/min and 0.5 ml of fraction volume.

Crystallization: Hanging drop vapor diffusion technique was used for the crystallization of protesome. The best diffracting crystals (Figure 1) were obtained under following conditions: 0.03 M Magnessium acetate, 0.1 M MES 7.2, 12% (v/v) MPD. Protein concentration used for experiment was 2.5 mg/ml and data were collected using advances photon source – beam 19ID (Argonne National Laboratory, Argonne, IL). Structure was

solved using molecular replacement technique where proteasome (3RYP) structure as a model was used (refinement still in progress).

Activity of designed peptides and digestion experiment

Synthesized compounds are based on the sequences of 11S activator, protein HIV-1 Tat and PR39 peptide respectively. Synthesis was carried out on solid phase according to SPPS procedure on automatic peptides synthesizer Millipore 9050 Plus Pepsynthesizer or microwave reactor Plazmatronika RM800. Biological studies shown that following peptides are able to activate latent proteasome with high effectiveness (data not shown).

Even if peptides are able to regulate proteasome activity, there is a need to check their degradation by multicatalytic complex. To determine stability of mentioned compounds, digestion experiment was performed as follows: peptides concentration used for experiment - 100μM, proteasome concentration 0.01 mg/ml, reaction buffer: 50 mM Tris-Cl pH 8.0, 0.005% SDS. Results are shown on MALDI-MS spectra (Figure 2).

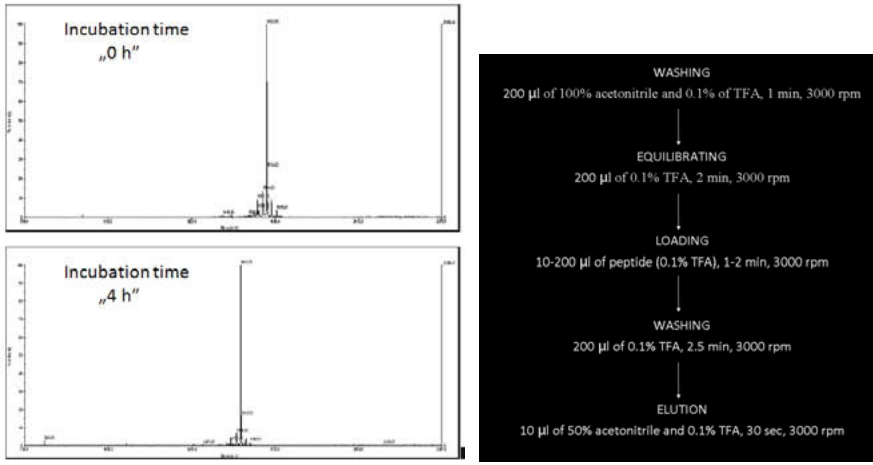

Fig. 2. MALDI MS spectra of digestion experiment and procedure of experiment.

Conclusions

Since precise regulation of proteasome functioning plays very important role in keeping organisms in homeostasis, there is a need to find selective and specific inhibitors or activators of its activity. High level of activity and allosteric character of synthesized peptides gave the idea to crystallize the protein itself and in complex with those regulators. That allows us to compare conformational changes between proteasome in native state and interrupted state caused by interaction with peptide molecule (crystallization of protein complexes in progress). Digestion experiment indicated that used compounds were not digested by enzyme. To make conditions most suitable for substrate degradation, activated proteasome was used. Even after 4h of incubation there were no traces of any other compound except used peptide – MS spectra above. Comparison of structures of protein complex and protein itself should give an answer about mechanism of regulator-proteasome interaction.

Acknowledgments

Supported by grant DS/8440-4-0172-0.

References

1. Juryszyn, A., Skotnicki, A. *Adv. Clin. Exp. Med.* **15**, 309-320 (2006).
2. Rechsteiner, M., Realini, C., Ulster V. *Biochem. J.* **345**, 1-15 (2000).
3. Ciechanover, A., Iwai, K. *IUBMB Life* **56**, 193-201 (2004).
4. Debirage, R., Price, R. *Am. J. Physiol. Renal Physiol*. **285**, F1-8 (2003).

Proceedings of the 31st European Peptide Symposium
Michal Lebl, Morten Meldal, Knud J. Jensen, Thomas Hoeg-Jensen (Editors)
European Peptide Society, 2010

Characterisation of the Minimal Epitope Detecting Autoantibodies in Multiple Sclerosis by Surface Plasmon Resonance

Feliciana Real-Fernández[1,2], Irene Passalacqua[1,2], Elisa Peroni[3], Francesco Lolli[1,4], Paolo Rovero[1,5], and Anna Maria Papini[1,2,3]

[1]Laboratory of Peptide & Protein Chemistry & Biology, Polo Scientifico e Tecnologico, University of Florence; [2]Department of Chemistry "Ugo Schiff" and CNR ICCOM, Via della Lastruccia 3/13, University of Florence, I-50019 Sesto Fiorentino (FI), Italy; [3]Laboratoire SOSCO-EA4505, University of Cergy-Pontoise, 5 mail Gay-Lussac, Neuville sur Oise, 95031 Cergy-Pontoise cedex, France; [4]Department of Neurological Sciences & Azienda Ospedaliera Careggi, Viale Morgagni 34, University of Florence, I-50134 Firenze, Italy; [5]Department of Pharmaceutical Sciences, Via Ugo Schiff 6, University of Florence, I-50019 Sesto Fiorentino (FI), Italy

Introduction

With the aim of developing efficient tools for autoimmune diseases diagnostics, several studies have been focused on the use of synthetic peptides. Peptides have several advantages: they are relatively easy to produce and may retain chemical stability over time. Moreover, reproduction of co- or post-translational modifications in peptides, synthetically speaking, is a quite easy task compared to recombinant techniques. As a proof-of-concept we have previously developed by a "Chemical Reverse Approach" the synthetic glycopeptide CSF114(Glc), able to detect specific autoantibodies circulating in blood by Enzyme Linked Immunosorbent Assay (ELISA) on Multiple Sclerosis patients' sera [1]. This glycopeptide contains a β-D-glucopyranosyl moiety linked to an Asn residue on the tip of a β-hairpin structure probably reproducing a native post-translational modification.

In order to identify the minimal epitope of the glycopeptide, we previously synthesized a series of shortened sequences of CSF114(Glc). All the shortened glycopeptide sequences inhibited anti-CSF114(Glc) Abs in competitive ELISA. The modified amino acid Asn^7(Glc) was demonstrated to be fundamental for an optimal antigen-antibody interaction, and a seven amino-acid sequence having Asn(Glc) in middle position was the minimal epitope able to inhibit anti-CSF114(Glc) antibodies in competitive ELISA. Nevertheless, short peptides displayed poor coating efficiency into the solid-phase conditions of the polystyrene ELISA plate [2]. Therefore these short peptides were not useful as antigens for developing a solid phase ELISA. In this context, we decided to modify the shortened sequences in order to facilitate peptide immobilization. The new modified sequences have been studied in competition and solid phase ELISA. Moreover, surface plasmon resonance (SPR) technology has been used to control in real time the peptide immobilization process on a gold sensor chip. SPR technology monitors in real time with a microfluidic system immobilization and binding interactions.

Results and Discussion

Shortened penta- and heptapeptide sequences were synthesized by solid phase peptide synthesis (SPPS) following the Fmoc/tBu strategy. Moreover, penta- and heptapeptides were modified by coupling the spacer Fmoc-NH-$(PEG)_2$-COOH (Figure 1) at the N-terminal. The commercially available spacer was specially protected for the SPPS.

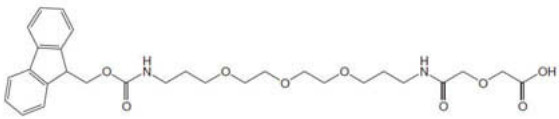

Fig.1. Protected spacer Fmoc-NH-$(PEG)_2$-COOH.

All peptides were cleaved from the resin, purified by solid phase extraction, and further characterized by mass spectrometry. Sequences and analytical data of new peptides are summarized in Table 1.

The synthetic penta- and heptapeptide sequences were used as antigens to measure their binding interactions with autoantibodies in MS patients' sera in inhibition experiments both in ELISA and SPR. At this purpose, the original glycopeptide sequence CSF114(Glc)

Table 1. Sequences and analytical data of synthesized peptides

Peptide	*Sequence*	*ESI-MS; $[M+H]^+$ (m/z)*	
		calculated	*found*
Penta	ERN(Glc)GH-NH_2	773.35	773.64
Peg-Penta	NH_2-Peg-ERN(Glc)GH -NH_2	1091.35	1091.42
Hepta	VERN(Glc)GHS-NH_2	959.45	959.76
Peg-Hepta	NH_2-Peg-VERN(Glc)GHS-NH_2	1278.05	1278.32

was coated in a polystyrene microplate and the shortened penta- and heptapeptides were tested in a competition assay to evaluate their affinity to specific antibodies. All the synthesized shortened peptides were able to inhibit antibodies presenting similar IC_{50}. Therefore, the autoantibody recognition in ELISA is not affected by Peg modifications.

Moreover, competition assay was also performed by SPR instrumentation. Immobilization of CSF114(Glc) was performed on the sensor chip surface following the amine coupling strategy. This sensor chip was used to test the inhibition of specific autoantibodies in Multiple Sclerosis patients' sera with the synthesized shortened penta- and heptapeptide sequences. Results showed that the new modified peptides were able to recognize autoantibodies in patients' sera by a SPR biosensor.

The new shortened peptides containing Peg spacer were able to detect specific anti-CSF114(Glc) antibodies in both competition ELISA and SPR, then modifications have not modified the epitope of recognition. Further experiments to facilitate shortened peptide sequences immobilization will be performed in ELISA. Moreover, SPR technology will be useful for monitoring the peptide coating on the sensor surface. The possibility of monitoring immobilization of synthetic probes in real-time directly on the sensor chip surface will enable to develop new sequences for antibody detection. Binding interactions with autoantibodies in MS patients' sera will be measured using all the synthetic shortened glucosylated peptide sequences.

Acknowledgments

Ente Cassa Risparmio di Firenze, PRIN 2008, and ANR Chaire d'Excellence PepKit 2009-2013 (France) are gratefully acknowledged.

References

1. (a) Lolli, F., et al. *Proc. Natl. Acad. Sci. U.S.A.* **102**, 10273-10278 (2005); (b) Lolli, F., et al. *J. Neuroimm.* **167**, 131-137 (2005); (c) Papini, A.M. *Nat. Med.* **11**, 13 (2005); (d) Carotenuto, A., et al. *J. Med. Chem.* **49**, 5072-5079 (2006); (e) Papini, A.M., Rovero, P., Chelli, M., Lolli, F. Granted U.S.A. Patent & PCT Application WO 03/000733 A2; (f) Carotenuto. A., et al. *J. Med. Chem.* **51**, 5304-5309 (2008).
2. Nuti, F., Mulinacci, B., Peroni, E., Alcaro, M.C., Paolini, I., Benedetti, F., Carotenuto, A., Ciolli, F., Lolli, F., Chelli, M., Rovero, P., Papini, A.M. *Adv. Exp. Med. Biol.* **611,** 431-432 (2009).

Proceedings of the 31st European Peptide Symposium
Michal Lebl, Morten Meldal, Knud J. Jensen, Thomas Hoeg-Jensen (Editors)
European Peptide Society, 2010

Antigenic Probes for Autoantibody Detection in Multiple Sclerosis: Synthetic Peptides versus Recombinant Proteins

Francesca Gori[1,2], Barbara Mulinacci[1,2,*], Lara Massai[1,2], Francesco Lolli[1,3], Anna Maria Papini[1,4,5], and Paolo Rovero[1,2]

[1]Laboratory of Peptide & Protein Chemistry & Biology, University of Florence, Sesto Fiorentino (Fi), I-50019, Italy; [2]Department of Pharmaceutical Sciences, University of Florence, Sesto Fiorentino (Fi), I-50019, Italy; [3]Department of Neurological Sciences, University of Florence, Azienda Ospedaliero-Universitaria Careggi, Firenze, I-50134, Italy; [4]Department of Chemistry ''Ugo Schiff'' and CNR-ICCOM, University of Florence, Sesto Fiorentino (Fi), I-50019, Italy; [5]Laboratoire SOSCO-EA4505, University of Cergy-Pontoise, Cergy-Pontoise cedex, 95031, France

[*]present address: Max-Planck Institut für Biochemie, Martinsried, München, Germany

Introduction

Autoimmune diseases are a class of disorders that need early diagnosis and efficient prognosis for setting up therapeutic treatments. Multiple sclerosis is the most common central nervous system inflammatory demyelinating disease. Its pathogenesis has not been yet elucidated, but an autoimmune mechanism against myelin antigens is thought to contribute to its immunopathological mechanisms.

The identification of autoantibodies as specific biomarkers is a relevant target and, up to now, most of the diagnostic immunoassays are based on native antigens as immunological probes.

One of the most studied antigen targets in Multiple Sclerosis is Myelin Oligodendrocyte Glycoprotein (MOG), a glycoprotein of the myelin sheath [1]. MOG is considered a putative autoantigen and interesting data are focused on the diagnostic and prognostic role of the detection of antibodies to MOG in adults' serum [2].

However, post-translational modifications of proteins, either native or aberrant, may play a fundamental role for specific and sensitive autoantibody detection in autoimmune diseases. So antigens characterization should take into account the chemical modification introduced on side chains of amino acids. The use of chemically modified synthetic peptides can be useful for this purpose.

We demonstrated that a 'chemical reverse approach' is efficient in developing specifically modified synthetic peptides, able to fishing out autoantibodies from patients' biological fluids. In particular a specific antigenic probe, termed CSF114(Glc), was developed to identify autoantibodies, as biomarkers correlating with disease activity, in a population of Multiple Sclerosis patients [3,4].

We decided to focus our attention on recombinant MOG with the aim of comparing the relative merit of this protein versus synthetic modified peptides as antigenic probes for autoantibody detection in ELISA.

Results and Discussion

The full-length MOG consists of 218 amino acids; the encephalitogenic properties of this protein are believed to result from the extracellular IgV-like domain (amino acids 1-125).

The cDNA of the extracellular domain of rat MOG was subcloned into the His-tag expression vector pQE12. $rMOG_{ED}(His)_6$ was overexpressed in inclusion bodies in *E. coli*. After disruption of the cells by sonication, the inclusion bodies were purified by repetitive steps of centrifugation and resuspension in 50 mM Tris, 0.5 M NaCl, 0.5% lauryldimethylamine oxide, pH 8.0. The inclusion bodies were solubilized in a denaturating buffer (100 mM NaH_2PO_4, 10 mM Tris, 6 M guanidine·HCl, 40 mM mercaptoethanol, pH 8.0).

$rMOG_{ED}(His)_6$ was loaded onto an affinity chromatography column (Chelating Sepharose Fast Flow; GE Healthcare) and the refolding of the protein was achieved under a gradient of denaturating buffer (100 mM NaH_2PO_4, 10 mM Tris, 6 M guanidine·HCl, pH 8.0) versus nondenaturating solution (100 mM NaH_2PO_4, 10 mM Tris, 3 mM reduced glutathione, pH 8.0) over 10 h. The folded protein was subsequently eluted with 0.5 M imidazole in 100 mM NaH_2PO_4, 10 mM Tris, 0.2 M NaCl (pH 8.0). Finally the protein was dialyzed against PBS, pH 8.

Identity of the protein was checked by mass spectrometry, while the proper refolding was checked by Circular Dichroism measurements.

The antibody absorbance (Figure 1) to the expressed $rMOG_{ED}(His)_6$ was evaluated by indirect ELISA using patients [Multiple Sclerosis sera (MS) and cerebrospinal fluid (MS-CSF)] and controls [other neurological diseases (OND), rheumatoid arthritis (RA), and blood donors (BD)].

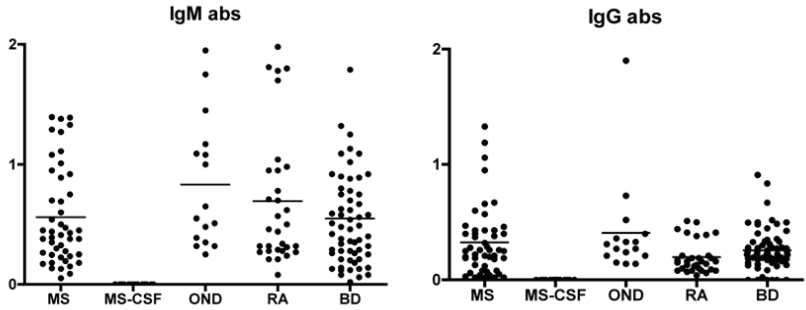

Fig. 1. Column scatter of the ELISA absorbance values to the $rMOG_{ED}(His)_6$ in MS, MS-CSF, OND, RA, BD.

Antibodies were detected in a few sera and in no CSF. No difference existed between both the groups for IgM while for IgG there were borderline differences among sera groups (Kruskal-Wallis Test, $p<0.03$). The Dunn test showed no differences between MS versus BD or OND. Only a few patients (MS or controls) presented increased IgG or IgM antibodies in serum, and no CSF displayed evidence for IgG or IgM antibodies in MS.

In conclusion, although an efficient refolding procedure has been applied to $rMOG_{ED}(His)_6$, autoantibodies were detected in a few sera. These results validated the hypothesis that it is necessary to obtain MOG (or other myelin proteins) in the native state with the proper post-translational modifications in order to understand the role of anti-MOG (or anti-myelin) autoantibodies in Multiple Sclerosis patients' sera.

References

1. Johns, T.G., Bernard, C.C.A, *J. Neurochem*. **72**, 1-9 (1999).
2. Berger, T. et al. *N. Engl. J. Med.* **349**, 139-145 (2003).
3. Lolli, F., et al. *Proc. Natl. Acad. Sci. U.S.A.* **102**, 10273 (2005).
4. Papini, A.M., Rovero, P., Chelli, M., Lolli, F. *PCT International Patent Application WO 03/000733*.

Proceedings of the 31st European Peptide Symposium
Michal Lebl, Morten Meldal, Knud J. Jensen, Thomas Hoeg-Jensen (Editors)
European Peptide Society, 2010

The Metabolisation of Different Iodinated Peptide Species

Bart De Spiegeleer[1], Sylvia Van Dorpe[1], and Ewald Pauwels[2]
[1]Drug Quality and Registration (DruQuaR) group, Faculty of Pharmaceutical Sciences, Ghent University, Ghent, 9000, Belgium; [2]Department of Subatomic and Radiation Physics, Faculty of Sciences, Ghent University, Ghent, 9000, Belgium

Introduction

Radio-iodinated peptides are frequently used in biomedical research (*e.g.* blood-brain barrier transport studies) and diagnostic-therapeutic clinical applications. Up till now, only two enzyme systems are known to be responsible for dehalogenation: iodotyrosine deiodinase (IYD) and iodothyronine deiodinase (ID) [1-3]. However, currently, only iodinated amino acids and thyroid hormones have been investigated [4], but no systematic study on the metabolisation of iodinated peptides has been published. It is reported that enzymatic degradation and deiodination occurs *in vitro* as well as *in vivo* [5,6]. Therefore, the *in vitro* stability of different iodinated mouse obestatin peptides was characterised in the main metabolic compartments: plasma, liver and kidney. The degradation kinetics and metabolites of the iodinated obestatin peptides arising from both enzymatic proteolysis and dehalogenation is evaluated.

Results and Discussion

The *in vitro* first order degradation kinetics results obtained on the different iodinated obestatin peptides in different biological matrices using HPLC with UV detection at 195 nm are summarized in Table 1. Although iodine incorporation is considered to potentially hinder peptide breakdown by protease activity, a statistically significant (*i.e.* based upon the 95% confidence intervals) increase in half life time was only observed for (DIP (Tyr))-obestatin in plasma and for (MIP (Tyr))-obestatin in liver homogenate. Several obestatin metabolites arising from proteolytic activity were observed using (tandem) mass spectrometry (Figure 1).

Fig. 1. A graphical overview of the proteolytic cleavages observed at T_{20min} in plasma (left) and liver (right). Significant proteolysis is indicated by ┃, followed by less important cleavage ┆ and least important ┊.

Both in plasma and liver homogenate, the peptide bond between Phe[5] and Asp[6] was found to be more susceptible to proteolytic cleavage for the iodinated peptide with reference to the native peptide. In plasma, the abundance of cleavages near the C-terminus of the sequence (*i.e.* Leu[11] to Leu[23]) was found to decrease upon peptide iodination, *e.g.* Arg[21]-Ala[22]. In liver, a similar effect was observed for the cleavage at Gly[20]-Arg[21], together with an inhibition of the Tyr[16]-Gln[17] peptide bond proteolysis for the two Tyr[16]-iodinated obestatin derivatives.

Table 1. In-vitro metabolic stability half-lives and dehalogenation of iodinated obestatin

Tissue	*Half-life (min) [% dehalogenation]*			
	NIP[a]	*MIP (Tyr)*[b]	*DIP (Tyr)*[c]	*DIP (His)*[d]
Plasma	16.8	14.7 [14.4]	26.9 [59.8]	16.7 [69.3]
Liver	15.7	41.5 [9.2]	14.2 [13.5]	18.4 [37.2]
Kidney	7.0	10.9 [0.0]	18.8 [3.5]	13.2 [2.9]

[a]*NIP = non iodinated peptide*

[b]*MIP (Tyr)= mono-iodinated peptide on the tyrosine residue*

[c]*DIP (Tyr) = di-iodinated peptide on the tyrosine residue*

Additionally, significant dehalogenation was observed for the iodinated derivatives as well, especially for (DIP (His))-obestatin incubated in plasma (Table 1). Iodine atom(s) removal in plasma was found to increase in the following order: MIP (Tyr), DIP (Tyr) and DIP (His). The percentage of peptide degradation solely attributed to deiodinase activity was estimated to reach up to 69.3%, the remainder being proteolysis. *In vitro* dehalogenation was also observed in liver and kidney homogenates, although to a lesser extent when compared to plasma. Especially when the percentage of deiodination was found to be rather high, several metabolites arising from a combination of dehalogenation and proteolysis were observed as well.

In conclusion, this study demonstrated that the pharmacokinetic profile of tyrosine- and histidine-iodinated mouse obestatin derivatives is not only severely compromised through rapid degradation by systemic proteolytic enzymes, but also by dehalogenases. Also, the site-specificity of the proteases is altered by incorporation of iodine atoms. Hence, their use to predict the *in vivo* pharmacokinetics of unmodified peptide is questionable.

Acknowledgments

This research is funded by a PhD grant (no. 73402) of "Agency for Innovation by Science and Technology in Flanders (IWT)".

References

1. Thomas, S.R., McTamney, P.M., Adler, J.M., LaRonde-LeBlanc, N., Rokita, S.E. *J. Biol. Chem.* **284**, 19659-19667 (2009).
2. Friedman, J.E., Watson, J.A., Lam, D.W.H., Rokita, S.E. *J. Biol. Chem.* **281**, 2812-2819 (2006).
3. Dentice, M., Ambrosio, R., Salvatore, D. *Expert Opin. Ther. Targets* **13**, 1363-1373 (2009).
4. Goldberg, E.R., Cohen, L.A. *Bioorg. Chem.* **21**, 41-48 (1993).
5. Solis-S, J.C., Villalobos, P., Orozco, A., Valverde-R, C. *J. Endocrinol.* **181**, 385-392 (2004).
6. Vergote, V., Van Dorpe, S., Peremans, K., Burvenich, C., De Spiegeleer, B. *Peptides* **29**, 1740-1748 (2008).

Proceedings of the 31st European Peptide Symposium
Michal Lebl, Morten Meldal, Knud J. Jensen, Thomas Hoeg-Jensen (Editors)
European Peptide Society, 2010

Rational Design and Optimization of the Newly Designed Glycopeptide Sequence to Develop the Diagnostic/Prognostic Assay for Multiple Sclerosis

Shashank Pandey[1,2], Elisa Peroni[3], Paolo Rovero[1,5], Francesco Lolli[1,4], Mario Chelli[1,2], Anna Maria D'Ursi[6], and Anna Maria Papini[1,2,3]

[1]Laboratory of Peptide & Protein Chemistry & Biology, University of Florence, I-50019, Sesto Fiorentino (FI), Italy; [2]Department of Chemistry "Ugo Schiff" and CNR ICCOM, Via della Lastruccia 3/13, University of Florence, I-50019, Sesto Fiorentino (FI), Italy; [3]Laboratoire SOSCO-EA4505, Universitè de Cergy-Pontoise, Neuville-sur-Oise, F-95031, Cergy-Pontoise, France; [4]Department of Neurological Sciences & Azienda Ospedaliera Careggi, Viale Morgagni 34, University of Florence, I-50134, Firenze, Italy; [5]Department of Pharmaceutical Sciences Via Ugo Schiff 6, University of Florence, I-50019, Sesto Fiorentino (FI), Italy; [6]Deptartment of Pharmaceutical Sciences, University of Salerno, I-84084, Fisciano, Italy

Introduction

Fig. 1. Ribbon diagram of the lowest energy conformer of 50 calculated structures of designed glycopeptide analogs derived from NMR data in micelles of DPC/SDS.

Circulating autoantibodies are interesting biomarkers of patients affected by autoimmune diseases. These specific autoantibodies can be used as diagnostic, prognostic, and theragnostic tools for autoimmune diseases.

In previous studies, we have already demonstrated the ability of an N-glucosylated peptide [i.e., CSF114(Glc)] as an efficient probe to detect, isolate, and characterize autoantibodies as biomarkers of Multiple Sclerosis. In fact, CSF114(Glc) is a simple, reliable, and efficient tool, based on an aberrant N-glucosylation possibly involved in triggering autoantibodies in Multiple Sclerosis [1-4]. This glycopeptide is characterized by a type I′ β-turn surrounding the minimal but fundamental epitope Asn(Glc) that allows an efficient exposure of this moiety for antibody recognition in the context of a solid-phase immunoenzymatic assay [5].

We report herein, how once again a structurally designed glycopeptides could display increased antibody recognition (IgMs and IgGs) compared to CSF114(Glc) in the solid-phase conditions of ELISA on MS patients' sera for the development of MS PepKit (Figure 1).

Results and Discussion

With the aim of optimizing autoantibody recognition in MS patients' sera, we designed a new glycopeptide to develop an efficient MS PepKit. Some fragments of nervous system proteins, containing *N*-glycosylation consensus sequences (Asn-Xaa-Ser/Thr), were selected from SwissProt database. Maintaining Asn(Glc) at position 7 and modifying amino acids sequence to increase homology towards native fragments of nervous system proteins (Table1).

Table 1. Design of the new glycopeptide analogue via primary structure alignment of nervous system protein fragments containing N-glycosylation sites

Neo-peptide epitopes	*Sequences*
[Asn641(Glc)]FAN(635-655)	G I T V S R N G S S V F T T S Q D S T L K
[Asn192(Glc)]]OMgp(186-204)	T L I N L T N L T H L Y L H N N K F T F I
[Asn179(Glc)]]NogoR(173-191)	T F R D L G N L T H L F L H G N R I S S V
CSF114(Glc)	T P R V E R N G H S V F L A P Y G W M V K
Newly designed glycopeptide for MS PepKit	T F R V L R N G T S V F L H P N K W T V K

*The new designed analog appeared to have 9/21, 9/21, 10/21, and 14/21 residues homology with [Asn^{641}(Glc)]FAN(635-655), [Asn^{192}]OMgp(186-204), and [Asn^{179}] NogoR(173-191), and CSF114(Glc) respectively. **N**: Asn(Glc).*

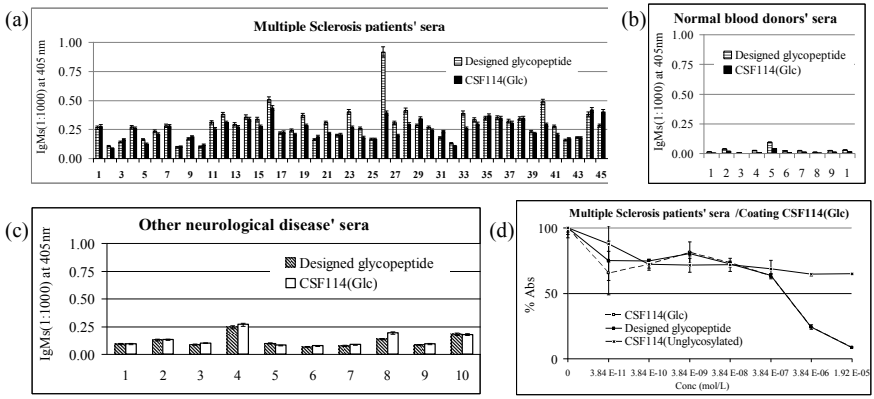

Fig. 2 SP-ELISA of autoantibodies (IgMs) recognition of CSF114(Glc) and designed peptide (Glc) in (a) MS patients' sera. (b) Normal blood donors' sera (c) Other auto-immune sera. (d) Inhibition ELISA of anti-CSF114(Glc) IgGs, designed peptide(Glc) showed IC_{50}=7.6 E-07

The newly designed glycopeptide-based MS PepKit showed increased activity in IgMs recognition in MS patients' sera (SP-ELISA), as well as a competitive ELISA (IC^{50} = 7.6 E-07) using IgGs (Figure 2).

Thus the newly designed glycopeptide appears the most promising diagnostic/ prognostic tool to start the validation in large cohort of Multiple Sclerosis patients under different therapeutic treatments.

Acknowledgments

Italian government scholarship for biotechnology 2008 (India) and MIUR scholarship 2009 (Italy) to S.P. are kindly acknowledged. Moreover we are grateful to Ente Cassa Risparmio di Firenze (Italy) and ANR Chaire d'Excellence 2009-2013 (France) to A.M.P for financial support.

References

1. Papini, A.M., et al. *Granted U.S.A. Patent & PCT WO 03/000733 A2*.
2. Lolli, F., et al. *P.N.A.S.* **102**, 10273 (2005).
3. Lolli, F., et al. *J. Neuroimmuno.* **167**, 131(2005).
4. Papini, A.M. *Nat. Med*. **11**, 13 (2005).
5. Carotenuto, A., et al. *J. Med. Chem*. **51**, 5304 (2008).

Proceedings of the 31st European Peptide Symposium
Michal Lebl, Morten Meldal, Knud J. Jensen, Thomas Hoeg-Jensen (Editors)
European Peptide Society, 2010

Structure-Function Relationships of a Hexapeptide Fragment of the Carcinoembryonic Antigen

Sándor Lovas, Nicholas Y. Palermo, Peter Thomas, and Richard F. Murphy

Department of Biomedical Sciences, Creighton University Medical Center, Omaha, NE, 68178, U.S.A.

Introduction

Carcinoembryonic antigen (CEA), a 180,200 kD glycoprotein, binds to the heterogeneous ribonucleoprotein M (hnRNP M) which acts as a cell surface receptor in Kupffer cells [1]. The binding induces release of inflammatory cytokines and promotes colorectal cancer metastasis to the liver [2]. The amino acid sequence in CEA which binds the hnRNP M receptor is Tyr-Pro-Glu-Leu-Pro-Lys. In this study, the structure-function relationships of Ac-Tyr-Pro-Glu-Leu-Pro-Lys-NH_2 (YPELPK) was investigated by binding of the peptide and its Ala-scan analogs (Table 1) to hnRNP M using molecular docking calculations. Peptides were synthesized at the 0.1 mmol scale on a CEM Liberty microwave peptide synthesizer using N^{α}-Fmoc-protected amino acids. The structure of peptides were determined by 100 ns replica-exchange molecular dynamics (REMD) simulations [3] using the OPLS-AA/L force field [4] as implemented in the GROMACS package [5]. Peptides were docked to the structure of hnRNP M (pbd id 2DGV) using the GLIDE program (Version 4.5, Schrödinger, LLC, New York, NY, 2007). The biological activity of YPELPK and its analogs were studied using differentiated human THP-1 cells, which express hnRNP M on their surface and secrete IL-6 when stimulated by CEA.

Table 1. Relative free energy (ΔG_{rel}) of binding of YPELPK and its Ala-scan analogs

Peptide	*Sequence*	ΔG_{rel} / *kcal mol*$^{-1}$
YPELPK	Ac-Tyr-Pro-Glu-Leu-Pro-Lys-NH_2	0.00[b]
A1[a]	Ac-Ala-Pro-Glu-Leu-Pro-Lys-NH_2	0.80
A2	Ac-Tyr-Ala-Glu-Leu-Pro-Lys-NH_2	0.39
A3	Ac-Tyr-Pro-Ala-Leu-Pro-Lys-NH_2	0.75
A4	Ac-Tyr-Pro-Glu-Ala-Pro-Lys-NH_2	1.11
A5	Ac-Tyr-Pro-Glu-Leu-Ala-Lys-NH_2	3.33
A6	Ac-Tyr-Pro-Glu-Leu-Pro-Ala-NH_2	0.98

[a]*Residues of YPELPK replaced with Ala are indicated in boldface fonts.* [b]*Energies of binding are relative to that of YPELPK. A positive value indicates less binding affinity.*

Results and Discussion

The REMD simulation of the structure of YPELPK folds the peptide into a stable PPII helix conformation, since the trajectory of the simulation has one dominant backbone conformation and 93.4% of the structures belong to a single cluster.

In docking, analogs **A1**, **A2**, **A3** and **A6** have lower affinity for hnRNP M than does YPELPK; the difference in energy is less than 1.0 kcal mol^{-1} (Table 1). **A4** and **A5** have the least affinity for hnRNP M. The best ligand pose for YPELPK (Figure 1) is stabilized by a mix of two hydrogen bonds, two salt bridges and four weakly polar interactions. The binding of YPELPK to the C-terminal region of hnRNP M which does not associate with the cell membrane, indicates that no steric constraints would be imposed on binding. The smaller loss of binding energy, 0.80 kcal mol^{-1} in response to the replacement of the Tyr

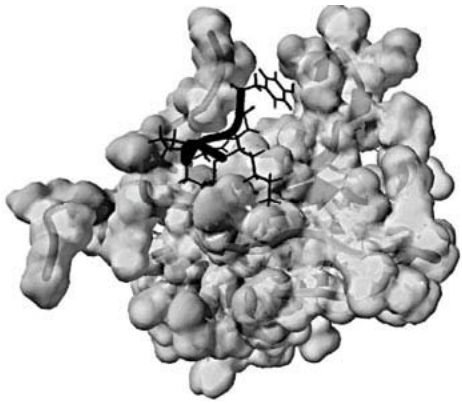

Fig. 1. The best ligand pose of YPELPK (black) with hnRNP M. The van der Waals surface of hnRNP M is in gray.

side-chain in A1, than when the side-chain of Leus and Pro are replaced in A4 and A5, respectively, was unexpected. The Tyr residue participates in a hydrogen bond and two weakly-polar interactions, whereas the Leu and Pro residues in positions 4 and 5 do not have any direct interactions with the receptor. Even replacing the charged side-chains, as in peptides A2 and A6 has less loss of binding energy, 0.39 kcal mol^{-1} and 0.98 kcal mol^{-1}, respectively, than replacing the Leu and Pro residues. Thus, the conformational rigidity given by the Leu and Pro residues seems to be more important to binding than that by other side-chains, although, these may also participate in electrostatic or weakly polar interactions. YPELPK at µM concentrations, significantly increases IL-6 production by differentiated THP-1 cells (Figure 2). The Ala-scan analogs of YPELPK activate THP-1 cells less than the parent peptide. **A1** and **A6**, however, are still able to stimulate IL-6 production (Figure 2). In summary, YPELPK, **A1** and **A6** are biologically active at concentrations low enough that they can be used as core compounds to develop an antagonist of CEA at the hnRNP M receptor.

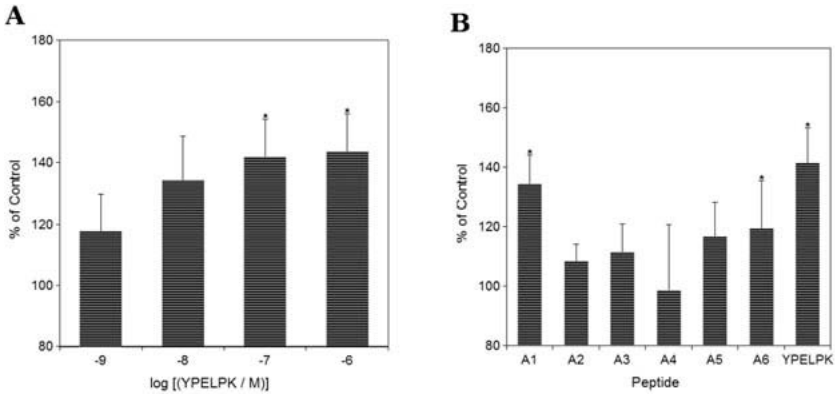

*Fig. 2. IL-6 production of THP-1 cells treated with YPELPK and analogs. **A**, YPELPK; **B**, YPELPK and Ala-scan analogs. Significance of $p < 0.05$ is marked with a *.*

Acknowledgments
This work was supported by the NIH-INBRE grant P20 RR016469.

References

1. Bajenova, O.V., Zimmer, R., Stolper, E., Salisbury-Rowswell, J., Nanji, A., Thomas, P. *J. Biol. Chem.* **276**, 31067-31073 (2001).
2. Gangopadhyay, A., Bajenova, O., Kelly, T. M., Thomas, P. *Cancer Res.* **56**, 4805-4810 (1996).
3. Sugita, Y., Okamoto, Y. *Chem. Phys. Lett.* **314**, 141-151 (1999).
4. Kaminski, G.A., Friesner, R.A., Tirado-Rives, J., Jorgensen, W.L. *J. Phys. Chem. B*. **105**, 6474-6487 (2001).
5. van der Spoel, D., Lindahl, E., Hess, B., Groenhof, G., Mark, A.E., Berendsen, H.J.C. *J. Comput. Chem*. **26**, 1701-1718 (2005).

Proceedings of the 31st European Peptide Symposium
Michal Lebl, Morten Meldal, Knud J. Jensen, Thomas Hoeg-Jensen (Editors)
European Peptide Society, 2010

Tying Up Loose Ends: β Capping Units as Non-covalent Staples for Loops and as a Dynamics Probes

Brandon L. Kier, Irene Shu, Jackson Kellock, and Niels H. Andersen
Department of Chemistry, University of Washington, Seattle, WA, 98195, U.S.A.

Introduction

We recently reported [1] a β capping unit for hairpin structures that increases hairpin fold stabilities by 6 – 9 kJ/mol. As a result, it is now possible to design hairpin folds that are 98+% folded in water at 280 – 300K as measured by backbone NH exchange protection factors. The capping unit consists of an N-terminal Ac-W and a C-terminal WTG(-NH_2) sequence positioned such that the two Trp residues occupy terminal cross-strand positions that are not H-bonded in an antiparallel hairpin alignment. The C-terminal NH_2 is not required for the stabilizing interaction, but the N-terminal acetyl (or, even better, a propanoyl) is essential. The hairpin stabilization is attributed to the synergistic combination of: an edge-to-face W/W indole ring interaction, the acetyl carbonyl forming H-bonds with both the backbone NH and the sidechain hydroxyl of the cross-strand threonine, and hydrophobic burial of a Gly-NH to indole ring H-bond. The latter results in a 3 – 3.5 ppm upfield (ring current) shift of the Gly-NH. In the present account, we apply this "β cap" to longer peptides with a variable length loop connecting two β strands and examine alternative capping motifs. The folding dynamics of the longer peptides provide loop closure kinetics and data which cannot be rationalized by the "turn-formation followed by H-bond zippering" mechanism [2] often assumed for hairpin structure formation.

Results and Discussion

Additional studies regarding the requisites for β cap formation have been performed. As previously noted, deletion of the N-terminal acetyl results in fold destabilizations on the order of 5 – 8 kJ/mol, essentially the full stabilizing increment of the cap. Replacing the acetyl with a glycine or an extended peptide chain is nearly as destabilizing ($\Delta\Delta G$ = 4 – 5 kJ/mol) as acetyl deletion; peptide extension beyond the WTG unit, however, is fully tolerated but mutations at the Thr and particularly the Gly sites in the C-terminal cap were found, in most part, to be highly destabilizing. We have now established that favorable Coulombic interactions can replace the hydrophobic and H-bonding interactions within the cap (*vide infra*).

In our initial *PNAS* article [1] on the β cap we reported the following sequence (Ac-WITVTI-HG-KKIRVWTG-NH_2, with an IHGK β-turn) as a >98.5% folded hairpin and that a folded hairpin (χ_F = 0.57 at 300K) formed even when the -HG- unit was replaced by a long flexible loop (-GGGGKKGGGG-). For the long loop construct, removing the N-terminal acetyl reduced the fractional population of the hairpin state to undetectable levels ($\chi_F \leq 0.08$). The length of the β strands is also an important feature; Ac-WVTI-$G_4K_2G_4$-KKIWTG-NH_2 has a much less stable fold ($\chi_F \approx 0.2$). As a result, a series of constructs of type Ac-WITVTI-loop-KKIRVWTG-NH_2 appeared to be ideally suited for studies of the contact order dependence of folding rates. Two hairpin formation mechanisms have been proposed [2] (Scheme 1); the more commonly cited "turn-nucleation-H-bond-zippering" mechanism should be precluded for long loop constructs making loop search for the formation of the terminal hydrophobic cluster the rate determining process. The Hε3 signal of the Trp in the WTG unit of the cap was upfield by 2 ppm in the folded state due to ring current effects and displayed exchange broadening suitable for NMR dynamics experiments at temperatures for which an equilibrium population of the unfolded state is present. The chemical shift of this probe provides an

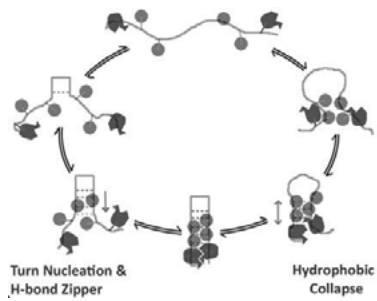

Scheme 1. Two hairpin formation mechanisms.

Table 1. Folding dynamics of Ac-WITVTI-loop-KKIRVWTG-NH_2 peptides at 300K

loop =	*$\delta(H\varepsilon 3)$[a]*	*K_F*	*$1/k_F$ (μs)*	*$1/k_U$ (μs)*	*Entry#*
HG or **p**G	5.66	≥ 60	<1.2	n.d.	
GG	5.69	23.9	3.1	74.1	1
GGGG	6.20	2.57	13.5	34.7	2
GI**p**GKG	5.77	13.2	9.4	124	3
GGGGKKGGGG	6.55	1.33	24.5	32.5	4
GGGI**p**GKGGG	6.01	4.56	14.7	67.0	5

[a]*The Hε3 shifts of the WTG Trp, the edge indole in the EtF interaction, is given; the random coil shift for this proton is 7.58 ppm. Note -* ***p*** *= D-Pro*

accurate measure of χ_F and how this changes with temperature and loop substitutions. Some of the loop substitution that have been examined are, loop, (χ_F at 300K): GGSGSGSG (χ_F = 0.67), GNPDGKG (χ_F = 0.70), GNPATGKG (χ_F = 0.75), and GI**p**GKG (χ_F = 0.93). Additional examples are included in Table 1.

NMR dynamics experiments have been performed for a number of loops; the results appear in Table 1. As expected, longer loops (and thus higher contact order) resulted in slower folding (longer folding times). The changes in K_F and k_U can be rationalized by ΔS considerations. When a tight turn (IpGK) replaced the central four residues of the flexible 10-residue loop (entries #4 and 5), folding sped up by 80% while unfolding was twice as slow. Of some note, the loop search times we observe, even for loops containing stable turn units, are at least 30-fold longer than prior measures [3] of "loop contact times".

Further stabilization of the hairpin-closed loop structure will be required to extend these studies to longer loops. To date two new designs have emerged from our studies; these are compared to the prior construct below (Table 2). The HW - - WE cap serves to demonstrate that the hydrophobic burial contribution within the cap can be replaced by attractive Coulombic interactions. The direct comparison above demonstrates that the HW - - WE cap is more robust than the Ac-W - - WTG cap. The longer hairpin system incorporates a W/W-flanked loop as well as a β cap and is also a more robust folding system; in this case, the two distinct EtF W/W probes may provide differentiation of distinct stages in the folding process.

Table 2. Fractional population of the hairpin state at 320K

Structure	*χ_F*
Ac-WITVTI-G4K2G4-KKIRVWTG-NH_2	0.32
HWITVTI-G4K2G4-KKIRVWE	0.53
Ac-WITVRIW-loop-WKTIRVWTG-NH_2	>0.80

We anticipate that these capped loop structures will be useful for preparing models of biorecognition loops as well as for determining the sequence and length dependence of loop search dynamics.

Acknowledgments
Supported by grants CHE-0650318 (NSF) and GM59658 (NIH).

References

1. Kier, B.L., Shu, I., Eidenschink, L.A., Andersen, N.H. *P.N.A.S. U.S.A.* **107**, 10466-10471 (2010).
2. a) zipper mechanism – Muñoz, V., Henry, E.R., Hofrichter, J., Eaton, W.A. *P.N.A.S. U.S.A.* **95**, 5872-5879 (1998); b) hydrophobic collapse - Dinner, A.R., Lazaridis, T., Karplus, M. *P.N.A.S. U.S.A.* **96**, 9068-9073 (1999); Dyer, R.B., Andersen, N.H., et al. *Biochemistry* **43**, 11560-11566 (2004).
3. a) Lapidus, L.J., et al. *J. Phys. Chem. B* **106**, 11628-11640 (2002); b) Krieger, F., et al. *J. Mol. Biol.* **332**, 265-274 (2003).

Proceedings of the 31st European Peptide Symposium
Michal Lebl, Morten Meldal, Knud J. Jensen, Thomas Hoeg-Jensen (Editors)
European Peptide Society, 2010

Two Short Peptides that Arise in Inflammation Demonstrated Strong Neuroprotective Effects *In Vitro*

Vsevolod G. Pinelis[1], Tatyana N. Storozhevykh[1], Kristina V. Glebova[2], Tatyana N. Danyukova[2], Yana E. Senilova[1], Stanislav I. Schramm[2], and Nikolay F. Myasoedov[2]

[1]Laboratory of Membranology and Genetic Research, Scientific Center for Children Health, Russian Academy of Medical Sciences, Moscow, 119991, Russia; [2]Laboratory of Neuropharmacology, Institute of Molecular Genetics, Russian Academy of Sciences, Moscow, 123182, Russia

Introduction

Several studies have shown that tripeptide *N-acetyl*-Pro-Gly-Pro (*N-acetyl*-PGP) endogenously derived from collagen or other extracellular matrix proteins is an important mediator of inflammation in the lungs [1,2]. This activity is due to the ability of the peptide to activate neutrophils through chemokine receptors CXCR1 and CXCR2 [2]. Another peptide, PGP, also demonstrated chemotactic activity, but weaker than *N-acetyl*-PGP [3]. It is also known that cerebral ischemia progression in the brain leads to matrix metalloproteinases activation and, perhaps, to accumulation of long-living products, especially Pro- and Gly-rich peptides [4]. Meanwhile, we have previously shown that PGP-treatment has a neuroprotective effect after experimental focal brain ischemia in rats [5]. Based on these and some other data, we assume that ischemia-generated PGP-like peptides can be actively involved both in inflammation and neuroprotection through interaction with neuronal or glial CXCR1/2. Thus, in this study we attempted to better understand the nature of revealed neuroprotective effect using various *in vitro* models of neuron damage, as well as cell cultures in which CXCR1/2 expression differs.

Results and Discussion

Two neuronal cell cultures one of which does not express CXCR1/2 (rat pheochromocytoma PC12 cell line) and the other one – well express CXCR1/2 (primary culture of cerebellar granule neurons - CGNs) were used for modeling three different neuron damage mechanisms: 1) oxidative stress-stimulated necrosis (Oxidative stress model - PC12 cells, 1 mM H_2O_2, 30 min); 2) growth factors deprivation-induced apoptosis (Deprivation model - CGNs, B-27 Supplements withdrawal, 24 h); and 3) glutamate receptor hyperactivation (Glu-toxicity model - CGNs, 100 μM Glu, 1 h) resulting in both necrosis and apoptosis.

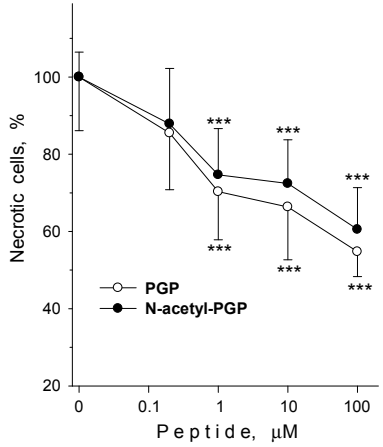

*Fig. 1. Cytoprotective effects of PGP and N-acetyl-PGP on neuronal PC12 cells after H_2O_2-induced oxidative stress. ***p<0.001.*

It was shown that peptides PGP and N-acetyl-PGP in the range of 1-100 μM increased PC12 cells survival after H_2O_2-induced oxidative stress (Figure 1). There were no significant differences in activity of these two peptides at all concentrations used. These data indicate that apart from CXCR1/2 receptors one or more other unknown targets may be involved in neuroprotective effects of PGP-like peptides. Similar protective effect of PGP (100 μM) was observed in CGNs on deprivation model, too (data not shown).

Further we investigated whether PGP influences the cytotoxic effects of Glu on cultured CGNs. Treatment of CGNs with 100 μM Glu for 1 h led to a significant reduction in cell viability and to intracellular Ca^{2+} deregulation (Figures 2A and 2C). As we and other authors

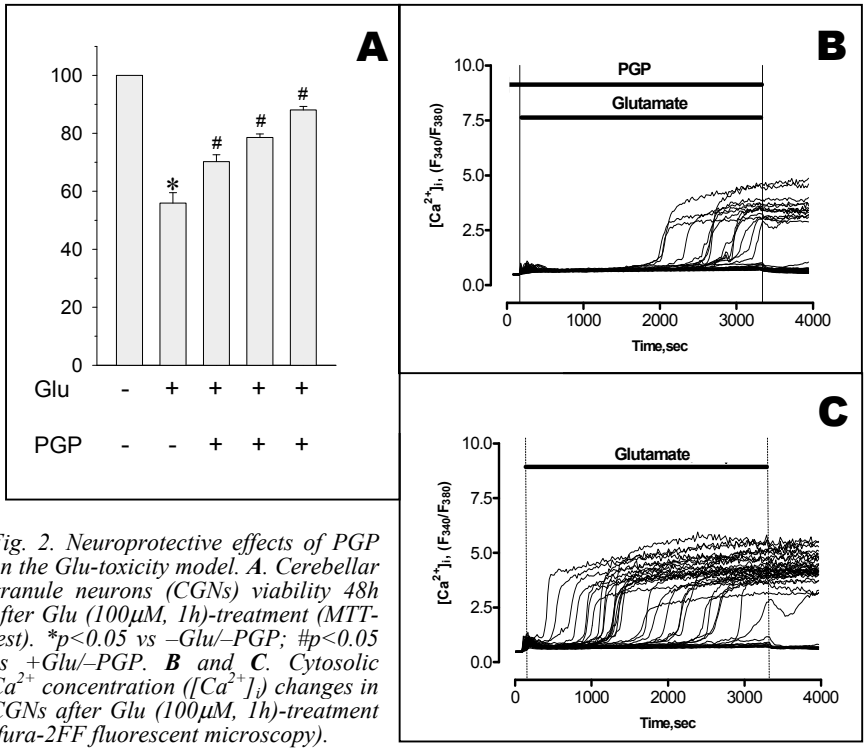

*Fig. 2. Neuroprotective effects of PGP on the Glu-toxicity model. **A**. Cerebellar granule neurons (CGNs) viability 48h after Glu (100μM, 1h)-treatment (MTT-test). *p<0.05 vs –Glu/–PGP; #p<0.05 vs +Glu/–PGP. **B** and **C**. Cytosolic Ca^{2+} concentration ($[Ca^{2+}]_i$) changes in CGNs after Glu (100μM, 1h)-treatment (fura-2FF fluorescent microscopy).*

have shown previously, Glu-treatment causes two rises in cytosolic Ca^{2+} concentration ($[Ca^{2+}]_i$) in CGNs: an initial transient $[Ca^{2+}]_i$ rise that is followed by secondary sustained $[Ca^{2+}]_i$ rise which is referred to as delayed calcium deregulation [6]. As it can be seen in Figure 2B PGP at concentration 100 μM notably delayed calcium deregulation in most CGNs tested. Incubation with 100 μM PGP also increased viability of CGNs after glutamate treatment but the effectiveness of PGP strongly depended on the time of cells incubation with peptide after Glu-treatment (Figure 2A). Moreover, PGP in concentration-dependent manner stimulates neurotrophins (NGF and BDNF) and tyrosine kinase receptors (TrkA and TrkB) mRNA synthesis in cortical neurons (data not shown). Thus, the results obtained indicate that the peptides PGP and *N-acetyl*-PGP under pathological conditions may be involved in the neuroprotective mechanisms, which are triggered in the brain due to various damaging factors.

Acknowledgments

The work has been partly supported by the Russian Foundation for Basic Research (grants 08-04-01760 and 09-04-13813).

References

1. O'Reilly, P.J., et al. *Current Opinion in Pharmacology* **8**, 242-248 (2008).
2. Weathington, N.M., et al. *Nature Medicine* **12**, 317-323 (2006).
3. Haddox, J.L., et al. *Invest. Ophthal. Visual Science* **40**, 2427-2429 (1999).
4. Gasche, Y., et al. *Front Biosci*. **11**, 1289-1301 (2006).
5. Silachev, D.N., et al. *Abstract Book of the Kuopio Stroke Symp. 2007* (Kuopio, Finland, June 6-8, 2007), 2007, p. 18.
6. Khodorov, B.I. *Progress in Biophysics & Molecular Biology* **86**, 279-351 (2004).

Proceedings of the 31st European Peptide Symposium
Michal Lebl, Morten Meldal, Knud J. Jensen, Thomas Hoeg-Jensen (Editors)
European Peptide Society, 2010

Neuroprotective Effect of Short Collagen-Related Peptides and Their Ability to Interact with ACE Reveal Structure-Activity Similarity

Stanislav I. Schramm, Tatyana N. Danyukova, Kristina V. Glebova, Igor Yu. Nagayev, Ludmila A. Andreeva, and Nikolay F. Myasoedov
Laboratory of Neuropharmacology, Institute of Molecular Genetics, Russian Academy of Sciences, Moscow, 123182, Russia

Introduction

Collagen and other similar proteins, both endogenous and exogenous, are a rich source of short peptides mainly consisting of proline, hydroxyproline and glycine residues [1]. It was found that a collagen-rich diet or chronic neutrophilic inflammation both lead to a multifold increase in the level of such short collagen-related (SCR) peptides in the body [2,3]. To date, various effects of naturally occurring and synthetic SCR peptides on cardiovascular, nervous, immune and digestive systems in health and disease have been reported [1,3,4]. However molecular bases of the effects discovered are not yet fully understood. Also it remains unclear whether activities of SCR peptides are mediated by single or diverse molecular target(s). Therefore it is of great importance to compare structure-activity data for SCR peptides obtained on different models and objects. We have previously found out that several SCR peptides are neuroprotective *in vivo* and *in vitro* [5,6]. The aim of this investigation is to identify structure-activity relationships of SCR peptides for both neuroprotective activity *in vitro* and their susceptibility to interact with bovine angiotensin-converting enzyme (ACE) as substrates/inhibitors.

Results and Discussion

Previously we have shown that *C*-terminal amino acid residues in the molecules of SCR peptides provide their neuroprotective effect in a model of oxidative stress-induced neuronal death [5]. On the other hand the nature of *C*-terminal peptide sequence is also important for ACE since this enzyme is a peptidyl dipeptide hydrolase that removes the carboxyl terminal dipeptide from certain oligopeptides. A series of peptides with a specific structure of the *C*-terminus was chosen for this study. One group consisted of peptides with the *C*-terminal sequence Gly-Pro, and another one with Pro-Gly (Table 1).

Neuroprotective activity of SCR peptides has been assessed on the basis of their ability to

Table 1. Neuroprotective activity of SCR peptides and their susceptibility to ACE hydrolysis

Peptide	*Neuroprotective activity*[a]	*Hydrolysis by ACE*[b]*, %*	*Peptide*	*Neuroprotective activity*[a]	*Hydrolysis by ACE*[b]*, %*
Peptides with Gly-Pro C-terminal sequence			*Peptides with Pro-Gly C-terminal sequence*		
GP	+	ND[c]	PG	−	ND
PGP	+	80 ± 3	GPG	+	ND
N-acetyl-PGP	+	100 ± 0	PGPG	−	14 ± 5
GPGP	+	100 ± 0	GPPG	−	18 ± 3
LPGP	ND	100 ± 0	GPGPG	−	ND
FPGP	ND	100 ± 0	PGPGPG	−	ND
RPGP	ND	100 ± 0	*Other peptides*		
PGGP	+	99 ± 2	PGPL	−	13 ± 6
PGPGP	−	ND			
GPGPGP	+	ND			
PGPPGP	−	100 ± 0			

[a] *PC-12 cells were incubated with 1mM H_2O_2 for 30 min; peptide - 1-100 μM.*
[b] *Peptide - 100 μM; ACE - 20 nM; 50 mM HEPES pH 7.5; 18h at 30°C.*
[c] *ND – not determined.*

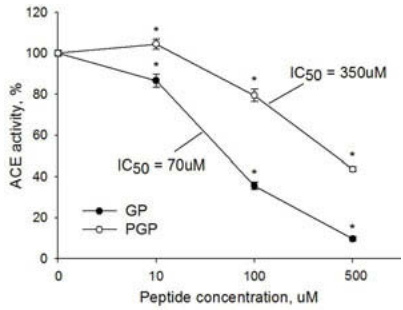

*Fig. 1. Inhibition of ACE by SCR peptides. Assay conditions: ACE - 0.8 nM; hippuryl-His-Leu - 100 μM; 20 min at 30°C. *p<0.01 versus control (Mann-Whithey U-test), n=4.*

increase survival of cultivated PC-12 cells after H_2O_2-induced oxidative stress [5]. It was shown that SCR peptides with *C*-terminal sequence Gly-Pro in the range of 1-100 μM reduced percent of necrotic cells except for PGPGP and PGPPGP (Table 1). Regarding the latter peptides we assumed that the *N*-terminal part of the peptide molecule hinder sterically the "active" *C*-terminal moiety from interaction with a target protein. On the contrary, all peptides with Pro-Gly *C*-terminal sequence did not show any neuroprotective activity except for GPG.

Recently it has been reported that several SCR peptides isolated from enzymatic collagen hydrolysate show a hypotensive effect in spontaneously hypertensive rats due to inhibition of ACE [4]. Therefore we studied several SCR peptides on their ability to interact with bovine ACE as substrates or inhibitors. To determine ACE hydrolysis products HPLC-analysis of dansylated peptides has been performed. After incubation with ACE for 18 hours SCR peptides with Gly-Pro *C*-terminal sequence appeared to break down releasing GP as a major product (Table 1). Meanwhile, peptides PGPG, PGPL, and GPPG were hydrolyzed to a much lesser extent.

Then we investigated inhibition of ACE by two SCR peptides – GP and PGP. It was shown that GP reduced ACE activity in a dose-dependent manner assuming competitive type inhibition with IC_{50} about 70μM (Figure 1). Peptide PGP demonstrated similar but weaker effect (IC_{50} about 350μM; Figure 1), whereas tetrapeptides PGPG, PGPL, and GPPG did not show any inhibitory activity (data not shown).

The data represented here suggest that *C*-terminal sequence Gly-Pro is crucial for SCR peptide neuroprotective activity as well as for its binding with ACE. The smallest peptide exhibiting both neuroprotective and ACE-inhibitory activity was GP. Similar results were obtained in the study of protective antistress effects of SCR peptides [7]. On the contrary, only PGP and its *N*-substituted analogs, but not PG or GP, demonstrated chemotactic activity for neutrophils [8]. However it is difficult to perform a deeper comparative analysis of structure-activity relationships for SCR peptides because of lack of experimental data. Nevertheless, on the basis of currently available data we can assume that peptides with *C*-terminal Gly-Pro sequence specifically interact with a variety of molecular targets, and therefore have a number of diverse biological activities. Thereby, *C*-terminal Gly-Pro sequence seems to be a short pharmacophore of biologically active SCR peptides, and production of more stable peptidomimetics based on GP dipeptide may be successful. In addition *N*-terminal modification of GP dipeptide is expected to be an approach for designing new substances with directed biological effects.

Acknowledgments

This study was supported by the Russian Foundation for Basic Research (Grants No. 08-04-01760 and 09-04-013813).

References

1. Samonina, G., et al. *Pathophysiology* **8**, 229-234 (2002).
2. Ichikawa, S., et al. *Int. J. Food Sci. Nutr.* **61**, 52-60 (2010).
3. Gaggar, A., et al. *J. Immunol*. **180**, 5662-5669 (2008).
4. Ichimura, T., et al. *Biosci. Biotechnol. Biochem*. **73**, 2317-2319 (2009).
5. Martynova, K.V., et al. *Bioorg. Khim. (Rus.)* **35**, 165-171 (2009).
6. Silachev, D.N., et al. *Abstract Book of the Kuopio Stroke Symp. 2007*, Kuopio, Finland, 2007, p.18.
7. Badmaeva, S.E., et al. *Neurosci. Behav. Physiol.* **36**, 409-413 (2006).
8. Haddox, J.L., et al. *Invest. Ophthalmol. Vis. Sci.* **40**, 2427-2429 (1999).

Proceedings of the 31st European Peptide Symposium
Michal Lebl, Morten Meldal, Knud J. Jensen, Thomas Hoeg-Jensen (Editors)
European Peptide Society, 2010

Design and Synthesis of Guanidinium-Rich Molecular Transporters for Drug Delivery

Tatyana Dzimbova[1], Kaloyan Georgiev[2], and Tamara Pajpanova[1]
[1]Institute of Molecular Biology, Bulgarian Academy of Sciences, Sofia, Bulgaria; [2]Medical University of Varna, Faculty of Pharmacy, Varna, Bulgaria

Introduction

For many therapeutic applications, it has become more important to find synthetic compounds that have ability to transport a variety of drugs and cargo molecules into cells and tissues.

Microscopic studies revealed that oligoarginines and other arginine-rich peptides are efficiently taken up by cells. The molecule with the highest efficiency turned out to be octaarginine, whereas peptides of < 5 and >12 arginine residues showed only negligible translocation. A direct comparison of nonamers composed of arginine, histidine, lysine or ornithine revealed that arginine residues were most effective in penetrating the plasma membrane because of their guanidinium group [1]. It was also shown that some branched oligoarginines exhibited potent *in vivo* antiangiogenic activity and powerful *in vitro* angiogenesis inhibition of basic fibroblast growth factor (bFGF)-stimulated proliferation. These results suggest that arginine oligomers may be a useful tool for angiogenic diseases.
To evaluate this hypothesis, a series of octamers were prepared that incorporated arginine mimetics with either, oxy- or sulfoguanidino side chain (Figure 1). In addition lysine oligomers were also synthesized.

Further antiproliferative and cytotoxic potential of the forming amino acid analogues were examined in a panel of human tumor cell lines, as well as against VEGF-stimulated human umbilical vein endothelial cells (HUVECs).

Results and Discussion

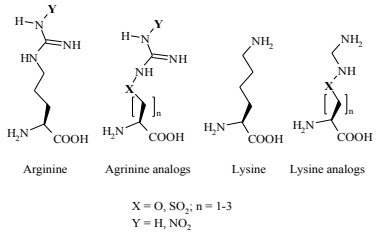

*Fig. 1. Arginine and lysine analogs (**Cav**: X=O, n=2; **NCav**: X=O, n=1; **sArg**: X=SO_2, n=2; **NsArg**: X=SO_2, n=1; **NNC**: X=O, Y=NO_2, n=2; **NNA**: Y=NO_2).*

Synthesis

Peptide oligomers $(Cav)_8$, $(NCav)_8$, $(sArg)_8$ and $(sLys)_8$ were obtained by conventional Fmoc solid phase chemistry on a Rink-amide resin with DIC/HOBt activation. Amino acids, Fmoc-Cav(Boc)-OH, Fmoc-Cav(NO_2)-OH, Fmoc-NCav-OH, Fmoc-sArg(Boc)-OH and Fmoc-sLys(Boc)-OH were synthesized as previously described with minor modification [2-4]. The Fmoc moiety was deprotected by 20% piperidine/DMF and the activation was catalyzed with NMP/DMF (0.4 M) for each cycle. The crude peptides were purified by C18 reverse-phase MPLC and their purity was checked by analytical HPLC. Electro-spray MS were in agreement with the expected results.

Antiproliferative and cytotoxic determination

The cytotoxic activity of compounds **Cav, NNC, NNA and NsArg** was studied in a panel of human tumor cell lines, as follows: HL-60 (acute myeloid leukemia), K-562 and LAMA-

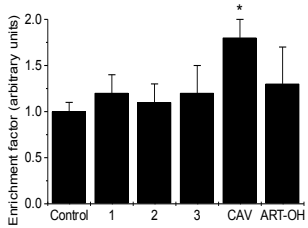

*Fig. 2. Enrichment of the cytosole of HUVECs with mono and oligonucleosomal DNA-fragments after treatment with compounds **NNC** (1), **NNA** (2), **NsArg** (3), and **Cav** (at 500 μM) or ART-OH (at 50 μM), as assessed by a "Cell Death Detection" ELISA kit. The asterisk indicates $p<0.05$ vs the untr. Control (Student t-test).*

84 (chronic myeloid leukemia), SKW-3 (human T-cell leukemia), HD-MY-Z (Hodgkin lymphoma), DOHH-2 (non-Hodgkin lymphoma), 5637 and EJ (human urinary bladder carcinoma). The effects were assessed by the MTT-dye reduction assay in a wide concentration range (1-500 μM) with varying the exposure periods (24, 48, 72 or 96 h). The reference angiostatic drug thalidomide (THAL) and the sesquiterpene lactone hydroxyartemisinine (ART-OH) (with established anticancer and antiangiogenic effects) were used as positive controls throughout the study (Table 1). The tested arginine analogues demonstrated only marginal effects and failed to cause 50% inhibition of cellular viability even after 3 days exposure.

Table 1. Antiproliferative effects of the tested compounds against a spectrum of human tumor cell lines, as assessed by the MTT-dye reduction assay

Cell lines	*IC_{50} values (μM)*									
	NNC		NNA		NsArg		CAV		THAL	ART-OH
	72 h	*96 h*	*72 h*	*96 h*	*72 h*	*96 h*	*72 h*	*96 h*	*72 h*	*72 h*
K-562	>500	>500	>500	>500	>500	>500	>500	>500	85	>100
HL-60	>500	>500	>500	>500	>500	>500	>500	>500	39	>100
HD-MY-Z	>500	>500	>500	>500	>500	>500	>500	>500	70	>100
DOHH-2	>500	>500	>500	>500	>500	>500	>500	>500	47	>100
5637	>500	>500	>500	>500	>500	>500	>500	>500	29	>100
EJ	>500	>500	>500	>500	>500	>500	>500	>500	90	>100

"Cell Death Detection" ELISA

In order to elucidate the mechanisms underlying the angiostatic effects of tested compounds we analyzed their propensity to induce apoptosis in VEGF-stimulated HUVEC (Figure 2). To meet this objective we assessed the oligonucleosomal fragmentation of DNA in treated vs non-treated cells after 24 h exposure at concentrations higher than TGI. Compounds **NNC, NNA** and **NCMe** did not trigger apoptosis, which is in line with the MTT-data showing lack of cytotoxic effects. Some increase of the level of histone associated DNA-fragments was evoked only with **CAV**, which indicates that the induction of apoptosis is at least partly implicated in the observed cytotoxic effects against VEGF-stimulated HUVEC.

In conclusion we could say that new polyarginines were synthesized. The abnormal proliferative activity of vascular endothelium is a crucial event in tumor-induced angiogenesis. The preliminary screening for antiproliferative and cytotoxic effects of tested building amino acids against a spectrum of six human cell lines revealed that the established inhibitory activity, together with the low cytotoxicity, give us reason to consider these compounds as prospective leads for development of antiangiogenic agents.

Acknowledgments

We are grateful to the the Bulgarian Ministry of Education and Science and NFSR of Bulgaria (Contract MY-FS-13-07).

References

1. Tung, C., Weissleder, R. *Adv. Drug Delivery Rev*. **55**, 281-294 (2003).
2. Pajpanova, T., Stoev, S., Golovinsky, E., Krauss, G.-J., Miersch, J. *Amino Acids* **12**, 191-204 (1997).
3. Videnov, G., Aleksiev, B., Stoev, M., Pajpanova, T., Jung, G. *Liebigs Ann. Chem*. 941-945 (1993).
4. Dzimbova, T., Pajpanova, T., Tabakova, S., Golovinsky, E. In: *5th Hellenic Forum on Bioactive Peptides*, TYPORAMA, Greece, Cordopatis P. (Ed.) 223-227 (2007).

Proceedings of the 31st European Peptide Symposium
Michal Lebl, Morten Meldal, Knud J. Jensen, Thomas Hoeg-Jensen (Editors)
European Peptide Society, 2010

Synthesis and Biological Evaluation of Daunorubicin-GnRH-III Prodrug

Rózsa Hegedüs[1], Erika Orbán[1], Ildikó Szabó[1], Marilena Manea[2,3], and Gábor Mező[1]

[1]Research Group of Peptide Chemistry, Hungarian Academy of Sciences, Eötvös L. University, Budapest, Hungary, [2]Laboratory of Analytical Chemistry and Biopolymer Structure Analysis, Department of Chemistry, University of Konstanz, Konstanz, Germany; [3]Zukunftskolleg, University of Konstanz, Konstanz, Germany

Introduction

Tumor targeting with the decapeptide gonadotropin-releasing hormone (GnRH) or its analogs is based on the discovery that GnRH receptors are highly expressed in many tumor cells (e.g., prostate, ovarian, breast, endometrial), compared with their expression in normal tissues. Therefore, these peptides could be used as carriers/targeting moieties to which therapeutic agents are attached leading to the formation of conjugates with increased selectivity and lower toxic side effects. The lamprey GnRH-III (<EHWSHDWKPG-NH_2, where <E is pyroglutamic acid) is especially suitable as a targeting moiety because of its antiproliferative effect and weak endocrine activity in mammals.

The anthracycline antibiotic daunorubicin (Dau) is an effective anticancer drug; however, its use is limited by severe cardiotoxicity. Dau can be conjugated through the amino group of the sugar moiety or through the oxo group on the 13C atom of the aglycon part [1,2]. However, the free amino group might be essential for the biological activity. Therefore, an enzymatic cleavable spacer should be incorporated between the amino group of the drug and the targeting moiety. It is known that Cathepsin B, a lysosomal enzyme overexpressed in cancer cells, cleaves peptide bonds in sequences such as ALAL, LALARR, YRRL, GFLG [3,4], that can be used as spacers.

Results and Discussion

Four new prodrug conjugates (Figure 1) were synthesized in which daunorubicin was attached to a GnRH-III derivative through different types of Cathepsin B cleavable peptide

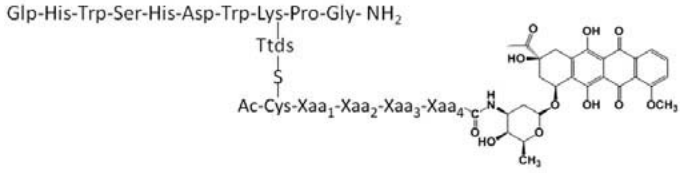

Fig. 1. GnRH-III(Dau-spacer) conjugates.

spacers (Ac-Cys-Xaa_1-Xaa_2-Xaa_3-Xaa_4 = Ac-CYRRL-COOH, Ac-CGGFL-COOH, Ac-CALAL-COOH, Ac-CGFLG-COOH). The peptides were synthesized manually by SPPS: the spacer sequences using Boc/Bzl strategy on Merrifield resin, while the chloro-acetylated GnRH-III-Ttds [5] carrier molecule by Fmoc/tBu strategy on Rink Amide

Table 1. In vitro antitumor activity of Daunorubicin-spacer-GnRH-III-Ttds conjugates IC50 values in μM determined by MTT assay

compounds / cells	GnRH-III-Ttds-(Dau-AcCYRRL)	GnRH-III-Ttds-(Dau-AcCGGFL)	GnRH-III-Ttds-(Dau-AcCALAL)	GnRH-III-Ttds-(Dau-AcCGFLG)
HT-29 human colon	19.2± 1.1	85.0±7.0	> 100	21.2±0.5
MCF-7 human breast	5.6±1.9	15.8±3.5	> 100	15.8±2.2

IC50 values for Daunorubicin are 0.1-0.3 μM on MCF-7 cells and 1-5 μM and HT-29 cells

Table 2. Enzymatic Digestion of GnRH-III(Dau-spacer) conjugates by Cathepsin B

a, GnRH-III-Ttds(Ac-CALAL-Dau)

Fragment	MW (calc)	MW (exp)
<EHWSHDWK-[Ttds-(Ac-CGFLG-Dau)]PG-NH_2	2648.6	2649.4
H-K-[Ttds-(Ac-CGFLG-Dau)]PG-NH_2	1690.6	1690.8
<EHWSHDWK-[Ttds-(Ac-CG)]PG-NH_2	1822.8	1823.4
H-FLG-Dau + Na^+	868.1	867.7
H-FLG-Dau	846.2	846.1

b, GnRH-III-Ttds(Ac-CGGFL-Dau)

Fragment	MW (calc)	MW (exp)
<EHWSHDWK-[Ttds-(Ac-CALAL-Dau)]PG-NH_2	2643.2	2643.6
H-K-[Ttds-(Ac-CALAL-Dau)]PG-NH_2	1684.6	1684.0
<EHWSHDWK-[Ttds-(Ac-CA)]PG-NH_2	1838.0	1838.2
H-LAL-Dau	826.2	826.5

MBHA resin. Daunorubicin was conjugated to the spacers *via* amide bond, while the spacer sequences were attached to the GnRH-III peptide *via* thioether bond. The peptides and the conjugates were purified by semi-preparative RP-HPLC and characterized by analytical RP-HPLC and mass spectrometry.

Racemization was observed at the conjugation of spacer molecules containing Leu at their C-terminus.

The influence of the spacer sequences on the *in vitro* antitumor ativity of the conjugates was investigated on MCF-7 human breast and HT-29 human colon cancer cells by MTT assay (Table 1).

The drug release from the amide bond-linked GnRH-III(Dau-spacer) conjugates was determined in the presence of Cathepsin B. In case of conjugates GnRH-III-Ttds-(Dau-AcCGFLG) and GnRH-III-Ttds-(Dau-AcCALAL), the smallest metabolites were Dau containing tripeptides (*H*-LAL-Dau, *H*-FLG-Dau). The GnRH-III-Ttds-(Dau-AcCGFLG) conjugate degraded in the highest rate, followed by the GnRH-III-Ttds-(Dau-AcCALAL).

No significant cleavage was observed in case of GnRH-III-Ttds-(Dau-AcCGGFL). The GnRH-III-Ttds-(Dau-AcCYRRL) conjugate has not been analyzed yet. Free Dau was not detected in the digestion mixtures.

Degradation of the bioconjugates in lysosomal homogenates will be performed. Further experiments are needed to determine the correlation between the cytostatic effect and the metabolites.

Acknowledgments

The authors thank to Hedvig Medzihradszky-Schweiger PhD, C.Sc. This study was supported by grants from the Hungarian National Science Fund (OTKA NK77485, F 67884, K 81596), the University of Konstanz (Zukunftskolleg, Project 879/08) and GVOP-3.2.1.-2004-04-0005/3.

References

1. Mező, G., et al. *Collection Symposium Series* **11**, 72-76 (2009).
2. Szabó, I., et al. *Bioconjug. Chem.* **20**, 656-665 (2009).
3. Calderon, M., et al. *Bioorg. Med. Chem. Lett.* **19**, 3725-3728 (2009).
4. Ajaj, K.A., et al. *Cancer Chemother. Pharmacol*. **64**, 413-418 (2009).
5. Bartos, Á., et al. *Biopolymers* **92**, 110-115 (2009).

Proceedings of the 31st European Peptide Symposium
Michal Lebl, Morten Meldal, Knud J. Jensen, Thomas Hoeg-Jensen (Editors)
European Peptide Society, 2010

[Tc(N)PNP] Metal Fragment Labeled Peptide for MC1 Receptors Imaging: Preliminary Studies

Barbara Biondi[1], Cristina Bolzati[2], Davide Carta[3], Nicola Salvarese[3], Fiorenzo Refosco[2], Andrea Calderan[1], and Paolo Ruzza[1]

[1]Institute of Biomolecular Chemistry of CNR, Padova Unit and Department of Chemical Sciences, University of Padova, Padova, 35131,Italy; [2]Institute of Inorganic Chemistry and Surfaces of CNR, Padova, 35020, Italy; [3]Department of Pharmaceutical Sciences, University of Padova, Padova, 35131, Italy

Introduction

Malignant melanoma is the most lethal form of skin cancer: melanoma metastases are very aggressive and no curative treatment exists for it due to its resistance to chemotherapy and immunotherapy regimens. Therefore, development of new melanoma-specific radiopharmaceuticals for early detection of primary melanoma tumours or internal radiotherapy is a subject of great interest. In this perspective, melanocortin type-1 receptors (MC1R) represent a promising target for the development of effective molecular probes for diagnosis or therapy. MC1R are overexpressed on the surface of melanoma cells and able to selectively recognise the peptide sequence His-D-Phe-Arg-Trp mimicking the melanocyte stimulating hormone (αMSH). The literature described several linear and cyclic radiolabeled αMSH analogues. In particular, the introduction of a cyclic constraint in a lead peptide restricts the flexibility and may favour peptide–receptor interactions, receptor selectivity and enzymatic stability [1].

In this work we synthesised linear and cyclic NAPamide analogues (Figure 1), in order to improve their affinity toward MC1R and to be used as ligands in the formation of ^{99m}Tc complexes with the $[^{99m}Tc(N)(PNPn)]^{2+}$ metal fragment [2]. We investigated the *in vitro* stability in phosphate buffer solutions (PBS), in cysteine and glutathione solutions as well as in rat liver (RLH) and kidney homogenates (RKH). Biodistribution studies were performed in female Sprague Dowley (S.D.) rats with $[^{99m}Tc(N)(NAP\text{-}NS1/2)(PNPn)]^{+}$ in order to evaluate their organ uptake and excretion pathways.

Results and Discussion

Peptides were synthesised according to standard Fmoc/tBu method using HBTU/HOBt as C-activation procedure. The Ahx-βAla sequence was conjugated to the N-terminus of both peptides as a spacer between the radiolabeled moiety and the binding region to avoid interference between the different portions of the molecule, while Cys residue is involved in complex formation. NAP-NS2 cyclization was performed on resin, using a Pd-mediated deprotection of Alloc/Allyl protecting groups of Lys[4] and Glu[10], respectively [3]. After HPLC purification, peptides were obtained in good yields with a purity >98%.

NAP-NS1: H-Cys-Ahx-βAla-Nle-Asp-**His-D-Phe-Arg-Trp**-Gly-Val-NH_2

NAP-NS2: H-Cys-Ahx-βAla-c[Lys-Glu-**His-D-Phe-Arg-Trp**-Glu]-Arg-Pro-Val-NH_2

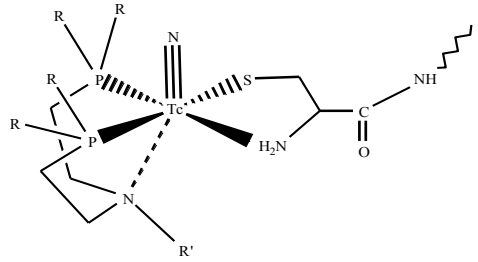

Fig. 1. Peptide sequences and structure of complexes.

The $[^{99m}Tc(N)(peptide)(PNPn)]^{+}$ complexes were prepared using two different methods. The first method is a two-step procedure: 1) the ^{99m}Tc–nitrido precursors $[^{99m}Tc{\equiv}N]^{2+}$ was prepared by reaction of $Na^{99m}TcO_4$ (50.0 MBq-3.0 GBq) with succinic dihydrazide (SDH), $SnCl_2$ and ethanol in 30 minutes at room temperature; 2) the PNPn ligand and NAP-NS1/2 were simultaneously added to $[^{99m}Tc{\equiv}N]^{2+}$, and the reaction mixture was heated at 80°C for

30 min at pH 7. Radiochemical yields (RCYs), as determined by TLC and HPLC chromatography, were around 90%.

The second method is a one-step procedure: $Na^{99m}TcO_4$ (50.0 MBq-3 GBq) was added to a vial containing SDH, $SnCl_2$, ethanol, NAP-NS1/2 and PNPn. RCYs determined by TLC and HPLC, after 60 min at 80 °C, were around 90%.

The $[^{99m}Tc(NNAP\text{-}NS1/2)(PNPn)]^+$ complexes isolated by HPLC were concentrated on a Sep Pack C18 column rinsed with H_2O and eluted using a mixture of EtOH/phosphate buffer 0.2 M, pH 7.4, 80/20. The second fraction containing all the activity was utilized for *in vitro* and *in vivo* studies. After purification, radiochemical purities (RCPs) evaluated by TLC and HPLC were > 90% [4].

The *in vitro* stability of the complexes was evaluated by transchelation experiments in presence of cysteine and glutathione solutions, at 37°C for 24 hours. At fixed times aliquots of the reaction mixture were withdrawn and the RCPs analysed by TLC and HPLC. We also assessed the *in vitro* stability monitoring the RCPs at different time points in presence of human serum (HS), rat serum (RS) and in rat liver and kidney homogenates (RLH, RKH). Complexes evidenced a good stability in challenge experiments and in human and rat sera while a partial degradation was observed in homogenates. Biodistribution studies were performed in healthy female S.D. rats with $[^{99m}Tc(N)(NAP\text{-}NS1/2)(PNPn)]^+$ to investigate their organ uptake and excretion pathways. Complexes present an extremely fast elimination from the blood and from significant organs; the renal excretion was extremely rapid and the activity was manly eliminated through the urinary tract.

NAP-NS1/2 were also tested for their affinity toward MC1R overexpressed on B16 murine melanoma cells. Cells were incubated in Avidin-ITC and the fluorescence intensity measured at increasing peptide concentration. Jurkat Human lymphoma cells were used as a reference. Peptides evidenced a selective binding to B16 melanoma cells (Figure 2).

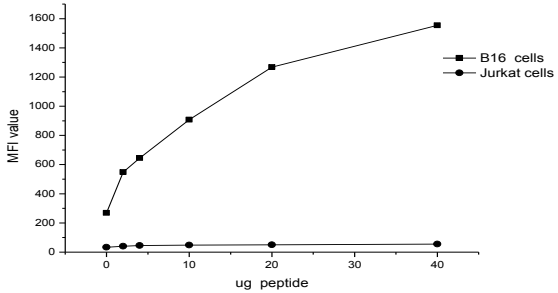

Fig. 2. Binding of NAP-NS1 toward B16 cells.

Future studies will be focused on the evaluation *in vitro* and *in vivo* of the ^{99m}Tc-complexes binding affinities in B16 melanoma cell line.

Acknowledgments
Supported by the Italian MIUR grant PRIN 2008 (2008F5A3AF_002).

References

1. Bolzati, C., et al. *Current Medicinal Chemistry* **17**, 2656-2683 (2010).
2. Cheng, Z., et al. *Bioconjugate Chem.* **18**, 765-772 (2007).
3. Grieco, P., et al. *J. Peptide Res.* **57**, 250-256 (2001).
4. Agostini, S., et al. *J. Pept. Sci.* **13**, 211-219 (2007).

Proceedings of the 31st European Peptide Symposium
Michal Lebl, Morten Meldal, Knud J. Jensen, Thomas Hoeg-Jensen (Editors)
European Peptide Society, 2010

Kinetic Studies on Cellular Uptake of Polyarginine Peptide Using FRET

Akihiro Ambo, Yasuyuki Suzuki, Motoko Minamizawa, and Yusuke Sasaki

Department of Biochemistry, Tohoku Pharmaceutical University, Sendai, 9818558, Japan

Introduction

Cell-penetrating peptides (CPPs) are known to be able to pass through the plasma membrane and are used as tools for delivery of hydrophilic molecules such as peptides, proteins, and oligonucleotides [1]. Endocytic mechanisms involving clathrin-mediated, caveolae-mediated, macropinocytosis, or a non-endocytic mechanism involving direct translocation have been suggested for cellular uptake of CPPs in live cells [2]. In either uptake mechanism, the cationic portion of CPPs is thought to initially interact with anionic substances present at the extracellular surface of the plasma membrane, such as proteoglycans. However, their transport mechanisms are still not clearly understood.

In the present study, we attempted to determine the cellular uptake of CPPs into cells using conjugated peptides by the fluorescence resonance energy transfer (FRET) technique. The FRET-peptide consists of FAM-Gab-Cys-(cargo or CPP)-NH_2 and Dabcyl-Gab-Cys-(CPP or cargo)-NH_2, which are covalently linked via an S-S bond (Table 1). The use of FRET-peptides has the advantage that undelivered peptides do not need to be removed from cells during the cellular uptake determination, and thus minimizes artifacts arising from incomplete washing of the undelivered peptide. We kinetically examined the cellular uptake of conjugated FRET-peptides into Jurkat cells under different incubation conditions by FACS analysis.

Table 1. Sequences of FRET-peptides

Abbr.	*Sequences*	*TOF-MS (m/z, $M+H^+$)*	
		found	*calcd.*
FRET-CR9	Dabcyl-Gab-Cys-$(Arg)_9$-NH_2 | FAM-Gab-Cys-His-His-NH_2	2698.95	2698.35
rev-FRET-CR9	FAM-Gab-Cys-$(Arg)_9$-NH_2 | Dabcyl-Gab-Cys-His-His-NH_2	2698.93	2698.35
FRET-CDR9	Dabcyl-Gab-Cys-$(Arg)_6$-D-Arg-$(Arg)_2$-NH_2 | FAM-Gab-Cys-His-His-NH_2	2698.77	2698.35

Results and Discussion

We designed and synthesized three FRET-peptides as listed in Table 1. Cys-His-His-NH_2 was employed as the cargo, which itself is not able to pass across the plasma membrane (data not shown). The conjugate peptides did not emit fluorescence due to quenching of the FAM group by the Dabcyl group, but after reduction with 1 mM glutathione, which exists abundantly in the cytosol, equally high fluorescence was measured with FRET-CR9 and rev-FRET-CR9. As shown in Figure 1, intracellular fluorescence intensities of three FRET-peptides rapidly increased for up to 15 min and then decreased after prolonged periods. The permeability of FRET-CDR9 was high, at least 1.4-fold better than that of

FRET-CR9. The efficiency of FRET-CDR9 may be due to improved resistance against degradative enzymes. Figure 2 shows the confocal microscope images of cells treated with FRET-CDR9. The time-course results coincided well with that of cellular uptake (Figure 1).

When cellular uptake was examined by FACS using FRET-CDR9 at 4°C, a slight intracellular fluorescence was detected. Interestingly, when cells were incubated at 20°C or hyperthermia-treated cells (42°C for 1 h) were used, uptake of FRET-CDR9 increased linearly, and the decrease of fluorescence intensity was not observed. From these results, it is most likely that the decrease of intracellular fluorescence after a prolonged time (~90 min) is attributable to elimination by exclusion processes such as exocytosis or metabolism.

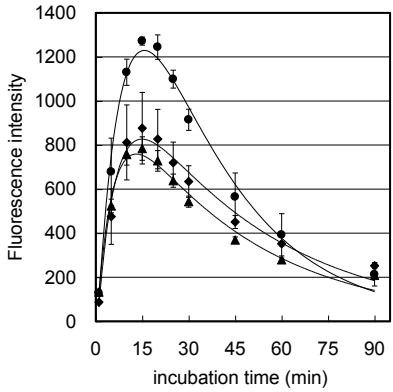

Fig. 1. Cellular uptake of FRET-peptides in Jurkat cells. Cells were incubated at 37°C with FRET-CR9 (▲), rev-FRET-CR9 (◆) and FRET-CDR9 (●).

The cellular uptake of FRET-CDR9 was effectively inhibited by the macropinocytosis inhibitor, EPIA (50 μM), but not by chlorpromazine (30 μM) which is an inhibitor of clathrin-mediated endocytosis. Under conditions of 10% FBS (but not FBS free conditions), methyl-β-cyclodextrin (2 mM) inhibited the cellular uptake. These results suggest that the FRET-peptide was delivered into cells mainly via a macropinocytosis mechanism, and partially via caveolae-mediated endocytosis. Under the FBS-free conditions, non-endocytic direct translocation would partially participate in cellular uptake of the FRET-peptide.

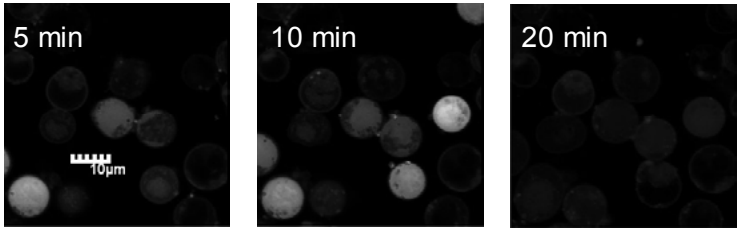

Fig. 2. Confocal microscopic appearance of FRET-CDR9 (5 μM) internalization at 37°C. Jurkat cells were incubated in 10% FBS/RPMI-1640 under 5% CO_2. The fluorescence signals were detected by excitation at 499 nm using a 519 nm emission filter.

Conclusion

In conclusion, the present study demonstrated the utility of FRET-nonaarginine peptides, especially FRET-CDR9, to investigate mechanisms of cellular uptake of oligoarginine peptides. The FRET-peptide was delivered into Jurkat cells efficiently. Kinetic studies using FRET-CDR9 revealed that fluorescein-labeled cargo peptide was delivered mainly by macropinocytosis into the cells. The intracellularly delivered peptides are probably excluded from cells or metabolized after prolonged periods.

References

1. Fonseca, S.B., Pereira, M.P., Kelley, S.O. *Adv. Deliv. Rev.* **61**, 953-964 (2009).
2. Schmidt, N., Mishra, A., Lai, G.H., Wong, G.C. *FEBS Lett.* **584**, 1806-1813 (2010).

Proceedings of the 31st European Peptide Symposium
Michal Lebl, Morten Meldal, Knud J. Jensen, Thomas Hoeg-Jensen (Editors)
European Peptide Society, 2010

Synthesis and *In Vitro* Antitumor Activity of New Daunomycin Containing GnRH-II Derivatives

Ildikó Szabó, Erika Orbán, Szilvia Bősze, and Gábor Mező
Research Group of Peptide Chemistry, Hungarian Academy of Sciences, Eötvös L. University, Budapest, Hungary

Introduction

Two isoforms of GnRH exist in humans, namely GnRH-I and GnRH-II [1]. The hypothalamic decapeptide gonadotropin-releasing hormone (GnRH-I; <EHWSYGLRPG-NH_2, where <E is pyroglutamic acid) is the central regulator of reproductive system through the stimulation of luteinizing hormone (LH) and follicle-stimulating hormone (FSH) from pituitary gonadotropes. The exact function of GnRH-II (<EHWSHGWYPG-NH_2) is unknown, but it may play a role in the maturation of sexual behaviour, the regulation of gonadotropin secretion and in the immunological process [2-4]. It was also indicated recently, that GnRH-II derivatives have more potent antiproliferative activity on human endometrial and ovarian cancer cell cultures *in vitro* than GnRH-I analogs [5]. Some types of tumor cells (e.g. breast, prostate, colon) produce both GnRH-I and GnRH-II, furthermore, their receptors are also expressed [6,7]. However, the presence of functionally active GnRH-II receptors on cancer cells is still not clear.

Our aims were to synthesize new GnRH-II derivatives and their conjugates with daunomycin as antineoplastic agent. We wanted to investigate cytostatic effect and cellular uptake of the drug molecule and daunomycin containing GnRH-II conjugates on MCF-7 (human breast adenocarcinoma cell culture) and HT-29 (human colon adenocarcinoma cell culture). We planned to determine the cytotoxicty of the GnRH-II conjugates on HepG2, human liver cancer cell culture.

Results and discussion

The sythesis of [D-Lys^6]GnRH-II, which is one of the most potent GnRH-II agonist, was carried out on solid phase using Fmoc/^{t}Bu strategy. The crude peptides were used to the conjugation with the daunomycin. The drug molecule was coupled to the peptide directly or through an enzyme (Cathepsin B) labile spacer (GFLG) in solution (0.2M NH_4OAc buffer, pH 5.1) *via* oxime bond formation (Figure 1). Conjugates were purified by semipreparative RP-HPLC and characterized by analytical RP-HPLC and ESI-MS.

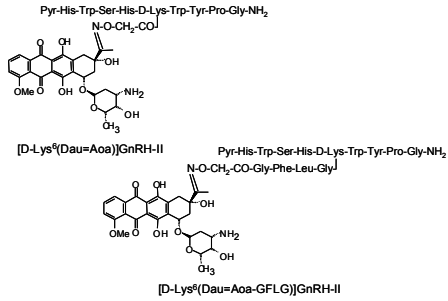

Fig. 1. Structure of GnRH-II conjugates.

In vitro cytostatic effect of the GnRH conjugates was cell type dependent. MCF-7 cells were more sensitive than the HT-29 cell culture. In case of MCF-7 cells [D-Lys^6(Dau=Aoa)]GnRH-II was as effective as GnRH-I and GnRH-III conjugates without spacer, that were prepared previously [8]. Cytostatic effect of the [D-Lys^6(Dau=Aoa-GFLG)]GnRH-II showed the same activity as the appropriate GnRH-III conjugate, while the [D-Lys^6(Dau=Aoa-GFLG)]GnRH-I was the less effective (Table 1). Similar cytostatic effect was observed in case of all conjugates on HT-29 cells except GnRH-III conjugate without spacer that showed significantly higher activity (Table 1). All of the conjugates were less effective than daunomycin on both cell cultures (Table 1). In contrast daunomycin, GnRH-II conjugates were not cytotoxic on HepG2 cell culture (Table 1).

The cellular uptake of the GnRH-II conjugates was concentration dependent on both cell cultures (Figure 2). Both type of cells internalized more effectively the conjugate with spacer. Unlike the GnRH-II conjugates, we could not observe any difference in the cellular uptake of the GnRH-I conjugates. They can be taken up in the same amount. There is no significant difference between the cellular uptake of the GnRH-I and GnRH-II conjugates.

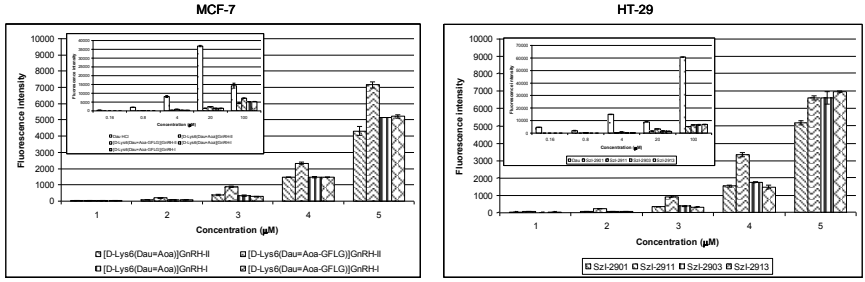

Fig. 2. Cellular uptake of the daunomycin and the GnRH conjugates.

In the case of both cell cultures the most effective compound was the free daunomycin. The results might be explained by the different mechanism of cellular uptake of the compounds. GnRH conjugates can be taken up by receptor mediated endocytosis, while daunomycin may enter the cell by passive diffusion. In Figure 2, fluorescence values are illustrated which are proportional with cellular uptake of the conjugates.

Table 1. Cytostatic and cytotoxic effect of the daunomycin and GnRH conjugates

	Cytostasis IC_{50} (μM)		Cytotoxicity IC_{50} (μM)
	MCF-7	**HT-29**	**HepG2**
Daunomycin Hydrochloride	0.1-0.3	1-5	toxic
[D-Lys^6(Dau=Aoa)]GnRH-II	4.27±0.05	19.27±3.10	non toxic
[D-Lys^6(Dau=Aoa-GFLG)]GnRH-II	6.29*	19.22±2.37	non toxic
[D-Lys^6(Dau=Aoa)]GnRH-I	4.1±0.40	20.21*	
[D-Lys^6(Dau=Aoa-GFLG)]GnRH-I	22.4±6.9	24.2±4.70	
GnRH-III(Dau=Aoa)	4.35±1.97	5.25±0.07	
GnRH-III(Dau=Aoa-GFLG)	4.53±1.54	15.90±5.50	

**Only one data point*

New GnRH-based drug containing conjugates were synthesized. These conjugates consist of daunomycin and GnRH-II molecules which are coupled to each other directly or *via* Cathepsin B labile spacer (GFLG). Cytostatic effect and cellular uptake of conjugates were determined on two different cancer cell cultures (MCF-7 and HT-29). Cytotoxicity of GnRH-II conjugates was also studied on HepG2, human hepatocellular carcinoma. Cytostatic effect of the conjugates was cell type dependent; [D-Lys^6(Dau=Aoa)]-GnRH-II had higher (IC_{50}: 4.27 μM) cytostatic activity on MCF-7 cells than the one with spacer (IC_{50}: 6.29 μM). This difference was not observed on HT-29 cells (IC_{50}: 19.29 and 19.22 μM). Cytostatic effect of the GnRH-II conjugates was similar than it was shown by the appropriate GnRH-I or GnRH-III conjugates. None of the GnRH-II conjugate was cytotoxic on HepG2 cell culture.

Conjugates can be internalized in a concentration dependent manner on MCF-7 and HT-29 cells. In the case both cell culture [D-Lys^6(Dau=Aoa-GFLG)]GnRH-II can be taken up more effectively than the [D-Lys^6(Dau=Aoa)]GnRH-II. No significant difference was observed when we compared the internalization ability of GnRH-I and GnRH-II conjugates. These conjugates will be potential candidate in the targeted tumor therapy.

Acknowledgement
This work was supported by grants from the Hungarian National Science Fund (OTKA NK 77485, F 67884, K 81596) and GVOP-3.2.1.-2004-04-0005/3.

References

1. White, R., et al. *PNAS* **95**, 305-309 (1998).
2. Millar, R.P. *Trends in Endocrinology and Metabolism* **14,** 35-43 (2003).
3. Joseffson, E., et al. *Immunology* **88,** 140-146 (1996).
4. Krontic, S., et al. *Peptides* **21,** 1941-1964 (2000).
5. Günthert, A., et al. *Eur. J. Endocrinol*.**153**, 613-625 (2005).
6. Neil, J., et al. *Trends Endorinol. Metab*. **15**, 383-392 (2004).
7. Gründker, C., et al. *Eur. J. Endorinol*. **151**, 141-149 (2004).
8. Szabó, I., et al. *Bioconj. Chem.* **20**, 656-665 (2009).

Proceedings of the 31st European Peptide Symposium
Michal Lebl, Morten Meldal, Knud J. Jensen, Thomas Hoeg-Jensen (Editors)
European Peptide Society, 2010

Anthracycline-Gonadotropin Releasing Hormone-III Bioconjugates: Synthesis, Antitumor Activity and *in vitro* Drug Release

Gábor Mező[1], Ulrike Leurs[2], Pascal Schlage[2], Erika Orbán[1], Ildikó Szabó[1], Szilvia Bősze[1], and Marilena Manea[2,3]

[1]*Research Group of Peptide Chemistry, Eötvös L University, Budapest, Hungary;*
[2]*Laboratory of Analytical Chemistry, University of Konstanz, Konstanz, Germany;*
[3]*Zukunftkolleg, University of Konstanz, Konstanz, Germany*

Introduction

Chemotherapy is still the main approach for the treatment of advanced or metastatic cancer. However, due to the lack of selectivity for tumor tissues, the application of free anticancer drugs can lead to severe side effects and low cure rates. Therefore, targeted delivery of anticancer drugs is one of the most actively pursued goals in cancer chemotherapy. Bioconjugates with receptor mediated tumor-targeting functions and carrying cytotoxic agents should enable the specific delivery of chemotherapeutics to malignant tissues, thus increasing their local efficacy while limiting the peripheral toxicity [1]. It was found that receptors for peptide hormones, such as gonadotropin-releasing hormone (GnRH), are expressed in higher amount on cancer cells compared to normal cells. Consequently, GnRH and its derivatives can be used as targeting moieties to deliver cytotoxic agents directly to tumor cells [2,3]. One of the most promising natural GnRH analogs is lamprey GnRH-III (Glp-His-Trp-Ser-His-Asp-Trp-Lys-Pro-Gly-NH_2) which specifically binds to GnRH receptors on cancer cells and has lower hormonal effect in mammals than the human GnRH [4,5]. It was shown that the modification of the side chain of ^{8}Lys or the replacement of ^{4}Ser by Lys or Lys(Ac) did not result in a significant change of the biological activity of GnRH-III [6,7]. In our previous work, the antineoplastic agent daunorubicin (Dau) was attached to GnRH-III via oxime linkage resulting in bioconjugates (Glp-His-Trp-Ser-His-Asp-Trp-Lys(Dau=Aoa-X)-Pro-Gly-NH_2, where X is 0 or Gly-Phe-Leu-Gly spacer) that had both in vitro and in vivo antitumor activity and no significant toxic side effects [8].

The major goal of the present work was to increase the antitumor activity of Daunorubicin – GnRH-III bioconjugates by modifying: (i) the GnRH-III in position 4; (ii) the number of drug molecules attached to the carrier; (iii) the linkage between the drug and GnRH-III hormone peptide.

Results and Discussion

Serine in position 4 of GnRH-III(Dau=Aoa) was replaced by N-MeSer or acetylated lysine (Lys(Ac), see Figure 1B). Both compounds showed not only increased enzymatic stability toward chymotrypsin, but also increased in vitro cytostatic effect on MCF-7 human breast and HT-29 human colon cancer cell lines (Table 1). The enzymatic stability of [N-^{4}MeSer]-GnRH-III(Dau=Aoa) was higher than that of [^{4}Lys(Ac)]-GnRH-III(Dau=Aoa). In case of GnRH-III(Dau=Aoa), the peptide bond Trp^{3}-Ser^{4} was almost completely cleaved by chymotrypsin within 6 hrs, while only 20% of [N-^{4}MeSer]-GnRH-III(Dau=Aoa) was degraded during this time.

The incorporation of an additional oxime-linked Dau to the side chain of ^{4}Lys (Glp-His-Trp-Lys(Dau=Aoa)-His-Asp-Trp-Lys(Dau=Aoa)-Pro-Gly-NH_2, Figure 1C) did not increase the in vitro antitumor activity further (Table 1). The reason might be the different metabolic pathway of the two Dau containing lysine residues, process which will be further investigated.

A bioconjugate containing the self-imolative PABC linker (Figure 1A) was also prepared according to Dubowchik, et al. [9]. Although the degradation of this compound by cathepsin B or in rat liver lysosomal homogenate showed free Dau release, its *in vitro* cytostatic effect was not higher than that observed in the case of oxime bond-linked bioconjugates (that do not provide free Dau under the same conditions). The determination of the *in vivo* toxicity and antitumor activity of the bioconjugates is in progress.

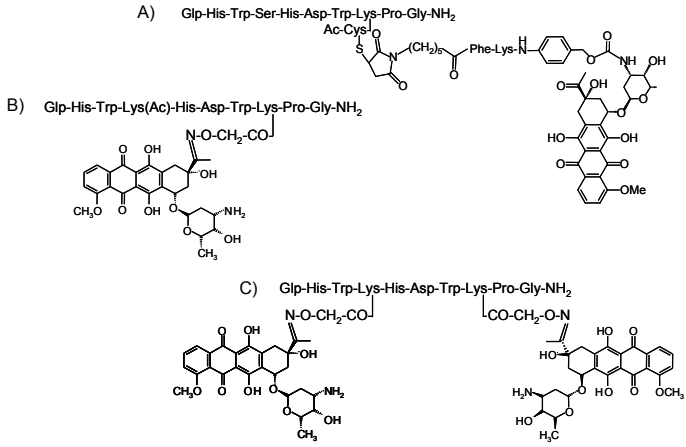

Fig. 1. Structure representation of Daunorubicin – GnRH-III bioconjugates.

Table 1. In vitro long term antitumor activity of daunorubicin-GnRH-III bioconjugates (IC_{50} values determined by MTT assay (μM))

Compounds	*MCF-7*	*HT-29*
Glp-His-Trp-Ser-His-Asp-Trp-Lys(Dau=Aoa)-Pro-Gly-NH_2	7.2 ± 2.8	14.2 ± 2.4
Glp-His-Trp-*N*-MeSer-His-Asp-Trp-Lys(Dau=Aoa)-Pro-Gly-NH_2	2.0 ± 0.5	9.2 ± 2.4
Glp-His-Trp-Lys(Ac)-His-Asp-Trp-Lys(Dau=Aoa)-Pro-Gly-NH_2	1.3 ± 0.3	3.8 ± 0.4
Glp-His-Trp-Lys(Dau=Aoa)-His-Asp-Trp-Lys(Dau=Aoa)-Pro-Gly-NH_2	2.1 ± 0.3	4.3 ± 0.5
Glp-His-Trp-Ser-His-Asp-Trp-Lys(Ac-Cys[MC-Phe-Lys-PABC-Dau])-Pro-Gly-NH_2	2.1 ± 0.4	n.d.

MCF-7: IC_{50} of Dau: 0.1-0.2 μM; HT-29: IC_{50} of Dau: 1-3 μM; n.d. not determined

Acknowledgments
This work was supported by grants from the Hungarian National Science Fund (OTKA NK 77485), the Ministry of Health (GVOP-3.2.1.-2004-04-0005/3) and University of Konstanz (Zukunftskolleg and AFF).

References

1. Singh, Y., Palombo, M., Sinko, P.J. *Curr. Med. Chem.* **15**, 1802-1826 (2008).
2. Nagy, A., Schally, A.V. *Biol. Reprod*. **73**, 851-859 (2005).
3. Mező, G., Manea, M. *Exp. Opin. Drug Deliv.* **7**, 79-96 (2010).
4. Lovas, S., Pályi, I., Vincze, B., Horváth, J., Kovács, M., Mező, I., et al. *J. Pept. Res.* **52**, 384-389 (1998).
5. Kovács, M., Vincze, B., Horváth, J.E., Seprődi, J. *Peptides* **28**, 821-829, (2007).
6. Mező, I., Lovas, S., Pályi, I., Vincze, B., Kálnay, A., Turi, G., et al. *J. Med. Chem.* **40**, 3353-3358 (1997).
7. Mező, G., Czajlik, A., Manea, M., Jakab, A., Farkas, V., Majer, Z., et al. *Peptides* **28**, 806-820 (2007).
8. Szabó, I., Manea, M., Orbán, E., Csámpai, A., Bősze, S., et al. *Bioconjugate Chem*. **20**, 656-665 (2009).

Proceedings of the 31st European Peptide Symposium
Michal Lebl, Morten Meldal, Knud J. Jensen, Thomas Hoeg-Jensen (Editors)
European Peptide Society, 2010

Design and Synthesis of Polyfunctional Spacers Based on Biodegradable Peptides

Lyubov A. Yarinich[1,2], Lyudmila S. Koroleva[1,2], Tatyana S. Godovikova[1,2], and Vladimir N. Silnikov[1]

[1]Institute of Chemical Biology and Fundamental Medicine, Novosibirsk, 630090, Russian Federation; [2]Novosibirsk State University, Novosibirsk, 630090, Russian Federation.

Introduction

Research of drug delivery into cells is actively carried out at present. Release of drug from carrier is necessary after uptake of therapeutic construction in target cells. Peptides – substrates for cathepsins taking part in cancer progression has been described in the literature [1]. Application of such peptides as biodegradable linkers let to release the therapeutic in transformed cells. Human serum albumin can be used as a carrier for drug delivery in tumor cells. Modification of Cys-34 sulfhydryl group in albumin permits to obtain bioconjugate of protein with the therapeutic [2]. Antisense oligonucleotides have a wide application in molecular biology, as they give an opportunity to have selective effect on gene expression. We propose such approach to delivery of antisense oligonucleotides to cells.

Results and Discussion

It is well known that cathepsin B is carboxypeptidase and cleaves Ala-Leu dipeptide fragments from *C*-terminal of substrate [3]. Therefore the peptides $(AlaLeu)_2Gly$, $(AlaLeu)_2$, $(AlaLeu)_3$ have been synthesized as the first step. Synthesis of peptides was carried out in solution using *Boc*-strategy. To obtain bifunctional compounds based on synthesized peptides, different constructs have been proposed. The first variant was coupling of diamine to the *C*-terminal of peptide and maleimide fragment to the *N*-terminal (Figure 1). 4,9-Dioxa-1,12-diaminododecane was coupled to peptide ***1*** as linker to increase hydrophilicity of the target conjugate. Further free amino group in ***2*** has been protected by ethyl trifluoroacetate with subsequent deblocking of α-amino group of alanine. Compound ***3*** was reacted with pentafluorophenyl ester of *N*-maleimidohexanoic acid. Finally bifunctional derivative of pentapeptide with trifluoroacetic protection (***4)*** has been synthesized. After removing of TFA-group, opening of maleimide cycle with loosing reactivity related to sulfhydryl group of cysteine has been noticed.

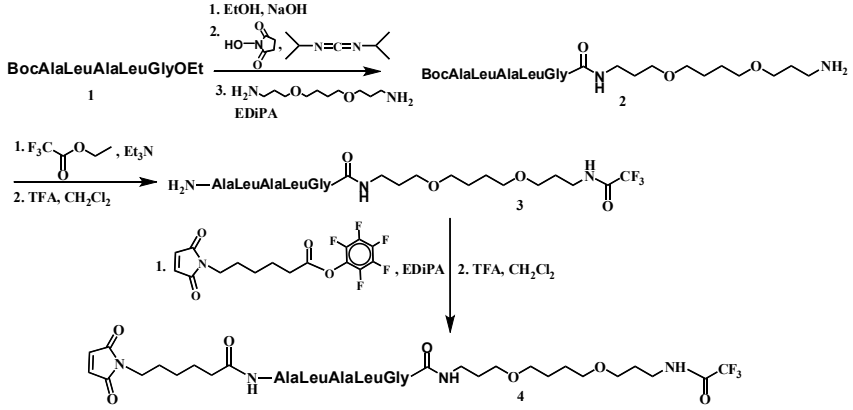

Fig. 1. Synthetic scheme of maleimide derivative of the AlaLeuAlaLeuGly.

The second variant was to couple flexible amino linker with maleimide fragment to *C*-terminus without modification of peptide *N*-terminal amino group (Figure 2). In this case maleimide cycle has remained and number of synthetic steps has been reduced. At first

step, benzyl protection has been removed, *Boc*-protected tetrapeptide ***5*** has been activated by *N*-hydroxysuccinimide in the presence of DCC with subsequent coupling with 4,9-dioxa-1,12-diaminododecane. After that, compound ***6*** was reacted with pentafluorophenyl ester of *N*-maleimidohexanoic acid. Deblocking of N^{α}-amino group led to bifunctional compound ***7***. The structures of the target compounds were confirmed by NMR spectroscopy and mass spectrometry.

Amino groups of obtained compounds can allow connecting antisense oligonucleotide to *N*-terminal of peptides. Maleimide residue in such peptide-oligonucleotide conjugates permits us to form covalent bond with albumin.

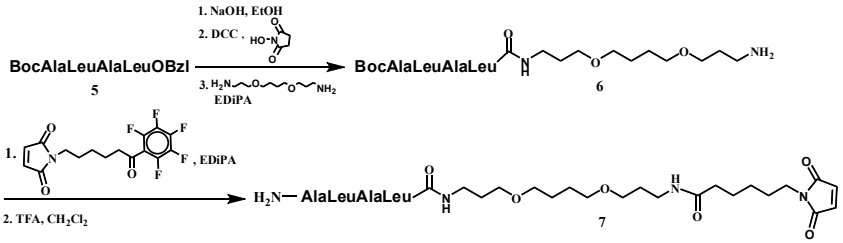

Fig. 2. Synthetic scheme of bifunctional reagent based on the tetrapeptide.

To verify substrate properties of obtained peptides, fluorescent derivatives **10** and **11** have been synthesized. To introduce fluorescein residue in AlaLeuAlaLeu or in compound **7** *N*-hydroxysuccinimide ester of 5(6)-carboxyfluorescein has been used (Figure 3).

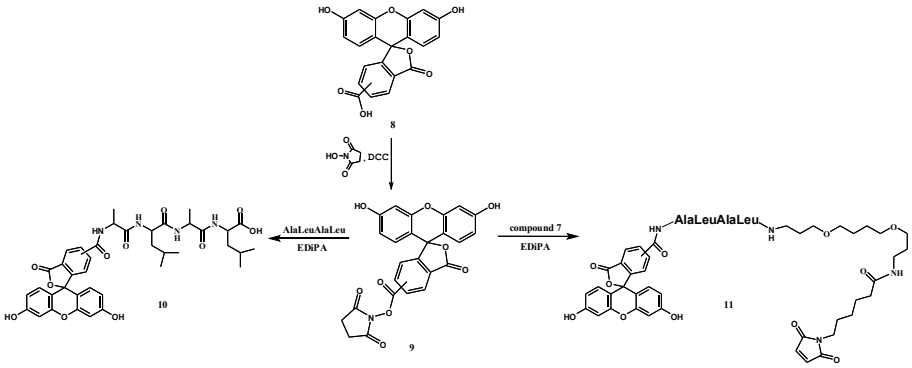

Fig. 3. Synthetic scheme of fluorescent derivatives of peptides.

Obtained fluorescently labeled substrate can be used to trace the transport of therapeutic constructs in the cells.

Acknowledgments

The work was supported by integration project of SB RAS №88, Carl Zeiss-2010, №SC-3185.2010 and grant of RFBR 09-04-01483-a.

References

1. Shiose, Y., Kuga, H., Ohki, H., Yamashita, F., Hashida, M. *Bioconjugate Chem.* **20**, 60-70 (2009).
2. Temming, K., Meyer, D., Zabinski, R., Dijkers, E., Poelstra, K., Molema, G., Kok, R. *Bioconjugate Chem.* **17**, 1385-1394 (2006).
3. Vasiljeva, O., Korovin, M., Gajda, M., Reinheckel, T., et al. *Oncogene* **27**, 4191-4199 (2008).

Proceedings of the 31st European Peptide Symposium
Michal Lebl, Morten Meldal, Knud J. Jensen, Thomas Hoeg-Jensen (Editors)
European Peptide Society, 2010

Amino Acids Esters of Acyclovir-Synthesis and Antiviral Activity

Ivanka Stankova[1], Stoyan Shishkov[2], Kalina Kostova[2], Daniel Todorov[2], Luchia Mukova[3], and Angel Galabov[3]

[1]Department of Chemistry, South-West University "Neofit Rilsky", Blagoevgrad, Bulgaria;[2]Laboratory of Virology, Faculty of Biology, University of Sofia "St. Kl. Ohridski", Sofia, Bulgaria; [3]The Stephan Angeloff Institute of Microbiology, Bulgarian Academy of Sciences, 1113, Sofia, Bulgaria

Introduction

Following the discovery of the first effective antiviral compound (idoxuridine) in 1959, nucleoside analogues, especially acyclovir (ACV) for the treatment of herpesvirus infections, have dominated antiviral therapy for several decades [1,2]. However, ACV and similar acyclic nucleosides suffer from low aqueous solubility and low bioavailability following oral administration. Derivatives of acyclic nucleosides, typically esters, were developed to overcome this problem and valacyclovir, the valine ester of ACV, was among the first of a new series of compounds that were readily metabolized upon oral administration to produce the antiviral nucleoside *in vivo*, thus increasing the bioavailility by several fold [3,4].

One of the known approaches in the treatment of viral infection is the application of a number of combinations of specific inhibitors with different mechanism of action, so the simultaneous use of inhibtors with immunomodulators. This action leads to reducing the dose of the drug and its resistance. There are distinct effects of combinations of acyclovir (9-(2-hydroxyethoxymethyl)guanine) and cisplatin, rimantadine and ribavirin, oseltamivir and rimantadine. A significant synergy between ribavirin and oseltamivir against influenza virus H9N2 in vivo is established [5-7].

We expect that the obtained new analogues by coupling of acyclovir with 4-F-Phenylalnine (R,S) could possess a greater antiviral effect due to synergy. A two new analogues of acyclovir and 4-F-Phenylalnine (R,S) were synthesized and screened for their activity in vitro against herpes simplex virus-1 (HSV-1) and influenza virus.

Results and Discussion

Synthesis of acyclovir analogues

A mixture of **1 a-b** and DDC in dimethylformamide (DMF) was stirred for 1h at 0°C under nitrogen atmosphere. A solution of acyclovir (Figure 1) and 4-*N*,*N*-(dimethylamino)-pyridine (DMAP) was added to the reaction mixture and stirred for 24h. Then DMF was evaporated *in vacuo* and the residue was chromatographed on silica gel. The resulting white solid, Boc–(4-F)-Phe–ACV (R, S) was dissolved in 20 ml of TFA and stirred at 0°C for 1h to remove the Boc group. Following removal of the TFA in vacuum, 20 ml of ethyl acetate was added to the oily reside. The solution was then added drop-wise to the cold diethyl ether. After filtration, 4-F-Phe–ACV (R,S) (TFA salt) was collected as white solid with high purity (>95%). Four milliliters of triethylamine (TEA) was added to 4-F-Phe–ACV (R,S) and kept for 15 min before dissolving it in 15 ml DMF. The ^{1}H and ^{13}C-NMR, mass-spectra were consistent with desired structure **(2 a-b).**

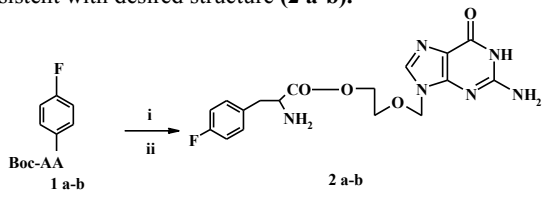

(i) acyclovir / DCC/DMAP ; (ii) TFA/CH_2CH_2

Protected AA: 1 a) Boc-(4-F)-Phenylalanine (R);1 b) Boc-(4-F)-Phenylalanine (S).

Fig. 1. Synthesis of acyclovir analogues with 4-F-Phenylalanine (R,S).

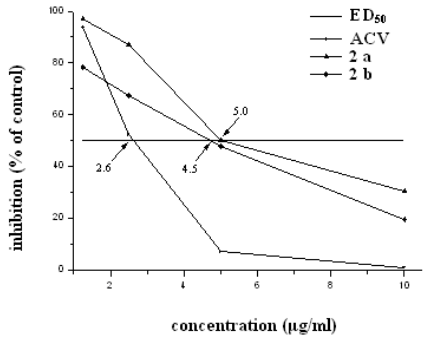

Fig. 2. Effects of compounds 2 (a-b) on the replication of HSV-1.

Biological Activity

Antiviral activity against HSV-1

Viruses: Herpes simplex virus type 1 (HSV-1), strain Vic. *Cell culture*: Cell line MDBK (Madin-Darby Bovine Kidney), grown in growth medium RPMI-1640 (Flow Laboratories) with 10% new born calf serum.

The compounds were explored in concentrations 10, 5, 2,5 and 1,25 µg / ml against HSV-1, strain Vic. The data suggested strong dose-depend effects on the viral replication. The inhibition was similar with antiviral effect of reference drug. According to expectation he 50% effective doses (ED50) were almost the same (Figure 2). It was for compound **(2 a)** 4,5 µg / ml and 5,0 µg / ml for compound **(2 b).** ED50 for ACV is at the same level – 2,6 µg / ml.

Antiviral activity against influenza virus A(H3N2)

Viruses: Influenza A virus [Aichi/2/68 (H3N2)] [IAV/H3N2], from the collection of the Stephan Angeloff Institute of Microbiology, BAS (Sofia, Bulgaria).

Determination of Cytotoxicity

The maximal tolerated concentration (MTC) is determined as the concentration at which no visible changes in the cell monolayer are observed. The 50% cytotoxic concentration (CC50) is calculated in comparison to the cell control by applying the regression analysis with the help of Origin 6.1 computer program. The compounds showed no effect against influenza virus A(H3N2).

In conclusion new acyclovir esters have been synthesized with (4-F)-Phe–OH (R, S) and their activity on the HSV-1and Influenza virus have been explored. The results in our investigations showed that 4-F-Phe–ACV (R), applied in 10µg/ml suppressed viral replication – 70% and the 4-F-Phe–ACV (S) – 80%. The studied compounds showed no effect against influenza virus A(H3N2).

Acknowledgments

For the support of this work we are grateful to the National Science Fund of Bulgaria (ContractsVUL-304/07) and South-West University 'Neofit Rilski'', Blagoevgrad, Bulgaria (SRP-C2/2010).

References

1. Beauchamp, L.M., Orr, G.F., de Miranda, P., Burnette, T., Krenitsky, T.A. *Antivir. Chem. & Chemoth.* **3**, 157-164 (1992).
2. Beauchamp, L.M., Krenitsky, T.A. *Drugs Future* **18**, 619-628 (1993).
3. Anand, B.S., Mitra, A.K. *Pharm. Res*. 1194-1202 (2002).
4. Anand, B.S., Katragadda, S., Mitra, A.K. *J. Pharmacol. Exp. Ther*. **311**, 659-667 (2004).
5. Coluccia, M., Boccarelli, L., Cermelli, C., Portolani, M., Natile, G. *downloads.hindawi.com/journals/mbd/1995/835735.pdf* **5**, 246-256, (1995).
6. Garozzo, A., Tempera, G., Ungheri, D., Timpanaro, R., Castro, A. *Int. J. Immun. Pharmacol.* **20**, 349-54 (2007).
7. Galabov, A., Simeonova, L., Gegova, G. *Antivir. Chem. & Chemoth.* **17**, 251-258 (2008).
8. Golankiewich, B., Ostrowski, T., Goslinski, P., Januszczyk, J., Zeidler, D., Baranowski, K., Clerq, E. *J. Med. Chem.* **44**, 4284-4287 (2001).

Proceedings of the 31st European Peptide Symposium
Michal Lebl, Morten Meldal, Knud J. Jensen, Thomas Hoeg-Jensen (Editors)
European Peptide Society, 2010

Homobivalent α–MSH Derivatives for Melanoma Imaging: ^{99m}Tc(CO)$_3$-Labeling and Biological Evaluation

Maurício Morais, Paula D. Raposinho, Maria Cristina Oliveira, João D.G. Correia, and I. Santos

Unit of Chemical and Radiopharmaceutical Sciences, Instituto Tecnológico e Nuclear, Estrada Nacional 10, 2686-953, Sacavém, Portugal

Introduction

Early detection of primary melanoma tumours is essential because current treatments do not enhance substantially patient survival once metastases have occurred. Since most human and murine melanoma cells over express melanocortin type 1 receptor (MC1R), radiolabelled α-MSH (α-Melanocyte Stimulating Hormone) analogs have been considered interesting tools for melanoma imaging or therapy [1,2]. Aimed at the targeting of MC1R *in vivo*, and based on the affinity enhancement expected when using a multivalent approach, herein, we report on the synthesis, characterization and biological evaluation of a novel homobivalent α–MSH derivative labeled with the *fac*-[^{99m}Tc(CO)$_3$]$^+$core [3,4].

Results and Discussion

The fully protected α–MSH analog NAPamide (Ac-Nle-Asp-His-*D*Phe-Arg-Trp-Gly-Lys) was synthesized by Fmoc-based Solid Phase Peptide Synthesis on a CEM Liberty automated peptide synthesizer, using the methyltrityl (Mtt) protecting group for Lys^{11} side chain and a Sieber Amide resin. The partially deprotected α-MSH analog was obtained after selective removal of the Mtt group and resin cleavage under mild acidic conditions (Scheme 1).

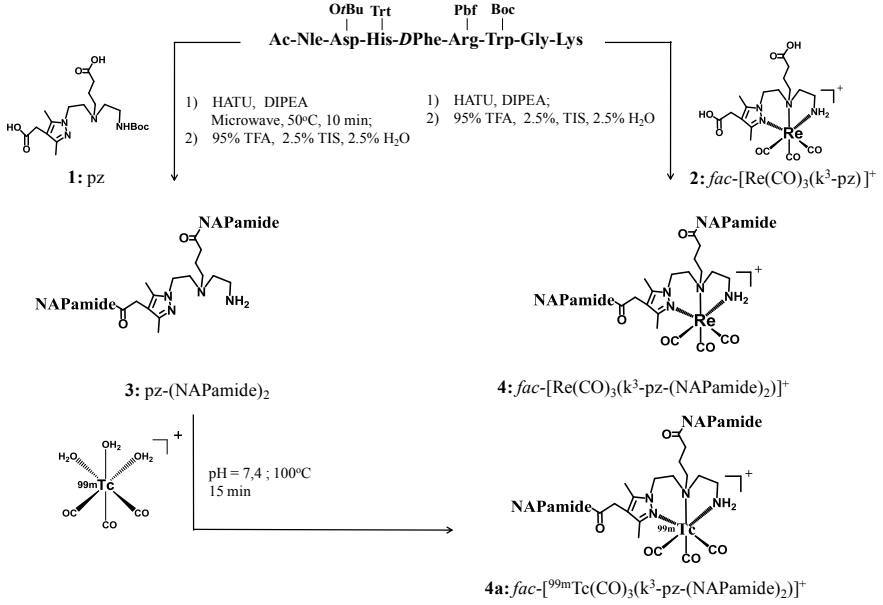

Scheme 1. Synthesis of homobivalent derivatives.

The peptide was coupled to **1** and **2** through Lys^{11} side chain, yielding the homobivalent derivatives **3** and **4** after full deprotection (Scheme 1). **3** and **4** were purified by semi-preparative RP-HPLC and characterized by ESI-MS (Table 1).

*Table 1. Analytical Data for Homobivalent Derivatives **3** and **4***

Compound	*Formula*	*Calculated [ion]*	*Found*	*t_R (purity)*
3	$C_{119}H_{170}N_{36}O_{24}$	1244.6 $[M+2H]^{2+}$	1244.6	15 min (98%)
4	$C_{122}H_{170}N_{36}O_{27}Re$	920.6 $[M+3H]^{3+}$	920.6	15.5 min (98%)

The binding affinity of **3** (IC_{50} = 0.33 ± 0.27 nM) to MC1R is very high and of the same order as NAPamide (IC_{50} = 0.78 ± 0.03 nM) and the monovalent ligand pz-NAPamide (IC_{50} = 0.66 ± 0.13 nM) prepared previously [3]. The metallation of **3** led to a complex **4** with slightly lower affinity (IC_{50} = 1.43 ± 1.54 nM).

The radioactive complex **4a** was prepared in high yield and radiochemical purity (98%) by reacting **3** with $[^{99m}Tc(CO)_3(H_2O)_3]^+$ (Scheme 1). The highly hydrophilic complex **4a** (log $P_{o/w}$= - 1.82 ± 0.02) was characterized/identified comparing its RP-HPLC chromatogram with the one obtained for **4**, synthesized as surrogate (Figure 1).

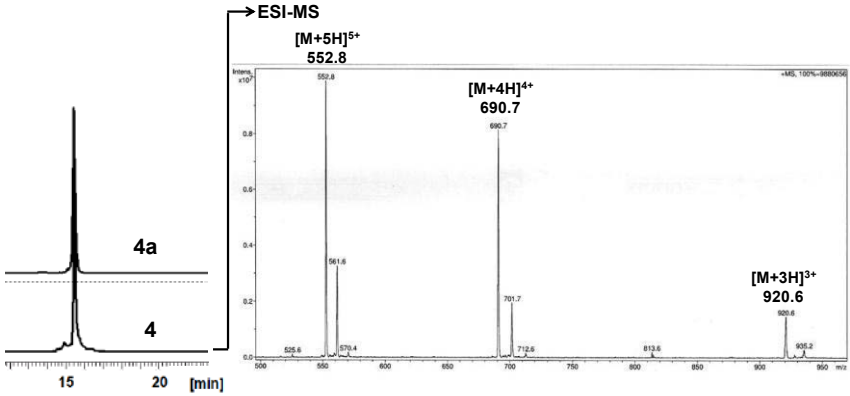

*Fig. 1. HPLC chromatograms of **4a** (γ - detection)/ **4** (UV-vis detection) and ESI-MS spectrum of **4**.*

In vitro studies have shown that **4a** is stable in fresh human serum (6h, 37°C). Internalization studies in B16F1 murine melanoma cells revealed that over 45% of the cell-associated activity was internalized after 4 h, at 37°C.

In conclusion, we have synthesized and characterized the novel homobivalent *fac*-$[M(CO)_3]^+$ complexes **4**/**4a** (M = Re/^{99m}Tc) containing the NAPamide. Preliminary studies have shown that the radioactive complex is enzymatically stable, displayed high affinity to MC1R and high cellular uptake. The biological evaluation of **4a** in tumour-bearing mice is currently underway.

Acknowledgments
M. Morais thanks FCT for a PhD grant (SFRH/BD/48066/2008). Covidean is acknowledged for the IsoLink® Kits. Dr. J. Marçalo is acknowledged for performing the ESI-MS analyses. The QITMS instrument was acquired with the support of the Programa Nacional de Reequipamento Científico (Contract REDE/1503/REM/2005 - ITN).

References

1. Miao, Y., Quinn, T. *Crit. Rev. Oncol/Hematol.* **67**, 213-228 (2008).
2. Raposinho, P.D., Correia, J.D.G., Cristina, M.C., Santos, I. *Biopolymers: Peptide Science* (2010).
3. Raposinho, P.D., Correia, J.D.G., Alves, S., Botelho, M.F., Santos, A.C., Santos, I. *Nucl. Med. Biol.* **35**, 91-99 (2008).
4. Vagner, J., Handl, H.L., Gillies, R., Hruby, V.J. *Bioorg. Med. Chem. Lett.* **14**, 211-215 (2004).

Proceedings of the 31st European Peptide Symposium
Michal Lebl, Morten Meldal, Knud J. Jensen, Thomas Hoeg-Jensen (Editors)
European Peptide Society, 2010

Development of Drug Delivery Systems for Targeted Cancer Chemotherapy Based on GnRH Antagonist and Agonist Peptides

Bence Kapuvári[1], Borbála Vincze[1], Marilena Manea[2], Miguel Tejeda[1], Ákos Schulcz[1], József Tóvári[1], Dezső Gaál[1], Erika Orbán [3], Ildikó Szabó[3], and Gábor Mező[3]

[1]National Institute of Oncology, Budapest, Hungary; [2]University of Konstanz, Zukunftskolleg and Department of Chemistry, Laboratory of Analytical Chemistry and Biopolymer Structure Analysis, Konstanz, Germany; [3]Research Group of Peptide Chemistry, Hungarian Academy of Sciences, Eötvös L. University, Budapest, Hungary

Introduction

Targeted cancer chemotherapy has been developed to overcome the drawbacks associated with the application of free anticancer drugs (e.g. lack of selectivity, toxic side effects, multi-drug resistance of cancer cells). Tumor targeting is achieved by conjugating a chemotherapeutic agent to a targeting moiety which is directed to specific binding sites on cancer cells [1]. Gonadotropin releasing hormone (GnRH) receptor expression was identified on different types of tumors, such as breast, ovarian, colon, endometrial, prostate, renal, brain, pancreatic, melanomas and non-Hodgkin's lymphomas [2].

The aim of our work was to use GnRH agonist and antagonist peptides as targeting moieties for the attachment of anticancer drugs. Bioconjugates in which the chemotherapeutic agent daunorubicin (Dau) was attached through an oxime bond to the GnRH analogs MI-1892 (Ac-wxwSkD(LQPa-NH_2)-DEA, where x is D-p-chlorophenyl-alanine, DEA is diethylamide, and small letters mean D-amino acids) [3] and GnRH-III (<EHWSHDWKPG-NH_2, where <E is pyroglutamic acid) [4] were prepared (Figure 1) and their biological properties were investigated. The drug was connected to the hormone peptide carrier either directly or through an enzymatic cleavable spacer [5].

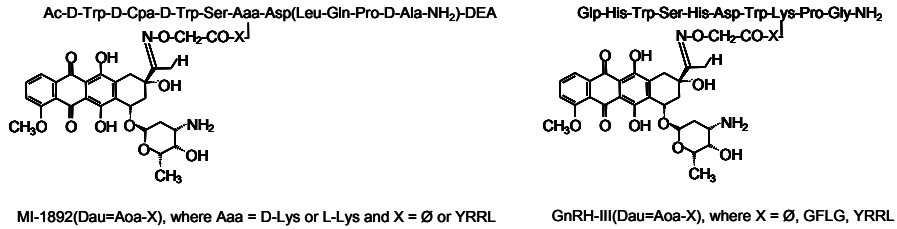

Fig. 1. Structure representation of GnRH derivative – daunorubicin bioconjugates.

Results and Discussion

Three GnRH antagonist peptide - daunorubicin bioconjugates have been prepared. Dau was attached via oxime linkage to aminooxyacetylated MI-1892 derivatives either directly or by insertion of an YRRL tetrapeptide spacer, leading to the bioconjugates MI-1892(Dau=Aoa) and MI-1892(Dau=Aoa-YRRL). The YRRL spacer is efficiently cleaved by Cathepsin B, a lysosomal enzyme overexpressed in cancer cells. In the third compound, D-Lys in position 5 was replaced by L-Lys ([Lys^5]-MI-1892(Dau=Aoa)). Interestingly, the latest bioconjugate showed one order of magnitude lower IC_{50} values (determined by MTT assay) both on MCF-7 human breast and HT-29 human colon cancer cell lines than the bioconjugates containing the original MI-1892 sequence (Table 1). The cytostatic effect of [Lys^5]-MI-1892(Dau=Aoa) is comparable to the activity of the free drug (IC_{50}: 0.10±0.30 μM and 0.23±0.03 μM on MCF-7 and 3.8±0.1 μM and 2.5±1.1 μM on HT-29, respectively). Neither MI-1892(Dau=Aoa) nor [Lys^5]-MI-1892(Dau=Aoa) were degraded in rat liver lysosomal homogenate. Therefore, the difference in bioactivity might not be derived from the produced metabolites. Comparative structural studies of the bioconjugates are in progress.

The GnRH-III based bioconjugates with or without spacer (GnRH-III(Dau=Aoa-GFLG), GnRH-III(Dau=Aoa-YRRL) and GnRH-III(Dau=Aoa)) showed similar cytostatic effect that was higher on MCF-7 cells (IC_{50}: 1-5 μM) than on HT-29 cells (IC_{50}: 10-30 μM) (Table 1). Because the stability of the YRRL spacer was fairly low in human serum, only the other two compounds were tested in vivo. The in vivo antitumor activity was evaluated on HT-29 human colon carcinoma bearing SCID mice. GnRH-III(Dau=Aoa) and GnRH-III(Dau=Aoa-GFLG) bioconjugates injected 3 times at a dose of 15 mg/kg Dau content had significant antitumor activity (tumor growth inhibition: 41% and 50%, respectively on the day 35 after tumor transplantation) (Figure 2). Mice treated with free Dau, 5 mg/kg or 2.5 mg/kg body weight, died before the second treatment (till the day 20 or 23, respectively).

Table 1. In vitro long term antitumor activity of Dau-GnRH derivative bioconjugates

Compounds	*HT-29 (IC_{50}/μM)*	*MCF-7 (IC_{50}/μM)*
Daunorubicin-HCl	2.5 ±1.1	0.23 ±0.03
GnRH-III	>100	>100
GnRH-III(GFLG)	>100	>100
GnRH-III(Dau=Aoa)	14.2± 3.2	2.2 ±1.2
GnRH-III(Dau=Aoa-GFLG)	19.4± 3.1	3.9 ±1.2
GnRH-III(Dau=Aoa-YRRL)	28.6 ±5.5	1.8 ±0.5
MI-1892	>100	>100
MI-1892(Dau=Aoa)	16.1± 1.9	7.4 ±0.5
MI-1892[^{5}Lys](Dau=Aoa)	3.8 ±0.1	1.0 ±0.3
MI-1892(Dau=Aoa-YRRL)	16.2 ±2.0	6.9 ±1.5

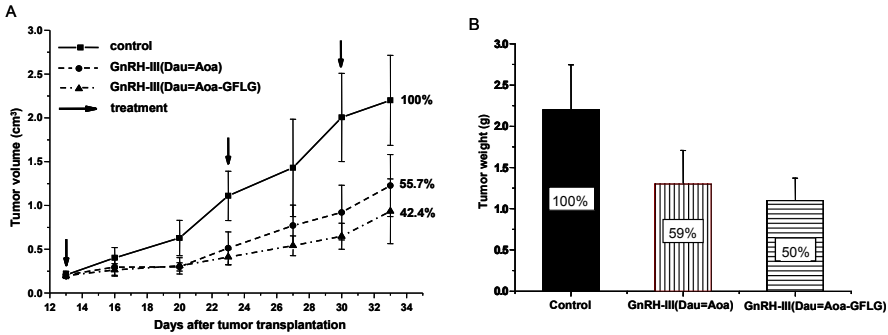

Fig. 2. In vivo antitumor effect of GnRH-III – daunorubicin bioconjugates discussion.

Our results indicate that oxime bond-linked daunorubicin-GnRH analog bioconjugates represent a promising drug delivery system with potential applications in targeted cancer chemotherapy.

Acknowledgments
This work was supported by grants from the Hungarian National Science Fund (OTKA NK 77485), the Ministry of Health (GVOP-3.2.1.-2004-04-0005/3) and the University of Konstanz (Zukunftskolleg and AFF).

References

1. Singh, Y., Palombo, M., Sinko, P.J. *Curr. Med. Chem.* **15**, 1802-1826 (2008).
2. Mező, G., Manea, M. *Exp. Opin. Drug Deliv.* **7**, 79-96 (2010).
3. Mező, I., et al. *Biochemical Peptides, Proteins & Nucleic Acids* **2**, 33-40 (1996).
4. Sower, S.A., Chiang, Y.-C., Lovas, S., Conlon, J.M. *Endocrinol.* **132**, 1125-31 (1993).
5. Szabó, I., Manea, M., Orbán, et al. *Bioconjugate Chem.* **20**, 656-665 (2009).

Proceedings of the 31st European Peptide Symposium
Michal Lebl, Morten Meldal, Knud J. Jensen, Thomas Hoeg-Jensen (Editors)
European Peptide Society, 2010

Miniprotein Engineering of the Knottin-like Scaffold Min-23- Solid-phase Synthesis and Oxidative Folding Strategies

Frederic Zoller[1], Christain Hauer[2], Annette Markert[1,2], Uwe Haberkorn[1,2], and Walter Mier[2]

[1]Clinical Cooperation Unit Nuclear Medicine, German Cancer Research Center, 69120, Heidelberg, Germany; 2Clinic for Nuclear Medicine, University Hospital Heidelberg, D-69120, Heidelberg, Germany

Introduction

Miniprotein scaffolds are currently emerging as novel recognition molecules and for the generation of epitope binding motifs for medical applications [1]. Owing to their extraordinary stable architecture that tolerates multiple amino acid substitutions or insertions, disufide-rich miniproteins are ideal scaffolds for combinatorial engineering [2]. The knottin-like peptide scaffold Min-23 is rationally designed from the plant-occurring cyclotide *ecballium elaterium trypsin inhibitor II* (EETI-II) (Figure 1). This 23-mer peptide incorporating a cystine-stabilised beta-sheet (CSB) motif frames an autonomous folding unit. The plasticity of the CSB motif allows the integration of a randomized affinity function into the stably folded framework [3]. These characteristics classify Min-23 as a peptide scaffold for lead generation using in vitro screening techniques, such as phage or ribosome display [4]. However, engineering of cystine-knotted miniproteins is a challenging process, which requires an efficient solid-phase synthesis and oxidative folding strategies.

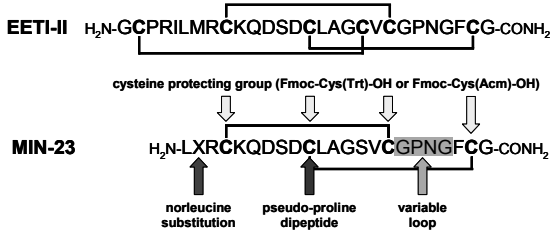

Fig. 1. Primary structure of EETI-II and Min-23. Key role amino acids for an optimized Fmoc/tBu-solid phase synthesis are highlighted.

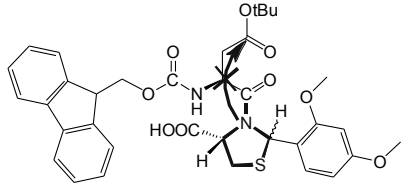

Fig. 2. Structure of Fmoc-Asp(OtBu)-Cys($\psi^{H,DMP}$pro)-OH. This pseudoproline building block avoids secondary structure formation. Moreover, it was shown to prevent aspartimide formation and it acts as orthogonal protecting group for cysteine.

Results and Discussion

The initial solid-phase peptide synthesis of Min-23 revealed a high aggregation during the chain elongation within the helical section. This drawback was overcome using commercially available Asp-Ser-pseudoproline. In addition, the tertiary amide backbone of the Asp-Cys-pseudoproline building block was shown to prevent aspartimide formation (Figure 2) [5]. This optimization results in a crude peptide purity of 76% compared to only 42% using standard SPPS-building blocks. For the subsequent oxidative peptide folding via disulfide formation two different strategies were developed. The simultaneous formation of two disulfide bridges was achieved by air oxidation in a DMSO-free, buffered solution in

24 hours. The native configuration of the disulfide core was obtained in 93% purity within the crude mixture. Using an orthogonal protecting group strategy, Min-23 could be folded into the desired configuration in a two step procedure. The uniformity of both folded peptides was verified by HPLC. High resolution mass spectrometry in combination with HPLC enables the identification of the separated peptide species.

The Fmoc-assisted solid-phase synthesis and the oxidative peptide folding of the scaffold Min-23 were optimized. In addition, the consecutive oxidation folding strategy allows both a directed peptide folding into the desired disulfide configuration and a control of the autonomous folding procedure. These achievements of the cystine peptide chemistry are used for engineering random peptide motifs incorporated in the disulfide-constrained Min-23 scaffold, which are identified by in vitro high-throughput screening techniques. Therefore, this chemical concept is a valuable approach for the miniprotein engineering of randomised Min-23 scaffolds.

Acknowledgments
The authors are grateful to the Bundesministerium für Bildung und Forschung (Grant No. 13N10269) for financial support.

References

1. Binz, H.K., Amstutz, P., Pluckthun, A. *Nat. Biotechnol.* **23**, 1257 (2005).
2. Nygren, P.A., Skerra, A. *J. Immunol. Methods* **3**, 290 (2004).
3. Heitz, A., Le-Nguyen, D., Chiche, L. *Biochemistry* **38**, 10615 (1999).
4. Souriau, C., Chiche, L., Irving, R., Hudson, P. *Biochemistry* **44**, 7143 (2005).
5. Wöhr, T., Wahl, F., Nefzi, A., Rohwedder, B., Sato, T., Sun, X., Mutter, M. *J. Am. Chem. Soc.* **19,** 9218 (1996).

Proceedings of the 31st European Peptide Symposium
Michal Lebl, Morten Meldal, Knud J. Jensen, Thomas Hoeg-Jensen (Editors)
European Peptide Society, 2010

Synthesis and Characterization of Novel Dipeptide Ester of Acyclovir

Ivanka G. Stankova[1], Ivanka B. Stoineva[2], and Michaela Schmidtke[3]
[1]Department of Chemistry, South-West University "Neofit Rilsky", Blagoevgrad, Bulgaria;
[2]Institute of Organic Chemistry, Bulgarian Academy of Sciences, 1113, Sofia, Bulgaria;
[3]Jena University Hospital, School of Medicine, Department of Virology and Antiviral Therapy, Jena, Germany

Introduction

The human peptide transporter (hPEPT1) displays broad substrate specificity and recognizes dipeptides and tripeptides, but not free amino acids, as its primary substrates. The peptide transporter not only carries nutrients across absorptive cell membranes but also functions in the transport of exogenous compounds that have peptide-like structures. Small dipeptides, angiotensin-converting enzyme inhibitors, and β-lactam antibiotics are known substrates for intestinal PEPT1 [1-5]. Strategies have been used to design prodrugs of various poorly absorbed drugs targeted toward receptors/transporters for improved bioavailability [6].

A series of water-soluble dipeptide ester prodrugs of acyclovir were synthesized [7] valyl-valine acyclovir (VVACV), tyrosinul-glycine acyclovir (YGACV), glycyl-valine acyclovir (GVACV), glycyl-glycine-acyclovir (GGACV), glycyl-tyrosine acyclovir (GYACV), valyl-tyrosine acyclovir (VYACV), and tyrosinyl-valine acyclovir (YVACV). The results of this study indicate that the dipeptide prodrugs of ACV, a poorly absorbed antiviral nucleoside, exhibit high affinity toward the intestinal oligopeptide transporter. The uptake of these prodrugs was efficiently mediated by hPEPT1 because they significantly inhibit the uptake of glycylsarcosine. These prodrugs hydrolyze readily to regenerate the active parent drug, acyclovir, thereby fulfilling the basic requirement of a prodrug. These prodrugs owing to their high affinity, excellent solution stability, and in vitro antiviral activity against herpes infections are promising drug candidates against oral and ocular herpes infections.

The aim of this study is synthesis of new dipeptide esters of acyclovir (Val-Pro-OH and Ile-Pro-OH) and explore antiviral activity against HSV-1.

Results and Discussion

Synthesis of dipeptide Boc-Val-Pro-OH and Boc-Ile-Pro-OH was according to [8].

*Synthesis of acyclovir analogues (**2a-b**)*

A mixture of dipeptide 1 a-b and DCC in dimethylformamide (DMF) was stirred for 1h at 0°C under nitrogen atmosphere. A solution of acyclovir (Figure 1) and 4-N, N-(dimethylamino)-pyridine (DMAP) was added to the reaction mixture and stirred for 24 h. Then DMF was evaporated *in vacuo* and the residue was chromatographed on silica gel, using 1:4 MeOH:CH_2CH_2.

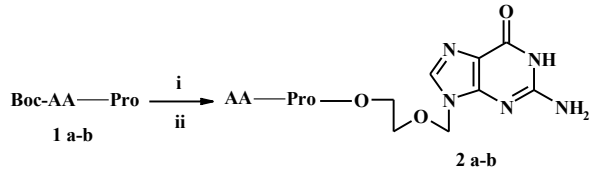

(i) acyclovir / DCC/DMAP ; (ii) TFA/CH_2CH_2

Protected AA: **1 a)** Boc-Val-OH;**1 b)** Boc-Ile-OH.

Fig. 1. Synthesis of dipeptide esters of acyclovir.

The Boc-Val-Pro-ACV and Boc-Ile-Pro-ACV was dissolved in 20 ml of TFA and stirred at 0°C for 1h to remove the Boc- group. Following removal of the TFA in vacuum, DIPEA was added to a solution of Val-Pro-ACV or Ile-Pro-ACV and solution stirred for 10 min.

Antiviral activity

Virus: Herpes simplex virus type 1 (HSV-1), strain DA.

Cytotoxicity and anti-herpetic activity against HSV-1 of the newly synthesized dipeptide esters of acyclovir was tested in GMK cells.

To exclude non-specific antiviral activities, the derivatives of acyclovir were tested for cytotoxicity on confluent monolayer's of host cells. The results demonstrate a good compatibility of the new acyclovir analogous for the tested cell lines. None of the compounds inhibited the HSV-1-induced cytopathic effect in GMK cells.

In conclusion, novel esters of acyclovir have been synthesized with dipeptide H-Val-Pro-OH and H-Ile-Pro-OH and their antiherpetic activity have been explored.

The results in our investigations showed that these modification of acyclovir reduced antiviral effect in comparison with modification of acyclovir with amino acids (valacyclovir).

Acknowledgments

For the support of this work we are grateful to the National Science Fund of Bulgaria (ContractsVUL-304/07) and South-West University 'Neofit Rilski'', Blagoevgrad, Bulgaria (SRP-C2/2010).

References

1. Dantzig, A.H., Bergin, L. *Biochim Biophys Acta*. **1027**, 211-217 (1990).
2. Hashimoto, N., Fujioka, T., Toyoda, T., Muranushi, N., Hirano, K. *Pharm. Res*. **11**, 1448-1451 (1994).
3. Ganapathy, M.E., Brandsch, M., Prasad, P.D, Ganapathy, V., Leibach, F.H. *J. Biol. Chem*. **270**, 25672-25677 (1995).
4. Han, H., de Vrueh, R.L., Rhie, J.K., Covitz, K.M, Smith, P.L., Lee, C.P., Oh, D.M., Sadee, W., Amidon, G.L. *Pharm. Res*. **15**, 1154-1159 (1998).
5. Inui, K., Terada, T., Masuda, S., Saito, H. *Nephrol. Dial Transplant*. **15**, 11-13 (2000).
6. Lupia, R.H., Ferencz, N., Lertora, J.J., Aggarwal, S.K., George, W.J., Agrawal, K.C. *Antimicrob. Agents Chemother*. **37**, 818-824 (1993).
7. Anand, B.S., Nashed, Y.E., Mitra, A.K. *Curr. Eye Res*. **26**,151-163 (2002).
8. Tantry, S.J., Vasanthakumar, G., Suresh Babu, V.V. *Lett. Peptide Sci*. **10,** 51-55 (2003).

Proceedings of the 31st European Peptide Symposium
Michal Lebl, Morten Meldal, Knud J. Jensen, Thomas Hoeg-Jensen (Editors)
European Peptide Society, 2010

New SOCS1-KIR Mimetic Peptides Through the Screening of Focused Simplified Combinatorial Libraries

Daniela Marasco[1,2], Nunzianna Doti[2], Pasqualina L. Scognamiglio[1], Stefania Madonna[3], Menotti Ruvo[2], Carlo Pedone[1,2], and Cristina Albanesi[3]

[1]Department of Biological Sciences, School of Biotechnological Sciences, University "Federico II", Naples, 80134, Italy; [2]Institute of Biostructures and Bioimaging –IBB-CNR, Naples, 80134, Italy; [3]IDI-IRCCS, Roma, 00167, Italy

Introduction

Suppressor Of Cytokine Signalling (SOCS) proteins are negative feedback regulators of several pathways involved in immune response, particularly the JAK/STAT (Janus kinase/Signal Transducer and Activator of Transcription) [1]. Usually their basal levels are low, but they can be selectively induced by cytokines, such as IFNγ. SOCS1 inhibits IFNγ signalling for its capacity to bind and inactivate JAK2 protein and consequently to block the IFNγ-induced tyrosine phosphorylation of IFNγ receptor (IFNγR) and STAT1 activation. It has been demonstrated that keratinocytes avoid the detrimental consequences of an excessive stimulation by IFN-γ over-expressing SOCS1 thus hindering the expression of many pro-inflammatory genes, including those involved in skin diseases, such as psoriasis and allergic contact dermatitis (ACD) [2]. A three-dimensional model of the complex between SOCS-1 and JAK2 [3] shows that the Kinase Inhibitory Region (KIR) of SOCS-1 protrudes towards the catalytic region of JAK2 and occupies the ATP binding site. In this work we identify new peptides mimicking KIR-SOCS-1 binding activity through an ELISA-based screening of a focused simplified combinatorial peptide library [4].

Results and Discussion

Through direct binding ELISAs, we confirmed the ability of KIR region (52-67) of SOCS1 to bind to JAK2 catalytic site (1001-1013) both in the phosphorylated (Tyr1007), named pJAK2, and in the non-phosphorylated form, JAK2) (Figure 1). We quantified this interaction in terms of KD values of about 100 μM (Table 1).

Then to investigate crucial residues of KIR 52-67 region involved in JAK2 recognition, we synthesized Ala-scanning peptides. Their binding capacities to both JAK2 peptides were analyzed through direct ELISAs. Data analysis suggested that the key residues of KIR for JAK2 recognition are localized in 52-61 region. Then we synthesized and analyzed the binding properties of this shorter sequence, named New-KIR. ELISA experiments provided K_D values in the low micromolar range. Therefore the deletion of six amino acids in the C-terminal region of KIR led to new-KIR, able to bind to JAK2 catalytic site with a 4-fold greater affinity.

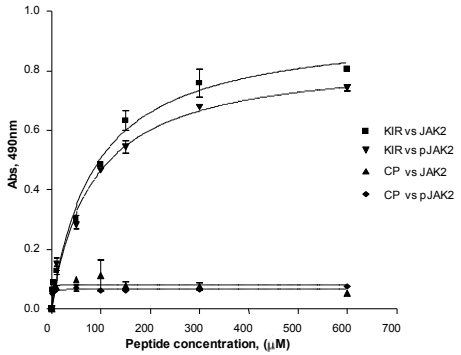

Fig. 1. ELISA direct binding between KIR peptide 52-67vs JAK2 and p-JAK2.

Table 1. K_D values (expressed in μM) of SOCS-KIR mimetic peptides in complex with JAK2 and pJAK2

	KIR	*New-KIR*	*PS-5*	*PS-12*	*PS-11*
JAK2	87±9	27±5	5.2±1.0	5.2±1.6	5.8±1.1
p-JAK2	81±8	16±4	0.8±0.1	4.7±0.5	NC

To further improve binding affinity of new-KIR sequence, following a combinatorial approach, we screened a "focused simplified peptide library", in postional scanning format, PS-SSPL [5]. This library was designed randomizing the three residues in positions 55-57 of New-KIR, that appeared not directly involved in the interaction with JAK2 catalytic region. The combination of identified amino acids in each randomized position led to the design of 12 new peptides. Their binding capacities to JAK2 peptides were analyzed through direct ELISA and we selected two peptides from the experiment involving JAK2 (PS-11 and PS-12), and one peptide (PS-5) from that vs pJAK2. Single peptides selected from PS-SSPL screening, were further analyzed in dose-response direct binding ELISA toward JAK2 peptides. Data fitting provided K_D values in the low micromolar range showing major affinities toward JAK2 region in respect to natural sequences (Table 1).

Then competition experiments were carried out employing PS-5 and PS-12 as competitors of the KIR-JAK2 peptide complexes and both inhibited the binding of JAK2 peptides to immobilized KIR in a dose-dependent fashion and data fitting provided IC50 values in the low micromolar range, fully consistent with estimated K_D values by direct binding, while new-KIR peptide resulted less able to compete with KIR, in the explored concentration range.

In order to perform cell-based experiments we conjuugated KIR sequences to Tat-CPP as carrier. To assess whether PS-5 peptide could inhibit JAK2/STAT1 signaling, we investigated the effect of these conjugated peptides on the phosphorylation of STAT1 and related genes expressions in human keratinocites. Cells pretreated with peptides and subsequently stimulated with INF-γ showed a sensible decrease of phosphorylation level of INF-γ-receptor, consequently, in IFN-γ-induced STAT1 tyrosine phosphorylation while the expression of ICAM1 was highly reduced in the presence of PS5.

In conclusion, here we show that SOCS-1-KIR binds to JAK2 catalytic site with about 80 μM affinity then, following an Ala-scanning approach, that the deletion of last six residues of SOCS-1 KIR (62SDYRRI67) improved the affinity of this domain to JAK2 peptides, providing lower K_D value of about 4-fold. Then we have opportunely designed a focused peptide library in which residues directly involved in complex with JAK2, (52-53, 57-61), remained unchanged, while positions 54-56 were randomized following our simplified approach. From the screening of PS-SSPL we have selected several new sequences with K_D values in the very low micromolar range (6-fold improvement in comparison to new-KIR). The ability to mime SOCS1 of these new peptide sequences were also evaluated in preliminary cellular assays confirming their capacity to interfere with IFN-γ-induced STAT1 phosphorylation and related genes expression, suggesting their potential application as modulators of disorders involving SOCSs over-expression. We selected new and more potent ligands as antagonists of SOCS-1 (K_D values are in the high nanomolar range that are 15-fold lower respect to w-t KIR) representing good candidate as therapuetic agents.

References

1. Alexander, W.S., et al. *Annu Rev Immunol.* **22**, 503-529 (2004).
2. Yoshimura, A., et al. *Nature Rev. Imm.* **7**, 454 (2007).
3. Giordanetto, F., et al. *Protein Engineering* **16**(2), 115 (2003).
4. Albanesi, C., et al. *Curr. Drug Targets Inflamm. Allergy* **4**(3), 329 (2005).
5. Marasco, D., et al. *Curr. Protein Pept. Sci.* **9**(5), 447 (2008).

Proceedings of the 31st European Peptide Symposium
Michal Lebl, Morten Meldal, Knud J. Jensen, Thomas Hoeg-Jensen (Editors)
European Peptide Society, 2010

Utilization of Enzymes from the Red King Crab Hepatopancreas for Obtainment of Cow Milk Protein Hydrolyzate

V. A. Mukhin[1], Yu. E. Trukhacheva[2], and V. Yu. Novikov[1]
[1]Knipovich Polar Research Institute of Marine Fisheries and Oceanography (PINRO), Murmansk, Russia; [2]Murmansk State Technical University (MSTU), Murmansk, Russia

Introduction

Waste from fishery and processing of marine invertebrates is used partly, mainly as feed for fur-bearing animals. However, its weight can comprise up to 90% of a catch [1].

Sufficient quantity of these raw materials as well as the possibility to use them as sources of enzymes open new prospects for their application. We demonstrated how these enzymatic agents can be used to derive protein hydrolyzates for different purposes [1,2].

Nowadays development of new organic forms of digestible essential cationic microelements (EM), such as manganese, zinc, copper and chromium, is an acute problem in medicine, particularly in dietology. One of the ways to solve this problem is to conjugate essential cationic microelements with peptide structures which are formed as a result of enzymatic hydrolysis of alimentary proteins [3,4].

The aim of the paper is to present comparative analysis of molecular-weight distribution of peptide fractions in hydrolyzates of cow milk protein concentrate derived by proteolysis using different enzymatic agents, particularly enzymes of marine origin as well as to estimate suitability of obtained hydrolyzates as complexing agents with essential microelements.

Results and Discussion

Cow milk protein concentrate (CMPC) (BE 8527, Denmark) was used as substrate. Such reagents as "Flavourzyme" (Denmark), "Pancreatin" (Germany) and the enzymatic agent from the red king crab hepatopancreas (EARKCH, Russia) were used as enzymatic agents.

"Flavourzyme" is a proteinase complex produced by fungus *Aspergillus oryzae*. "Pancreatin" is an enzymatic agent which is extracted from the pancreatic glands of cattle. The enzymatic agent from the red king crab hepatopancreas (EARKCH) is not a commercial one. We obtained it as an acetone powder. The previous papers give a detailed description of its characteristics and production [5].

Molecular-weight distribution of the derived hydrolyzates was studied applying medium-pressure exclusion chromatography and using "Superose-12" column (1.6×50 cm). The column was precalibrated with standard globular water-soluble proteins by the firm "Serva" (FRG). 0.2 M sodium chloride with azide was used as eluent. Optical density was registered using the Pharmacia UV-1 FPLC detector (Sweden) with 280 nm wave-length.

During our experiments we studied how temperature of the reaction medium, duration of hydrolysis, correlation between protein substrate and enzymatic agents affected molecular-weight distribution of peptide fractions contained in hydrolyzate of CMPC and derived using EARKCH, "Flavourzyme" and "Pancreatin".

We studied how EARKCH activity depended on the incubating temperature. And the results have shown that rise in temperature from 25 °C to 50 °C results in much more efficient proteolysis. Indicative of that is the reduced specific content of high-molecular structures (more than 28 kD) in hydrolyzate derived at 50 °C.

Increase in enzyme-to-substrate ratio owing to rise in EARKCH concentration from 0.2 % to 5.0 % with 22-hour enzymolysis and unstable pH in water at the temperature of 50 °C caused more than a triple reduction in the content of high-molecular structures (more than 28 kD) in the derived hydrolyzate. At the same time the specific content of fraction with minimal molecular weight (under 1,4 kD), which included relatively short-chain peptides and free amino acids, increased from 35.5% to 63.8%. Conversion of chromatograms, obtained for CMPC hydrolyzate at different EARKCH concentrations, into weight are shown in Figure 2. Hydrolysis took 22 hours at 50 °C and unstable pH.

It was found that EARKCH-induced hydrolysis of protein-containing raw materials is the most efficient when it takes 5-6 hours with 6.8-8.2 pH, 50-55 °C and 5-7 g of the enzymatic agent per 1 kg of protein-containing substrate.

We studied molecular-weight distribution of CMPC hydrolyzates which were derived using such enzymatic agents as "Flavourzyme", "Pancreatin" and EARKCH. Their concentrations varied from 0.5% to 5.0%. It was found that in the hydrolyzate obtained with 5.0 % Flavourzyme concentration the percentage of high-molecular structures halved, whereas the fraction of short-chain peptides and free amino acids increased by 1,7 times compared to the relevant indices for the hydrolyzate derived with 0.5% Flavourzyme concentration.

Cow milk protein concentrate was fermented by "Pancreatin" with two concentrations (0.5% and 2.0%) and stable 7.5 pH for 8 hours. With 0.5% concentration and optimal pH the fraction of high-molecular structures in hydrolyzate did not exceed 6% and the low-molecular fraction reached nearly 60%. Similar values were recorded for hydrolyzate derived by proteolysis of CMPC with 2% "Flavourzyme".

Thus, the lowest content of high-molecular structures in obtained products is recorded for hydrolysis with "Pancreatin" and stable pH for 8 hours when concentration of all the tested enzymatic agents is 0.5%. However, "foreign" macroelements, such as sodium or potassium, occurred at optimal pH are undesirable to further application of enzymolyzate as a complex with EM [6,7].

With low concentration (0.5%) EARKCH is more efficient than "Flavourzyme". When enzyme-to-substrate ratio increases the efficiency of proteolysis with these enzymatic agents is similar if to estimate it by molecular-weight distribution of peptide fractions of derived hydrolyzates.

High content of peptides with molecular weight under 1.4 kD in essential microelement complexes with enzymolyzate of cow milk proteins is unwanted for some reasons.

First of all, abundant low-molecular fractions in the complex increase osmomolarity of the obtained agent which is extremely undesirable to its further application for food fortification [7,8].

Secondly, these fractions make products bitter which will have a significant influence on their application in food industry [9,10].

Thirdly, we demonstrated earlier that cow milk protein structures with molecular weight under 1 kD and above 10 kD are less efficient in microelement binding [4,11,12]. The latter is probably dependent on the features of steric structure of peptide molecules.

It should be mentioned that EARKCH utilization is more efficient in respect to technology and microbiological control since this enzyme is active at low temperatures which considerably delay the development of microflora including pathogenic one.

Thus, formation of EM complexes containing peptides with molecular weight from 1.4 kD to 11.2 kD derived by proteolysis using the enzymatic agent from the red king crab hepatopancreas is considered to be the most optimal and efficient.

References

1. Mukhin, V.A., Novikov, V.Yu. 2001. Enzymatic protein hydrolyzate of tissues of marine hydrobionts: obtainment, characteristics and practical use. PINRO Press, Murmansk. 97 pp. (in Russian).
2. Mukhin, V.A., Novikov, V.Yu., Ryzhikova, L.S. *Appl. Biochem. Microbiol.* **37** (*3*), 292-296 (2001).
3. Vegarud, G.E., Langsrud, T., Svenning, C. *British J. Nutr*. **84** (*1*), 91-98 (2000).
4. Swain, J.H., Tabatabai, L.B., Reddy, M.B. *The J. Nutr*. **132** (*2*), 245-251 (2002).
5. Mukhin, V.A., Novikov, V.Yu. Proteolysis and proteolytic enzymes in the tissues of marine invertebrates. PINRO Press, Murmansk, 2002 (in Russian).
6. Manual for methods of analysis of food product quality and safety. Ed. by I. M. Skurikhin and Tutelyan. Brandes-medicine Press, Moscow. P. 183-185 (in Russian).
7. Popova, T.S., Tamazashvily, T.Sh., Shestopalov, A.E. *Parenteral and enteral nutrition in surgery*. "M-CITY" Press, Moscow, 1996 (in Russian).
8. Neklyudov, A.D., Ivankin, A.N., Berdutina, A.V. *Appl. Biochem. Microbiol*. **36** (*5*), 452-459 (2000).
9. Mahmoud, M.I. *Food Technol*. **48** (*10*), 89-95 (1994).
10. Pedersen, P. *Food Technol*. **48** (*10*), 96-98 (1994).
11. Etcheverry, P., Miller, D.D., Glahn, R.P. *The J. Nutr*. **134** (*1*), 93-98 (2004).
12. Serfass, R.E., Reddy, M.B. *The J. Nutr*. **133** (*2*), 449-455 (2003).

Proceedings of the 31st European Peptide Symposium
Michal Lebl, Morten Meldal, Knud J. Jensen, Thomas Hoeg-Jensen (Editors)
European Peptide Society, 2010

Isovaline Containing Peptides: Configurational Assignment Using 2D-NMR Spectroscopy

Marta De Zotti[1], Elisabetta Schievano[1], Stefano Mammi[1], Bernard Kaptein[2], Quirinus B. Broxterman[2], Sheo B. Singh[3], Hans Brückner[4], and Claudio Toniolo[1]

[1]ICB, Padova Unit, CNR, Department of Chemistry, University of Padova, Padova, 35131, Italy; [2]DSM Innovative Synthesis, BV, Geleen, 6160 MD, The Netherlands; [3]Medicinal Chemistry, Merck Research Laboratories, West Point, 07065, NJ, U.S.A.; [4]Department of Food Sciences, University of Giessen, Giessen, 35392, Germany

Introduction

The non-coded, C^{α}-tetrasubstituted, chiral α-amino acid isovaline (Iva) is a characteristic marker of a class of fungal peptide antibiotics termed peptaibiotics [1]. The unequivocal determination of the position and configuration of the Iva residues in peptides is imperative if their total chemical syntheses are attempted [2]. In peptaibiotics, Iva can be of L(*S*)- or D(*R*)- configuration [3].

Results and Discussion

By 2D-NMR we investigated the naturally occurring and chemically synthesized 16-mer integramides A and B, belonging to a group of bioactive, fungal peptides (peptaibiotics) that are characterized by an abundance of Aib as well as D- and L-Iva residues. Their primary structures are:

Ac-D-Iva[1]-L-Hyp[2]-L-Ile[3]-L-Iva[4]-L-Leu[5]-Aib[6]-Aib[7]-Aib[8] (L-Iva[8])

HO-Gly[16]-D-Iva[15]-L-Iva[14]-L-Hyp[13]-Aib[12]-L-Iva[11]-L-Leu[10]-L-Hyp[9]

Integramide A (B)

The chemical shifts of the C^{α}-alkyl groups in the Iva enantiomers depend on the α-carbon chirality and on the helical screw sense of the peptides, the latter determined by CD.

In the full-length, right-handed helical, integramides, as well as in the partial sequences exploited for their total chemical syntheses, the γ-methyl protons of the ethyl side chain of the D-Iva residues located near the C-terminus are significantly more shielded (δ <0.90 ppm) than those of the L-Iva residues (δ >0.95 ppm) (Figure 1).

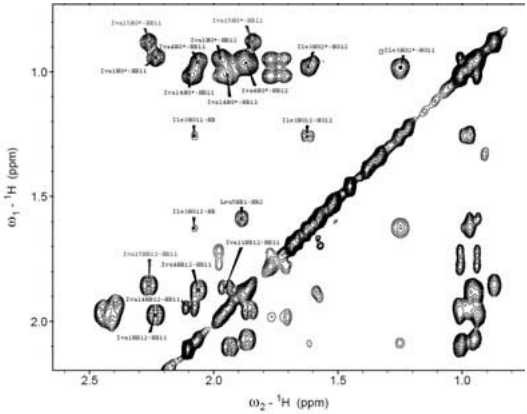

Fig. 1. Side-chain region of the TOCSY spectrum of integramide A in TFE-d_2 solution.

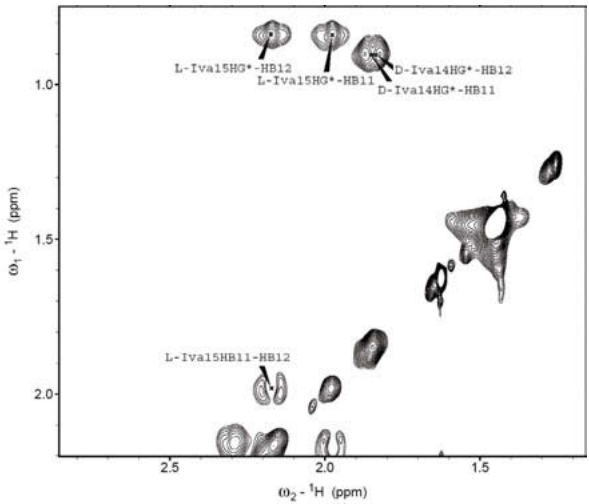

Fig. 2. Side-chain region of the TOCSY spectrum of the left-handed tetrapeptide Z-L-Hyp-D-Iva-L-Iva-Gly-OtBu in $CDCl_3$ solution.

The opposite behavior is observed for the left-handed, synthetic, intermediate Z-Aib-L-Hyp-L-Iva[14]-D-Iva[15]-O*t*Bu (Z, benzyloxycarbonyl; O*t*Bu, *tert*-butoxy) (Figure 2). Here, the γ-methyl protons of L-Iva[14] are more shielded (0.838 ppm) than those of D-Iva[15] (0.905 ppm).

The chemical shift difference between the diastereotopic β-methylene protons of the Iva side chains in the right-handed helical peptides is much larger for D-Iva than for L-Iva. For D-Iva[14/15], the values range from 0.38 to 0.63 ppm, whereas for D-Iva[1] the value is between 0.26 and 0.31 ppm. In each case, the difference is always larger for the D-Iva than for the L-Iva residues (which is always ≤ 0.19 ppm). Again, an opposite behavior is seen for the left-handed tetrapeptide.

Overall, our method enables the non-destructive assignment of the configuration of each Iva residue in peptides of known helical screw sense.

References

1. Toniolo, C., Brückner, H. (Eds.) *Peptaibiotics: Fungal Peptides Containing α-Dialkyl α-Amino Acids,* Verlag Helvetica Chimica Acta, Zürich, Switzerland and Wiley-VCH, Weinheim, Germany, 2009.
2. De Zotti, M., Damato, F., Formaggio, F., Crisma, M., Schievano, E., Mammi, S., Kaptein, B., Broxterman, Q.B., Felock, P.J., Hazuda, D.J., Singh, S.B., Kirschbaum, J., Brückner, H., Toniolo, C. *Chem. Eur. J.* **16**, 316-327 (2010).
3. Degenkolb, T., Brückner, H. *Chem. Biodivers.* **5**, 1817-1843 (2008).

Proceedings of the 31st European Peptide Symposium
Michal Lebl, Morten Meldal, Knud J. Jensen, Thomas Hoeg-Jensen (Editors)
European Peptide Society, 2010

Cyclic PDZ-Binding Peptides as Neuroprotective Agents Against Excitotoxic Brain Damage

Brian M Austen[1], Kate Duberley[1], Paul Turner[2], and Ruth Empson[2]
[1]Dept of Biomedical Sciences, St George's University of London, London, SW17 ORE, UK;
[2]Dept of Physiology, Otago University, Otago, New Zealand

Introduction

Post-synaptic density protein 95, a scaffold protein, regulates signaling in glutaminergic neurons by providing attachment points for NMDA receptors, calcium channels and signaling enzymes [1]. Interactions are made via SH3 and PDZ domains. PDZ domains, consisting of a 5-membered β-barrel and an α-helix, bind the C-termini of interacting proteins, in a grove between one of the β-strands and the α-helix (Figure 1). Excitotoxic neuronal death occurring by over-activation of NMDA receptors, and influx of calcium is involved in neurodegerative disease. We have synthesized stable cyclic peptide analogues of the C-terminal sequences of PMCA2 and NR2B, containing additional cell penetration sequences. Cell staining and immunoprecipitation show that the peptides are internalized and bind PSD95. These peptides have potential as neuroprotective agents.

Results and Discussion

A cyclised form of an analogue C-terminal sequence of PMCA2b Ser-Leu-Glu-Thr-Lys-Leu-COOH was synthesised, by incorporating a β-alanine bridge between Lys^{-2} and Glu^{-4} in the extended sequence:, acetyl-DArg-DArg-DArg-DArg-DArg-DArg-Gly-Gly-Lys(Biotin)Ser-Leu-c[Glu(βAla)Thr-Lys]-Leu-COOH (R2). R2 was synthesized on FmocLeu Peg-PS resin (ABI) using temporary α-amino Fmoc protected residues. The cyclised C-terminal sequence of PMCA2 was extended at the N-terminus by six D-Arg residues to act as a cell penetration sequence, and finally N-acetylated to block the N-terminus against protease degradation. Orthogonally protected residue FmocLys(ivDde) was coupled at step 2 and FmocGlu((2-PhiPr) at step 4. Pior to final deprotection, the ivDde group was removed with 2% hydrazine in DMF for 3x3 min. Fmoc-β-Ala was coupled with PyBOP. The 2-PhilPr group was then removed by treatment with 1% TFA and 0.5% ethanedithiol in dichloro-methane for 4x3 min, and the final Fmoc group removed by 20% piperidine in DMF. Subsequent ring closure, as monitored by ninhydrin reaction, was performed by treatment with 4 equivalents of PyBOP in 0.9M diisopropylamine in DMF. The peptidyl-resin was deprotected and cleaved in 90% TFA, 2.5% water, 2.5% triisopropyl silane, and 0.5% ethanedithiol, for 2hrs. The peptide was purified by HPLC and characterised by MALDI mass spectrometry (MH=2192.1; calc 2193). Affinity for PSD95 was shown by co-immunoprecipitation experiments and co-localisation of the biotin tag on R2, with PSD-95 in human neuroblastoma SHSY-5Y cells using TRITC-avidin and FITC-anti-rabbit antibody with a Rb antibody to human PSD-95 (Abcam) (Figure 2).

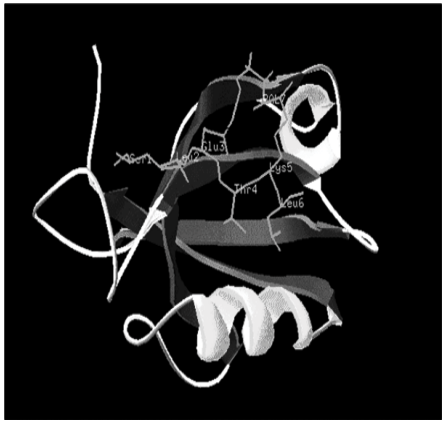

Fig. 1. R2 binding to PDZ domain of PSD95 [2].

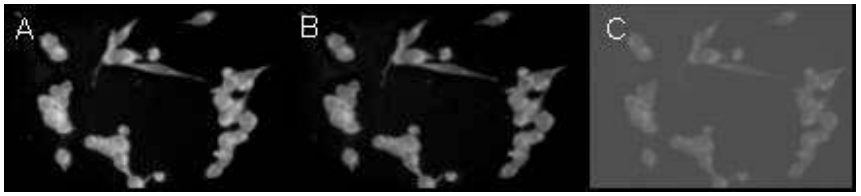

Fig. 2. Staining of SHSY-5Y cells incubated with R2 using TRITC-avidin (plate c), PSD-95 using FITC-anti-rabbit and PSD-95 rabbit antibody (Abnova) (plate b), showed co-localisation (plate a).

The peptide R2 was readily internalized, showing that the hexa-D-Arg sequence acted as an effective cell penetration peptide. The biotin moiety in R2 co-stained with an antibody binding to PSD-95 (Figure 2), indicating that the PDZ domain in PSD-95 was targeted by R2. SHSY-5Y cells challenged with 2mM glutamate were effectively protected against cell death by 2µM, 20µM and 200µM of the N-acetylated and non-acetylated forms of R2 in human non-differentiated SHSY-5Y neuroblastoma cells (Figure 3). Further modifications are required, however, to increase affinity and give rise to an effective therapeutic that will cross the blood-brain barrier.

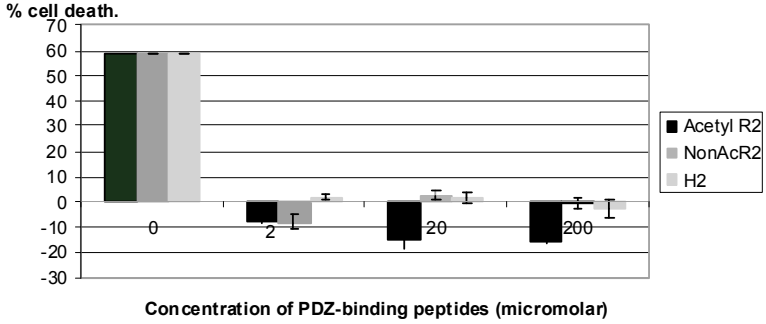

Fig. 3. Protection against cell death of glutamic acid (2mM) treated SHSY-5Y cells.

Acknowledgments
We acknowledge the awarding of a Biochemical Society (UK) travel grant to Kate Duberley.

References
1. Garside, M.L., Turner, P.R., Austen, B., Strehler, E.E., Beesley, P.W., Empson, R.M. *Neuroscience* **162**, 383-395 (2009).
2. Piserchio, A., Salinas, G.D., Li, T., Marshall, J., Spaller, M.R., Mierke, D.F. *Chem.Biol*. **11**, 469-473 (2004).

Proceedings of the 31st European Peptide Symposium
Michal Lebl, Morten Meldal, Knud J. Jensen, Thomas Hoeg-Jensen (Editors)
European Peptide Society, 2010

Cellular Expression of the Human Angiotensin II Type 1 Receptor Containing the Non-Canonical Photolabelling Amino Acid Bpa

Jason Arsenault, Julie Lehoux, Brian J. Holleran, Marilou Lefrançois, Gaetan Guillemette, Richard Leduc, and Emanuel Escher
Universitee de Sherbrooke, Sherbrooke, J1H 5N4, Canada

Introduction

The incorporation of non-coded amino acids into functional proteins in mammalian cells has recently been achieved by several laboratories, mostly through engineered tRNA-aminoacyl-tRNA synthetase pairs for the specific incorporation of unnatural amino acids through recognition of an AMBER codons [1]. We applied this approach to a G Protein Coupled Receptors (GPCR) in order to ultimately identify the binding partners (e.g. ligands, signal transduction- and regulatory proteins) of these receptors through photocross-linking. The human angiotensin II type 1 receptor (hAT_1), a peptidergic GPCR, has been extensively studied using synthetic Angiotensin II (AngII) analogues containing the photoreactive residue p-Benzoyl-L-Phenylalanine (Bpa). This has allowed to map the ligand binding domain of hAT_1 and to deduce its structure. Previous results have identified transmembrane domain (TMD) 7 as interacting with position 8 of the AngII analogue ^{125}I-[Sar^1, Bpa^8] AngII [2,3]. Residues 293 and 294 were the principal contact points [2]. As a proof-of-concept for later protein-receptor interaction studies we applied this approach in the aim of an inverse labeling study. The Amber codon TAG was inserted in a site-specific manner into the hAT_1 receptor gene at known ligand-interaction residues. Following co-transfection of this gene, together with a CUA bst tRNA, its engineered cognate Bpa specific aminoacyl-tRNA synthetase, and in presence of free Bpa, the mammalian cell line COS-7 was able to expressed hAT_1 mutants. TAG mutants were prepared in a site-specific fashion in the proximal location to the AngII binding environment. Since Bpa has been shown to react to methionine with a preferential kinetic [3], the [Sar^1, Met^8] AngII analogue was synthesized. However, synthesis of nonoxidized ^{125}I-[Sar^1, Met^8] Ang II as a Bpa selective bait ligand was not successful and an alternative identification strategy had to be found. The constitutively active N111G hAT_1 template tolerates N-terminal ligand modifications [4]. For this purpose, [Iminobiotinyl-Aca^0, Gly^1, Met^8] AngII was synthesized and N111G hAT_1 was mutated with the same TAG codons to produce the N111G/F293Bpa and N111G/C296Bpa hAT_1. N-terminal flag and C-terminal V5 epitopes were also added for immunoblotting.

Results and Discussion

All of the F293Bpa and C296Bpa receptor mutants displayed native hAT_1 like binding affinity towards Ang II and [Sar^1, Ile^8] Ang II albeit with reduced expression rates (1/3 to 1/10 of WT expression rates). In absence of either one of the transfection elements or of free Bpa, no receptor expression was observed. As expected, all of the tested AngII analogues had low nM affinity towards the WT hAT_1 receptor while the N-terminal iminobiotinylated AngII analogues had nM affinity towards the N111G hAT_1 receptor only. The hAT_1 and the Bpa mutant receptors were photolabeled at a constant 25^{o}C with ^{125}I-[Sar^1, Bpa^8] Ang II for 1h. Figure 1 shows that photoaffinity labeling can quickly distinguish between complete and incomplete receptors. Receptors having a truncation at residue 293 or 296 above the highly conserved NPxxY motif do not express at the plasma membrane nor can they bind AngII analogues. CNBr digestion as well as western blotting confirmed the integrity of the engineered protein. The two iminobiotinylated peptides did not produce sufficient yields to show specific N111G/F293Bpa and N111G/C296Bpa hAT_1 receptor labeling by streptavidine HRP chemiluminescence. Subsequent receptor purification could permit the positive identification of ligand-labeled receptor complexes. However, interestingly the CNBr digestion of the ^{125}I-[Sar^1, Bpa^8] AngII labeled C296Bpa hAT_1 receptor showed a slight elevation of molecular sizes in SDS-PAGE electrophoresis (see Figure 2A). According to the molecular weight ladders this would be an addition of 1 to 2 kDa on the TMD 7 fragments. This thus suggested that we were tagging a small auxiliary receptor binding protein. To confirm this finding we also submitted our receptor

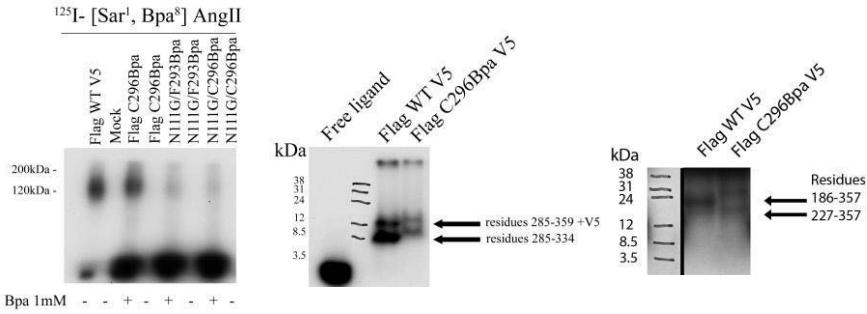

Fig. 1. Photoaffinity labeling. Fig. 2A. CNBr digestion. Fig. 2B. Enzymatic digestion.

to Glu C enzymatic digestion that should highlight larger migrated fragments (see Figure 2B). Again this digestion showed an elevation of 5 to 6 kDa on SDS-PAGE electrophoresis. We can also exclude intramolecular cross-linking due to the fact that only the intracellular fragment of TMD 4 could account for the CNBr digestion's gain in mass, yet according to molecular models, this region is over 20 Å away from the Bpa and thus too far to form a covalent bond even at extreme temperatures [5].

We have shown that the expression of hAT_1 containing the non-canonical amino acid Bpa can be accomplished with reasonable yields. These receptors can easily be identified using photoaffinity labeling. We are also able to identify an auxiliary hAT_1 binding protein, which has at least one CNBr digestion fragment of 1 to 2 kDa and a Glu C digestion fragment of 5 to 6 kDa. Subsequent immunoblotting experiments could be used to positively identify this hAT_1 binding protein. Furthermore, this method can easily be extrapolated to use other non-canonical amino acids that have been developed by the P.G. Schultz group by using the same tRNA and mutated receptor sequences.

Acknowledgments
We thank Marie-Reine Lefebvre for her expert knowledge and expertise. Funding was supported by the CIHR.

References

1. Liu, W., et al. *Nature Methods* **4(3)**, 239-244 (2007).
2. Perodin, J., et al. *Biochemistry* **41(48)**, 14348-14356 (2002).
3. Rihakova, L., et al. *J. Recept Signal Transduct. Res*. **22(1-4),** 297-313 (2002).
4. Fillion, D., et al. *J. Med. Chem*. **55(5),** 2073-2075 (2010).
5. Arsenault, J., et al. *Biochem. Pharmacol*. **80(7),** 990-999 (2010).

Proceedings of the 31st European Peptide Symposium
Michal Lebl, Morten Meldal, Knud J. Jensen, Thomas Hoeg-Jensen (Editors)
European Peptide Society, 2010

The Synthesis of Some Peptides Intended to Be Inhibitors of the RNA-Polymerase of Influenza A Virus

Oleg V. Matusevich[1] and Oleg I. Kiselev[2]
[1]*Saint-Petersburg State University, Chemical Faculty, St. Petersburg, 198504, Russia;*
[2]*Russian Academy of Medical Sciences, Research Institute of Influenza, St. Petersburg, 197376, Russia*

Introduction

The limited choice of anti-viral drugs is the reason of low efficiency of acute and persistent infection treatment [1]. The major drawback of modern anti-viral drugs is low virus-specific targeting [2]. Considerable possibilities in drug design are connected with development of peptides homologous to functional domains of virus-specific proteins [3].

The work presented here is concerned with the synthesis of some peptides appearing to be the potential inhibitors of the RNA-polymerase of influenza A virus. The effect of these peptides is based on the competitive inhibition of virus RNA-polymerase complex organization, said RNA-polymerase consisting of three subunits, namely PB1, PB2, and PA [4].

Results and Discussion

The choice of peptides to synthesize was premised on the data both on tertiary structure of the complex and from biological experiments on strains of Hong Kong isolate and Californian isolate. The former is the ancestor of the world outbreak of bird flu while the latter is known as swine flu and caused boom in 2009.

Sixteen fragments from the PB1 subunit of said viruses RNA-polymerase were synthesized, namely 1-5, 1-20, 1-25, 6-13, 6-25, 14-25, 26-30, 271-290, 381-386, 381-390, 391-400, 381-400, 395-400, 411-420, 525-530, and 525-535 fragments. The amino acid sequences of these fragments are represented in the table below.

N	*Designation*	*Amino Acid Sequence*
1	PB1 (1-5)	H-Met-Asp-Val-Asn-Pro-OH
2	PB1 (1-20)	H-Met-Asp-Val-Asn-Pro-‖-Thr-Leu-Leu-Phe-Leu-Lys-Val-Pro-Ala-Gln-Asn-Ala-Ile-Ser-Thr-OH
3	PB1 (1-25)	H-Met-Asp-Val-Asn-Pro-‖-Thr-Leu-Leu-Phe-Leu-Lys-Val-Pro-‖-Ala-Gln-Asn-Ala-Ile-Ser-Thr-Thr-Phe-Pro-Tyr-Thr-OH
4	PB1 (6-13)	H-Thr-Leu-Leu-Phe-Leu-Lys-Val-Pro-OH
5	PB1 (6-25)	H-Thr-Leu-Leu-Phe-Leu-Lys-Val-Pro-‖-Ala-Gln-Asn-Ala-Ile-Ser-Thr-Thr-Phe-Pro-Tyr-Thr-OH
6	PB1(14-25)	H-Ala-Gln-Asn-Ala-Ile-Ser-Thr-Thr-Phe-Pro-Tyr-Thr-OH
7	PB1 (26-30)	H-Gly-Asp-Pro-Pro-Tyr-OH
8	PB1(271-290)	H-Leu-Pro-Val-Gly-Gly-Asn-Glu-Lys-Lys-Ala-Lys-Leu-Ala-Asn-Val-Val-Arg-Lys-Met-Met-OH
9	PB1 (381-386)	H-Phe-Asn-Glu-Ser-Thr-Arg-OH
10	PB1(381-390)	H-Phe-Asn-Glu-Ser-Thr-Arg-Lys-Lys-Ile-Glu-OH
11	PB1 (381-400)	H-Phe-Asn-Glu-Ser-Thr-Arg-‖-Lys-Lys-Ile-Glu-Lys-Ile-Arg-Pro-‖-Leu-Leu-Val-Glu-Gly-Thr-OH
12	PB1(391-400)	H-Lys-Ile-Arg-Pro-Leu-Leu-Val-Glu-Gly-Thr-OH
13	PB1 (395-400)	H-Leu-Leu-Val-Glu-Gly-Thr-OH
14	PB1 (411-420)	H-Met-Phe-Asn-Met-Leu-Ser-Thr-Val-Leu-Gly-OH
15	PB1 (525-530)	H-Ile-Gly-Val-Thr-Val-Ile-OH
16	PB1 (525-535)	H-Ile-Gly-Val-Thr-Val-Ile-Lys-Asn-Asn-Met-Ile-OH

Solid-phase synthesis on the 2-Cl-Trt resin was performed by Fmoc-/t-Bu strategy both using standard methods of the sequential chain elongation and in a convergent manner [5], the corresponding fragments selection is marked in the table by the || sign.

DIC, HOBt, HOAt, and PyBOP served as condensing agents, reactions were run in DMF and NMP. The conversion of reactions was estimated using the Kaiser test and bromophenol blue.

The purification of the compounds obtained was carried out via preparative reversed-phase HPLC. Their purity turned to be not less than 95%. The molecular ion peaks in mass-spectra MALDI-TOF were in accordance with calculated peaks for all synthesized peptides.

At the moment the peptides under discussion are undergoing biological tests on the base of the Research Institute of Influenza situated in Saint-Petersburg.

References

1. De Clercq, E. *Nature Rev. Microbiol.* **2**, 704-720 (2004).
2. Kiselev, O.I., Deeva, E.G., Slita, A.V., Platonov, V.G. *Anti-viral medications for influenza and acute respiratory disease therapy. Drug design based on polymer carriers*. Publishing house of Information and Analysis Center "Vremya", St-Petersburg, 2000, p.132. (Published in Russian).
3. Trivedi, V.D., Cheng, S.-F., Wu, C.-W., Karthikeyan, R., Chen, C.-J., Chang, D.-K. *Protein Engineering* **16**, 4, 311-317 (2003).
4. Ghanem, A., Mayer, D., Chase, G., Tegge, W.F., Ronald, K.G., García-Sastre, A., Schwemmle, M. *Journal of Virology* **81**, 14, 7801-7804 (2007).
5. Chan, W.C., White, P.D. *Fmoc solid phase peptide synthesis*, Oxford University press, 2004.

Proceedings of the 31st European Peptide Symposium
Michal Lebl, Morten Meldal, Knud J. Jensen, Thomas Hoeg-Jensen (Editors)
European Peptide Society, 2010

The Adjuvant Activity of Glucosaminyl Muramyl Dipeptide (GMDP) is Linked to the Beta-Anomer Configuration and N-Acetylglucosamine (GlcNac) Uptake System

Elena A. Meshcheryakova, Elena P. Dobrushkina, Tatiana M. Andronova, and Vadim T. Ivanov
Shemyakin-Ovchinnikov Institute of Bioorganic Chemistry RAS, Moscow, 117997, Russian Federation

Introduction

Glucosaminyl muramyl dipeptide (GMDP, Figure 1) is the minimum unit of bacterial cell wall peptidoglycan which is the most potent activator of mammalian innate immune system. Numerous biological activities of GMDP including adjuvanticity, make it attractive for medical practice and GMDP has been used successfully in Russian Federation as the medicine Licopid® during more than ten years.

Recently it has been revealed that GMDP stimulates the innate immunity via activation of NF-kB signal pathway by means of intracellular NOD2 receptor [1], but the way by which this glycopeptide penetrates the cell and conformational requirements of this process are poorly understood. In this work we studied the influence of alfa-, beta-anomers equilibrium of GMDP molecule on their adjuvant activity. Besides, in order to highlight the mechanism of GMDP uptake we measured the GMDP adjuvant activity in the presence of Gly-Sar (agonist peptide transporter PEPT1) and N-acetylglucosamine (GlcNac) which models the terminal unit of GMDP.

We found that only beta-conformer of GMDP stimulates adjuvant activity and only GlcNac but not Gly-Sar competed with GMDP during uptake process.

Results and Discussion

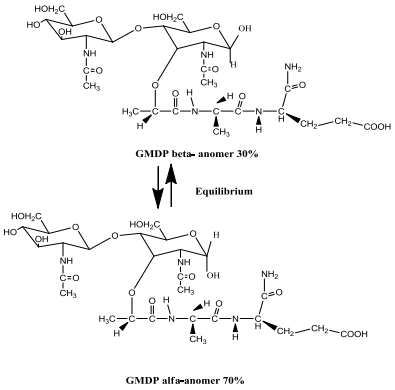

Fig. 1. GMDP anomer equilibrium.

Isolation of GMDP samples with 82% beta-anomer and 95% alfa-anomer.

The possibility to isolate GMDP fractions with 82% beta-anomer strongly depended on the injected quantity of GMDP to the preparative column (reversed phase column 100x600 mm, filled by sorbent Polygoprep 100-30, C18 (Macherey-Nagel). When injected quantity of GMDP was 46 g, the zone 5 on chromatogram was absent, but a little excess up to 50 g caused the appearance of zone 5 which contained 82% beta-anomer of GMDP (Figure 2A). 95% alfa-anomer of GMDP was collected at 36 min (zone 6, Figure 2A) of preparative chromatographic process. Figures 2B and C demonstrate the analytical chromatograms of isolated 82% beta-anomer and 95% alfa-anomer of GMDP.

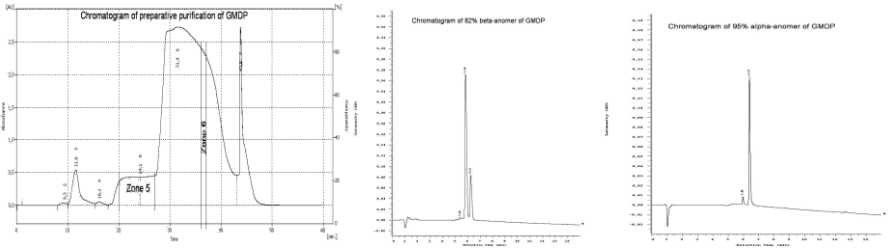

Fig. 2. Preparative (left) and analytical (middle, right) HPLC chromatograms.

Table 1. Stimulation of antibody production to ovalbumine[*]

Substance	*Fold over control*
GMDP	6.09±2.32
GMDP 95% alfa-anomer	1.35±1.2
GMDP 82% beta-anomer	5.87±2.62
GMDP + Gly-Sar (1:10 mol/mol)	6.2±1.93
GMDP + GlcNac (1:10 mol/mol)	0.84±0.19
Gly-Sar	0.84±0.38
GlcNac	1.01±0.26

**BALB/c, 6 animals/group, each mouse was immunized by25μg OVA and 0.144μM of GMDP sample i.p. Two boostings were done with 12.5μg OVA only. Antiserum from each mouse was tested by ELISA. Control group received only OVA.*

Rate of GMDP anomers conversion.

The investigation of rate GMDP anomers conversion by analytical HPLC revealed that for isolated samples with 82% beta- and 95% alfa-anomers standard equilibrium state (30% beta- and 70% alfa-anomers*)* in solution arose not so fast as we thought earlier: 82% beta-anomer 40 min later of dissolution converted only to 59.6% beta-anomer and standard GMDP anomer's equilibrium was achieved during 120 min interval. This rate of GMDP anomer's conversion was enough for studying of presumed difference in biological activities of alfa- and beta- anomers.

Adjuvant activities of alfa- and beta-anomers of GMDP.

We measured *in vivo* stimulation of antibody production by 82% beta- and 95% alfa-anomers GMDP samples in comparison with standard GMDP sample (30% beta- and 70% alfa-anomers). Obtained results showed (Table 1) that adjuvant activities of 82% beta-anomer and standard sample of GMDP were equal but 95% alfa-anomer did not demonstrate adjuvant activity.

Influence of GMDP competition with Gly-Sar and GlcNac on adjuvant activity.

We suggested that such strong conformational restriction of GMDP activity demonstrated above might be related to receptor binding specificity or existence of special sterical gate of GMDP transport system. In order to highlight the mechanism of GMDP uptake we measured the adjuvant activity of standard GMDP sample in the presence of Gly-Sar (agonist of peptide transporter PEPT1) and N-acetylglucosamine (GlcNac, terminal part of saccharide unit of GMDP) which possibly interferes with carbohydrate transporter(s). We concluded from data Table 1 that Gly-Sar was inactive while GlcNac completely inhibited the GMDP activity**.**

Taking together, the data obtained direct further research to investigation of possible GMDP phosphorylation by GlcNac kinase since this enzyme demonstrates high preference for the beta-anomer of GlcNac [2].

Acknowledgments
This work was supported by joint stock company "PEPTEK".

References

1. Meshcheryakova, E., et al. *Vaccine* **25**, 4515-4520 (2007).
2. Blume, A., et al. *Biochemistry* **47**, 13138-13146(2008).

Proceedings of the 31st European Peptide Symposium
Michal Lebl, Morten Meldal, Knud J. Jensen, Thomas Hoeg-Jensen (Editors)
European Peptide Society, 2010

Peptide Inhibitors of the Intrinsic Pathway of Apoptosis Targeting CARD-CARD Interactions

Yadira Palacios-Rodríguez[1,2], Guillermo García-Lainez[1], Mar Orzáez[1], and Enrique Pérez-Payá[1,2]

[1]Laboratory of Peptide and Protein Chemistry, Centro de Investigación Príncipe Felipe, Valencia, E-46012, Valencia, Spain; [2]Instituto de Biomedicina de Valencia IBV –CSIC, E-46010, Valencia, Spain

Introduction

The caspase recruitment domain (CARD) is a module present in proteins that play pivotal roles in programmed cell death (apoptosis) and inflammation. In the apoptotic intrinsic pathway, the interaction between the CARD domain of Apaf-1 (apoptotic protease-activating factor) and the CARD domain of procaspase 9 (PC9) is essential for the apoptosome activation [1]. In inflammation, proteins as those of the NLR family in particular NOD-1, NOD-2 and Nalp-1 also allow binding to a downstream effector molecule through CARD-CARD interaction [2,3]. Although the topology between CARD domains is identical, the primary sequence conservation is generally low; however, as some interface resident amino acids show a high degree of conservation, they were selected as basis for the synthesis of peptide apoptosome inhibitors.

Results and Discussion

Peptides derived from Apaf-1, PC9 and the counterpart sequences of NOD-1 and Nalp-1 CARD were synthesized by Fmoc chemistry, characterized by mass spectrometry and purified by HPLC. We have selected the helices interacting between Apaf-1 CARD and PC9 CARD which include strongly conserved amino acids between several CARDs. The panel of four peptides homologues to CARD from Apaf-1 and PC9 were inhibitors of apoptosome in two *in-vitro* assay formats (Table 1), the first of them was with the recombinant active mini Apaf-1 depleted from WD40 domain [4] and determining the PC9 activity by Ac-LEHD-afc substrate degradation. In the second assay format, cytosolic extracts of 293 cells were depleted from endogenous Apaf-1 by chromatography (FT fraction) and the effect of each peptide was evaluated with recombinant Apaf-1 full length supplemented externally, the result is reported as effect of caspase-3 activity inhibition by Ac-DEVD-afc substrate degradation (Figure 1A and 1B).

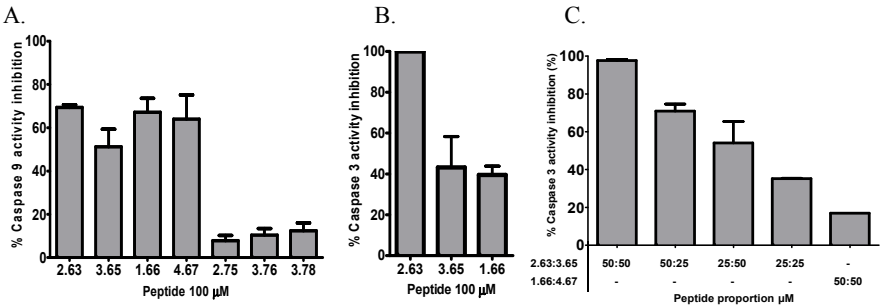

Fig. 1. Peptide inhibitory effect. A. Caspase-9 activity inhibition using rApaf-1 amino acids 1-591 and rPC9 in presence of dATP. B. Caspase-3 activity on FT extracts reconstituted with rApaf-1-XL. C. Synergic peptide effect. The peptides were combined at different proportions in micro molar range. The inhibitory effect was potentiated only by synergism between Apaf-1 CARD-derived peptides (2.63 and 3.65).

Table 1. Inhibitory effect of CARD-derived synthetic peptides in apoptosome reconstitution in-vitro assays

CARD protein-derived	*Helix.[a]Peptide[b]*	*Sequence*	*IC_{50} (μM)[c]*	*IC_{50} (μM)[d]*
Apaf-1	2.63	YIMDHMISDG	90	66
	3.65	FLTISEEEKV	102	84
PC9	1.66	LRRCRLRLVE	68	108
	4.67	RDQARQLII	81	(-)
Nod-1	2.75	TQCLVDNLLKND	(-)	(-)
	3.76	YFSAEDAEIVCA	(-)	(nd)
Nalp-1	3.78	VVLDKLHGQ	(-)	(-)

[a]Represent the helix in the corresponding CARD domain. [b]Peptide code assigned. [c]Determined as Caspase-9 activity inhibition in apoptosome reconstitution with recombinant proteins. [d]Determined as Caspase-3 activity inhibition in cell-free extracts; nd: not determined

In both assays (Figure 1A and B) the peptides 2.63 and 3.65 derived from Apaf-1 CARD were the most active as inhibitors, the IC_{50} was around 60-100 uM (Table 1). The peptides derived from Nod-1 and Nalp-1 did not present activity, confirming the specificity and selectivity from apoptosome derived peptides. Finally, at equimolar concentration the peptides derived from CARD Apaf-1 presented synergic effect and inhibit at 100% the apoptosome in opposition to the lack of contribution of peptides derived from CARD-PC9 (Figure 1C).

The designed mimetic peptides presented inhibitory activity at moderate but selective level and may represent the first generation of specific peptide apoptosome inhibitors.

Acknowledgments

Y. P.-R. was supported by a postdoctoral fellowship from National Autonomous University of Mexico and Consejo Superior de Investigaciones Científicas de España (UNAM-CSIC). The project was supported by MICINN BIO2007-60066 and Generalitat Valenciana PROMETEO/2010/005.

References

1. Qin, H., Srinivasula, S.M., Wu, G., Fernandes-Alnemri, T., Alnemri E.S., Shi, Y. *Nature* **399**, 549-557 (1999).
2. Inohara, N., Nuñez, G. *Nat. Rev. Immunol.* **3**, 371-382 (2003).
3. Proell, M., Riedl, S., Fritz, J.H., Rojas, A. M., Schwarzenbacher, R. *Plos one* **3**, e2119 (2008).
4. Riedl, S.J., Li, W., Chao, Y., Schwarzenbacher, R.S., Shi, Y. *Nature* **434**, 926-933 (2005).

Proceedings of the 31st European Peptide Symposium
Michal Lebl, Morten Meldal, Knud J. Jensen, Thomas Hoeg-Jensen (Editors)
European Peptide Society, 2010

Secondary Structure Modifications of Serine Protease Inhibitor Upain-1 to Improve Binding Affinity

Renée Roodbeen[1,3], Peter A. Andreasen[2,3], and Knud J. Jensen[1,3]
[1]IGM – bioorganic chemistry, Faculty of Life Sciences, University of Copenhagen, Frederiksberg, 1871, Denmark; [2]Department of Molecular Biology, University of Århus, Århus, 8000, Denmark; [3]Danish-Chinese Centre for Proteases and Cancer

Introduction

Cancer is a leading cause of death with a predicted 12 million casualties in 2030 worldwide [1]. Treatment is often complicated due to the formation of metastatic tumors. Metastasis occurs through the degradation of the extracellular matrix in which the plasminogen activation system has a key role (Figure 1) [2,3]. It has been shown that inhibition of this pathway reduces tumor growth and the formation of metastases in mice [4].

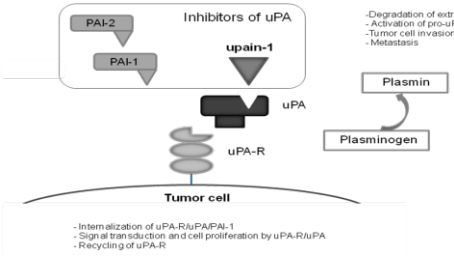

Fig. 1 Simplified overview of the urokinase plasminogen activation system, adapted from [3].

Plasminogen is activated by urokinase plasminogen activator (uPA). A specific cyclic peptidylic inhibitor of uPA, upain-1, was previously isolated from a phage-displayed peptide Library [5].

Upain-1 is a selective inhibitor of uPA and shows negligible affinity towards other serine proteases *e.g.* trypsin [5]. Upain-1 is a dodecameric peptide cyclized by a disulfide bridge between the terminal cysteines [5]. An equally potent analogue, Ac-CSWRGLENHAAC-NH_2, has already been synthesized [6]. Even though upain-1 is a very specific inhibitor, its K_i for uPA is 32 μM, which is too high for an application as a peptide drug.

We hypothesize that the low binding affinity is caused by a significant loss of entropy during the binding event. Therefore we aim to improve the affinity of upain-1 for uPA by making more rigid head-to-tail and sidechain-to-backbone monocyclic and bicyclic analogues of upain-1.

Results and discussion

All peptides were synthesized by sidechain-anchoring of Fmoc-Asp-OAll on a Rink amide resin (Figure 2).

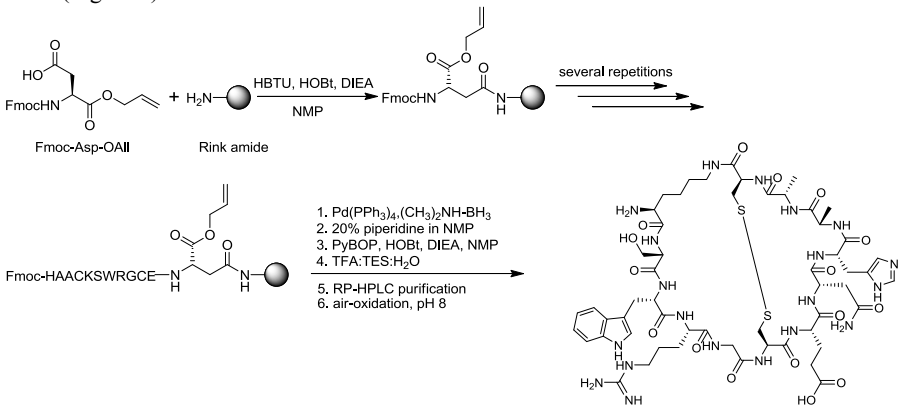

Fig. 2. SPPS-approach to obtain bicyclic upain-1 analogues.

Sidechain-to-backbone cyclized peptides were obtained by using Boc-Lys(Fmoc)-OH. The bicyclic peptides were made by introducing two cysteine-residues in the sequence.

The K_D values for binding of the upain-1 analogues to uPA were determined by displacement of the fluorescent *p*-aminobenzamidine from uPA (Table 1).

Table 1. K_D values for monocyclic (even entries) and bicyclic (uneven entries > 1) upain-1 analogues

Entry	*Sequence*	*K_D (μM)*
1	Ac-CSWRGLENHAAC-NH_2	16
2	ASWRGLENHAAA	>200
3	ASWRGCENHAAC	N.D.
4	PSWRGLENHAAA	>200
5	PSWRGCENHAAC	872
6	PSWRGLENHAAAA	117
7	PSWRGCENHCAAA	676
8	H-KSWRGLENHAAP	173
9	H-KSWRGCENHAPC	>200
10	H-KSWRGLENHAAA	363
11	H-KSWRGCENHAAC	31

N.D. = not determined

All monocyclic analogues show a reduced affinity for uPA. The bicyclic peptides show a further reduced affinity, except for entry 11 (Table 1). This bicyclic peptide binds ~10 times better than its monocyclic precursor and shows similar affinity as the synthetic upain-1 analogue (entry 1).

We conclude that remodeling the structure of upain-1 to form head-to-tail and sidechain to-backbone cyclized analogues has reduced the binding affinity for uPA. Bicyclization of these analogues by introducing a disulfide bridge has improved the affinity of a single analogue by a factor ~10, resulting in a similar affinity as synthetic upain-1. Introducing rigidity can thus improve binding affinity, but only if the binding enthalpy is preserved.

Acknowledgments
We gratefully acknowledge Anni Christensen, Århus University, for performing the displacement studies. The Danish-Chinese Centre for Proteases and Cancer and KU LIFE are thanked for funding.

References

1. Retrieved from: http://www.who.int/mediacentre/factsheets/fs297/en/ (August 5, 2010).
2. Andreasen, P.A., Egelund, R., Petersen, H.H. *Cell. Mol. Life Sci.* **57**, 25-40 (2000).
3. Schmitt, M., et al. *Fibrinilysis & Proteolysis* **14**, 114-132 (2000).
4. Henneke, I., et al. *Am. J. Respir. Crit. Care Med*. **181**, 611-619 (2010).
5. Hansen, M., et al. *J. Bio. Chem.* **280**, 38424-38437 (2005).
6. Hosseini, M., et al. manuscript in preparation.
7. Zhao, G., et al. *J. Struct. Bio.* **160**, 1-10 (2007).

Proceedings of the 31st European Peptide Symposium
Michal Lebl, Morten Meldal, Knud J. Jensen, Thomas Hoeg-Jensen (Editors)
European Peptide Society, 2010

Structural and Biophysical Studies of Ribose-5-Phosphate Isomerase A from Francisella Tularensis

R. Rostankowski[1,2], M. Orlikowska[1,2], D. Borek[2], C. Brautigam[2], T. Scheuermann[2], and Z. Otwinowski[2]

[1]*Faculty of Chemistry, Department of Medicinal Chemistry, University of Gdansk, Poland;*
[2]*Department of Biochemistry, UT Southwestern Medical Center at Dallas, TX, U.S.A.*

Introduction

Ribose-5-phosphate isomerase A (RpiA; EC 5.3.1.6, COG0120) catalyzes the interconversion of ribose-5-phosphate and ribulose-5-phosphate. This intracellular enzyme is essential in the pentose phosphate pathway and in the Calvin cycle of plants. It is ubiquitous and its sequence is highly conserved in species ranging from archaea and bacteria to plants and animals. Whether RpiA is viewed as an anabolic or catabolic enzyme depends on the particular metabolic circumstances. When ribose-5-phosphate is abundant, the reaction runs in the "forward" direction as part of the nonoxidative branch of the pentose phosphate pathway. This ultimately converts the phosphosugar into intermediates for glycolysis, and so provides precursors for the synthesis of amino acids, vitamins, nucleotides, and cell wall constituents. In plants, ribulose-5-phosphate is phosphorylated to form ribulose-1,5-bisphosphate, the vital acceptor of CO2 in the first dark reaction of photosynthesis. Running "in reverse," RpiA is the final step in converting glucose-6-phosphate into the ribose-5-phosphate required for synthesis of nucleotides and cofactors; the previous steps, which comprise the oxidative branch of the pentose phosphate pathway, are a major source of the NADPH needed for reductive biosynthesis. Despite its central role in metabolism, many details of RpiA's action have to date remained poorly understood, largely because of a lack of structural data [1].

Results and Discussion

Crystal structure determination

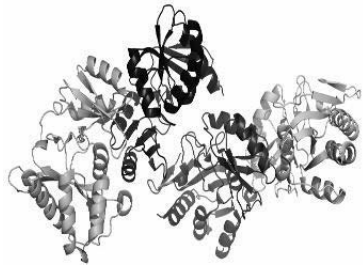

Fig. 1. Crystal structure of Ribose-5-phosphate Isomerase A (3KWM).

Sitting drop vapor diffusion technique was used for the crystallization of RpiA. Structure was solved using molecular replacement technique with substrate and inhibitor complexes of ribose-5-phosphate isomerase A from Vibrio vulnificus YJ016 (3ENQ) as a model. The model was rebuilt in the electron density map. Structure was deposited in Protein Data Bank - 3KWM (Figure 1).

Hanging drop vapor diffusion method was used for crystallization of the protein complex with R-5-P. Structure was solved using molecular replacement method where RpiA (3KWM) structure as a model was used [2].

Analytical Ultracentrifugation experiment

AUC sedimentation velocity run was carried out at room temperature using a Beckman XLI analytical ultracentrifuge equipped with UV absorption optics (Beckman Coulter, Brea, CA). Experiment was obtained in conventional double-sector cells. Protein solution contained 50 mM HEPES, 200 mM NaCl, 1 mM DDT. The concentrations of protein were 0.1 OD, 0.5 OD and 1 OD [3].

Isothermal Titration Calorimetry studies

Titrations of ligand into a protein solution were carried out at 30°C using a VP-ITC instrument (MicroCal LLC, Northcampton, MA). Both ligand and protein solutions contained 50 mM pH 7.5HEPES, 50 mM NaCl and 1 mM DTT. The concentrations of ligand and protein were 1mM and 0.05 mM respectively. Experiments were done in triplicate at given temperature and consisted of 25 injections of 10µl (first injection 1 µl).

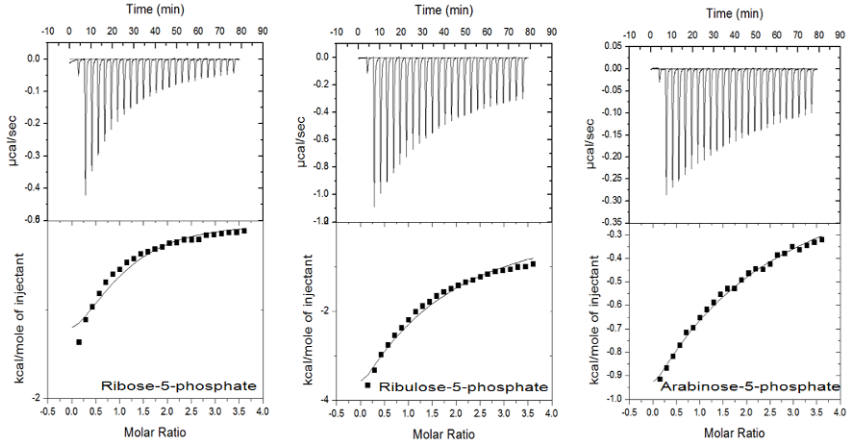

Fig. 2. ITC characterization of Ribose-5-phosphate, Ribulose-5-phosphate and Arabinose-5-phosphate binding to RpiA.

Injections were made at rate of 0.5 µl/s and at intervals of 180 s. The first injection peak was discarded from the isotherm. Areas under thermogrampeaks were calculated and fit to a one-site binding model using Origin (Figure 2) [4].

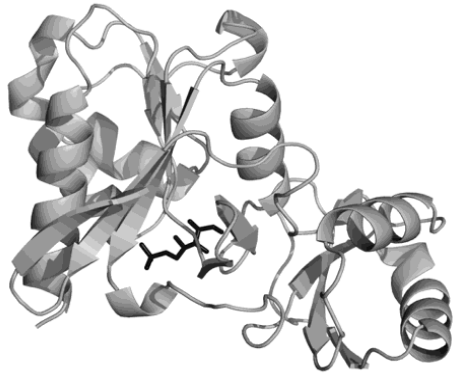

Fig. 3. Binding site of RpiA (ribose-5-phosphate depicted in black).

Conclusions

According to AUC experiment results Ribose-5phosphate isomerase A is a stable dimer. ITC experiments confirmed that ribose-5-phosphate bind to the active site of protein, however lower affinity was observed for other sugars such as arabinose-5-phosphate and ribulose-5-phosphate. Crystal structure of protein complex (RpiA+R5P) should allow us to determine a mechanism of interaction between protein molecule (RpiA) and ligand molecule (R5P) (Figure 3).

Reference

1. Zhang, R., Andersson, C.E., Savchenko, A., Skarina, T., Evdokimova, E., Beasley, S., Arrowsmith, C.H., Edwards, A.M. *Structure* **11** (1), 31-42 (2003).
2. Kim, T.G., Kwon, T.H., Min, K., Dong, M.S., Park, Y.I., Ban, C. *Mol. Cells.* **27** (1), 99-103 (2009).
3. Behike, J., Ristau, O. *Biophysical Journal* **72**, 428-434 (1997).
4. Demers, J.P., Mittermaier, A. *J. Am. Chem. Soc*. **131**, 4355-4367 (2009).

Proceedings of the 31st European Peptide Symposium
Michal Lebl, Morten Meldal, Knud J. Jensen, Thomas Hoeg-Jensen (Editors)
European Peptide Society, 2010

Simplified Θ-Defensins: Search for New Antivirals

Piotr Ruchala[1], Sylvia Cho[3], Amy L. Cole[4], Chun-Ling Jung[1], Hai T. Luong[1], Ewa D. Micewicz[2], Alan J. Waring[1], Alexander M. Cole[4], Betsy C. Herold[3], and Robert I. Lehrer[1]

[1]Department of Medicine;[2]Radiation Oncology, David Geffen School of Medicine, University of California at Los Angeles, Los Angeles, CA, 90095, U.S.A.; [3]Department of Pediatrics and Microbiology-Immunology, Albert Einstein College of Medicine of Yeshiva University, New York, NY, 10461, U.S.A.; [4]Department of Molecular Biology and Microbiology, Biomolecular Science Center, University of Central Florida, Orlando, FL, 32816, U.S.A.

Introduction

Three subfamilies of defensins exist in vertebrates, and are known as α-, β-, and θ-defensins [1]. They are small, amphipathic and cationic peptides with largely β-sheet structures which are stabilized by 3 intramolecular disulfide bonds. Human α- and β-defensins have broad antibacterial and antifungal activity as well as prominent antiviral activity against HIV-1, HSV-2 and influenza A [1]. The third subfamily, θ-defensins, is not expressed in humans. It was initially isolated from the leukocytes and bone marrow of nonhuman primates, specifically Old World monkeys. Subsequent numerous studies established that θ-defensins are effective primarily against viruses acting as potent entry inhibitors for HIV-1, HSV-2 and influenza A [2,3]. Despite small size (18 Xaa), θ-defensins are difficult to synthesize. Chemically, they belong to cysteine-rich peptides and in addition contain a circular backbone. Such structure requires 2 post-synthetic steps: oxidation (disulfide bonds formation) and cyclization (circularization via amide bond) resulting in a low final yield of desired product. Development of an expression system capable of delivering recombinant θ-defensins was also unsuccessful to date hampering greatly their development as potential antiviral drugs. Therefore our current studies focused on modification of θ-defensins with the general goal to simplify their structure and preserve or possibly enhance their antiviral properties.

Results and Discussion

We hypothesized that the anti-viral properties of retrocyclins might rely largely on structural features located in the central β-sheet region, which is defined by three disulfide bridges. Accordingly, we designed and synthesized two mini-libraries of smaller analogues called Hapivirins (HpVs) and Diprovirins (DpVs). The HpVs and DpVs consist of 13 residues and do not possess a cyclic backbone. In the case of DpVs, the β-turn and hairpin structure resulted from an introduction of (D)Pro-(L)Pro dipeptide moiety. HPVs and DpVs are easier to produce, and in the case of DpVs, may potentially be made and oxidized entirely on the resin, reducing post-synthetic work considerably, giving high final yields of desired compound(s).

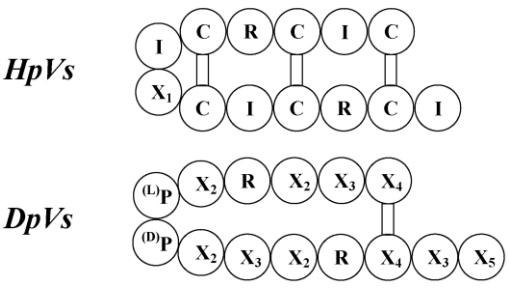

Fig. 1. Structure of Hapivirins (HpVs) and Diprovirins (DpVs). X_1, X_2, X_3, X_4, X_5 - variable residues.

HpVs and DpVs (Figure 1, 70 variants) were screened for activity against HIV-1 and HSV-2 using TZM-bl assay and plaque assay respectively (Table 1). The most active compound, DpV16, possesses antiviral activity comparable to parental θ-defensins (RC1 and RC101). Hydrophobicity in positions X_2 and X_3 is important for antiviral activity since only analogues carrying Ile and Leu in X_2 and Ach, Tle, Cpg, Chg and Tyr in X_3 were active. Only one additional permissive substitution utilizing Arg residues was found (DpV1622). Oxidation via disulfide bond

Table 1. Antiviral activity of HpVs and DpVs. For DpVs, only results for analogues with bioactivity of 50% and higher are shown

X_1	Peptide	% Inhibition±SEM HIV-1 at 10 μg/ml	% Inhibition±SEM HSV-2 at 50 μg/ml	X_1	Peptide	% Inhibition±SEM HIV-1 at 10 μg/ml	% Inhibition±SEM HSV-2 at 50 μg/ml
Gly	HpV1	25.4±2.3	100.0±0.0	X_2			
βAla	HpV2	3.5±1.5	11.3±7.1	**Chg**	DpV20	-8.4±2.6	96.7±0.8
GABA	HpV3	20.4±3.5	8.5±7.9	**D-Chg**	DpV21	-2.3±5.4	100.0±0.0
Ava	HpV4	43.5±2.9	8.1±5.2	X_3	**X_2 = Leu**		
Ahx	HpV5	57.3±2.8	94.1±4.2	**Val**	DpV1606	79.4±2.2	16.8±3.6
Ahp	HpV6	60.1±1.8	96.6±1.2	**Thr**	DpV1607	36.4±0.7	78.1±1.0
Aoc	HpV7	56.0±1.3	98.1±1.1	**Tle**	DpV1609	84.1±1.0	99.5±0.5
L-Pro	HpV8	N.T.	99.0±1.3	**Ach**	DpV1614	87.0±3.1	73.5±1.0
D-Pro	HpV9	14.7±4.6	99.2±1.3	**Cpg**	DpV1615	96.3±0.3	99.0±0.0
Idc	HpV10	16.0±3.2	100.0±0.0	**Chg**	DpV1616	97.4±0.2	99.5±0.5
Oic	HpV11	N.T.	10.7±0.0	**His**	DpV1619	-20.6±5.6	50.8±0.8
Tic	HpV12	38.6±1.8	100.0±0.0	**Tyr**	DpV1620	53.6±24.2	18.8±0.0
Ach	HpV13	14.2±1.9	100.0±0.0	**Arg**	DpV1622	87.9±0.2	97.4±0.5
L-Chg	HpV14	N.T.	100.0±0.0	X_4	**X_2 = Leu**	**X_3 = Ile**	
D-Chg	HpV15	37.2±2.3	85.4±3.5	**Cys^{SH}**	DpV1623	85.3±1.5	60.2±4.1
DGK	HpV16	26.2±1.7	21.7±11.3	**Thr**	DpV1625	23.9±0.2	64.1±0.0
X_2				X_5	X_2 = Leu	X_3 = Ile	X_4= Cys (oxid)
Val	DpV9	-15.3±4.1	82.2±4.6	**Mes**	DpV1630	88.8±1.1	98.7±1.3
Ile	DpV13	88.8±0.0	95.4±2.6	**PEG_5**	DpV1631	83.3±0.8	99.6±0.4
Leu	**DpV16**	**93.4±0.2**	**91.3±4.6**	**Aoa-PEG_5**	DpV1632	73.7±0.3	98.2±0.9

Abbreviations: Aib - α-Aminoisobutyric acid, Chg - Cyclohexylglycine, Abu - 4-Aminobutyric acid, Ava - 5-Aminoheptanoic acid, Ahx - 6-Aminohexanoic acid, Ahp - 7-Aminoheptanoic acid, Aoc - 8-Aminooctanoic acid, Idc - (S)-Indoline-2-carboxylic acid, Oic - (S)-Octahydroindole-2-carboxylic acid, Tle – tertLeucine, Tic - (3S)-1,2,3,4-Tetrahydroisoquinoline-3-carboxylic acid, Ach - 1-Amino-1-cyclohexane-carboxylic acid, Cpg – Cyclopentylglycine, Ach - 1-Amino-1-cyclohexane-carboxylic acid, hSer - Homoserine, Nle - Norleucine, Mes - Methanesulphonyl, Aoa - Aminooxyacetic acid

appears not to be crucial for activity, however the presence of cysteines in positions X_4 is. N-terminal modifications in parental molecule are generally permissive and may be used to introduce fairly large moieties, such as PEG5 spacer. Synthesis of HpVs and DpVs is much more efficient than these of θ-defensins, and in the case of DpV16 can be carried out entirely on resin with final yield ~200 mg per 0.5 mM scale. Mechanistically, new peptides mimic parental θ-defensins and bind to heptad repeat 2 (HR2) of gp41. DpV16 binds to glycoprotein D of HSV-2 (gpD2) with high affinity (Kd~400 nM), which is essential for viral entry and for cell-to-cell spread of HSV. It binds also to HR2 of gpH but not HR1, and does not bind to gpB. DpV16 based analogues appear to be a suitable template for new antivirals.

Acknowledgments

These studies were supported, in part, by funds from the Adams and Burnham endowments provided by the Dean's Office of the David Geffen School of Medicine at UCLA (P.R.) and by NIH grants AI-052017 and AI-082623 (to A.M.C.).

References

1. Lehrer, R.I. *Nat .Rev. Microbiol.* **2(9),** 727-738 (2004).
2. Owen, S.M., et al. *AIDS Res. Hum. Retroviruses* **20(11),** 1157-1165 (2004).
3. Cole, A.M. *Protein Pept. Lett.* **12(1),** 41-47 (2005).

Proceedings of the 31st European Peptide Symposium
Michal Lebl, Morten Meldal, Knud J. Jensen, Thomas Hoeg-Jensen (Editors)
European Peptide Society, 2010

Venomics: Targeted Drug Discovery and Lead Optimisation Using Animal Venoms

Reto Stöcklin*, Estelle Bianchi, Daniel Biass, Cécile Cros, Dominique Koua, Frederic Perret, Aude Violette, and Philippe Favreau

Atheris Laboratories, case postale 314, CH-1233, Bernex-Geneva, Switzerland

Introduction

Venoms are rich mixtures of peptides and proteins evolved by Nature to catch and digest preys or for protection against predators. They represent extensive sources of potent and selective bioactive compounds to discover and develop new drugs. Conventional bioactivity-guided strategies are time consuming and require large amounts of material. In contrast, state-of-the-art proteomic, transcriptomic and post-genomic technologies coupled to bioinformatics can swiftly generate abundant and valuable data using minimal sample amounts.

Strategy and Case Studies

In a typical drug discovery project, we use our databases to select venoms offering higher chances to generate hits for a given target. The venoms are pre-fractionated using specific methods and natural libraries are made ready for bioassays. The fraction composition is often investigated in parallel on our mass spectrometry and bioinformatics platform with database matching. Stringent criteria are used to pick out fractions for deconvolution, and hits are synthesised at an early stage to generate synthetic libraries of bioactive candidates. After deeper evaluations, selected leads undergo optimisation through drug design and structure-function studies. Here again, we developed an original approach: our platform is designed to screen related venoms and other organisms to identify natural analogues of the lead compound in order to exploit what nature has optimised through million years of natural selection.

Our bioactivity-guided, structure-driven and biocomputing-assisted Venomics strategies are illustrated through the discovery of novel sarafotoxins (endothelin-type peptides), bradykinin-potentiating peptides (BPP's) and novel antimicrobial peptides. The presentation will also focus on "CONCO – the cone snail genome project for health", the first fully integrated Venomics project, which is devoted to venomous marine snails.

Endothelins are mini-proteins of 21 amino acids with two disulfide bonds that play a key role in vascular homeostasis and are strong vasoconstrictors. Their over-expression leads to hypertension and vascular diseases. Sarafotoxins from burrowing asp snake toxins are homologous to endothelin peptides but lethal. By screening the proprietary database ToxEnter, a closely related species (*Atractaspis microlepidota*) was identified [1]. LC-ESI-MS and *de novo* MS/MS analysis of the venom revealed typical C-terminal sequences of sarafotoxins and endothelins prolonged by additional tripeptide (Figure 1). The structure revealed an additional C-terminal alpha-helix region crucial for interaction with endothelin receptors. The preliminary studies suggested binding to endothelin receptors with no induction of activity (inhibitory effect). Endothelin

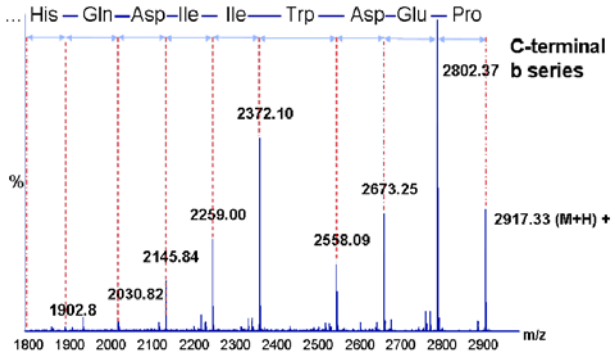

Fig. 1. MS/MS spectrum of sarafotoxin C-terminal sequence.

receptor antagonists may serve medicinal chemists in novel drug design or be used as drug candidates themselves [1].

Bee, wasp and ant venoms are available in a relatively limited number of species (except for social honeybees). The venom analyses of a few specimens of the solitary bee *Osmia rufa* by LC-ESI-MS and nanoESI-MS showed more than 50 different compounds with molecular masses ranging from 400 to 4000 Da [2]. The major component, at 1924.20 Da, was revealed after sequencing by *de novo* MS/MS and Edman degradation to be a 17-residue cysteine-free peptide, named osmin. Preliminary assays showed that osmin inhibits bacterial and fungal growth at micromolar concentrations and 3D models with alpha-helical structure showed an amphipathic pattern typical of antimicrobial peptides (AMPs) [2].

Bradykinin-potentiating peptides (BPPs) are angiotensin-converting enzyme inhibitors identified in several species. Originally discovered in the '60s, they led to the development of Captopril, a drug to treat hypertension. The characteristic structural features are invariable N-terminal pyroglutamate residues and two consecutive C-terminal proline residues. The development and validation of original methodology for high throughput discovery of BPPs in venoms combined to LC-ESI-MS/MS in precursor ion scan mode, 20 BPP-like sequences were discovered in venom of *Bothrops moojeni* snake [3].

Finally, the genome, venom transcriptome and proteome of *Conus consors* (Figure 2) are currently exhaustively studied. Identification, characterisation and synthesis of novel bioactive compounds are investigated [4]. After high throughput bioactivity screening, selected peptides are further characterised *in vivo* and their potential as novel biopharmaceutical drug candidates is evaluated. Additionally, the biodiversity, ecology and molecular evolution of a wide range of venomous gastropod species are studied.

We believe that our unique techniques, combining mass spectrometry to *in silico* data and text mining strategies, are a straightforward discovery approach for novel biomolecules from animal venoms and other natural sources.

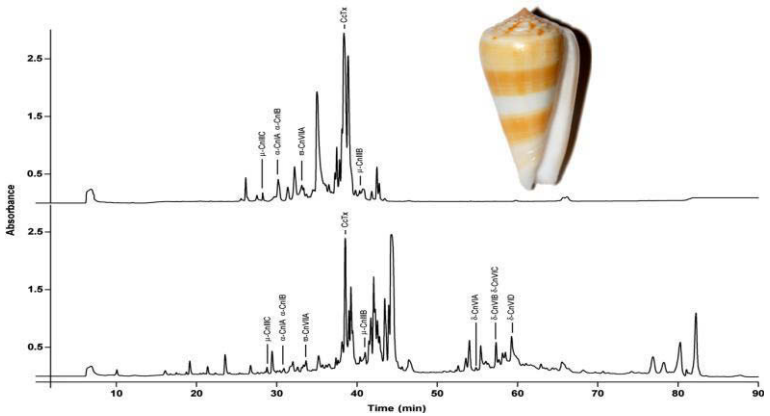

Fig. 2. HPLC UV of milked venom (MV) and dissected venom (DV) of Conus consors cone snail (bottom figure).

Acknowledgments

CONCO, the cone snail genome project for health, is funded by the European Commission: LIFESCIHEALTH-6 Integrated Project LSHB-CT-2007-037592. We are grateful to the governments of New Caledonia and French Polynesia.

References

1. Hayashi, et al. *Peptides* **25**(8), 1243-1251 (2004).
2. Stöcklin, et al. *Toxicon.* **55**(1), 20-27 (2010).
3. Menin, et al. *Toxicon.* **51**(7), 1288-1302 (2008).
4. Biass, et al. *J. Proteomics* **72**(2), 210-218 (2009).

Proceedings of the 31st European Peptide Symposium
Michal Lebl, Morten Meldal, Knud J. Jensen, Thomas Hoeg-Jensen (Editors)
European Peptide Society, 2010

Application of Conjugated Glutamic Acid Peptide (GAP) to a Novel 4-Anilinoquinoline EGFR Inhibitor for Tumor-Targeted Imaging

Chumpol Theeraladanon[1], Nobukazu Takahashi[1], Masaaki Shiina[2], Keisuke Hamada[2], Yuuki Takada[1], Hisashi Endo[3], Ukihide Tateishi[1], Takashi Oka[1], Kazuhiro Ogata[2], David J. Yang[4], and Tomio Inoue[1]

[1]Department of Radiology, Graduate School of Medicine, Yokohama City University, Yokohama, 236-0004, Japan; [2]Department of Biochemistry, Graduate School of Medicine, Yokohama City University, Yokohama, 236-0004, Japan; [3]Department of Pharmacy, Yokohama City University Hospital, Yokohama, 236-0004, Japan; [4]Division of Diagnostic Imaging, The University of Texas M. D. Anderson Cancer Center, Houston, Texas, 77030, U.S.A.

Introduction

Glutamic Acid Polypeptide (GAP) is a targeted drug delivery peptide. It would be suitable to conjugate anti-cancer as well as chelate to radiometal with its acid residues for imaging or radiotherapeutic application. Despite the fact that GAP is commercially available, various ranges of peptide chain (MW 750-50,000) leads to occasionally difficult explanation of experiment results when it exerts action though glutamate receptors. Herein, we designed the decapeptide GAP (MW 1309.16) as an optimized homing agent to carry a novel 4-anilinoquinoline epidermal growth factor receptor (EGFR) inhibitor aiming to develop ^{68}Ga-GAP-YCU07 to image functional ER(+) diseases such as breast cancer.

Results and Discussion

Decapeptide GAP was synthesized by peptide synthesizer. This well characterized GAP is a potential decapeptide targeted carrier and chelator, which conjugates rationally designed novel 4-anilinoquinoline EGFR Tyrosine Kinase Inhibitor, [6,7-dimethoxyethoxy]-quinolin-4-yl]-(3-ethynylphenyl)-amine (YCU07) via peptide linkage (Figure 1).

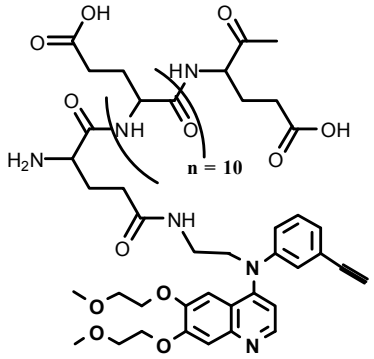

Fig. 1. GAP-YCU07.

According to the pharmacophore model for inhibitor competing at EGFR binding site, the quinoline nucleus of YCU07 was successfully synthesized employing Ring-Closing Metathesis (RCM) methodology. Facile radiolabeling with GAP technology provided ^{68}Ga-GAP-YCU07 which one molecule of GAP-YCU07 possibly chelated a maximum of three ^{68}Ga ions. Injection of ^{68}Ga labeled conjugated GAP-YCU07 to nude mice implanted with A431 evaluated the biodistribution and was imaged by using animal PET camera and CT resulting in accumulation of ^{68}Ga-GAP-YCU07 in the receptor positive tumor with uptake values of 1.50±0.09, 2.36±0.36 %ID/g at 30 and 90 min, respectively.

Acknowledgments
We thank Fuji Film RI Pharma Co., Ltd. for conducting the mass spectroscopy measurements. This research was supported in part by a 2007 Strategic Research Project grant (Fund Number K19016) of Yokohama City University, Japan.

References
1. Theeraladanon, C., Takahashi, N., Shiina, M., Hamada, K., Takada, Y., Endo, H., Tateishi, U., Oka, T., Ogata, K., Inoue, T. *Cancer Biother. Radiopharm.* **25**, 479-486 (2010).

Proceedings of the 31st European Peptide Symposium
Michal Lebl, Morten Meldal, Knud J. Jensen, Thomas Hoeg-Jensen (Editors)
European Peptide Society, 2010

Quantifying Molecular Partition of Charged Molecules by Zeta-Potential Measurements

João Miguel Freire, Marco M. Domingues, Joana Matos, Manuel N. Melo, Ana Salomé Veiga, Nuno C. Santos, and Miguel A.R.B. Castanho

Instituto de Medicina Molecular, Faculdade de Medicina da Universidade de Lisboa, Lisbon, Portugal; e-mail: joaofreire@fm.ul.pt

Introduction

Many cellular phenomena occur at the biomembranes level. Biomolecules, such as several peptides (e.g., antimicrobial peptides - AMP) and proteins, exert their effects at the cell membrane level. This feature creates the need of investigating their interactions with lipids to clarify their mechanisms of action and side effects [1].

The determination of molecular lipid/water partition constants (K_p) is frequently used to quantify the extension of the interaction, which has been achieved by using different spectroscopic and chromatographic methodologies [2-4].

In this work, we derived and tested a mathematical model to determine the K_p from ζ-potential data [3]. The values obtained with this method were compared with those obtained by fluorescence spectroscopy, a regular technique used to quantify the interaction of intrinsically fluorescent peptides with selected biomembrane model systems.

Two antimicrobial peptides (BP100 and pepR [5,6] were evaluated by this new method. The results obtained by this new methodology show that ζ-potential is a powerful technique to quantify peptide/lipid interactions of a wide variety of charged molecules, overcoming some of the limitations inherent to other techniques, such as the need for fluorescent labeling.

Results and Discussion

The quantification of partition can be tackled considering the distribution of a solute between immiscible phases [2]. Briefly, the partition constant can be formulated by equation 1 [2]. When using fluorescence spectroscopy, the variation of the fluorescence intensity emitted by the peptide with the concentration of lipid ([L]), is a linear combination of the contribution of the molecules in the aqueous or on the lipid phase [2]. The fraction of membrane-bound (X_L) solute can be related to K_p by Equation 2:

$$K_P = \frac{[P]_L}{[P]_W} \Leftrightarrow K_P = \frac{\frac{n_{s,L}}{V_L}}{\frac{n_{s,W}}{V_W}} \qquad \text{Eq. 1.}$$

$$\frac{I_f}{I_W} = \frac{1 + K_P \gamma_L [L] \frac{I_L}{I_W}}{1 + K_P \gamma_L [L]} \qquad \text{Eq. 2.}$$

Where K_p represents the partition constant, $n_{s,i}$ and $[P]_i$ are respectively the moles of solute and the peptide concentration in each environment i (i = W, water; i = L, Lipid) and γ_L is the molar volume of the lipid. I_W and I_L are the fluorescence intensities arising when all the peptide is in the aqueous and on the lipid phases, respectively.

Here we present a mathematical formalism to determine partition constants of polyelectrolytes, such as charged peptides (a characteristic shared by almost all AMP for instance), to lipid vesicles (LUVs) by ζ-potential measurements [3,7]. The basic assumption of this method is that the particle under study can be electrophoretically displaced, which is a consequence of its global net charge [7]. This method relies on electrostatic interactions, which have an important role in partition phenomena [3,8].

To determine the K_P value by this methodology, it is necessary to know in advance the net charge of the peptide and the proportion and effective charge of the ionic phospholipids in the vesicles. The reduction of global net charge of LU Vs induced by the peptide is proportional to the fraction of charged lipids that are neutralized, given by Equation 3:

In Equation 3 $|\Delta\zeta/\zeta_0|$ is the relative reduction in ζ-potential, which is dependent on the global peptide concentration, [P]; $n_{PL_{neutralized}}$ is the number of charged phospholipids that

Table 1. Values of the partition constants of BP100 and pepR to liposomes with different lipid compositions, at pH 7.4, obtained by ζ-potential and fluorescence spectroscopy measurements. (K_p ± standard deviation)

Peptide	*Lipid Mixture*	$K_p / 10^3$	
		Fluorescence Spectroscopy	*ζ-Potential*
BP100	POPC:POPG 1:2	50.7 ± 9.30	56.7 ± 0.70
pepR	POPC:POPG 4:1	0.44 ± 0.08	1.70 ± 0.06
	POPC:POPG 3:2	4.50 ± 1.06	5.50 ± 1.30

were perturbed by the peptide interaction and $n_{PL_{total}}$ is the total amount of charged phospholipids. Assuming that each nominal peptide charge, when interacting with the lipid membrane, neutralizes one nominal phospholipid charge, it is possible rearrange Equation 3 to Equation 4. z_{lipid} is the absolute charge of the lipid and ζ_{final} is the ζ-potential value for each titration with peptide. Plotting ζ_{final}/ζ_0 vs [P], it is possible to determine the value of K_P from the slope, using and Equation 4, where X_L is a function of K_P (*2*).

$$\left|\frac{\Delta\zeta}{\zeta_0}\right| = \frac{n_{PL^-_{neutralized}}}{n_{PL^-_{total}}} \qquad \text{Eq. 3.}$$

$$\frac{\zeta_{final}}{\zeta_0} = 1 + \frac{X_L z_{Peptide}}{f_{PL}[L] z_{Lipid}}[P] \qquad \text{Eq.4.}$$

We developed a new mathematical formalism to determine K_p from ζ-potential data and compared the retrieved values with those obtained by fluorescence spectroscopy. The K_p values calculated are summarized in Table 1. The net charges considered were -1, +12 and +6 for the anionic phospholipids, pepR and BP100 [6], respectively. Both methods retrieved comparable K_p values. ζ-potential measurements prove to be a reliable method for studying peptide/lipid interactions and for K_p determination. ζ-potential is a powerful approach when studying charged molecules that are also good scatterers; however charged particles are mandatory. When using fluorescence spectroscopy, a fluorescent reporter in the membrane-active molecule is needed. Nevertheless, there are some cases where no reporter is available in the native molecule. With this novel approach, it is possible to quantify the partition of molecules with no intrinsic fluorescent reporter, as long as they are charged, which is an almost universal condition in some areas of study, such as antimicrobial peptides.

Acknowledgments
The authors thank Rafael Ferre, Marta Planas, Lidia Feliu and Eduard Bardají (Department of Chemistry, University of Girona, Spain) for the synthesis of BP100 and to Wioleta Kowalczyk and David Andreu (Department of Experimental and Health Sciences, Pompeu Fabra University, Barcelona, Spain) for the synthesis of pepR. This work was partially supported by project PTDC/QUI/69937/2006 from FCT-MCTES, Portugal. JMF also thank FCT-MCTES for grant IMM/BT/37-2010 and EPS for the travel grant.

References
1. Reddy, K., et al. *Int. J. Antimicrob. Agents* **24**, 536 (2004).
2. Santos, N.C., et al. *Biochim Biophys Acta* **1612**, 123 (2003).
3. Domingues, M.M., et al. *J. Pep. Sci.* **14**, 394 (2008).
4. Matos, P.M., et al. *Biochim Biophys Acta* **1798**, 1999 (2010).
5. Alves, C., et al. *J. Biol. Chem.* **285**, 27536 (2010).
6. Ferre, R., et al. *Biophys. J.* **96**, 1815 (2009).
7. Kaszuba, M., et al. *Philos Transact. A Math Phys. Eng. Sci.* **368**, 4439 (2010).
8. White, S., Wimley, W. *Biochim Biophys Acta* **1376**, 339 (1998).

Proceedings of the 31st European Peptide Symposium
Michal Lebl, Morten Meldal, Knud J. Jensen, Thomas Hoeg-Jensen (Editors)
European Peptide Society, 2010

CcdB Toxin Peptides Derivatives and its Interactions with an Analogue of Bacterial CcdA Antitoxin

Saulo S. Garrido, Camila Ap. Cotrim, Davi B. Delfino, Anderson Garcia, Luiz C.B. Barbosa, and Reinaldo Marchetto
Institute of Chemistry, UNESP – Univ Estadual Paulista, Dept. Biochemistry and Chemistry Technology, Araraquara – São Paulo, Brazil

Introduction

DNA gyrase is an essential enzyme for maintaining the topological state of DNA in bacterial cells, making it a potential target for various antibacterial agents, including CcdB toxin [1]. CcdB is a protein of 11.7 kDa, which together with its antidote CcdA, constitute a programmed cell death system in bacteria. Cell death is prevented when the antidote is present, which forms a stable complex with CcdB toxin. The design and synthesis of peptide analogues of CcdB, structurally modified to prevent the formation of CcdA-CcdB complex could result in a new family of peptide DNA gyrase inhibitors. In this context, we have synthesized by solid phase methodology, a series of linear peptides derived from CcdB protein, and studied if the loop formed by Arg40-Leu50 sequence is really important in the process of interaction with the CcdA.

Results and Discussion

As an approach to understanding the CcdA-CcdB interactions, CcdA41, a polypeptide derived from CcdA, was synthesized and its interaction with CcdB peptide fragments analyzed. The CcdB peptide fragments (Figure 1) were built based on crystal structure of the natural CcdB including the C-terminal α-helix, the loop Arg40-Leu50 of the wing sheet, the N-terminal β-sheet (Met1 to Leu9) and the residues Gly100 and Ile101 that seem to play a key role in the formation of CcdB-GyrA complex [2]. All peptides were synthesized by solid phase methodology employing Fmoc/tBu strategy and were analyzed and purified by high performance liquid chromatography (HPLC) with final yield in the range of 20% for all sequences. The chemical identity was confirmed by mass spectrometry (positive ES-MS): 4942, 4872, 3459 and 2633 g/mol (*CcdA41*, *CcdBET2*, *CcdBET3* and *CcdBCC1* respectively).

^{32}MQNEARRLRAERWKAENQEGMAEVARFIEMNGSFADENRDW^{72} ***CcdA41***

^{1}MQFKVYTYK^{9}-Z-^{40}RLLSDKVSREL^{50}-Z-^{84}SHRENDIKNAINKMFWGI^{101} ***CcdBET2***

^{1}MQFKVYTYK^{9}-Z-^{84}SHRENDIKNAINKMFWGI^{101} ***CcdBET3***

^{34}IPLASARLLSDKVSRELYPVVHIG^{57} ***CcdBCC1***

Fig. 1. Primary structure of CcdA41 and synthetic peptides based on CcdB toxin.

The peptides immobilized on Sepharose resin were used as supports for affinity chromatography studies, a way to evaluate the CcdA-CcdB interactions [3]. The chromatographic behaviors of CcdA41 using the three columns containing immobilized *CcdBET2*, *CcdBET3* and *CcdBCC1*, respectively are shown in Figure 2. CcdA41 had affinity for the columns of immobilized *CcdBET2* and *CcdBCC1* and was eluted by addition of 0.4 mol.L^{-1} NaCl in Tris buffer (10 mol.L^{-1} Tris.HCl / 20 mmol.L^{-1} NaCl / 5 mmol.L^{-1} $MgCl_2$, pH 7.2). When the Arg40-Leu50 sequence was absent (column of immobilized *CcdBET3*), the CcdA41 had no affinity to the column.

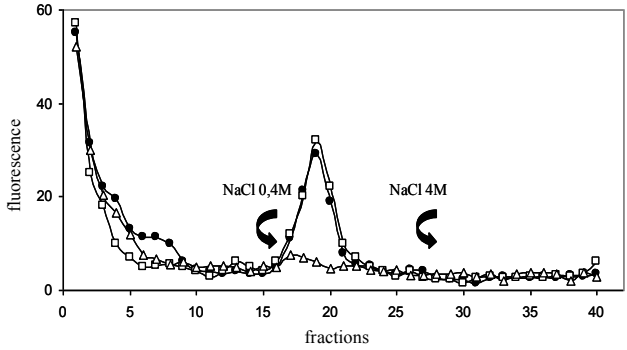

Fig. 2. CcdA41 affinity chromatography assays in columns containing immobilized CcdBET2 (●), CcdBET3 (Δ) and CcdBCC1 (□).

The affinity chromatography studies revealed interactions among the CcdA41 and the peptides fragments of CcdB. The interesting point was that the interactions were dependent on the Arg40-Leu50 sequence. This result prompted us to determine the binding parameters for the systems mentioned above. The binding parameters were studied by following the quenching of the intrinsic fluorescence of the CcdA41 upon binding of the *CcdBCC1* as has already described for *CcdBET2* [4]. The plot of the relative CcdA41 fluorescence intensity at the emission wavelength of 350 nm (λ_{ex}= 280 nm) as a function of total *CcdBCC1* was performed. The association constant (K_a) values to the CcdA41-*CcdBCC1* were obtained from the slope of the Stern-Volmer plot for identified static quenching [5], according to equation $F_0/F = 1 + K_a$ [*CcdBCC1*]. The obtained values of 416 mmol/L^{-1} for K_a are the means of at least five measurements. The ability of the CcdB fragments to inhibit the supercoiling reaction of DNA gyrase was investigated by titrating CcdB fragments into a fixed concentration of enzyme and DNA. The minimum concentration that produced complete inhibition of supercoiling activity was termed the IC_{100} [6]. In standard supercoiling assays at 37°C with 3.4 nM of gyrase, a relaxed DNA (500 ng) substrate is completely negatively supercoiled in 1 h. *CcdBET2* and *CcdBET3* inhibited this reaction with an IC_{100} value of 15 and 120 μM, respectively. *CcdBCC1* did not inhibit the DNA gyrase. This finding supports the theory that the three terminal residues (WGI) of CcdB plays a crucial role in DNA gyrase-CcdB complex formation [2].

Acknowledgments
This work was supported by FAPESP, in the form of research assistance (03/04492-3) and scholarship (IC 07/08052-9 - Cotrim C.Ap.) and CNPq in the form of PhD scholarships (Garrido S.S. and Trovatti E.) and research (Marchetto R.).

References

1. Couturier, M., Bahassi, E.M., Van Melderen, L. *Trends in Microbiology* **6,** 269 (1998).
2. Loris, R., Dao-Thi, M., Bahassi, EM.,Van Melderen, L., Poortmans, F., Liddington, R., Couturier, M., Wyns, L. *J. Mol. Biol*. **285**, 1667 (1999).
3. Marchetto, R., Nicolás, E., Castillo, N., Bacardit, J., Navia, M., Vila, J., Giralt, E. *J. Pep. Sci.* **7**, 27 (2001).
4. Cotrim, C.A., Garrido, S.S., Trovatti, E., Marchetto, R. *Quim. Nova.* **33**, *4*, 841, (2010).
5. Garrido, S.S., Scatigno, A., Trovatti, E., Marchetto, R. *J. Pep. Res*. **65**, *5*, 502, (2005).
6. Trovatti, E., Cotrim, C. Ap., Garrido, S.S., Barros, R., Marchetto, R. *Bioorg. Med. Chem. Lett.* **18**, 6161-6164 (2008).

Proceedings of the 31st European Peptide Symposium
Michal Lebl, Morten Meldal, Knud J. Jensen, Thomas Hoeg-Jensen (Editors)
European Peptide Society, 2010

A Regulatory Role for the Muramyl Peptide (GMDP) in a Murine Model of Allergic Asthma

Svetlana V. Guryanova[1], Marina A. Shevchenko[1], Ivan G. Kozlov[2], and Tatyana M. Andronova[1]

[1]Shemyakin and Ovchinnikov Institute of Bioorganic Chemistry RAS, Moscow, 117997, Russian Federation; [2]Russian State Medical University, Moscow, 117997, Russian Federation

Introduction

N-acetylglucosaminyl-N-acetylmuramyl dipeptide (GMDP) (Figure 1) – fragment of bacterial cell wall peptidoglycan is known to possess immunomodulatory activity against viral and bacterial infection [1,2].

Positive effect of based on GMDP pharmaceutics Licopid application was shown at the treatment of children with bronchial asthma and atopic dermatitis [3]. Previously we reported that *in vitro* studies on periphery blood mononuclear cells of allergic bronchial asthma patients demonstrated the ability of GMDP to shift Th1/Th2 balance towards Th1 and IFN-γ production [4].

In the present study we evaluated the ability of GMDP to modulate allergic airway inflammation both on the stage of sensitization and during ongoing airway inflammation. These results suggest that antiasthmatic activity of GMDP in OVA-induced lung inflammation may occur in part *via* downregulation of IgE production and eosinophil airway infiltration.

Results and Discussion

The standard well-characterized OVA-induced mouse model of asthma [5] (OVA/OVA) was utilized to assess the immunomodulatory effect of GMDP. Mice were immunized with GMDP in the stage of sensitization (GMDP/OVA/OVA) – two days before each intraperitoneal (i.p.) OVA/Alum injection or during effector stage of the airway inflammation - three consequent i.p. injections between the second and the last OVA challenge (OVA/OVA/GMDP).

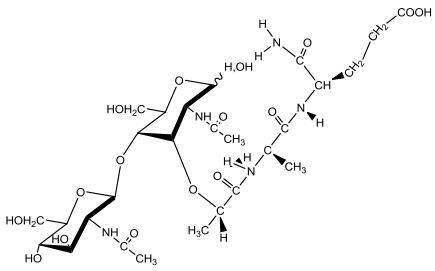

Fig. 1. N-acetylglucosaminyl-N-acetyl-muramyl dipeptide (GMDP).

Twofold decrease of serum total IgE and broncho-alveolar lavage fluid (BALF) IgA was detected in GMDP/OVA/OVA mice compared to the OVA/OVA group (Figure 2B). At the same time such route of

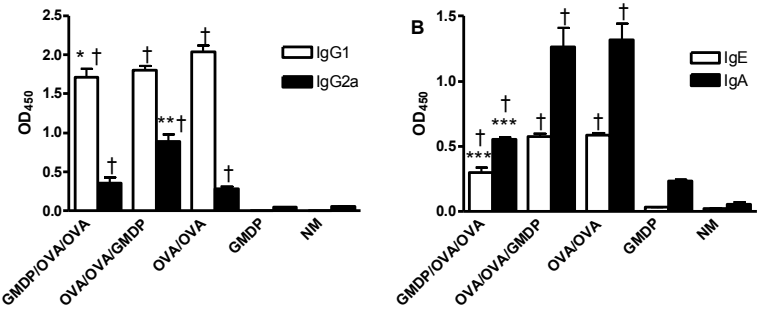

*Fig. 2. Immunoglobulin production. For IgG detection sera were diluted 1:1000, for IgE 1:10. IgA was detected in BALF (1:1). *P < 0.05, **P < 0.01, ***P < 0.005 vs. OVA/OVA; † P < 0.005 vs NM.*

Table 1. Differential cell counts in BALF

	Macrophages ($\times 10^5$ *cells)*	*Neutrophils* ($\times 10^5$ *cells)*	*Lymphocytes* ($\times 10^5$ *cells)*	*Eosinophils* ($\times 10^5$ *cells)*
GMDP/OVA/OVA	0.88±0.03*	0.12±0.02	0.235±0.003	2.46±0.005***
OVA/OVA/GMDP	2.33±0.13	0.94±0.16*	0.31±0.005	0.54±0.004***
OVA/OVA	**1.68±0.284**	**0.27±0.07**	**0.29±0.008**	**1.74±0.006**
GMDP	1.74±0.36	0.08±0.04	0.2±0.004	0.02±0.001***
NM	1.12±0.01	0.8±0.07	0.18±0.003	0.08±0.001***

*Results are expressed as means (n=8 for each group) ± SEM. *P < 0.05, ***P < 0.005 vs OVA/OVA*

GMDP application didn't alter the IgG1/IgG2a balance, hence didn't promote Th1 response (Figure 2A). Application of GMDP on the stage of ongoing airway inflammation increased OVA-specific IgG2a serum level (Figure 2A), which correlated with our previous *in vitro* results [4]. However this IgG2a elevation wasn't accompanied by serum total IgE or BALF IgA decrease (Figure 2A, B), and therefore couldn't be considered as an allergic response protection.

Analyses of total cell infiltration to the airways of mice from GMDP/OVA/OVA and OVA/OVA/GMDP group didn't reveal significant alteration of inflammation compared to OVA/OVA mice (data not shown). Comparison of infiltrating cells population composition showed significant eosinophilia decrease in group of mice, receiving GMDP during OVA challenge compared to OVA/OVA mice (Table 1). Neutrophil level in this group was significantly higher then in mice with allergic airway inflammation. Application of GMDP during the sensitization phase, which revealed protective decrease of serum IgE level, induced, however, a rise of eosinophil infiltration, the level of which was significantly higher than in OVA/OVA mice (Table 1).

Thus, GMDP application during sensitization phase reduced the proallergic IgE production, but was impotent to decrease airway eosinophilia. GMDP treatment of ongoing allergic airway inflammation initiated Th1-mediated decrease of eosinophil airway infiltration. These data point to a dual protective effect of GMDP: preventive application reduces IgE production whereas treatment of ongoing airway inflammation with muramyl peptide suppresses eosinophilia.

Acknowledgments
This work was supported by joint stock company PEPTEK.

References

1. Kozlov, A., Klimova, R.R., Shingarova, L.N., et al. *Mol. Biol. (Mosk)* **39**(3), 504-512 (2005).
2. Turánek, J., Ledvina, M., Kasná, A., et al. *Vaccine* **12**(24), Suppl. 2:S2, 90-91 (2006).
3. Kolesnikova, N.V., Kokove, A., Andronova, T.M., et al. *Russian J. of Allergology* **5,** 5-555 (2008).
4. Guryanova, S.V., Kozlov, I.G., Mesheryakova, E.A., et al. *Immunologia (Russian J.)* **5**(30), 305-308 (2009).
5. Braun, A., Lommatzsch, M., Mannsfeldt, A., et al. *Am. J. Respir. Cell Mol. Biol.* **21(**4), 537-546 (1999).

Proceedings of the 31st European Peptide Symposium
Michal Lebl, Morten Meldal, Knud J. Jensen, Thomas Hoeg-Jensen (Editors)
European Peptide Society, 2010

Molecular Dynamics of Amylin Amyloid Single and Multiple Beta Sheets

Dmitrijs Lapidus[1], Salvador Ventura[2], Cezary Czaplewski[3], Adam Liwo[3], and Inta Liepina[1]

[1]Latvian Institute of Organic Synthesis, Aizkraukles str. 21, Riga, LV1006, Latvia; [2]Institut de Biotecnologia i de Biomedicina, Universitat Autonoma de Barcelona, E-08193, Bellaterra, Spain; [3]Department of Chemistry, and University of Gdansk, ul. Sobieskiego 18, 80-952, Gdansk, Poland

Introduction

Amyloidosis is progressive metabolic conformational disease caused by misfolding and aggregation of soluble proteins in insoluble fibrils which impair cell functioning or cell-to-cell connectivity [1]. Amylin or Islet Amyloid Polypeptide (IAPP) is a 37 residue peptide hormone secreted by pancreatic β-cells. Amylin forms deposits in pancreas and is a non-insulin-dependent type II diabetes disease agent [2].

Six-stranded single β-sheets of amylin 10-29 (**Amyl 10-29**),

Gln^{10}-Arg^{11}-Leu^{12}-Ala^{13}-Asn^{14}-Phe^{15}-Leu^{16}-Val^{17}-His^{18}-Ser^{19}-Ser^{20}-Asn^{21}-Asn^{22}-Phe^{23}-Gly^{24}-Ala^{25}-Ile^{26}-Leu^{27}-Ser^{28}-Ser^{29}

reverse amylin 10-29 (**RevAmyl 10-29**)

Ser^{10}-Ser^{11}-Leu^{12}-Ile^{13}-Ala^{13}-Gly^{15}-Phe^{16}-Asn^{17}-Asn^{18}-Ser^{19}-Ser^{20}-His^{21}-Val^{22}-Leu^{23}-Phe^{24}-Asn^{25}-Ala^{26}-Leu^{27}-Arg^{28}-Gln^{29}

and a scrambled version (**ScrambAmyl 10-29**),

Leu^{10}-Ile^{11}-Gln^{12}-Ser^{13}-Ala^{14}-Phe^{15}-Gly^{16}-Asn^{17}-Val^{18}-Asn^{19}-His^{20}-Leu^{21}-Ser^{22}-Arg^{23}-Phe^{24}-Asn^{25}-Ser^{26}-Ser^{27}-Ala^{28}-Leu^{29}

as well as six β-sheet stacks **6xAmyl 10-29, 6xRevAmyl 10-29, 6xScrambAmyl 10-29** (Figure 1**),** of the all three systems were simulated by molecular dynamics (MD) with Amber 9.0, f99 force field, NTP protocol (constant number of particles, temperature, pressure), using a periodic water box of explicit water molecules 5 Å layer over the solute for single β-sheets and 10 Å layer for the β-sheet stacks. The systems were supplemented by chlorine counterions for the neutral charge. For single β-sheets the system temperature was raised stepwise from 10 K to 309 K in 40 ns of the MD run, then the systems were simulated at the temperature of 309 K. The total MD run was 187 ns for Amyl 10-29, 140 ns for RevAmyl 10-29 and 116 ns for ScrambAmyl 10-29. The β-sheet stack MDs were started from 309 K, and the simulation time is 41 ns for 6xAmyl 10-29, 38 ns for 6xRevAmyl 10-29 and 39 ns for 6xScrambAmyl 10-29.

Results and Discussion

Single β-sheets. All three systems show stable single β-sheet structures. **Amyl 10-29** ß-sheet stretches across the regions Arg^{11}-Val^{17} and time to time expands till Ser^{19}, besides two strands have stable β-sheet over the region Asp^{22}-Leu^{27}. In the Amylin 10-29 region Ser^{19}-Ser^{20}-Asn^{21}-Asn^{22} the β-sheet has W-shaped bend with the deeper vertex on Ser^{20} and smaller vertex on Asn^{22}, suggesting that also the bent β-sheet could be possible. Apart from backbone hydrogen bonding the β-sheets of Amyl 10-29 are stabilized by side chain hydrogen bonding between asparagine residues and between residues Ser^{20} and Asp^{22}. The β-sheets of Amyl 10-29 are glued together by leucine, isoleucine, valine residues and by phenylalanine residues, which together with asparagine residues form a sub-stack kept together by mild polar interactions. The β-sheet of the backward amylin **RevAmyl 10-29** is more flat and stronger than that one of Amyl 10-29. β-sheet of the scrambled amylin **ScrambAmyl 10-29** is strong, suggesting that for this sequence the order of amino acids is not important regarding the capability to create the β-sheet.

The distances between the mass centers of the nearby amino acid residues is of the same magnitude for the Amylin10-29 β-sheet and the RevAmyl 10-29, confirming that the alteration of the direction of the peptide chain does not change the compactness of the β-sheet.

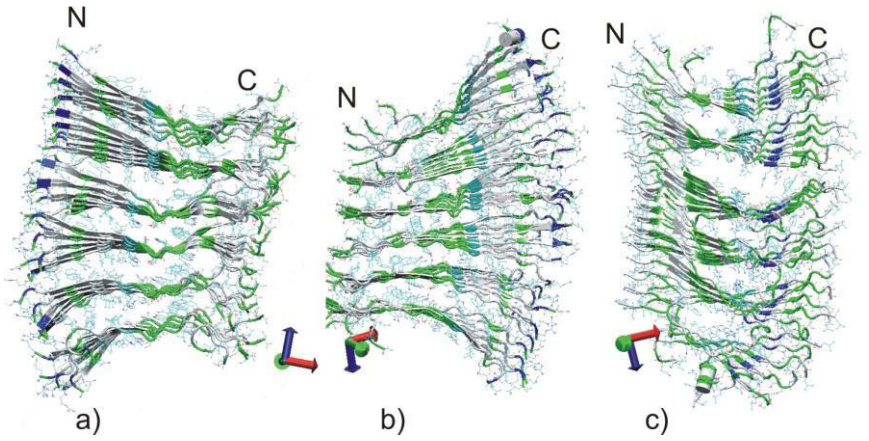

Fig. 1. The β-sheet stacks 6xAmyl 10-29, 6xRevAmyl 10-29 and 6xScrambAmyl 10-29 after 41ns, 38ns and 39ns of MD run respectively. N and C denote the N- and C-ends of the peptides.

The β-sheet stacks 6xAmyl 10-29, 6xRevAmyl 10-29 and 6xScrambAmyl 10-29 (Figure 1):
In the amylin stack **6xAmyl 10-29** C^{β} methylene groups of Asn^{21}, and Asn^{22} are pointed towards Phe^{23} of the nearby β-sheets. The asparagine Asn^{21}, Asn^{22} sidechains make intra-sheet hydrogen bondings and sandwiches Phe^{23} between them. Also Asn^{14} sidechains make intra-sheet hydrogen bonding, and a sandwich is made from Asn^{14}, and Phe^{15} of the nearby β-sheet. Hydrophobic cores keeping together the β-sheet stack is made by Phe^{15}, Leu^{16}, Val^{17}, and by Ile^{26}, Leu^{27}. The inter-sheet hydrogen-bonding is made by the neighbour-sheets residues Ser^{20} and Asn^{21}, Asn^{21} and Asn^{22}, His^{18} and Ser^{19}, Ser^{28} or Ser^{29} and the COO- terminal, Gln^{10} and Arg^{11}, Gln^{11} and NH_3-terminal, Arg^{11} and backbone carbonyl of Gln^{10}. The role of the semi-regular asparagine-phenyl sandwiches seems to order the whole stack, and this could explain the importance of Asn^{14}, Asn^{21} in fibril formation [3]. In the backward amylin stack **6xRevAmyl** there is no asparagine-phenyl sandwiches, the Phe^{24} and Leu^{23} makes one hydrophobic core, and the Leu^{12}, Ile^{13} – another one, not very tight. The inter-sheet hydrogen bonding is made by Asn^{17} and Asn^{18}, Ser^{19} and Asn^{17} or Asn^{18}, Ser^{10}-NH_3 terminal, Arg^{28}-COO- terminal. The scrambled amyline stack **6xScrambAmyl 10-29** is kept together by not very compact hydrophobic and hydrophilic inter-sheet (vertical) layers.

Acknowledgments
This work was supported by ESF project 2009/0197/1DP/1.1.1.2.0/09/APIA/VIAA/014, European Economic Area block grant "Academic Research" LV0015.EEZ09AP - 68 "Molecular modelling of amyloid formation". Calculations were performed on computers of the Gdansk Academic Computer Center TASK.

References
1. Westermark, P. *FEBS Journal* **272**, 5942-2949 (2005).
2. Hoppener, J.W.M., Ahren, B., Lips, C.J.M. *New England J. of Medicine* **343**, 411-419 (2000).
3. Koo, B.W., Hebda, A., Miranker, D. *Protein Engineering, Design & Selection* **21**, 147-154, (2008).

Proceedings of the 31st European Peptide Symposium
Michal Lebl, Morten Meldal, Knud J. Jensen, Thomas Hoeg-Jensen (Editors)
European Peptide Society, 2010

Molecular Modeling of Single and Multiple Beta-Sheets of Amyloid Beta Protein 25 – 35

Vita Duka[1,2], Isabella Bestel[3], Cezary Czaplewski[4], Adam Liwo[4], and Inta Liepina[2]

[1]Faculty of Physics and Mathematics, University of Latvia, Zellu iela 8, Riga LV1002, Latvia, [2]Latvian Institute of Organic Synthesis, Aizkraukles str. 21, Riga LV1006, Latvia, [3]Victor Segalen University of Bordeaux II, 146 rue Leo-Saignat, 33076, Bordeaux cedex, France, [4]Department of Chemistry, and University of Gdansk, ul. Sobieskiego 18, 80-952, Gdansk, Poland

Introduction

Amyloidosis is misfolding and self-assembled aggregation of soluble proteins in insoluble fibrils which replace the functional cells or block connections between the cells. The mechanism of amyloid formation is still unclear [1]. Amyloid beta protein 1-42 is responsible for formation of human amyloidosis leading to Alzheimer disease [2].

The present work studied the formation of amyloid β-structure of the amyloid beta protein fragment 25-35 (**Abeta 25-35**):

Gly25-Ser26-Asn27-Lys28-Gly29-Ala30-Ile31-Ile32-Gly33-Leu34-Met35

A flat, paralel single six-stranded beta-sheet (**6Abeta 25-35**) and ten-stranded beta-sheet (**10Abeta 25-35**) of Abeta 25-35 were constructed using a single strand of Abeta 25-35 peptide. Both systems, 6Abeta 25-35 and 10Abeta 25-35, were surrounded by chlorine counterions to neutralize the system, and by a 5 Å layer of explicit water molecules and subjected to molecular dynamics (MD) simulations in a periodic box using Amber 9.0, f99 force field and isothermal-isobaric ensemble, NTP protocol (constant temperature, pressure and the number of particles). Raise from 10K to 200K took 90ns, then for 90ns systems were kept at 200K, then in 35ns the temperatures were risen to 309K. Afterwards 6Abeta 25-35 system was simulated for 95 ns of MD run at 309K.

The multiple β-sheet stack consisting of six 6Abeta 25-35 parallel β-sheets (Figure 1) was built and subjected to 58 ns MD by similar protocol as that one for single β-sheets. The temperature was risen stepwise from 10 K to 200 K during 31 ns, then the system were kept at 200 K for 18 ns, and then the temperature was risen to 309 K.

Results and Discussion

Results of the single sheet MD of 6Abeta 25-35 and 10Abeta 25-35 show the stable β-sheet across the β-sheet region from Ile31 to Leu 34. The β-sheet region over region Ser26-

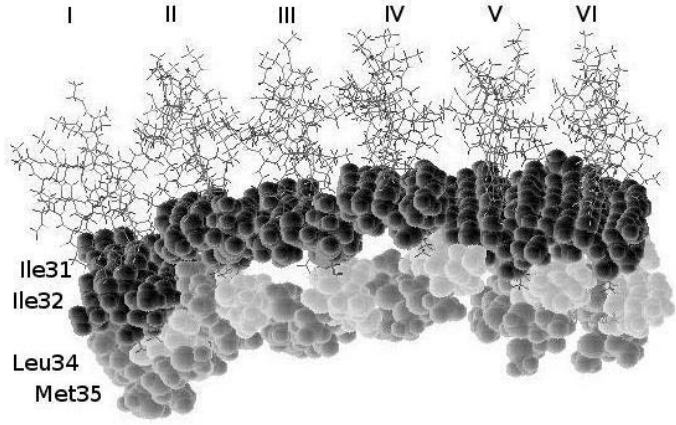

Fig. 1. Hydrophobic core of 6Aβ 25-35 stack (β-sheets I-VI). Ile31, Ile32- black, space fill. Leu34 – light gray, space fill. Met35 – dark gray, space fill.

Lys28 is fluctuating with the β-sheet melting time to time. The middle strands 3-6 of the six-stranded β-sheet form β-structure also across the Ser26-Lys28 region, while the β-structure over the Ser26-Lys28 region is melting at the β-sheet side strands 1-2 and 5-6.

- Both single and multiple systems are kept together by backbone hydrogen bonding.
- 6Aβ 25-35 and 10Aβ 25-35 systems show the stable β-structure at 200K temperature.
- 6Aβ 25-35 and 10Aβ 25-35 systems collapse loosing β-structure at 309K temperature, indicating that supplementary β-sheets are required for β-structure stabilization.
- Both single β-sheets (6Aβ 25-35 and 10Aβ 25-35) tend to cooperate alongside with β-sheets in nearby periodic boxes.
- To examine single β-sheet, more than 5 Å layer periodic water box is needed.

Results of the MD of the multiple β-sheet stack at 200 K show stable β-sheet (from Ile31 – Leu34), and the β-sheet is melting time to time from Gly25 – Ser26 and Lys28 - Ala30.

- Intra-sheet backbone hydrogen bonding keeps the β-sheets together.
- The strongest intra β-sheet gluing in the stack is realized by Ile31 and Ile32 forming the main part of the hydrophobic core (Figure 1).
- Apart from that, the β-sheets are kept together by Leu34 and Met35 hydrophobic interactions and Ser25 and Asn27 electrostatic interactions.
- In several cases the sidechain of Lys28 makes hydrogen bonding with the backbone carbonyl of Gly29 in the nearby β-sheet (Figure 2).

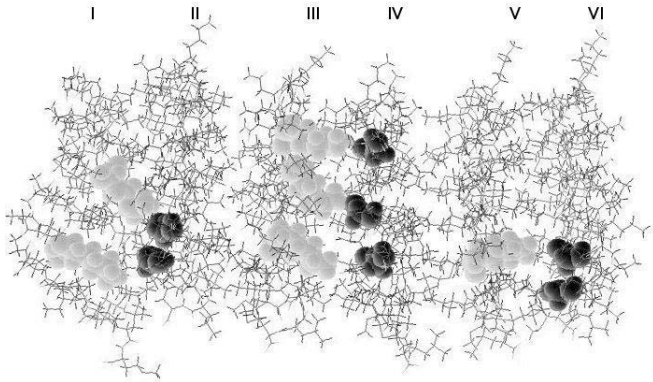

Fig. 2. Hydrogen bonding of Gly29 and Lys28 of 6Aß 25-35 stack (ß-sheets I-VI). Gly29-black, space fill. Lys28 – dark gray, space fill.

During the course of rising temperature from 200K till 309K the β-sheet stack tends to associate with the stack in a nearby periodic box. At 309K the β-sheet is kept mainly in the C-terminal part of the system over the region Ile31 to Leu34 and time to time over Ser26-Asn27 in the N-terminal part.

Apart from forming the β-structure a single strand of Abeta 25-35 stack tends to jump away from the stack and turns from β-structure to coil conformation with the further perspective to turn to α-helix. This is in accordance with literature data suggesting the dual structure of Abeta 25-35 peptide inhering both β-structure in fibrils and α-helical structure in water and membrane environment [3].

Acknowledgments

This work was supported by European Economic Area block grant ”Academic Research” LV0015. EEZ09AP-68 ”Molecular modeling of amyloid formation”, and by France-Latvia project ”Osmose”. Calculations were performed on computers of the Gdansk Academic Computer Center TASK.

References

1. Lei., H. *Protein & Cell* **1(4)**, 312-314 (2010).
2. Sarroukh, R., Cerf, E., Derclaye, S., Yves, F., Dufrene, F., Goormaghtigh, E., Ruysschaert, J.-M., Raussens, V. *Transformation of amyloid b(1-40) oligomers into fibrils is characterized by a major change in secondary structure. Cellular and Molecular Life Sciences*, Springer Basel AG 2010.
3. Di Carlo, M. *Eur. Biophys. J.* **39**, 877-888 (2010).

Proceedings of the 31st European Peptide Symposium
Michal Lebl, Morten Meldal, Knud J. Jensen, Thomas Hoeg-Jensen (Editors)
European Peptide Society, 2010

New Hybrid and Mutant PIA and MII Toxins with Greater Affinty and Selectivity for the α6* Subtype

Renato Longhi[1], Luca Pucci[2], Luca Rizzi[3], Giovanni Grazioso[3], Clelia Dallanoce[3], Francesco Clementi[2], and Cecilia Gotti[2]

[1]CNR, ICRM, Via Mario Bianco 9, Milano, 20131, Italy; [2]CNR, Istituto di Neuroscienze, Via Vanvitelli 32, Milano, 20129, Italy; [3]Dipartimento di Scienze Farmaceutiche "Pietro Pratesi", Unimi, Via Mangiagalli 25, Milano, 20133, Italy

Introduction

Neuronal nicotinic receptors (nAChRs) [1] make up a heterogeneous family of ligand-gated cation channels found in the central and peripheral nervous systems. The different nAChRs are involved in various physiological functions and the *in vivo* presence of a multitude of subtypes underlines the importance of their diversity in the fine tuning of the cholinergic transmission. The α6* receptors have aroused particular interest because recent studies have shown that they are involved in nicotine-elicited locomotion, acute and chronic nicotine self-administration and other brain activities [2]. At present, the compounds that are α6* selective belong to the α-conotoxin family [3]. The marine cone snail peptides α–conotoxin PIA and MII both bind the α6β2* receptors: MII binds and antagonises α6β2*and α3β2* subtypes with relatively high affinity, whereas the PIA toxin only binds the α6β2* subtype with lower affinity than MII. The lack of selectivity of MII is not surprising given the very high sequence homology in the extracellular binding domain of the α6 and α3 subunits. In this study, we analysed the role of the *N*-terminal amino acids in defining the affinity and potency of the PIA toxin for the α6β2* subtype; then we constructed a hybrid between the PIA and MII peptides that is more potent and selective for the native α6* subtype. Subsequently, by means of molecular modelling analysis, we aimed at identifying amino acid residues in MII which are relevant to the molecular recognition by the α3β2* subtype, thus achieving new structural analogues whose affinity for the α3β2* nAChRs is significantly reduced.

Results and Discussion

The small disulfide-rich α–conotoxins PIA and MII are both competitive antagonists of the α6β2* neuronal nicotinic receptor (nAChR) subtype, albeit with different affinity and selectivity. Both toxins have a common "ω–shaped" topology but, PIA is characterized in the N-terminal region by a tail containing three amino acids (RDP), which forms a type I β-turn. In order to obtain PIA and MII synthetic conotoxins of high quality, care and attention were devoted to the synthesis and peptides folding: The Cysteine residues were orthogonally protected: 1-3 Trt, 2-4 Acm. SS connectivity 1-3 was obtained using two equivalents of hydrogen peroxide in 60 minutes (Figure 1) and connectivity 2-4 in 30 minutes using 5 equivalents of iodine in 50% aqueous methanol. We than synthesised a group of PIA-related peptides in which RDP motif was gradually removed and the first amino acid mutated. Binding and functional studies showed that the RDP tripeptide is essential for high affinity of the PIA at the native rat α6β2*subtype (Figure 2A), with the major role being played by the Arginine residue R1. A molecular modeling study showed that the recognition process by α6β2* nAChR is mainly guided by a salt bridge involving the guanidine group of R1 and the highly negatively charged D166-D167 residues of the β2 subunit. Then, we inserted the RDP sequence at the *N*-terminus of the α-conotoxin MII (RDP-MII). When compared with the native α-conotoxin, the new hybrid-type peptide showed increased affinity (10-fold) and potency (5-fold) for the α6β2* nAChRs (Figure 2B) whereas its pharmacological profile was marginally

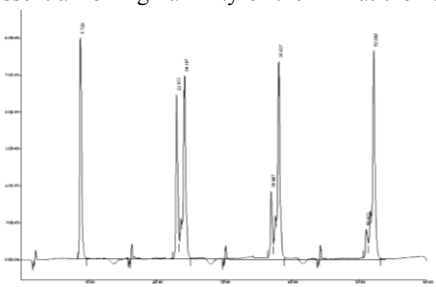

Fig. 1. H_2O_2 mediated folding of RDP-MII at t=0, 14, 28 and 42 min. after H_2O_2 addition.

Entry	Sequence
PIA	RDPCCSNPVCTVHNPQIC
MII	GCCSNPVCHLEHSNLC
ΔR-PIA	DPCCSNPVCTVHNPQIC
ΔRD-PIA	PCCSNPVCTVHNPQIC
ΔRDP-PIA	CCSNPVCTVHNPQIC
RDP-MII	RDPCCSNPVCHLEHSNLC
[E11R]MII	GCCSNPVCHLRHSNLC
[E11R]RDP-MII	RDPCCSNPVCHLRHSNLC

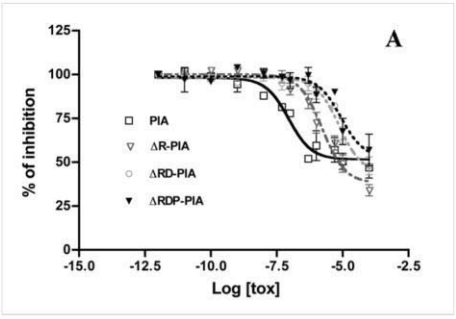

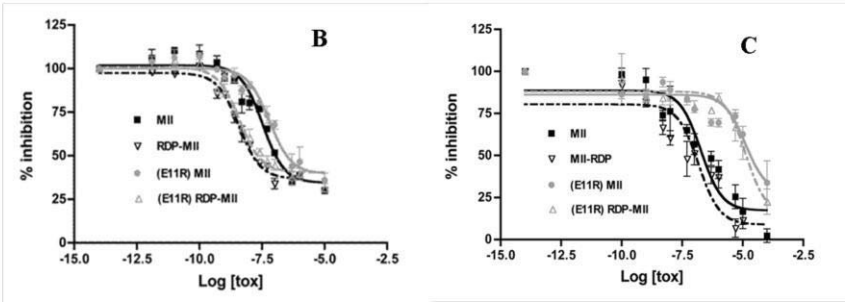

Fig. 2. Synthesized peptides and (A) Inhibition of [^{125}I]Epibatidine binding to immunoimmobilised striatal α6β2 receptors induced by native PIA, ΔR-PIA, ΔRD-PIA and ΔRDP-PIA peptides; (B)Affinity of [E11R]MII and [E11R]RDP-MII peptides for α6β2*; (C) affinity of [E11R]MII and [E11R]RDP-MII peptides for the native α3β2*.*

affected at the α3β2* subtype (Figure 2C). Unlike PIA, MII also binds the α3β2 subtype with relatively high affinity, and molecular modeling investigations showed that the glutamic acid (E) residue in position 11 plays a primary role in piloting molecular recognition. We therefore designed and synthesised new analogues of MII in which E11 was replaced by R [i.e., (E11R)MII and (E11R)RDP-MII)], and found that they displayed the same potency and affinity for native rat α6β2* as MII and RDP-MII (Figure 2B), but lower affinity and potency for the native and heterologously expressed α3β2* subtype (Figure 2C). Hence, the novel (E11R)MII and (E11R)RDP-MII peptides are potent and selective α6β2* antagonists.

In conclusion, we designed and synthesised new analogues of MII in which E11 was replaced by R (i.e., [E11R]MII and [E11R]RDP-MII), and found that they displayed a) the same potency and affinity for native rat α6β2* nAChRs as MII and RDP-MII, and b) lower affinity and potency for the native and heterologously expressed α3β2* subtype. Hence, the novel [E11R]MII and [E11R]RDP-MII peptides are potent and selective α6β2* vs. α3β2* antagonists.

Acknowledgments
This study was financially supported by the Italian research grants: FIRB # RBNE03FH5Y002 and PRIN # 20072BTSR2

References
1. Gotti, C., Zoli, M., Clementi, F. *Trends Pharmacol. Sci.* **27**, 482-491 (2006).
2. Gotti, C., et al. *Biochem. Pharmacol.* **78**, 703-711 (2009).
3. Olivera, B.C., et al. *Channels (Austin)* **2**, 143-152 (2008).

Proceedings of the 31st European Peptide Symposium
Michal Lebl, Morten Meldal, Knud J. Jensen, Thomas Hoeg-Jensen (Editors)
European Peptide Society, 2010

Molecular Modeling of Novel GnRH Analogues Using NMR Spectroscopy and Relation with Their Anti-Cancer Activities

F. Tahoori[1], M. Erfani Moghaddam[2], A. Arabanian[1], and S. Balalaie[1*]
[1]Peptide Chemistry Research Center, K.N. Toosi University of Technology, Tehran, P.O. Box 15875-4416, Iran; [2]Department of Biological Science, Tarbiat Modares University, Tehran, P.O. Box 14115-111, Iran; balalaie@kntu.ac.ir*

Introduction

Gonadotropin Releasing Hormone (pGlu-His-Trp-Ser-Tyr-Gly-Leu-Arg-Pro-Gly-NH_2, GnRH) plays a significant role in the controlling of gonadotropins and steroid hormones [1]. Considerable effort has been dedicated to the synthesis of peptide mimetic structures to overcome the unfavorable properties and also therapeutic deficiencies of peptides [2].

Among them is insertion of some chemical groups in the peptide sequences to increase their activity. In the present work, new GnRH analogues were designed, synthesized and analyzed for its anti-cancer activity in comparison with triptorelin acetate. The new analogue structure is similar to triptorelin acetate with two extra chemical groups inserted between Leu7 and Arg8 in order to increase peptide hydrophobic properties without any change in peptide active sites (**I**).

Results and Discussion

In a continuation of our research work for the synthesis of pharmaceutical peptides, and in order to study the effect of modification in triptorelin acetate structure, the new triptorelin analogue was designed, and synthesized *via* an efficient Ugi-4MCR (Figure 1) [3]. Reaction of heptapeptide which contained free carboxylic acid and tripeptide with free amino group, 4-pyridine carbaldehyde and cyclohexyl isocyanide leads to the desired compound (**I**). The heptapeptide was synthesized using Fmoc SPPS standard strategy in good yield. The anti-cancer activity of analogue (**I**) was studied. It showed better anti-cancer activity compared to triptorelin acetate. In the extra pituitary compartment GnRH and its receptor act as part of the autocrine regulatory system of cell proliferation, resulting in its anticancer activity. The inhibitory efficiency of this new analogue is proved to be higher than the original triptorelin [4].

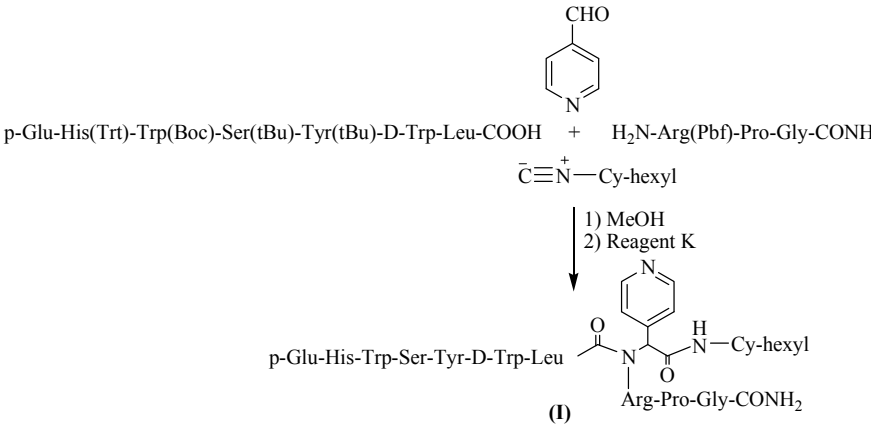

Fig. 1. Synthesis of novel GnRH analogue using Ugi-4MCR.

Herein, the sample was dissolved in DMSO-d6 and TOCSY and NOESY 2D spectra were recorded using a Bruker Avance DRX-500 spectrometer. The data acquisition were

performed at 25 ^{o}C with mixing times of 120 and 200 ms, and number of scans of 96 and 216 respectively (Figure 2).

The standard Wüthrich method was used for frequency resonance assignment. The peptide structure was calculated using CYANA by achieving molecular dynamic simulation in the torsion angle space on 300 random starting structures which resulted in 20 structures with a backbone RMSD of 1.3A^{o}. This analogue has a turn like structure between amino acids 4 and 6 (Figure 3).

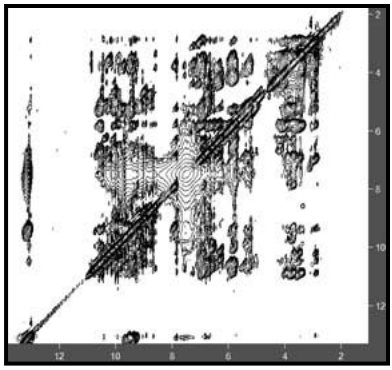

Fig. 2 The NOESY 2D spectra (DMSO-d6, 25^{o}C, mixing time 200ms).

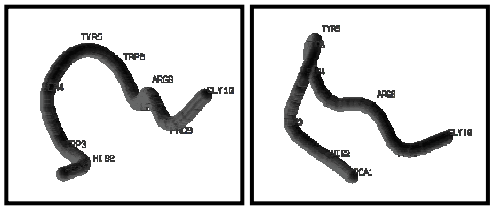

Fig. 3. Stereoview of triptorelin analogue (I).

Results indicate that proliferation of human breast and ovarian cancer cell lines is dose-dependently inhibited. The inhibitory efficiency of this new analogue is proved to be higher than the original triptorelin. It seems that the existence of a new functional group or the shape of the molecule could increase its biological activity compared to triptorelin. The design and synthesis of some novel analogues and investigation of their anti-cancer activity is in progress in our laboratory.

Acknowledgments

The authors would like to thank K. N. Toosi University of Technology research office for financial support. They also gratefully acknowledgement Kimia Exir for chemical donation and financial support.

References

1. Maudsley, S., Davidson, L., Pawson, A.J., Chan, R., Lopez de Maturana, R. *Cancer Research* **64**, 7533-7544 (2004).
2. Tourwé, D., Van Hemel, J., Piron, J. *In Synthesis of peptides and peptidomimetics*; Eds. Felix, A., Moroder, M., Toniolo, C., Thieme: Stuttgart**,** 2004, E22C, 606.
3. Arabanian, A., Mohammadnejad, M., Balalaie, S., Gross, J.H. *Bioorg. Chem. Lett.* **19**, 887-890 (2009).
4. Mirzaei Saleh-Abady, M., et al. *Biopolymers (Peptide Science*) **94** (3), 292-298 (2009).

Proceedings of the 31st European Peptide Symposium
Michal Lebl, Morten Meldal, Knud J. Jensen, Thomas Hoeg-Jensen (Editors)
European Peptide Society, 2010

Synthesis of Novel Peptides Containing Unusual γ-Amino acids and Investigation of Their Nanostructures

B. Talaei, A. Arabanian, and S. Balalaie*
Peptide Chemistry Research Center, K. N. Toosi University of Technology, Tehran, P.O. Box 15875-4416, Iran

Introduction

It was shown that insertion of an unusual amino acid in a peptide sequence could affect the secondary structure and also their biological activities. Self-assembled protein and peptide nanostructures are envisioned to serve as important building blocks in future nanotechnological devices and assemblies. Meanwhile, there are some reports about the mechanism of amyloid fibril formation which led to the unexpected discovery that diphenylalanine, NH_2-Phe-Phe-COOH, is core recognition motif of the Alzheimer's β-amyloid [1-2]. Investigations have shown that the Phe-Phe dipeptide rearranges due to the appropriate π-stacking interactions such that 6 species make a ring with a hydrophilic interior and hydrophobic exterior [3]. Numerous experiments performed by Gazit, et al. have investigated the effect of aromatic groups and the capabilities of the resulting molecule in the rearrangement process by using homoaromatic compounds instead of phenylalanine [4] or by addition of an aromatic species such as Fmoc to the F-F structure. They investigated the π interactions and the formations of the associated nanostructures [5]. On the other hand, other experiments which added molecules such as PEG [6] or aliphatic compounds to the end of the amino acid side chains and achieved nanofibril or other structures, made us utilize amino acids in our molecule which could induce more aliphatic properties to the phenylalanine-phenylalanine molecule. γ-Amino acids have important biological properties (as regulatory molecules, intermediary metabolities, storage compounds, and defensive weapons). γ-Aminobutyric acid (GABA) is a major physiological inhibitor of neuro-transmission in the brain [7]. Meanwhile, gabapentin, baclofen and other γ-amino acids are used for the treatment of CNS diseases. According to these findings, we were encouraged to synthesize some novel peptides which contained γ- amino acids such as baclofen and gabapentin in their backbones.

Results and Discussion

Due to the existence of aromatic moiety in the structure of baclofen it was selected as candidate for our investigation. Gabapentin's structure has a non polar property due to a cyclohexyl ring connected to its β-carbon atom. Dipeptide (F-F) was synthesized according to the known solution phase peptide synthesis methodology, and additional unusual amino acids were added to the peptide chain. By connecting these two unusual amino acids to di-phenylalanine, new analogues were synthesized which could play important roles in the formation of molecular assemblies due to π-stacking interactions. The *di- tri-* and *tetra-*peptides were synthesized in solution phase and with consideration of orthogonality and using of suitable protection and deprotection strategy.

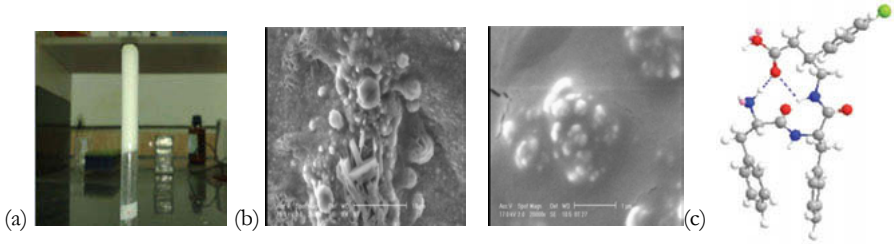

Fig. 1. a) Gel formation for compound 15; b) SEM micrographs of the compounds 6 and 8; c) Optimized structure of compound 9.

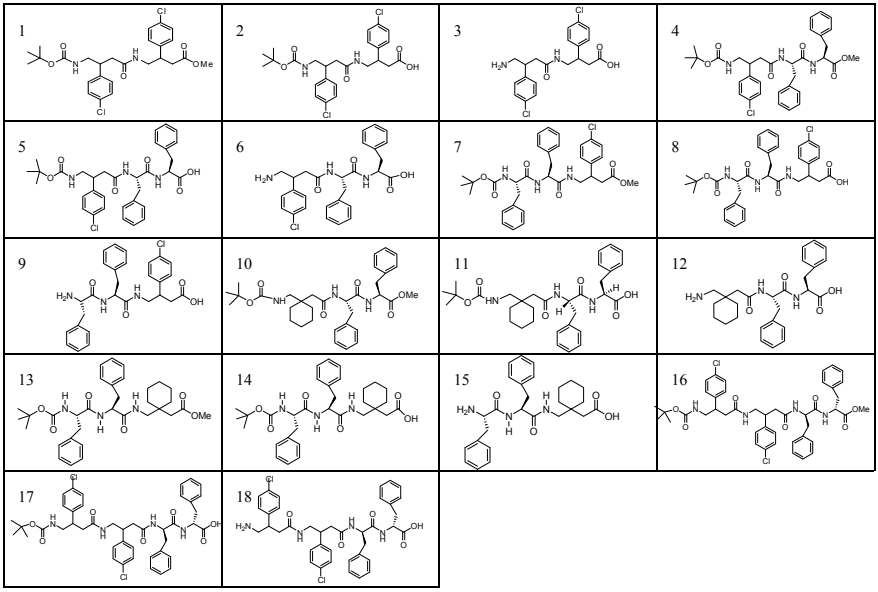

Fig. 2. Schematic representation of the molecular structures of the synthesized peptides.

Figure 2 shows the structure of synthesized peptides. The ability of synthesized peptides to make appropriate hydrogen bonding in aqueous media and organic solvents were investigated. First, the compounds were dried up completely and made into a fine powder using ultrasonication for five minutes. Then TFE solvent was added to the powder until it forms a saturated solution. White precipitates appear after adding water. With adjusting the pH, the precipitate becomes soluble and by becoming more acidic, the precipitate formation was increased. In a particular pH the precipitates assemble completely and do not pour down by turning the container upside down (Figure 1-a). This point is absolutely temperature dependent and the gel easily dissociates even with warmth from the hands. SEM results could show the nanostructure of the compounds **6** and **8** (Figure 1-b).

Molecular dynamic calculations for compound **9** could show the high capabilities of the compounds in establishing hydrogen bonds and appropriate π-stacking interactions (Figure 1-c). It seems, that *tri-* or *tetra-* peptides which contained γ-amino acids, the ability of hydrogen bonding could decrease, but on the other hand the helical structure of the products could be stable and therefore formation of π-stacking could increase.

In conclusion, we described the synthesis of some novel peptides which contained one or two γ-amino acids in the sequence structure of desired peptides. The existence of γ-amino acids could affect the self-assembly of the molecules and also the type of hydrogen bonding. The research for finding the biological activities of the synthesized peptides is in progress.

Acknowledgments

We thank Iran Nanotechnology Initiative Council for financial support. We also acknowledge Kimia Exir Company for chemical donation.

References

1. Petkova, A.T., Leapman, R.D., Guo, Z. *Science* **307**, 262-265 (2005).
2. Reches, M., Gazit, E. *Science* **300**, 625-627 (2003).
3. Gorbitz, C.H. *Chem. Eur. J.* **7**, 5153 (2001).
4. Reches, M., Gazit, E**.** *Phys. Biol*. **3**, S10-S19 (2006).
5. Andrew, M.S., et al. *Adv. Mater*. **20**, 37-41 (2008).
6. Castelletto, V., Hamley, L.W. *Biophys. Chem*. **141**, 169-174 (2009).
7. Schousboe, A., Sarup, A., Bak, L.H., Larsson, O.M., et al. *Neurochem. Int.* **45**, 521-527 (2004).

Proceedings of the 31st European Peptide Symposium
Michal Lebl, Morten Meldal, Knud J. Jensen, Thomas Hoeg-Jensen (Editors)
European Peptide Society, 2010

Structural Control of Diastereomeric Leu-Leu-Aib-Leu-Leu-Aib Sequences

Yosuke Demizu[1], Mitsunobu Doi[2], Yukiko Sato[1], Masakazu Tanaka[3], Haruhiro Okuda[1], and Masaaki Kurihara[1]

[1]Division of Organic Chemistry, National Institute of Health Sciences, Tokyo, 158-8501, Japan; [2]Osaka University of Pharmaceutical Sciences, Osaka, 569-1094, Japan; [3]Graduate School of Biomedical Sciences, Nagasaki University, Nagasaki, 852-8521, Japan

Introduction

The *de novo* design of peptides that fold into well-defined secondary structures is crucially important in a wide variety of fields such as organic chemistry and biological and material sciences. As templates for stabilizing the secondary structures of peptides, α,α-disubstituted α-amino acids have been widely used [1]. Among them, α-aminoisobutyric acid (Aib) has been found to be particularly useful as a helical promoter [2]. We have recently reported that the placement of Aib residues in an L-leucine-based hexapeptide (L-Leu-L-Leu-Aib-L-Leu-L-Leu-Aib) stabilized its right-handed (*P*) 3_{10}-helical structure [3]. Incidentally, the placement of L-amino acids in a helical sequence containing enantiomeric D-amino acids generally destabilizes the helical structure [4]. However, the accurate design of hybrid peptides with an effective combination of L- and D-amino acids is useful for constructing novel specific conformations [5]. Therefore, we speculated that new secondary structures could be built by appropriate design of Leu-based hexapeptides with a primary structure of Leu-Leu-Aib-Leu-Leu-Aib containing D-Leu residue in various combinations. Here, we designed three diastereomeric peptides using the same contents of L-Leu, D-Leu, and Aib residues; Boc-L-Leu-L-Leu-Aib-D-Leu-D-Leu-Aib-OMe (**1**), Boc-L-Leu-D-Leu-Aib-L-Leu-D-Leu-Aib-OMe (**2**), and Boc-L-Leu-D-Leu-Aib-D-Leu-L-Leu-Aib-OMe (**3**), and studied their preferred conformations in the crystalline state (Figure 1).

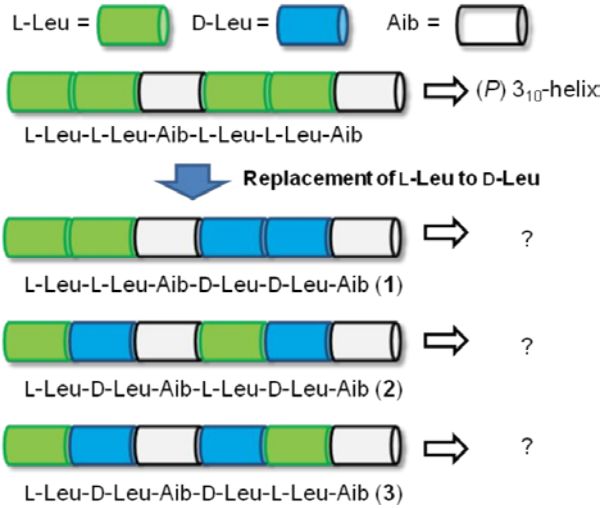

*Fig. 1. The design of peptides **1**, **2**, and **3**.*

Results and Discussion

Peptides **1**, **2**, and **3** were synthesized by conventional solution-phase methods according to a fragment condensation strategy using *O*-benzotriazole-*N*,*N*,*N*',*N*'-tetramethyluronium hexafluorophosphate (HBTU) and 1-hydroxybenzotriazole (HOBT) as coupling reagents. The conformation of peptides **1**, **2**, and **3** in the crystalline state was studied by X-ray crystallographic analysis. The preferred conformation of **1** was a left-handed (*M*)

3_{10}-helical structure, that of **2** was a β-hairpin nucleated by a type II' β-turn like structure, and that of **3** was an *S*-type turn structure nucleated by type II/III β-turns (Figure 2) [6].

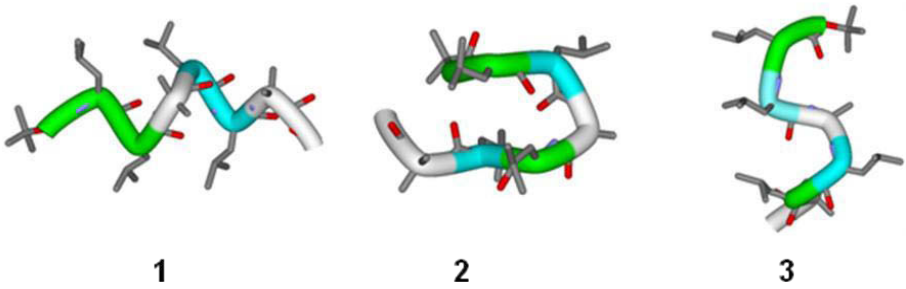

*Fig. 2. Illustrative structures of peptides **1**, **2**, and **3**.*

Acknowledgments
This work was supported in part by a Grant-in-Aid for Young Scientists (B) from the Ministry of Education, Culture, Sports, Science and Technology, Japan (MEXT), the Kurata Memorial Hitachi Science and Technology Foundation, and the Travel Grant from the Japan Society for the Promotion of Science (JSPS).

References

1. (a) Nagano, N., Tanaka, M., Doi, M., Demizu, Y., Kurihara, M., Suemune, H. *Org. Lett.* **11**, 1135-1137 (2009); (b) Tanaka, M., Anan, K., Demizu, Y., Kurihara, M., Doi, M., Suemune, H. *J. Am. Chem. Soc.* **127**, 11570-11571 (2005); (c) Tanaka, M., Demizu, Y., Doi, M., Kurihara, M., Suemune, H. *Angew. Chem. Int. Ed.* **43**, 5360-5363 (2004).
2. (a) Demizu, Y., Tanaka, M., Doi, M., Kurihara, M., Okuda, H., Suemune, H. *J. Pept. Sci.* in press; (b) Demizu, Y., Yamagata, N., Sato, Y., Doi, M., Tanaka, M., Okuda, H., Kurihara, M. *J. Pept. Sci.* **16**, 153-158 (2010); (c) Oba, M., Demizu, Y., Yamagata, N., Sato, Y., Doi, M., Tanaka, M., Suemune, H., Okuda, H., Kurihara, M. *Tetrahedron* **66**, 2293-2296 (2010); (d) Demizu, Y., Shiigi, H., Mori, H., Matsumoto, K., Onomura, O. *Tetrahedron: Asymmetry* **19**, 2659-2665 (2010).
3. Demizu, Y., Tanaka, M., Nagano, M., Kurihara, M., Doi, M., Maruyama, T., Suemune, H. *Chem. Pharm. Bull.* **55**, 840-842 (2007).
4. (a) Krause, E., Bienert, M., Schmieder, P., Wenschuh, H.L. *J. Am. Chem. Soc.* **122**, 4865-4870 (2000); (b) Fairman, R., Anthony-Cahill, S.J., DeGrado, W.F. *J. Am. Chem. Soc.* **144**, 5458-5459 (1992).
5. (a) Karle, I.L., Hosahudya, G.N., Balaram, P. *Proc. Natl. Acad. Sci. U.S.A.* **100**, 13946-13951 (2003); (b) Dhanasekaran, M., Fabiola, F., Pattabhi, V., Durani, S. *J. Am. Chem. Soc.* **121**, 5575-5576 (1999); (c) Haque, T.S., Little, J.C., Gellman, S.H. *J. Am. Chem. Soc.* **118**, 6975-6985 (1996).
6. Demizu, Y., Doi, M., Sato, Y., Tanaka, M., Okuda, H., Kurihara, M. *J. Org. Chem.* **75**, 5234-5239 (2010).

Proceedings of the 31st European Peptide Symposium
Michal Lebl, Morten Meldal, Knud J. Jensen, Thomas Hoeg-Jensen (Editors)
European Peptide Society, 2010

Optical Spectroscopy and Conformational Analysis of Peptide Aggregates. The Role of Aromatic Interactions and Conformational Flexibility

Mario Caruso[1], Ernesto Placidi[2], Emanuela Gatto[1], Lorenzo Stella[1], Antonio Palleschi[1], Gianfranco Bocchinfuso[1], Fernando Formaggio[3], Claudio Toniolo[3], and Mariano Venanzi[1]

[1]Department of Chemical Sciences and Technologies, University of Rome "Tor Vergata", Rome, 00133, Italy; [2]CNR, Department of Physics, University of Rome "Tor Vergata", Rome, 00133, Italy; [3]ICB, Padova Unit, CNR, Department of Chemistry, University of Padova, Padova, 35131, Italy

Introduction

Peptide aggregation is the basic process underlying a number of phenomena like sparkling of neuropathologies, formation of peptide films, and structuration of mesoscopic structures like fibrils or dendrimers. Experimental evidence indicates that aggregation is determined by a complex interplay of intermolecular interactions and structural effects, with a specific role played by aromatic residues.

Results and Discussion

In this study, the aggregation propensities of Aib (α-aminoisobutyric acid) homo-oligopeptides, of general formula Z-Aib$_n$-N (Z, benzyloxycarbonyl, N, naphthyl), with n=6, 12 and 15, were investigated by optical spectroscopy and atomic force microscopy techniques. From structural studies in solution and in the crystal state, Aib homo-peptides are well-known to populate 3_{10}- or α-helical structures depending, among other factors, on the length of the peptide chain [1,2].

The functionalization of the peptide scaffold with an N group allowed for optical spectroscopy techniques to be applied, particularly steady-state and time-resolved fluorescence. In methanol solution, all peptides investigated were found to exhibit emission spectra typical of the isolated N chromophores (Figure 1a). On the other hand, in the 30:70 (v/v) water/methanol mixture, while the shortest peptide shows an emission spectrum indicative of a monomeric species, the Z-Aib$_{15}$-N spectrum is characterized by a broad emission (Figure 1b), typical of excimer-like species, *i.e.* excited-state homo-dimeric complexes requiring the two interacting groups be located at short distances. This finding strongly suggests that hydrophobic effects are mainly responsible for the formation of the fluorescent aggregated species. A high fluorescence quantum yield is characteristic of J-type aggregates, *i.e.* stacked arrays of aromatic groups characterized by a slip angle $0 \leq \alpha < \pi/2$.

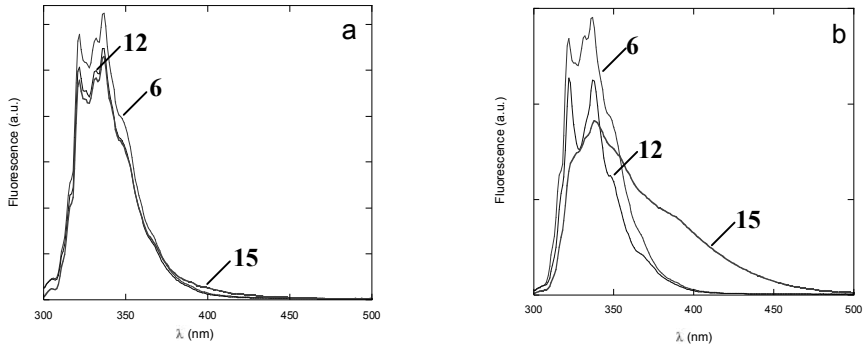

Fig. 1. Emission spectra of Z-Aib$_n$-N (n=6,12,15) in methanol (a) and in the 30:70 (v/v) water/methanol solvent mixture (b).

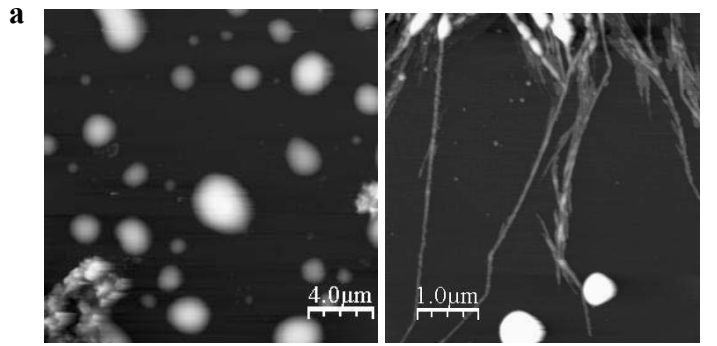

Fig. 2. AFM images of Z-Aib$_6$-N (a) and Z-Aib$_{15}$-N (b), both deposited on mica from the 30:70 (v/v) water/methanol solvent mixture.

Excimer emission can also be detected by time-resolved fluorescence measurements: Z-Aib$_{15}$-N showed decay time components of *ca.* 60ns for the N chromophore embedded as a monomer in the aggregate and 87ns for the excimer. Interestingly, the excimer time decay was also characterized by a short rise time component (≈3ns), associated to a negative pre-exponential factor that represents a measure of the dynamics of the nuclear motions leading to excimer formation.

AFM measurements were carried out on dried peptide films supported on mica and obtained by deposition of a 10μM 30:70 (v/v) water/methanol solvent mixture. Z-Aib$_6$-N (Figure 2a) showed globular structures characteristics of a specific aggregation, driven by hydrophobic interactions and promoted by the presence of the aromatic groups. On the contrary, Z-Aib$_{15}$-N exhibited, more extensively than Z-Aib$_{12}$-N, fibrillar structures several microns long and about 100nm thick (Figure 2b), suggesting that in this case interchain peptide interactions are the driving force that determines the morphology of the peptide aggregates. Both FTIR absorption spectroscopy and thioflavine test measurements indicated that the filaments are formed by microfibrils generated by entwined peptide helical chains.

References

1. Toniolo, C., Crisma, M., Formaggio, F., Peggion, C. *Biopolymers (Pept.Sci.)* **60**, 396-419 (2001).
2. Karle, I.L., Balaram, P. *Biochemistry* **29**, 6747-6756 (1990).

Proceedings of the 31st European Peptide Symposium
Michal Lebl, Morten Meldal, Knud J. Jensen, Thomas Hoeg-Jensen (Editors)
European Peptide Society, 2010

Mapping Charge Delocalization in a Peptide Chain Triggered by Oxidation of a Terminal Ferrocene Moiety

Vanessa Marcuzzo, Alessandro Donoli, Roberta Cardena, Alessandro Moretto, Claudio Toniolo, and Saverio Santi
Department of Chemical Sciences, University of Padova, Padova, 35131, Italy

Introduction

Electron transfer is one of the most relevant processes in chemistry and biology. Long-range electron transfer (ET) through proteins and enzymes is a fundamental step for all living organisms. The spatial organization of the electron donor and electron acceptor in peptides and proteins, as well as the dynamics of the ET between them, critically depends on the structure-directing and charge-transmitting properties of hydrogen bonds. ET through peptide helices has attracted much attention because their assemblies are universal motifs found in biological ET systems.

Results and Discussion

Two series of peptides of different length and rigidity, based on the strongly helicogenic α-aminoisobutyric acid (Aib) residue and containing a terminal ferrocene (Fc) unit, Fc–CO-$(Aib)_n$–OMe (A_n, n = 1–5, OMe, methoxy) and Z–$(Aib)_n$–NH–Fc (B_n, n = 1–5, Z, benzyloxycarbonyl), were prepared and investigated. We utilized the oxidation-state sensitive, spectroscopic tags of peptides, the CO and NH groups, to map charge delocalization triggered by oxidation of the terminal ferrocene, induced and monitored by Vis-IR-NIR spectroelectrochemistry. The rigid and well-defined 3_{10}-helical structure of $(Aib)_n$ homo-peptides [1,2] is advantageous for the study of the distance dependence of charge delocalization. The orientation of the carbonyl groups in the 3_{10}-helix produces a dipole with the positive end at the N-terminus and the negative end at the C-terminus. Thus, the A_n and B_n peptides series are characterized by an opposite-direction macrodipole towards the redox Fc/Fc^+ probe.

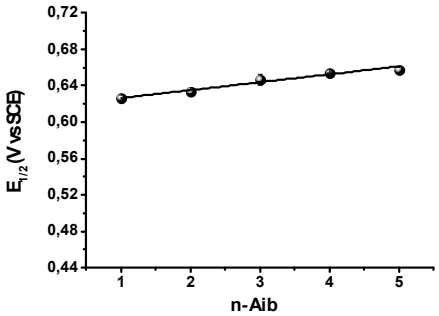

Fig. 1. Redox potentials vs saturated calomel electrode (SCE) of the Z-$(Aib)_n$-NHFc (n=1-5) peptide series recorded at a 0.5 mm diameter gold disk electrode in CH_2Cl_2 with 0.1 M nBu_4NPF_6 as supporting electrolyte.

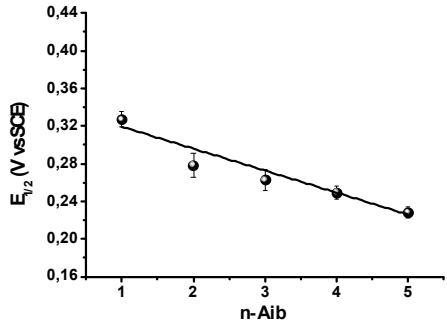

Fig. 2. Redox potentials vs SCE of the Fc-CO-(Aib)$_n$-OMe (n=1-5) peptide series recorded at a 0.5 mm diameter gold disk electrode in CH_2Cl_2 with 0.1 M nBu_4NPF_6 as supporting electrolyte.

The effect of the different orientation of the dipole moment (the latter increasing with the number of Aib residues in the backbone) was investigated by means of electrochemical and spectroscopic techniques. The oxidation potential dramatically depends on the dipole direction and the number of Aib units (the latter tunes intramolecular hydrogen-bond formation) (Figures 1 and 2). Moreover, the dependence of current intensity on peptide length was also explored. Finally, the shift and pattern of the C=O and N-H vibrations upon oxidation were used for mapping charge delocalization in the peptide chains, and estimating efficacy and time scale of intramolecular ET.

References

1. Karle, I.L., Balaram, P. *Biochemistry* **29**, 6747-6756 (1990).
2. Toniolo, C., Benedetti, E. *Macromolecules* **24**, 4004-4009 (1991).

Proceedings of the 31st European Peptide Symposium
Michal Lebl, Morten Meldal, Knud J. Jensen, Thomas Hoeg-Jensen (Editors)
European Peptide Society, 2010

Paternò-Yang Photocyclization Reaction in Bpa/Met 3_{10}-Helical Peptides: Role of Spacer Length

Anna Cupani, Alessandro Moretto, Fernando Formaggio, and Claudio Toniolo

ICB, Padova Unit, CNR, Department of Chemistry, University of Padova, Padova, 35131, Italy

Introduction

The 3-(4-benzoylphenyl)alanyl (Bpa) residue is extensively used as a photoaffinity label, particularly for studies of *intermolecular* (peptide)ligand-receptor(protein) interaction, where it is believed to most frequently remove a hydrogen atom from the side chain of a Met residue followed by covalent C-C bond formation of the resulting radical pair [1,2]. We are currently carrying out an extensive and detailed investigation of this Paternò-Yang *intramolecular* photochemical reaction in a series of backbone rigified, 3_{10}-helical [3] hexapeptides of general sequences Boc-$U_xBU_yMU_z$-OMe and Boc-$U_xMU_yBU_z$-OMe, where B=(*S*)-Bpa, U=Aib, M=(*S*)-Met, and $U_x+ U_y+ U_z=4$. We aim at determining the effects induced by the spacer length (U_y=0-3) on the chemical and 3D-structures of the resulting products and their ratios. We have already reported our results for the UBU_2MU hexapeptide substrate 1 [4].

1 Boc-Aib-**Bpa**-Aib-Aib-**Met**-Aib-OMe ($i \rightarrow i+3$)

2 Boc-Aib-**Bpa**-Aib-**Met**-Aib-Aib-OMe ($i \rightarrow i+2$)

3 Boc-Aib-**Bpa**-**Met**-Aib-Aib-Aib-OMe ($i \rightarrow i+1$)

4 Boc-Aib-**Met**-Aib-Aib-**Bpa**-Aib-OMe ($i \leftarrow i+3$)

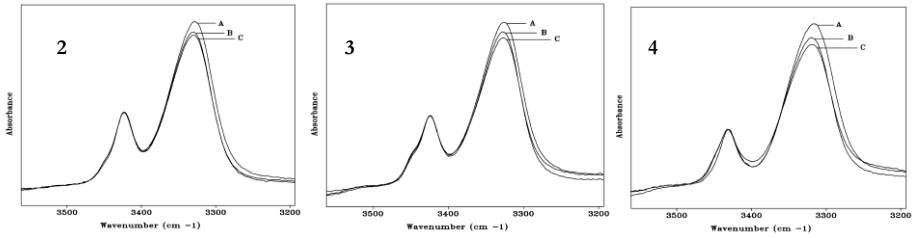

*Fig. 1. FTIR absorption spectra in the N-H stretching region of hexapeptides **2**, **3** and **4** in $CDCl_3$ solution. Peptide concentrations: 10 (A), 1 (B), 0.1 (C) mM.*

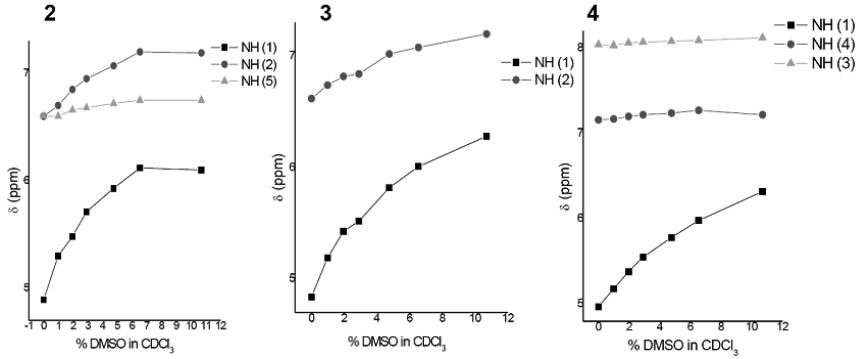

*Fig. 2. Plots of chemical shifts of the visible NH protons in the ^1H NMR spectra of hexapeptides **2-4** as a function of increasing percentages of DMSO (v/v) added to the $CDCl_3$ solution. Peptide concentration: 1mM.*

Results and Discussion

Here, we describe our recent FT-IR absorption (Figure 1) and ^1H NMR data (Figure 2) on the conformational analyses of the linear hexapeptides **2**-**4**. The huge IR absorption band near 3330 cm^{-1} and the sensitivity to the addition of the perturbing agent DMSO of the chemical shifts of only the NH(1) and NH(2) protons clearly support the view that stable 3_{10}-helical structures are formed by all three hexapeptides examined. These results are in good accord with those already reported [4] for the related hexapeptide **1**.

Moreover, in a prelimimary investigation (still underway) of the Paternò-Yang photocyclization on the hexapeptide substrates **2**-**4** we already demonstrated the significant effects induced by the distance and relative orientation of the Bpa/Met side chains on the isomeric product ratios and on the regio- and stereospecificities of the reaction.

References

1. Kauer, J.C., Erickson-Viitanen, S., Wolfe, H.R., Jr., DeGrado, W.F. *J. Biol. Chem.* **261**, 10695-10700 (1986).
2. Deseke, E., Nakatani, Y., Ourisson, G. *Eur. J. Org. Chem.* 243-251 (1998).
3. Toniolo, C., Benedetti, E. *Trends Biochem. Sci.* **16**, 350-353 (1991).
4. Moretto, A., Crisma, M., Formaggio, F., Huck, L.A., Mangion, D., Leigh, W.J., Toniolo, C. *Chem. Eur. J.* **15**, 67-70 (2009).

Proceedings of the 31st European Peptide Symposium
Michal Lebl, Morten Meldal, Knud J. Jensen, Thomas Hoeg-Jensen (Editors)
European Peptide Society, 2010

Experimental and Theoretical Spectroscopy Study of 3_{10}-Helical Peptides Using Isotopic Labeling

Ahmed Lakhani[1], Anjan Roy[1], Marcelo Nakaema[1], Matteo De Poli[2], Fernando Formaggio[2], Claudio Toniolo[2], and Timothy A. Keiderling[1]
[1]Department of Chemistry, University of Illinois at Chicago, Chicago, 60607-7061, IL, U.S.A.; [2]ICB, Padova Unit, CNR, Department of Chemistry, University of Padova, Padova, 35131, Italy

Introduction

Combined experimental and theoretical studies of IR absorption, vibrational circular dichroism (VCD), and Raman spectra are very useful for the unequivocal assignment of peptide conformation. In this work, an analysis has been performed on 3_{10}-helical [1] peptides with two different main-chain lengths: hexapeptide (*i*PrCO-Aib-L-Ala-Aib-L-Ala-L-Ala-Aib-NH*i*Pr) (*i*PrCO, *iso*propylcarbonyl; Aib, α-aminoisobutyric acid; NH*i*Pr, *iso*propylamino) and octapeptide (Ac-Aib-L-Ala-Aib-L-Ala-L-Ala-Aib-Aib-Aib-OMe) (Ac, acetyl; OMe, methoxy). These peptides are characterized by isotopic labeling ($^{13}C{=}O$) of the L-Ala residue on the following positions: *A4* and *A5*, (single labeled); *A4A5*, *A2A4* and *A2A5* (double labeled) for the hexapeptide, and *A4A5* for the octapeptide. Aib favors the 3_{10}-helix due to restriction of the backbone (ϕ, ψ) torsion angles by its α-carbon tetrasubstitution [2].

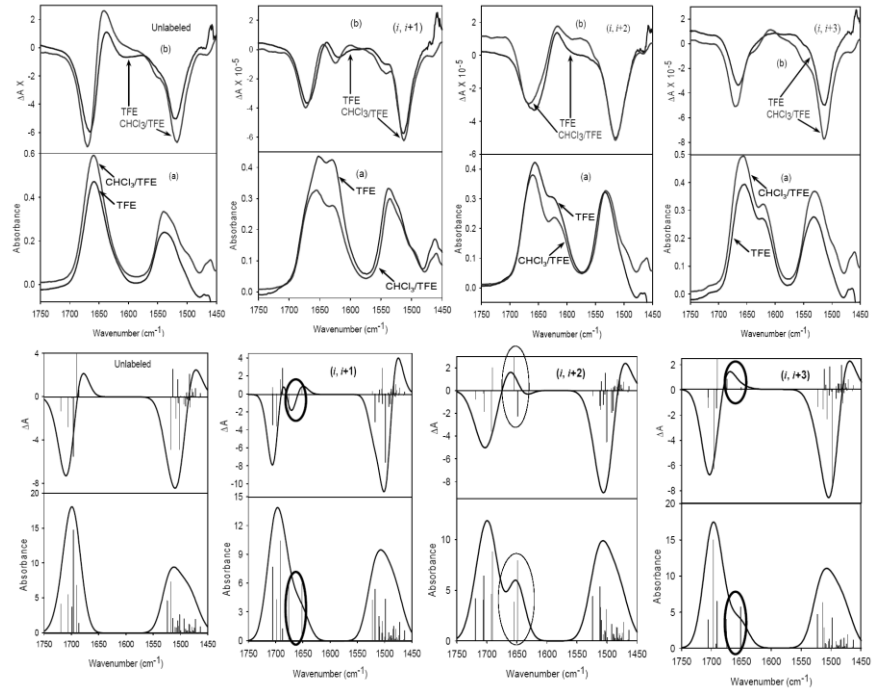

Fig. 1. (a) IR absorbance and (b) VCD spectra of the hexapeptide series (i,i+1: A4A5; i,i+2: A2A4; i,i+3: A2A5) in TFE and in $CHCl_3$/TFE solutions (amide I and II regions). Peptide concentration: ca. 20 mg/ml. The experimental (top) and simulated (bottom) spectra are reported.

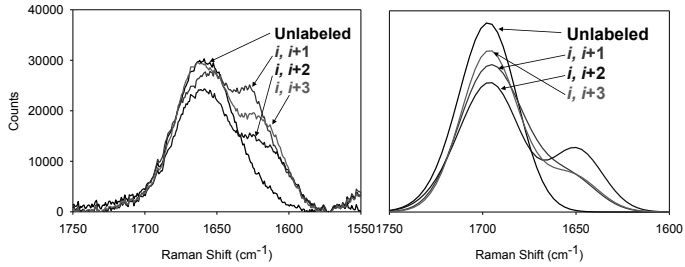

Fig. 2. Experimental (left) and simulated (right) Raman spectra of the hexapeptide series (i,i+1: A4A5; i,i+2: A2A4; i,i+3: A2A5) in TFE solution (peptide concentration: ca. 100 mg/ml).

Results and Discussion

Theoretical IR absorption and VCD (Figure 1), and Raman (Figure 2) simulations were performed on sequences identical to the synthesized ones with ϕ, ψ torsion angles constrained to an ideal 3_{10}-helical geometry (-60°, -30°), but with all the other coordinates fully optimized.

All calculations were carried out for peptides *in vacuo* using the DTF BPW91/6-31G* levels of theory. The simulations predicted the conformational dependence of the relative separations of ^{13}C=O and ^{12}C=O features, and the exciton splitting of the ^{13}C=O band in the doubly labeled species to be in agreement with those seen experimentally (Figures 1 and 2), with the exception that fraying at the N- and C-termini causing a change in diagonal force field are not well represented in the theoretical modeling.

Experimental spectra for the octapeptide (*A4A5*) confirmed the source of deviation for the related hexapeptides. Comparison of IR absorption and VCD intensity patterns helped sort out the vibrational coupling constants sensed in the ^{13}C=O modes. The isotopic labeled group vibrations are coupled to each other most strongly when they are degenerate and are effectively uncoupled from those of the unlabeled groups.

References

1. Toniolo, C., Benedetti, E. *Trends Biochem. Sci.* **16**, 350-353 (1991).
2. Toniolo, C., Crisma, M., Formaggio, F., Peggion, C. *Biopolymers (Pept. Sci.)* **60**, 396-419 (2001).

Proceedings of the 31st European Peptide Symposium
Michal Lebl, Morten Meldal, Knud J. Jensen, Thomas Hoeg-Jensen (Editors)
European Peptide Society, 2010

Oostatic Peptides Containing D-Amino Acids: Degradation, Accumulation in Ovaries and NMR Study

Jan Hlaváček[1], Blanka Bennettová[2], Bohuslav Černý[3], Věra Vlasáková[4], Josef Holík[4], Miloš Buděšínský[1], Jiřina Slaninová[1], and Richard Tykva[1]

[1]Institute of Organic Chemistry and Biochemistry, Czech Academy of Sciences, Prague, 166 10, Czech Republic; [2]Institute of Entomology, Czech Academy of Sciences, České Budějovice, 37 005, Czech Republic;[3]1st Medical Faculty, Charles University, Prague, 11 636, Czech Republic;[4]Institute of Experimental Botany, Czech Academy of Sciences, Prague, 142 20, Czech Republic

Introduction

Oostatic pentapeptide H-Tyr-Asp-Pro-Ala-Pro-OH (5P) (1a) is the C-terminus shortened analog of decapeptide H-Tyr-Asp-Pro-Ala-Pro-Pro-Pro-Pro-Pro-Pro-OH from mosquito *Aedes aegypti* [1]. This pentapeptide inhibits a development of eggs in the flesh fly *Neobellieria bullata* [2] by decreasing their hatchability. In this study, we focused our interest on the oostatic activity of analogs of the pentapeptide 1a, containing corresponding D-amino acids: H-D-Tyr-Asp-Pro-Ala-Pro-OH (1b), H-Tyr-D-Asp-Pro-Ala-Pro-OH (1c), H-Tyr-Asp-D-Pro-Ala-Pro-OH (1d), H-Tyr-Asp-Pro-D-Ala-Pro-OH (1e), H-Tyr-Asp-Pro-Ala-D-Pro-OH (1f), all D-(H-Tyr-Asp-Pro-Ala-Pro-OH) (1g) and on accumulation of radioactivity from tritium labeled pentapeptides H-Tyr-Asp-[^{3}H]Pro-Ala-Pro-OH (2a), H-Tyr-D-Asp-[^{3}H]Pro-Ala-Pro-OH (2b) and H-Tyr-Asp-[^{3}H]Pro-D-Ala Pro-OH (2c) in ovaries of *N. bullata*, and on the labeled pentapeptides degradation [3,4].

Results and Discussion

Peptide sequences were assembled on 2-chlorotrityl polystyrene resin, compatible with C-terminal Pro residue, using Fmoc/OtBu strategy. Fmoc deprotection was performed by 20% piperidine in DMF and a coupling by DIC/HOBt in DMF. The peptide detachment from the resin and the side-chain deprotection were carried out simultaneously by a TFA/TIS (10:1) mixture for 30 min. Radiolabeled peptides were obtained by addition of tritium gas to the double bond of $^{\Delta}$Pro residue in corresponding precursors, in the presence of $PdO/BaSO_4$.

Assay on the oostatic activity of the pentapeptides 1b-1g in the flesh fly *N. bullata* has shown a significant decrease of hatchability in the 1st gonotrophic cycle, comparable with the parent pentapeptide 1a, and no hatchability in the 2nd gonotrophic cycle. Morphology changes in ovaries correspond to a large resorption of oocytes of treated flies after application of the pentapeptides 1b, 1c and 1g. Even if the pentapeptides 1d-1f exhibit low

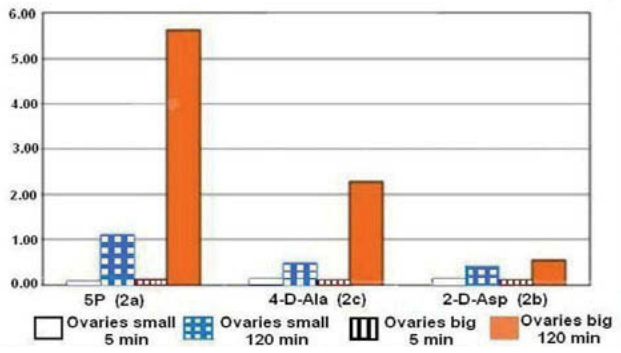

Fig. 1. Radioactivity of N.bullata ovaries (in kBq) after incubation with pentapeptides 2a - 2c. Small means 5th-6th and big means 11th-12th of the 14 developmental stages, based on the deposition of the yolk in oocytes [5].

resorption, this effect interferes with the embryogenesis, so that hatching is impossible and the changes in female reproductive system of *N. bullata* are degenerative.

An incubation of *N. bullata* ovaries with labeled pentapeptides 2a-2c shows different results. Contrary to the quick degradation of the peptide 2a**,** its analogs 2b and 2c were degraded much slower. Just 2 hours after incubation, the pentapeptide 2b and its degradation product Tyr-D-Asp-Pro have been still present in ovaries as detected by radio-HPLC. Similarly, the pentapeptide 2c degrades slowly to Asp-Pro-D-Ala-Pro and Pro-D-Ala-Pro. With these analogs, the total radioactivity accumulation in ovaries was significantly decreased in comparison with the parent peptide 2a (Figure 1). An imbalanced decrease, however, might be ascribed to position of D-amino acid residue toward to Tyr^1 residue and to changed conformation of D-amino acid containing analogs.

To rationalize the results of degradation and accumulation studies with labeled pentapeptides 2a-2c**,** we utilized NMR spectroscopy for molecular modeling and estimation of conformational changes in corresponding peptides**.** NOEs measured were used as distance restrains and applied on previously unrestrained optimized structures. The energy minimization (AMBER; for all NOE restraints distance limit 4A) provided the structures shown in Figure 2. Peptide 1e adopts the most extended form that differs from 1a mainly by orientation of Pro^5 residue. The most compact seems to be a molecule of 1c that could be stabilized with the H-bond between OH group of Tyr^1 and C=O of Pro^3 (see dotted line).

The metabolic stabilization of the molecules with D-amino acids is linked to changed conformation, which might perturb peptides interaction with enzyme and prolong their half-life. The analogs with partially restricted structures, due to the presence of D-amino acids, are flexible enough to maintain and even potentiate oostatic effect in *N. bullata*. Thus, the presence of D-amino acids in oostatic peptides results in more oocytes influenced during the period of their development, which enhances the regulatory potency of corresponding analogs.

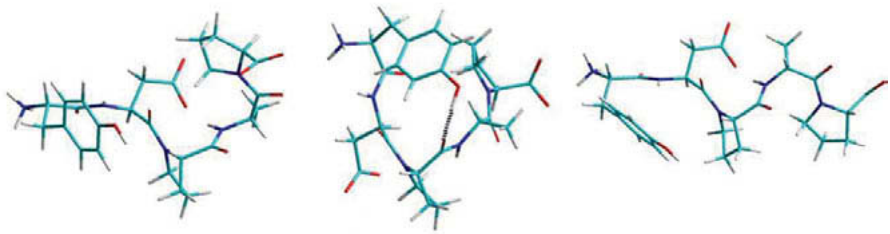

Fig. 2. The calculated energy minimized structures of 1a, 1c and 1e (NOE distance restraints applied).

Acknowledgments

Supported by the Research Project Z4 055 0506 of the Institute of Organic Chemistry and Biochemistry CAS, v.v.i. and by the Czech Science Foundation (Grant No. 203/06/1272)

References

1. Borovsky, D., Carlson, D.A., Griffin, P.R., Shabanowitz, J., Hunt D.F. *FASEB J*. **4**, 3015-3020 (1990).
2. Hlaváček, J., Tykva, R., Bennettová, B., Barth, T. *Bioorg. Chem*. **26**, 131-140 (1998).
3. Tykva, R., Hlaváček, J., Vlasáková, V., Černý, B., Borovičková, L., Bennettová, B., Holík, J., Slaninová, J. *J. Chrom. B*. **848**, 258-263 (2007).
4. Hlaváček, J., Černý, B., Bennettová, B., Holík, J., Tykva, R. *Amino Acids* **33**, 489-497 (2007).
5. King, R.C., *Ovarian Development in Drosophila melanogaster*, 33-54. Academic Press, New York, 1970.

Proceedings of the 31st European Peptide Symposium
Michal Lebl, Morten Meldal, Knud J. Jensen, Thomas Hoeg-Jensen (Editors)
European Peptide Society, 2010

Dendrimeric Peptides with Affinity to Opioid Receptors – Complexation Studies

Marta Sowińska[1], Anna Leśniak[2], Andrzej W. Lipkowski[2], and Zofia Urbanczyk-Lipkowska[2]

[1]Institute of Organic Chemistry, PAS, Warsaw 01-224, Poland;
[2]Medical Research Centre, PAS, Warsaw, 02-106, Poland

Introduction

A pharmaceutical formulation improving bioavailability or cellular uptake gained recently a lot of attention [1]. Biphalin, dimeric enkephalin analogue (Tyr-D-Ala-Gly-Phe-NH)$_2$ has unique properties, i.e. high antinociceptive effects. It has limited permeability of blood-brain barrier [2]. Several reports were published on design of analogs or conjugates of biphalin with improved bioavailability [3,4]. Here we present preparation of $(Lys)_2Lys$ dendrons functionalized with terminal Tyr-Gly- and investigate complex formation with biphalin. ESI MS studies have been applied to study complex stoichiometry. Opioid receptor binding was performed for these derivatives alone and in the complex.

Results and Discussion

It has been discovered recently, that short amphipatic peptides act as an efficient carriers of oligonucleotides due to formation of noncovalent complex between the two species [4]. Analogously, it is expected that properties of any biologically active peptide (i.e. 3D structure, hydrophobicity, solubility, etc.) can be modified by formation of molecular complex with another peptide that has affinity to the same receptor. To check this hypothesis, two peptides with branched structure, functionalized with enkephalin fragment were synthesized using convergent strategy. Initially synthesized $(Lys)_2Lys$ dendron **A** (Figure 1) containing phenylethylamino group at C-end was coupled with two equivalents of dipeptide Boc-Tyr-Gly-OH yielding neutral compound **A-1**, that after deprotection of amino groups yielded compound **A-2**, bearing double charge. Dendrimers were purified with size exclusion chromatography using Sephadex LH-20 (in MeOH). Their structure was confirmed by ESI MS and NMR spectroscopy. Possibility of formation of the dendrimer/biphalin (BIPH) complex was checked by taking ESI MS spectra of the mixtures containing 0.5, 1, 1.5 and 2.0 molar dendrimer/biphalin ratios in water. ESI MS spectra revealed ions belonging to $[\mathbf{A} + BIPH + 2H]^{2+}$ ions, thus both dendrimers form in gas phase associates with 1:1 stoichiometry. Fragmentation study of the complex between neutral **A-1** and biphalin is shown in Figure 2.

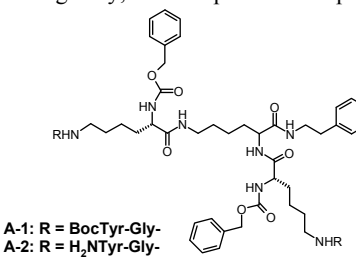

Fig. 1. Structure of peptide dendrimers.

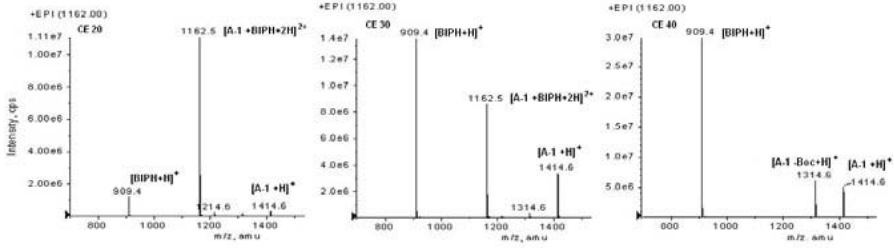

*Fig. 2. MS/MS spectra of the 1:1 complex between **A-1** and biphalin, measured at various collision energies (CE).*

Table 1. Affinity to μ and δ opioid receptor subtypes[a]

Compound	*Affinity to μ receptor (nM)*	*Affinity to δ receptor (nM)*
A-1	>1000(96)	>1000(102)
A-1 + BIPH	0.39(2)	1.56(2)
BIPH	0.40(2)	1.26(1)
A-2	630(62)	794(70)
A-2 + BIPH	0.31(2)	0.80(5)

[a]*rat brain homogenate*

Tandem mass spectrometry method has been used (4000 Q TRAP mass spectrometer) to confirm relative strength of the complex between **A-1** and **A-2** and biphalin. The resulting spectra (Figure 2) of **A-1**/biphalin after raising energy of collisions (CE) from 20 to 40 eV's gave gradual disappearance of the ion with 1162.5 mass and increase of intensity of the two monoprotonated ions belonging to individual peptides (BIPH - 909.4 and **A-1** -1414.6). However, in case when both peptides are positively charged (i.e. **A-2** and biphalin), intensity of the cumulative peak is very low (ca. 10%) and disappears when CE equals to 30 eV. In conclusion, positively charged dendrimer associates much weaker with biphalin.

In vitro binding to μ and δ opioid receptors was performed for neutral and charged dendrimers, as well as for their mixture with biphalin (Table 1). Dendrimers **A-1** and **A-2** have ca 10^3 times lower affinity to μ and δ opioid receptors than biphalin. However, they do not have impact on resulting affinity when mixed with biphalin. It is interesting to note that water solubility of the (1:1) compositions was ca 30% higher than that of biphalin alone.

Presented data show that the designed dendrimeric peptides can be used as prospective carriers for biphalin. They form associates with biphalin with improved solubility in water. Multiple hydrogen bonds that can be formed between uncharged central fragments of both molecules are probably the driving forces of this process.

Acknowledgments
Supported by EC grant "Normolife" and Grant N204 239436 from Ministry of Science and Higher Education of Poland.

References

1. Crombez, L., Charnet, A., Morris, M.C., Aldrian-Herrada, G., Heitz, F., Divita, G.**,** *Biochem. Soc. Trans.* **35,** 44-46 (2007).
2. Kosson, D., Klinowiecka, A., Kosson, P., Bonney , I., Carr, D.B., Mayzner-Zawadzka, B., Lipkowski, A.W. *Eur. J. Pain* **12**, 611-616 (2008).
3. Witt, K., Huber, J.D., Egleton, R.D., Davis, T.D. *J. Pharm. Exp. Therapy* **303**, 760-767 (2002).
4. Laufer, S.D., Recke, A.L., Veldhoen, S., Trampe, A., Restle, T. *Oligonucleotides* **19**, 63-80 (2009).

Proceedings of the 31st European Peptide Symposium
Michal Lebl, Morten Meldal, Knud J. Jensen, Thomas Hoeg-Jensen (Editors)
European Peptide Society, 2010

NMR-Based Conformational Studies of the C-Terminal Heptadecapeptide(101-117) of Human Cystatin C

Martyna Maszota, Paulina Czaplewska, Anna Śladewska, Marta Spodzieja, and Jerzy Ciarkowski
Faculty of Chemistry, University of Gdańsk, Gdańsk, 80-952, Poland

Introduction

Human cystatin C (hCC) is a small (13 kDa, 120 amino acid residues) protein inhibitor of cysteine proteases [1]. It is the most widespread cystatin in mammalian body fluids. hCC is involved in various diseases including the Alzheimer's disease; it binds amyloid β (Aβ) and reduces its aggregation and deposition [2]. Recent *in vitro* epitope extraction/excision mass spectrometry studies including Aβ and hCC revealed that the C-terminal heptadecapeptide of the latter, hCC (101-117) is the minimal Aβ-binding epitope of hCC [3]. NMR-based conformational studies of hCC (101-117) will help to understand oligomerization of hCC, possibly including its self-aggregation and interactions with Aβ and, in the next step, design the new potential inhibitors of hCC oligomerization.

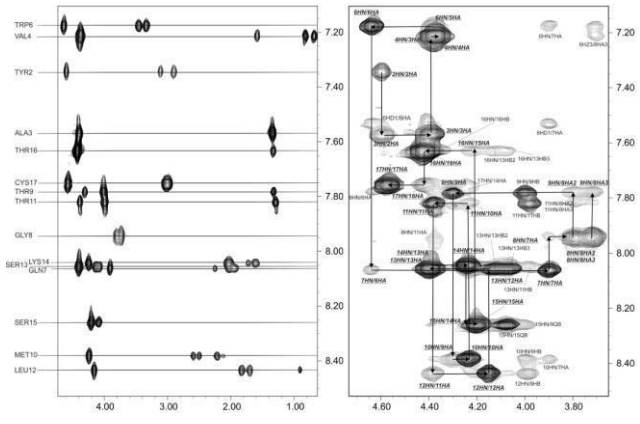

Fig. 1. Left – fingerprint region of a TOCSY spectrum; Right – the NH-Hα region of TOCSY (black) and NOESY (grey) with indicated connectivities.

Results and Discussion

Complete assignment of the proton spectra of hCC(101-117) was achieved according to the

Fig. 2. The backbone represents the final 300 structures; the side-chains represent the averaged conformation of hCC(101-117).

Table 1. Proton chemical shifts and vicinal coupling constants of hCC(101-117)

Residue	3J NH-Hα [Hz]	Chemical shift [ppm]					
		NH	α - CH	ε - CH	β - CH	δ - CH	γ -CH
ILE1	-	-	3.62	-	1.86	1.31 1.11	0.94
TYR2	12.8	7.35	4.59	-	3.11 2.90	7.05	-
ALA3	7.3	7.58	4.39	-	1.35	-	-
VAL4	8.3	7.22	4.37	-	1.60	-	0.84 0.73
PRO5	-	-	4.38	-	2.35 2.09	3.71 3.55	2.05
TRP6	7.7	7.18	4.63	7.45 7.19	3.45 3.34	7.54	-
GLN7	6.1	8.06	3.91	-	1.94	-	2.25
GLY8	16.2	7.95	3.80 3.73	-	-	-	-
THR9	-	7.78	4.30	-	4.01	-	1.34
MET10	5.1	8.38	4.24	-	2.23 2.13	-	2.60 2.51
THR11	-	7.82	4.38	-	3.99	-	1.31
LEU12	5.9	8.44	4.16	-	1.84	0.92	1.72
SER13	7.6	8.06	4.39	-	4.12 4.07	-	-
LYS14	8.0	8.05	4.24	3.05	2.04	1.73	1.63
SER15	8.4	8.26	4.21	-	4.08	-	-
THR16	9.6	7.63	4.42	-	4.41	-	1.35
CYS17	8.2	7.76	4.57	-	3.01	-	-

standard Wüthrich procedure [4] using DQF-COSY, TOCSY and NOESY spectra. The fingerprint region of the TOCSY spectrum and the diagnostic region of TOCSY and NOESY, including the sequential assignments, are given in Figure 1. There is only one set of chemical shifts, indicative of only one (time-averaged) state of hCC(101-117). Small values of $^3J_{NHH\,\alpha}$, typical of helix, were found for Met10 and Leu12 (Table 1). Vicinal coupling constants typical of a β-sheet were found only for Tyr2 and Gly8. Most of the amino acid residues have $^3J_{NHH\alpha}$ values near 7Hz, suggesting a statistical-coil conformation; some $^3J_{NHH\alpha}$ could not be measured. Analyzes of NOE $d_{\alpha N(i,i+3)}$ intensities point at helical 6-11 and 12-17 fragments of hCC(101-117). A $d_{NN(i,i+1)}$ connectivities suggesting helical conformation are present for most residues.

The last 300 snapshots of MD with restraints are shown in Figure 2. RMSD value is 0.71 Å for all atoms, 0.56 Å for heavy atoms and 0.35 Å for the backbone atoms. All conformations have unordered N-termini with bends in their central part and very similar helical structures in the (12-17) fragment. All the features of the calculated structures obtained for the C-terminal fragment of hCC(101-117) are in very good agreement with the qualitative predictions from the NMR data.

Acknowledgments
The work was supported by Polish Ministry of Science grant no. 1264/B/H03/2009/37 and BW 8372-5-0647-0. The calculations were carried out in the Academic Computer Centre (TASK) in Gdańsk, Poland.

References

1. Levy, E., Jaskólski, M., Grubb, A. *Brain Pathol.* **16,** 60-70 (2006).
2. Kaeser, S.A., Herzig, M.C., Coomaraswamy, J., et al. *Nat. Genet.* **39,** 1437-1439 (2007).
3. Juszczyk, P., Paraschiv, G., Szymańska, A., et al. *J. Med. Chem.* **52**, 2420-2428 (2009).
4. Wüthrich, K. *NMR of Proteins and Nucleic Acids*, John Wiley & Sons, New York (1986).

Proceedings of the 31st European Peptide Symposium
Michal Lebl, Morten Meldal, Knud J. Jensen, Thomas Hoeg-Jensen (Editors)
European Peptide Society, 2010

Beta-Aspartic Acid Impairs the Ability to Bind Metal Ions by Immunosuppresory Fragment of Ubiquitin and Other Peptides as Studied by ESI-MS/MS

Marek Cebrat, Marlena Zajączkowska, Piotr Stefanowicz, and Zbigniew Szewczuk
Faculty of Chemistry, University of Wrocław, Wrocław, 50-383, Poland

Introduction

Recently ubiquitin was suggested as a promising anti-inflammatory protein therapeutic [1]. We found that a peptide fragment corresponding to the ubiquitin 50–59 sequence (LEDGRTLSDY, Ubq^{50-59}) possessed the immunosuppressive activity comparable with that of ubiquitin. The peptide was much less toxic than cyclosporine, particularly at higher doses [2]. The cyclic peptide designed to mimic the ubiquitin 50–59 loop strongly suppressed the immune response, suggesting that ubiquitin and its LEDGRTLSDY fragment may interact with the same hypothetical receptors [3].

It is known that the formation of complexes of proteins and peptides with metal ions often plays a significant role in their interaction with the respective receptors [4]. Our earlier studies indicated that the mass spectrometry can provide reliable information on the stoichiometry and a possible binding mode of the peptide-metal complexes [5,6]. Therefore, we applied high-resolution mass spectrometry to study the interaction of LEDGRTLSDY fragment analogues with Cu^{2+} and Zn^{2+} ions. A series of the peptide analogues, which included acetylated and amidated peptides and sequences with Asp residue replaced by beta-aspartic acid (βAsp), was synthesized. A model tetrapeptide H-βAsp-His-Gly-His-OH as well as analogues of natural, biologically active peptides (angiotensin, AT; fibrinopeptide A, FPA; thymopentin, TP-5; osteonectin, SPARC) with Asp to βAsp substitution were also synthesized and tested:

Ubiquitin50-59 fragment analogues:

H-Leu-Glu-Asp-Gly-Arg-Thr-Leu-Ser-Asp-Tyr-OH	Ubq^{50-59}
Ac-Leu-Glu-Asp-Gly-Arg-Thr-Leu-Ser-Asp-Tyr-OH	$AcUbq^{50-59}$
H-Leu-Glu-Asp-Gly-Arg-Thr-Leu-Ser-Asp-Tyr-NH_2	Ubq^{50-59}-NH_2
Ac-Leu-Glu-Asp-Gly-Arg-Thr-Leu-Ser-Asp-Tyr-NH_2	$AcUbq^{50-59}$-NH_2
H-Leu-Glu-βAsp-Gly-Arg-Thr-Leu-Ser-Asp-Tyr-OH	$[\beta Asp^3]Ubq^{50-59}$
Ac-Leu-Glu-βAsp-Gly-Arg-Thr-Leu-Ser-Asp-Tyr-OH	$[\beta Asp^3]AcUbq^{50-59}$

Other peptides:

H-βAsp-His-Gly-His-OH	$[\beta Asp^1]$DHGH
H-βAsp-Arg-Val-Tyr-Ile-His-Pro-Phe-OH	$[\beta Asp^1]$AT
H-Ala-βAsp-Ser-Gly-OH	$[\beta Asp^2]$FPA
H-Arg-Lys-βAsp-Val-Tyr-OH	$[\beta Asp^3]$TP-5
Ac-Thr-Leu-Glu-Gly-Thr-Lys-Lys-Gly-His-Lys-Leu-His-Leu-βAsp-Tyr-NH_2	$[\beta Asp^{14}]$AcSPARC-NH_2

Results and Discussion

Peptides were synthesized by a manual solid phase peptide synthesis using standard Fmoc protocol. Peptide solutions were mixed with the metal ions solutions (1:1) and incubated for 24 hours at 5°C before MS experiments. Interaction of the peptides with metal ions were studied on Bruker apex ultra 7T FT-ICR mass spectrometer equipped with an ESI source using standard instrument settings. Positive ions were analyzed.

The analysis of ESI-MS spectra of the studied peptides containing βAsp residue clearly shows that they are poor ligands for Cu^{2+} and even worse for Zn^{2+} ions. In a case of the LEDGRTLSDY peptide (Ubq^{50-59} fragment) and its analogues the substitution of Asp^3 residue by βAsp^3 as well as N-terminal acetylation drastically reduces the ability to form a peptide-metal complex. For example, peaks of the Ubq^{50-59} fragment complexed with Cu^{2+} ion is very intense (peaks at m/z 615.22 and 1229.43) whereas they are almost completely absent for $[\beta Asp^3]Ubq^{50-59}$ (Figure 1). C-terminal amidation does not influence binding of Cu^{2+} ions.

The presence of βAsp residue in position three of the peptide chain (Ubq^{50-59} fragment analogues and $[\beta Asp^3]$TP-5 peptide) completely prevents the formation of the complexes

with Zn^{2+} ions. Peptides containing βAsp in position 1 or 2 ([βAsp^1]DHGH, [βAsp^1]AT, [βAsp^2]FPA) have a very low affinity towards Zn^{2+} but the complexes that are formed are much more stabile than those with Cu^{2+}. Surprisingly, [βAsp^{14}]AcSPARC-NH_2 peptide was a poor ligand for Cu^{2+} and Zn^{2+} ions even though it contains two His residues.

The analysis of CID ESI-MS/MS spectra of the peptide-metal ion complexes allowed us to draw some conclusions on the most probable sites of the metal ion binding. For example, in case of the Ubq$^{50-59}$ fragment analogues Cu^{2+} ions interact mainly with the N-terminal amino group and the Glu^2 residue. For the model peptide [βAsp^1]DHGH and [βAsp^{14}]AcSPARC-NH_2 the major binding sites for Cu^{2+} are both His residues.

Presented results are in a very good agreement with those obtained by more traditional methods applied to study peptide–metal interactions (potentiometry, UV-Vis). This proves that the mass spectrometry may provide reliable information not only on the stoichiometry of the peptide-metal complexes, but also on the binding mode and the localization of the metal ion within the complex.

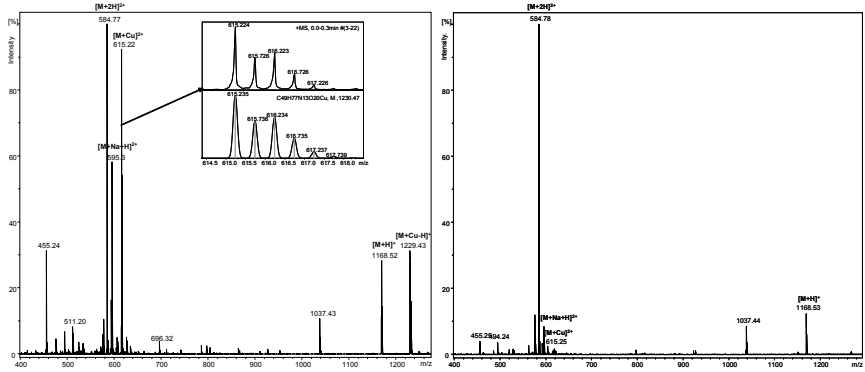

Fig. 1. ESI-MS spectra of Ubq$^{50-59}$ (left) and [β-Asp^3]Ubq$^{50-59}$ (right) in the presence of Cu^{2+}. Inserts show isotopic patterns of the indicated peak; top spectra was measured, the bottom one was calculated.

Acknowledgments

This work was supported in part by grant No. N N401 222734 from the Ministry of Science and Higher Education (Poland).

References

1. Earle, S.A., El-Haddad, A., et al. *Transplantation* **82**, 1544-1546 (2006).
2. Szewczuk, Z., Stefanowicz, P., et al. *Biopolymers* **74**, 325-362 (2004).
3. Jaremko, L., Jaremko, M., et al. *Biopolymers* **91**, 423-4314 (2009).
4. Liu, D., Seuthe, A.B., et al. *J. Am. Chem. Soc.* **127**, 2024-2025 (2005).
5. Brasun, J., Cebrat, M., et al. *J. Inorg. Bioch.* **103**, 1033-1038 (2009).
6. Brasun, J., Cebrat, M., et al. *Dalton Trans.* 853-4857 (2009).

Proceedings of the 31st European Peptide Symposium
Michal Lebl, Morten Meldal, Knud J. Jensen, Thomas Hoeg-Jensen (Editors)
European Peptide Society, 2010

Ensemble Fit of Conformational Equilibria of Restrained Peptides to NMR Data. Dependence on Force fields: Amber8 vs ECEPP/3

J. Ciarkowski[1], S. Łuczak[1], M. Oleszczuk[2], and J. Wójcik[3]
[1]Faculty of Chemistry, University of Gdańsk, 80-952 Gdańsk, Poland; [2]Department of Biochemistry, University of Alberta, T6G 2H7CA, Canada; [3]Institute of Biochemistry and Biophisics, PAS, 02-106, Warsaw, Poland

Introduction

Searching an optimal method for conformational analysis of flexible peptides, we used two dermorphin analogs Tyr-D-Daa-Phe-Daa-NH_2 comprising combinations of D-Dab[2] (α,γ-diaminobutyryl) with Lys[4], **1**, and of D-Dap[2] (α,β-diaminopropionyl) with Orn[4], **2.** They had side chain amino groups bridged with >C=O, restraining **1** and **2** with 16- and 14-membered rings and leading to potent and impotent μ/δ opioid peptides, respectively [1]. The conformational equilibria of **1** and **2** were found by fitting their ensembles to the NOE and J NMR data using the method introduced by Groth, et al. [2], implementing the maximum entropy principle to avoid overfit. The latter turns up when a physical quantity (here equilibrium), is fitted to data charged with inherent statistical uncertainty (here NOE and J). In the procedure quoted, the overfit is dispersed by the introduction of the scaled entropy term (scaling factor α), favoring uniform distribution of conformers [2]. Typically, for α=0 (no entropy term), a fit delivers a few conformations, the standard deviation (SD) of the objective function is ≤ than that transposed from the measured SD in J and NOE, and we arrive at effectively fitting a good share of noise (overfit). On the opposite side, e.g. α≈2, thousands of conformers are found, SD grows larger and more realistic, χ^2 test becomes excellent. For flexible peptides, an objective is a compromise between these two options to be reached by trial-and-error, featured with SD ≥ than that transposed from parameter errors and with a handy conformational distribution meeting χ^2 criterion.

Results and Discussion

The Authors [1] provided us with their NMR NOE- and J-data in H_2O/D_2O, and with the results of fitting conformational equilibria of **1** and **2** to their NMR data using an ensemble generated by means of EDMC/ECEPP/3 (rigid-valence geometry) methodology [2]. We submitted **1** and **2** to the 4 ns molecular dynamics (AMBER v.8, flexible-valence) in the periodic boundary conditions at constant pressure, using the locally enhanced sampling (LES-MD, 5 copies) for more efficient sampling. The time step was 2 fs, the coordinates saved every 2000 steps and put together. In the time range 0.48-4 ns every fifth set was collected, resulting with 880 conformers per **1** and/or **2**.

Earlier use of EDMC/ECEPP methodology [2] by some of us resulted with 7 structures for **1** and 11 for **2** [1], hereby applied as a reference. The structures were received from the fits restoring the NMR parameters to ~94% and *not* employing the entropy term, α=0 [1], see Table 1. Currently, using fits to the LES-MD/AMBER [3] ensemble, we selected the entropy factor α=0.001 by trial-and-error. The choice resulted in 154 structures

*Fig. 1. Macrocycle-fitted overlap of LES-MD/AMBER (grey) for EDMC/ECEPP (black) structures: left – for **1** and;right – for **2**.*

*Table 1. Root mean square (RMS) deviation values, characterizing conformational clusters of **1** and **2** and the differences between both fitting approaches*

	LES-MD/AMBER confidence level 0.8	*EDMC/ECEPP [1] confidence level 0.94*	*AMBER vs ECEPP*
	1		
No of structures:	154/23(α=0.001/α=0)	7(α=0)	154/7
σ_J [a]	0.011/0.003	0.88	
σ_{NOE} [b]	0.13/0.13	0.32	
RMS [c]: All	2.33/2.27	1.22	2.52
Macrocycle	1.02/1.01	0.66	1.31
	2		
No of structures:	26/3(α=0.001/α=0)	11(α=0)	26/11
σ_J [a]	0.007/0.003	0.78	
σ_{NOE} [b]	0.05/0.05	0.18	
RMS [c]: All	2.40/2.01	1.79	2.46
Macrocycle	0.96/0.91	0.77	1.49

[a] in Hz; [b] unitless; [c] "heavy" C, N atoms, in Å

for **1** and 26 for **2,** restoring the NMR parameters to about 80%. The value of α=0.001 certainly have not eliminated overfit (e.g. $^3J_{NC\alpha}$-s were restored to an astonishing *apparent* accuracy of ~0.01 Hz, see Table 1), yet, mere introduction of α has dispersed conformational variability from 23 to 154 for **1**, and from 3 to 26 for **2**, as referred to α=0 (Table 1). The representative structures of **1** and **2** are shown in Figure 1. The RMS deviation values calculated using all the heavy atoms and those of the restraining rings (see above) are shown in Table 1.

In agreement with the work of Groth, at al. [2], the overfit falls down rapidly with the introduction of even the slightest share of entropy to the objective function (comp. higher RMS for α=0.001 than for α=0, Table 1). Intriguing is startlingly small $\sigma_J \approx 0.01$ Hz at α=0.001 for LES-MD/AMBER methodology, as compared to σ_J =0.8-0.9 Hz for EDMC/ECEPP at α=0. A similar feature is not the case when comparing σ_{NOE} in both methods. Hence, at minute entropy contributions, it follows that J does or does not transpose "overfitted" into the final SD in the AMBER or ECEPP ensemble, respectively. This is apparently an effect of softness of the AMBER vs ECEPP force field and its effect on ensemble sampling. A further corollary is that using AMBER ensemble for fitting flexible peptides, J restraints may be omitted with a minute loss in quality of fit. As NOE contributes to structure determinations from NMR in a major way while $^3J_{NC\alpha}$ is less significant [4] this is not a concern and comparisons between equilibria resultant from ECEPP [1] and AMBER are justified. Thus, both methodologies give similar conformational equilibria, in which the restraining rings fit well within 1,31Å for **1** and 1,49Å for **2** (Table 1). Apparent differences seen in Tyr and Phe (Figure 1) arise from conformational freedom of their side chains.

Acknowledgments

This work was supported by Polish Ministry of Science grant DS 8360-4-01330-0. The calculations were carried out in the Academic Computer Centre (TASK) in Gdańsk, Poland.

References

1. Filip, K., et al. *J. Peptide Sci.* **11**, 347-352 (2005).
2. Groth, M., et al. *J. Biomolec. NMR* **15**, 315-330 (1999).
3. Case, D.A., Darden, T.A., Kollman, P.A. *AMBER8 Manual*, University of California, San Francisco; and references therein (2004).
4. Rule, G.S., Hitchens, T.K. *Fundamentals of Protein NMR Spectroscopy*, Springer 2006, Chapter 27.

Proceedings of the 31st European Peptide Symposium
Michal Lebl, Morten Meldal, Knud J. Jensen, Thomas Hoeg-Jensen (Editors)
European Peptide Society, 2010

Understanding and Modulation of the Folding of a Helix-Loop-Helix Dimerization Domain

Michael Beisswenger[1], Sara Pellegrino[2], Roberto Fanelli[2], Nicola Ferri[3], Maria L. Gelmi[2], and Chiara Cabrele[1]

[1]Fakultät für Chemie und Biochemie, Ruhr-Universität Bochum, Bochum, 44801, Germany; [2]DISMAB-Sez. di Chimica Organica, Università degli Studi di Milano, Milan, 20133, Italy; [3]Dip. di Scienze Farmacologiche, Università degli Studi di Milano, 20133, Milan, Italy

Introduction

The helix-loop-helix (HLH) domain is the characteristic dimerization domain of the HLH transcription factors family [1]. This domain triggers the formation of protein dimers that display a parallel four-helix bundle [2]. This type of protein-protein interaction is essential for the biological function of the HLH proteins. For example, the Id proteins are HLH transcription factors that inhibit the action of other HLH factors by sequestering them in inactive heterodimers [3]. By using this mechanism, the Id proteins promote cell proliferation and inhibit cell differentiation during development and tumorigenesis. We are interested in the inhibition of Id protein dimerization with their endogenous partners (i.e. E47 and MyoD). Our work focuses on the identification of the structural prerequisites for the correct HLH folding, as well as of short peptide sequences targeting the Id HLH domain and altering its folding/dimerization properties.

Results and Discussion

Studies based on amino-acid substitutions [4] and backbone modifications [5,6] have underlined the role of some primary-structure elements on the secondary and tertiary structures adopted by a synthetic Id HLH peptide. Side-chain packing and backbone direction are both crucial for the optimal fold. For example, two *O*-acyl-isopeptide analogs of the Id1 HLH domain (residues 66-106) bearing the backbone and side-chain modification at one of the two helix-loop junctions are disordered at pH 4-5, whereas the native Id1 HLH peptide is structured (though less than at pH 7). This indicates that the chemical changes at the junctions destabilize both the tertiary and secondary structures. However, these are fully restored upon conversion of the *O*-acyl-isopeptide analogs into the native peptide at pH 7 [5,6].

Further, we have evaluated the ability of short peptides to interact with the Id1 HLH domain and prepared some peptidic constructs that have been tested on vascular smooth muscle cells expressing the Id1 protein. Two constructs (**2a** and **2b**) based on covalent dimers of the Id1 fragment 91-101 have been shown to be active in the micromolar range, reducing cell growth and migration, stimulating cell differentiation and considerably decreasing the cellular level of the Id1 protein [7] (Figure 1). The covalent linkage is represented by the building block *N*-benzoyl *cis*-3-carboxy-cyclopentylglycine [8] in the

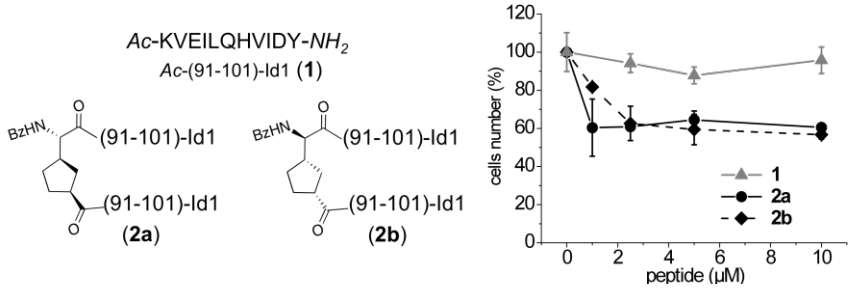

*Fig. 1. Effect on the Id1 fragment 91-101 as monomer (**1**) or covalent dimer (**2a** and 2b) on the proliferation of vascular smooth-muscle cells.*

configuration (1'S, 1S, 3R) in the dimer **2a**, and in the configuration (1'R, 1R, 3S) in the dimer **2b**. The dose-response curves of the two constructs obtained in the cell proliferation assay are comparable, suggesting that the stereochemistry of the linker does not significantly affect the biological activity. Interestingly, the monomeric form of the Id1 fragment 91-101 (**1**) has not decreased cell proliferation in the concentration range, in which its dimeric form has been found to be active (Figure 1). Therefore, converting the short peptide from a monomer to a covalent homodimer has allowed obtaining an active compound, probably due to increased avidity towards its biological target.

Acknowledgments
This work was supported by the DFG (Emmy-Noether Grant CA296), the DAAD-Vigoni and in part by the EU FP6 Grant LSHM-CT-2006-037498.

References

1. Massari, M.E., Murre, C. *Mol. Cell Biol.* **20**, 429-440 (2000).
2. Ma, P.C., Rould, M.A., Weintraub, H., Pabo, C.O. *Cell* **77**, 451-459 (1994).
3. Perk, J., Iavarone, A., Benezra, R. *Nat. Rev. Cancer* **5**, 603-614 (2005).
4. Kiewitz, S.D., Cabrele, C. *Biopolymers (Peptide Sci.)* **80**, 762-774 (2005).
5. Kiewitz, S.D., Kakizawa, T., Kiso, Y., Cabrele, C. *J. Peptide Sci.* **14**, 1209-1215 (2008).
6. Beisswenger, M., Yoshiya, T., Kiso, Y., Cabrele, C. *J. Peptide Sci.* **16**, 303-308 (2010).
7. Pellegrino, S., Ferri, N., Colombo, N., Cremona, E., Corsini, A., Fanelli, R., Gelmi, M.L., Cabrele, C. *Bioorg. Med. Chem. Lett.* **19**, 6298-6302 (2009).
8. Cabrele, C., Clerici, F., Gandolfi, R., Gelmi, M.L., Molinari, F., Pellegrino, S. *Tetrahedron* **62**, 3502-3508 (2006).

Proceedings of the 31st European Peptide Symposium
Michal Lebl, Morten Meldal, Knud J. Jensen, Thomas Hoeg-Jensen (Editors)
European Peptide Society, 2010

2D IR Spectroscopy of Oligopeptides Conformationally Restrained by $C^{\alpha,\alpha}$-Dialkylated Glycyl Residues

Hiroaki Maekawa[1], Matteo De Poli[2], Gema Ballano[2], Fernando Formaggio[2], Claudio Toniolo[2], and Nien-Hui Ge[1]

[1]Department of Chemistry, University of California at Irvine, Irvine, 92697-2025, CA, U.S.A.; [2]ICB, Padova Unit, CNR, Department of Chemistry, University of Padova, Padova, 35131, Italy

Introduction

Recent advances in ultrafast two-dimensional infrared (2D IR) spectroscopy have demonstrated its unique capabilities in elucidating peptide structures. To develop these techniques with full rigor and to establish spectrum-structure relationships, studies of model systems are needed. To this end, oligopeptides composed of $C^{\alpha,\alpha}$-dialkylated Gly residues serve as ideal model systems because of their well-defined peptide backbone conformations. Here, we report the amide-I/II 2D IR spectra of two series of peptides in $CDCl_3$ solution: (1) unlabeled and ($^{13}C{=}O^{18}$-Leu and ^{15}N-Gly) isotope labeled Aib-rich hexapeptides, Z-Aib-L-Leu-$(Aib)_2$-Gly-Aib-O*t*Bu (Z, benzyloxycarbonyl; Aib, α–aminoisobutyric acid; O*t*Bu: *tert*-butoxy) and (2) Ac-$(Deg)_n$-O*t*Bu (Ac, acetyl; Deg, $C^{\alpha,\alpha}$-diethylglycine, n = 2–5). We demonstrate how 2D IR spectral signatures reveal the underlying 3_{10}-helical conformation [1] in peptides (1) and fully-extended (multiple C_5) conformation [2] in peptides (2).

Results and Discussion

In the study of Aib-rich hexapeptides, a novel isotope labeling scheme was devised to probe vibrational couplings between amide-I and -II modes on specific residues. The 2D IR spectra of $^{13}C{=}O^{18}$-Leu mono-labeled and $^{13}C{=}O^{18}$-Leu/^{15}N-Gly bis-labeled isotopologues (Figure 1) exhibit isotope-dependent amide-I/II cross peaks, clearly indicating that the second and fourth peptide linkages are vibrationally coupled as they are in proximity, forming a 3_{10}-helical turn. Theoretical calculations, based on an expanded vibrational exciton model, reasonably reproduce the experimental results. In contrast, the *semi*-extended, poly-$(Pro)_n$ type II-like structure is predicted to exhibit no isotope shifts in the amide-I/II cross peaks. This conformational sensitivity indicates that 2D IR is promising for detecting nascent helix formation.

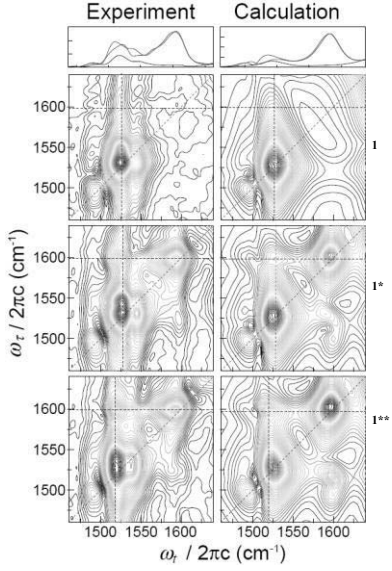

Fig. 1. Amide-I/II region of the experimental and calculated 2D IR spectra of unlabeled (1), $^{13}C{=}O^{18}$-Leu mono-labeled (1) and $^{13}C{=}O^{18}$-Leu/^{15}N-Gly bis-labeled (1**) hexapeptides. The ^{15}N substitution red-shifts the amide I/II cross peaks.*

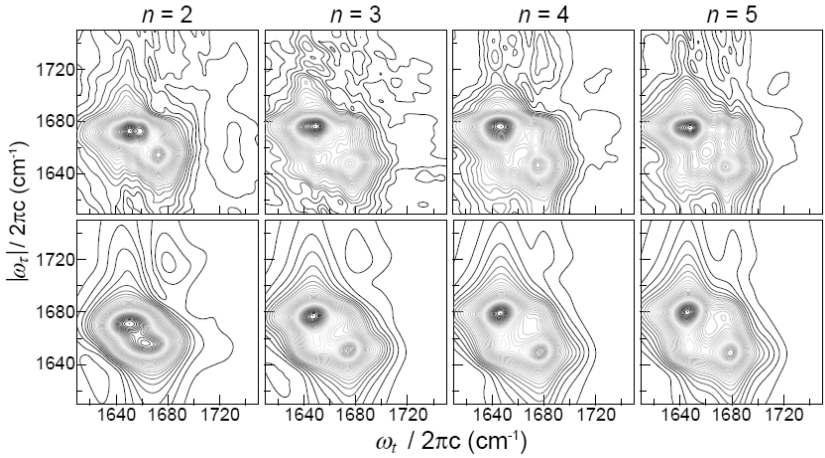

Fig. 2. Amide-I region of the 2D IR spectra acquired for Ac-(Deg)$_n$-OtBu, with n=2-5, showing the characteristic pattern of the fully-extended conformation.

The Deg homo-peptides exhibit unusual spectroscopic features: the amide-II band is more intense than the amide-I band and it red shifts with increasing main-chain length. We have performed detailed analysis of the peptide conformation through stringent comparisons of measured and simulated amide-I and -II 2D IR spectra (Figure 2). The results indicate that the backbones of these homo-peptides are fully extended regardless of their main-chain length. This conclusion is corroborated by molecular dynamics simulations and density functional theory calculations. The complete characterization of the vibrational properties of the amide-I and II modes in the fully-extended structure will facilitate the conformational analysis of other peptides involving C_5 motifs.

Acknowledgments
This research was supported by grants from the American Chemical Society Petroleum Research Fund (39148-G6) and the National Science Foundation (CHE-0450045, CHE-0802913, and DMS-0835863) to N.-H. G.

References

1. Toniolo, C., Benedetti, E. *Trends Biochem. Sci.* **16**, 350-353 (1991).
2. Toniolo, C., Crisma, M., Formaggio, F., Peggion, C., Broxterman, Q.B., Kaptein, B. *Biopolymers (Pept. Sci.)* **76**, 162-176 (2004).

Proceedings of the 31st European Peptide Symposium
Michal Lebl, Morten Meldal, Knud J. Jensen, Thomas Hoeg-Jensen (Editors)
European Peptide Society, 2010

In Vitro Antiviral Properties of Alloferon, *Any*-GS and Their Analogues against *Human Herpes Virus* and Coxsackie B2 Virus

Mariola Kuczer[1], Anna Midak-Siewirska[2], Renata Zahorska[2], Mirosław Łuczak[2], and Danuta Konopińska[1]
[1]*Faculty of Chemistry, University of Wroclaw, Wroclaw, Poland; e-mail: km@wchuwr.pl*
[2]*Department of Microbiology, Medical University of Warsaw, Warsaw, Poland*

Introduction

The present study was carried out to search for new antiviral activity among selected peptides originating from the insect such as alloferon (HGVSGHGQHGVHG), yamamarin (DILRGa) (*Any*-GS) and series of their analogues.

Alloferon has been isolated from the blow fly *Calliphora vicina* [1]. *In vitro* alloferon stimulates natural killer lymphocytes and *in vivo* this peptide has antiviral and antitumor capabilities. Pentapeptide *Any*-GS has been isolated from the wild silkmoth *Antheraea yamamai* [2]. This peptide suppresses the proliferation of the rat hepatoma cells [3]. In preliminary investigations we found that alloferon and *Any*-GS inhibit the replication of *Human Herpes Virus* type 1 (HHV-1) [4]. Continuing our studies on these peptides we performed a further search for their other antiviral activity.

We obtained the following peptides: 1/ alloferon and its analogues modified at position 1 of the peptide chain - HGVSGHGQHGVHG (I), AGVSGHGQHGVHG (II), KGVSGHGQHGVHG (III), RGVSGHGQHGVHG (IV); 2/ *Any-GS* and its shortened derivatives - DILRGa (V), ILRGNa (VI), DILRa (VII), DILa (VIII); 3/ analogues of *Any-GS* modified at position 1 of the peptide chain - RILRGa (IX), QILRGa (X), GILRGa (XI), KILRGa (XII), AILRGa (XIII).

Peptides I-IV were synthesized by the classical solid phase method according to the Fmoc-procedure. Other peptides (V-XIII) were synthesized by classical solid-phase method according to the Boc-procedure. All peptides were purified by preparative HPLC. Peptides were tested *in vitro* for the antiviral activity in respect to DNA (*Human Herpes Virus* type 1 and wild-type HHV), and RNA viruses (971 PT Coxsackie type B2 and wild-type Coxsackie type B2) and cytotoxic activity using a Vero and HEp-2 cell lines. The herpesviruses were propagated in Vero or HEp-2 cells. The coxsackieviruses were propagated in HEp-2 cells. Antiviral and cytotoxic activities were assessed *in vitro* according to [4]. Antiviral activity of tested peptides was finally expressed as the compound concentration that reduces virus yield by 50% (IC_{50}).

Results and Discussion

Microscopic observations showed that no changes occurred in Vero and HEp-2 cells growth or morphology in the presence of tested peptides. The MTT assay also proved that they had no effect on cell proliferation. The antiviral bioassay showed that most of investigated peptides inhibit in vitro the replication of viruses in Vero or HEp-2 cells (Table 1). We found that alloferon inhibits the replication of viruses HHV-1MC and wild-type HHV-1 in Vero cells with IC_{50} values 305.50 μg/ml and 479.00 μg/ml, respectively. Among analogues of alloferon, only [Lys^1]-alloferon (III) was very active against herpesviruses in Vero cells (IC_{50}=147.09 μg/ml and 4.95 μg/ml) and coxackieviruses in HEp-2 cells (IC50=74.0 μg/ml and 107.04 μg/ml). *Any*-GS (V) inhibits also the replication of HHV-1MC and wild-type HHV-1 in Vero cells. The IC_{50} values were 235.30 μg/ml and 216.6 μg/ml respectively. A similar activity was observed for four peptides X-XIII. However, [Arg^1]-*Any*-GS (IX) was very active against HHV-1MC and wild-type HHV-1 in Vero cells. Moreover, the shortened derivatives (peptides VI and VIII) were very active only against the wild-type HHV-1. During the investigation of the influence of *Any*-GS and its derivatives on the replication of viruses in HEp-2 cells, we found that [Gly^1]-*Any*-GS (XI) was very active against HHV-1MC, wild-type HHV-1, 971 PT Coxsackie and wild-type Coxsackie B2 with IC_{50} values 191.62 μg/ml, 102.76 μg/ml, 197.92 μg/ml and 158.92 μg/ml, respectively. A similar activity was observed for peptides VII and XIII. However, these peptides show a weak inhibitory effect on the replication of HHV-1MC and Coxsackie B2.

Table 1. Antiviral activity of alloferon, Any-GS and their analogues (IC_{50}[μg/ml])

Peptides	*Vero cells*		*HEp-2 cells*			
	HHV-1_{MC}	wild-type HHV-1	HHV-1_{MC}	wild-type HHV-1	*971 PT CVB2*	*wild-type CVB2*
alloferon (I)	305.00	479.00	*	*	*	*
[Ala^1]-alloferon (II)	#	#	#	#	#	#
[Lys^1]-alloferon (III)	147.09	4.95	241.90	230,00	107.04	74,00
[Arg^1]-alloferon (IV)	321.10	928.2	#	#	629.33	#
Any-GS (V)	235.30	216.60	*	*	*	*
[2-5]-*Any*-GS (VI)	469.37	187.17	315.07	166.08	199.45	128.91
[1-4]-*Any*-GS (VII)	235.50	371.00	*	*	*	*
[1-3]-*Any*-GS (VIII)	283.78	198.96	521.66	*	342.03	232.10
[Arg^1]-*Any*-GS (IX)	176.65	58.56	277.40	222.40	217.98	121.08
[Gln^1]-*Any*-GS (X)	238.95	220.42	214.98	148.45	429.58	346.98
[Gly^1]-*Any*-GS (XI)	410.94	213.64	191.62	102.76	197.92	158.92
[Lys^1]-*Any*-GS (XII)	281.56	409.59	417.52	659.55	275.45	206.93
[Ala^1]-*Any*-GS (XIII)	409.47	310.57	90.88	179.97	287.20	138.56

** not determined, # without effect*

Moreover, peptides IX was very active only against 971 PT Coxsackie (IC_{50} = 121.08 μg/ml) but peptide X was active against wild-type HHV-1 (IC_{50} = 148.45 μg/ml).

Our results indicate that the antiviral activity of tested peptides depends upon the virus and cell line used. Further studies are planned to elucidate the antiviral mechanism of tested peptides in different cell-virus models.

Acknowledgments

This work was supported by the Polish Ministry of Science and Higher Education (Grant No. N N204 085638), the University of Wroclaw (Grant No. 2237/W/WCh/09) and by the Medical University of Warsaw grants AM20/W1 and W2/2008–2009.

References

1. Chernysh, S., Kim, S.I., Bekker, G., Pleskach, V.A., Filatova, N.A., Anikin, V.B., Platonov, V.G., Bulet, P. *PNAS* **99**, 12628-12632 (2002).
2. Suzuki, K., Minagawa, T., Minakawa, T., Kumagai, T., Naya, S., Endo, Y., Osanai, M., Kuwano, E. *J. Insect Physiol.* **36,** 855-860 (1990).
3. Yang, P., Abe, S. Zhao, Y., An, Y., Suzuki, K. *J. Insect Biotech. Sericology* **73**, 7-13 (2004).
4. Kuczer, M., Dziubasi, K., Midak-Siewirska, A., Zahorska, R., Łuczak, M., Konopińska, D. *J. Pept. Sci.* **16**, 186-92 (2010).

Proceedings of the 31st European Peptide Symposium
Michal Lebl, Morten Meldal, Knud J. Jensen, Thomas Hoeg-Jensen (Editors)
European Peptide Society, 2010

Novel Calpain Inhibitors

Zoltán Bánóczi[1], Levente E. Dókus[1], Ágnes Tantos[2], Attila Farkas[2], Péter Tompa[2], Péter Friedrich[2], and Ferenc Hudecz[1,3]

[1]Research Group of Peptide Chemistry, Eötvös L. University Hungarian Academy of Sciences, Budapest, Hungary; [2]Institute of Enzymology, Biological Research Center, Hungarian Academic of Sciences, Budapest, Hungary; [3]Department of Organic Chemistry, Eötvös L. University, Budapest 112 POB 32, H-1518, Hungary

Introduction

Calpains are intracellular cysteine proteases and are of considerable interest due to their implication in numerous physiological events. Besides physiological functions, they play a key role in some well-studied pathological processes. The overactivation of calpains, which results in the disorder in Ca^{2+} homeostasis, increases the degradation of the enzyme substrates and could contribute to the development of the Alzheimer and/or Huntington diseases and also to death of nervous cells caused by traumatic brain injury, spinal cord injury [1].

One of the main methods to study the calpain function is to inhibit the enzyme. Unfortunately, there is only one specific calpain inhibitor of native origin known, the calpastatin protein. Other inhibitors, mentioned in the literature, are not specific. Use of these inhibitors might confuse the interpretation of the results [2]. The use of calpastatin or its region B as specific inhibitors, is compromised by limited cell-penetration. The calpain inhibition may be important not only in the functional studies, but also in blocking of calpain overactivation in different diseases. These claims require more selective inhibitors, and trigger intensive research in this field.

Results and Discussion

Our aim is to develop new, specific and cell-permeable calpain inhibitor(s), to be used for analysis of calpain function under different conditions and also for the development of drugs to treat different calpain dependent diseases. For this, our plan was to synthesize azapeptide inhibitors based on the calpain substrate (TPLKSPPPSPR) described by us [3]. In these new inhibitors, the Lys residue after which the calpain cleaves the substrate was replaced by azaglycine (aGly) moiety. Besides this azapeptide, which is similar to the substrate sequence (TPLaGlySPPPSPR), shorter peptides were prepared (TPLaGlySPPPS and TPLaGlySP) to study the role of the amino acids at the *C*-terminal in inhibition. For examining the importance of amino acids in the position P_2 and P_3 aGlySPPPS, TPVaGlySPPPS, TPTaGlySPPPS, TSLaGlySPPPS and TWLaGlySPPPS azapeptides were synthesized based on the preference matrix [3]. The azapeptides containing aGly were produced by solid phase peptide synthesis on MBHA resin using Boc/Bzl strategy (Figure 1). The azaglycine moiety was incorporated with the reaction of 1,1'-carbonyldiimidazole (CDI) and Boc-hydrazide. The cleaved peptides were purified by RP-HPLC and were characterized by analytical RP-HPLC and ESI-MS (Table 1).

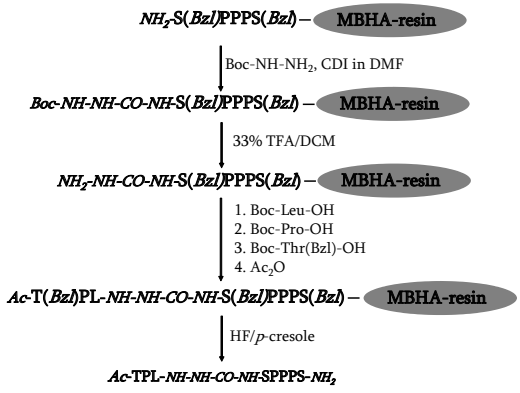

Fig. 1. Outline of a typical synthesis of azapeptide inhibitors.

The inhibitory effect of peptides was determined in calpain buffer (10 mM HEPES, 150 mM NaCl, 1 mM EDTA, 5 mM benzamidine, 0.5 mM phenylmethylsulfonyl fluoride, 10 mM β-mercaptoethanol, pH

Table 1. Characteristics, K_i and IC_{50} values of azapeptides

Compound	R_t *(min)*[a]	*MS [M]*[b]		K_i (μM)	IC_{50} (μM)
		calc.	*meas.*		
Ac-TPLaGlySP-NH_2	18.3	612.3	612.4	-	-
Ac-TPLaGlySPPPS-NH_2	18.8	893.5	893.5	8.7	8.5
H-TPLaGlySPPPSPR-NH_2	18.0	1104.6	1104.6	20.3	n.d.
Ac-TPVaGlySPPPS-NH_2	19.0	879.4	879.8	-	-
Ac-TPTaGlySPPPS-NH_2	17.4	881.4	881.5	-	-
Ac-TSLaGlySPPPS-NH_2	20.0	883.4	883.7	3.5	9.5
Ac-TWLaGlySPPPS-NH_2	27.1	982.4	982.5	5.8	9.8
Ac-aGlySPPPS-NH_2	12.6	582.3	582.3	-	-

[a] *Column:Phenomenex Jupiter C18, 250 x 4.6 mm, 5 μm, 300Å; Gradient:0 min-0%, 5 min 0%, 50 min 90%B, eluents 0.1% TFA/H_2O (A), 0.1% TFA /acetonitrile-water(80:20, v/v) (B); flow rate: 1 ml/min, $\lambda_{det.}$=220 nm;* [b] *ESI-MS*

7.5) contained 5 mM substrate, various inhibitor concentrations (10-100 μM) and 3 mM $CaCl_2$. The enzyme concentrations used were 0.2 μM m-calpain. Data were analyzed by the MicroCal Origin data analysis software to determine the initial slope of fluorescence change. First, all peptides were studied at 100 μM concentration. Peptides showing inhibition were examined at lower concentration and the K_i and IC_{50} values were determined (Table 1).

Four peptides, *Ac*-TPLaGlySPPPS-NH_2, *H*-TPLaGlySPPPSPR-NH_2, *Ac*-TSLaGlySPPPS-NH_2 and *Ac*-TWLaGlySPPPS-NH_2, inhibited the m-calpain at 100 μM concentration. The short peptides; *Ac*-aGlySPPPS-NH_2 and *Ac*-TPLaGlySP-NH_2, had no inhibitory effect. It seems that a number of amino acid residues at the *C*- and *N*-terminal are necessary for the inhibition. The data show that the Leu residue is highly important; the derivatives with other amino acid tested in the P_2 position did not exhibit inhibition. Contrarily, the amino acid in position P_3 might have no influence on the inhibitory activity, although only the best three amino acids in the preference matrix [3] were tested.

In summary, new and effective azapeptide based calpain inhibitors were prepared and characterized. It turned out that the presence of amino acid residues at the *C*- and *N*-terminal could increase the inhibition, and also that the Leu residue in the P_2 position is important.

Acknowledgments
This study was supported by grants: OTKA K-68285 and GVOP-3.2.1-2004-04-0352/3.0. Bánóczi, Z. acknowledges the support of Bolyai János Scholarship.

References
1. Huang, Y., Wang, K.K.W. *Trends Mol. Med*. **7**, 355-362 (2001).
2. Wells, G.J., Bihovsky, R. *Exp. Opin. Ther. Patents* **8**, 1707-1727 (1998).
3. Tompa, P., et al. *J. Biol. Chem.* **279**, 20775-20785 (2004).

Proceedings of the 31st European Peptide Symposium
Michal Lebl, Morten Meldal, Knud J. Jensen, Thomas Hoeg-Jensen (Editors)
European Peptide Society, 2010

PNA-Peptide Conjugates for Regulation of DNA and RNA G-Quadruplex Structures Depending on a Particular Protease Concentration

Kenji Usui[1,2], Keita Kobayashi[1], and Naoki Sugimoto[1,2]
[1]Faculty of Frontiers of Innovative Research in Science and Technology (FIRST), Konan University; [2]Frontier Institute for Biomolecular Engineering Research (FIBER), Konan University, Kobe, 6500047, Japan

Introduction

It has been elucidated in the last few decades that some DNA and RNA secondary structures modulate a variety of cellular events. It is recently suggested that a G-quadruplex structure, which is one of the secondary structures, also regulates cellular events such as transcription, translation, pre-RNA splicing and telomerase elongation, and these events are related to serious diseases and aging [1,2]. Therefore, systems that could control DNA and RNA G-quadruplex structures when needed, would be able to modulate various cellular events, and as a result the systems could provide biological effects. Although many G-quadruplex-targeting ligands including phthalocyanine derivatives [3] were proposed so far, next generation ligands should have more specificity to a particular G-quadruplex and more functionality including switching, cellular penetrating and organelle-targeting. From this point of view, we attempted to construct a system using alternative small molecules to regulate G-quadruplex structures with an on-off switching module depending on cellular environments.

Results and Discussion

First of all, the small molecule (Lmyc) was designed (Figure 1). The molecules consisted of two parts. One part was composed of guanine PNA-rich sequences to induce G-rich DNA/RNA sequences to form G-quadruplex structures with the PNAs. PNAs have some advantages not only that PNAs have enzyme resistance but also that functions such as cell-penetrating or switching can be introduced. In this study, a switching module depending on a particular cellular environment was adopted into the other part and we selected a particular protease concentration as the cellular environment. Therefore, this system would induce DNA/RNA to form G-quadruplex structure when the protease would not be expressed in cells, and once expressing the protease, these conjugates would be digested and simultaneously loose the induction ability resulting in collapse of a DNA-PNA quadruplex structure (Figure 2). Calpain I, which is related with serious diseases such as Dystrophia and Alzheimer's disease, was chosen as a model particular protease. Thus a calpain I substrate sequence was put into the center of the small molecule as the switching module.

After synthesis of the peptides by Fmoc chemistry [4], we checked the G-quadruplex structure induction by far-UV CD spectroscopy using a model DNA sequence halfTG (Figure 1), which was a part of c-Myc promoter. The DNA with the PNA peptide showed a similar spectrum including a positive maximum in ellipticities at 260 nm to other PNA-DNA parallel G-quadruplexes as previously described [5]. CD melting curves of the target DNA with/without the conjugate showed that *T*m of the PNA-DNA structure at 260 nm was ca. 10 ºC higher than that of the DNA alone. This implied that a G-rich DNA could be induced to form PNA-DNA G-quadruplex by the PNA peptide.

Also we attempted to demonstrate the switch function depending on the protease

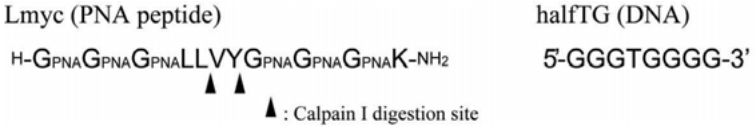

Fig. 1. Sequences of the PNA peptide and the target DNA.

concentration. We at first checked by HPLC and MS whether calpain I could digest the Lmyc smoothly. Then digestion experiments using the DNA-PNA quadruplex were conducted. It was found that *T*m of the DNA with digested peptides by calpain I was almost equal to that of DNA alone. This implied that quadruplex structure of halfTG and Lmyc is destabilized by calpain I.

With more improvement of binding-specificity and adding other functions such as cellular penetrating, this system may lead to controls of the DNA and/or RNA events including RNA expression. Throughout this study, these PNA-peptide conjugates would be one of the promising tools for regulation of important cellular events toward cell engineering and tissue engineering.

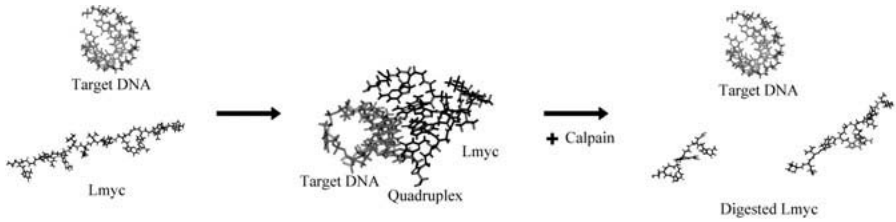

Fig. 2. Outline drawing of the switching system for regulation of G-quadruplex structure using Lmyc.

Acknowledgments

This study was in part supported by the Grants-in-Aid for Scientific Research, the "Core research" project (2009-2014) from the Ministry of Education, Culture, Sports, Science and Technology (MEXT). K. U. is grateful to Grant-in-Aid for Research Activity Start-up from MEXT.

References

1. Miyoshi, D., Matsumura, S., Nakano, S., Sugimoto, N. *J. Am. Chem. Soc.* **126**, 165-169 (2003).
2. Yu, H.Q., Miyoshi, D., Sugimoto, N. *J. Am. Chem. Soc.* **128**, 15461-15468 (2006).
3. Yaku, H., Murashima, T., Miyoshi, D., Sugimoto, N. *Chem. Commun.* **46**, 5740-5742 (2010).
4. Sano, S., Tomizaki, K.-Y., Usui, K., Mihara, H. *Bioorg. Med. Chem. Lett.* **16**, 503-506 (2006).
5. Roy, S., Tanious, F.A., Wilson, W.D. Ly, D.H. Armitage, B.A. *Biochemistry* **46**, 10433-10443 (2007).

Proceedings of the 31st European Peptide Symposium
Michal Lebl, Morten Meldal, Knud J. Jensen, Thomas Hoeg-Jensen (Editors)
European Peptide Society, 2010

Structure of a New Stable Cu(III)/Cyclopeptide Complex by Cu K-Edge XAS Study

Alessandro Pratesi[1,2*], Gabriele Giuli[3], Maria Rita Cicconi[3], Tsu-Chien Weng[4], Giovanni Pratesi[5], and Mauro Ginanneschi[1,2]

[1]Laboratory of Peptide & Protein Chemistry & Biology, Polo Scientifico e Tecnologico, University of Florence, Italy ;[2]Department of Chemistry "Ugo Schiff", University of Florence, 50019, Sesto Fiorentino, Italy; [3]Dipartimento di Scienze della Terra, University of Camerino, 62032, Camerino, Italy; [4]European Synchrotron Radiation Facility - ESRF, F-38043, Grenoble, France; [5]Dipartimento di Scienze della Terra, University of Florence, 50121, Florence, Italy; [*]alessandro.pratesi@unifi.it

Introduction

Cyclic peptides are important tools in medicinal chemistry, as their constrained geometry allows conformational investigations for structure-activity relationship studies in the characterization of the active site of proteins. Cyclopeptides are useful versatile scaffolds, as they can be used for conformational investigations in the search of epitope/pharmacophore models, or metals coordinating ligands. Some cyclic tetrapeptides, containing the sequence Xaa-His-Yaa-His mimicking metalloprotein binding sites, have been synthesized by using a rapid and flexible method based on pseudodiluition SPPS. Cyclic tetrapeptides *cyclo*(Lys-His-βAla-His) (LK13), *cyclo*(Lys-DHis-βAla-His) (DK13) and *cyclo*(Gly-βAla-Gly-Lys) (GK13) have been prepared using SPPS. When the copper(II) coordination compounds of DK13 in aqueous solution were investigated, it was noticed that, differently from the preceding ligands, the equilibrium mixture at alkaline pH gave an absorption band in the near UV range and showed a red-orange color. Complete spectroscopic analysis (UV, NMR, MS, EPR) and electrochemical experiments demonstrated that, at alkaline pH, stable coordinated copper(III) species were formed, probably by dioxygen action on the added Cu(II) ions [1]. In order to confirm the presence of Cu^{3+} species and to clarify the role of peptide structure in the mechanism of the copper oxidation, Cu K-edge XANES and EXAFS spectra have been collected for three different cyclo-peptides.

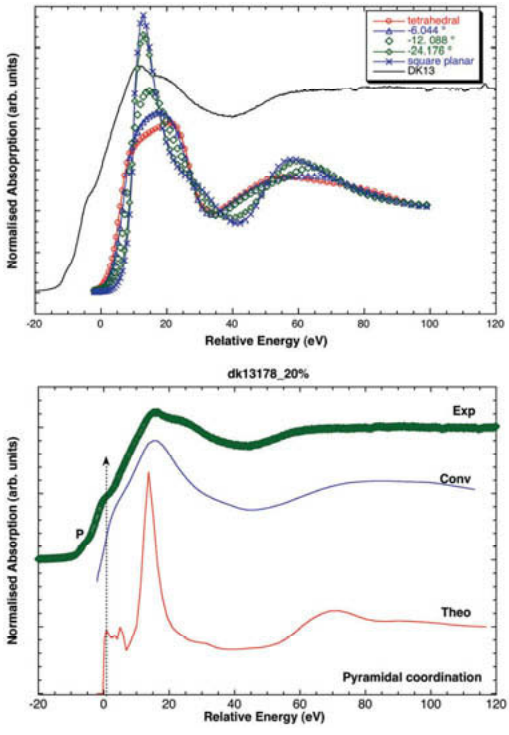

Fig. 1. Theoretical XANES curves.

Results and Discussion

X-Ray Absorption Spectroscopy (XAS) data have been collected at the ID26 beamline of the ESRF storage ring (Grenoble, F). Cu K-edge XANES and EXAFS step scan spectra were acquired in fluorescence mode, monitoring the emitted fluorescence signal with a high-purity multi-element Ge detector. Radiation was monochromatised by means of a double-crystal Si(311) monochromator to achieve high-energy resolution at the Cu K-edge. In order to reduce radiation induced damage of the peptide samples, spectra have been collected at 10 K in a He cryostat, and the intensity of the incident radiation at the sample has been adjusted by means of Al filters.

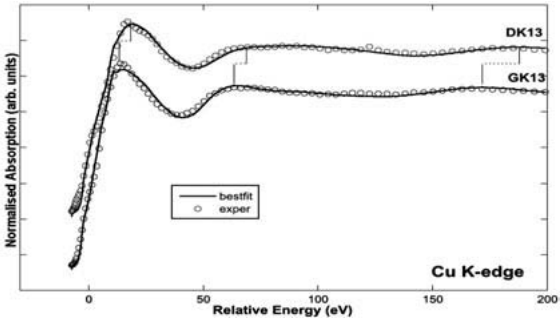

Fig. 2. Structural refinements.

Preliminary time scans allowed to ascertain that the samples suffered no damage within 1300 seconds exposure to the X-ray beam. For each sample 1000 seconds long spectra have been acquired at different sample positions in order not to alter the sample. Average of 10 scans allowed to obtain a good signal to noise ratio for all the samples.

Comparison of pre-edge peak features with those of Cu model compounds, allowed to determine the Cu oxidation state in the three peptides: Cu is purely divalent in GK13, purely trivalent in DK13 and present as both Cu^{2+} and Cu^{3+} in LK13. Also edge energies and EXAFS derived Cu-N distances (1.79 Å and 1.90 Å for DK13 and GK13, respectively) are consistent with the XANES determined Cu oxidation states. Theoretical XANES spectra have been calculated by means of the MXAN code. The initial structural model has been calculated according to a DFT code; the structural refinement with the MXAN code allowed finding optimised values of the overlap between Muffin-Tin spheres; to refine the coordinates of the neighbouring N atoms and refine the coordinates of all other atoms. The good agreement between theoretical and experimental XANES data (Figure 1) allows to assume that the refined structure, at least in the first coordination shell around Cu, is a good approximation of the peptide/Cu^{3+} complex structure. These results suggest that the CuN_4 unit is not planar but form a slightly distorted pyramid [2]. Figure 2 shows the experimental XANES curves for DK13 and GK13, compared with those obtained after the structural refinements (solid lines). The simulations obtained with the proposed structures are in good agreement with the experimental ones. Figure 3 depicts the proposed models for the peptide complexes DK13/Cu^{3+} and GK13/Cu^{2+}. The DK13/Cu^{3+} shows a slight variation from square planar geometry, with Cu out of the plane, that justifies the loss of centrosymmetry and causes the high absorbance in the pre-peak zone, due to a strong ^1s-^3d transition.

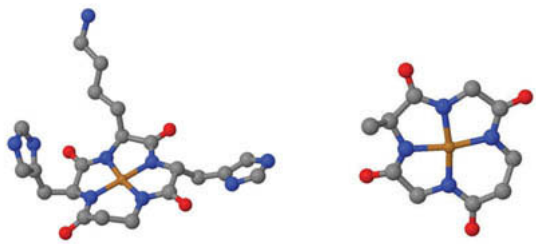

Fig. 3. Proposed models for DK13/Cu^{3+} and GK13/Cu^{2+}.

Even though no clear explanation can be provided yet, available data strongly suggest that imidazole side chains have an important role in the formation of the final Cu^{3+} complex in DK13 peptide.

Acknowledgments
This work was supported by Ente Cassa di Risparmio di Firenze and MIUR funds (Prin 2005).

References

1. Pratesi, A., Zanello, P., Giorgi, G., Messori, L., Laschi, F., Casini, A., Corsini, M., Gabbiani, C., Orfei, M., Rosani, C., Ginanneschi, M. *Inorg. Chem.* **46**, 10038-10040 (2007).
2. Pratesi, A., Giuli, G., Cicconi, M.R., Weng, T.C., Pratesi, G., Ginanneschi, M. *14th International Conference on X-ray Absorption Fine Structure*, p. 239, Camerino (Italy), July 26-31 (2009).

Proceedings of the 31st European Peptide Symposium
Michal Lebl, Morten Meldal, Knud J. Jensen, Thomas Hoeg-Jensen (Editors)
European Peptide Society, 2010

Stability of CLIPS Peptides in Human Serum

Wim Schaaper, Peter van Dijken, and Peter Timmerman
Pepscan Therapeutics B.V., Zuidersluisweg 2, 8243RC, Lelystad, The Netherlands

Introduction

Small peptides generally do not express high biological activity due to their flexible random structure. Many methods have been developed to introduce a more rigid conformation. Our proprietary CLIPS™ technology [1,2] (**C**hemical **LI**nkage of **P**eptides onto **S**caffolds) was used to develop a bicyclic enzyme inhibitor specific for human plasma kallikrein [3]. This CLIPS peptide (S905/T3, IC_{50} = 1.7 nM) was > 5000-fold more active than the linear peptide. Here, we present the results of an enzyme degradation study in human serum of the bicyclic S905/T3 peptide. We also tested both monocyclic loops, either as CLIPS construct, as cyclic disulfide, or as the Cys-blocked linear analogue. Furthermore, the bicyclic retro-inverso peptide, based on D-amino acids and inversed sequence, was also tested.

The CLIPS peptides, especially the bicyclic products, were found to be superior in stability against enzymatic degradation compared to their linear analogues.

Results and Discussion

Four peptides (S905: ACSDRFRNCPADEALCG-amide, S906: ACSDRFRNC, S907: CPADEALCG-amide, and P431: Gclaedapcnrfrdsca-amide) were synthesized using Fmoc chemistry and purified using preparative RP-HPLC. The peptides were modified by one of the following routes: a) cyclisation by overnight air oxidation at pH 8 (for S906 and S907), b) blocking of the free cysteines by reaction with iodoacetamide at pH 8 for 2 hours (all peptides), c) CLIPS reaction (Figure 1) by reaction with 1,3,5-tris(bromomethyl)benzene (for S905 and P431) or with α,α'-dibromo-m-xylene (for S906 and S907) in 0.02M ammonium bicarbonate/acetonitrile for 1 hour. All products were purified using preparative RP-HPLC to yield a final purity of >95%.

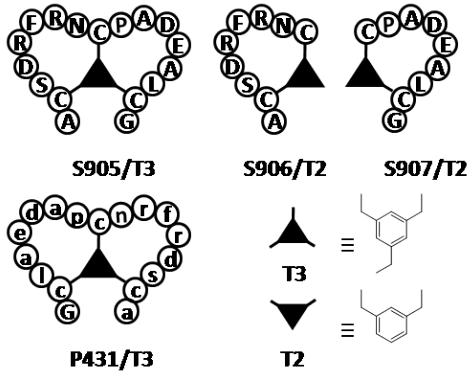

Fig. 1. CLIPS constructs: S905/T3: bicyclic T3, S906/T2, cyclic N-terminal T2, S907/T2: cyclic C-terminal T2, P431/T3: bicyclic retro-inverso T3.

In the stability study, the CLIPS peptides (Figure 1) and their linear counterparts in which the cysteines were blocked with iodoacetamide were dissolved in PBS, pH 7.2 [4] at a concentration of 2 mg/mL. This solution was mixed with human serum (Sigma) 1:1 (v/v) or, as reference samples, with PBS 1:1 (v/v) to a final concentration of 1 mg/mL. All samples were stored at 37°C and 50 µL samples were taken at several time intervals for analysis. These samples were mixed with 50 µL of 10% TFA/water. Precipitated proteins in the serum samples were separated by centrifugation.

Stability of bicyclic T3 constructs: in S905/T3 the N-terminal Ala, which was outside the ring structure, was slowly cleaved in serum ($t_{½}$ = 113 hr), however, the ring structure itself was far more stable ($t_{½}$ = 240 hr). Ring cleavage occurred slowly at the carboxyl group of Arg-7 and at the amino group of Asp-12. Finally, after 1060 hours, most of the peptide was digested to yield Cys_3/T3. The linear Cys-blocked peptide was digested very rapidly ($t_{½}$ = 0.9 hr).

As expected, the retro-inverso peptides were extremely resistant against enzymatic degradation, since they are composed of D-amino acids. Nevertheless, the T3 CLIPS construct (P431/T3), is even more stable ($t_{½}$ = 5165 hr) than the linear Cys-blocked product ($t_{½}$ = 2174 hr). For the retro-inverso products no specific degradation products could be identified by LC-MS within 1060 hours.

Table 1. Half lives of the tested peptide constructs in human serum

product	*half life ($t_{1/2}$ in hours)*			
	CLIPS-T3	*CLIPS-T2*	*linear*	*Cyclic SS*
S905	113/240*	-	0.9	-
S907	-	9.6	0.5	12.4
S906	-	1.9	0.5	1.2
P431	5165	-	2174	-

** half-life of the des-Ala-1 peptide*

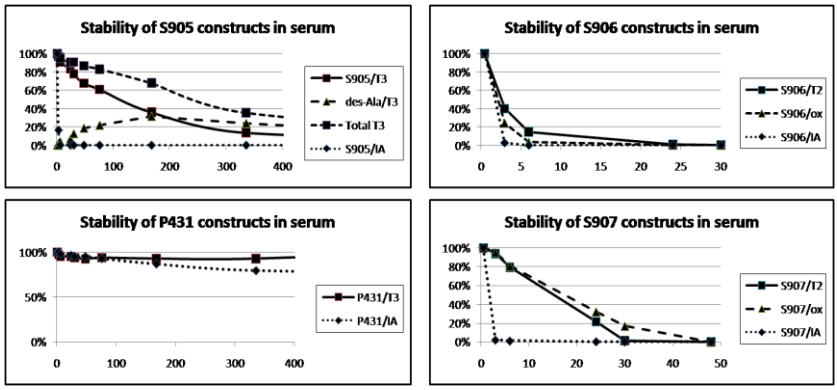

Fig. 2. Concentration of T3 (left) and T2 (right) CLIPS constructs, compared to their linear, Cys-blocked counterparts in human serum in time. Starting concentration was 1 mg/mL in 50% human serum/PBS, time in hours.

Stability of cyclic T2 constructs (Table 1, Figure 2*):* in S906/T2, the N-terminal Ala, which was outside the ring, again was the first to be cleaved ($t_{½}$ = 1.9 hr). However, shortly after, the ring was opened at Arg-7 and this resulted after 168 hours in an almost complete digestion to Cys_2/T2. The disulfide loop S906/ox was digested somewhat faster ($t_{½}$ = 1.2 hr) and the linear Cys-blocked peptide almost completely disappeared within 6 hours ($t_{½}$ = 0.5 hr).

In S907/T2 and S907/ox, the ring was preferentially cleaved at Ala-3, and both products could not be detected anymore at 48 hours ($t_{½}$ = 9.6 resp. 12.4 hr). For the T2 construct again Cys_2/T2 was the final product. From the linear Cys-blocked peptide, only 3% was left after 3 hours ($t_{½}$ = 0.5 hr). An intramolecular cyclization reaction of the N-terminal S-carbamoylmethyl-cysteine [5] in this peptide generated a more enzyme-resistant product which could be identified by LC-MS up to 24 hrs.

The CLIPS technology was developed in order to constrain a variety of peptides in a "loop-like" conformation that adequately mimics β-turns, hairpins or β-sheets. Here we showed that the CLIPS technology is also very effective in stabilizing peptides against enzymatic degradation. The T3 scaffold, which forms bicyclic peptides, is superior in generating stability in human serum, even in retro-inverso peptides. The T2 scaffold peptides show similar stability as cyclic disulfide peptides, but are more stable than their linear analogues. After ring opening, the CLIPS constructs are ultimately digested to Cys_3/T3 or Cys_2/T2.

References

1. Timmerman, P., Beld, J., Puijk, W.C., Meloen, R.H. *ChemBioChem* **6**, 821-824 (2005).
2. Timmerman, P., Puijk, W.C., et al. *Open Vacc. J.* **2**, 56-67 (2009).
3. Heinis, C., Rutherford, T., Freund, S., Winter, G. *Nat. Chem. Biol.* **5**, 502-507 (2009).
4. Tugyi, R., Uray, K., Ivan, D., Fellinger, E., Perkins, A., Hudecz, F. *PNAS* **102**, 413-418 (2005).
5. Geoghegan, K.F., Hoth, L.R., Tan, D.H., Borzilleri, K.A., Withka, J.M., Boyd, J.G., *J. Proteome Res.* **1**, 181-187 (2002).

Proceedings of the 31st European Peptide Symposium
Michal Lebl, Morten Meldal, Knud J. Jensen, Thomas Hoeg-Jensen (Editors)
European Peptide Society, 2010

Tryptophan Interactions that Stabilize Folding Motifs: A Guide to Placement, Dynamics Applications, and Optimizing Fold Stabilization

Irene Shu, Michele Scian, Brandon L. Kier, D. Victoria Williams, and Niels H. Andersen
Department of Chemistry, University of Washington, Seattle, WA, 98195, U.S.A.

Introduction

Trp/Trp interactions in proteins have been observed by CD since at least 1994 [1], with an exciton couplet centered at 222 nm. The melting of such a CD couplet in a hairpin with a W-turn-W motif is illustrated in Figure 1. This feature is the result of a chiral edge-to-face (EtF) interaction geometry between the indole rings of the Trp residues. This feature has been used in designing hairpin folds since 1999 [2 and references cited therein]. More recently a capping unit for hairpin structures that also contains an EtF W/W interaction has been developed [3]. In the present report, we detail how to place W/W pairs in hairpin so as to enhance fold stability. In addition, the EtF W/W interaction produces large chemical shift deviations (CSDs) in the folded state. The protons with very large chemical shift changes between the folded and unfolded state also serve as probes for NMR dynamics studies based on exchange broadening data. This allows access to hairpin folding and unfolding rates in the μsec timescale [6]. We illustrate unexpected changes in hairpin folding rates, with a dependence on both loop sequence and the presence or absence of Coulombic interactions at the hairpin termini being observed.

Results and Discussion

In our continuing studies, four distinct EtF W/W interaction geometries have been observed; these are illustrated in Figure 2. Geometry A is observed when P12 of the Trp-cage is replaced by an additional Trp residue [4 and unpublished studies at UW by Williams and Kier]. The other geometries are observed for cross-strand W/W pairs in hairpins [2,3,5]. Panel B represents two geometries as the "edge Trp" can either be at the *N*- or *C*-terminus of a sequence. The geometry in panel C has been observed in hairpins only in the presence of fluoroalcohol co-solvents. All of these geometries produce a far upfield indole ring-H in the NMR spectrum. In the case of geometry B, Hε3 (indole H4) on the edge-indole is upfield by 2-2.5 ppm. In less stable versions of hairpins, the Hε3 CSD provides the extent of folding.

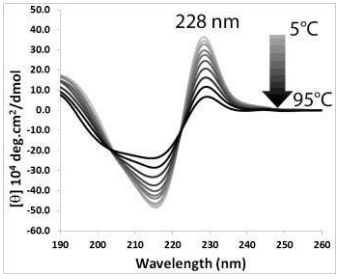

Fig.1. The melting of a W/W exciton couplet in a hairpin.

EtF W/W interaction only appear when the W/W pair is placed at non-H-bonded hairpin strand positions: the positions which also produce fold

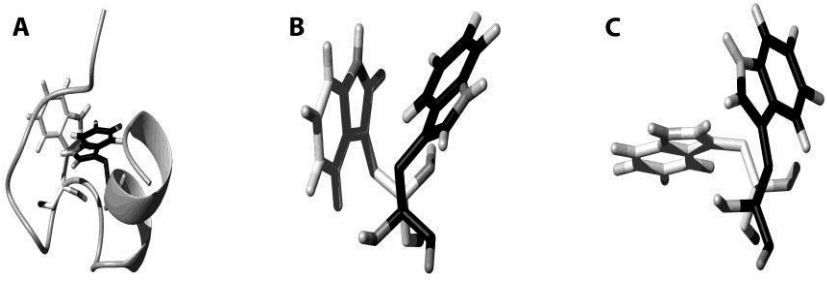

Fig. 2. Trp-Trp geometries observed in miniprotein and hairpin constructs.

stabilization are the non-H-bonded sites closest to the turn and closest to the chain termini. In the case of the turn-flanking W/W interaction, the fold stabilization is most dramatic for [4:6]- and [2:4]-hairpins with a type I' turn. The stabilization that results when the W/W pair, together with essential flanking interactions, is present at the non-H-bonded site at the hairpin termini is discussed in an accompanying report.

The [4:6]-hairpin series provides examples of the extent to which a turn-flanking W/W can provide stabilization and also some of the more interesting hairpin dynamics results that have come from "edge-Hε3" exchange broadening data. The

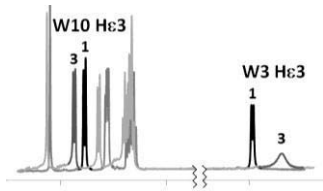

Fig. 3. Lineshapes of the two Hε3.signals for entries #1 and #3.

Table 1. Folding dynamics of KTW-NXXXXX-WTX peptides ([4:6]-hairpins) at 300K

Peptide sequence	δ *(Hε3)*	Δ^{ex} *(Hz)*	$1/k_F$ *(μs)*	$1/k_U$ *(μs)*	*Entry#*
KTW-NPATGK-WTE [a]	5.49 [a]	1.67	0.34	1.89	1
KTW-NAAAGK-WTE	5.28	5.89	2.15	27.26	2
KTW-NAAAKK-WTE	5.34	34.27	9.83	89.61	3
KTW-NPATGK-WTA-NH_2	5.99	12.79	2.00	3.47	4
KTW-NAAAKT-WTE [a]	5.49 [a]	42.42	8.72	47.25	5
at pH 3	6.13	101.20	16.37	23.00	6

[a] *The identical Hε3 shifts indicate equivalent fold stability even though the folding rates differ by a factor of 25*

optimized NPATGK turn sequence [5] can replace a variety of 5- and 4-residue sequences in other hairpins without loss of fold stability. However, the NAAAXX sequences shown in Table 1 require the turn-flanking W/W in order to display significant hairpin formation. For example, while KTW-NAAAKK-WTE is nearly as stable as the corresponding NPATGK compound, KKLWVS-NAAAKK-KIWVSA (with the W/W unit moved to a central rather than the turn-flanking non-H-bonded site) does not display a detectable hairpin fold population even though KKLWVS-INGK-KIWVSA has a stable hairpin fold.

In previous studies of hairpin folding dynamics with identical strands, the fold stabilizing effects of turn mutations are reflected in increases in k_F. The data in Table 1 indicates that loop sequence can have dramatic effects on folding rates even for systems with identical fold stabilities. The line width data that affords these rates appear in Figure 3. In contrast the folding retardation seen in going from entry #1 to entry #4 (a C-terminal E to A-NH_2 mutation) reflects the deletion of an attractive Coulombic interaction between the extreme termini of the hairpin strands. The acidification induced folding rate retardation (entries #5/6) provides additional evidence that this Coulombic interaction effects an increase in folding rates. The dynamics data in Table 1 is viewed as inconsistent [6] with a "turn-formation first then zipper-up" mechanism for hairpin formation. We anticipate that hairpin constructs with W/W pairs will continue to be valuable systems for elucidation folding mechanisms and requisites.

Acknowledgments
Supported by grants CHE-0650318 (NSF) and GM59658 (NIH).

References

1. Grishina, I., Woody, R. *Faraday Discuss.* **99**, 245 (1994).
2. Eidenschink, L., Kier, B., Huggins, K., Andersen, N. *Proteins Struct. Funct. Bioinf.* **75**, 308 (2009).
3. Kier, B., Shu, I., Eidenschink, L., Andersen, N. *Proc. Natl. Acad. Sci. U.S.A.* **107**, 10466 (2010).
4. Bunagan, M., Yang, X., Saven, J., Gai, F. *J. Phys. Chem. B* **110**, 3759 (2006).
5. Andersen, N., Olsen, K., Fesinmeyer, R., et al. *J. Am. Chem. Soc.* **128**, 6101 (2006).
6. Olsen, K., Andersen, N., et al. *Proc. Natl. Acad. Sci. U.S.A.* **102**, 15483(2005) and refs cited therein.

Proceedings of the 31st European Peptide Symposium
Michal Lebl, Morten Meldal, Knud J. Jensen, Thomas Hoeg-Jensen (Editors)
European Peptide Society, 2010

Au_{25} Nanoclusters Capped by Photoactive Aib-based Azopeptides

Ivan Guryanov, Sabrina Antonello, Mahdi Hesari, Martina Zamuner, and Flavio Maran

Department of Chemistry, University of Padova, Padova, 35131, Italy

Introduction

The study of novel phenomena and processes at the molecular level provides useful knowledge for designing a wide range of tools, materials, devices, and systems with specific characteristics. Monolayer-protected gold nanoclusters (MPC) of small size (< 1.5 nm) are of particular interest because they are rather complex hybrid systems but still display quasi-molecular features, such as the presence of a well-defined HOMO-LUMO gap [1,2]. The introduction of different ligands into the nanoparticle-capping monolayer can significantly affect the properties of the nanoparticle, such as the redox or optical behavior. For this purpose, rigid 3_{10}-helical peptides based on the α-aminoisobutyric (Aib) acid unit are very interesting molecules because they are stiff, possess a strong dipole moment, and are capable of mediating electron tunneling very efficiently [3,4]. In this work, we used the ligand place-exchange approach to introduce a thiolated Aib-peptide, containing an azo-fragment, into the monolayer of preformed phenylethanthiolate-protected gold nanoclusters $Au_{25}(SCH_2CH_2Ph)_{18}$. Upon irradiation at 366 nm, *trans→cis* isomerization of the –N=N– bond was expected to change the spatial orientation of the peptide dipole moment as well as the distance between the peptide and the nanoparticle core (Figure 1).

Results and Discussion

Two azo-group containing ligands were synthesized, one with the peptide fragment (compound **1**) and the other with a methyl ester group (compound **2**) (Figure 2A). By studying the optical behavior of the free trityl (Trt) protected ligands (*trans* form), we

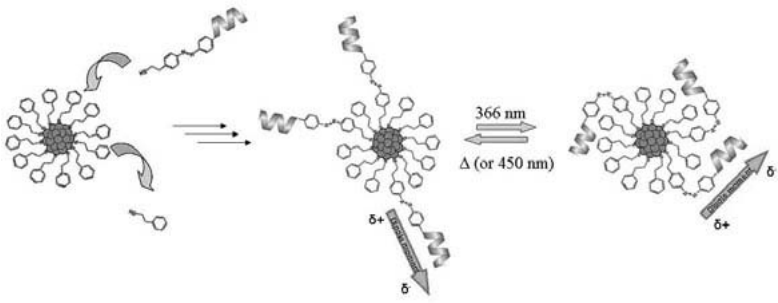

Fig. 1. Ligand exchange reaction with thiolated azopeptides.

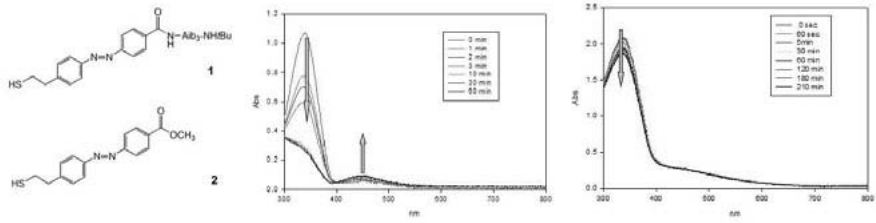

*Fig.2. Ligands used for nanoparticle modification (A) and trans→cis isomerization of **1** (B) or the 20% substituted Au nanoparticle (C) at 366 nm.*

Table 1. Gold nanoparticles obtained by ligand-exchange reaction

Ligand	*Ligand/Ph(CH$_2$)$_2$SH Ratio Used for the Exchange Reaction*	*Extent of Exchange ("death reaction")*	*Percentage of Exchange*
1	1.72	16-17	~90%
1	0.7	5-6	~30%
1	0.2	3-4	~20%
2	0.7	7-8	~40%

observed that irradiation at 366 nm leads to formation of a mixture of the *cis* and *trans* isomers with, under our experimental conditions, a *cis* to *trans* ratio of about 70% (Trt-protected **1**, Figure 2B) and 40% (**2**). Upon *trans*→*cis* transition, the peptide 3_{10}-helical structure remained intact, as indicated by FT-IR, but we observed noticeable changes in the ^{1}H NMR spectrum, including peaks of the peptide moiety (CH_3 groups of Aib). Thermal decay experiments at r.t. showed that the spontaneous *cis* to *trans* conversion (in the dark) has a $t_{1/2}$ of 29.6 hours for Trt-protected **1**.

Different amounts of **1** or **2** were used to carry out the ligand-exchange reaction. The percentage of substitution was determined by destruction of the so-obtained MPCs with iodine, and calculation of the ratio between the resulting oxidized phenylethanethiol and exogenous ligand by ^{1}H NMR ("death reaction") (Table 1).

We also carried an analytical HPLC separation of the MPCs containing 90% of **1**, whereas the MPCs with 20 and 30% of **1** showed a single broad peak. Irradiation of the substituted MPCs also led to spectral changes related to *trans*→*cis* isomerization. Under otherwise identical conditions, the decrease of the intensity of the main band was much less pronounced than for the free ligand (Figure 2C). We also observed that the decrease was less marked for more substituted MPCs. The *cis*→*trans* thermal decay was about 3 times faster than observed for the free ligand. These observations are in agreement with sterical hindrance affecting the isomerization process when the ligands are in the MPC monolayer.

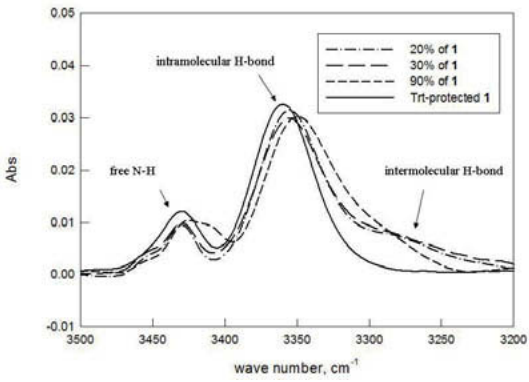

Fig.3. FT-IR analysis of the substituted MPCs.

FT-IR analysis of N-H stretch region (Amide A) showed the presence of inter- and intra-molecular H-bonds as well as free N-H groups (Figure 3). Whereas the stretch frequency of the free N-H groups does not change significantly, the band of intra-molecular H-bonds red-shifts when the ligand is in the MPC monolayer. This is attributed to enhancement of the stiffness of the 3_{10}-helical structure when the peptide ligand is in the monolayer. Further shift takes place upon irradiation causing *trans*→*cis* isomerization, but the effect vanishes when the nanoparticle is heavily substituted (90%).

Differential Pulse Voltammetry (DPV) showed that for the MPCs with 20% and 30% of **1** as well as 40% of **2** the two main oxidation peaks are located at more positive potentials and are more separated with respect to the corresponding oxidation peaks of the native nanoparticle, $Au_{25}(SCH_2CH_2Ph)_{18}$. The positive shift is in line with the expected peptide dipole-moment effect on the charging behavior. In particular, the potential shift is more evident for the 30% substituted MPC.

References

1. Murray, R.W. *Chem. Rev.* **108**, 2688-2720 (2008).
2. Antonello, S., et al. *J. Am. Chem. Soc.* **129**, 9836-9837 (2007).
3. Fabris, L., et al. *J. Am. Chem. Soc.* **128**, 326-336 (2006).
4. Holms, A.H., et al. *Langmuir* **22**, 10584-10589 (2006).

Proceedings of the 31st European Peptide Symposium
Michal Lebl, Morten Meldal, Knud J. Jensen, Thomas Hoeg-Jensen (Editors)
European Peptide Society, 2010

Photocurrent Generation Through Mono- and Bicomponent Peptide Self-Assembled Monolayers: Antenna and Junction Effects

Alessandro Porchetta[1], Emanuela Gatto[1], Mario Caruso[1], Marco Crisma[2], Fernando Formaggio[2], Claudio Toniolo[2], and Mariano Venanzi[1]

[1]Department of Chemical Sciences and Technologies, University of Rome "Tor Vergata", Rome, 00133, Italy; [2]ICB, Padova Unit, CNR, Department of Chemistry, University of Padova, Padova, 35131, Italy

Introduction

Hybrid materials obtained by functionalizing metals or semiconductors with biomolecules or bioinspired molecular systems have been recently synthesized, paving the way for the fast-growing field of bionanoelectronics. The photocurrent generation properties of mono- and bicomponent, peptide-based self-assembled monolayers (SAMs) immobilized on a gold surface were studied by electrochemical and spectroscopic techniques. The peptides investigated were exclusively formed by C^{α}-tetrasubstituted α-amino acids. These residues, due to their peculiar conformational properties [1,2], constrain the peptide in a helical conformation, as confirmed by X-ray diffraction structure determinations, and circular dichroism and NMR experiments in solution.

Results and Discussion

An Aib (α-aminoisobutyric acid) homo-hexapeptide was functionalized at the N-terminus with a lipoic group for immobilization to a gold substrate exploiting the strong Au-S affinity (≈40kcal·mol^{-1}). The peptide was further functionalized with a pyrene chromophore (SSA6Pyr) strongly absorbing in the UV-Vis region to enhance the molecular photon capture cross-section. A peptide with the same backbone, but lacking the pyrene chromophore (SSA6), was also synthesized as a reference compound.

SSA6

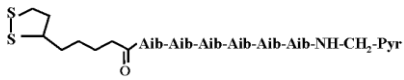

SSA6Pyr

A photoactive octapeptide (A8Pyr), formed exclusively by C^{α}-tetrasubstituted residues and comprising a pyrene chromophore but *not* linked to the gold surface as it lacks the lipoic group, was additionally prepared for photocurrent studies of a peptide SAM:

Z-Aib-Api(Pyr)-L-(αMe)Val-Aib-L-(αMe)Val -L-(αMe)Val -Aib-Api(Boc)-NHtBu (A8Pyr) where Z is benzyloxycarbonyl, (αMe)Val is C^{α}-methyl valine, Boc is *tert*-butyloxy-carbonyl, and Api is 4-aminopiperidine-4-carboxylic acid.

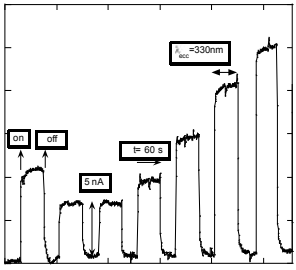

Fig. 1. Photocurrent generation experiment on a gold electrode modified by deposition of an SSA6Pyr film.

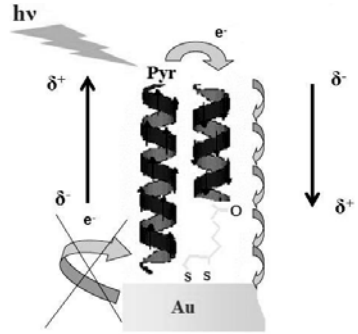

Fig. 2. Schematic representation of the ET pathway in the A8Pyr/SSA6 bicomponent SAM.

In a photocurrent generation experiment, photo-excitation of the pyrene chromophore triggers an electron transfer (ET) event across the peptide chain to the gold electrode (anodic current). The cycle is closed by a second ET step from a sacrificial electron donor in solution (triethanolamine) to the pyrene radical cation. In the presence of an electron acceptor in solution (methylviologen), the electronic current direction can be easily reversed, producing a cathodic current, *i.e.* Au→Pyr ET. On/off cycles of the electronic photocurrent generated by excitation at different wavelengths of the SSA6Pyr SAM immobilized on a gold electrode in a triethanolamine aqueous solution are shown in Figure 1 (*antenna effect*).

In the case of A8Pyr, the photoactive peptide is embedded in a bicomponent peptide SAM formed by an equimolar A8Pyr and SSA6 solution, and it is not linked to the gold surface. Direct ET from the pyrene excited state to the gold surface is therefore inhibited by the high activation energy required for a through-space ET step. A possible mechanism forecasts that the ET process would take place through an intermolecular A8Pyr*→SSA6 interchain ET step followed by multiple ET steps across the SSA6 peptide chain linked to gold (*junction effect*). This mechanism is pictorially sketched in Figure 2.

References

1. Toniolo, C., Crisma, M., Formaggio, F., Peggion, C. *Biopolymers (Pept.Sci.)* **60**, 396-419 (2001).
2. Karle, I.L., Balaram, P. *Biochemistry* **29**, 6747-6756 (1990).

Proceedings of the 31st European Peptide Symposium
Michal Lebl, Morten Meldal, Knud J. Jensen, Thomas Hoeg-Jensen (Editors)
European Peptide Society, 2010

Vibrational Energy Transport in a Peptide Capping Layer over Gold Nanoparticles

Marco Schade[1], Paul M. Donaldson[1], Peter Hamm[1], Alessandro Moretto[2], and Claudio Toniolo[2]

[1]Institute of Physical Chemistry, University of Zűrich, Zűrich, 8057, Switzerland; [2]ICB, Padova Unit, CNR, Department of Chemistry, University of Padova, Padova, 35131, Italy

Introduction

Gold nanoparticles have found numerous applications in life sciences as labels, where they are often covered by biocompatible capping agents [1-3]. Thermal relaxation processes [4] in metal nanoparticles and the subsequent energy transfer process into a solvent have reached considerable interest in current research.

Results and Discussion

To obtain site-selective information about different positions in a 3_{10}-helical [5] peptide capping layer, we used ^{13}C isotope labeling. The two peptides studied were HS-CH_2CH_2-O-CO-NH-Aib-Ala*-Aib_6-OMe (**1**) and HS-CH_2CH_2-O-CO-NH-Aib_3-Ala*-Aib_4-OMe (**2**) (Figure 1). The N-terminal HS-groups of these peptides allow covalent attachment to the gold nanoparticles. Due to a difference in the metal core diameter (sample **1**, 1.2 nm; sample **2**, 2 nm) the plasmon resonance in the Vis spectrum of **2** is more pronounced. Because of the size-dependent surface/volume ratio, a higher absolute concentration of **2** is needed to reach the same effective peptide concentration as that of **1**.

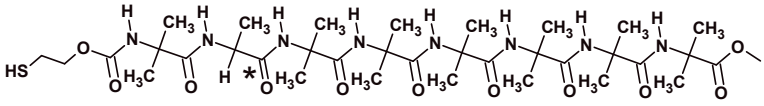

peptide **1**

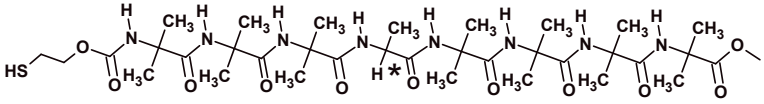

peptide **2**

Fig. 1. The two capping agents used in this study are the 3_{10}-helical octapeptides HS-$(CH_2)_2$-O-CO-Aib-L-Ala-$(Aib)_6$-OMe (peptide **1**) and HS-$(CH_2)_2$-O-CO-$(Aib)_3$-L-Ala*-$(Aib)_4$-OMe (peptide **2**), where Aib stands for α-aminoisobutyric acid and an asterisk (*) indicates a ^{13}C=O label. A urethane moiety was inserted between the linking group and the actual peptide to have an intrinsically spectrally resolved C=O group at the beginning of the helical chain.*

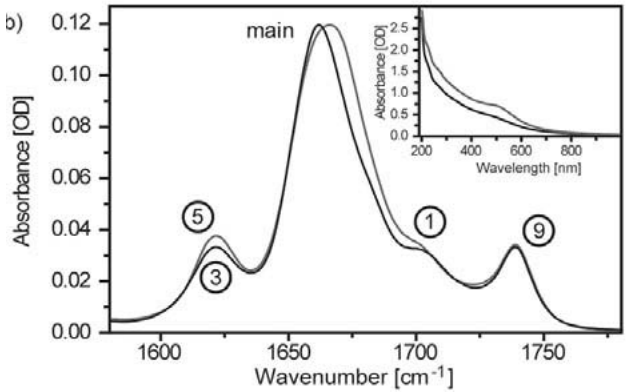

*Fig. 2. FTIR and UV-vis (inset) spectra in acetonitrile-d_3 recorded for nanoparticles coated with peptide **1** (black line) and peptide **2** (gray line) at equal effective peptide concentration. The spectrally resolved C=O bands are labeled according to their positions in the peptide chain. Bands 1: urethane C=O; bands 3 and 5: labeled amide ^{13}C=O; bands 9: methyl ester C=O; main band: amide C=O. Inset: in the UV-vis spectra the plasmon resonance appearing around 520 nm is more pronounced for the nanoparticles coated with peptide **2** (gray line) due to the bigger diameter of its gold core.*

In a VIS pump /IR probe experiment we deposited vibrational excess energy in the gold nanoparticles by exciting their plasmon resonance and monitored the responses of spectrally resolved C=O *thermometers* in the backbone of the helical peptides. The sequential appearance of the bleach maxima of the different C=O reporter units nicely showed the propagation of vibrational energy trough the capping layer: the further a reporter unit is away from the heated gold nanoparticle, the later and the less vibrational energy arrives (Figure 2). We observed that the cooling behavior depends on the particle size: due to a lower surface/volume ratio, bigger particles cool slower. To analyze the structural distribution and its dynamics, we recorded the 2D-IR spectra of the capping layer. From the distinct tilt of the 2D-IR peaks, in particular that of the isotope labelled one, we concluded that the transitions are strongly inhomogenously broadened. The increased inhomogeneous broadening, compared to that of the isolated peptides in solution, suggests strong interactions among the aligned peptides in the capping layer or between the peptides and the gold nanoparticles.

References

1. Giljohann, D.A., Seferos, D.S., Daniel, W.L., Massich, M.D., Patel, P.C., Mirkin, C.A. *Angew. Chem. Int. Edit.* **49**, 3280-3294 (2010).
2. Bunz, U.H.F., Rotello, V.M. *Angew. Chem. Int. Edit.* **49**, 3268-3279 (2010).
3. Klajn, R., Fraser Stoddart, J., Grzybowski, B.A. *Chem. Soc. Rev.* **39**, 2203-2237 (2010).
4. Backus, E.H.G., Bloem, R., Moretto, A., Crisma, M., Toniolo, C., Hamm, P. *J. Phys. Chem.* **B113**, 13405-13409 (2009).
5. Toniolo, C., Benedetti, E. *Trends Biochem. Sci.* **16**, 350-353 (1991).

Proceedings of the 31st European Peptide Symposium
Michal Lebl, Morten Meldal, Knud J. Jensen, Thomas Hoeg-Jensen (Editors)
European Peptide Society, 2010

Cyclic Amino Acid-Containing α-helical Peptide-Catalyzed Enantioselective Epoxidation Reaction

Masakazu Tanaka[1], Masanobu Nagano[2], Mitsunobu Doi[3], Masaaki Kurihara[4], and Hiroshi Suemune[2]

[1]Graduate School of Biomedical Sciences, Nagasaki University, 1-14 Bunkyo-machi, Nagasaki, 852-8521, Japan; [2]Graduate School of Pharmaceutical Sciences, Kyushu University, 3-1-1 Maidashi, Higashi-ku, Fukuoka, 812-8582, Japan; [3]Division of Organic Chemistry, National Institute of Health Sciences, Tokyo, 158-8501, Japan; [4]Osaka University of Pharmaceutical Sciences, Osaka, 569-1094, Japan

Introduction

Poly L-α-amino acid-catalyzed asymmetric epoxidation of chalcone was reported by Juliá, Colonna and co-workers [1]. They studied the generality of substrates, reaction conditions, effect of the length of oligomers, and reaction mechanisms. In the reaction, poly L-α-amino acids might form α-helical structures, and their α-helical *N*-termini are important for asymmetric induction. To stabilize the α-helical structure of catalyst, polyethyleneglycol and resin-attached L-Leu oligomers have been developed, and thus, the high molecular weight and insolubility of catalysts were in part overcome [2].

Also, α,α-disubstituted amino acids (dAAs) were used to induce a helical structure, but dAA-containing oligomers formed not α-helices but 3_{10}-helices, which did not give epoxide of high enantiomeric excess [3]. Recently, we have disclosed that cyclic amino acid-containing L-Leu-based peptides preferentially formed right-handed (*P*) α-helices [4]. Thus, we reasoned that cyclic amino acid-containing L-Leu-based peptides would catalyze the asymmetric epoxidation of (*E*)-chalcone. Here we demonstrate the enantioselective epoxidation of (*E*)-chalcone, and the relationship between the secondary structure of catalysts and the enantiomeric excesses of epoxides [5].

Results and Discussion

We prepared chiral cyclic dAA-containing oligomers R-{L-Leu-L-Leu-dAA}$_n$-OMe {R = Boc, or H; n = 2, 3, 4; dAA = Aib, (*R*,*R*)-Ac$_5$c^{dOM}, (*S*,*S*)-Ac$_5$c^{dOM}, (1*R*,3*S*)-Ac$_5$c^{OM}, and (1*S*,3*S*)-Ac$_5$c^{OM}} using solution phase-methods.

First, asymmetric epoxidation of (*E*)-chalcone using 25 mol % of Boc-{L-Leu-L-Leu-dAA}$_n$-OMe was examined under conditions of urea-H_2O_2 (1.1 equiv) and DBU (5.6 equiv) in THF at 0 °C to room temperature for 24 h. Although the reactions catalyzed by hexamers afforded epoxide of low enantiomeric excesses (7–11% ee) in 77–91% conversion yield (not shown), elongation of the peptide chain improved enantiomeric excesses, except for Aib-containing peptides. It should be noted that side-chain chiral centers affected enantiomeric excesses, and those by (1*S*,3*S*)-Ac$_5$c^{OM}-containing nonamer and dodecamer were 82–83% ee, which are in contrast to other cases. X-ray crystallographic analysis revealed that the (1*S*,3*S*)-Ac$_5$c^{OM} hexamer assumed a mixture of (*P*) 3_{10}-/α-helix, where intramolecular hydrogen bonds of *i*←*i*+3 type are formed on the *N*-terminal side (*i* = 0, 1) and those of *i*←*i*+4 type are formed on the *C*-terminal side (*i* = 1, 2). Three crystallographic independent conformers, which are similar in the peptide backbone, exist in asymmetric units. Contrary to the 3_{10}-/α-helix of hexamer, the (1*S*,3*S*)-nonamer formed fully developed right-handed α-helices, where *i*←*i*+4-type hydrogen bonds were observed.

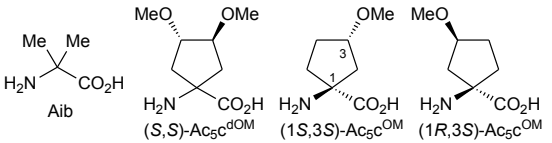

Fig. 1. Structure of dAAs.

In Boc-protected 3_{10}-helical peptides, intramolecular hydrogen bonds of *i*←*i*+3 type are formed, and the two *N*-terminal NH protons are not involved in intramolecular hydrogen bonding. On the other hand, in α-helical peptides, intramolecular hydrogen bonds of *i*←*i*+4 type are formed, and the first three *N*-terminal NH protons are free of intramolecular hydrogen bonding. According to Roberts' model [2], the three N-terminal

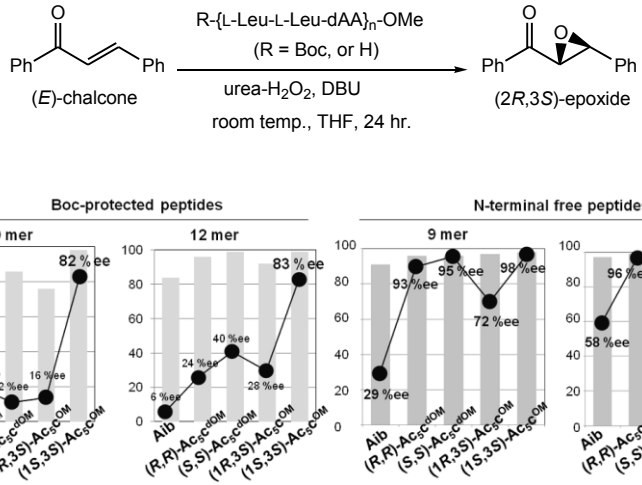

Fig. 2. Epoxidation of chalcone using helical oligopeptides.

N(2)H, N(3)H and N(4)H protons are crucial for asymmetric induction, and the N(1)H proton is less important. In Boc-protected α-helical peptides, the N(4)H proton forms an intramolecular hydrogen bond with the C=O of the protecting group, and thus, the N(4)H proton may not be available for interaction with chalcone intermediate. Thus, next we examined epoxidation using 5 mol % of *N*-terminal free oligomers.

Except for hexamers having Aib and (*R*,*R*)-Ac_5c^{dOM}, *N*-terminal free peptides gave better enantiomeric excesses than Boc-protected ones. In particular, the reaction by (*S*,*S*)-Ac_5c^{dOM} and (1*S*,3*S*)-Ac_5c^{OM} containing nonamers and dodecamers afforded epoxides of >95% ee in good yield. Furthermore, the (1*S*,3*S*)-Ac_5c^{OM} containing α-helical nonamer can be applied to epoxidation of various α,β-unsaturated ketones.

Acknowledgments

This work was supported in part by a Grant-in-Aid (B) from JSPS, by a Grant-in-Aid for Scientific Research on Priority Areas (No. 20037054, "Chemistry of Concerto Catalysis") from MEXT, and also by a Grant-in-Aid from the ASAHI GLASS Foundation.

References

1. (a) Juliá, S., Masana, J., Vega, J.C. *Angew. Chem., Int. Ed.* **19**, 929 (1980); (b) Juliá, S., Colonna, S., et al. *J. Chem. Soc. Perkin Trans.* **1** 1317 (1982).
2. (a) Porter, M.J., Roberts, S.M., Skidmore, J. *Bioorg. Med. Chem*. **7**, 2145 (1999); (b) Roberts, S.M., et al. *TRENDS in Biotechnology* **23**, 507 (2005); (c) Kelly, D.R., Roberts, S.M. *Biopolymers (Peptide Sci.)* **84**, 74 (2006); (d) Toniolo, C., et al. *Biopolymers (Peptide Sci.)* **84**, 90 (2006); (e) Geller, T., Roberts, S.M. *J. Chem. Soc., Perkin Trans. I.* 1397 (1999); (f) Roberts, S.M., et al. *Tetrahedoron Lett*. **45**, 3885 (2004). Also, references cited therein.
3. (a) Ohkata, K., et al. *Chem. Lett.* 366 (2000); (b) Toniolo, C., Scrimin, P., et al. *Biopolymers (Peptide Sci.)* **84**, 97 (2006).
4. (a) Demizu, Y., Tanaka, M., et al. *Chem. Pharm. Bull*. **55**, 840(2007); (b) Nagano, M., Tanaka, M., et al. *Org. Lett.* **11**, 1135 (2009).
5. Nagano, M., Tanaka, M., et al. *Org. Lett.* **12**, 3564 (2010).

Proceedings of the 31st European Peptide Symposium
Michal Lebl, Morten Meldal, Knud J. Jensen, Thomas Hoeg-Jensen (Editors)
European Peptide Society, 2010

Design and Synthesis of Bipyridyl-Containing Peptide Dendrimers as Iron Protein Models

Piero Geotti-Bianchini, Nicolas A. Uhlich, Tamis Darbre, and Jean-Louis Reymond*
Department of Chemistry and Biochemistry, University of Berne, Freiestrasse 3, 3012, Berne, Switzerland

Introduction

Peptide dendrimers, containing diamino acids as branching units [1], possess suitable properties as soluble protein models, such as a hindered, solvent-shielded core and multiple peripheral groups [2]. Since peptide dendrimers are composed of amino acids, their chemico-physical properties, hence their activity, are easily tunable by sequence modification or introduction of non-natural amino acids [3]. Bipyridyl is a bidentate ligand with high affinity for late transition metals, forming very stable 3:1 complexes with Fe(II). In such complexes the valence of the metal center is saturated, whereas in iron enzymes coordinative unsaturatation is required for activity [4]. Therefore, in our research on metalloenzyme models, we have studied the effect of the incorporation of bipyridyl units in peptide dendrimers, aiming at a control of binding selectivity and stoichiometry.

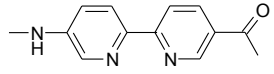

Bpy

Fig. 1. The bipyridyl derived amino acid Bpy.

We have recently reported [5] the synthesis of a bipyridyl-based amino acid (**Bpy**, Figure 1) and its incorporation in the focal point of a combinatorial library of peptide dendrimers (Figure 2, top left, structure **1**). Metal binding experiments showed that 3:1 dendrimer/Fe(II) complexes were formed by negatively charged sequences, but not by strongly positively charged ones.

Results and Discussion

We have then prepared second generation peptide dendrimers carrying Bpy in the two first-generation branches (Figure 2, bottom left, structure **2**), expecting stronger metal binding and a more pronounced effect of the dendrimer composition on the metal complexation properties.

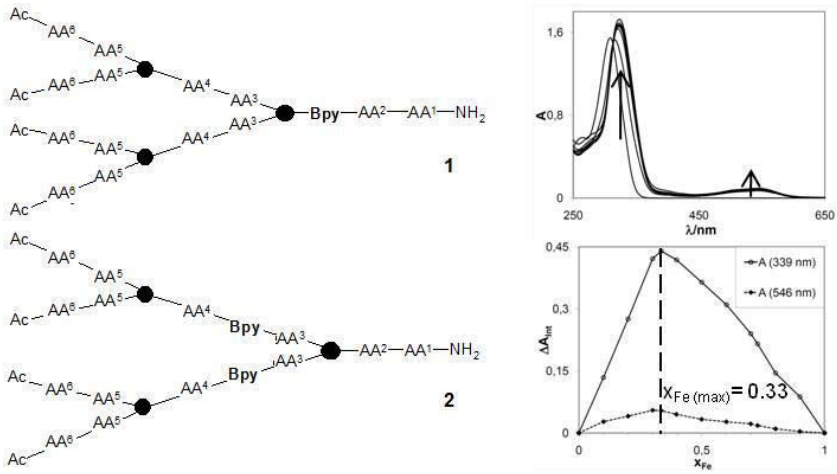

*Fig. 2. Left: Structure of the peptide dendrimers carrying one Bpy residue in the focal point (**1**, top) or two Bpy residues in the two first generation branches (**2**, bottom). Black dots represent the branching residues (2,3-diamino-propionic acid), AA^n (n= 1-6) represent the variable amino acids (specified in Table 1). Right: Spectrophotometric titration of dendrimer **2a** (30 μM) with Fe(II) in HEPES buffer (top); Job plot analysis of Fe(II) binding for the same dendrimer at a total concentration of 30 μM (bottom).*

Table 1. Sequences and properties of the peptide dendrimers synthesized

	AA^1	AA^2	AA^3	AA^4	AA^5	AA^6	*MS calc.*	*Yield (%)*	*MS found*	*Charge (pH 7)*
2a	Asp	Ala	Val	Ala	Thr	Glu	2285.3	13.0	2285.2	- 5
2e	Asp	Ala	Val	Glu	Thr	Glu	2401.4	13.2	2401.0	- 7
2h	Ser	His	Ala	His	Thr	Gln	2463.6	2.2	2463.5	0
2p	Lys	Ala	Val	Leu	Lys	Arg	2599.1	12.9	2599.0	+ 9

Negatively charged (**2a**, **2e**), neutral hydrophilic (**2h**) and strongly positively charged (**2p**) sequences have been synthesized on solid-phase and purified by RP-HPLC (Table 1).

The metal binding properties of the peptide dendrimers have been tested by UV-Vis measurements, detecting bipyridyl/metal interactions by the shift in the bipyridyl absorption band. Spectrophotometric titrations with Cu(II), Ni(II) and Zn(II) in HEPES buffer, pH 6.5, have detected the formation of stable 1:1 complexes (K_f 10^5 -10^6 M^{-1}) for all dendrimers tested.

By titrating neutral or negatively charged dendrimers with Fe(II), the characteristic MLCT band of low-spin tris-bipyridyl iron complexes is observed in the visible region (Figure 2, top right). Moreover, from the presence of isosbestic points it can be deduced that such complexes are the only species formed. The 2:1 dendrimer/metal stoichiometry required for interaction of an iron center with three bipyridyl ligands has been confirmed by Job plot analyses [6] of complex formation (Figure 2, bottom right). On the other hand, for the positively charged dendrimer **2p**, neither the shift in the bipyridyl absorption band nor the band in the visible region are observed under the same conditions, suggesting that this dendrimer does not bind the metal.

Some metal/dendrimer mixtures have been analyzed by LC-MS: in addition to the peaks of the free dendrimers formed by complex hydrolysis under the acidic elution conditions, peaks due to metal complexes with the stoichiometry predicted by the UV experiments have been detected. Interestingly, in the case of the **2e**/Fe(II) mixture, peaks due to different regio- and stereo-isomers of the 2:1 complex appear, as well as peaks due to 1:1 complexes formed as hydrolysis intermediates.

In the 2:1 dendrimer/Fe(II) complexes the two dendrimer ligands are not equivalent: the first one has both bipyridyl moieties bound to the metal, the second one has one bipyridyl bound to the metal and the other not engaged in binding. The two free coordination sites of such bipyridyl could chelate a further metal ion, allowing the formation of more complex molecular architectures.

Acknowledgments

Financial support from the Swiss National Science Fondation for the research project, as well as from the Nachwuchsförderungskommission of the Faculty of Natural Philosophy of the University of Berne for the participation of Piero Geotti-Bianchini to the Symposium, are gratefully acknowledged.

References

1. Crespo, L., Sanclimens, G., Pons, M. Giralt, E., Royo, M., Albericio, F. *Chem. Rev.* **105**, 1663-1681 (2005).
2. Darbre, T., Reymond, J.-L. *Acc. Chem. Res.* **39**, 925-934 (2006).
3. Javor, S., Delort, E., Darbre, T., Reymond, J.-L. *J. Am. Chem. Soc.* **129**, 13238-13246 (2007).
4. Costas, M., Mehn, M.P., Jensen, M.P., Que, L. Jr. *Chem. Rev.* **104**, 939-986 (2004).
5. Uhlich, N.A., Sommer, P., Bühr, C., Schürch, S., Reymond, J.-L., Darbre, T. *Chem. Commun.* 6237-6239 (2009).
6. Huang, C.Y. *Meth. Enzymol.* **87**, 509-525 (1982).

Proceedings of the 31st European Peptide Symposium
Michal Lebl, Morten Meldal, Knud J. Jensen, Thomas Hoeg-Jensen (Editors)
European Peptide Society, 2010

Synthesis of Self-Assembled Glycolipopeptide and Its Activation of Peritoneal Macrophages

Ayumi Suzuki[1], Yasushi Suzuki[1], Naoya Kojima[2], and Toshiyuki Inazu[1,3]*

[1]Department of Applied Chemistry, School of Engineering; [2]Department of Applied Biochemistry, School of Engineering; [3]Institute of Glycoscience, Tokai University, Kitakaname 4-1-1, Hiratsuka, Kanagawa, 259-1292, Japan

Introduction

Glycoconjugates have important roles in cell function, such as intercellular recognition, cell proliferation control, and the information transmission. We generated liposomes coated with a neoglycolipid constructed from mannotriose and dipalmitoylphosphatidyl-ethanolamine (Man3-DPPE), and showed that resident peritoneal macrophages (PEMs) mature together with up-regulation of MHC class II and co-stimulatory molecules and produce IL-12 in response to intraperitoneal uptake of Man3-DPPE coated liposomes (OMLs), leading to antigen-specific Th1 immunity sufficient to reject tumors and parasites[1,2]. Our attention was focused on not only the large size of OMLs but also the surface morphology of the mannose(Man) cluster to develop a more suitable materials instead of OMLs.

Results and Discussion

We synthesized the glycolipopeptide, Ac-Tyr-Ser-Gln-Glu(Hda)-Gln-Ser-Ser(Man)-Ser-Ser-Gln-Glu(Hda)-Gln-Ser-Gly-NH_2 (**1**) by solid-phase synthesis using Fmoc-Glu(Had)-OH shown in Figure 1 [3]. The synthesis was carried out using the corresponding Fmoc-amino acids by the Mpt-MA method [4] starting from Fmoc-NH-resin (Rink Amide™ resin; Fmoc 0.43 mmol/g resin). After deprotection of the Fmoc group with 20% piperidine in *N*-methyl-2-pyrrolidinone (NMP), the resin was reacted twice with a 4-fold excess of Fmoc-amino acid Mpt-MA, (Fmoc-AA-OP(S)Me_2) in the presence of *N,N*-diisopropylethylamine (DIEA) by a double coupling method. Finally, the treatment of lipopeptide resin with 95% trifluoroacetic acid (TFA) gave a crude peptide. The desired pure lipopeptide with a Man residue was obtained by decantation using MeOH in 27% yield from Fmoc-NH-resin. It was purified by reverse-phase high-performance liquid chromatography (HPLC). The characterization of the synthetic peptide was performed by MALDI-TOF MS (*m/z* Calcd for $C_{111}H_{193}N_{21}O_{47}$ for $[M + Na]^+$ 2595.2, found 2597.6). These solid-phase reactions are shown in Figure 2.

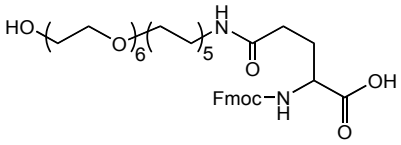

Fig. 1. Structure of Fmoc-Glu(Hda)-OH.

*Fig. 2. Solid-phase synthesis of glycolipopeptide **1**.*

The particle size distribution of this synthetic glycolipopeptide **1** measured by dynamic light scattering (DLS) in H_2O/MeOH (3:1) suggested that it may have some self-assembly capability. We used Transmission Electron Microscopy (TEM) to study the structure in detail. The glycolipopeptide solution was placed on carbon grids and stained with an aqueous solution of 1% by weight of RuO_4 at room temperature for 5 min. We observed spherical vesicle and planar bilayer morphologies as shown in Figure 3. These results suggest the self-assembled molecular size of **1** would be similar to that of OML.

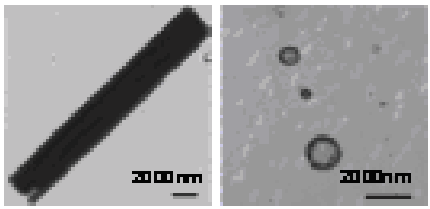

*Fig. 3. TEM images of glycolipopeptide **1**.*

Next, we investigated the activation of peritoneal macrophages by the synthesized glycolipopeptide **1** and the induction of IL-12 production. C57BL/6 mice (female, 6-8 weeks old) were intraperitoneally injected once with 300 μg from 1mg/mL solution of the synthesized **1**. The peritoneal cells (PECs) were harvested from the peritoneal cavity of mice 1 h after the injection, and the production of IL-12 from PEMs was assessed by enzyme-linked immunosorbent assay (ELISA). We found glycolipopeptide **1** induced production of significant levels of IL-12 from PEMs, suggesting that synthesized glycolipopeptide **1** may have an activity for PEM activation.

Further detailed assay of IL-12 production and investigation of the structure-activity relationship of glycolipopeptide **1** are now in progress.

Acknowledgments

We thank Prof. Tomokazu Iyoda and Dr. Kaori Kamata from Chemical Resources Laboratory, Tokyo Institute of Technology for the measurement of TEM images. We would also like to thank Mr. Cheol, Min Yun, and Prof. Yu Nagase from our Department for their helpful discussion and measurement of AFM and TEM images. We also thank Technical Service Coordination Office Tokai University for the technical support of the measurement of AFM images. Part of this work was supported by the Program for Promotion of Basic Research Activities for Innovative Biosciences (PROBRAIN), a grant for Hi-tech research program from Tokai University, and Research and Study Project of Tokai University Educational System General Research Organization.

References

1. Ikehara, Y., Shiuchi, N., Kabata-Ikehara, S., Nakanishi, H., Yokoyama, N., Takagi, H., Nagata, T., Koide, Y., Kuzushima, K., Takahashi, T., Tsujimura, K., Kojima, N. *Cancer Lett.* **260**, 137-145 (2008).
2. Takagi, H., Furuya, N., Kojima, N. *Cytokine* **40**, 241-250 (2007).
3. Suzuki, A., Suzuki, Y., Kuramochi, M., Inazu, T. *"Peptide Science 2008: Proceeding of 45th Japanese Peptide Symposium"* Ed. by M. Nomizu, The Japanese Peptide Society, Osaka, (2009) pp.151-154.
4. Mizuno, M., Haneda, K., Iguchi, R., Muramoto, I., Kawakami, T., Aimoto, S., Yamamoto, K., Inazu, T. *J. Am. Chem. Soc*. **121**, 284-290 (1999).

Proceedings of the 31st European Peptide Symposium
Michal Lebl, Morten Meldal, Knud J. Jensen, Thomas Hoeg-Jensen (Editors)
European Peptide Society, 2010

Computational Studies of the Stability and Chirality of Self-Assembled Complexes of a Novel Iron(II)-Binding Insulin Derivative

Niels Johan Christensen[1], Henrik K. Munch[2], Søren Thiis Heide[1], Thomas Hoeg-Jensen[3], Peter Waaben Thulstrup[1] and Knud J. Jensen[2]

[1]*Bioinorganic Chemistry, Department of Basic Sciences and Environment, Faculty of Life Sciences, University of Copenhagen, Frederiksberg C, 1871, Denmark;*
[2]*Bioorganic Chemistry, Department of Basic Sciences and Environment, Faculty of Life Sciences, University of Copenhagen, Frederiksberg C, 1871, Denmark;*
[3]*Novo Nordisk, Maaloev, 2760, Denmark*

Introduction

In a concurrent study, we demonstrate experimental evidence for the Fe(II) directed self-assembly of a novel insulin derivative (human insulin (B9Asp + B27Glu) [1]) functionalized with bipyridine through the B29Lys side-chain or through the N-terminal of the A-chain (Figure 1). In the following, these engineered insulin monomers shall be referred to as B29 and A1, where no confusion will arise. Here we present initial computational studies on self-assembled states involving the chelation of Fe(II) by three B29 or A1 monomers.

Results and Discussion

Measurements confirm that the self-assembled insulin structures are trimers containing a Fe(II) ion coordinated by three bipyridine ligands. This information is consistent with four modes of association, as illustrated with tentative *in silico* models in Figure 2 in the case of B29. We have employed time-dependent density functional theory (TDDFT) calculations at the RB3lYP/6-31G(d) level of theory on the coordination environment around the Fe(II) ion to predict circular dichroism (CD) spectra of the four stereoisomers of the self-assembled insulin trimer. The TDDFT calculations were carried out on small models truncated close to the bipyridine moiety, allowing representation of the Fe(II) coordination environment of both A1 and B29 trimers. The RB3LYP/6-31G(d) geometries and relative SCF energies are shown in Figure 3. It is evident that the meridional arrangement is disfavored by 2.1 kJ/mol with respect to the facial arrangement for these models. With the chosen truncation, the Λ and Δ forms are enantiomers and thus have identical energies. This is not the case for the actual insulin trimers, and we are currently studying more realistic models to elucidate Λ/Δ preferences. Figure 4 shows the measured CD spectra and spectra predicted from the model systems. Although the calculated spectra are blue-shifted

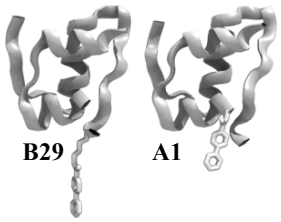

Fig. 1. Models of insulin X2 monomers functionalized with bipyridine at the B29 or A1 position.

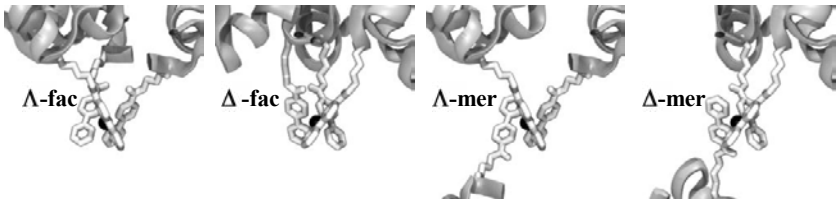

Fig. 2. Three insulin X2 monomers funtionalized with bipyridine (B29 or A1 of Figure 1) can form four types of coordination complex with Fe(II), differing in the chirality (Λ or Δ) of the tris-bipyrdine complex and the facial (fac) or meridional (mer) arrangement of substituents. The complexes shown are tentative in silico models corresponding to B29-bipy functionalized insulin.

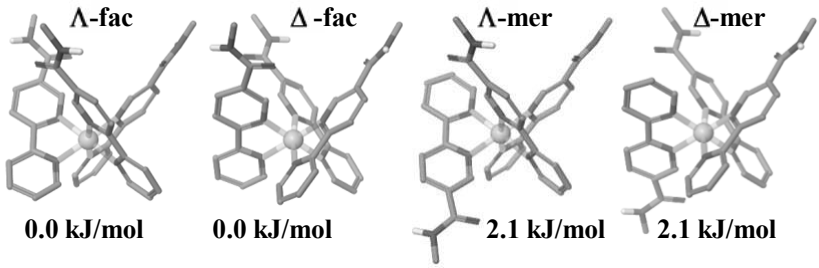

Fig. 3. Truncated model systems representing the insulin trimers in Figure 2. The geometries were obtained at the B3LYP/6-31G(d) level of theory. Relative SCF energies are given.

25-50 nm relative to the measured spectra, the change of sign of the CD signal is reproduced by the calculations in the two characteristic spectral regions (240-350 nm) and (400-700 nm). Since the spectra calculated for Λ and Δ models agree with CD measurements for B29 and A1, respectively, the dominating enantiomer in solution has been determined in each case. The calculated spectra for *mer* and *fac* configurations are

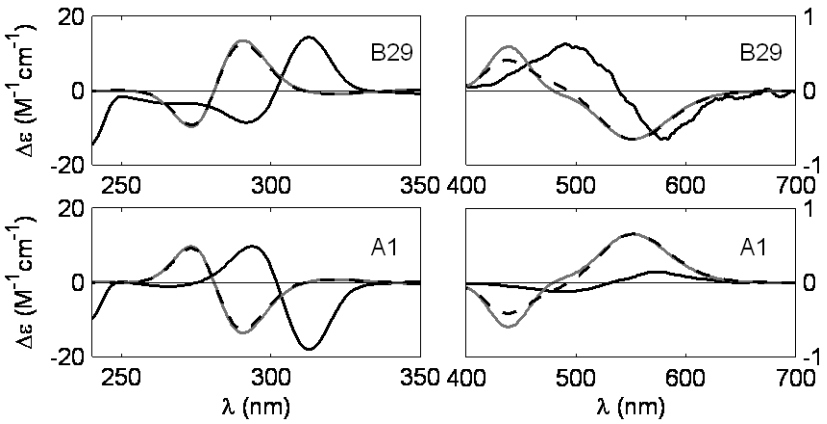

Fig. 4. Measured and calculated CD spectra for engineered insulin trimers. Solid black lines: Measured spectra. Solid grey and dashed black lines: Calculated (RB3LYP/6-31G(d), 100 electronic states) spectra for fac and mer species, respectively. Top panel: Measured CD spectrum for B29 and calculated spectra for fac and mer Λ models. Bottom panel: Measured CD spectrum for A1 and calculated spectra for fac and mer Δ models.

nearly identical, and the preference for *fac* suggested by the relative SCF energies in Figure 3 can therefore not be confirmed from the comparison with measurement. In summary we have shown from comparison with small model systems that the dominating enantiomer in solution for the novel insulin trimers is Λ for B29 and Δ for A1. The structural basis for the differences in enantioselectivity, as well as *mer* and *fac* preferences are currently under investigation.

Acknowledgments
Supported by NABIIT grant 2106-07-0024 (The Danish Council for Strategic Research).

References

1. Brange, J., Ribel, U., Hansen, J.F., Dodson, G., Hansen, M.T., Havelund, S., Melberg, S.G., Norris, F., Norris, K., Snel, L., Sørensen, A.R. *Nature* **333**, 679-682 (1988).

Proceedings of the 31st European Peptide Symposium
Michal Lebl, Morten Meldal, Knud J. Jensen, Thomas Hoeg-Jensen (Editors)
European Peptide Society, 2010

Tubomicelle of Gene Transfection Agent 1,4-Dihydropyridine Lipid and Its Binding with DNA

Inta Liepina[1], Ainars Zemitis[1], Gunars Duburs[1], Cezary Czaplewski[3], and Adam Liwo[3]

[1]*Latvian Institute of Organic Synthesis, Aizkraukles str. 21, Riga LV1006, Latvia,*
[2]*Department of Chemistry, and University of Gdansk, ul. Sobieskiego 18, 80-952 Gdansk, Poland*

Introduction

Artificial lipids are in wide use for gene and drug delivery [1-3]. In our prior work [4] we showed with molecular dynamics (MD) simulation, that the gene transfection agent, 1,1'-{[3,5-bis(dodecyloxycarbonyl)-4-phenyl-1,4-dihydropyridin-2,6-diyl]dimethylene} bispyridinium dibromide (1,4-DHP lipid) (Figure 1) [5,6] formed a tubular micelle, if started from a lipid bilayer, and the existence of worm-like structures was confirmed by electron microscopy.

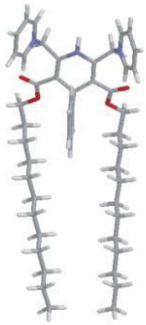

Fig. 1. 1,4-DHP lipid.

The present work investigates the stability of the tubular micelle and its binding with the 15-mer DNA: TGG-CGT-CTT-CCA-TTT.1,4-DHP lipid tubomicelle was taken from [4] and:

1) immersed in a bigger amount of water (**system 1**) and subjected for 22 ns of MD run,

2) four tubomicellaes were put together (**system 2**) and simulated by MD for 63 ns,

3) four tubomicellaes were surrounded by additional water (**system 3**) and subjected to MD for 42 ns,

4) System of five tubomicellaes was complexed with the 15-mer DNA double helix (**system 4**) and simulated by MD for 32 ns.

All the systems were subjected to MD with AMBER 9.0 program package, f99 force field, NTP protocol (constant number of particles, temperature, pressure), using a periodic water box of explicit water molecules, MD simulation were started at T=10K and heated up till T=309K, and then the calculations were continued at constant temperature of T=309K.

Results and Discussion

System 1, 1,4-DHP lipid tubomicelle in the bigger amount of water. During the course of simulation a gap appeared in the tubomicelle, - after about 6 ns of MD, then after about 12 ns the classical micellae split away from the tubular structure. After about 17 ns the rest of the tubula split into two round micellaes.

System 2, four tubomicellaes together, showed the stability of tubular structure during the whole simulation time of 63 ns.

System 3, four tubomicellaes surrounded by water, kept their tubular structure during the whole course of MD simulation of 42 ns, however there few cuts are formed in the tubulas suggesting that with the time some round micellae form could emerge.

System 4, five tubomicellaes complexed with the DNA, showed that the DNA double helix is stable during the whole course of simulation. The DNA rod was put aside from the five tubomicallaes, during the 1 ns of MD simulation it edged between two tubular micellaes, become squeezed there, and then, after about 12 ns the part of the third tubular micelle started to move towards the DNA rod.

Conclusions

A 1,4-DHP lipid tubomicelle is stable in water, but in smaller 1,4-DHP lipid concentrations classic micelle can split from the tubomicelle, and tubomicelle can transform to round micellaes. This is in agreement with electron microscopy showing both tubular and round structures.

The DNA could be bound between two tubular micellaes maintaining its double helical structure and showing stability during the course of simulation. The 1,4-DHP rings tend to take tangential position towards the tubular micellaes' surface.

The fact that 1,4-DHP lipid molecules moved from the initial bilayer structure to the tubular one and turned to micellaes suggests that the supramolecular structure of the 1,4-DHP lipid depend on external conditions, in high 1,4-DHP lipid concentrations very probably the gene transfection with 1,4-DHP lipid is performed by means of the tubular lipoplex in micellar hexagonal structure or complexed inverted hexagonal structure.

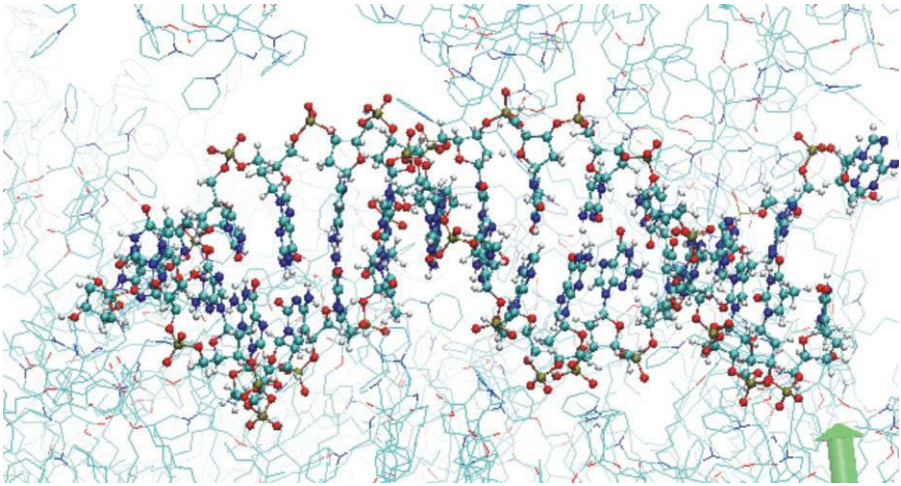

Fig. 2. Binding of DNA between two tubomicelaes after 12676 ps of MD run.

Acknowledgments

This work was supported by European Economic Area block grant "Academic Research" LV0015.EEZ09AP- 68, and by ESF project 2009/0197/1DP/1.1.1.2.0/09/APIA/VIAA/014. Calculations were performed on computers of the Gdansk Academic Computer Center TASK.

References

1. Tresset, G., Cheong, W.C.D., Tan, Y.L.S., Boulaire, J., Lam, Y.M. *Biophysical Journal* **93**, 637-644 (2007).
2. Luo, D., Saltzman, M. *Nature Biotechnology* **18**, 33-37 (2000).
3. Belguise-Valladier, P., Behr, J.-P. *Cytotechnology* 35, 197-201, 2001.
4. Liepina, I., Czaplewski, C., Ose, V., Danne, R., Duburs, G. *Proceedings of NIC Workshop From Computational Biophysics to System Biology, Julich, May 19-21, 2008, Germany., NIC, v40,* (Ulrich H.E. Hansman, Jan H., Meinke, Sandipan Mohanty, Walter Nadler, Olav Zimmermann, Eds), pp 305-307.
5. Hyvonen, Z., Plotniece, A., Reine, I., Chekavichus, B., Duburs, G., Urtti, A. *Biochim. Biophys. Acta* **1509**, 451-466 (2000).
6. Hyvonen, Z., Ronkko, S., Toppinen, M.-R., Jaaskelainen, I., Plotniece, A., Urtti, A. *Journal of Controlled Release* **99**, 177-190 (2004).

Subject index

Author index